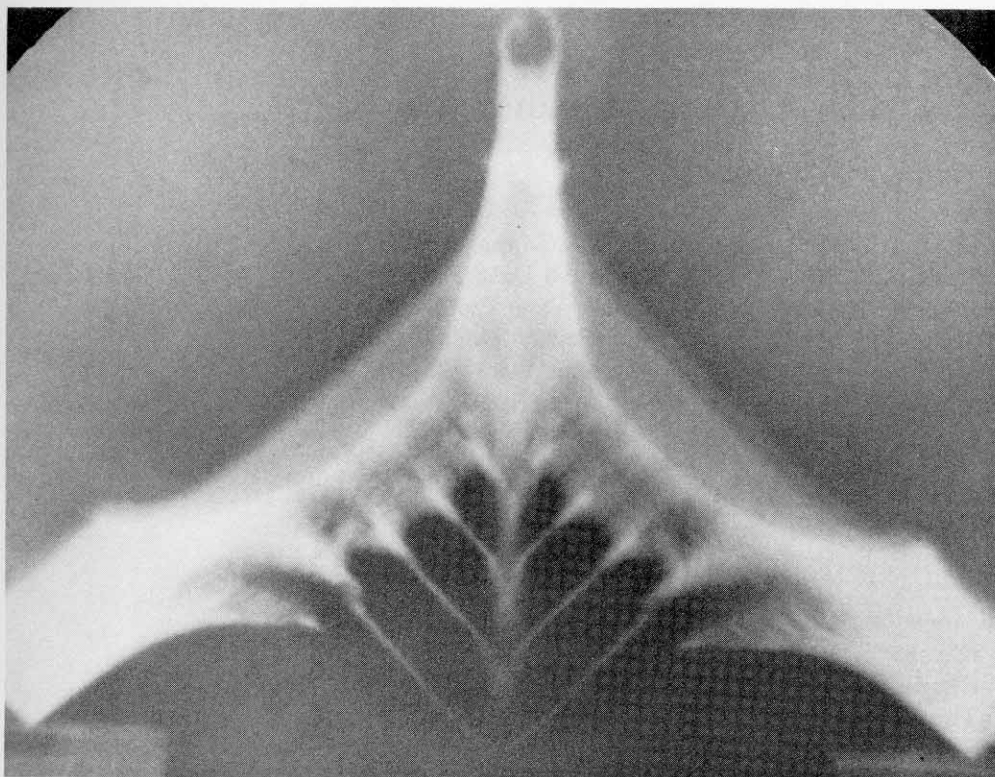


LASL PHERMEX DATA

VOLUME I



UNIVERSITY OF CALIFORNIA, SAN DIEGO
La Jolla, California 92037

LOS ALAMOS SERIES ON DYNAMIC MATERIAL PROPERTIES

LOS ALAMOS DATA CENTER FOR DYNAMIC MATERIAL PROPERTIES

TECHNICAL COMMITTEE

Charles L. Mader	Program Manager
Terry R. Gibbs	Explosive Data Editor
John W. Hopson, Jr.	Shock Wave Profile Editor
Stanley P. Marsh	Equation of State Editor
Alphonse Popolato	Explosive Data Editor
Martha S. Hoyt	Computer Applications Analyst
Kasha V. Thayer	Technical Editor

John F. Barnes
Bobby G. Craig
William E. Deal, Jr.
Richard D. Dick
James N. Johnson
Elizabeth Marshall
Charles E. Morris
Timothy R. Neal
Suzanne W. Peterson
Raymond N. Rogers
Melvin T. Thieme
Jerry D. Wackerle
John M. Walsh

LASL PHERMEX DATA VOLUME I

**Editors - Charles L. Mader
Timothy R. Neal
Richard D. Dick**



UNIVERSITY OF CALIFORNIA PRESS
Berkeley · Los Angeles · London

University of California Press
Berkeley and Los Angeles, California

University of California Press, Ltd.
London, England

Copyright © 1980 by
The Regents of the University of California

ISBN: 0-520-04009-0

Series ISBN: 0-520-04007-4

Library of Congress Catalog Card Number: 79-66580

Printed in the United States of America

1 2 3 4 5 6 7 8 9

CONTENTS

INTRODUCTION	1
THE PHERMEX FACILITY	2
PHERMEX Machine Design and Operating Characteristics	2
The Accelerator	3
The Electron Source and Injection	9
The RF Power System	9
Timing, Firing, and Signal Detection	11
Radiographic Procedures	14
DATA PRESENTATION	16
REFERENCES	25
CATALOG OF SHOT SUBJECTS, PHERMEX SHOTS 1 THROUGH 400. .	28

INTRODUCTION

About 15 years ago, a unique and important flash-radiographic facility became operational at the Los Alamos Scientific Laboratory. This facility is known as PHERMEX, which is an acronym for *Pulsed High Energy Radiographic Machine Emitting X* rays. The PHERMEX machine is a high-current, 27-MeV, linear electron accelerator that produces very intense but short-duration bursts of bremsstrahlung from a thin tungsten target for flash radiographic studies of explosives and explosive-driven metal systems. The facility was built in the early 1960s to complement other hydrodynamics facilities at Los Alamos and to implement studies of shock waves, jets, spalling, detonation characteristics of chemical explosives, and other hydrodynamic phenomena.

Flash radiography has been used in diagnosing explosive-driven systems for about 40 years and has provided direct observation of dynamic processes. The size of systems that could be radiographed dynamically using conventional equipment has always been severely limited by the poor ability of the available x-ray flux to penetrate the blast protection devices. PHERMEX, however, was designed and built to overcome these limitations and to permit precise radiography of large explosive systems containing materials of high atomic number.

PHERMEX has been used to study materials in various geometries under a variety of shock conditions. Over 1800 unclassified radiographs will be described in the LASL PHERMEX data collection. This is the first of the five volumes scheduled for publication by the LASL Data Center.

A description of the PHERMEX facility is followed by a general description of the data to be presented. These data include the purpose of the shot, the timing data, any literature references, the experimenter's name, the shot geometry, and copies of the static and dynamic radiographs.

THE PHERMEX FACILITY

PHERMEX encompasses several subsystems used to generate a precisely timed radiation burst for radiographing explosive events with submicrosecond time resolution. These are the rf power source and control, the electron accelerator and electron source, fire control and signal detection, and data acquisition. Each is equally important to the overall quality of the radiographic data and is discussed in the succeeding sections.

PHERMEX Machine Design and Operating Characteristics

Before describing the linear electron accelerator, we should briefly discuss a few experimental objectives as an aid in understanding the design requirements. PHERMEX was constructed to obtain flash radiographs of large explosive systems that contained high atomic number materials such as iron and, particularly, uranium.* The intent was to provide direct observation of hydrodynamic events to complement the contactor-pin and high-speed-camera coverage of explosive systems. In the early and mid 1950s, detailed study (Boyd et al., 1965; Venable, 1967) of such a radiographic requirement indicated that precise determination of areal distribution of mass density in very thick sections was feasible, given adequate flux. Study also indicated that precise radiography required careful attention to alignment, penumbra effects, scattered radiation, film latitude, etc. for sections as thick as ten mean-free-path lengths in a variety of object configurations. Further, for good penetration, the radiation must be rich in 3- to 4-MeV quanta for uranium and 4- to 8-MeV quanta for iron. The studies also indicated that a pulsed electron accelerator could be constructed to meet these radiographic objectives. The radiation pulse duration was selected to provide the optimum motion blur versus space resolution relationship. The flux had to be adequate to capture the hydrodynamic events of interest and still maintain 0.5- to 1.0-mm space resolution when object velocities up to 10 km/s were encountered. A very short x-ray burst produces inadequate flux for large systems, whereas a long burst permits unacceptable motion blur. Space resolution without the complication of motion blur is achieved by controlling the beam diameter.

*The words "uranium" and "tuballoy" are used interchangeably here.

Careful consideration of all the radiographic objectives showed that a 20-MeV electron beam delivering 5 to 10 μCi to a tungsten target in a 3-mm-diam spot in 0.1 to 0.2 μs should generate adequate bremsstrahlung flux in a single-pulse radiograph. The machine, designed and built according to these guidelines produced its first x rays in 1963. Since then, it has been upgraded to produce an electron beam energy of about 30 MeV, and it delivers approximately 15 μCi to the tungsten target in a 0.3-mm-diam spot in 0.2 μs .

The PHERMEX machine is diagrammed in Figure 1 and its subsystem characteristics are summarized in Table I. It is housed in a thick-walled concrete structure called the PHERMEX Chamber, shown in Figure 2. The hemicylindrical structure is about 30 m long, 10 m wide, and 10 m high. The round nose at the target end is also concrete, 1.5 m thick and covered with expendable steel matting and sandbags. Behind the PHERMEX Chamber is the Power Control Building. Conduits connecting the two buildings contain the rf transmission lines used to energize the cavities.

The Accelerator

PHERMEX is a standing-wave, linear accelerator that operates at an injected power of 13.5 MW for 3 ms. Three cylindrical resonant cavities connected in tandem and operating in the TM_{010} mode serve as the energy-storage chambers for exchanging energy between the electromagnetic field and an axially injected electron beam. Each 4.6-m-diameter by 2.6-m-long cavity is made of copper-clad steel with a water-cooled copper bulkhead at each end. However, water cooling is not used at present power levels because of the low duty cycle. During the initial design phase,

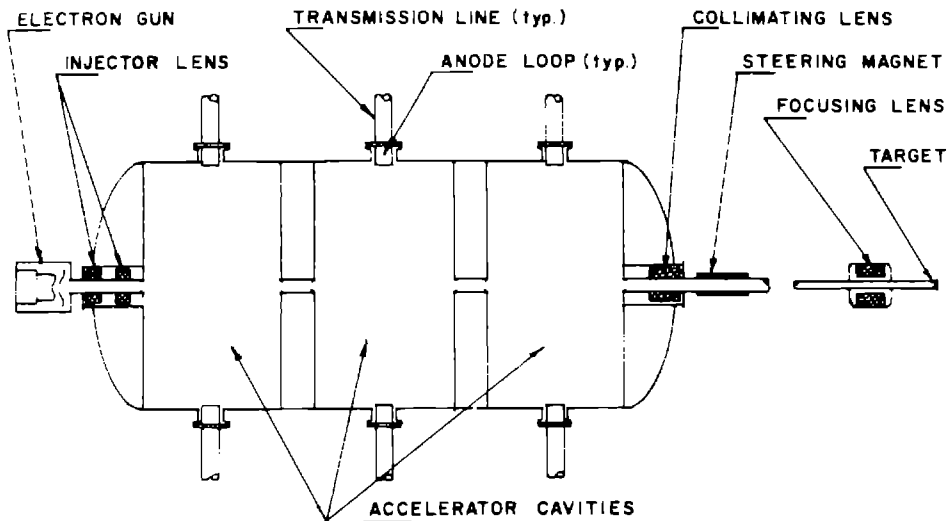


Fig. 1. The PHERMEX machine.

TABLE I
CHARACTERISTICS OF PHERMEX SUBSYSTEMS

Electron beam source	
Injection charge	500 A for 200-ns pulse 500 A for 100-ns pulse 500 A for 40-ns pulse
Injection voltage	600 kV
Injection diameter	25 mm
Confining magnetic lenses	2
rf power source	
Final stage amplifier type	RCA 6949 triodes
Total dc power demand (9 stages)	27 MW
Total power delivered (9 stages)	13.5 MW
dc plate power unit	100- μ F capacitor at 25-35 kV
Frequency	50 MHz
Pulse length	3 ms
Duty cycle	1 pulse/s
Accelerator	
Type	Three-cavity standing wave
Resonant frequency	50 MHz
Mode	TM ₀₁₀
Cavity diameter	4.6 m
Cavity length	2.6 m
Cavity Q	125,000
α cavity	
Stored energy	1200 J
Power required	6 MW
Beam current	500 A in, 250 A out
Field strength	5-5.5 MV/m
Electron energy gain	10 MeV
β cavity	
Stored energy	1600 J
Power required	4.5 MW
Beam current	250 A in, 180 A out
Field strength	6-7 MV/m
Electron energy gain	13 MeV
γ cavity	
Stored energy	800 J
Power required	3 MW
Beam current	180 A in, 150 A out
Field strength	4 MW/m
Electron energy gain	7 MeV

Table I (cont)

Target beam

Final beam energy	30 MeV
Final beam current	60 A
Spot diameter	1 mm
Charge	15 μ C
Radiation intensity per burst	100 R at 1 m, 200 ns 40 R at 1 m, 100 ns 15 R at 1 m, 40 ns

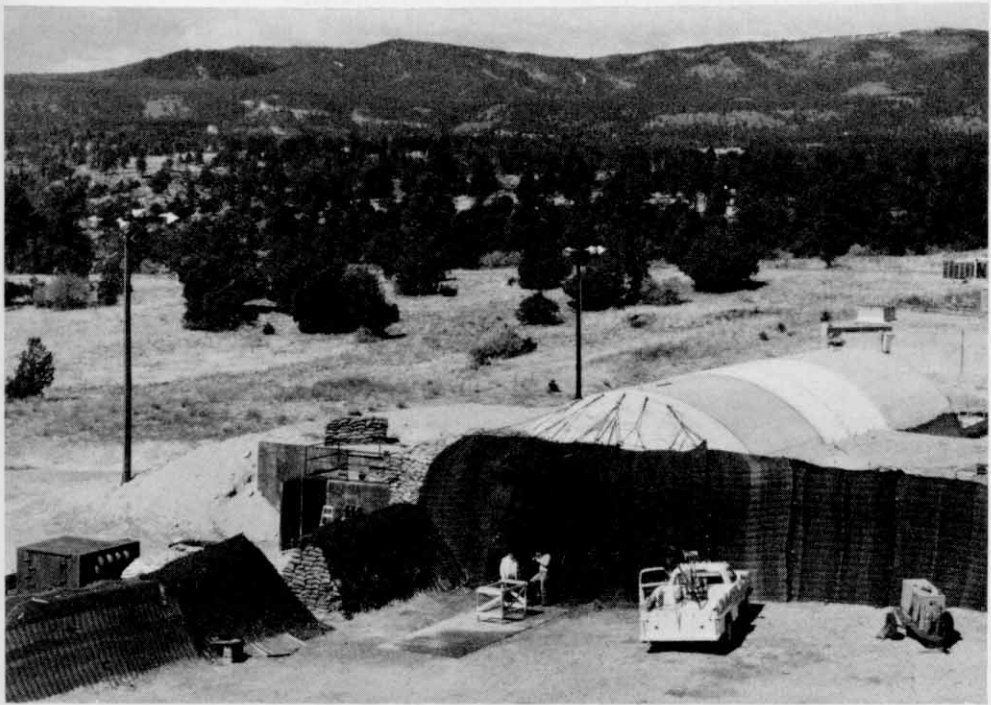


Fig. 2. The PHERMEX Chamber, Power Control Building, transmission line conduits, and firing site.

a 50-MHz rf power source was chosen to excite the cavities because it was readily available at reasonable cost. This frequency dictated the cavity diameter, because the resonant frequency of a cylindrical cavity operating in the TM_{010} mode depends only on its diameter. The length was chosen to ensure minimal momentum spread among electrons delivered to the gamma-ray converter and to provide the most efficient energy transfer to an electron, per cycle, from a given field strength in the cavity at a specified injection energy. This arrangement allows power to be transferred to the beam from the cavities at a rate that depends on electron injection parameters, not on the rate at which the power source supplies energy to the cavity. This feature permits use of conventional rf amplifiers.

The vessel that contains the activities is approximately 11.3 m long by 4.6 m inside diameter and it weighs about 10^6 kg. Figure 3 shows the three-cavity vessel. There are seven sections: three cavities, the two ends, and the spaces between the cavities which divide the vessel into "hard" (1.3×10^{-6} -Pa) and "soft" (7×10^{-2} -Pa) vacuum. Each cavity has six 458-mm-diameter ports to provide a choice of positions for the rf driving loops and vacuum attachments.

The first cavity in the chain (α cavity) operates at a field strength of 5 to 5.5 MV/m; the second (β cavity) is supplied with a field strength of 6 to 7 MV/m, and the third (γ cavity) has a field strength of 4 to 4.5 MV/m derived from the high-power, 50-MHz rf amplifiers. A 25-cm-diameter electron beam of approximately 500-A current is injected into the machine from the electron source. As the electrons

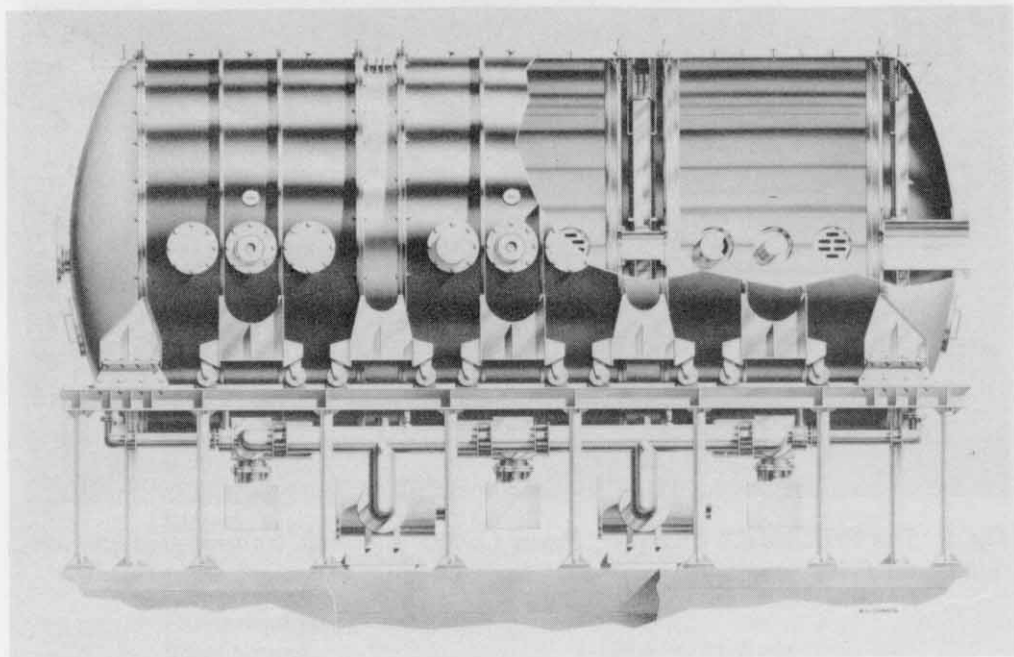


Fig. 3. Cutaway illustration of the three-cavity vessel.

traverse α cavity, the beam is chopped into bunches because only part of the electrons are in proper phase with the rf source to be accelerated. Figure 4 shows an oscilloscope trace of these subbursts. For example, a 200-ns pulse length contains 10 bunches of electrons 20 ns apart. The other electrons are lost to the cavity walls. Although the peak current is preserved, because of improper phasing, the average current per cycle is reduced to about 250 A at the time the electron subbursts enter β cavity. Loss of more electrons reduces the average beam current into γ cavity to about 180 A. At the exit aperture of γ cavity, the electrons are highly relativistic and have a beam energy of about 30 MeV and a current of about 150 A. A short drift section between cavity pairs requires that the electromagnetic fields be phased properly to accept the electron bunches from the previous cavity without significant loss.

Downstream from the final cavity, a lens collimates most of the high-energy beam for passage through a 25-mm-diameter aperture. This is the first step toward convergence to a 1-mm spot diameter. Figure 5 shows the ejection section of the accelerator. Beyond the collimating lens is a steering quadrupole magnet for moving the electron beam a few millimeters radially to improve its centering on the target. Next the beam travels through a drift tube and two thick beryllium collimators, one with a 25-mm and the other with a 13-mm-diameter hole. Finally, the beam leaves the PHERMEX machine chamber and is brought to a <1-mm-diameter spot on the target by a final focusing lens. A thick steel blast shield protects the focusing lens and the target assembly. An expendable aluminum cone is attached to the blast protector to shield the target from the explosive experiment.

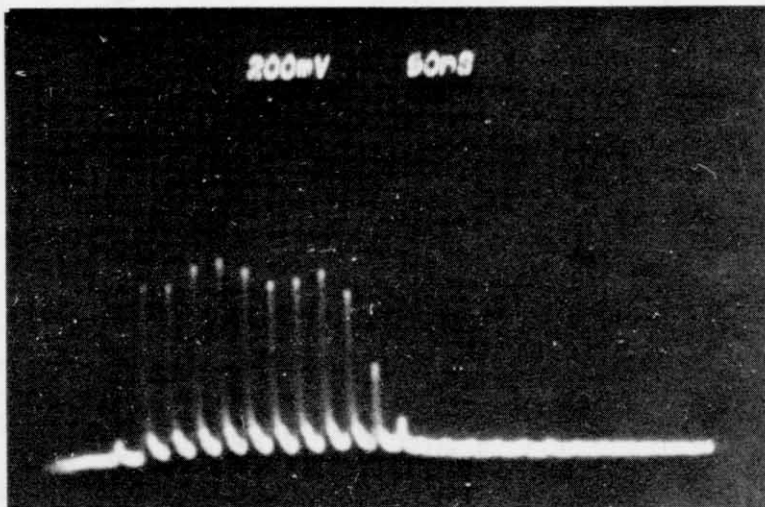


Fig. 4. An oscilloscope trace of the subbursts of x rays resulting from the electron train.

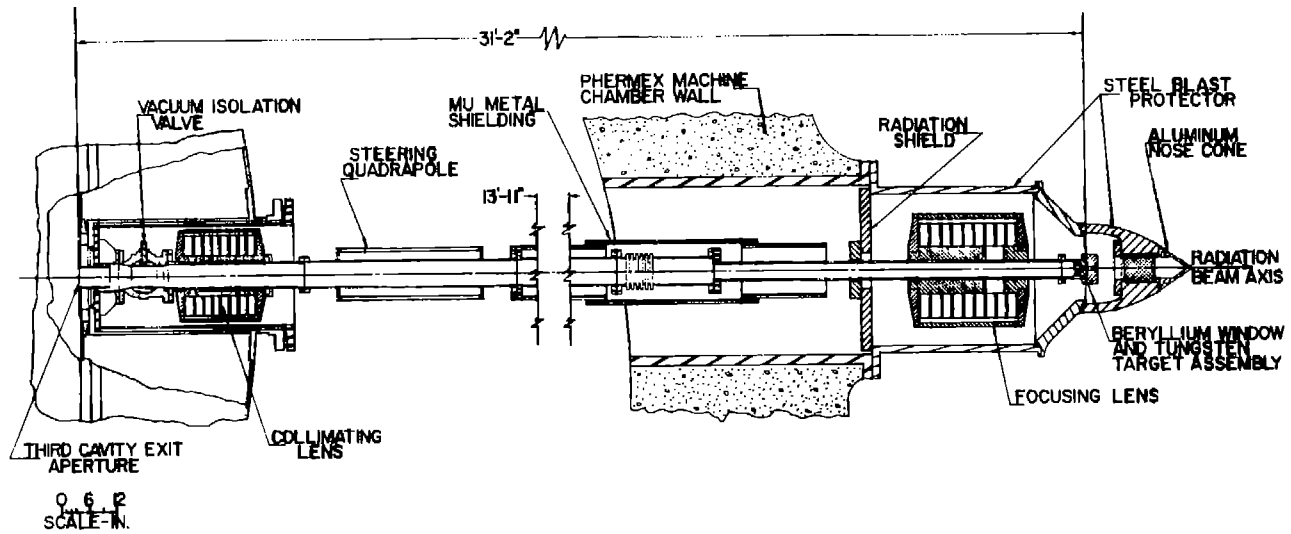


Fig. 5. Ejection section of the PHERMEX accelerator.

The target is a 1.75-mm-thick tungsten disk that is rotated remotely after each pulse. The bremsstrahlung that results from stopping the electrons in the tungsten target has a highly directional radiation pattern. A plot of the x-ray intensity as a function of angle indicates that most of the radiation is included in a 20° apex angle. A 200-ns pulse of electrons deposits about 200 joules of energy into the target, and the resulting radiation level is about 100 R at 1 m. Shorter duration pulses give proportionately smaller amounts of radiation.

The Electron Source and Injection

The electron source is a space-charge limited, 102-mm-diameter, spherical-segment cathode, diode gun (Pierce gun) with selectable pulse lengths of 200, 100, and 40 ns at an injection voltage of 600 kV. The gun is designed with a perveance [beam current \div (anode voltage)^{3/2}] of about 10⁻⁶. In operation, the commercially available, 102-mm-diameter, sintered tungsten cathode is heated to about 1200 K. Upon application of the 200-ns, 600-kV pulse, a conical electron beam of approximately 500 A is accelerated and converges through the anode aperture. The first magnetic lens controls the first beam expansion caused by strong space charge forces. After passage through the vacuum valve, the electron beam is controlled by a second magnetic lens. These two lenses control the entrance diameter and convergence angle of the electron beam into α cavity. Figure 6 shows the electron beam injector and the two magnetic lenses.

The 600-kV pulsers that drive the gun are commercially available items manufactured by Hewlett-Packard, formerly Femcor. The pulsers are Marx generators that use transmission lines as energy-storage elements of a specific length to provide the desired pulse duration. A large pulse transformer and trigger pulse amplifier deliver a very energetic spark to trigger the Femcor pulser at the appropriate time for an explosive experiment.

The RF Power System

To achieve an electron beam energy of 30 MeV, four amplifier chains drive α cavity, three drive β cavity, and two drive γ cavity. Figure 7 shows the rf flow for buildup to high power levels. To introduce rf power to the cavities, the variable frequency oscillator (VFO) shown in the diagram is gated "on" for 3 ms at a specific time. Power from the amplifiers is coupled to the cavity by rotatable magnetic coupling loops at the cavity walls. The electromagnetic fields reach steady-state amplitudes in about 1.5 ms. During tuneup, the field amplitude and phase of the cavities are sampled, and, if they are satisfactory, a signal is generated which triggers the electron injector.

Each final amplifier shown in Figure 8 provides approximately 1.5 MW of rf power for use by the cavities at a duty cycle of one pulse per second. The total dc plate power demand for the nine amplifiers is 27 MW during each driving period; it is derived from nine 100- μ F capacitor banks, one for each amplifier. The rf power from each final amplifier is supplied by an RCA 6949 shielded-grid beam triode.

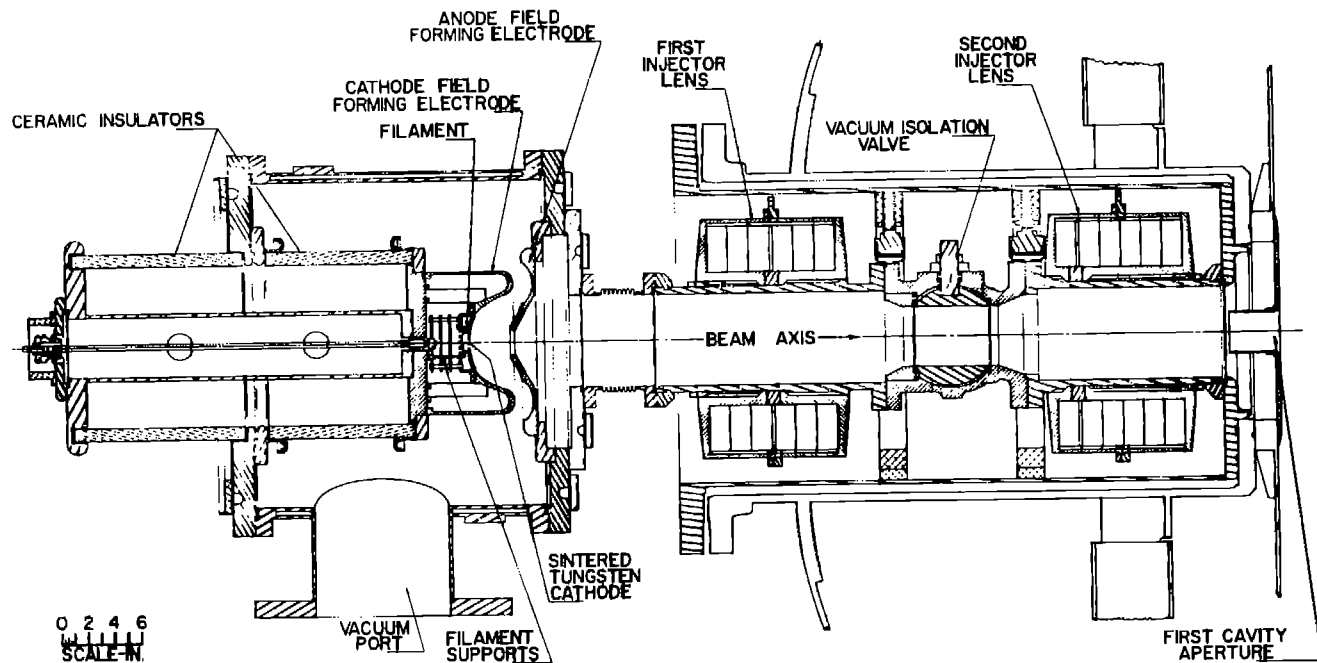


Fig. 6. Electron beam injector and the magnetic lenses.

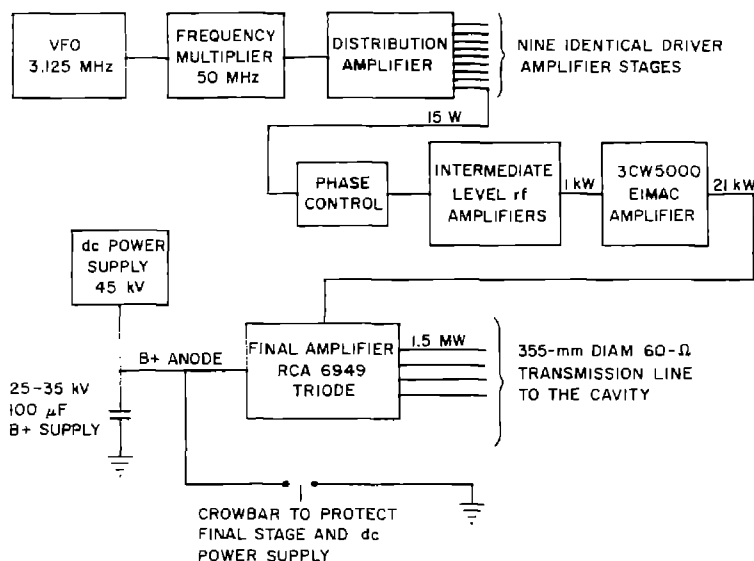


Fig. 7. PHERMEX rf flow.

Precise frequency tuning and phase adjustment are necessary for optimum electron acceleration. The frequency is tuned by setting the variable frequency master oscillator and frequency multiplier to 49.9472 MHz; then dual-bellows tuning slugs in α , β , and γ cavities are adjusted so that each cavity resonates with the drive frequency. Once the drive frequency and resonant frequency have been regulated, the proper phase relationships are established by adjusting the phase shifter mechanism in each amplifier chain for maximum final electron beam current at the target as determined by the charge collection. The phase control is basically a distributed transmission line that allows the phase angle in each amplification state to be changed before the rf power is applied to the cavities.

The rf energy generated by each of the nine amplifiers is transferred to the three cavities by large-diameter transmission lines whose electrical lengths are integral multiples of a half-wavelength, to within about 50 mm; see Figure 8. The diameter of the outer conductor of each 60- Ω coaxial line is 355 mm, and that of the inner conductor is 127 mm. Finally, the rf energy is coupled to the azimuthal magnetic fields in the cavities through rotatable loops at the ends of the transmission lines.

The rf power is generated, controlled, and monitored in the Power Control Building. That building also contains the energy storage (nine capacitor banks), the control console, the nine rf amplifier chains, and a deionized-water cooling system for cooling the amplifiers and the electron gun.

Timing, Firing, and Signal Detection

Important aspects of the PHERMEX facility are its capabilities for producing radiation, detonating explosive charges at the desired time, and recording various

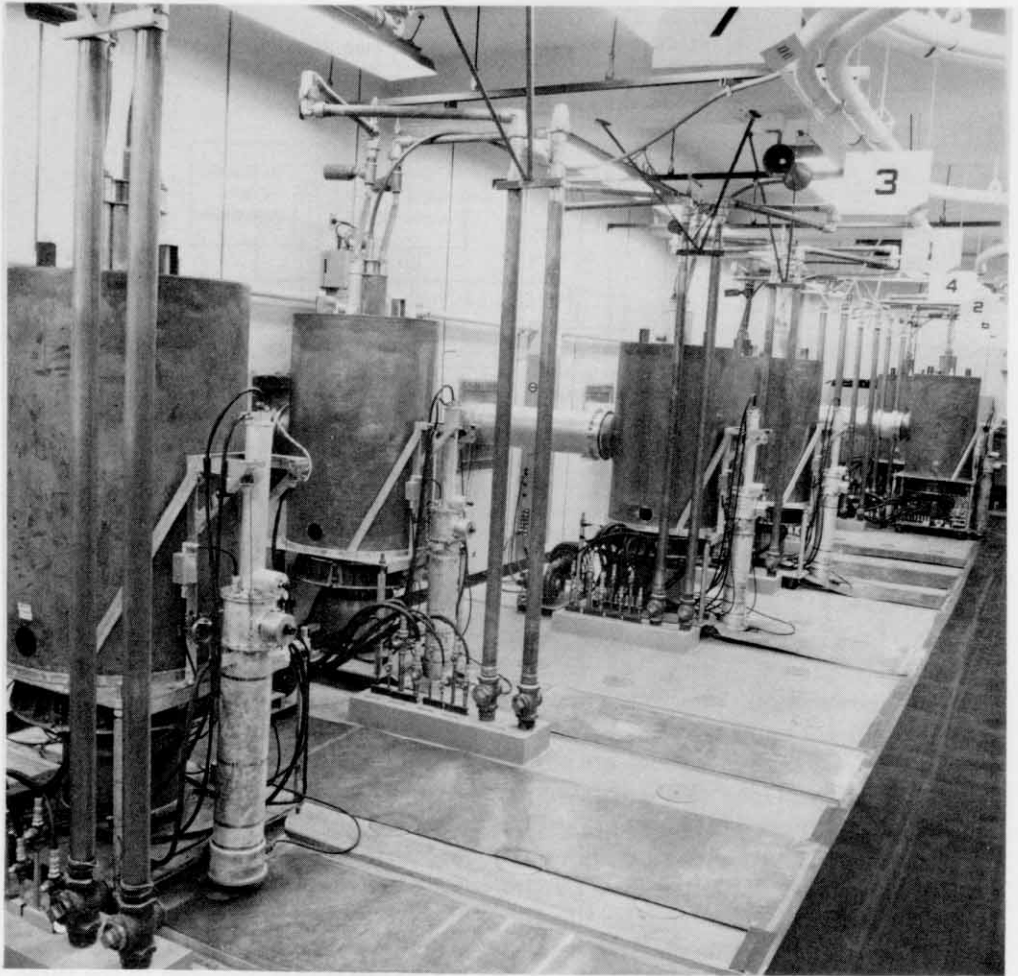


Fig. 8. The final amplifier stages.

signals. The required electronic equipment is housed in the Detection Chamber, which is interconnected with the Power Control Building and PHERMEX Chamber. Two principal functions are carried out from the Detection Chamber. One is the triggering and monitoring needed to detonate the shot and to activate the electron gun pulser to generate radiation. The other is recording of the time and amplitude of the radiation pulse from a suitable x-ray detector and the signals from other diagnostic equipment.

In an explosive experiment, the PHERMEX machine excitation time of 3 ms is very long compared to the microseconds needed for data acceptance. The triggering chain needed to radiograph an event is diagrammed in Figure 9. Activation of the

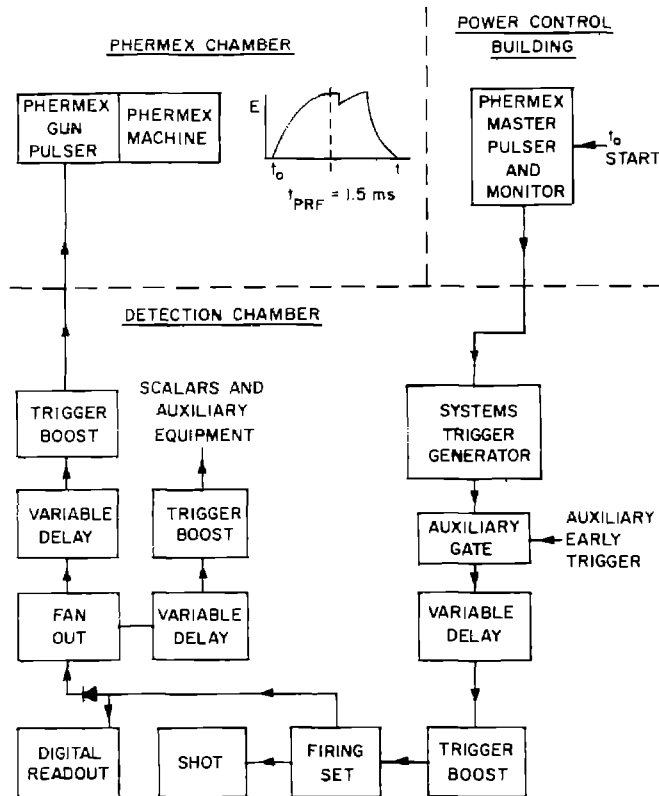


Fig. 9. PHERMEX triggering chain.

chain begins with a start pulse from the master pulser. At this time, each rf power channel energizes the cavities, causing the fields to grow approximately as shown in the field (E) versus time (t) plot of Figure 9. Then the fields are sampled and a PHERMEX Ready Fire (PRF) trigger is sent to the trigger generator for eventual firing of the detonators and the explosive. Finally, a trigger is sent from the firing set through a delay unit to the electron gun injector pulser. In this way radiation can be produced to radiograph the hydrodynamic event at a specific time. Gun pulser trigger delays of 10 to 100 μ s after detonation often are required for proper timing. The trigger signal from the gun pulser and the radiation signal are displayed on scalars and other recording equipment to provide accurate timing information.

Signals from other instruments, such as contactor pins, piezoresistive pressure gauges, and quartz gauges, are recorded by a variety of high-speed digital and analog electronic devices. Further, most of these devices are interfaced with a computer that can store data on disks or tape, manipulate it by use of resident codes, and print out the information.

Radiographic Procedures

Given the radiation levels that PHERMEX provides, an explosive event can be radiographically recorded easily using industrial x-ray films, such as Kodak X-Ray Film T, AA, or KK (SO-142), with a suitable screen. Film densities achieved in typical conditions range from 1 to 3. The purpose and makeup of an experiment dictate the choice of radiation pulse length, shot orientation, and shot geometry.

Figure 10 shows a flash radiographic geometry used for many explosive experiments. Target protection also is shown. Because the data are recorded on x-ray film, a blast- and shrapnel-proof cassette must be used. Two basic types of film protectors are in normal use. One is a hollow aluminum cone that accepts 355-mm-diameter film; the other is a 560- by 710-mm rectangular cassette with various thicknesses of aluminum in front for protection. Figure 11 shows a conical protector. These cassettes can protect film from the effects of about 30 kg of explosive when the film plane is as close as 900 mm to the charge center.

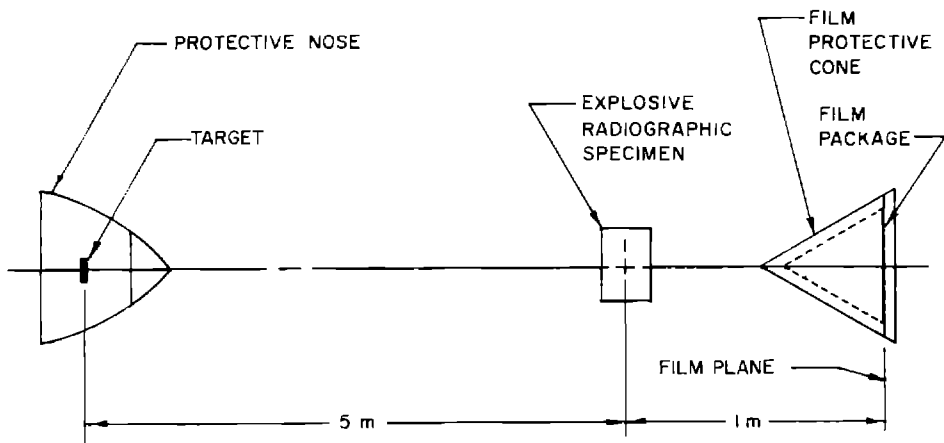


Fig. 10. Firing site geometry of a typical flash radiographic experiment.

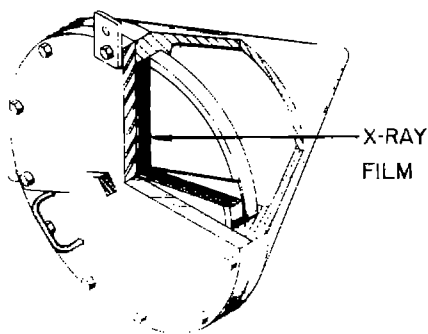


Fig. 11. Conical film protector.

Careful alignment of the experiment on the firing pad with the axis of the bremsstrahlung beam is important. It is accomplished by using an alignment telescope cradled in a precision fixture attached to the steel target protector to make the beam and sight axes coincide. An observer sights away from the PHERMEX machine at a sighting target located beyond the experiment and film protector. After the target center is adjusted to coincide with the telescope line of sight, a second telescope is substituted for the sighting target. The experiment is then set in place and aligned with respect to the beam axis by use of the telescopes and a leveling table. After alignment, the telescopes are removed and the film cassette is put in place. This method has proven reliable, accurate, and quick.

Several film and screen combinations may be used in one film package to record the wide range of radiation intensity transmitted in an experiment. For example, a typical film and screen combination might include one Kodak KK film intensified with two 1-mm-thick lead screens, one Kodak AA film with two such screens, and another Kodak KK film with one such screen. A large variety of film and screen combinations is available to the experimenter, as is a variety of x-ray film-processing procedures—normal 5- and 8-min development times at 293 K, forced processing by the X-omat technique, and the hydrazine process (Sandoval and Kearns, 1973) to increase the speed and contrast of industrial x-ray films.

The PHERMEX machine's resolution when a typical shot geometry is used (see Figure 10) varies from 0.3 mm on Kodak AA film to 1.0 mm on Kodak KK film. This is illustrated in Figure 12, a radiograph on Kodak AA film of a 6-mm-thick tungsten resolution plate with square teeth of a different size, 4, 3, 2, and 1 mm, machined on each edge. The 1-mm teeth are easily resolved on the actual radiograph.

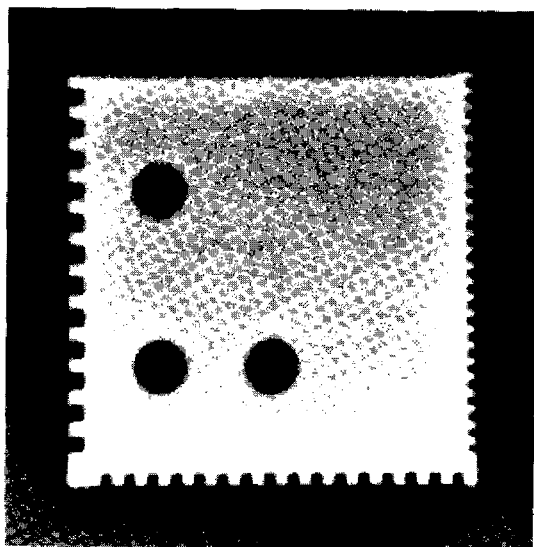


Fig. 12. A tungsten resolution plate. The smallest teeth are 0.040 in. (1.0 mm) square.

DATA PRESENTATION

The PHERMEX data are presented by increasing shot number, which increases according to the date the shot was planned, not necessarily the date on which it was fired. A few shots either failed or were never completed. A descriptive shot title is presented, along with the date the shot was fired. The name of the person who originated the experiment is given. The radiographic time is that from initiation of the detonator to the middle of the radiograph pulse. The radiograph pulse width is $0.2 \mu\text{s}$. The plane-wave lens and detonator burning times (typical of the PHERMEX firing system) used to estimate other times were

P-040	13.5 μs ,
P-081	22.5 μs ,
P-120	29.5 μs .

Literature that describes a shot or its general purpose is cited. The purpose of the shot and important features of the radiograph are discussed. The experimental setup is sketched, and certain dimensions appropriate for each shot are given in millimeters. The distance, h , of the beam axis from some shot geometry location is given. All available static radiographs are presented, and the dynamic radiographs are shown on the same scale as the static radiographs.

The first few hundred shots were designed to survey various topics of interest in the fields of shock hydrodynamics and detonations. The process of jet formation from grooved aluminum and steel plates was investigated extensively. Table II summarizes the aluminum jet studies; Table III, the steel jet studies.

Table IV summarizes the dynamic fracture shots, and Table V lists the observed spalling thicknesses in aluminum, copper, nickel, thorium, uranium, beryllium, and lead. Some of the data was obtained from shots to be described in future volumes of LASL PHERMEX data.

Table VI summarizes the measured reflected shock velocities of colliding detonations of Composition B-3, Cyclotol, PBX-9404, and Octol. Table VII presents the gaseous Munroe jet shots.

TABLE II
ALUMINUM JET SHOT TIME SEQUENCE
90° Groove Angle

Time (μs)	Shot No.	Comments
0	28	static film
7.3	24	10.41 mm into P-040
12.5	10	37.59 mm into P-040
14.5	11	7.94 mm into Composition B-3
16.7	28	25.4 mm into Composition B-3
19.9	8	50.8 mm into Composition B-3
26.3	22	top edge of aluminum
27.2	9	6.35 mm into aluminum
28.1	23	12.7 mm into aluminum
29.11	148	19.8 mm into aluminum
29.28	149	21.0 mm into aluminum
29.4	7, 141, 197	22.2 mm into aluminum
29.9	12, 142, 198	bottom edge of aluminum
30.4	16, 144	0.5 μ s free run
30.9	13, 143, 199	1.0 μ s free run
31.4	17, 145	1.5 μ s free run
31.9	18, 36, 37, 146	2.0 μ s free run
32.2	19, 147	2.5 μ s free run
32.8	20	3.0 μ s free run
33.1	1,6	3.2 μ s free run
33.4	21	3.5 μ s free run
34.9	29	5.0 μ s free run
36.9	30	7.0 μ s free run
39.9	32	10.0 μ s free run
42.9	25	13.0 μ s free run

TABLE III
1019 STEEL JET SHOT TIME SEQUENCE
90° Groove Angle

Time (μs)	Shot No.	Comments
31.3	51	0.0 μ s free run
33.3	47	2.0 μ s free run
34.9	44	3.5 μ s free run
36.3	46	5.0 μ s free run
39.3	48	8.0 μ s free run
42.2	49	11.0 μ s free run
45.3	50	14.0 μ s free run

TABLE IV
DYNAMIC FRACTURE SHOTS^a

Shot No.	Composition B-3 Thickness (mm)	Material	Material Thickness (mm)	Radiographic Time (μs)
60	101.6	2024 aluminum	25.4	34.1
61	101.6	2024 aluminum	25.4	37.9
62	101.6	2024 aluminum	25.4	46.0
63	101.6	2024 aluminum	25.4	53.9
68	101.6	2024 aluminum	24.5	28.9
69	101.6	2024 aluminum	24.6	31.4
70	101.6	2024 aluminum	24.6	33.9
76	101.6	2024 aluminum	25.1	28.0
77	101.6	2024 aluminum	25	32.9
78	101.6	2024 aluminum	25	32.9
79	101.6	2024 aluminum	25.1	27.3
80	101.6	2024 aluminum	25	30.9
81	101.6	2024 aluminum	25	30.8
82	101.6	2024 aluminum	25	33.9
83	101.6	2024 aluminum	1	30.5
84	101.6	2024 aluminum	3	30.7
85	101.6	2024 aluminum	6	31.2
88	101.6	2024 aluminum	6	32.0
89	101.6	2024 aluminum	25	33.9
97	101.6	2024 aluminum	25	33.9
102	101.6	aluminum	3	34.3
103	101.6	aluminum	3	38.3
104	101.6	aluminum	6	38.4
105	101.6	aluminum	6	34.29
107	101.6	aluminum	6	28.43
108	101.6	aluminum	12	34.30
109	101.6	aluminum	12	30.43
110	101.6	aluminum	12	42.29
115	101.6	nickel	25.4	38.0
116	101.6	nickel	25.4	45.29

^aA P-040 lens was used throughout, except in Shots 245-247, for which a P-081 lens was used.

TABLE IV (cont)

Shot No.	Composition B-3 Thickness (mm)	Material	Material Thickness (mm)	Radiographic Time (μ s)
129	101.6	uranium	1	34.4
130	101.6	thorium	1	34.41
131	101.6	uranium	25	43.28
132	101.6	thorium	25	41.44
133	101.6	uranium	12	39.64
165	101.6	uranium	25	39.39
166	38.1	uranium	25	33.40
167	101.6	uranium	25	41.42
168	101.6	uranium	12	33.8
169	19.05	uranium	12	25.35
170	6.35	uranium	12	25.72
171	101.6	uranium	6	30.55
172	101.6	thorium	25	37.41
173	50.8	thorium	25	32.89
174	38.1	thorium	25	31.33
175	101.6	thorium	12	32.76
176	19.05	thorium	12	29.27
177	12.7	nickel	25	27.28
178	12.7	nickel	12	25.05
179	101.6	thorium	6	29.56
191	101.6	water	25.4	34.83
211	6.35	aluminum	25	18.28
212	6.35	aluminum	6	16.39
213	101.6	aluminum	6	37.53
222	101.6	aluminum	25	26.95
223	101.6	aluminum	25	27.88
224	101.6	aluminum	25	28.90
226	101.6	aluminum	25	29.89
227	101.6	aluminum	25	30.41
228	101.6	aluminum	25	30.92
229	101.6	aluminum	25	31.41
230	101.6	aluminum	25	32.40
231	101.6	aluminum	25	32.92
232	101.6	aluminum	25	33.42
234	101.6	aluminum	25	36.43

TABLE IV (cont)

Shot No.	Composition B-3 Thickness (mm)	Material	Material Thickness (mm)	Radiographic Time (μ s)
235	101.6	aluminum	25	36.40
236	101.6	aluminum	25	26.93
238	101.6	aluminum	25	32.43
239	19.05	copper	12	26.64
240	12.7	copper	12	25.25
241	19.05	aluminum	12	22.50
242	25.4	nickel	25	28.89
245	101.6	aluminum	6	38.24
246	6.35	aluminum	6	28.24
247	101.6	aluminum	6	37.51
270	19.05	nickel	12	25.91
271	50.8	beryllium	25	28.34
305	101.6	aluminum	25	33.38
348	50.8	aluminum	25	24.77
349	38.1	aluminum	25	23.02
355	50.8	aluminum	25	25.25
356	50.9	aluminum	25	25.71
357	50.8	aluminum	25	26.23
358	38.1	aluminum	25	25.07
359	38.1	aluminum	25	23.53
360	38.1	aluminum	25	24.02
361	38.1	aluminum	25	24.52
379	6.35	beryllium	25	21.52
380	25.4	beryllium	25	23.94
381	50.8	beryllium	25	27.04
382	38.1	beryllium	12	24.33
383	19.05	beryllium	12	21.95
384	12.7	beryllium	12	21.07
385	6.35	beryllium	6	19.60
386	25.4	aluminum	25	23.73
387	213.2	aluminum	25	46.10
389	50.8	copper	25	32.38
390	38.1	copper	25	31.00
391	25.4	copper	25	29.2
392	50.8	nickel	25	32.10

TABLE IV (cont)

Shot No.	Composition B-3 Thickness (mm)	Material	Material Thickness (mm)	Radiographic Time (μs)
393	38.1	nickel	25	30.55
394	25.4	nickel	25	28.88
395	25.4	thorium	25	29.70
396	12.7	thorium	25	28.09

TABLE V
OBSERVED SPALL LAYER THICKNESSES
(mm)

<u>HE^a/Metal</u> <u>(mm)</u>	<u>Aluminum^b</u>	<u>Copper^c</u>	<u>Nickel^d</u>	<u>Thorium^e</u>	<u>Uranium^f</u>	<u>Beryllium^g</u>	<u>Lead^h</u>
200/25	2.5 ± 0.1						
100/25	2.6 ± 0.2	2.4 ± 0.2	3.3	none	2.2 ± 0.2	2.5 ± 0.2	1.3 ± 0.2
51/25	2.4 ± 0.2	2.2 ± 0.2	2.9 ± 0.2	1.6 ± 0.2	2.0 ± 0.3	3.3 ± 0.2	1.1 ± 0.2
38.1/25	2.1 ± 0.2	1.95 ± 0.2	2.9 ± 0.2	1.7 ± 0.1	1.9 ± 0.3	2.2 ± 0.2	0.85 ± 0.2
25/25	1.85 ± 0.2	1.7 ± 0.2	2.6 ± 0.2	1.4 ± 0.1	1.95 ± 0.2	2.0 ± 0.2	1.0 ± 0.2
12.7/25	1.8 ± 0.1	1.65 ± 0.2	2.2 ± 0.1	1.7 ± 0.1	2.0 ± 0.3	1.8 ± 0.2	1.2 ± 0.1
19/12	1.45 ± 0.1	1.3 ± 0.2	1.85 ± 0.1	1.2 ± 0.1	1.6 ± 0.2	1.3 ± 0.2	0.75 ± 0.2
12.7/12	1.5 ± 0.1	1.2 ± 0.2	1.7 ± 0.2	1.15 ± 0.1	1.7 ± 0.2	1.0 ± 0.2	0.4 ± 0.1
6.37/25	none					2.4 ± 0.2	
6.37/6	0.7 ± 0.2	0.85 ± 0.1			1.45 ± 0.1	0.9 ± 0.1	
100/12	2.2 ± 0.2			none	2.2		
100/6	2.3 ± 0.2			none	none		
100/3	none						
100/1	none				none		

^aThe HE driver was Composition B-3 whose initial density was about 1.73 g/cm³.

^bAluminum specimens were Type 1100-F.

^cElectrolytic tough pitch (ETP) copper was used.

^dCommercially pure "A" nickel was used.

^eHigh-purity (11.66-g/cm³) thorium was supplied by Oak Ridge.

^fThe uranium was 99.9% pure, at 18.93 g/cm³.

^gGeneral Astrometals Corporation Grade B-2 beryllium was used. This resembles Brush Corporation beryllium S-200-C. Several shots with beryllium used vacuum-cast material. The data for this material lay within the error flags for the GB-2 beryllium.

^hLead plates were formed from commercially pure deep-rolled material.

TABLE VI
REFLECTED SHOCK VELOCITIES

<u>Explosive</u>	<u>Reflected Shock Velocity (mm/μs)</u>	<u>Shot No.</u>	<u>Detonation Velocity (mm/μs)</u>
Composition B-3	6.115 \pm 1.61%	86, 87, 91, 92, 273-277	7.882
Cyclotol	6.142 \pm 1.09%	203-206, 291	8.252
PBX-9404	6.892 \pm 0.16%	207-210, 292	8.732
Octol	6.234 \pm 2.09%	294-297	8.480

TABLE VII
GASEOUS MUNROE JET SHOTS

<u>Shot No.</u>	<u>Gap (mm)</u>	<u>Jet Run (mm)</u>	<u>Time (μs)</u>
258	5.0	50.8	32.24
248	10.0	50.8	32.37
283	10.0	203.2	51.47
315	10.0	406.4	76.95
255	20.0	25.4	29.07
249	20.0	50.8	32.30
260	20.0	50.8	32.36
256	20.0	76.2	35.45
341	20.0	86.0	36.68
342	20.0	94.0	37.69
362	20.0	98.0	38.18
257	20.0	101.6	38.65
343	20.0	101.6	38.60
262	20.0	152.4	45.10
261	20.0	203.2	51.35
264	40.0	12.75	27.52
265	40.0	25.40	29.15
259	40.0	50.80	32.24
266	40.0	76.2	35.46
267	40.0	101.6	38.68
263	80.0	50.8	32.30

TABLE VII (cont)

<u>Shot No.</u>	<u>Gap (mm)</u>	<u>Jet Run (mm)</u>	<u>Time (μs)</u>
285	20.0	Expanding	52.92
286	20.0	Expanding	53.8
287	20.0	Expanding	55.06
344	20.0	Interacting	41.65
345	20.0	Interacting	43.97
346	20.0	Interacting	45.97
322	Diverging, 5°		30.71
323	Diverging, 5°		34.96
324	Diverging, 5°		39.25
325	Diverging, 10°		31.28
326	Diverging, 10°		35.49
327	Diverging, 10°		39.72
328	Diverging, 20°		32.40
329	Diverging, 20°		36.54
330	Diverging, 20°		40.70
363	Converging, 5°		26.41
364	Converging 10°		26.43
365	Converging, 20°		26.39

REFERENCES

John F. Barnes, Patrick J. Blewett, Robert G. McQueen, Kenneth A. Meyer, and Douglas Venable, "Taylor Instability in Solids," *Journal of Applied Physics* **45**, No. 2, 727 (1974).

T. J. Boyd, Jr., B. T. Rogers, F. R. Tesche, and Douglas Venable, "PHERMEX—a High-Current Electron Accelerator for Use in Dynamic Radiography," *Review of Scientific Instruments* **36**, No. 10, 1401 (1965).

B. R. Breed, Charles L. Mader, and Douglas Venable, "Technique for the Determination of Dynamic-Tensile-Strength Characteristics," *Journal of Applied Physics* **38**, No. 8, 3271 (1967).

B. R. Breed and Douglas Venable, "Dynamic Observations of the Course of a Shock-Induced Polymorphic Phase Transition in Antimony," *Journal of Applied Physics* **39**, No. 7, 3222 (1968).

W. C. Davis and Douglas Venable, "Pressure Measurements for Composition B-3," p. 13 in *Fifth Symposium (International) on Detonation, Pasadena, California, August 1970*, Office of Naval Research Symposium Report ACR-184 (1970).

Richard D. Dick, "Insensitive Explosive Study Using PHERMEX," p. 179 in *Proceedings of the Flash Radiography Symposium, Houston, Texas, September 1976*, Larry Bryant, Ed. (American Society for Nondestructive Testing, 1978).

Charles L. Mader, "The Two-Dimensional Hydrodynamic Hot Spot—Volume II," Los Alamos Scientific Laboratory report LA-3235 (1965).

Charles L. Mader, "The Two-Dimensional Hydrodynamic Hot Spot—Volume III," Los Alamos Scientific Laboratory report LA-3450 (1966) (a).

Charles L. Mader, "An Equation of State for Iron Assuming an Instantaneous Phase Change," Los Alamos Scientific Laboratory report LA-3599 (1966) (b).

Charles L. Mader, "Numerical Studies of Regular and Mach Reflection of Shocks in Aluminum," Los Alamos Scientific Laboratory report LA-3578 (1967).

Charles L. Mader, Roger W. Taylor, Douglas Venable, and James R. Travis, "Theoretical and Experimental Two-Dimensional Interactions of Shocks with Density Discontinuities," Los Alamos Scientific Laboratory report LA-3614 (1967).

Charles L. Mader, "Detonations Near the Water Surface," Los Alamos Scientific Laboratory report LA-4958 (1972) (a).

Charles L. Mader, "Two-Dimensional Detonations," Los Alamos Scientific Laboratory report LA-4962 (1972) (b).

Charles L. Mader and James D. Kershner, "Two-Dimensional, Continuous, Multi-component Eulerian Calculations of Interactions of Shocks with V Notches, Voids, and Rods in Water," Los Alamos Scientific Laboratory report LA-4932 (1972).

Charles L. Mader, "Detonation Induced Two-Dimensional Flows," *Acta Astronautica* 1, 373 (1974).

Charles L. Mader and B. G. Craig, "Nonsteady-State Detonations in One-Dimensional Plane, Diverging, and Converging Geometries," Los Alamos Scientific Laboratory report LA-5865 (1975).

Charles L. Mader and Charles A. Forest, "Two-Dimensional Homogeneous and Heterogeneous Detonation Wave Propagation," Los Alamos Scientific Laboratory report LA-6259 (1976).

Charles L. Mader, *Numerical Modeling of Detonations* (University of California Press, Berkeley, 1979).

T. Neal, "Mach Waves and Reflected Rarefactions in Aluminum," *Journal of Applied Physics* 46, No. 6, 2521 (1975).

T. Neal, "Dynamic Determinations of the Grüneisen Coefficient in Aluminum and Aluminum Alloys for Densities up to 6 Mg/m³," *Physical Review B* 14, No. 12, 5172 (1976) (a).

T. Neal, "Perpendicular Explosive Drive and Oblique Shocks, p. 602 in *Sixth Symposium (International) on Detonation, San Diego, California, August 1976*, Office of Naval Research Symposium Report ACR-221 (1976) (b).

T. Neal, "Second Hugoniot Relationship for Solids," *Journal of Physical Chemistry of Solids* 38, 225 (1977).

T. Neal, "Determination of the Grüneisen γ for Beryllium at 1.2 to 1.9 Times Standard Density," in *High Pressure Science and Technology*, Volume 1 (Plenum Publishers, New York, 1979).

W. C. Rivard, D. Venable, W. Fickett, and W. C. Davis, "Flash X-Ray Observation of Marked Mass Points in Explosive Products," p. 3 in *Fifth Symposium (International) on Detonation, Pasadena, California, August 1970*, Office of Naval Research Symposium Report ACR-184 (1970).

E. M. Sandoval and J. P. Kearns, "Use of Hydrazine Compounds to Increase the Speed and Contrast of Industrial Radiographic Film," Los Alamos Scientific Laboratory report LA-5198-MS (1973).

R. W. Taylor and Douglas Venable, "An Aluminum Splash Generated by Impact of a Detonation Wave," *Journal of Applied Physics* **39**, No. 10, 4633 (1968).

Rodney S. Thurston and William L. Mudd, "Spallation Criteria for Numerical Computations," Los Alamos Scientific Laboratory report LA-4013 (1968).

Douglas Venable, "PHERMEX," *Physics Today* **17**, No. 12, 19 (1964).

Douglas Venable and T. J. Boyd, Jr., "PHERMEX Applications to Studies of Detonation Waves and Shock Waves," p. 639 in *Fourth Symposium (International) on Detonation, White Oak, Maryland, October 1965*, Office of Naval Research Symposium Report ACR-126 (1966).

Douglas Venable, Ed., "PHERMEX: A Pulsed High-Energy Radiographic Machine Emitting X-Rays," Los Alamos Scientific Laboratory report LA-3241 (1967).

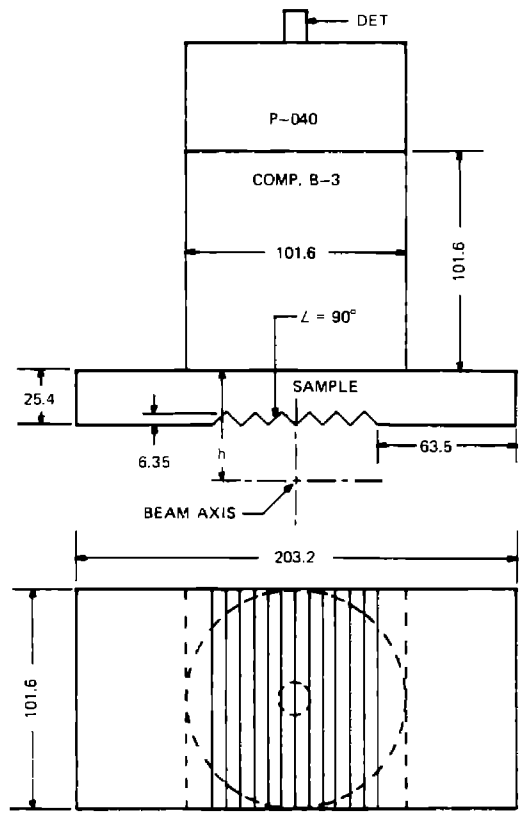
CATALOG OF SHOT SUBJECTS, PHERMEX SHOTS 1 THROUGH 400

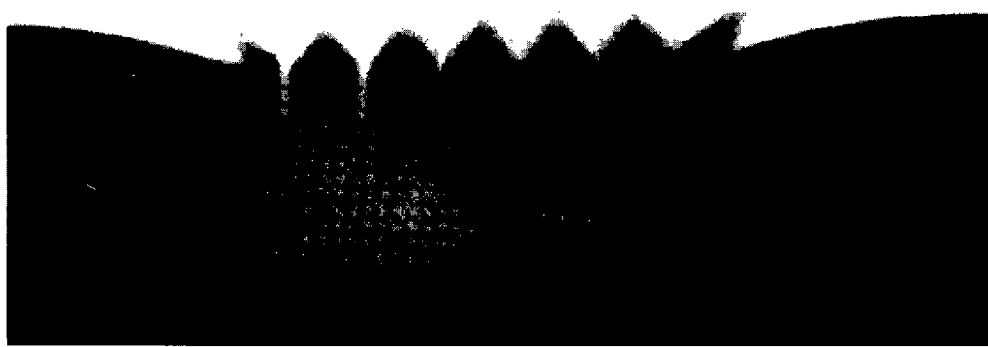
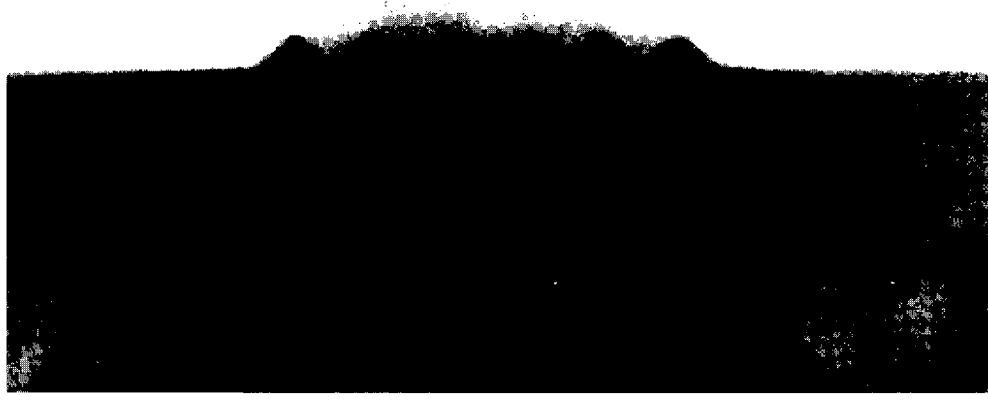
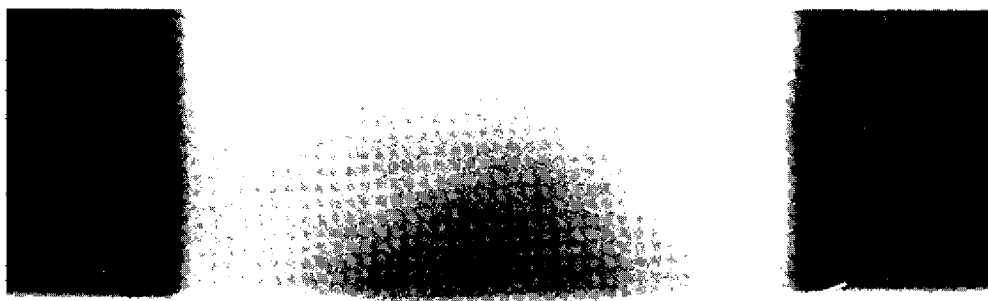
ALUMINUM JETS	1, 6-13, 16-25, 28-30, 32, 36, 37, 141-149, and 197-199
ALUMINUM JETS FROM 40° GROOVES	161 and 162
ALUMINUM JETS FROM 60° GROOVES	159 and 160
ALUMINUM JETS FROM 120° GROOVES	157 and 158
ALUMINUM JETS FROM 140° GROOVES	155 and 156
ALUMINUM JETS FROM 160° GROOVES	153 and 154
ALUMINUM JETS FROM 170° GROOVES	151 and 152
ALUMINUM JETS PENETRATING URANIUM	150 and 201
ALUMINUM ROD IN WATER	189, 190, 269, 281, and 282
ALUMINUM WEDGE	39, 135-138, 193, and 214-217
ARMCO IRON SPLASH WAVE	57
COLLIDING COMPOSITION B-3 DETONATION PRODUCTS	139, 140, 195, and 196
COLLIDING COMPOSITION B-3 DETONATIONS	86, 87, 91, 92, and 273-277
COLLIDING CYCLOTOL DETONATIONS	203-206 and 291
COLLIDING OCTOL DETONATIONS	294-297
COLLIDING PBX-9404 DETONATIONS	207-210 and 292
COMPOSITION B-3 TURNING A 15° CORNER	377 and 378
COMPOSITION B-3 TURNING A 30° CORNER	375 and 376
COMPOSITION B-3 TURNING A 45° CORNER	373 and 374
COMPOSITION B-3 TURNING A 60° CORNER	371 and 372
COMPOSITION B-3 TURNING A 75° CORNER	369 and 370
COMPOSITION B-3 TURNING A 90° CORNER	366-368
COMPOSITION B-3 WITH EMBEDDED TANTALUM FOILS	220, 221, 272, 290, and 352-354
CONVERGING MUNROE JET	363-365
COPPER JETS	43
COPPER SPLASH WAVE	54
CYLINDRICAL HOLE IN POLYETHYLENE	314 and 351
CYLINDRICAL HOLE IN WATER	187, 188, 278-280, 300, and 318
DETONATION OF TWO P-040 LENSES	14
DIVERGING MUNROE JET	322-330

DYNAMIC FRACTURE OF ALUMINUM	60-63, 68-70, 76-85, 89, 97, 102-105, 107-110, 211-213, 222-224, 226-232, 234-236, 238, 241, 245-247, 305, 348, 349, 355-361, 386, and 387
DYNAMIC FRACTURE OF BERYLLIUM	271 and 379-385
DYNAMIC FRACTURE OF COPPER	239, 240, and 389-391
DYNAMIC FRACTURE OF NICKEL	115, 116, 177, 178, 242, 270, and 392-394
DYNAMIC FRACTURE OF THORIUM	130, 132, 172-176, 179, 395, and 396
DYNAMIC FRACTURE OF URANIUM	123, 129, 131, 133, and 165-171
EXPANSION OF COMPOSITION B-3 PRODUCTS INTO A VACUUM	93 and 94
EXPLOSIVE DRIVER FOR MULTIPLE PLATE FRACTURE	334 and 347
INTERACTING ALUMINUM JETS	41, 42, and 59
INTERACTION OF COMPOSITION B-3 AND BARATOL PRODUCTS	2
LEAD JETS	45
LUCITE AND WATER CORNER	112 and 114
LUCITE SHOCK WAVE	75
MACH REFLECTION IN BARATOL	3-5, 15, and 55
MACH REFLECTION IN COMPOSITION B-3	101
MAGNESIUM JETS	321
MULTIPLE PLATE FRACTURE	308-313, 319, 331-333, 335-339, and 385
MUNROE JET	240, 249, 255-267, 283, 285-287, 315, 341-343, and 362
MUNROE JET INTERACTING WITH ALUMINUM	334-336
OBLIQUE ALUMINUM PLATE IMPACT	90 and 96
OBLIQUE ALUMINUM PLATE IMPACT ON COMPOSITION B-3	98 and 99
PERLITE SHOCK VELOCITY	320
PLANE WAVE ALUMINUM GUN	250-252
REGULAR REFLECTION IN COMPOSITION B-3	100
SHOCKED ALUMINUM GROOVES INTERACTING WITH MERCURY	27
SHOCKED MERCURY INTERACTING WITH ALUMINUM GROOVES	26 and 184-186
SPHERICAL HOLE IN WATER	56 and 95
STEEL JETS	44 and 46-51
STEEL SPLASH WAVE	58
THORIUM JETS	125-128
TWO COMPOSITION B-3 DETONATIONS	35, 38, 40, and 64
TWO COMPOSITION B-3 DETONATIONS COLLIDING WITH ALUMINUM	33 and 34
TWO OFFSET COMPOSITION B-3 DETONATIONS	31 and 71-73
URANIUM JETS	74, 117, 122, and 180-182
URANIUM JETS PENETRATING ALUMINUM	118 and 124
VERMICULITE SHOCK VELOCITY	340
WATER FREE SURFACE MOTION	191
WATER JET	192, 298, and 299
WATER SHOCK	32, 53, 111, 113, 253, and 254

SHOT 1: **Aluminum Jets**
Date: August 27, 1963
Experimenter: Douglas Venable
Radiographic Time: 33.1 μ s

Formation of metallic jets. The explosively induced shock wave in the aluminum plate interacts with the grooves to produce the jets. The free surface of the plate has run for 3.2 μ s. h is 12.7 mm. The white lines on the static radiograph are from cracks in the negative.





SHOT 2:

Interaction of Composition B-3 and Baratol Products

Date:

October 21, 1963

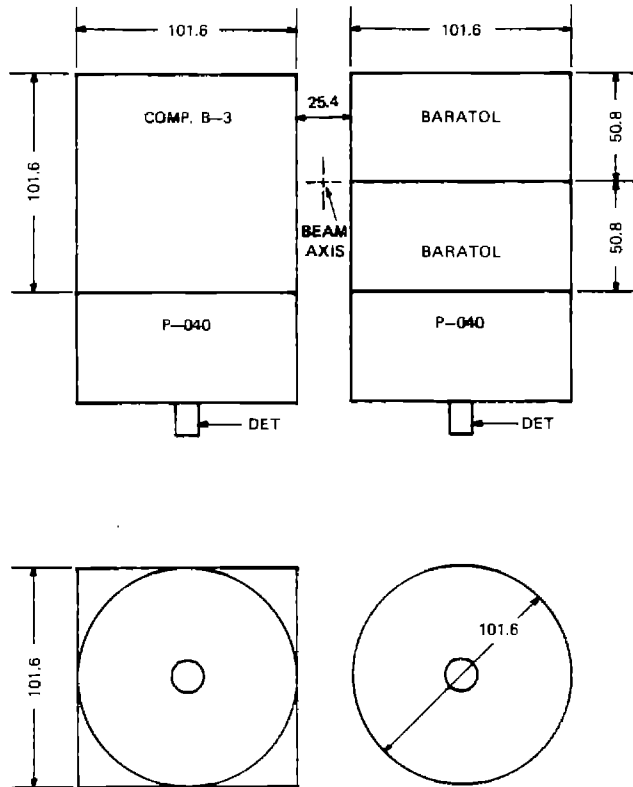
Experimenter:

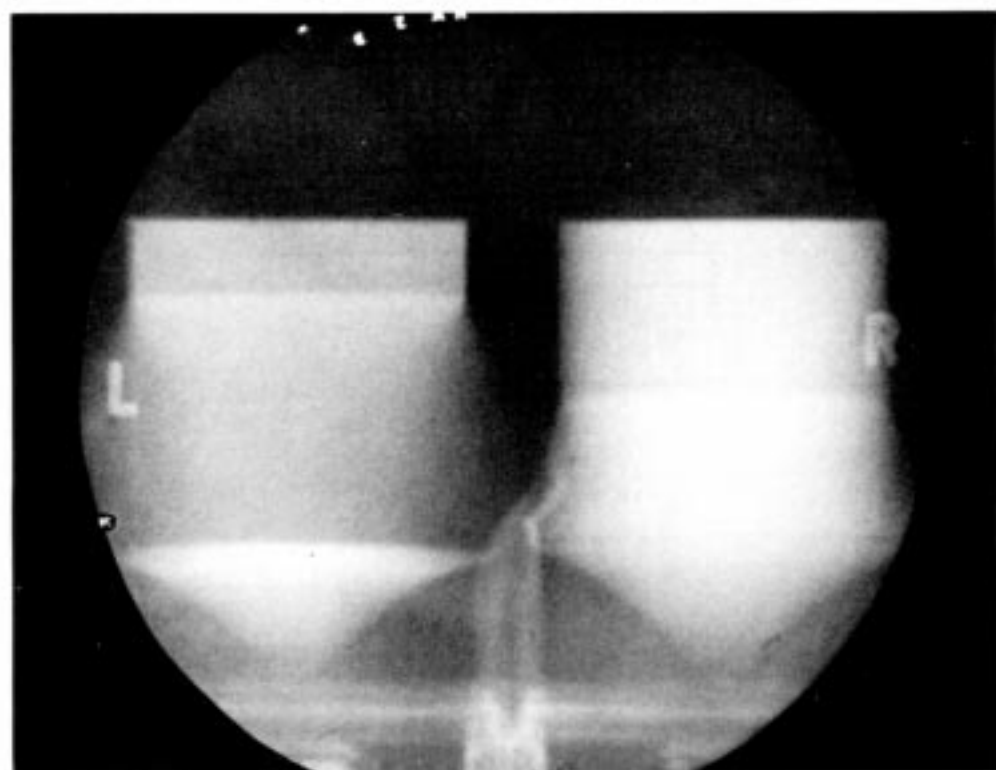
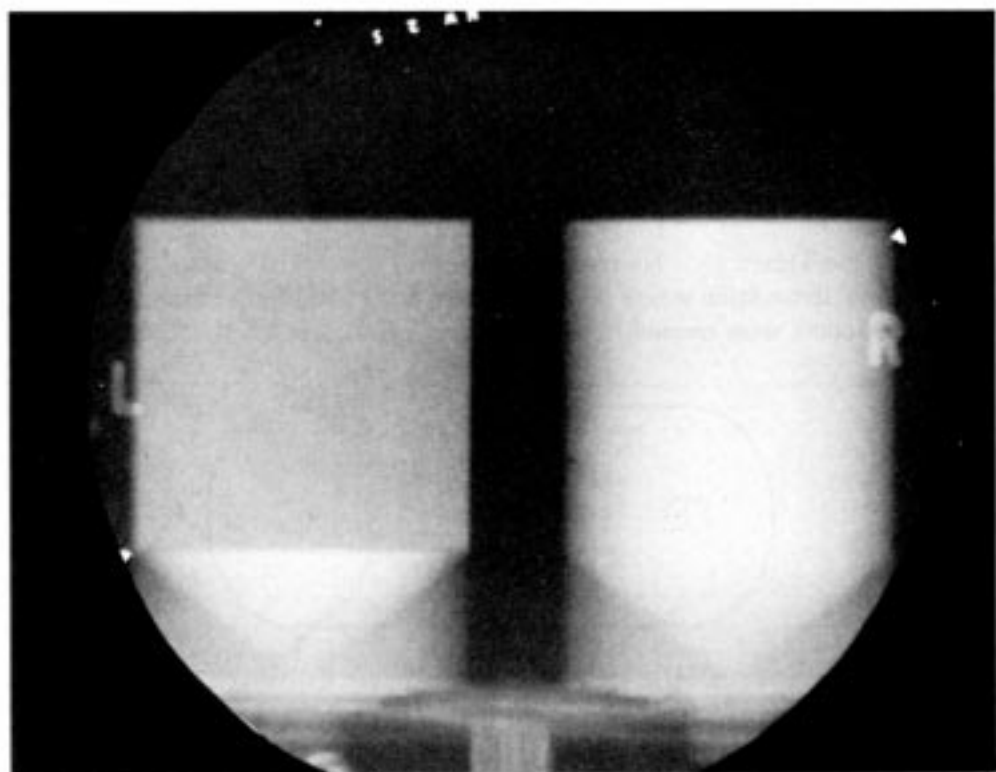
Douglas Venable

Radiographic Time:

23.4 μ s.

Interaction of the detonation products of a Composition B-3 block and a Baratol cylinder placed 25.4 mm apart and simultaneously bottom-initiated.





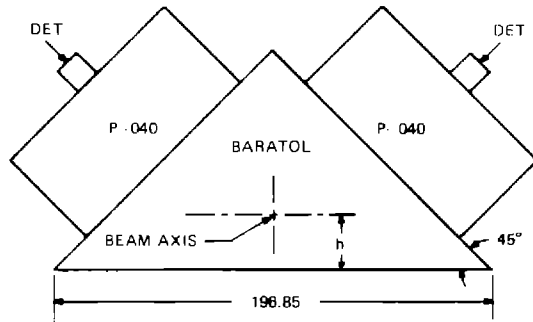
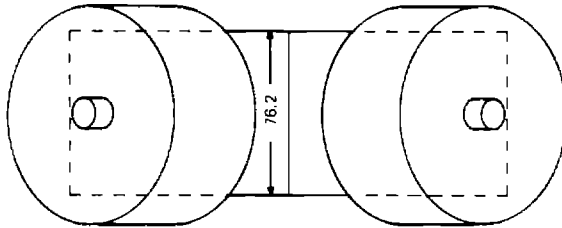
SHOT 3: Mach Reflection in Baratol

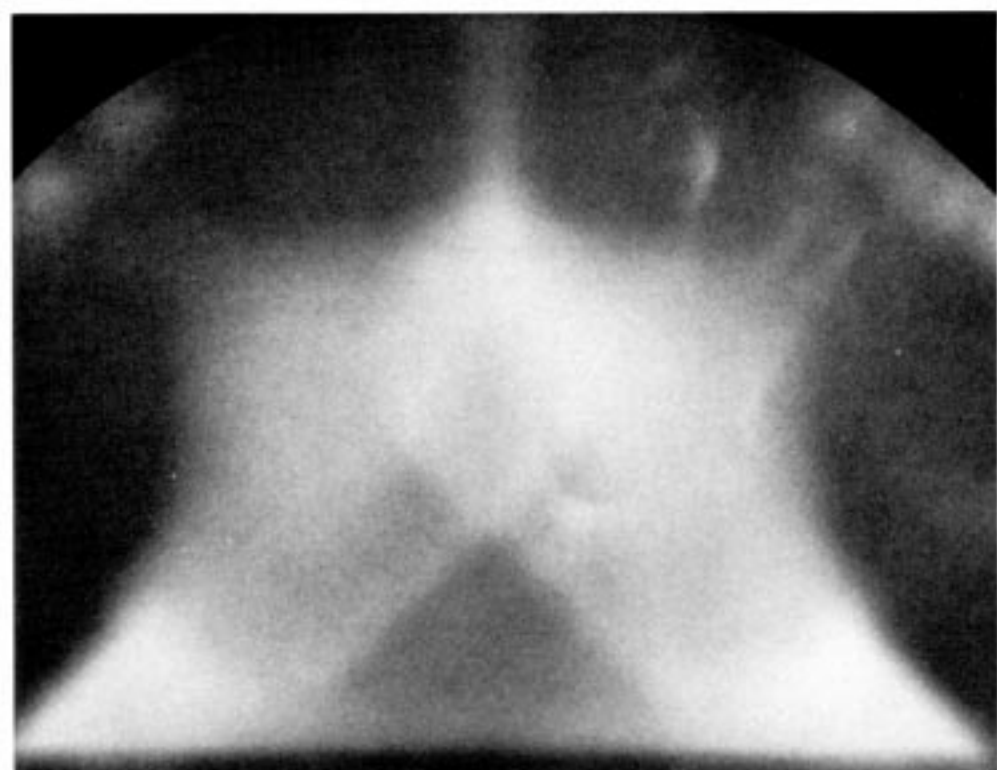
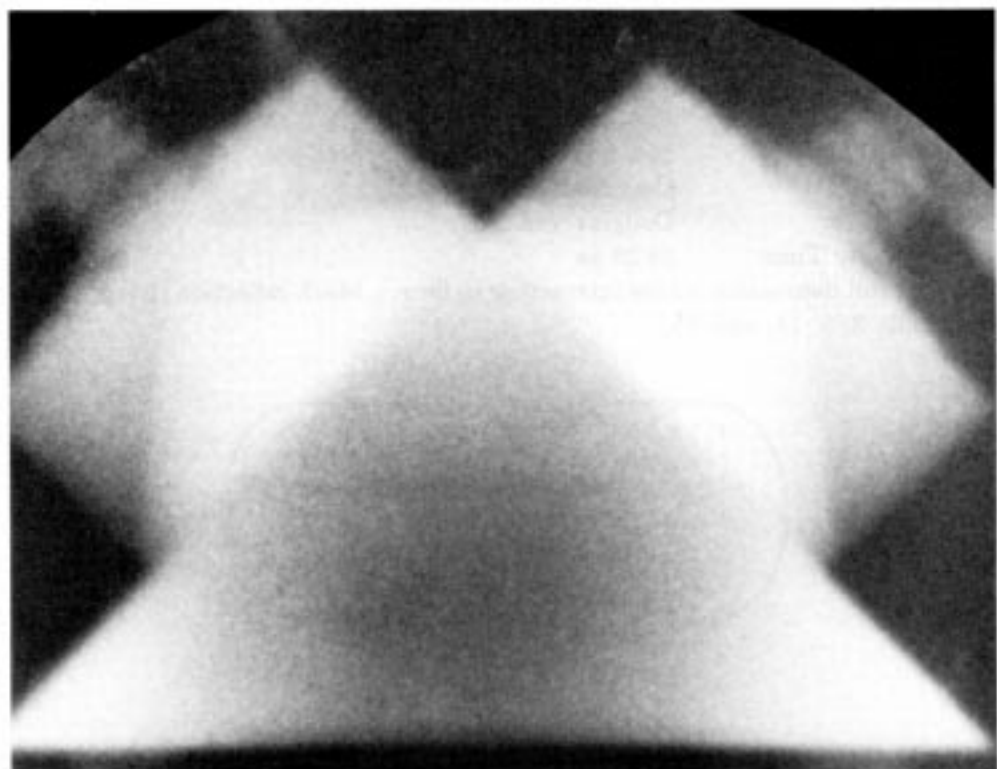
Date: November 5, 1963

Experimenter: Douglas Venable

Radiographic Time: No record

Two Baratol detonation waves interacting to form a Mach reflection. h is 25.4 mm. The black spots were caused by shot shrapnel. See Shots 4, 5, 15, and 55.





SHOT 4:

Mach Reflection in Baratol

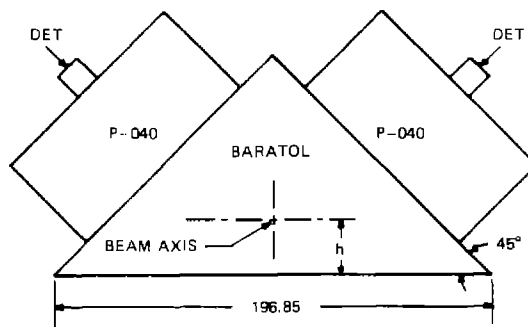
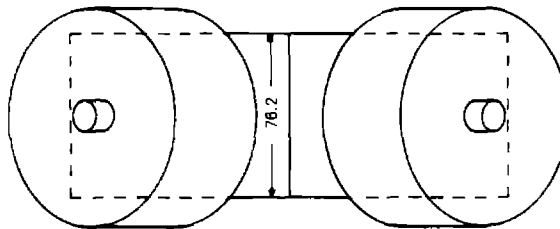
Date: December 4, 1963

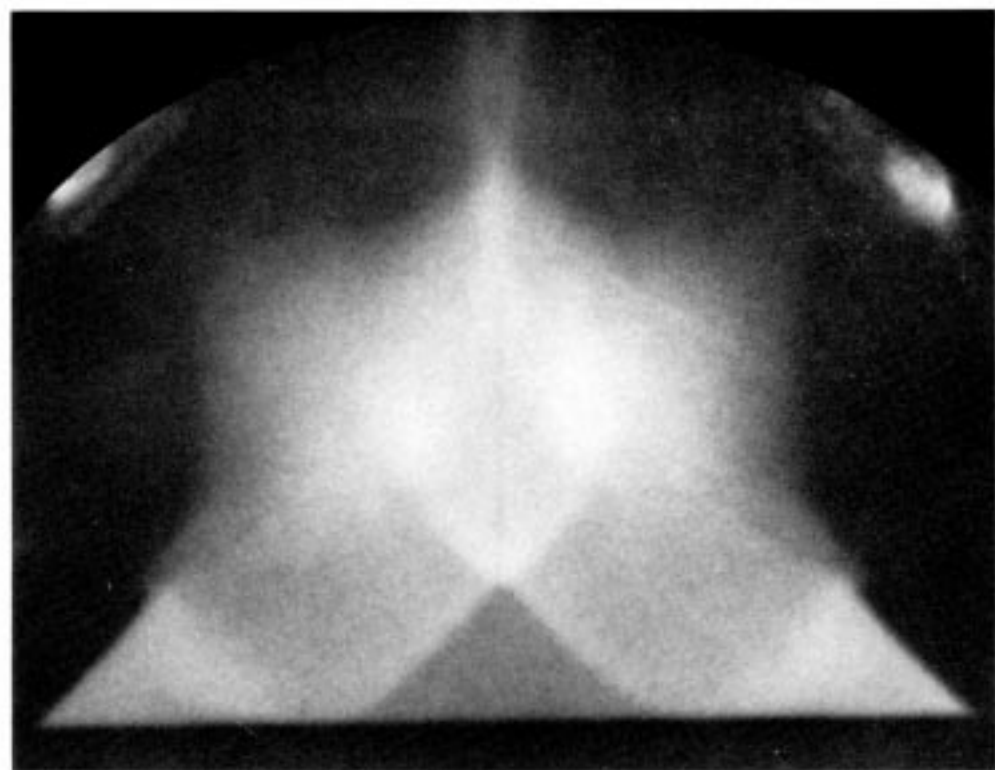
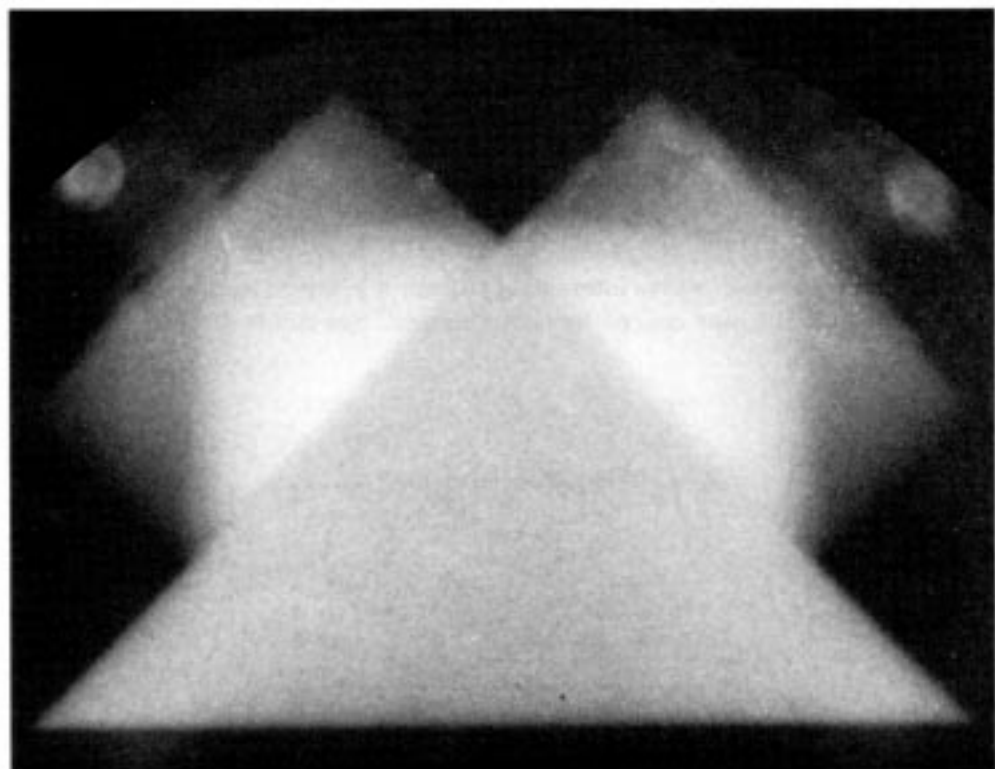
Experimenter: Douglas Venable

Radiographic Time: 24.28 μ s

Two Baratol detonation waves interacting to form a Mach reflection. h is 15.9 mm.

See Shots 3, 5, 15, and 55.





SHOT 5:

Mach Reflection in Baratol

Date:

December 18, 1963

Experimenter:

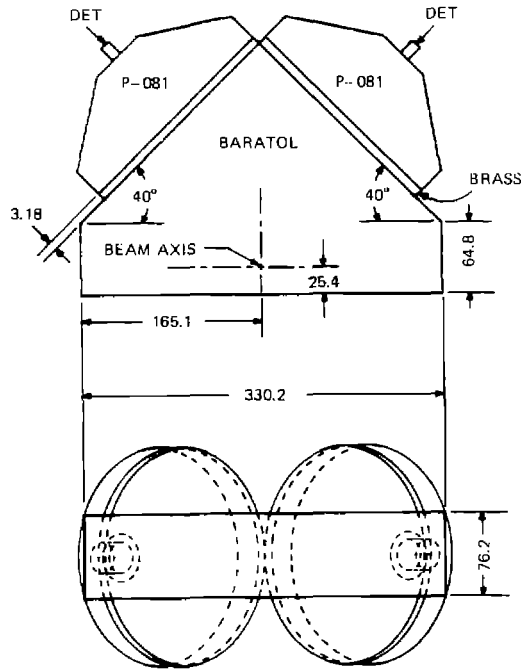
Douglas Venable

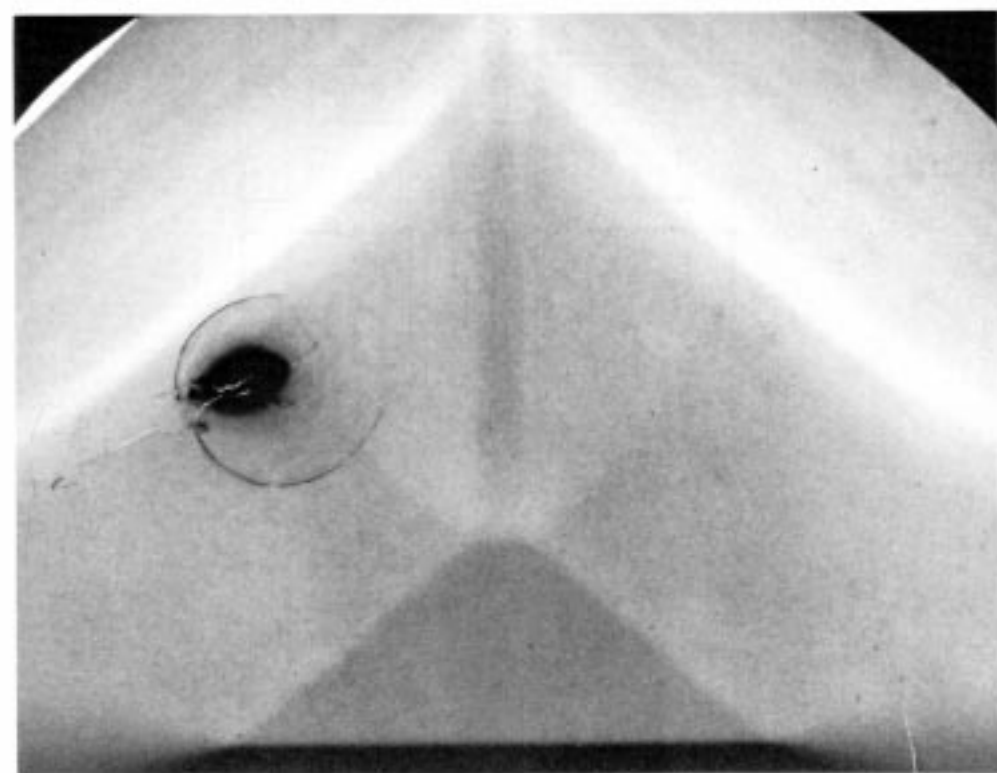
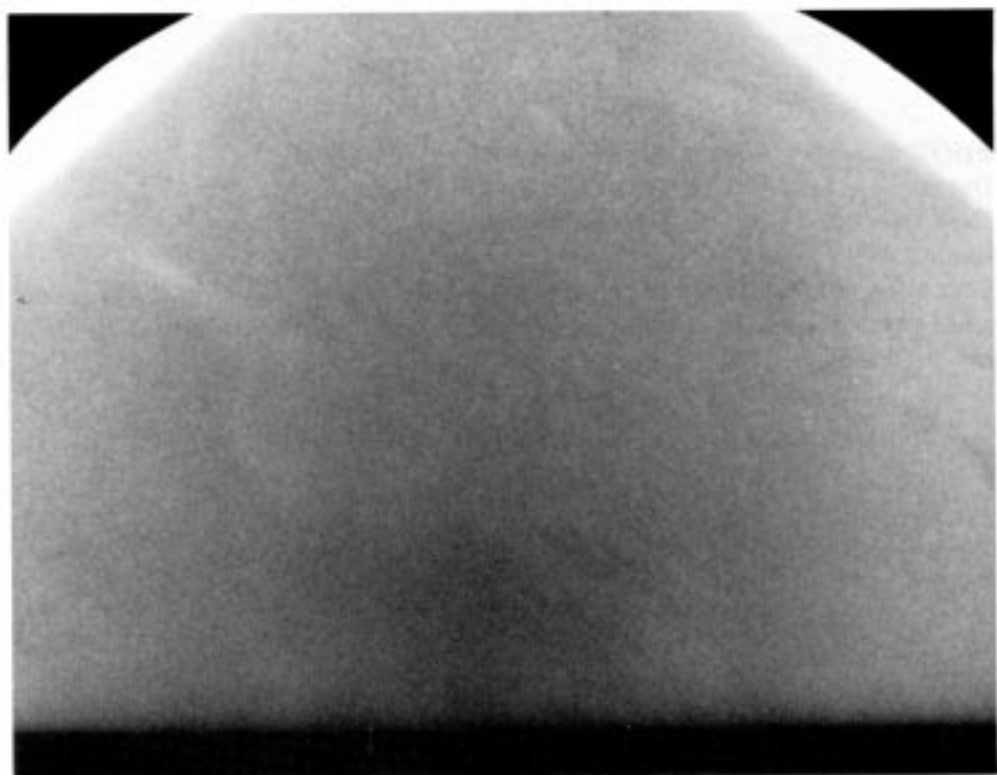
Radiographic Time:

No record

Two Baratol detonation waves interacting to form a Mach reflection. h is 25.4 mm.

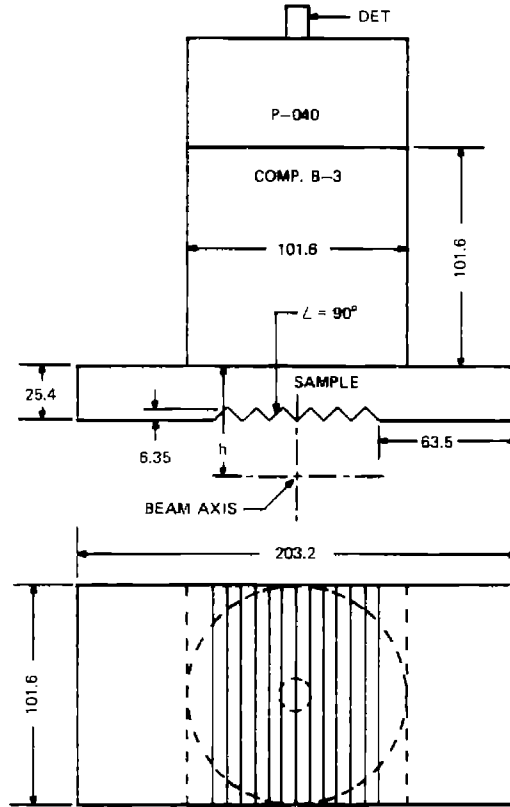
The hole in the film was caused by shot shrapnel. See Shots 3, 4, 15, and 55.

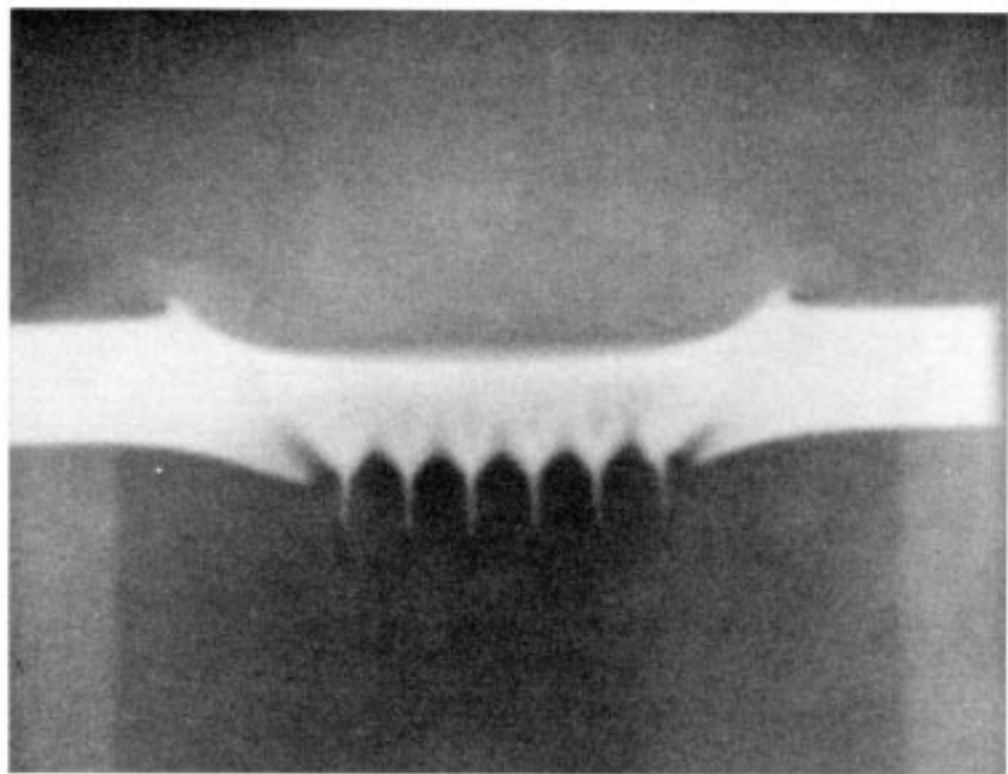




SHOT 6: **Aluminum Jets**
Date: February 13, 1964
Experimenter: Douglas Venable
Radiographic Time: 33.1 μ s

Formation of metallic jets. The explosively induced shock wave in the aluminum plate interacts with the grooves to produce the jets. The free surface of the plate has run for 3.2 μ s. h is 12.7 mm.





SHOT 7:

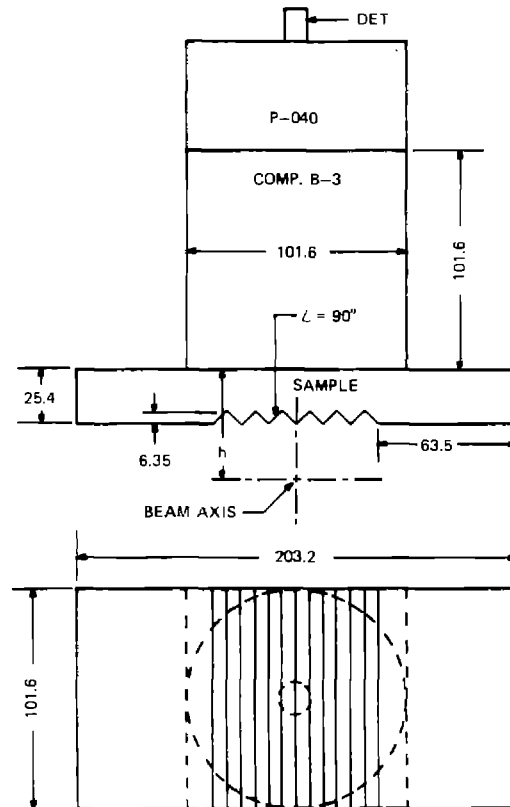
Aluminum Jets

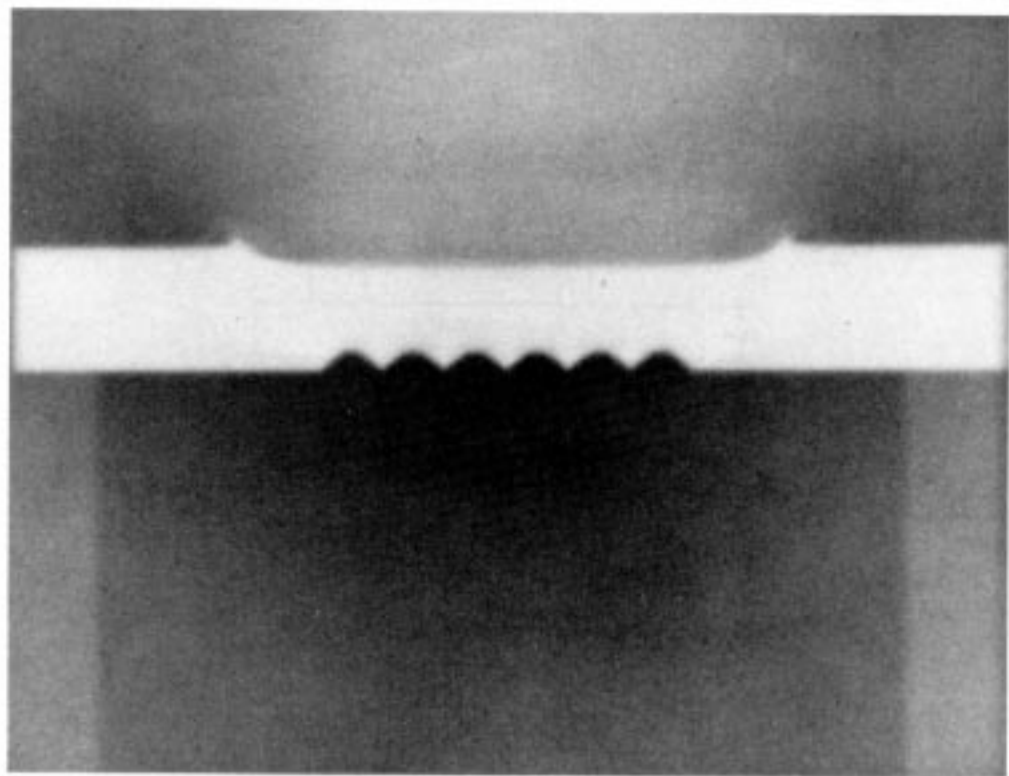
Date: February 18, 1964

Experimenter: Douglas Venable

Radiographic Time: 29.46 μ s

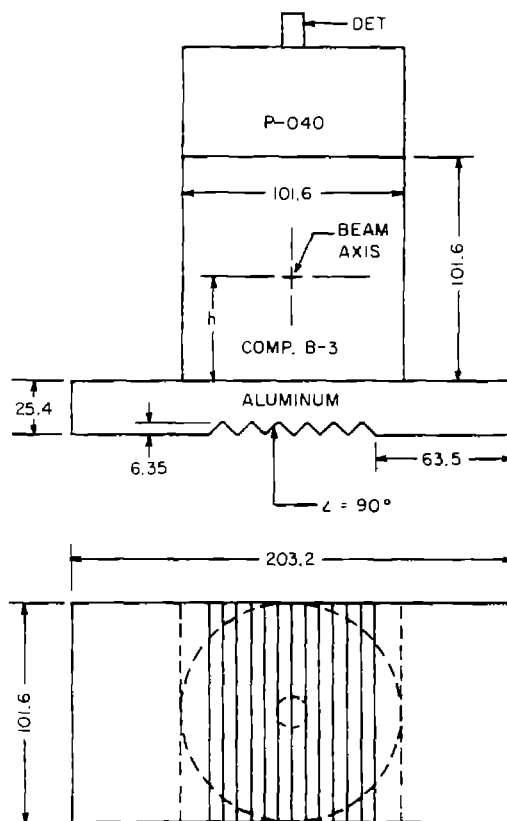
The shock wave used to form metallic jets has traveled 22.2 mm into the aluminum plate. h is 22.22 mm. Duplicated in Shots 141 and 197.

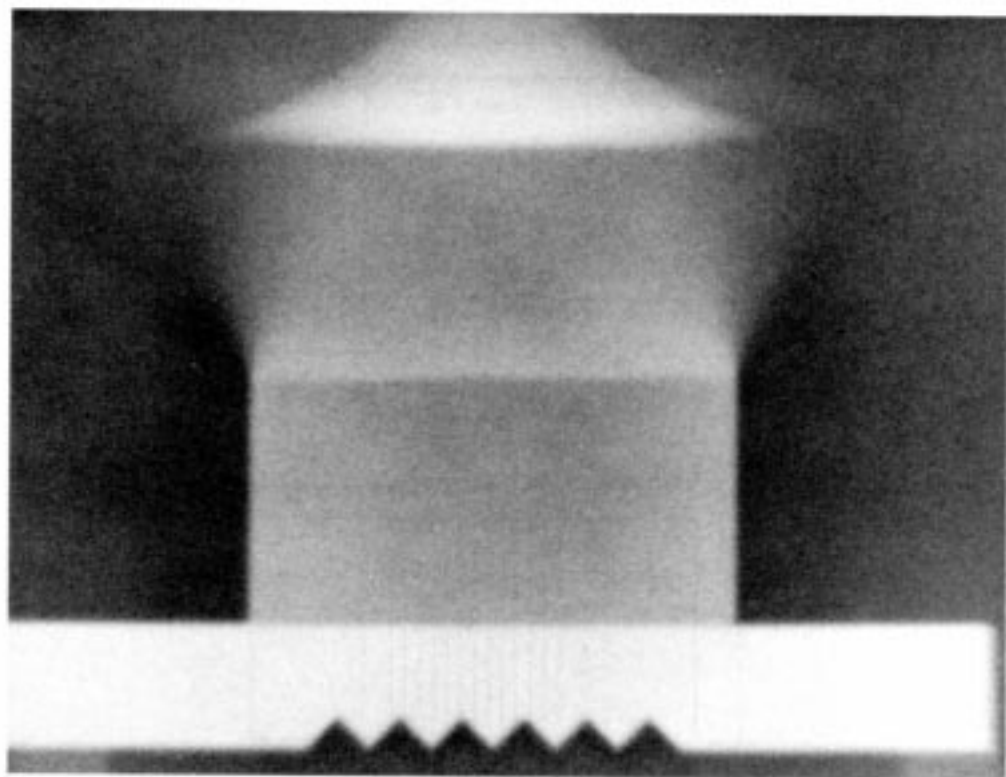




SHOT 8: **Aluminum Jets**
Date: **February 18, 1964**
Experimenter: **Douglas Venable**
Radiographic Time: **19.96 μ s**

The explosive system used to form metallic jets. The Composition B-3 detonation wave has run 50.8 mm in 6.4 μ s. h is 50.8 mm.





SHOT 9:

Aluminum Jets

Date:

February 18, 1964

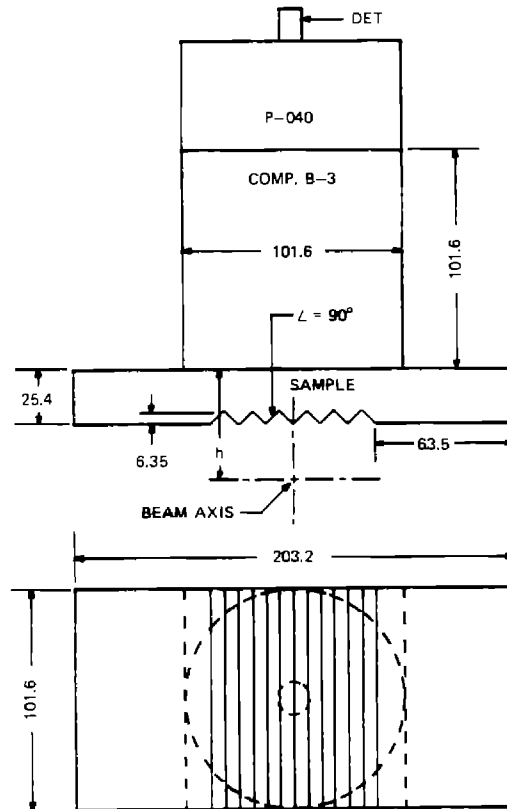
Experimenter:

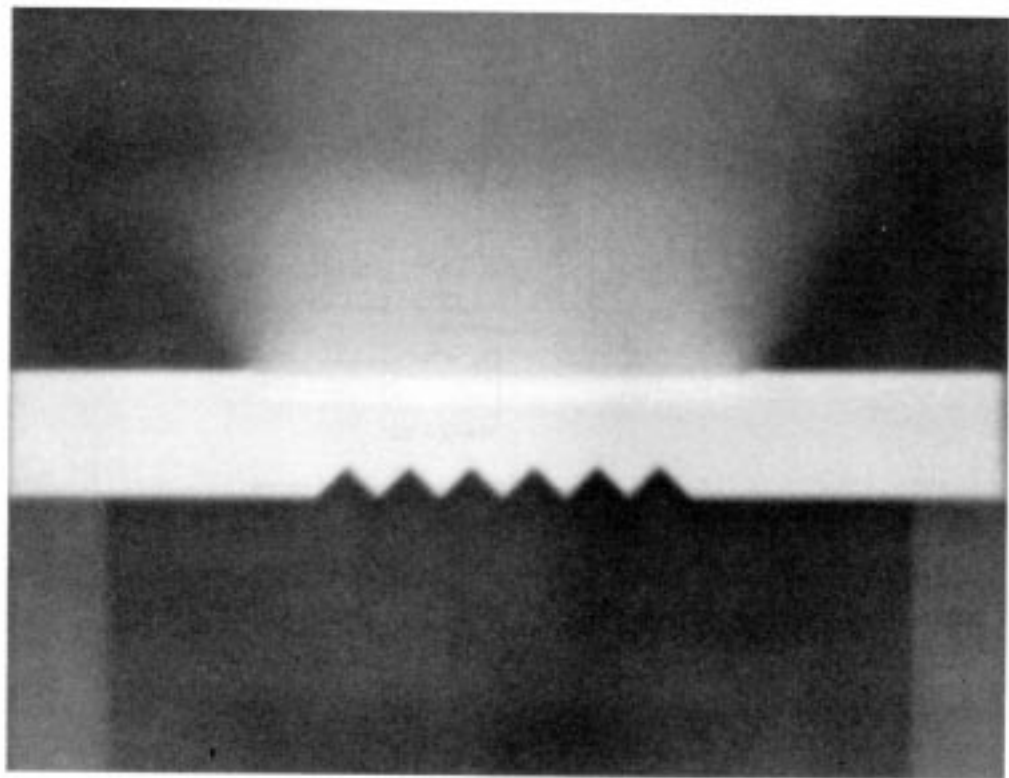
Douglas Venable

Radiographic Time:

27.2 μ s

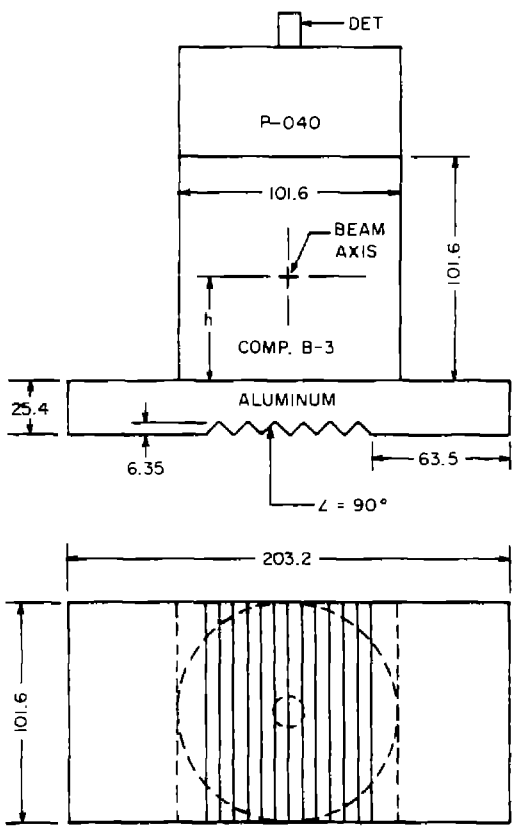
The shock wave used to form metallic jets has traveled 6.35 mm into the aluminum plate in 0.9 μ s. h is 6.35 mm.

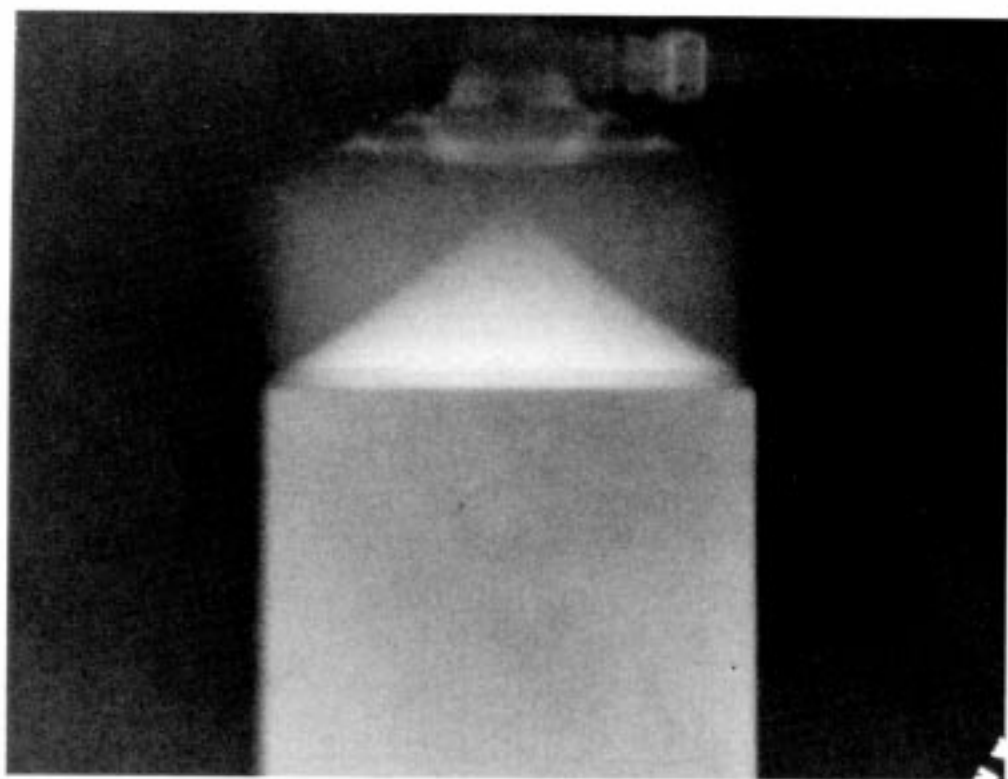




SHOT 10: **Aluminum Jets**
Date: **February 18, 1964**
Experimenter: **Douglas Venable**
Radiographic Time: **12.55 μ s**

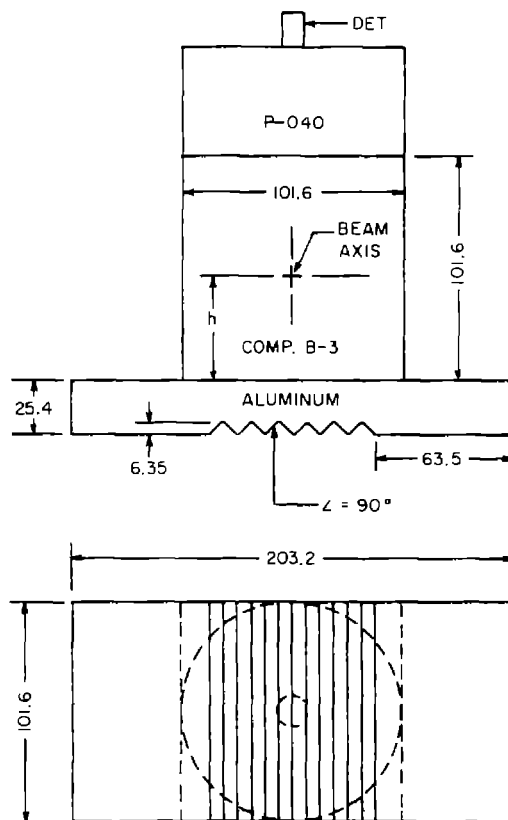
The explosive system used to form metallic jets. The detonation wave has run 37.6 mm into the P-040 lens in 7.2 μ s. h is 106.8 mm.

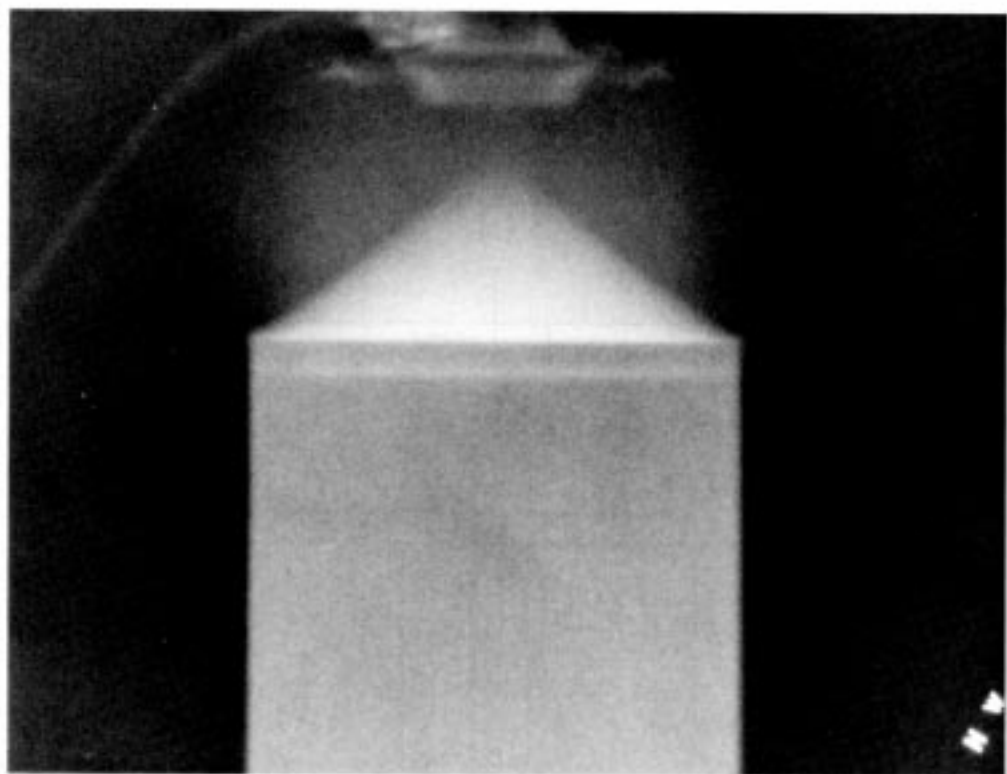




SHOT 11: **Aluminum Jets**
Date: **March 3, 1964**
Experimenter: **Douglas Venable**
Radiographic Time: **14.55 μ s**

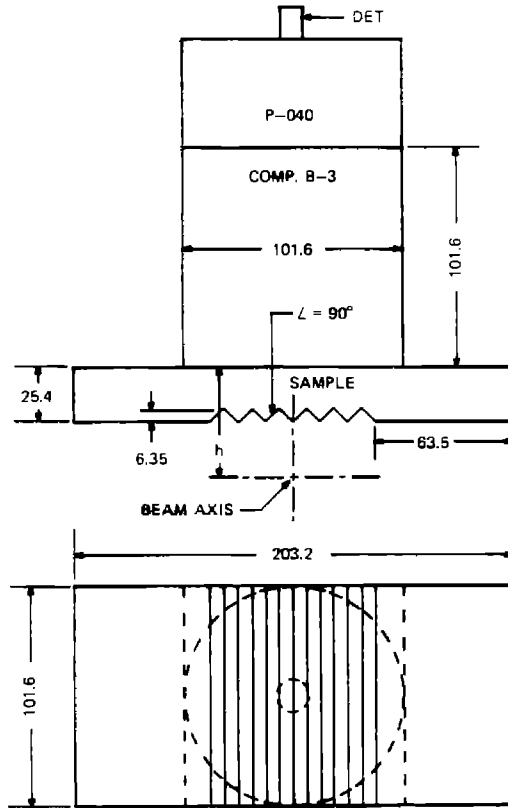
The explosive system used to form metallic jets. The Composition B-3 detonation wave has run 7.9 mm in 1.0 μ s. h is 93.66.

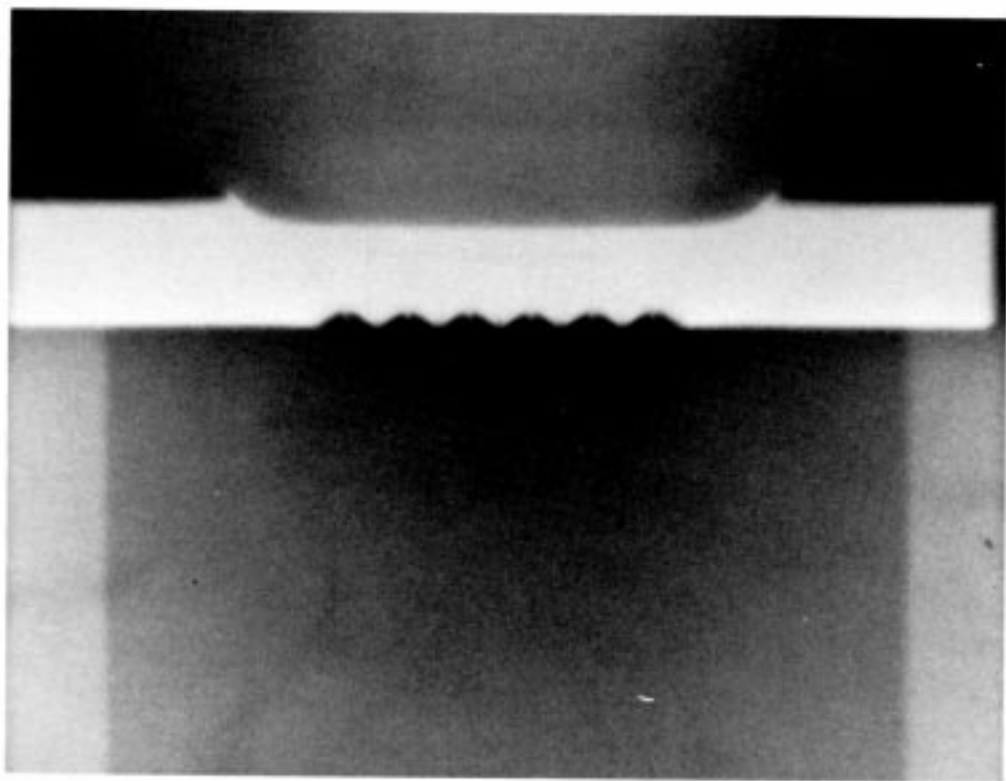




SHOT 12: **Aluminum Jets**
Date: March 3, 1964
Experimenter: Douglas Venable
Radiographic Time: 29.9 μ s

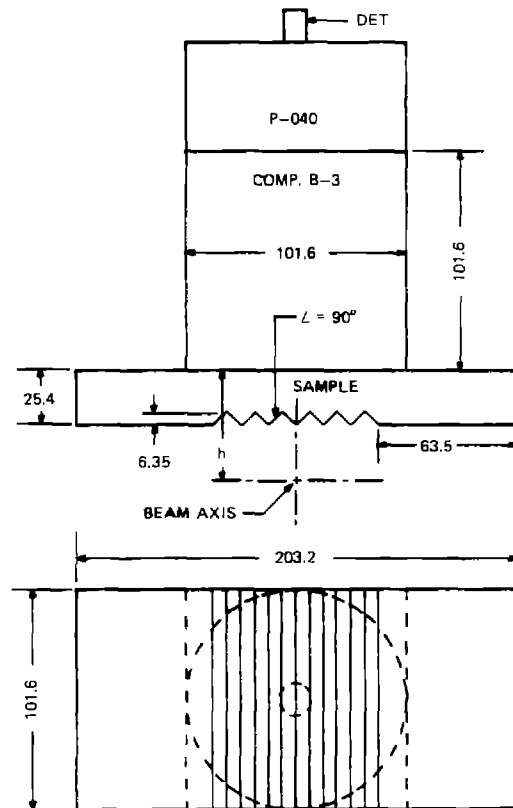
Formation of metallic jets. The explosively induced shock wave in the aluminum plate interacts with the grooves to produce the jets. The shock wave has reached the plate free surface. h is 25.4 mm. Duplicated in Shots 142 and 198.

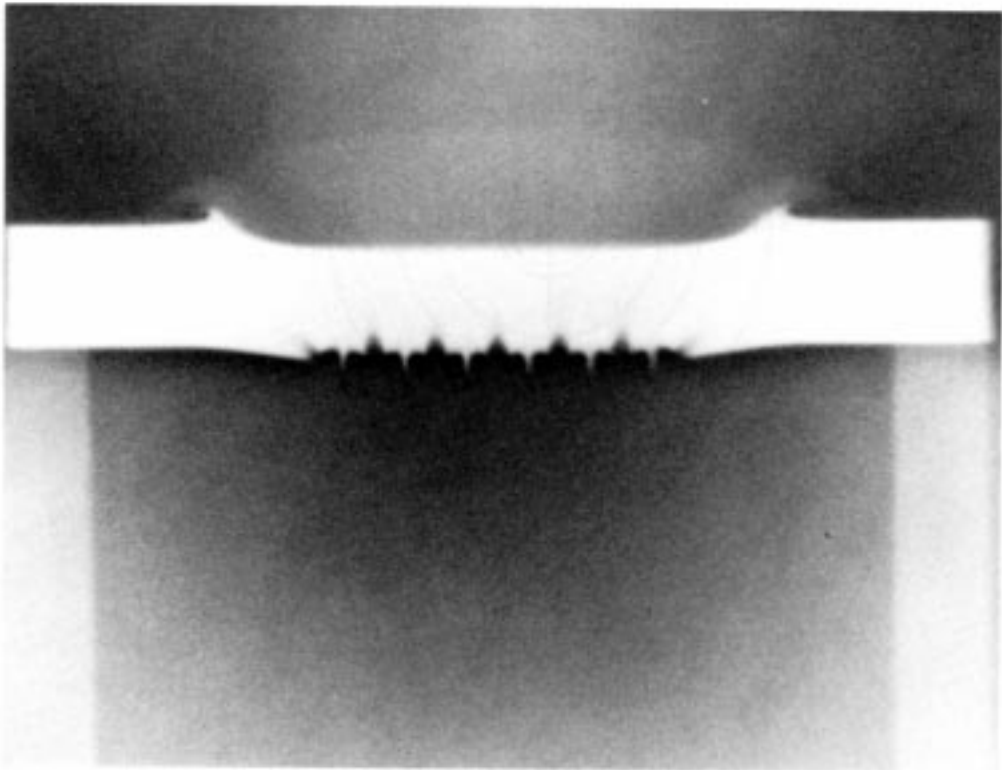




SHOT 13: **Aluminum Jets**
Date: **March 10, 1964**
Experimenter: **Douglas Venable**
Radiographic Time: **30.88 μ s**
Reference: **Venable, 1964**

Formation of metallic jets. The explosively induced shock wave in the aluminum plate interacts with the grooves to produce the jets. The free surface of the plate has run for 1.0 μ s. h is 25.4 mm. Duplicated in Shot 143.





SHOT 14:

Detonation of Two P-040 Lenses

Date:

March 10, 1964

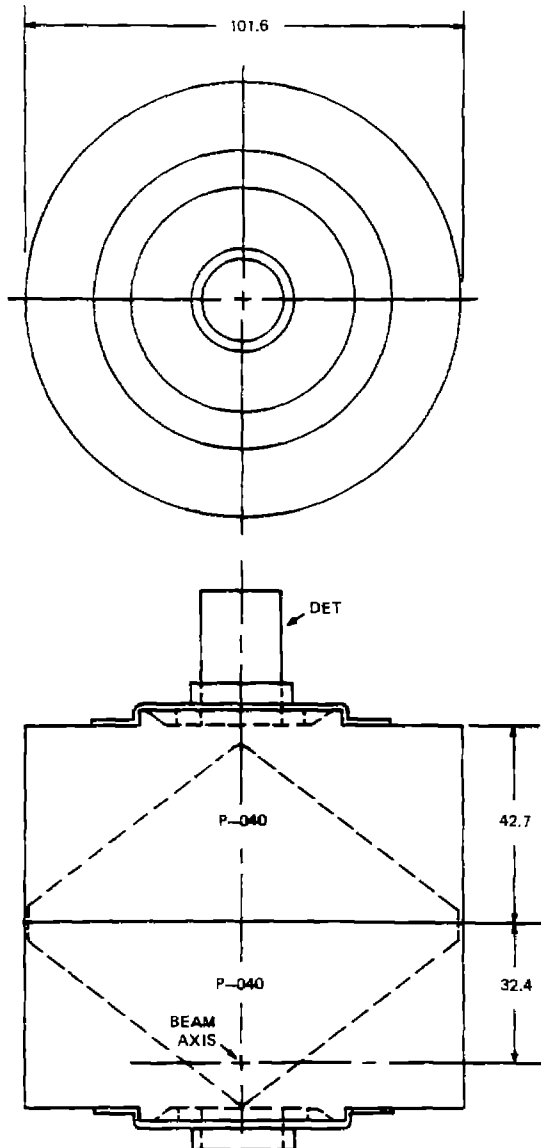
Experimenter:

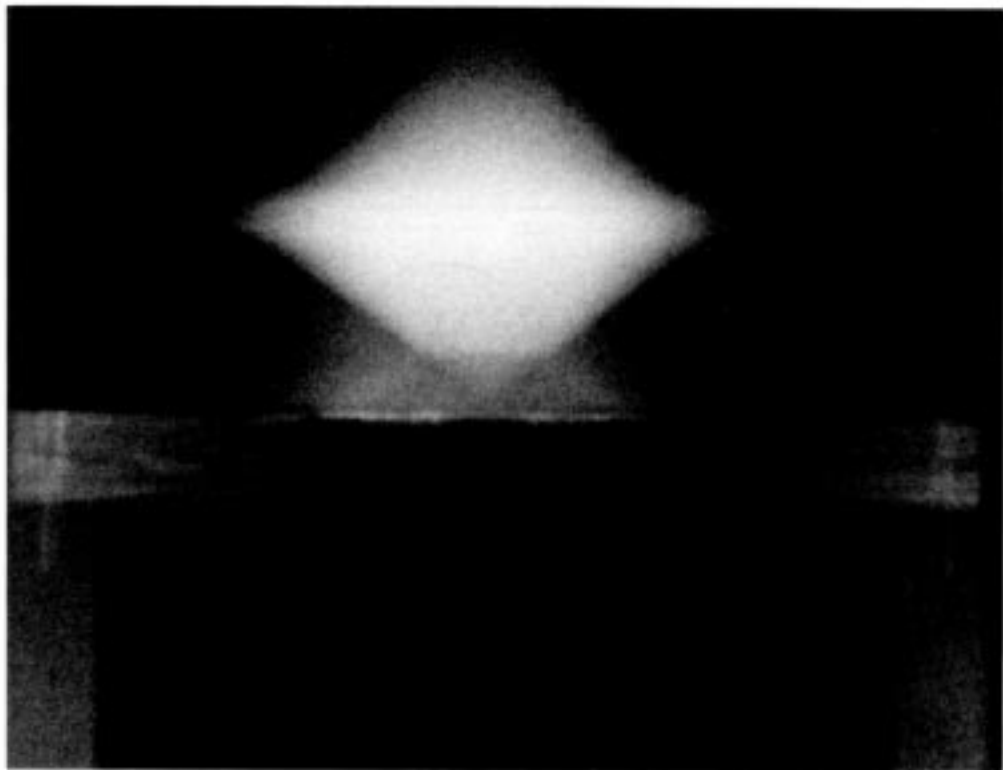
Douglas Venable

Radiographic Time:

19.69 μ s

Two P-040 plane-wave lenses detonated by the top lens. The detonation wave is 10.0 mm from the bottom of the lower lens.





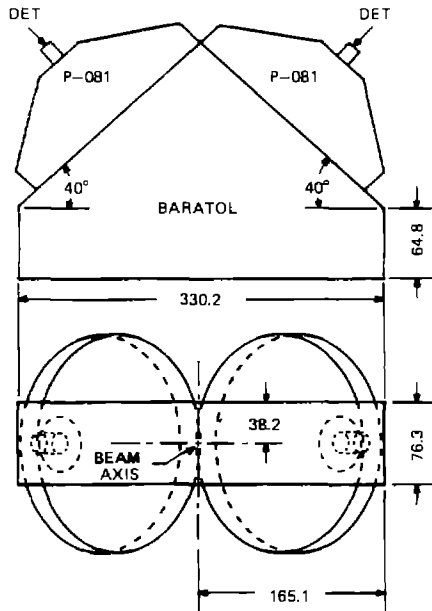
SHOT 15: Mach Reflection in Baratol

Date: March 10, 1964

Experimenter: Douglas Venable

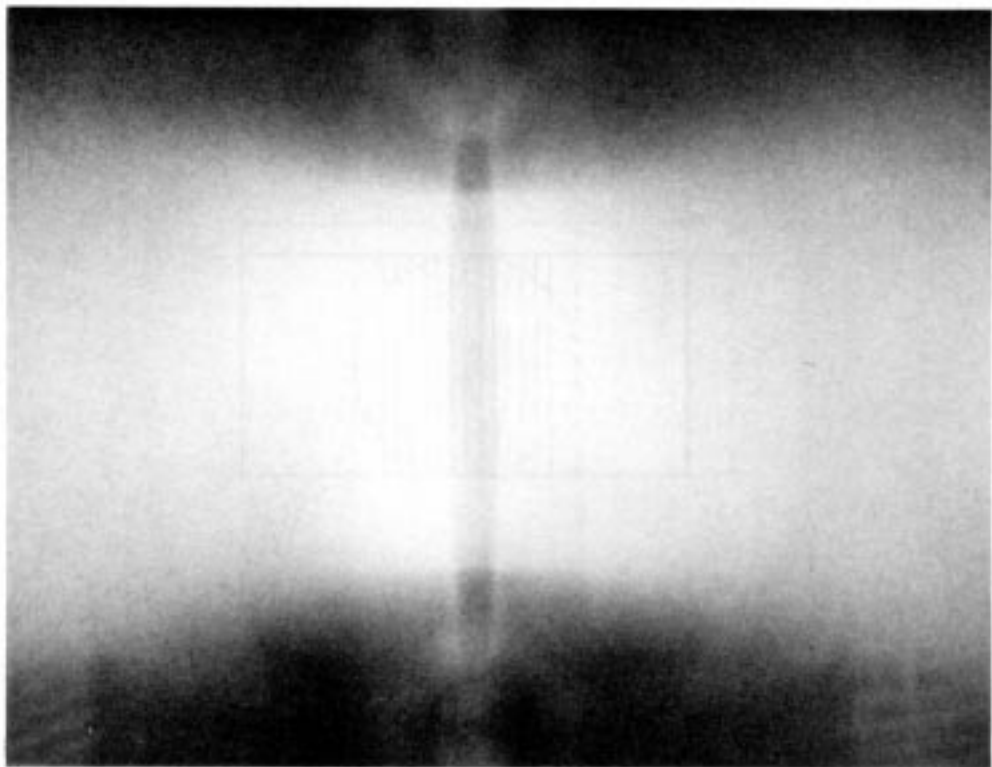
Radiographic Time: 53.0 μ s

Two Baratol detonation waves interacting to form a Mach reflection. The shot is identical to Shot 5 except for the beam orientation. See Shots 3-5 and 55.



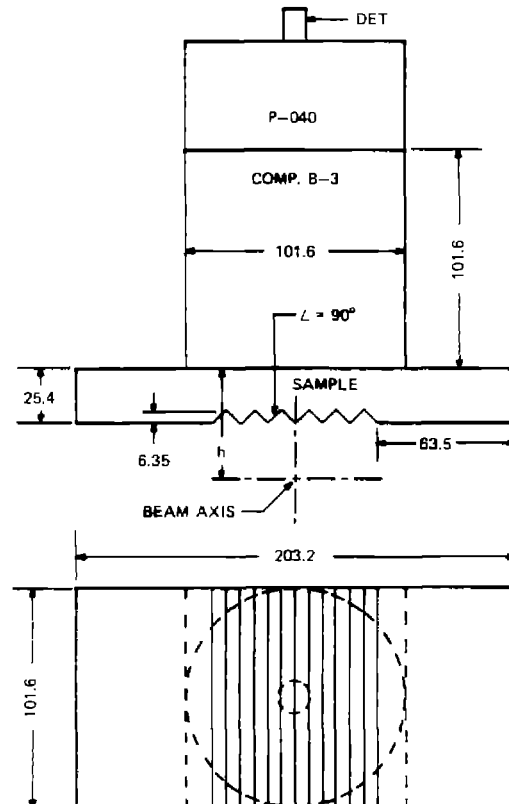


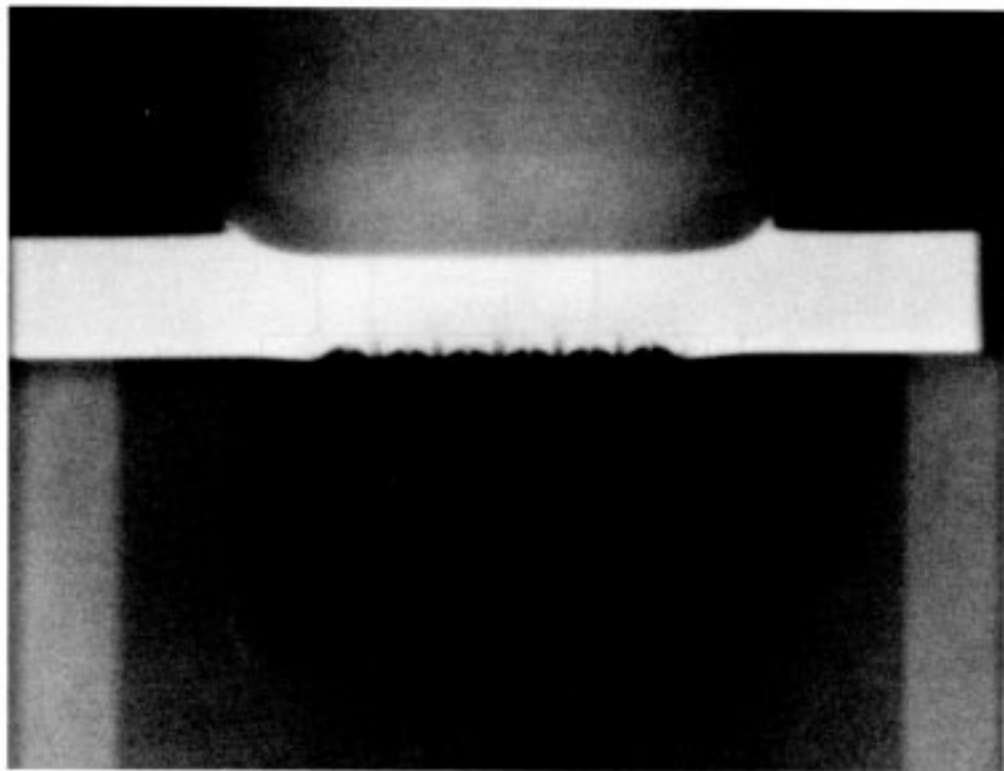
Faint, illegible text, possibly bleed-through from the reverse side of the page. The text is centered and appears to be a short paragraph or a list of items.



SHOT 16: **Aluminum Jets**
 Date: March 17, 1964
 Experimenter: Douglas Venable
 Radiographic Time: 30.32 μ s
 Reference: Venable, 1964

Formation of metallic jets. The explosively induced shock wave in the aluminum plate interacts with the grooves to produce the jets. The free surface of the plate has run for 0.5 μ s. h is 25.4 mm. Duplicated in Shot 144.





SHOT 17:

Aluminum Jets

Date:

March 17, 1964

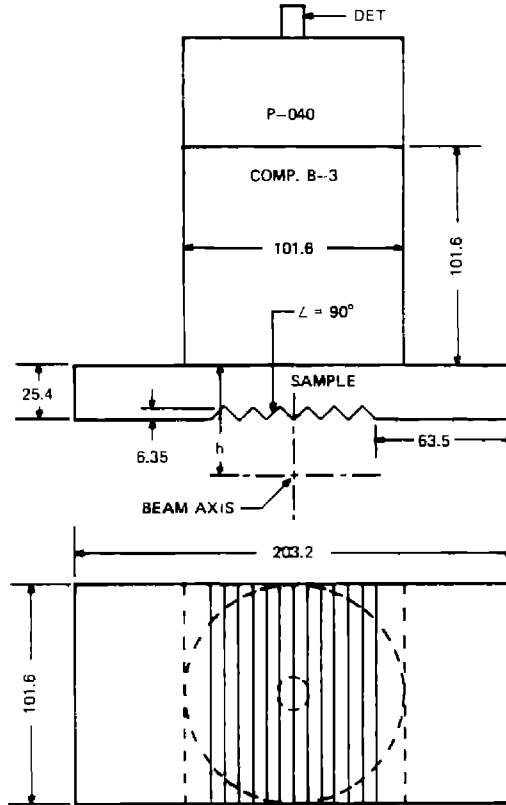
Experimenter:

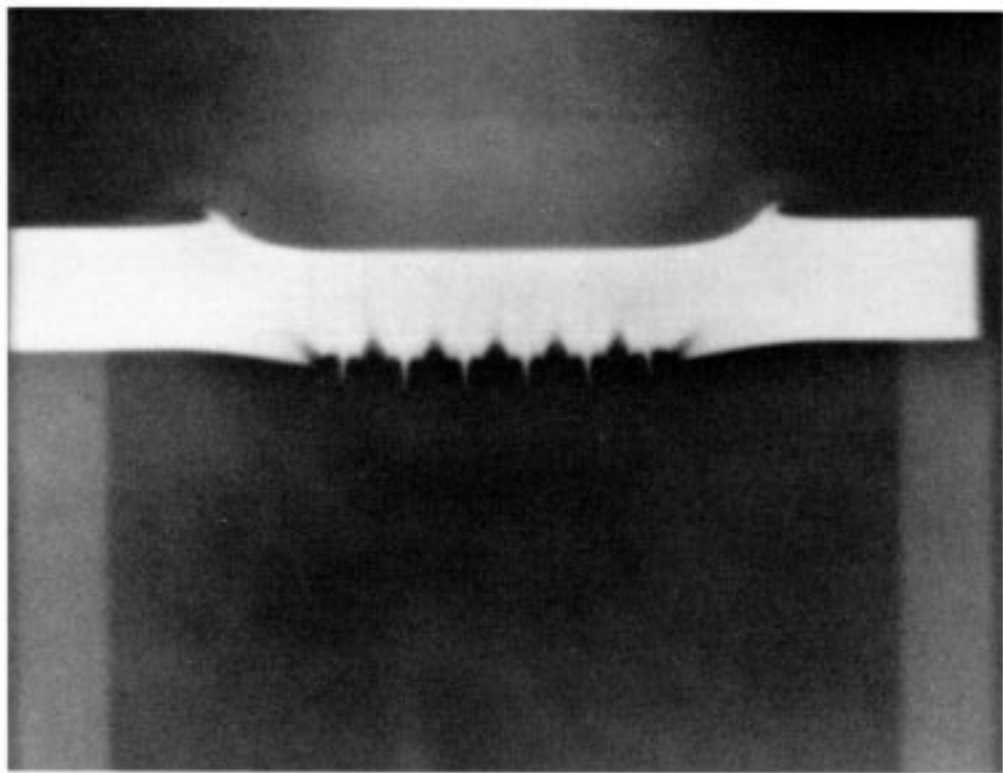
Douglas Venable

Radiographic Time:

31.33 μ s

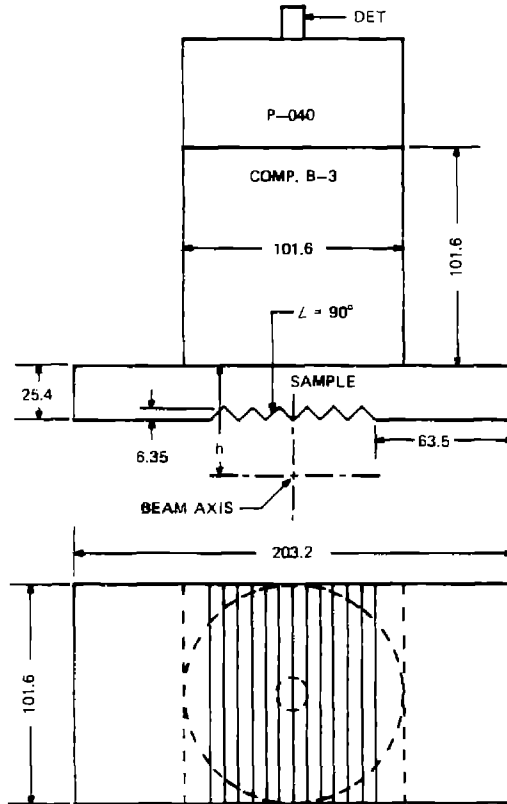
The formation of metallic jets. The explosively induced shock wave in the aluminum plate interacts with the grooves to produce the jets. The free surface of the plate has run for 1.5 μ s. h is 25.4 mm. Duplicated in Shot 145.

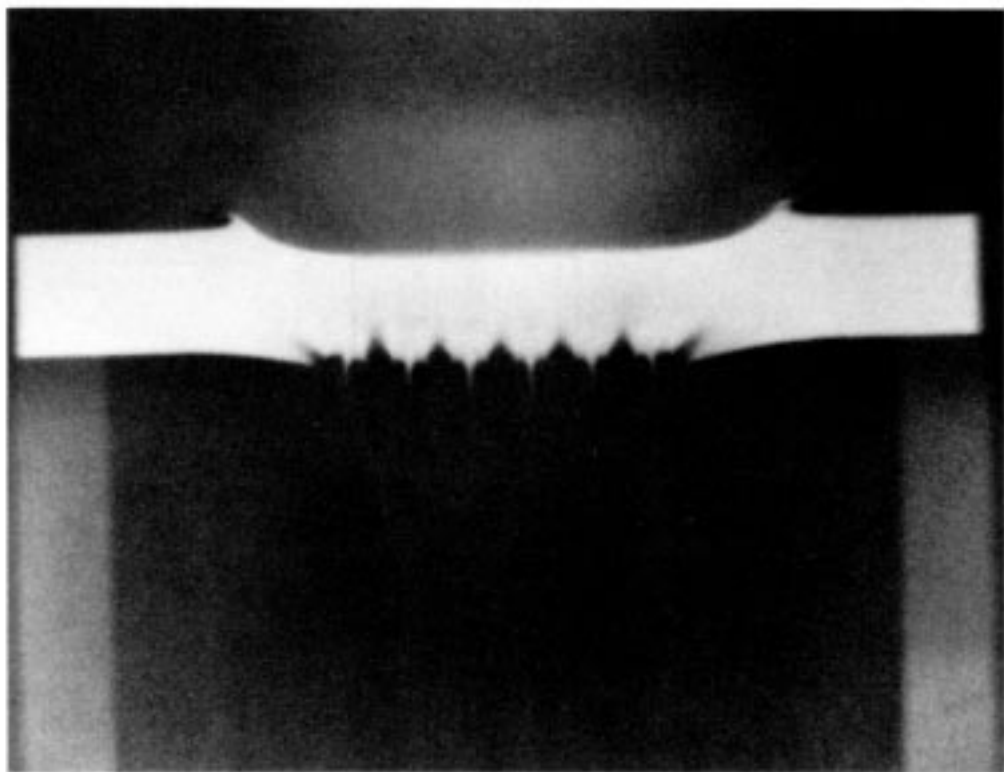




SHOT 18: **Aluminum Jets**
Date: **March 17, 1964**
Experimenter: **Douglas Venable**
Radiographic Time: **31.83 μ s**

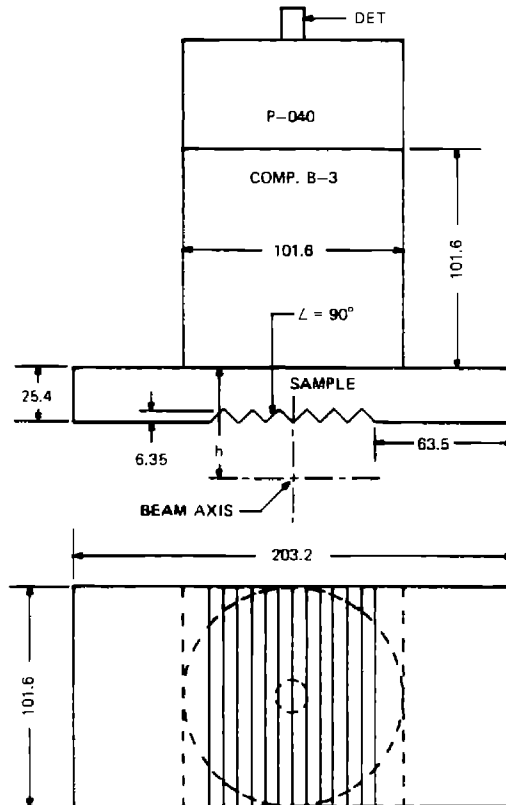
Formation of metallic jets. The explosively induced shock wave in the aluminum plate interacts with the grooves to produce the jets. The free surface of the plate has run for 2.0 μ s. h is 25.4 mm. Duplicated in Shot 146.

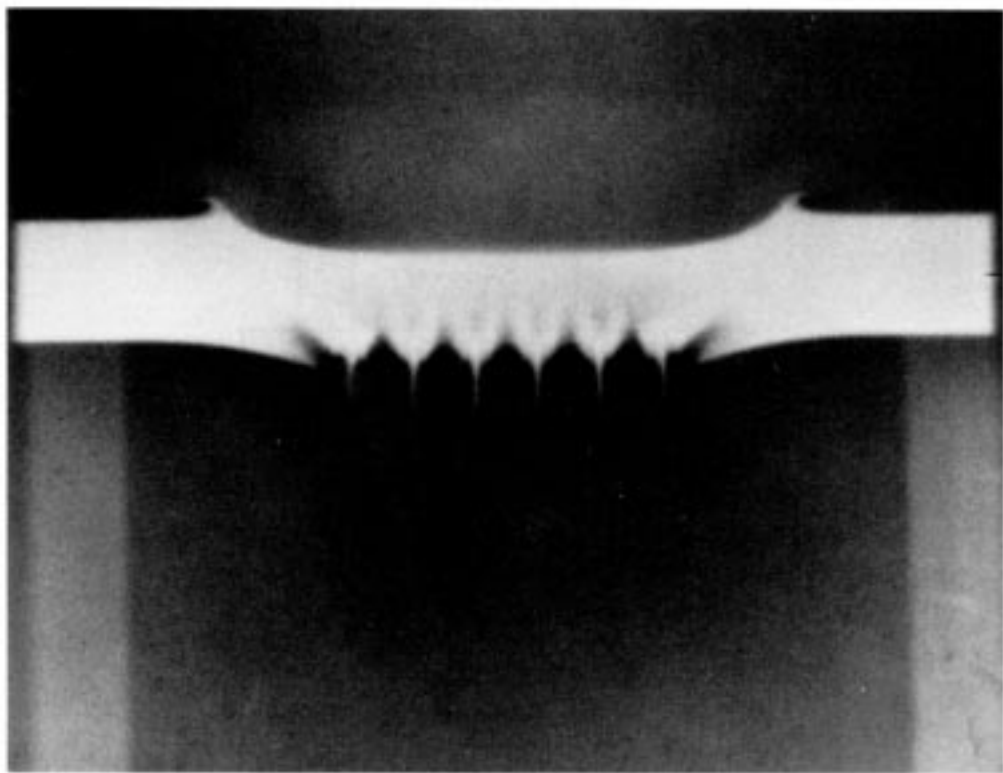




SHOT 19: **Aluminum Jets**
Date: **March 24, 1964**
Experimenter: **Douglas Venable**
Radiographic Time: **32.26 μ s**
Reference: **Venable, 1964**

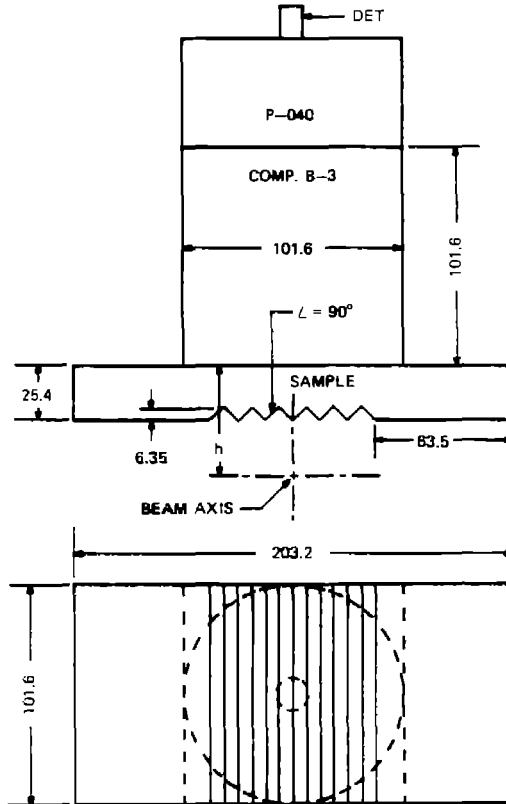
Formation of metallic jets. The explosively induced shock wave in the aluminum plate interacts with the grooves to produce the jets. The free surface of the plate has run for 2.5 μ s. h is 25.4 mm. Duplicated in Shot 147.

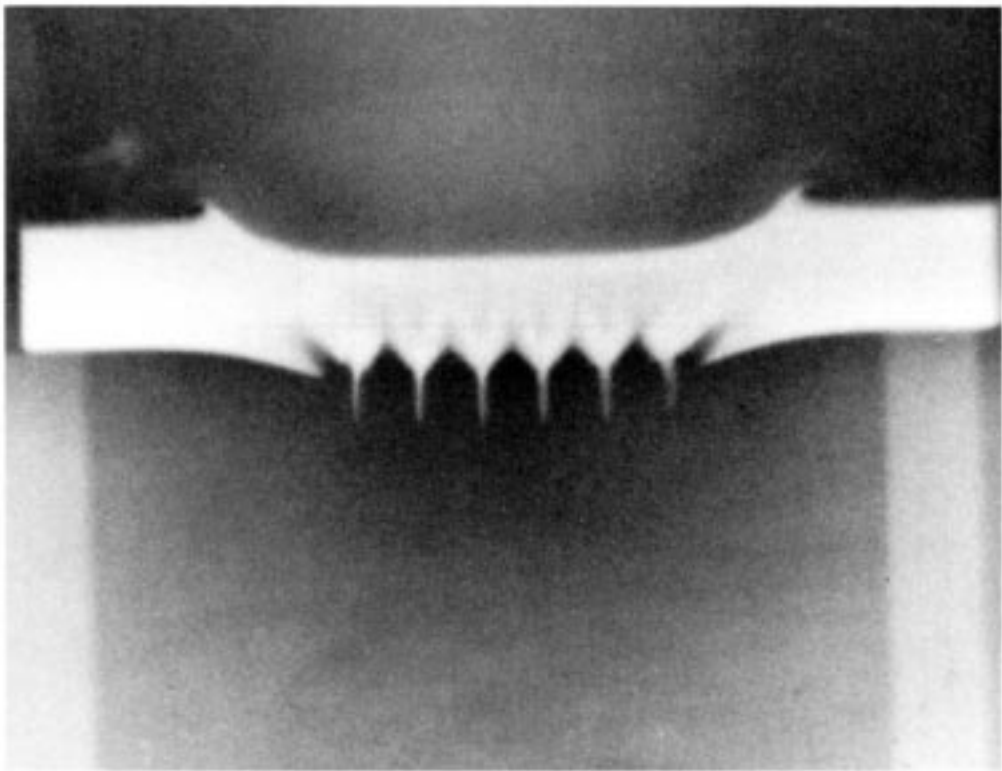




SHOT 20: **Aluminum Jets**
Date: **March 24, 1964**
Experimenter: **Douglas Venable**
Radiographic Time: **32.8 μ s**

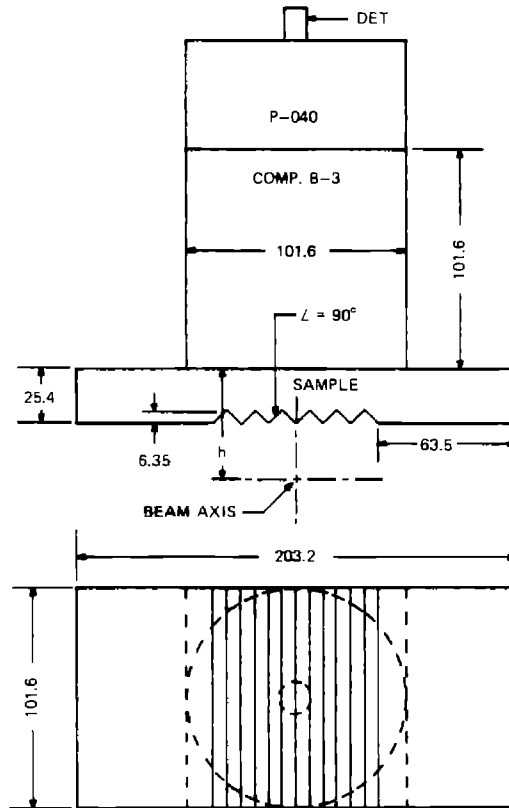
Formation of metallic jets. The explosively induced shock wave in the aluminum plate interacts with the grooves to produce the jets. The free surface of the plate has run for 3.0 μ s. h is 25.4 mm.

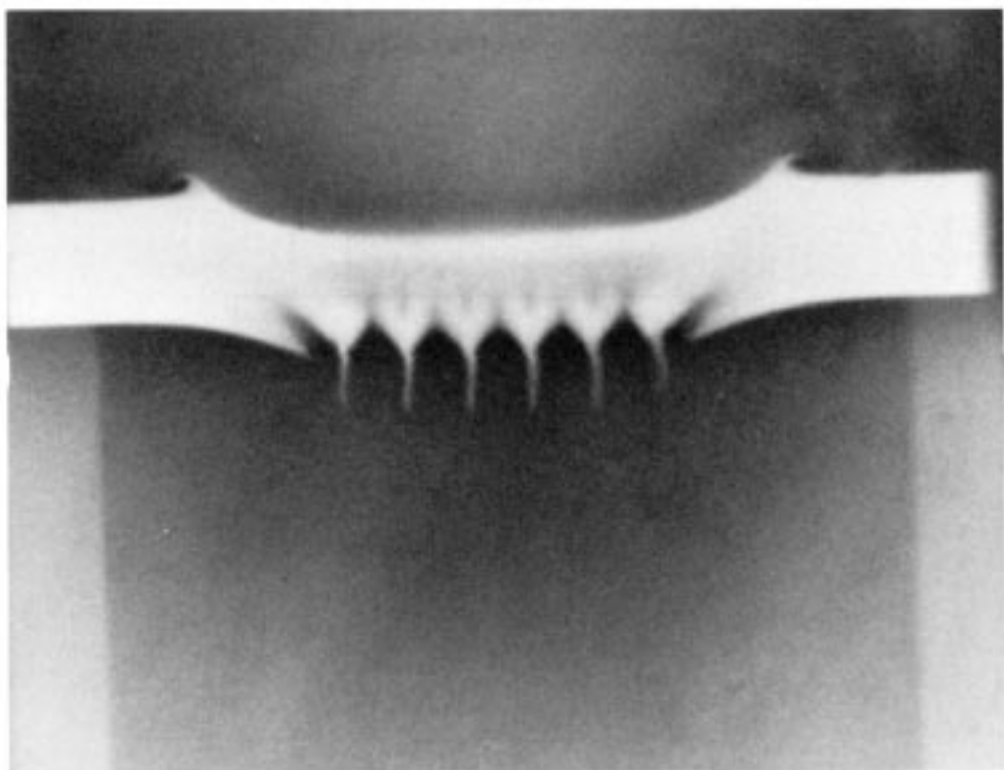




SHOT 21: **Aluminum Jets**
 Date: March 24, 1964
 Experimenter: Douglas Venable
 Radiographic Time: 33.32 μ s

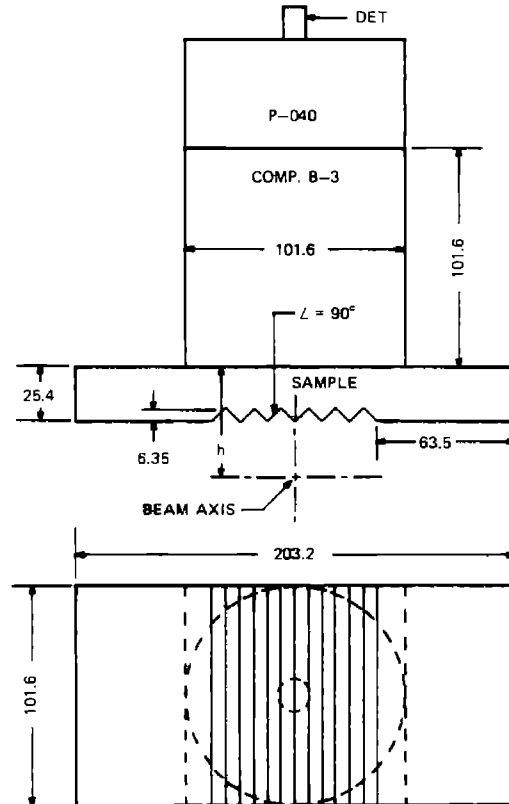
Formation of metallic jets. The explosively induced shock wave in the aluminum plate interacts with the grooves to produce the jets. The free surface of the plate has run for 3.5 μ s. h is 25.4 mm.

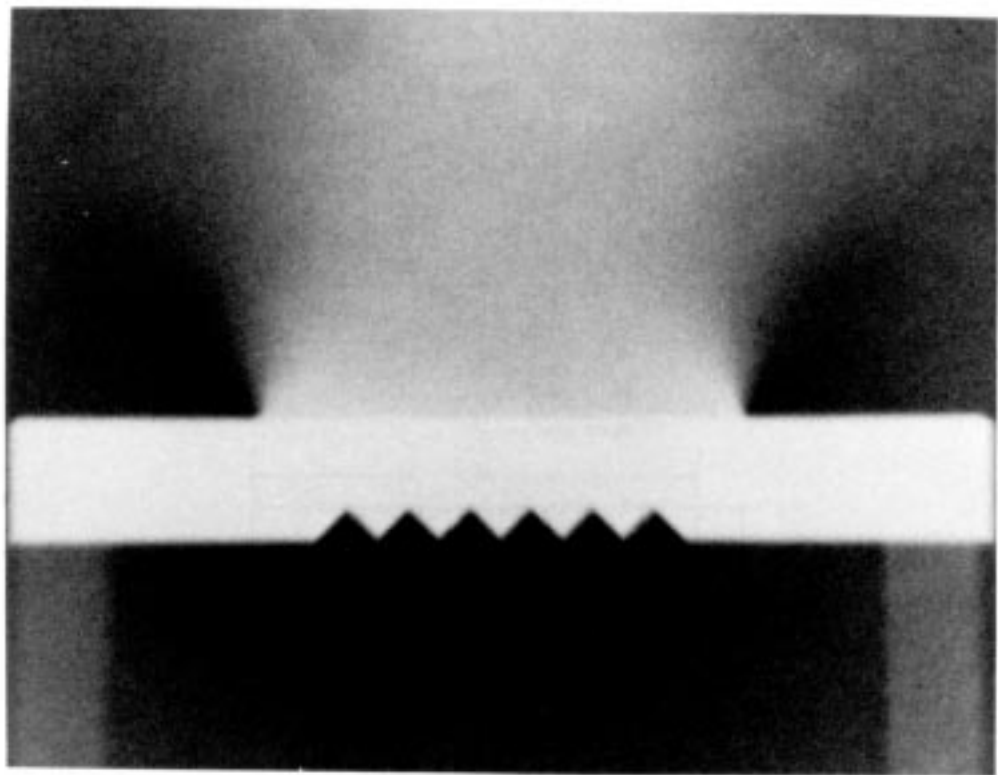




SHOT 22: **Aluminum Jets**
Date: March 31, 1964
Experimenter: Douglas Venable
Radiographic Time: 26.36 μ s

The shock wave used to form metallic jets has reached the top edge of the aluminum plate. h is 0.0 mm.





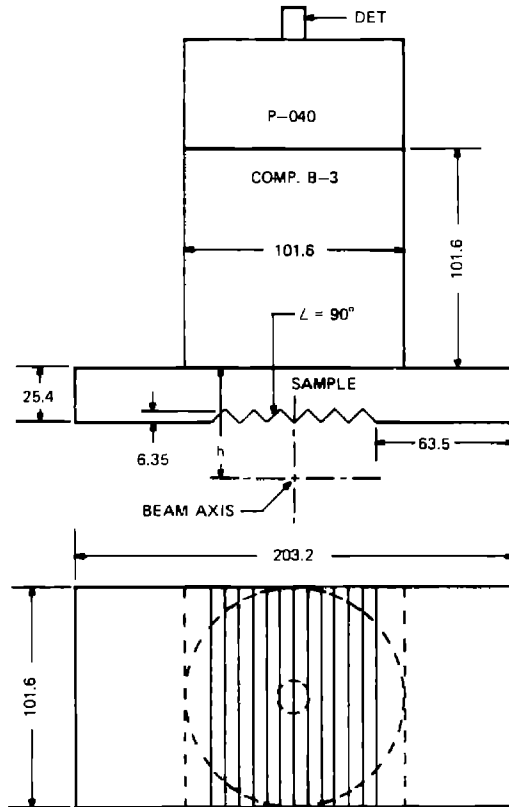
SHOT 23: Aluminum Jets

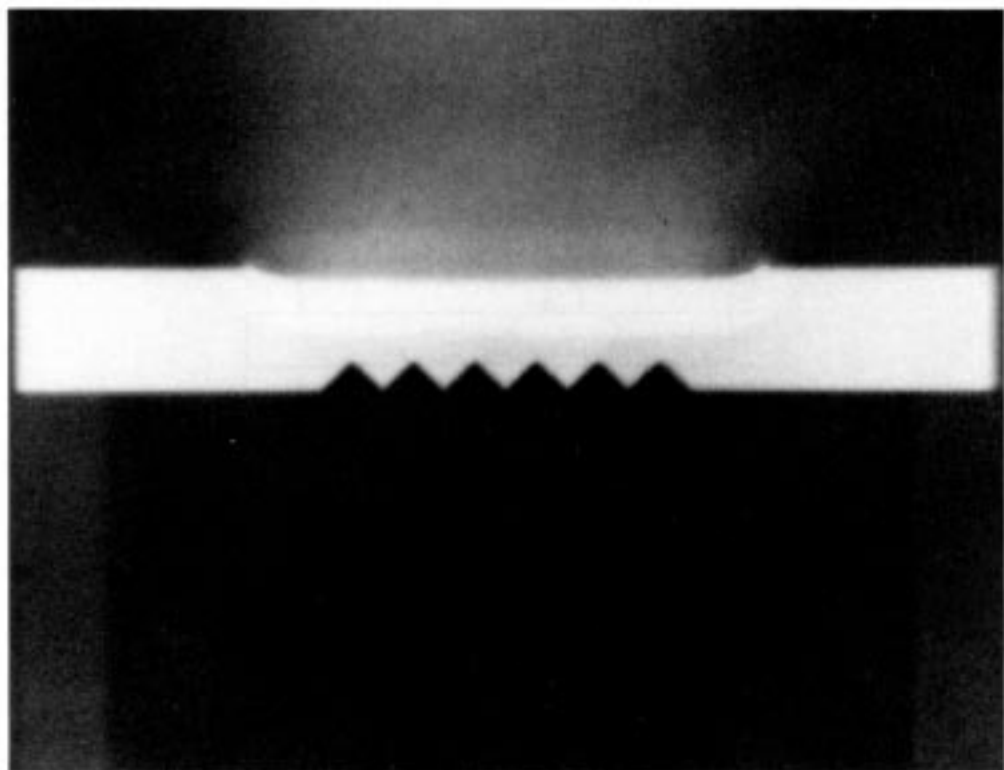
Date: March 31, 1964

Experimenter: Douglas Venable

Radiographic Time: 28.15 μ s

The shock wave used to form metallic jets has traveled 12.7 mm in 1.8 μ s into the aluminum plate. h is 12.7 mm.





SHOT 24:**Aluminum Jets**

Date:

March 31, 1964

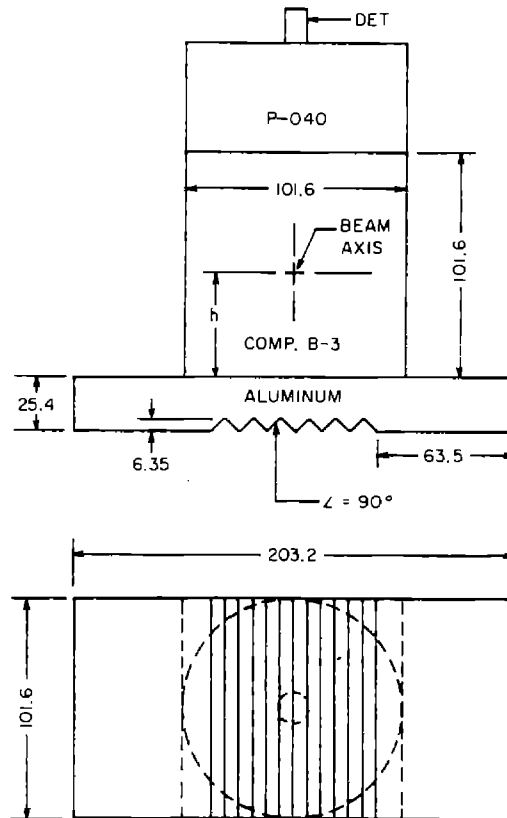
Experimenter:

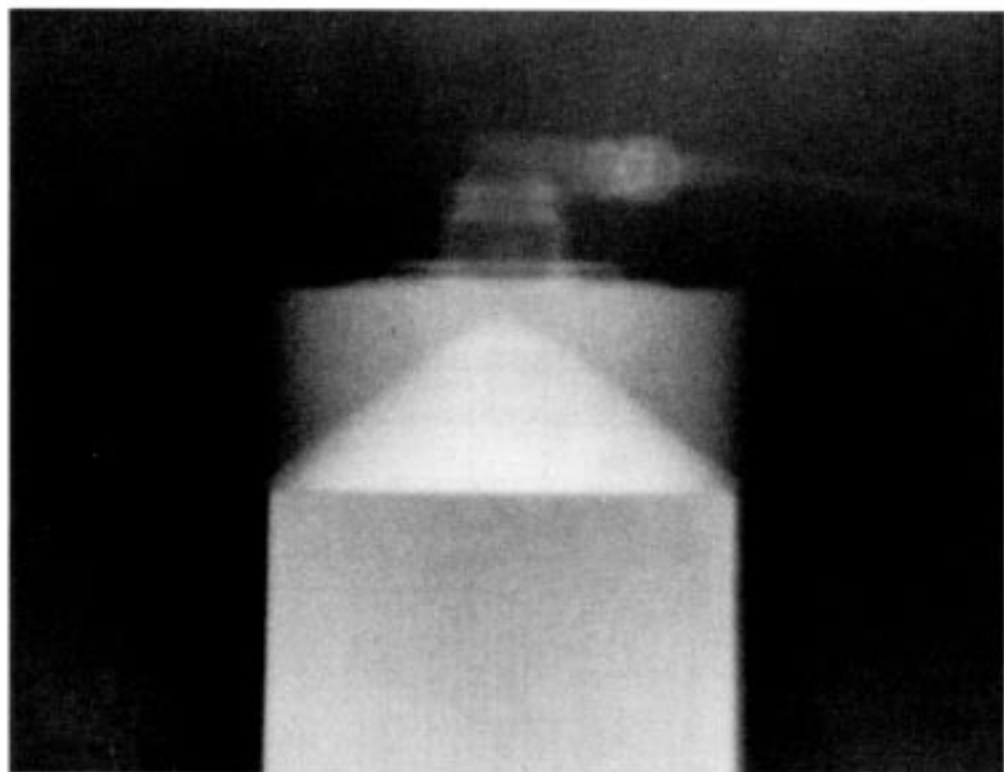
Douglas Venable

Radiographic Time:

7.3 μs

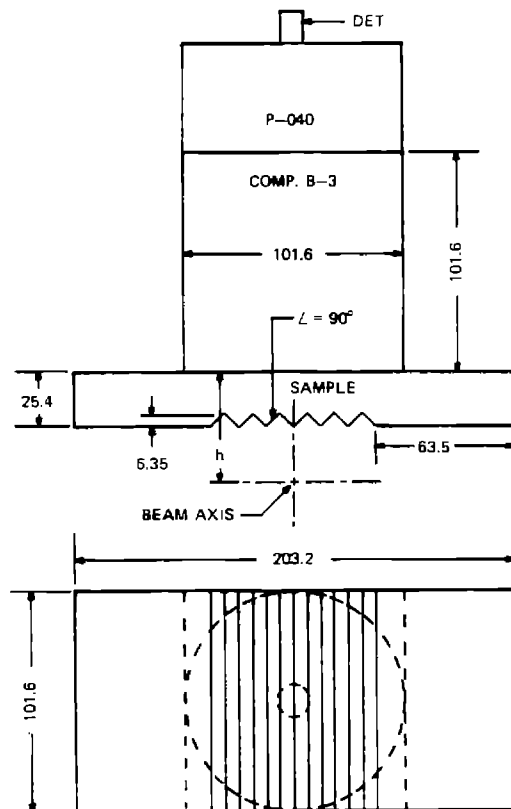
The explosive system used to form metallic jets. The detonation wave has run 10.41 mm into the P-040 lens in 2.0 μs . h is 134.0 mm.

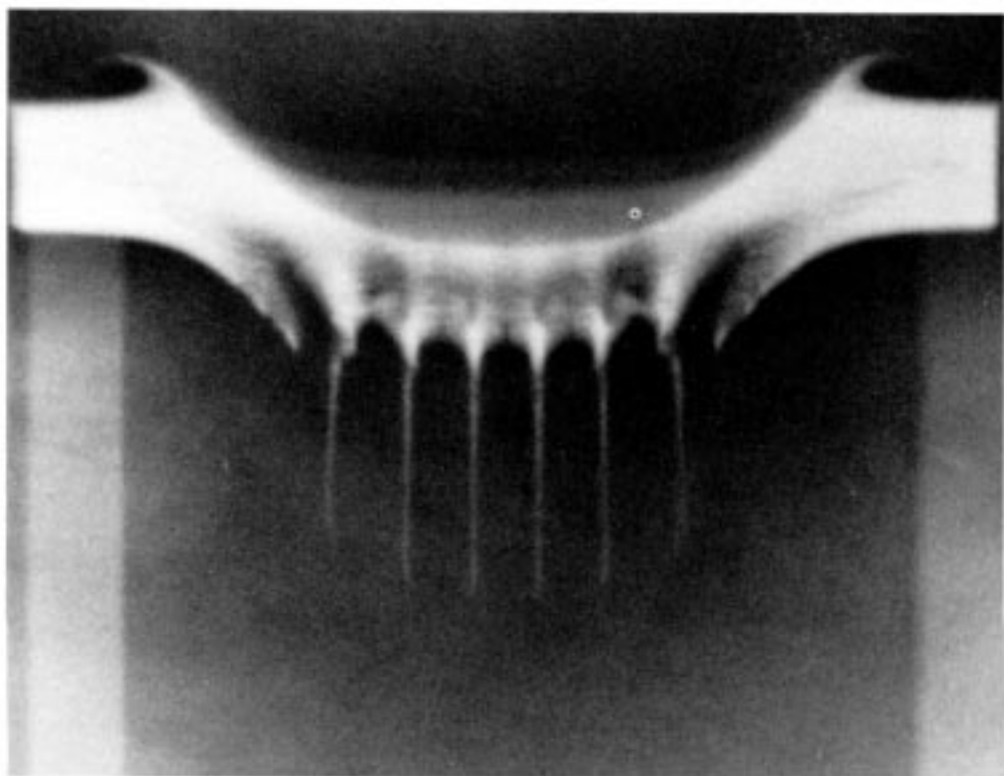




SHOT 25: Aluminum Jets
Date: April 7, 1964
Experimenter: Douglas Venable
Radiographic Time: 42.87 μ s
Reference: Venable, 1964

Formation of metallic jets. The explosively induced shock wave in the aluminum plate interacts with the grooves to produce the jets. The free surface of the plate has run for 13.0 μ s. *h* is 57.15 mm.





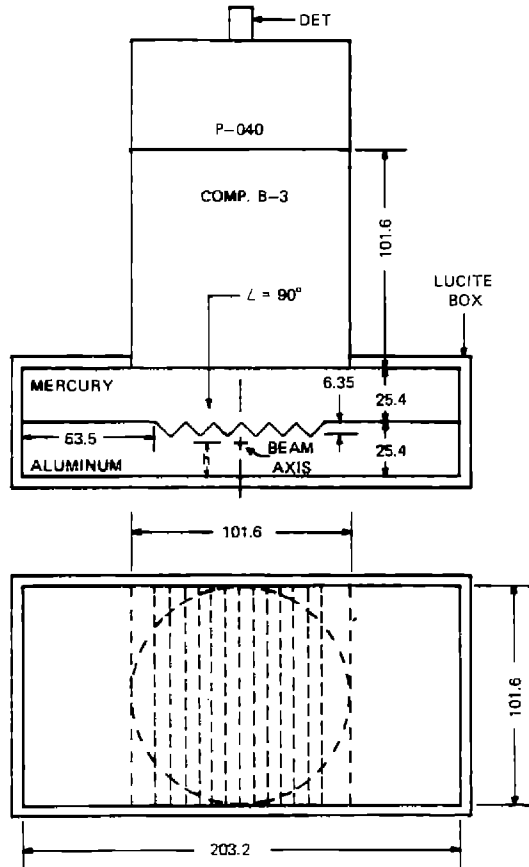
SHOT 26: Shocked Mercury Interacting with Aluminum Grooves

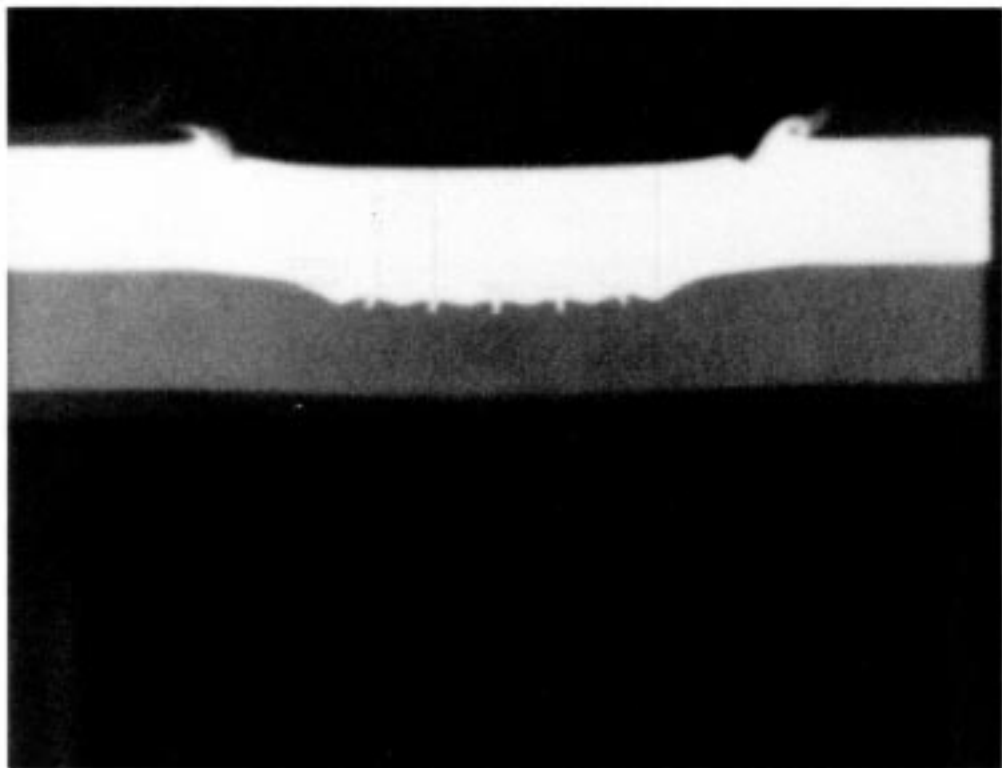
Date: April 7, 1964

Experimenter: Douglas Venable

Radiographic Time: 40.62 μ s

Shocked mercury interacting with a 90°-grooved aluminum plate. Compare with Shot 27. h is 19.05 mm. See Shots 184-186 for other times.





SHOT 27:

Shocked Aluminum Grooves Interacting with Mercury

Date:

April 7, 1964

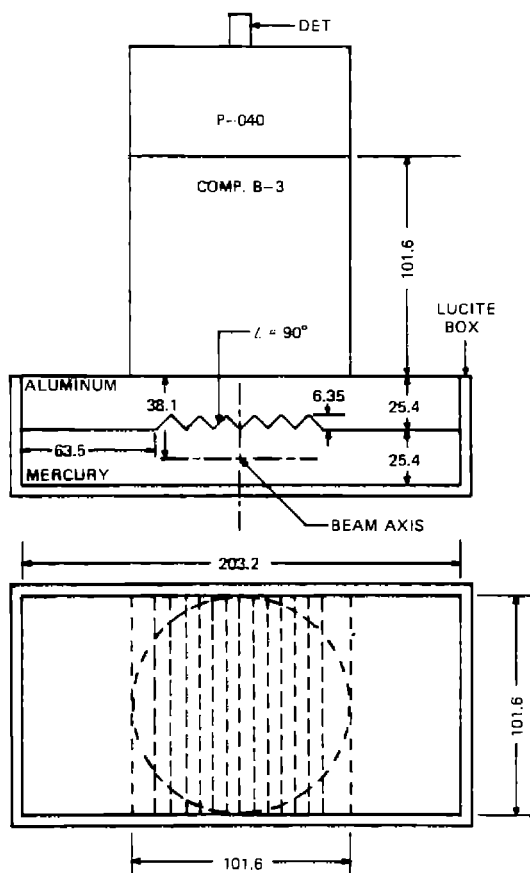
Experimenter:

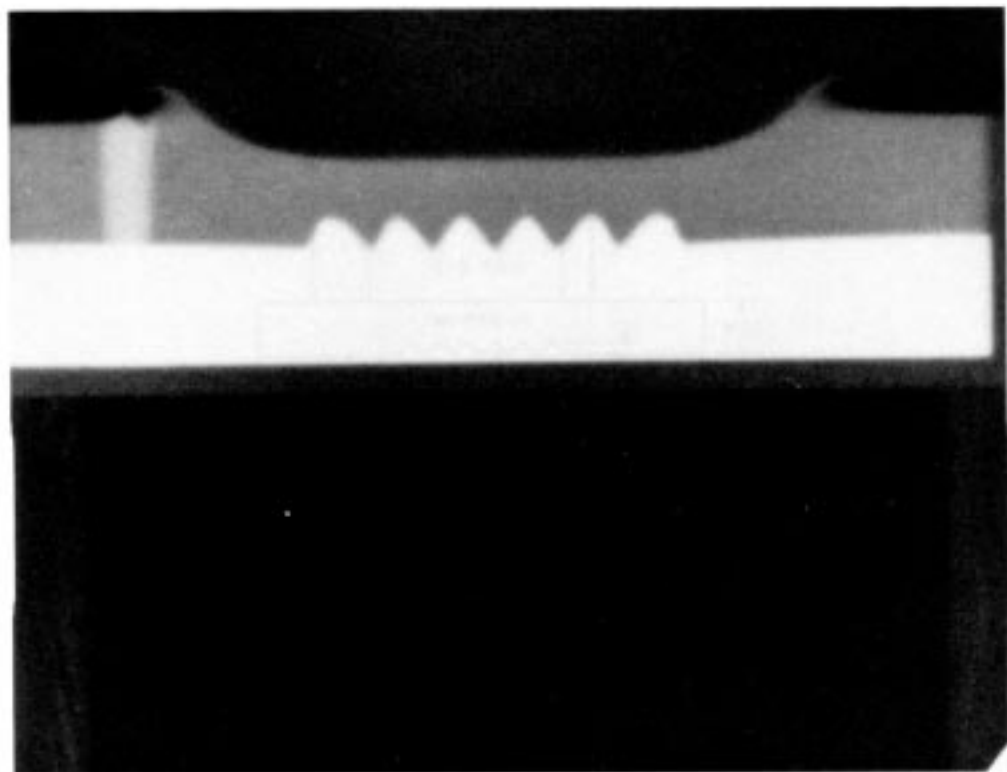
Douglas Venable

Radiographic Time:

37.1 μ s

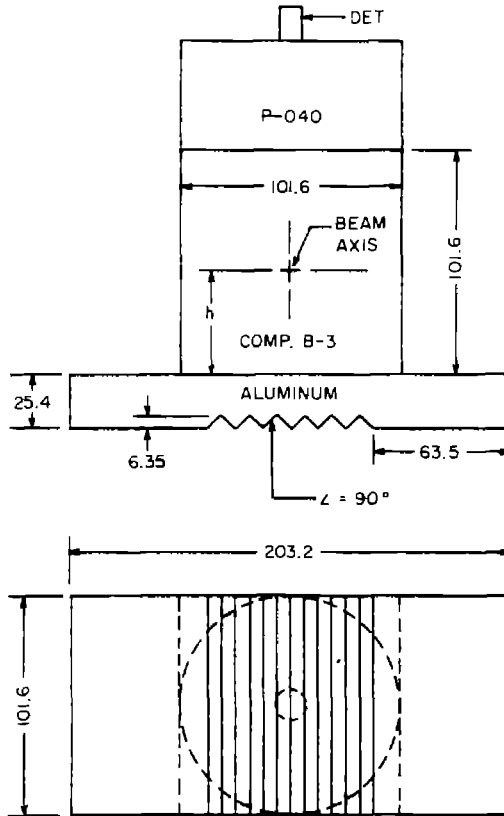
A shocked 90°-grooved aluminum plate interacting with mercury. Compare with Shot 26.

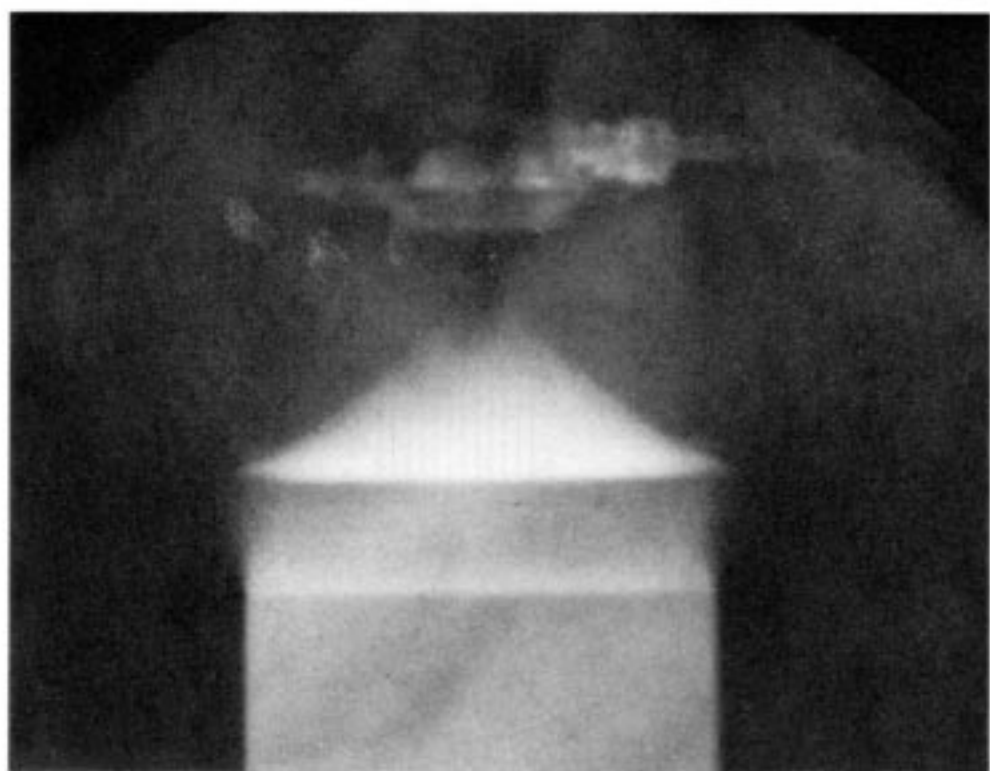
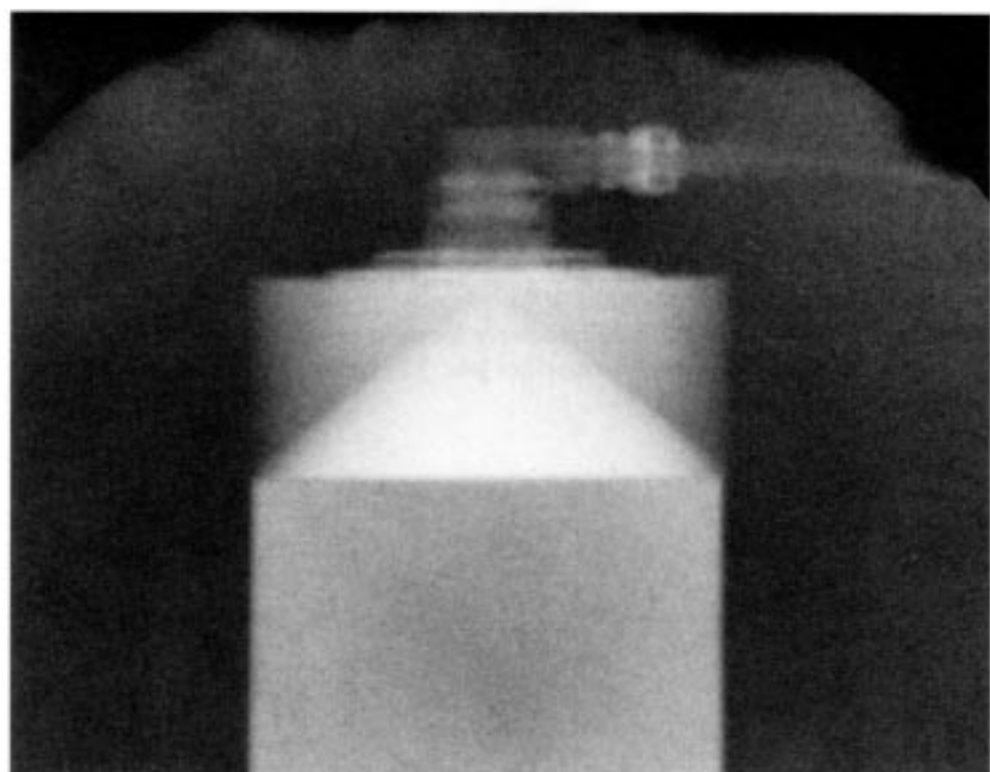


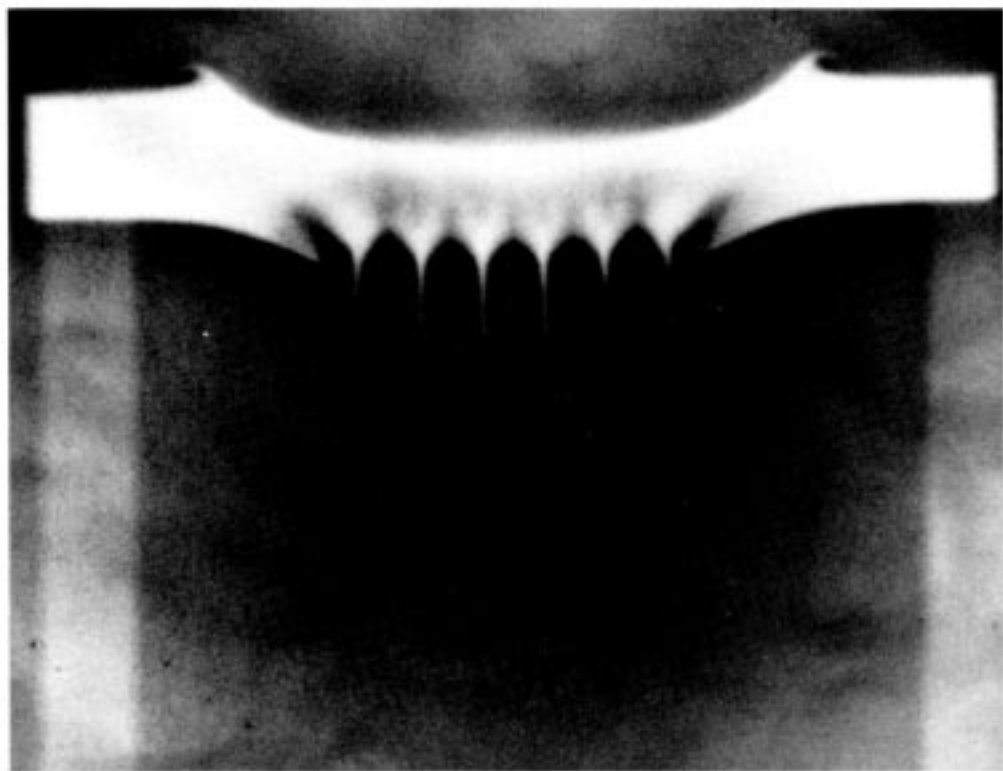


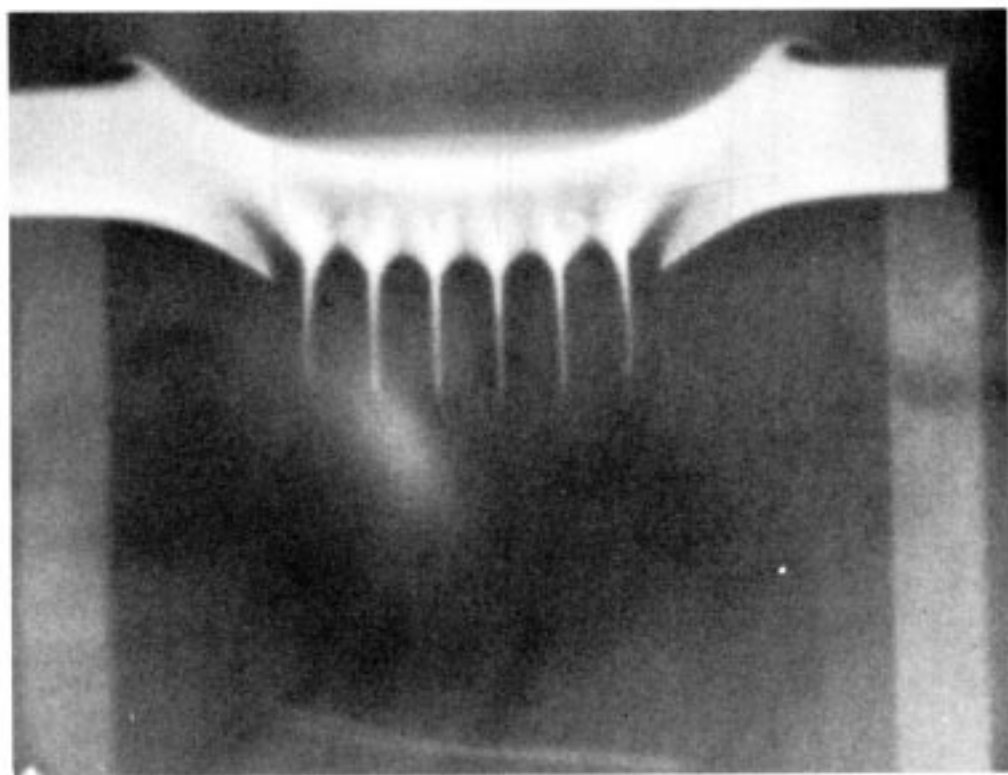
SHOT 28: **Aluminum Jets**
Date: April 14, 1964
Experimenter: Douglas Venable
Radiographic Time: 16.7 μ s

The explosive system used to form metallic jets. The Composition B-3 detonation wave has run 25.4 mm in 3.2 μ s. h is 76.2 mm.









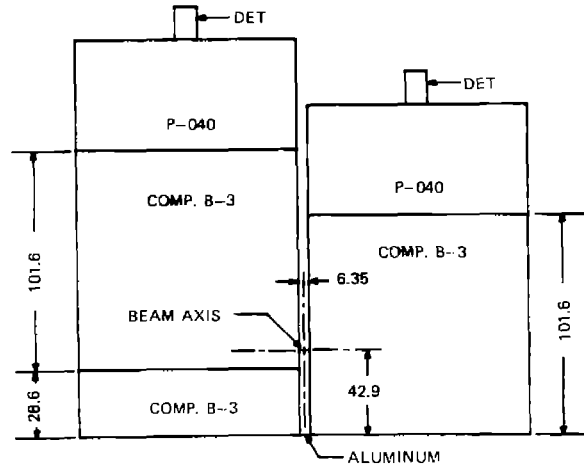
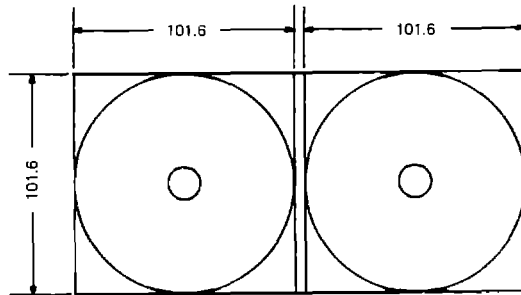
SHOT 31: Two Offset Composition B-3 Detonations

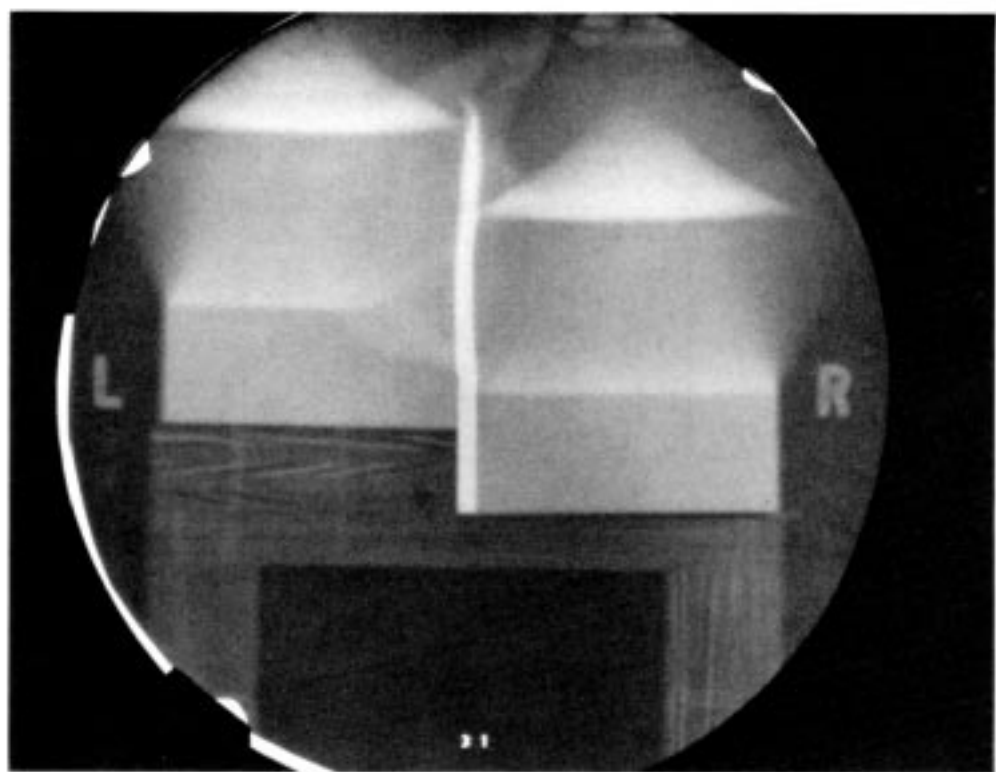
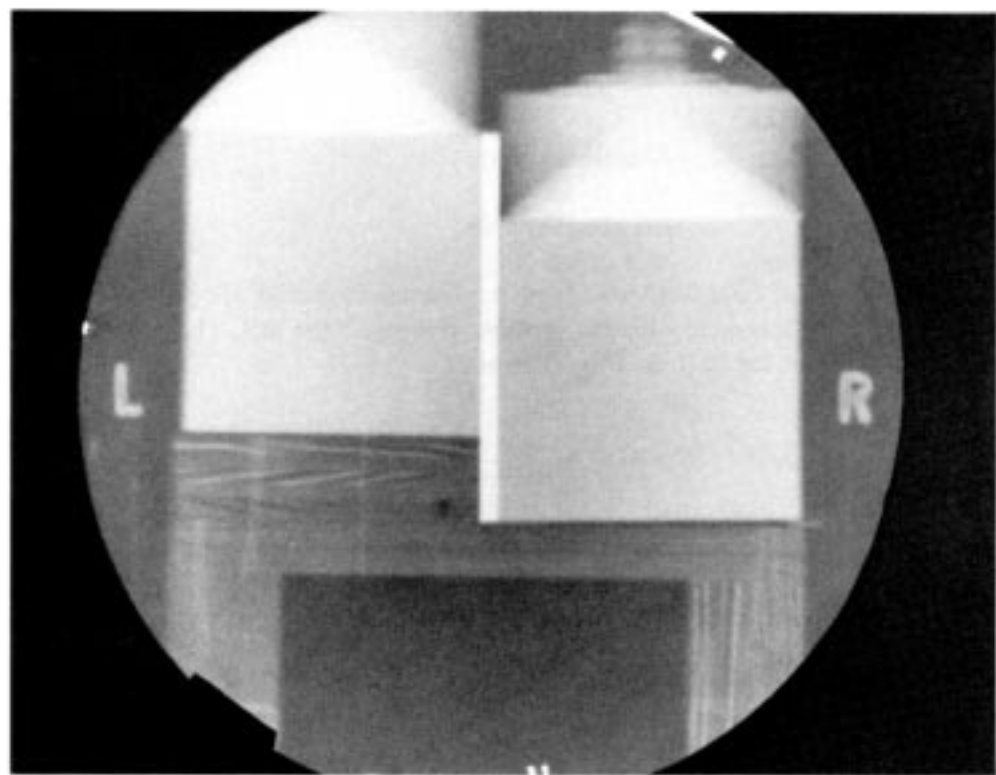
Date: April 16, 1964

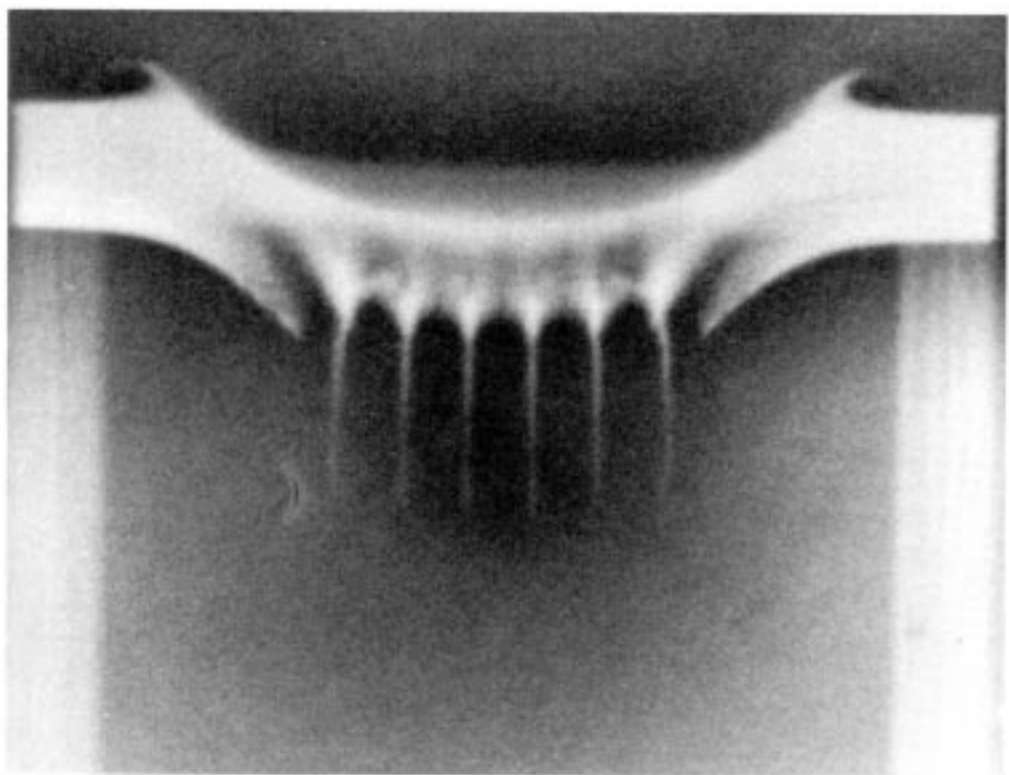
Experimenter: Douglas Venable

Radiographic Time: 21.25 μ s

Simultaneous detonation of two blocks of Composition B-3 offset by 28.6 mm. A 6.35-mm-thick aluminum plate was placed between the explosive blocks perpendicular to the direction of detonation wave travel. The detonations have run 60.19 mm in the Composition B-3.







SHOT 33:

Two Composition B-3 Detonations Colliding with Aluminum

Date:

May 5, 1964

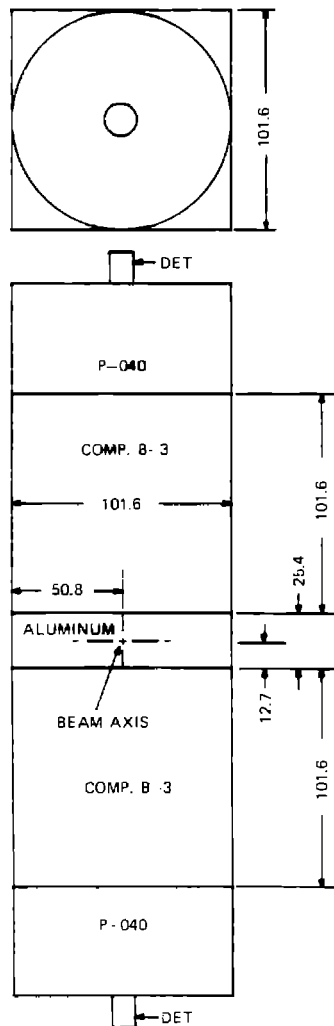
Experimenter:

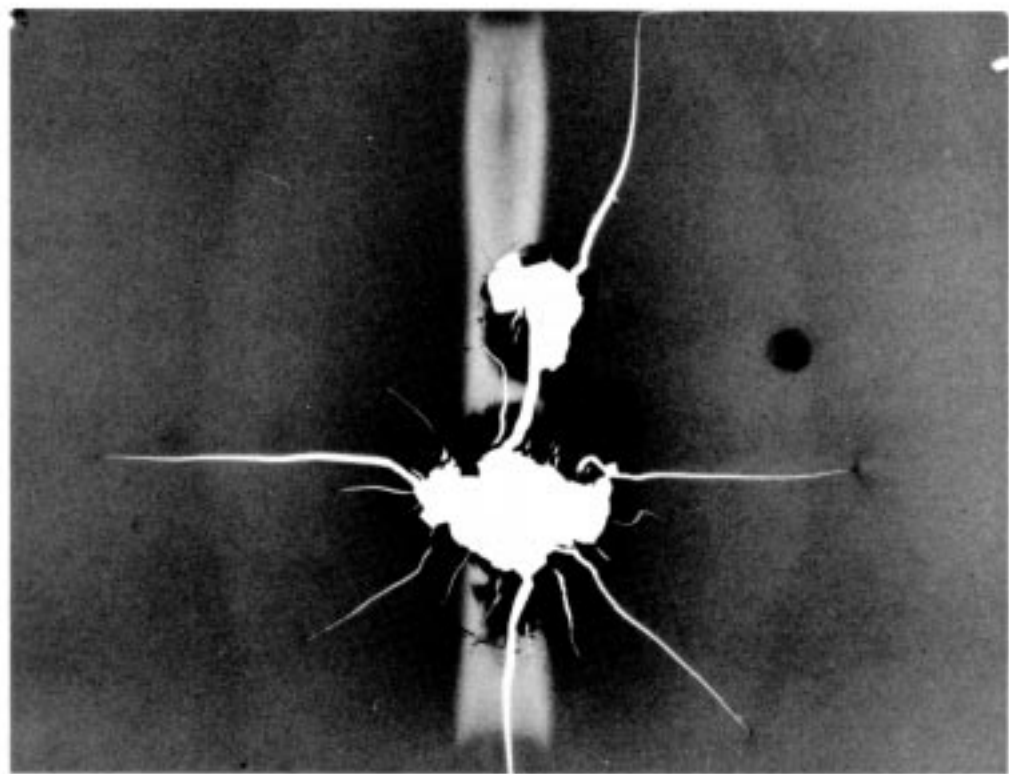
Douglas Venable

Radiographic Time:

40.6 μ s

Two blocks of Composition B-3 were detonated simultaneously and the detonation waves collided with a 25.4-mm-thick aluminum plate. The compressed aluminum plate and the shock waves reflected back into the detonation products are shown. The holes in the film were caused by shot shrapnel. See Shot 34 for an earlier time.





SHOT 34:

Two Composition B-3 Detonations Colliding with Aluminum

Date:

May 5, 1964

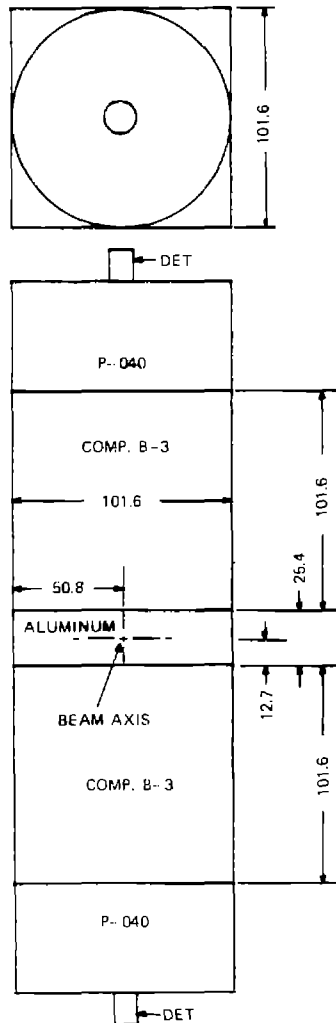
Experimenter:

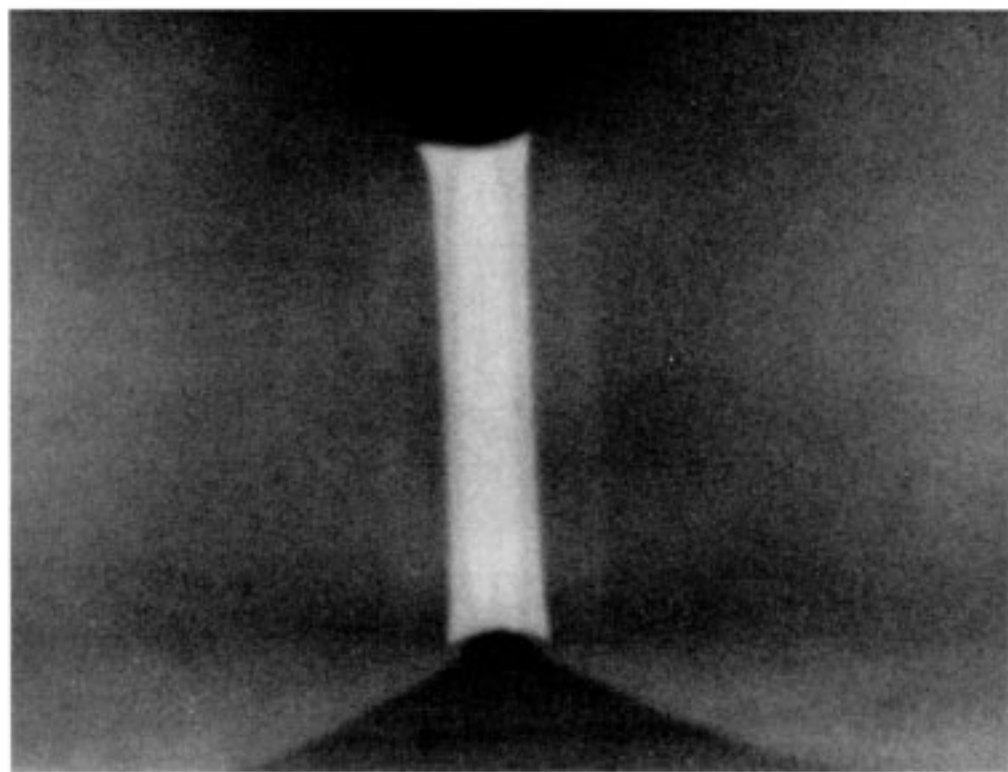
Douglas Venable

Radiographic Time:

28.69 μ s

Two blocks of Composition B-3 were detonated simultaneously and the detonation waves collided with a 25.4-mm-thick aluminum plate. The compressed aluminum plate and the shock waves reflected back into the detonation products are shown. See Shot 33 for a later time.





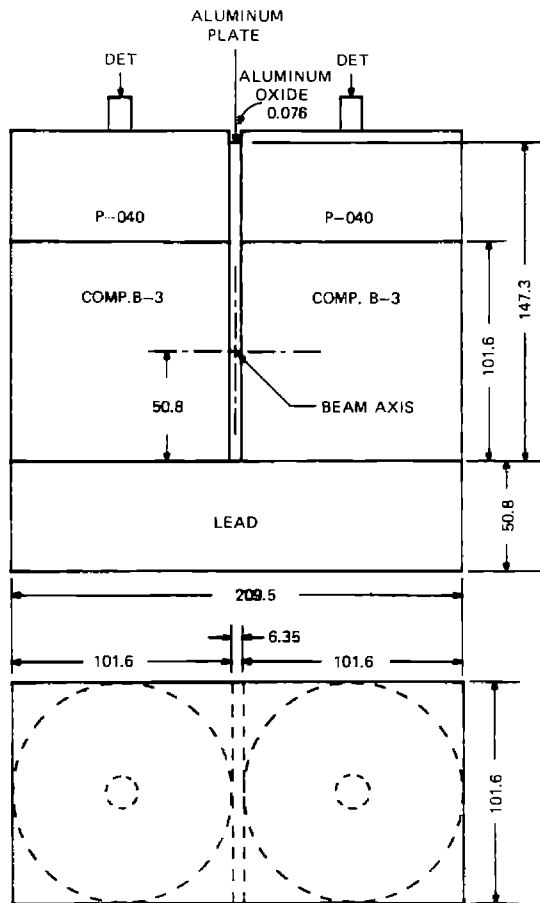
SHOT 35: Two Composition B-3 Detonations

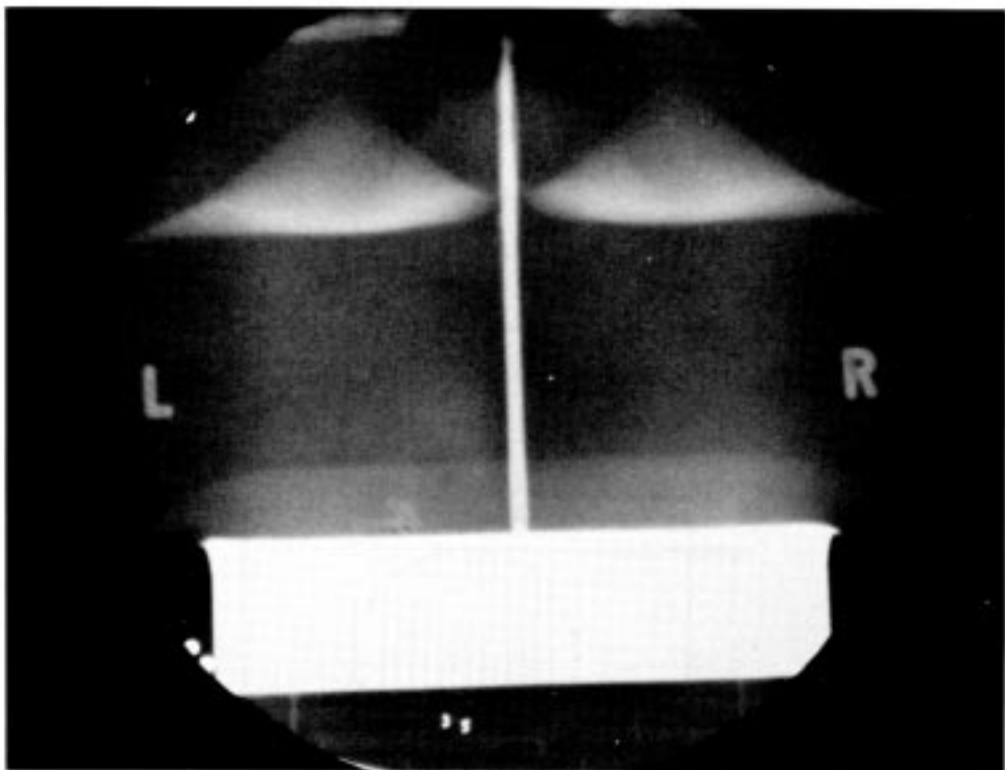
Date: May 6, 1964

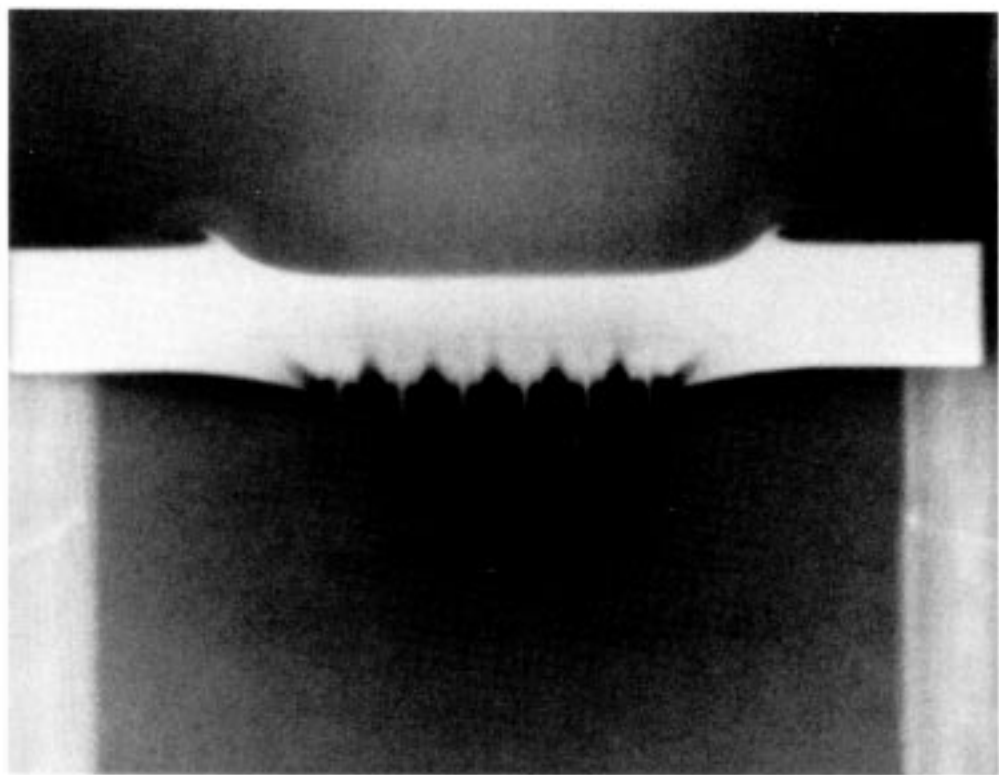
Experimenter: Douglas Venable

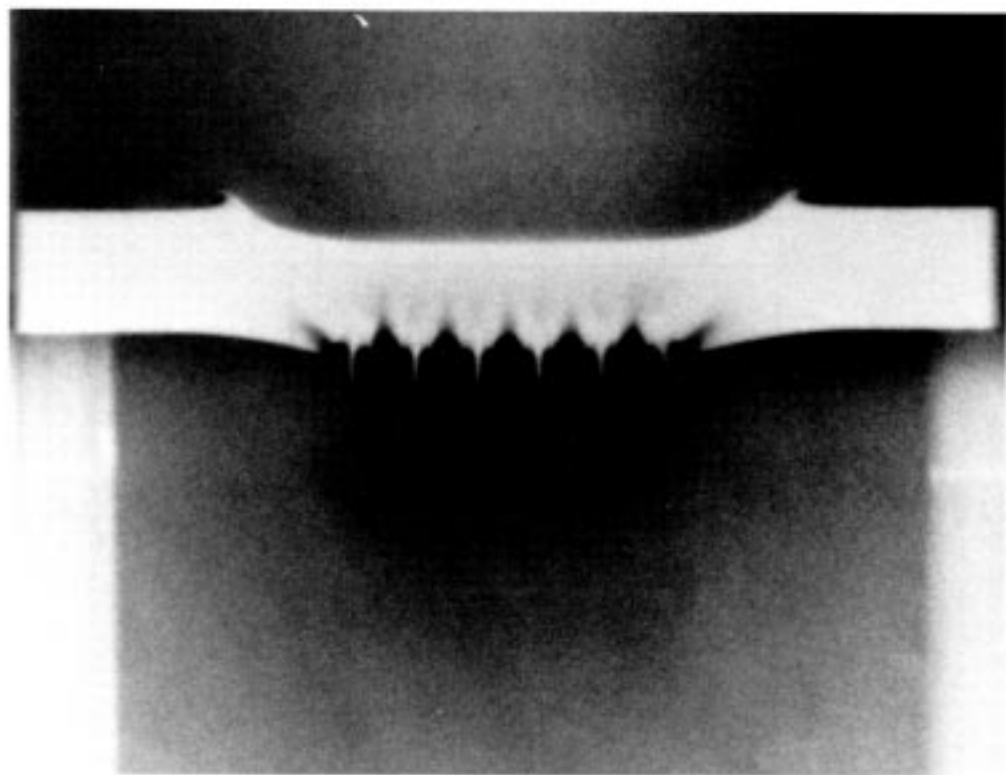
Radiographic Time: 31.3 μ s

Two blocks of Composition B-3 were detonated simultaneously. A 6.35-mm-thick aluminum plate, one side of which was coated with aluminum oxide, was placed between the explosive blocks perpendicular to the direction of detonation wave travel.





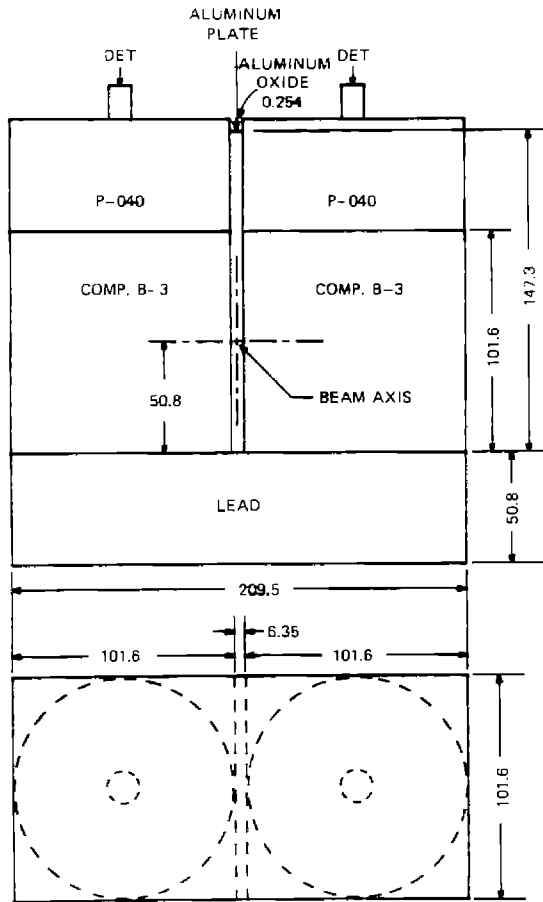


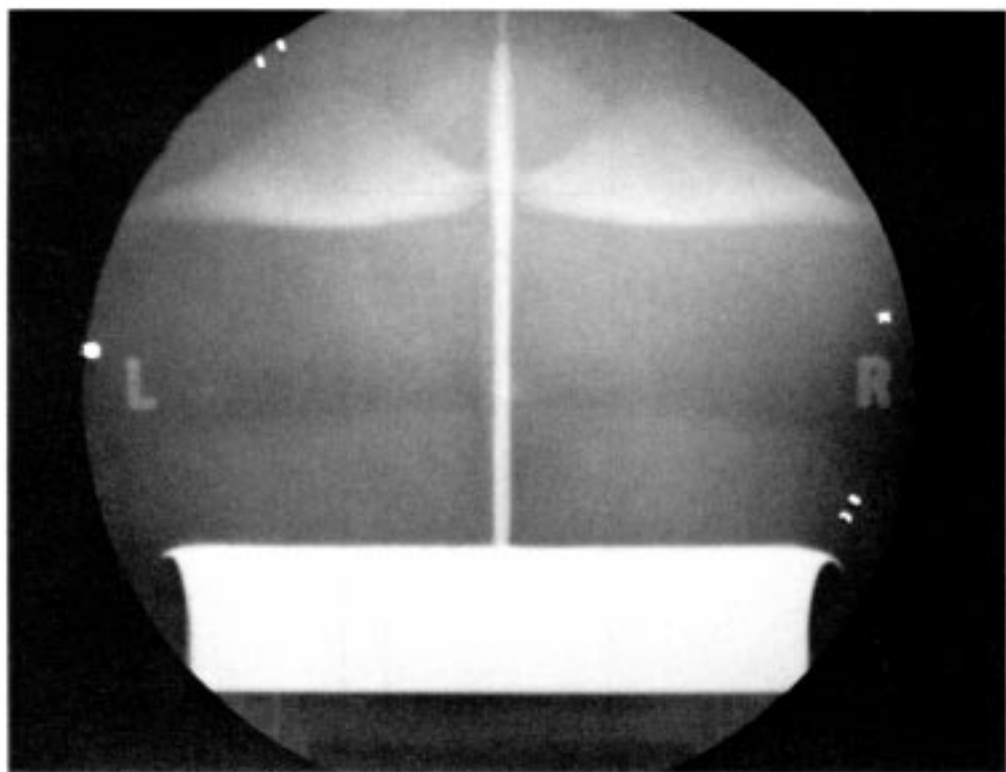


SHOT 38: Two Composition B-3 Detonations

Date: May 12, 1964
Experimenter: Douglas Venable
Radiographic Time: 36.3 μ s

Two blocks of Composition B-3 were detonated simultaneously. A 6.35-mm-thick aluminum plate with an aluminum oxide coating on one side was placed between the explosive blocks perpendicular to the direction of detonation wave travel. The detonation waves collided with a lead plate, and a reflected shock was sent back into the detonation products. The reflected shock wave has traveled for 10 μ s.





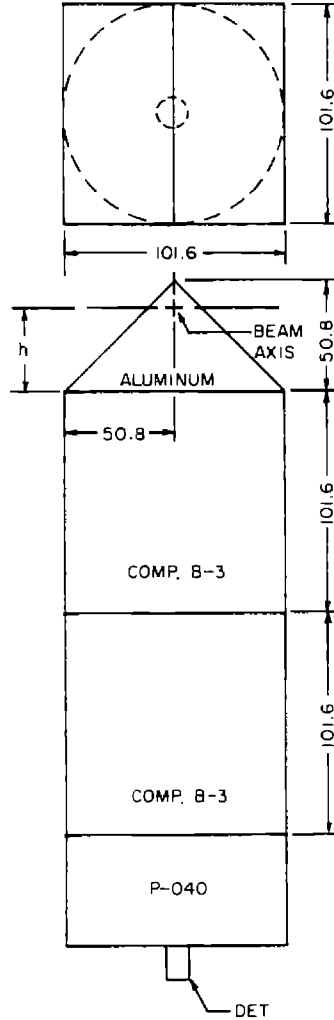
SHOT 39: Aluminum Wedge

Date: May 12, 1964

Experimenter: Douglas Venable

Radiographic Time: 44.5 μ s

A shock wave generated by a Composition B-3 detonation wave interacting with a 90° aluminum wedge, h is 38.1 mm. The shock wave has traveled 38.1 mm into the wedge in 5.37 μ s. See Shots 135-138 and 214-217 for other times.

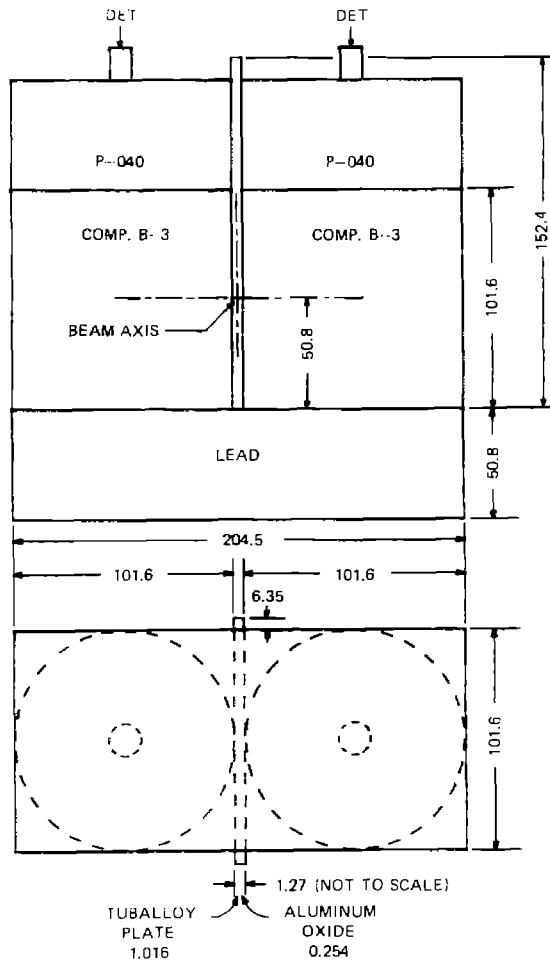


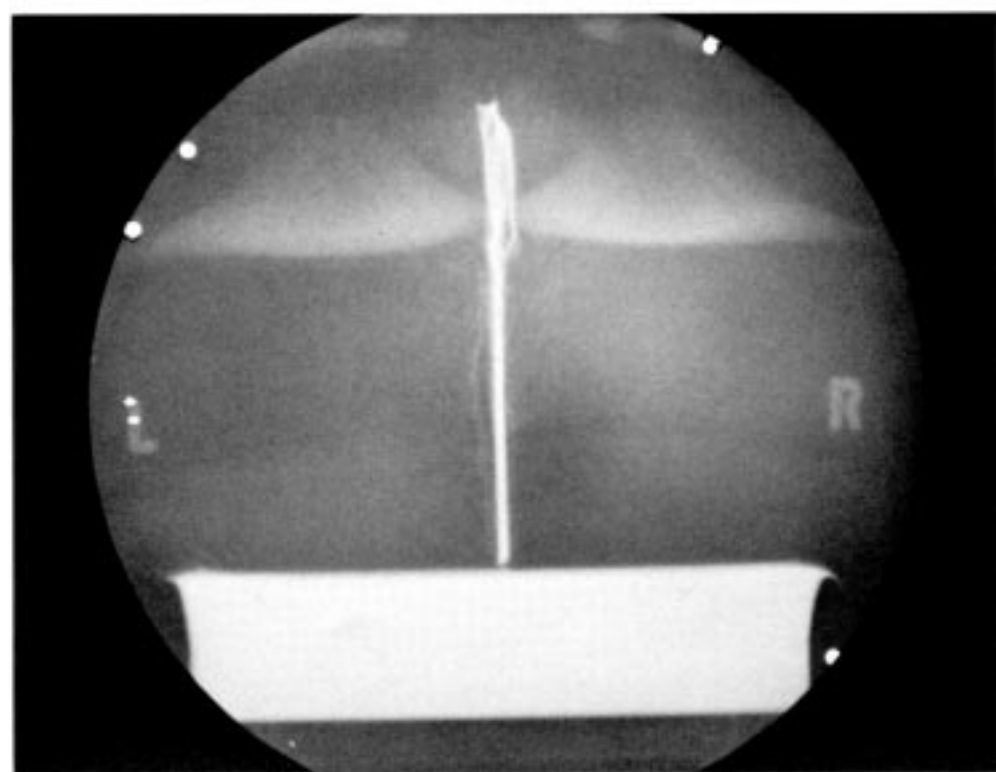
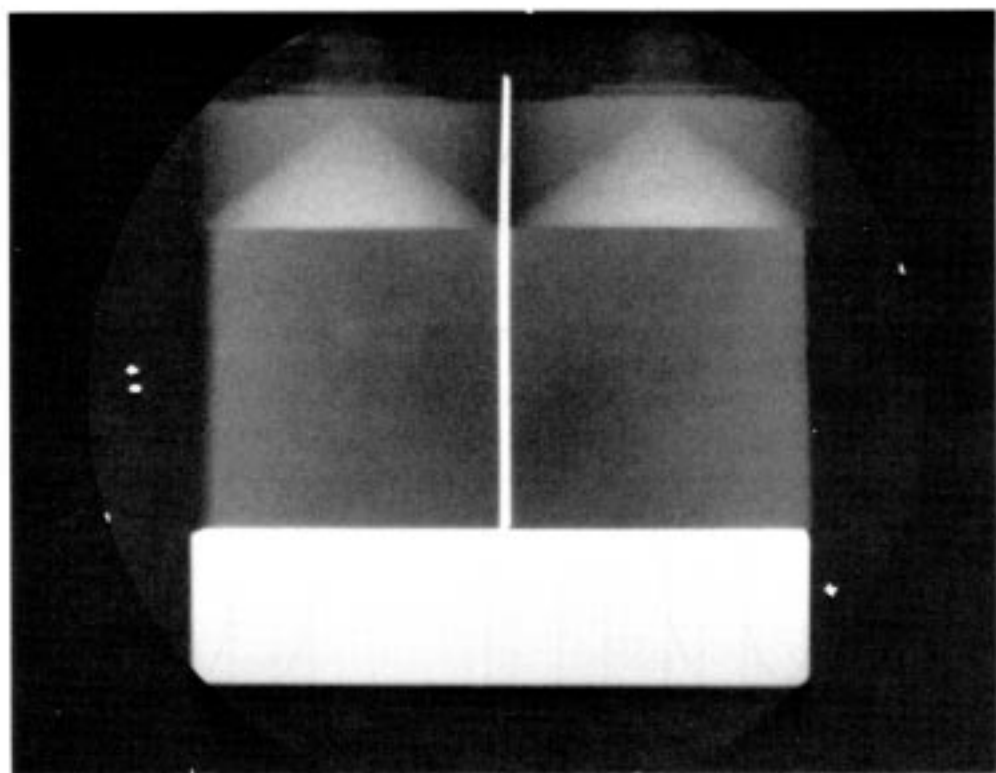


SHOT 40: Two Composition B-3 Detonations

Date: May 12, 1964
Experimenter: Douglas Venable
Radiographic Time: 36.3 μ s

Two blocks of Composition B-3 were detonated simultaneously. A 6.35-mm-thick uranium plate with an aluminum oxide coating on one side was placed between the explosive blocks perpendicular to the direction of detonation wave travel. The detonation waves collided with a lead plate, and a reflected shock of 10- μ s duration was sent back into the detonation products. See Shot 64 for a different beam orientation.





SHOT 41: Interacting Aluminum Jets

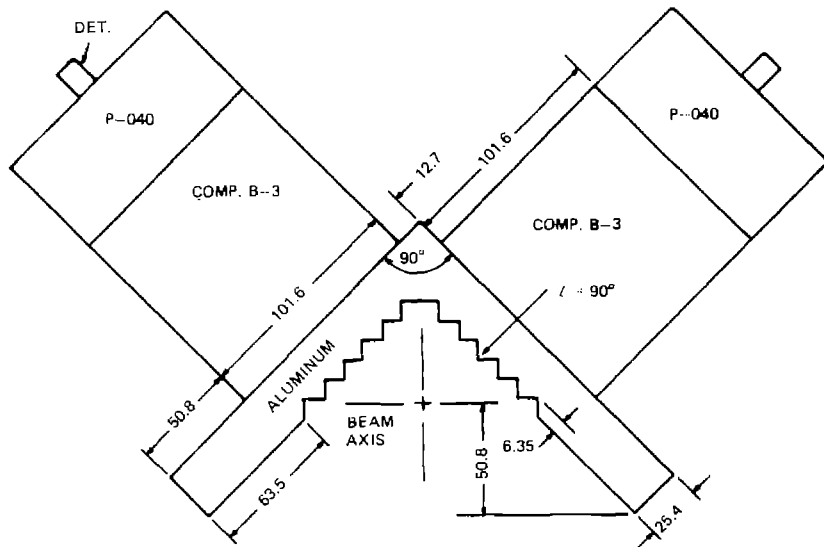
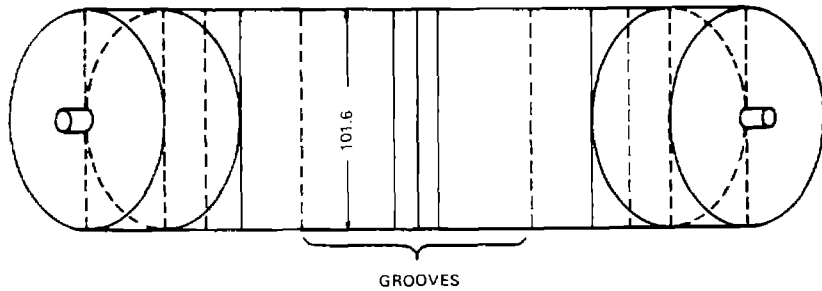
Date: June 16, 1964

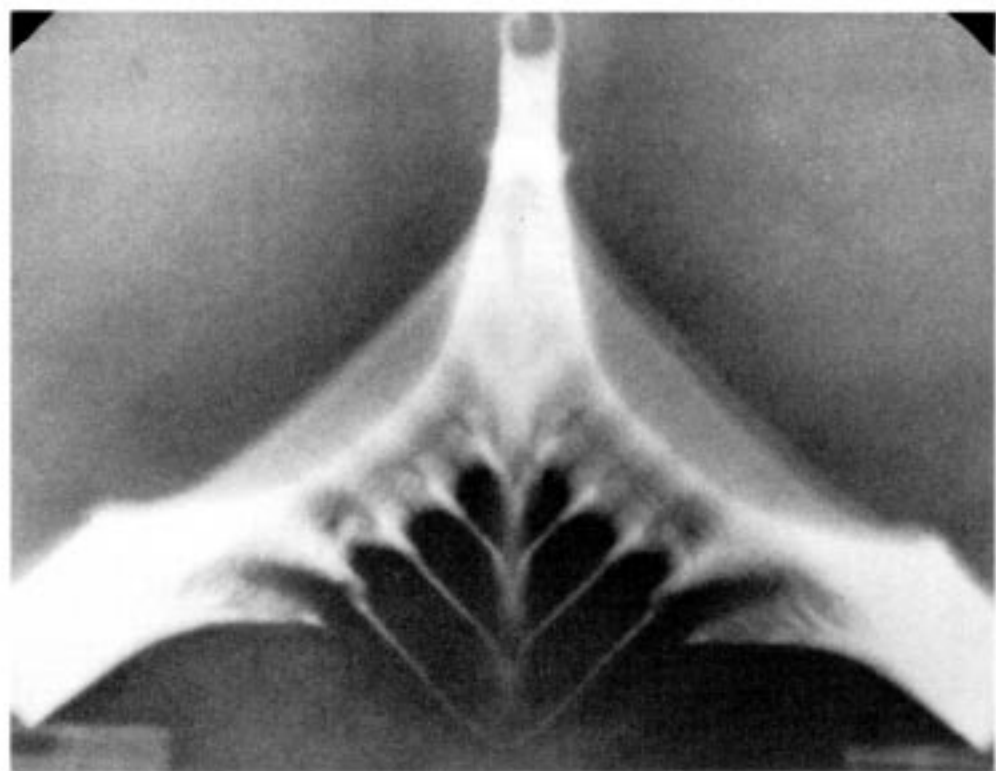
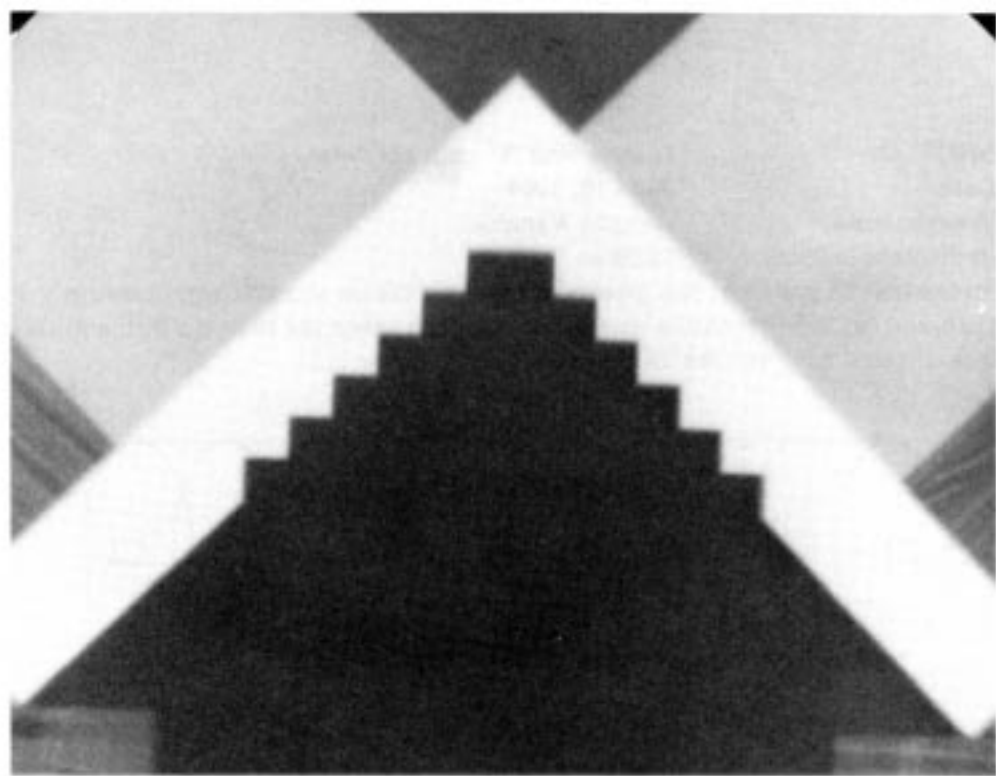
Experimenter: Douglas Venable

Radiographic Time: 42.93 μ s

Reference: Venable, 1964

Interaction of jets from two grooved aluminum plates shocked simultaneously by Composition B-3 detonation waves. The plates were perpendicular to each other. The free surfaces of the plates have run for 13.0 μ s. See Shot 59.





SHOT 42:

Interacting Aluminum Jets

Date:

June 16, 1964

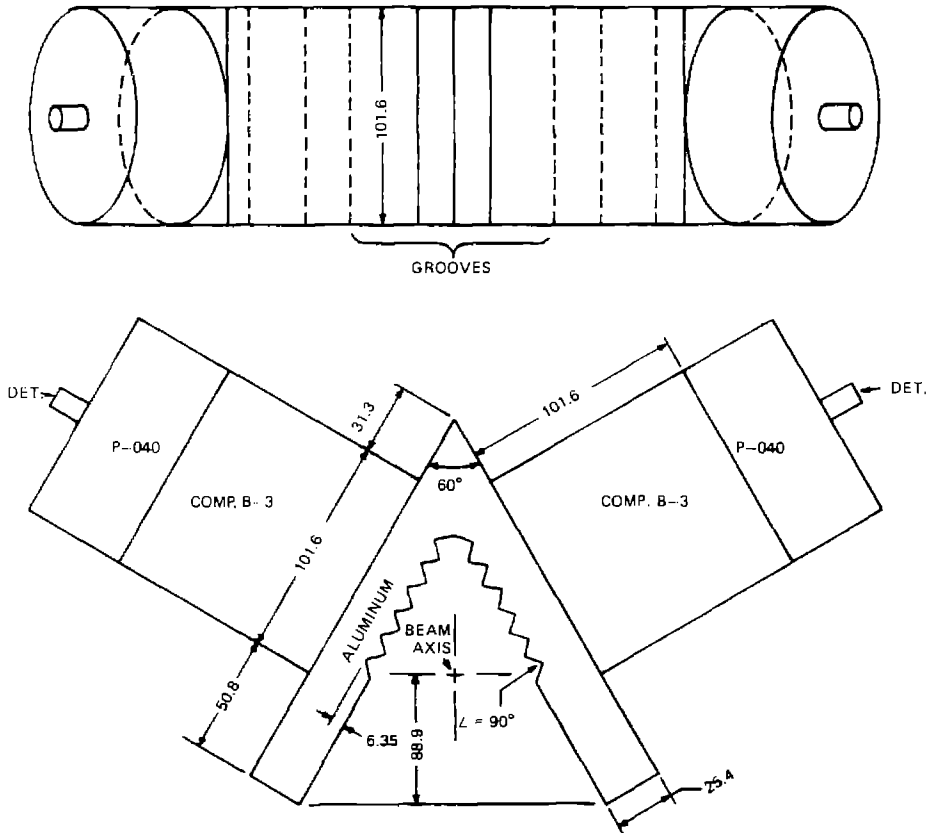
Experimenter:

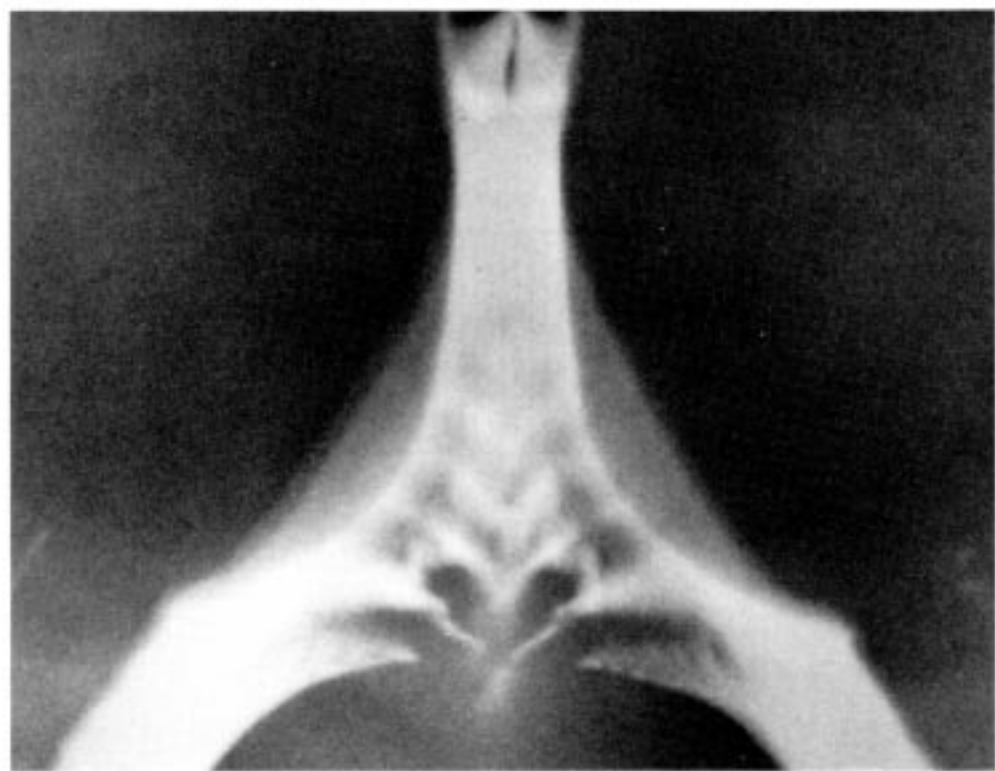
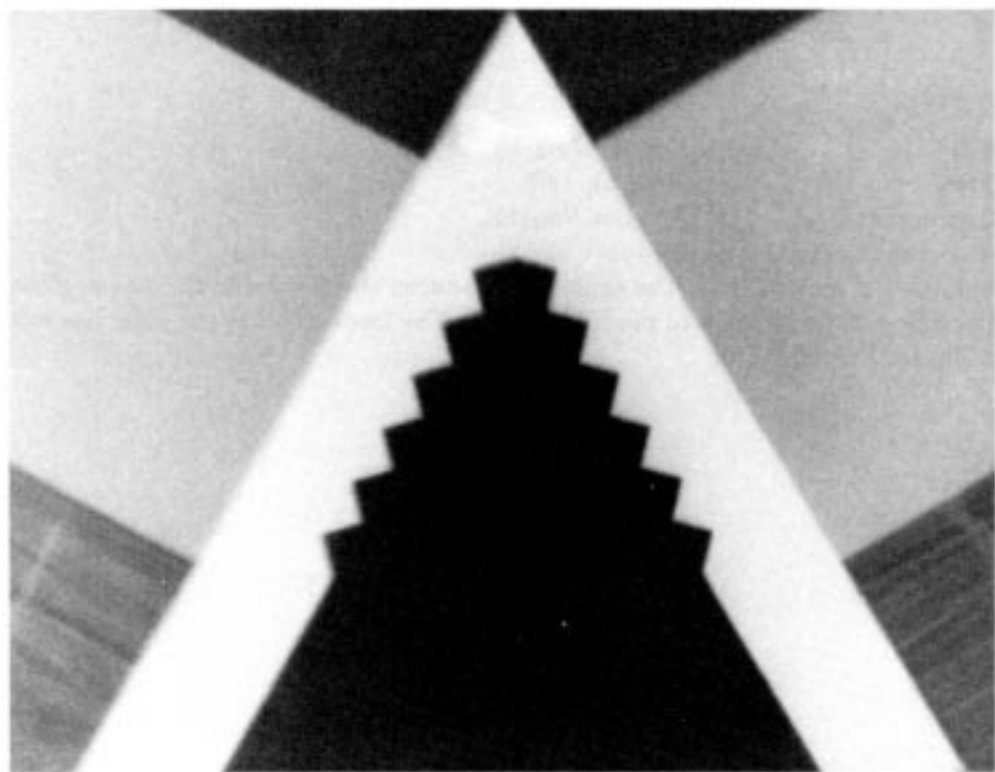
Douglas Venable

Radiographic Time:

42.99 μ s

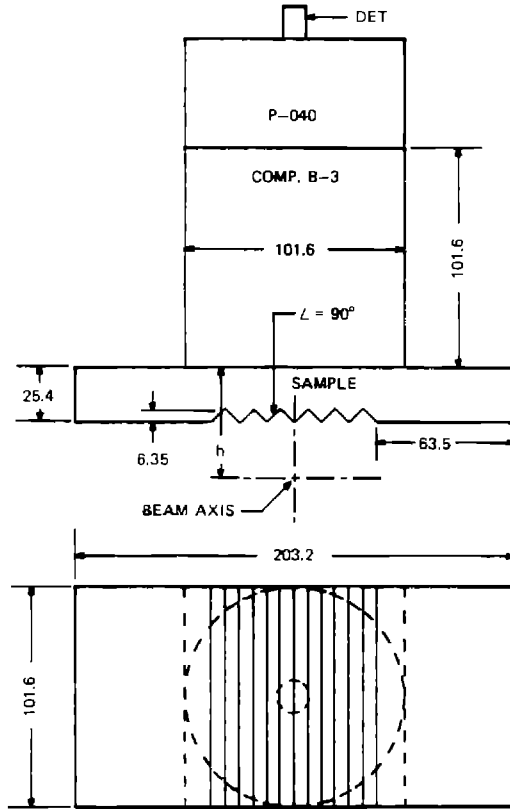
Interaction of jets from two grooved aluminum plates shocked simultaneously by Composition B-3 detonation waves. The angle between the plates is 60° , and their free surfaces have run for 13.0 μ s.

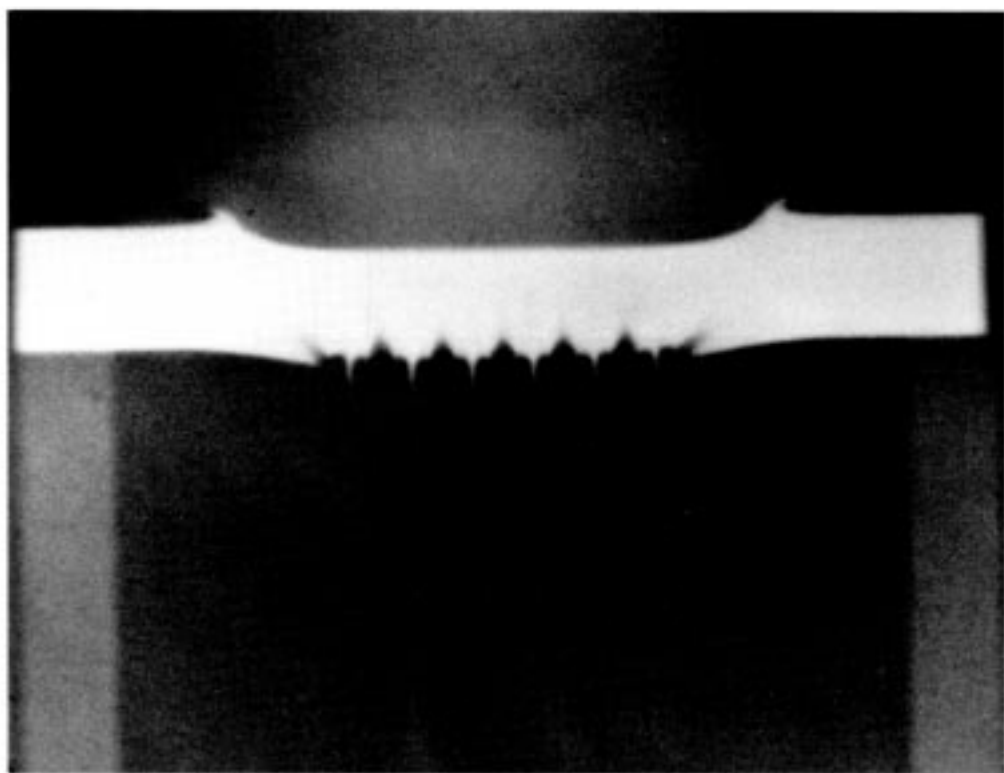




SHOT 43: **Copper Jets**
Date: **June 23, 1964**
Experimenter: **Douglas Venable**
Radiographic Time: **34.8 μ s**

Formation of metallic jets. The explosively induced shock wave in the copper plate interacts with the grooves to produce the jets. The free surface of the plate has run for 3.5 μ s. h is 25.4 mm.





SHOT 44:

Steel Jets

Date:

June 23, 1964

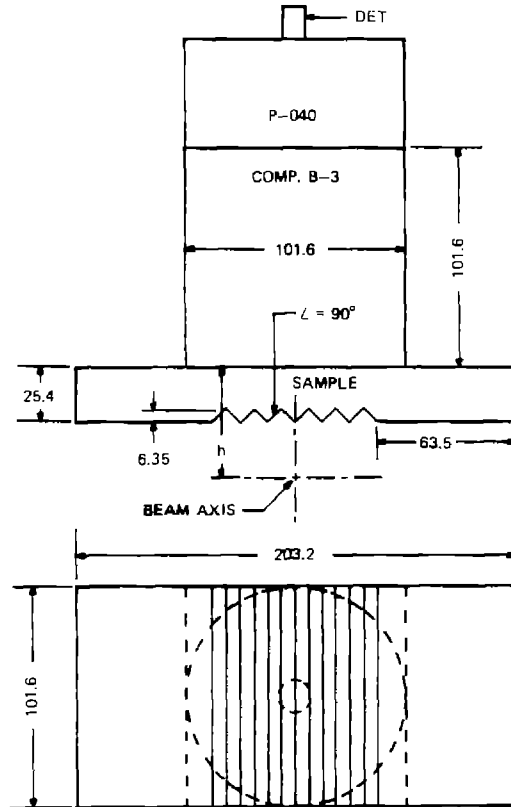
Experimenter:

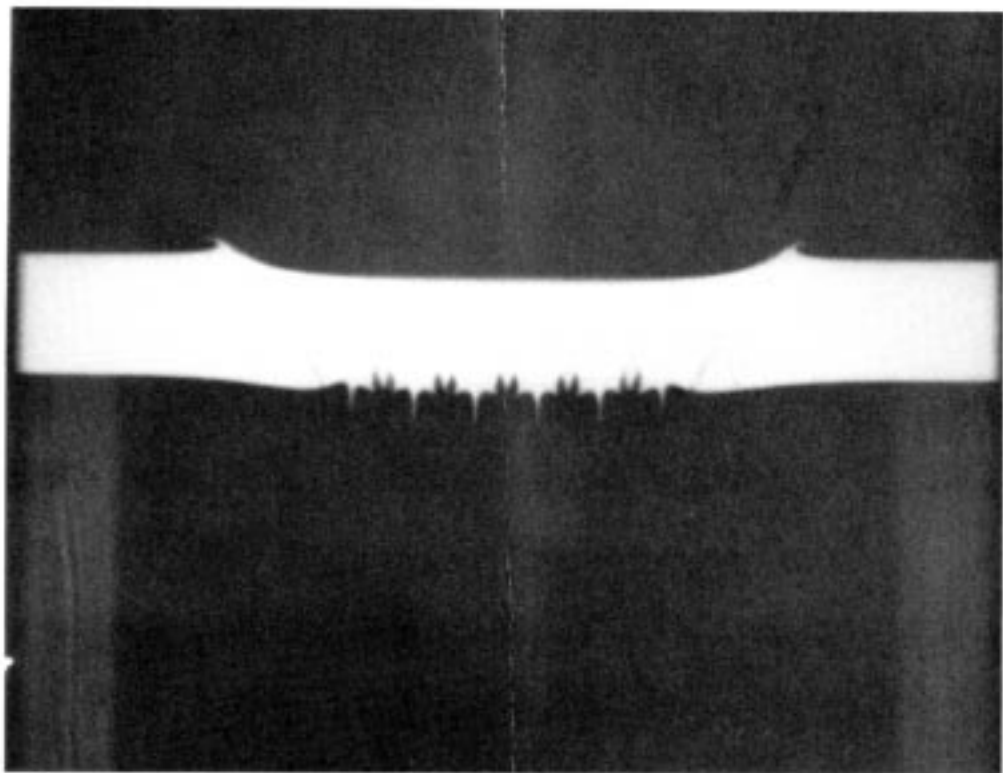
Douglas Venable

Radiographic Time:

34.9 μ s

Formation of metallic jets. The explosively induced shock wave in the 1019 steel plate interacts with the grooves to produce the jets. The free surface of the plate has run for 3.5 μ s. h is 25.4 mm.





SHOT 45:

Lead Jets

Date:

June 23, 1964

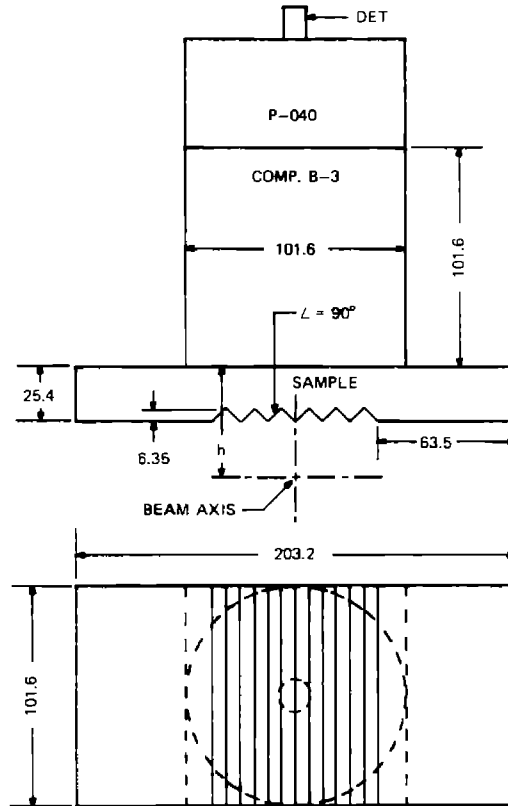
Experimenter:

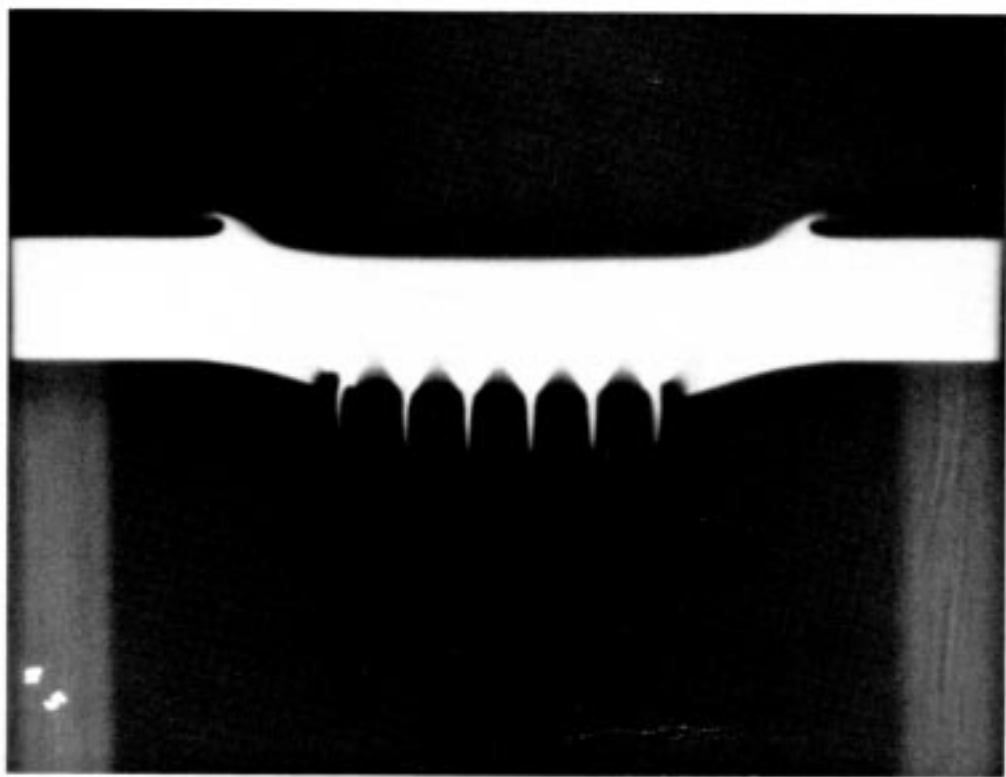
Douglas Venable

Radiographic Time:

39.4 μ s

Formation of metallic jets. The explosively induced shock wave in the lead plate interacts with the grooves to produce the jets. The free surface of the plate has run for 3.5 μ s. h is 25.4 mm.





SHOT 46:

Steel Jets

Date:

June 30, 1964

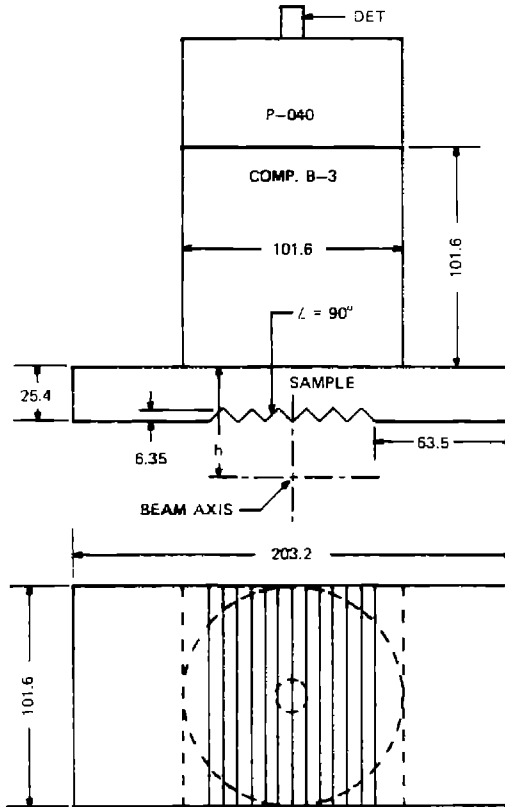
Experimenter:

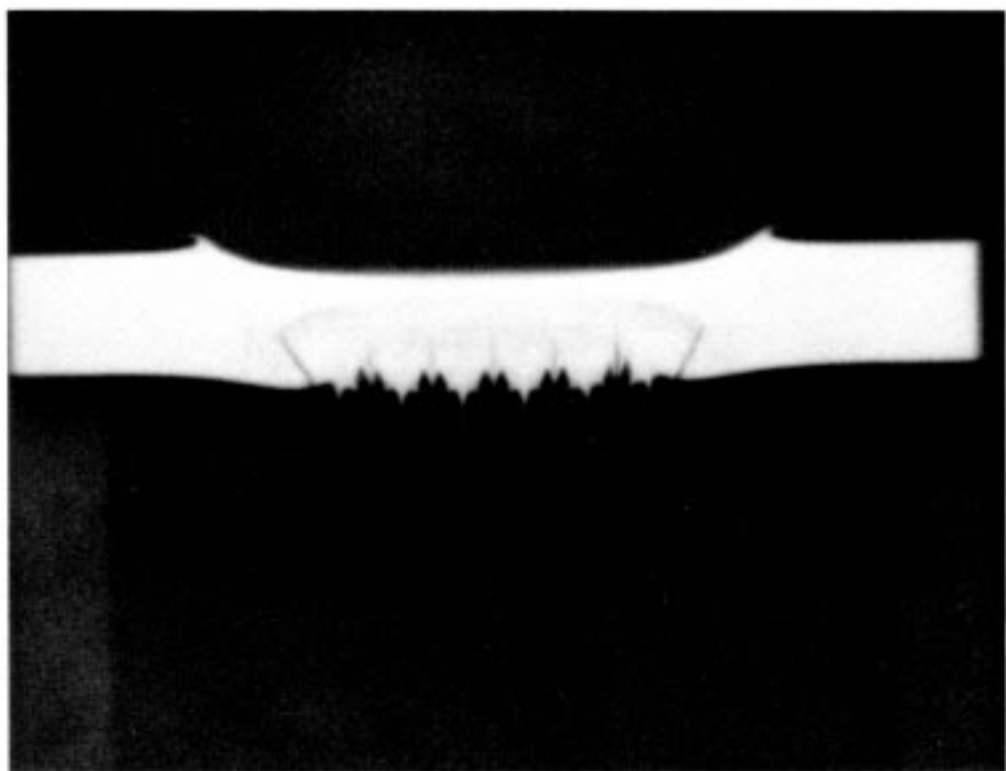
Douglas Venable

Radiographic Time:

36.28 μ s

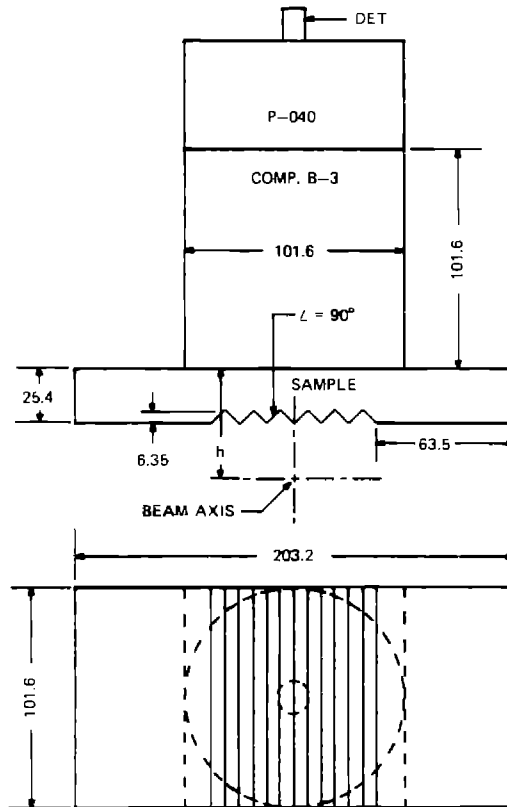
Formation of metallic jets. The explosively induced shock wave in the 1019 steel plate interacts with the grooves to produce the jets. The free surface of the plate has run for 5.0 μ s. h is 25.4 mm.

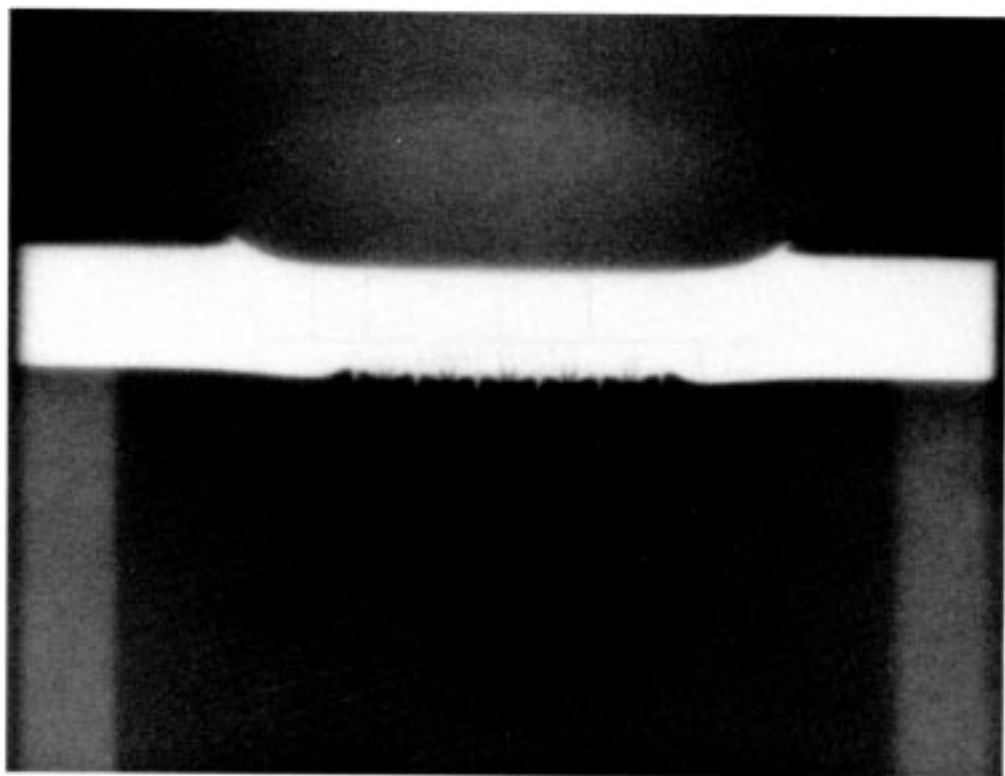




SHOT 47: **Steel Jets**
Date: June 30, 1964
Experimenter: Douglas Venable
Radiographic Time: 33.32 μ s

Formation of metallic jets. The explosively induced shock wave in the 1019 steel plate interacts with the grooves to produce the jets. The free surface of the plate has run for 2.0 μ s. h is 25.4 mm.





SHOT 48:

Steel Jets

Date:

June 30, 1964

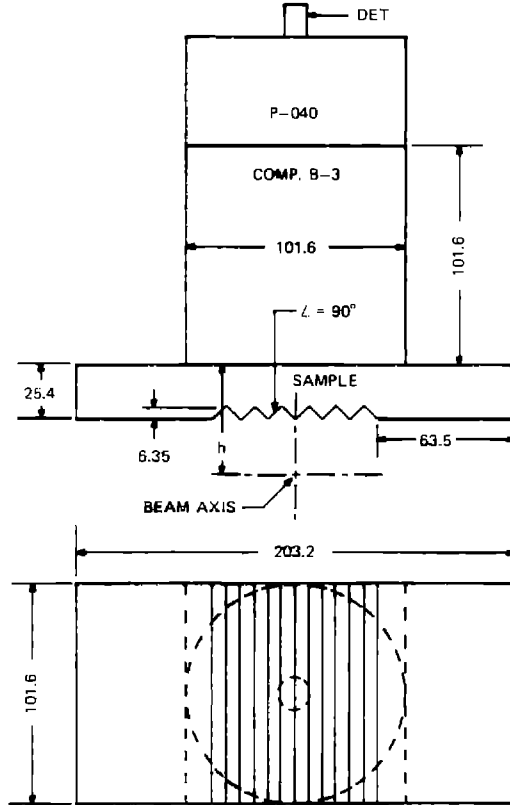
Experimenter:

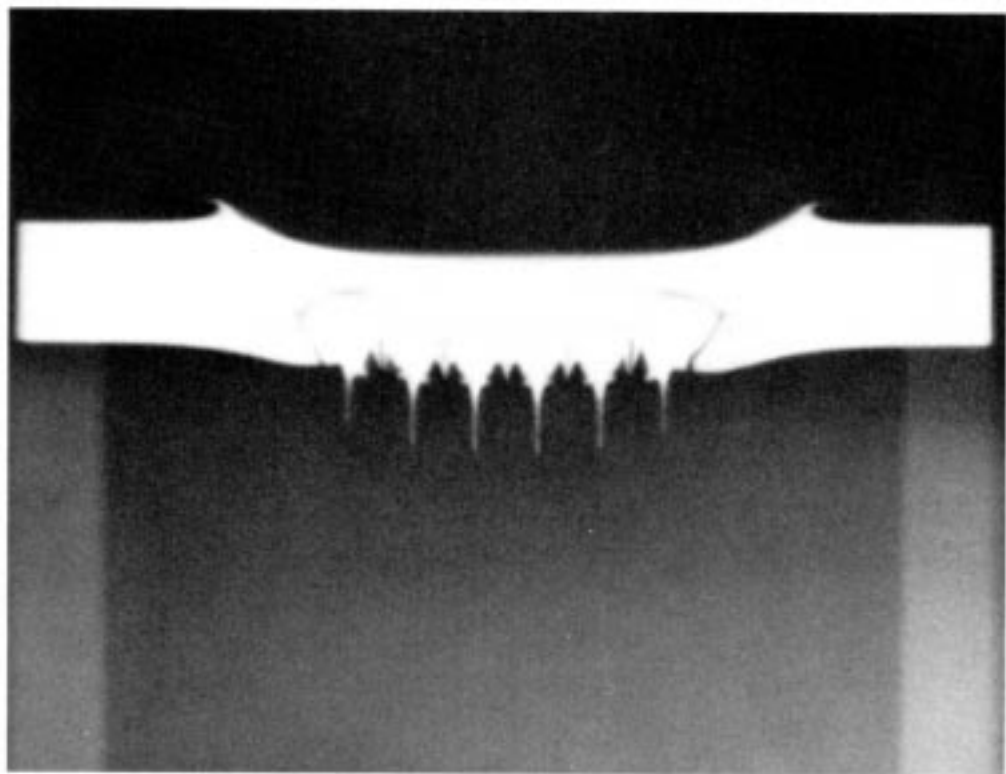
Douglas Venable

Radiographic Time:

39.32 μ s

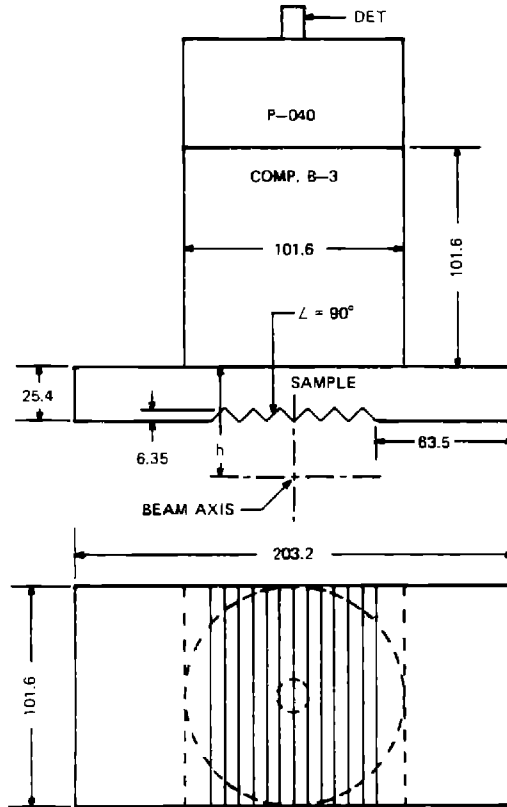
Formation of metallic jets. The explosively induced shock wave in the 1019 steel plate interacts with the grooves to produce the jets. The free surface of the plate has run for 8.0 μ s. h is 25.4 mm.

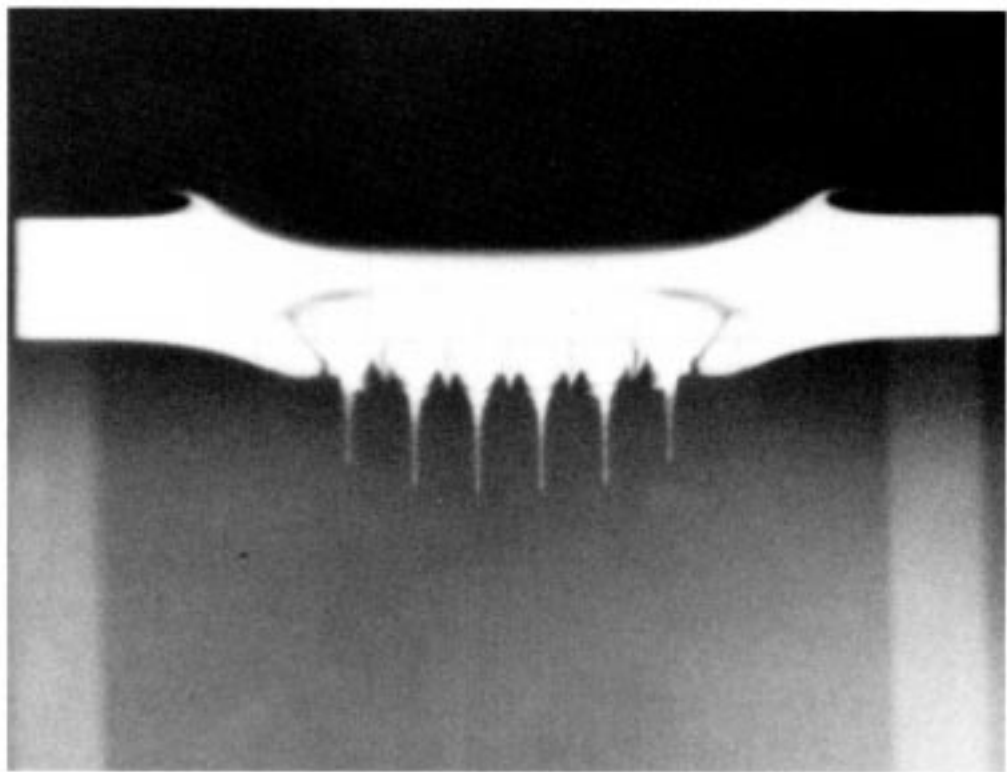




SHOT 49: **Steel Jets**
Date: **July 7, 1964**
Experimenter: **Douglas Venable**
Radiographic Time: **42.2 μ s**

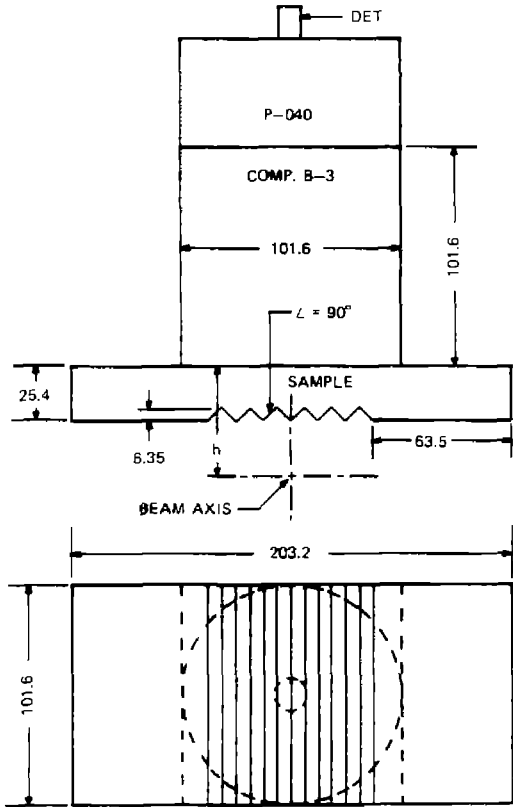
Formation of metallic jets. The explosively induced shock wave in the 1019 steel plate interacts with the grooves to produce the jets. The free surface of the plate has run for 11.0 μ s. h is 25.4 mm.

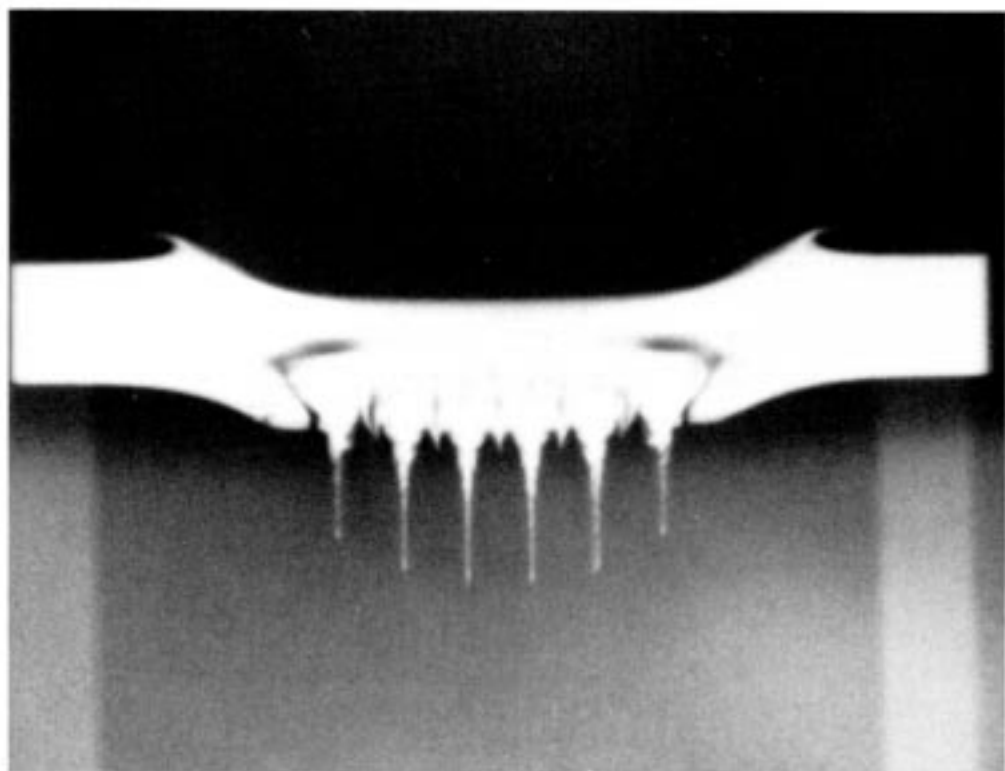




SHOT 50: Steel Jets
Date: July 7, 1964
Experimenter: Douglas Venable
Radiographic Time: 45.3 μ s

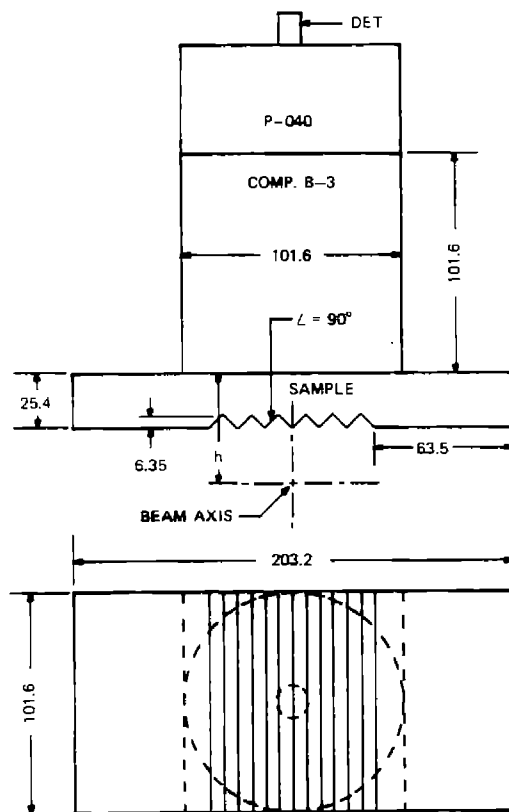
Formation of metallic jets. The explosively induced shock wave in the 1019 steel plate interacts with the grooves to produce the jets. The free surface of the plate has run for 14.0 μ s. h is 25.4 mm.

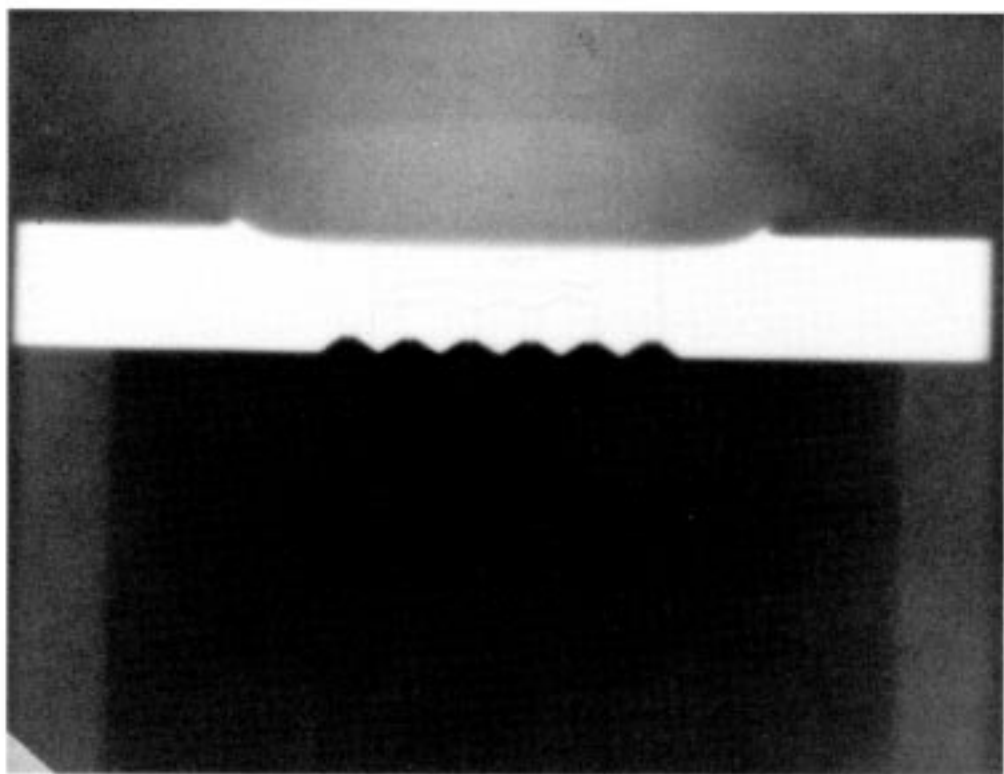




SHOT 51: **Steel Jets**
Date: July 7, 1964
Experimenter: Douglas Venable
Radiographic Time: 31.3 μ s

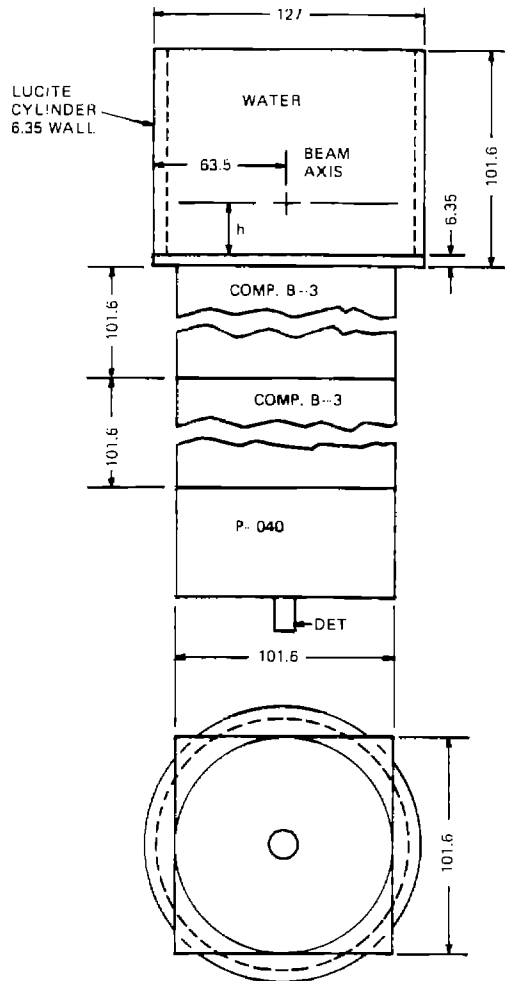
Formation of metallic jets. The explosively induced shock wave in the 1019 steel plate interacts with the grooves to produce the jets. The shock wave has reached the plate free surface. h is 25.4 mm.

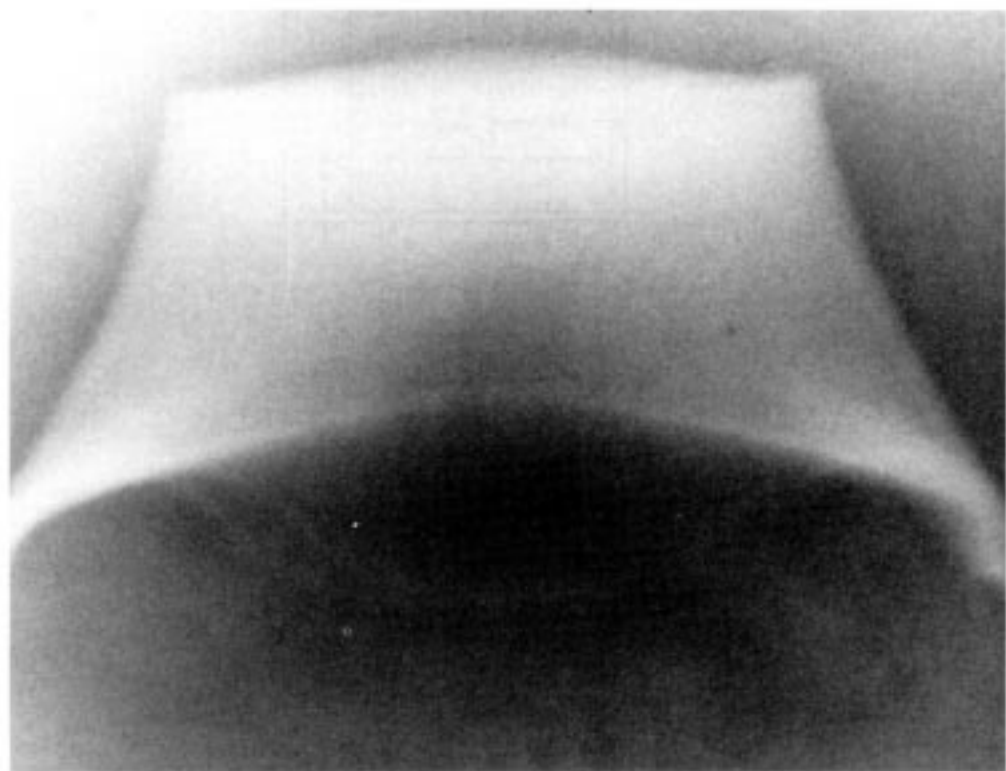




SHOT 52: **Water Shock**
Date: July 9, 1964
Experimenter: Douglas Venable
Radiographic Time: 67.1 μ s
Reference: Mader, 1965

The shock wave formed in water by a Composition B-3 detonation wave has reached the water-free surface. h is 25.4 mm.





SHOT 53:

Water Shock

Date:

July 14, 1964

Experimenter:

Douglas Venable

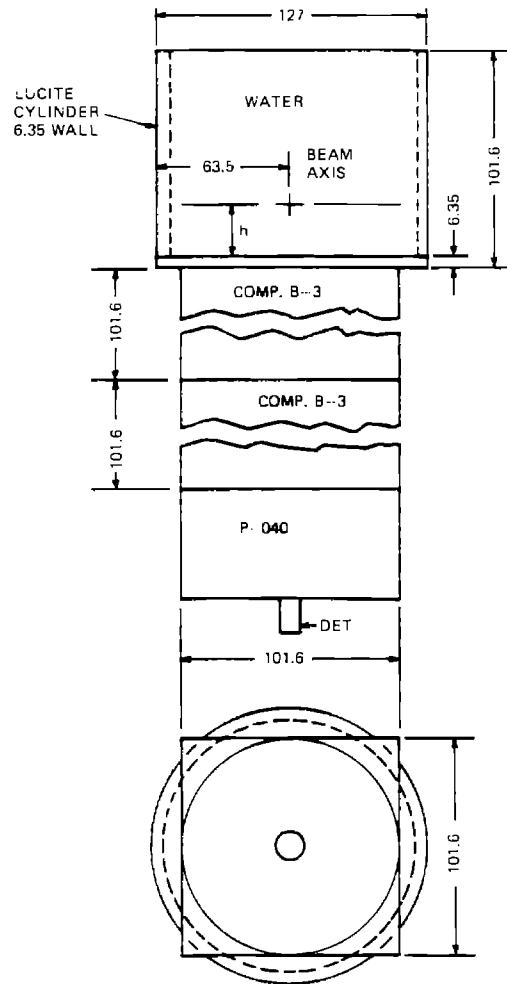
Radiographic Time:

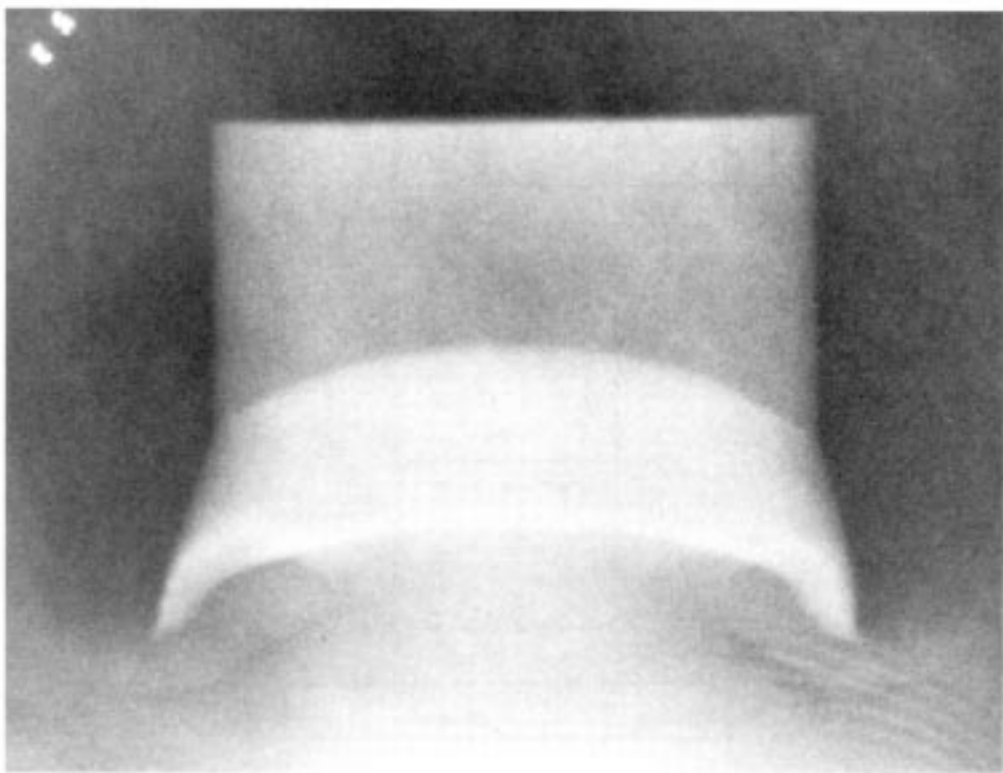
49.5 μ s

Reference:

Mader, 1965

The shock wave formed in water by a Composition B-3 detonation wave. h is 50.8 mm.





SHOT 54:

Copper Splash Wave

Date:

July 14, 1964

Experimenter:

Douglas Venable

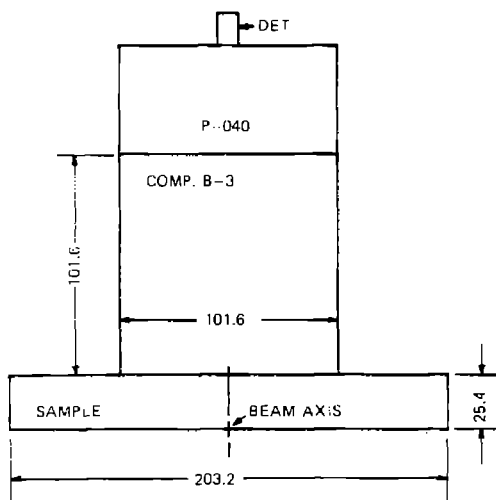
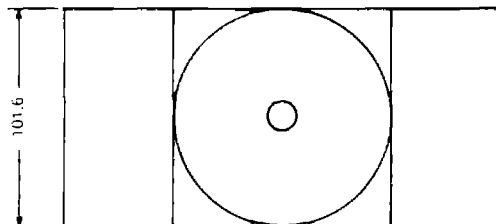
Radiographic Time:

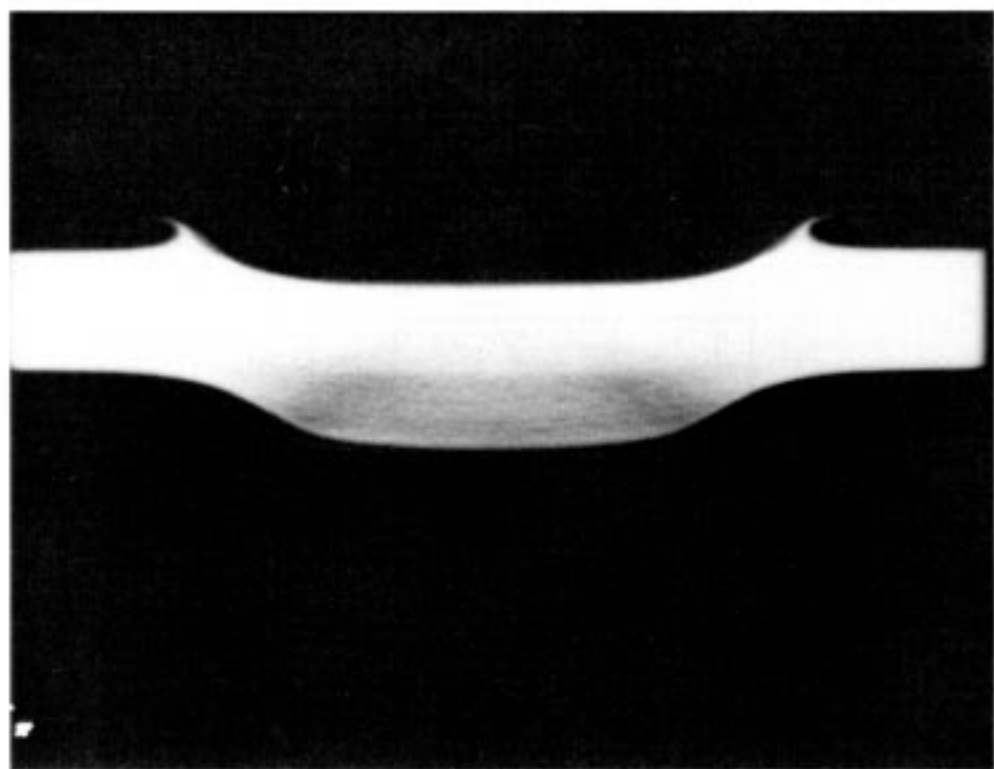
42.2 μ s

References:

Taylor and Venable, 1968

Copper splash wave and dynamic fracture generated by 101.6 mm of detonated Composition B-3 initiated by a P-40 lens. The copper plate was coated with solder.





SHOT 55:

Mach Reflection in Baratol

Date:

July 14, 1964

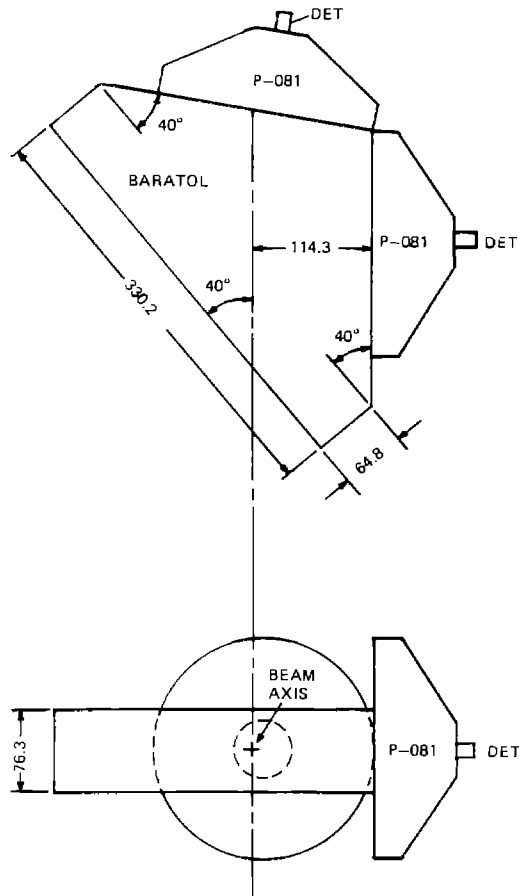
Experimenter:

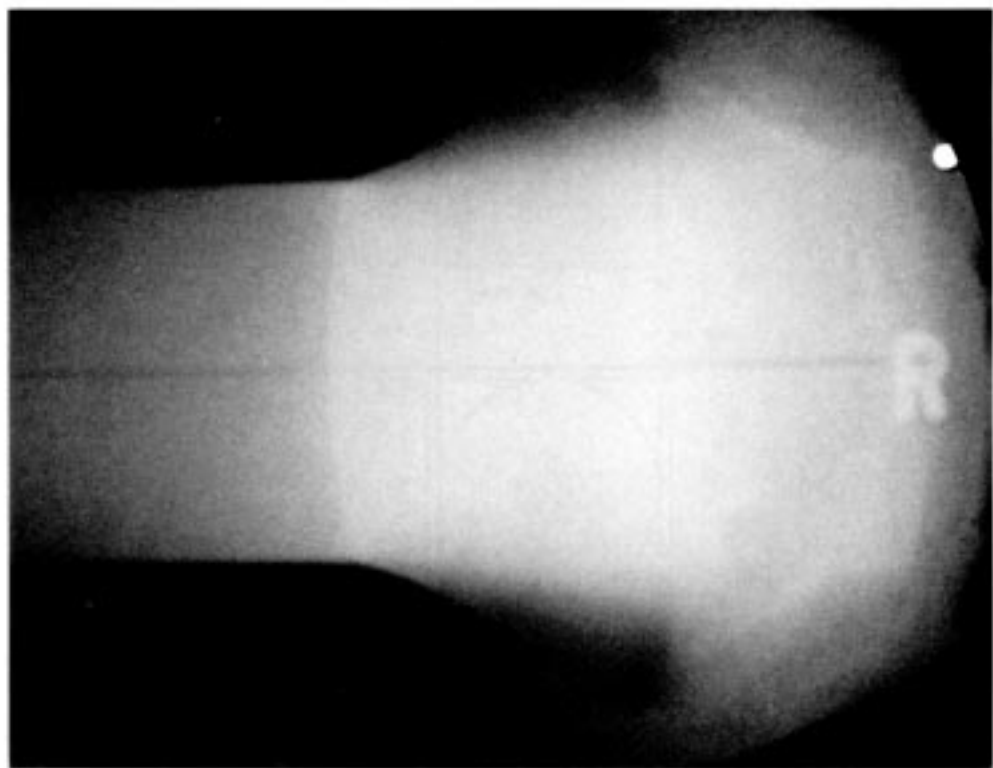
Douglas Venable

Radiographic Time:

46.2 μ s

Two Baratol detonation waves interacting to form a Mach reflection. Similar to Shots 5 and 15, but the beam orientation is different. See Shots 3-5 and 15.





SHOT 56:

Spherical Hole in Water

Date:

July 14, 1964

Experimenter:

Douglas Venable

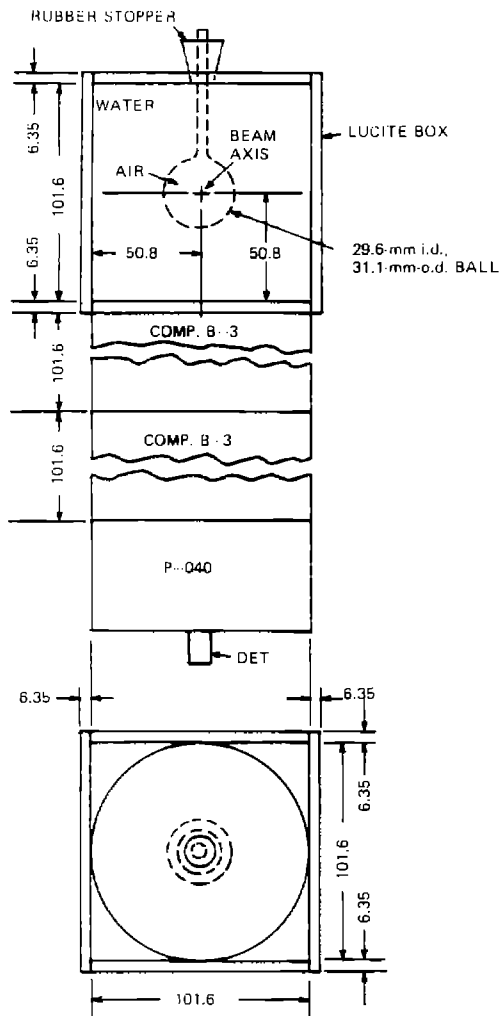
Radiographic Time:

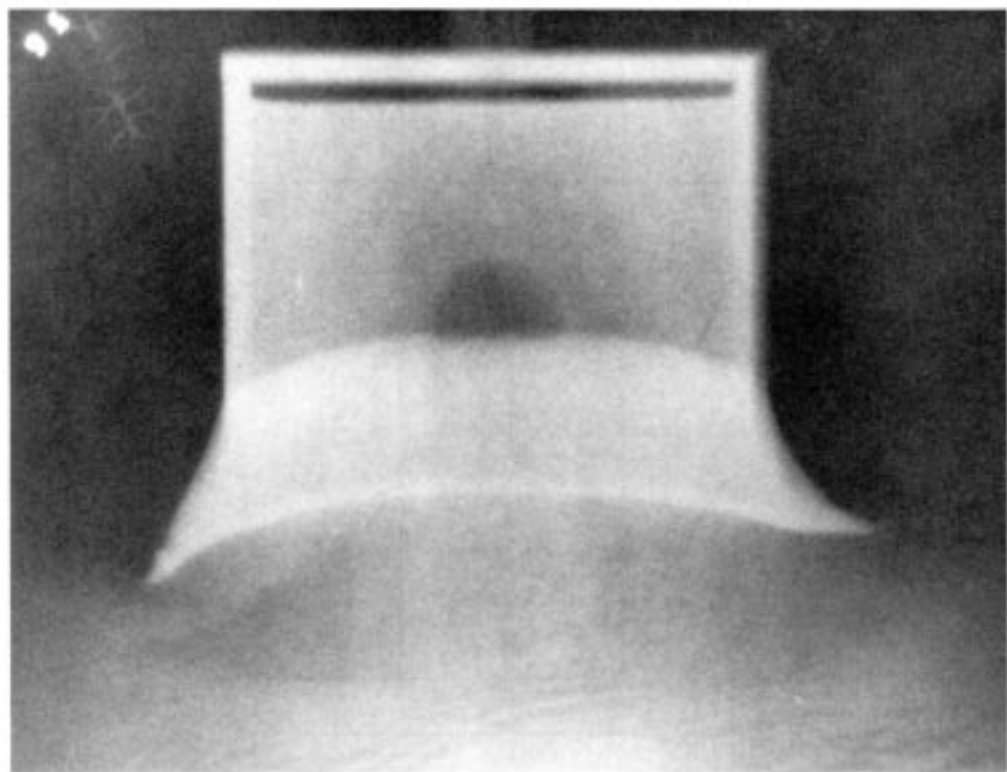
49.2 μ s

Reference:

Mader, 1965

A shock wave formed in water by a Composition B-3 detonation wave (see Shot 53) interacts with a spherical air bubble. See also Shot 95.





SHOT 57:

Armco Iron Splash Wave

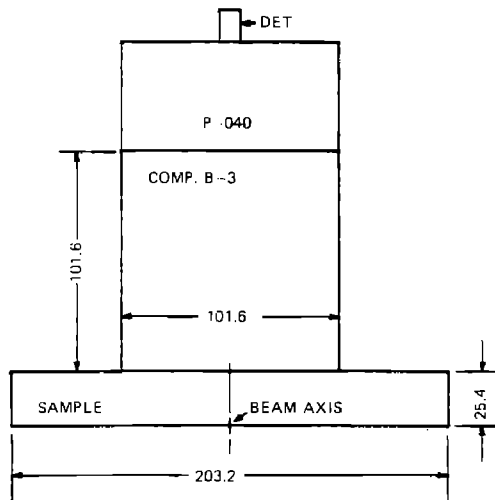
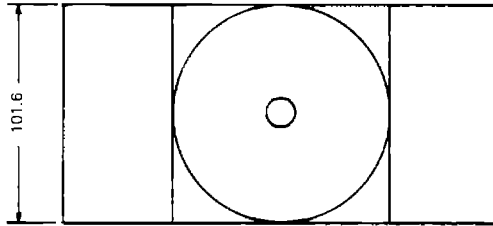
Date: July 21, 1964

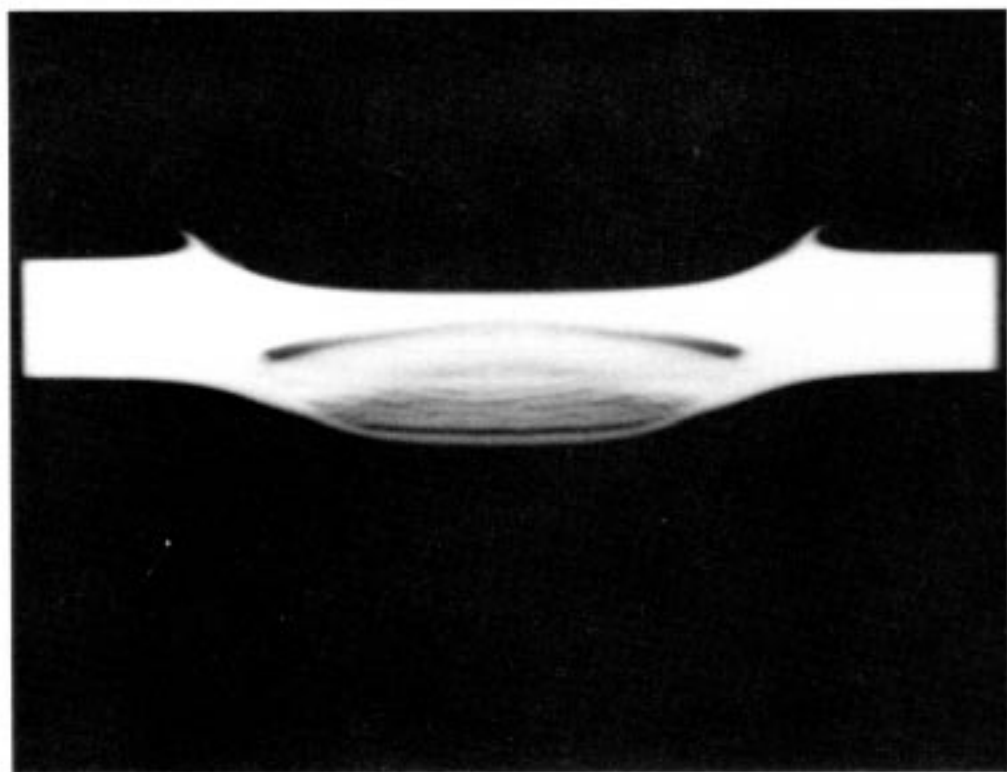
Experimenter: Douglas Venable

Radiographic Time: 42.68 μ s

Reference: Taylor and Venable, 1968

Armco iron splash wave and dynamic fracture generated by 101.6 mm of detonated Composition B-3 initiated by a P-40 lens.





SHOT 58:

Steel Splash Wave

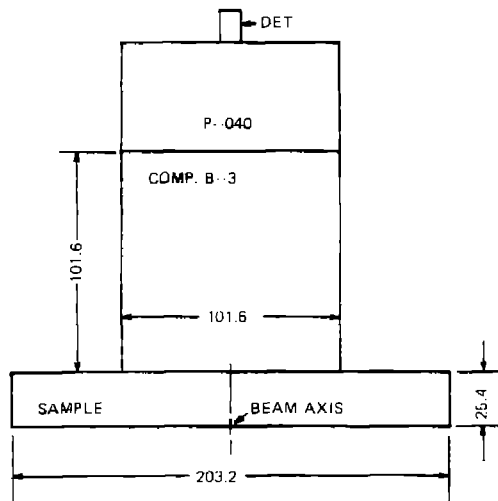
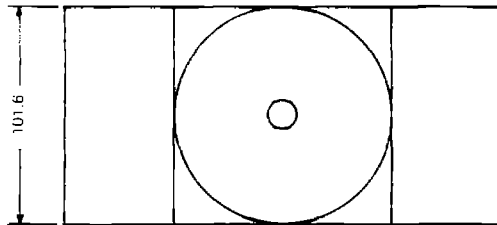
Date: July 21, 1964

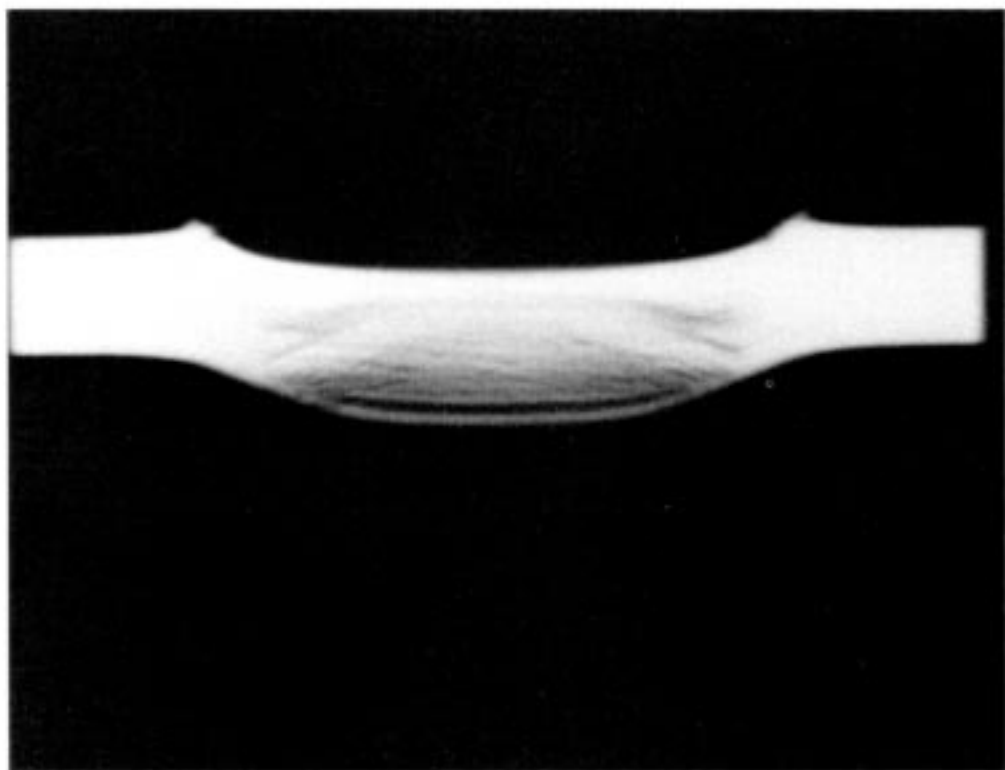
Experimenter: Douglas Venable

Radiographic Time: 42.01 μ s

Reference: Taylor and Venable, 1968

AISI O-2 tool steel splash wave and dynamic fracture generated by 101.6 mm of detonated Composition B-3 initiated by a P-40 lens.

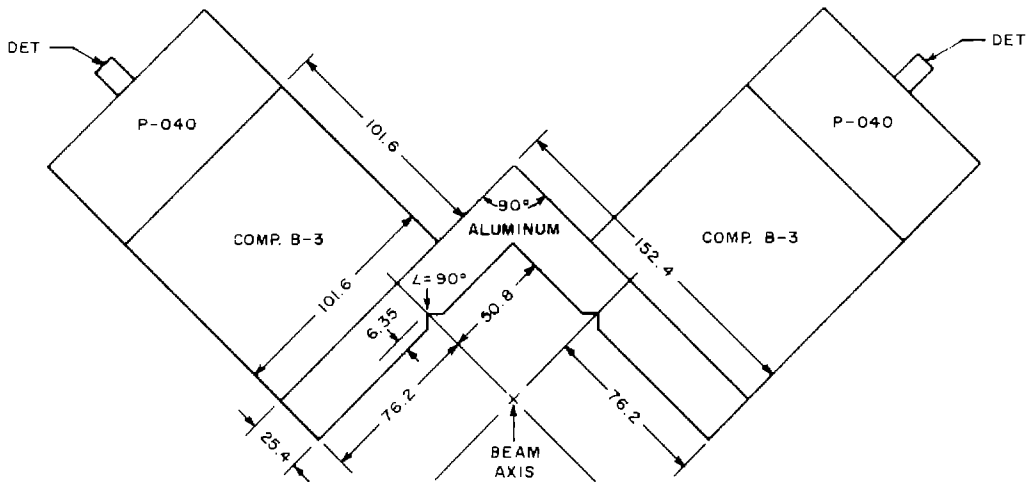
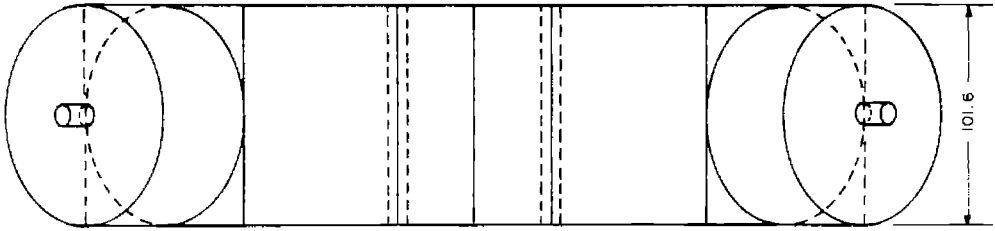


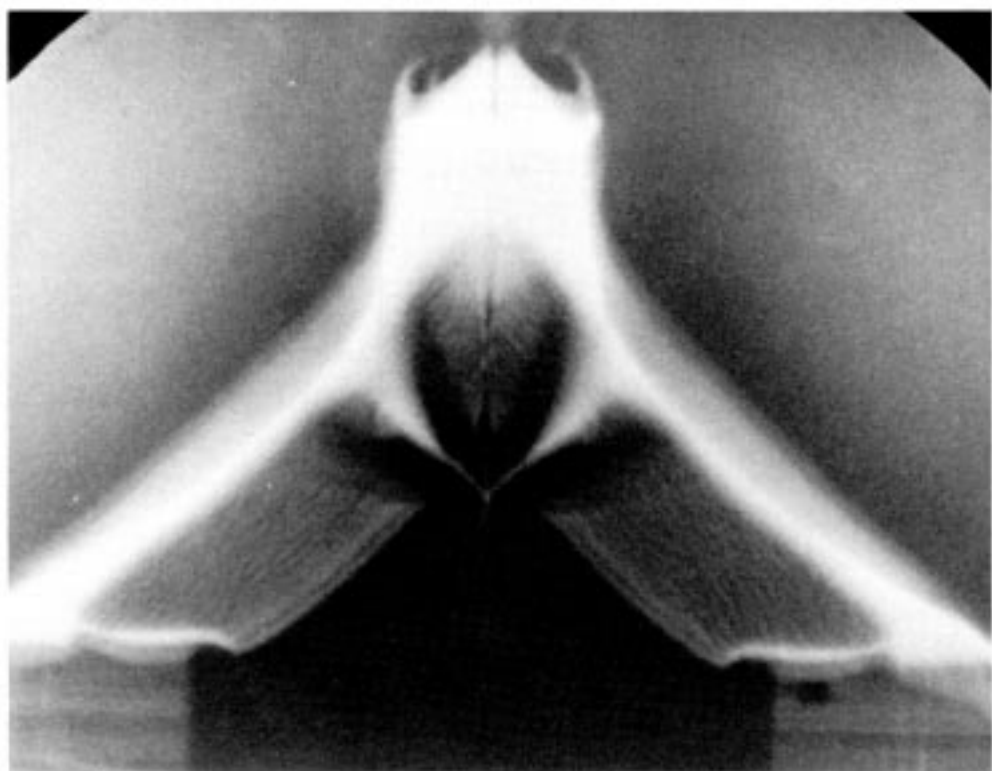
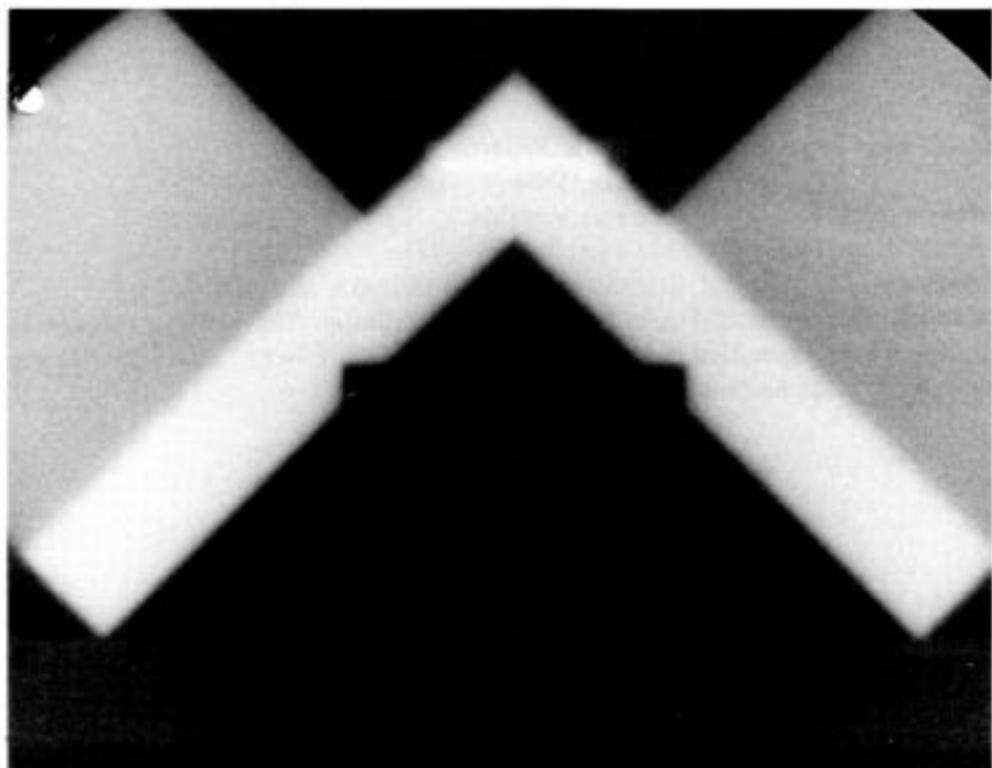


SHOT 59: Interacting Aluminum Jets

Date: July 21, 1964
Experimenter: Douglas Venable
Radiographic Time: 42.47 μ s
Reference: Venable, 1965

Interaction of the jets produced by two aluminum plates shocked simultaneously by Composition B-3 detonation waves. The plates were perpendicular to each other, and their free surfaces have run for 13.0 μ s. See Shot 41.





SHOT 60:

Dynamic Fracture of Aluminum

Date:

July 28, 1964

Experimenter:

Douglas Venable

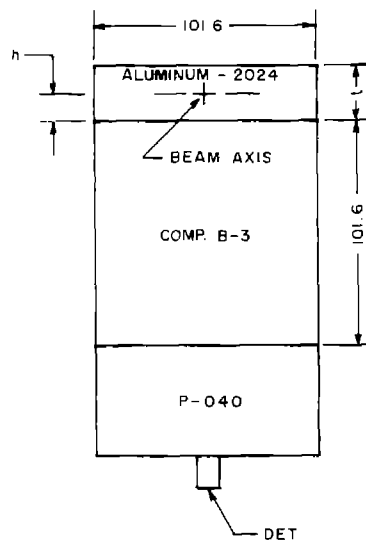
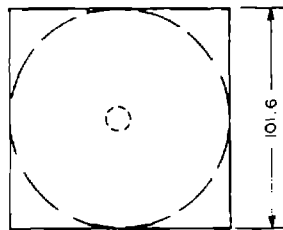
Radiographic Time:

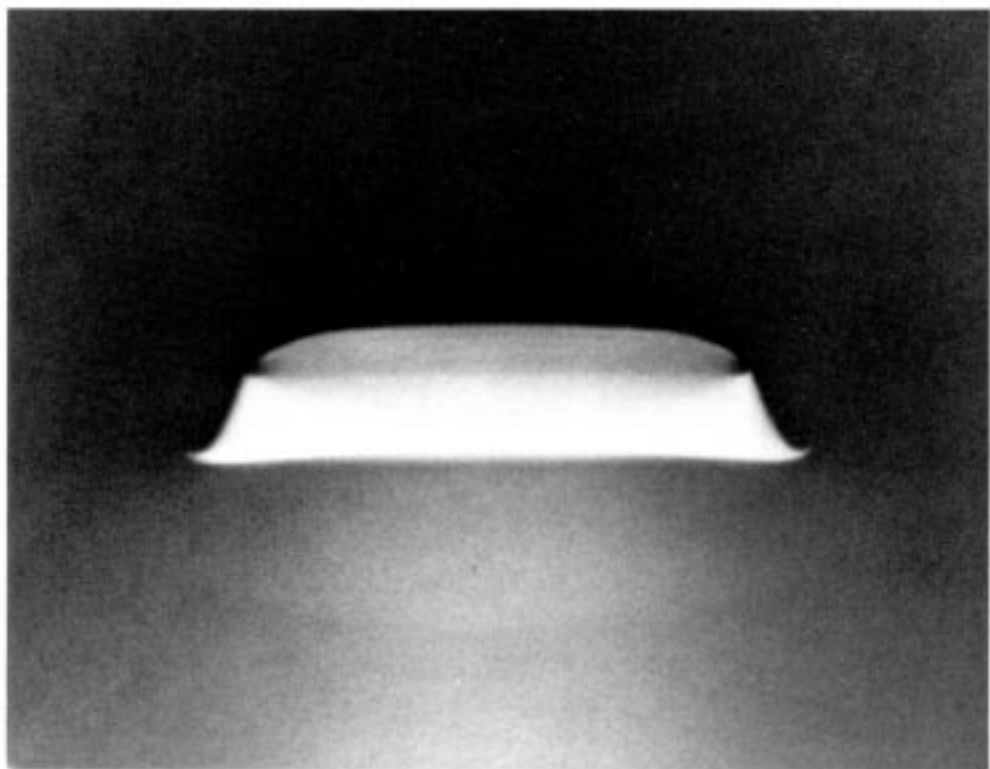
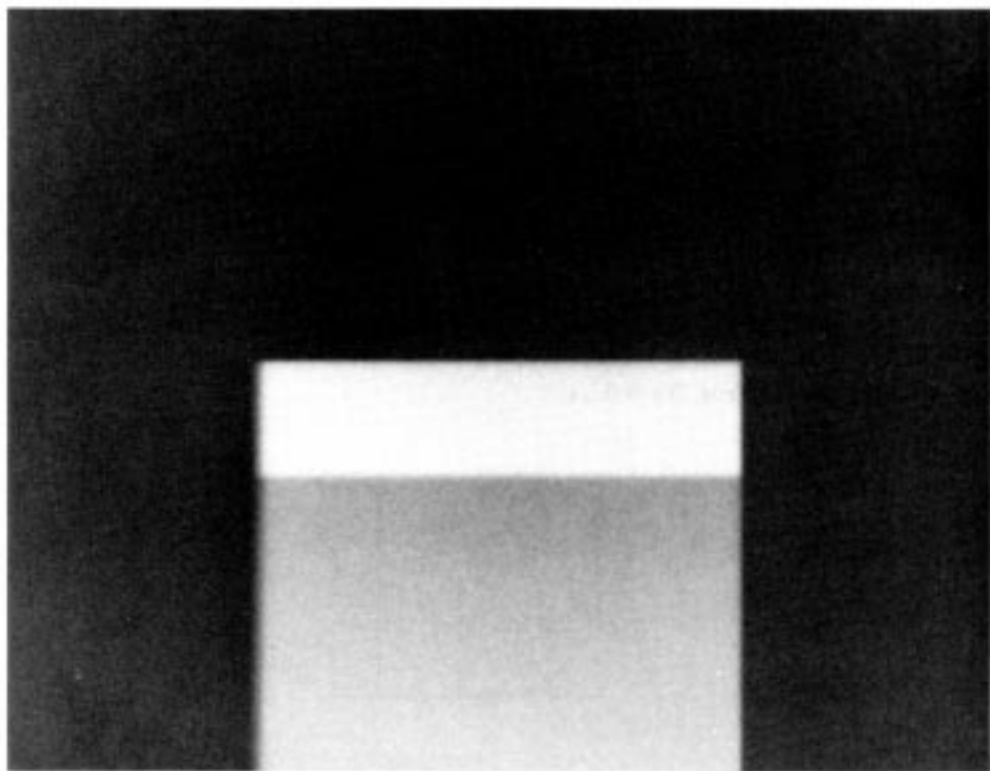
34.07 μ s

References:

Breed et al., 1967; Thurston and Mudd, 1968

Dynamic fracture of 25.4-mm-thick, t, 2024 aluminum. The plate is shocked by 101.6 mm of Composition B-3 initiated by a P-040 lens. h is 12.7 mm. The free surface of the plate has run 25.4 mm in 4.0 μ s.





SHOT 61:

Dynamic Fracture of Aluminum

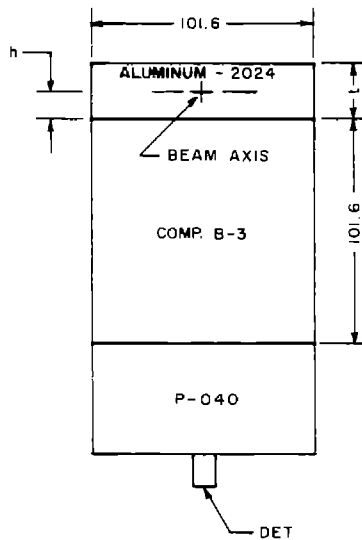
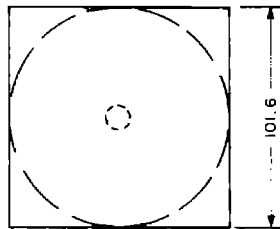
Date: July 28, 1964

Experimenter: Douglas Venable

Radiographic Time: 37.86 μ s

References: Breed et al., 1967; Thurston and Mudd, 1968

Dynamic fracture of 25.4-mm-thick, t, 2024 aluminum. The plate is shocked by 101.6 mm of Composition B-3 initiated by a P-040 lens. h is 25.4 mm. The free surface of the plate has run for 8.0 μ s.





SHOT 62:

Dynamic Fracture of Aluminum

Date:

July 28, 1964

Experimenter:

Douglas Venable

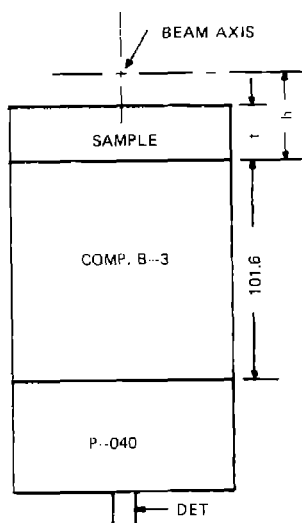
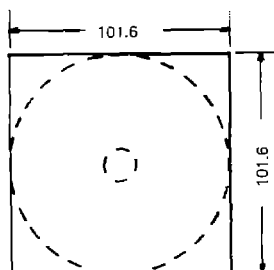
Radiographic Time:

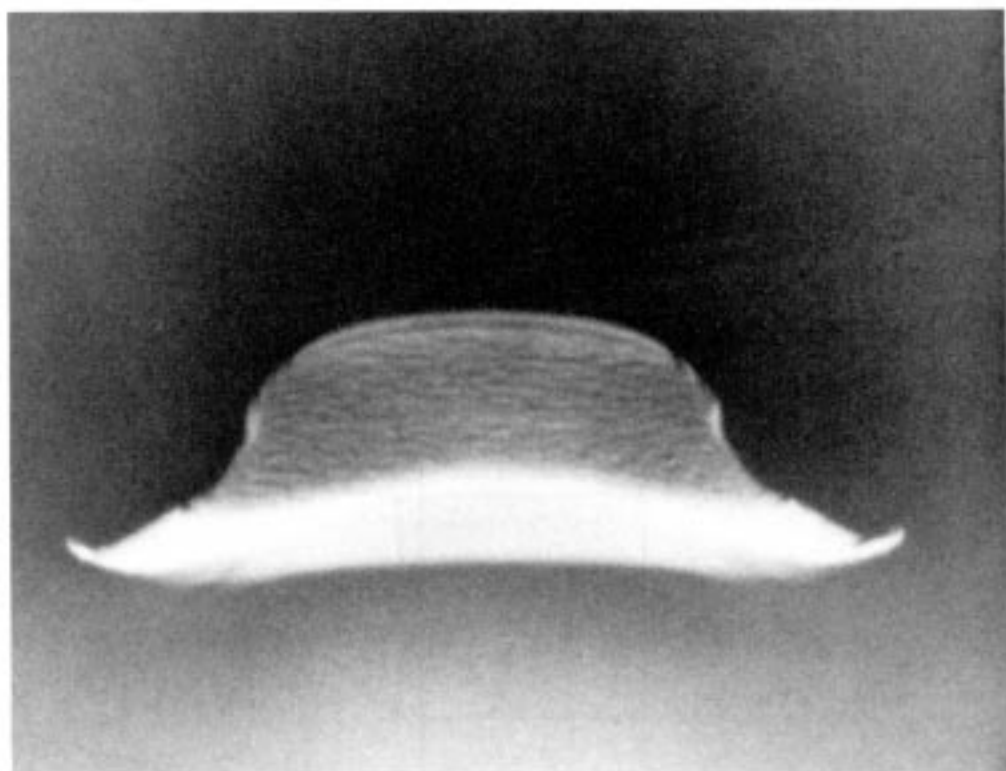
45.98 μ s

References:

Breed et al., 1967; Thurston and Mudd, 1968

Dynamic fracture of 25.4-mm-thick, t, 2024 aluminum. The plate is shocked by 101.6 mm of Composition B-3 initiated by a P-040 lens. h is 50.8 mm. The free surface of the plate has run for 16.0 μ s.





SHOT 63:

Dynamic Fracture of Aluminum

Date:

July 28, 1964

Experimenter:

Douglas Venable

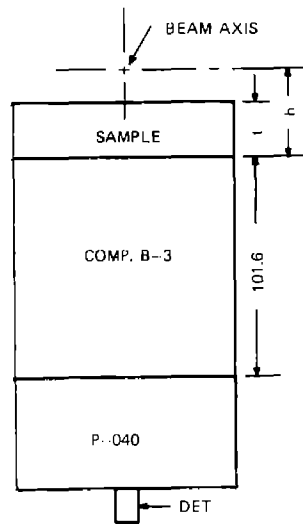
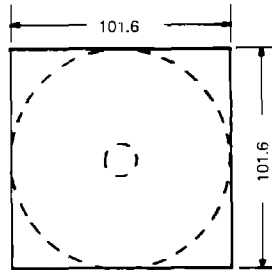
Radiographic Time:

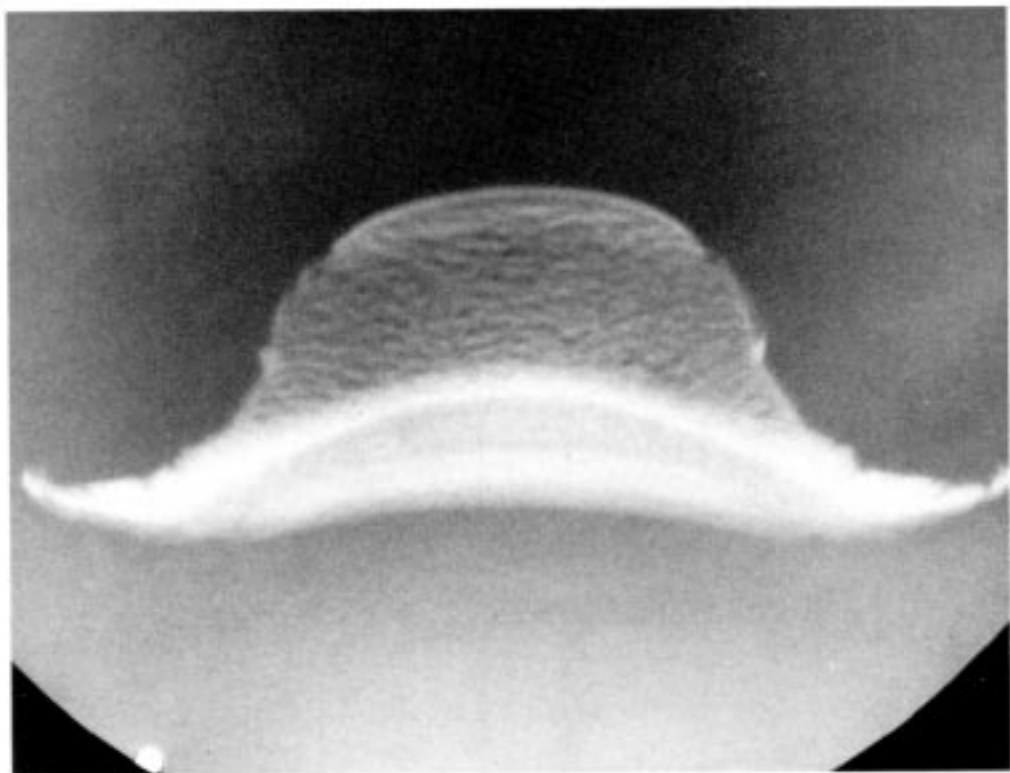
53.88 μ s

References:

Breed et al., 1967; Thurston and Mudd, 1968

Dynamic fracture of 25.4-mm-thick, t , 2024 aluminum. The plate is shocked by 101.6 mm of Composition B-3 initiated by a P-040 lens. h is 76.2 mm. The free surface of the plate has run 76.2 mm in 24.0 μ s.

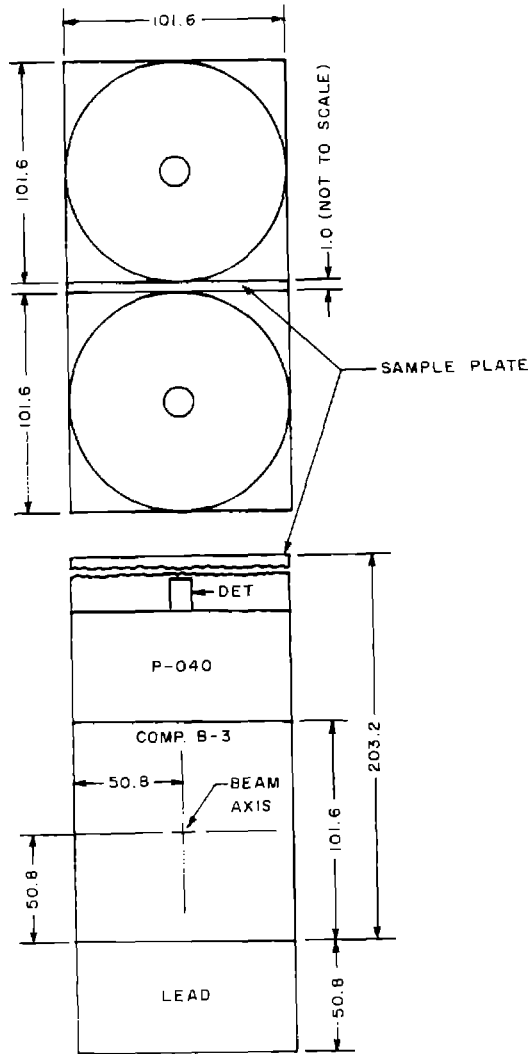


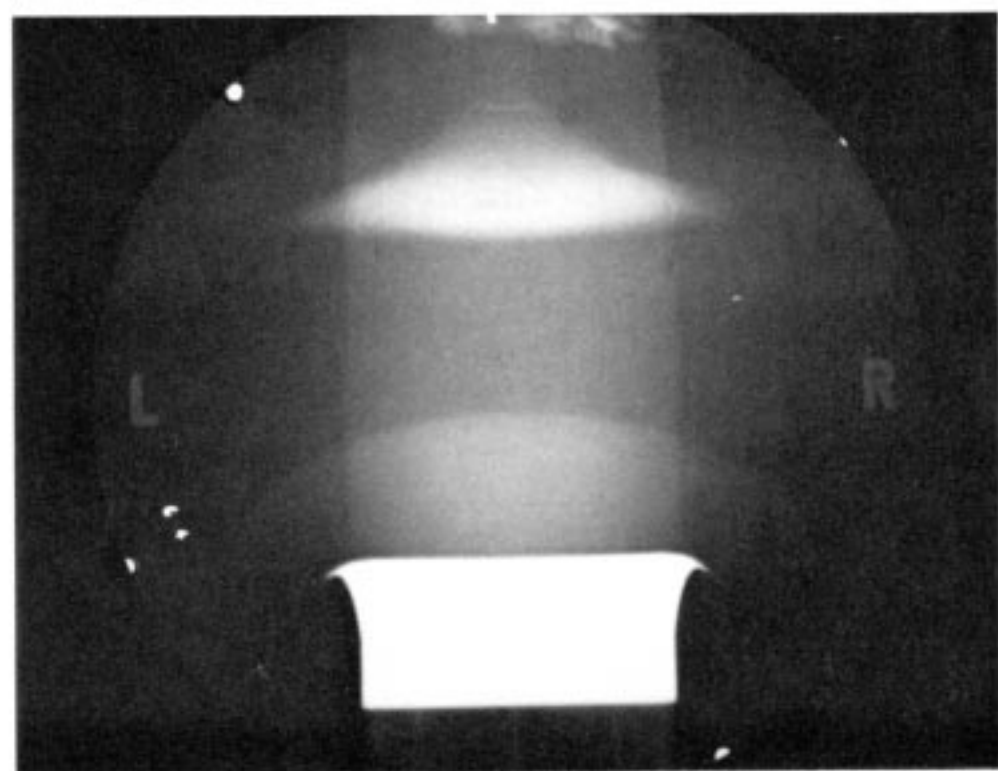
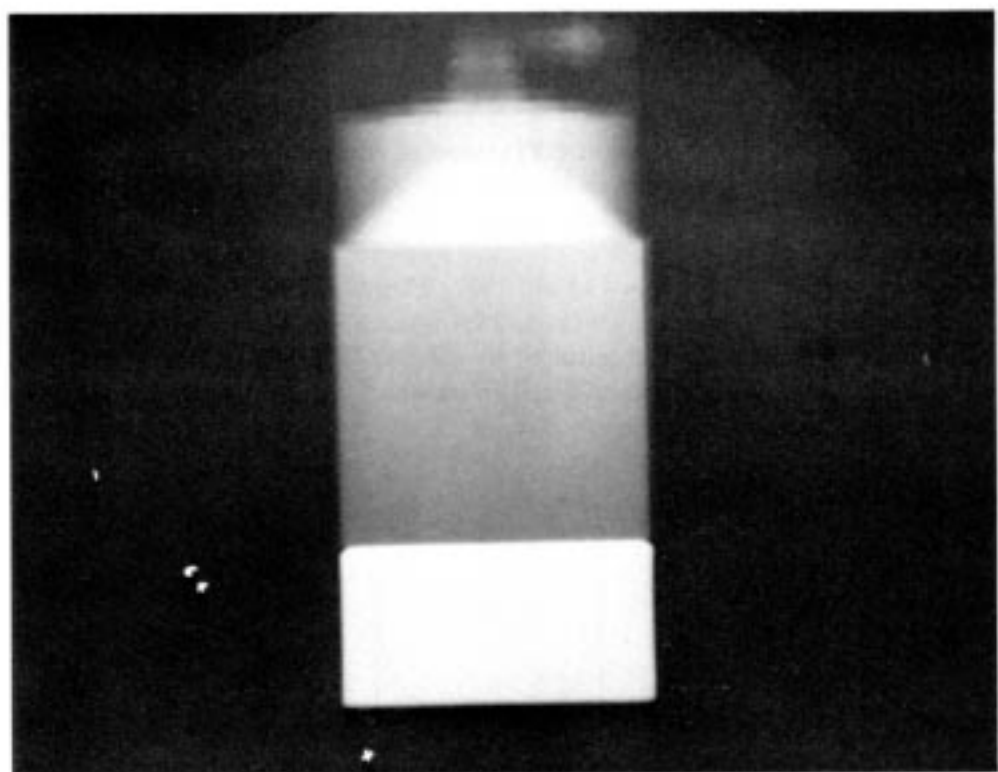


SHOT 64: Two Composition B-3 Detonations

Date: August 6, 1964
Experimenter: Douglas Venable
Radiographic Time: 36.49 μ s

Two blocks of Composition B-3 were detonated simultaneously. A 1.0-mm-thick uranium plate was placed between the explosive blocks perpendicular to the direction of detonation wave travel. The detonation waves collided with a lead plate, and a reflected shock was sent back into the detonation products. See Shot 40 for a different beam orientation.





SHOT 68: Dynamic Fracture of Aluminum

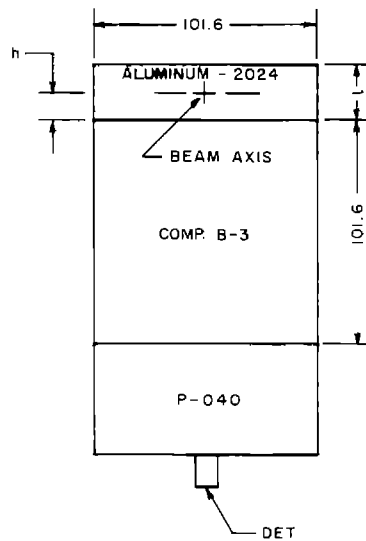
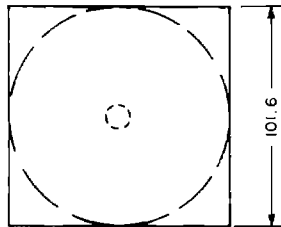
Date: August 18, 1964

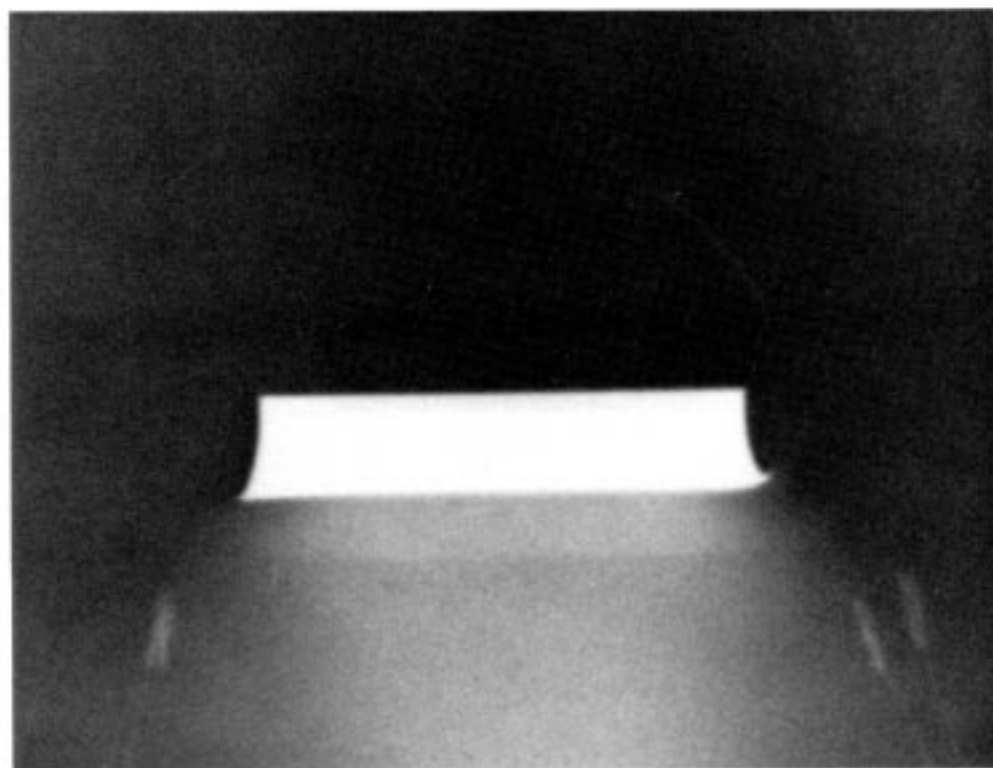
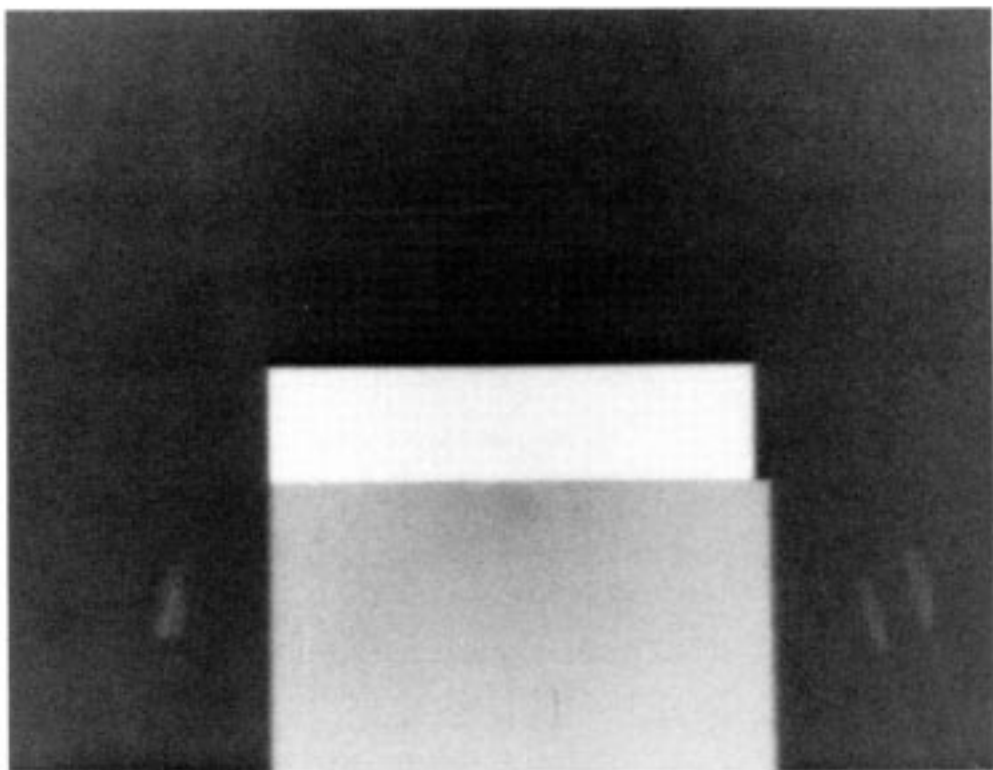
Experimenter: Douglas Venable

Radiographic Time: 28.93 μ s

References: Breed et al., 1967; Thurston and Mudd, 1968

Dynamic fracture of 24.5-mm-thick, t, 2024 aluminum. The plate is shocked by 101.6 mm of Composition B-3 initiated by a P-040 lens. h is 12.7 mm. The shock wave in the aluminum and the reflected shock wave in the detonation products are visible.





SHOT 69:

Dynamic Fracture of Aluminum

Date:

August 18, 1964

Experimenter:

Douglas Venable

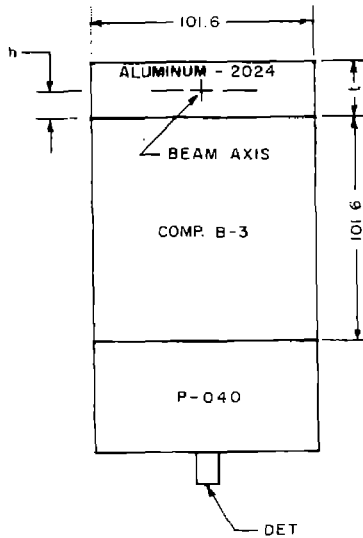
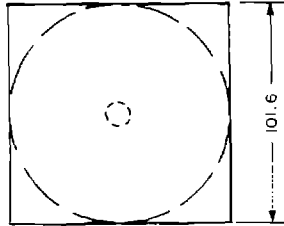
Radiographic Time:

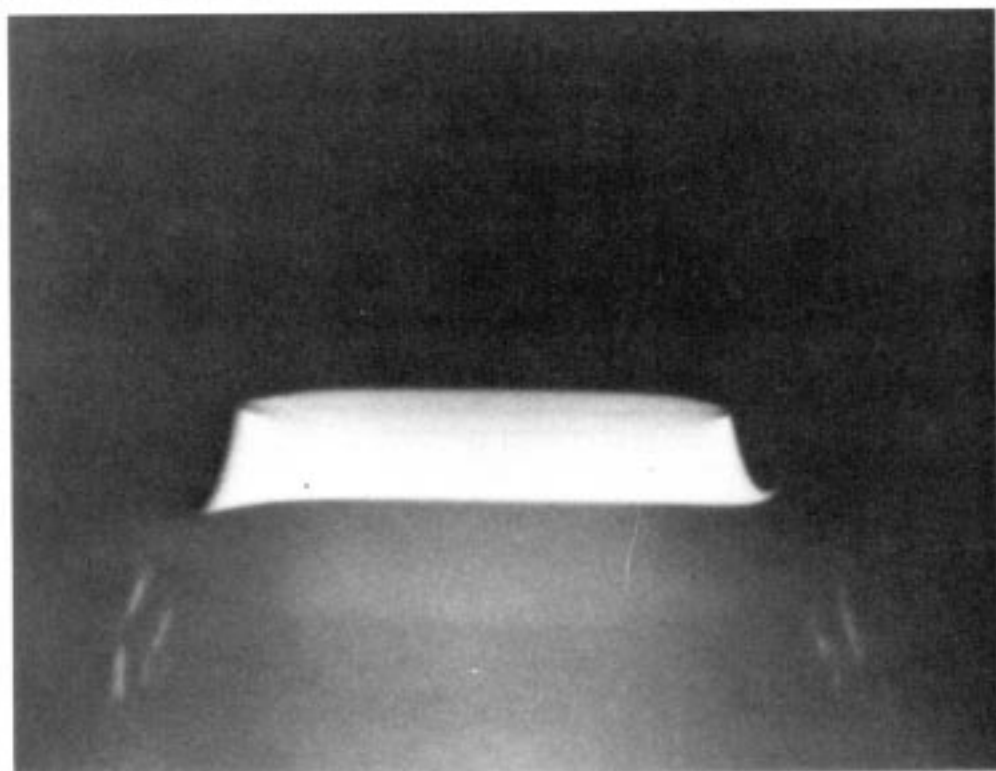
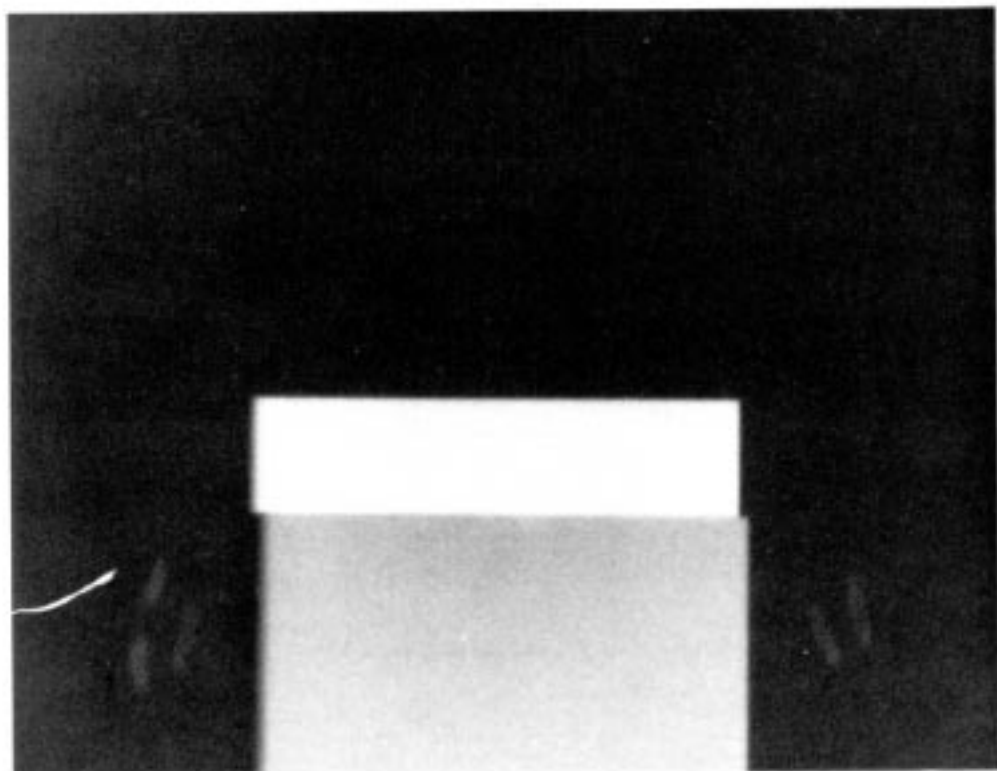
31.38 μ s

References:

Breed et al., 1967; Thurston and Mudd, 1968

Dynamic fracture of 24.6-mm-thick, t , 2024 aluminum. The plate is shocked by 101.6 mm of Composition B-3 initiated by a P-040 lens. h is 12.7 mm.





SHOT 70:

Dynamic Fracture of Aluminum

Date:

August 18, 1964

Experimenter:

Douglas Venable

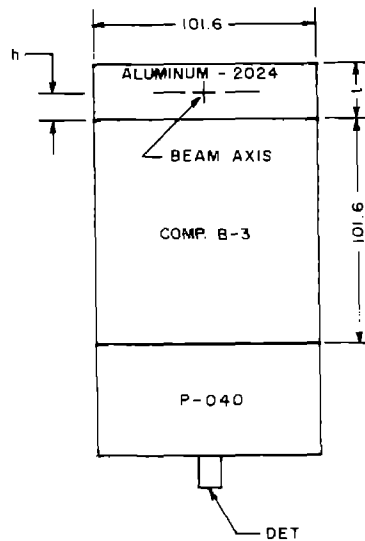
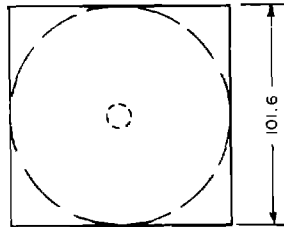
Radiographic Time:

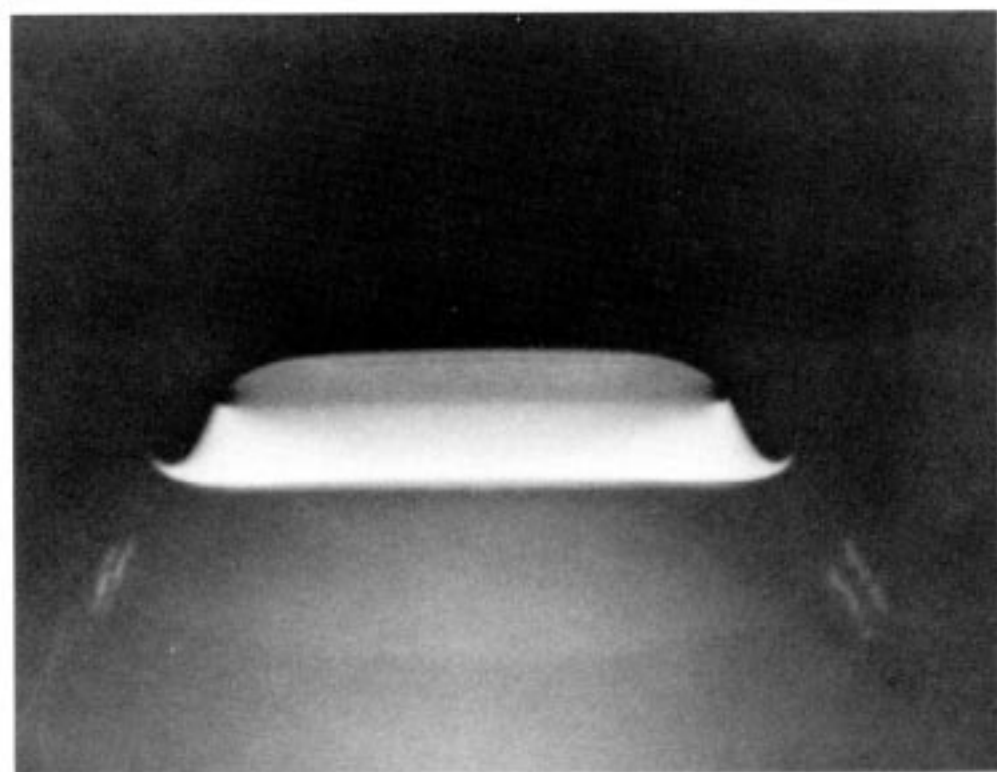
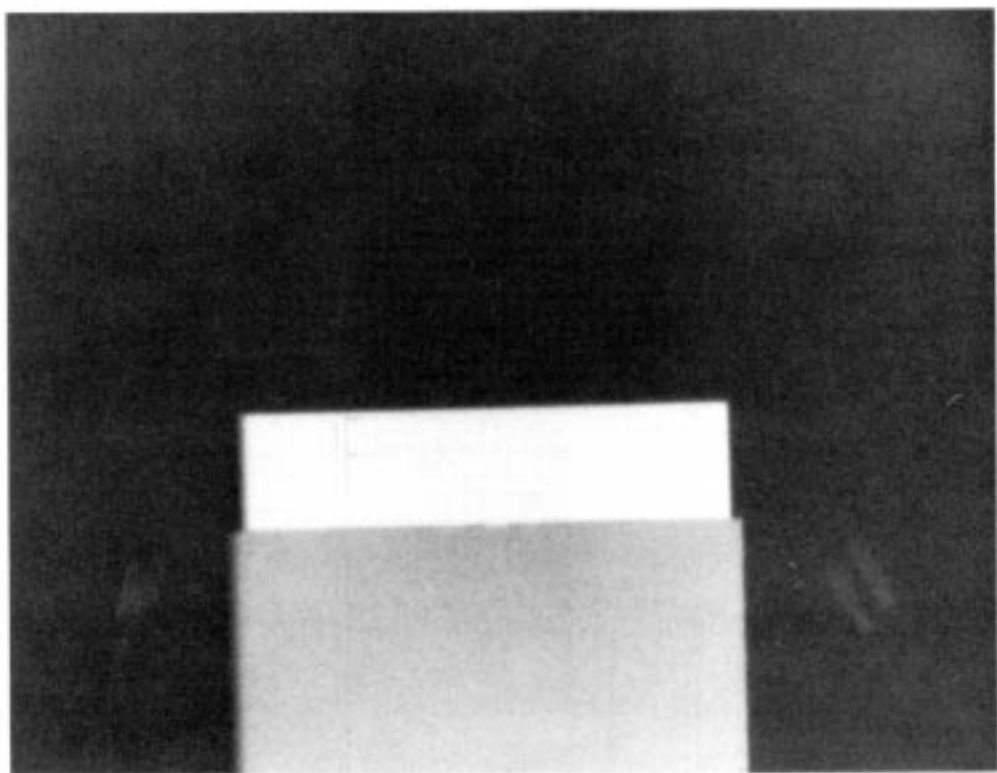
33.86 μ s

References:

Breed et al., 1967; Thurston and Mudd, 1968

Dynamic fracture of 24.6-mm-thick, *t*, 2024 aluminum. The plate is shocked by 101.6 mm of Composition B-3 initiated by a P-040 lens. *h* is 12.7 mm.





SHOT 71:

Two Offset Composition B-3 Detonations

Date:

August 11, 1964

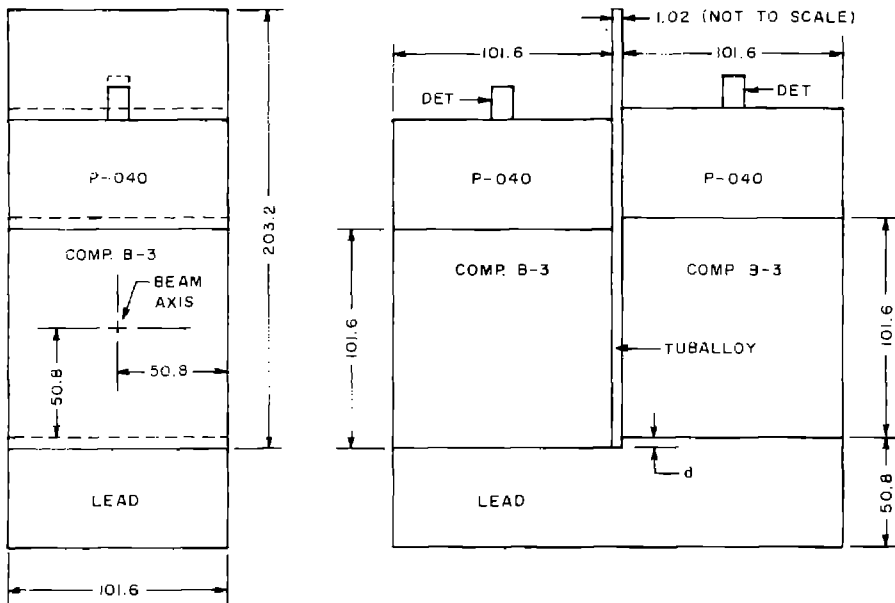
Experimenter:

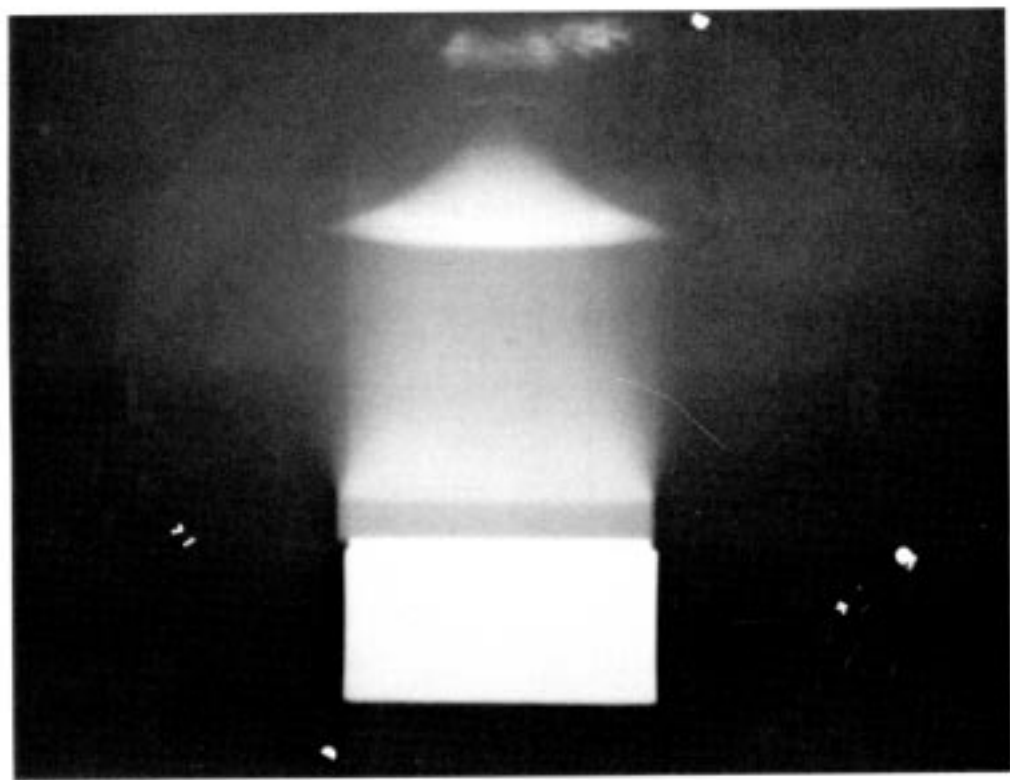
Douglas Venable

Radiographic Time:

24.53 μ s

Two Composition B-3 detonations separated by 1.02-mm-thick uranium and offset, d, 1.02 mm.





SHOT 72:

Two Offset Composition B-3 Detonations

Date:

August 11, 1964

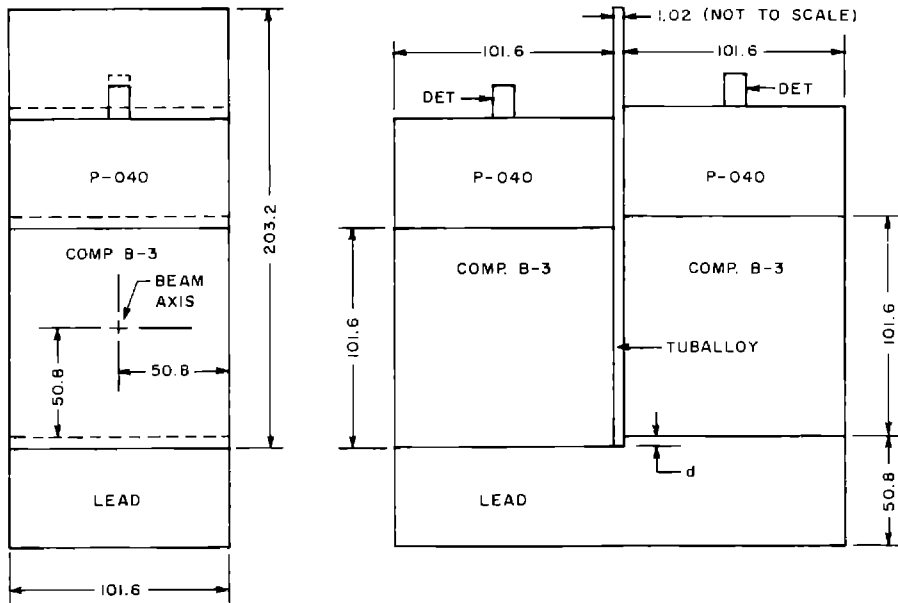
Experimenter:

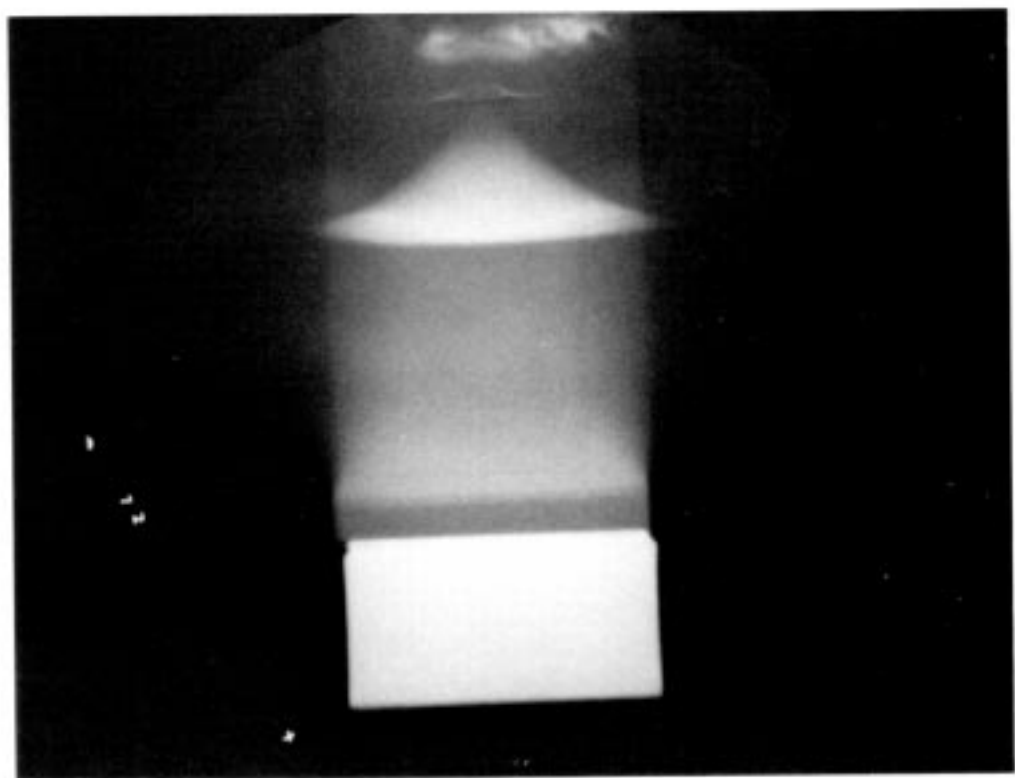
Douglas Venable

Radiographic Time:

24.52 μ s

Two Composition B-3 detonations separated by 1.02-mm-thick uranium and offset, d, 2.03 mm.





SHOT 73:

Two Offset Composition B-3 Detonations

Date:

August 11, 1964

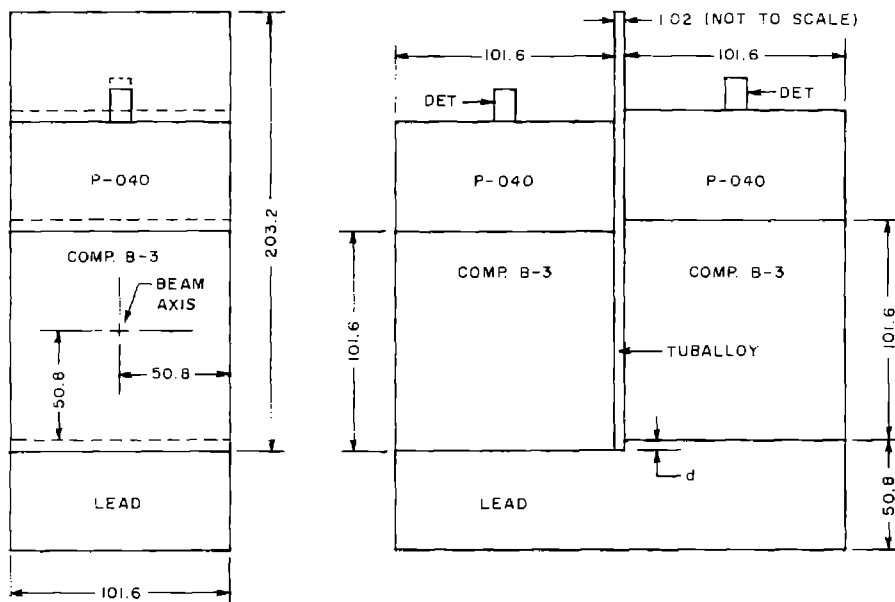
Experimenter:

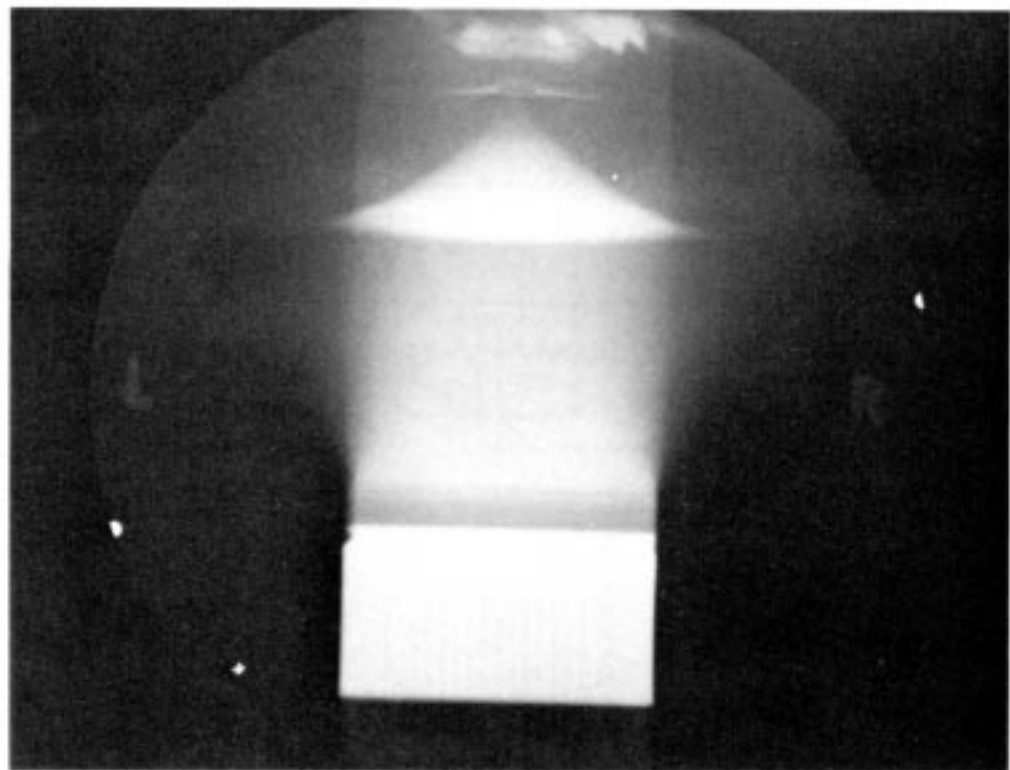
Douglas Venable

Radiographic Time:

24.49 μ s

Two Composition B-3 detonations separated by 1.02-mm-thick uranium and offset, d, 3.05 mm.





SHOT 74:

Uranium Jets

Date:

August 11, 1964

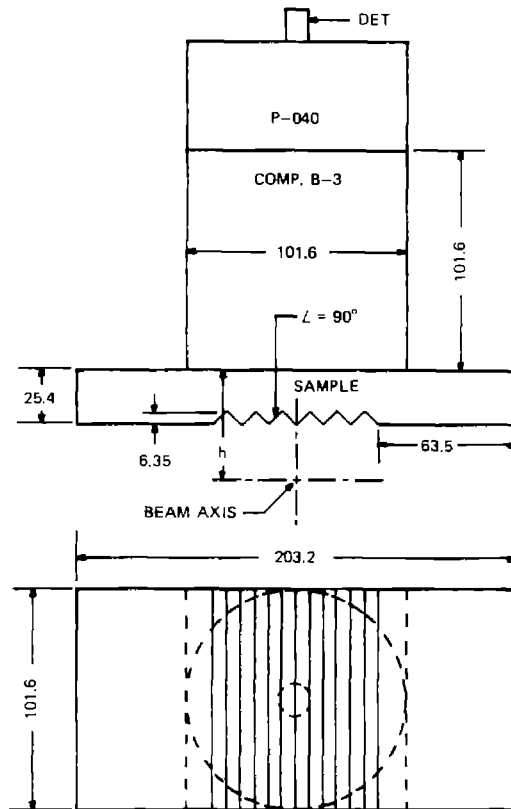
Experimenter:

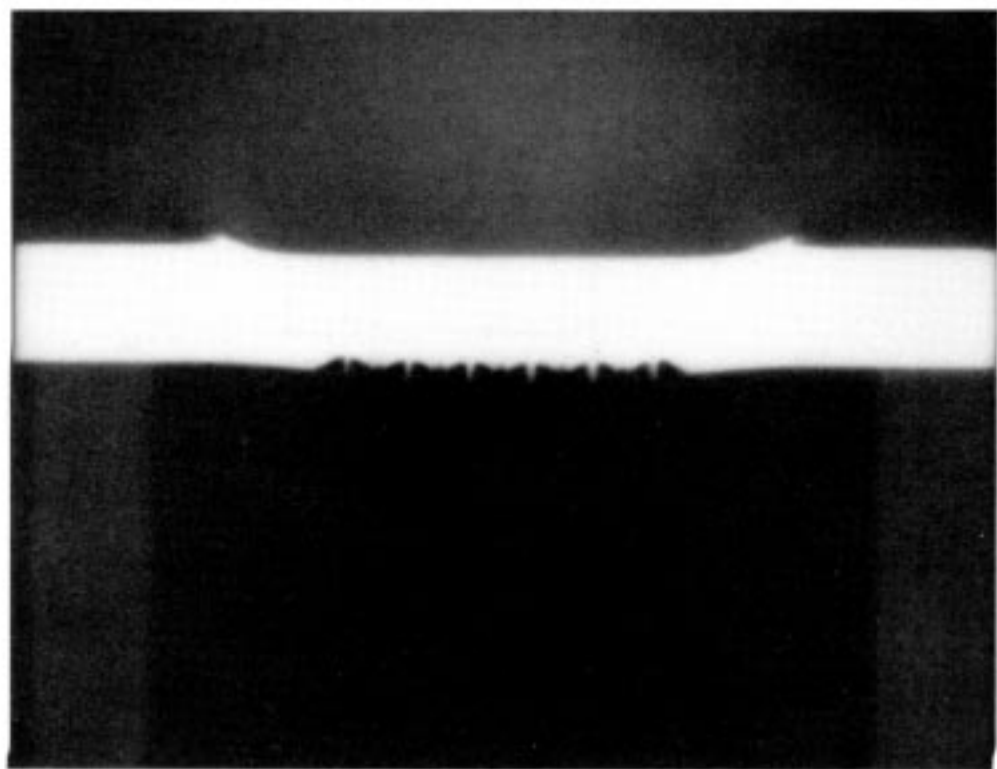
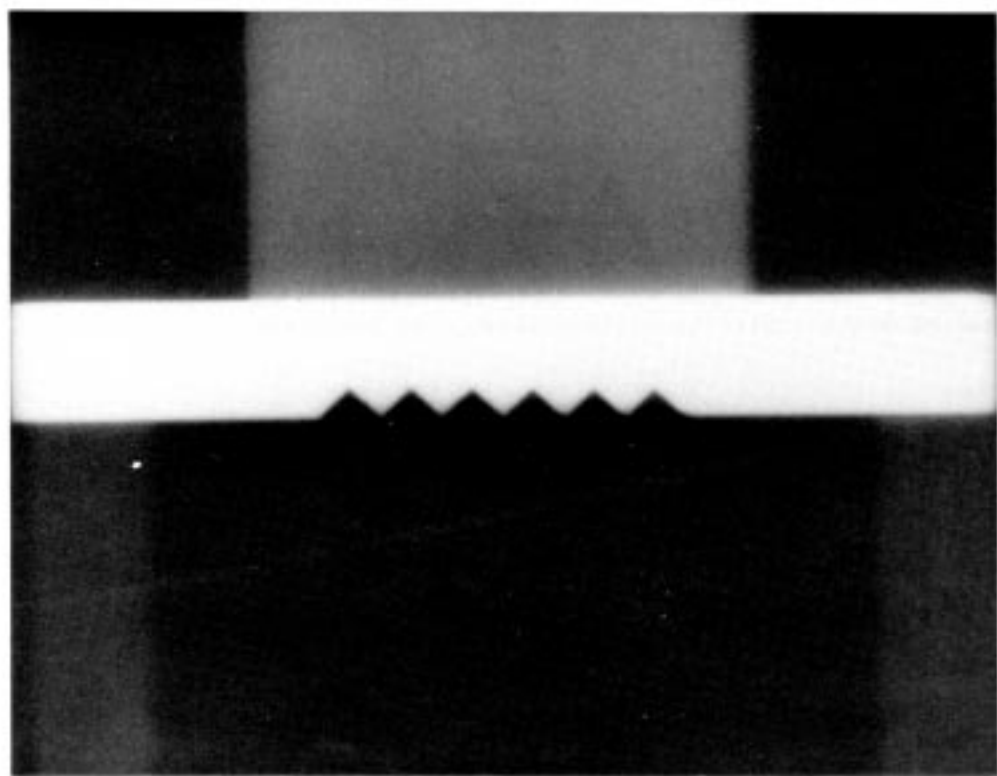
Douglas Venable

Radiographic Time:

35.9 μ s

Formation of metallic jets. The explosively induced shock wave in the uranium plate interacts with the grooves to produce the jets. h is 25.4 mm.





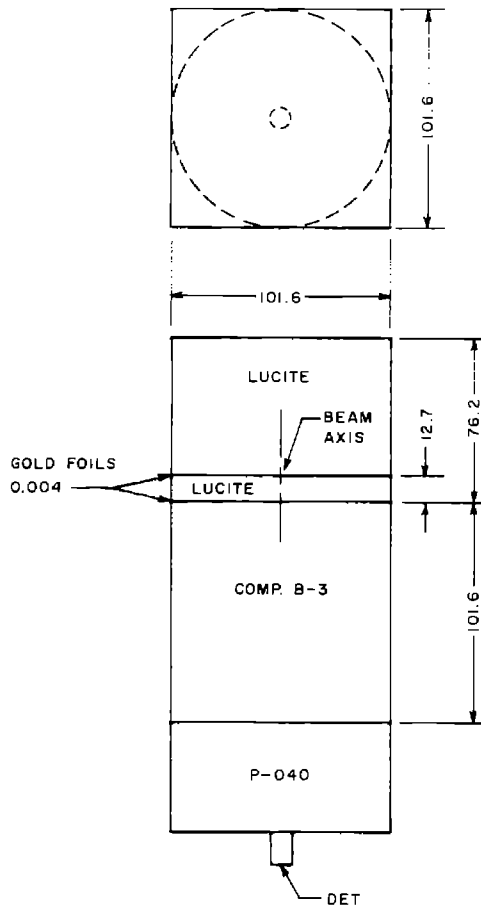
SHOT 75: Lucite Shock Wave

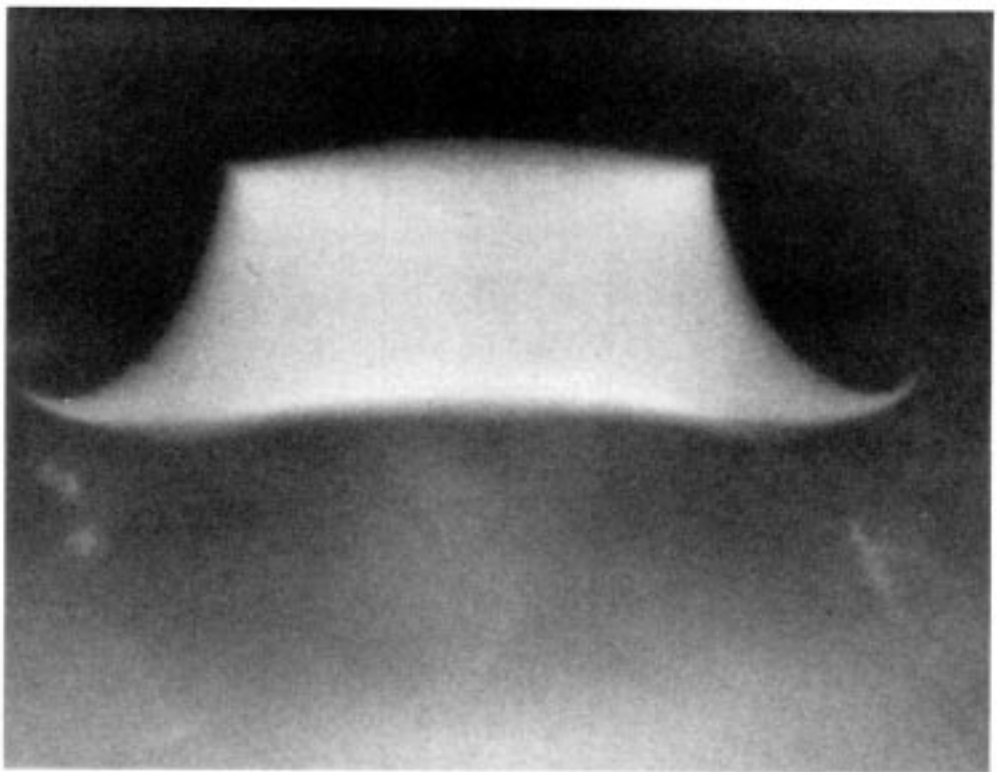
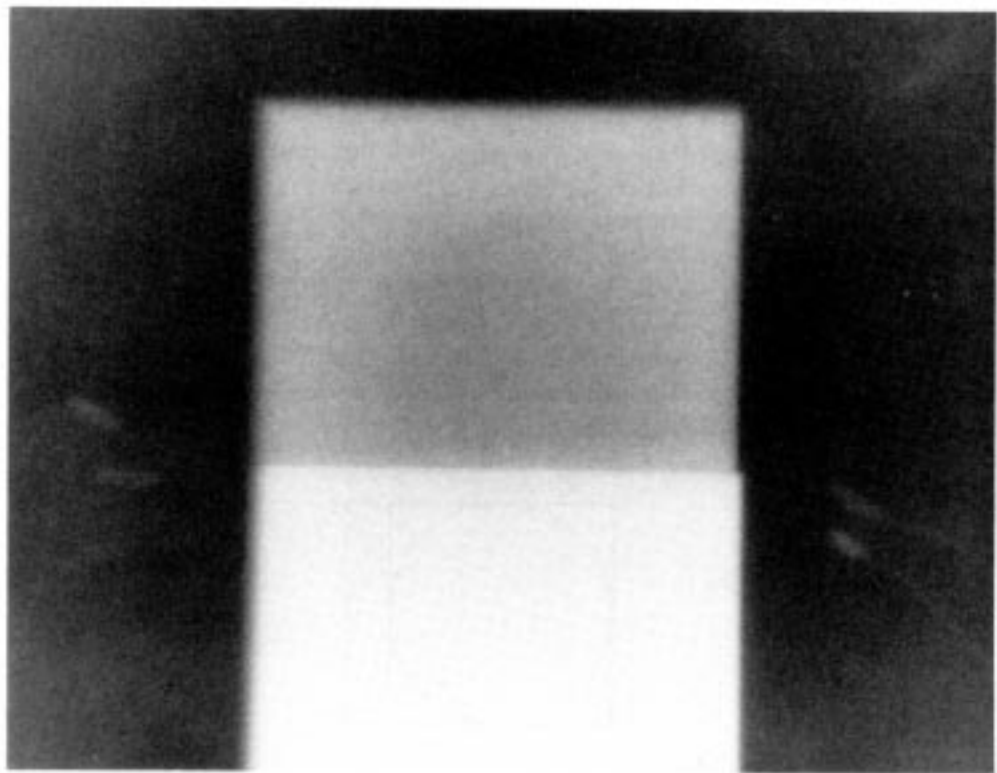
Date: August 19, 1964

Experimenter: Douglas Venable

Radiographic Time: 42.37 μ s

The shock wave formed in Lucite by a Composition B-3 detonation wave. The resulting deformation of the Lucite block could not be examined using gold foils.





SHOT 76:

Dynamic Fracture of Aluminum

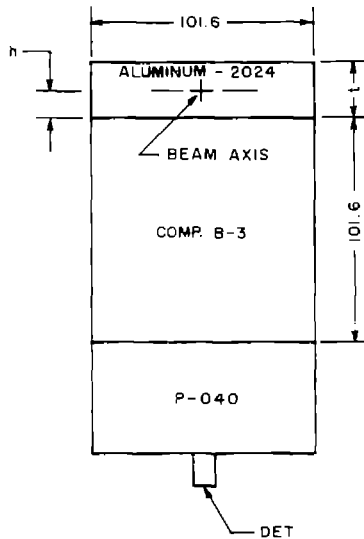
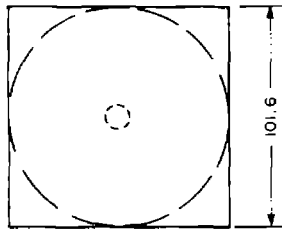
Date: August 25, 1964

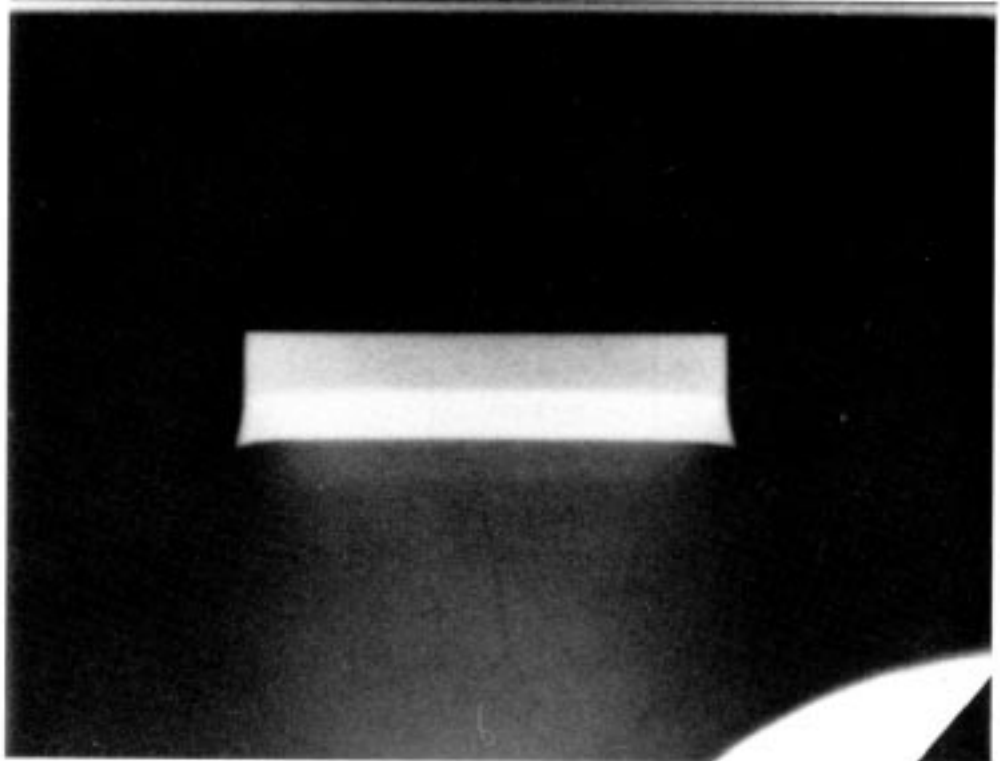
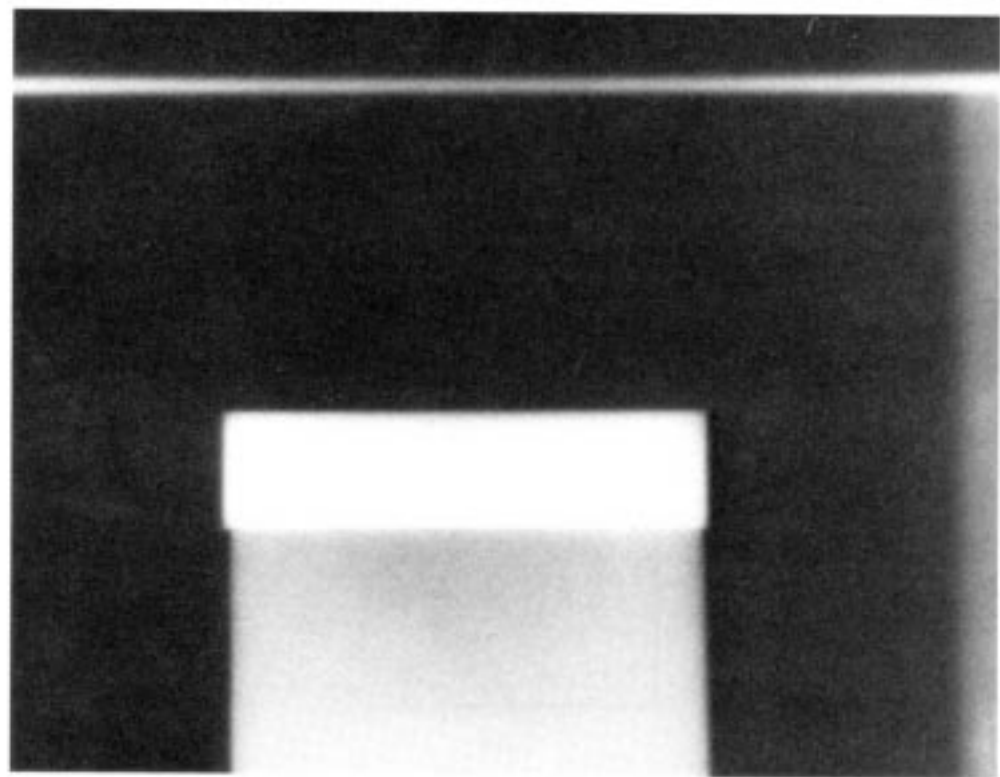
Experimenter: Douglas Venable

Radiographic Time: 28.0 μ s

References: Venable, 1965; Breed et al., 1967; Thurston and Mudd, 1968

Dynamic fracture of 25.1-mm-thick, t, 2024 aluminum. The plate is shocked by 101.6 mm of Composition B-3 initiated by a P-040 lens. h is 12.7 mm. The shock wave is about half way through the aluminum.





SHOT 77:

Dynamic Fracture of Aluminum

Date:

August 25, 1964

Experimenter:

Douglas Venable

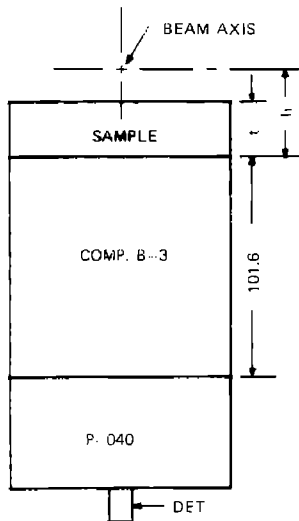
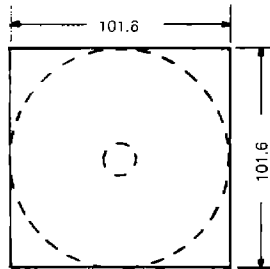
Radiographic Time:

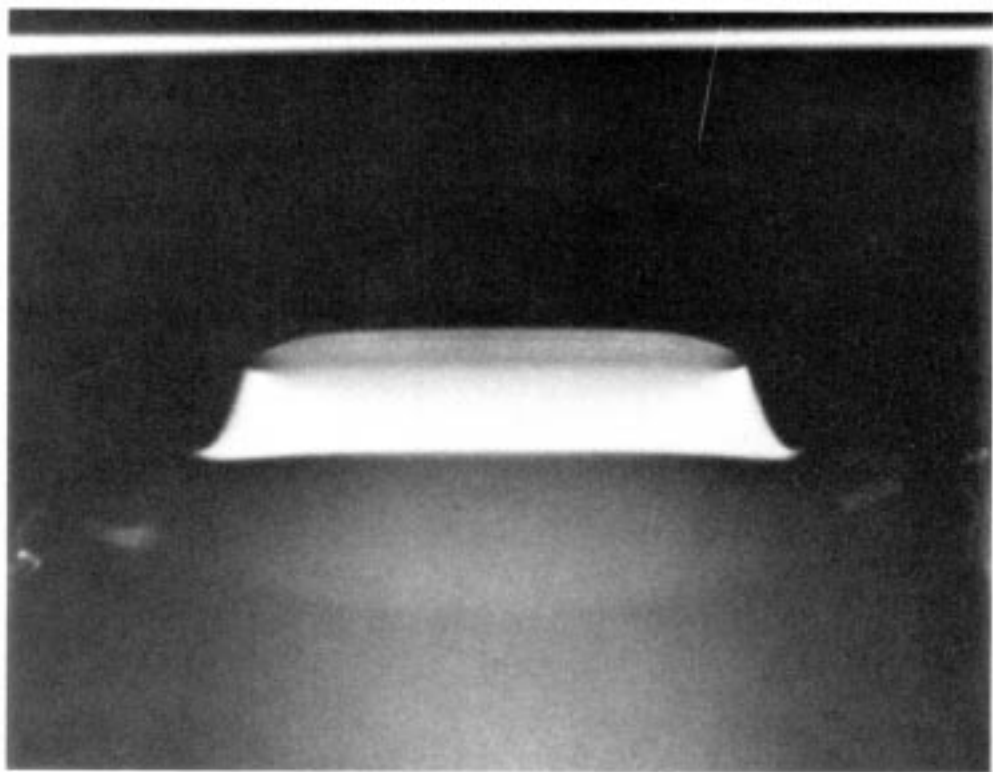
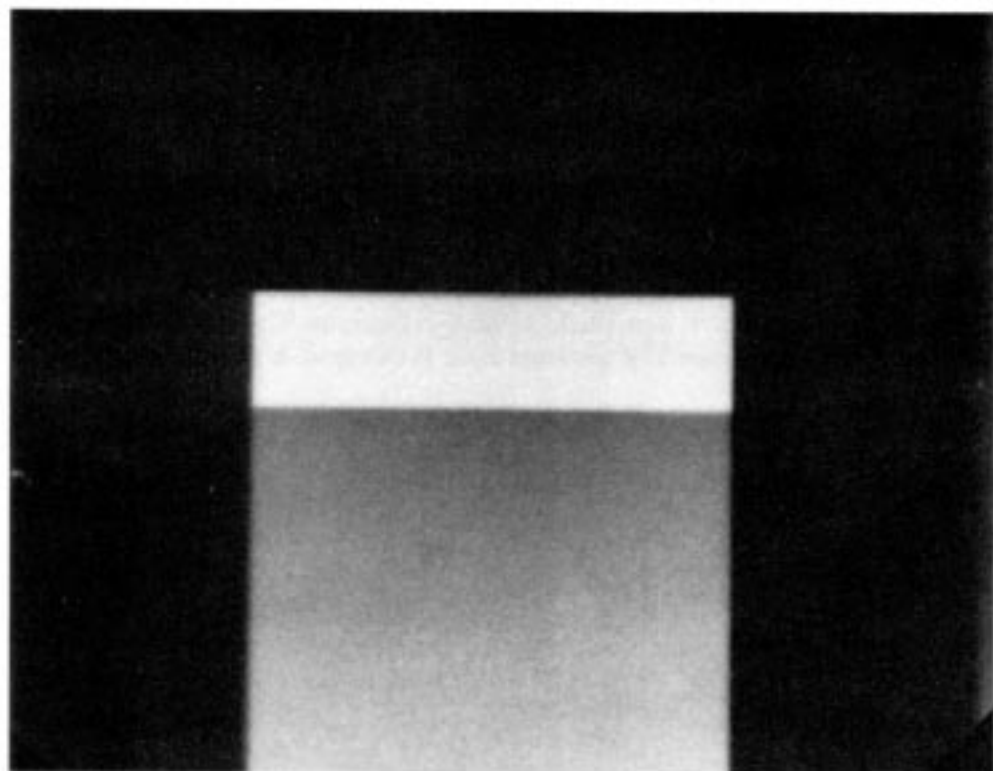
32.92 μ s

References:

Breed et al., 1967; Thurston and Mudd, 1968

Dynamic fracture of 25.0-mm-thick, t , 2024 aluminum. The plate is shocked by 101.6 mm of Composition B-3 initiated by a P-040 lens. h is 31.8 mm.





SHOT 78:

Dynamic Fracture of Aluminum

Date:

August 25, 1964

Experimenter:

Douglas Venable

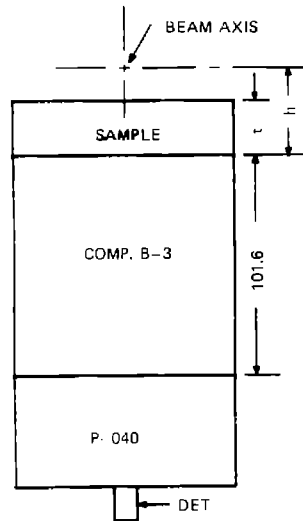
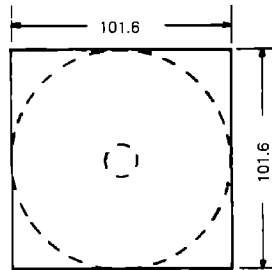
Radiographic Time:

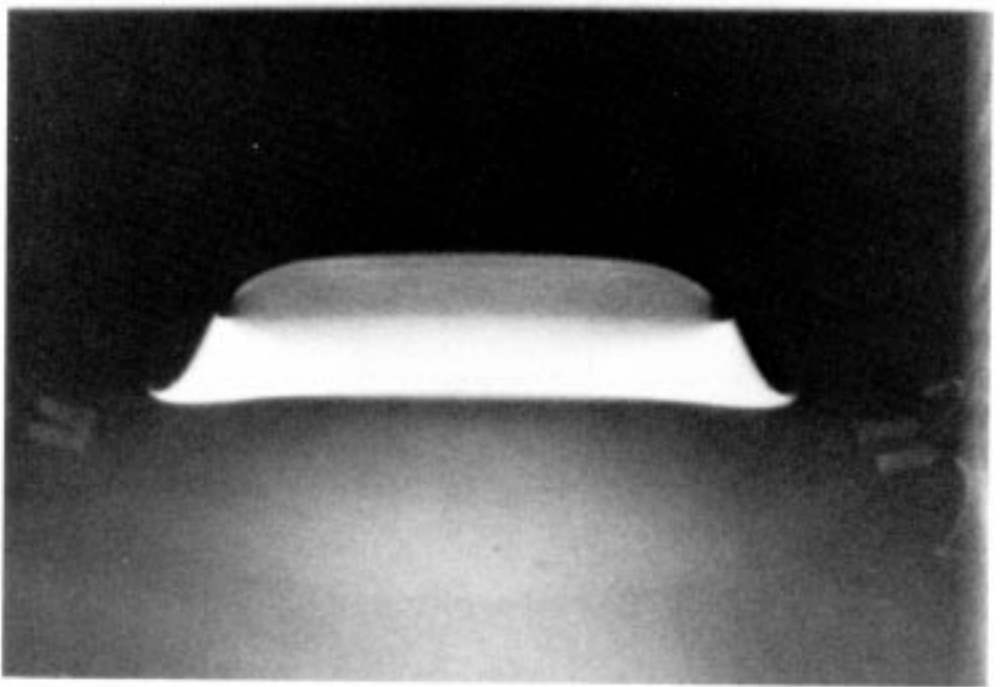
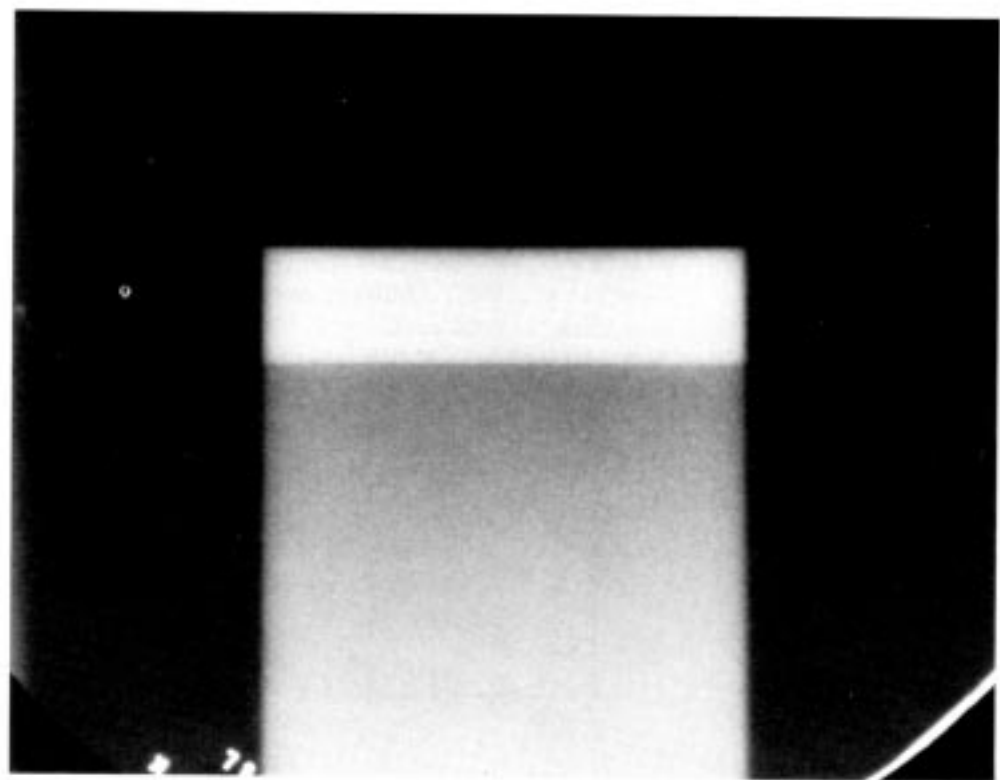
32.93 μ s

References:

Breed et al., 1967; Thurston and Mudd, 1968

Dynamic fracture of 25.0-mm-thick, t , 2024 aluminum. The plate is shocked by 101.6 mm of Composition B-3 initiated by a P-040 lens. h is 38.1 mm.





SHOT 79:

Dynamic Fracture of Aluminum

Date:

September 1, 1964

Experimenter:

Douglas Venable

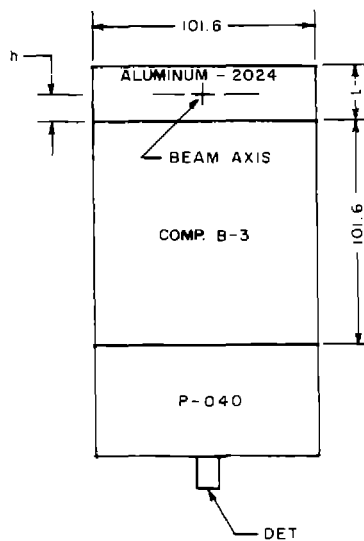
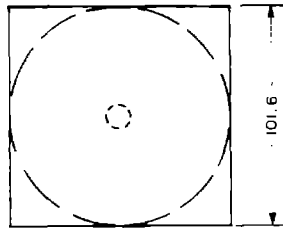
Radiographic Time:

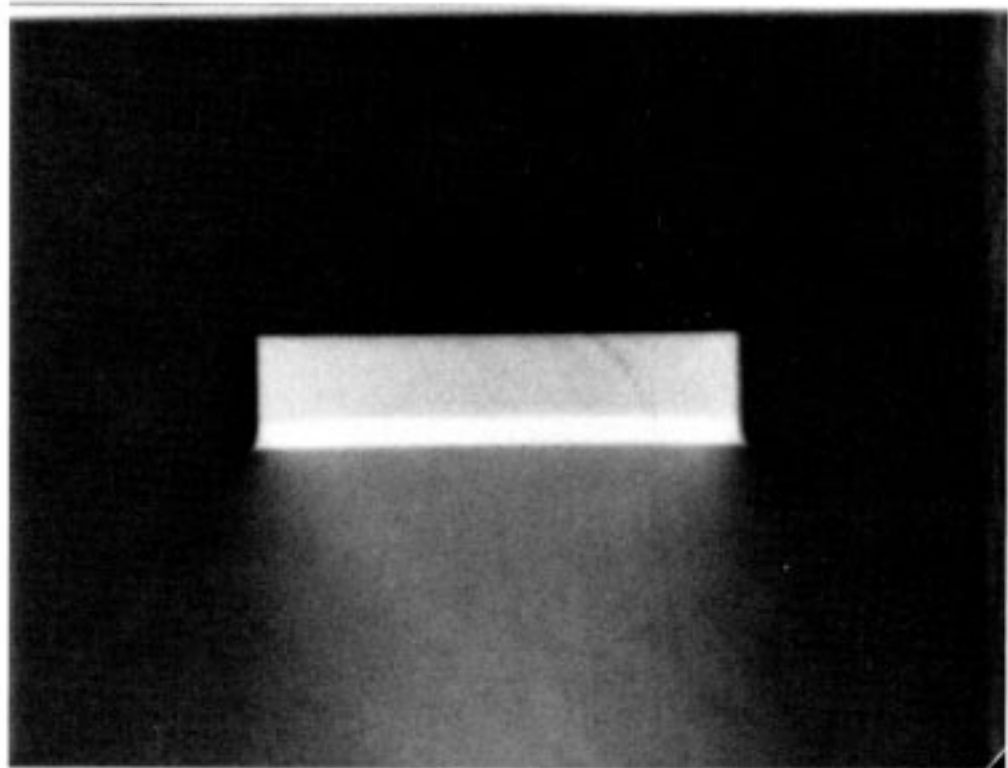
27.33 μ s

References:

Breed et al., 1967; Thurston and Mudd, 1968

Dynamic fracture of 25.1-mm-thick, t, 2024 aluminum. The plate is shocked by 101.6 mm of Composition B-3 initiated by a P-040 lens. h is 6.4 mm. The shock wave is about one-fourth through the aluminum.





SHOT 80:

Dynamic Fracture of Aluminum

Date:

September 1, 1964

Experimenter:

Douglas Venable

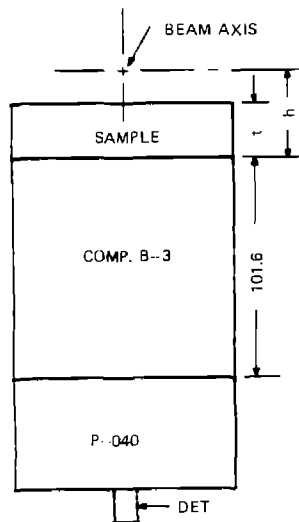
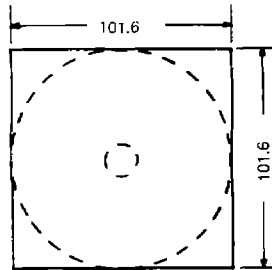
Radiographic Time:

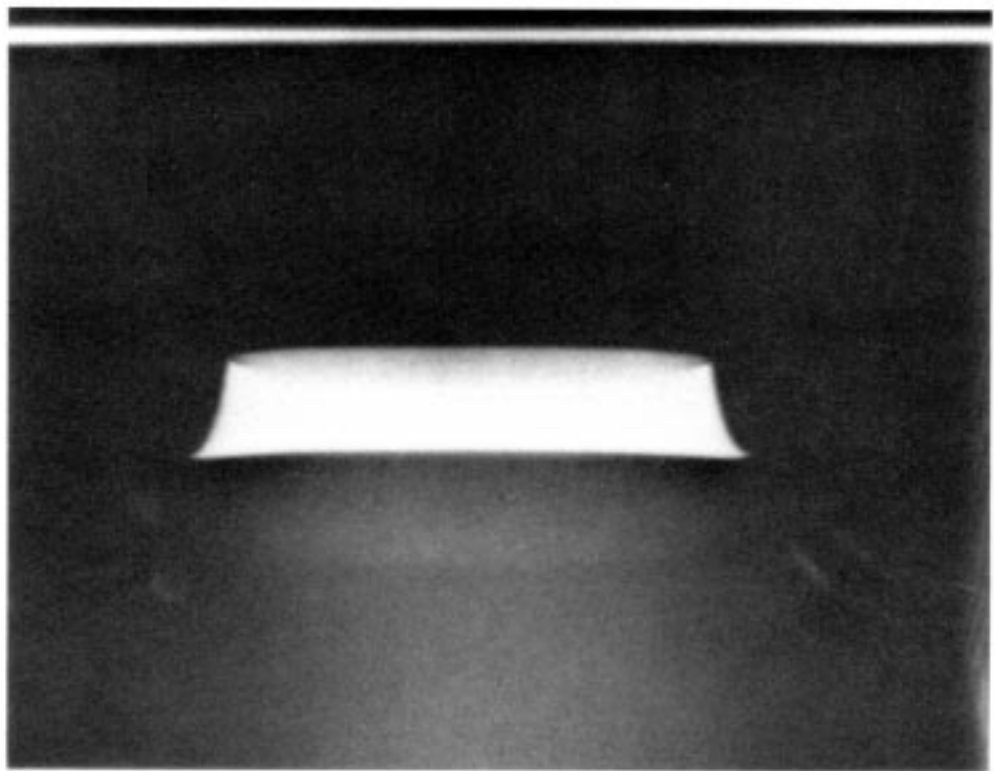
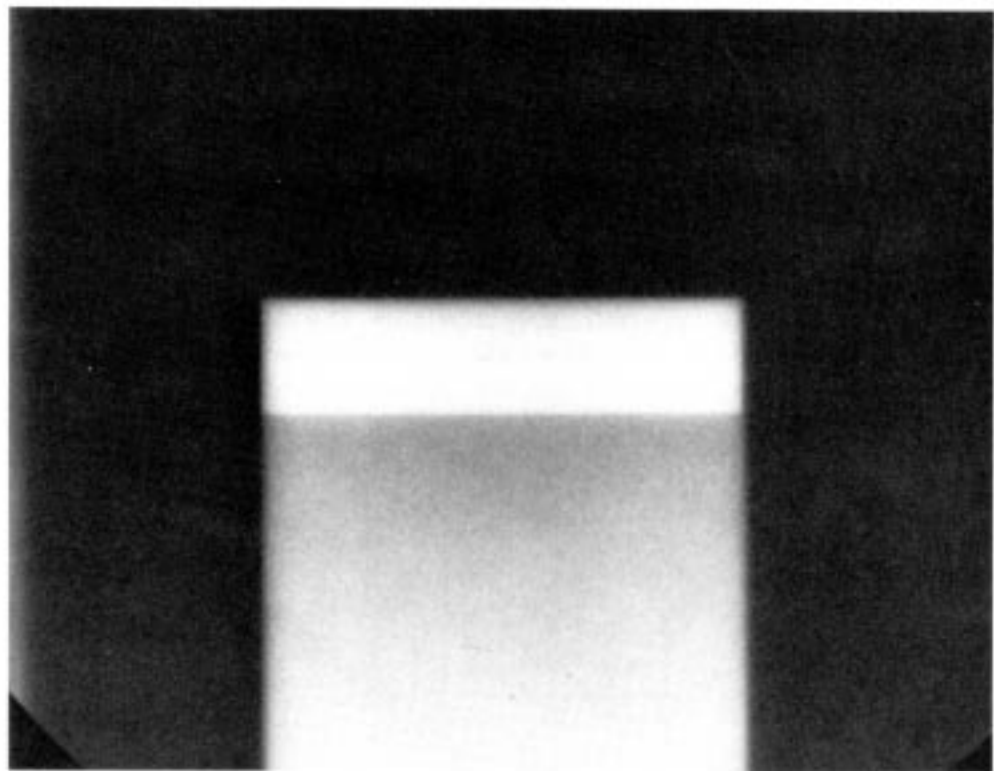
30.87 μ s

References:

Breed et al., 1967; Thurston and Mudd, 1968

Dynamic fracture of 25.0-mm-thick, t , 2024 aluminum. The plate is shocked by 101.6 mm of Composition B-3 initiated by a P-040 lens. h is 31.8 mm.





SHOT 81:

Dynamic Fracture of Aluminum

Date:

September 1, 1964

Experimenter:

Douglas Venable

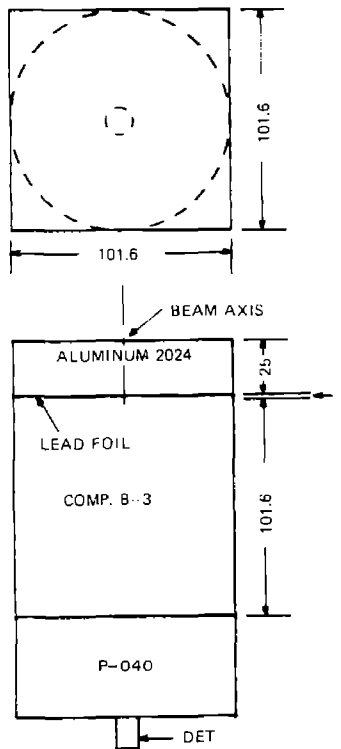
Radiographic Time:

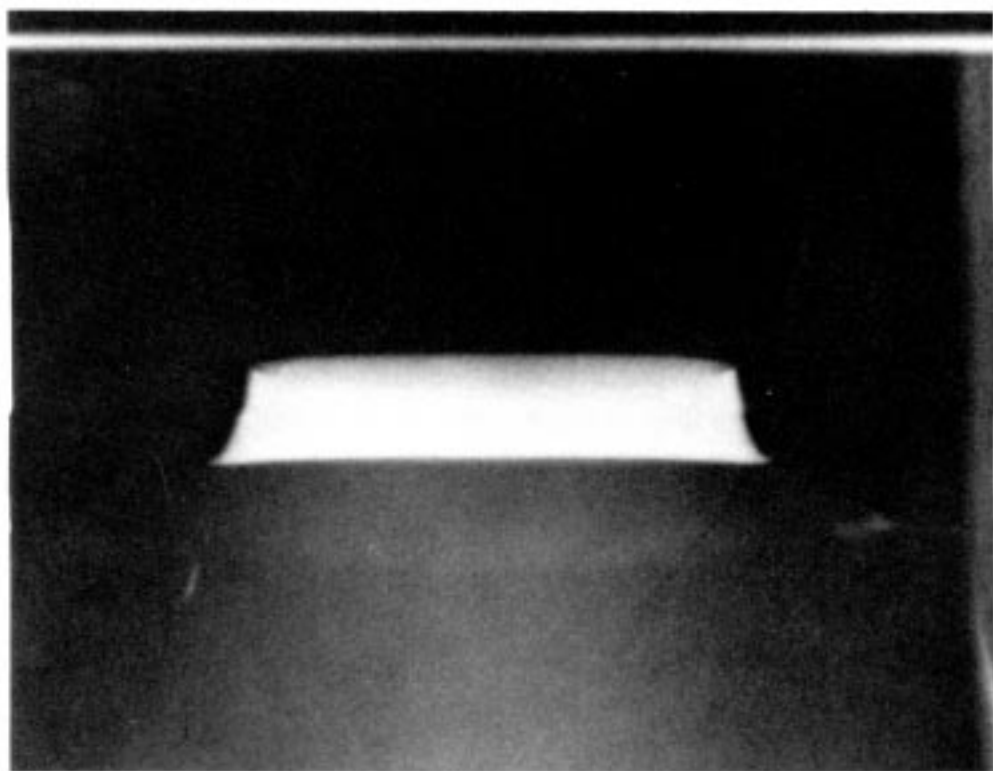
30.86 μ s

References:

Breed et al., 1967; Thurston and Mudd, 1968

Dynamic fracture of 25.0-mm-thick 2024 aluminum. The plate is shocked by 101.6 mm of Composition B-3 initiated by a P-040 lens. There is a 0.05-mm-thick, t , lead foil between the Composition B-3 and the aluminum plate.





SHOT 82: Dynamic Fracture of Aluminum

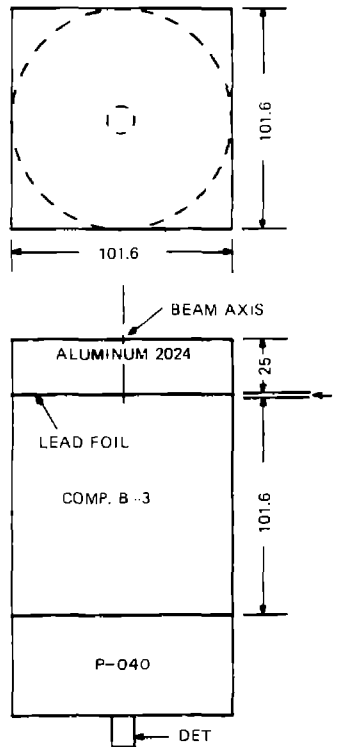
Date: September 15, 1964

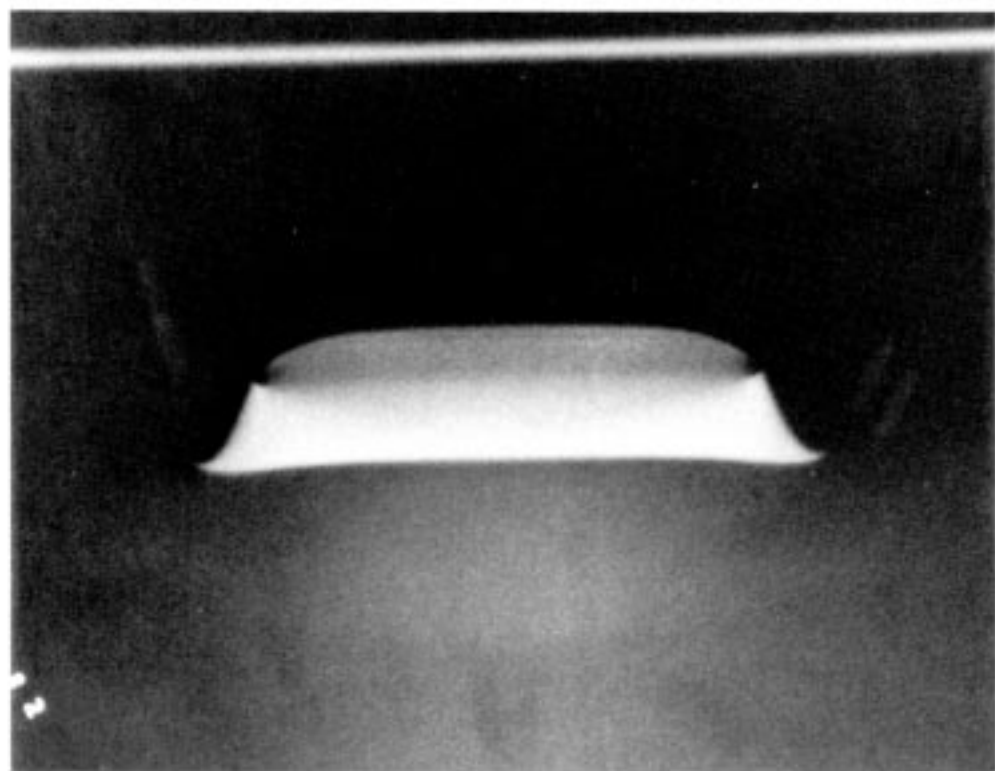
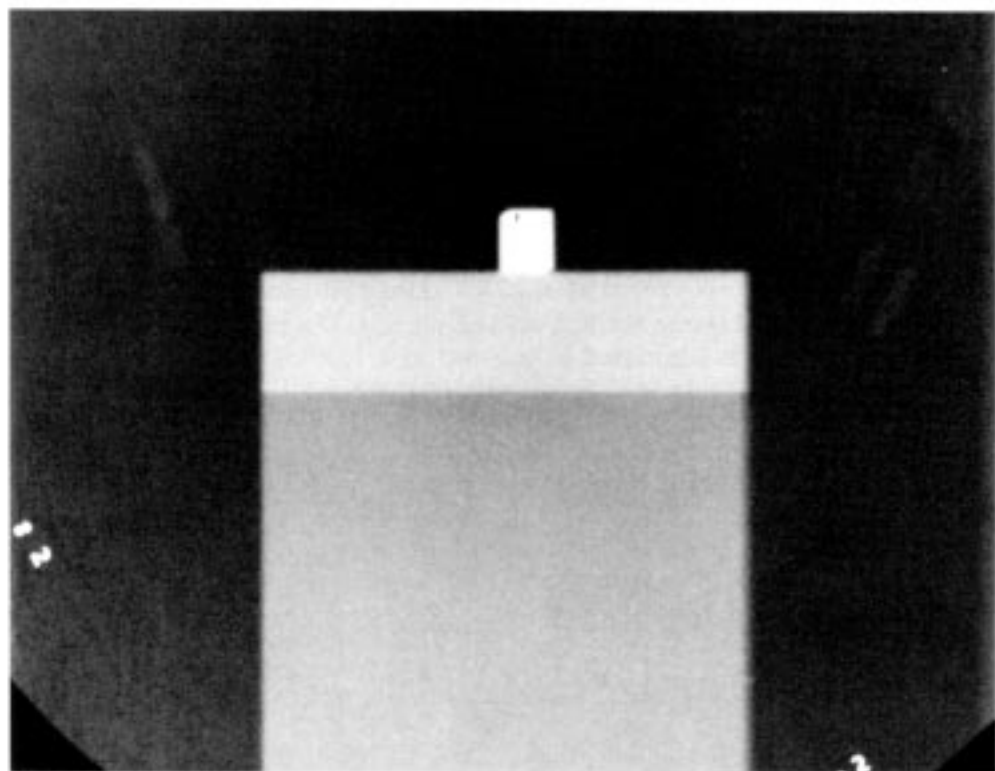
Experimenter: Douglas Venable

Radiographic Time: 33.94 μ s

References: Breed et al., 1967; Thurston and Mudd, 1968

Dynamic fracture of 25.0-mm-thick 2024 aluminum. The plate is shocked by 101.6 mm of Composition B-3 initiated by a P-040 lens. There is a 0.05-mm-thick, t , lead foil between the Composition B-3 and the aluminum plate.





SHOT 83: Dynamic Fracture of Aluminum

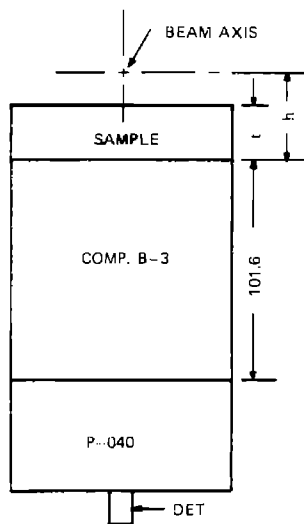
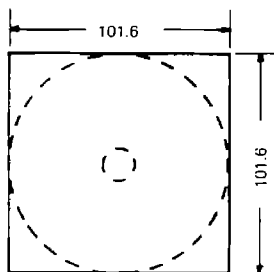
Date: September 15, 1964

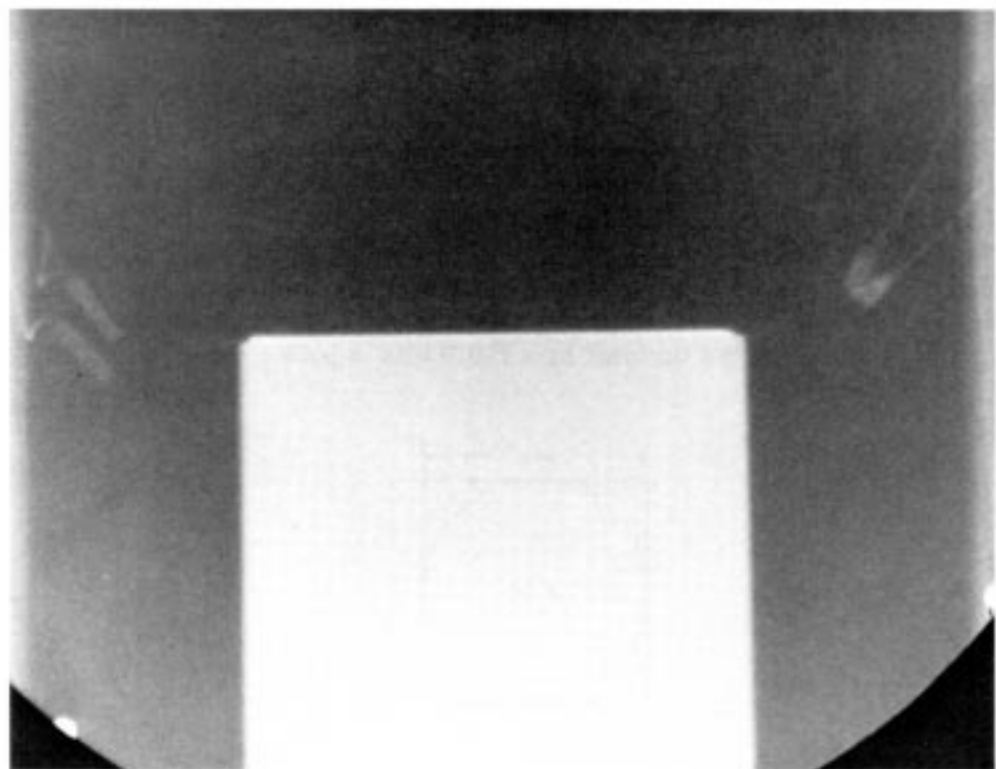
Experimenter: Douglas Venable

Radiographic Time: 30.53 μ s

References: Breed et al., 1967; Thurston and Mudd, 1968

Dynamic fracture of 1.0-mm-thick, t , 2024 aluminum. The plate is shocked by 101.6 mm of Composition B-3 initiated by a P-040 lens. h is 25.4 mm.





SHOT 84: Dynamic Fracture of Aluminum

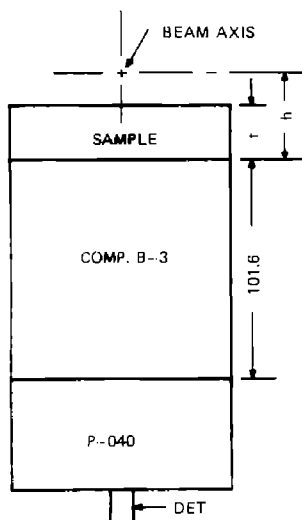
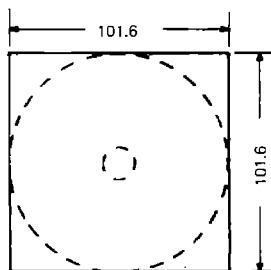
Date: September 15, 1964

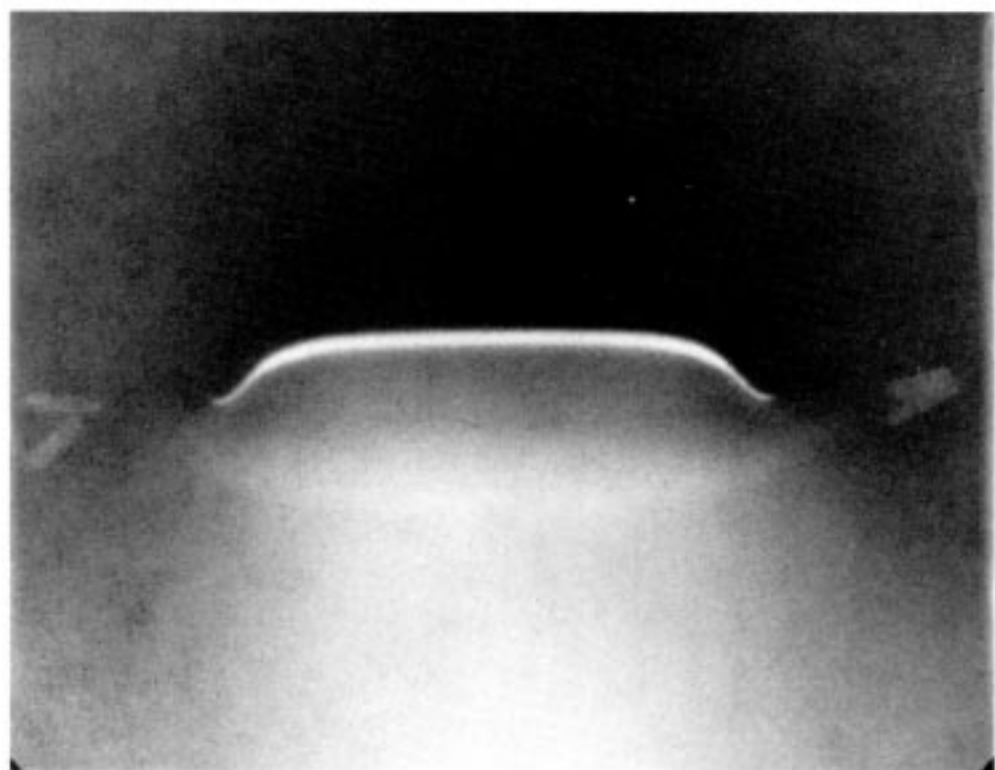
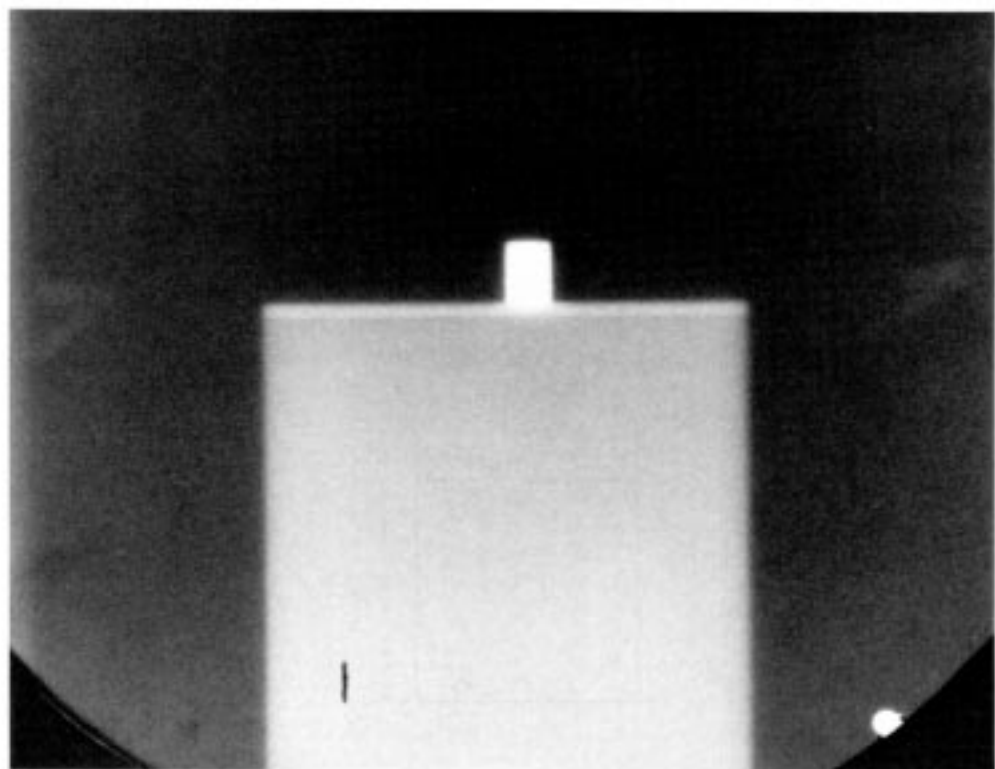
Experimenter: Douglas Venable

Radiographic Time: 30.74 μ s

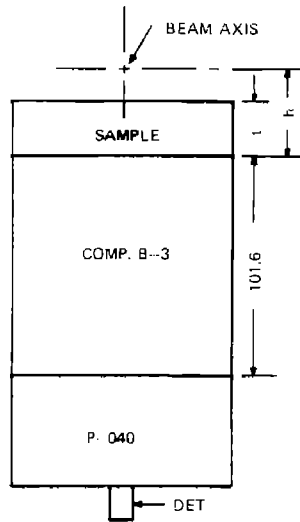
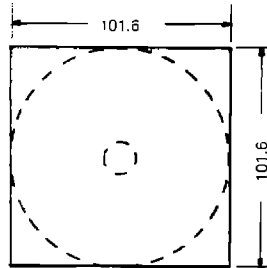
References: Breed et al., 1967; Thurston and Mudd, 1968

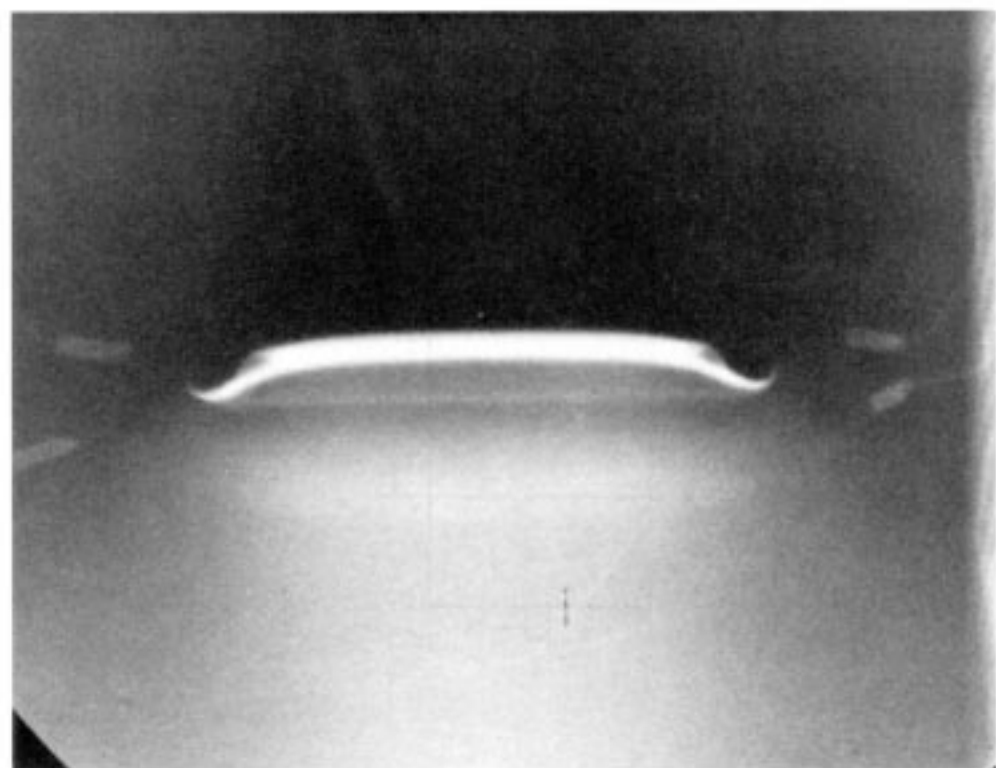
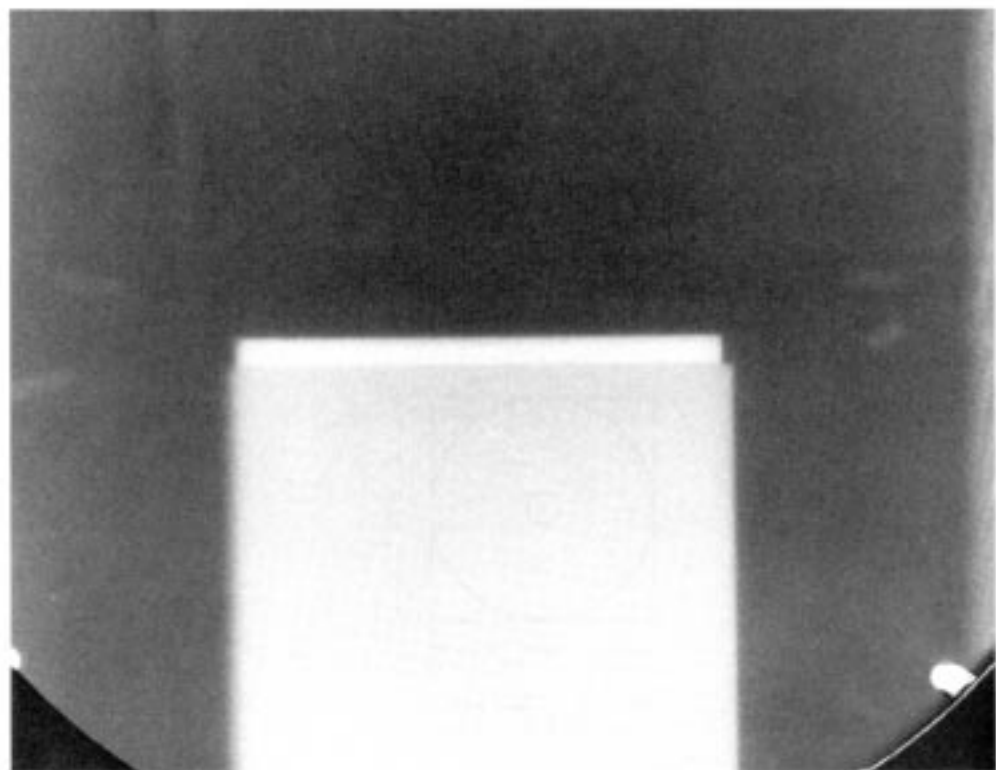
Dynamic fracture of 3.0-mm-thick, t, 2024 aluminum. The plate is shocked by 101.6 mm of Composition B-3 initiated by a P-040 lens. h is 25.4 mm.





SHOT 85: Dynamic Fracture of Aluminum
Date: September 15, 1964
Experimenter: Douglas Venable
Radiographic Time: 31.18 μ s
References: Breed et al., 1967; Thurston and Mudd, 1968
Dynamic fracture of 6.0-mm-thick, t, 2024 aluminum. The plate is shocked by 101.6 mm of Composition B-3 initiated by a P-040 lens. h is 25.4 mm.





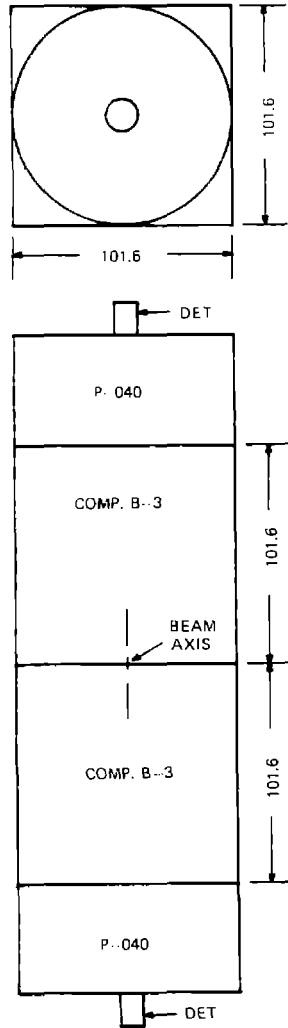
SHOT 86: Colliding Composition B-3 Detonations

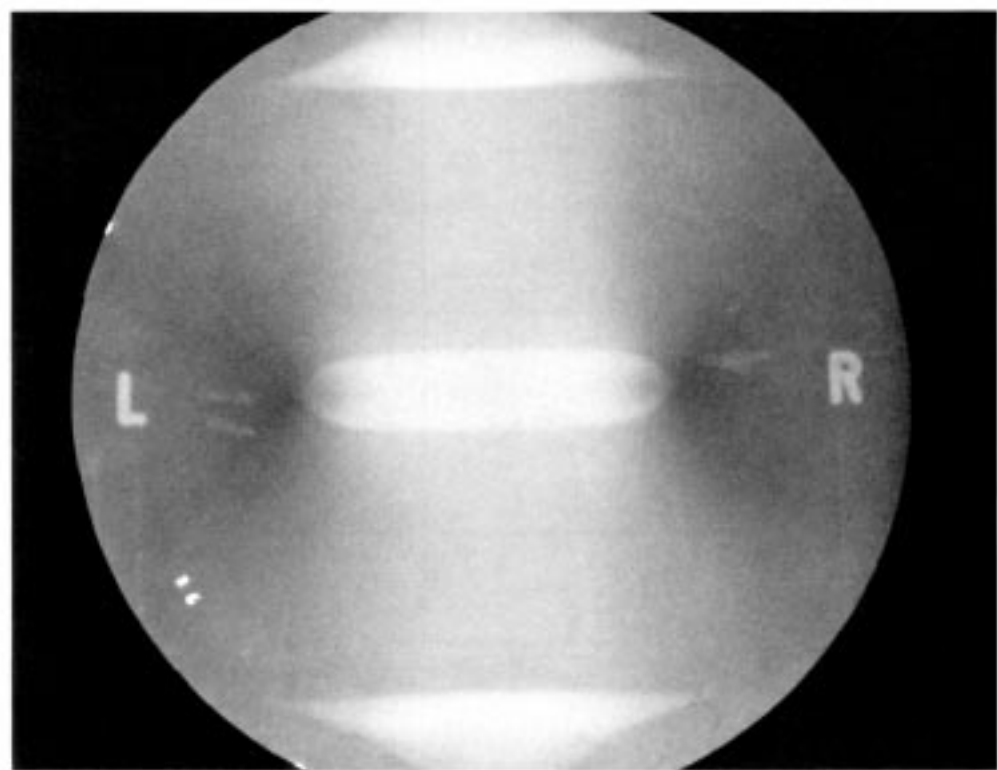
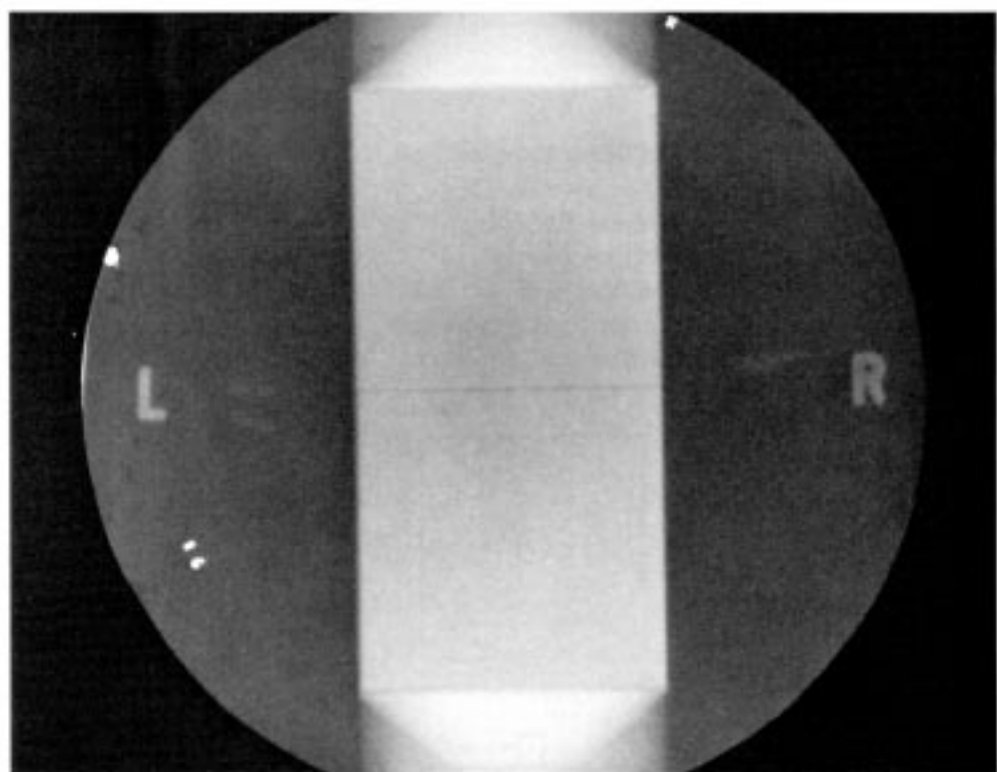
Date: September 22, 1964

Experimenter: Douglas Venable

Radiographic Time: 28.42 μ s

The reflected shocks in Composition B-3 detonation products 2.0 μ s after collision of the detonation waves. See Shots 87, 91, 92, and 273-277.





SHOT 87:

Colliding Composition B-3 Detonations

Date:

September 22, 1964

Experimenter:

Douglas Venable

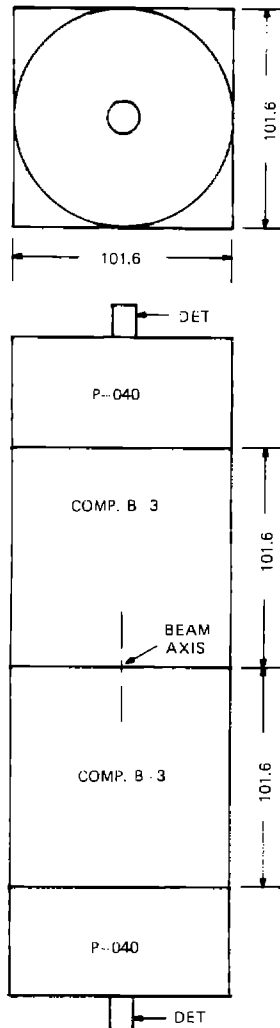
Radiographic Time:

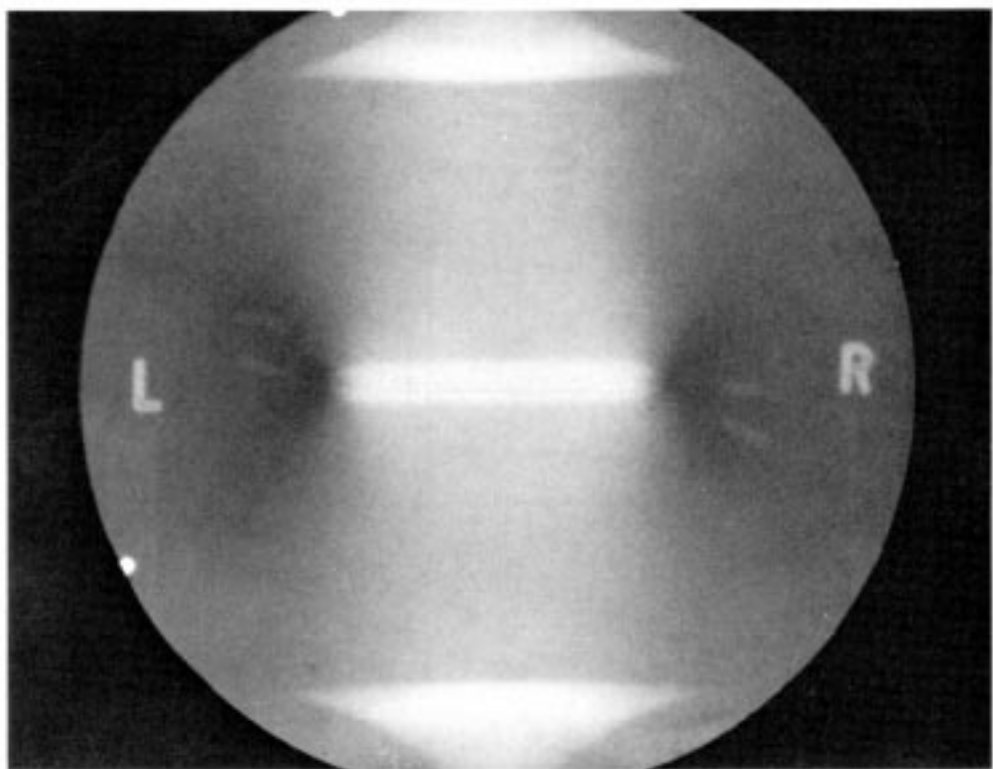
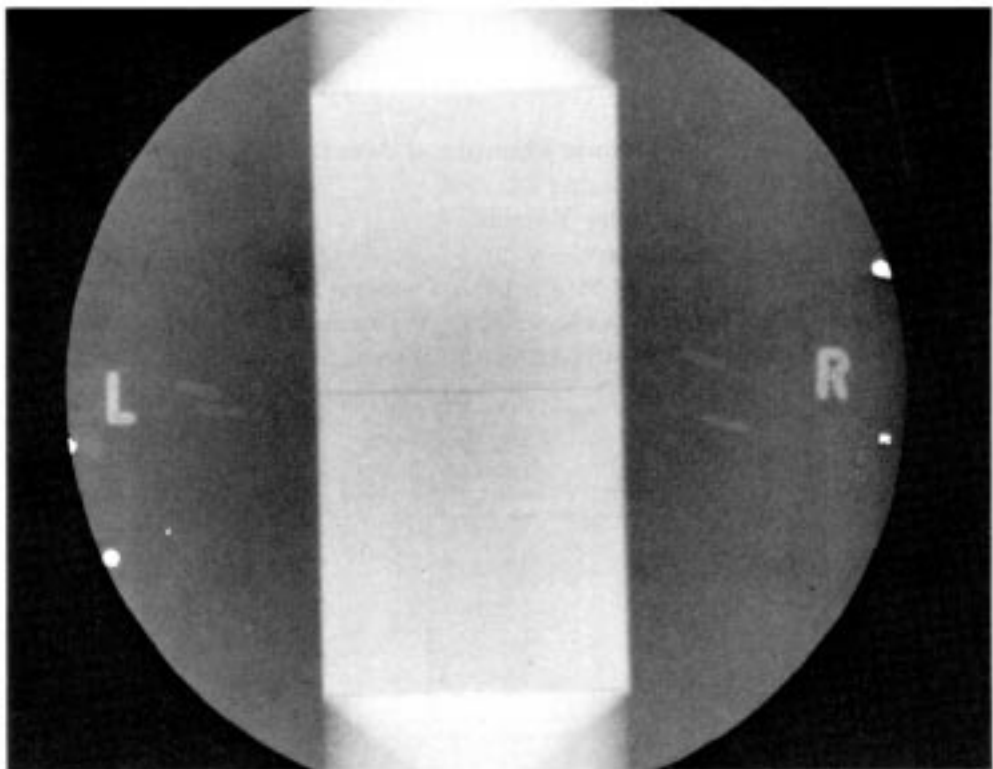
27.41 μ s

Reference:

Venable, 1965

The reflected shocks in Composition B-3 detonation products 1.0 μ s after collision of the detonation waves. See Shots 86, 91, 92, and 273-277.





SHOT 88:

Dynamic Fracture of Aluminum

Date:

September 22, 1964

Experimenter:

Douglas Venable

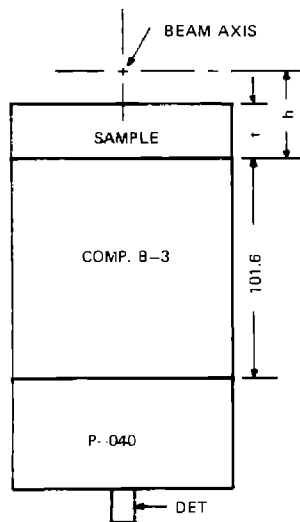
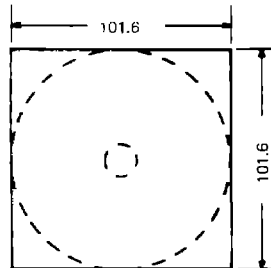
Radiographic Time:

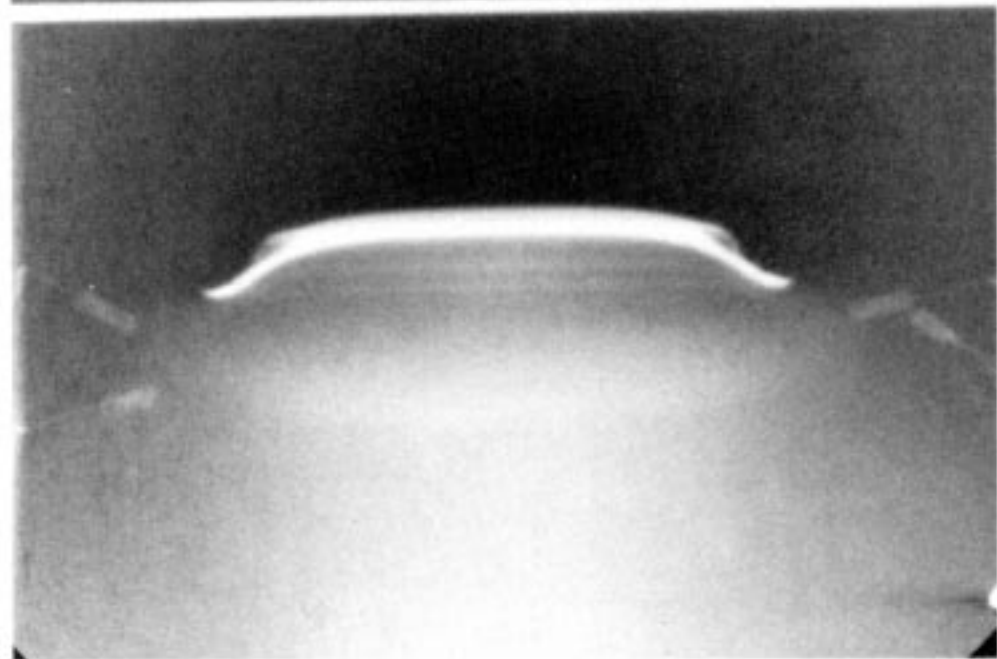
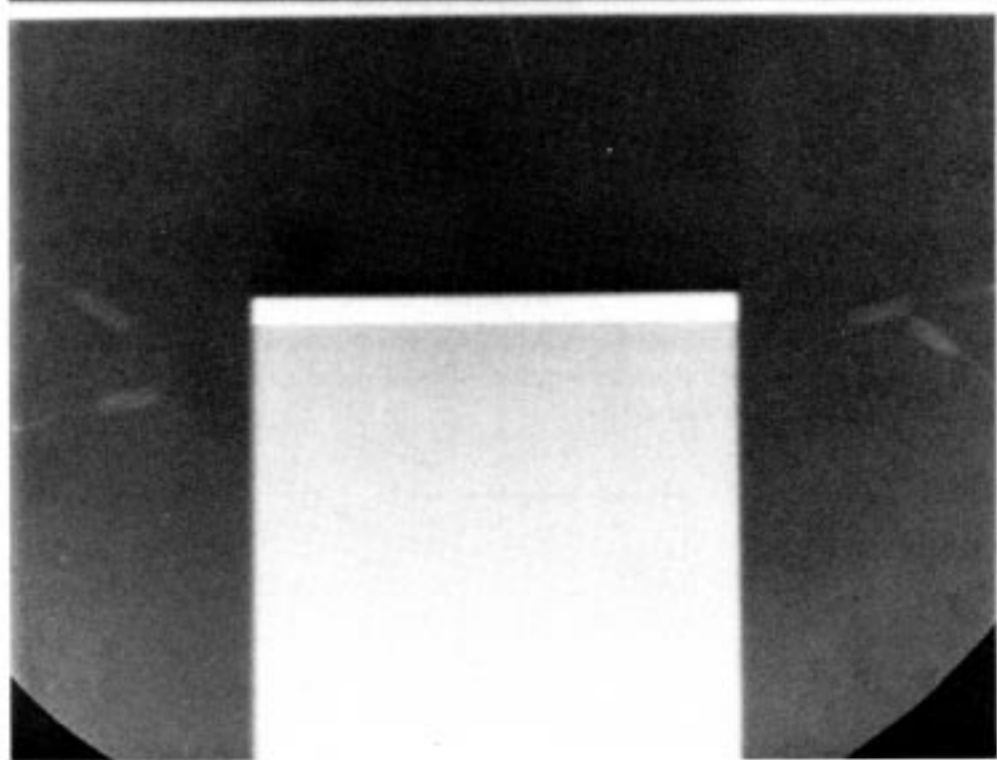
32.0 μ s

References:

Breed et al., 1967; Thurston and Mudd, 1968

Dynamic fracture of 6.0-mm-thick, t , 2024 aluminum. The plate is shocked by 101.6 mm of Composition B-3 initiated by a P-040 lens. h is 25.4 mm. The free surface of the plate has run 4 μ s.





SHOT 89:

Dynamic Fracture of Aluminum

Date:

September 22, 1964

Experimenter:

Douglas Venable

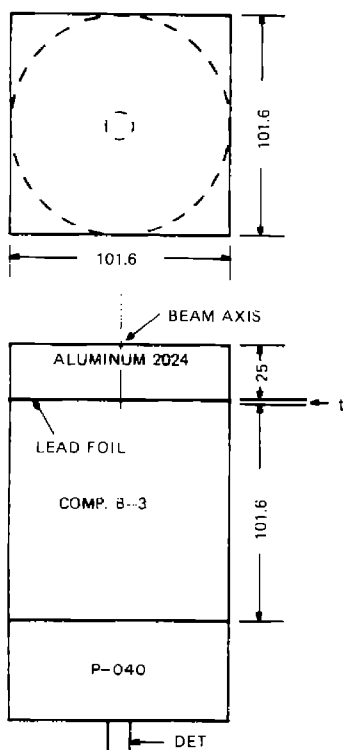
Radiographic Time:

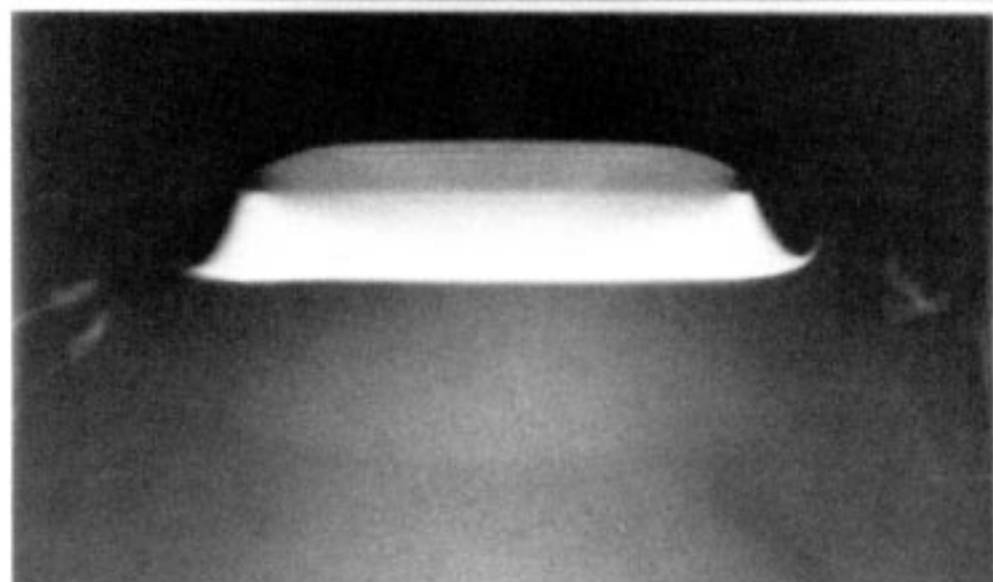
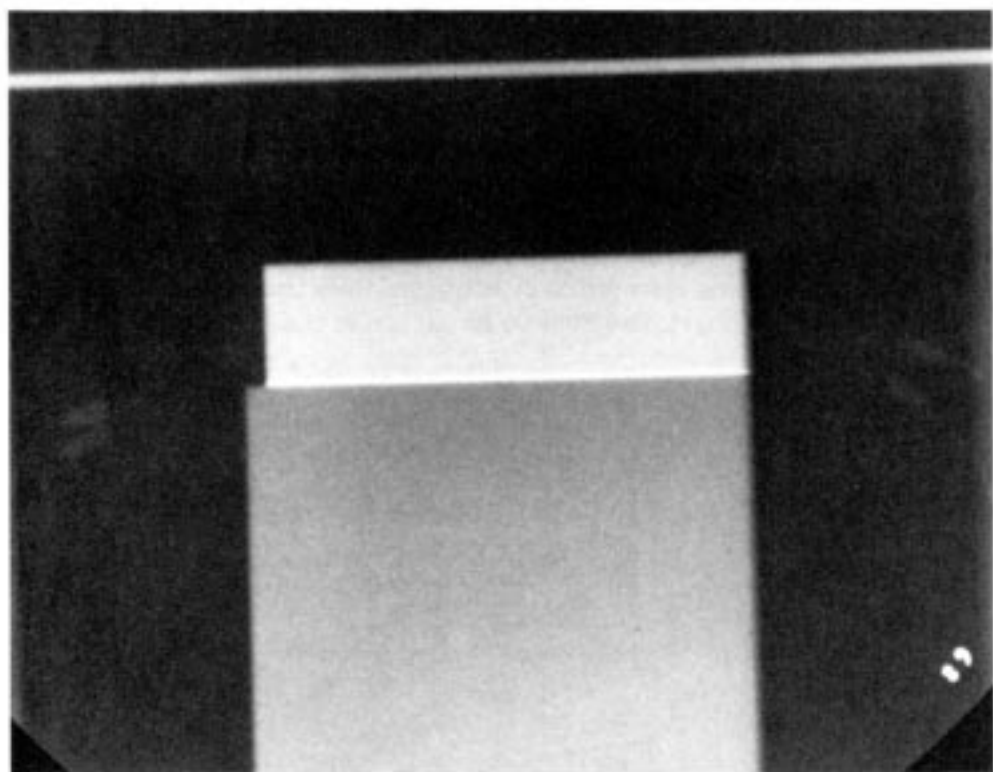
33.9 μ s

References:

Breed et al., 1967; Thurston and Mudd, 1968

Dynamic fracture of 25.0-mm-thick 2024 aluminum. The plate is shocked by 101.6 mm of Composition B-3 initiated by a P-040 lens. h is 25.0 mm. There is a 0.25-mm-thick, t , lead foil between the Composition B-3 and the aluminum plate. The free surface of the plate has run 4.0 μ s.





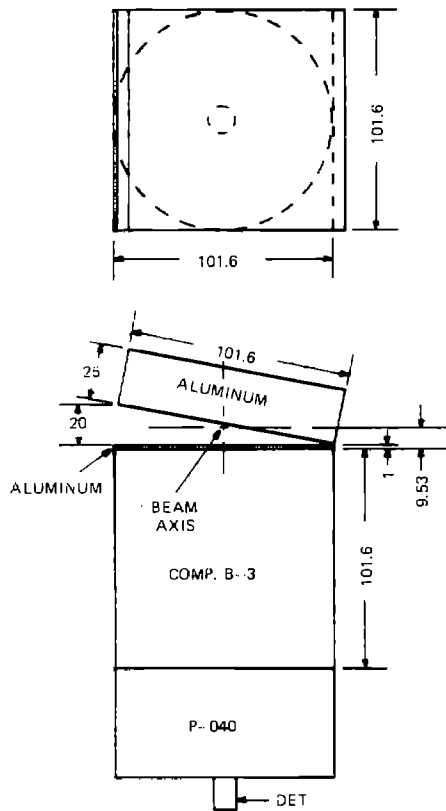
SHOT 90: Oblique Aluminum Plate Impact

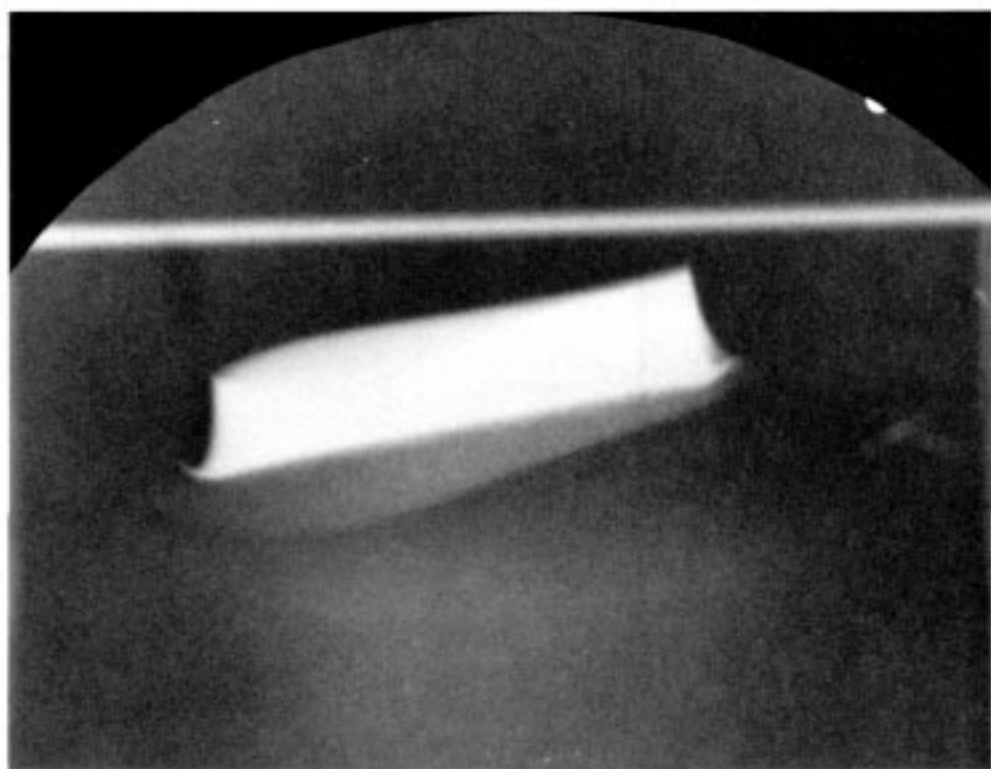
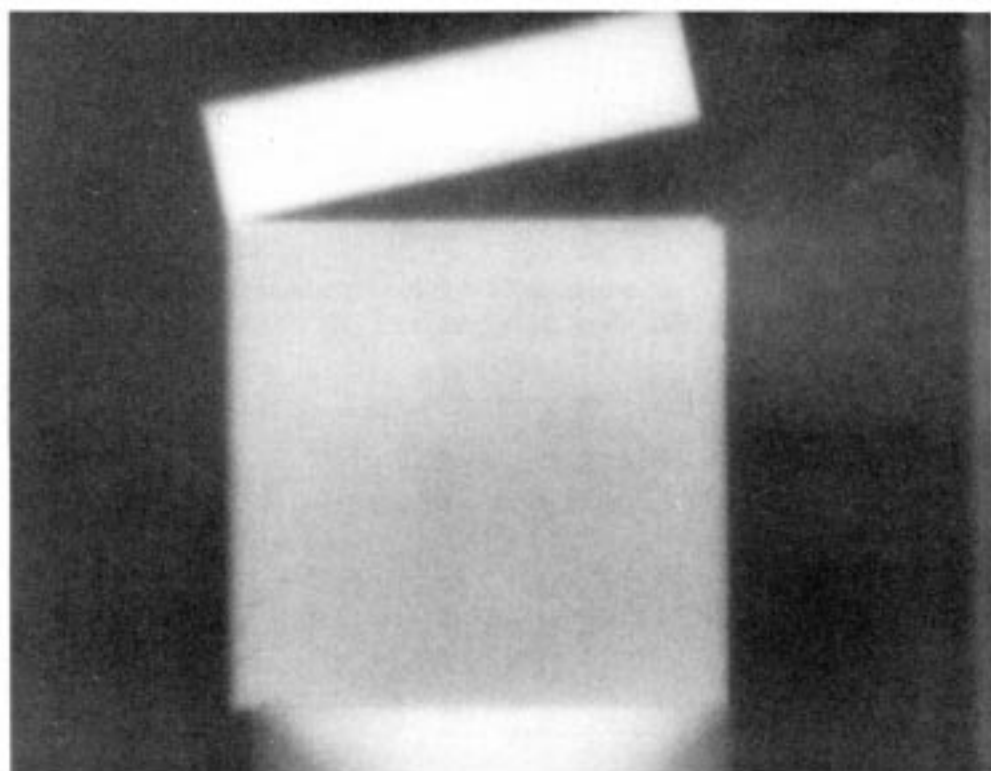
Date: September 22, 1964

Experimenter: Douglas Venable

Radiographic Time: 32.60 μ s

A 1.0-mm-thick aluminum plate driven by 101.6-mm-thick Composition B-3 strikes an oblique aluminum target. See Shot 96 for an earlier time.





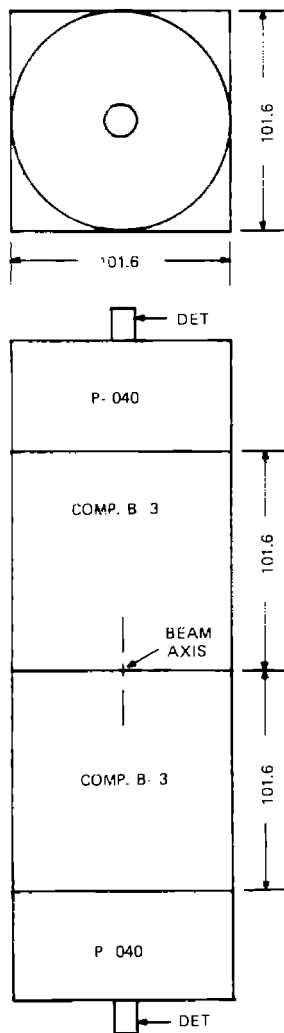
SHOT 91: Colliding Composition B-3 Detonations

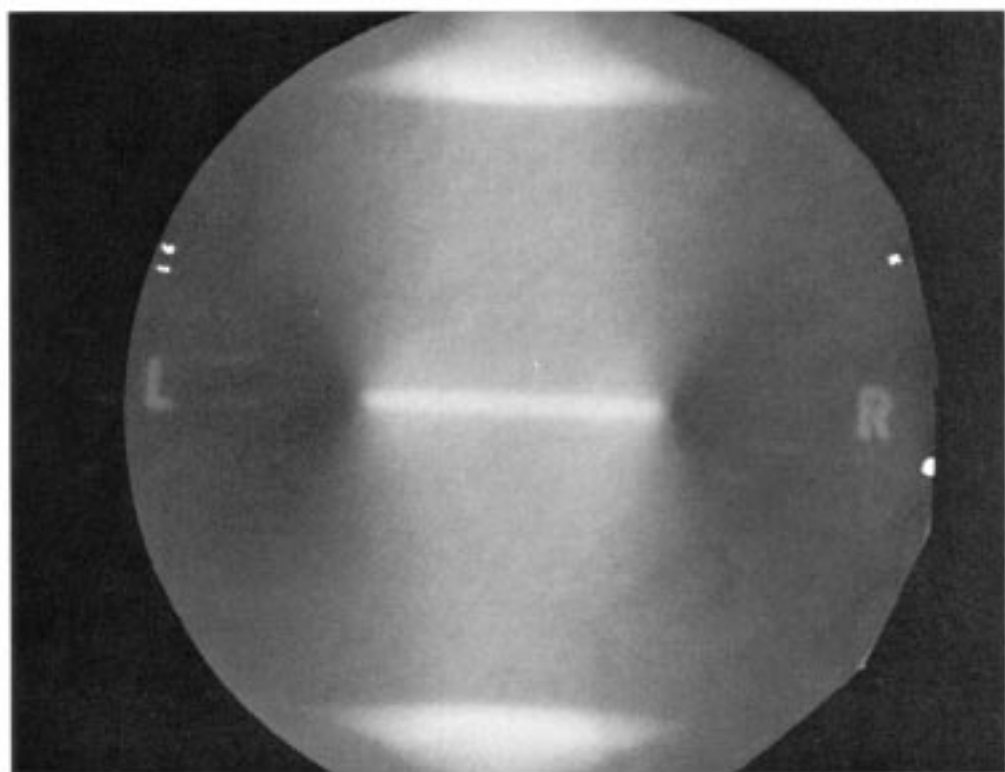
Date: September 29, 1964

Experimenter: Douglas Venable

Radiographic Time: 26.8 μ s

The reflected shocks in Composition B-3 detonation products 0.5 μ s after collision of the detonation waves. See Shots 86, 87, 92, and 273-277.





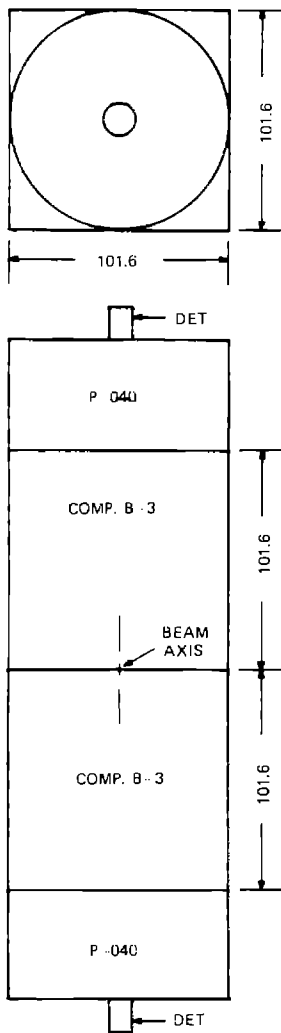
SHOT 92: Colliding Composition B-3 Detonations

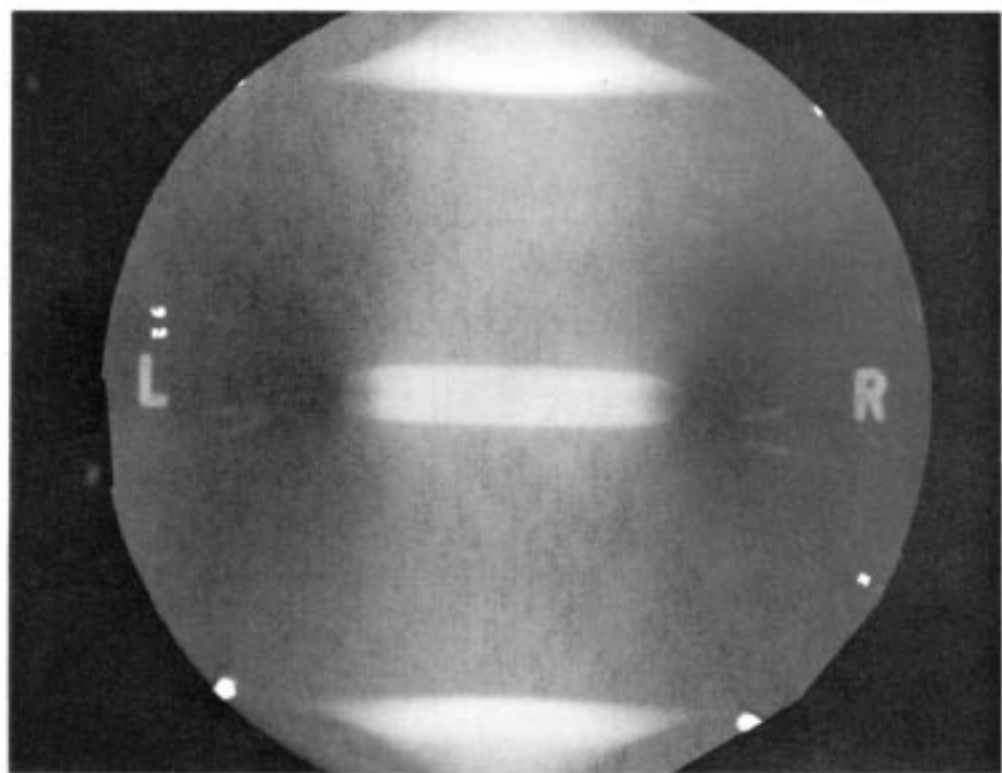
Date: September 29, 1964

Experimenter: Douglas Venable

Radiographic Time: 27.8 μ s

The reflected shocks in Composition B-3 detonation products 1.5 μ s after collision of the detonation waves. See Shots 86, 87, 91, and 273-277.





SHOT 93:

Expansion of Composition B-3 Products into a Vacuum

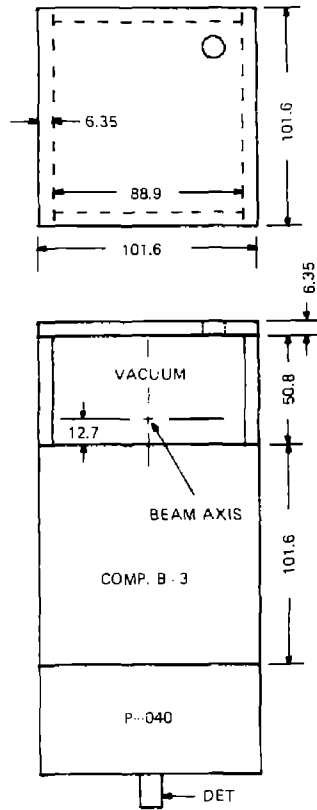
Date: September 29, 1964

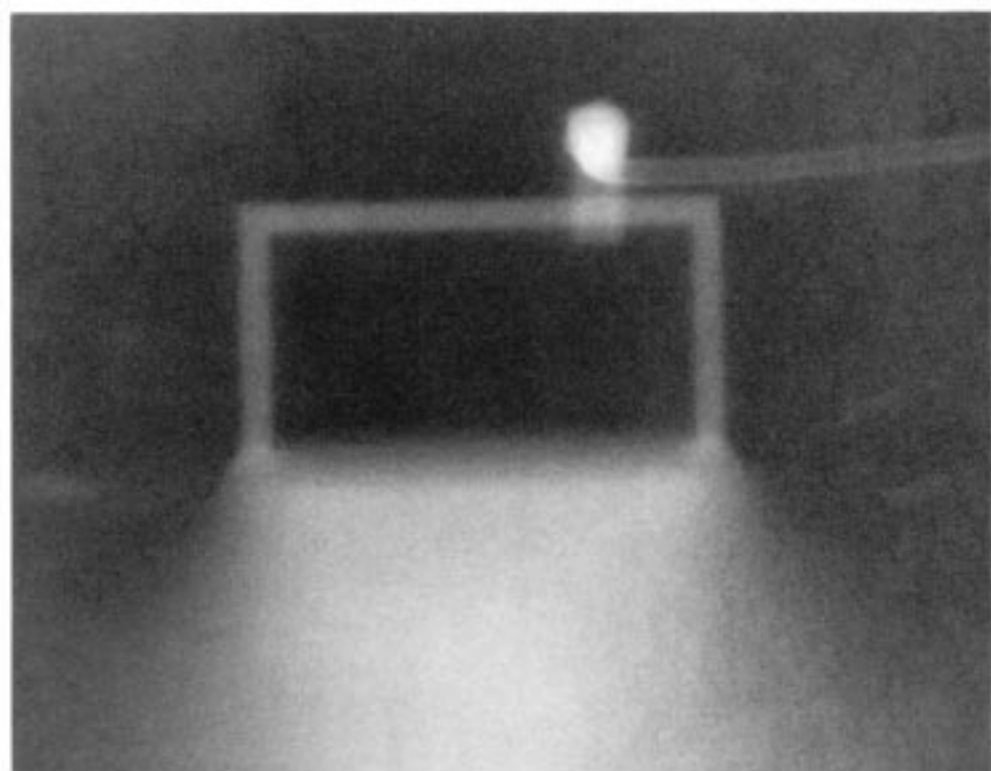
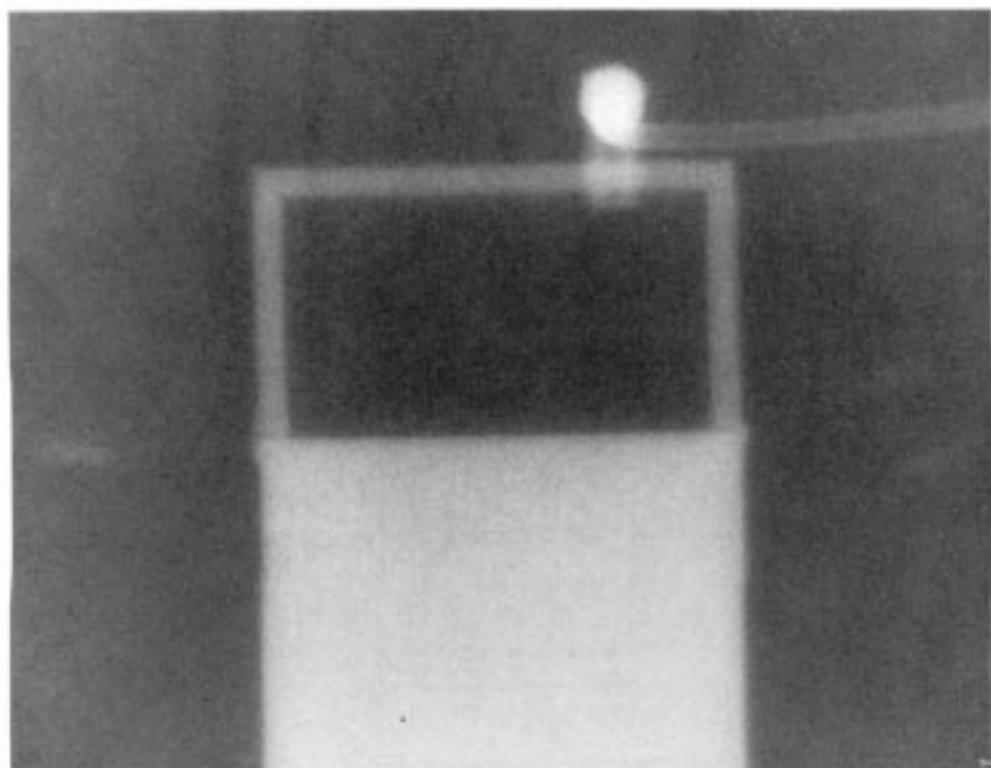
Experimenter: Douglas Venable

Radiographic Time: 27.3 μ s

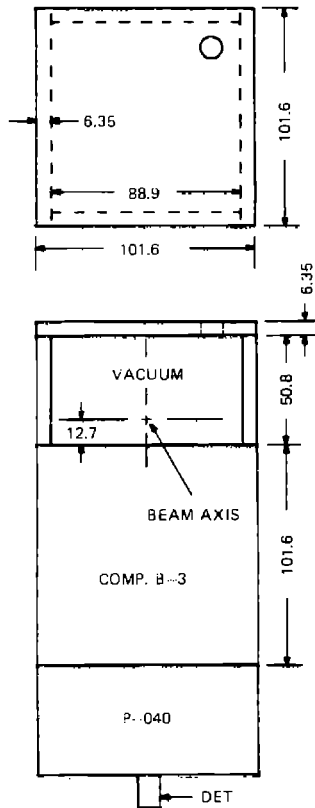
Reference: Venable, 1965

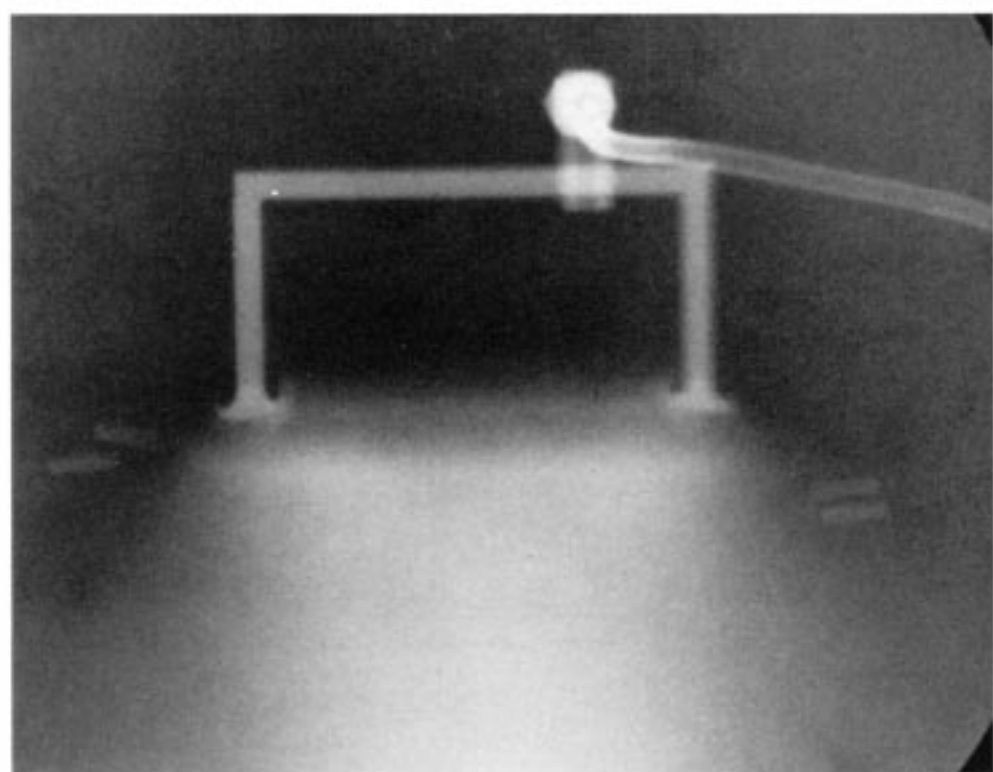
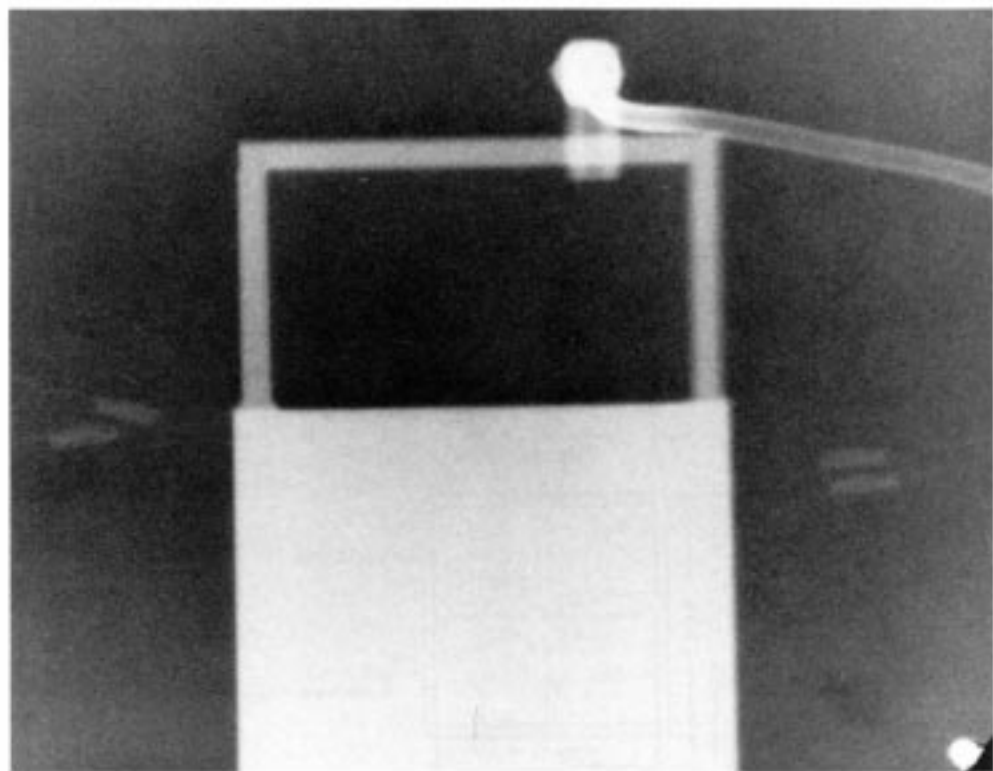
Expansion of Composition B-3 detonation products into a vacuum for 1.0 μ s. See Shot 94.





SHOT 94: **Expansion of Composition B-3 Products into a Vacuum**
Date: September 29, 1964
Experimenter: Douglas Venable
Radiographic Time: 28.3 μ s
Reference: Venable, 1965
Expansion of Composition B-3 detonation products into a vacuum for 2.0 μ s. See Shot 93.





SHOT 95: Spherical Hole in Water

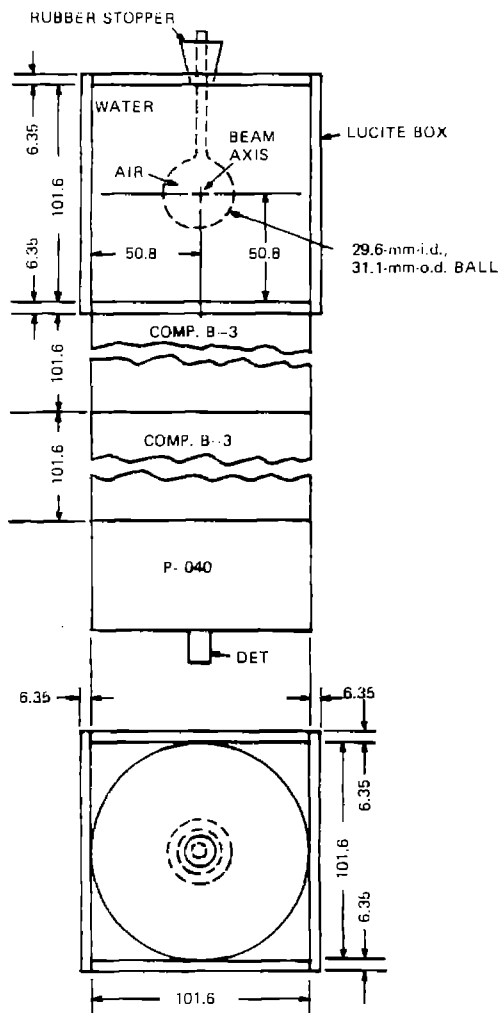
Date: September 29, 1964

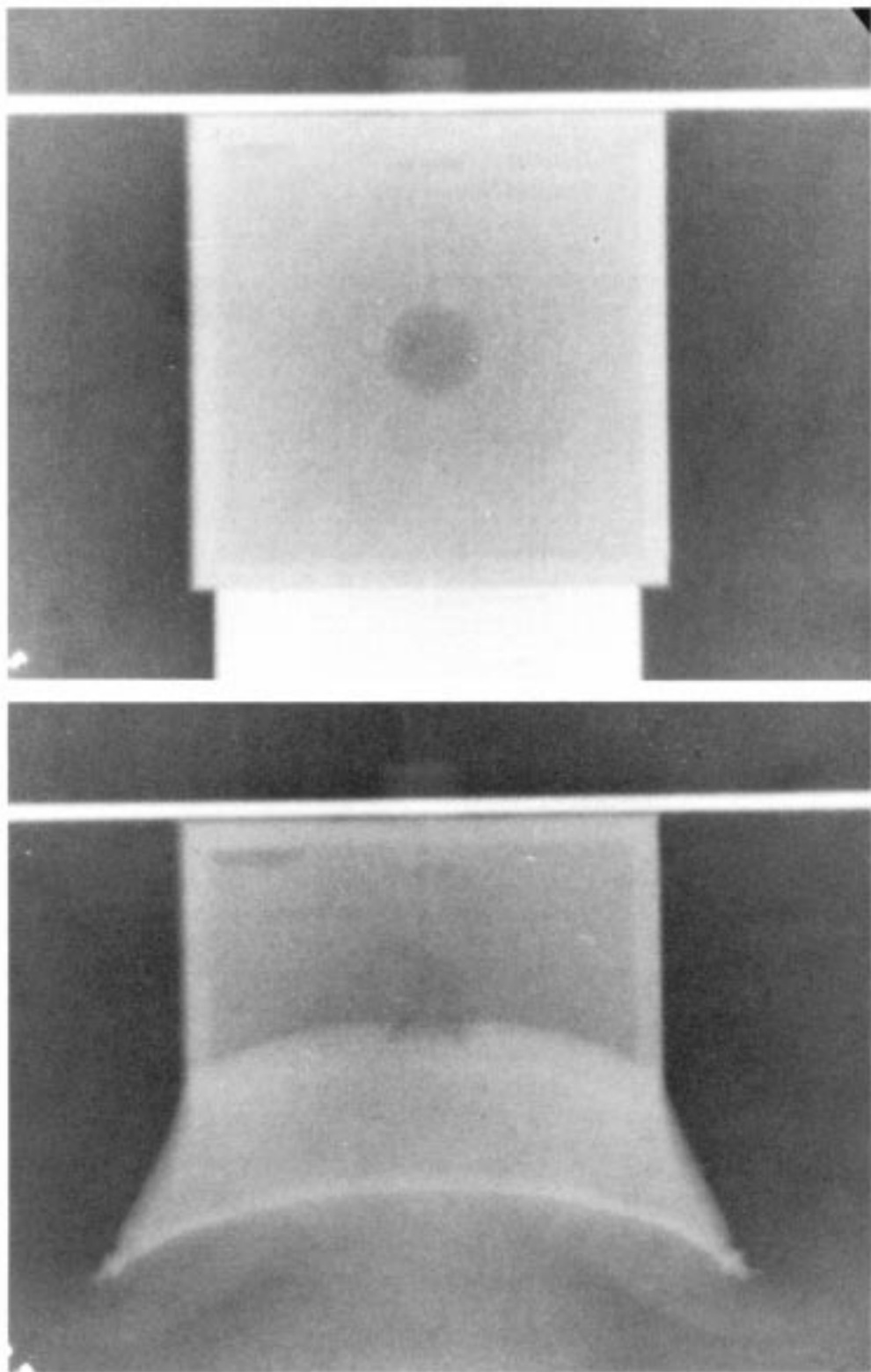
Experimenter: Douglas Venable

Radiographic Time: 50.6 μ s

Reference: Mader, 1965

A shock wave formed in water by a Composition B-3 detonation wave (see Shot 53) interacts with a spherical air bubble. See Shot 56.





SHOT 96: Oblique Aluminum Plate Impact

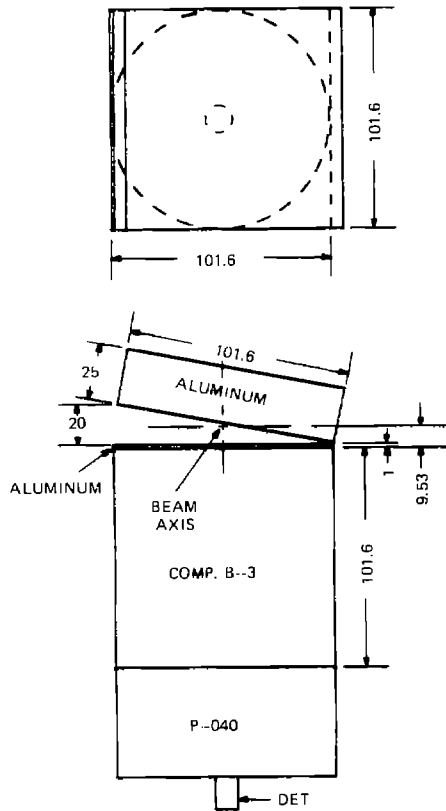
Date: October 2, 1964

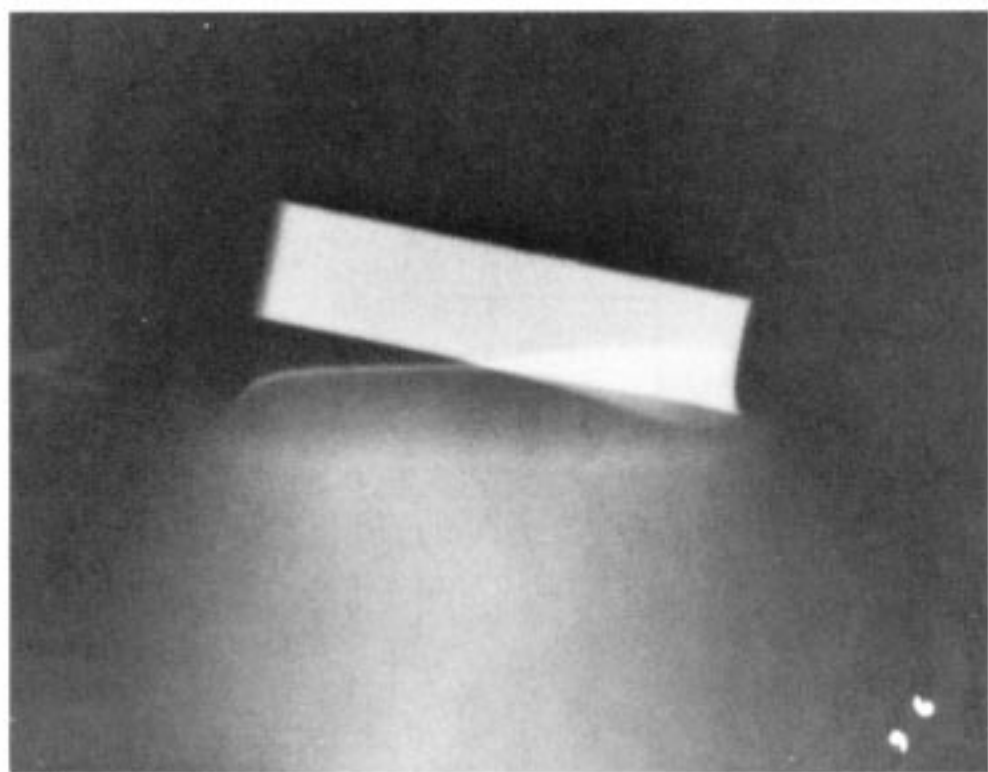
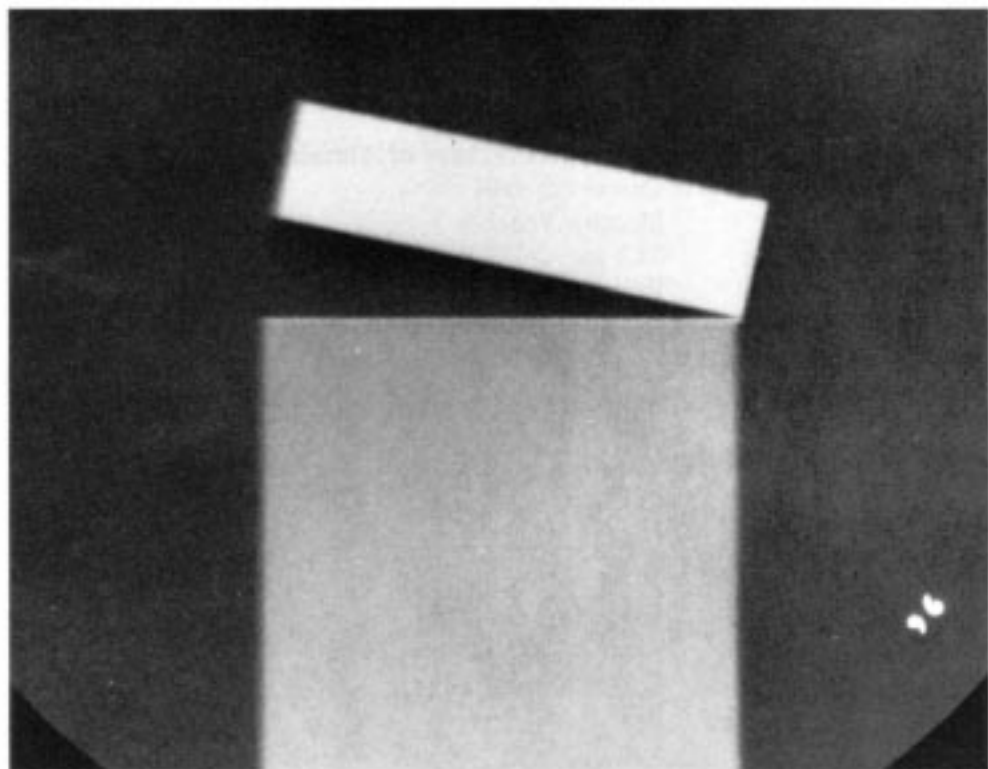
Experimenter: Douglas Venable

Radiographic Time: 28.5 μ s

Reference: Venable, 1965

A 1.0-mm-thick aluminum plate driven by 101.6-mm-thick Composition B-3 strikes an oblique aluminum target for 2.0 μ s. See Shot 90 for a later time.





SHOT 97: Dynamic Fracture of Aluminum

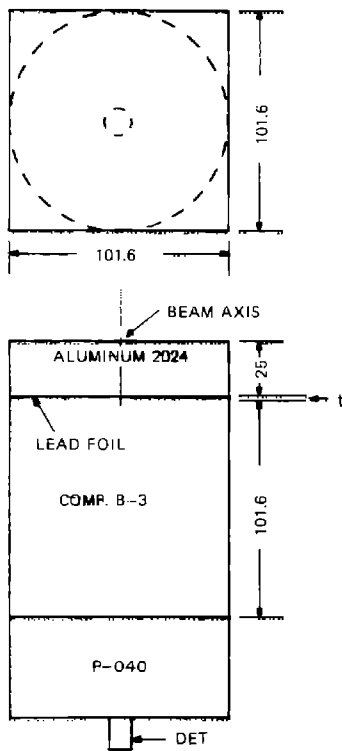
Date: October 2, 1964

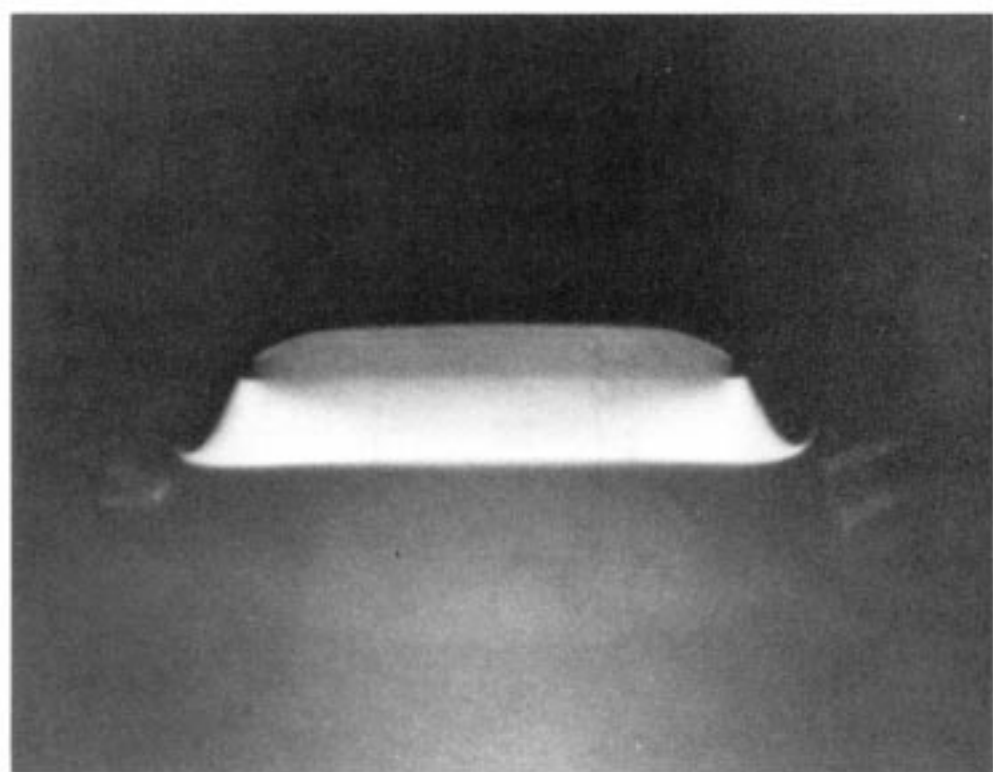
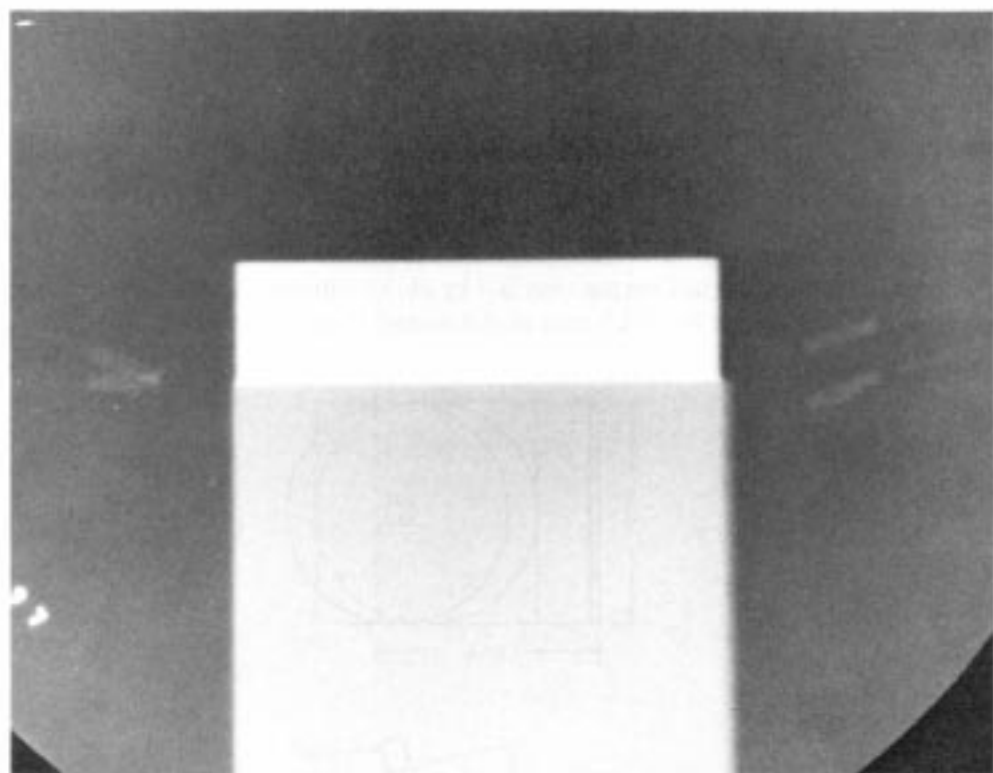
Experimenter: Douglas Venable

Radiographic Time: 33.9 μ s

References: Breed et al., 1967; Thurston and Mudd, 1968

Dynamic fracture of 25.0-mm-thick 2024 aluminum. The plate is shocked by 101.6 mm of Composition B-3 initiated by a P-040 lens. There is a 0.13-mm-thick, t , lead plate between the Composition B-3 and the aluminum plate.





SHOT 98:

Oblique Aluminum Plate Impact on Composition B-3

Date:

November 17, 1964

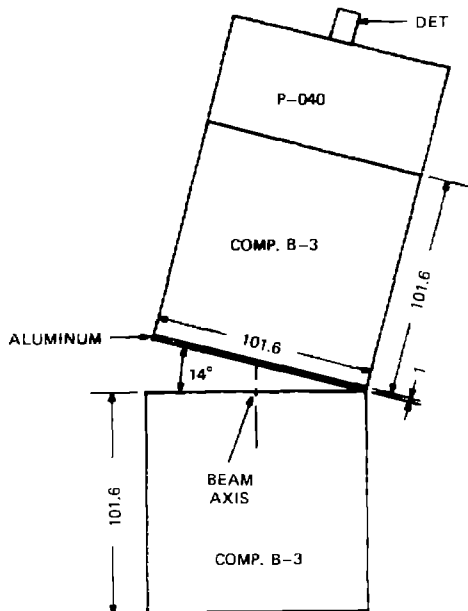
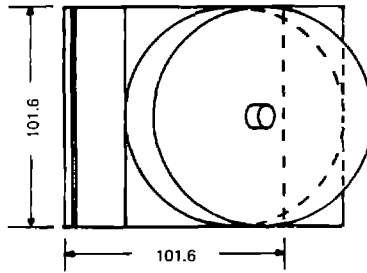
Experimenter:

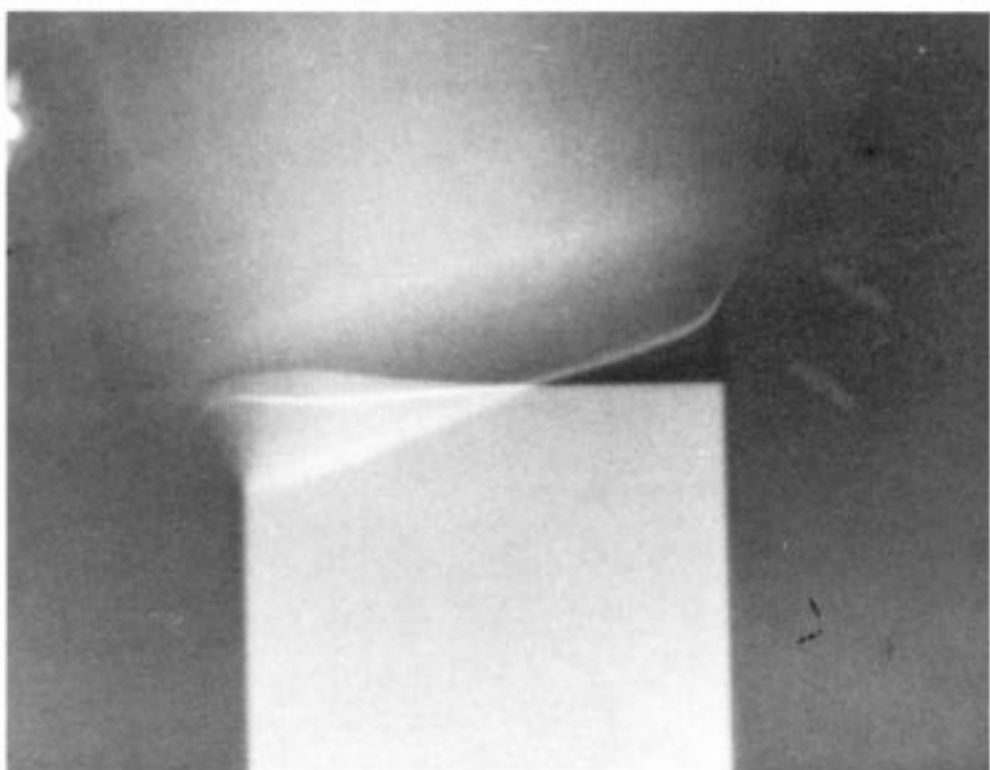
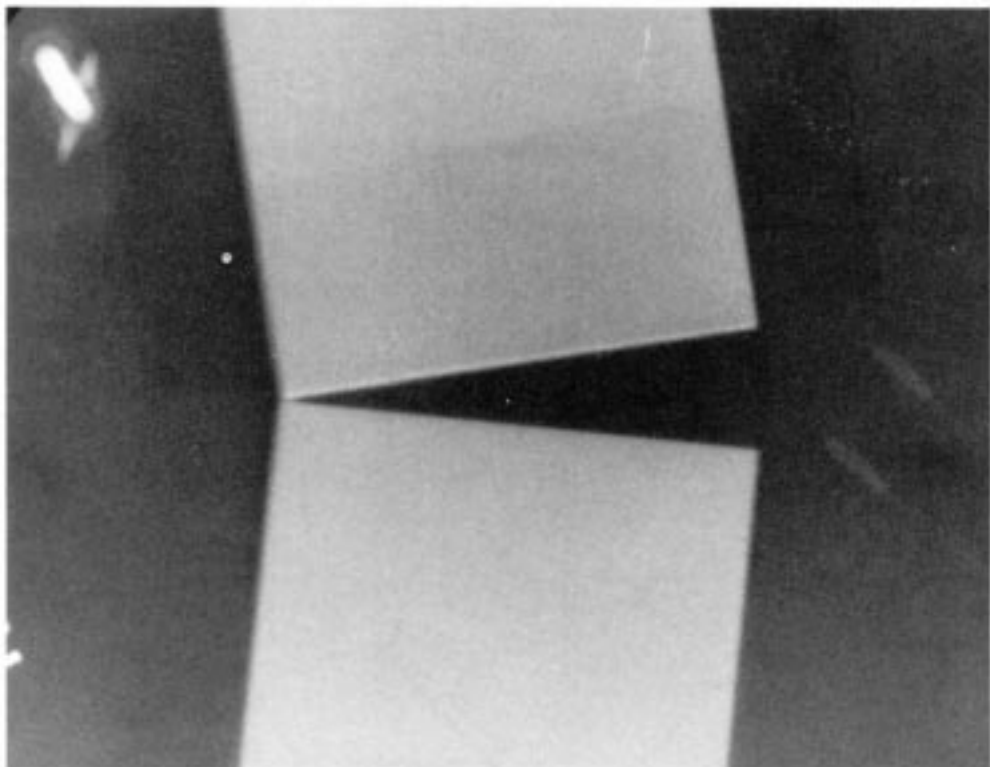
Douglas Venable

Radiographic Time:

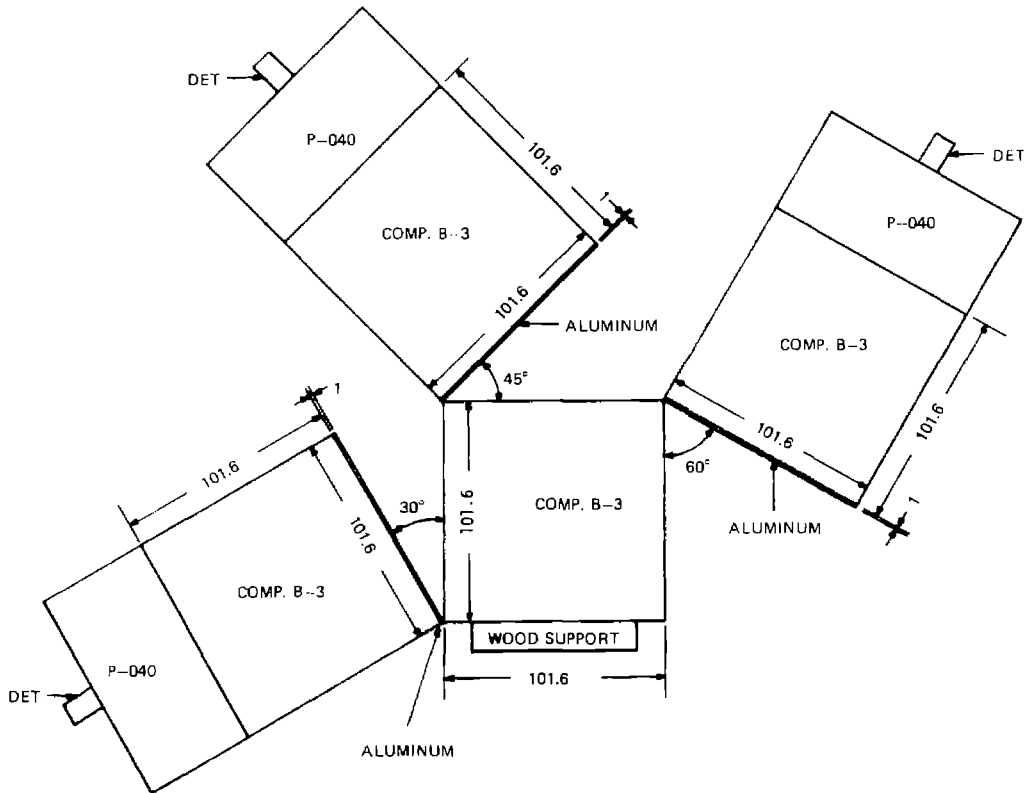
29.38 μ s

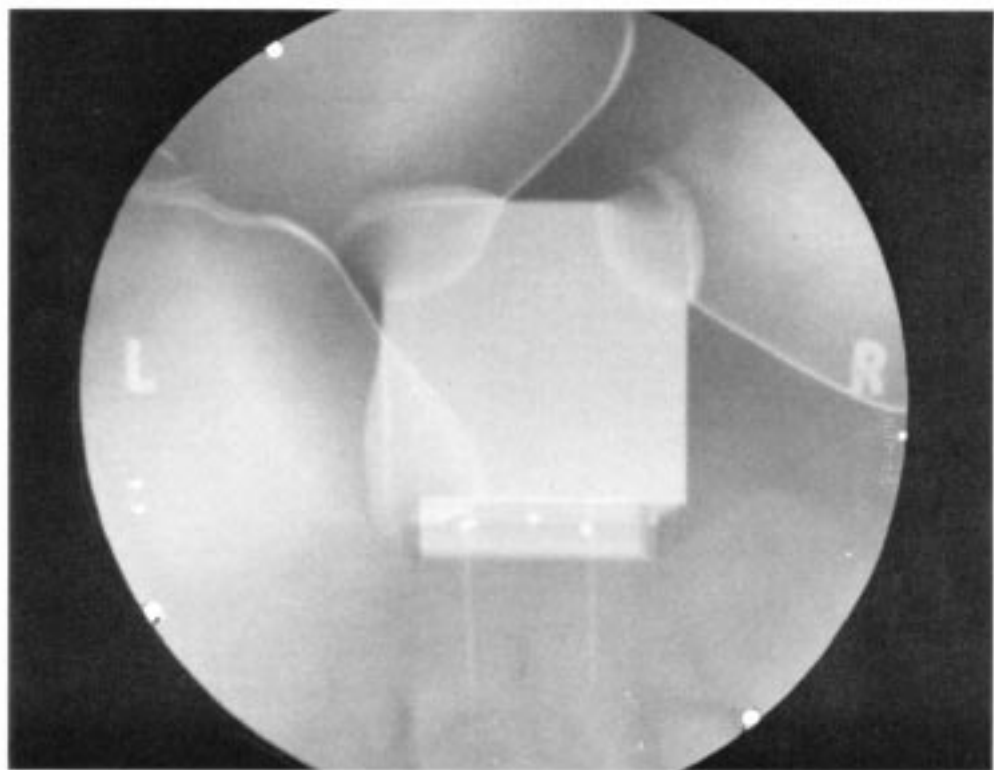
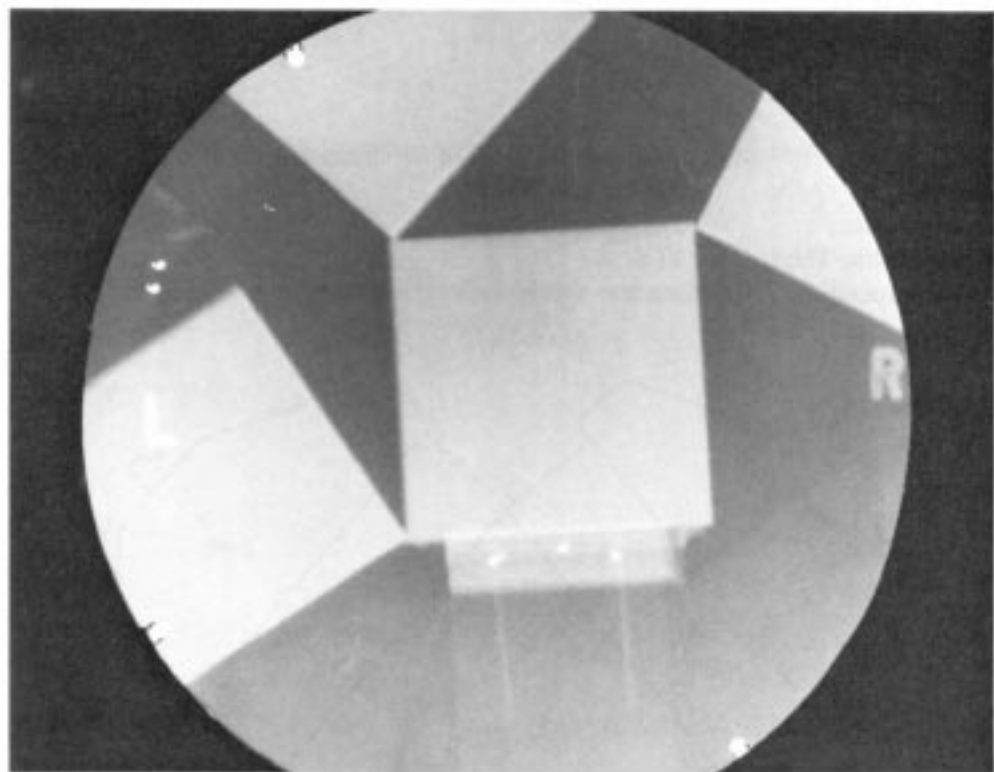
Initiation of detonation in Composition B-3 by oblique impact from a 1.0-mm-thick aluminum plate driven by 101.6 mm of detonated Composition B-3.





SHOT 99: Oblique Aluminum Plate Impact on Composition B-3
Date: November 17, 1964
Experimenter: Douglas Venable
Radiographic Time: 31.38 μ s
Multiple initiation of detonation in a block of Composition B-3 by oblique impact from three 1.0-mm-thick aluminum plates driven by blocks of detonating Composition B-3.





SHOT 100:

Regular Reflection in Composition B-3

Date:

November 17, 1964

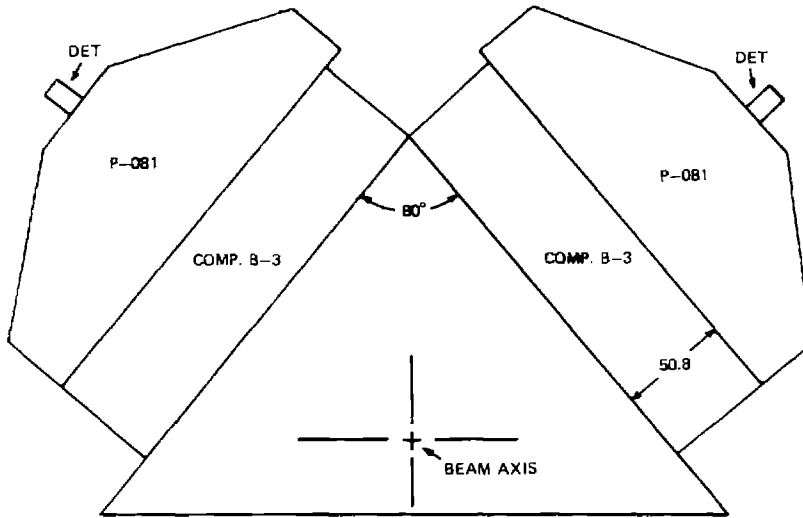
Experimenter:

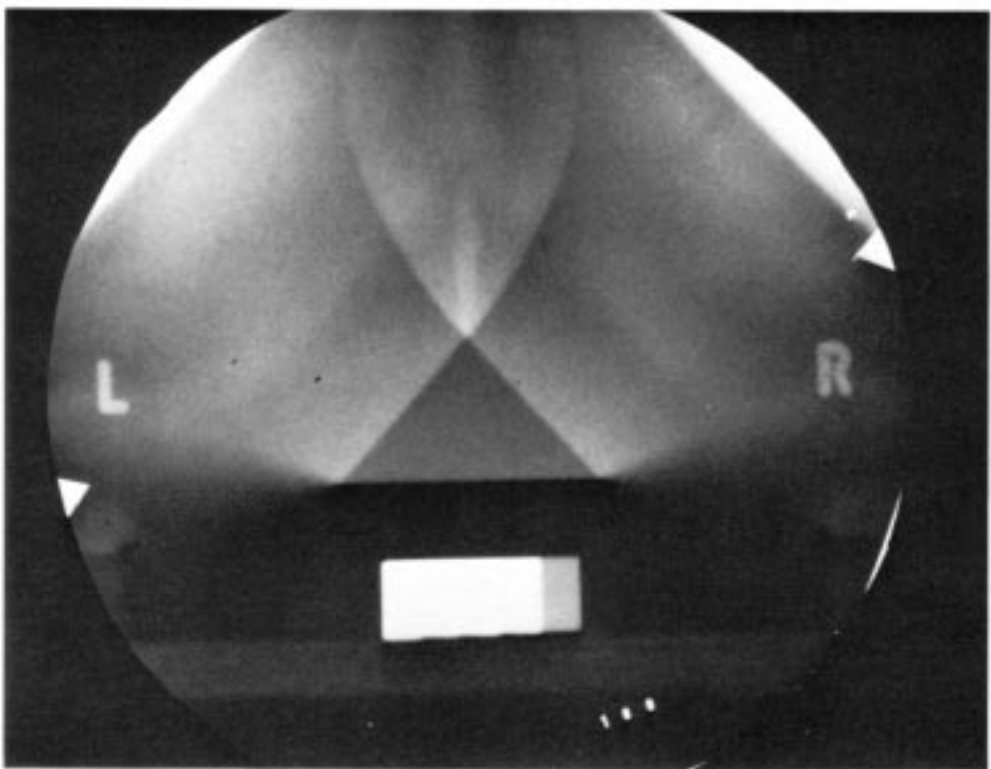
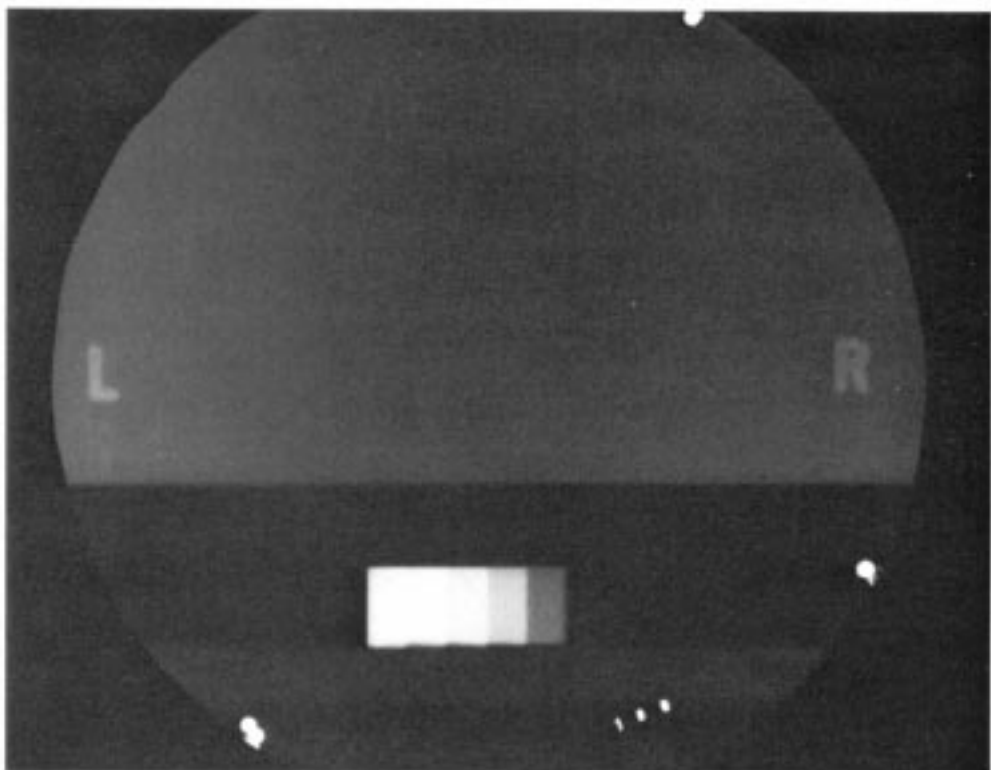
Douglas Venable

Radiographic Time:

37.9 μ s

Two Composition B-3 detonation waves interacting to form a regular reflection.





SHOT 101:

Mach Reflection in Composition B-3

Date:

November 17, 1964

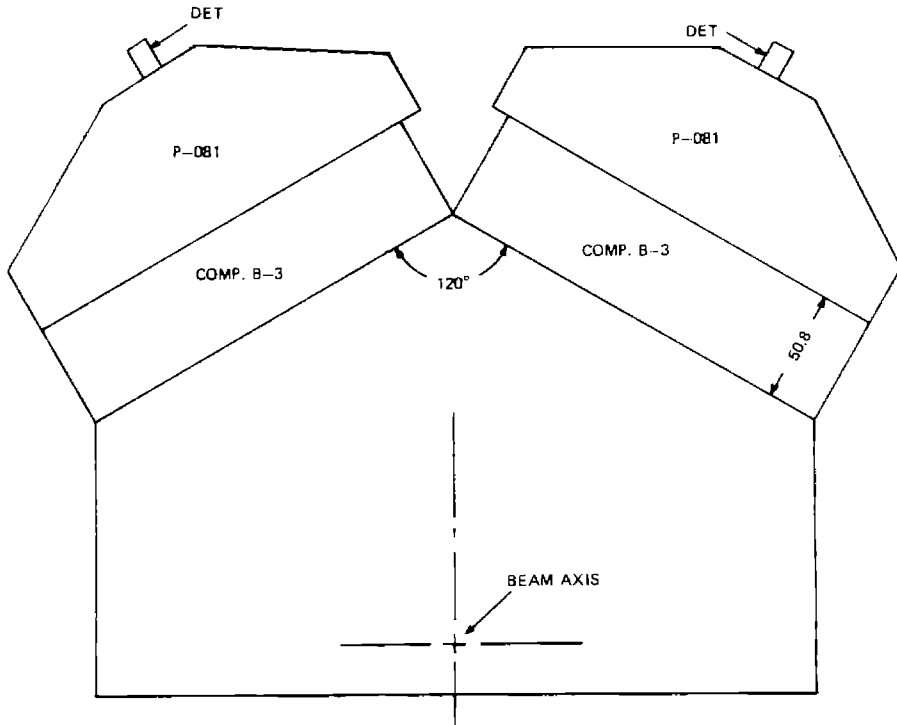
Experimenter:

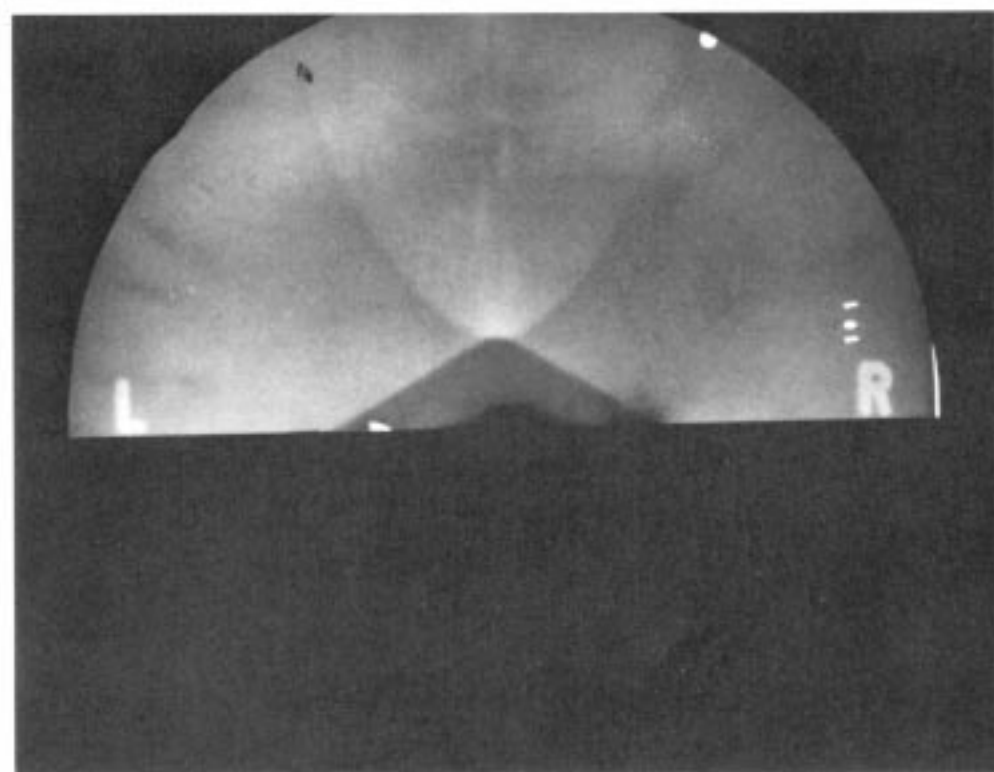
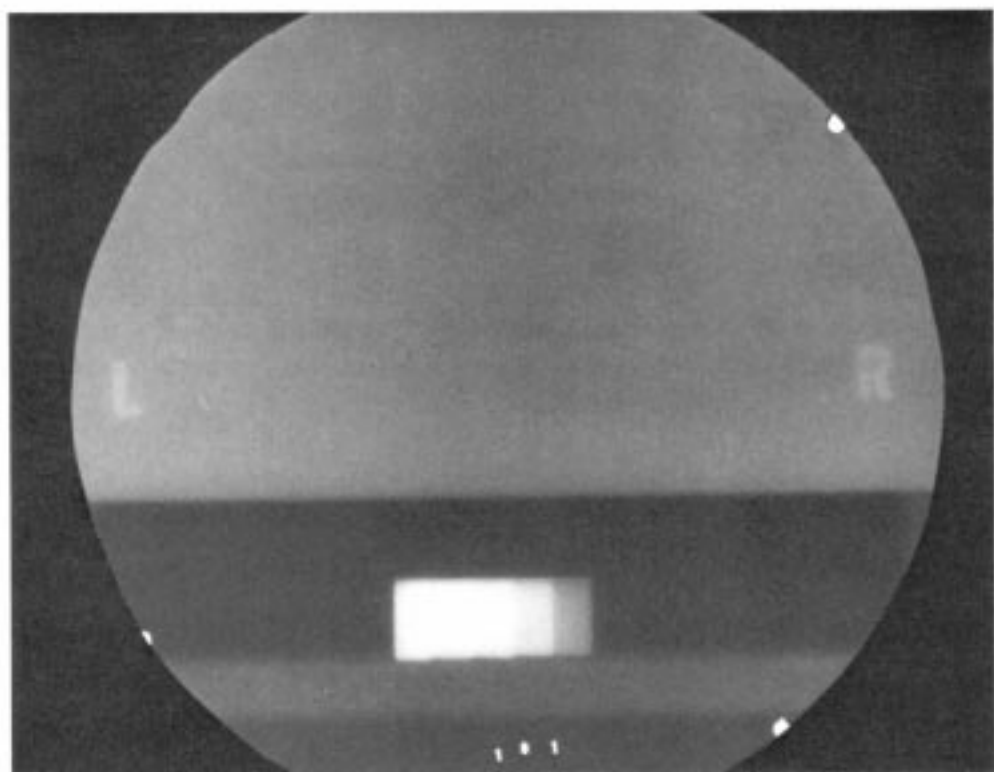
Douglas Venable

Radiographic Time:

44.8 μ s

Two Composition B-3 detonation waves interacting to form a Mach reflection. The series of density standards (step wedges) at the bottom of the static radiograph is for film density calibration.





SHOT 102:

Dynamic Fracture of Aluminum

Date:

November 24, 1964

Experimenter:

Douglas Venable

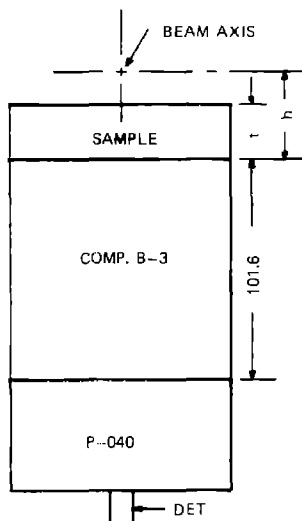
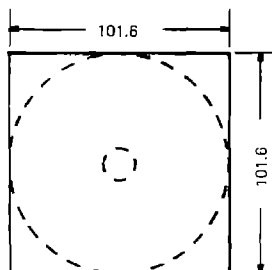
Radiographic Time:

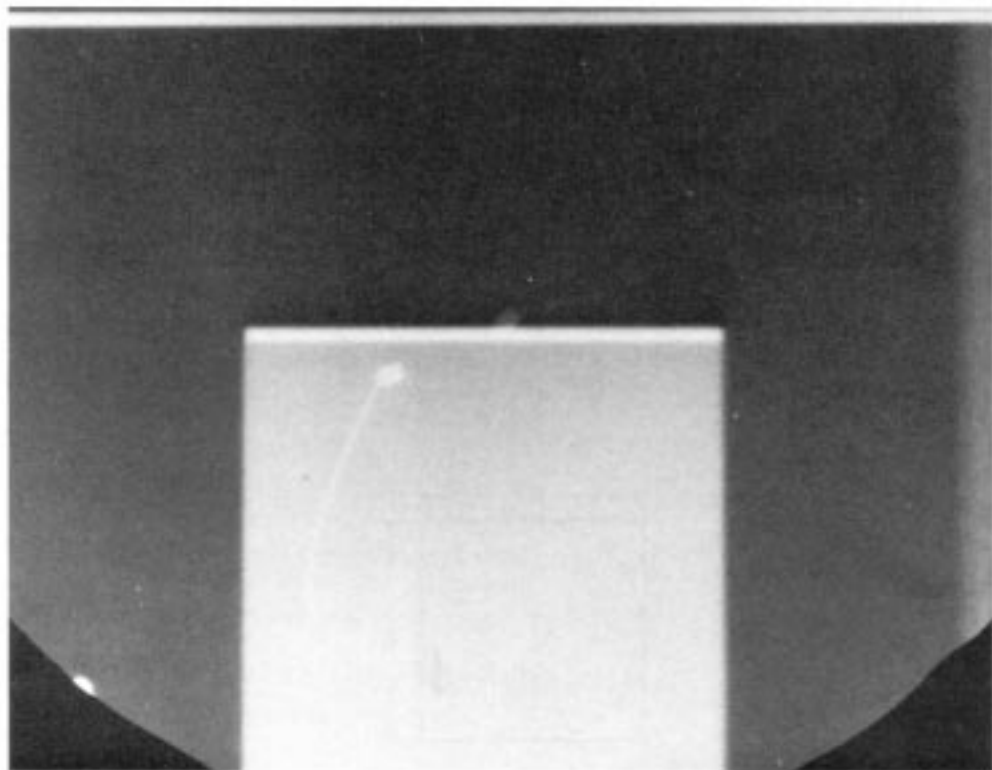
34.31 μ s

References:

Breed et al., 1967; Thurston and Mudd, 1968

Dynamic fracture of 3.0-mm-thick, t , aluminum. The plate is shocked by 101.6 mm of Composition B-3 initiated by a P-040 lens. h is 38.1 mm. No fracture layer was observed.





SHOT 103: Dynamic Fracture of Aluminum

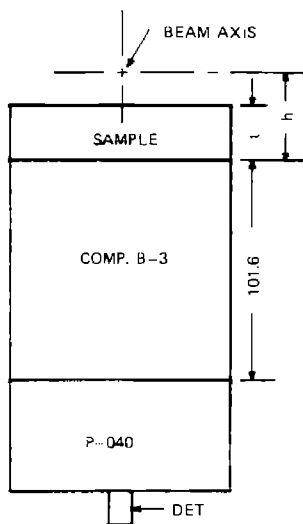
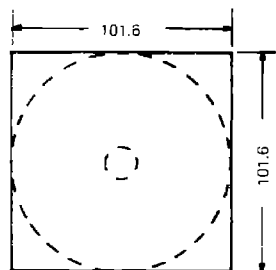
Date: December 8, 1964

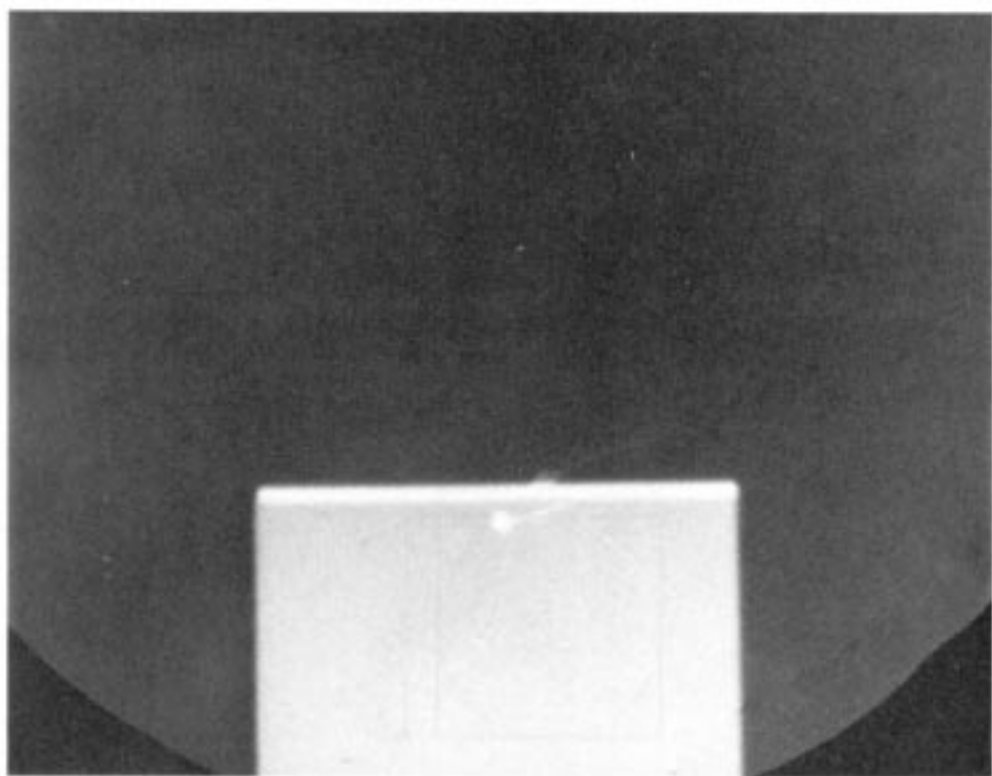
Experimenter: Douglas Venable

Radiographic Time: 38.42 μ s

References: Breed et al., 1967; Thurston and Mudd, 1968

Dynamic fracture of 3.0-mm-thick, t , aluminum. The plate is shocked by 101.6 mm of Composition B-3 initiated by a P-040 lens. No fracture layer was observed.





SHOT 104: Dynamic Fracture of Aluminum

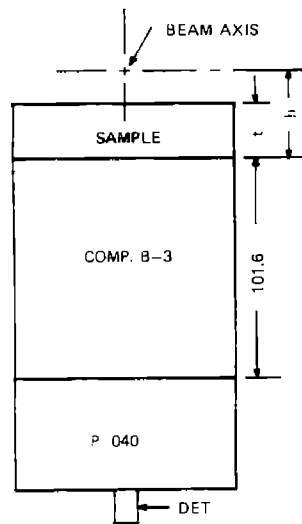
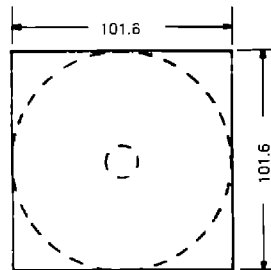
Date: January 6, 1965

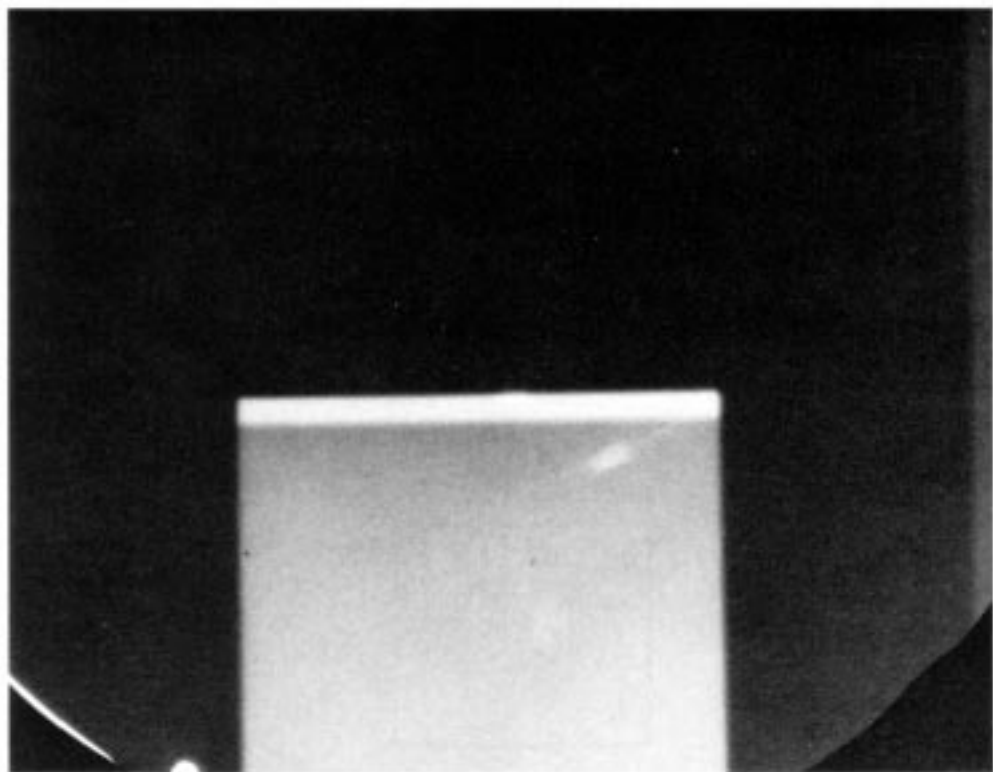
Experimenter: Douglas Venable

Radiographic Time: 38.33 μ s

References: Breed et al., 1967; Thurston and Mudd, 1968

Dynamic fracture of 6.0-mm-thick, t , aluminum. The plate is shocked by 101.6 mm of Composition B-3 initiated by a P-040 lens. h is 50.8 mm. No fracture layer was observed.





SHOT 105:

Dynamic Fracture of Aluminum

Date:

November 24, 1964

Experimenter:

Douglas Venable

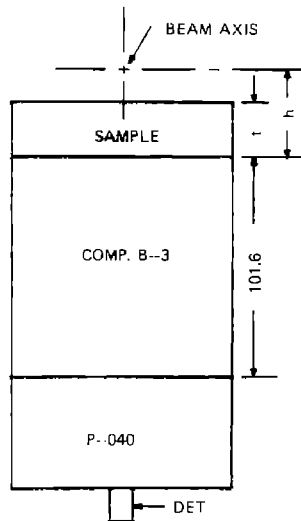
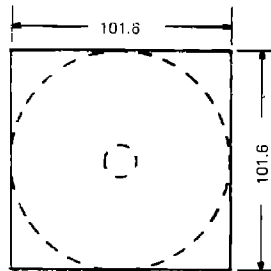
Radiographic Time:

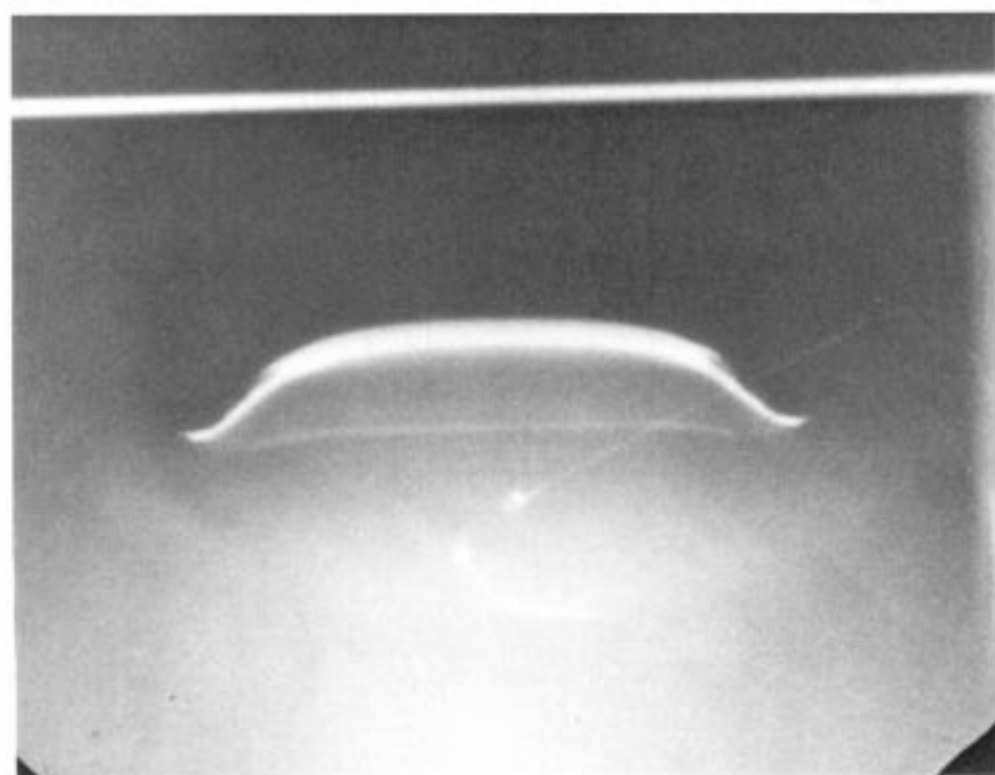
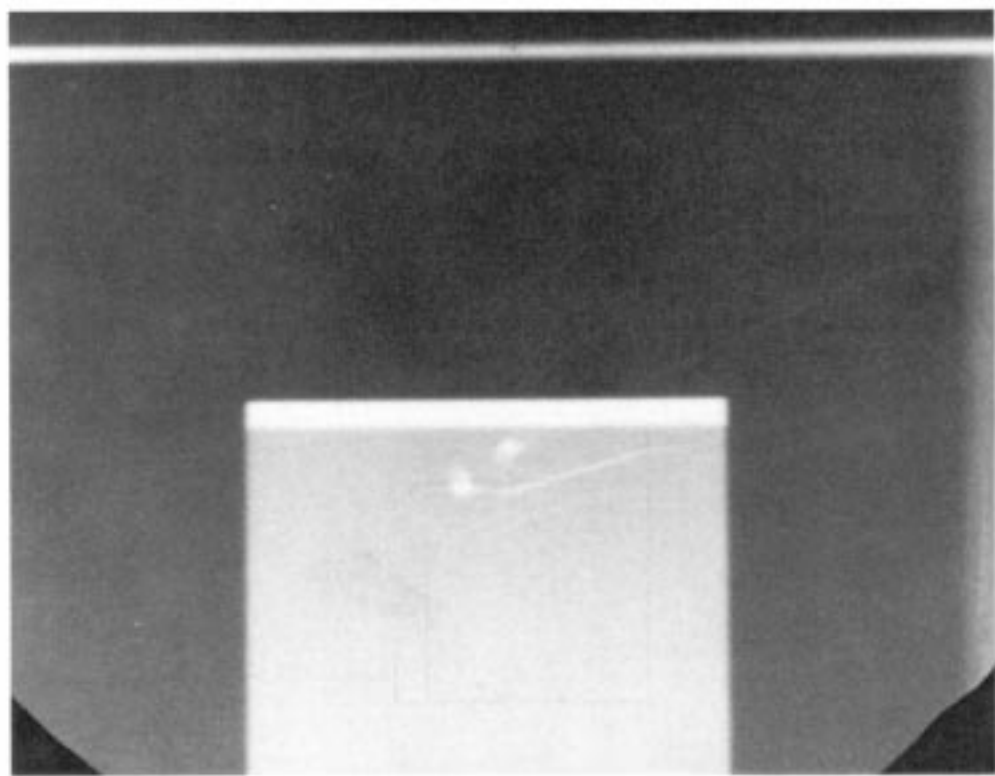
34.29 μ s

References:

Breed et al., 1967; Thurston and Mudd, 1968

Dynamic fracture of 6.0-mm-thick, t , aluminum. The plate is shocked by 101.6 mm of Composition B-3 initiated by a P-040 lens. h is 34.575 mm. No fracture layer was observed.





SHOT 107:

Dynamic Fracture of Aluminum

Date:

January 20, 1965

Experimenter:

Douglas Venable

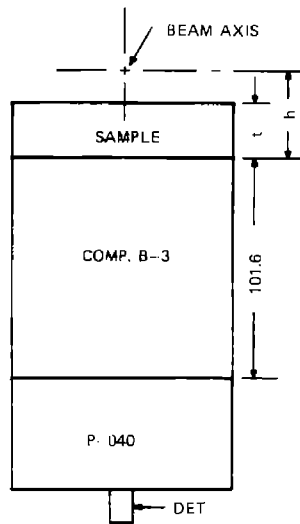
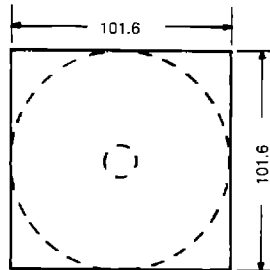
Radiographic Time:

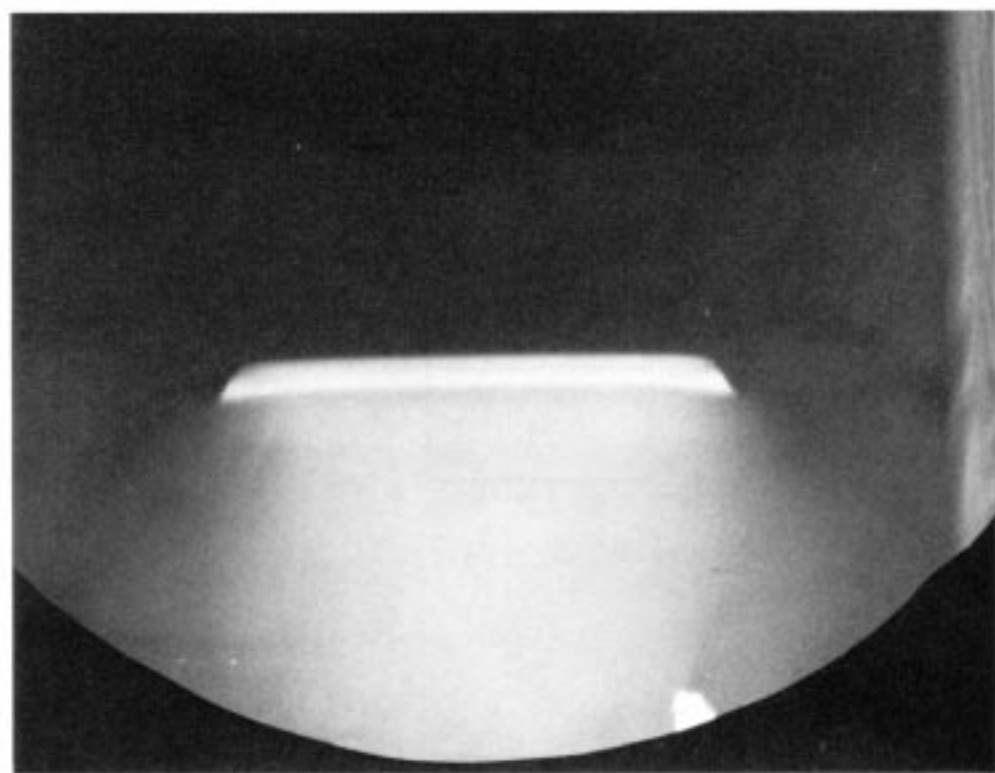
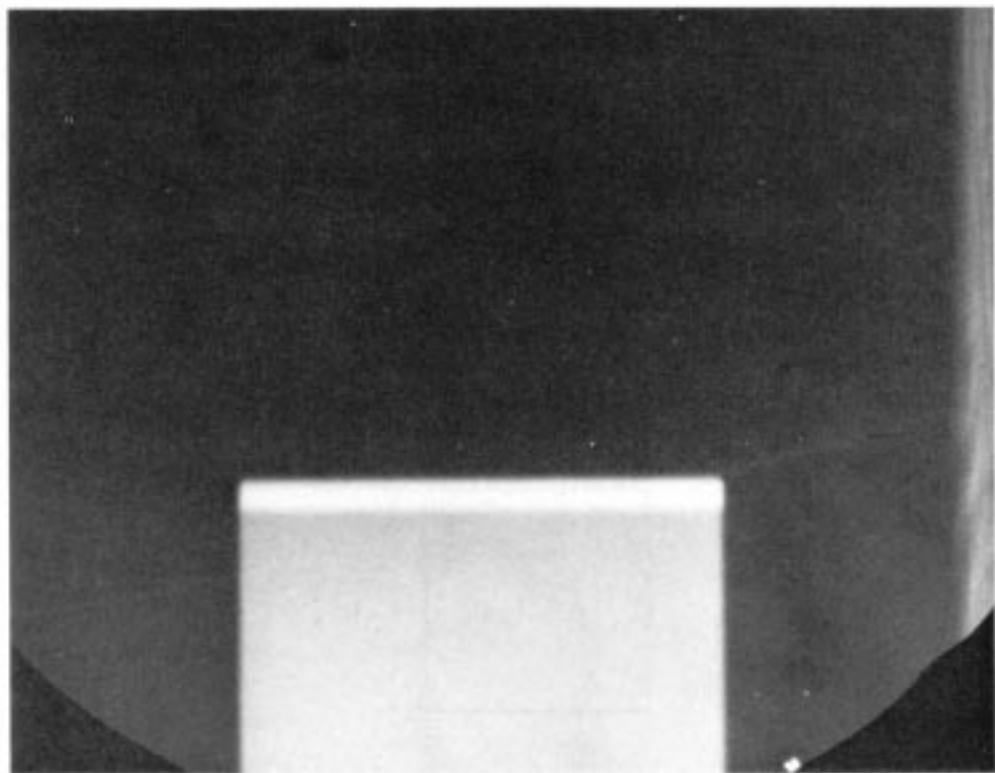
28.43 μ s

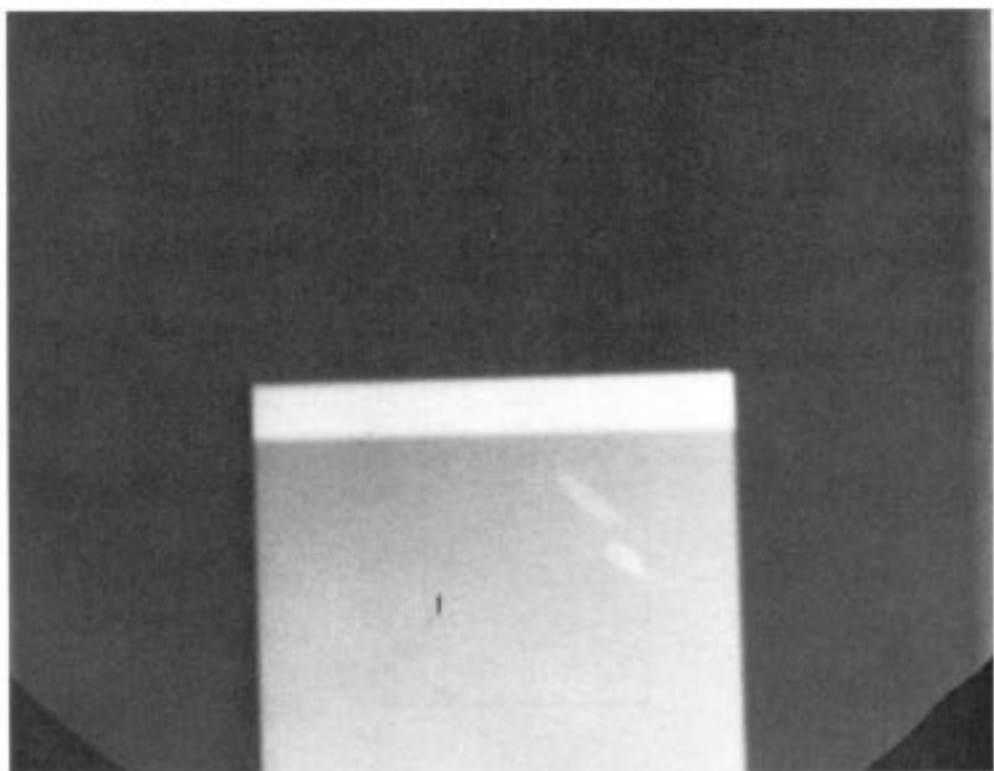
References:

Breed et al., 1967; Thurston and Mudd, 1968

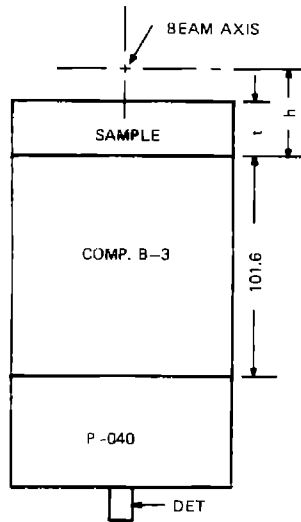
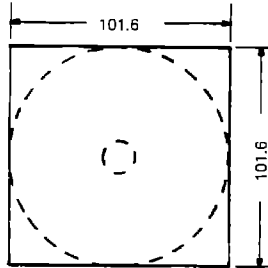
Dynamic fracture of 6.0-mm-thick, t , aluminum. The plate is shocked by 101.6 mm of Composition B-3 initiated by a P-040 lens. h is 57.15 mm.

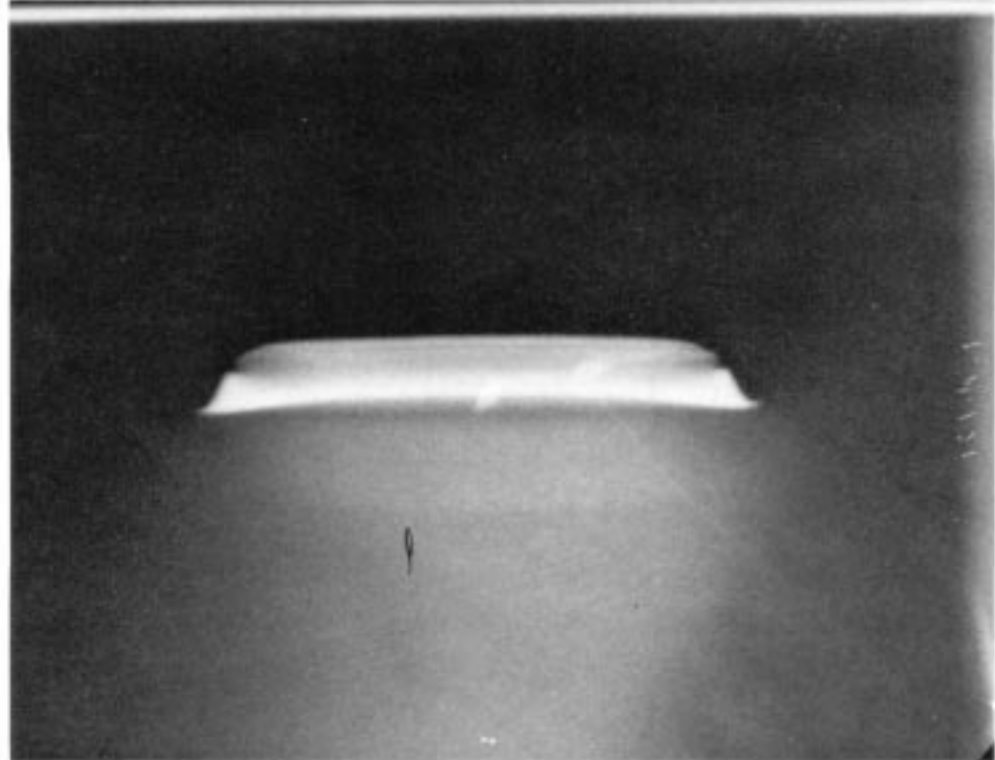
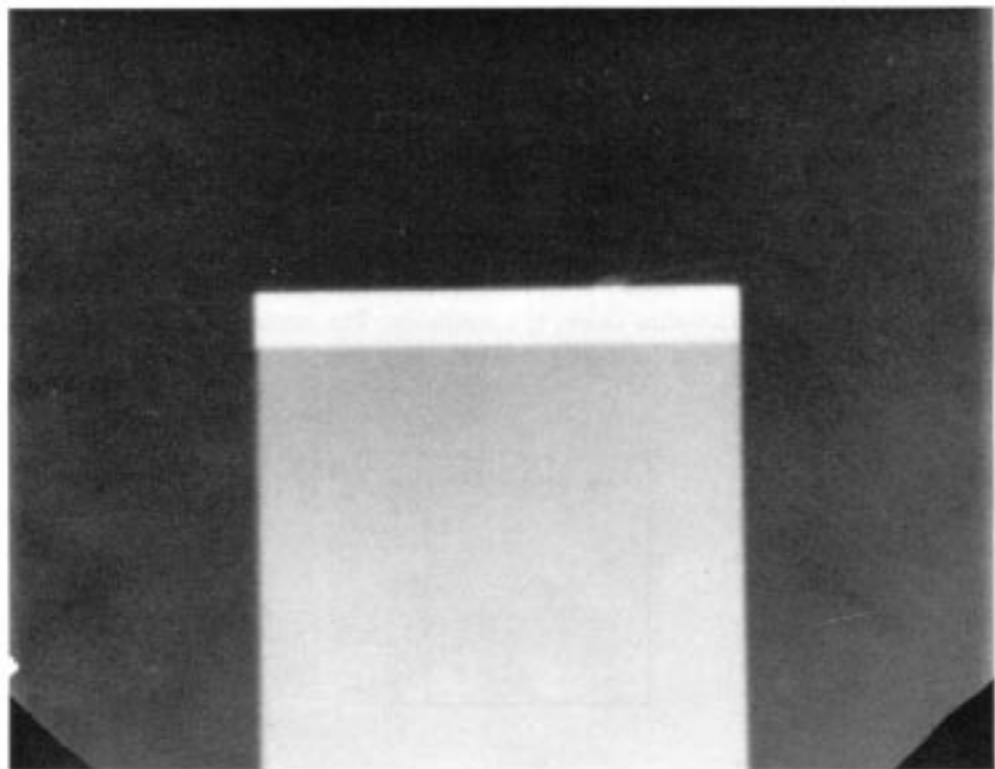






SHOT 109: Dynamic Fracture of Aluminum
Date: December 8, 1964
Experimenter: Douglas Venable
Radiographic Time: 30.43 μ s
References: Breed et al., 1967; Thurston and Mudd, 1968
Dynamic fracture of 12.0-mm-thick, t , aluminum. The plate is shocked by 101.6 mm of Composition B-3 initiated by a P-040 lens. h is 19.05 mm.





SHOT 110:

Dynamic Fracture of Aluminum

Date:

January 5, 1965

Experimenter:

Douglas Venable

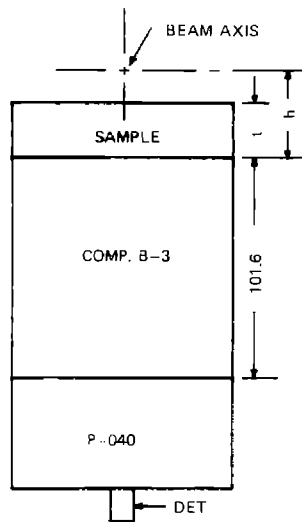
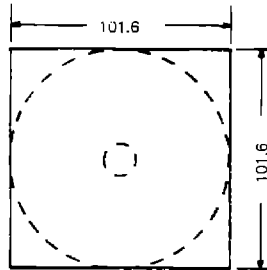
Radiographic Time:

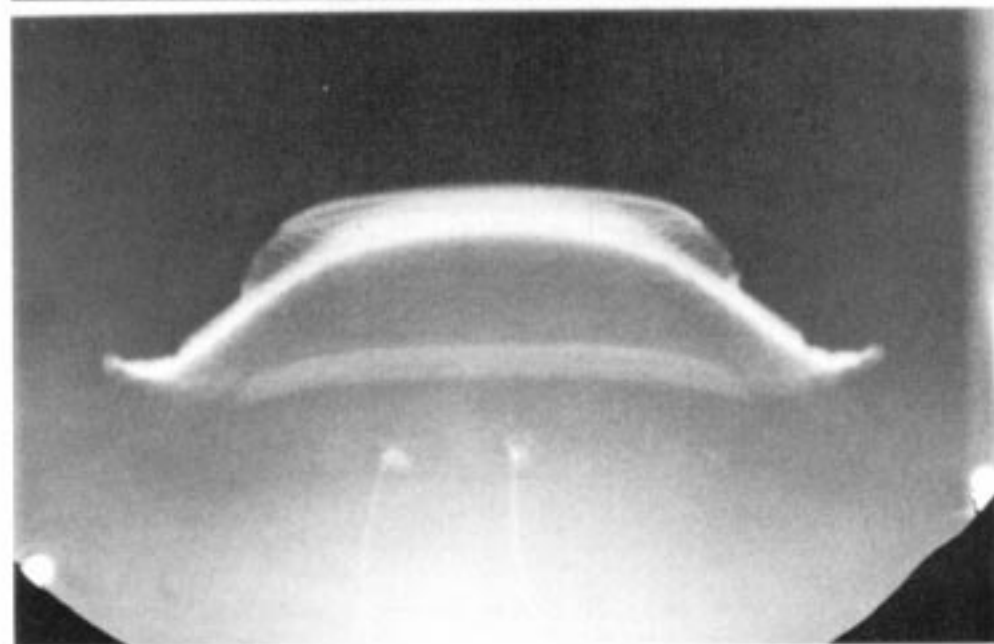
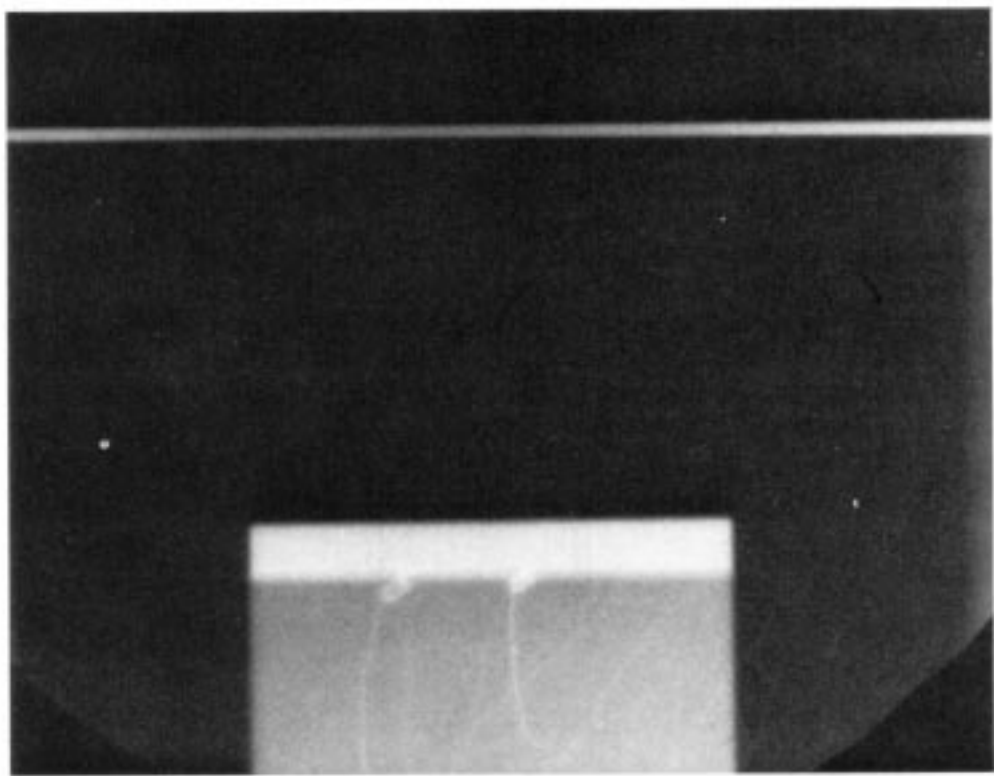
42.29 μ s

References:

Breed et al., 1967; Thurston and Mudd, 1968

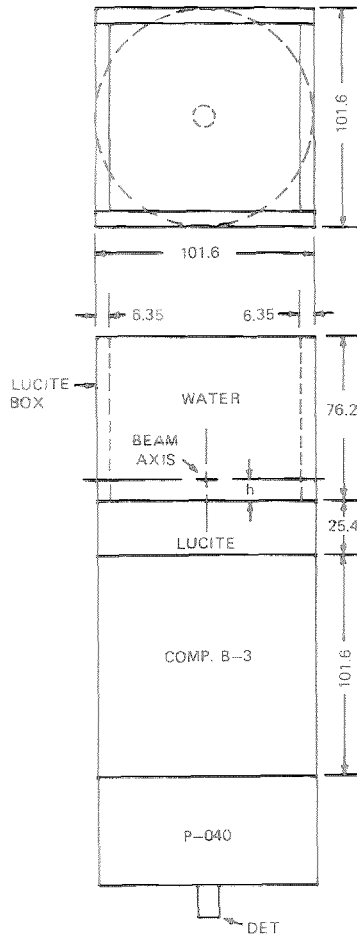
Dynamic fracture of 12.0-mm-thick, t , aluminum. The plate is shocked by 101.6 mm of Composition B-3 initiated by a P-040 lens. h is 75.5 mm.

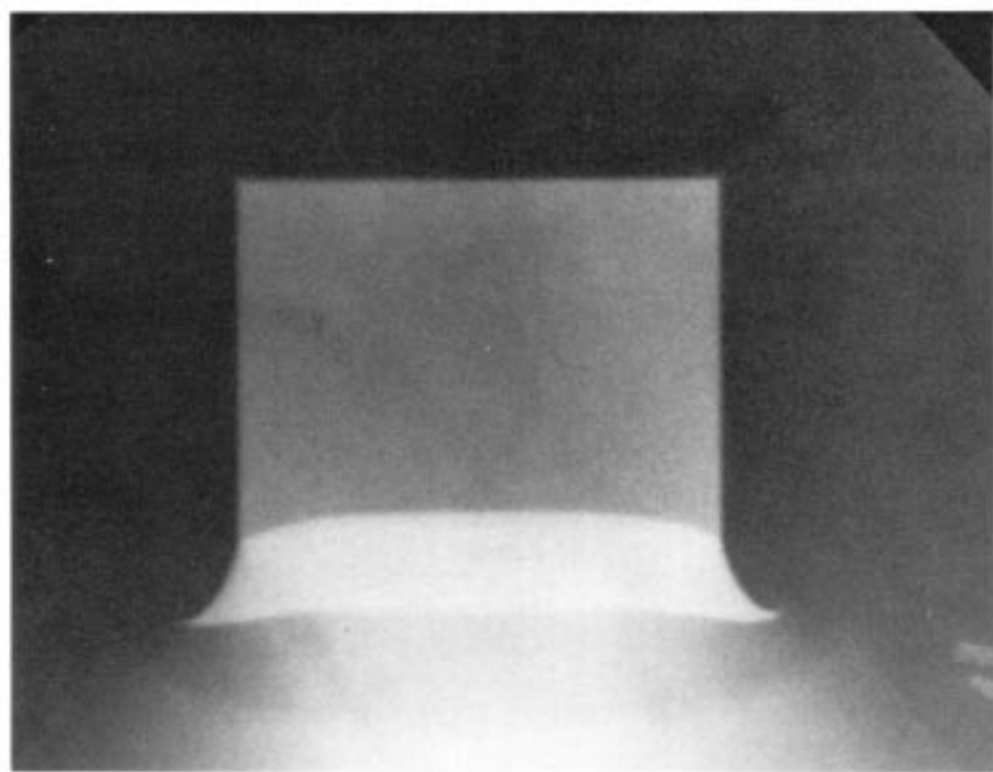
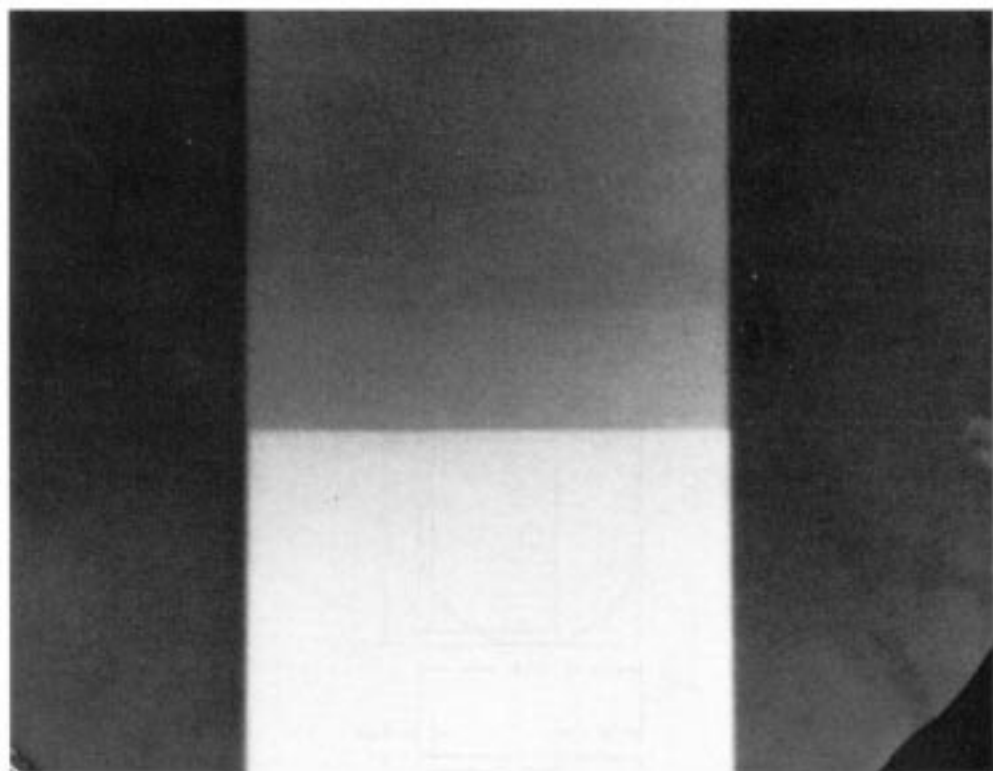




SHOT 111: Water Shock
 Date: December 21, 1964
 Experimenter: Douglas Venable
 Radiographic Time: 31.07 μ s
 Reference: Mader, 1966a

The shock wave formed in water by a Composition B-3 detonation wave driving 25.4-mm-thick Lucite. h is 5.08 mm. This shot shows the shock wave curvature for the Lucite and water corner shots, 112 and 114. Shot 113 shows the water shock wave at a later time.





SHOT 112: Lucite and Water Corner

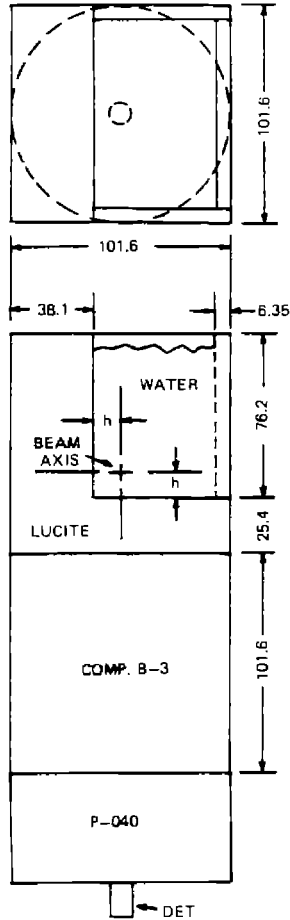
Date: December 22, 1964

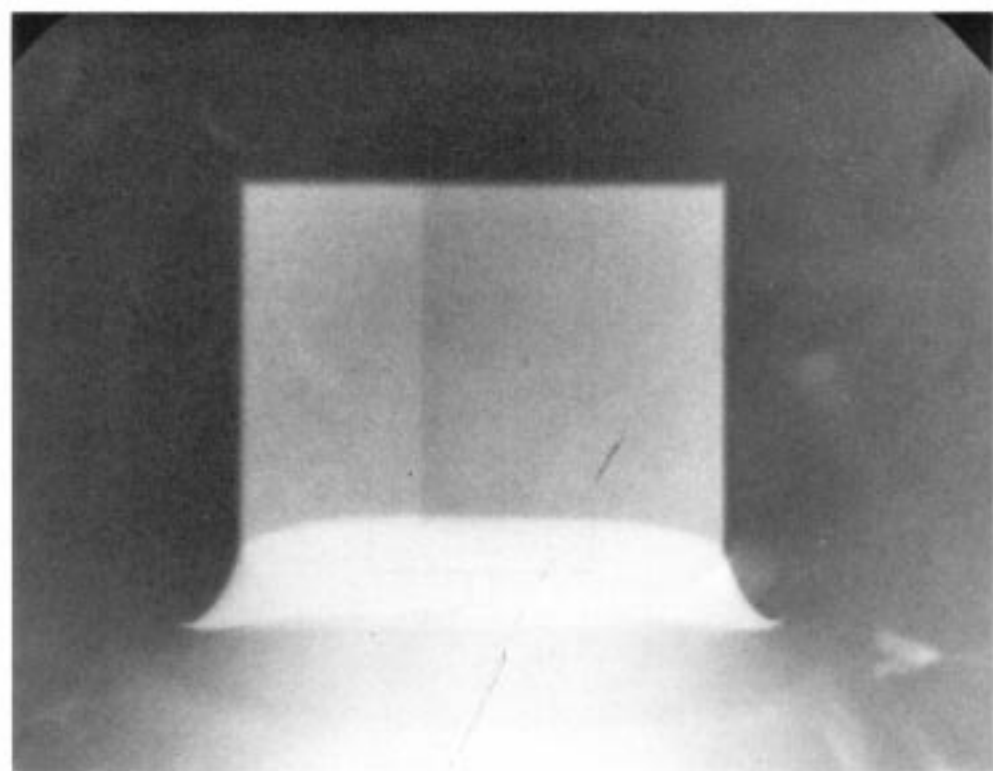
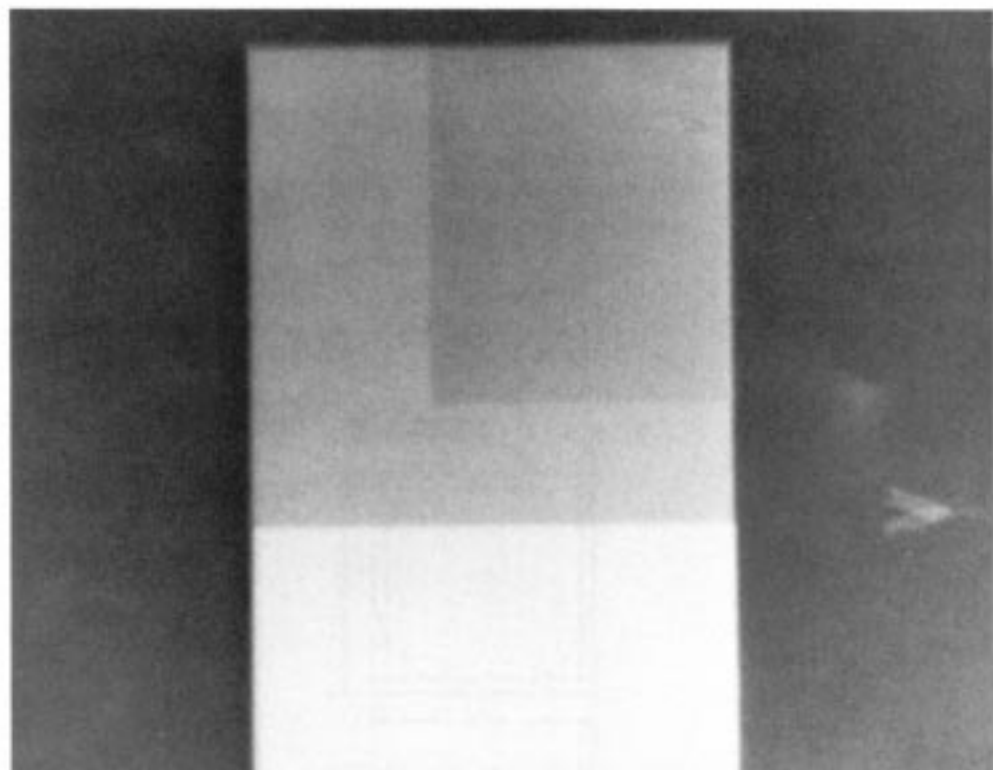
Experimenter: Douglas Venable

Radiographic Time: 31.13 μ s

Reference: Mader, 1966a

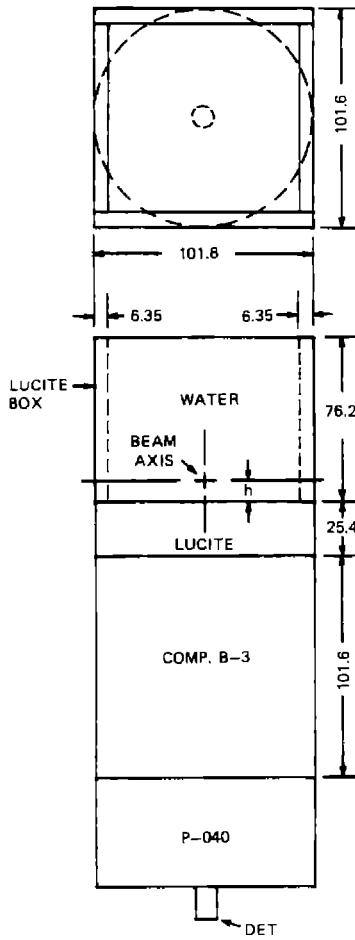
The shock wave formed by Composition B-3 driving 25.4-mm-thick Lucite interacts with a Lucite corner filled with water. See Shot 114 for a later time. h is 5.08 mm.

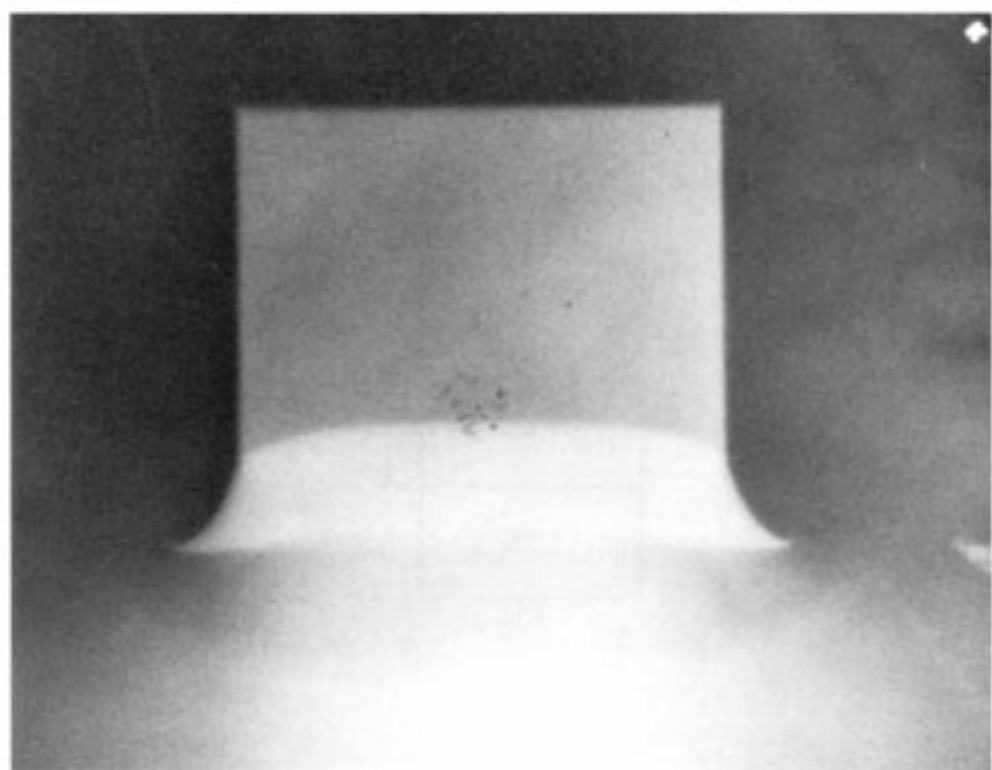
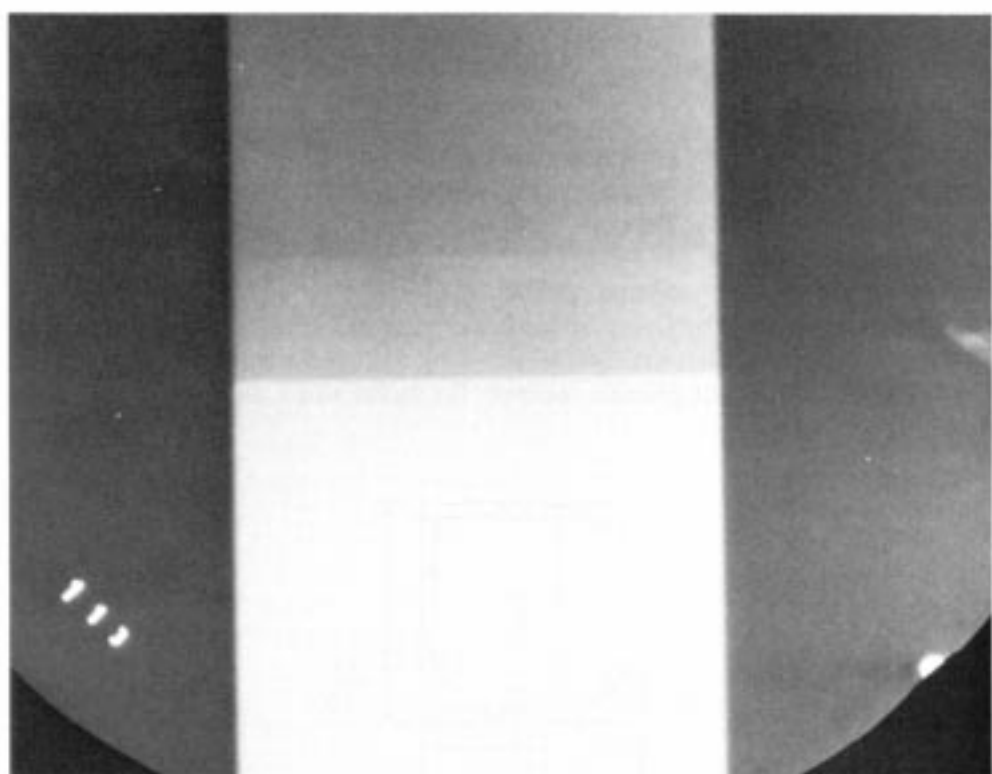




SHOT 113: **Water Shock**
Date: December 22, 1964
Experimenter: Douglas Venable
Radiographic Time: 31.86 μ s
Reference: Mader, 1966a

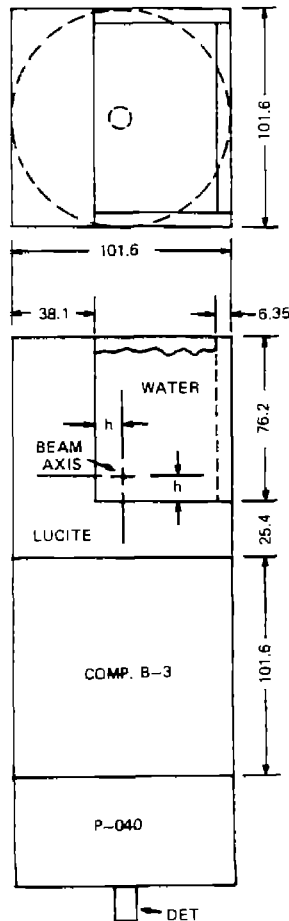
The shock wave formed in water by a Composition B-3 detonation wave drives 25.4-mm-thick Lucite. Shot 111 shows the water shock wave at an earlier time. h is 10.16 mm.

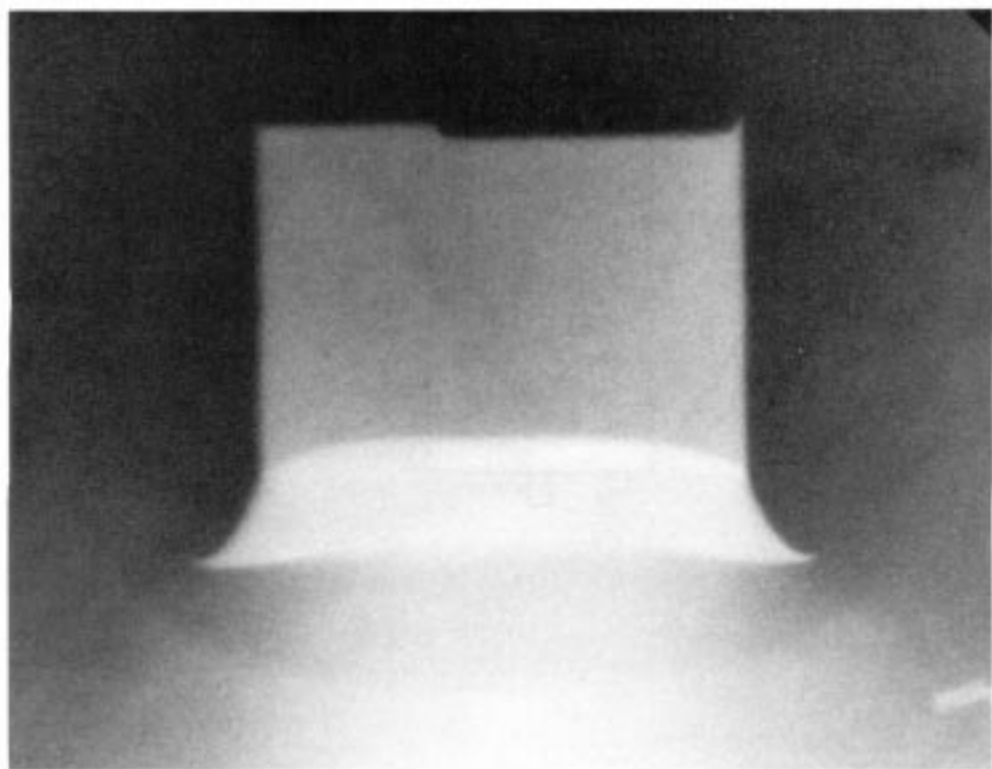
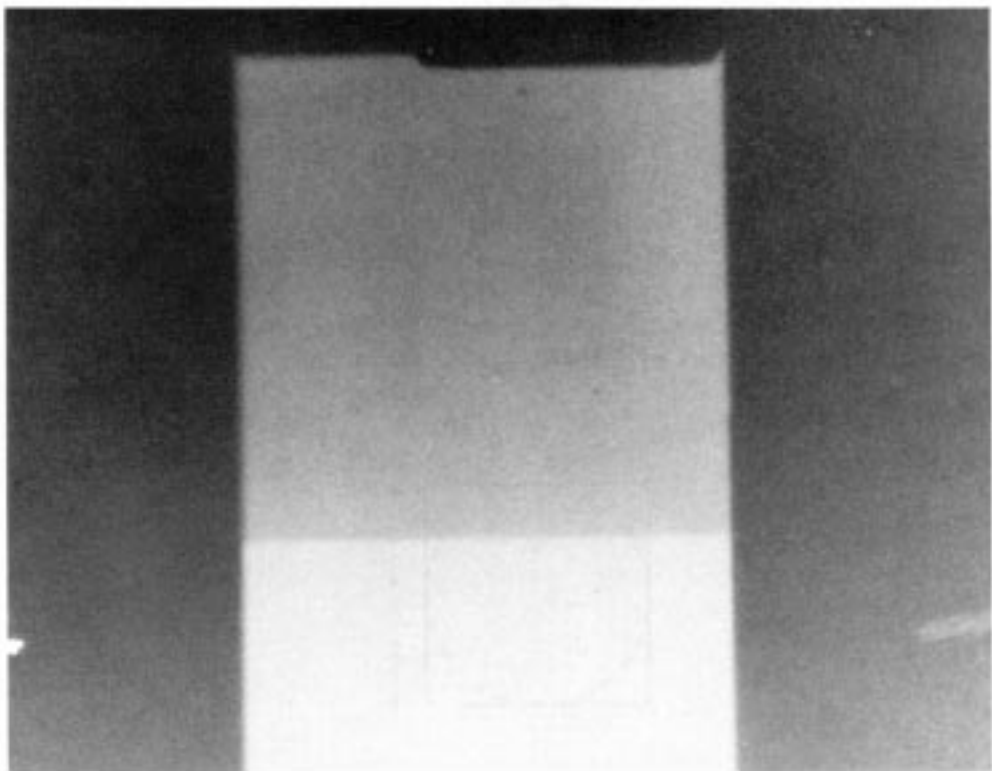




SHOT 114: Lucite and Water Corner
Date: December 29, 1964
Experimenter: Douglas Venable
Radiographic Time: 31.85 μ s
Reference: Mader, 1966a

The shock wave formed by Composition B-3 driving 25.4-mm-thick Lucite interacts with a Lucite corner filled with water. See Shot 112 for an earlier time. h is 10.16 mm. To increase the radiographic contrast, 0.4 molar zinc iodide was added to the water.





SHOT 115:

Dynamic Fracture of Nickel

Date:

January 7, 1965

Experimenter:

Douglas Venable

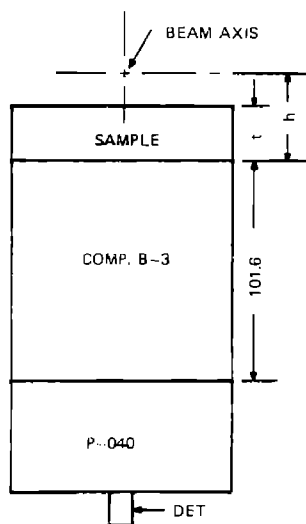
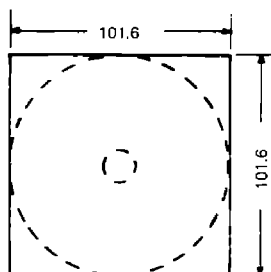
Radiographic Time:

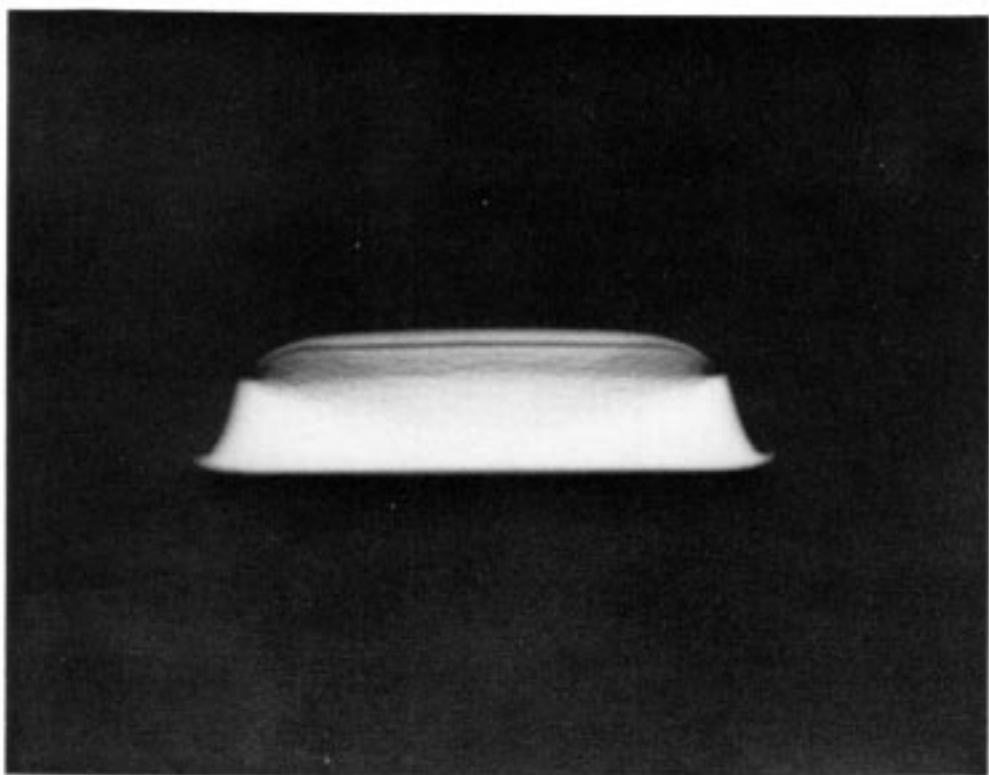
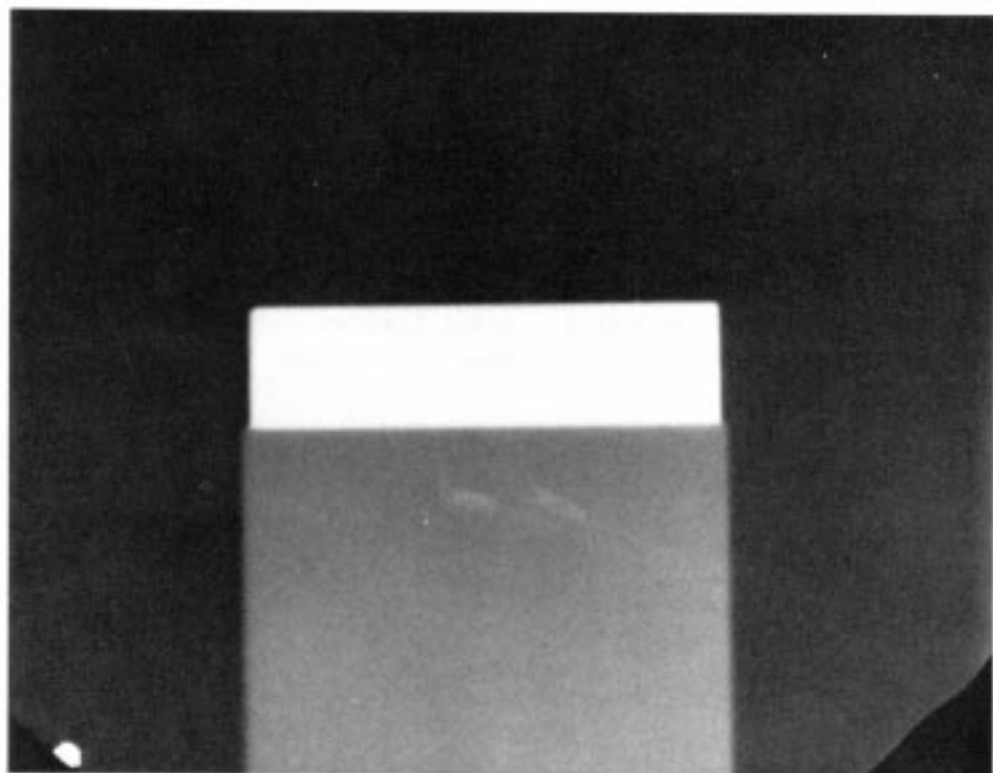
38.0 μ s

References:

Breed et al., 1967; Thurston and Mudd, 1968

Dynamic fracture of 25.4-mm-thick, t , nickel. The plate is shocked by 101.6 mm of Composition B-3 initiated by a P-040 lens. h is 38.1 mm.





SHOT 116:

Dynamic Fracture of Nickel

Date:

January 7, 1965

Experimenter:

Douglas Venable

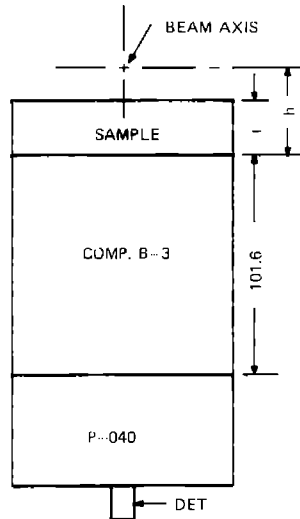
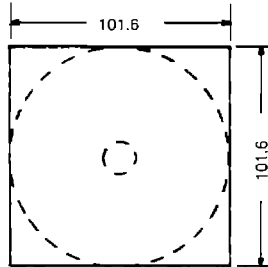
Radiographic Time:

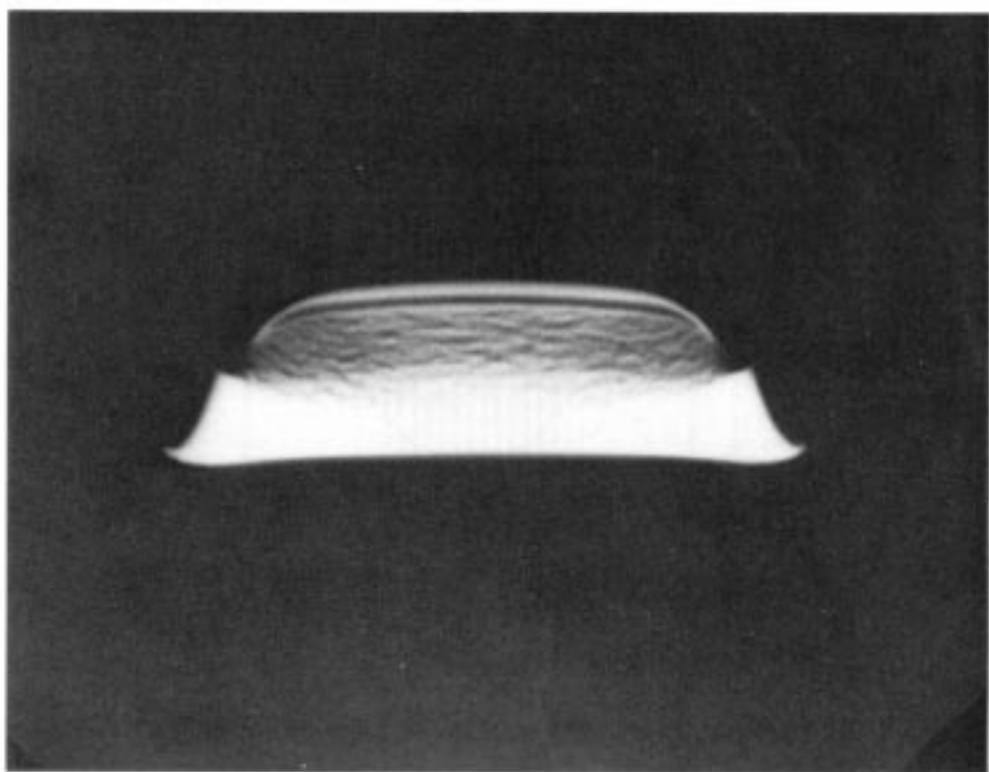
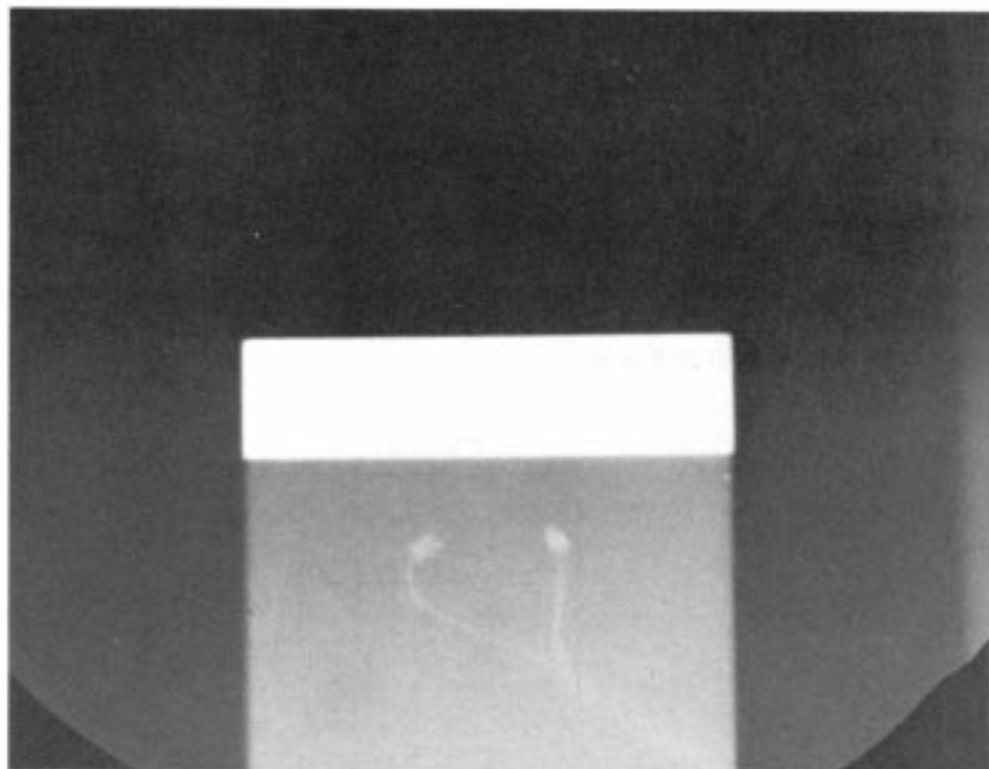
45.29 μ s

References:

Breed et al., 1967; Thurston and Mudd, 1968

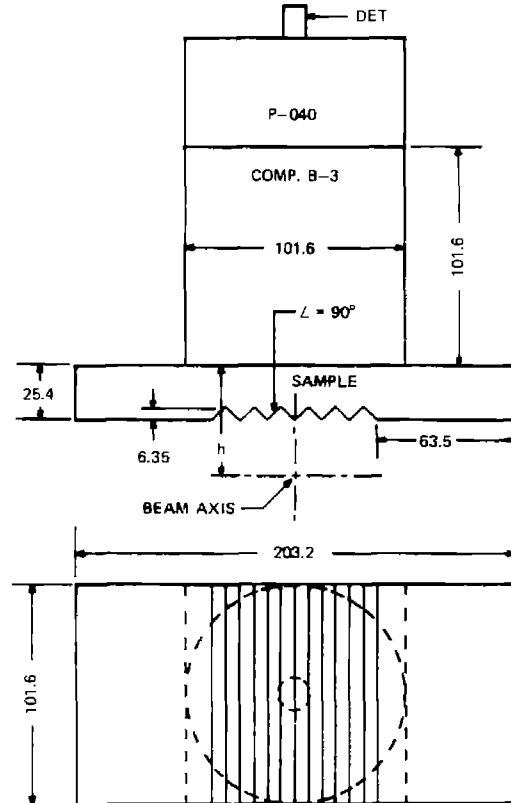
Dynamic fracture of 25.4-mm-thick, *t*, nickel. The plate is shocked by 101.6 mm of Composition B-3 initiated by a P-040 lens. *h* is 50.8 mm.

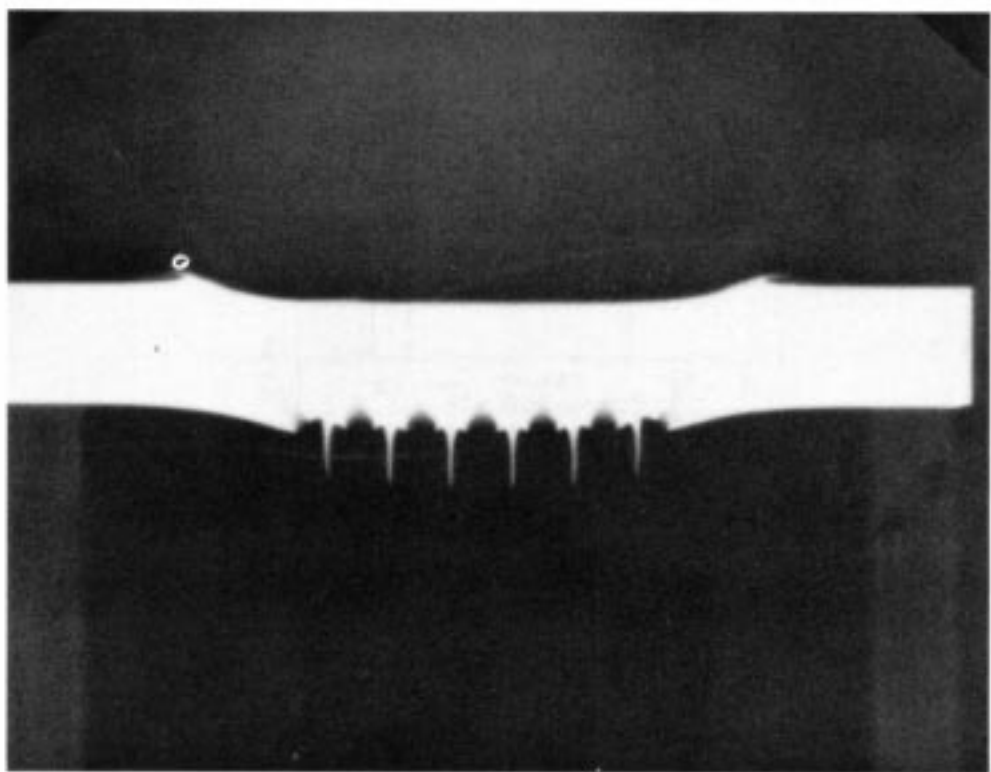
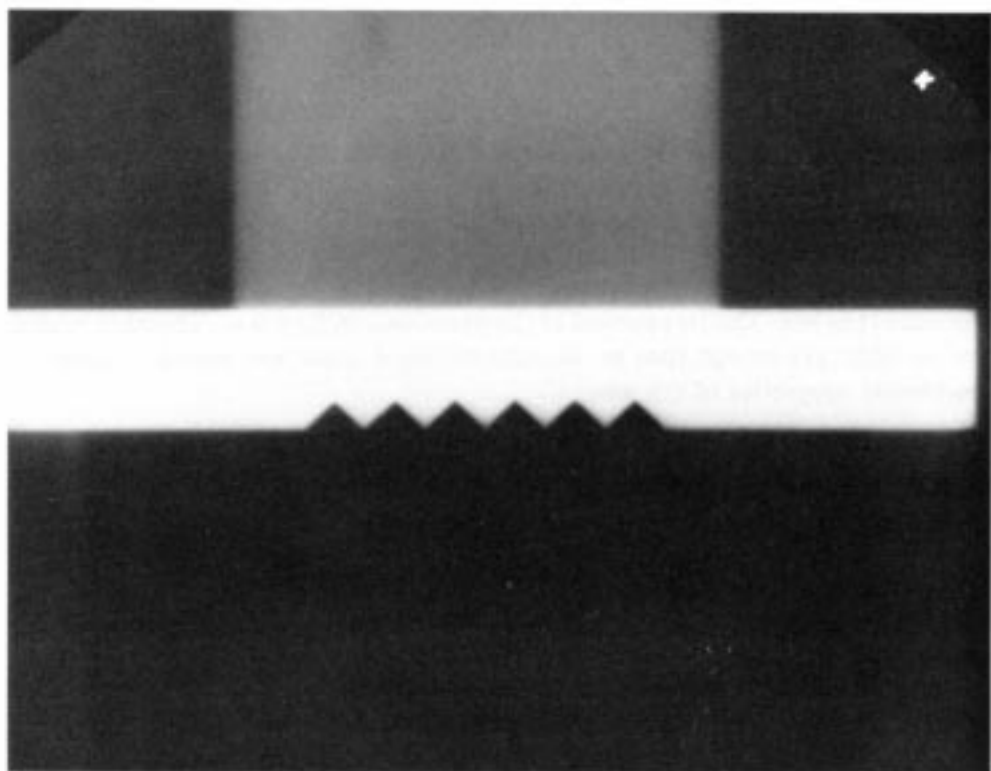




SHOT 117: **Uranium Jets**
Date: **November 24, 1964**
Experimenter: **Douglas Venable**
Radiographic Time: **41.46 μ s**

Formation of metallic jets. The explosively induced shock wave in the uranium plate interacts with the 90° grooves to produce the jets. The free surface of the plate has run for 9.9 μ s. h is 50.8 mm.





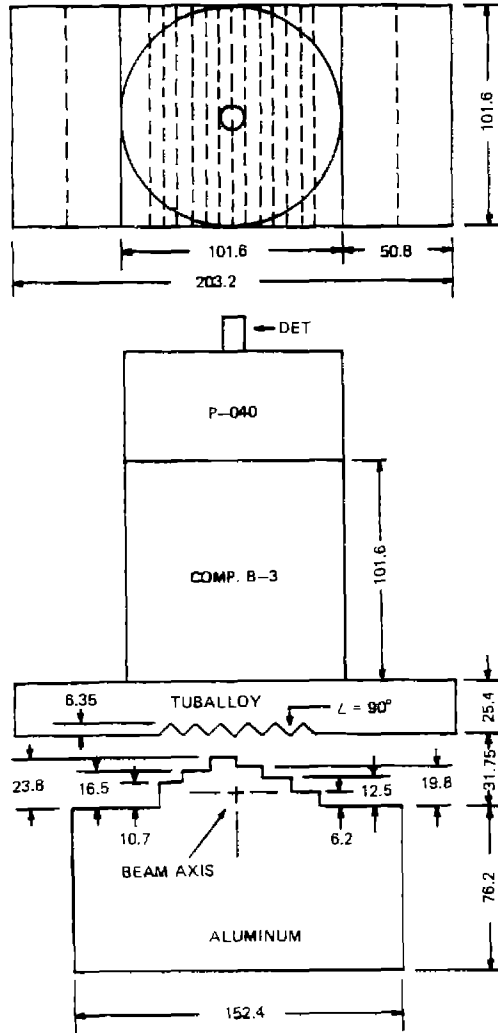
SHOT 118: Uranium Jets Penetrating Aluminum

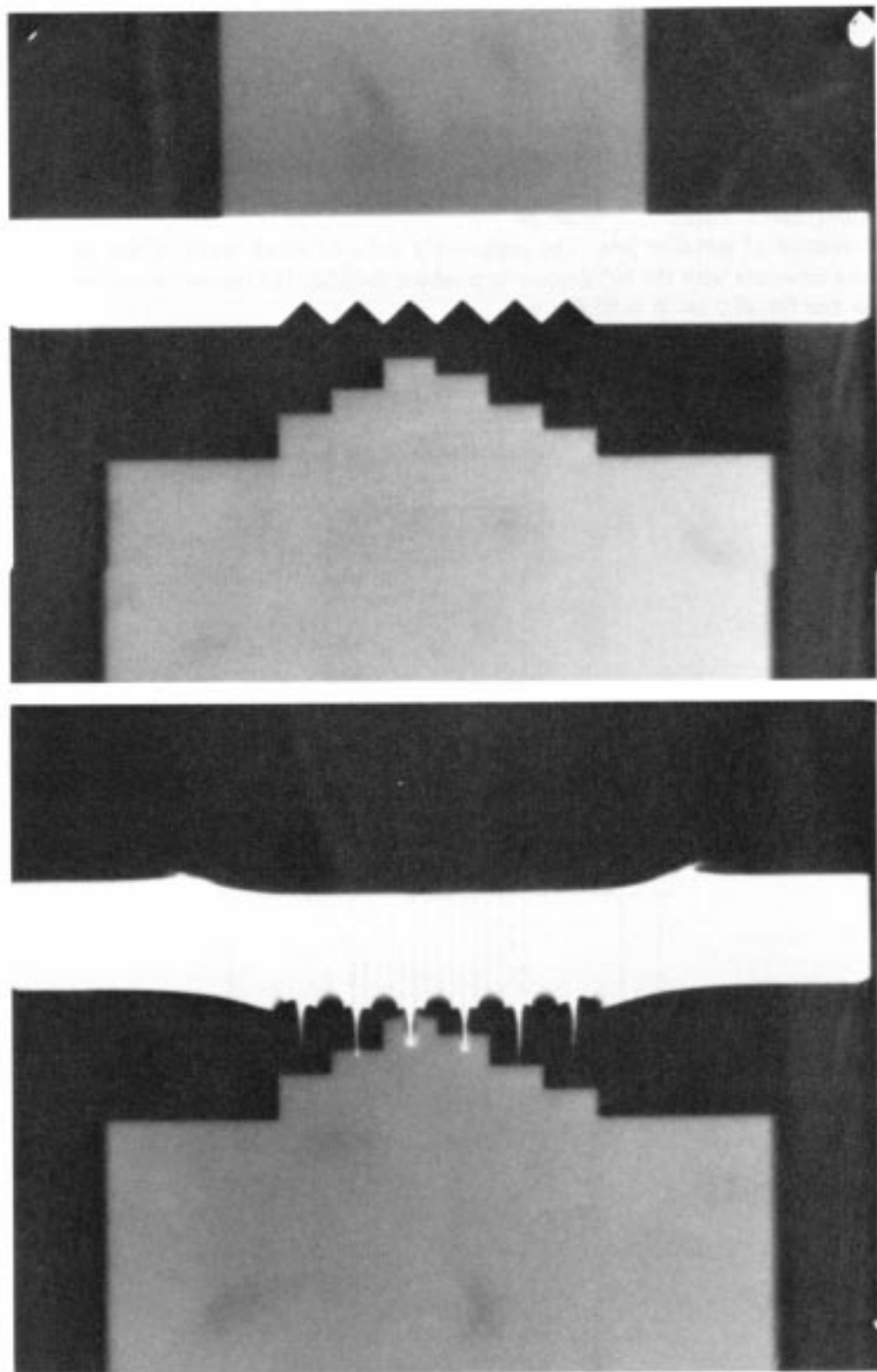
Date: December 3, 1964

Experimenter: Douglas Venable

Radiographic Time: 41.48 μ s

The explosively induced shock wave in the uranium plate interacts with the grooves to produce the jets. The free surface of the plate has run for 9.9 μ s. This shot is identical to Shot 117 except that an aluminum target plate was added to show the penetration properties of the jets.





SHOT 122:

Uranium Jets

Date:

December 8, 1964

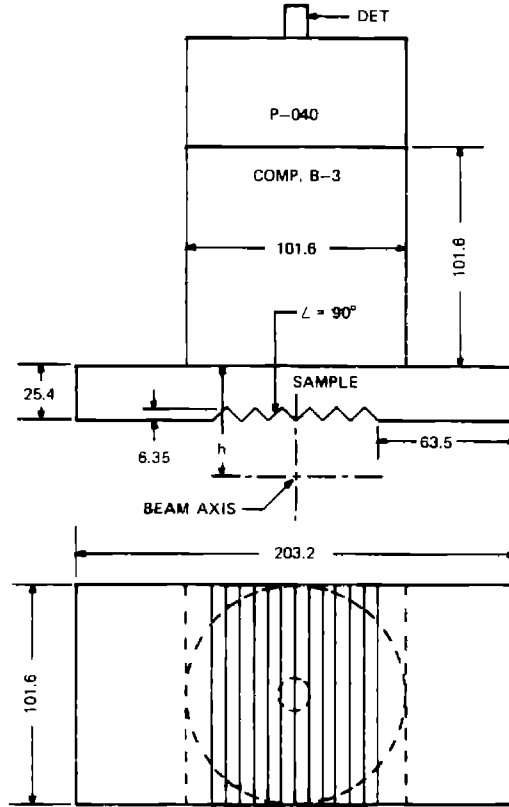
Experimenter:

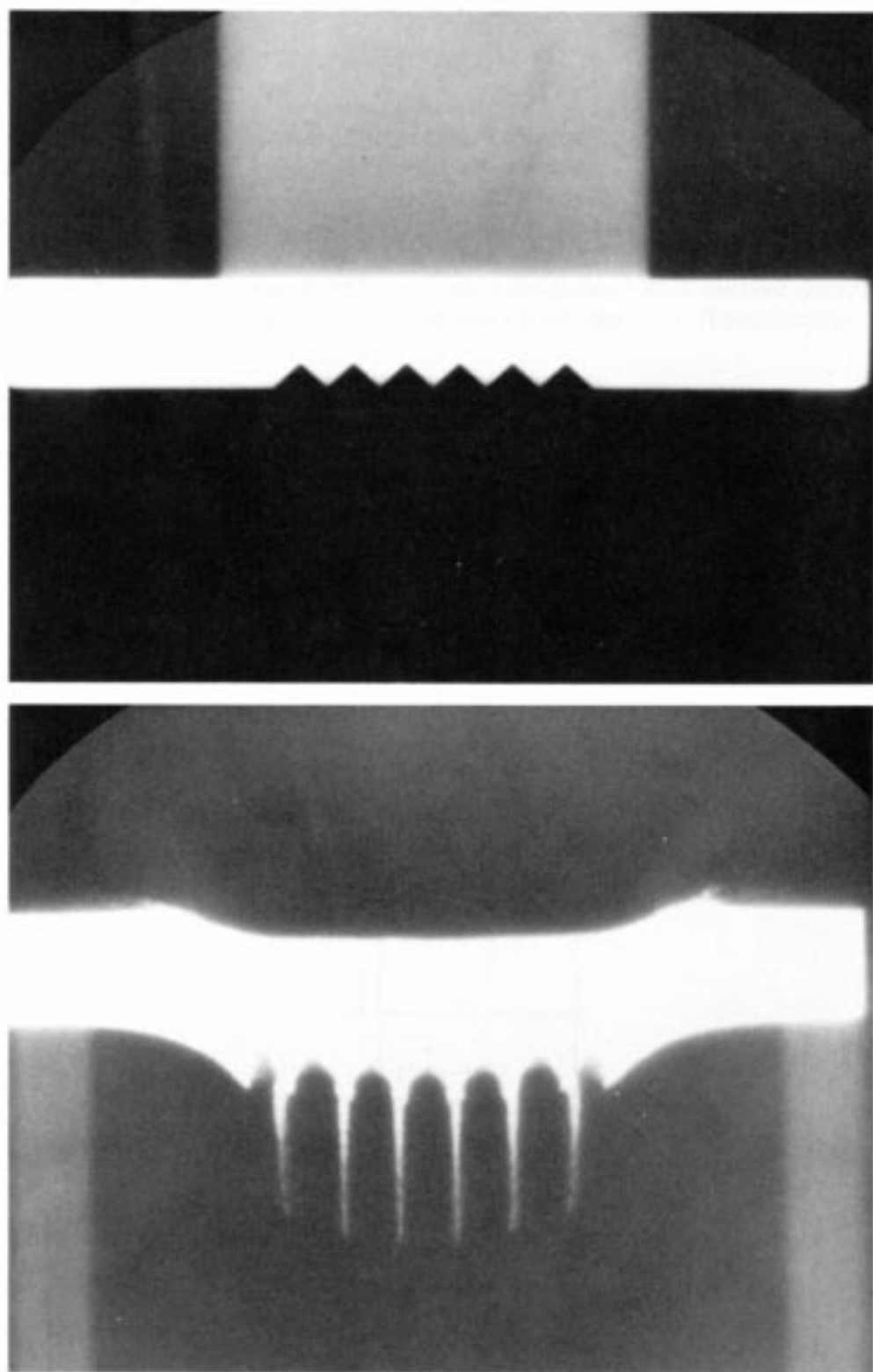
Roger W. Taylor

Radiographic Time:

56.58 μ s

Formation of metallic jets. The explosively induced shock wave in the uranium plate interacts with the 90° grooves to produce the jets. The free surface of the plate has run for 25.0 μ s. h is 63.5 mm.





SHOT 123:

Dynamic Fracture of Uranium

Date:

December 30, 1964

Experimenter:

Roger W. Taylor

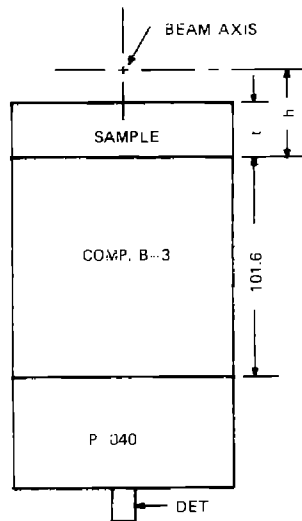
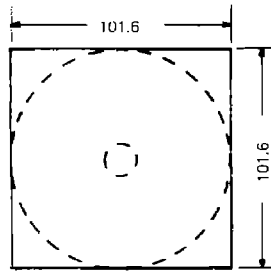
Radiographic Time:

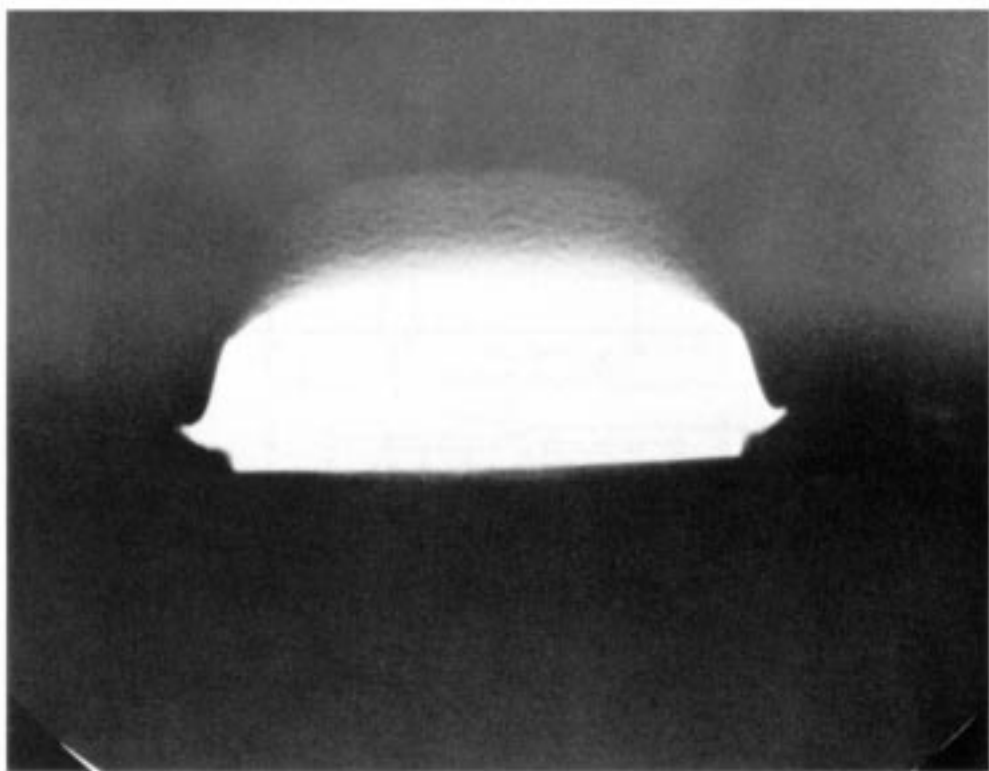
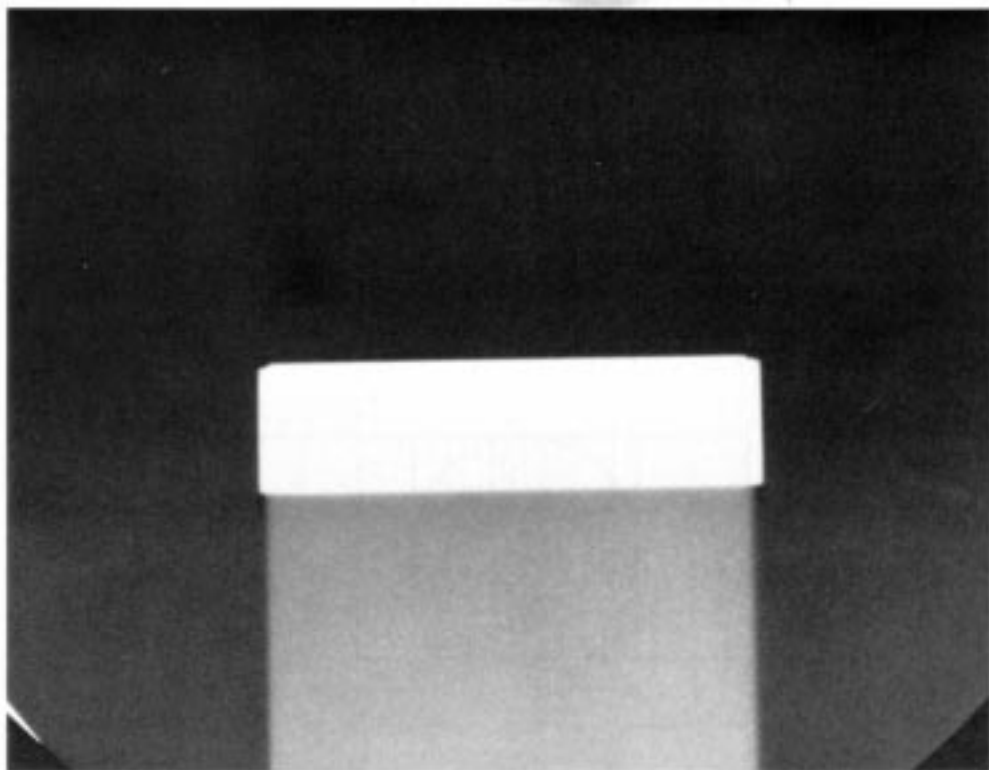
49.15 μ s

Reference:

Thurston and Mudd, 1968

Dynamic fracture of 25.4-mm-thick, t , uranium. The plate is shocked by 101.6 mm of Composition B-3 initiated by a P-040 lens. h is 50.8 mm.





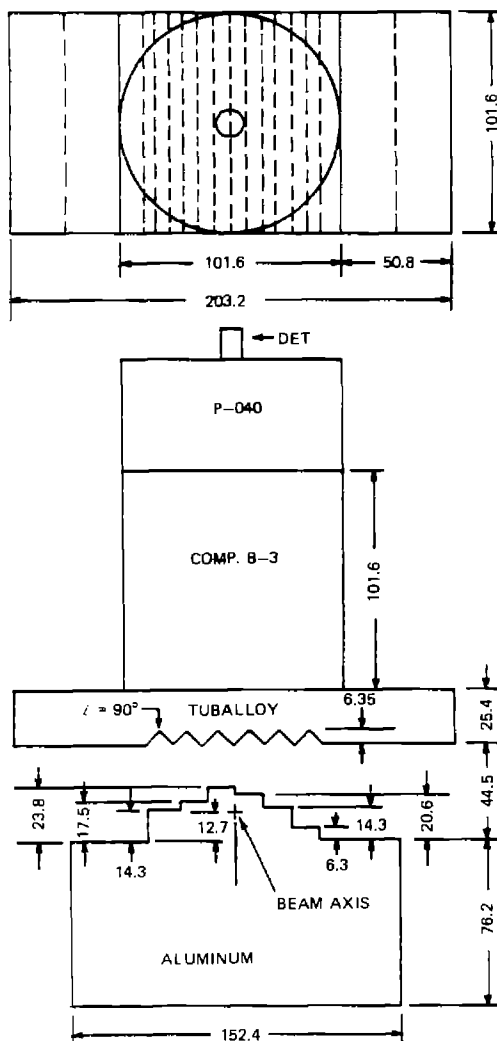
SHOT 124: Uranium Jets Penetrating Aluminum

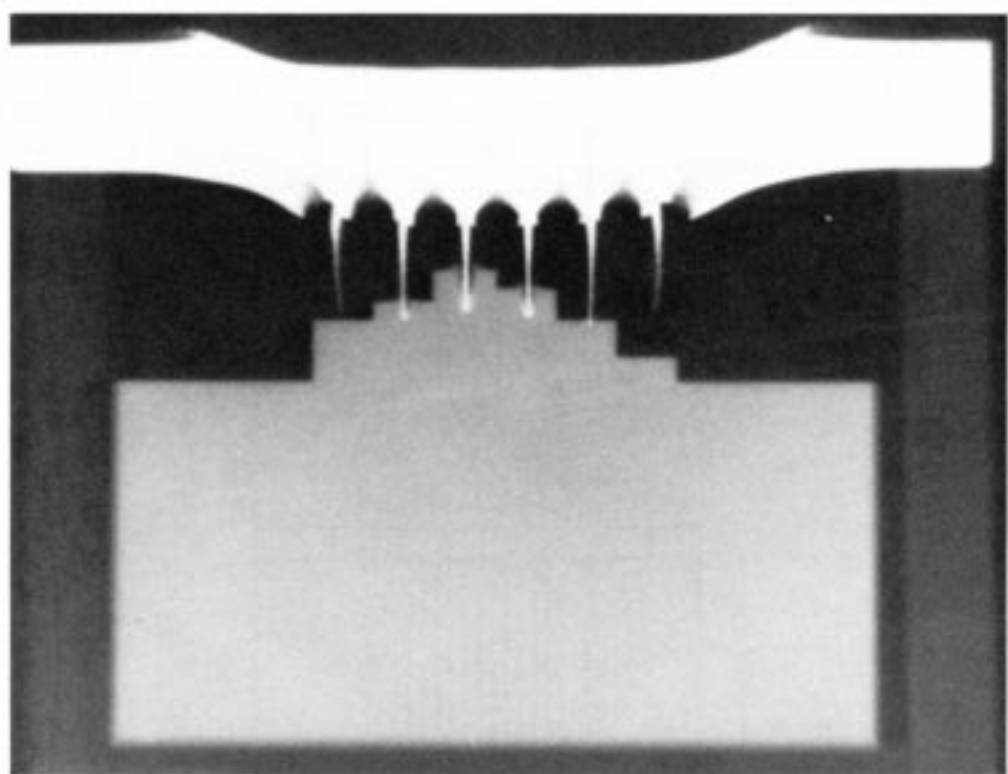
Date: December 31, 1964

Experimenter: Roger W. Taylor

Radiographic Time: 49.12 μ s

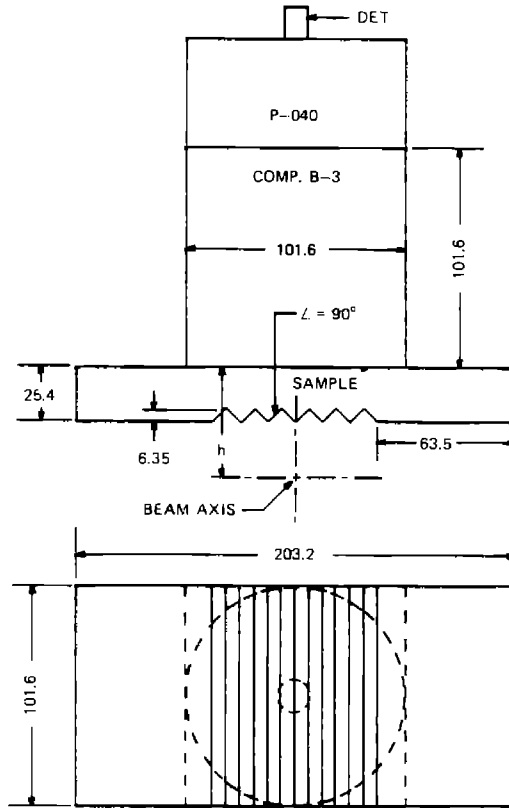
The explosively induced shock wave in the uranium plate interacts with the grooves to produce the jets. The free surface of the plate has run for 17.5 μ s. The aluminum target plate shows the penetration properties of the uranium jets.

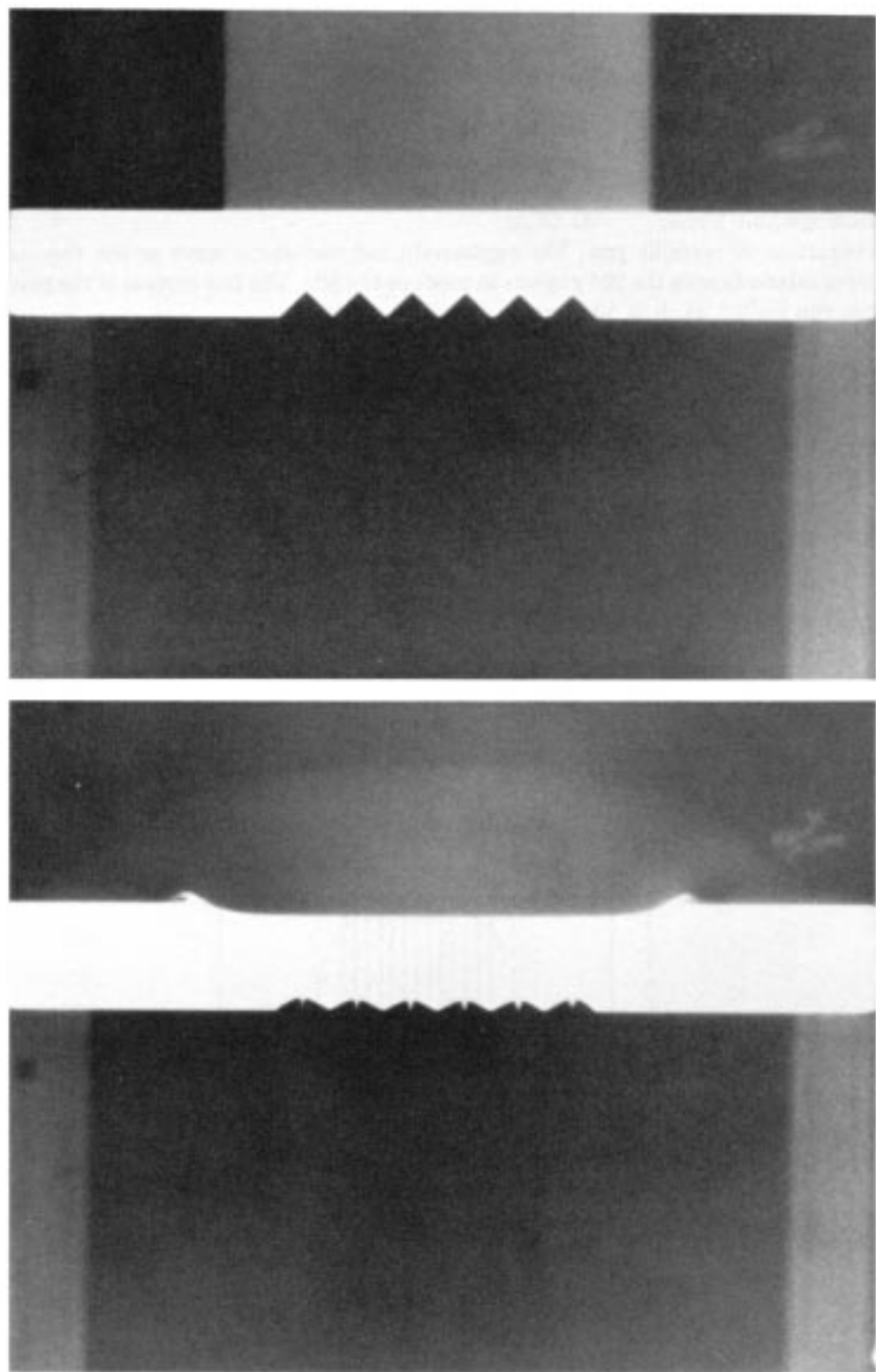




SHOT 125: **Thorium Jets**
 Date: January 26, 1975
 Experimenter: Roger W. Taylor
 Radiographic Time: 33.57 μ s

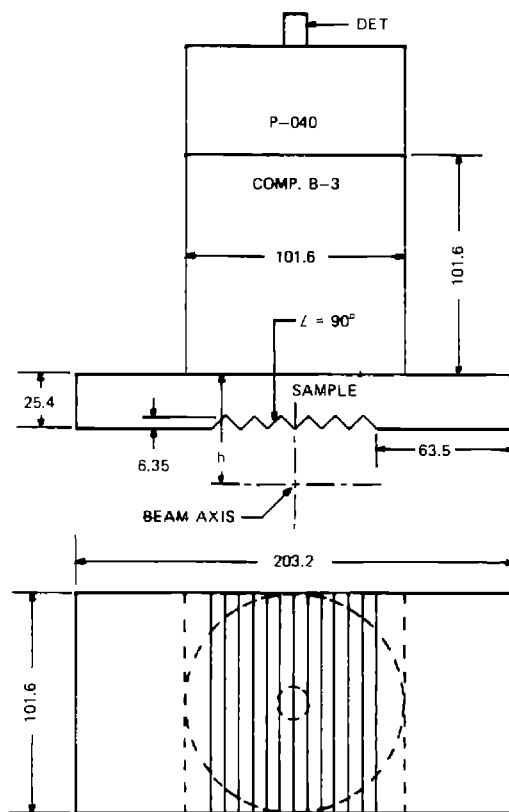
Formation of metallic jets. The explosively induced shock wave in the thorium plate interacts with the 90° grooves to produce the jets. h is 25.4 mm. The shock wave has arrived at the plate free surface.

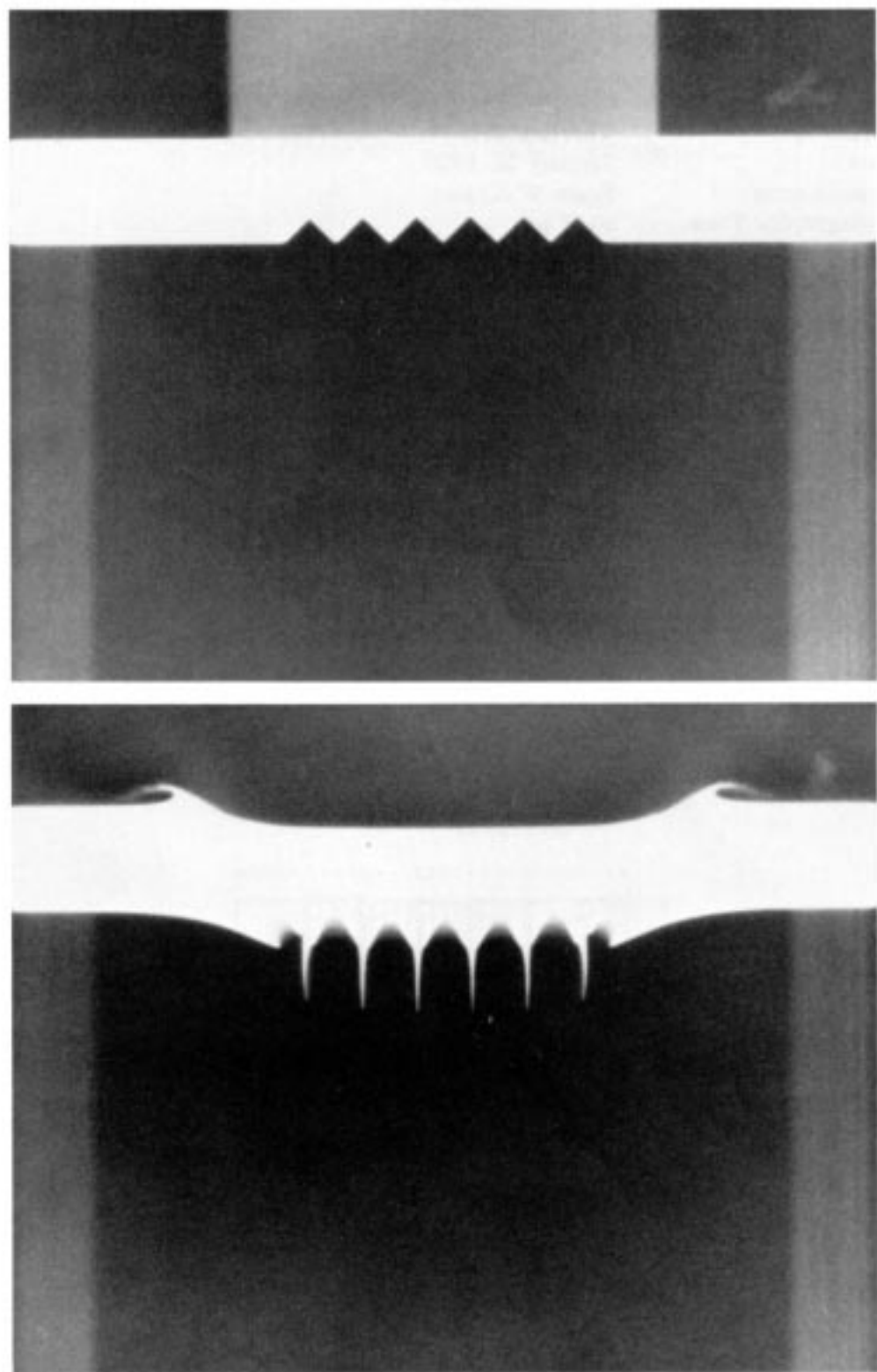




SHOT 126: **Thorium Jets**
Date: **December 31, 1964**
Experimenter: **Roger W. Taylor**
Radiographic Time: **41.68 μ s**

Formation of metallic jets. The explosively induced shock wave in the thorium plate interacts with the 90° grooves to produce the jets. The free surface of the plate has run for 8.1 μ s. h is 50.8 mm.





SHOT 127:

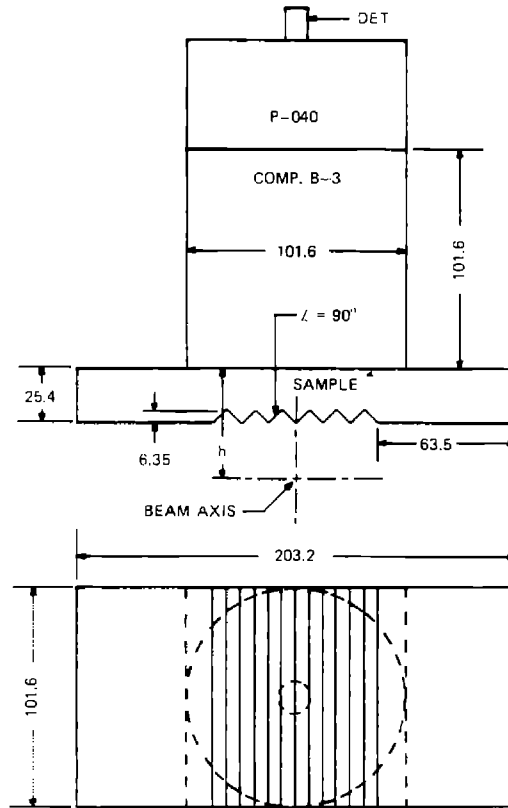
Thorium Jets

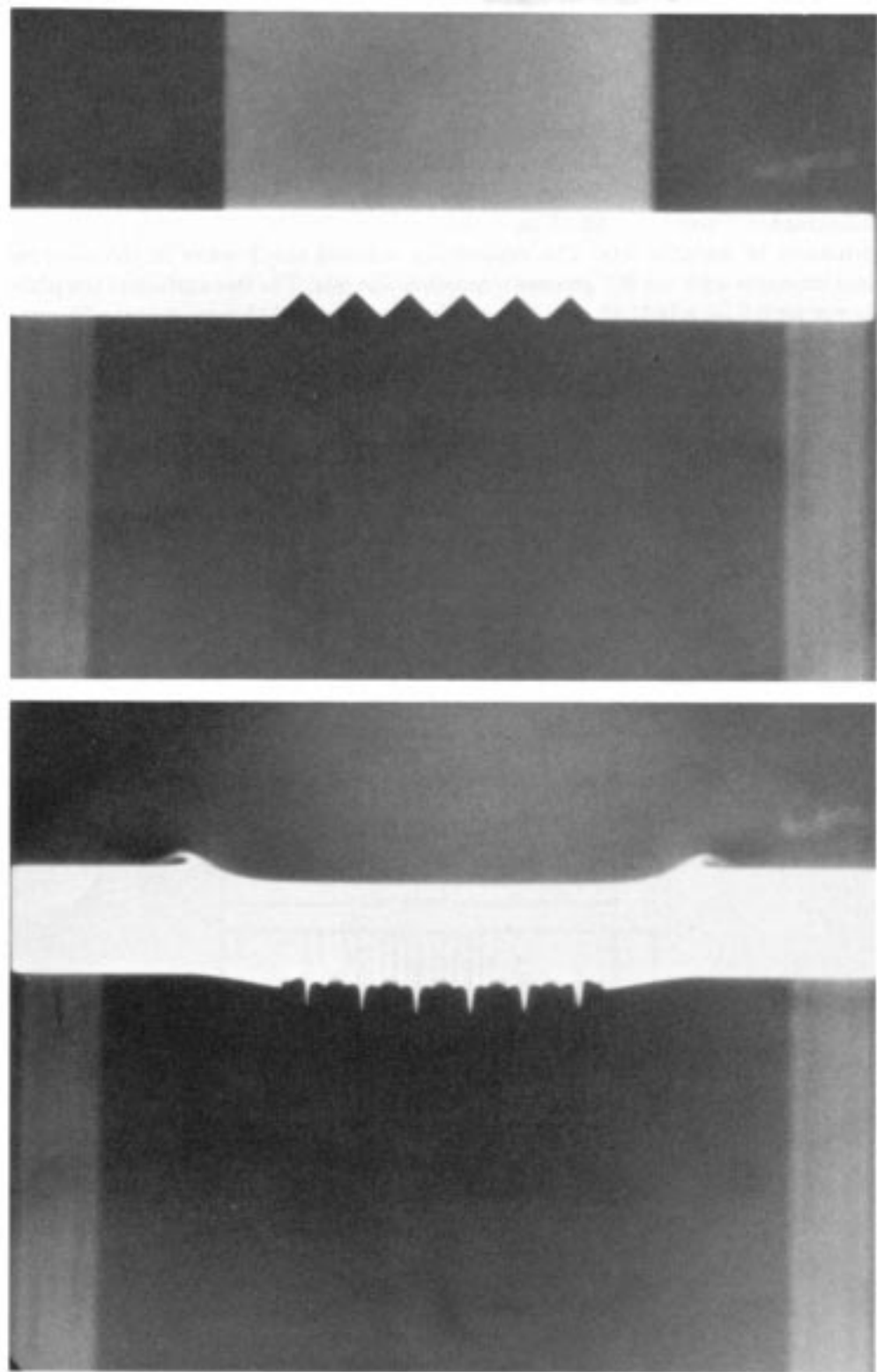
Date: January 26, 1965

Experimenter: Roger W. Taylor

Radiographic Time: 36.57 μ s

Formation of metallic jets. The explosively induced shock wave in the thorium plate interacts with the 90° grooves to produce the jets. The free surface of the plate has run for 3.0 μ s. h is 25.4 mm.





SHOT 128:**Thorium Jets**

Date:

January 26, 1965

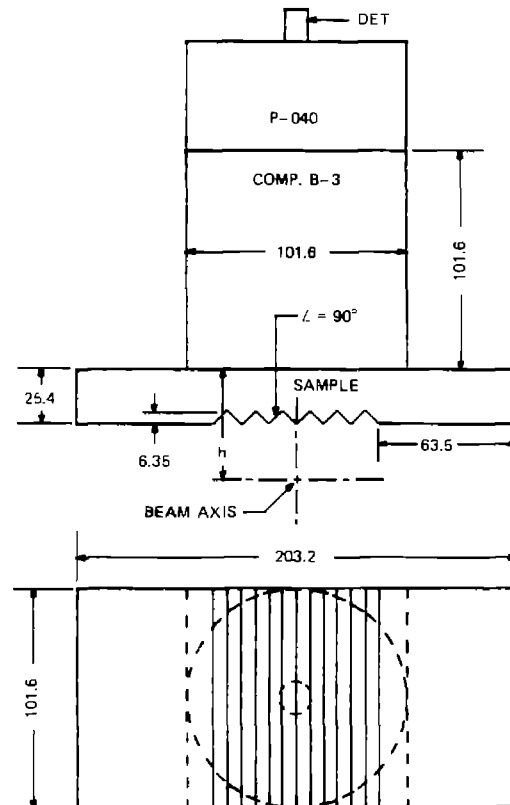
Experimenter:

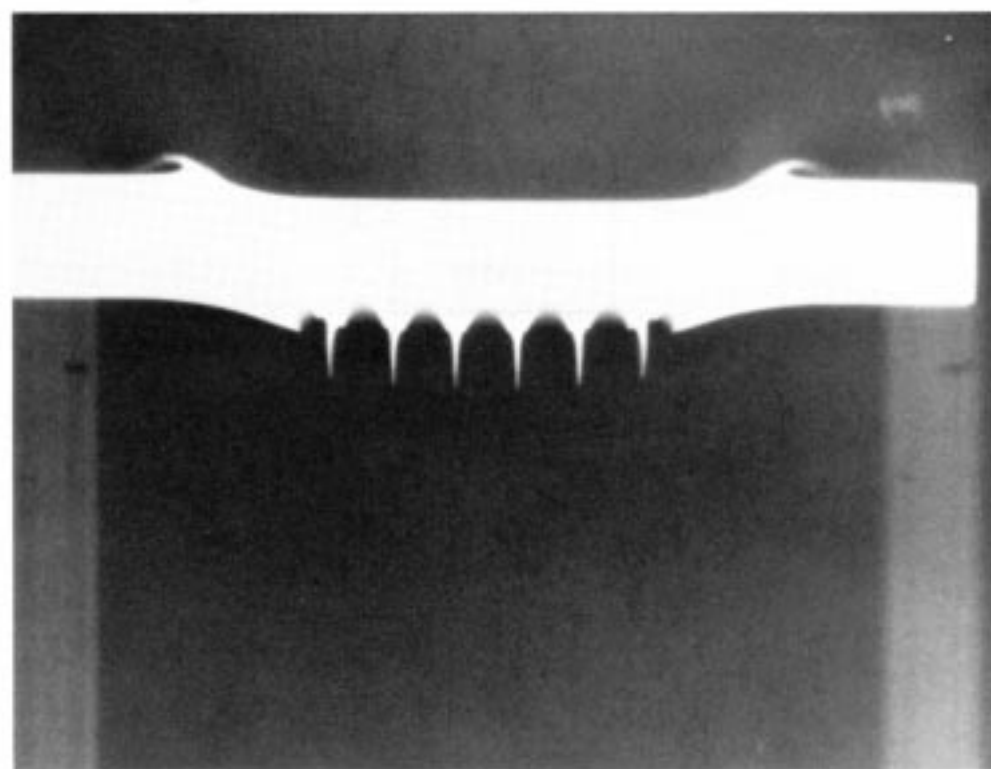
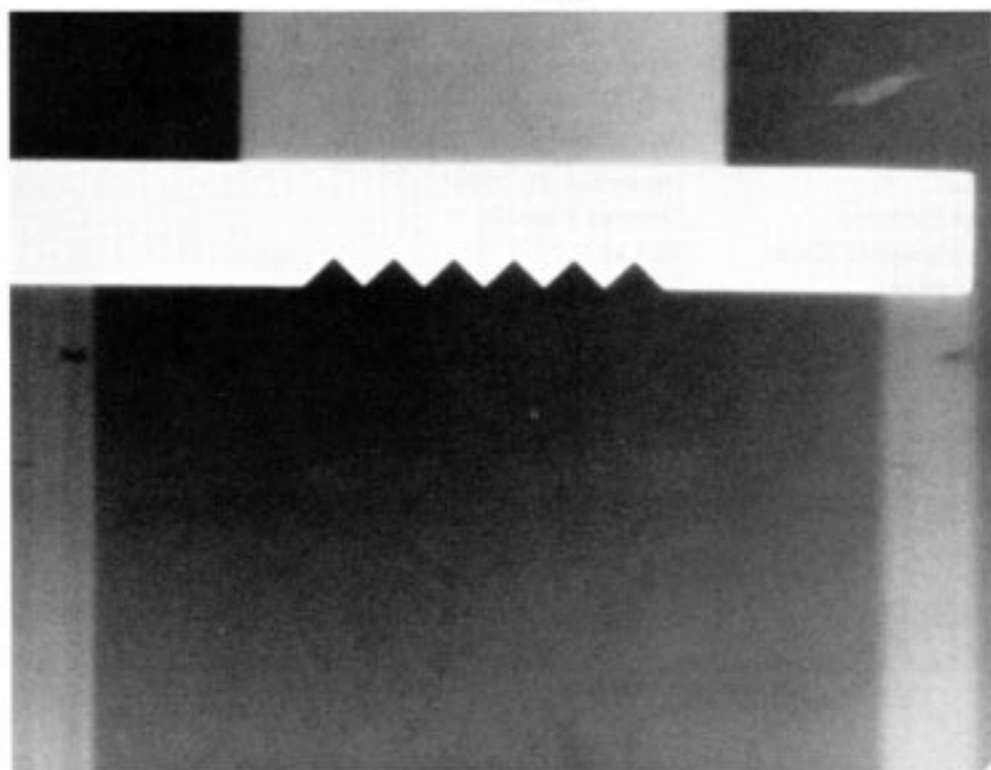
Roger W. Taylor

Radiographic Time:

39.53 μ s

Formation of metallic jets. The explosively induced shock wave in the thorium plate interacts with the 90° grooves to produce the jets. The free surface of the plate has run for 6.0 μ s. h is 31.75 mm. The jet tip velocity was 3.15 mm/ μ s over a 25-mm-long run.





SHOT 129:

Dynamic Fracture of Uranium

Date:

December 31, 1964

Experimenter:

Douglas Venable

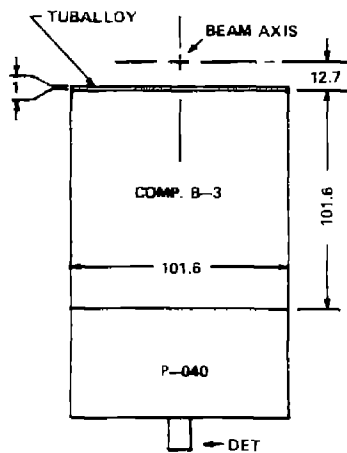
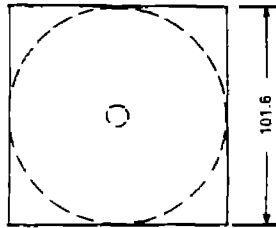
Radiographic Time:

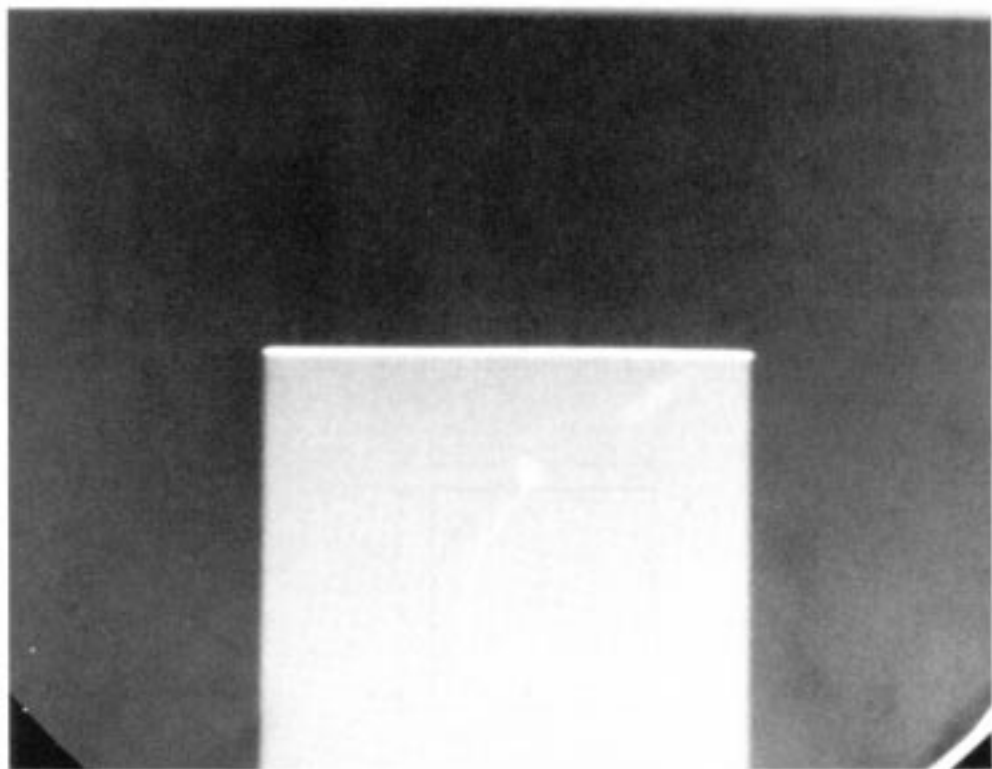
34.4 μ s

Reference:

Thurston and Mudd, 1968

Dynamic fracture of 1.0-mm-thick uranium. The plate is shocked by 101.6 mm of Composition B-3 initiated by a P-040 lens. h is 12.7 mm.





SHOT 130:

Dynamic Fracture of Thorium

Date:

December 30, 1964

Experimenter:

Douglas Venable

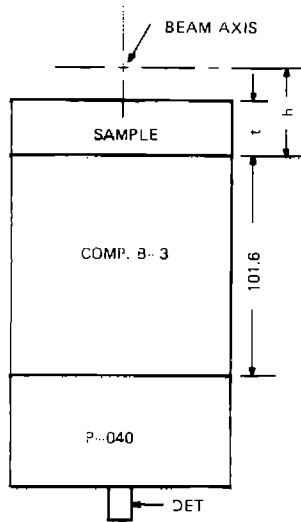
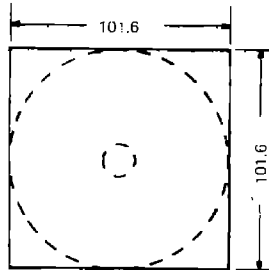
Radiographic Time:

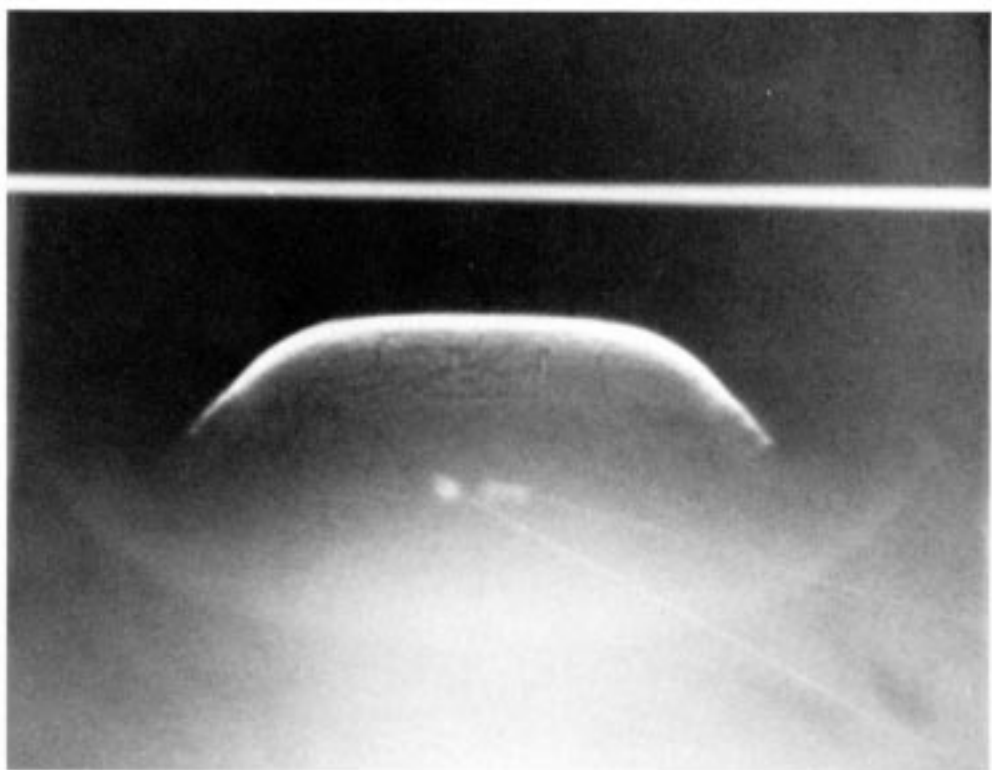
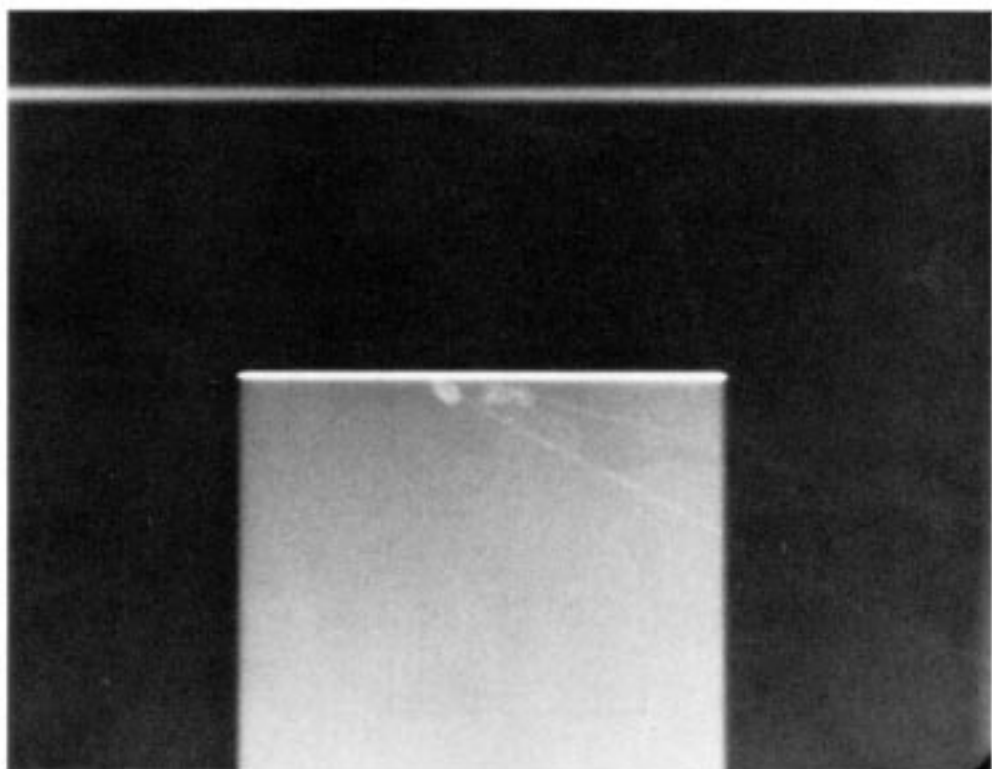
34.41 μ s

Reference:

Thurston and Mudd, 1968

Dynamic fracture of 1.0-mm-thick, t , thorium. The plate is shocked by 101.6 mm of Composition B-3 initiated by a P-040 lens. h is 12.7 mm.





SHOT 131:

Dynamic Fracture of Uranium

Date:

December 29, 1964

Experimenter:

Douglas Venable

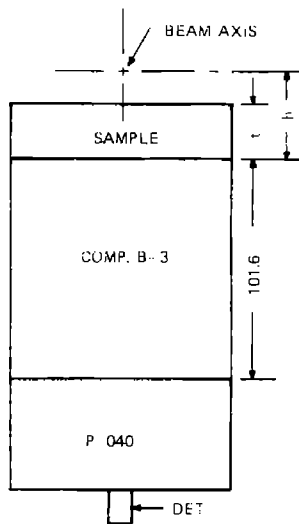
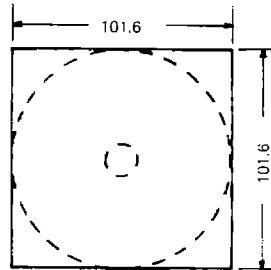
Radiographic Time:

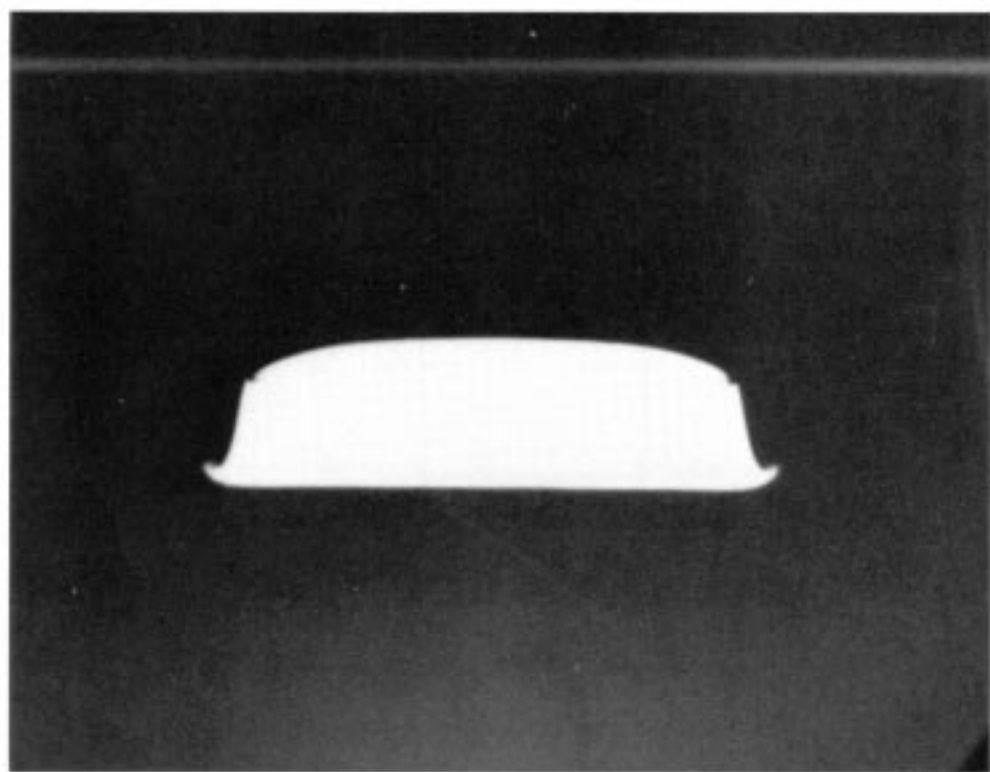
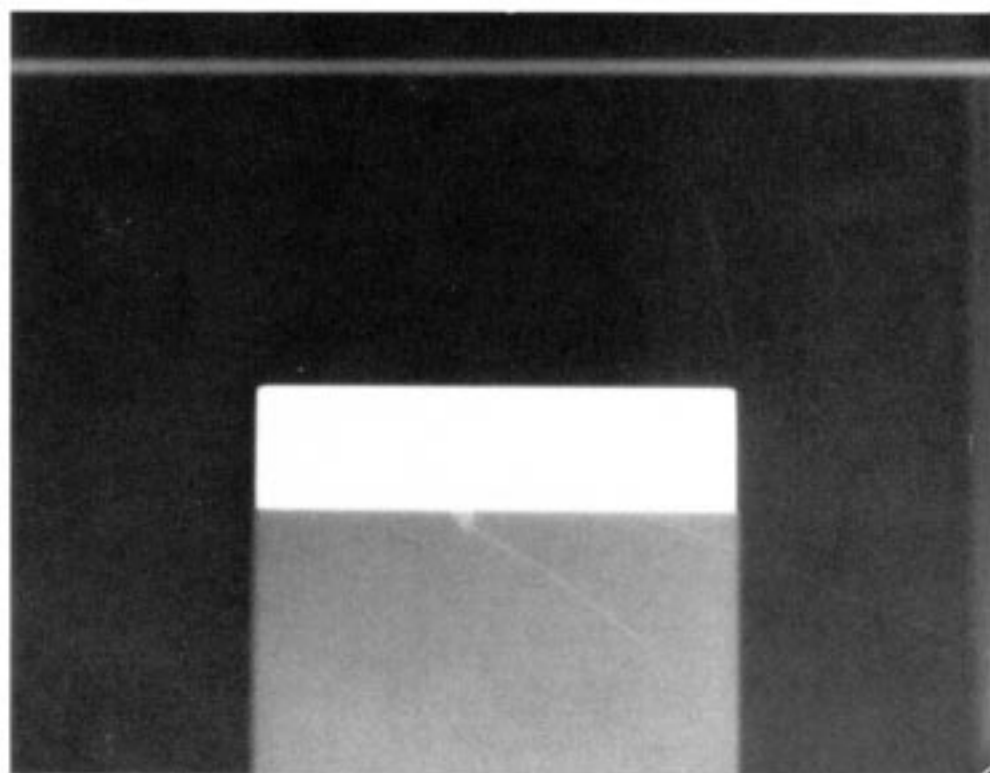
43.28 μ s

Reference:

Thurston and Mudd, 1968

Dynamic fracture of 25.0-mm-thick, t, uranium. The plate is shocked by 101.6 mm of Composition B-3 initiated by a P-040 lens. h is 38.1 mm.





SHOT 132:

Dynamic Fracture of Thorium

Date:

December 30, 1964

Experimenter:

Douglas Venable

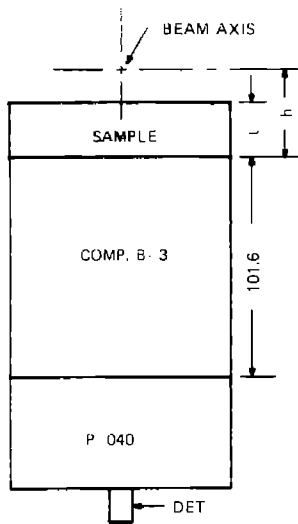
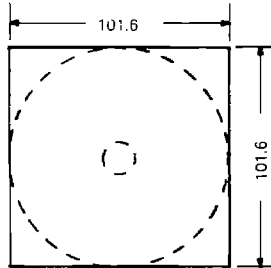
Radiographic Time:

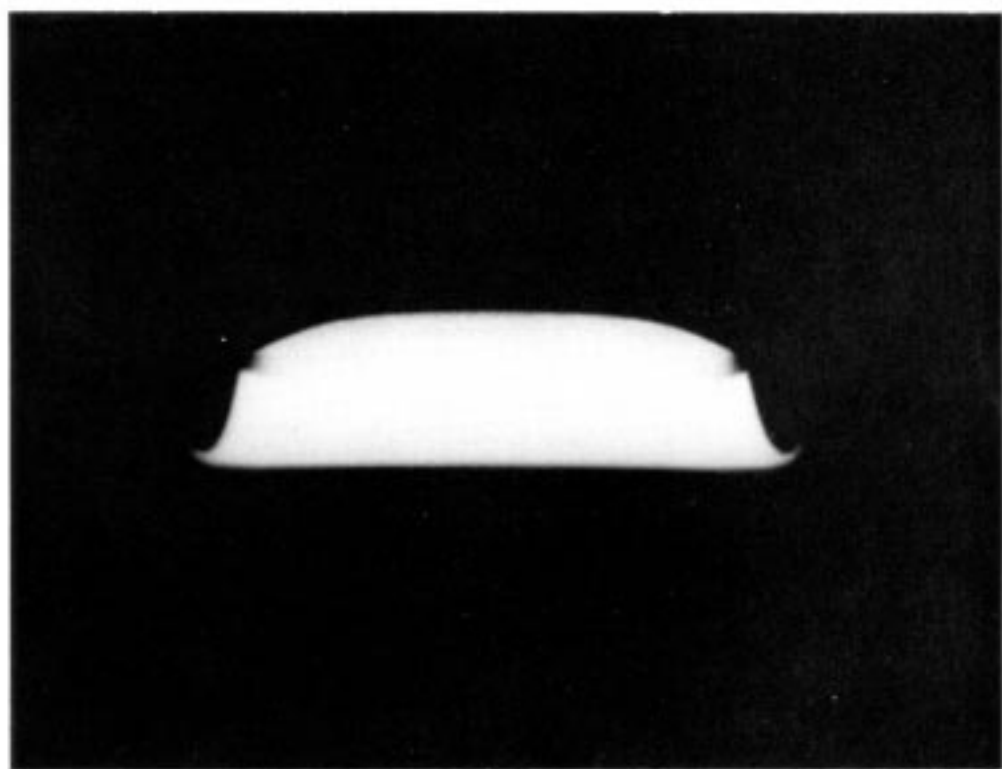
41.40 μ s

Reference :

Thurston and Mudd, 1968

Dynamic fracture of 25.0-mm-thick, t, thorium. The plate is shocked by 101.6 mm of Composition B-3 initiated by a P-040 lens. h is 41.3 mm.





SHOT 133:

Dynamic Fracture of Uranium

Date:

December 29, 1964

Experimenter:

Douglas Venable

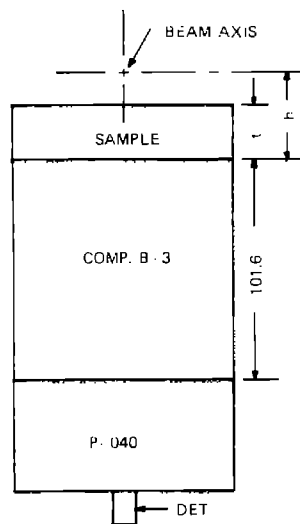
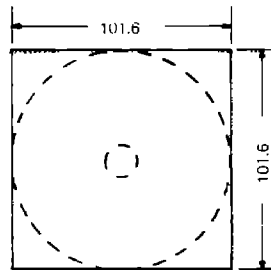
Radiographic Time:

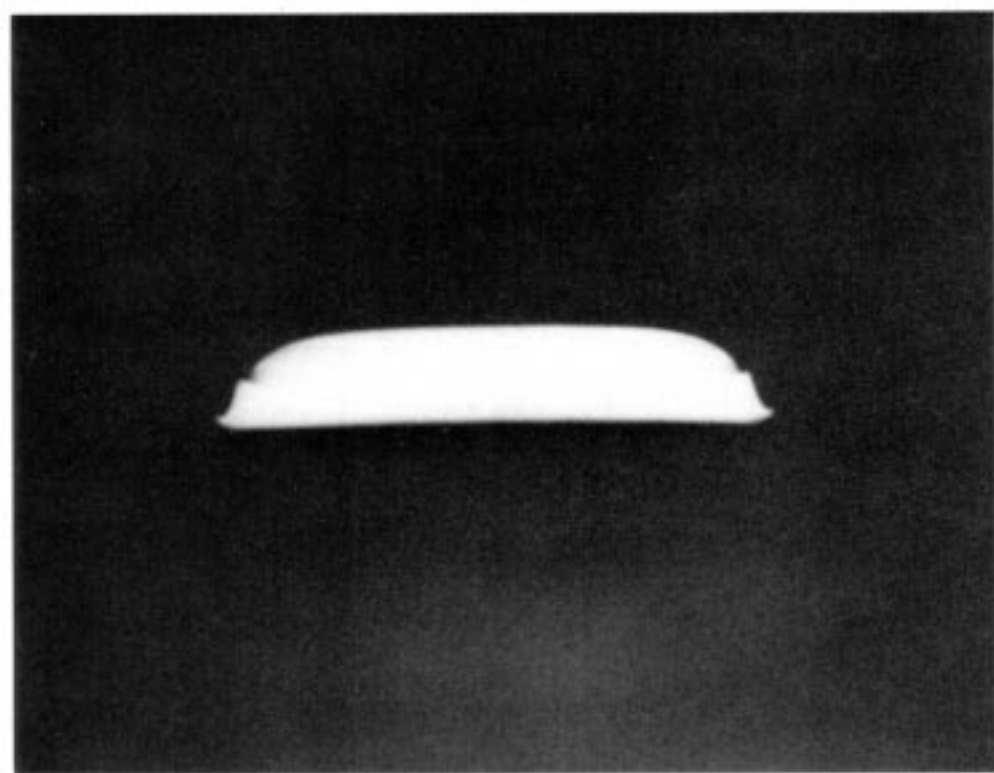
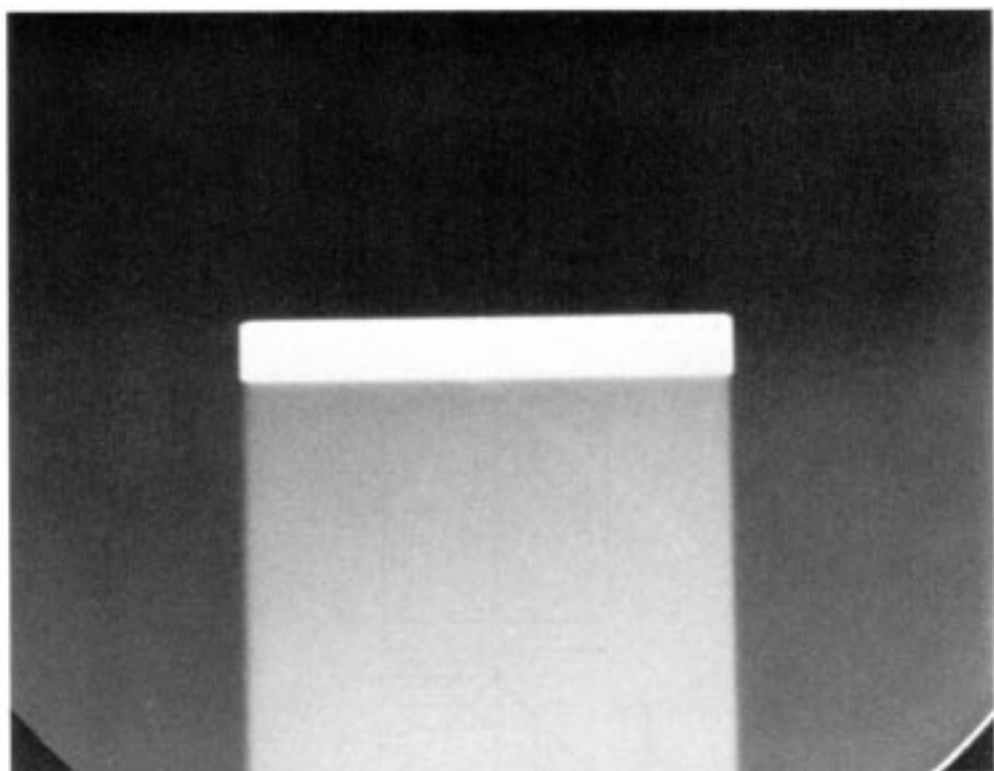
39.64 μ s

Reference:

Thurston and Mudd, 1968

Dynamic fracture of 12.0-mm-thick, t , uranium. The plate is shocked by 101.6 mm of Composition B-3 initiated by a P-040 lens. h is 25.4 mm.





SHOT 135:

Aluminum Wedge

Date:

January 21, 1965

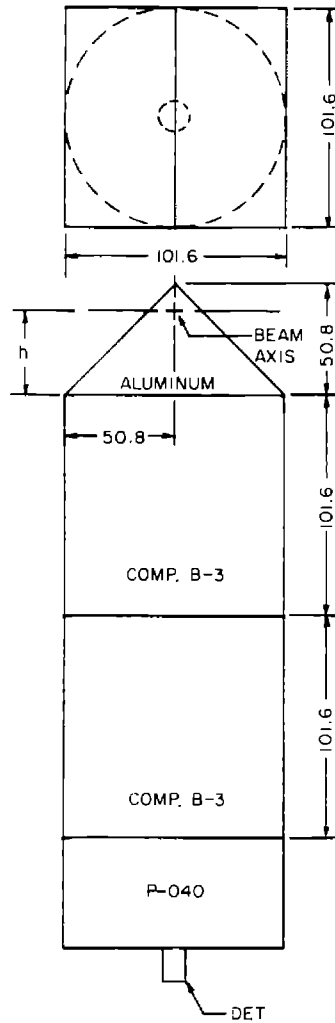
Experimenter:

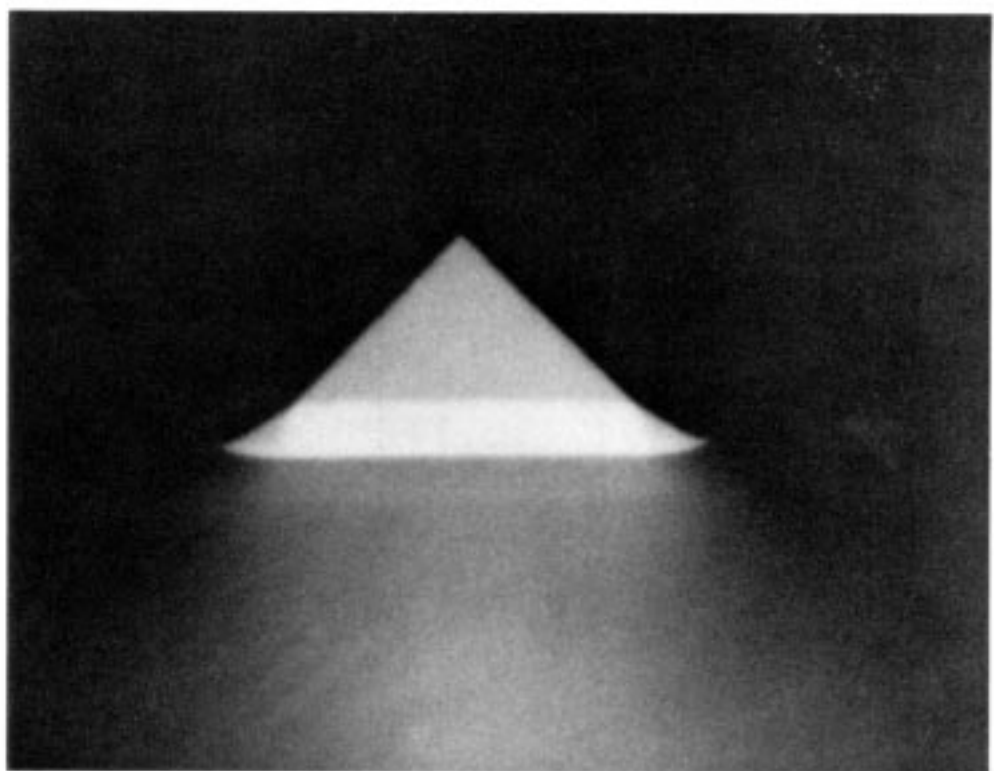
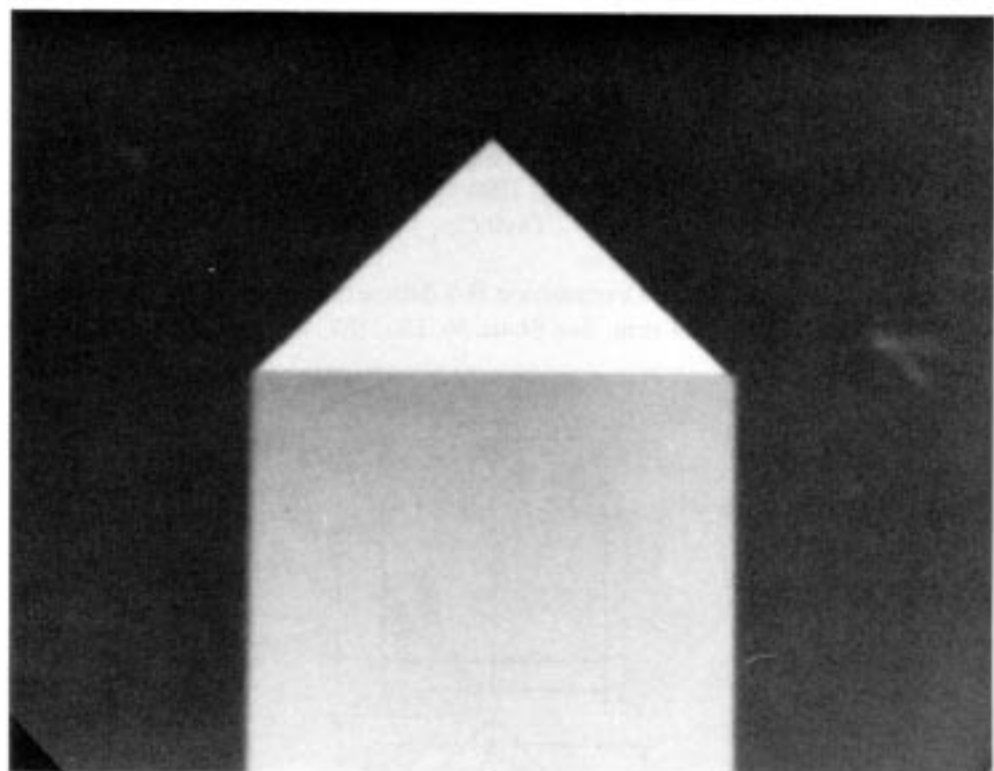
Roger W. Taylor

Radiographic Time:

40.79 μ s

A shock wave generated by a Composition B-3 detonation wave interacts with a 90° aluminum wedge. h is 12.7 mm. See Shots 39, 136-138, and 214-217 for other times.





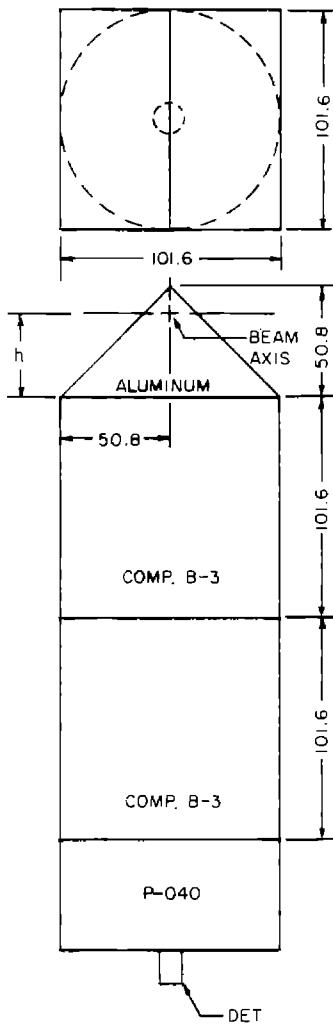
SHOT 136: Aluminum Wedge

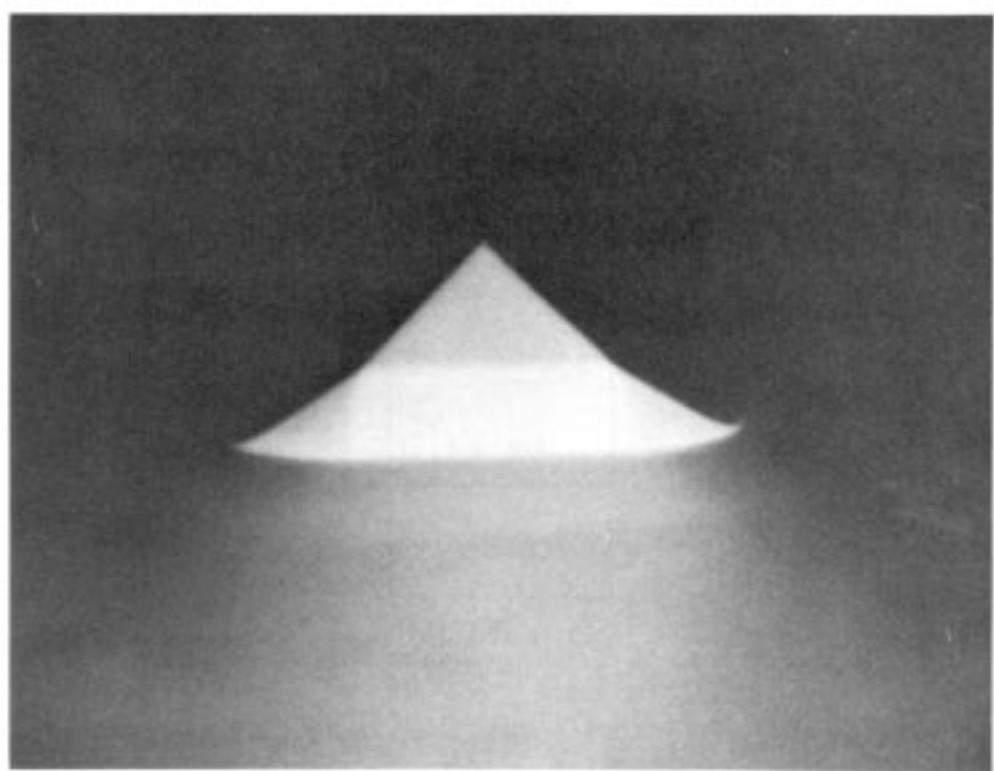
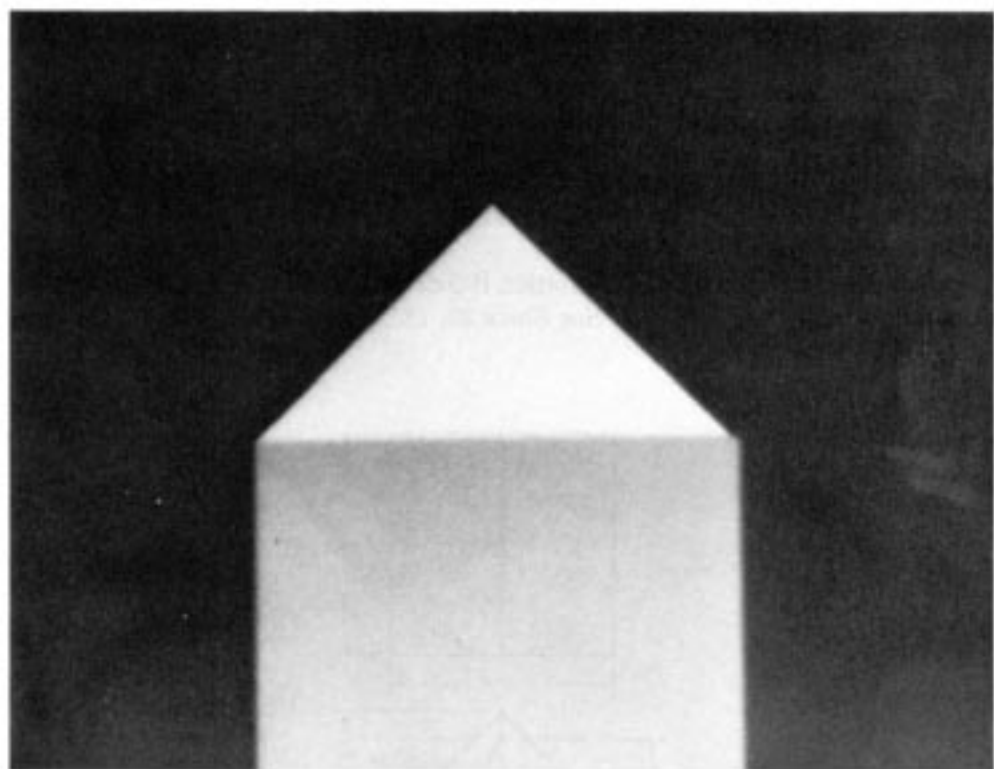
Date: January 21, 1965

Experimenter: Roger W. Taylor

Radiographic Time: 42.44 μ s

A shock wave generated by a Composition B-3 detonation wave interacts with a 90° aluminum wedge. h is 25.4 mm. See Shots 39, 135, 137, 138, and 214-217 for other times.





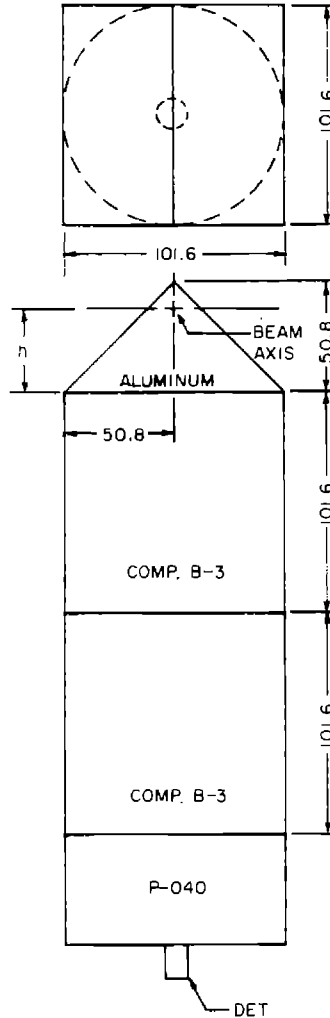
SHOT 137: Aluminum Wedge

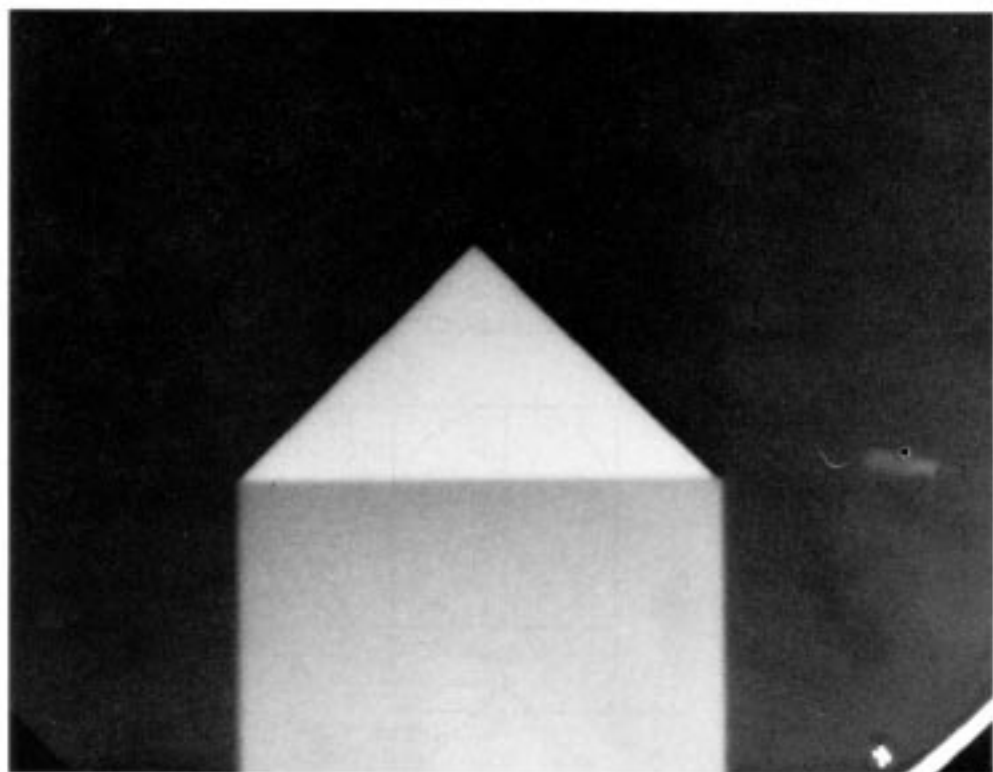
Date: January 21, 1965

Experimenter: Roger W. Taylor

Radiographic Time: 45.79 μ s

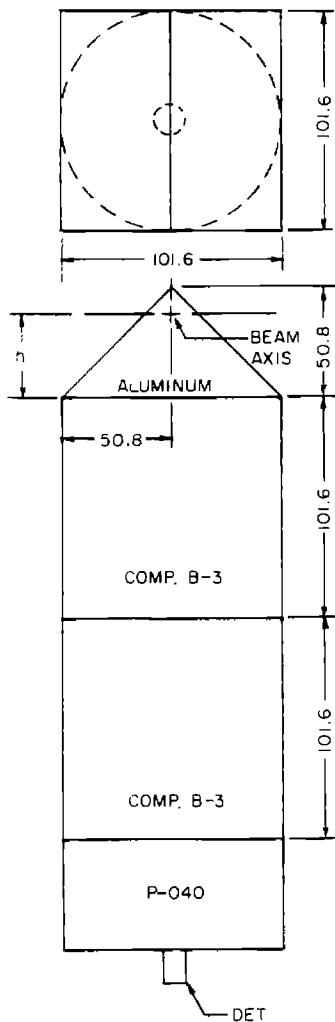
A shock wave generated by a Composition B-3 detonation wave interacts with a 90° aluminum wedge. h is 50.8 mm. See Shots 39, 135, 136, 138, and 214-217 for other times.

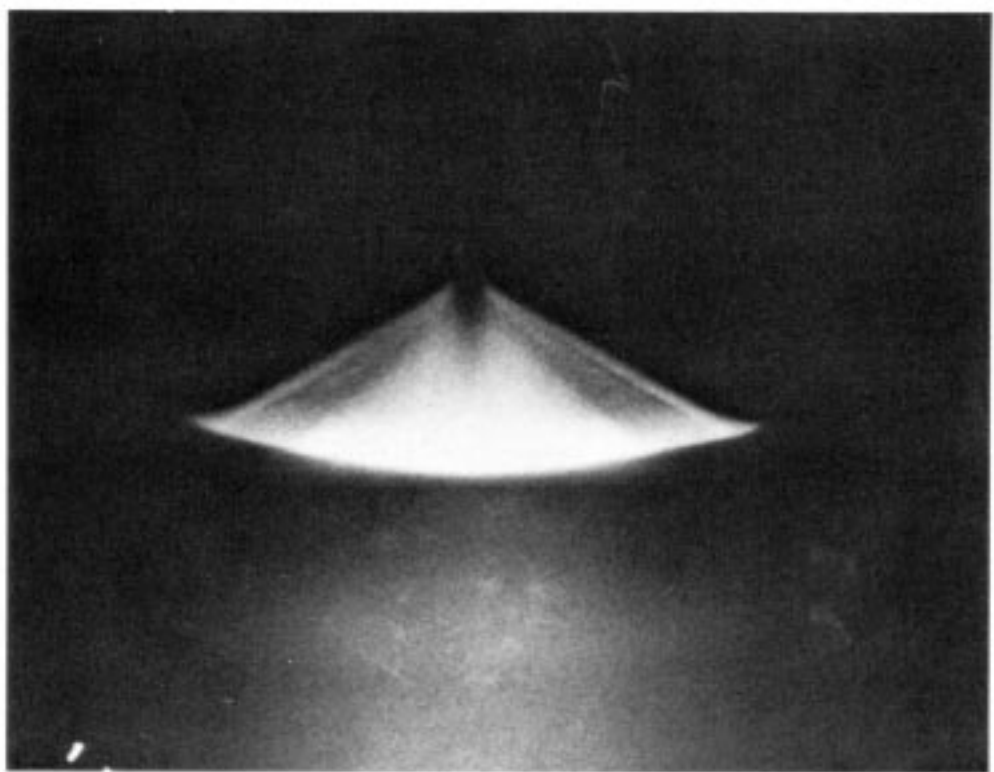
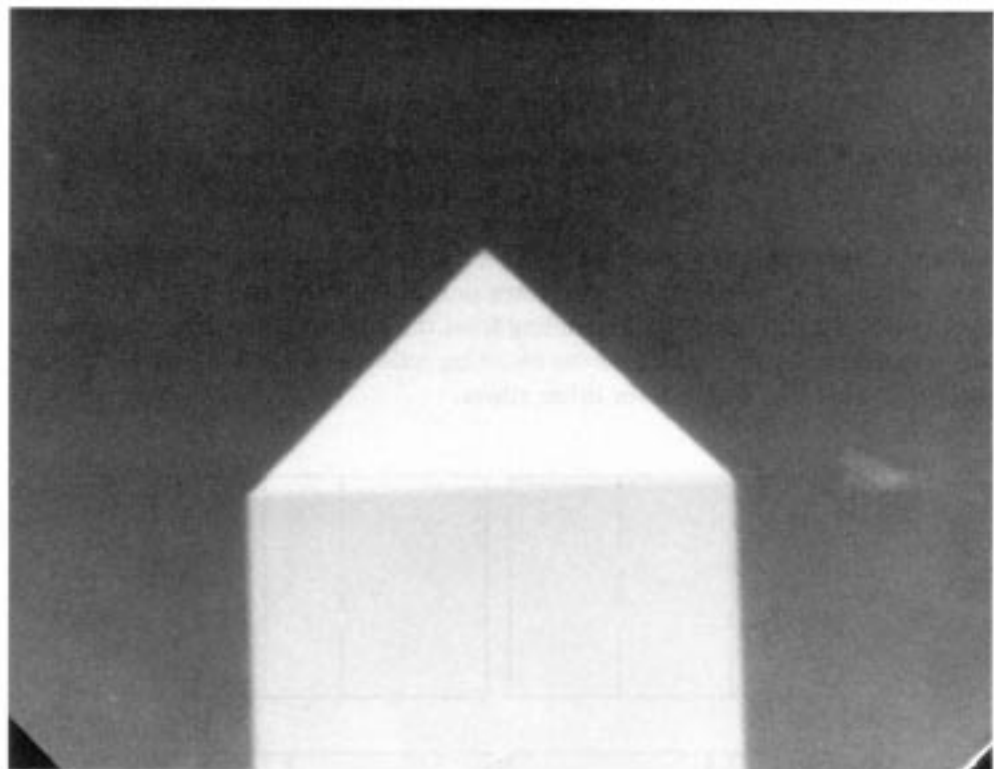




SHOT 138: **Aluminum Wedge**
Date: **January 6, 1965**
Experimenter: **Roger W. Taylor**
Radiographic Time: **47.44 μ s**

A shock wave generated by a Composition B-3 detonation wave interacts with a 90° aluminum wedge. h is 38.1 mm. See Shots 39, 135-137, and 214-217 for other times.





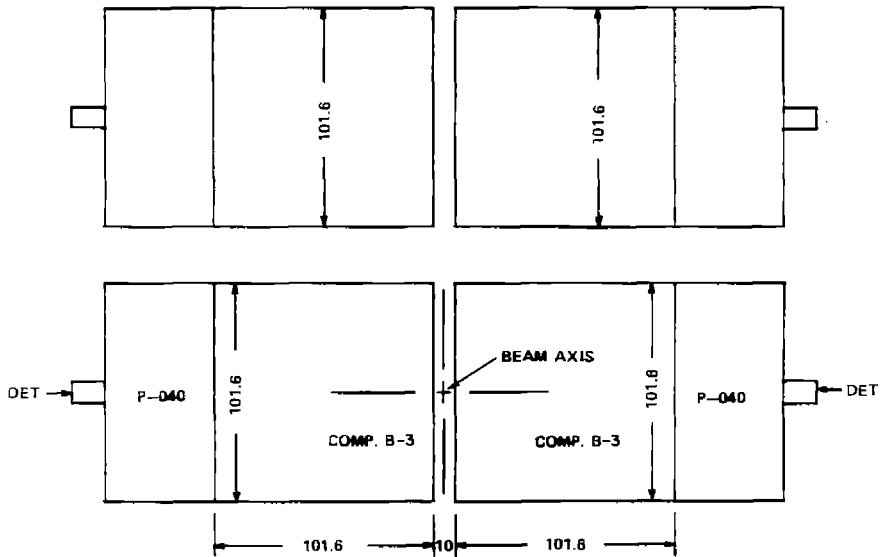
SHOT 139: Colliding Composition B-3 Detonation Products

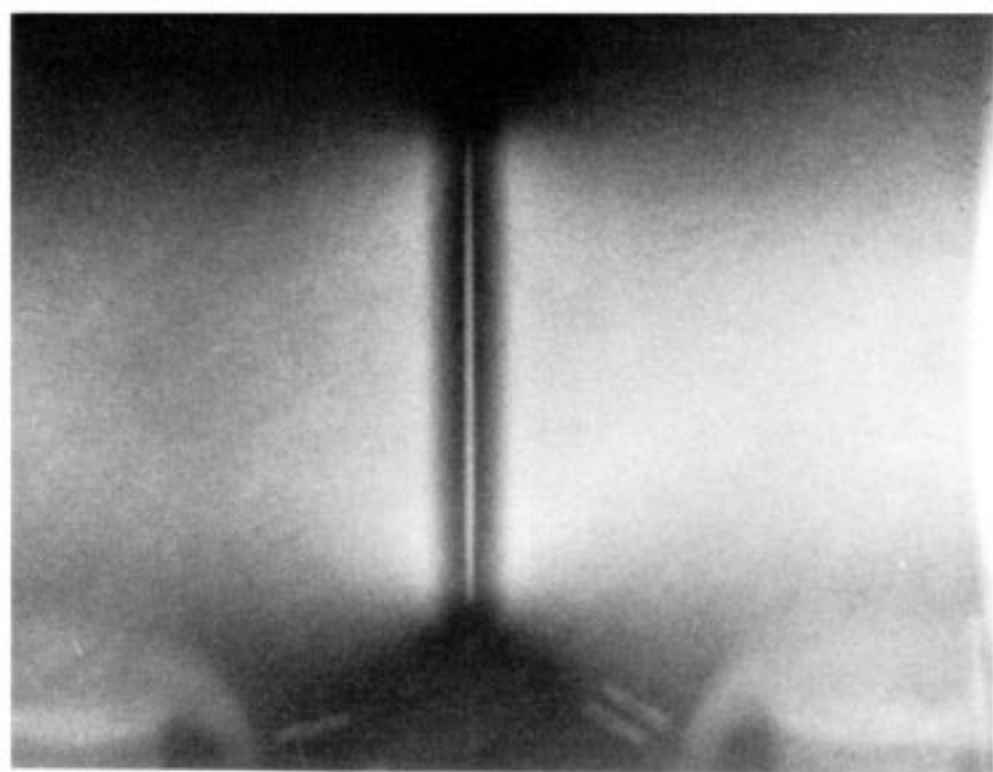
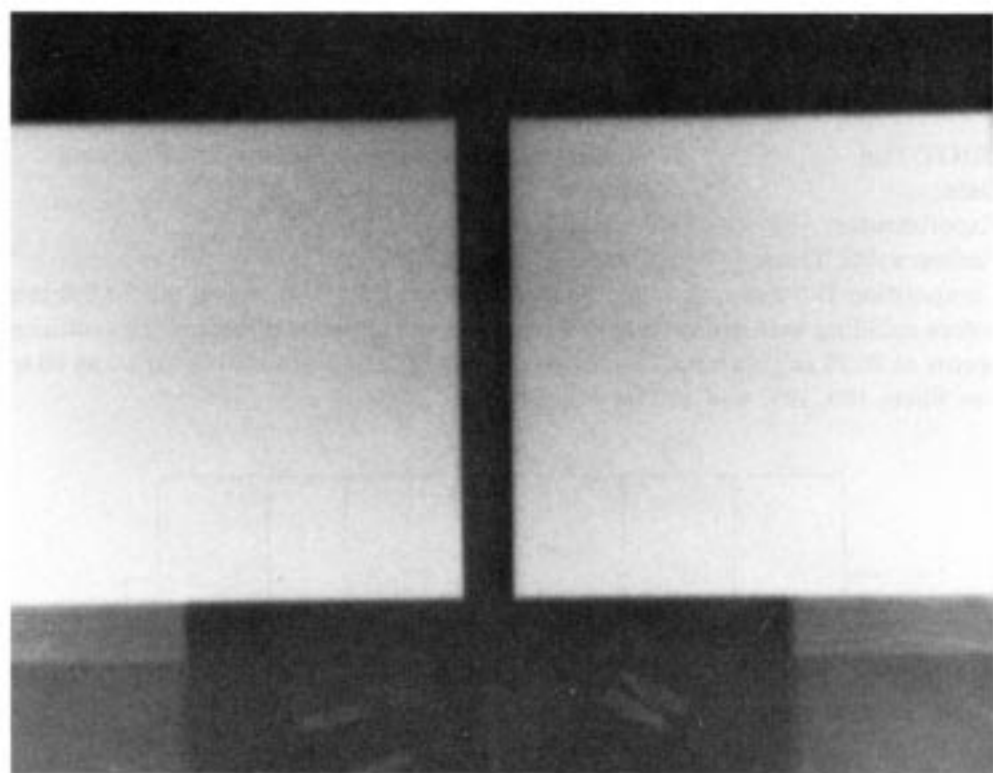
Date: January 6, 1965

Experimenter: Douglas Venable

Radiographic Time: 27.37 μ s

Composition B-3 detonation products are permitted to expand in air for 5.0 mm before colliding with products expanding from the opposite direction. The collision occurs at 26.25 μ s (pin data), and the resulting reflected wave is shown 1.0 μ s later. See Shots 140, 195, and 196 for other times.





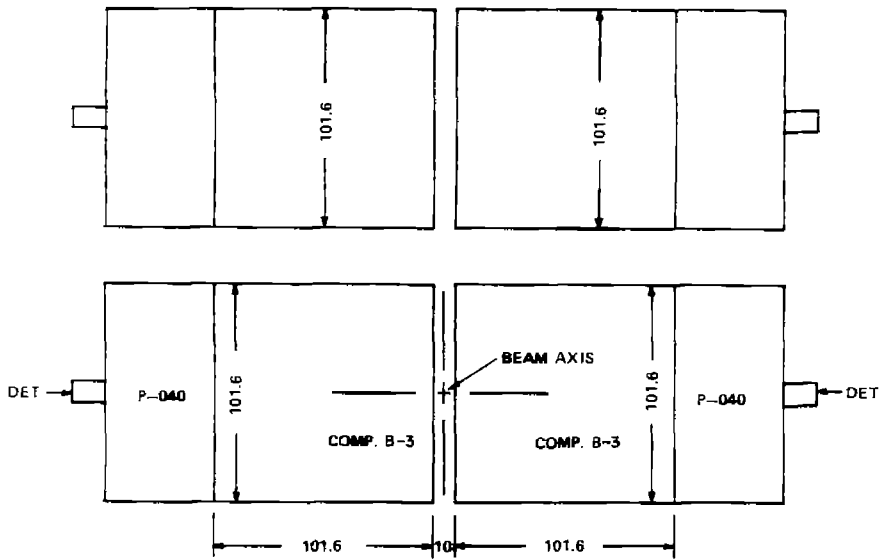
SHOT 140: Colliding Composition B-3 Detonation Products

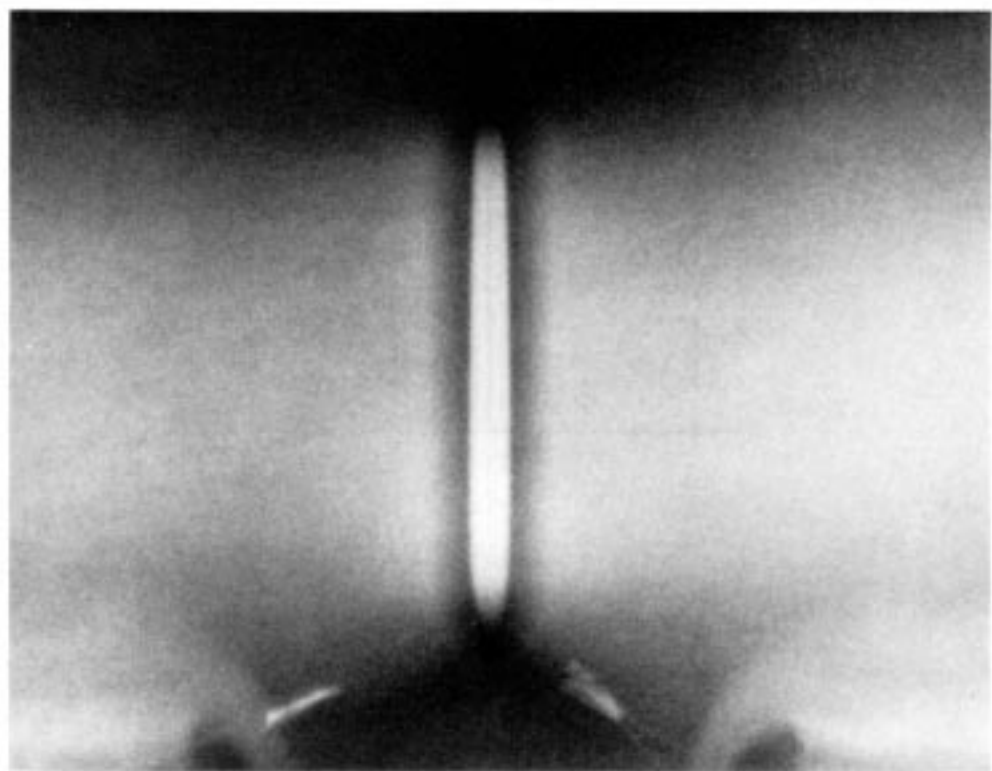
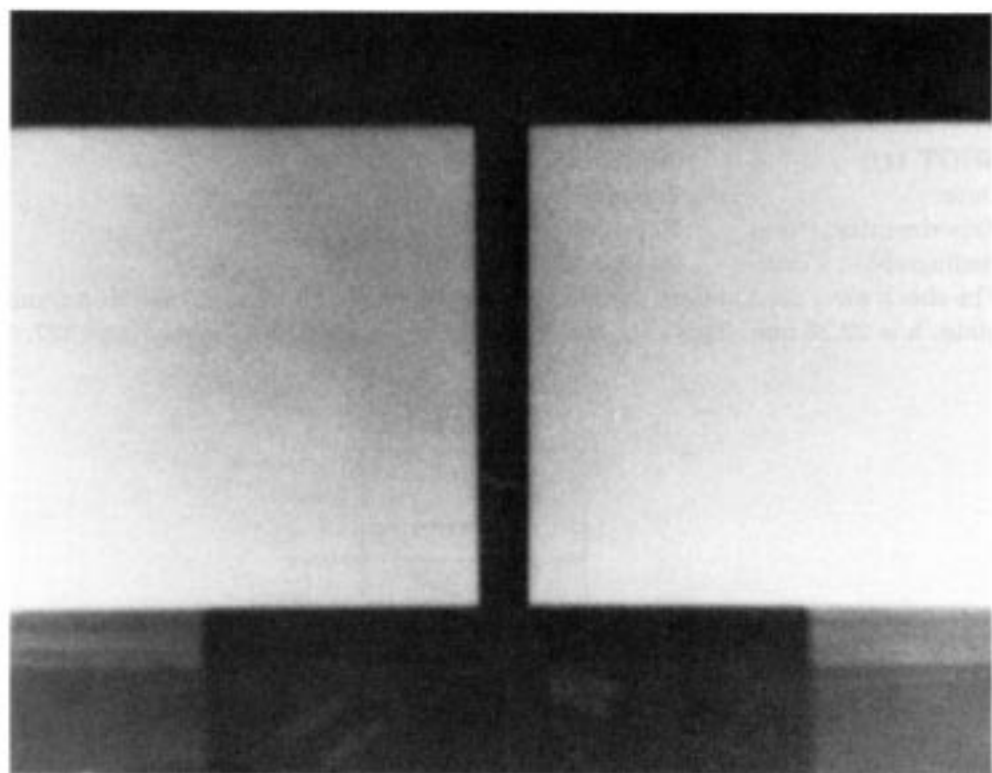
Date: January 6, 1965

Experimenter: Douglas Venable

Radiographic Time: 28.39 μ s

Composition B-3 detonation products are permitted to expand in air for 5.0 mm before colliding with products expanding from the opposite direction. The collision occurs at 26.25 μ s (pin data), and the resulting reflected wave is shown 2.0 μ s later. See Shots 139, 195, and 196 for other times.





SHOT 141:

Aluminum Jets

Date:

January 12, 1965

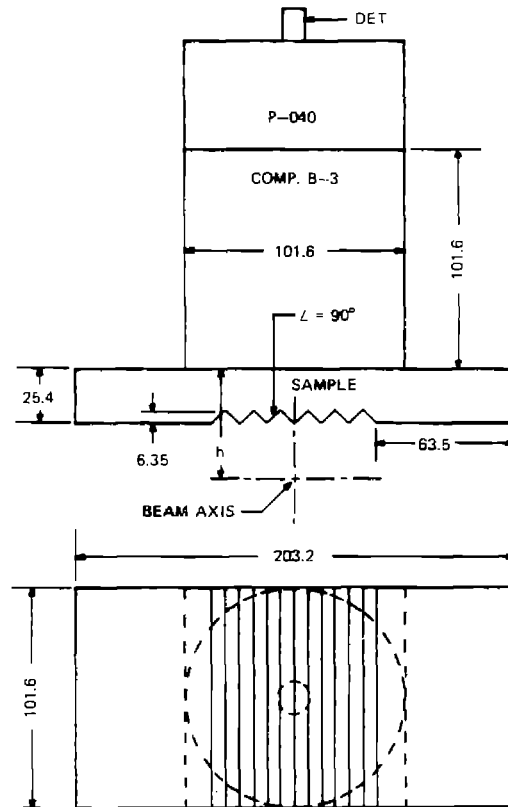
Experimenter:

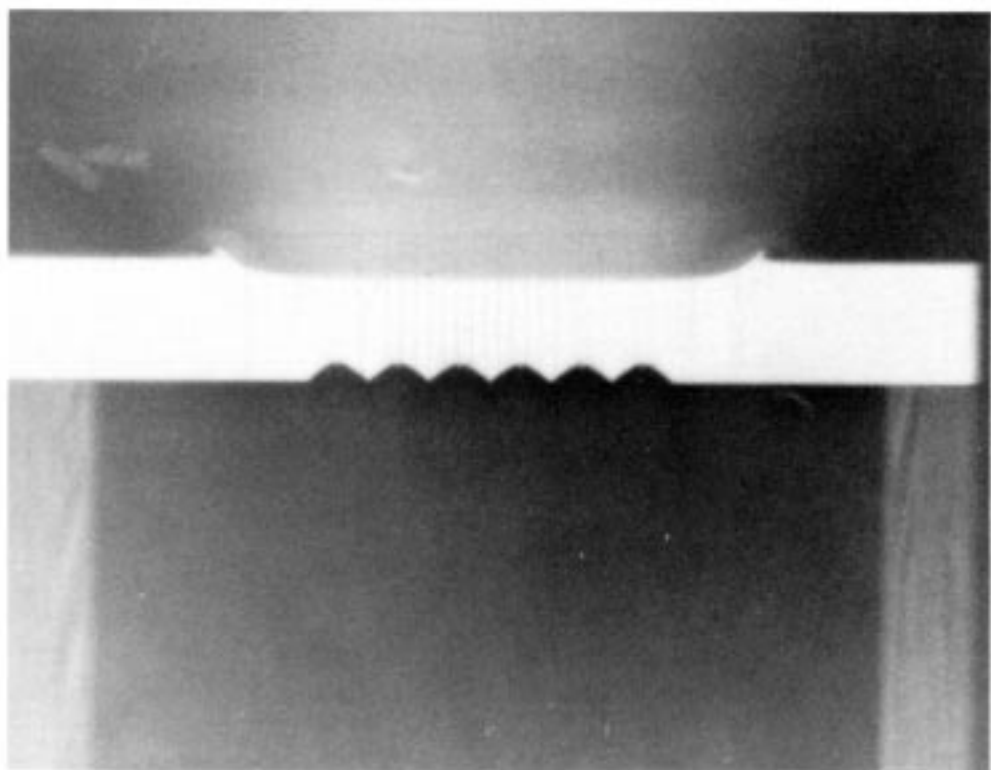
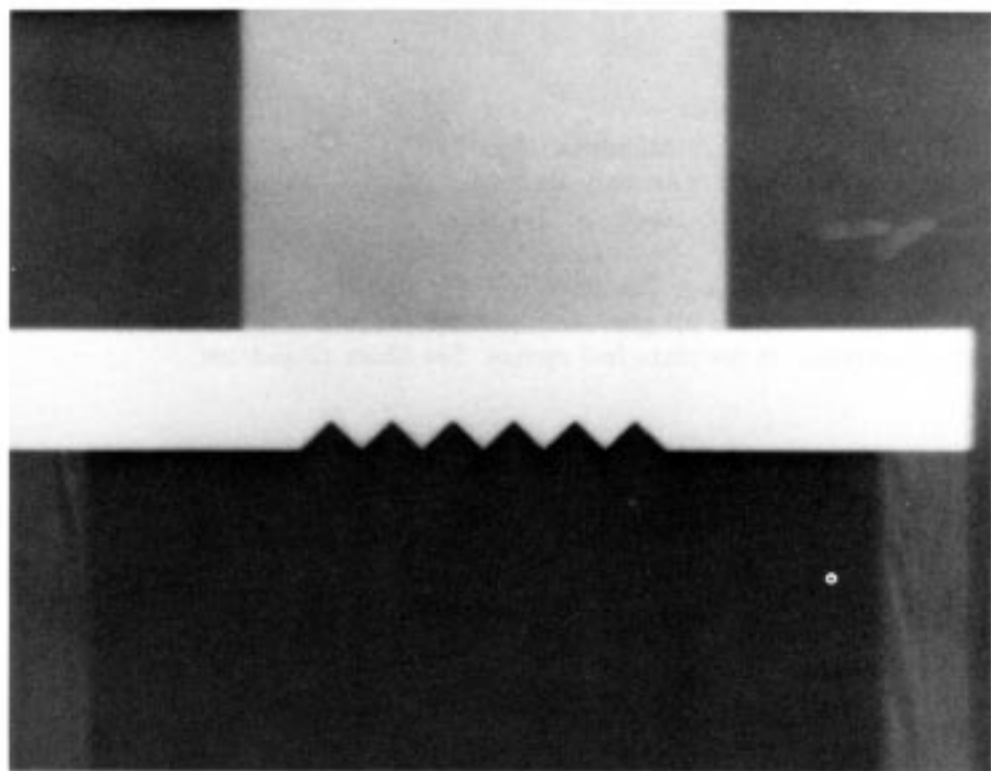
Roger W. Taylor

Radiographic Time:

29.52 μ s

The shock wave used to form metallic jets has traveled 22.7 mm into the aluminum plate. h is 22.23 mm. This shot had a low radiation level. See Shots 7 and 197.





SHOT 142:

Aluminum Jets

Date:

January 12, 1965

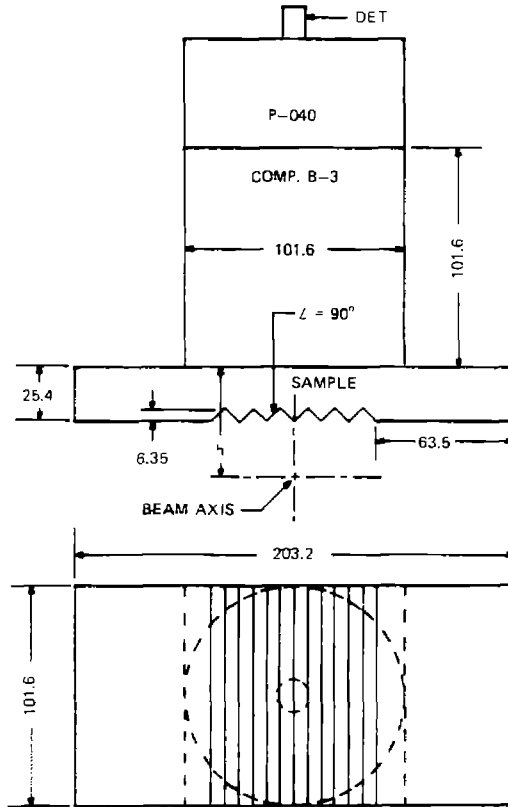
Experimenter:

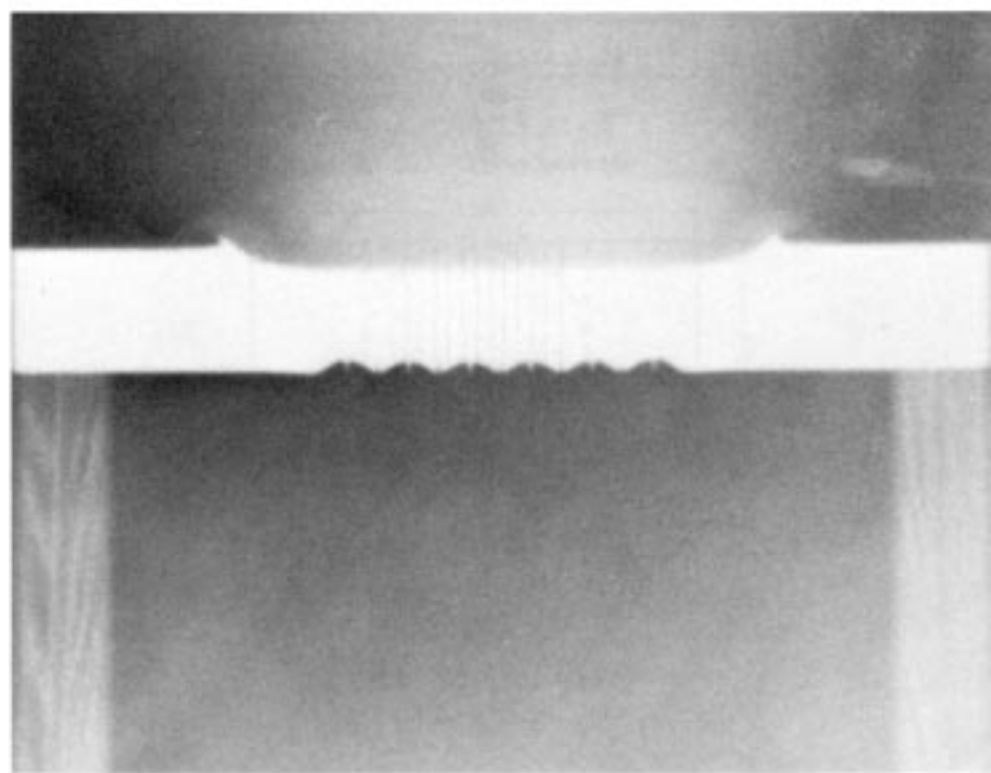
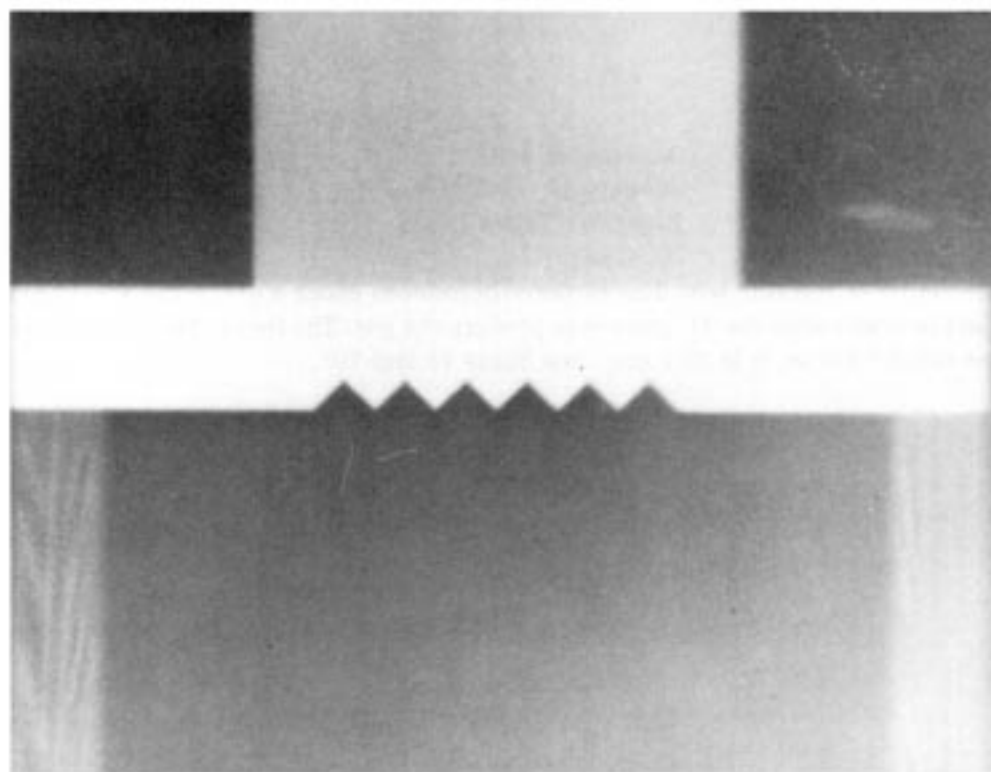
Roger W. Taylor

Radiographic Time:

30.0 μ s

Formation of metallic jets. The explosively induced shock wave in the aluminum plate interacts with the 90° grooves to produce the jets. h is 25.4 mm. The shock wave has arrived at the plate free surface. See Shots 12 and 198.





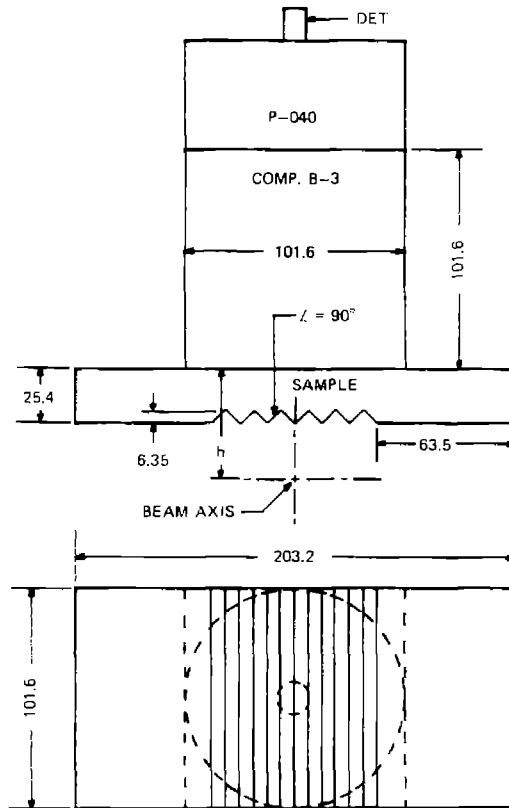
SHOT 143: Aluminum Jets

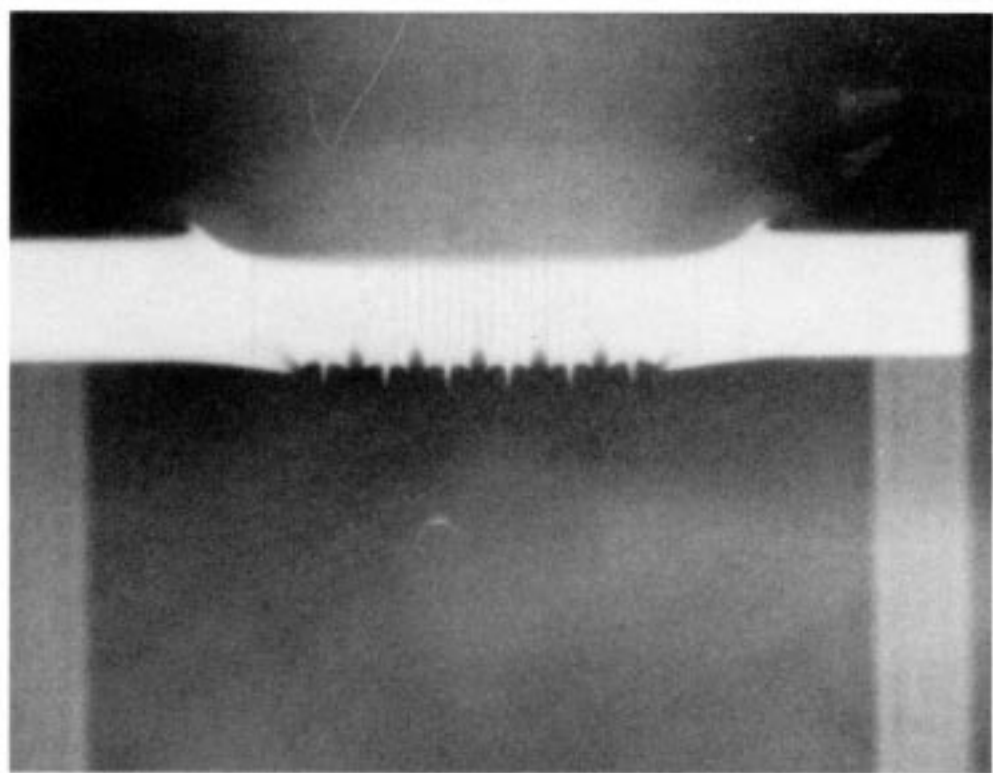
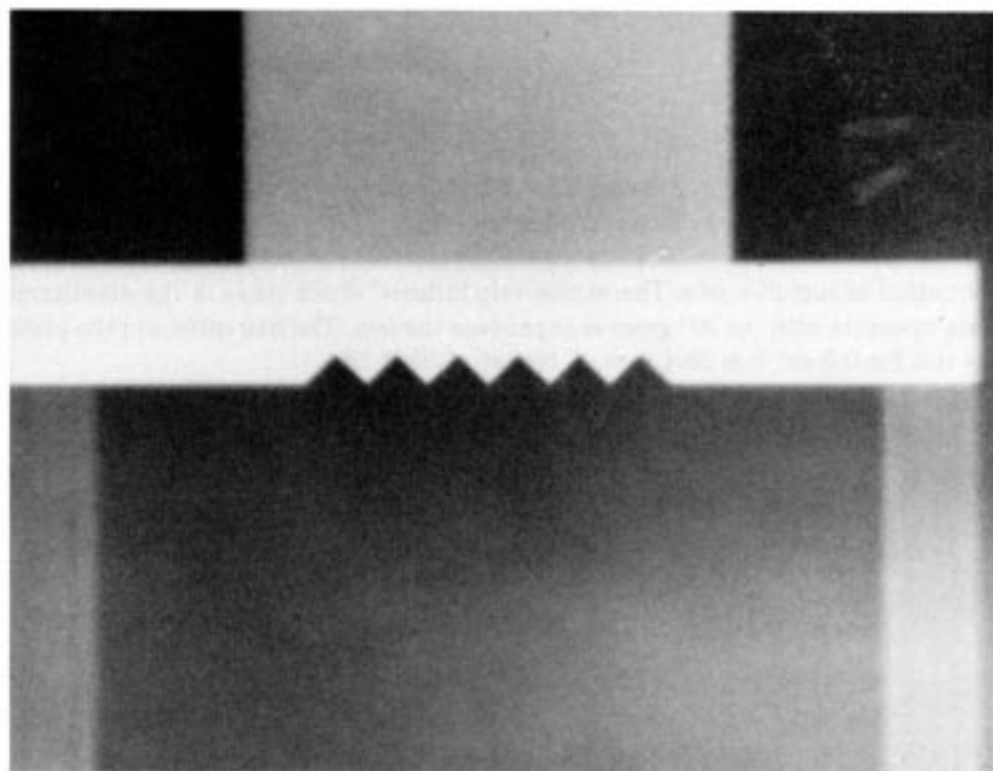
Date: January 12, 1965

Experimenter: Roger W. Taylor

Radiographic Time: 30.92 μ s

Formation of metallic jets. The explosively induced shock wave in the aluminum plate interacts with the 90° grooves to produce the jets. The free surface of the plate has run for 1.0 μ s. h is 25.4 mm. See Shots 13 and 199.





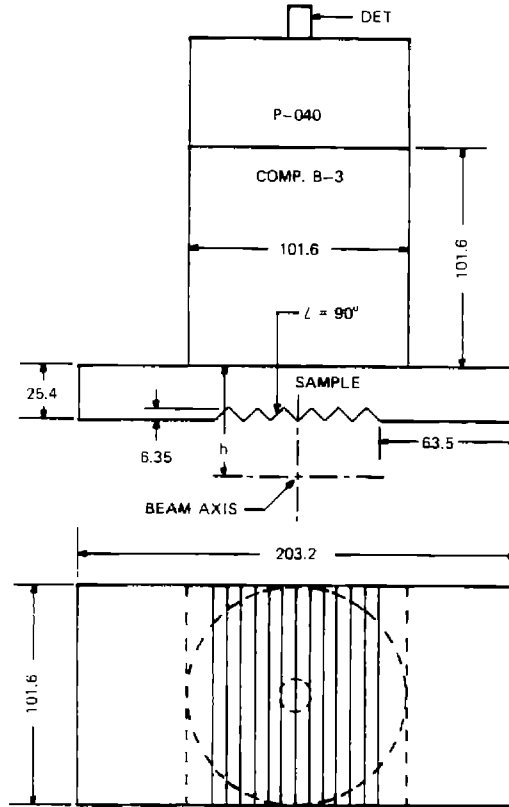
SHOT 144: Aluminum Jets

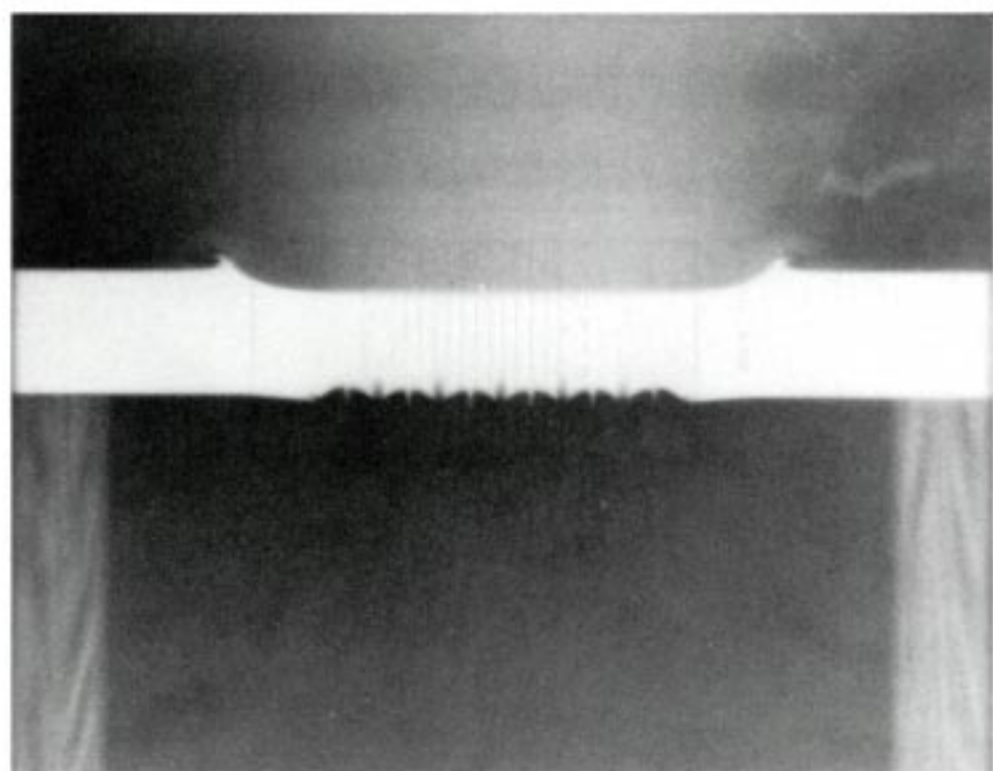
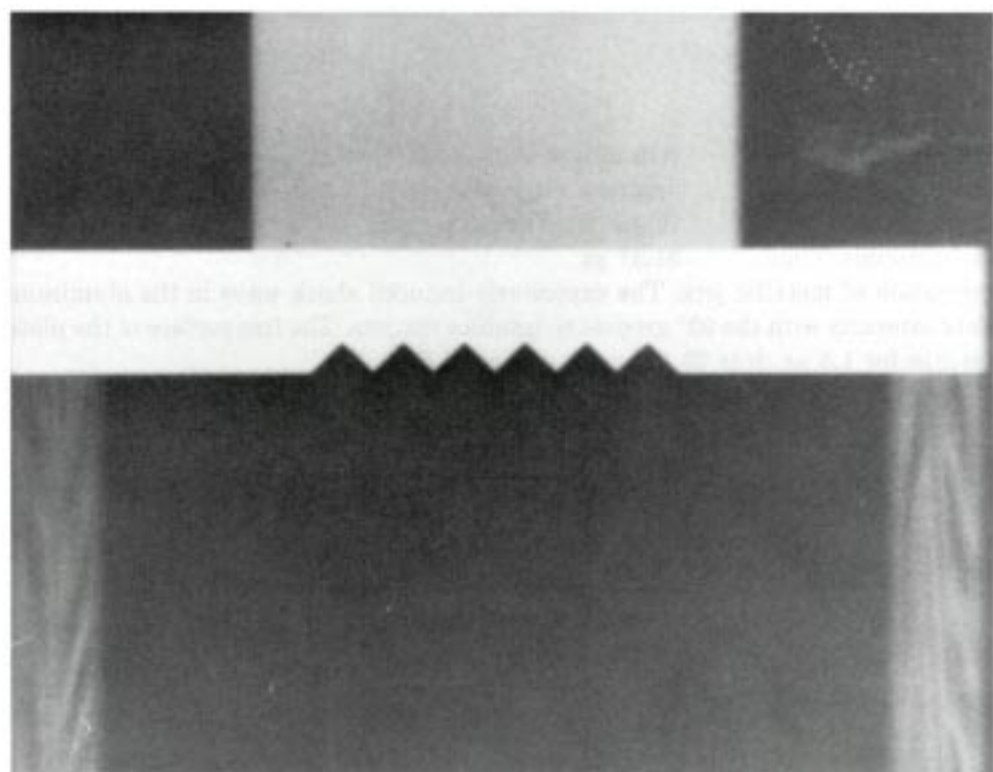
Date: January 15, 1965

Experimenter: Roger W. Taylor

Radiographic Time: 30.38 μ s

Formation of metallic jets. The explosively induced shock wave in the aluminum plate interacts with the 90° grooves to produce the jets. The free surface of the plate has run for 0.5 μ s. h is 25.4 mm. A repeat of Shot 16.





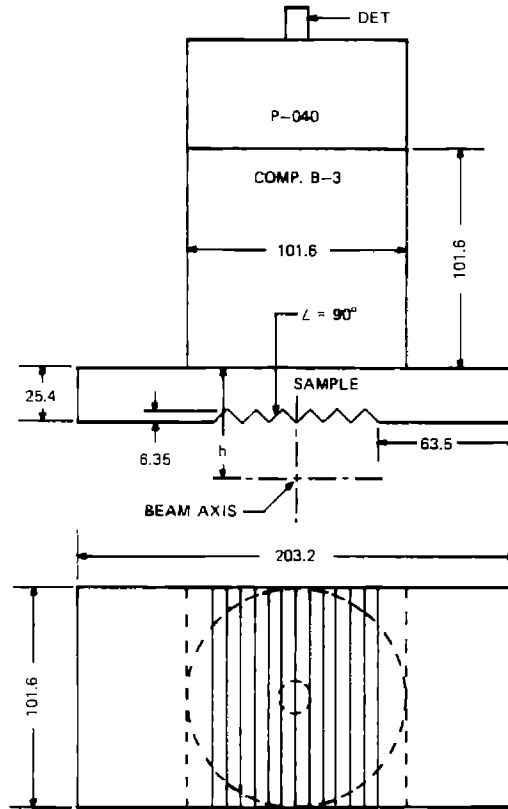
SHOT 145: Aluminum Jets

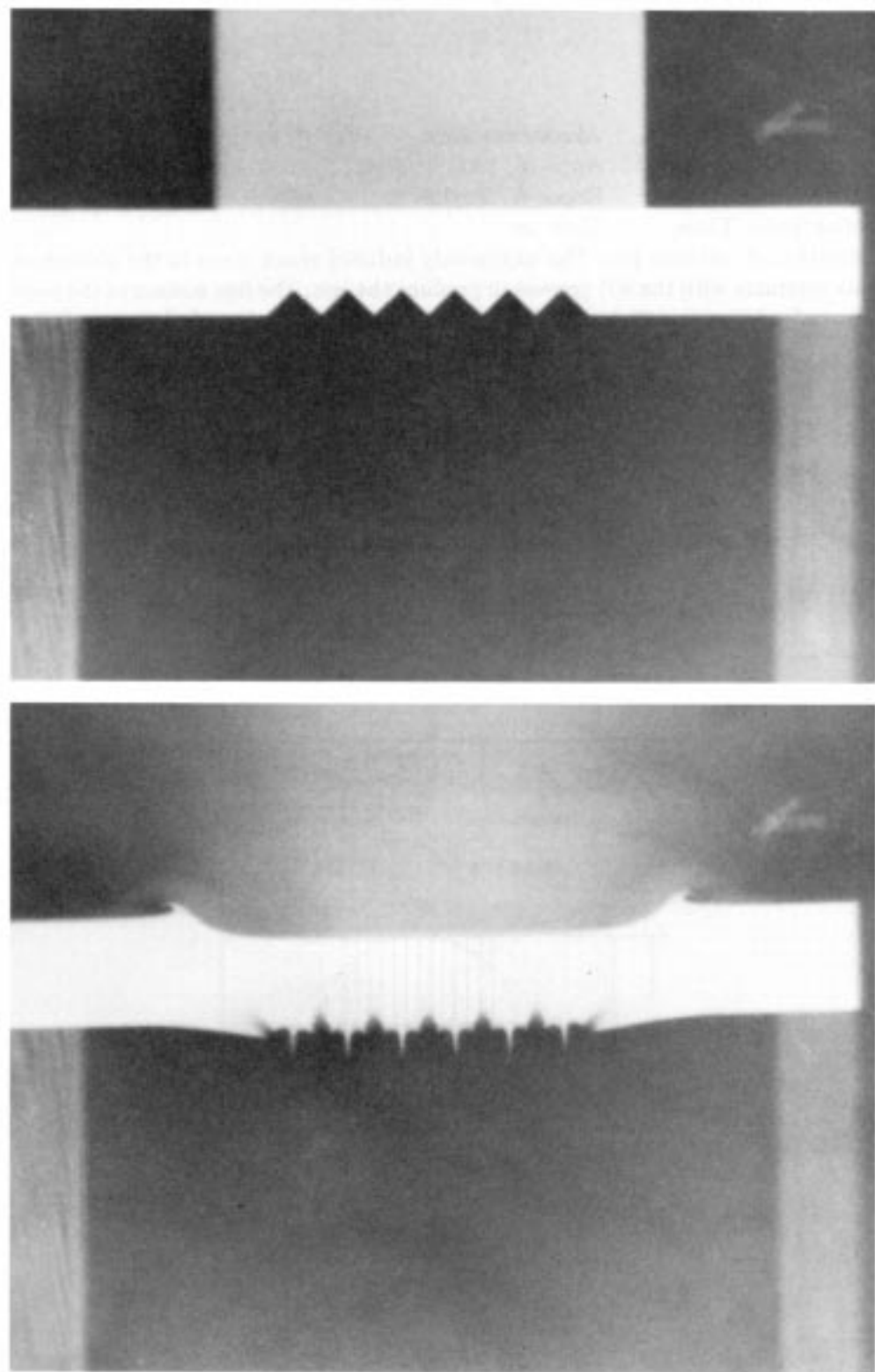
Date: January 13, 1965

Experimenter: Roger W. Taylor

Radiographic Time: 31.37 μ s

Formation of metallic jets. The explosively induced shock wave in the aluminum plate interacts with the 90° grooves to produce the jets. The free surface of the plate has run for 1.5 μ s. h is 25.4 mm. A repeat of Shot 17.





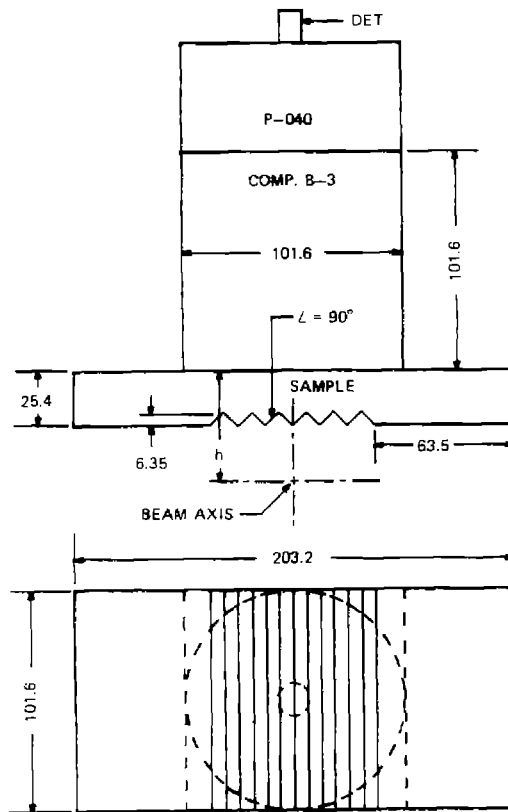
SHOT 146: Aluminum Jets

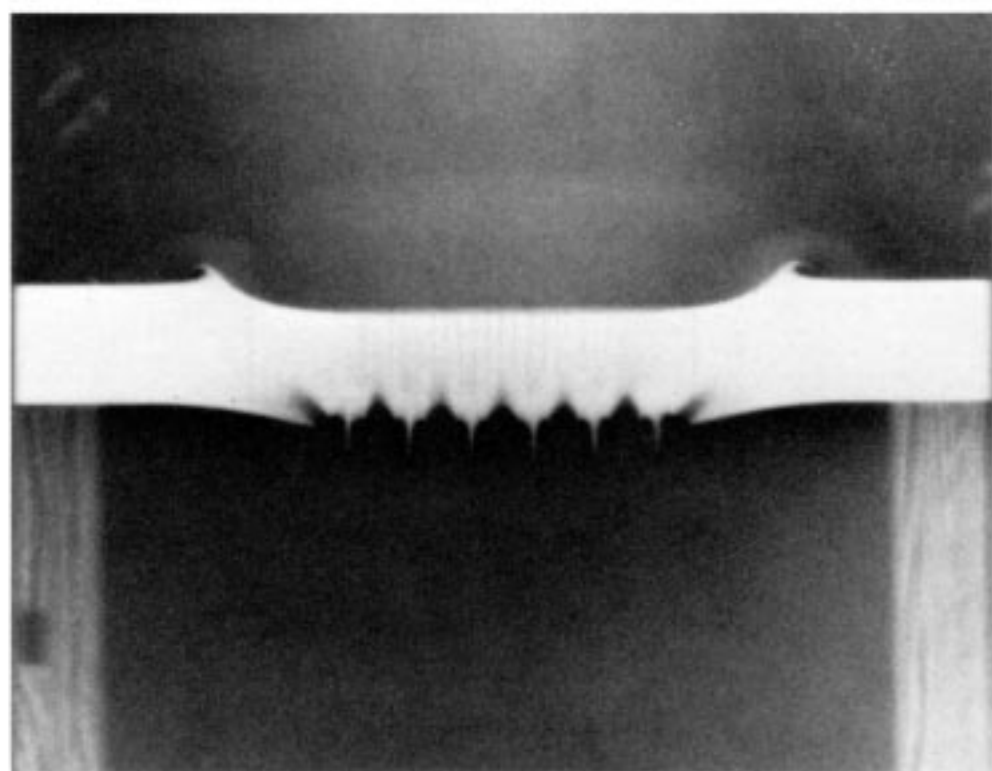
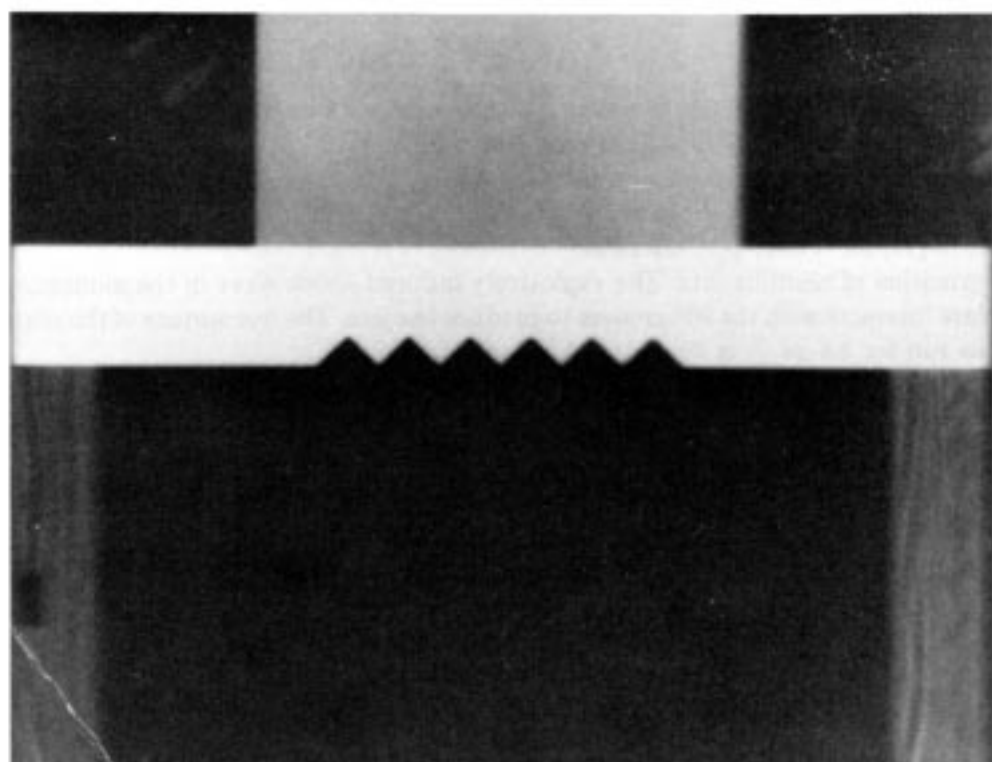
Date: April 26, 1965

Experimenter: Roger W. Taylor

Radiographic Time: 31.86 μ s

Formation of metallic jets. The explosively induced shock wave in the aluminum plate interacts with the 90° grooves to produce the jets. The free surface of the plate has run for 2.0 μ s. h is 25.4 mm. This shot was not properly aligned. A repeat of Shot 18.





SHOT 147:

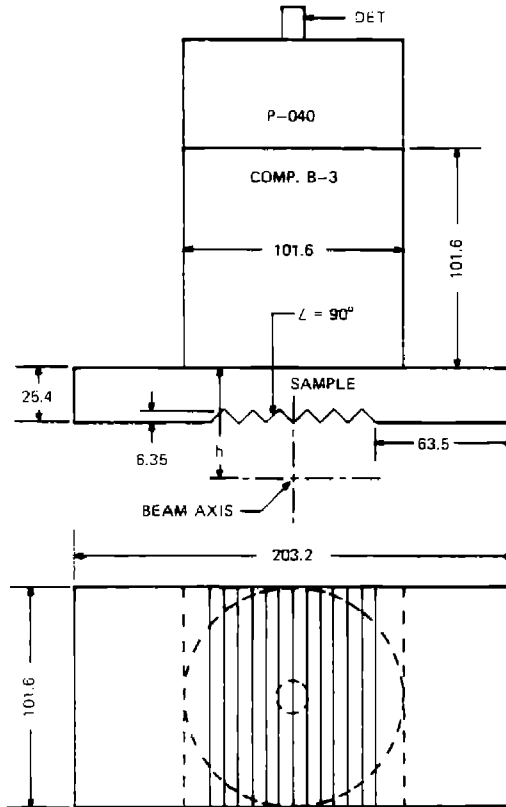
Aluminum Jets

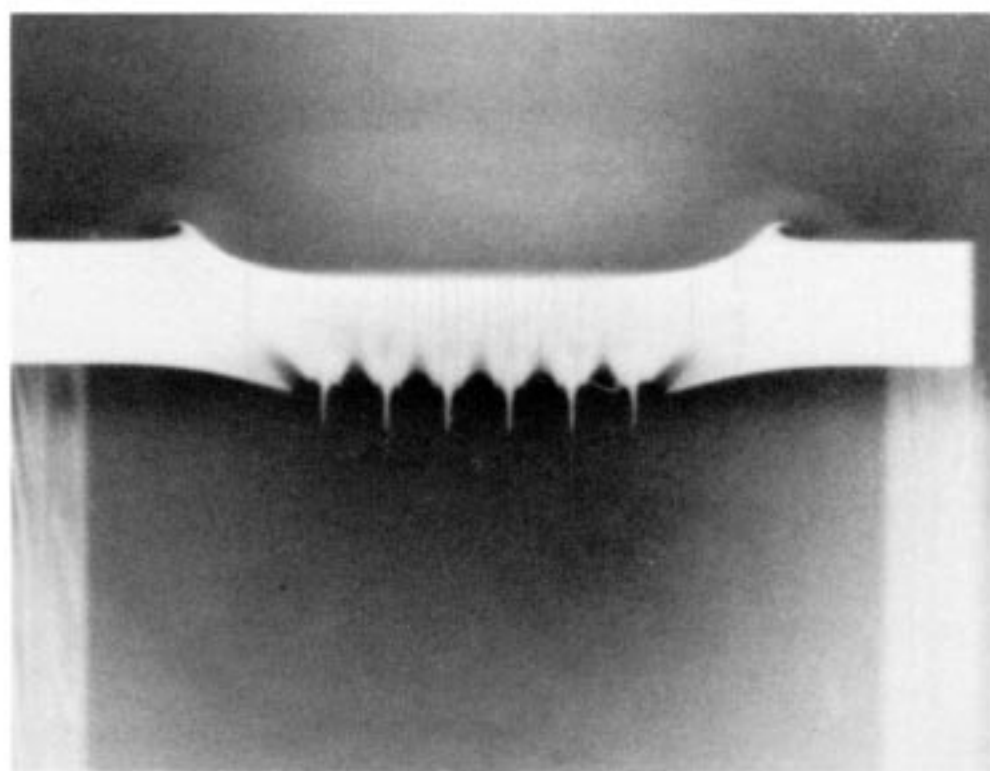
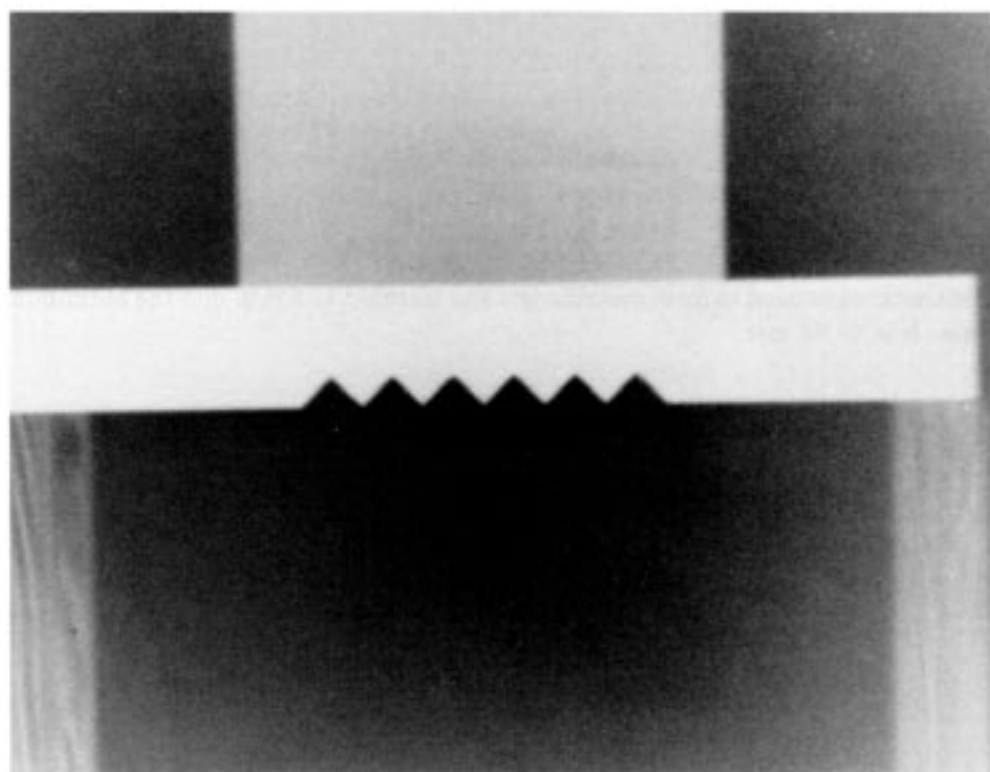
Date: November 2, 1965

Experimenter: Roger W. Taylor

Radiographic Time: 32.25 μ s

Formation of metallic jets. The explosively induced shock wave in the aluminum plate interacts with the 90° grooves to produce the jets. The free surface of the plate has run for 2.5 μ s. h is 25.4 mm. A repeat of Shot 19.





SHOT 148:

Aluminum Jets

Date:

January 4, 1966

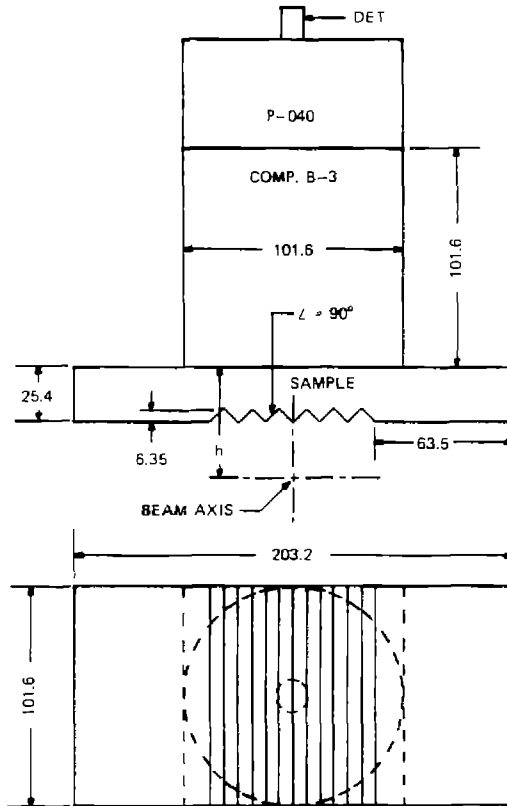
Experimenter:

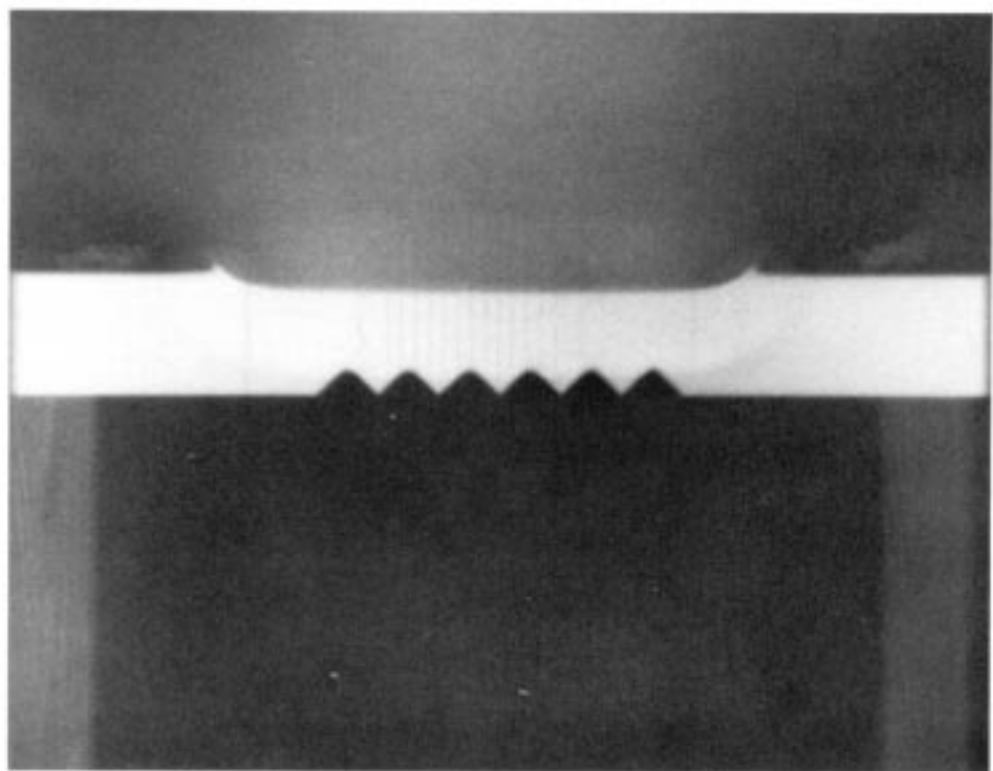
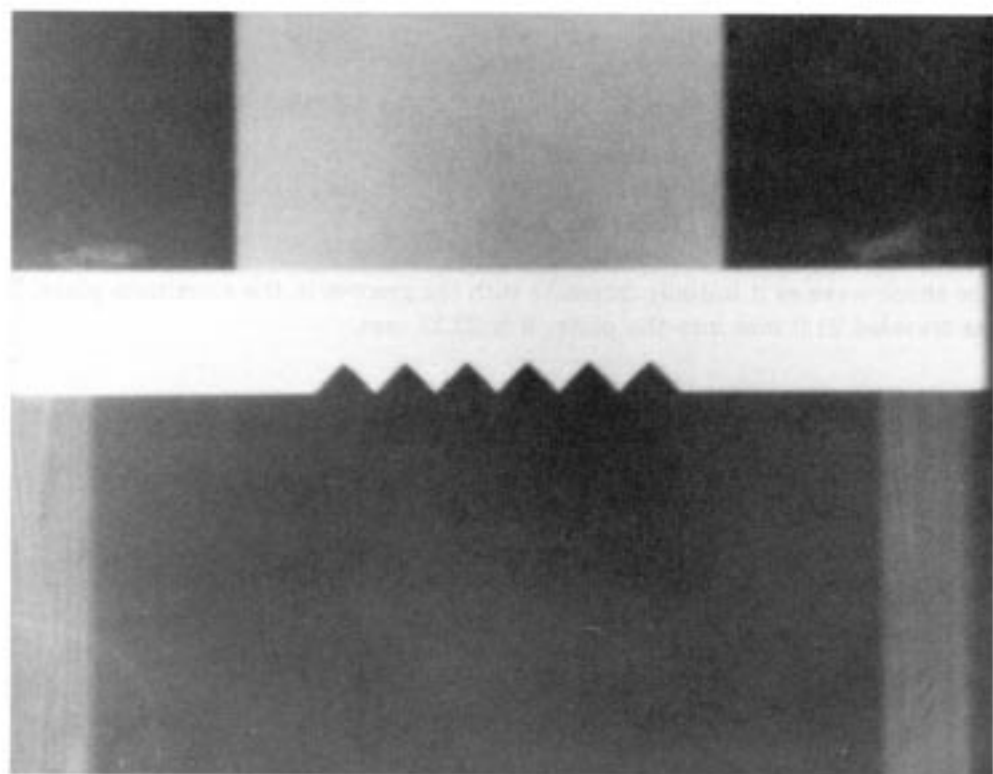
Roger W. Taylor

Radiographic Time:

29.11 μ s

The shock wave used to form metallic jets has traveled 19.8 mm into the aluminum plate. h is 20.64 mm.





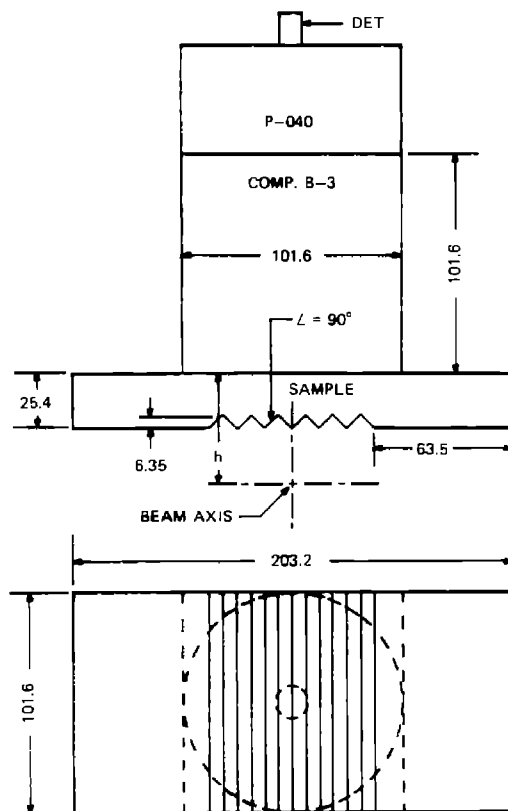
SHOT 149: Aluminum Jets

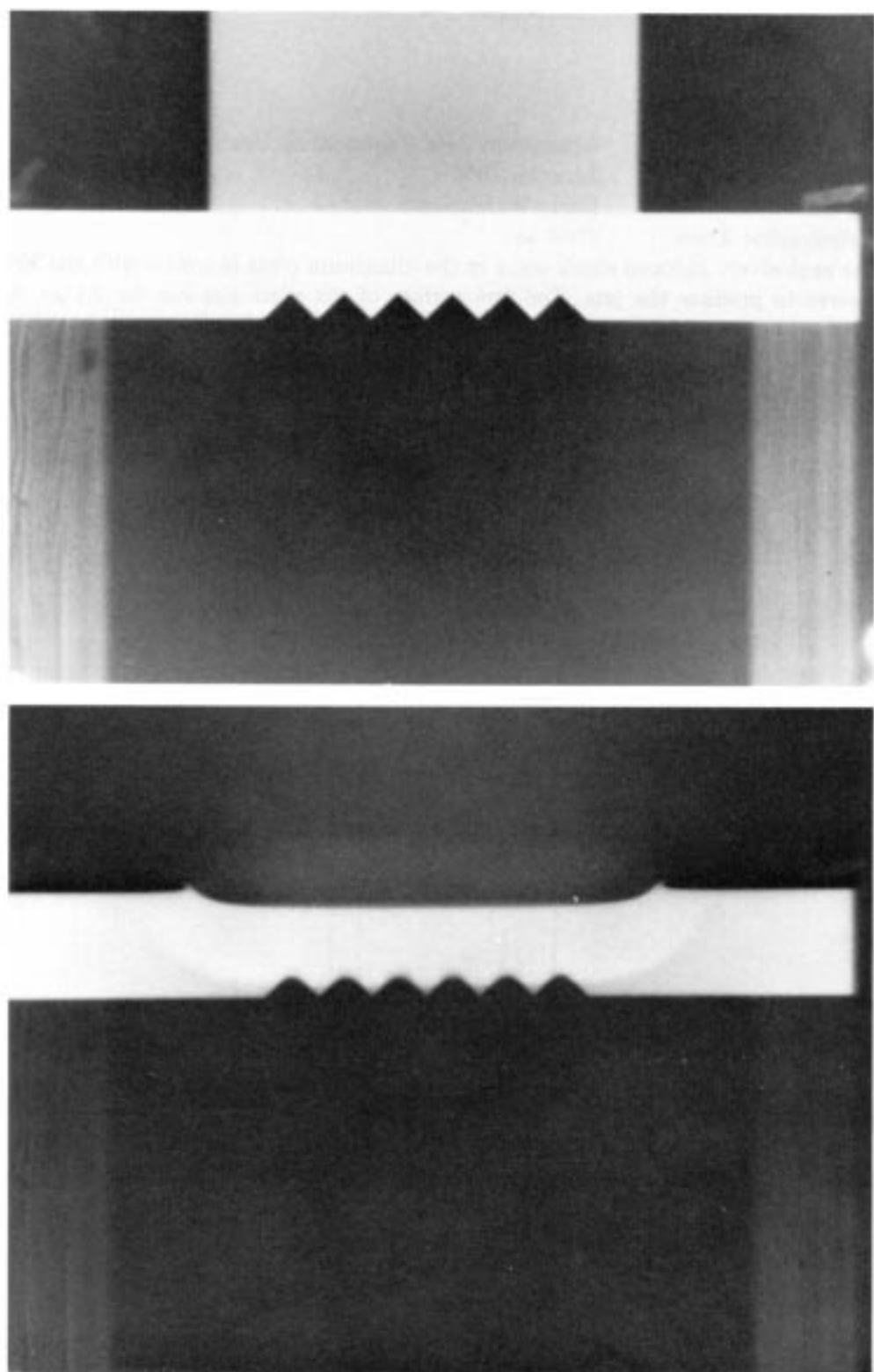
Date: March 23, 1966

Experimenter: Roger W. Taylor

Radiographic Time: 29.28 μ s

The shock wave as it initially interacts with the grooves in the aluminum plate. It has traveled 21.0 mm into the plate. h is 22.23 mm.





SHOT 150:

Aluminum Jets Penetrating Uranium

Date:

June 14, 1966

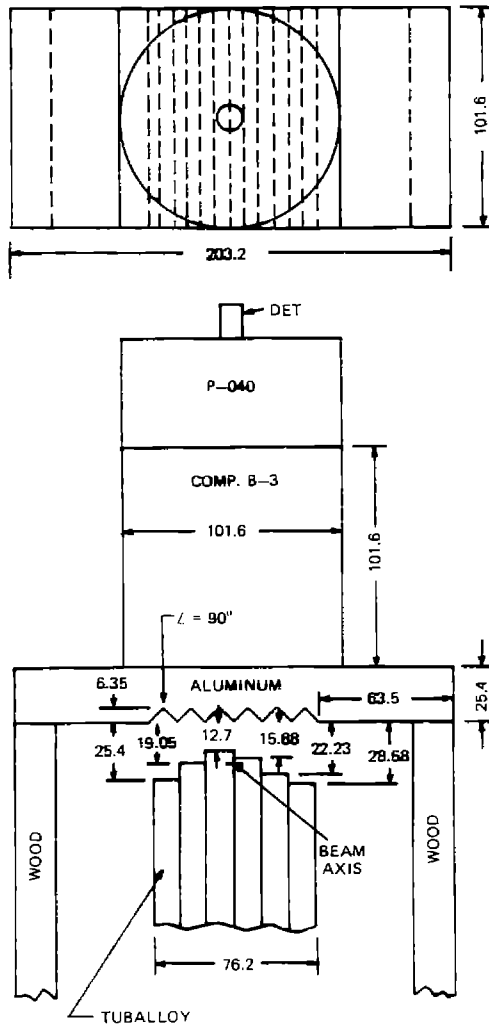
Experimenter:

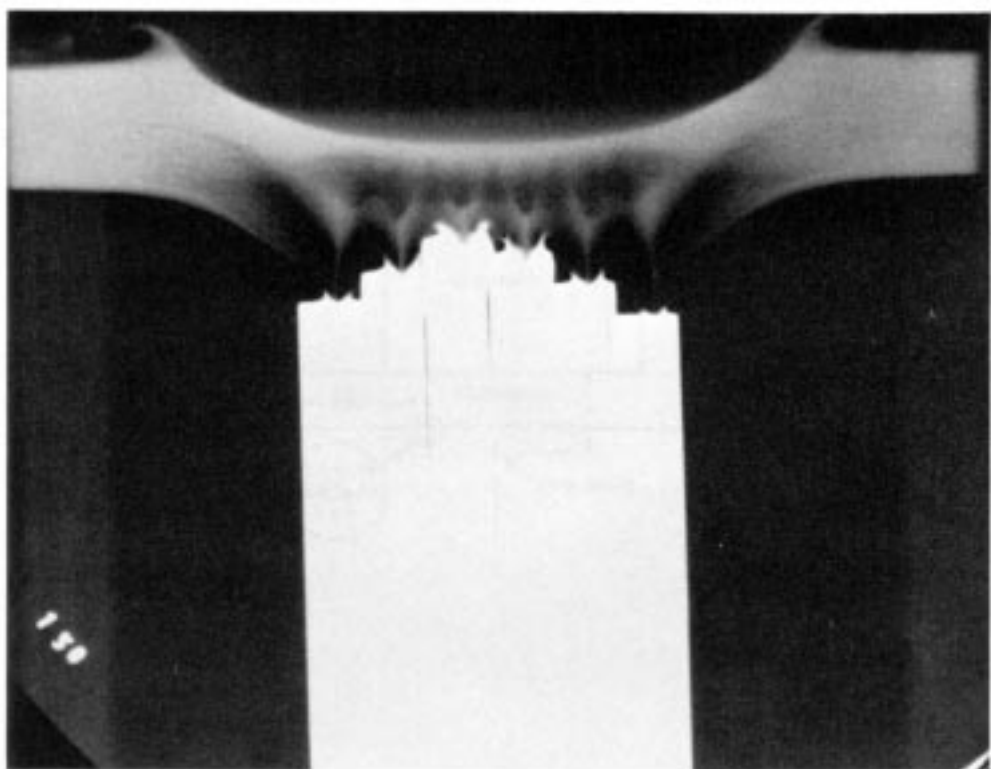
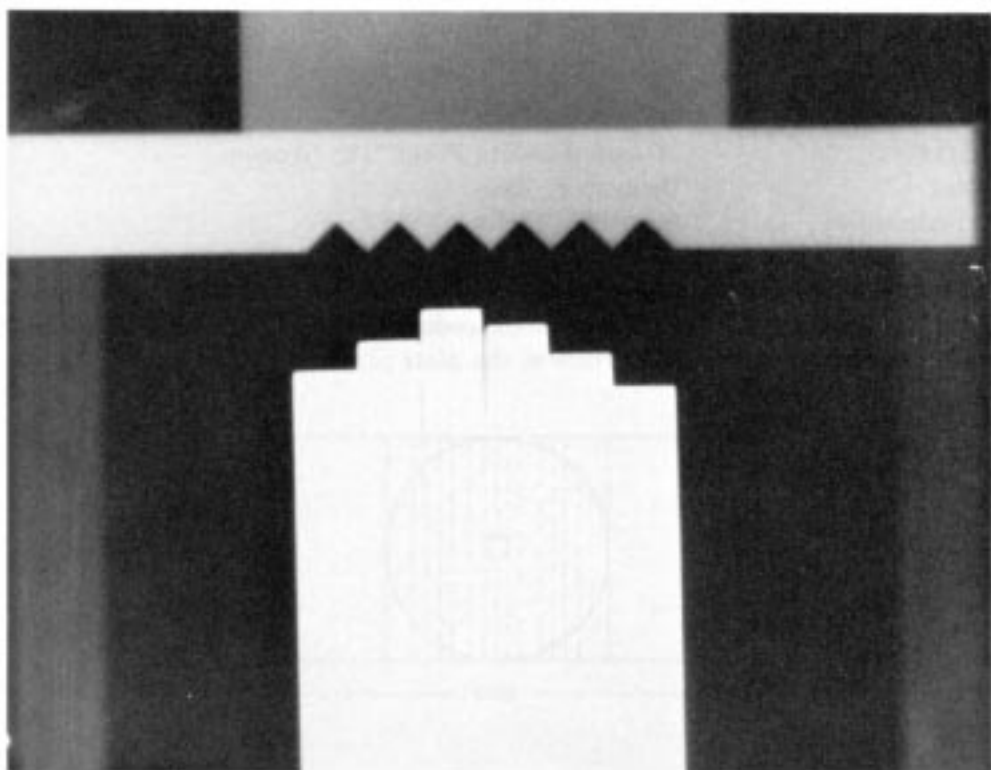
Roger W. Taylor

Radiographic Time:

37.06 μ s

The explosively induced shock wave in the aluminum plate interacts with the 90° grooves to produce the jets. The free surface of the plate has run for 7.1 μ s. A uranium target plate shows the penetration properties of the aluminum jets. See Shot 201.





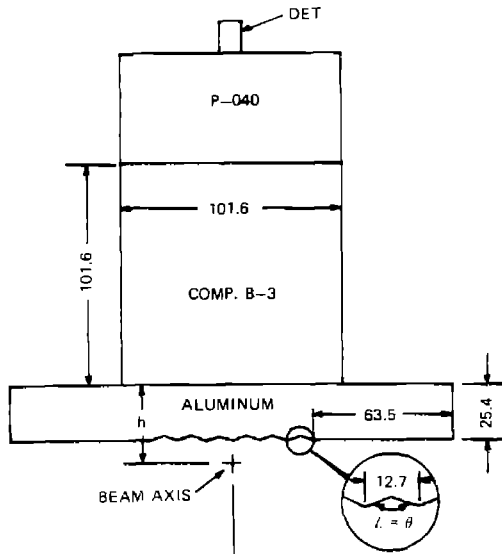
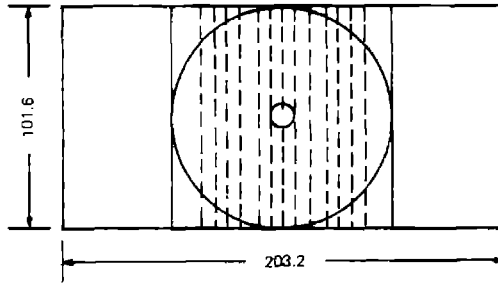
SHOT 151: Aluminum Jets From 170° Grooves

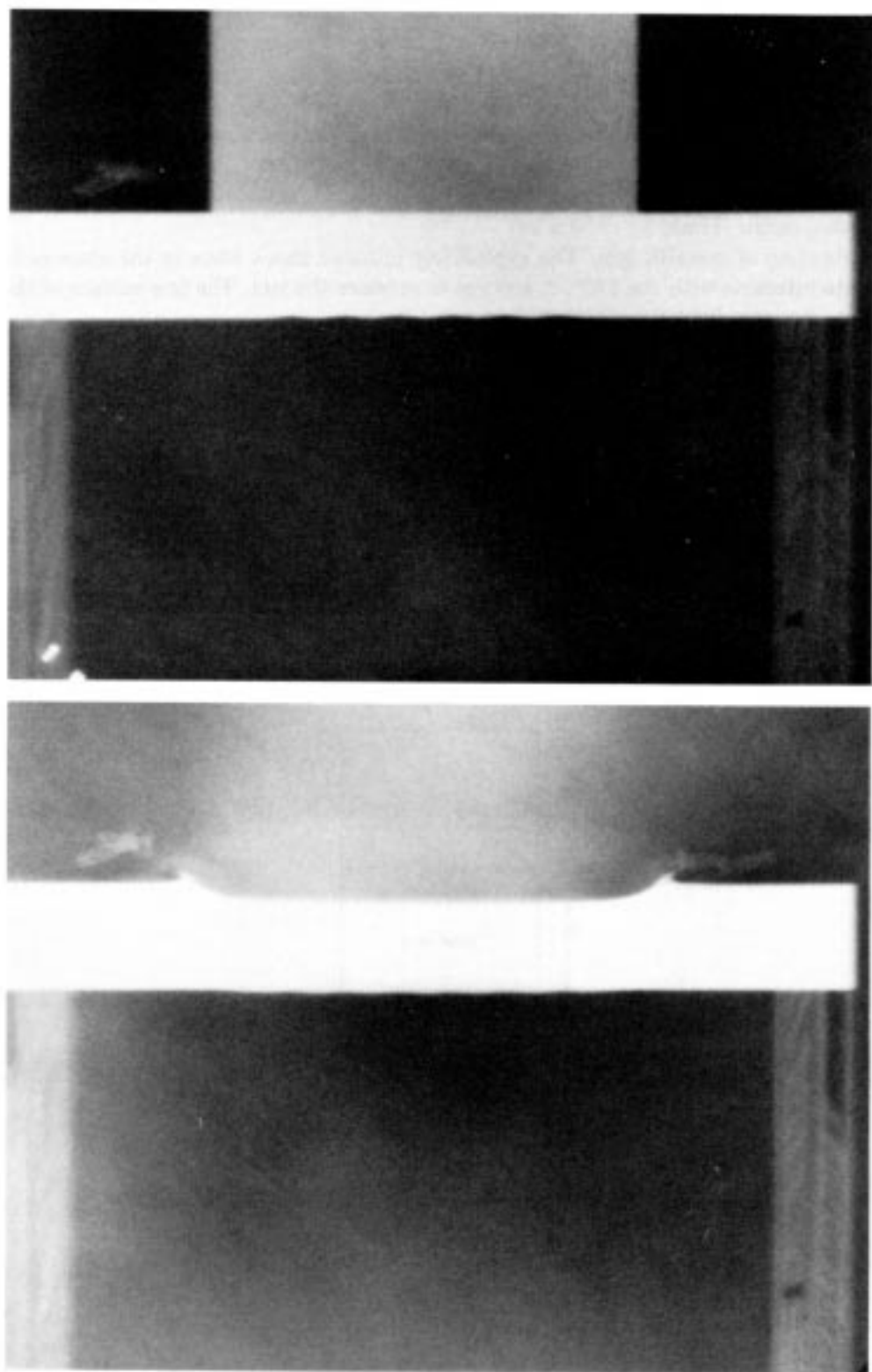
Date: January 4, 1966

Experimenter: Roger W. Taylor

Radiographic Time: 29.93 μ s

Formation of metallic jets. The explosively induced shock wave in the aluminum plate interacts with the 170°, θ , grooves to produce the jets. h is 25.4 mm. The shock wave has arrived at the free surface of the plate.





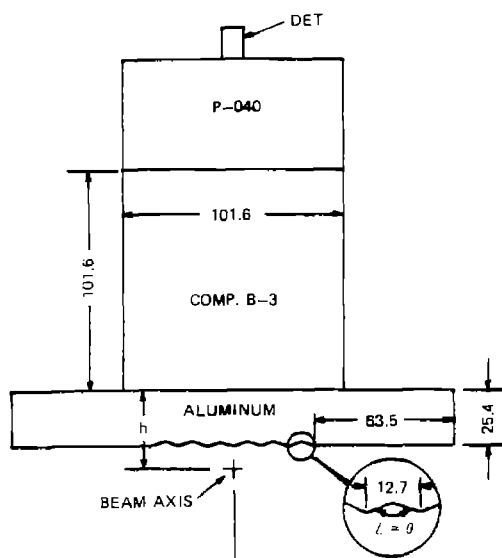
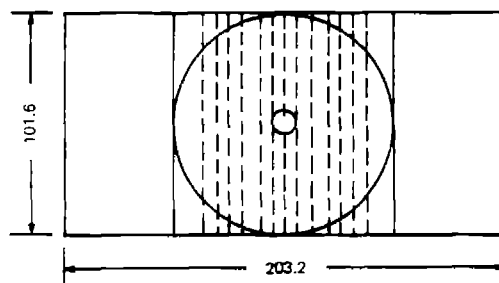
SHOT 152: Aluminum Jets From 170° Grooves

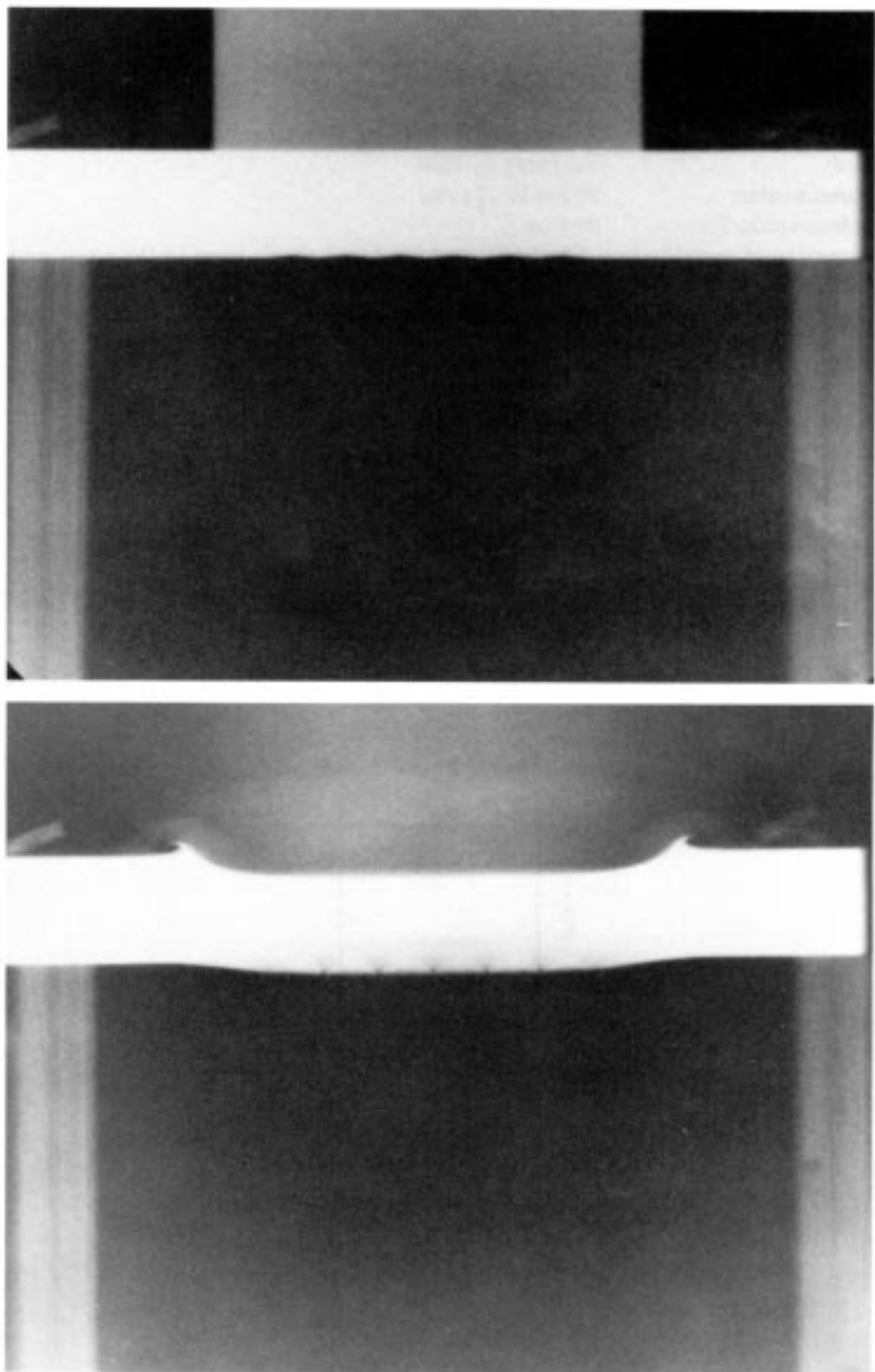
Date: March 29, 1966

Experimenter: Roger W. Taylor

Radiographic Time: 30.9 μ s

Formation of metallic jets. The explosively induced shock wave in the aluminum plate interacts with the 170°, θ , grooves to produce the jets. The free surface of the plate has run for 1.0 μ s. h is 28.5 mm.





SHOT 153:

Aluminum Jets from 160° Grooves

Date:

February 3, 1966

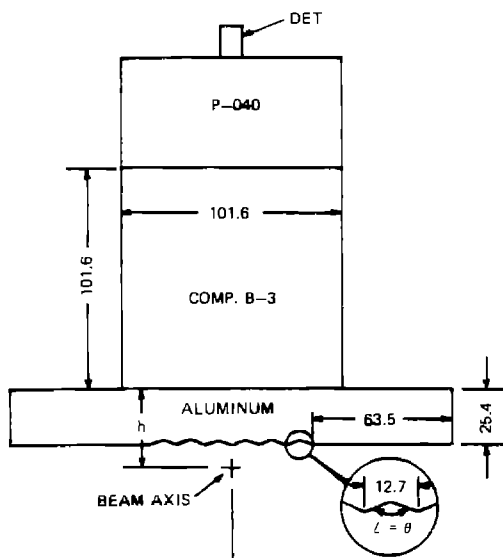
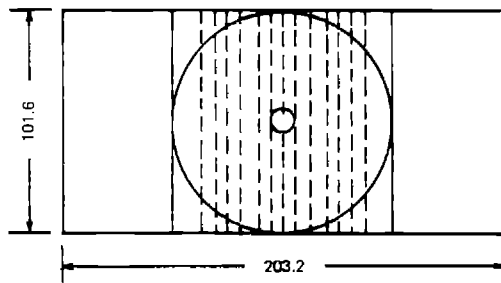
Experimenter:

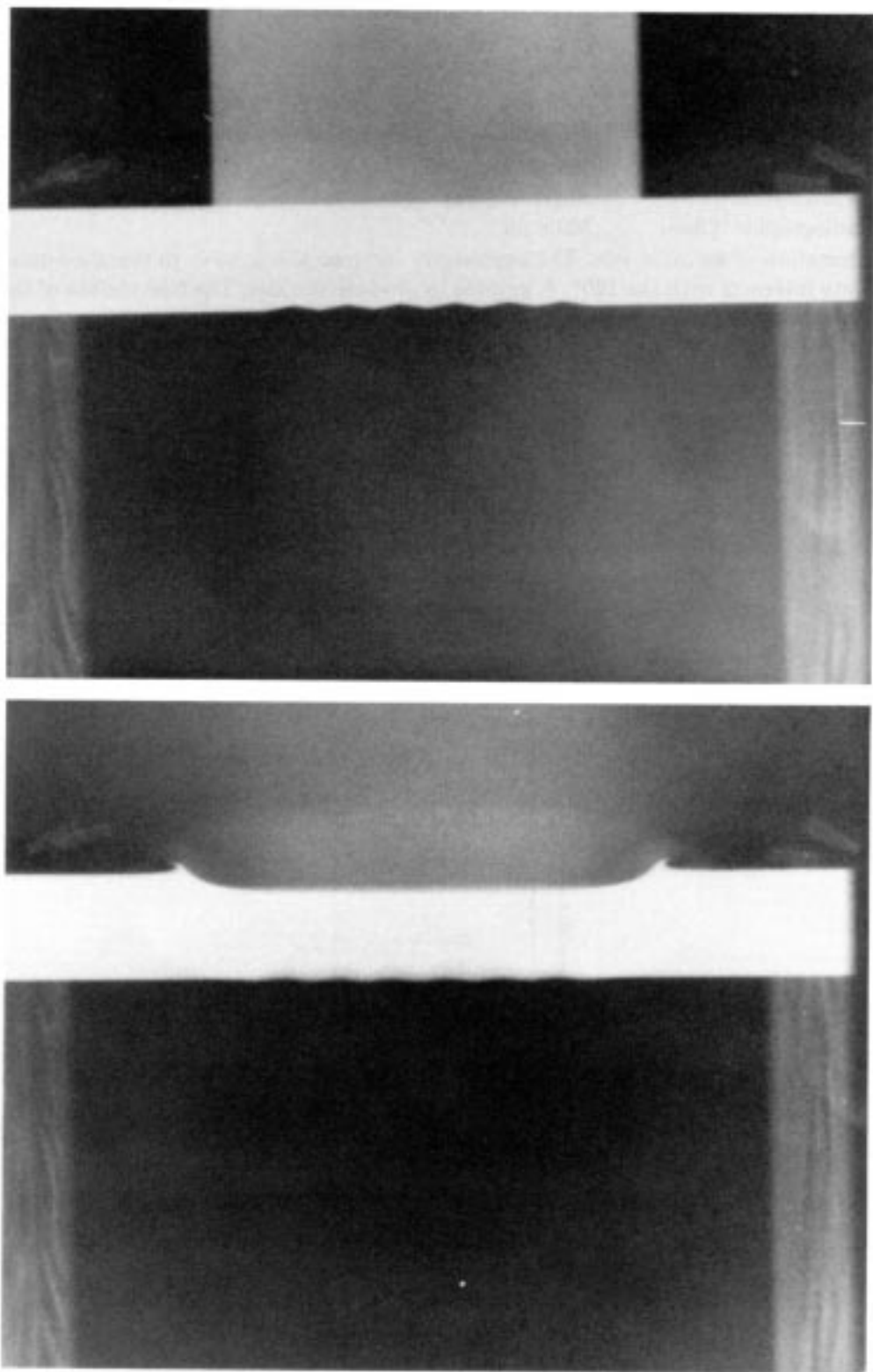
Roger W. Taylor

Radiographic Time:

29.9 μ s

Formation of metallic jets. The explosively induced shock wave in the aluminum plate interacts with the 160°, θ , grooves to produce the jets. The shock wave has arrived at the free surface of the plate. h is 25.4 mm.





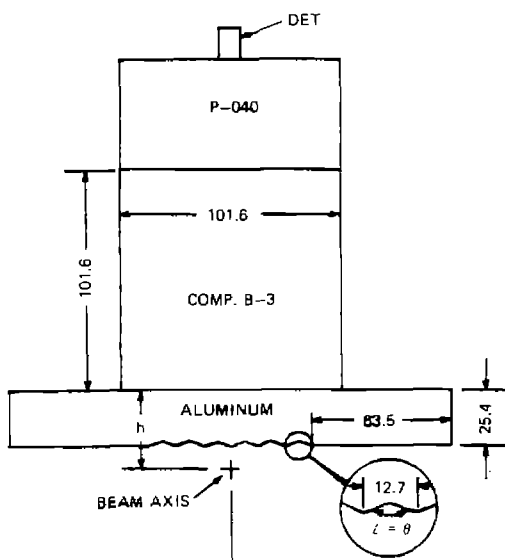
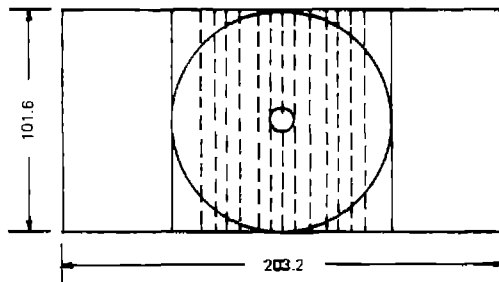
SHOT 154: Aluminum Jets From 160° Grooves

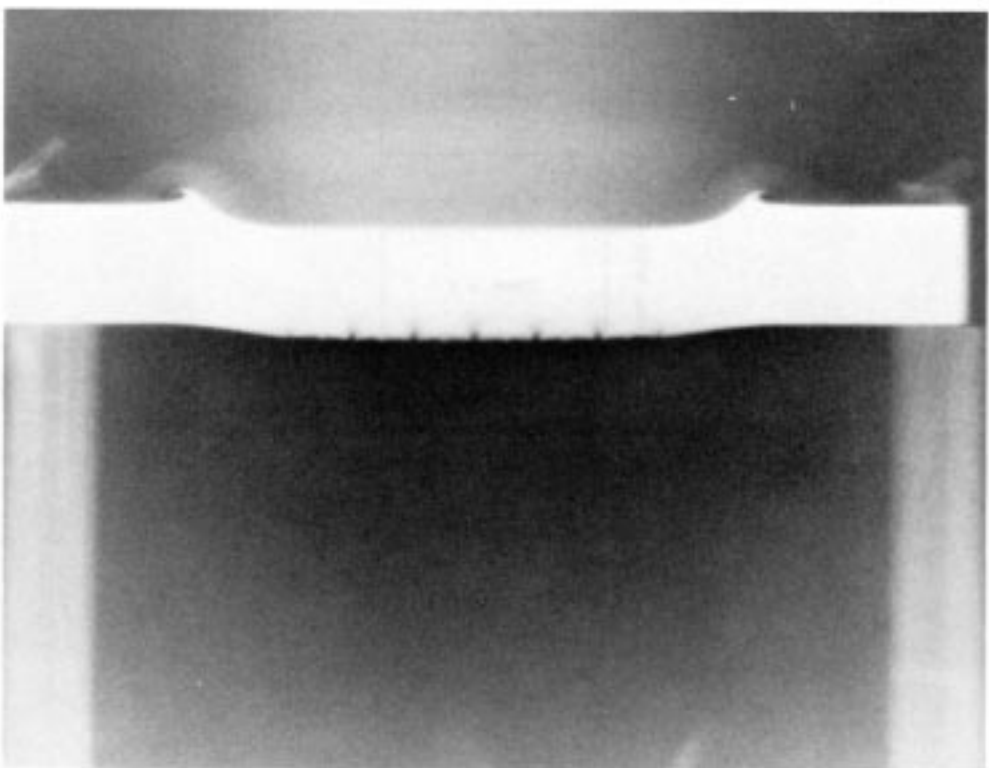
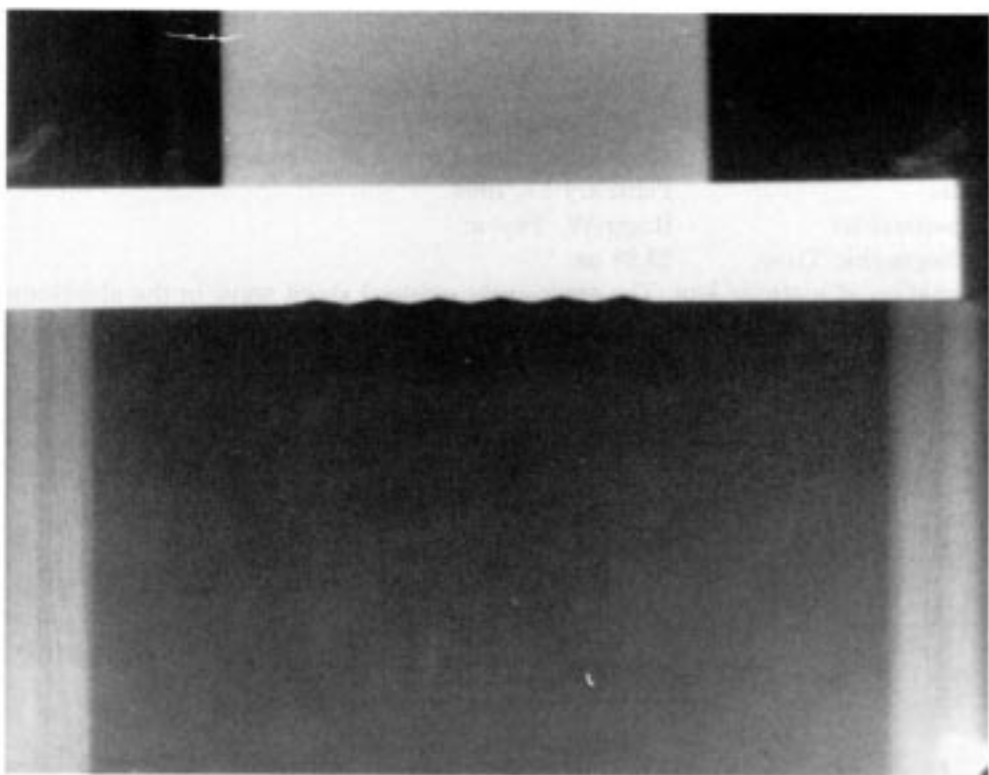
Date: March 29, 1966

Experimenter: Roger W. Taylor

Radiographic Time: 30.88 μ s

Formation of metallic jets. The explosively induced shock wave in the aluminum plate interacts with the 160°, θ , grooves to produce the jets. The free surface of the plate has run for 1.0 μ s. h is 28.5 mm.





SHOT 155:

Aluminum Jets From 140° Grooves

Date:

February 17, 1966

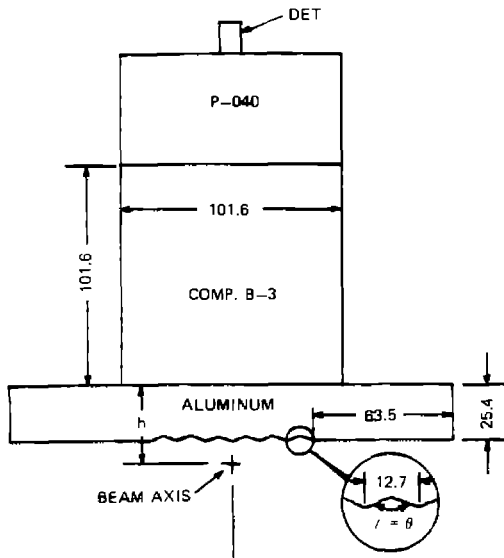
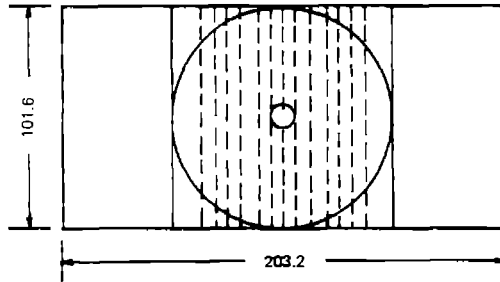
Experimenter:

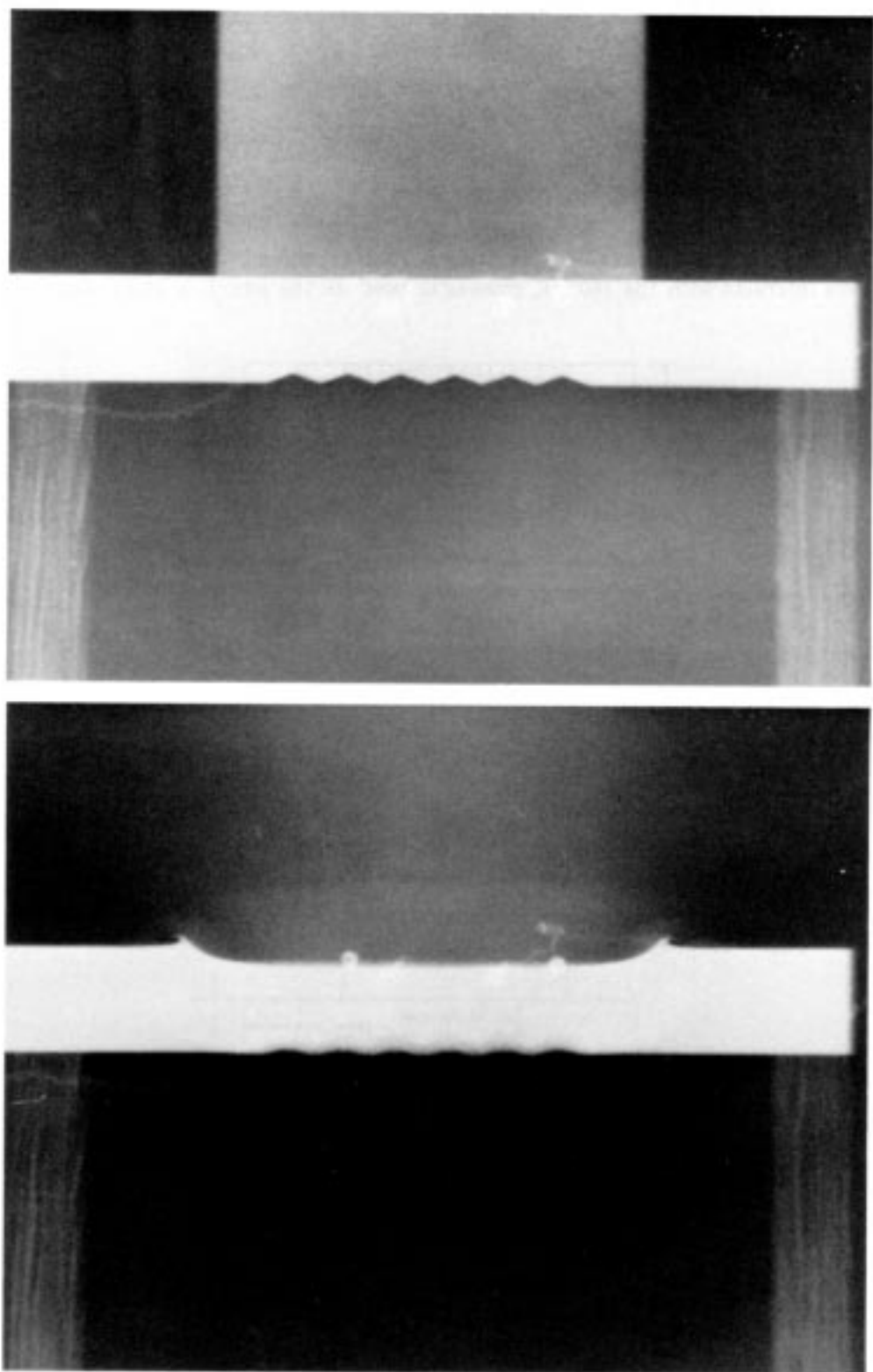
Roger W. Taylor

Radiographic Time:

29.88 μ s

Formation of metallic jets. The explosively induced shock wave in the aluminum plate interacts with the 140°, θ , grooves to produce the jets. The shock wave has arrived at the free surface of the plate. h is 25.4 mm.





SHOT 156:

Aluminum Jets From 140° Grooves

Date:

May 4, 1966

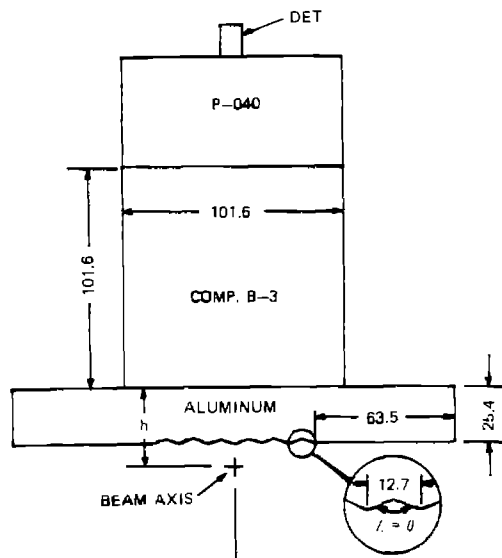
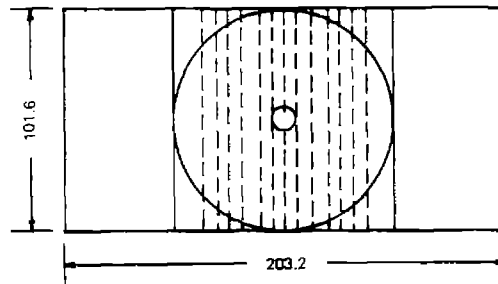
Experimenter:

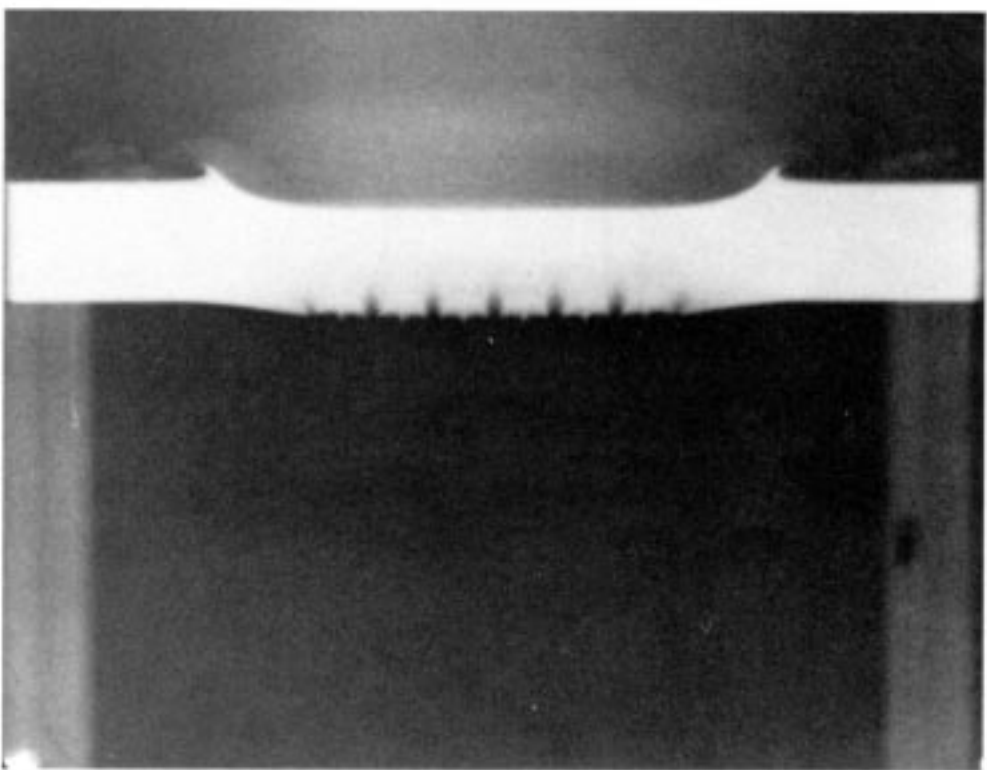
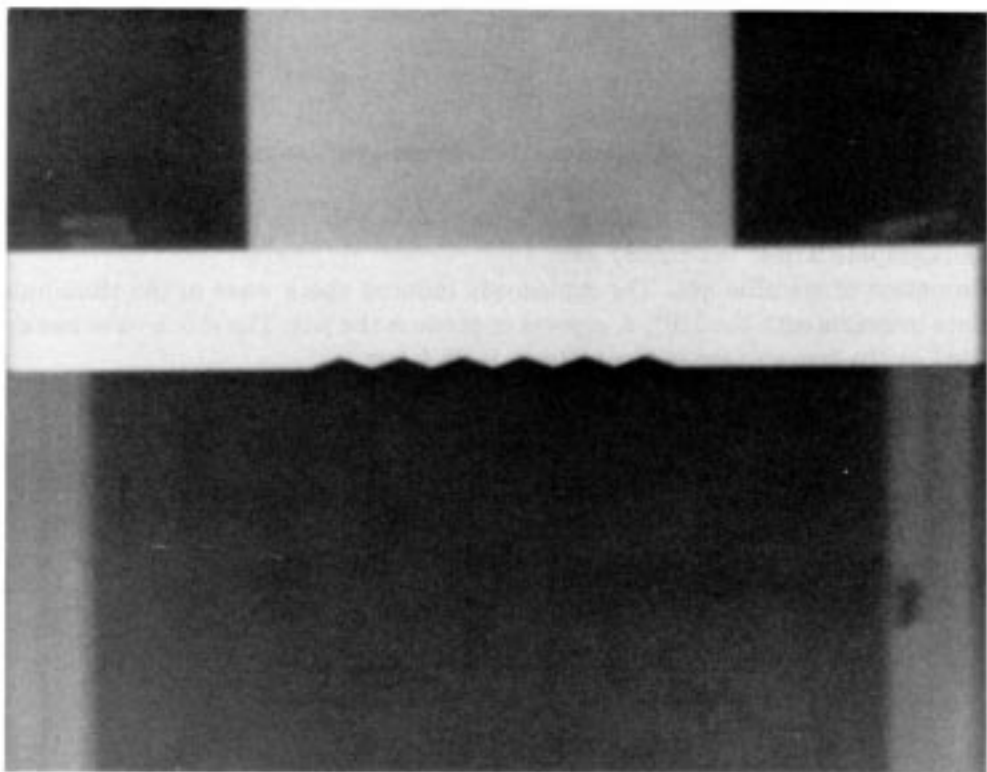
Roger W. Taylor

Radiographic Time:

30.9 μ s

Formation of metallic jets. The explosively induced shock wave in the aluminum plate interacts with the 140°, θ , grooves to produce the jets. h is 28.57 mm.





SHOT 157:

Aluminum Jets From 120° Grooves

Date:

February 17, 1966

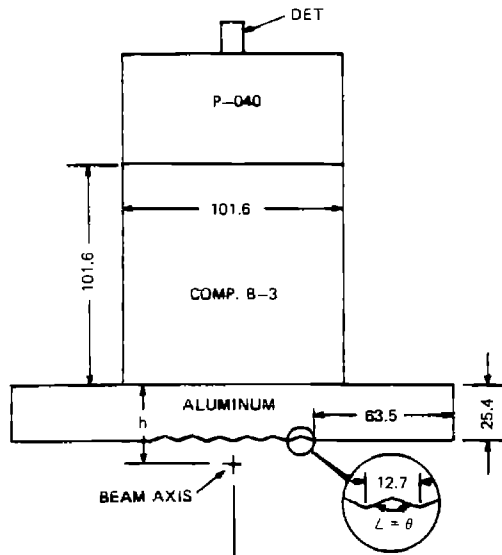
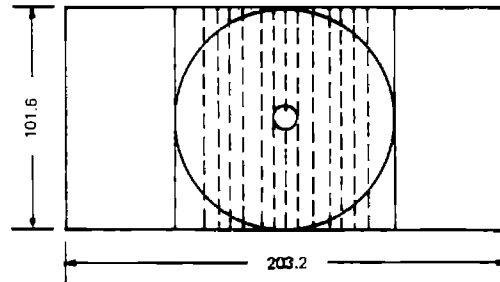
Experimenter:

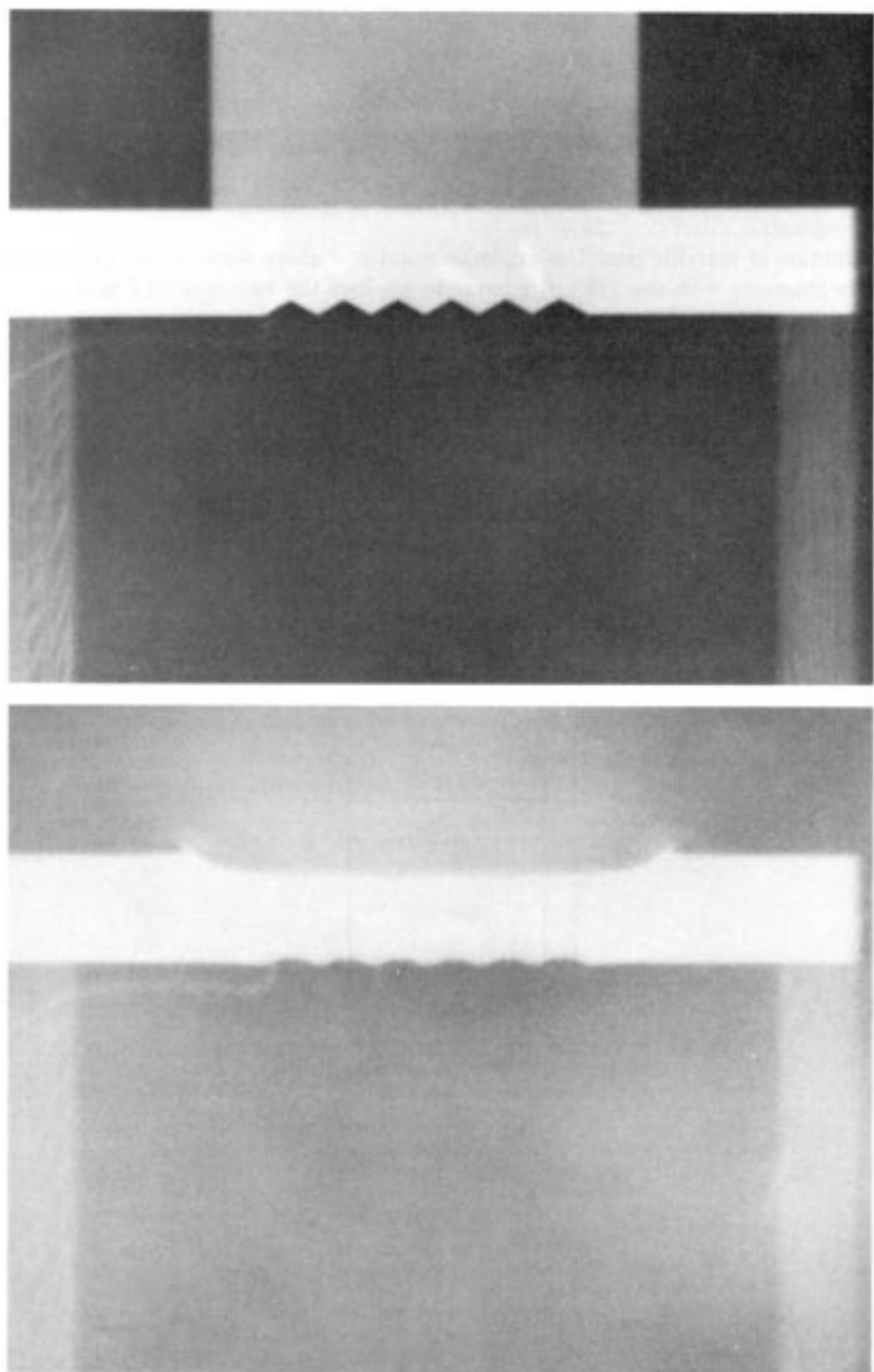
Roger W. Taylor

Radiographic Time:

29.87 μ s

Formation of metallic jets. The explosively induced shock wave in the aluminum plate interacts with the 120°, θ , grooves to produce the jets. The shock wave has arrived at the free surface of the plate. h is 25.4 mm.





SHOT 158:

Aluminum Jets From 120° Grooves

Date:

March 30, 1966

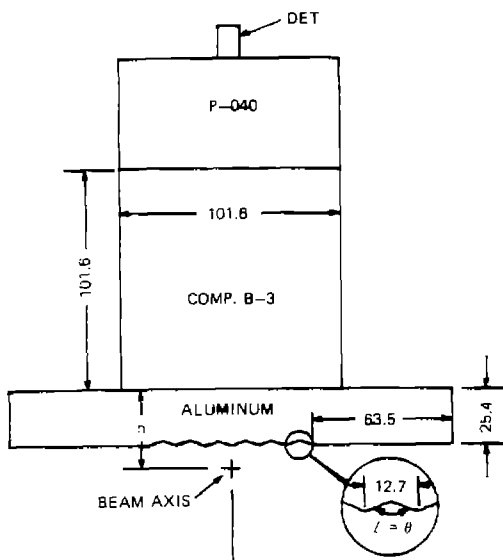
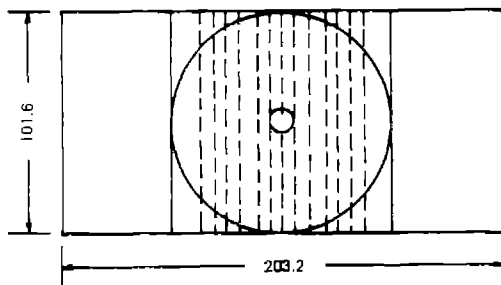
Experimenter:

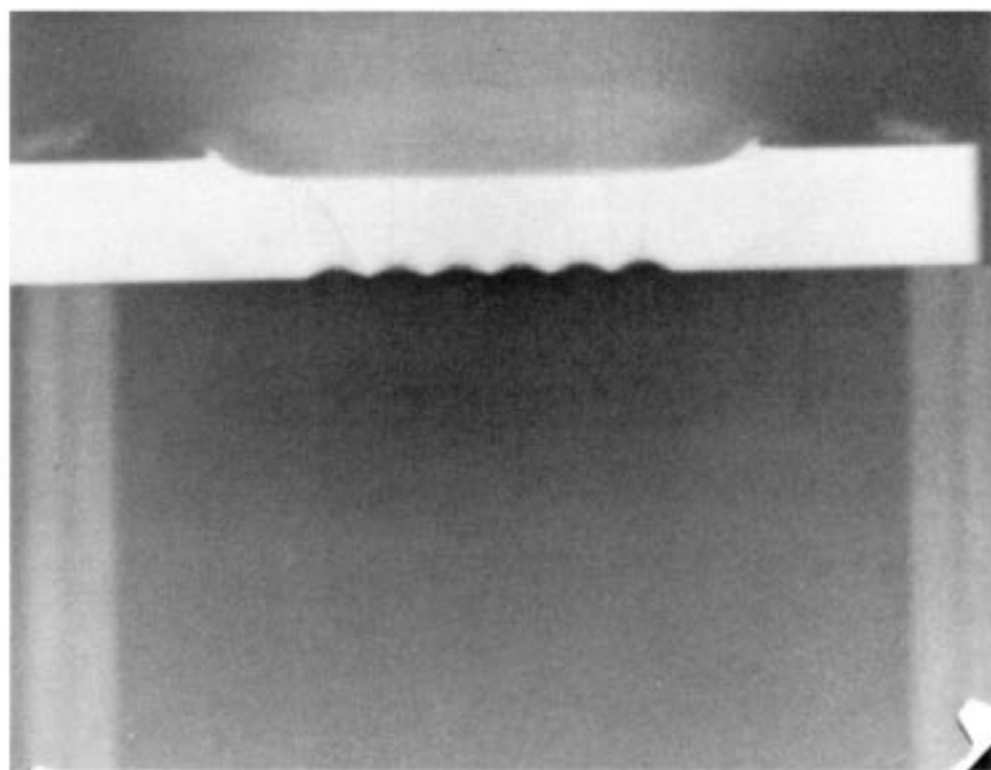
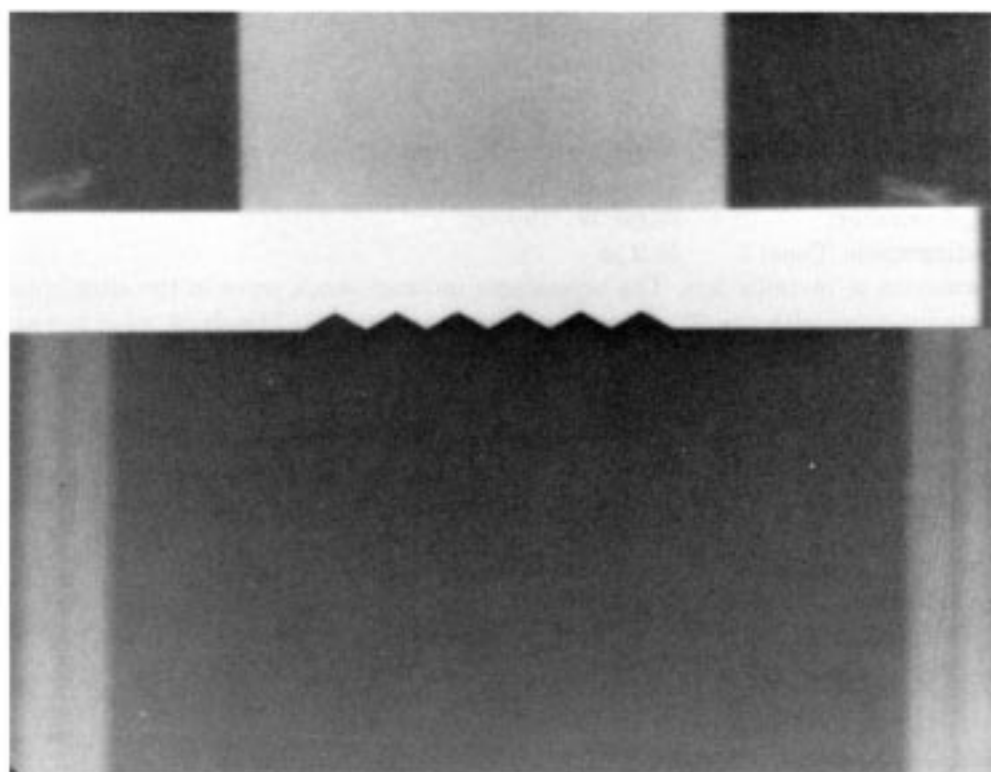
Roger W. Taylor

Radiographic Time:

29.58 μ s

Formation of metallic jets. The explosively induced shock wave in the aluminum plate interacts with the 120°, θ , grooves to produce the jets. h is 22.2 mm.





SHOT 159:

Aluminum Jets From 60° Grooves

Date:

March 9, 1966

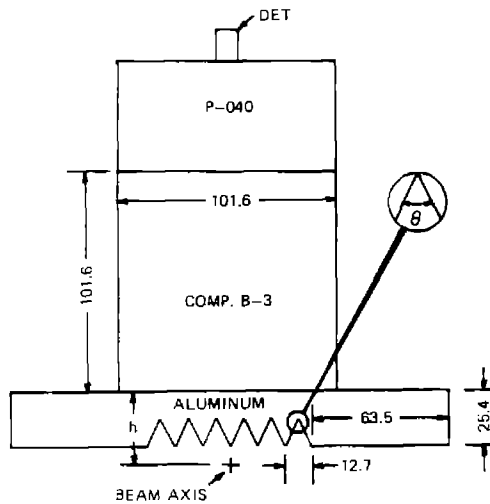
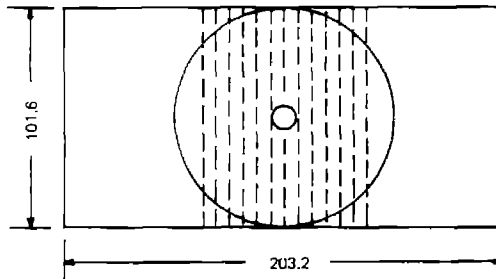
Experimenter:

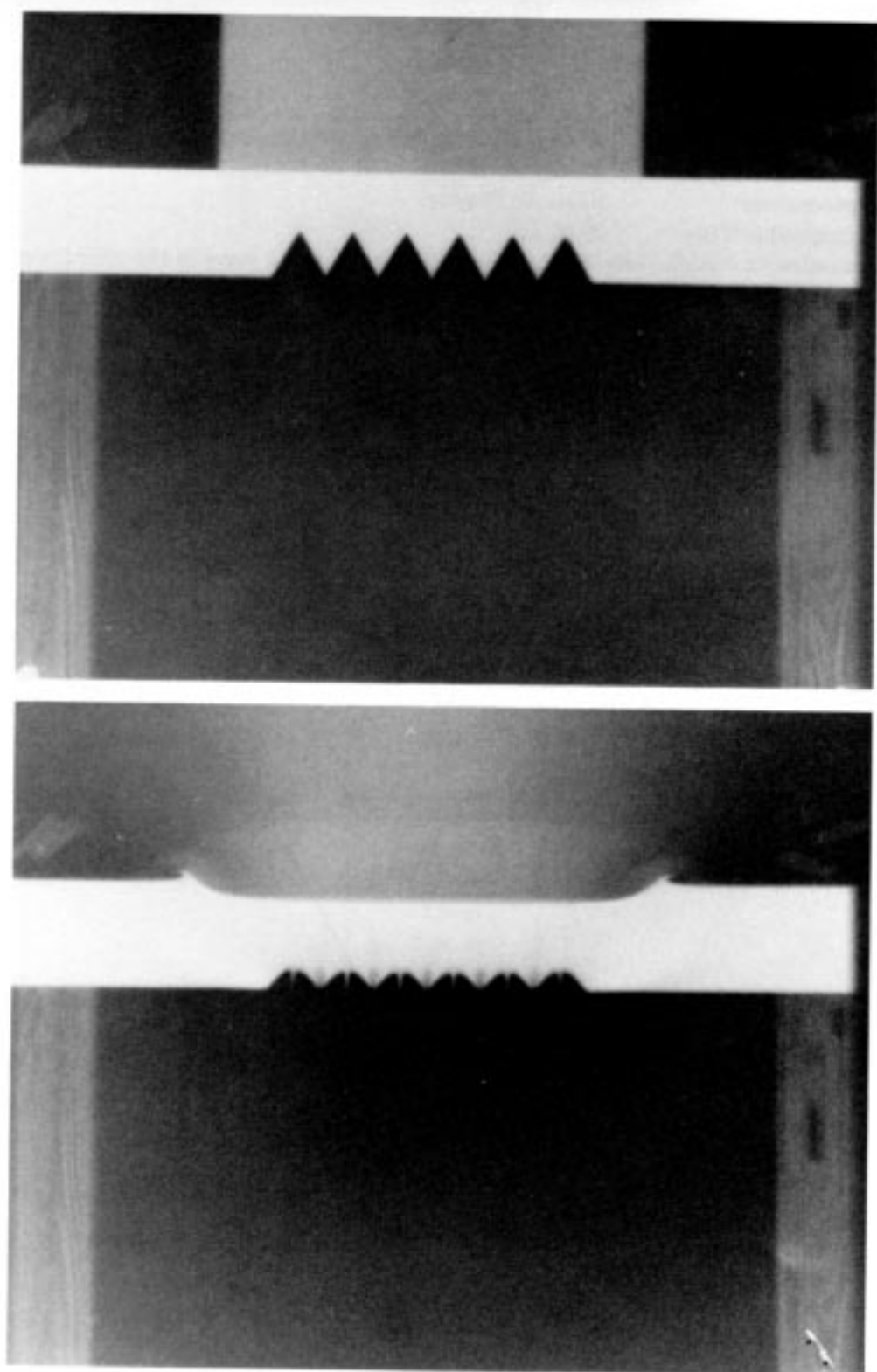
Roger W. Taylor

Radiographic Time:

29.9 μ s

Formation of metallic jets. The explosively induced shock wave in the aluminum plate interacts with the 60°, θ , grooves to produce the jets. The shock wave has arrived at the free surface of the plate. h is 25.4 mm.





SHOT 160:

Aluminum Jets From 60° Grooves

Date:

March 30, 1966

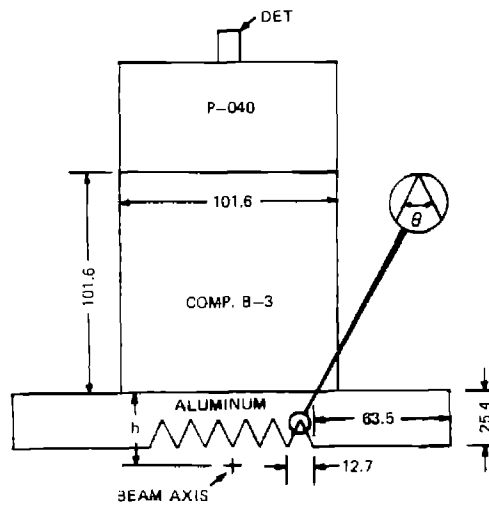
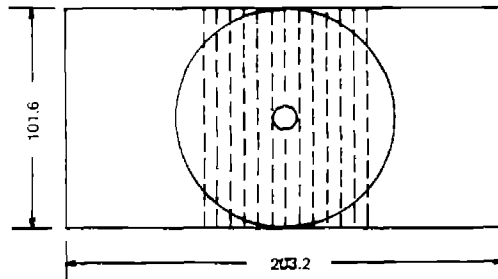
Experimenter:

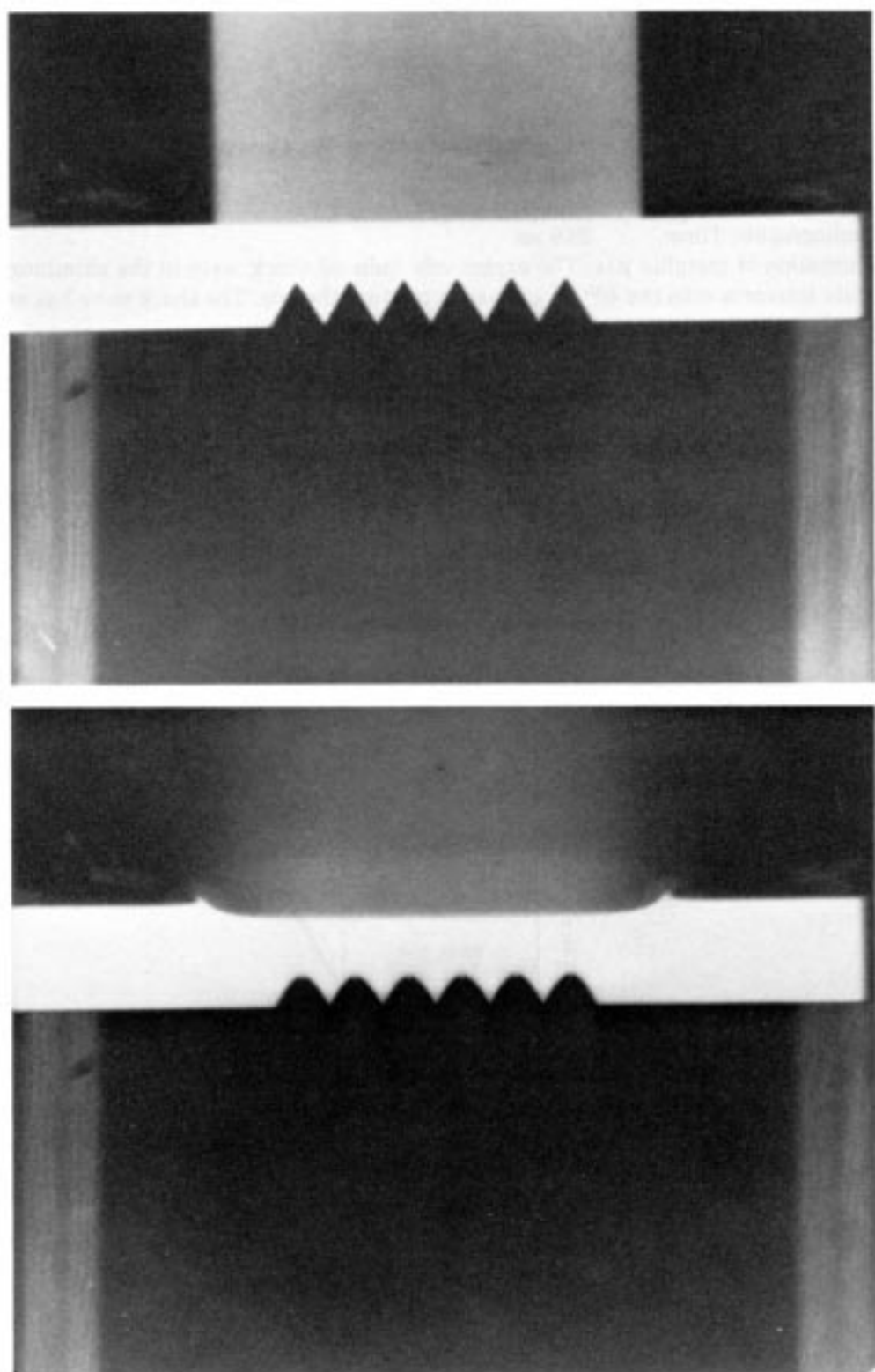
Roger W. Taylor

Radiographic Time:

29.06 μ s

Formation of metallic jets. The explosively induced shock wave in the aluminum plate interacts with the 60°, θ , grooves to produce the jets. h is 19.1 mm.





SHOT 161:

Aluminum Jets From 40° Grooves

Date:

March 10, 1966

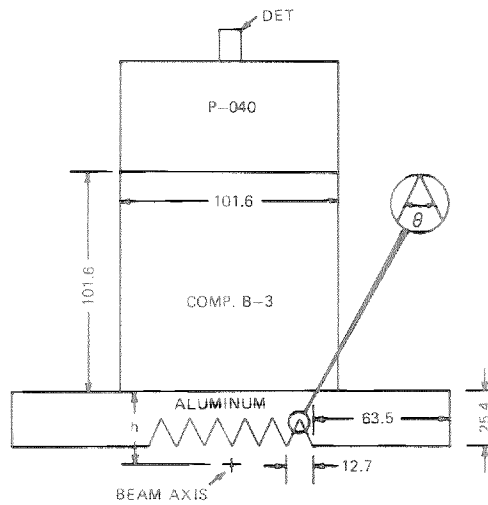
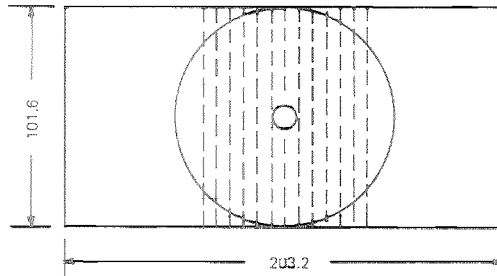
Experimenter:

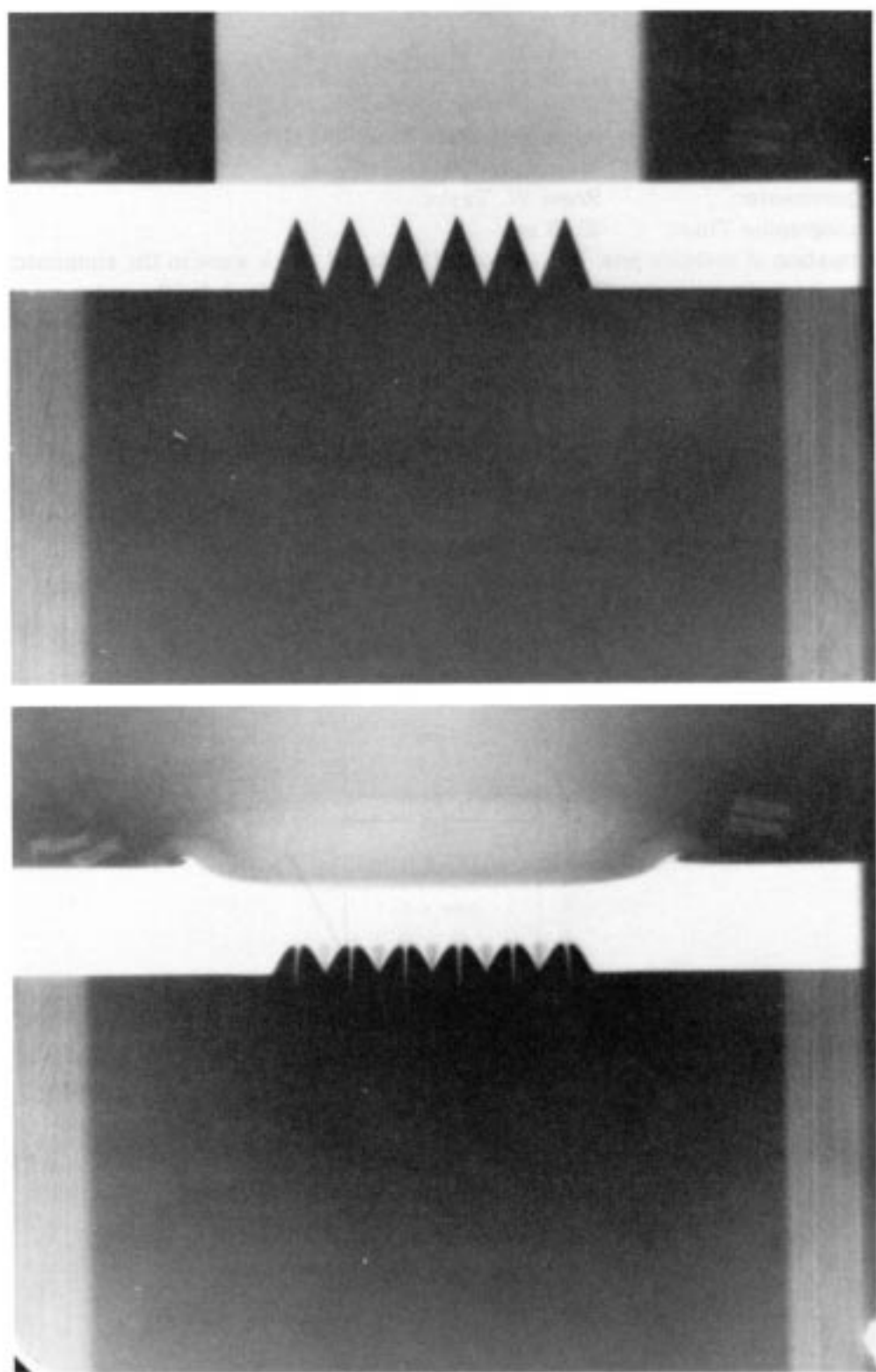
Roger W. Taylor

Radiographic Time:

29.9 μ s

Formation of metallic jets. The explosively induced shock wave in the aluminum plate interacts with the 40°, θ , grooves to produce the jets. The shock wave has arrived at the free surface of the plate. h is 25.4 mm.





SHOT 162:

Aluminum Jets From 40° Grooves

Date:

March 31, 1966

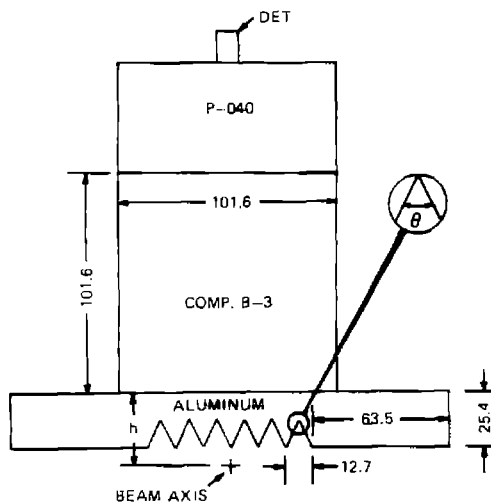
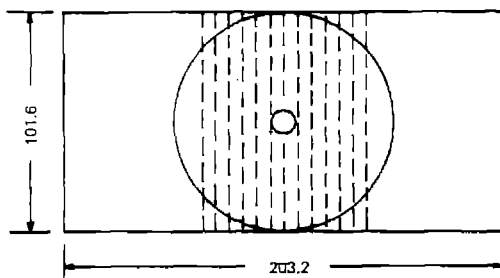
Experimenter:

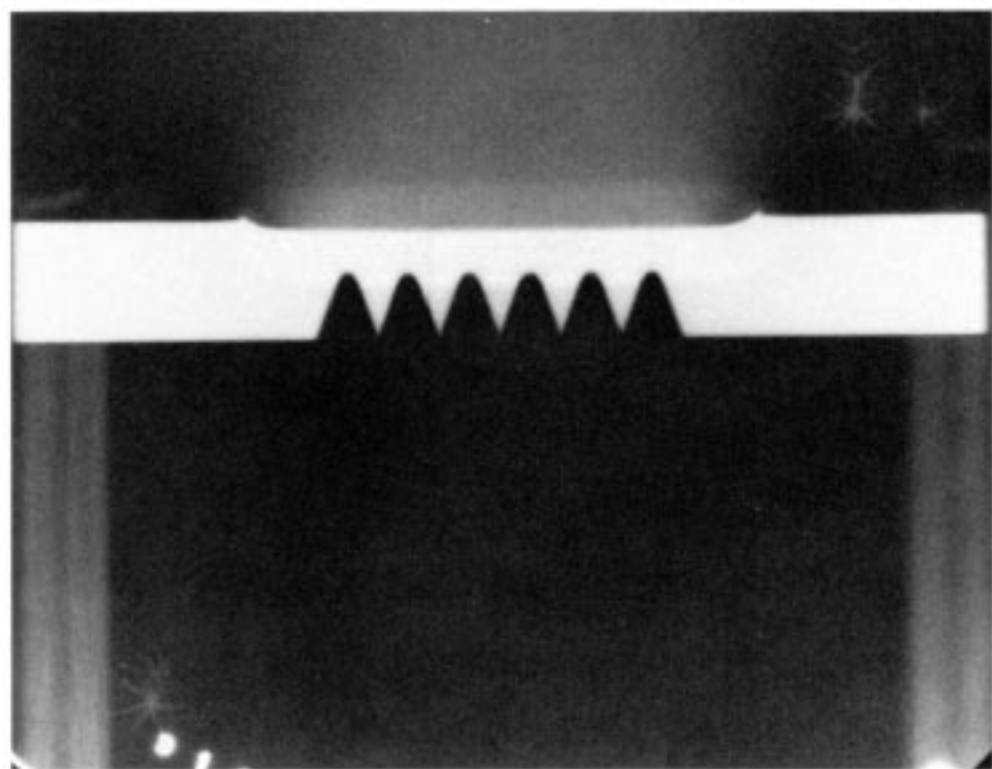
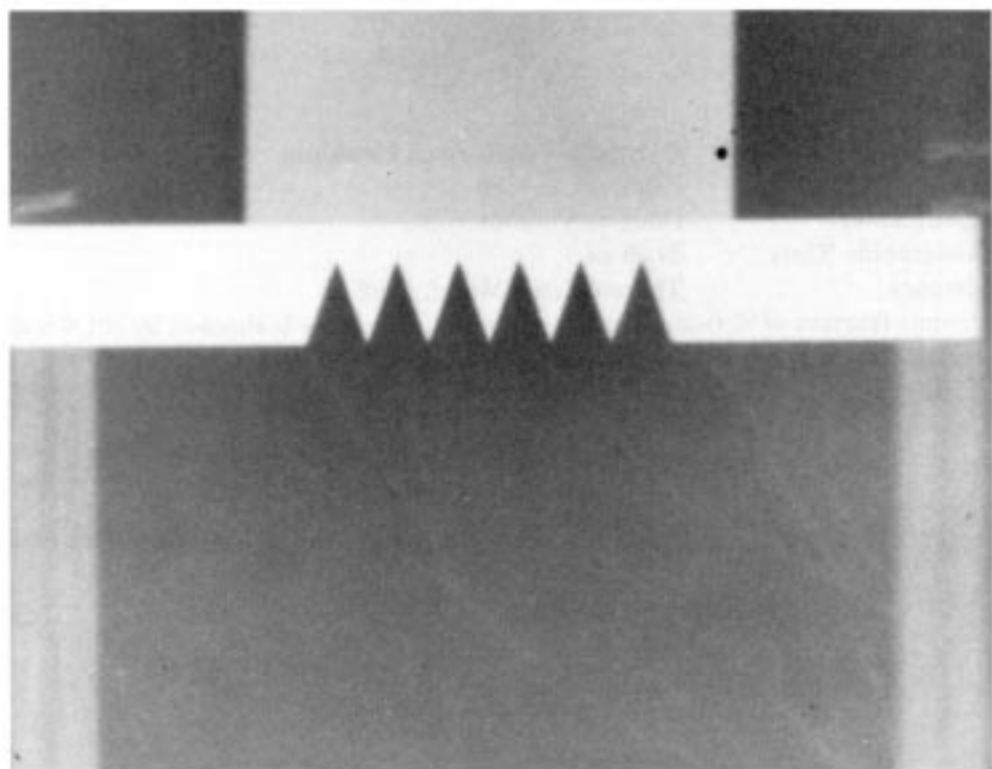
Roger W. Taylor

Radiographic Time:

28.09 μ s

Formation of metallic jets. The explosively induced shock wave in the aluminum plate interacts with the 40°, θ , grooves to produce the jets. h is 19.1 mm.





SHOT 165:

Dynamic Fracture of Uranium

Date:

February 2, 1965

Experimenter:

Douglas Venable

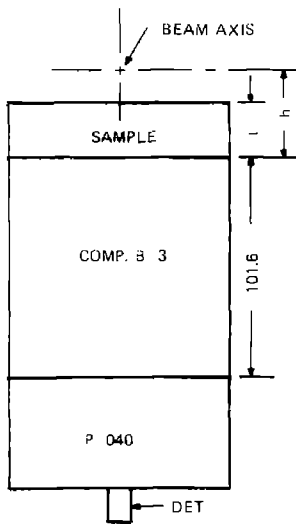
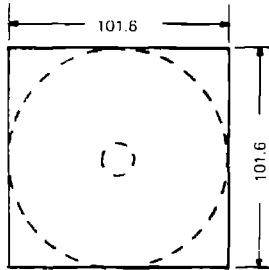
Radiographic Time:

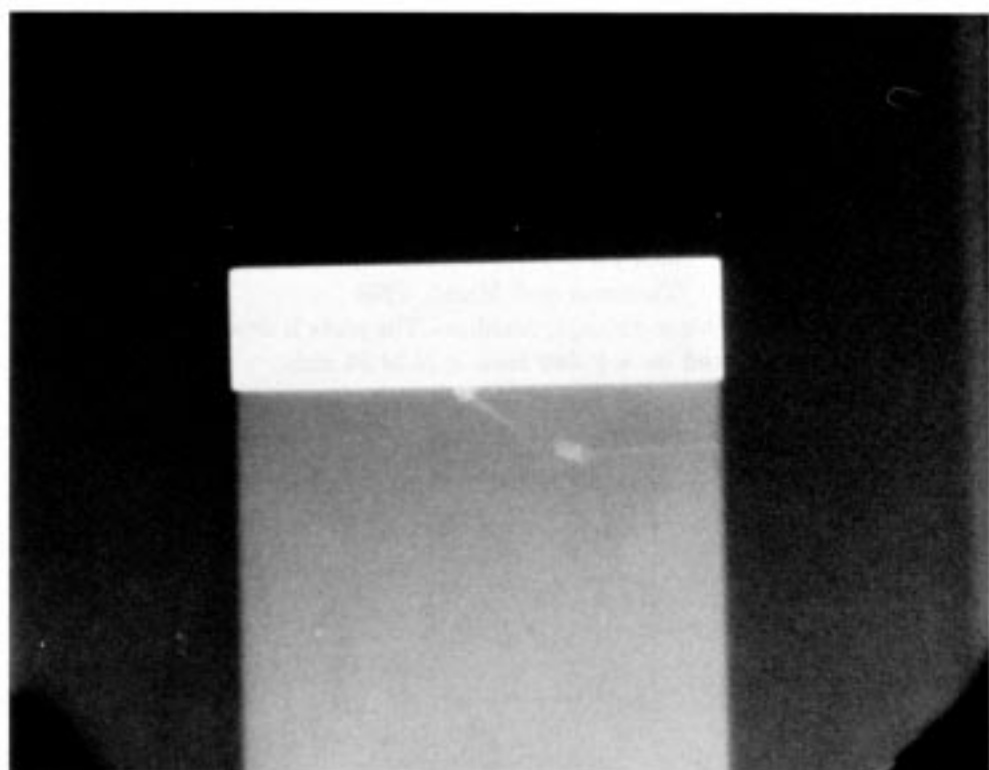
39.39 μ s

Reference:

Thurston and Mudd, 1968

Dynamic fracture of 25.0-mm-thick, t, uranium. The plate is shocked by 101.6 mm of Composition B-3 initiated by a P-040 lens. h is 34.93 mm.





SHOT 166:

Dynamic Fracture of Uranium

Date:

November 16, 1965

Experimenter:

Benny Ray Breed

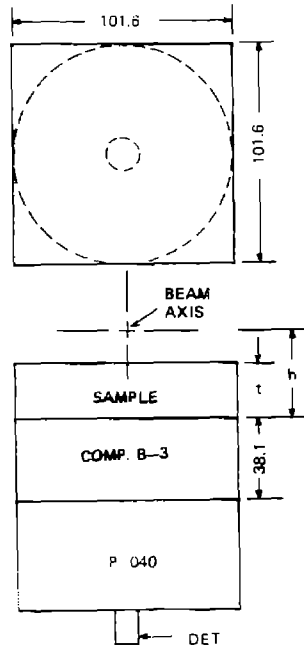
Radiographic Time:

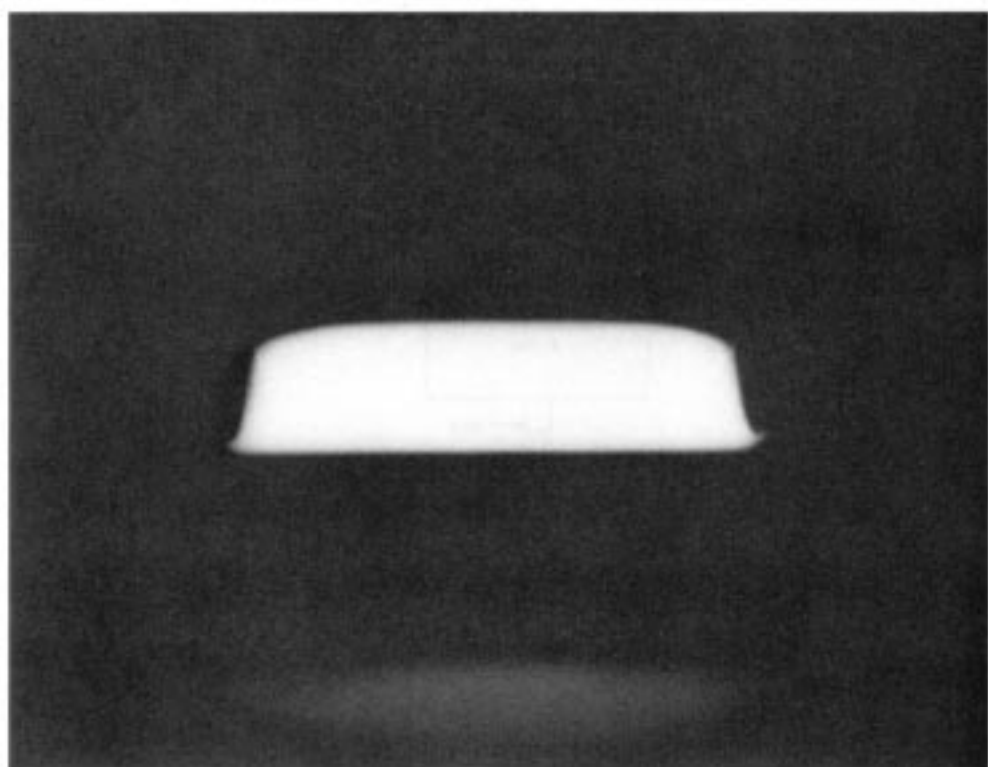
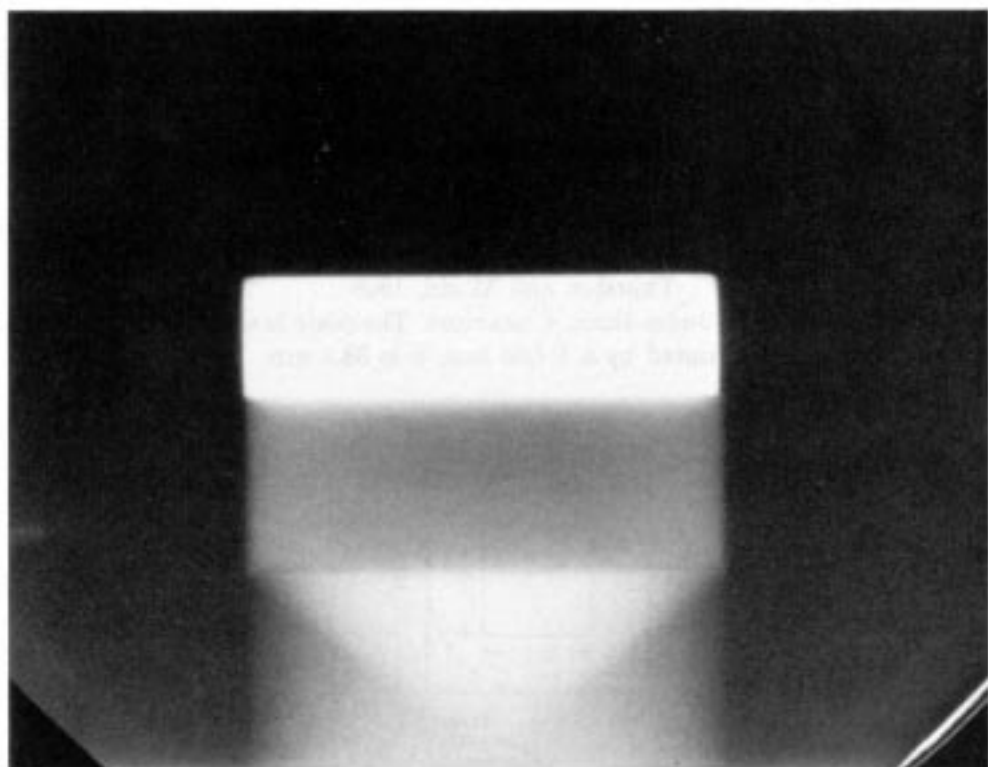
33.4 μ s

Reference:

Thurston and Mudd, 1968

Dynamic fracture of 25.0-mm-thick, t , uranium. The plate is shocked by 38.1 mm of Composition B-3 initiated by a P-040 lens. h is 34.93 mm.





SHOT 167:

Dynamic Fracture of Uranium

Date:

February 16, 1966

Experimenter:

Benny Ray Breed

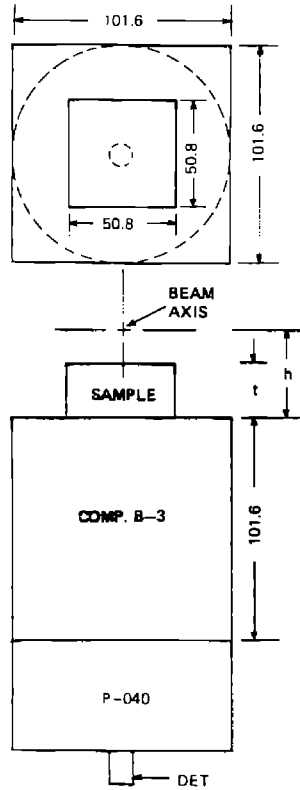
Radiographic Time:

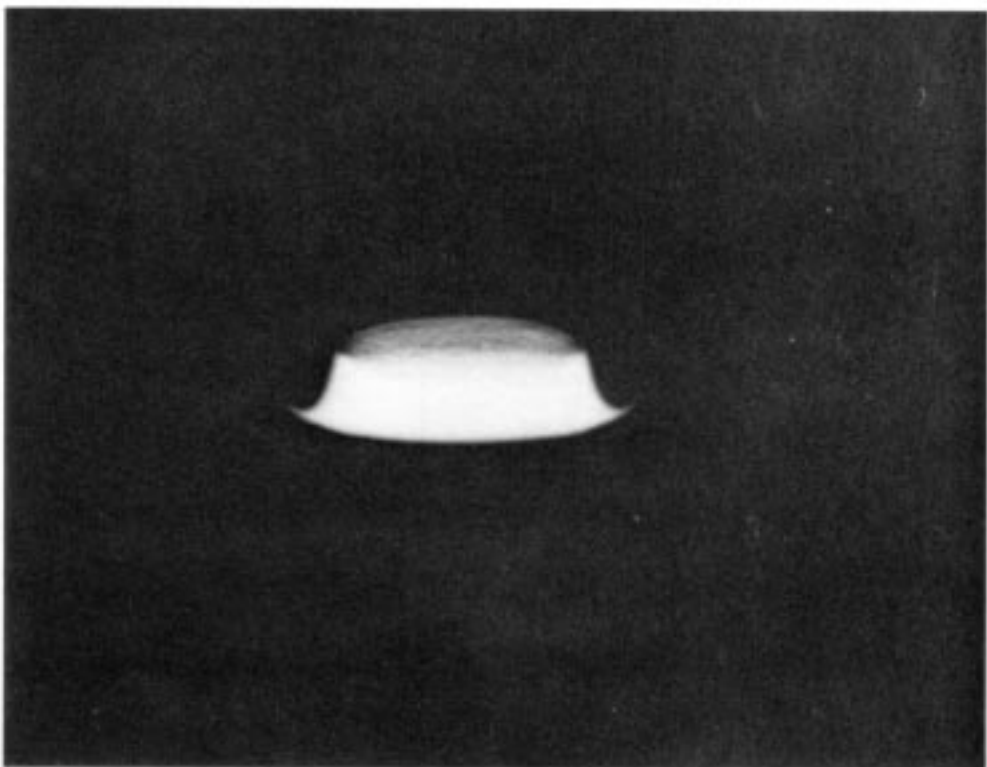
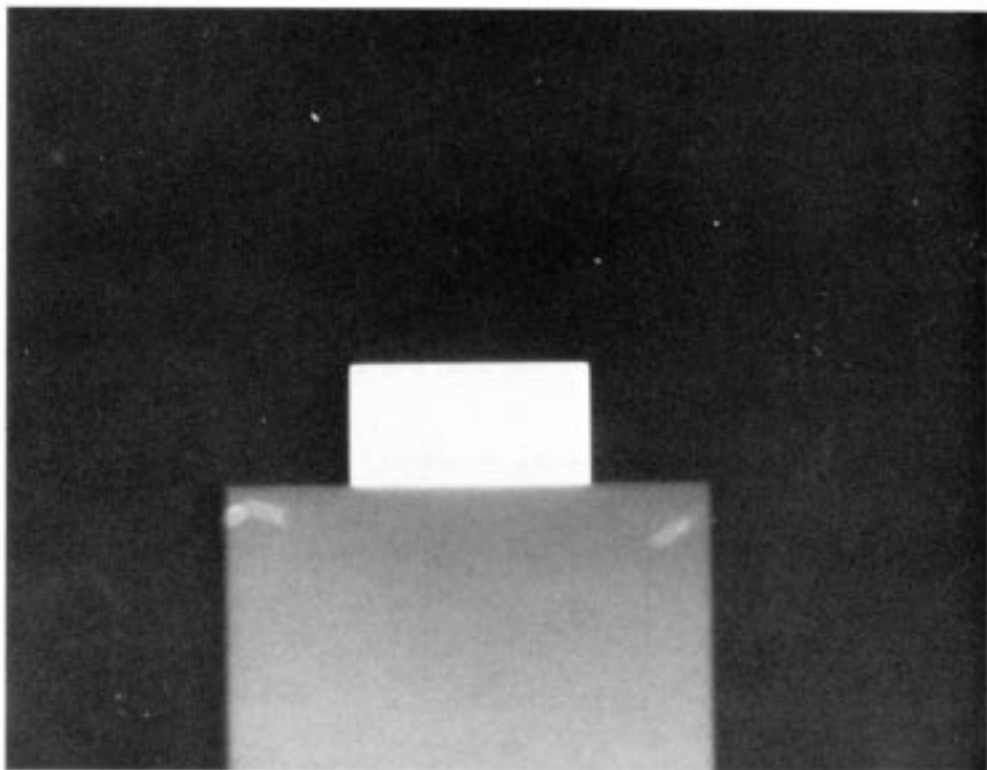
41.42 μ s

Reference:

Thurston and Mudd, 1968

Dynamic fracture of 25.0-mm-thick, t , uranium. The plate is shocked by 101.6 mm of Composition B-3 initiated by a P-040 lens. h is 38.1 mm.





SHOT 168:

Dynamic Fracture of Uranium

Date:

February 3, 1965

Experimenter:

Douglas Venable

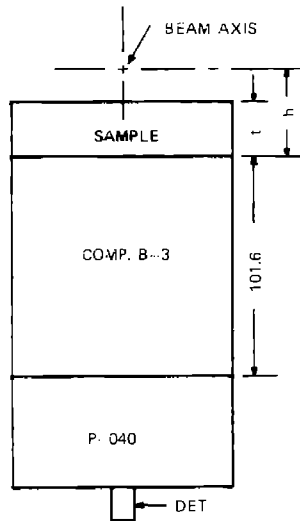
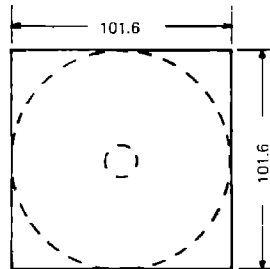
Radiographic Time:

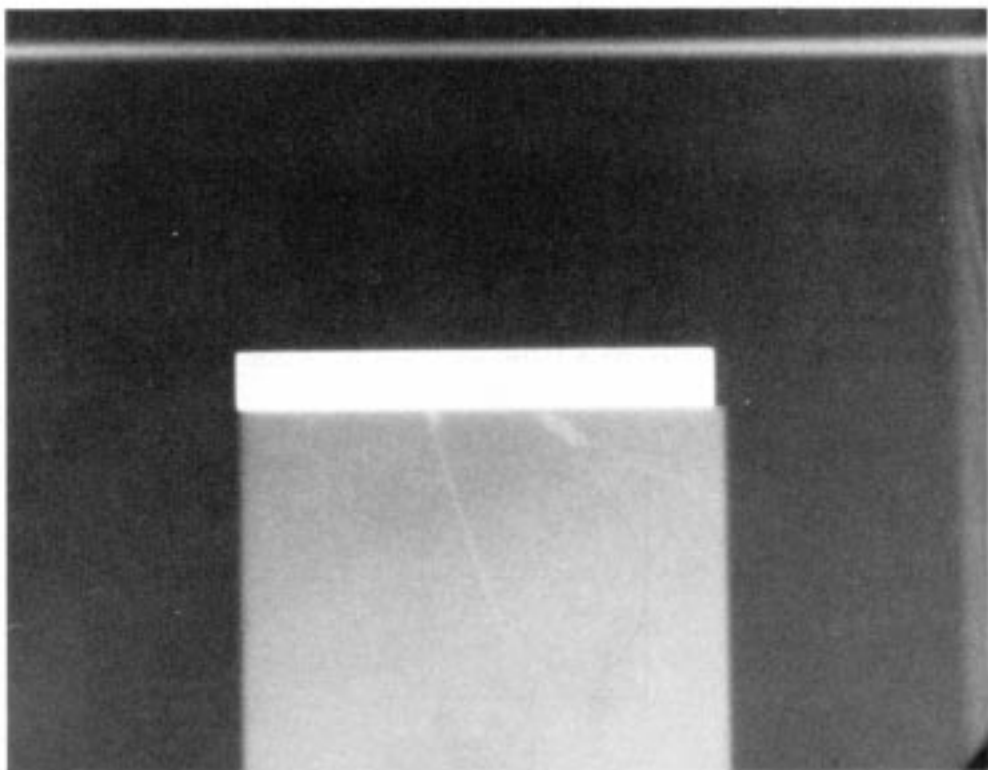
33.8 μ s

Reference:

Thurston and Mudd, 1968

Dynamic fracture of 12.0-mm-thick, t , uranium. The plate is shocked by 101.6 mm of Composition B-3 initiated by a P-040 lens. h is 19.1 mm.





SHOT 169:

Dynamic Fracture of Uranium

Date:

May 17, 1965

Experimenter:

Benny Ray Breed

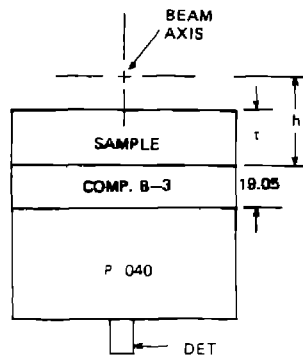
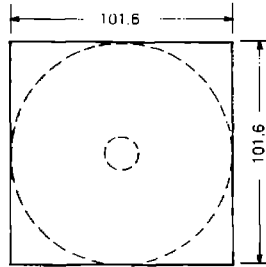
Radiographic Time:

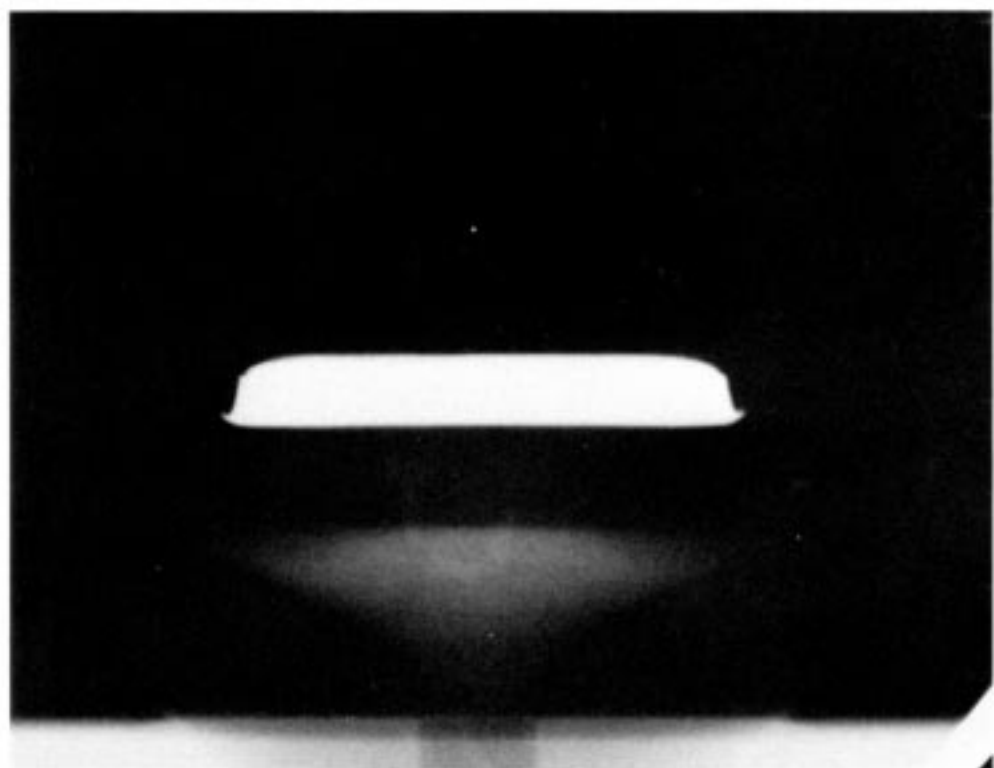
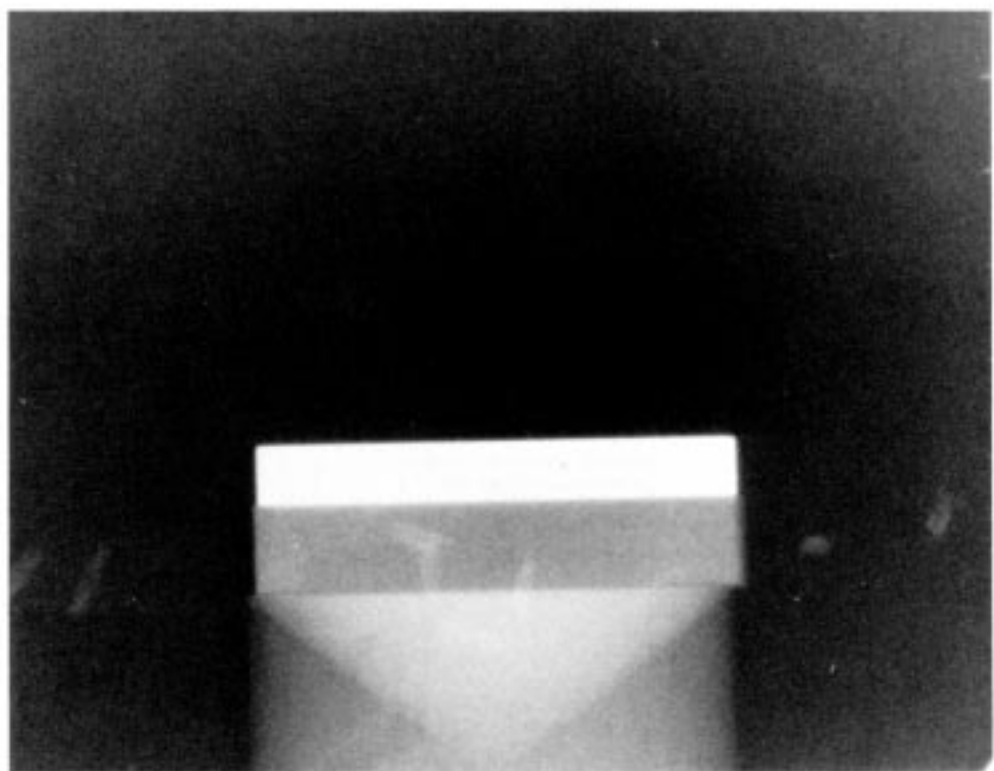
25.35 μ s

Reference:

Thurston and Mudd, 1968

Dynamic fracture of 12.0-mm-thick, t , uranium. The plate is shocked by 19.05 mm of Composition B-3 initiated by a P-040 lens. h is 20.64 mm.





SHOT 170:

Dynamic Fracture of Uranium

Date:

November 15, 1965

Experimenter:

Benny Ray Breed

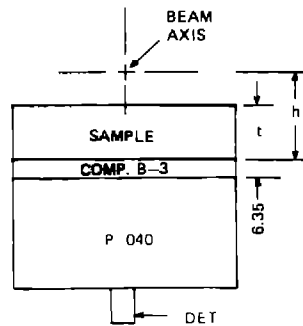
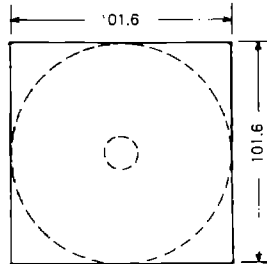
Radiographic Time:

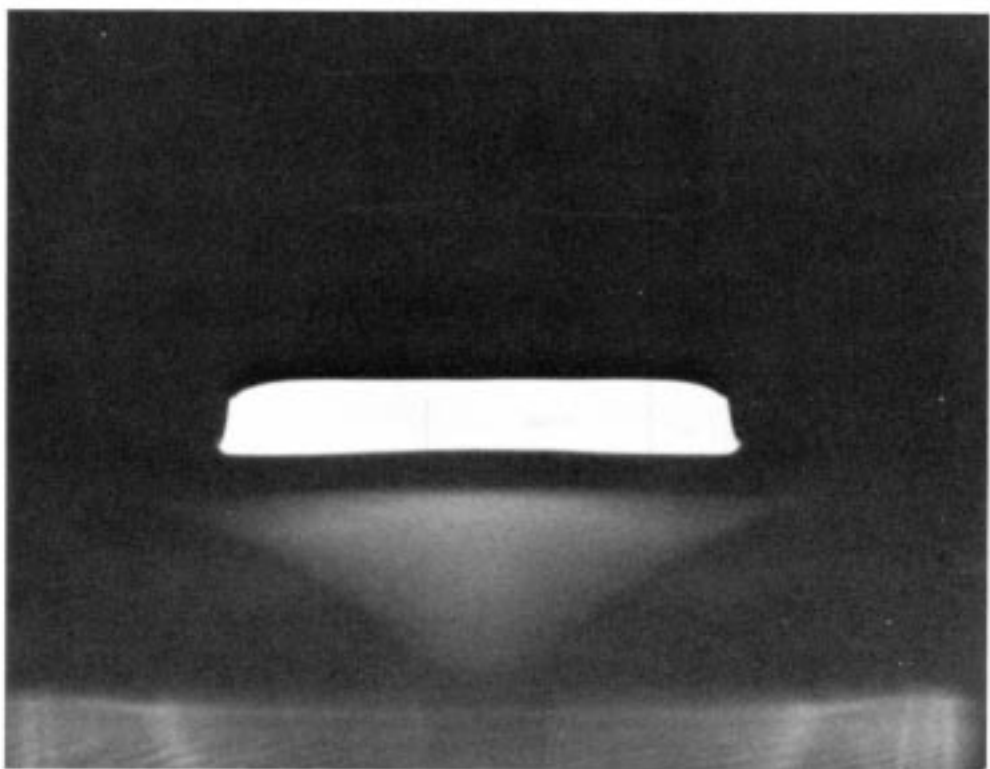
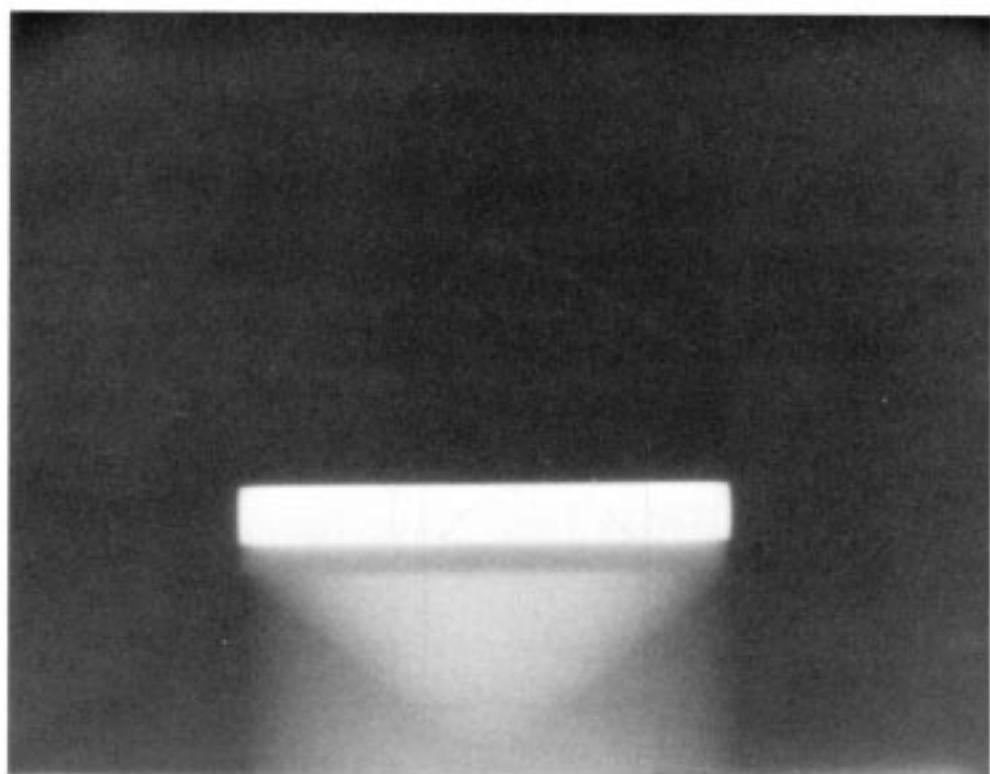
25.72 μ s

Reference:

Thurston and Mudd, 1968

Dynamic fracture of 12.0-mm-thick, t , uranium. The plate is shocked by 6.35 mm of Composition B-3 initiated by a P-040 lens. h is 25.4 mm.





SHOT 171: Dynamic Fracture of Uranium

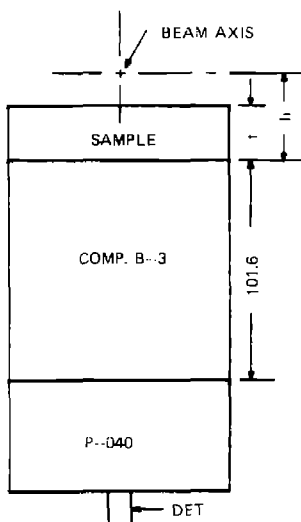
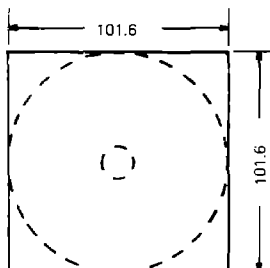
Date: February 3, 1965

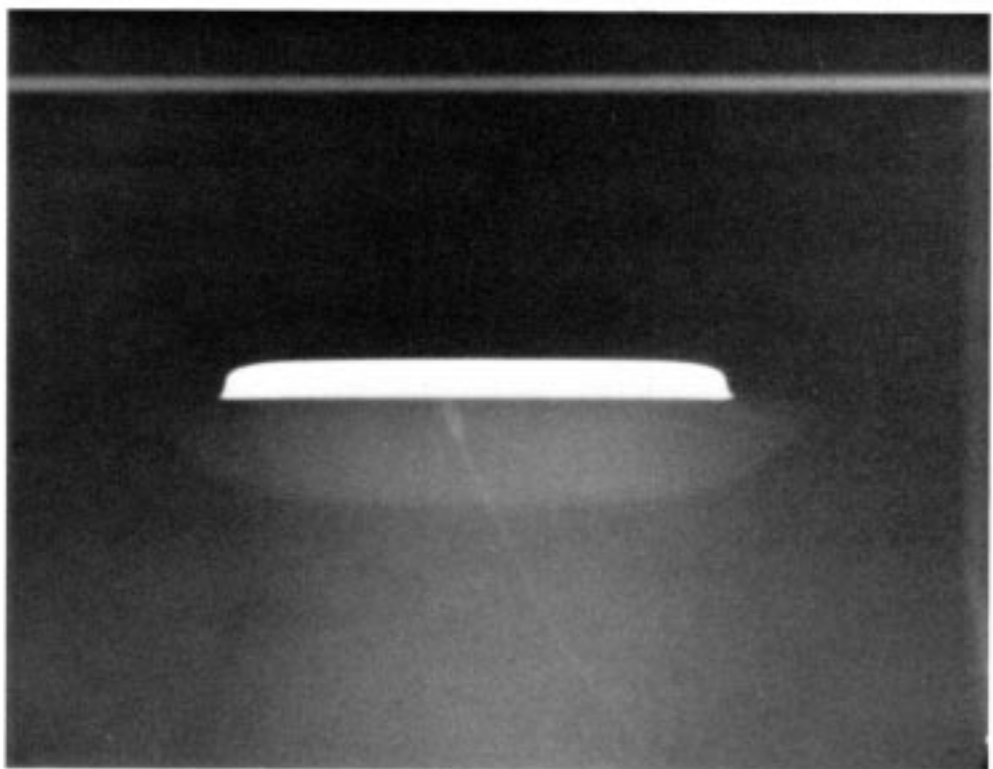
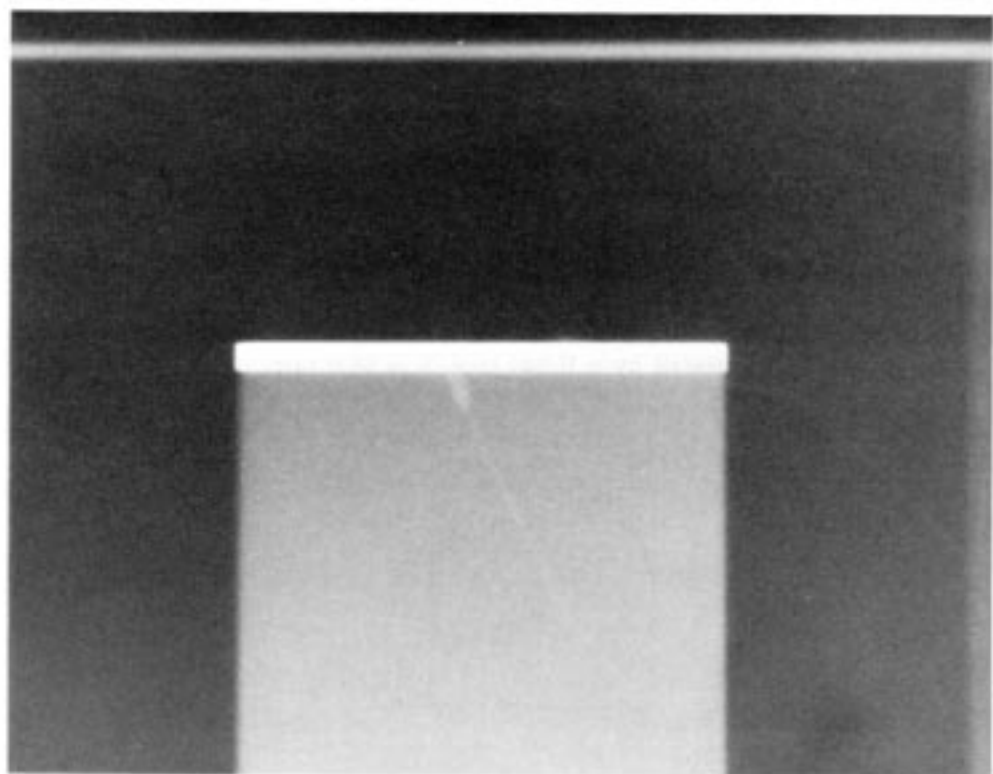
Experimenter: Douglas Venable

Radiographic Time: 30.55 μ s

Reference: Thurston and Mudd, 1968

Dynamic fracture of 6.0-mm-thick, t , uranium. The plate is shocked by 101.6 mm of Composition B-3 initiated by a P-040 lens. h is 9.5 mm.





SHOT 172:

Dynamic Fracture of Thorium

Date:

February 2, 1965

Experimenter:

Douglas Venable

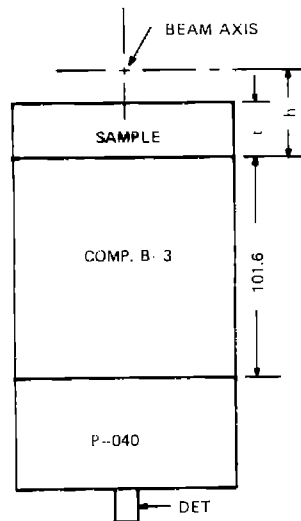
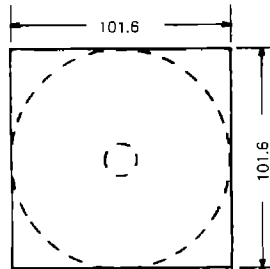
Radiographic Time:

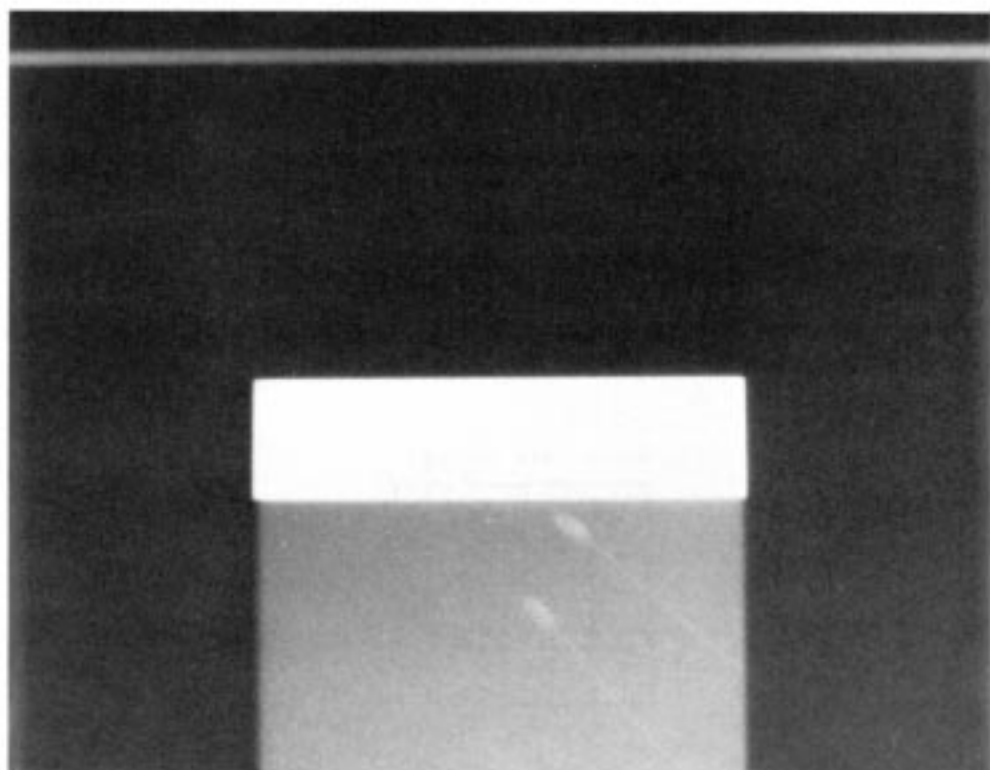
37.41 μ s

Reference:

Thurston and Mudd, 1968

Dynamic fracture of 25.0-mm-thick, t , thorium. The plate is shocked by 101.6 mm of Composition B-3 initiated by a P-040 lens. h is 34.9 mm.





SHOT 173:

Dynamic Fracture of Thorium

Date:

January 12, 1966

Experimenter:

Benny Ray Breed

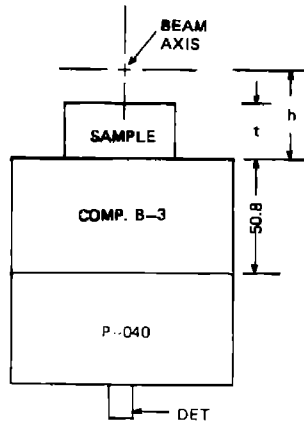
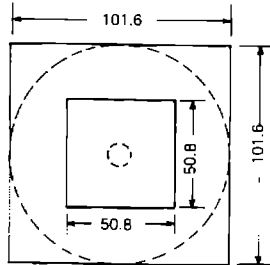
Radiographic Time:

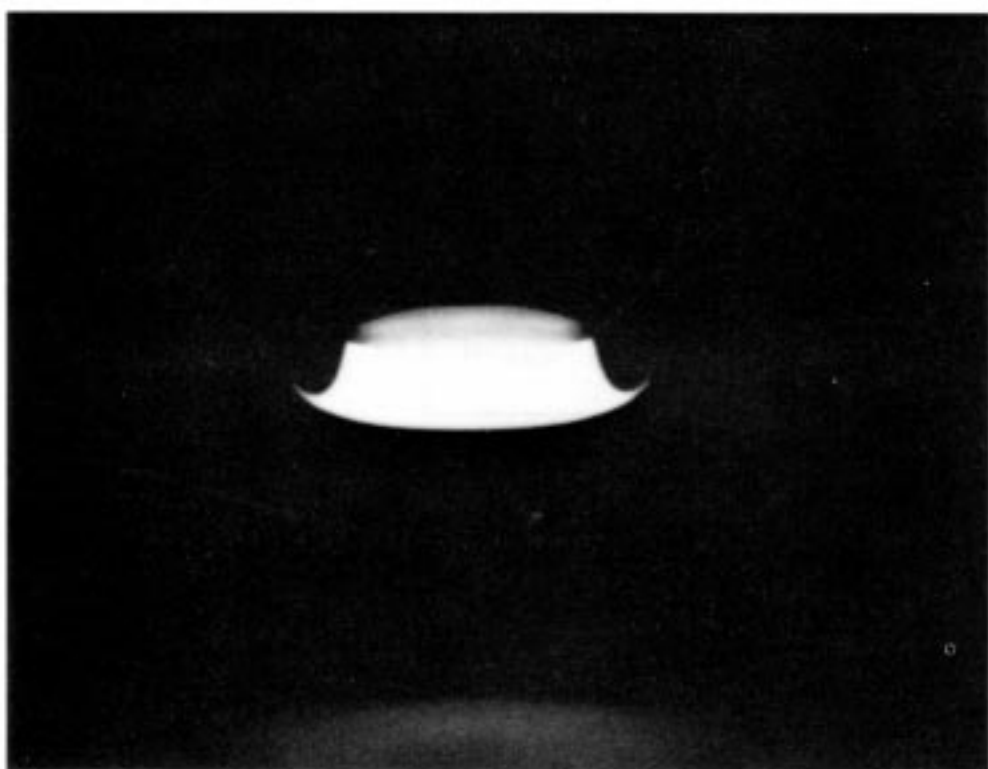
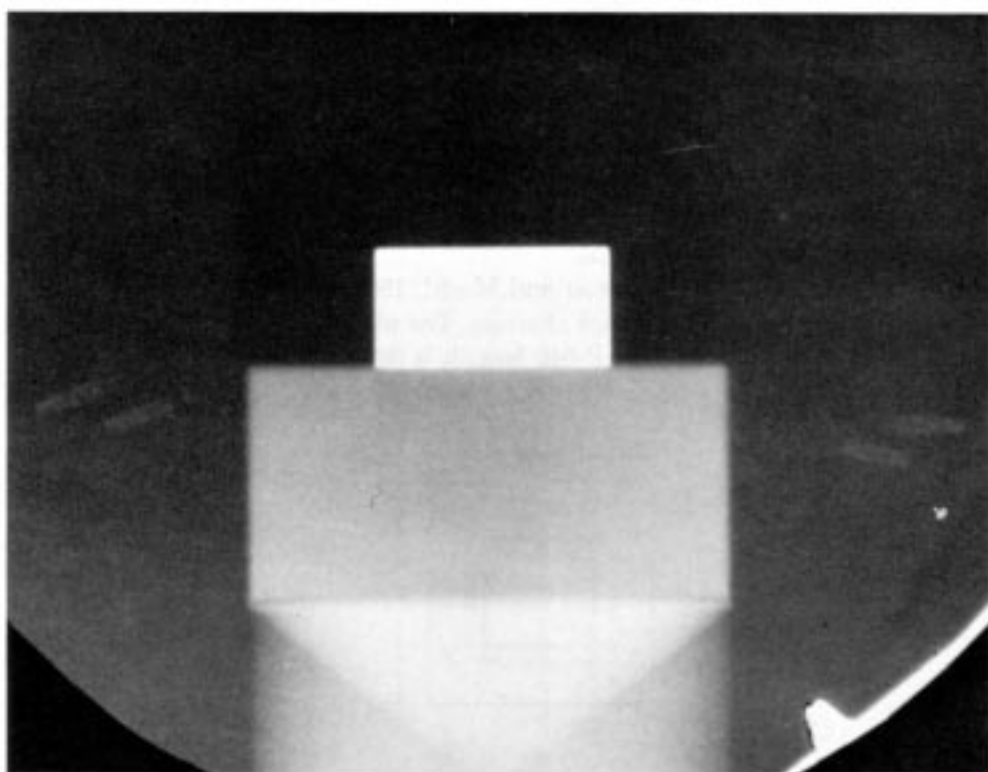
32.89 μ s

Reference:

Thurston and Mudd, 1968

Dynamic fracture of 25.0-mm-thick, t , thorium. The plate is shocked by 50.8 mm of Composition B initiated by a P-040 lens. h is 38.1 mm.





SHOT 174:

Dynamic Fracture of Thorium

Date:

January 12, 1966

Experimenter:

Benny Ray Breed

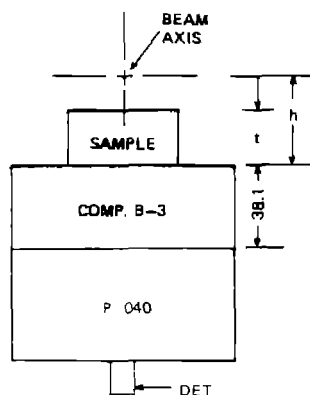
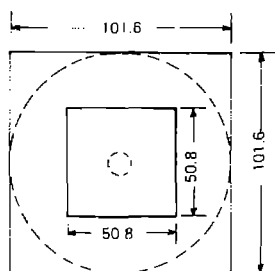
Radiographic Time:

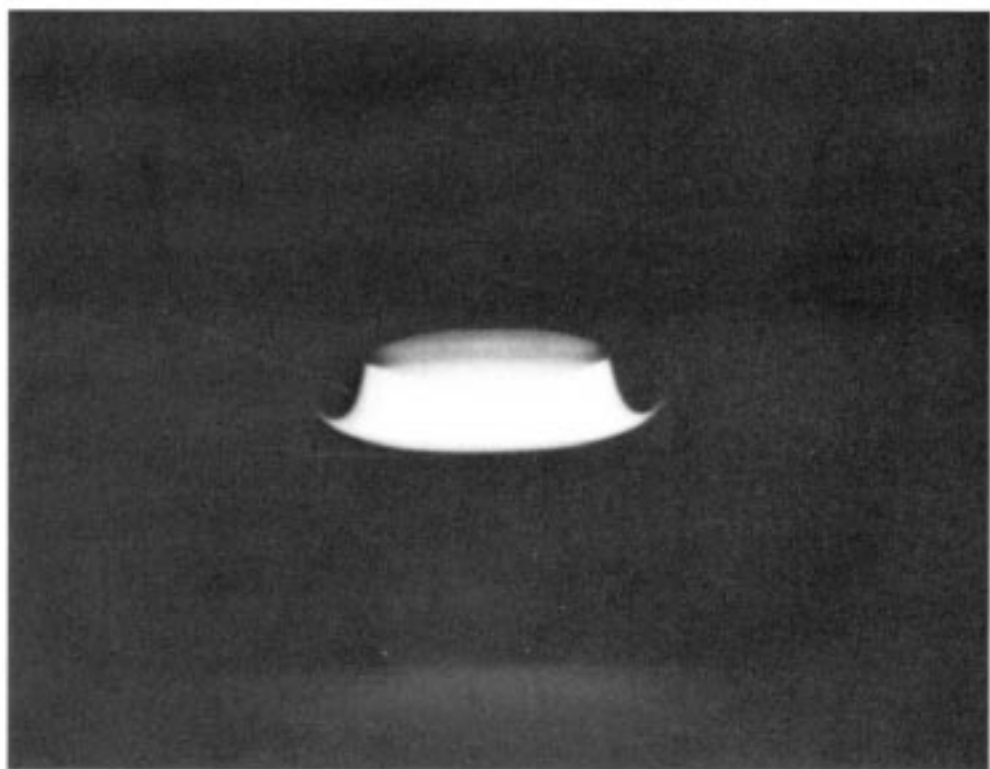
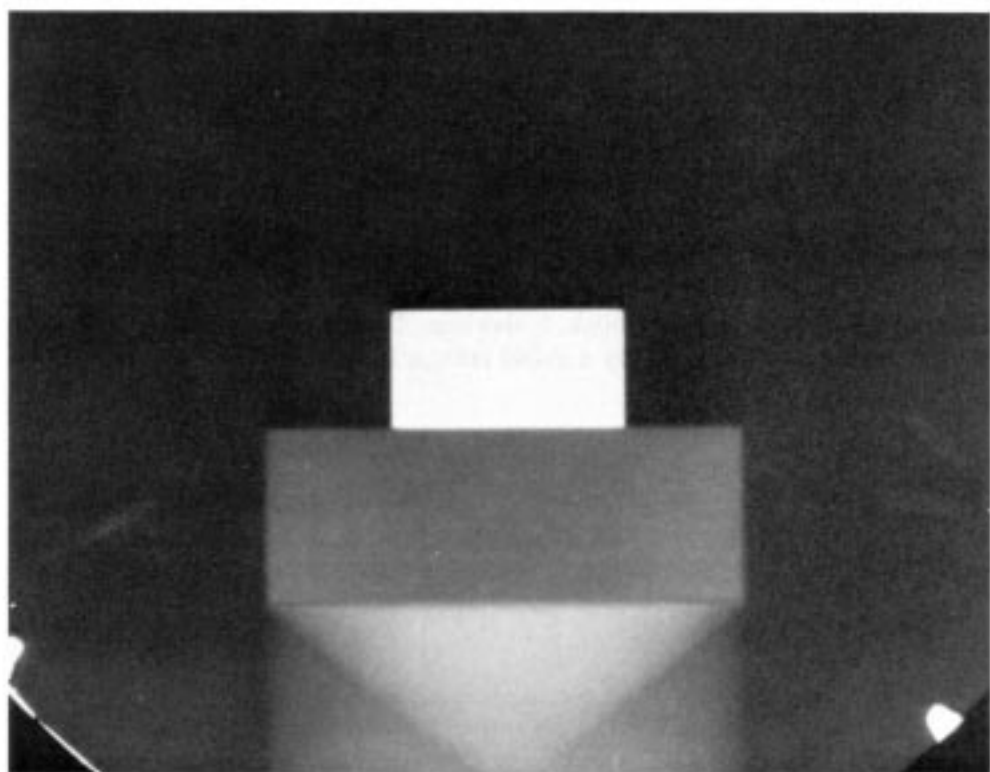
31.33 μ s

Reference:

Thurston and Mudd, 1968

Dynamic fracture of 25.0-mm-thick thorium. The plate is shocked by 38.1 mm, t, of Composition B-3 initiated by a P-040 lens. h is 38.1 mm.





SHOT 175: Dynamic Fracture of Thorium

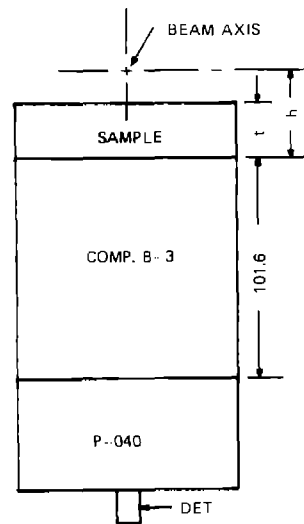
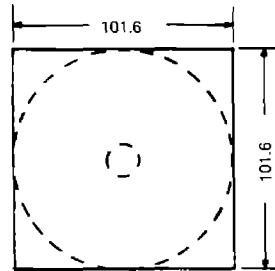
Date: February 2, 1965

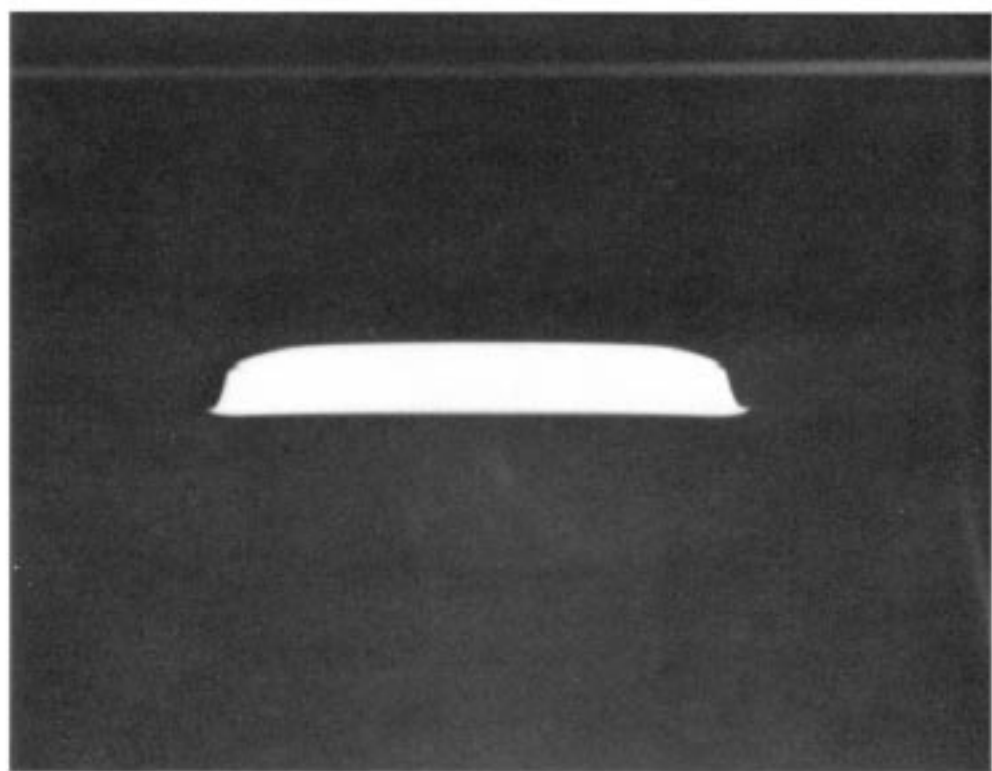
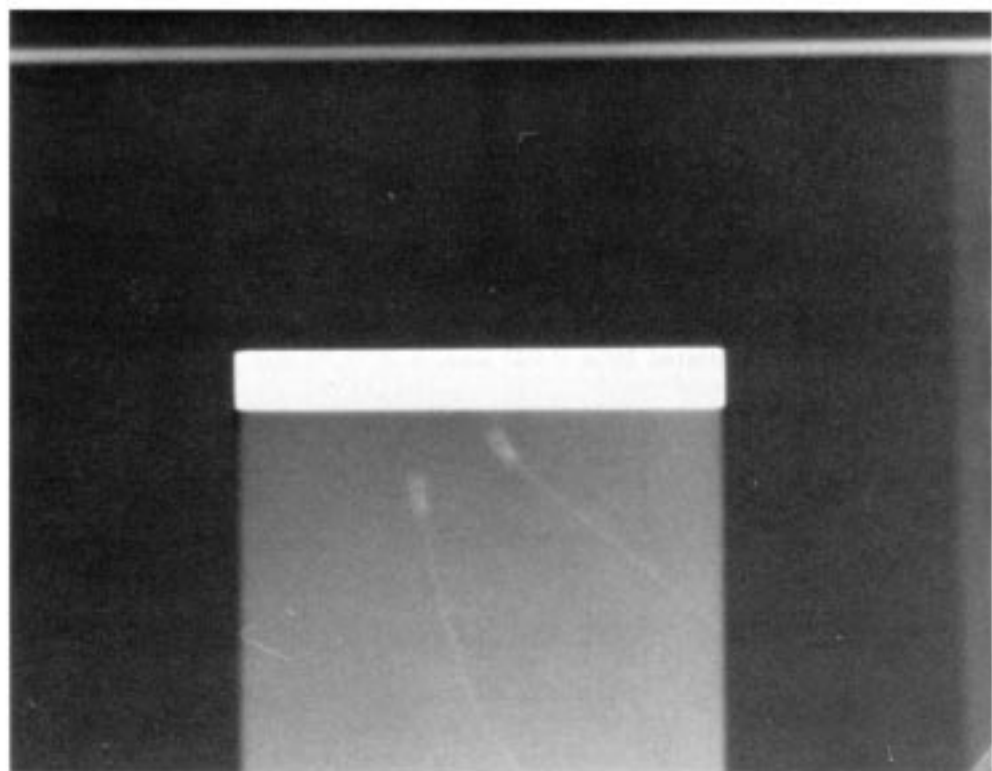
Experimenter: Douglas Venable

Radiographic Time: 32.76 μ s

Reference: Thurston and Mudd, 1968

Dynamic fracture of 12.0-mm-thick, t, thorium. The plate is shocked by 101.6 mm of Composition B-3 initiated by a P-040 lens. h is 19.1 mm.





SHOT 176:

Dynamic Fracture of Thorium

Date:

April 13, 1966

Experimenter:

Benny Ray Breed

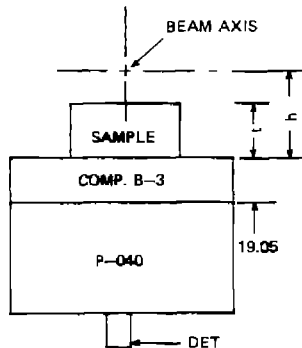
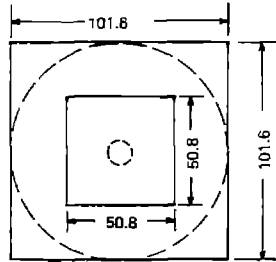
Radiographic Time:

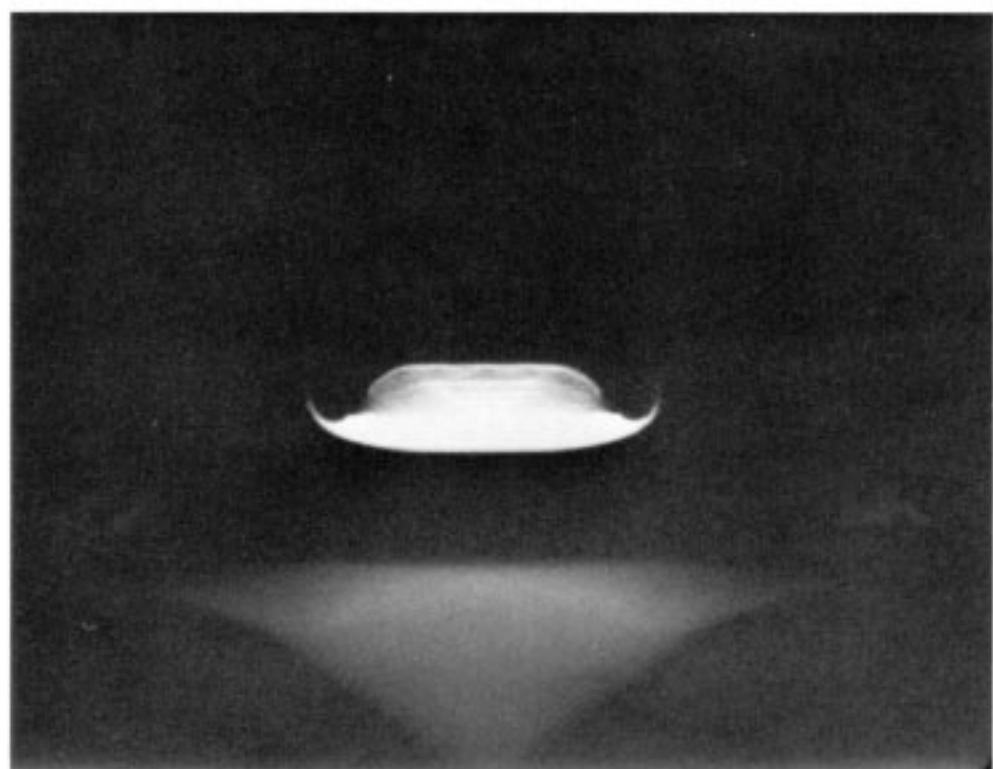
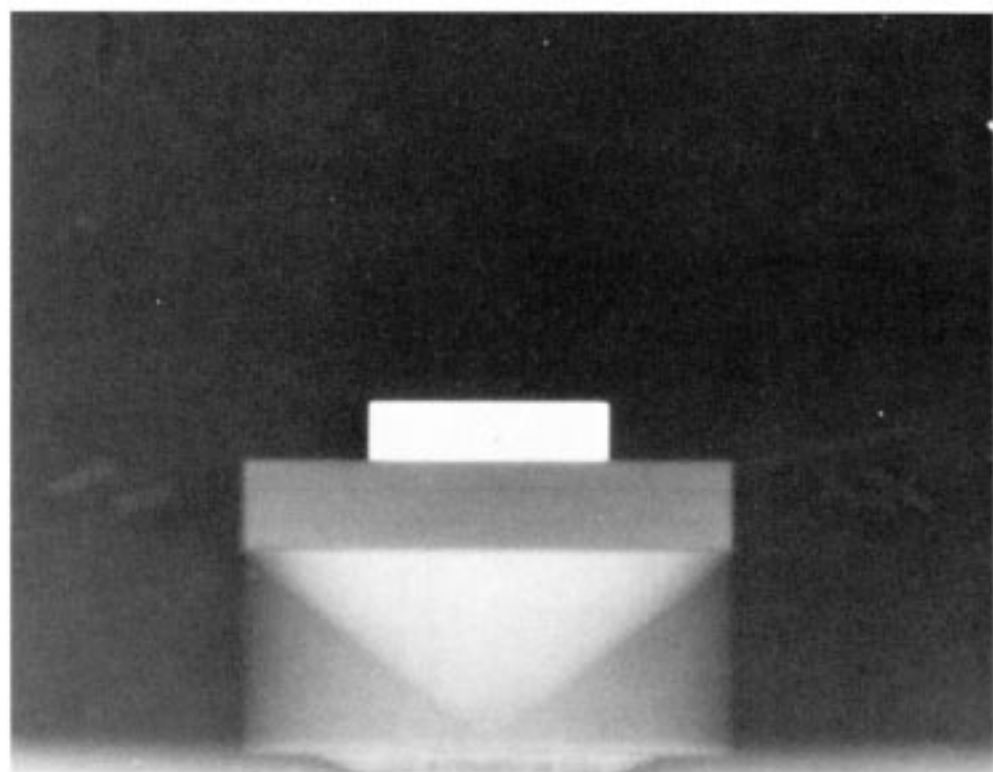
29.27 μ s

Reference:

Thurston and Mudd, 1968

Dynamic fracture of 12.0-mm-thick, t , thorium. The plate is shocked by 19.05 mm of Composition B-3 initiated by a P-040 lens. h is 31.75 mm.





SHOT 177:

Dynamic Fracture of Nickel

Date:

April 20, 1966

Experimenter:

Benny Ray Breed

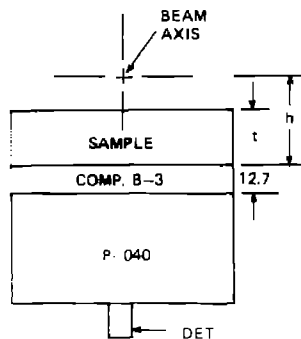
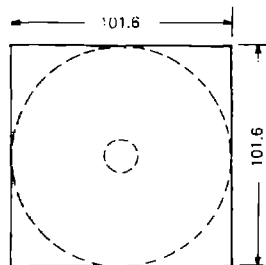
Radiographic Time:

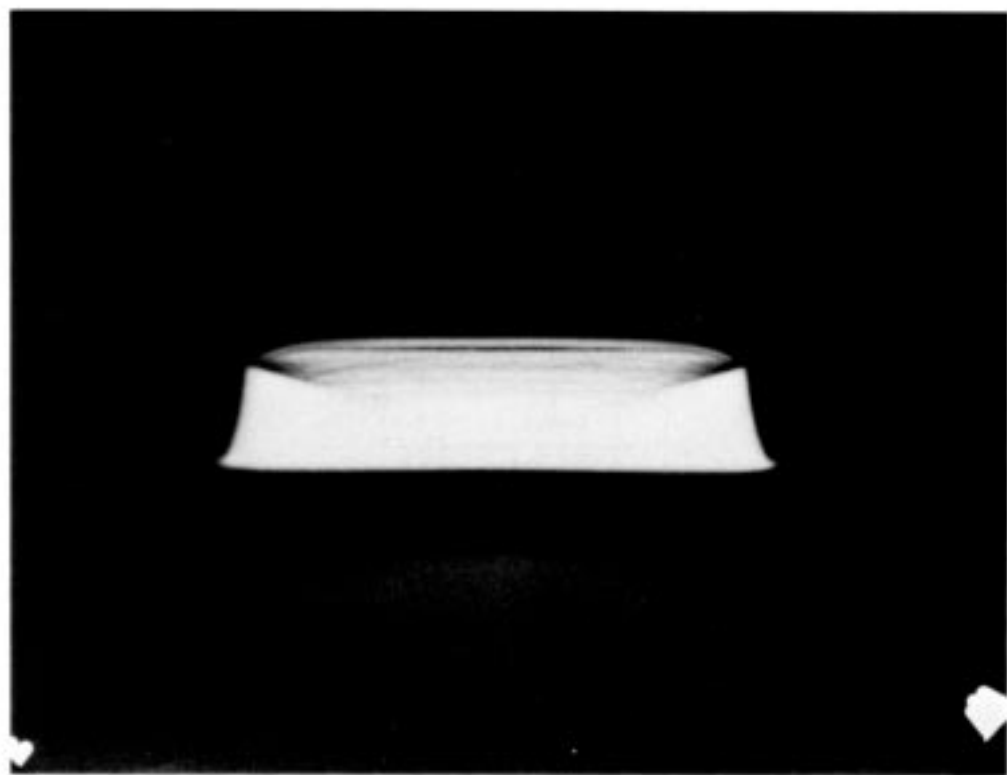
27.28 μ s

References:

Breed et al., 1967; Thurston and Mudd, 1968

Dynamic fracture of 25.0-mm-thick, t , nickel. The plate is shocked by 12.7 mm of Composition B-3 initiated by a P-040 lens. h is 41.3 mm.





SHOT 178:

Dynamic Fracture of Nickel

Date:

April 26, 1966

Experimenter:

Benny Ray Breed

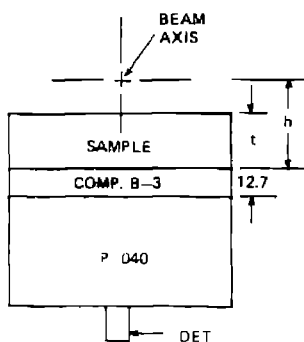
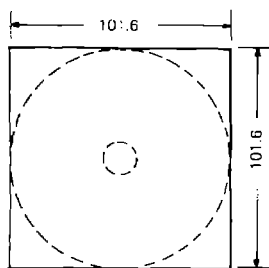
Radiographic Time:

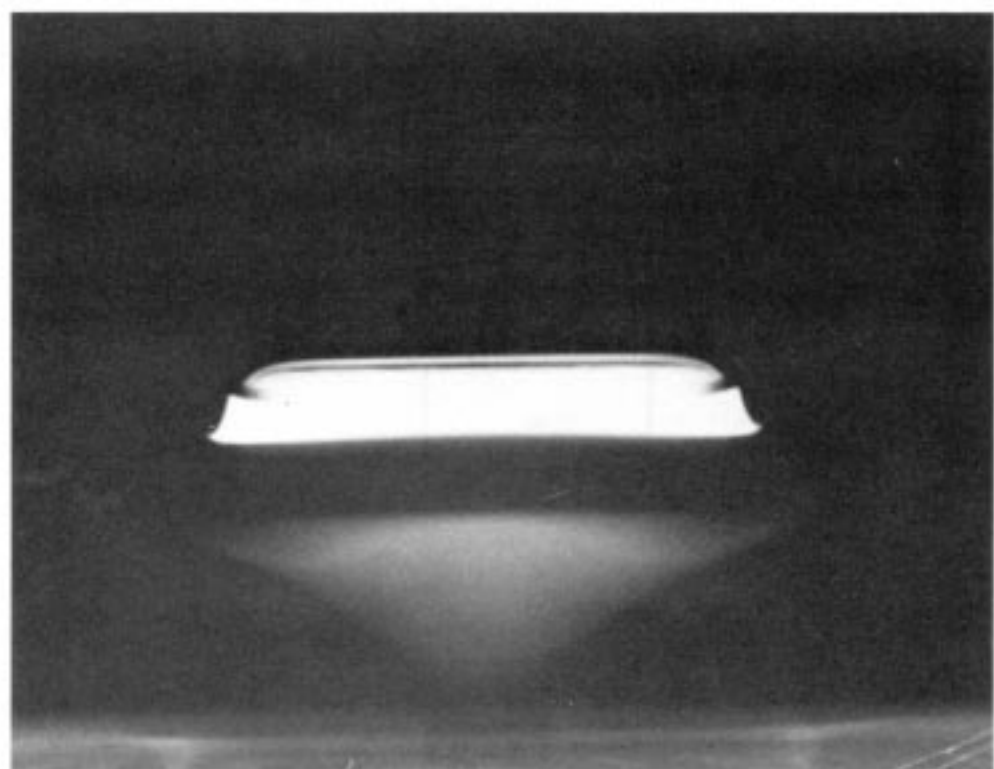
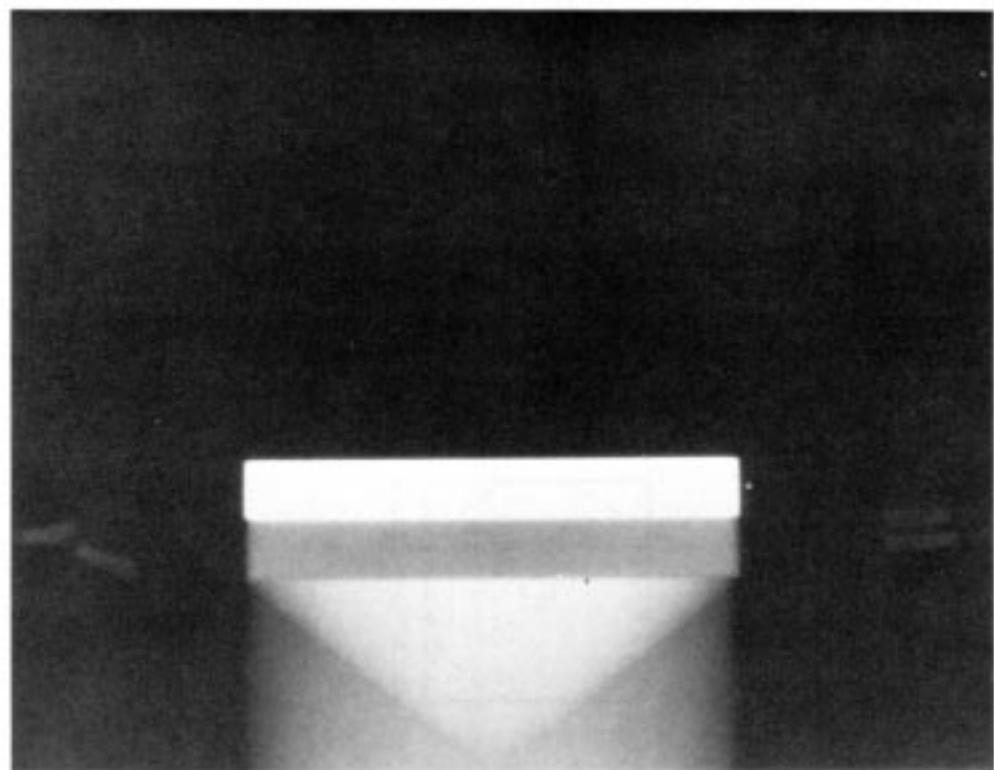
25.16 μ s

References:

Breed et al., 1967; Thurston and Mudd, 1968

Dynamic fracture of 12.0-mm-thick, *t*, nickel. The plate is shocked by 12.7 mm of Composition B-3 initiated by a P-040 lens. *h* is 28.57 mm.





SHOT 179:

Dynamic Fracture of Thorium

Date:

February 2, 1965

Experimenter:

Douglas Venable

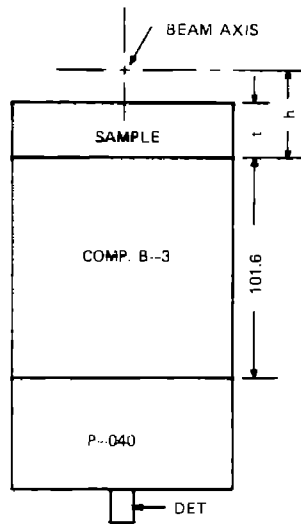
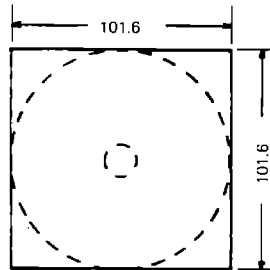
Radiographic Time:

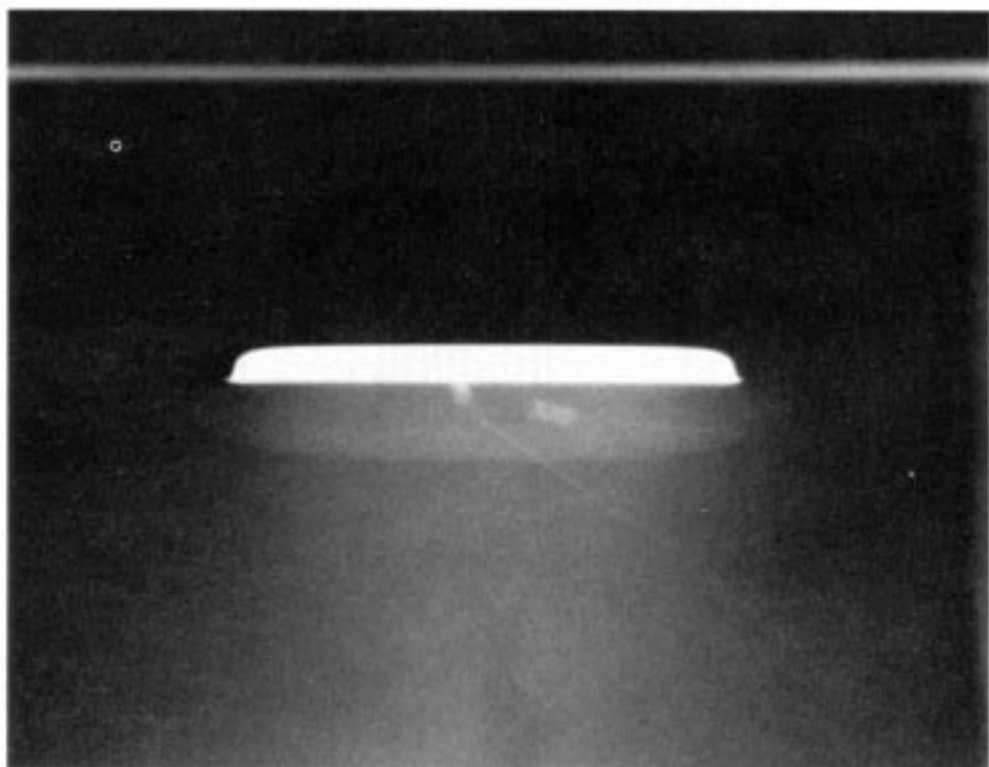
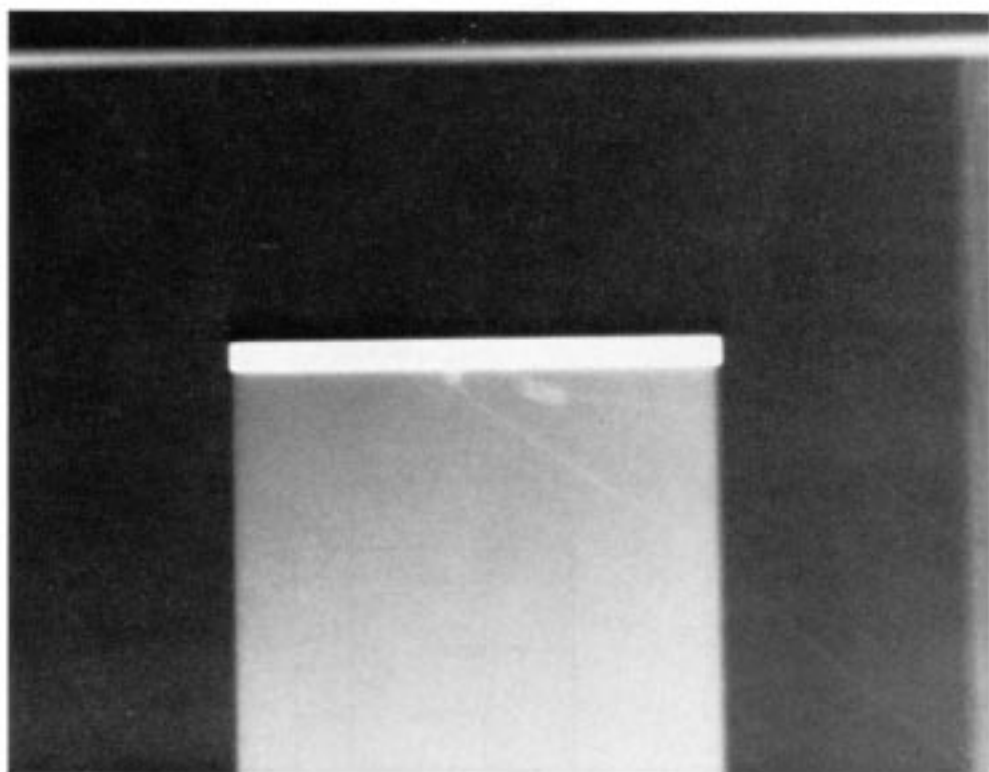
29.56 μ s

References:

Breed et al., 1967; Thurston and Mudd, 1968

Dynamic fracture of 6.0-mm-thick, t, thorium. The plate is shocked by 101.6 mm of Composition B-3 initiated by a P-040 lens. h is 9.5 mm.





SHOT 180:

Uranium Jets

Date:

April 13, 1966

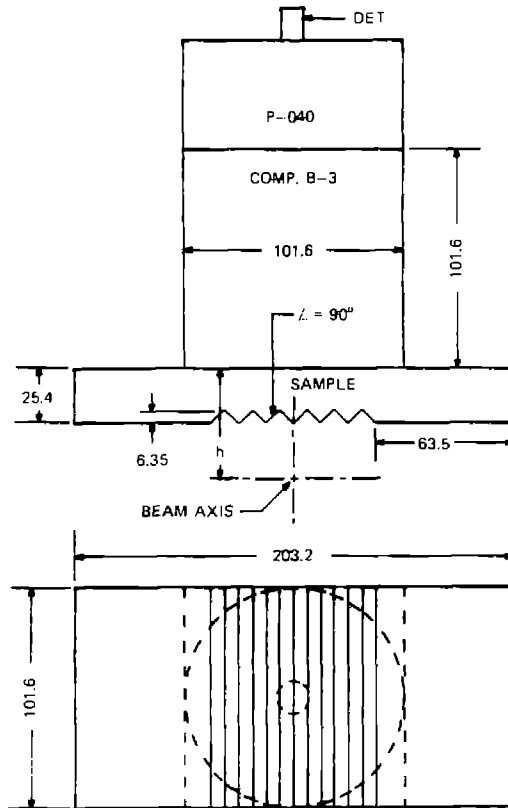
Experimenter:

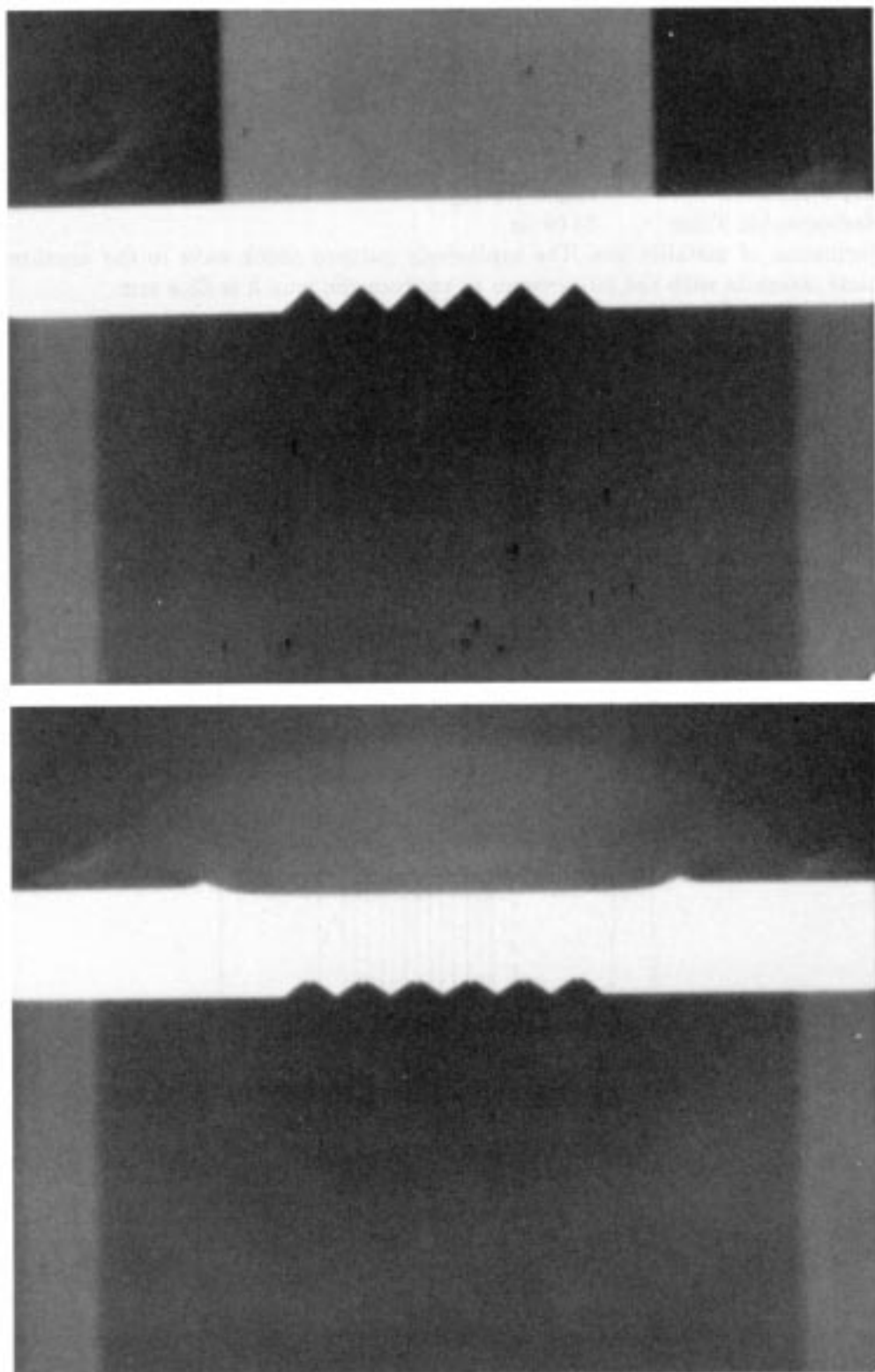
Roger W. Taylor

Radiographic Time:

33.51 μ s

Formation of metallic jets. The explosively induced shock wave in the uranium plate interacts with the 90° grooves to produce the jets. h is 25.4 mm.





SHOT 181:

Uranium Jets

Date:

May 11, 1966

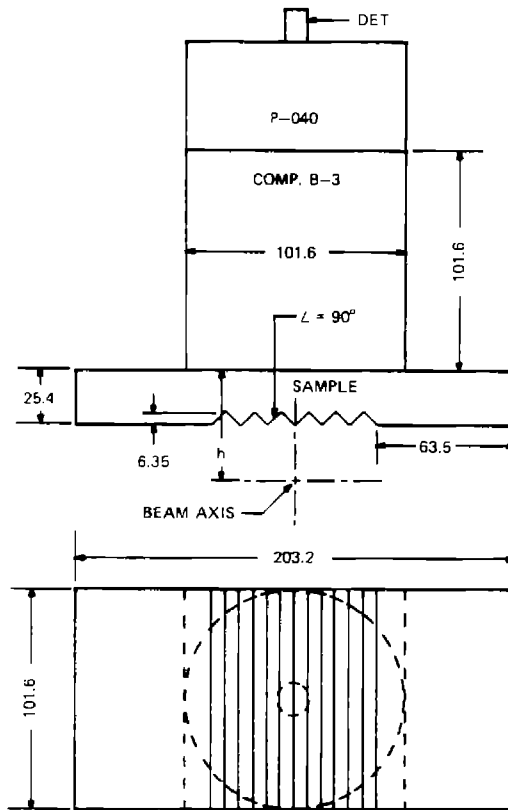
Experimenter:

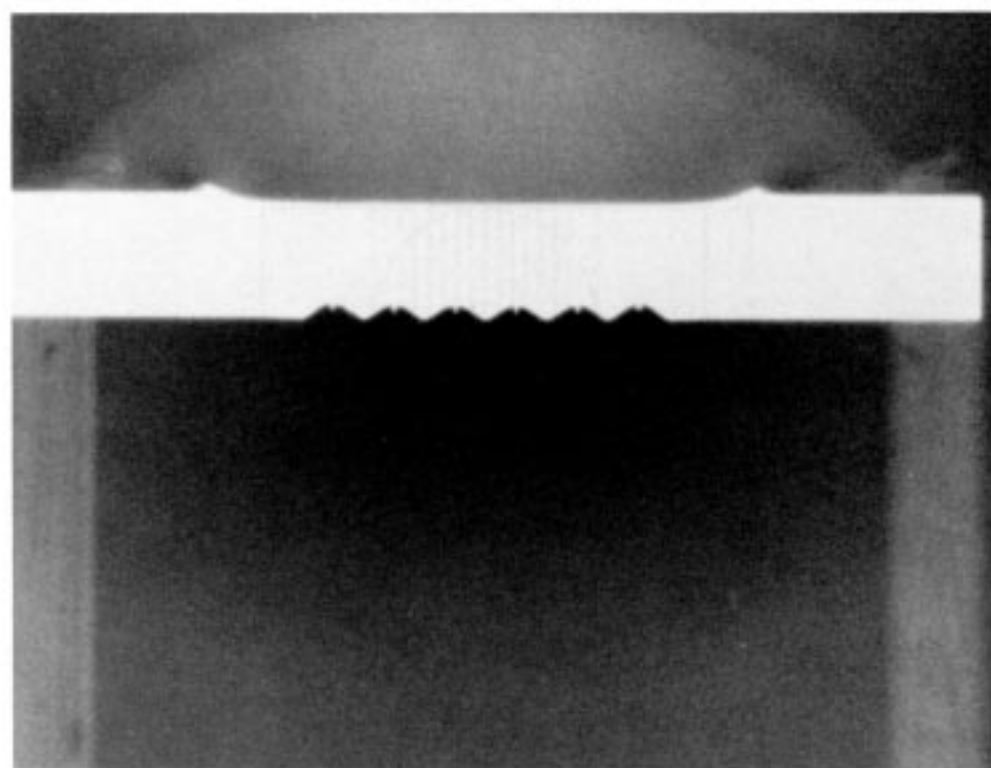
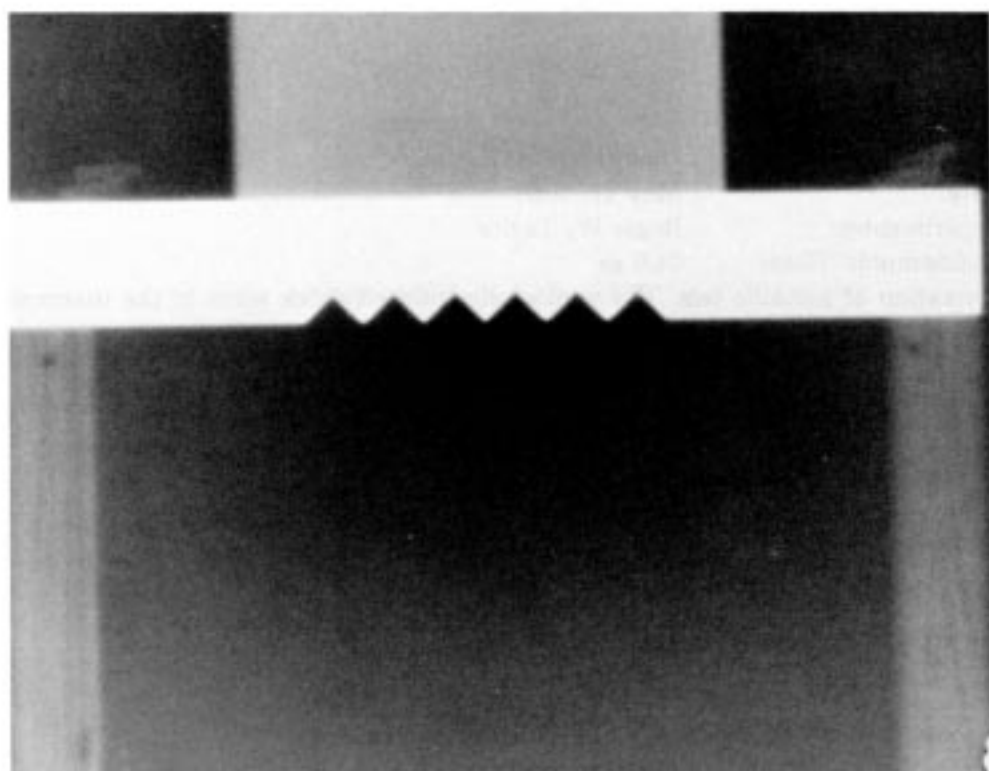
Roger W. Taylor

Radiographic Time:

34.09 μ s

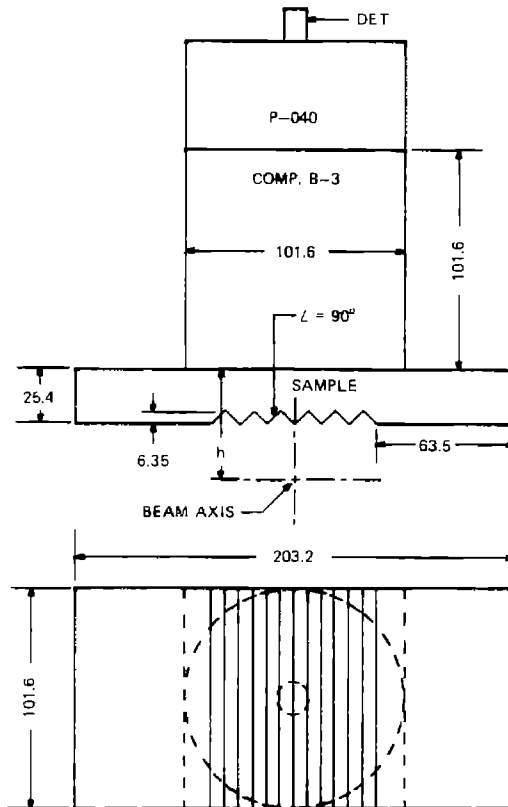
Formation of metallic jets. The explosively induced shock wave in the uranium plate interacts with the 90° grooves to produce the jets. h is 25.4 mm.

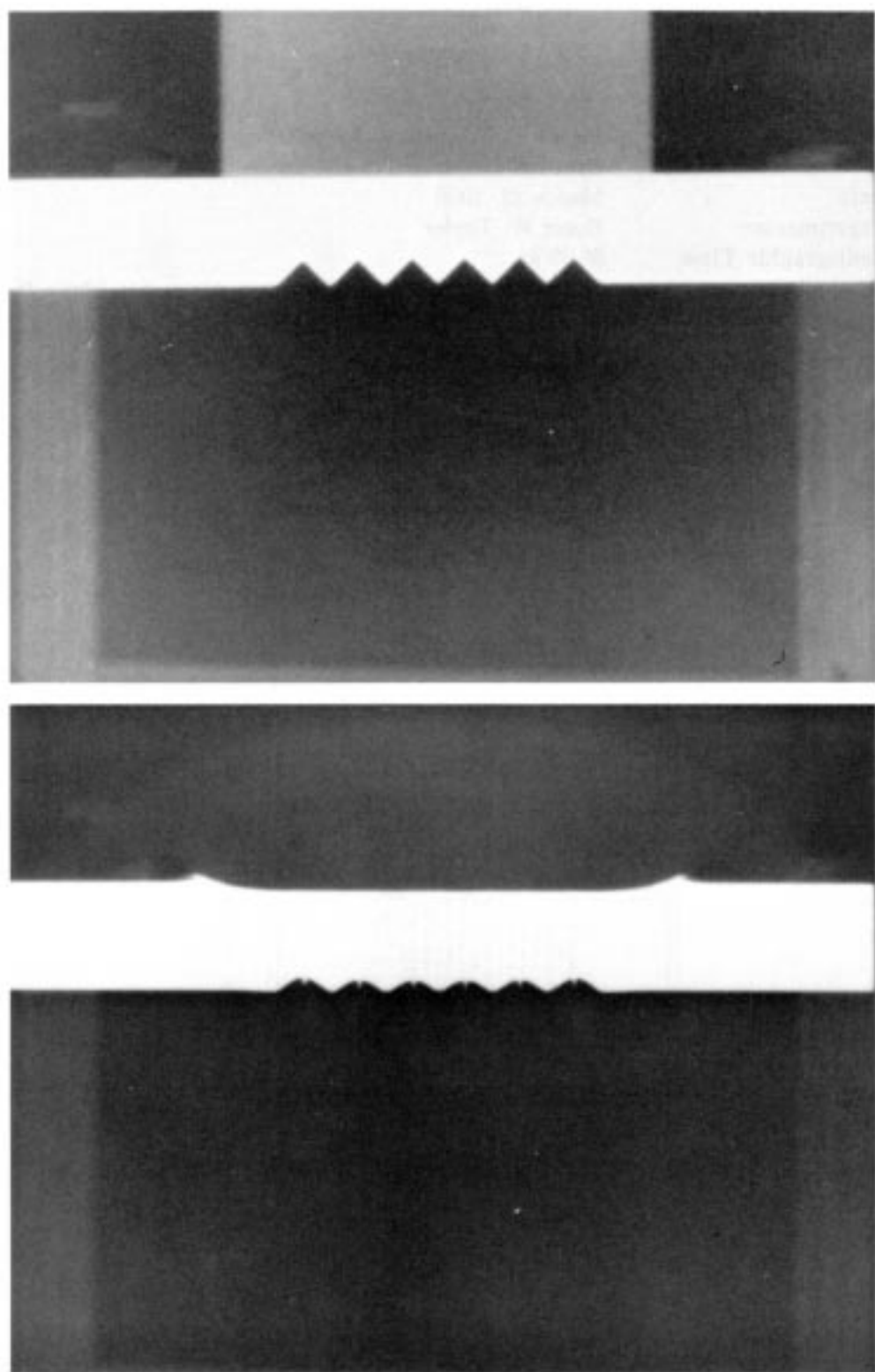




SHOT 182: **Uranium Jets**
Date: **May 11, 1966**
Experimenter: **Roger W. Taylor**
Radiographic Time: **34.5 μ s**

Formation of metallic jets. The explosively induced shock wave in the uranium plate interacts with the 90° grooves to produce the jets. h is 25.4 mm.





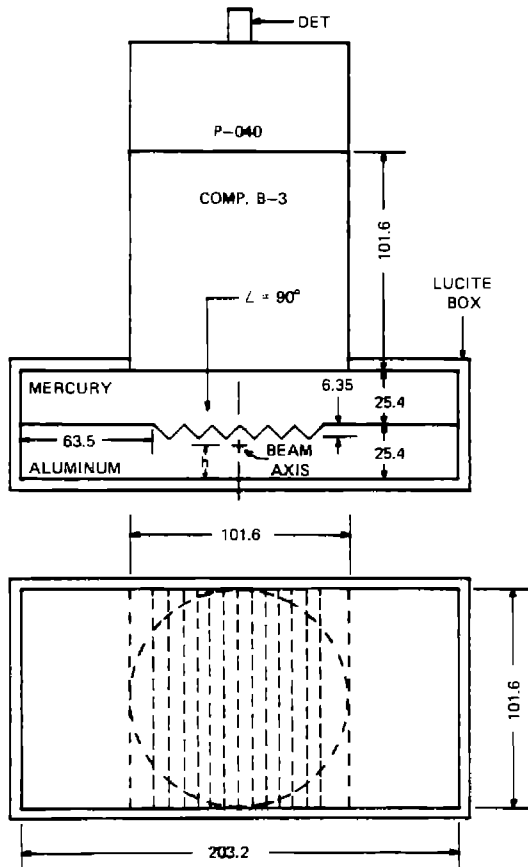
SHOT 184: Shocked Mercury Interacting with Aluminum Grooves

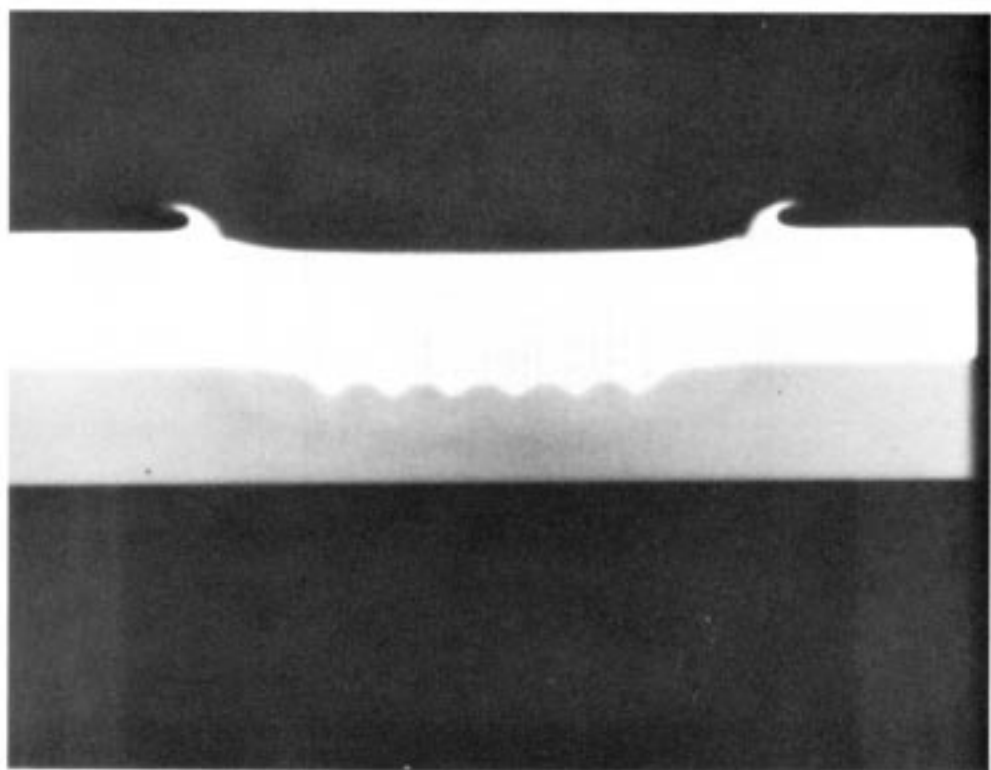
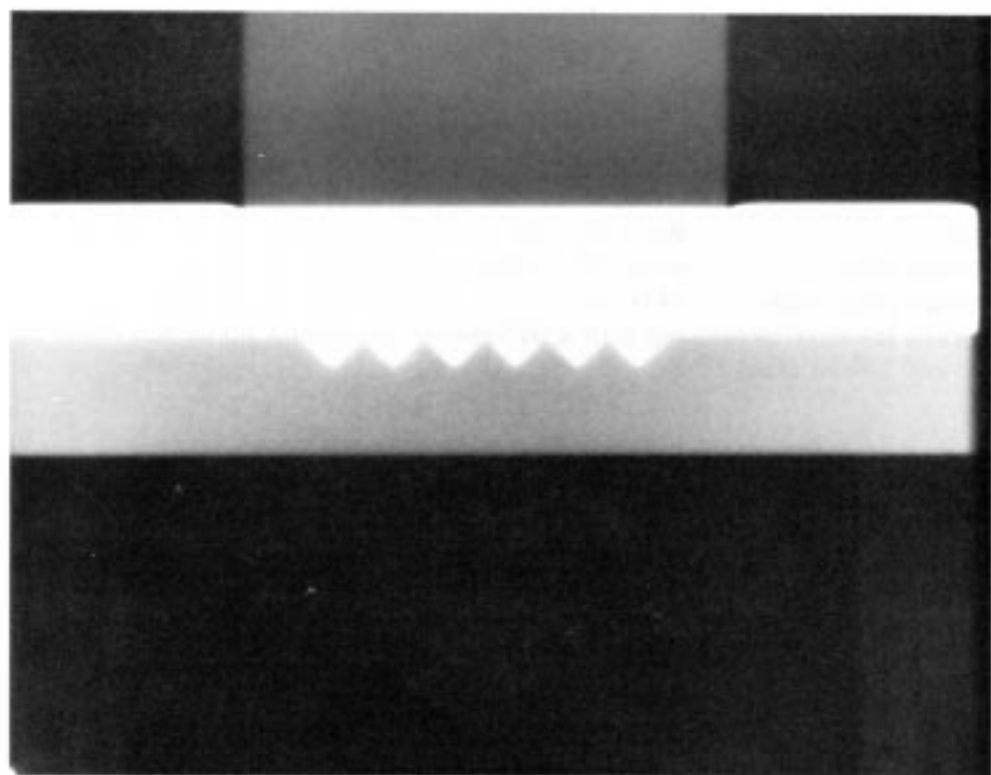
Date: March 22, 1966

Experimenter: Roger W. Taylor

Radiographic Time: 36.99 μ s

Shocked mercury interacting with a 90°-grooved aluminum plate. See Shots 26, 185, and 186 for other times.





SHOT 185:

Shocked Mercury Interacting with Aluminum Grooves

Date:

April 27, 1966

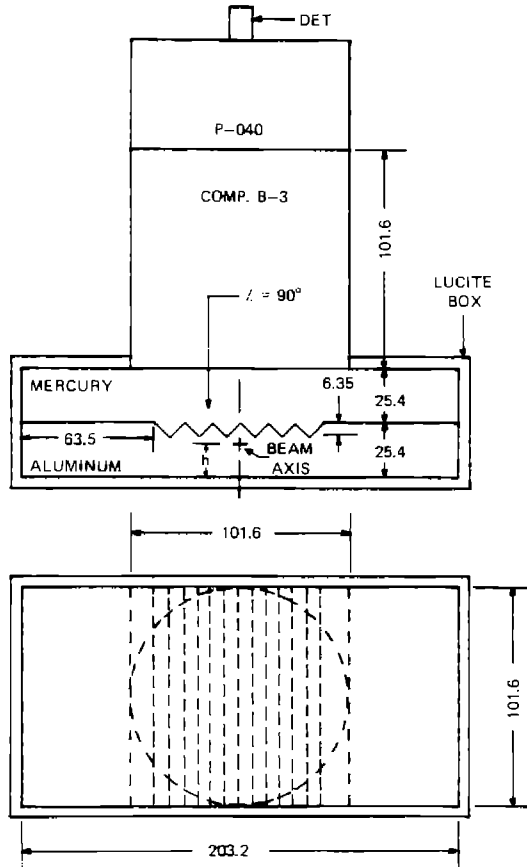
Experimenter:

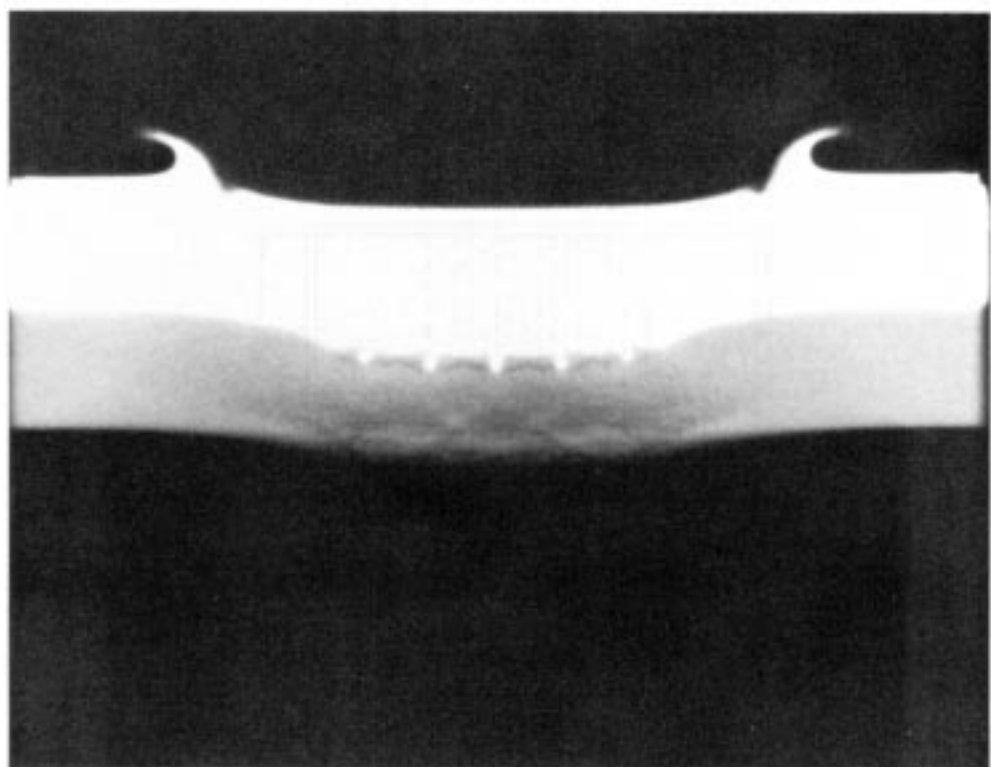
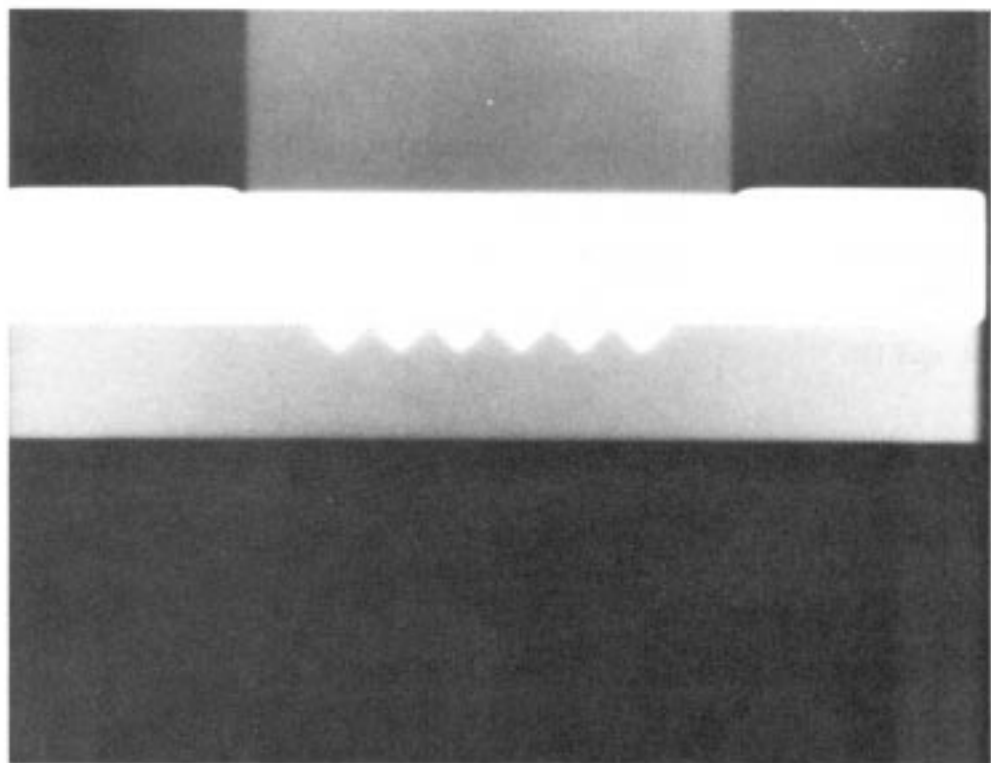
Roger W. Taylor

Radiographic Time:

44.06 μ s

Shocked mercury interacting with a 90°-grooved aluminum plate. See Shots 26, 184, and 186 for other times.





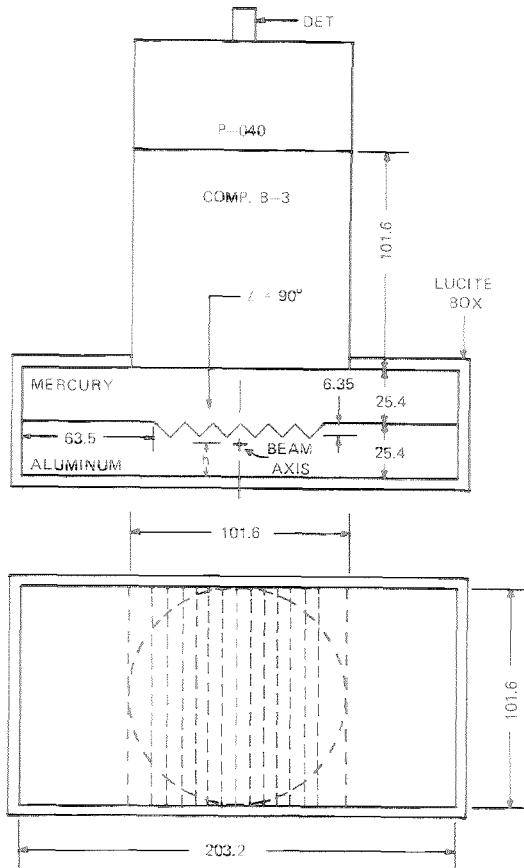
SHOT 186: Shocked Mercury Interacting with Aluminum Grooves

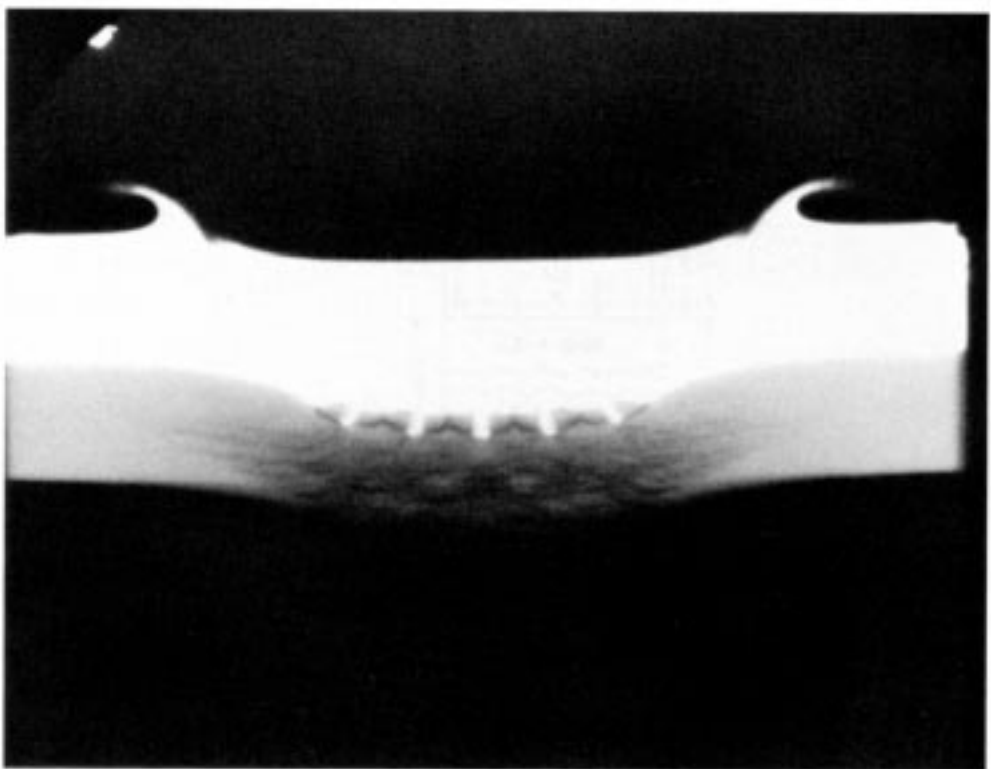
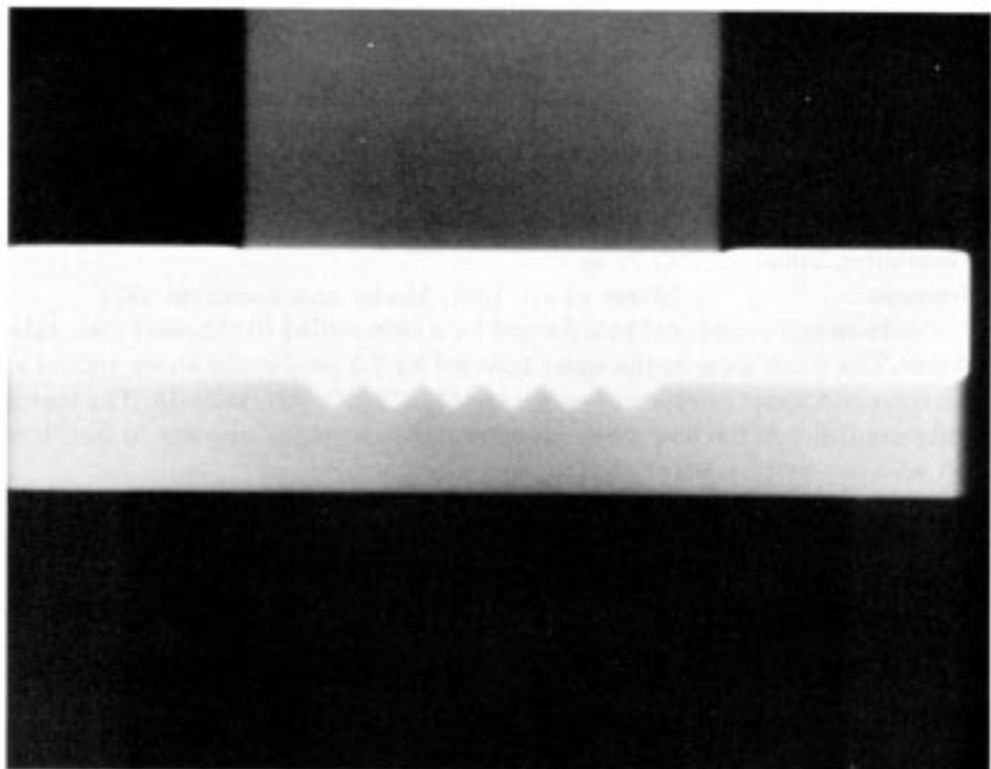
Date: May 18, 1966

Experimenter: Roger W. Taylor

Radiographic Time: 47.57 μ s

Shocked mercury interacting with a 90°-grooved aluminum plate. See Shots 26, 184, and 185





SHOT 187: Cylindrical Hole in Water

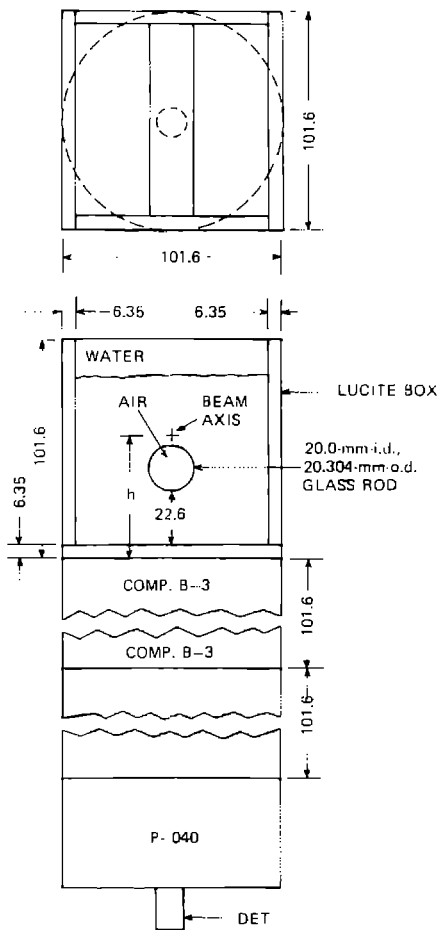
Date: August 19, 1965

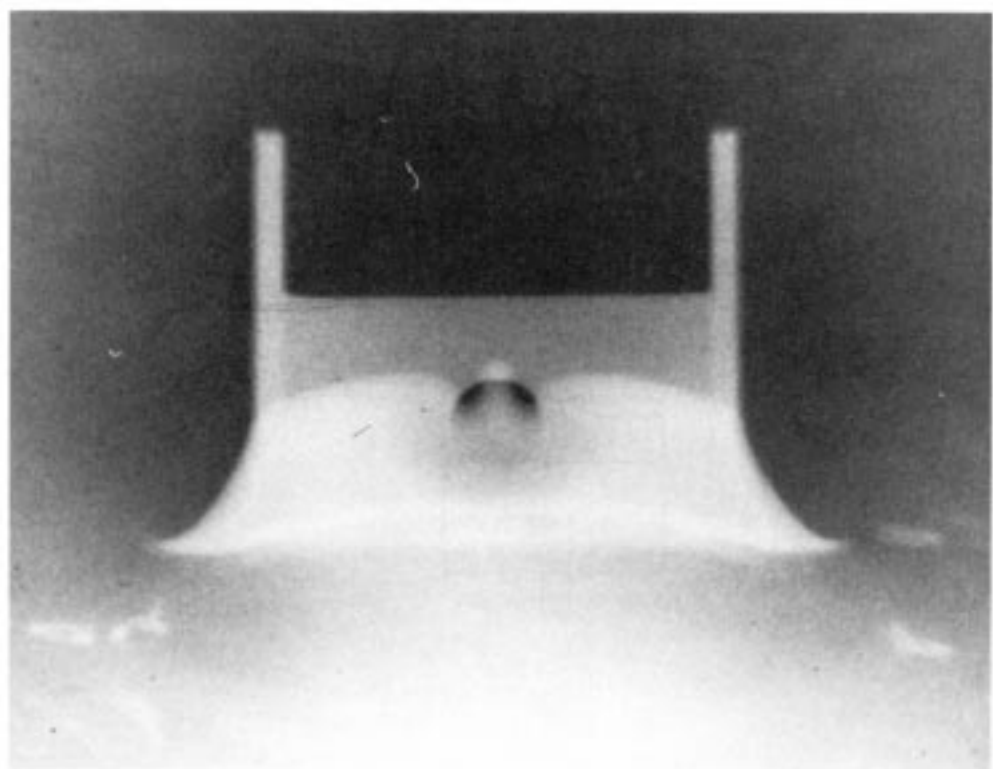
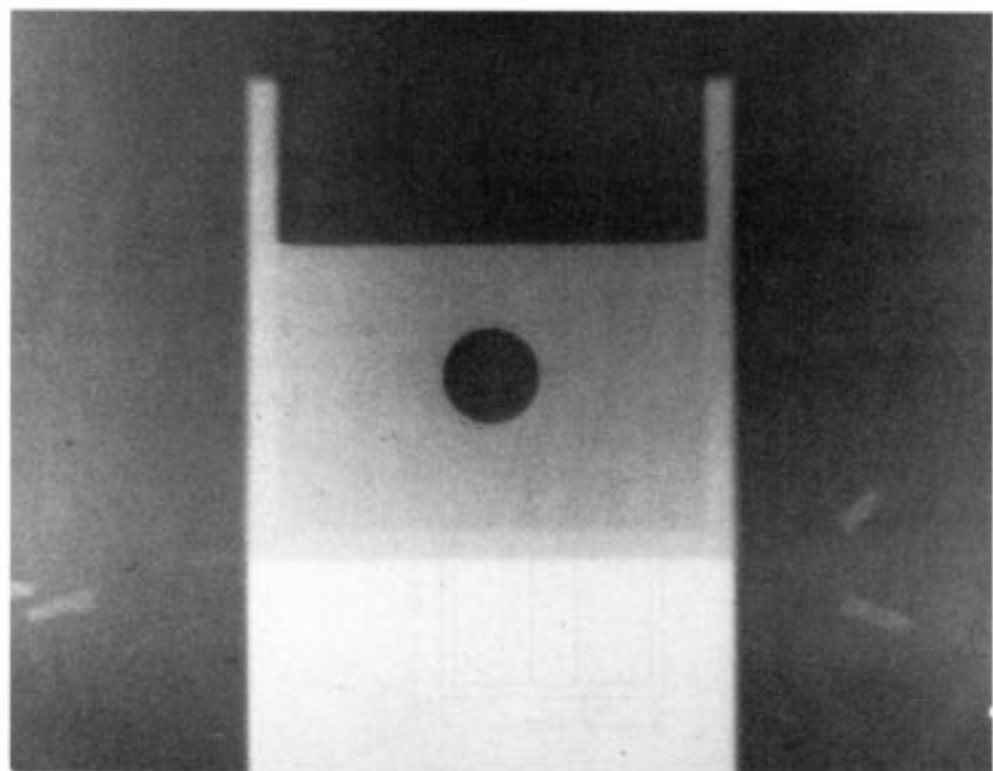
Experimenter: Roger W. Taylor

Radiographic Time: 47.72 μ s

References: Mader et al., 1967; Mader and Kershner, 1972

A 10.0-mm-radius cylindrical hole formed by a thin-walled (0.152-mm) glass tube in water. The shock wave in the water traveled for 7.5 μ s after the shock arrived at the Lucite and water interface. See Shots 188, 278-280, 300, and 318. The strong density gradients in the hole make its outer rim look empty whereas, in fact, it is filled with low-density water. h is 30.16 mm.





SHOT 188: Cylindrical Hole in Water

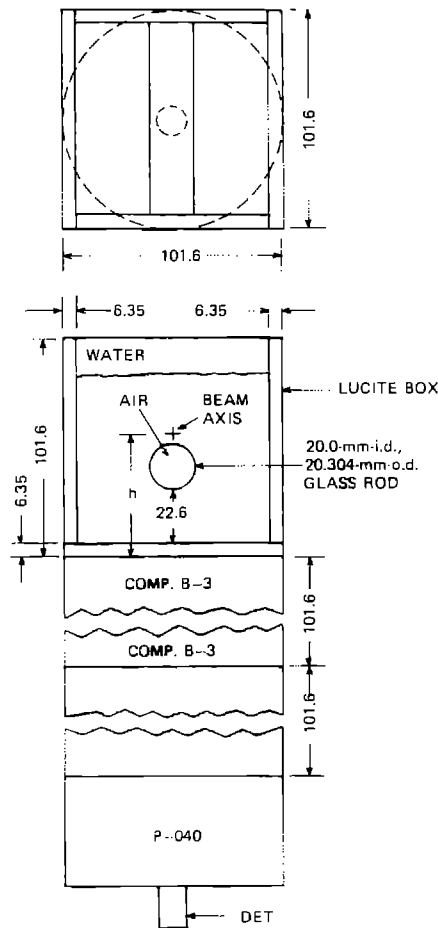
Date: August 19, 1965

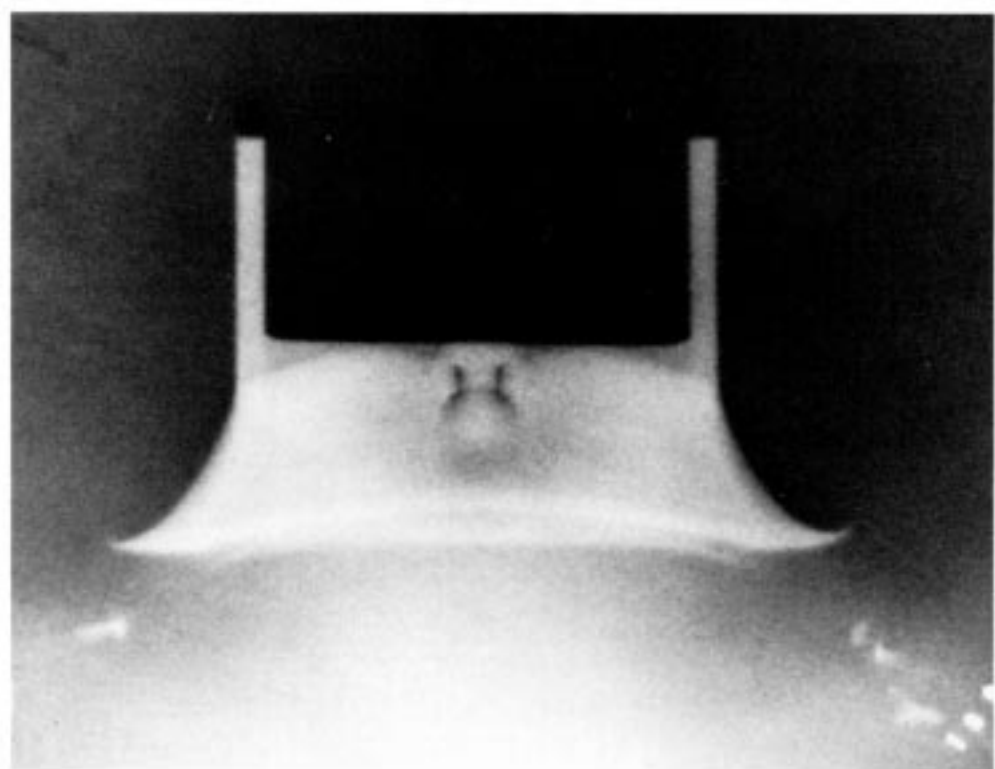
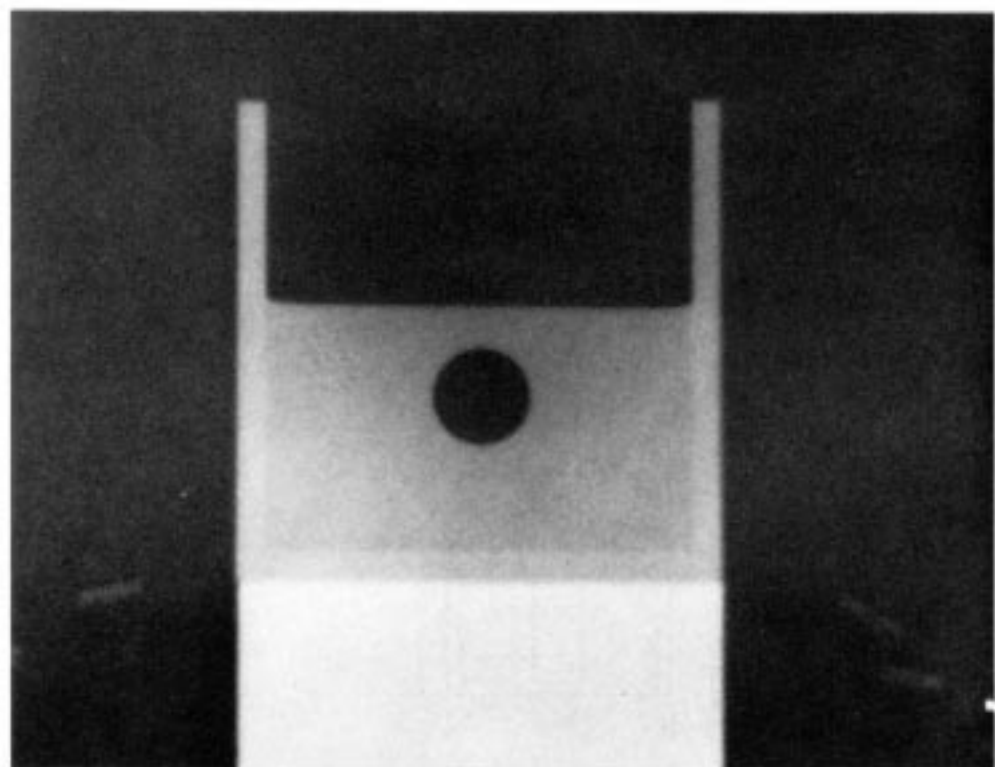
Experimenter: Roger W. Taylor

Radiographic Time: 49.20 μ s

References: Mader et al., 1967; Mader and Kirshner, 1972

A 10.0-mm-radius cylindrical hole formed by a thin-walled (0.152-mm) glass tube in water. The shock wave in the water traveled for 9.0 μ s after the shock arrived at the Lucite and water interface. See Shots 187, 278-280, 300, and 318. h is 53.97 mm.





SHOT 189:

Aluminum Rod in Water

Date:

September 13, 1965

Experimenter:

Roger W. Taylor

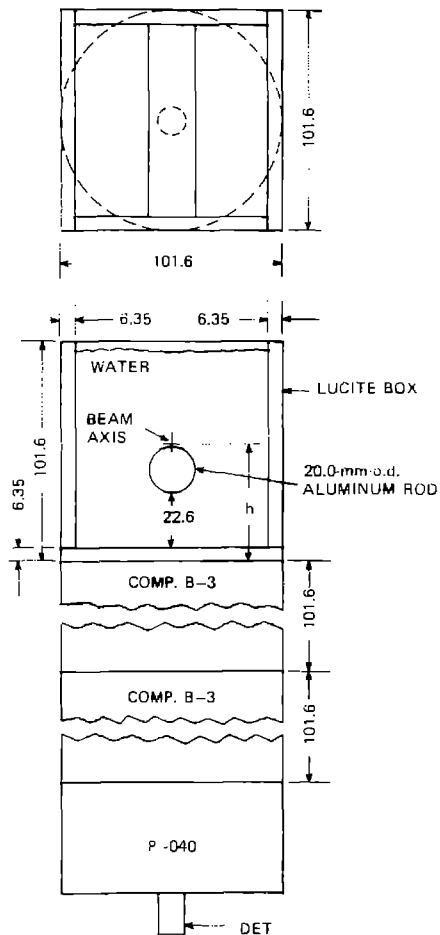
Radiographic Time:

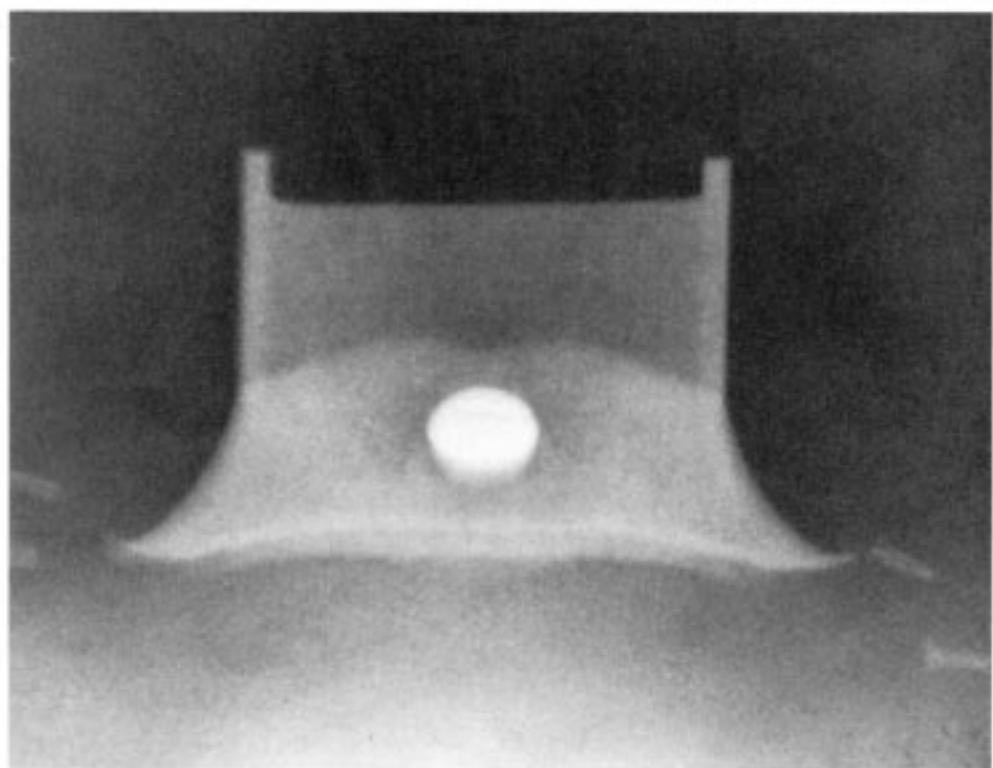
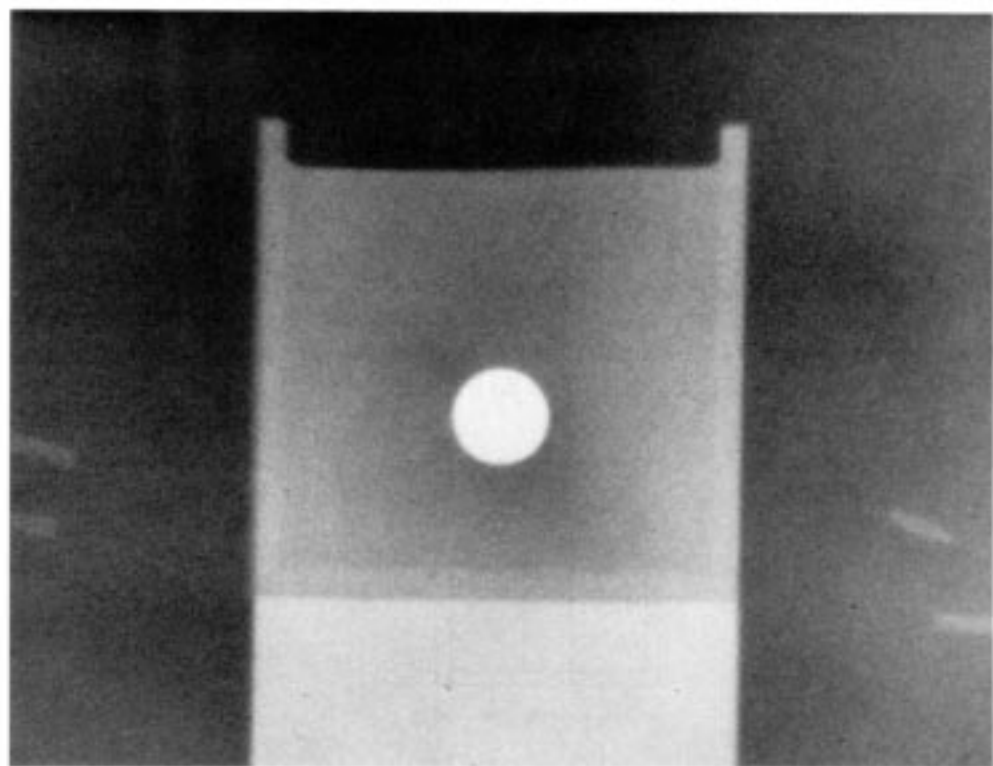
49.51 μ s

References:

Mader et al., 1967; Mader and Kershner, 1972

A shock wave in water interacts with a 10.0-mm-radius aluminum rod. The shock wave traveled 9.3 μ s after the shock arrived at the Lucite and water interface. See Shots 190, 269, 281, and 282. h is 46.03 mm.





SHOT 190: Aluminum Rod in Water

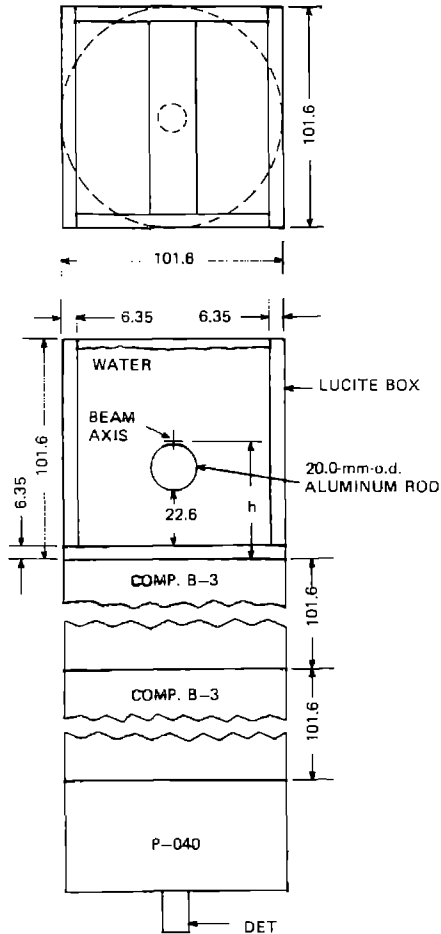
Date: August 25, 1965

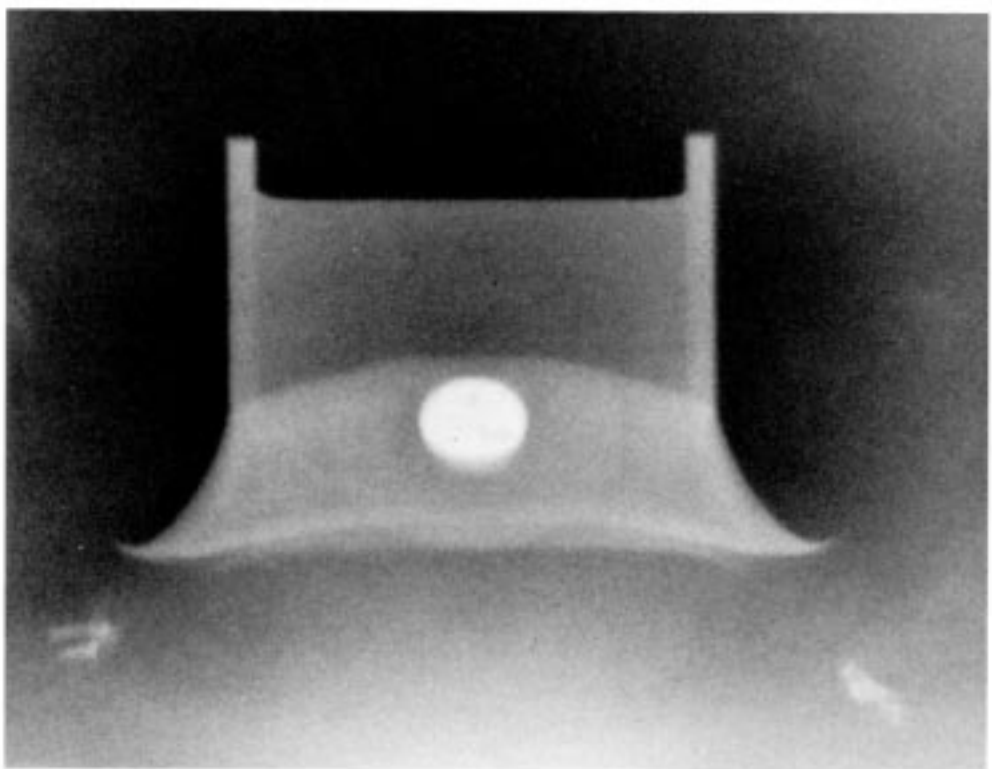
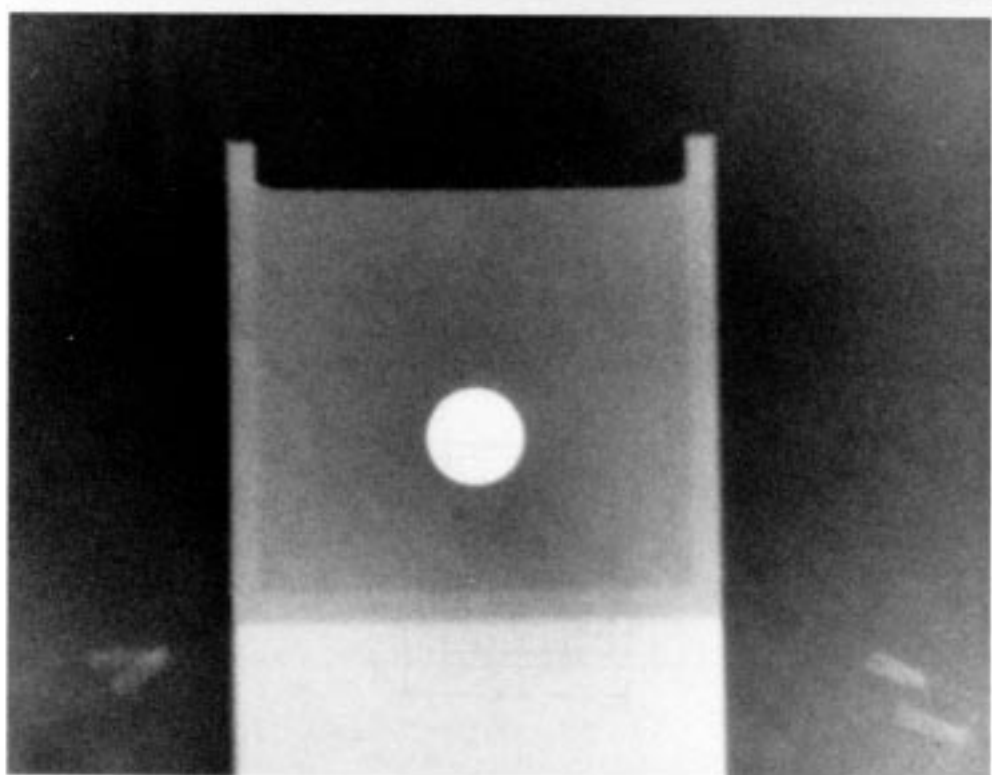
Experimenter: Roger W. Taylor

Radiographic Time: 48.19 μ s

References: Mader et al., 1967; Mader and Kershner, 1972

A shock wave in water interacts with a 10.0-mm-radius aluminum rod. The shock wave has traveled 8.0 μ s since the shock arrived at the Lucite and water interface. See Shots 189, 269, 281, and 282. h is 53.97 mm.





SHOT 191:**Water Free Surface Motion**

Date:

April 26, 1965

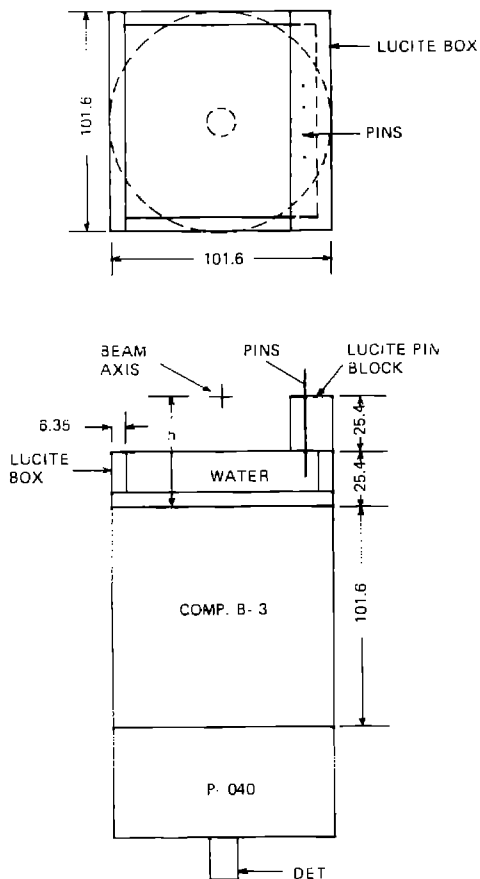
Experimenter:

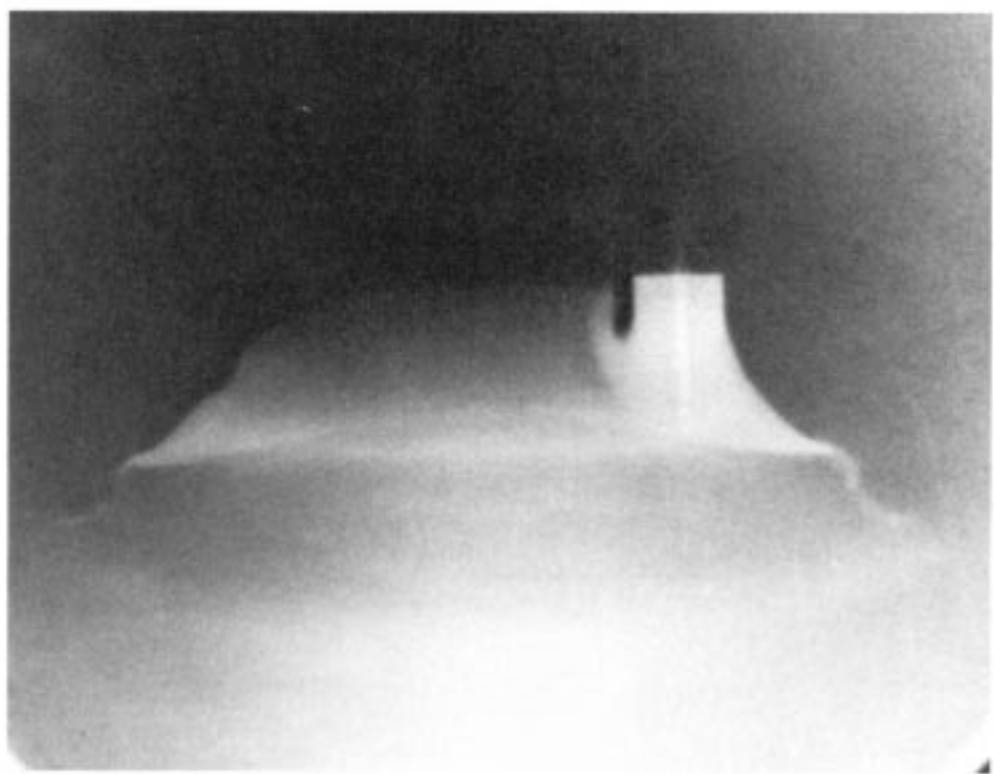
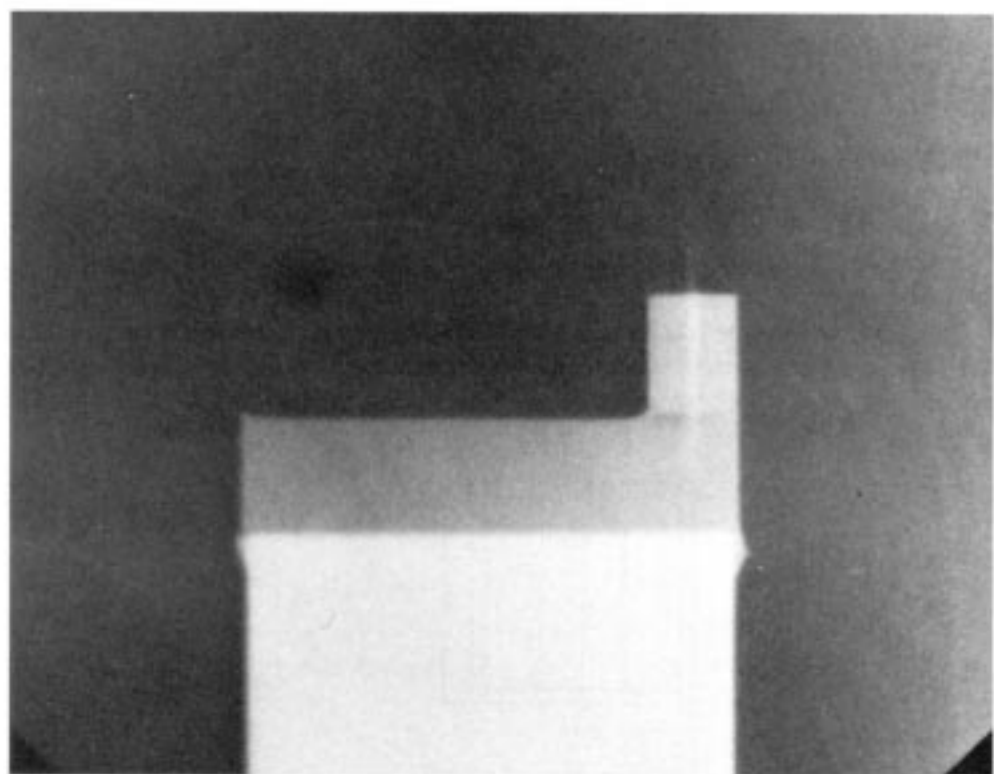
Roger W. Taylor

Radiographic Time:

34.83 μ s

The free surface motion of 25.4-mm-thick water shocked by 101.6 mm of Composition B initiated by a P-040 lens. h is 50.8 mm. The shock velocity was measured using pins located on the right side of the water container.





SHOT 192:**Water Jet**

Date:

July 22, 1965

Experimenter:

Roger W. Taylor

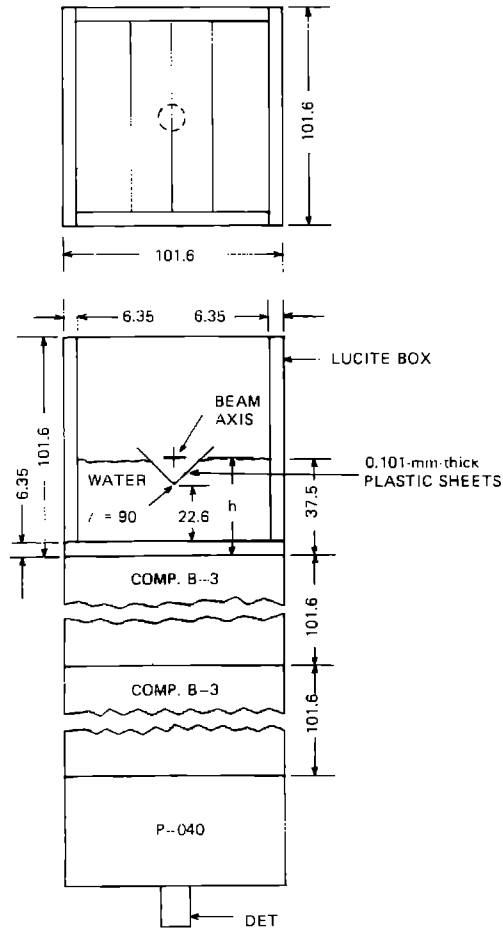
Radiographic Time:

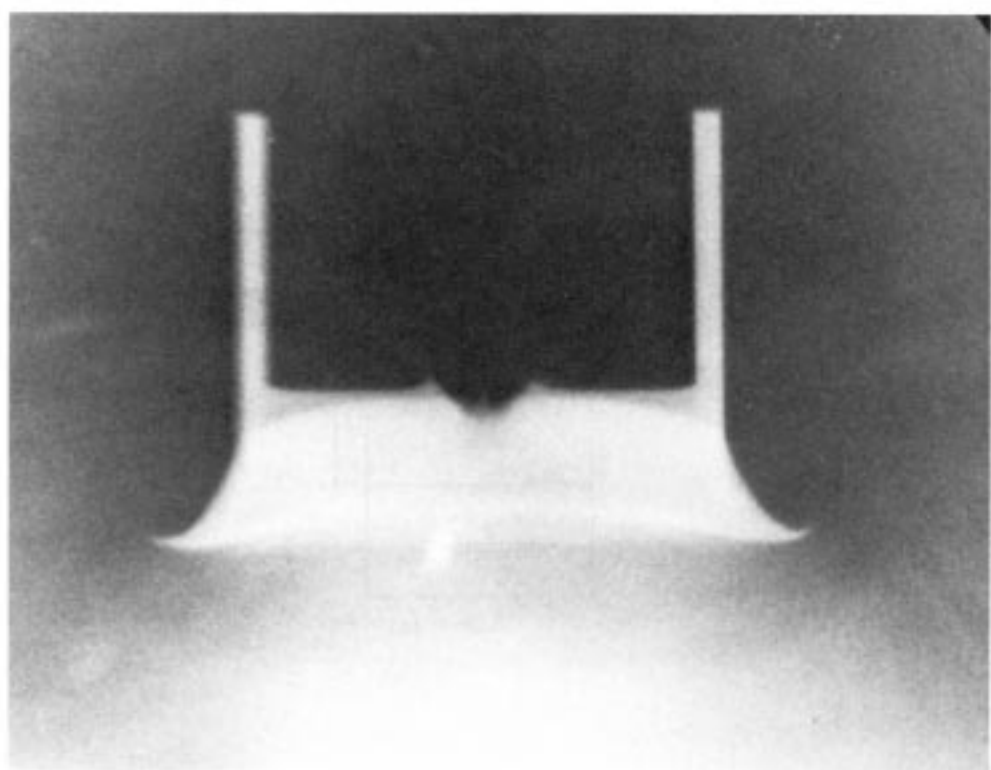
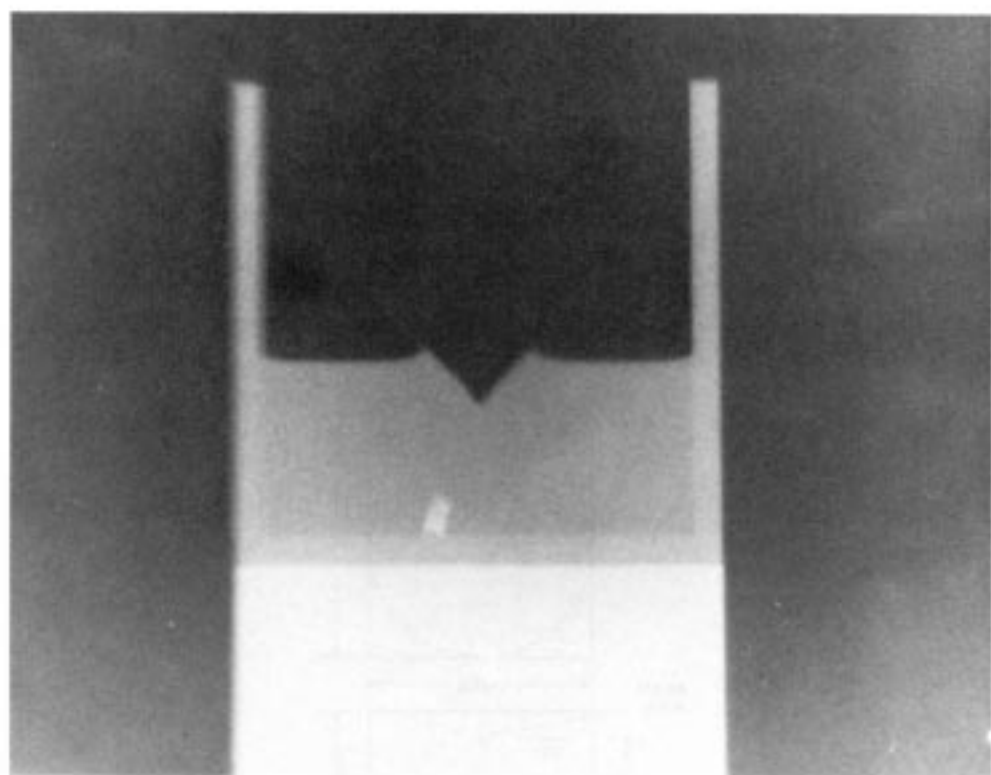
45.93 μ s

References:

Mader et al., 1967; Mader and Kershner, 1972

A shock wave in water interacts with a 9.0-mm-deep 90° groove formed by thin (0.101-mm) plastic sheets. The shock wave has traveled 5.7 μ s since the shock reached the Lucite and water interface. See Shots 298 and 299. h is 38.8 mm.





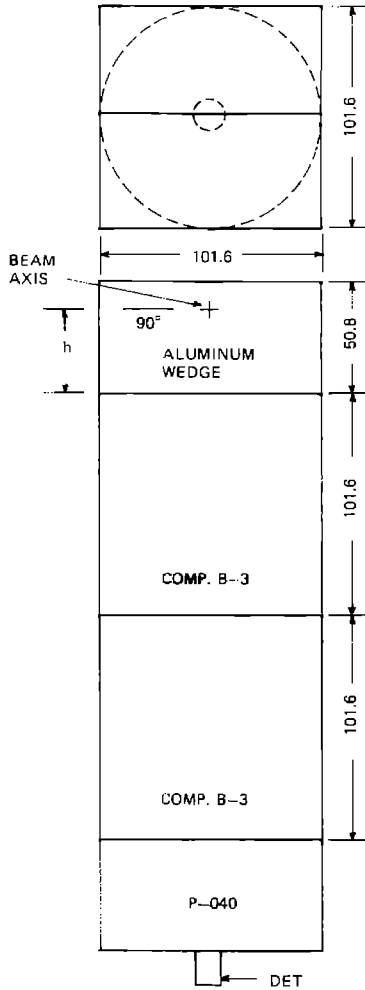
SHOT 193: Aluminum Wedge

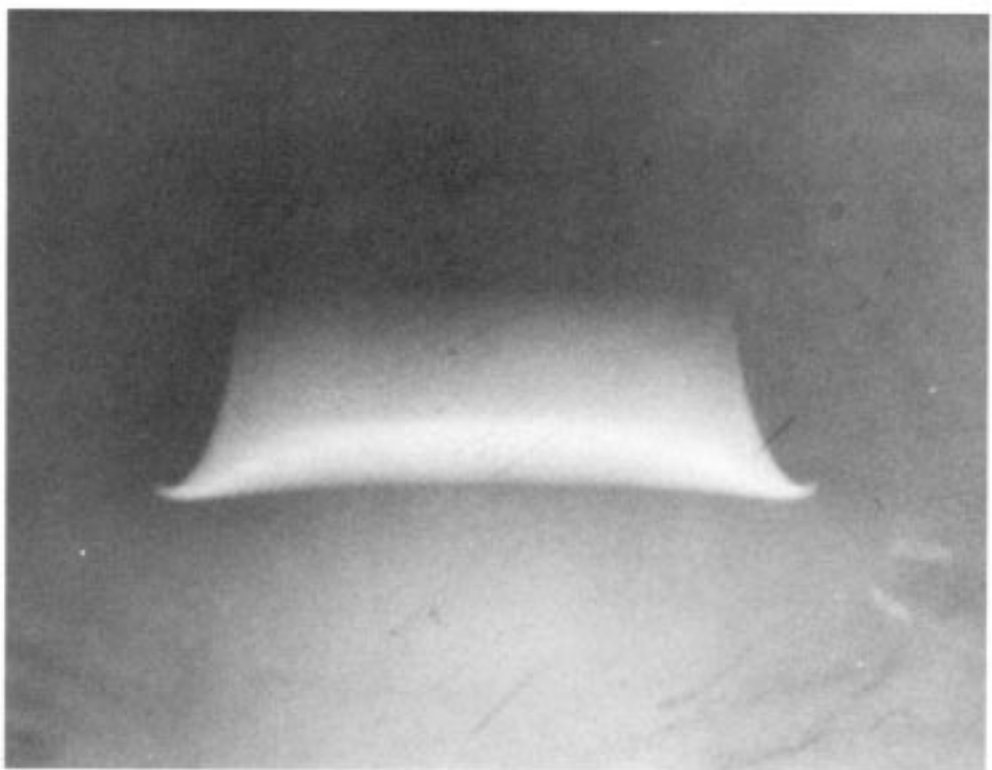
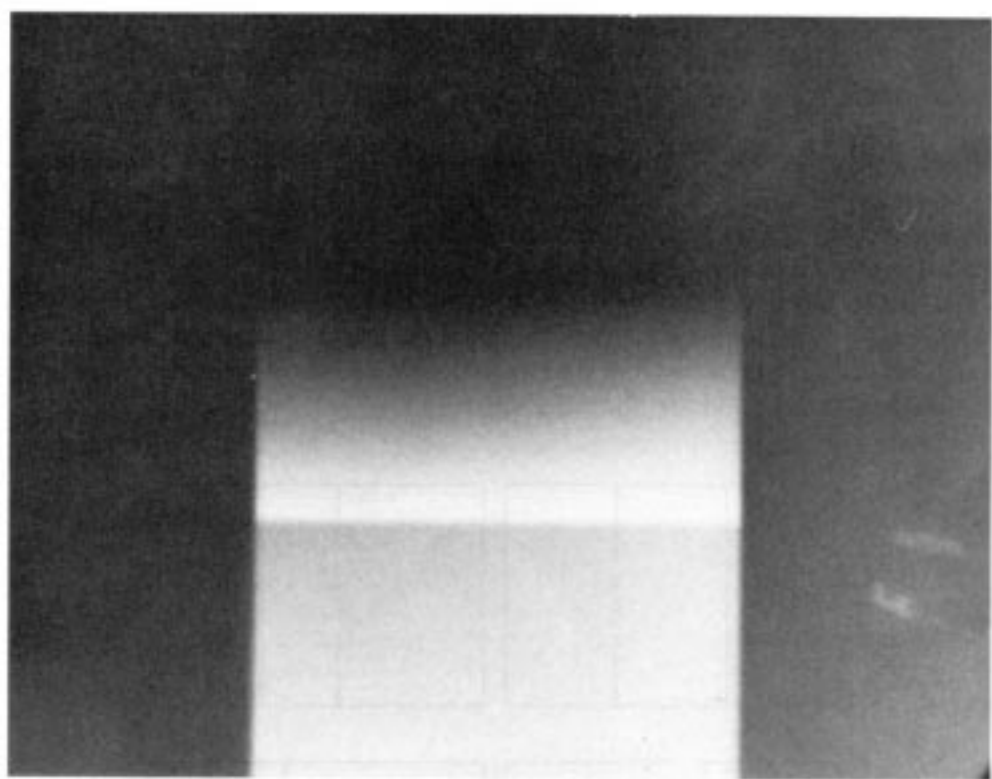
Date: January 12, 1965

Experimenter: Roger W. Taylor

Radiographic Time: 47.52 μ s

A shock wave generated by a Composition B-3 detonation wave interacts with a 90° aluminum wedge. Similar to Shot 138 except for beam orientation. h is 38.1 mm. See Shots 39, 135, 137, and 214-217.





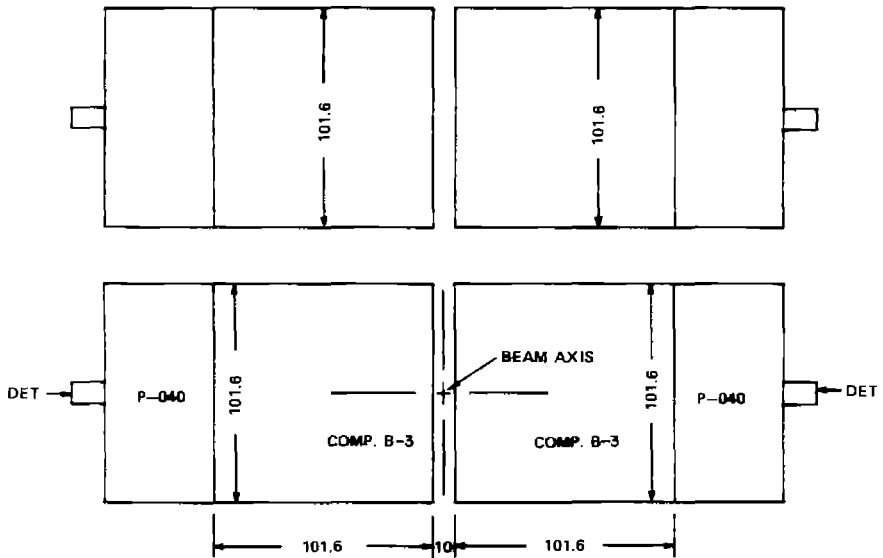
SHOT 195: Colliding Composition B-3 Detonation Products

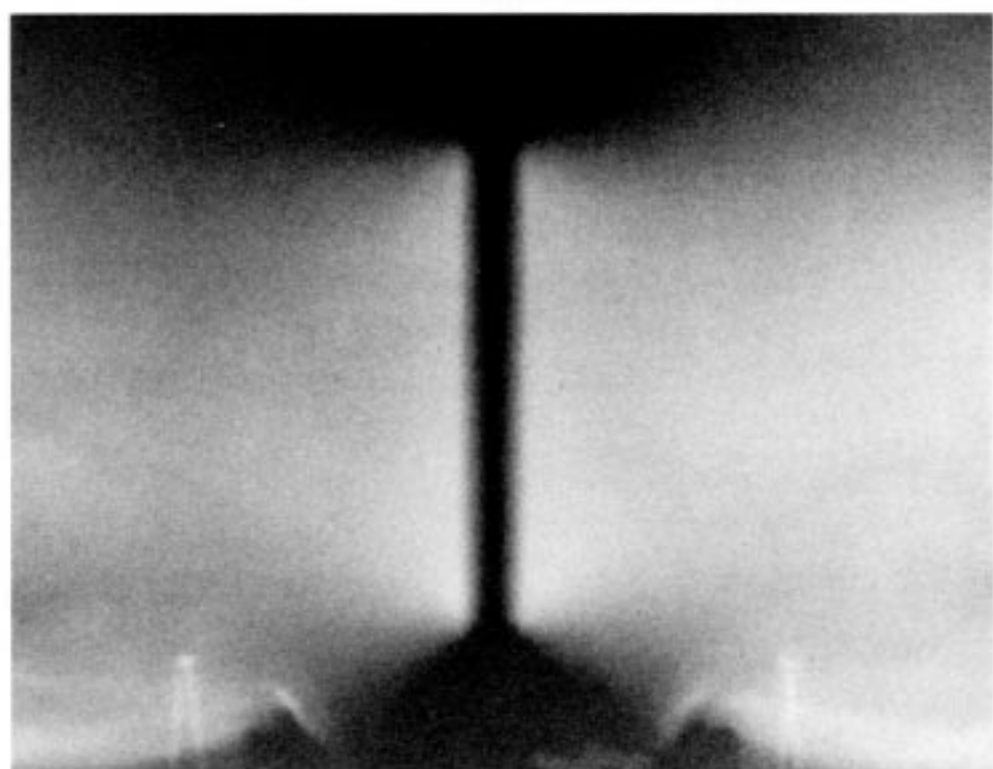
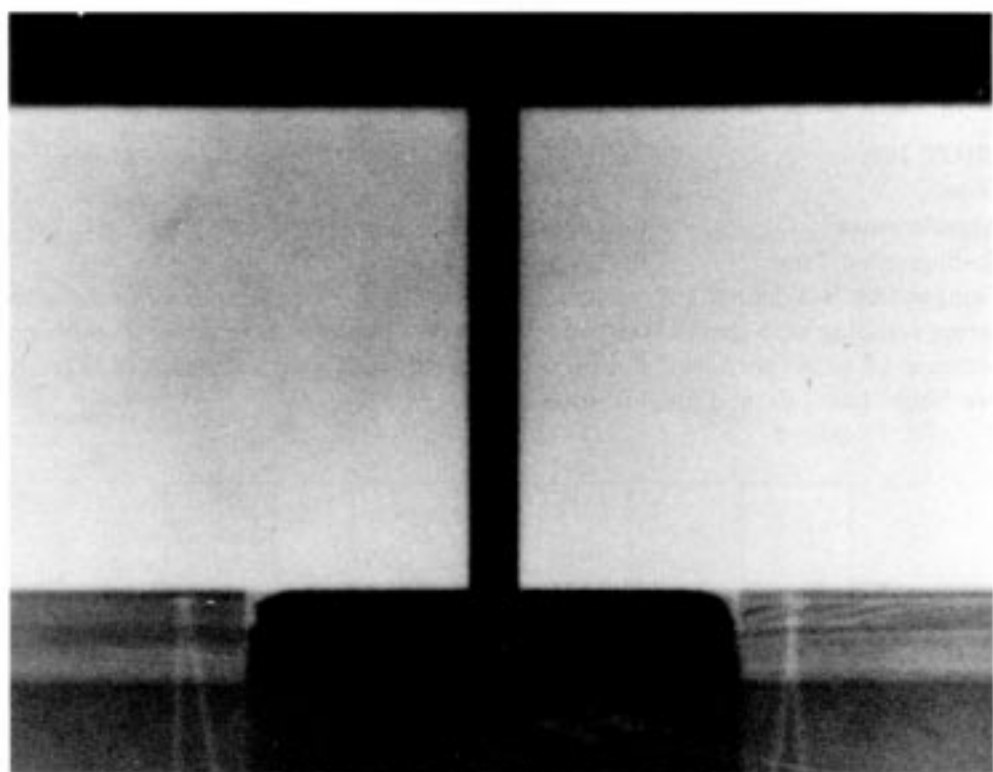
Date: February 9, 1965

Experimenter: Douglas Venable

Radiographic Time: 26.9 μ s

Composition B-3 detonation products are permitted to expand into air for 5.0 mm before colliding with products expanding from the opposite direction. The collision occurs at 26.25 μ s (pin data), and the resulting reflected wave is shown 0.55 μ s later. See Shots 139, 140, and 196 for other times.





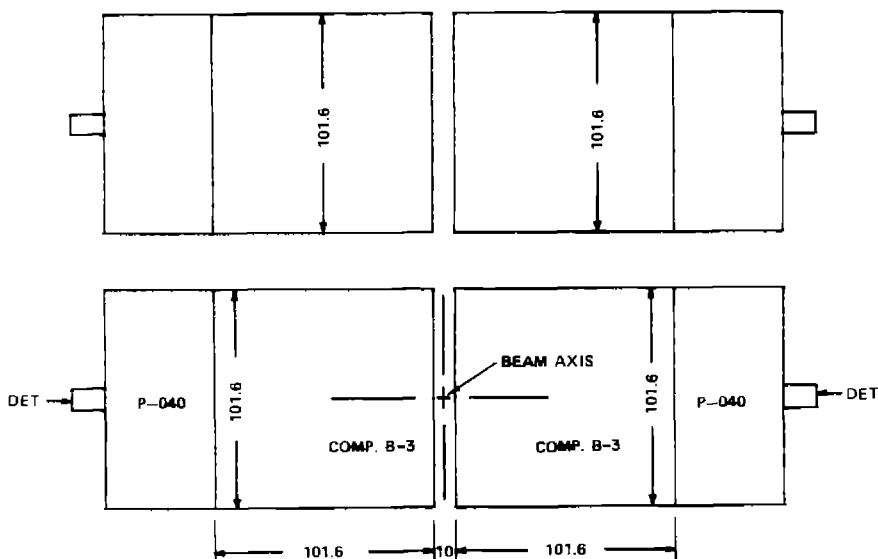
SHOT 196: Colliding Composition B-3 Detonation Products

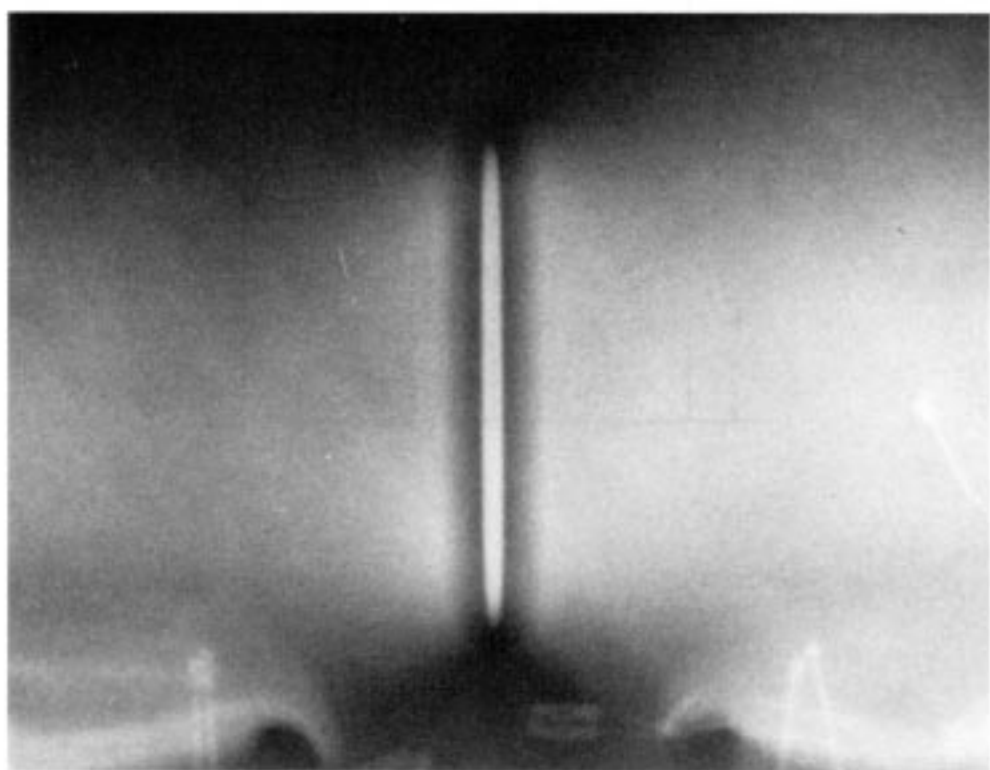
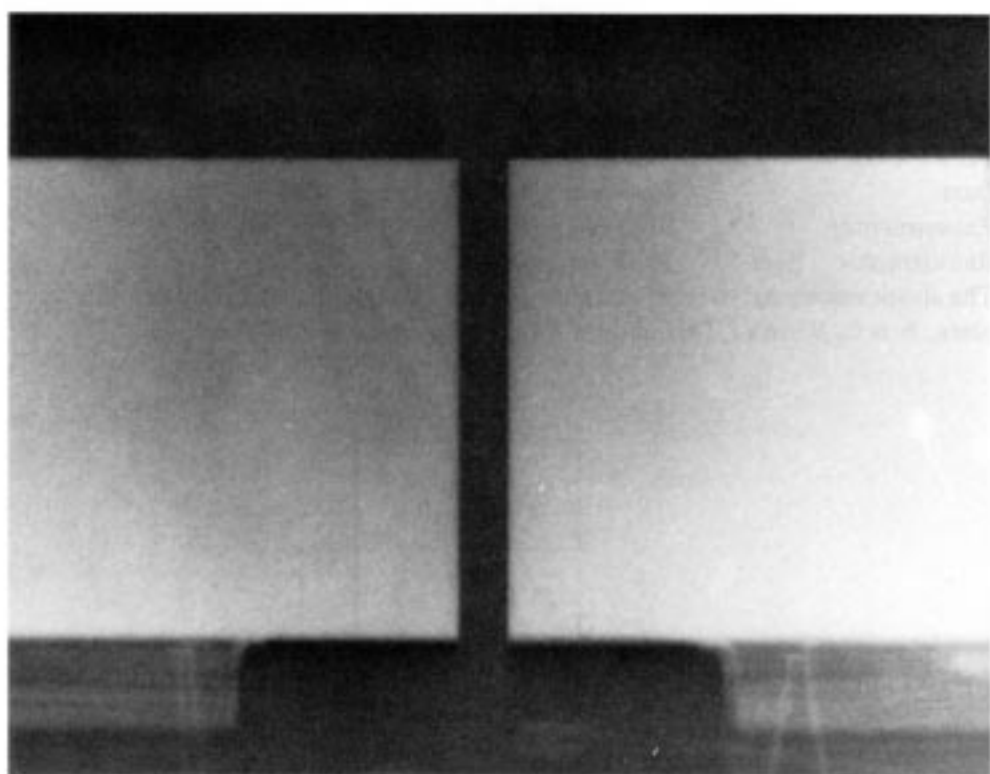
Date: February 9, 1965

Experimenter: Douglas Venable

Radiographic Time: 27.91 μ s

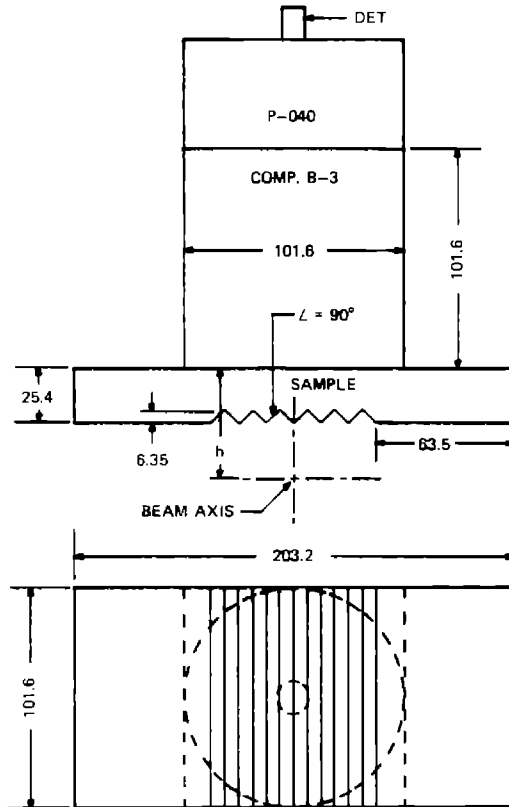
Composition B-3 detonation products are permitted to expand into air for 5.0 mm before colliding with products expanding from the opposite direction. The collision occurs at 26.25 μ s (pin data), and the resulting reflected wave is shown 1.65 μ s later. See Shots 139, 140, and 195 for other times.

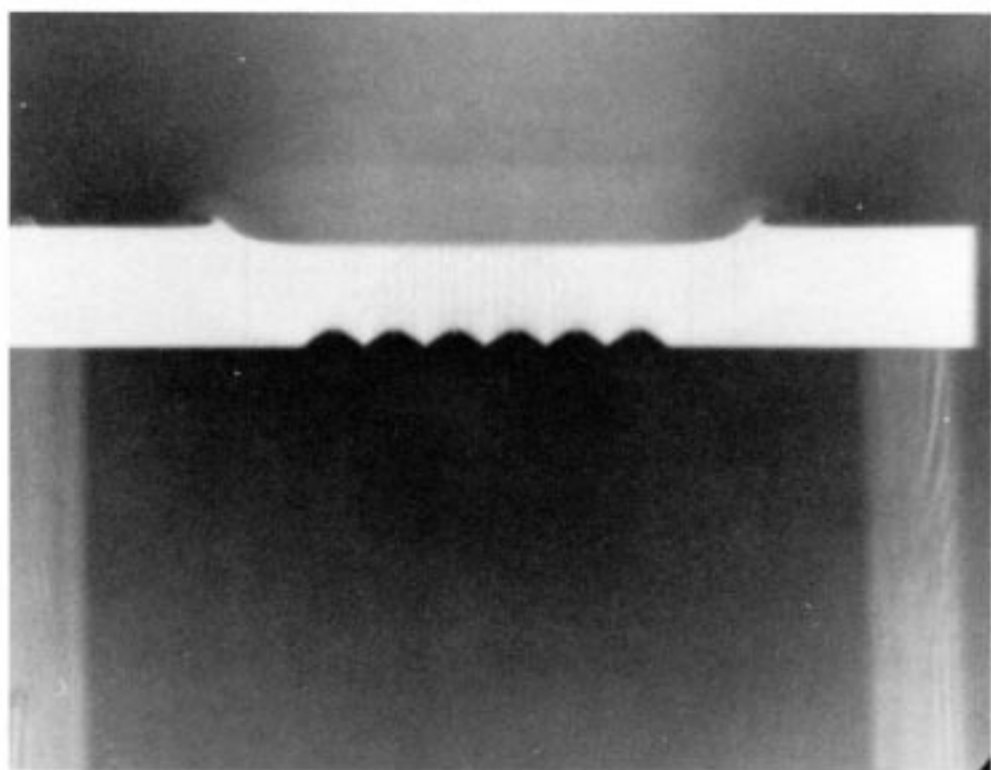
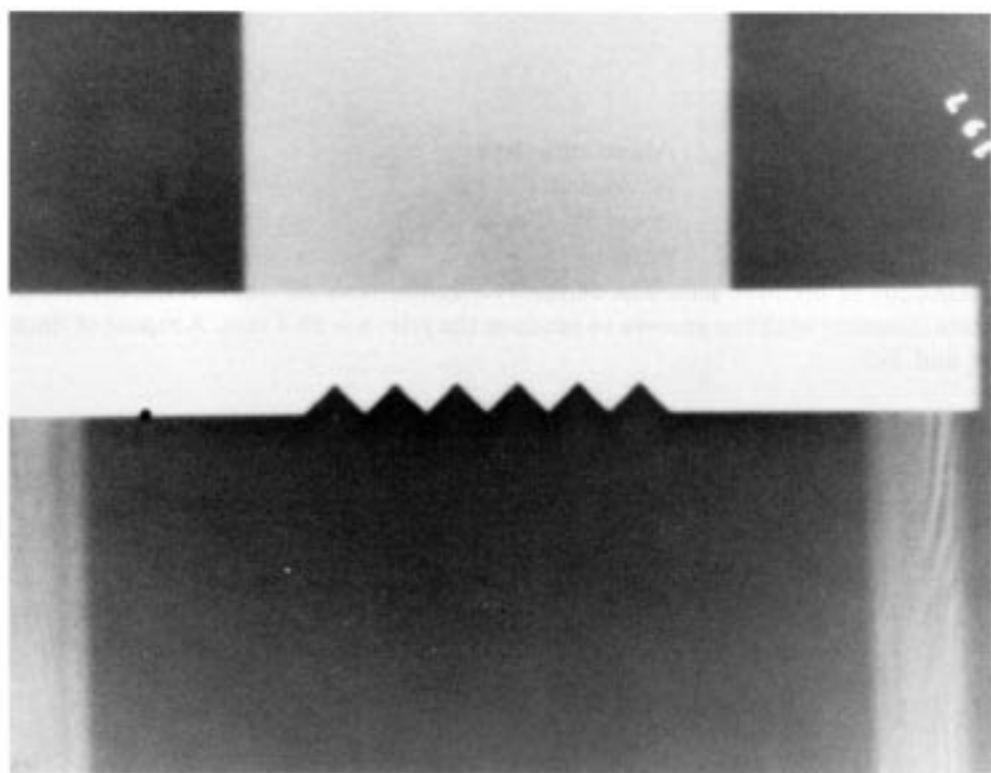




SHOT 197: **Aluminum Jets**
Date: November 4, 1965
Experimenter: Roger W. Taylor
Radiographic Time: 29.48 μ s

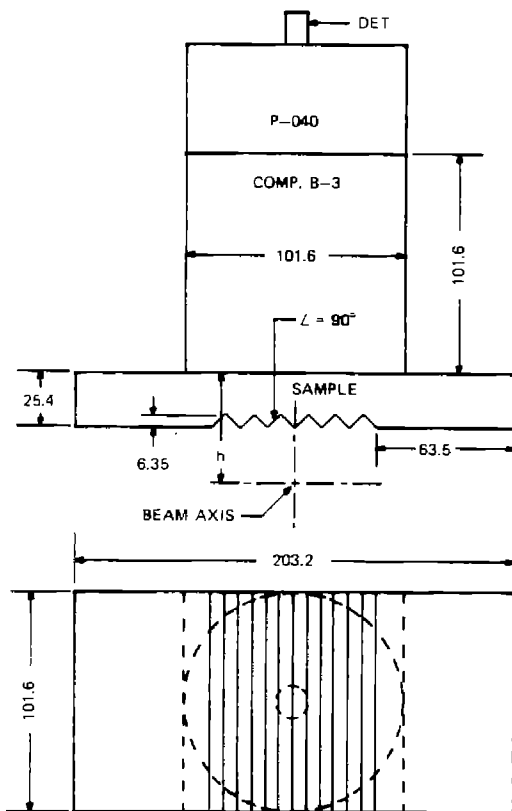
The shock wave used to form metallic jets has traveled 22.4 mm into the aluminum plate. h is 22.23 mm. This shot is a repeat of Shots 7 and 141.

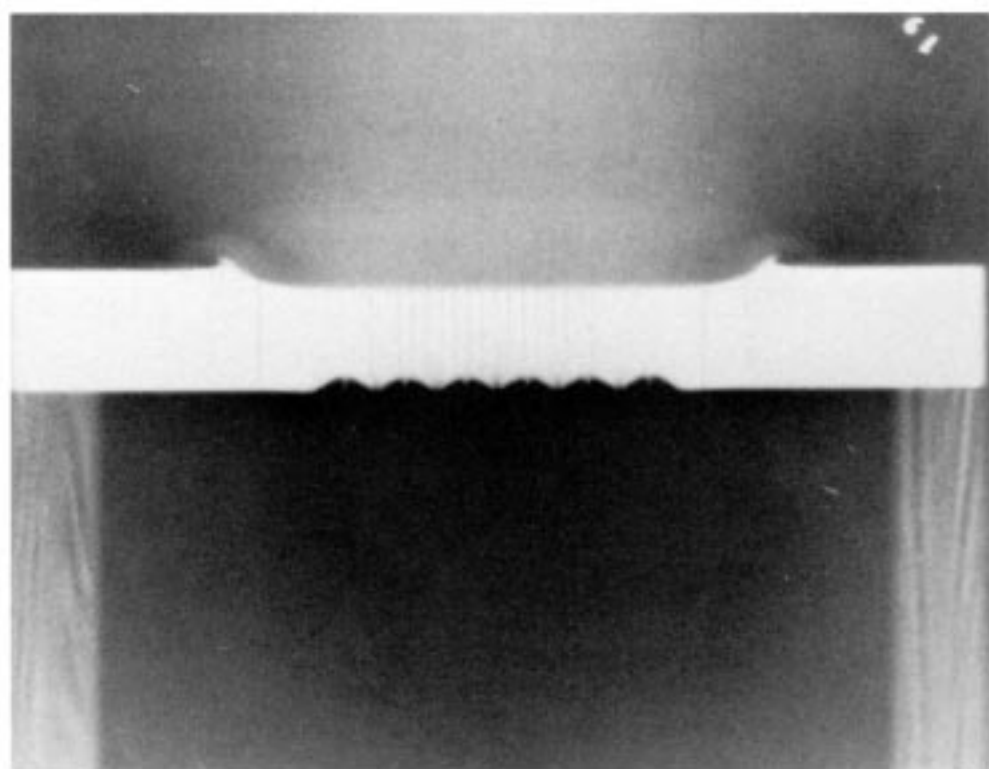
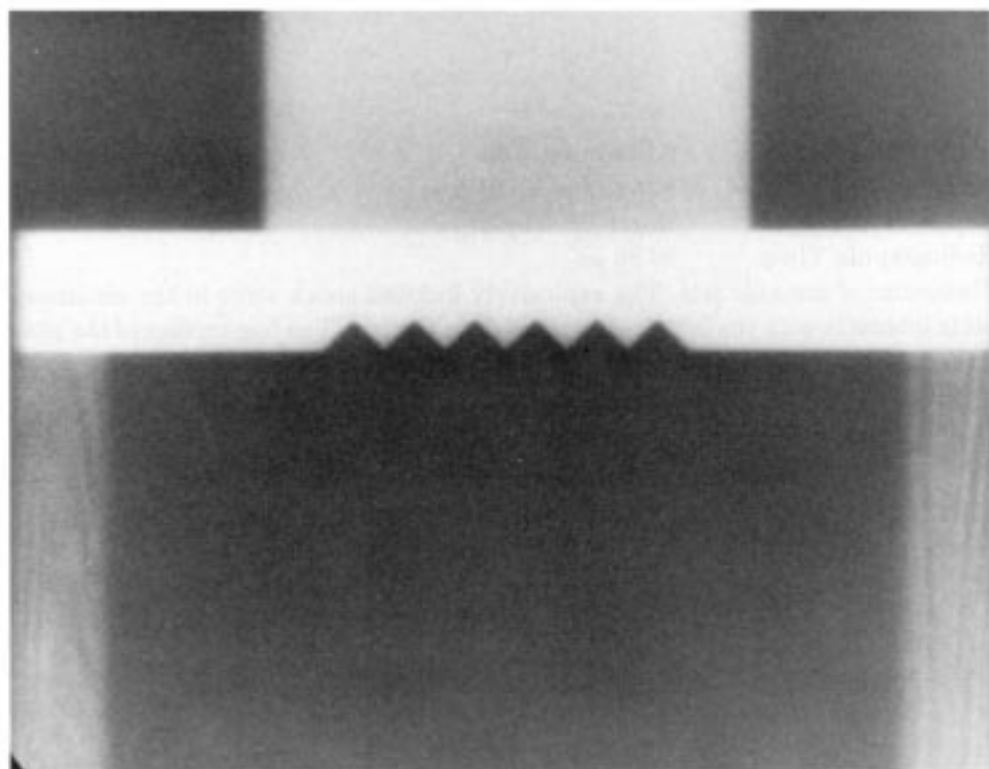




SHOT 198: **Aluminum Jets**
 Date: November 4, 1965
 Experimenter: Roger W. Taylor
 Radiographic Time: 29.94 μ s

Formation of metallic jets. The explosively induced shock wave in the aluminum plate interacts with the grooves to produce the jets. h is 25.4 mm. A repeat of Shots 12 and 142.





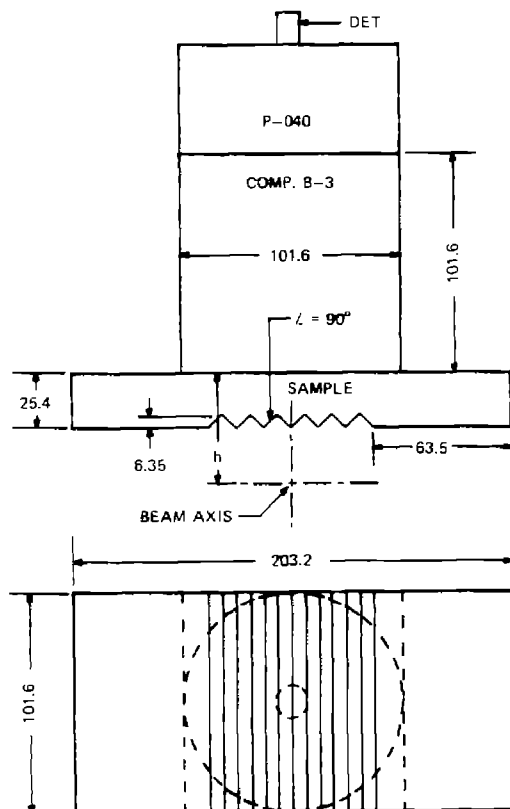
SHOT 199: Aluminum Jets

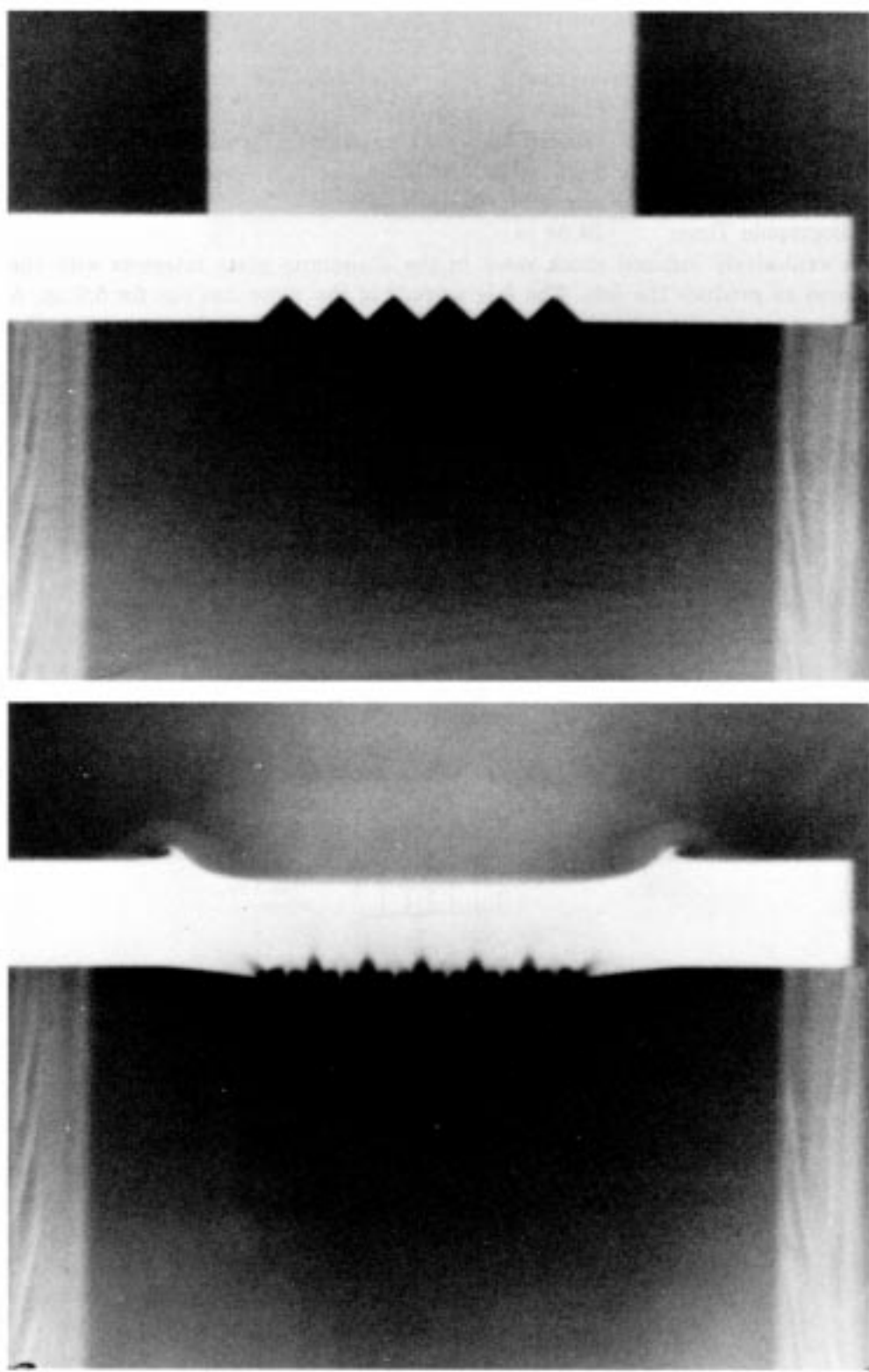
Date: November 4, 1965

Experimenter: Roger W. Taylor

Radiographic Time: 30.88 μ s

Formation of metallic jets. The explosively induced shock wave in the aluminum plate interacts with the 90° grooves to produce the jets. The free surface of the plate has run for 1.0 μ s. h is 25.4 mm. This is a repeat of Shots 13 and 143.





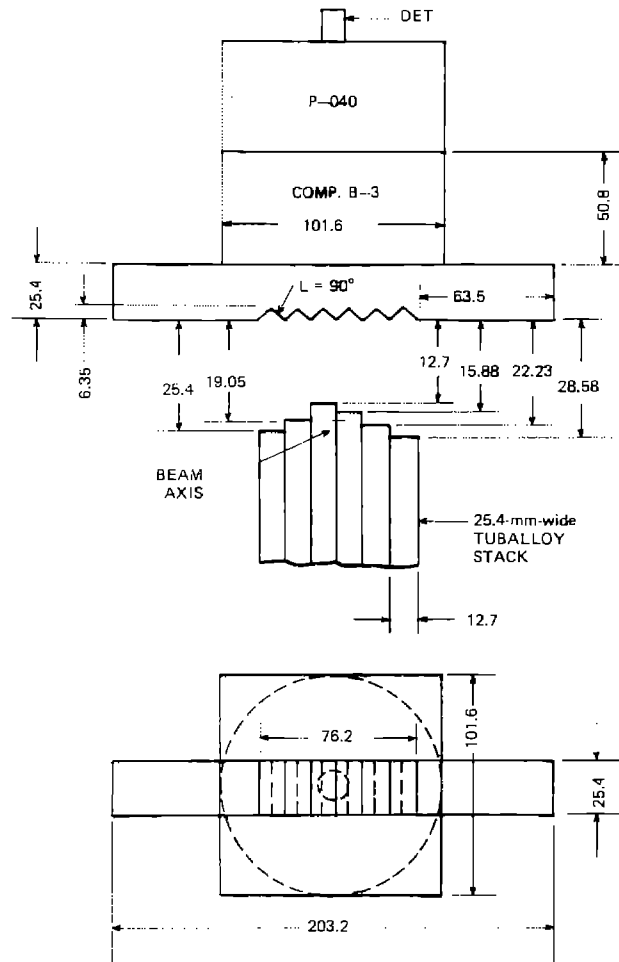
SHOT 201: Aluminum Jets Penetrating Uranium

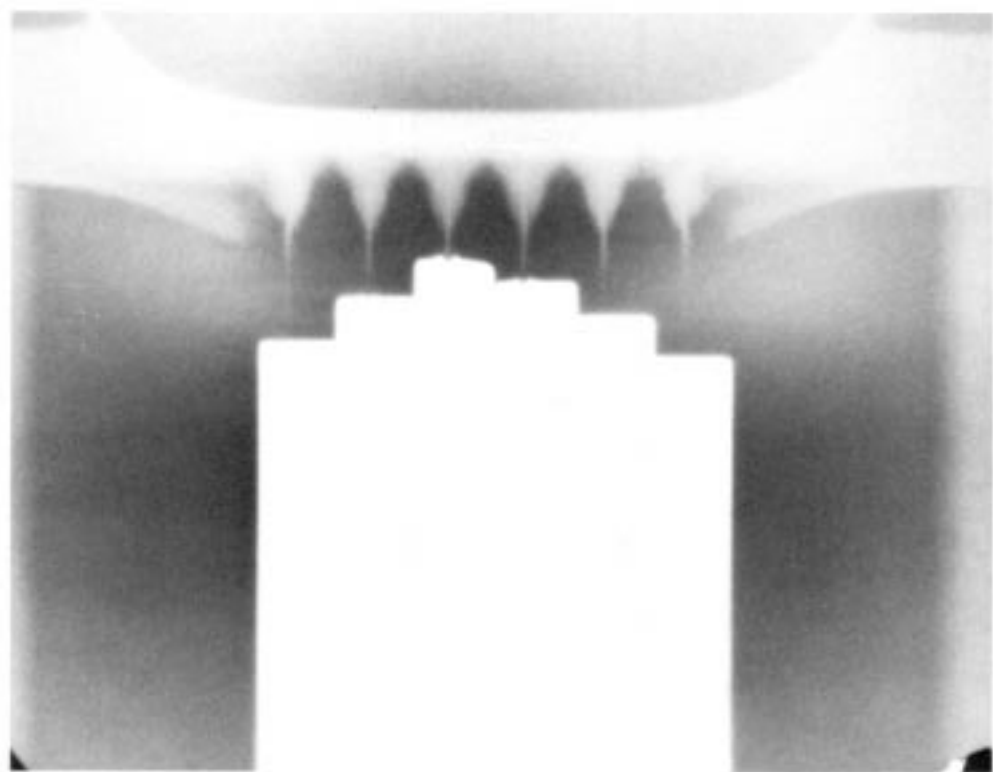
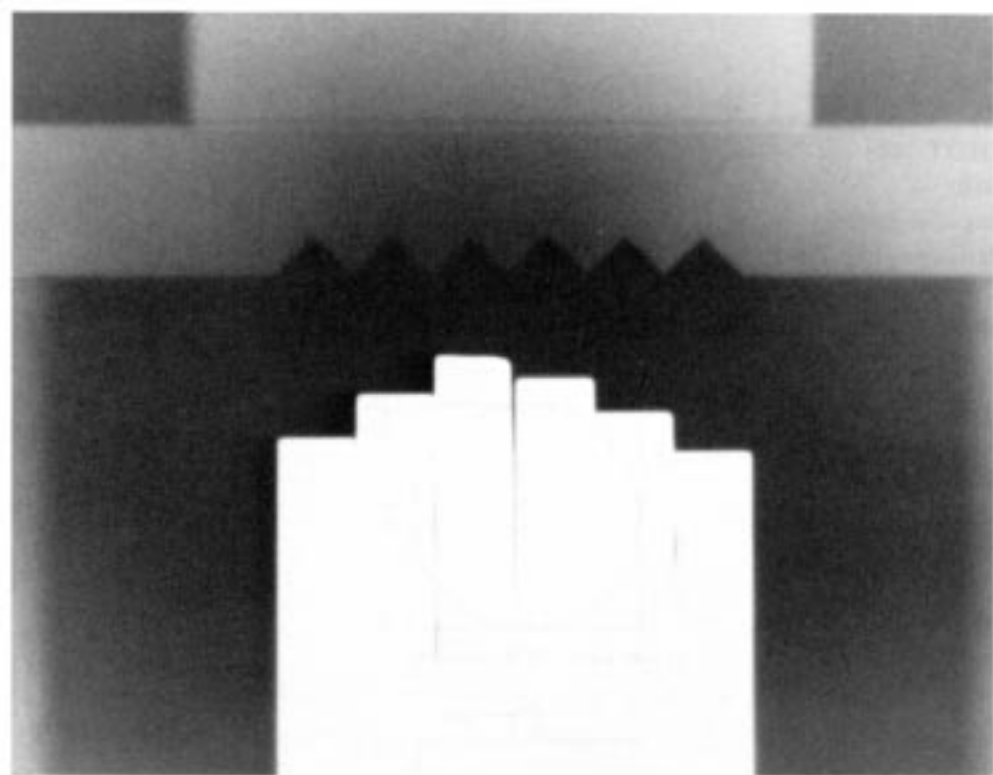
Date: September 7, 1966

Experimenter: Roger W. Taylor

Radiographic Time: 34.94 μ s

The explosively induced shock wave in the aluminum plate interacts with the grooves to produce the jets. The free surface of the plate has run for 5.0 μ s. A uranium target plate shows the penetration properties of the aluminum jets. See Shot 150.





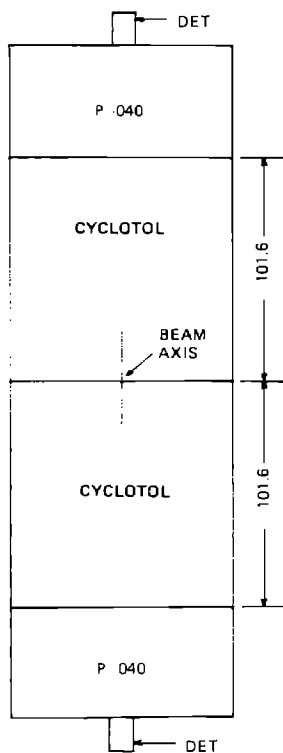
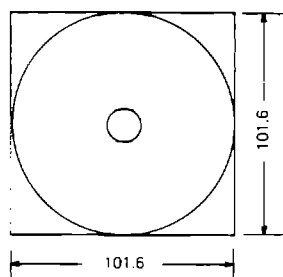
SHOT 203: Colliding Cyclotol Detonations

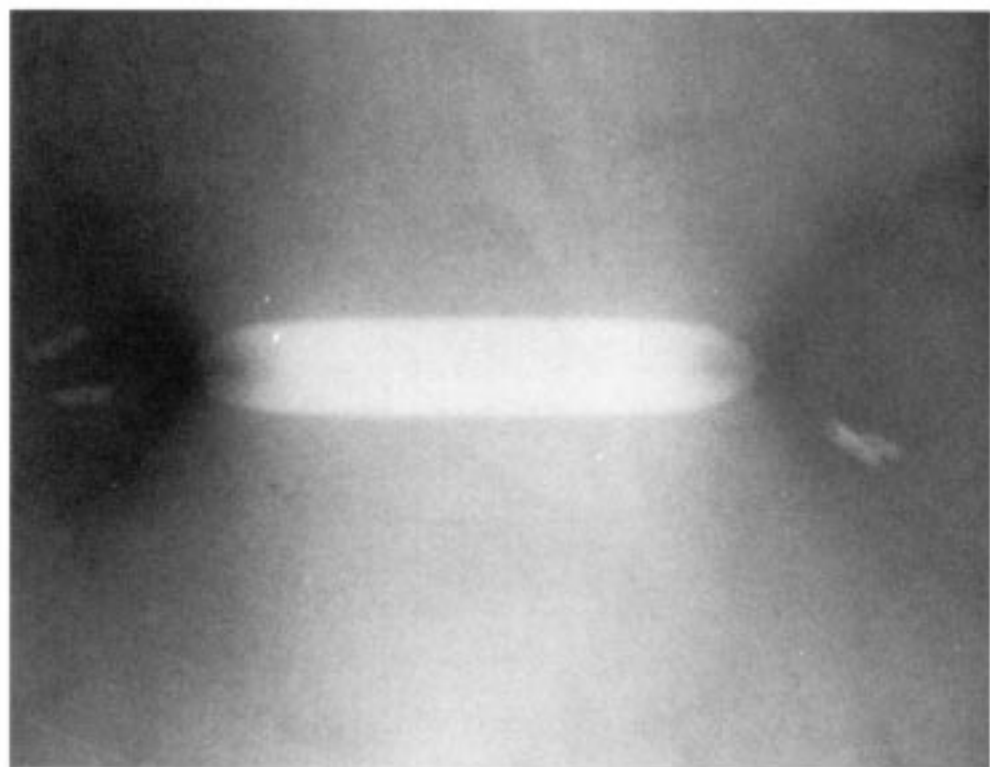
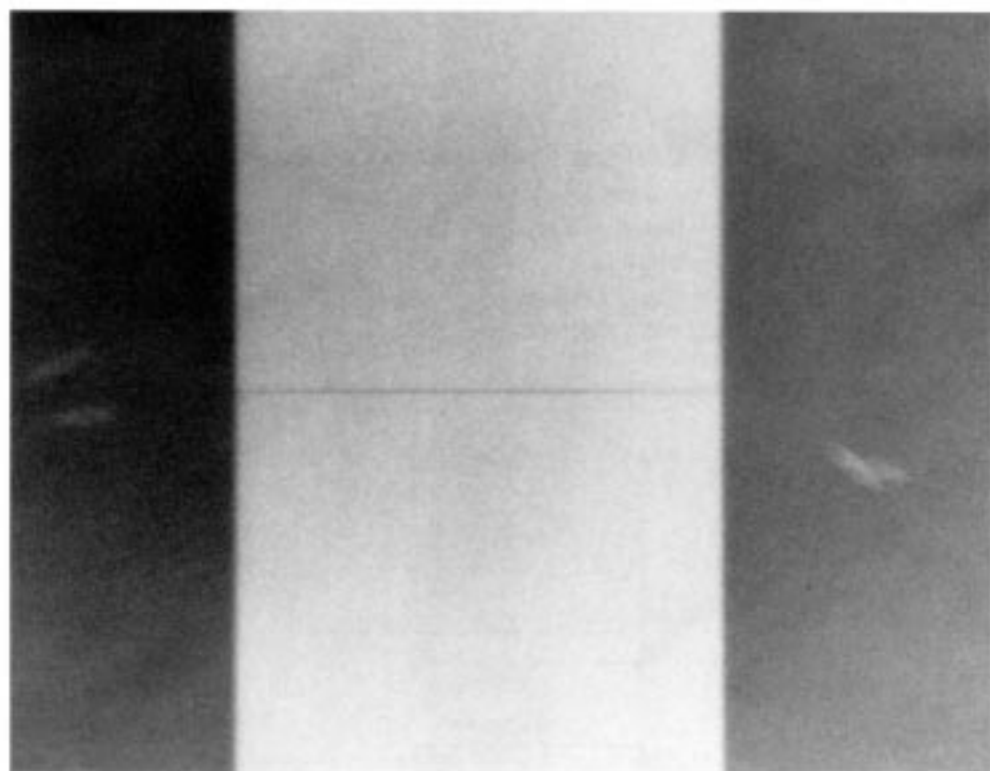
Date: January 27, 1965

Experimenter: Douglas Venable

Radiographic Time: 27.68 μ s

The reflected shocks in cyclotol detonation products 1.76 μ s after the detonation waves collided. See Shots 204-206 and 291.





SHOT 204:

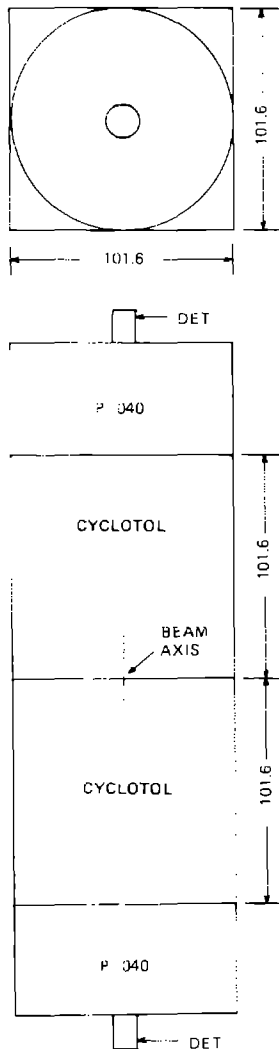
Colliding Cyclotol Detonations

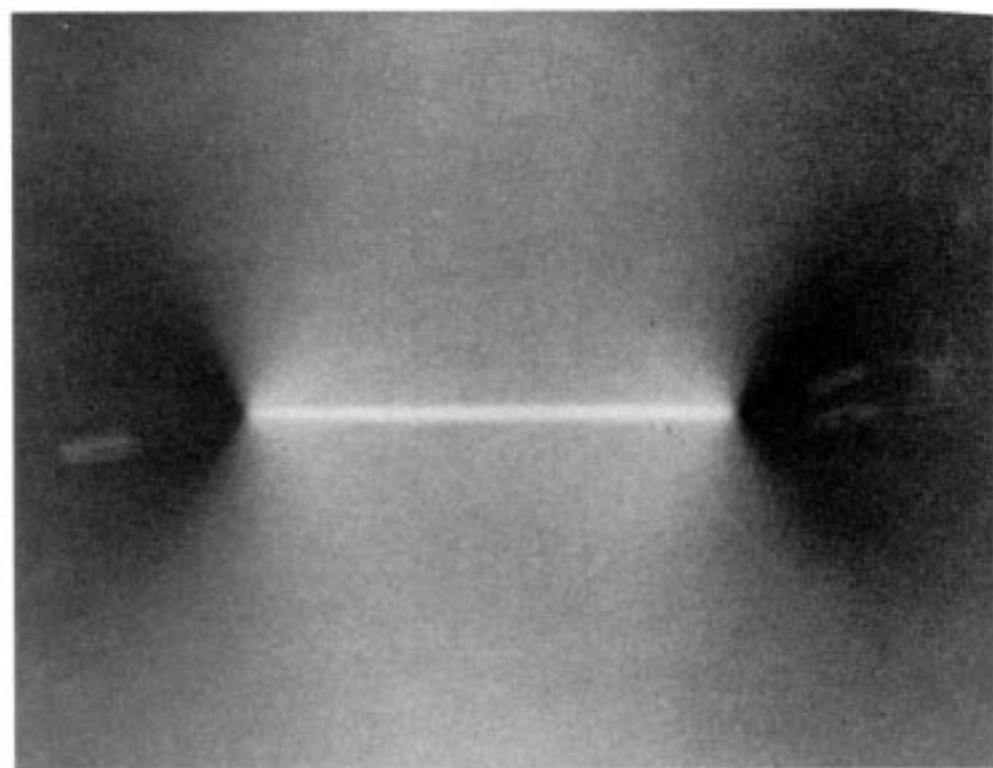
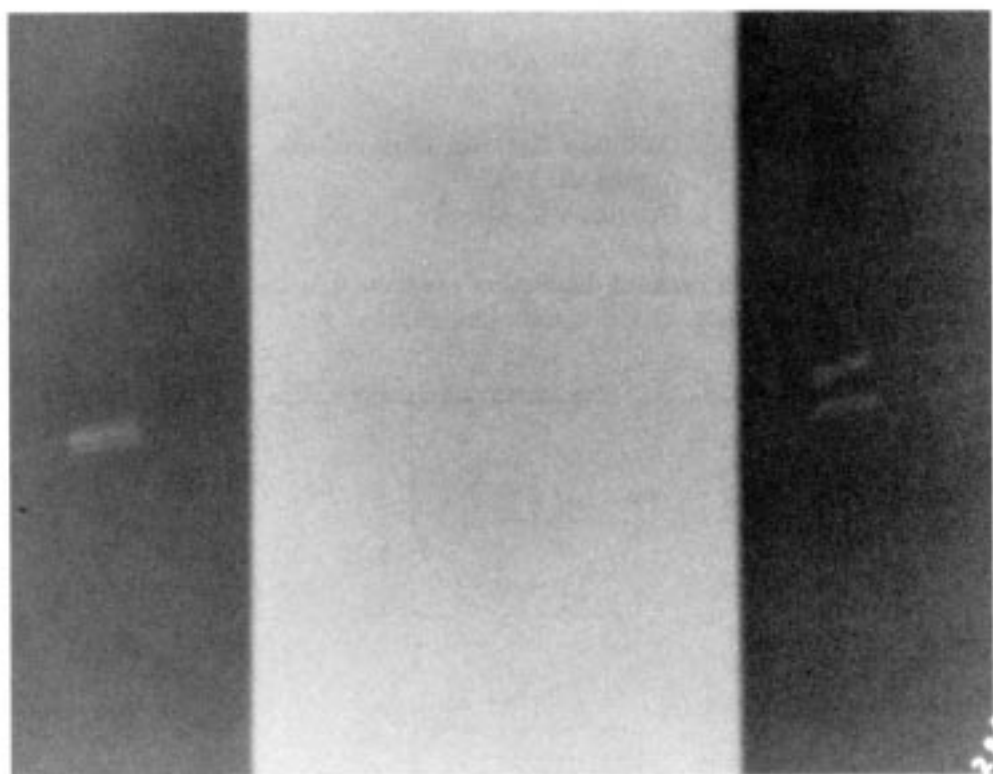
Date: August 24, 1965

Experimenter: Douglas Venable

Radiographic Time: 26.14 μ s

The reflected shocks in cyclotol detonation products 0.22 μ s after the detonation waves collided. See Shots 203, 205, 206, and 291.





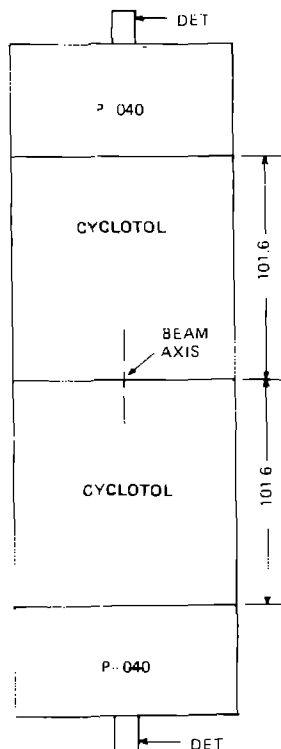
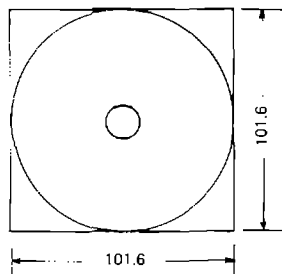
SHOT 205: Colliding Cyclotol Detonations

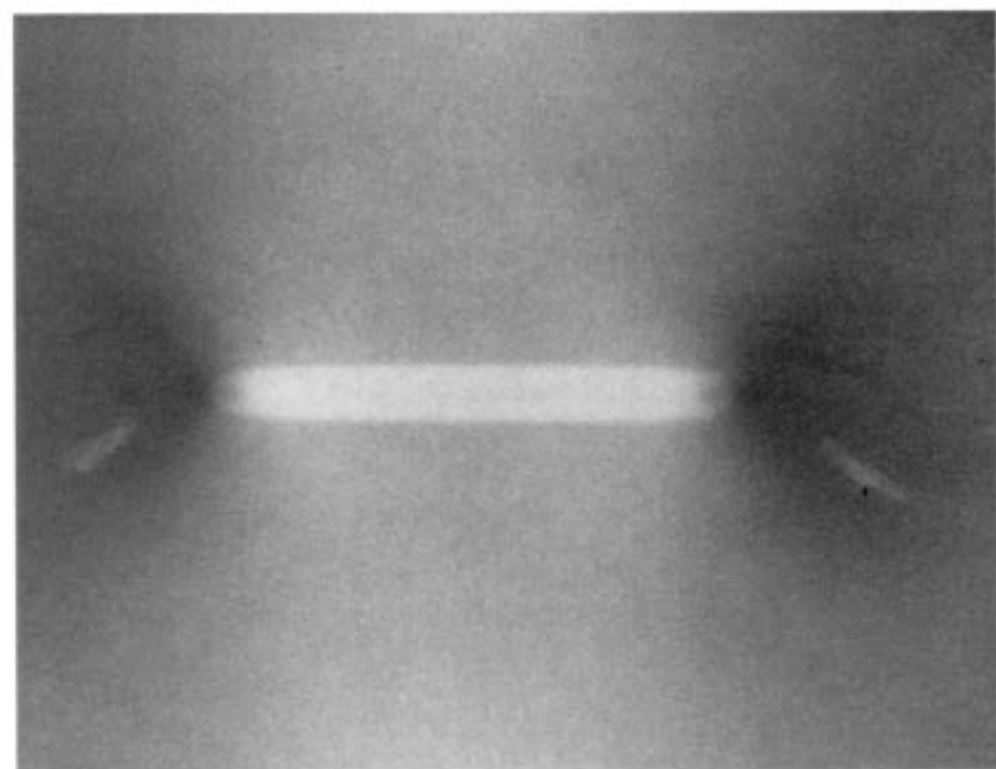
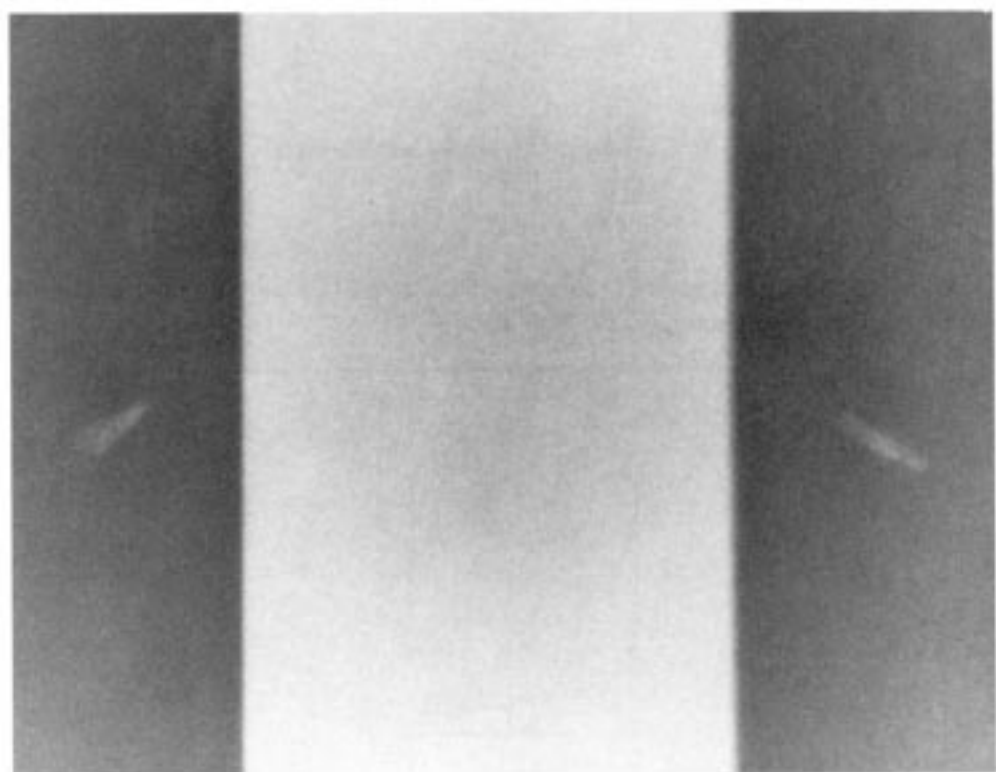
Date: August 24, 1965

Experimenter: Douglas Venable

Radiographic Time: 26.82 μ s

The reflected shocks in cyclotol detonation products 0.91 μ s after the detonation waves collided. See Shots 203, 204, 206, and 291.





SHOT 206:

Colliding Cyclotol Detonations

Date:

August 24, 1965

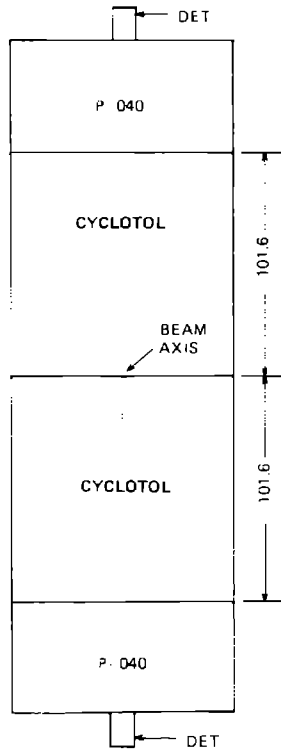
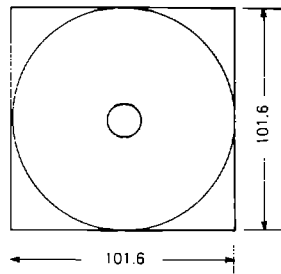
Experimenter:

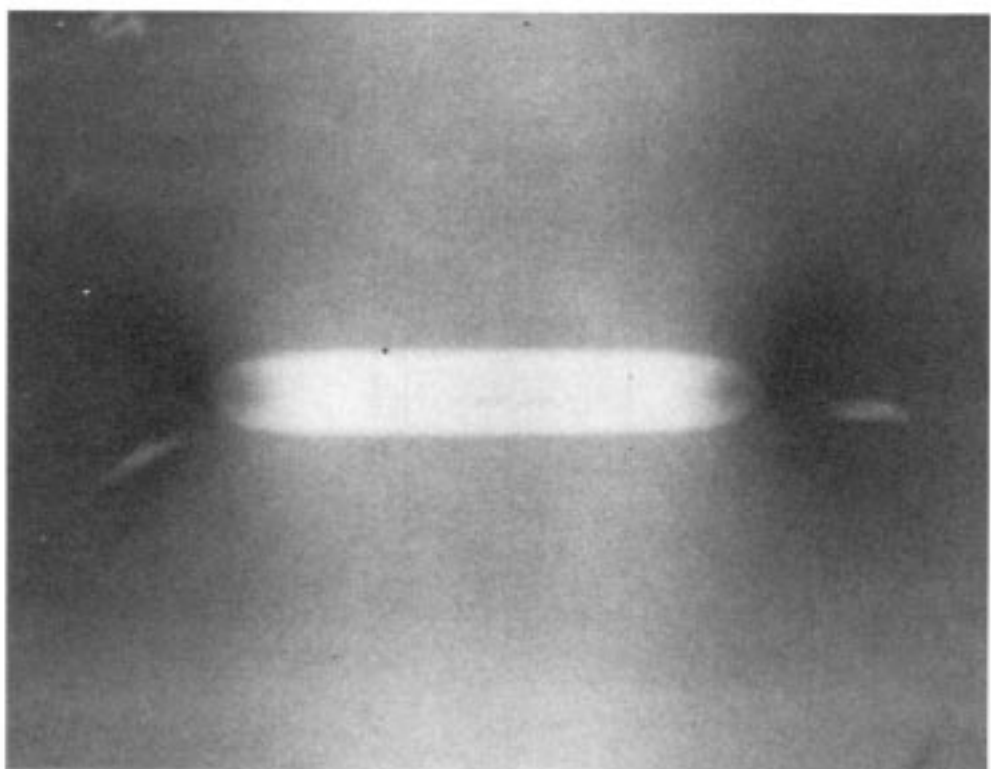
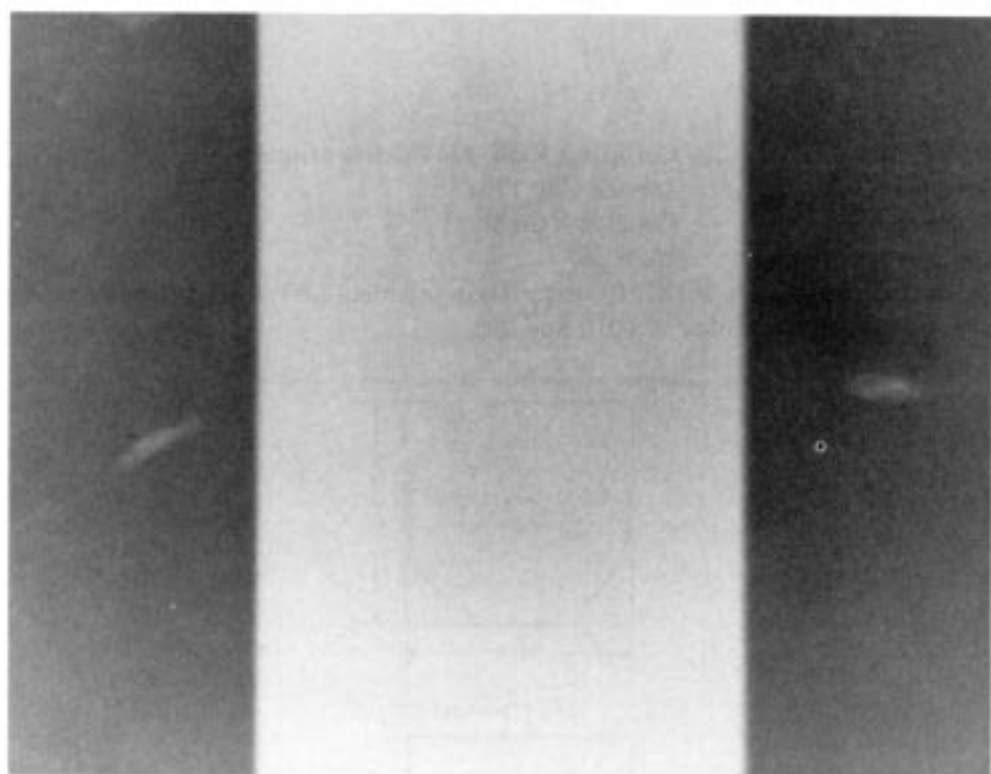
Douglas Venable

Radiographic Time:

27.29 μ s

The reflected shocks in cyclotol detonation products 1.38 μ s after the detonation waves collided. See Shots 203-205 and 291.





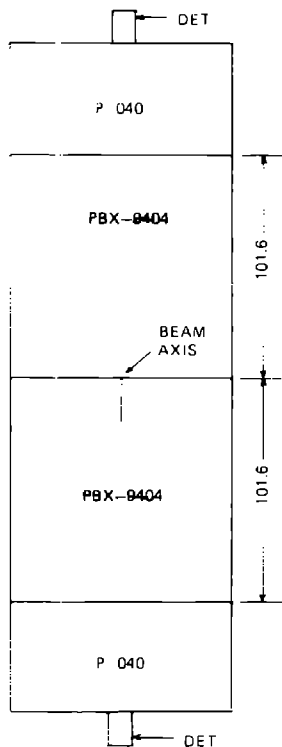
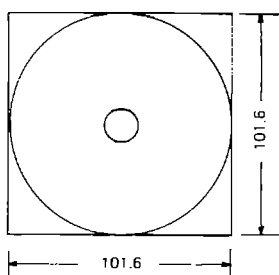
SHOT 207: Colliding PBX-9404 Detonations

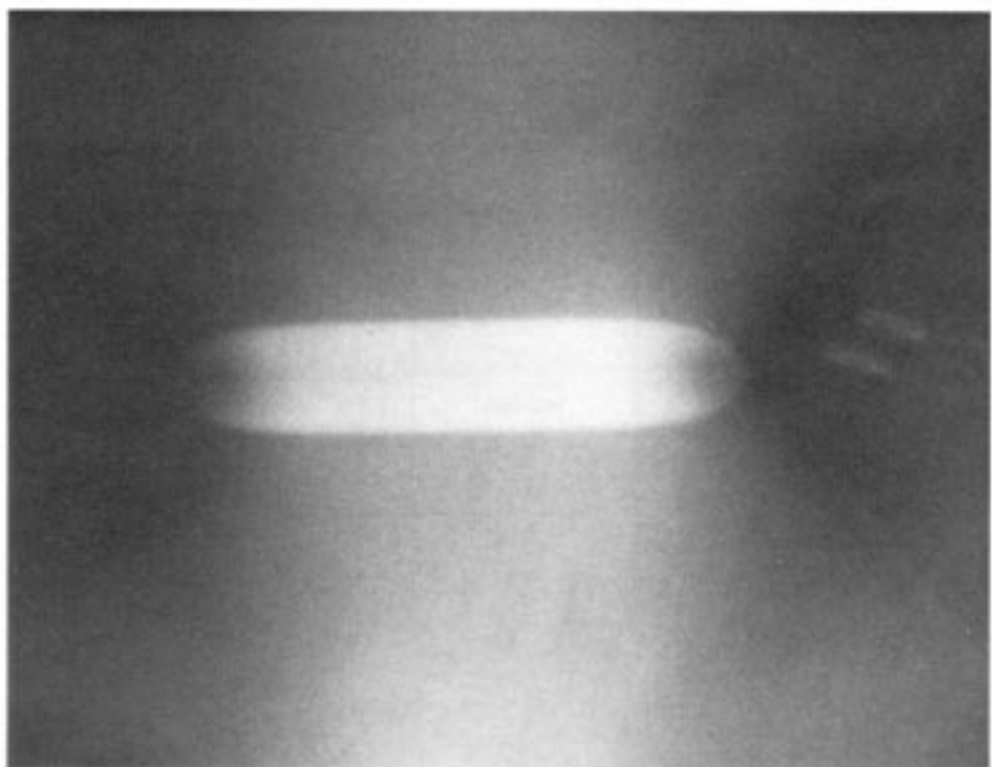
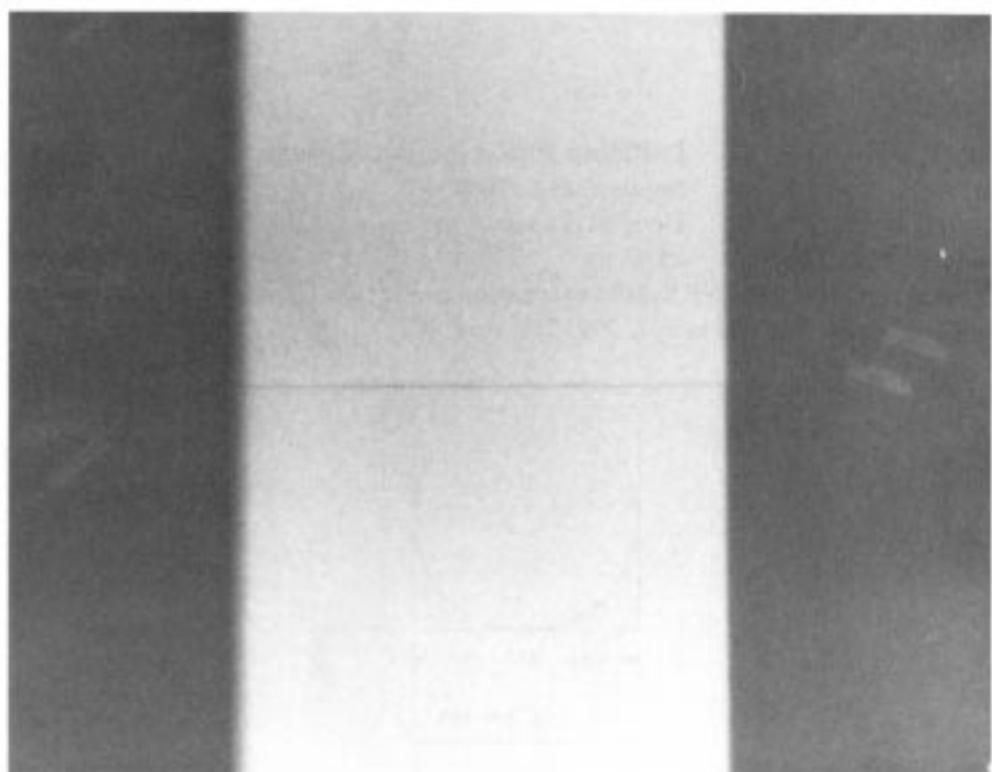
Date: January 28, 1965

Experimenter: Douglas Venable

Radiographic Time: 26.98 μ s

The reflected shocks in PBX-9404 detonation products 1.80 μ s after the detonation waves collided. See Shots 208-210 and 292.





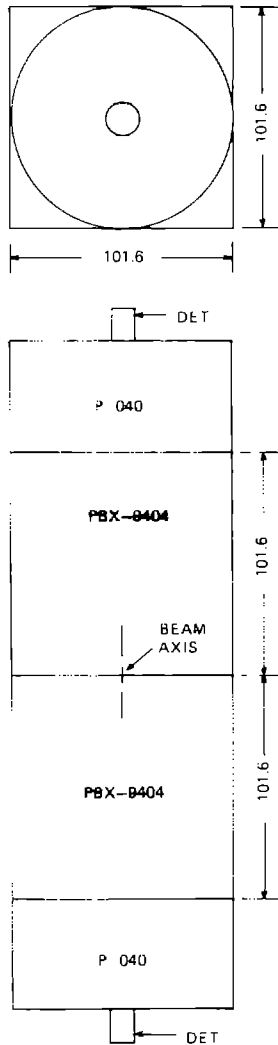
SHOT 208: Colliding PBX-9404 Detonations

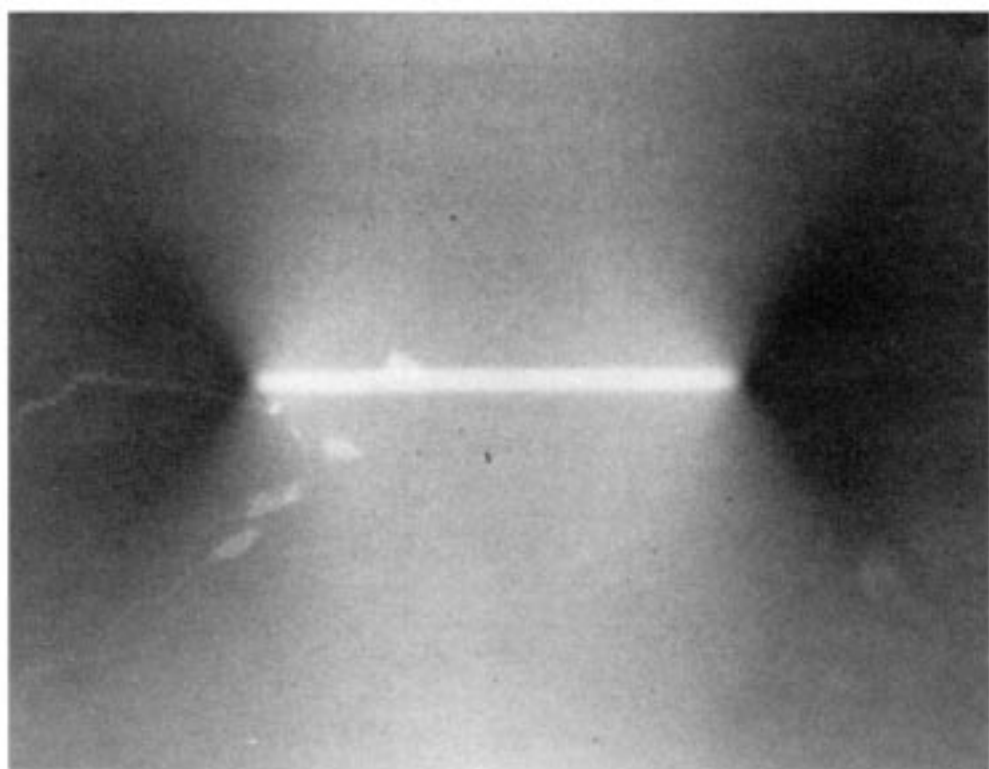
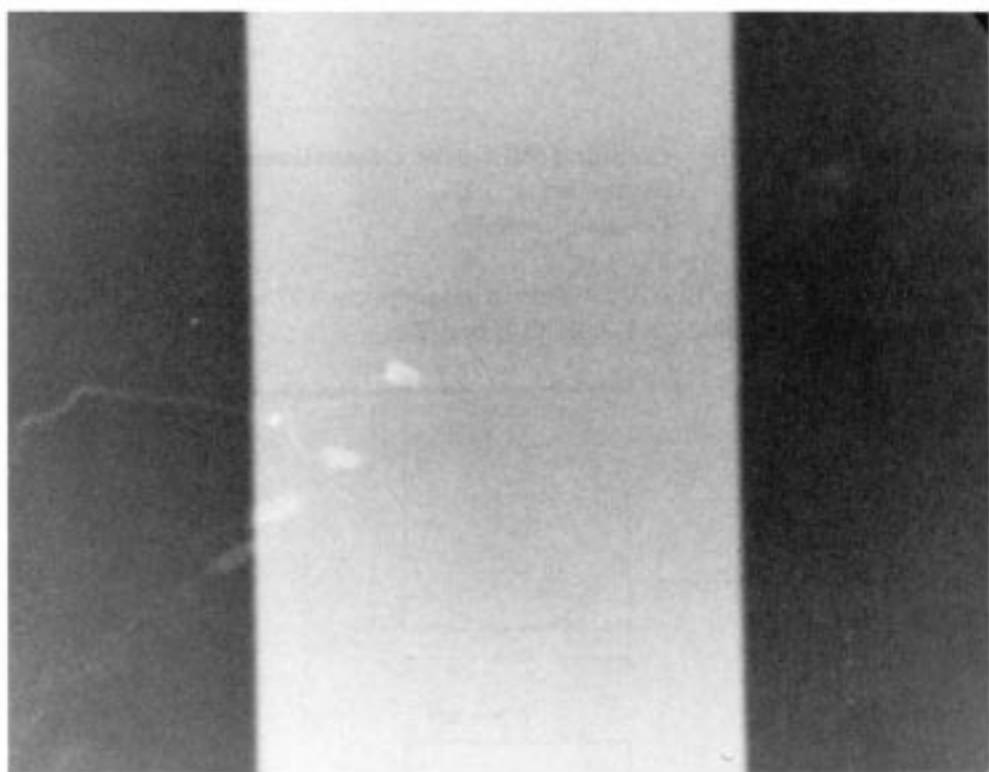
Date: September 1, 1965

Experimenter: Douglas Venable

Radiographic Time: 25.45 μ s

The reflected shocks in PBX-9404 detonation products 0.35 μ s after the detonation waves collided. See Shots 207, 209, 210, and 292.





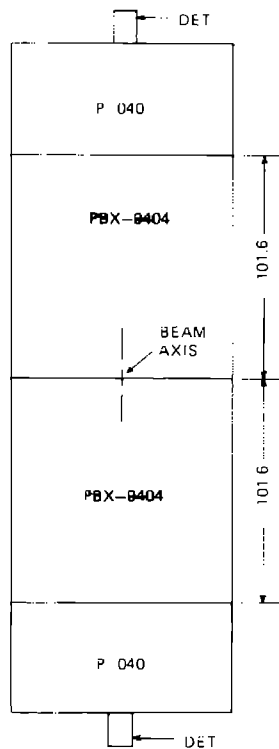
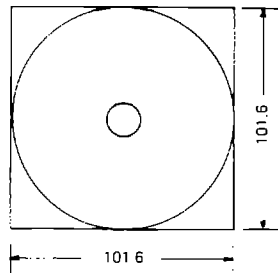
SHOT 209: Colliding PBX-9404 Detonations

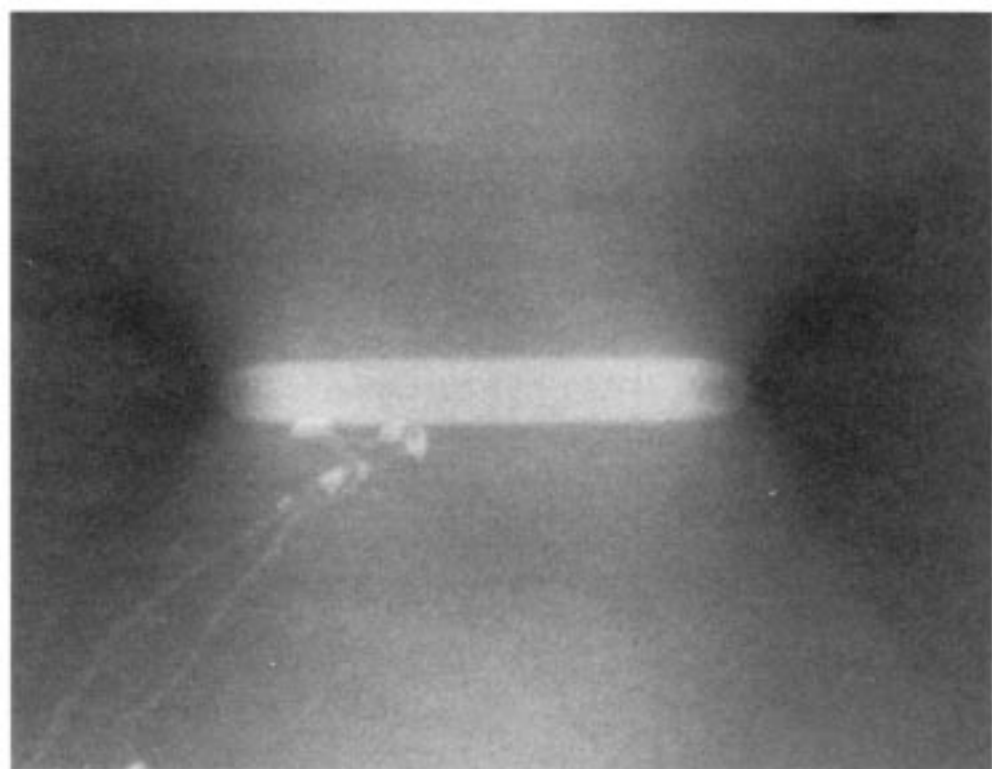
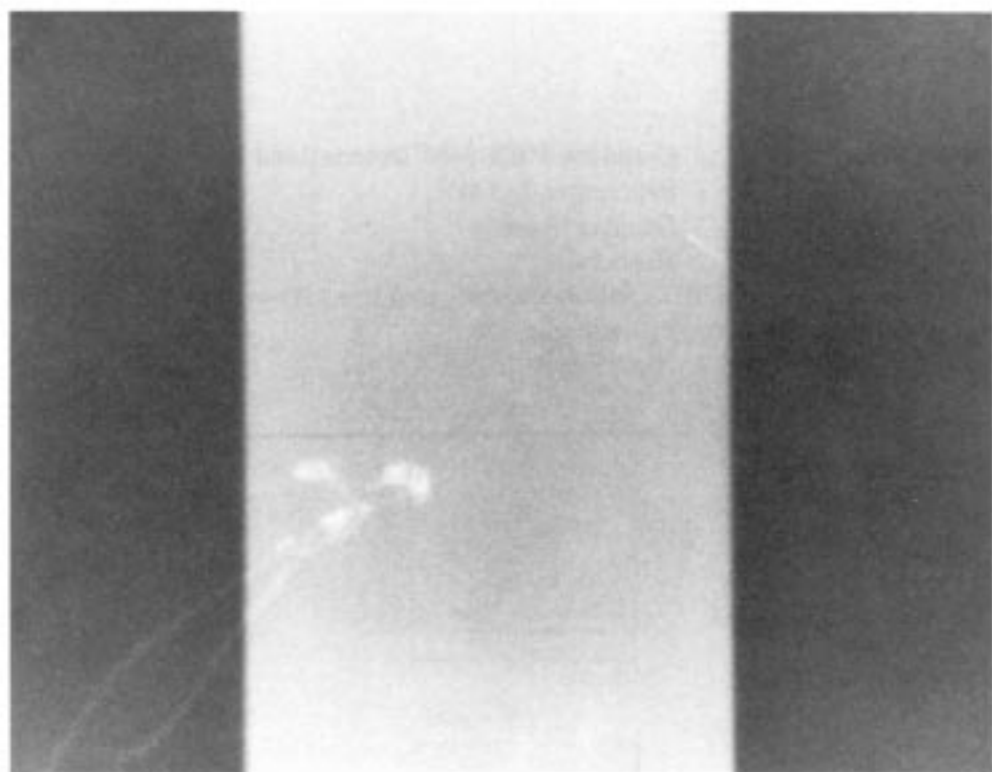
Date: September 1, 1965

Experimenter: Douglas Venable

Radiographic Time: 26.09 μ s

The reflected shocks in PBX-9404 detonation products 0.97 μ s after the detonation waves collided. See Shots 207, 208, 210, and 292.





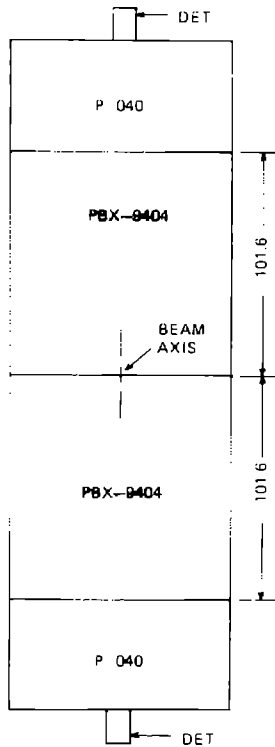
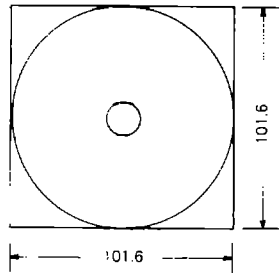
SHOT 210: Colliding PBX-9404 Detonations

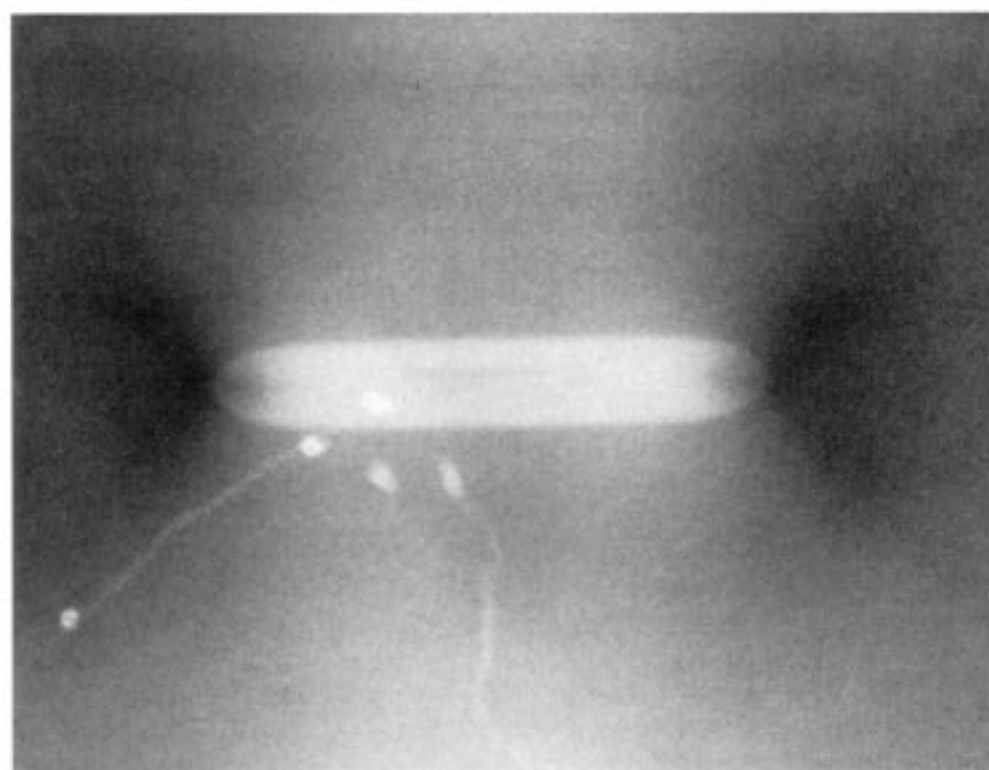
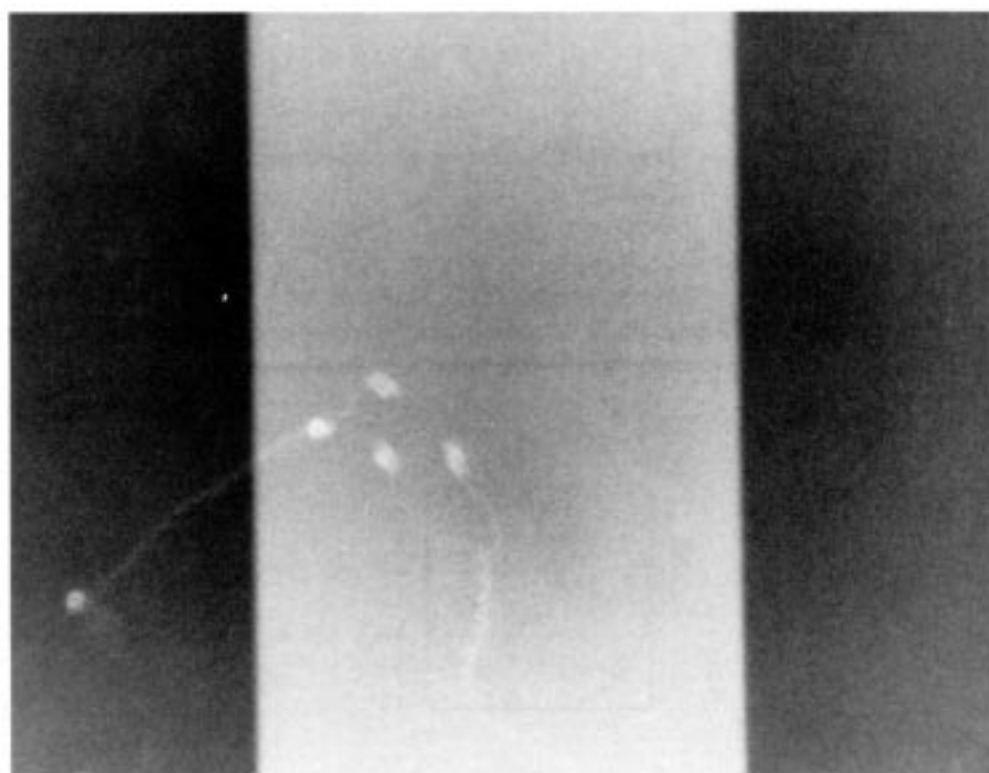
Date: September 1, 1965

Experimenter: Douglas Venable

Radiographic Time: 26.45 μ s

The reflected shocks in PBX-9404 detonation products 1.33 μ s after the detonation waves collided. See Shots 207-209 and 292.





SHOT 211:

Dynamic Fracture of Aluminum

Date:

January 27, 1965

Experimenter:

Douglas Venable

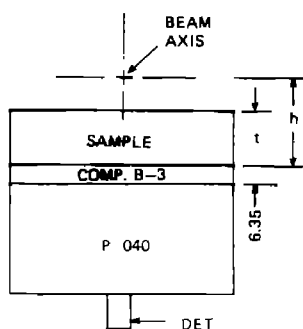
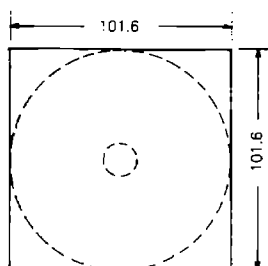
Radiographic Time:

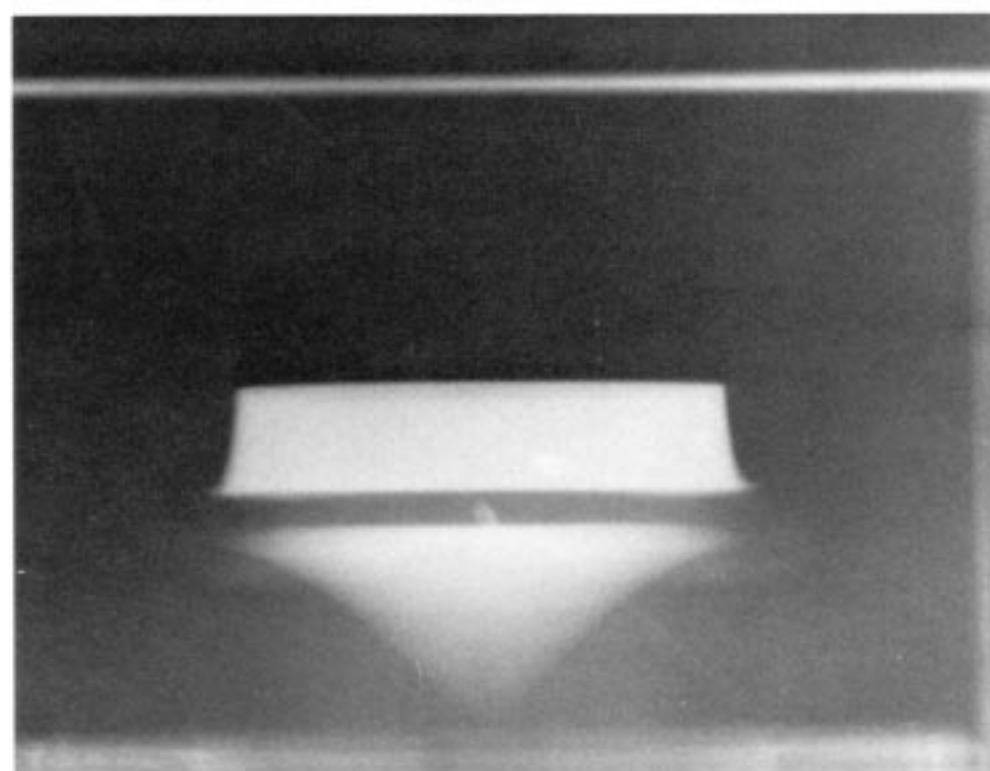
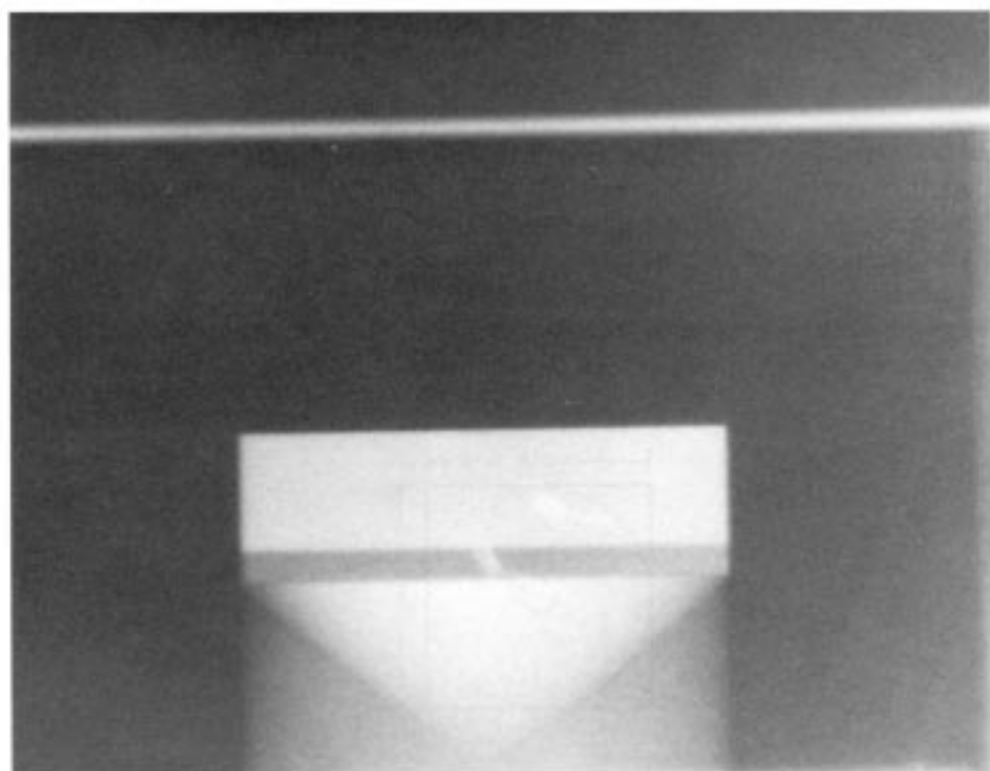
18.28 μ s

References:

Breed et al., 1967; Thurston and Mudd, 1968

Dynamic fracture of 25-mm-thick, t, aluminum. The plate is shocked by 6.35 mm of Composition B-3 initiated by a P-040 lens. h is 28.57 mm.





SHOT 212:

Dynamic Fracture of Aluminum

Date:

January 27, 1965

Experimenter:

Douglas Venable

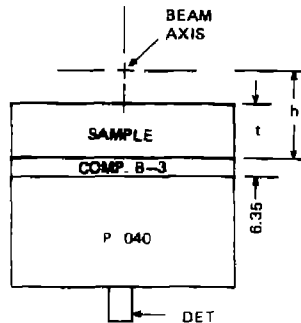
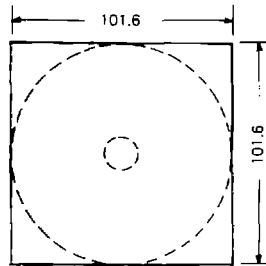
Radiographic Time:

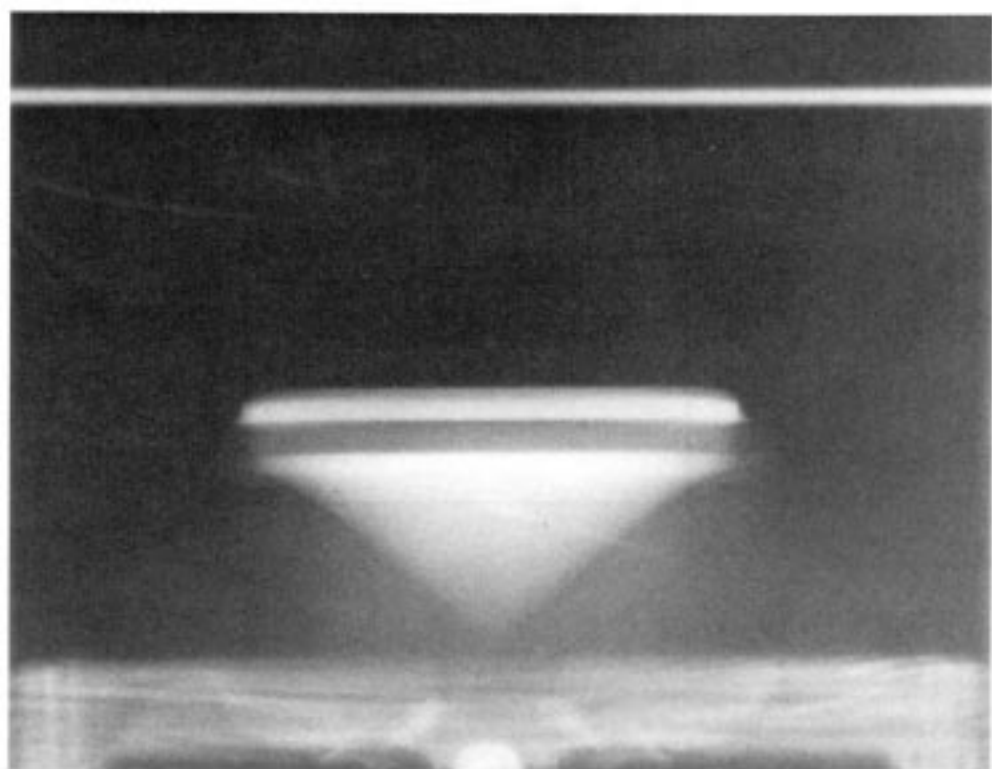
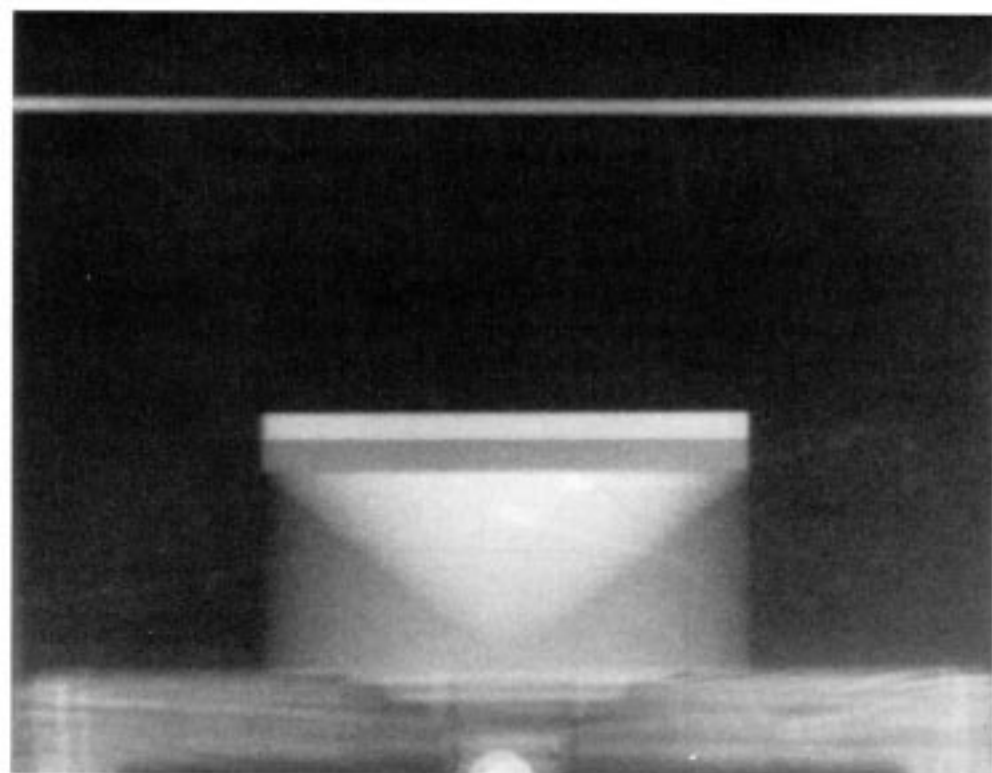
16.39 μ s

References:

Breed et al., 1967; Thurston and Mudd, 1968

Dynamic fracture of 6.0-mm-thick, t , aluminum. The plate is shocked by 6.35 mm of Composition B-3 initiated by a P-040 lens. h is 9.52 mm.





SHOT 213:

Dynamic Fracture of Aluminum

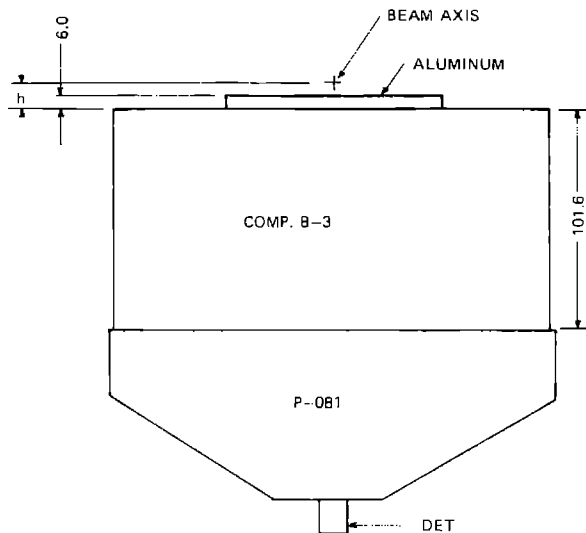
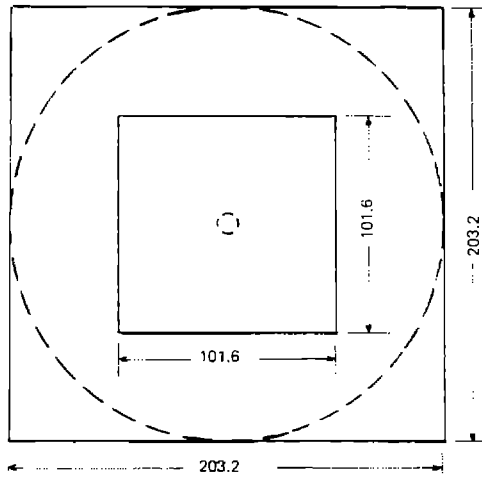
Date: January 26, 1965

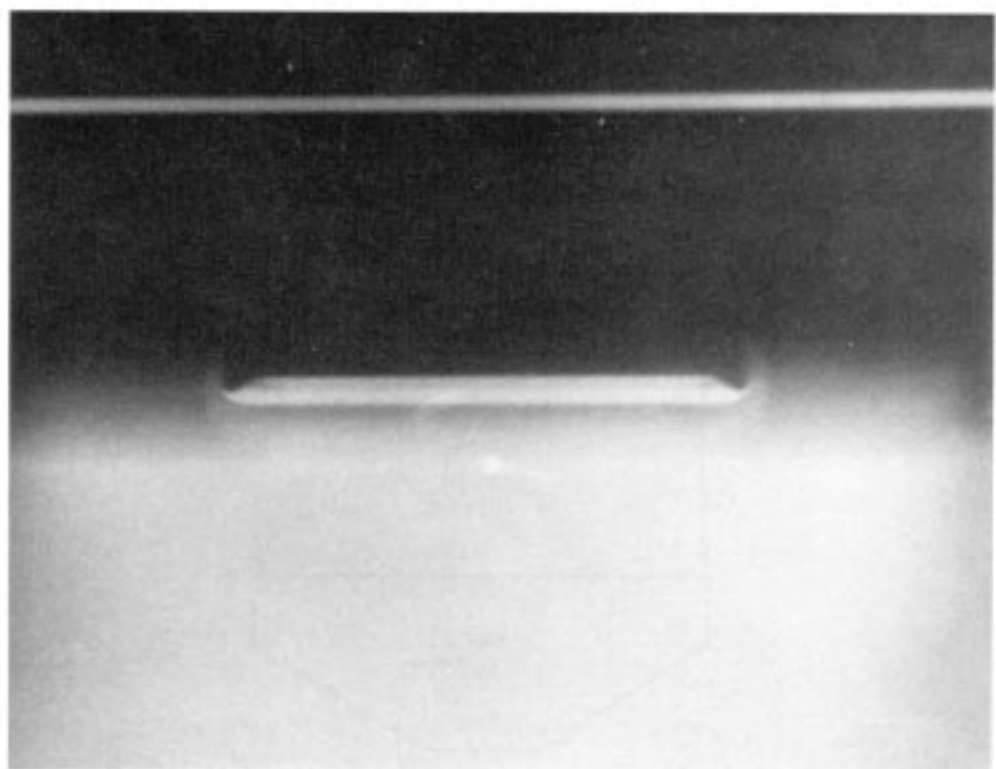
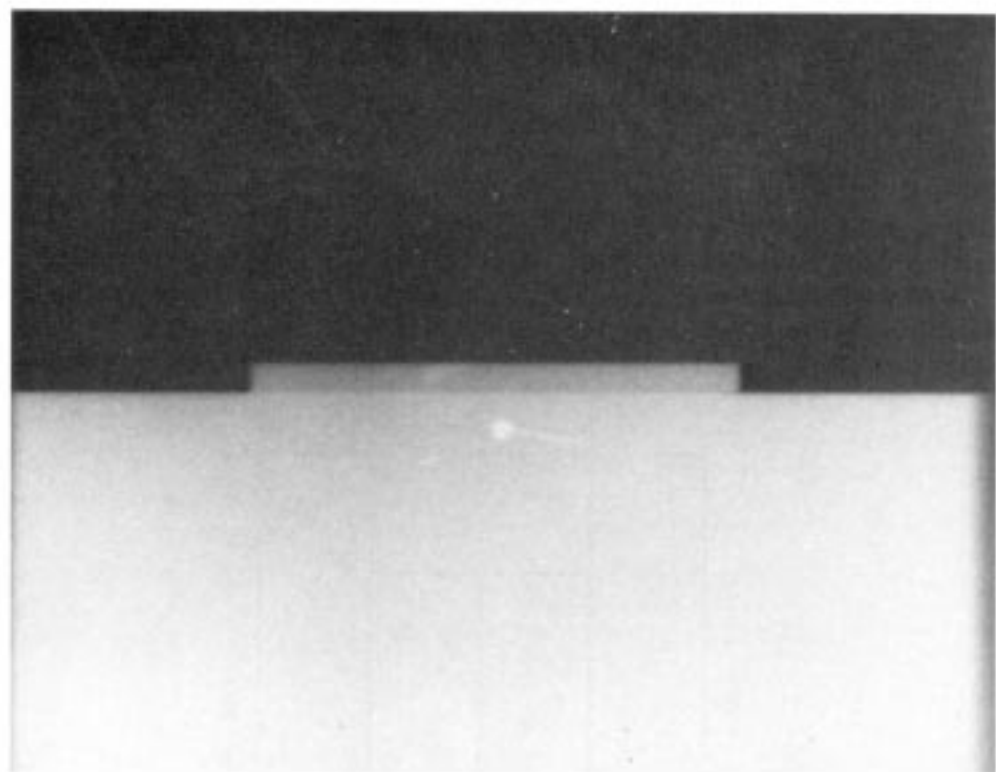
Experimenter: Douglas Venable

Radiographic Time: 37.53 μ s

References: Breed et al., 1967; Thurston and Mudd, 1968

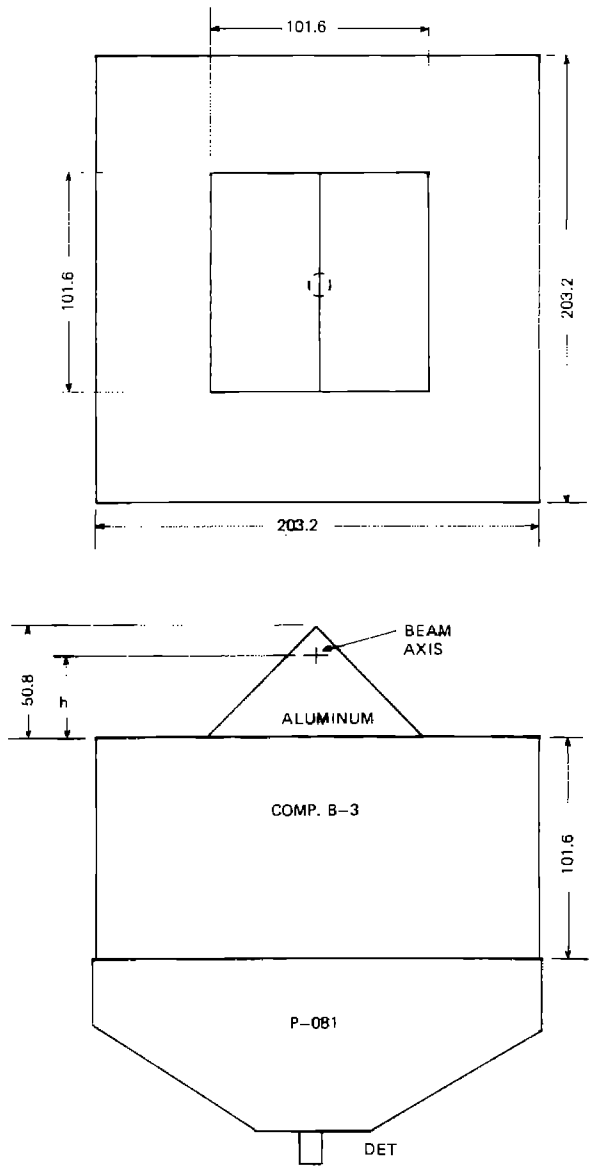
Dynamic fracture of 6.0-mm-thick aluminum. The plate is shocked by 101.6 mm of Composition B-3 initiated by a P-081 lens. h is 12.7 mm.

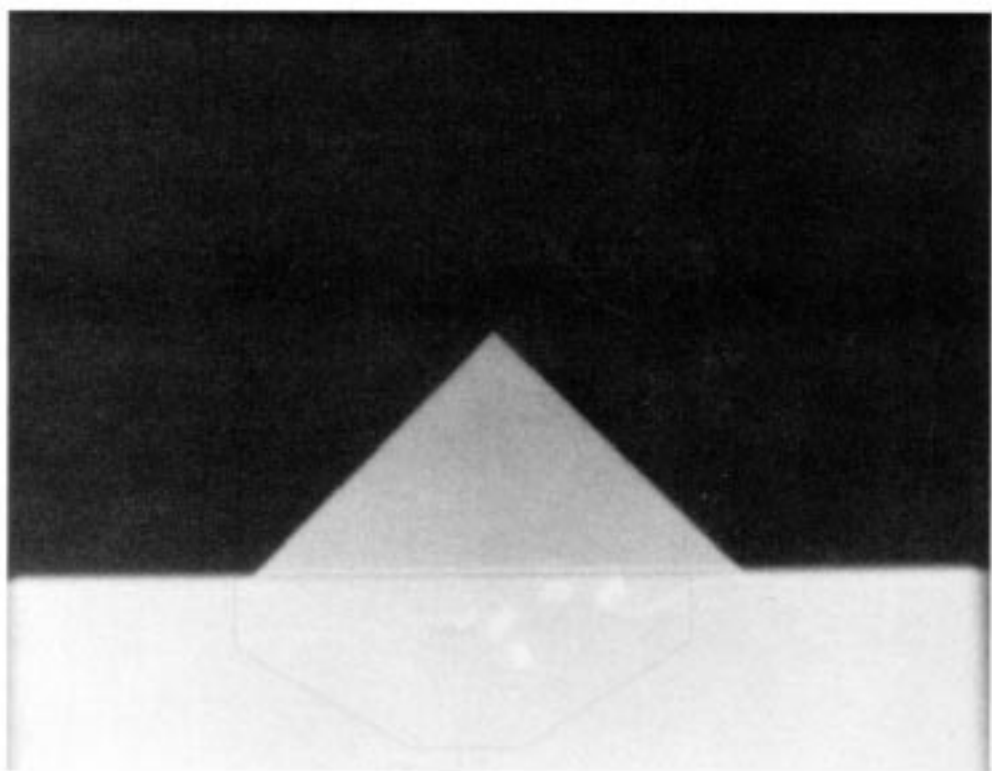
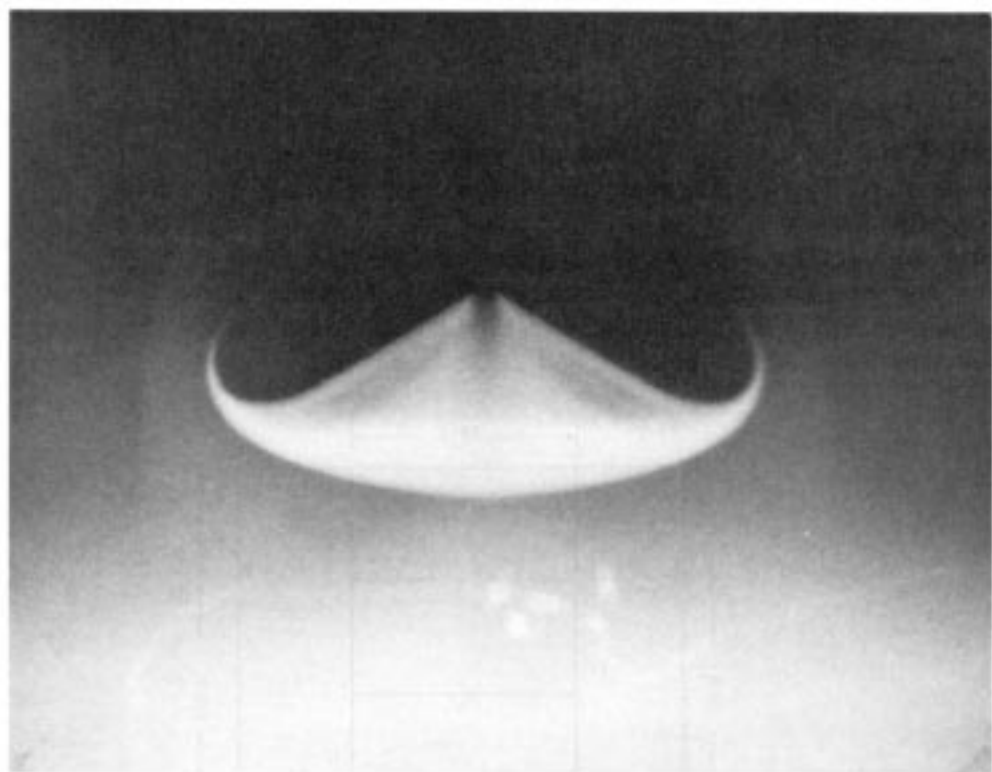




SHOT 214: **Aluminum Wedge**
Date: **September 2, 1965**
Experimenter: **Roger W. Taylor**
Radiographic Time: **43.84 μ s**

A shock wave generated by a Composition B-3 detonation wave interacts with a 90° aluminum wedge. h is 38.1 mm. See Shots 39, 135-138, and 215-217.





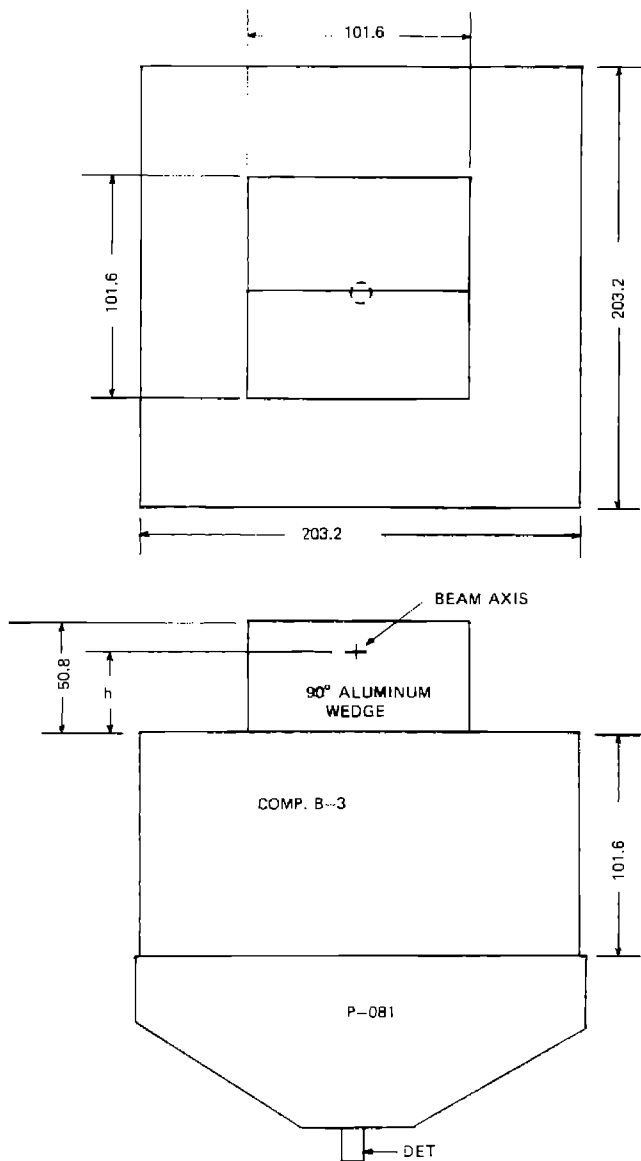
SHOT 215: Aluminum Wedge

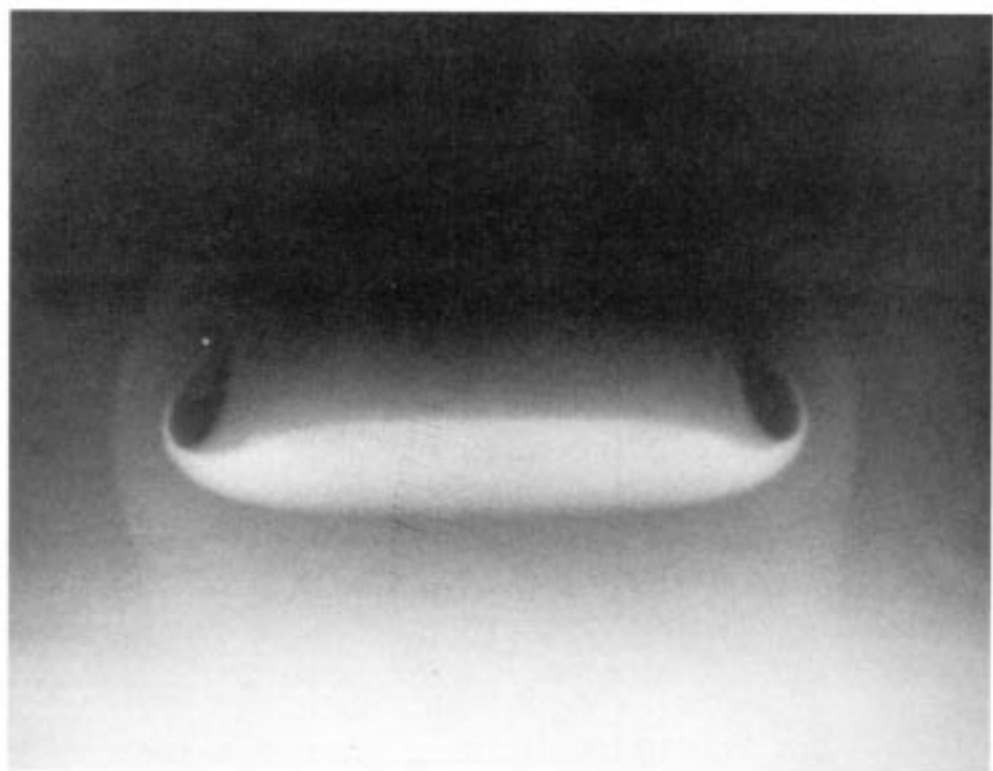
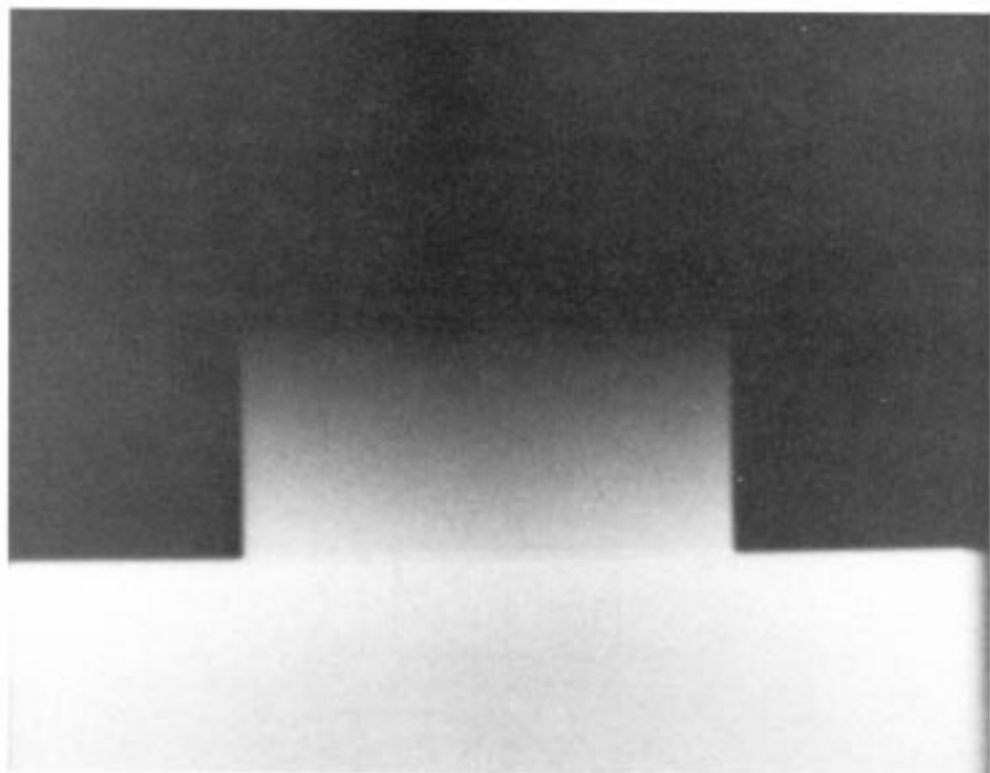
Date: September 7, 1965

Experimenter: Roger W. Taylor

Radiographic Time: 43.82 μ s

A shock wave generated by a Composition B-3 detonation interacts with a 90° aluminum wedge. This shot is identical to Shot 214 except for the beam orientation. See Shots 39, 135-138, 216, and 217. h is 38.1 mm.





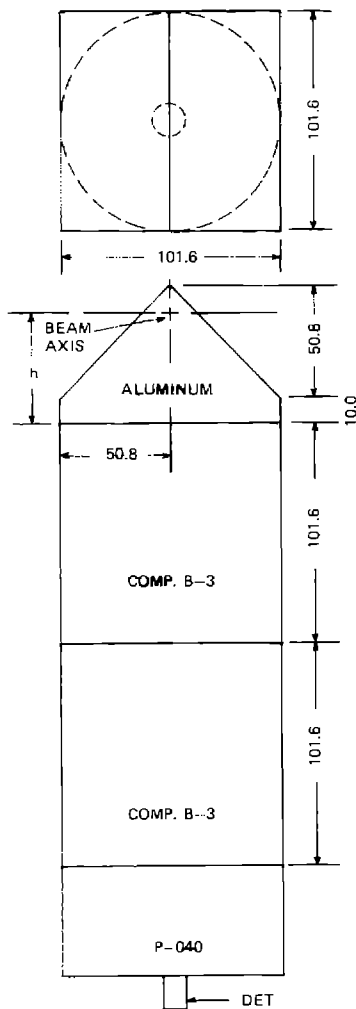
SHOT 216: Aluminum Wedge

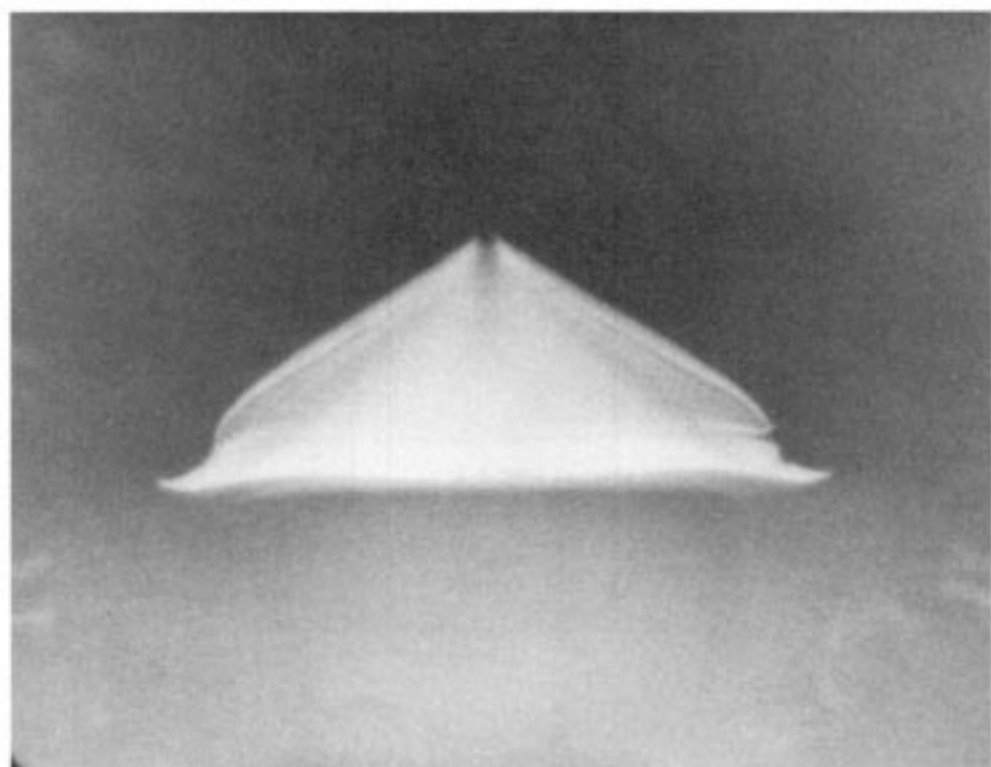
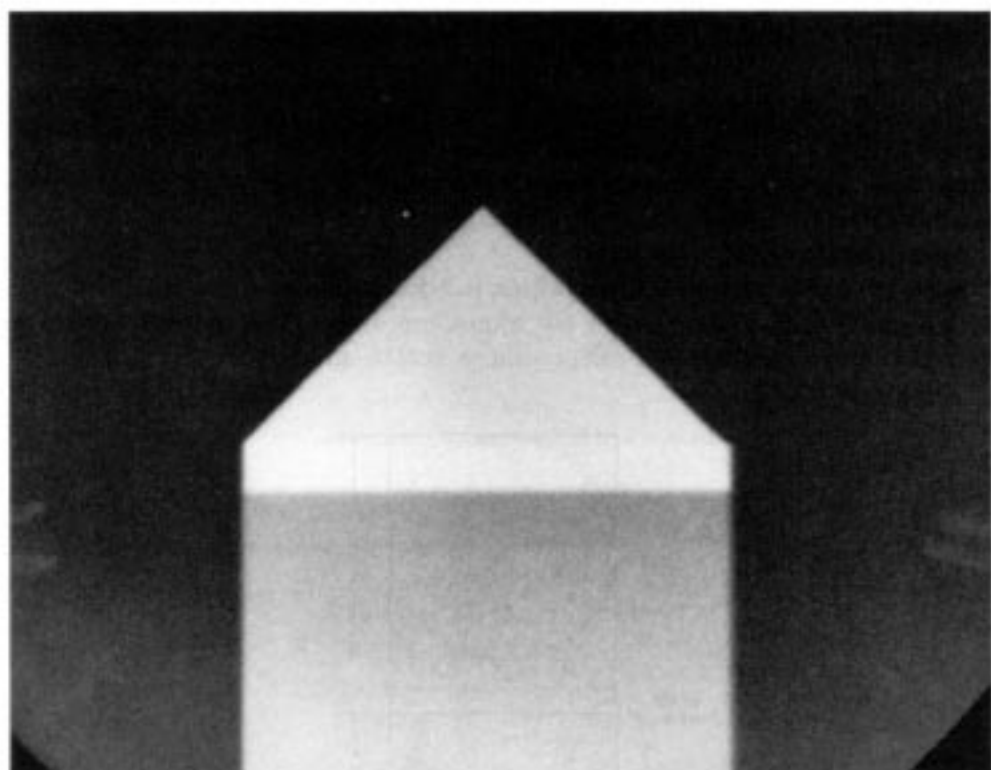
Date: September 7, 1965

Experimenter: Roger W. Taylor

Radiographic Time: 48.73 μ s

A shock wave generated by a Composition B-3 detonation interacts with 10.0-mm-thick aluminum in contact with a 90° aluminum wedge. h is 50.8 mm. See Shots 39, 135-138, 214, 215, and 217.





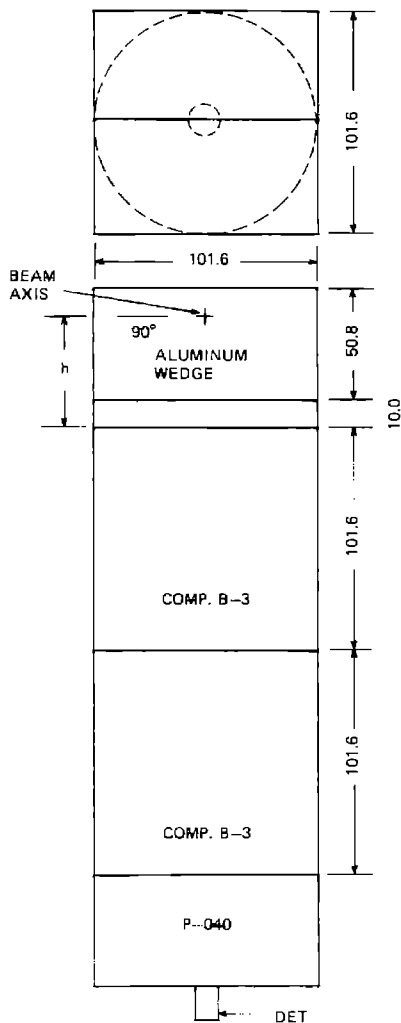
SHOT 217: Aluminum Wedge

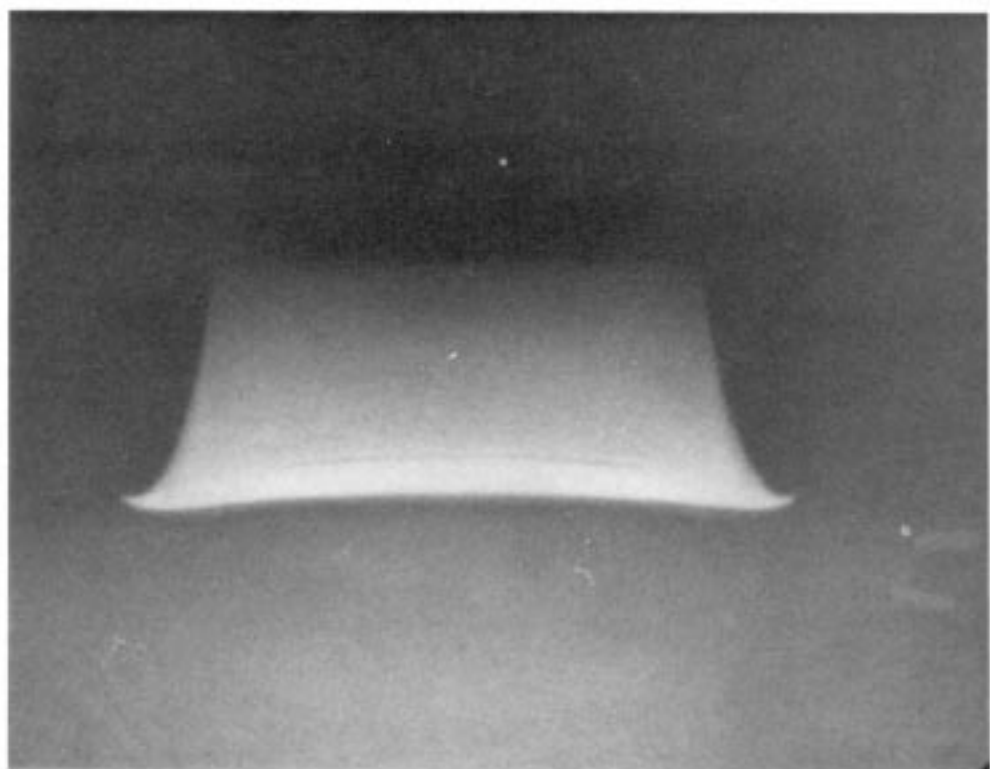
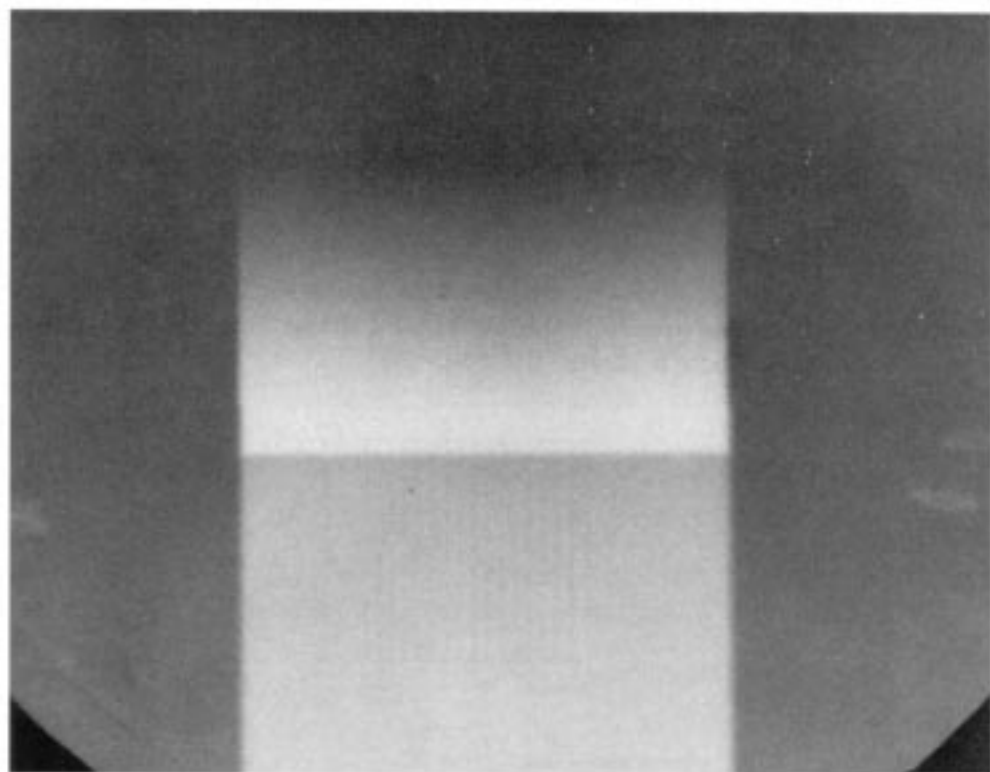
Date: September 9, 1965

Experimenter: Roger W. Taylor

Radiographic Time: 48.76 μ s

A shock wave generated by a Composition B-3 detonation interacts with 10.0-mm-thick aluminum in contact with a 90° aluminum wedge. The shot is identical to Shot 216 except for the beam orientation. h is 50.8 mm.





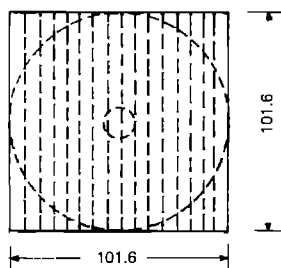
SHOT 220: **Composition B-3 with Embedded Tantalum Foils**

Date: July 19, 1965

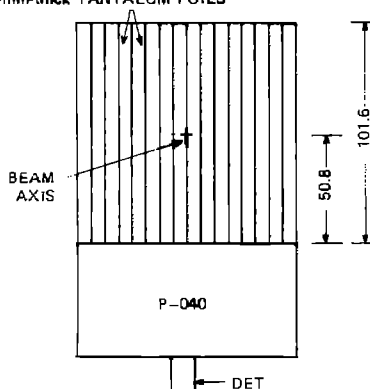
Experimenter: Douglas Venable

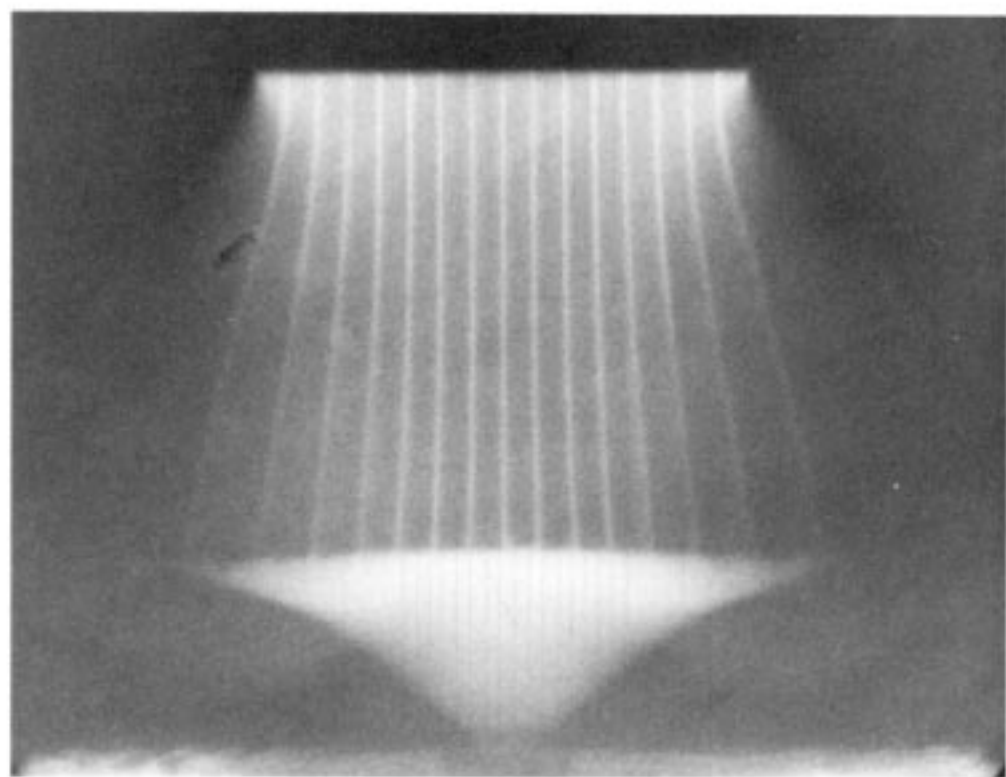
Radiographic Time: 26.32 μ s

Sixteen slabs of 6.35-mm-thick Composition B-3 separated by 0.025-mm-thick tantalum foils were initiated parallel to the foils by a P-040 lens. The flow of the unconfined detonation products is shown. See Shot 290.



SIXTEEN 6.35-mm-thick
COMP. B-3 SLABS SEPARATED BY
0.025-mm-thick TANTALUM FOILS





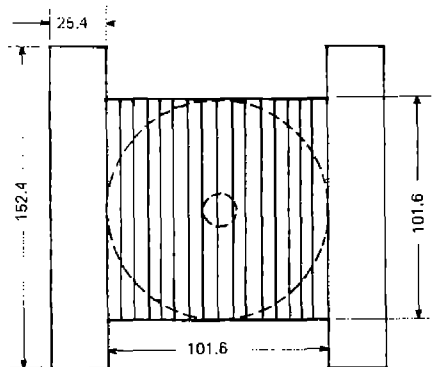
SHOT 221: Composition B-3 with Embedded Tantalum Foils

Date: July 19, 1965

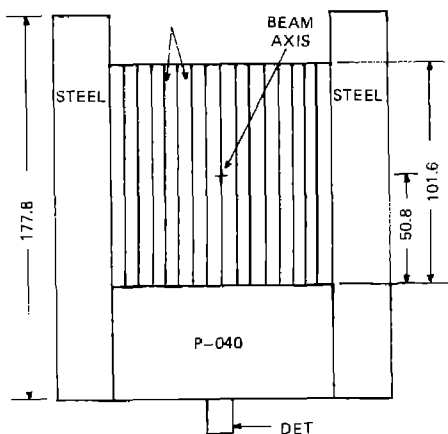
Experimenter: Douglas Venable

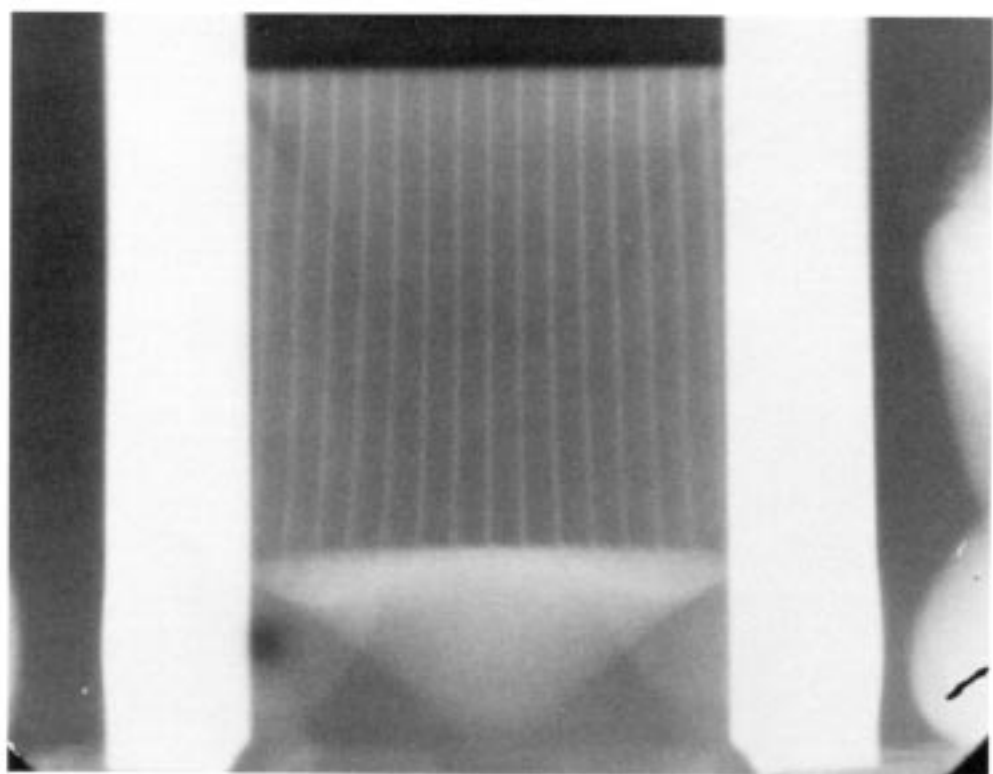
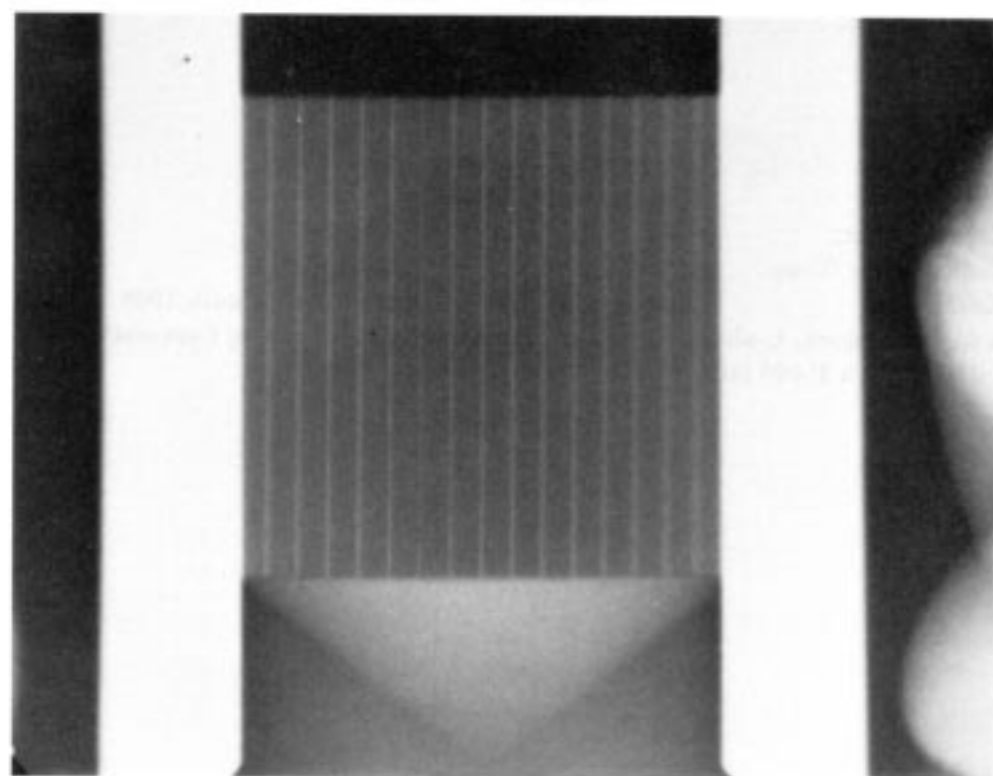
Radiographic Time: 26.32 μ s

Sixteen slabs of 6.35-mm-thick Composition B-3 separated by 0.025-mm-thick tantalum foils were initiated parallel to the foils by a P-040 lens. The flow of the detonation products confined by 25.4-mm-thick steel is shown. See Shot 272.



SIXTEEN 6.35-mm-thick
COMP. B-3 SLABS SEPARATED BY
0.025-mm-thick TANTALUM FOILS





SHOT 222:

Dynamic Fracture of Aluminum

Date:

September 9, 1965

Experimenter:

Roger W. Taylor

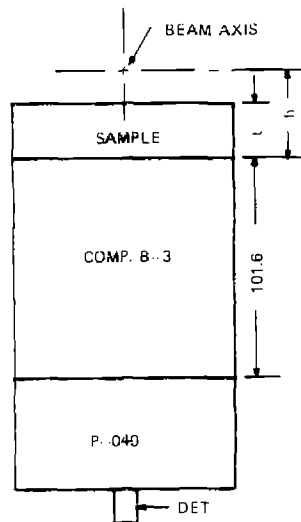
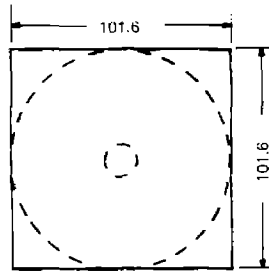
Radiographic Time:

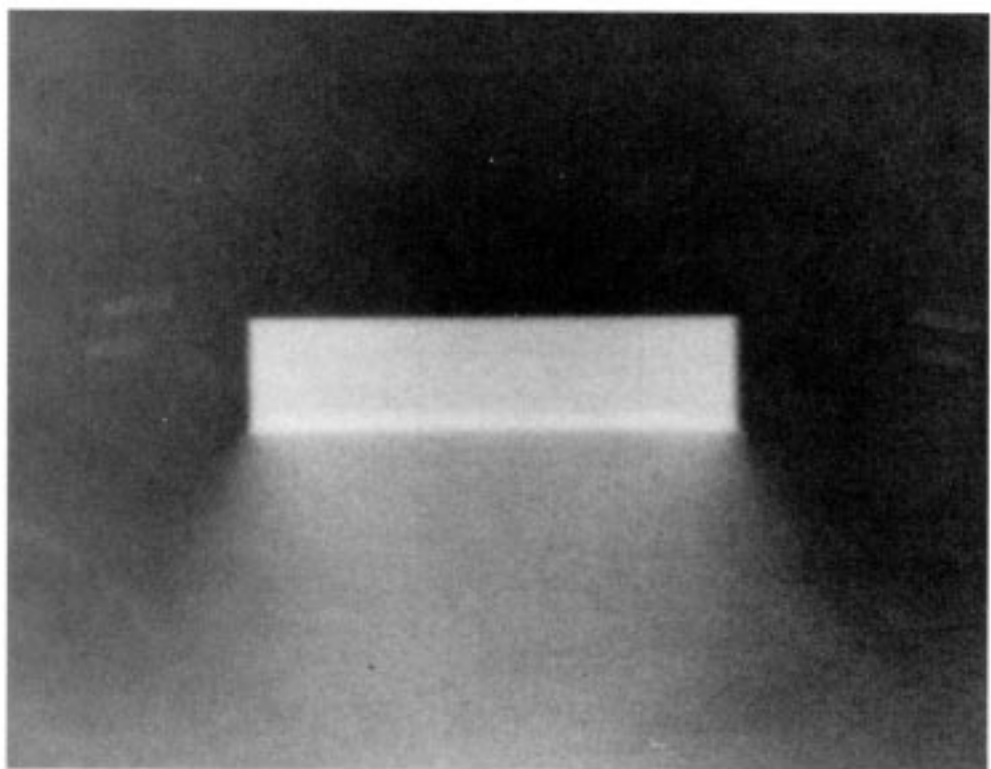
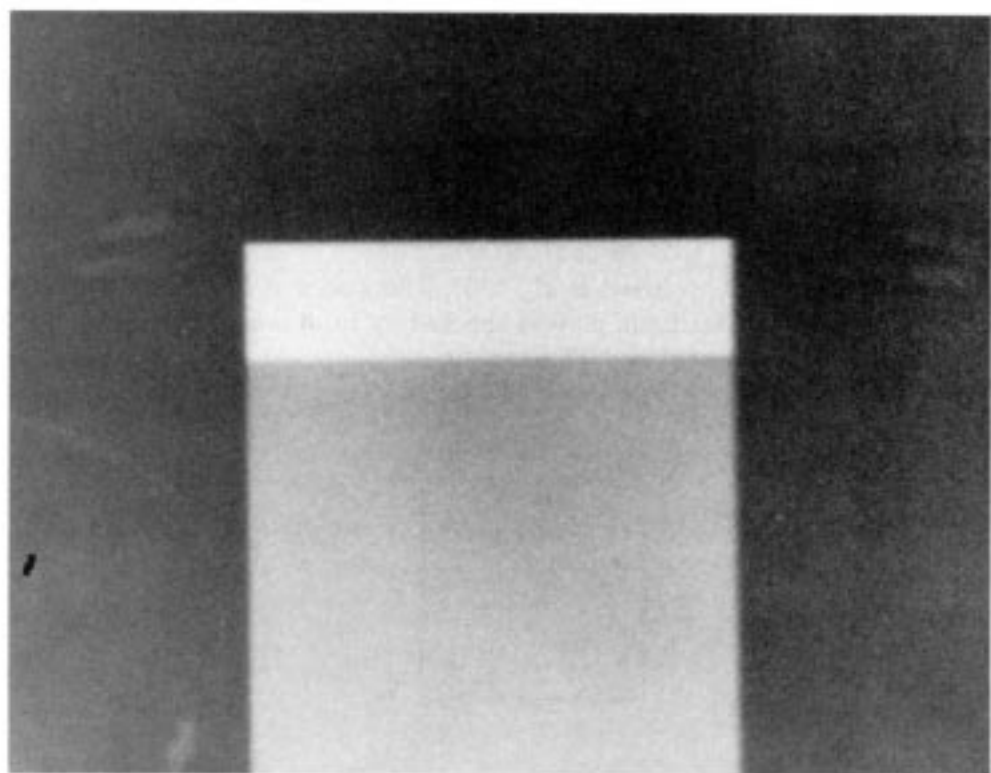
26.95 μ s

References:

Breed et al., 1967; Thurston and Mudd, 1968

A 25.0-mm-thick, t , aluminum plate is shocked by 101.6 mm of Composition B-3 initiated by a P-040 lens. h is 3.17 mm.





SHOT 223:

Dynamic Fracture of Aluminum

Date:

September 23, 1965

Experimenter:

Roger W. Taylor

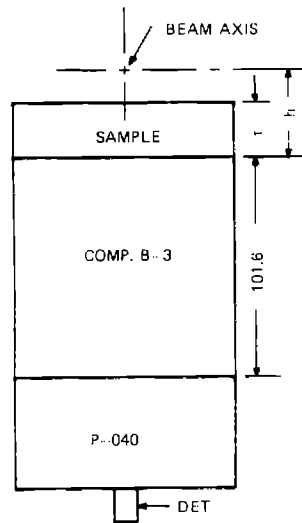
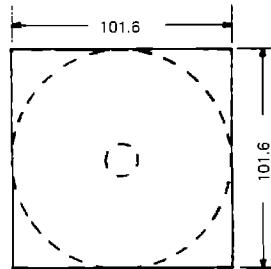
Radiographic Time:

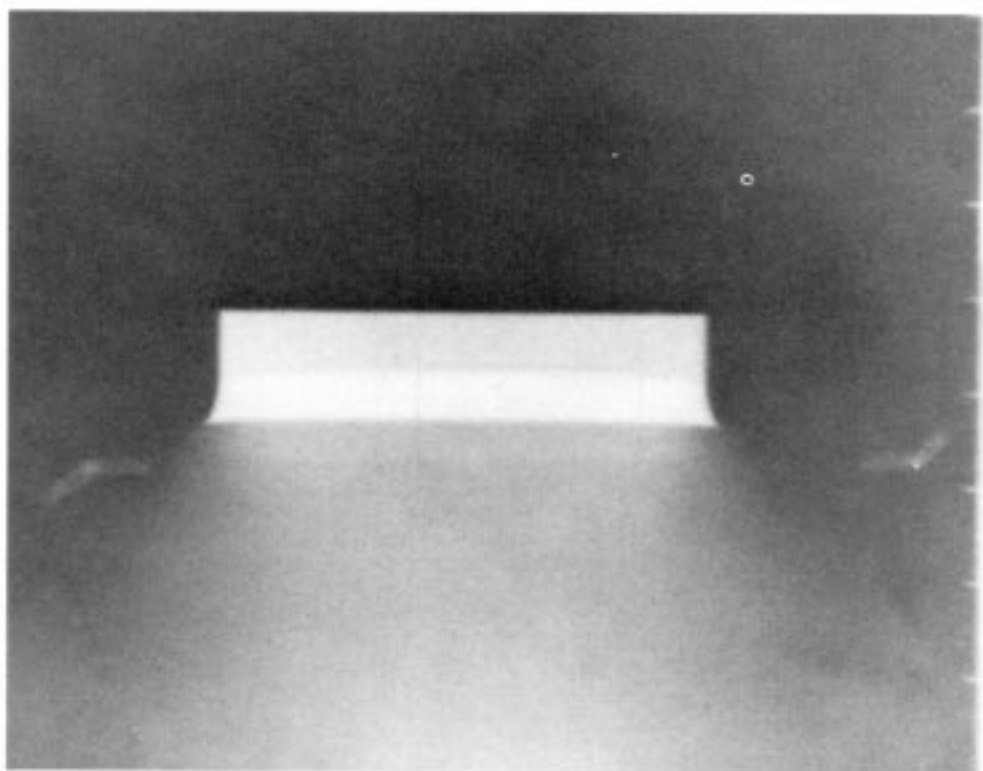
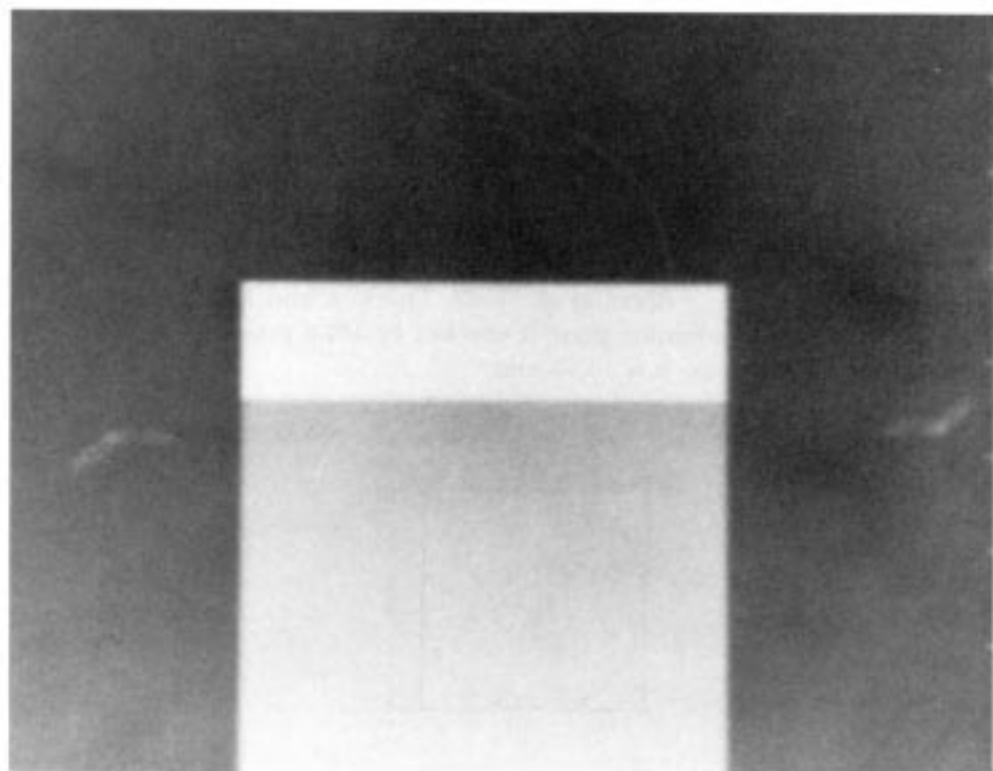
27.88 μ s

References:

Breed et al., 1967; Thurston and Mudd, 1968

A 25.0-mm-thick, t , aluminum plate is shocked by 101.6 mm of Composition B-3 initiated by a P-040 lens. h is 3.17 mm.





SHOT 224:

Dynamic Fracture of Aluminum

Date:

September 28, 1965

Experimenter:

Roger W. Taylor

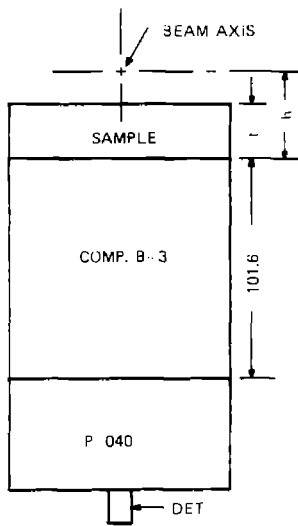
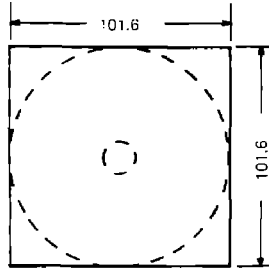
Radiographic Time:

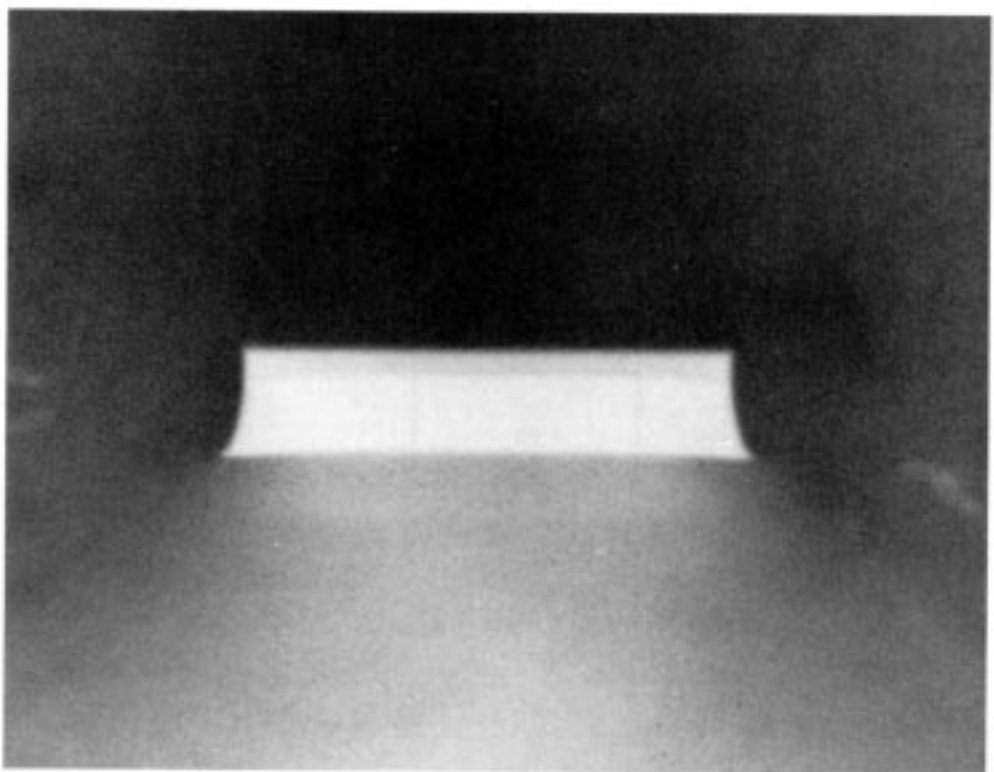
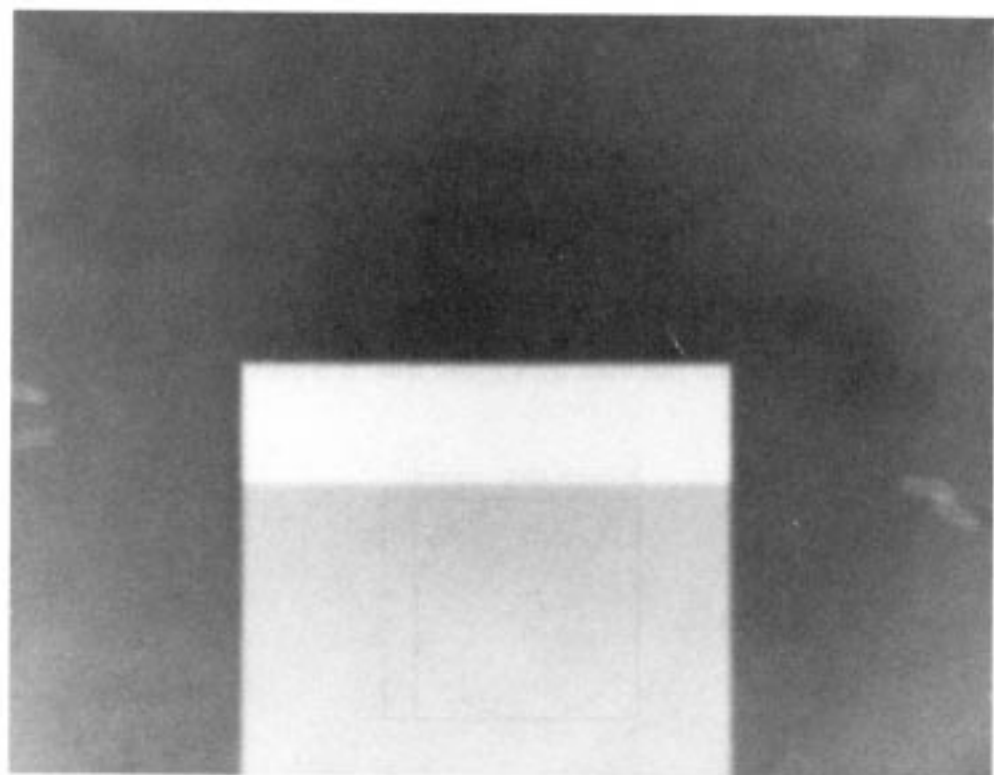
28.9 μ s

References:

Breed et al., 1967; Thurston and Mudd, 1968

A 25.0-mm-thick, t , aluminum plate is shocked by 101.6 mm of Composition B-3 initiated by a P-040 lens. h is 12.70 mm.





SHOT 226: Dynamic Fracture of Aluminum

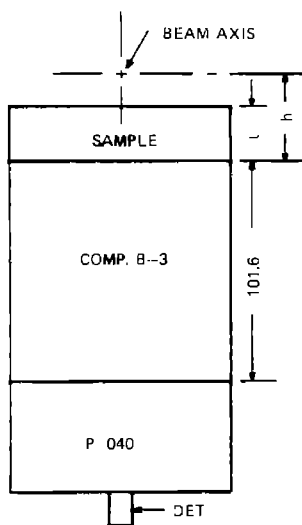
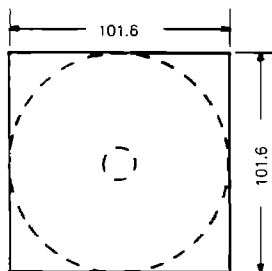
Date: October 5, 1965

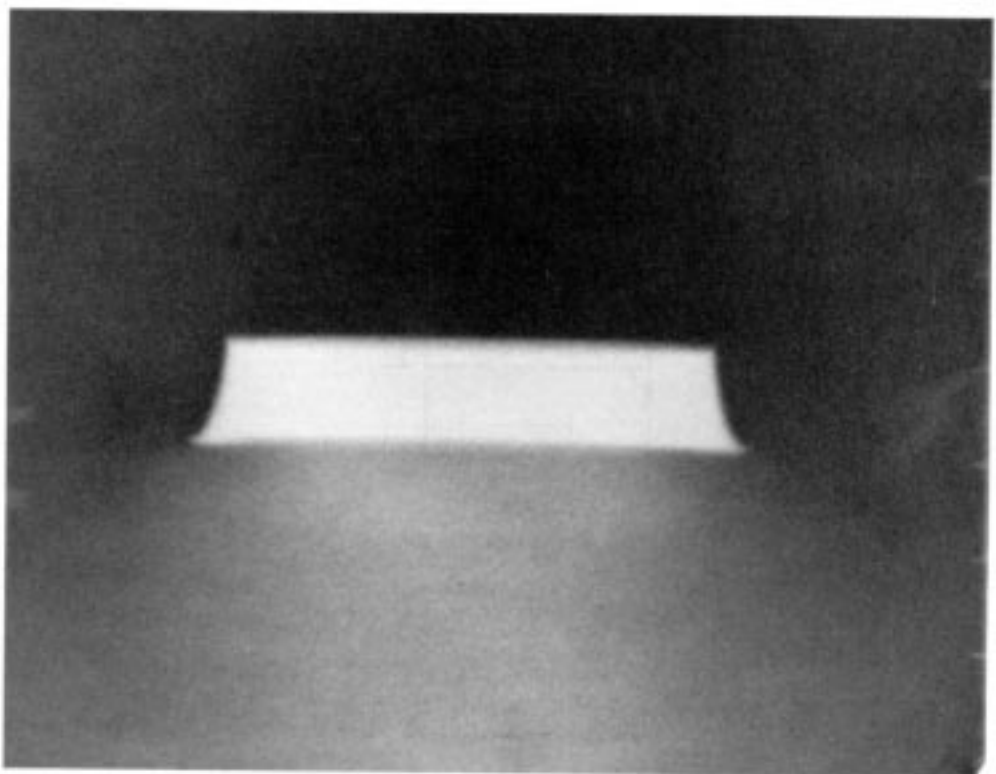
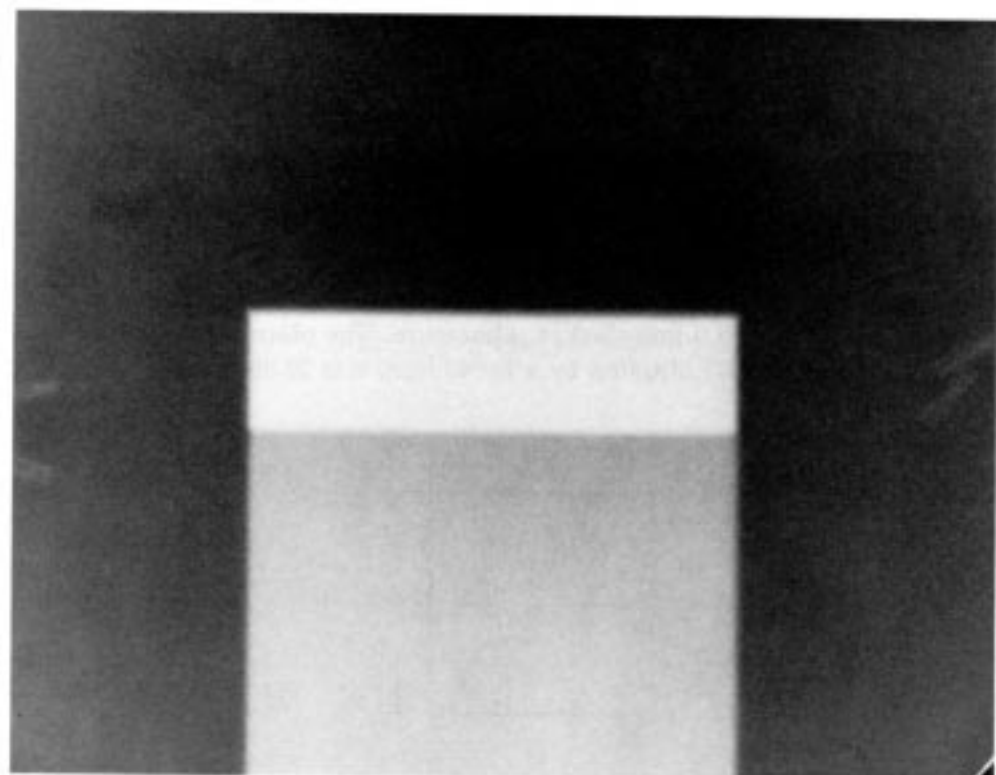
Experimenter: Roger W. Taylor

Radiographic Time: 29.89 μ s

References: Breed et al., 1967; Thurston and Mudd, 1968

Dynamic fracture of 25.0-mm-thick, t, aluminum. The plate is shocked by 101.6 mm of Composition B-3 initiated by a P-040 lens. h is 25.4 mm.





SHOT 227:

Dynamic Fracture of Aluminum

Date:

October 6, 1965

Experimenter:

Roger W. Taylor

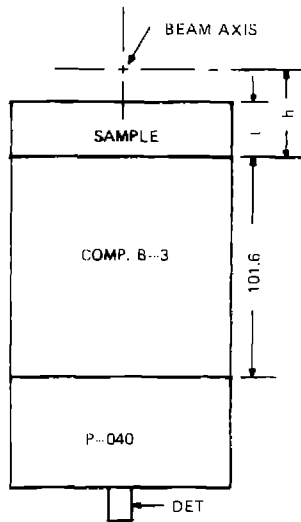
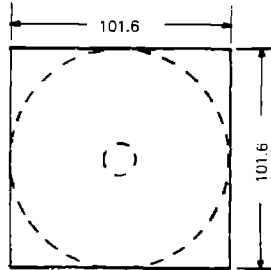
Radiographic Time:

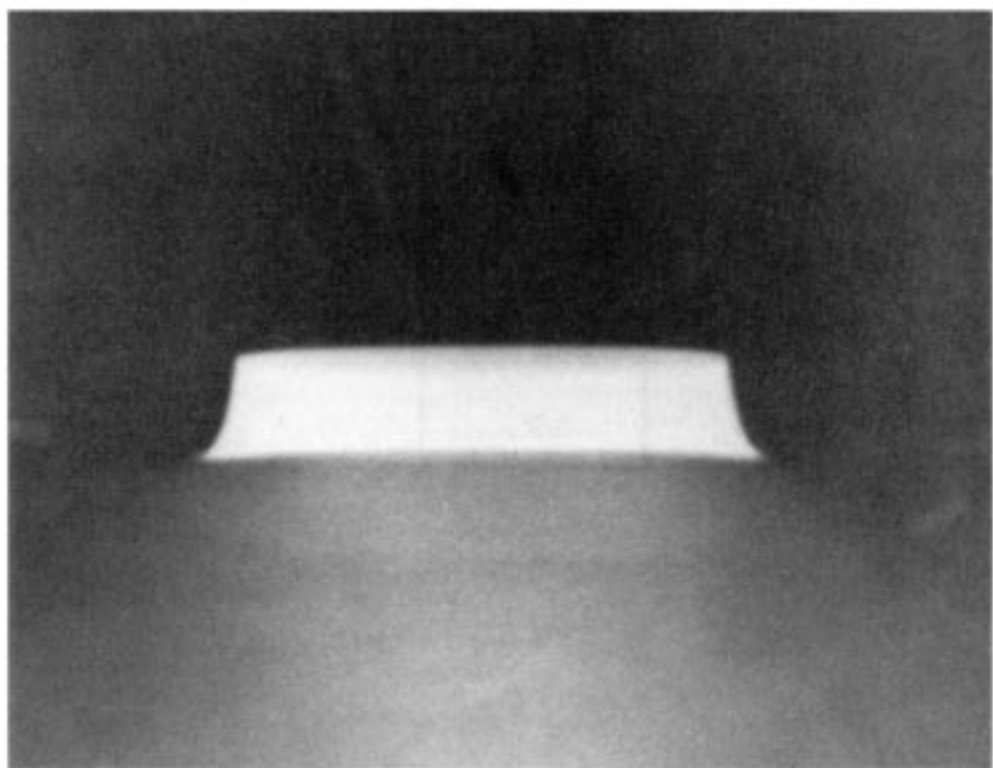
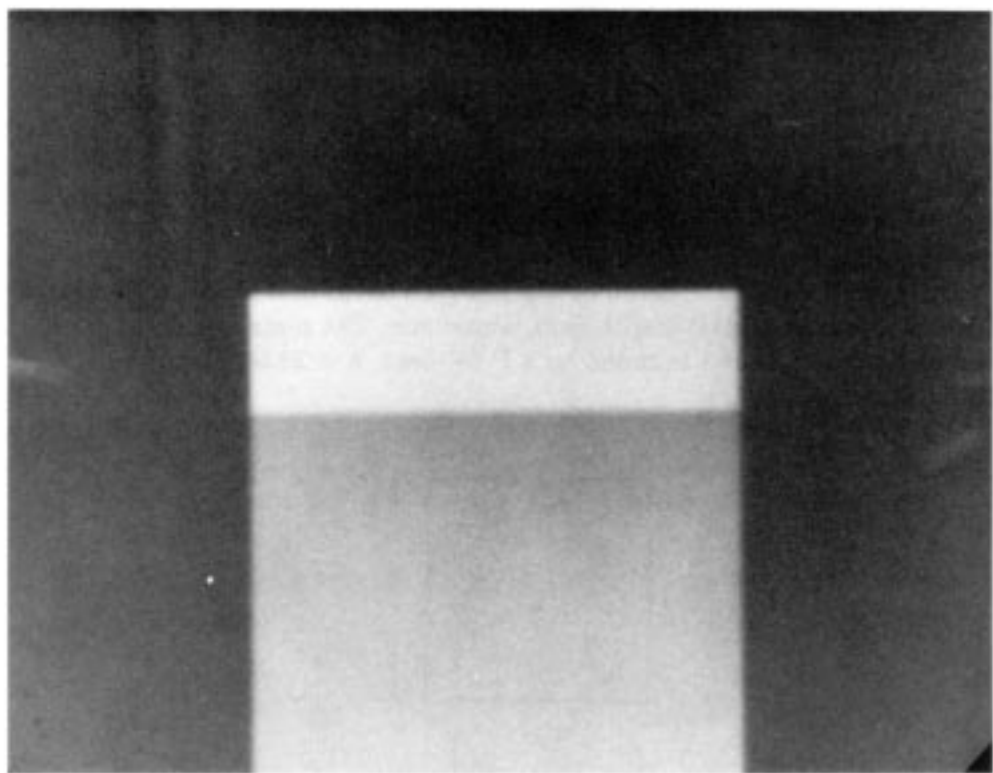
30.41 μ s

References:

Breed et al., 1967; Thurston and Mudd, 1968

Dynamic fracture of 25.0-mm-thick, *t*, aluminum. The plate is shocked by 101.6 mm of Composition B-3 initiated by a P-040 lens. *h* is 26.99 mm.





SHOT 228:

Dynamic Fracture of Aluminum

Date:

October 6, 1965

Experimenter:

Roger W. Taylor

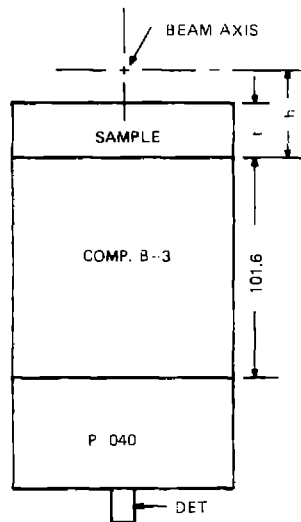
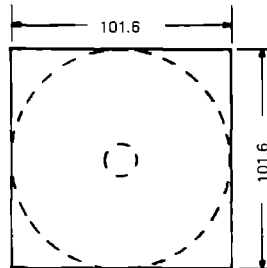
Radiographic Time:

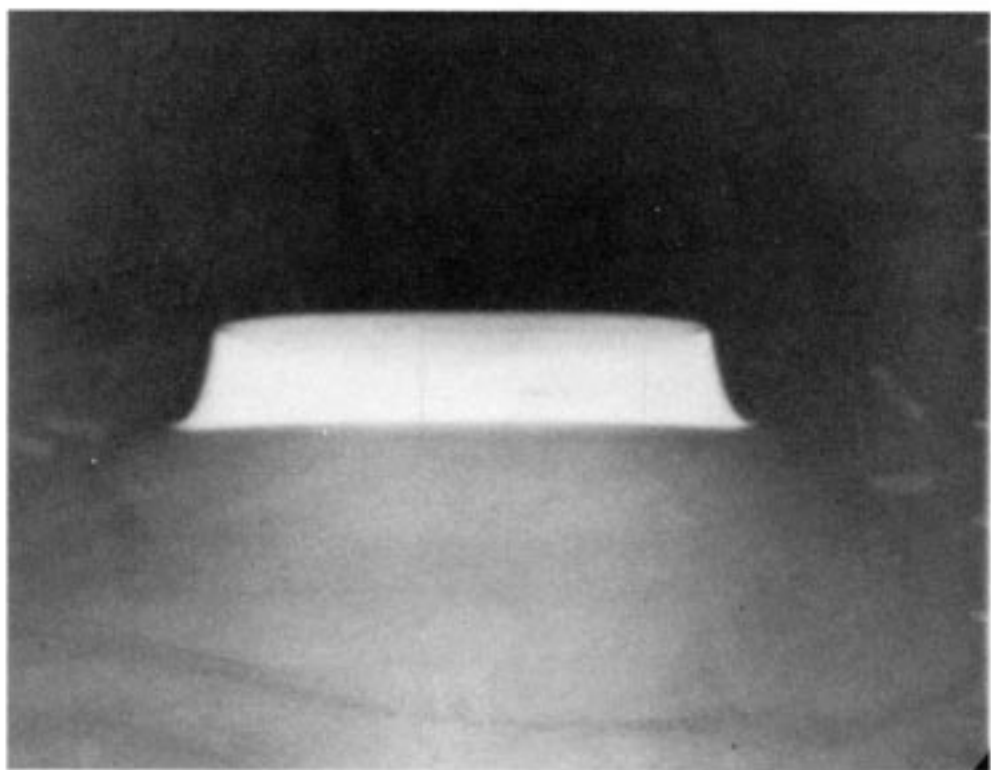
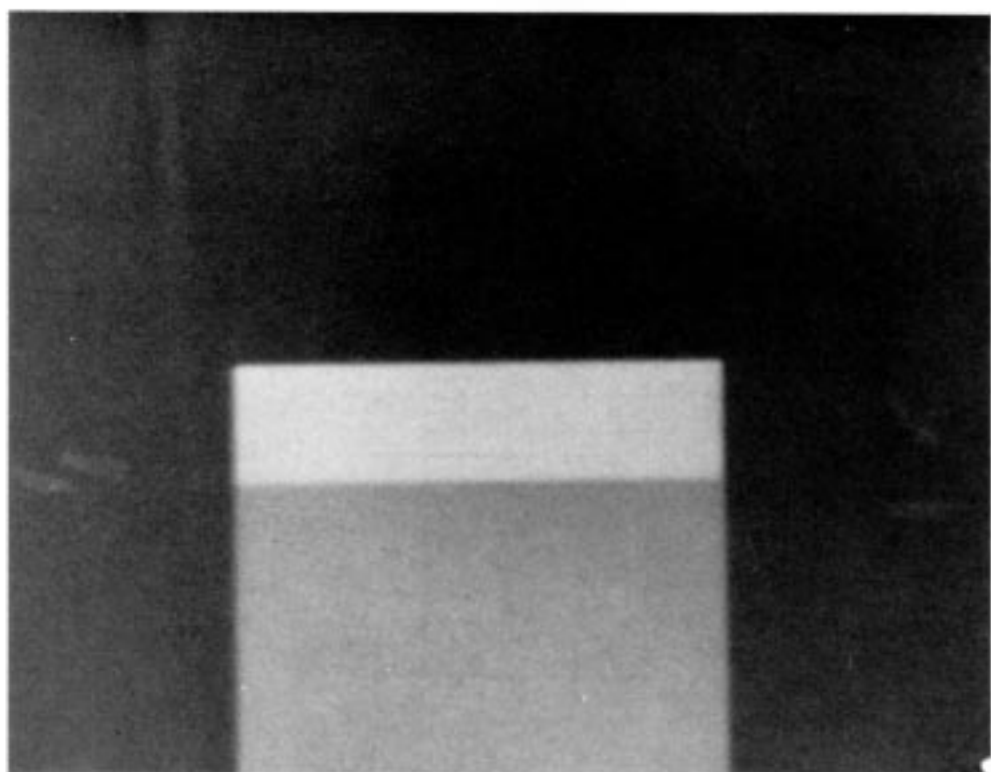
30.92 μ s

References:

Breed et al., 1967; Thurston and Mudd, 1968

Dynamic fracture of 25.0-mm-thick, *t*, aluminum. The plate is shocked by 101.6 mm of Composition B-3 initiated by a P-040 lens. *h* is 28.58 mm.





SHOT 229:

Dynamic Fracture of Aluminum

Date:

October 6, 1965

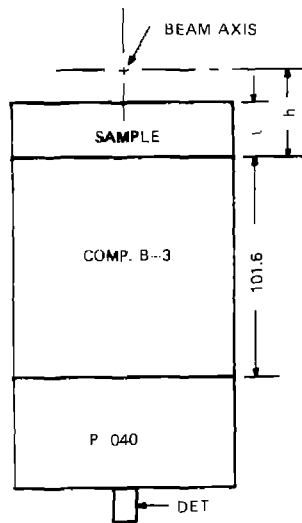
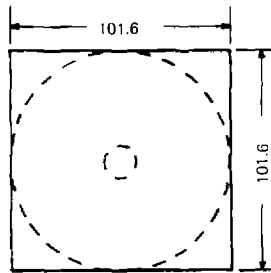
Experimenter:

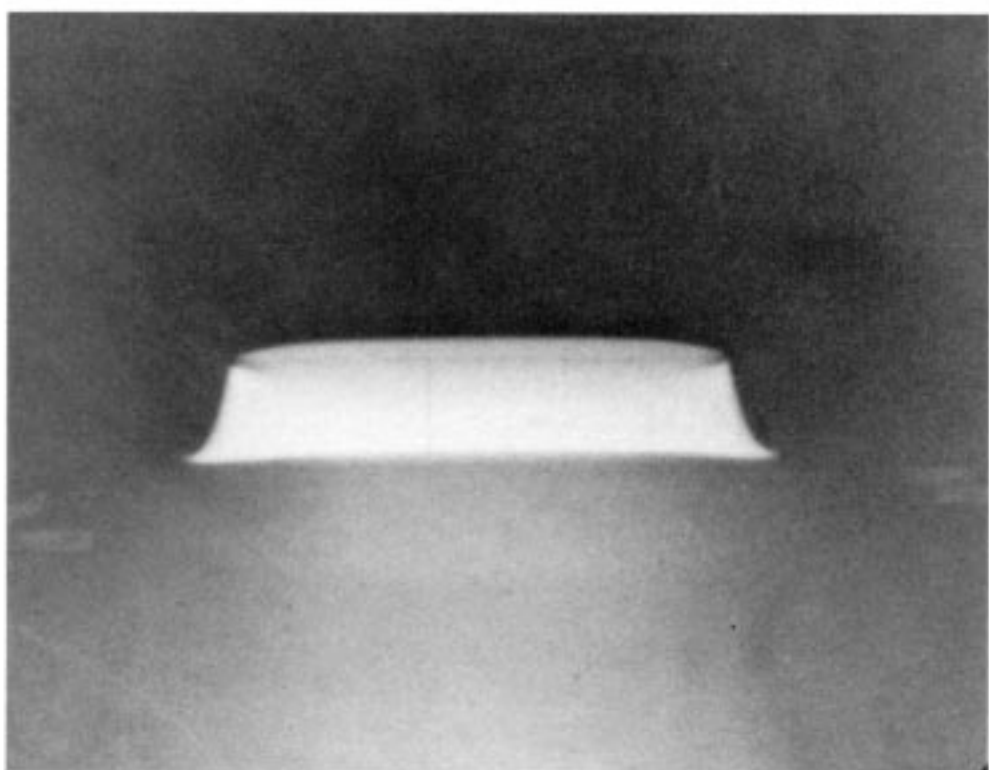
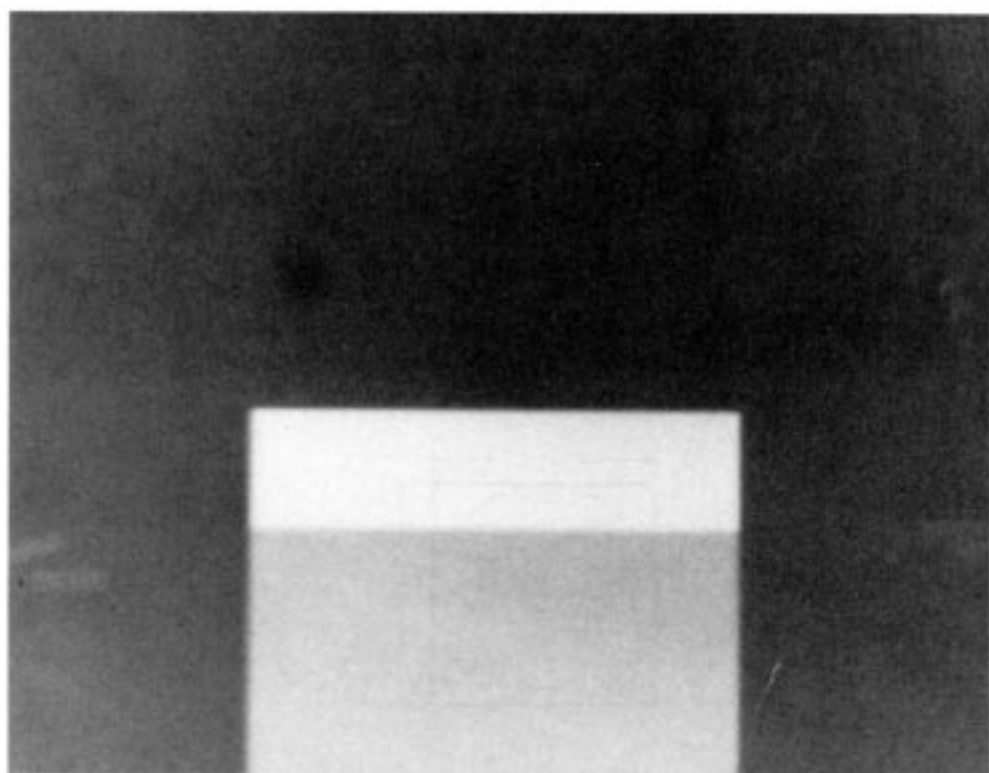
Roger W. Taylor

Radiographic Time:

31.41 μ s

Dynamic fracture of 25.0-mm-thick, *t*, aluminum. The plate is shocked by 101.6 mm of Composition B-3 initiated by a P-040 lens. *h* is 31.75 mm.





SHOT 230:

Dynamic Fracture of Aluminum

Date:

October 6, 1965

Experimenter:

Roger W. Taylor

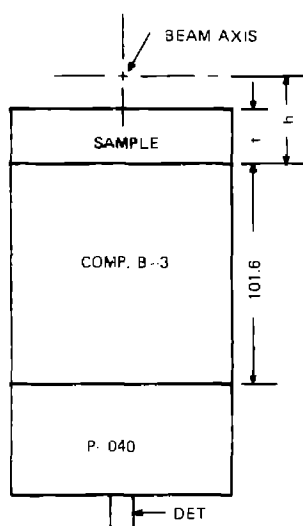
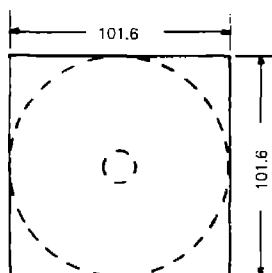
Radiographic Time:

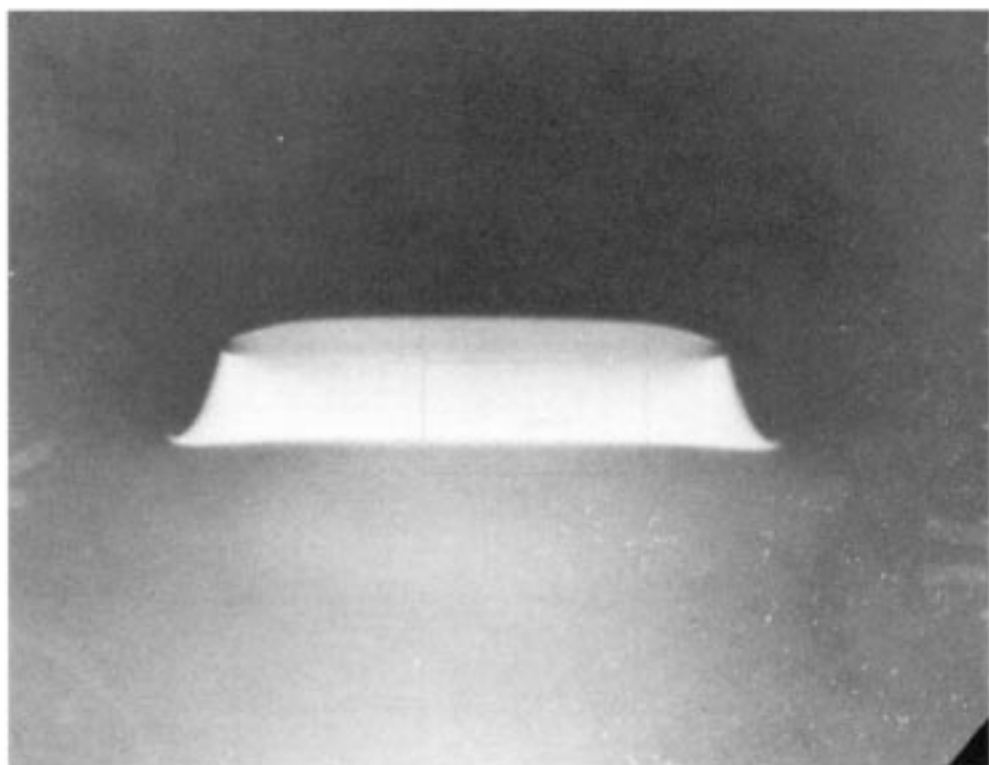
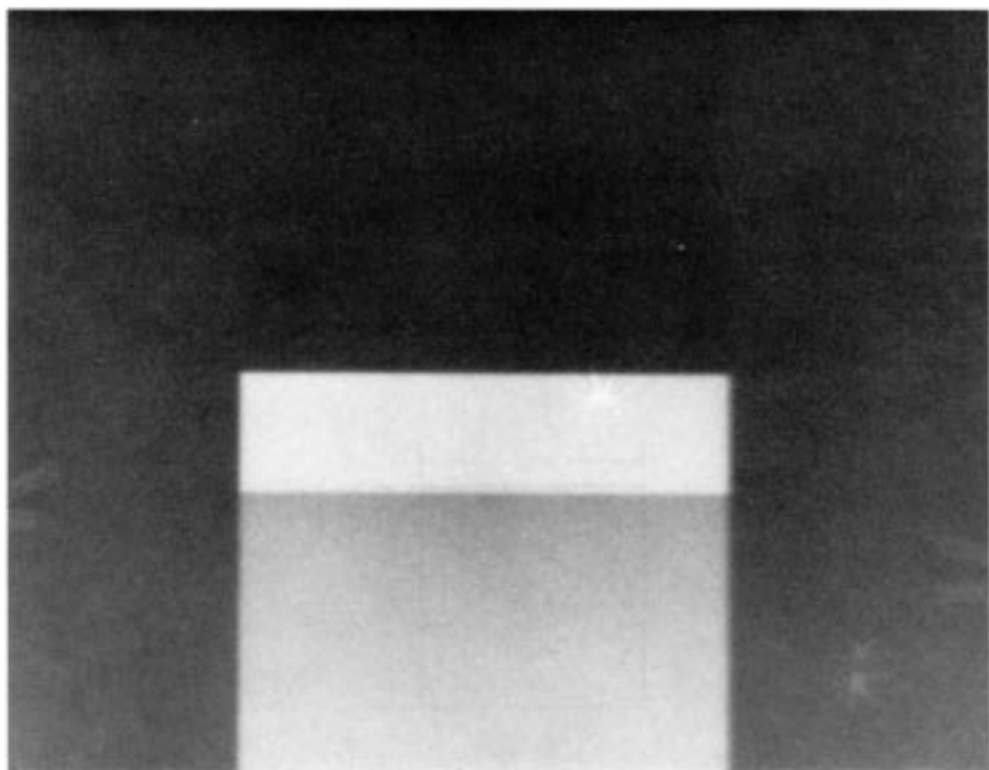
32.4 μ s

References:

Breed et al., 1967; Thurston and Mudd, 1968

Dynamic fracture of 25.0-mm-thick, t , aluminum. The plate is shocked by 101.6 mm of Composition B-3 initiated by a P-040 lens. h is 34.93 mm.





SHOT 231:

Dynamic Fracture of Aluminum

Date:

October 27, 1965

Experimenter:

Roger W. Taylor

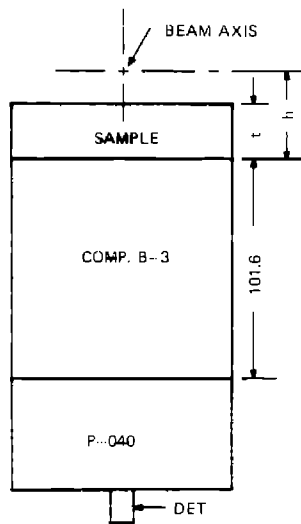
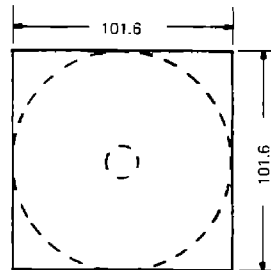
Radiographic Time:

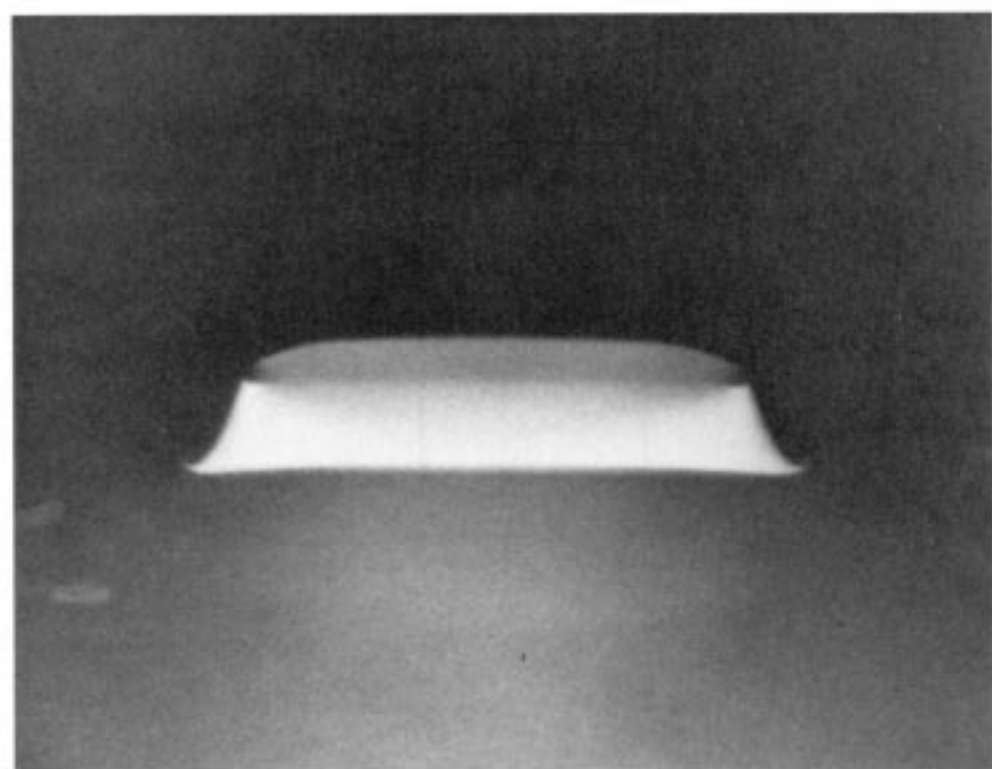
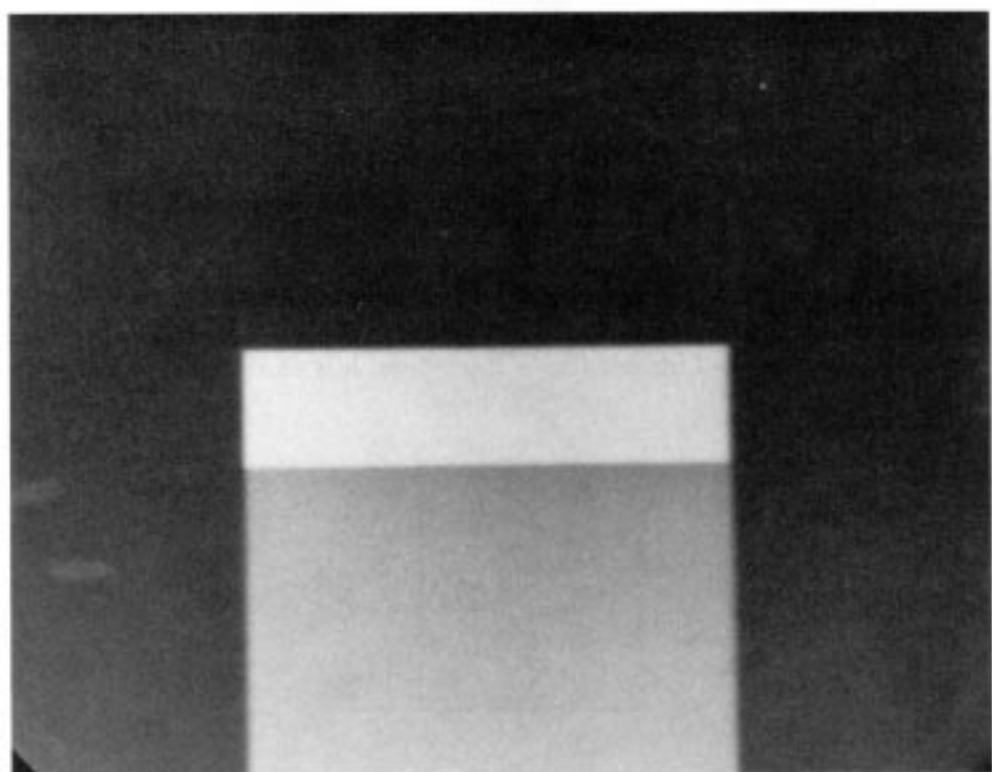
32.92 μ s

References:

Breed et al., 1967; Thurston and Mudd, 1968

Dynamic fracture of 25.0-mm-thick, t , aluminum. The plate is shocked by 101.6 mm of Composition B-3 initiated by a P-040 lens. h is 36.51 mm.





SHOT 232:

Dynamic Fracture of Aluminum

Date:

October 27, 1965

Experimenter:

Roger W. Taylor

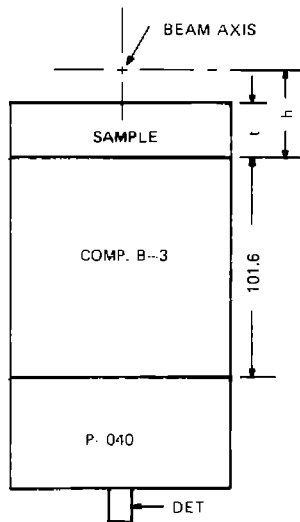
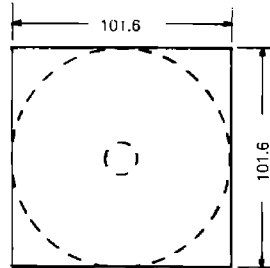
Radiographic Time:

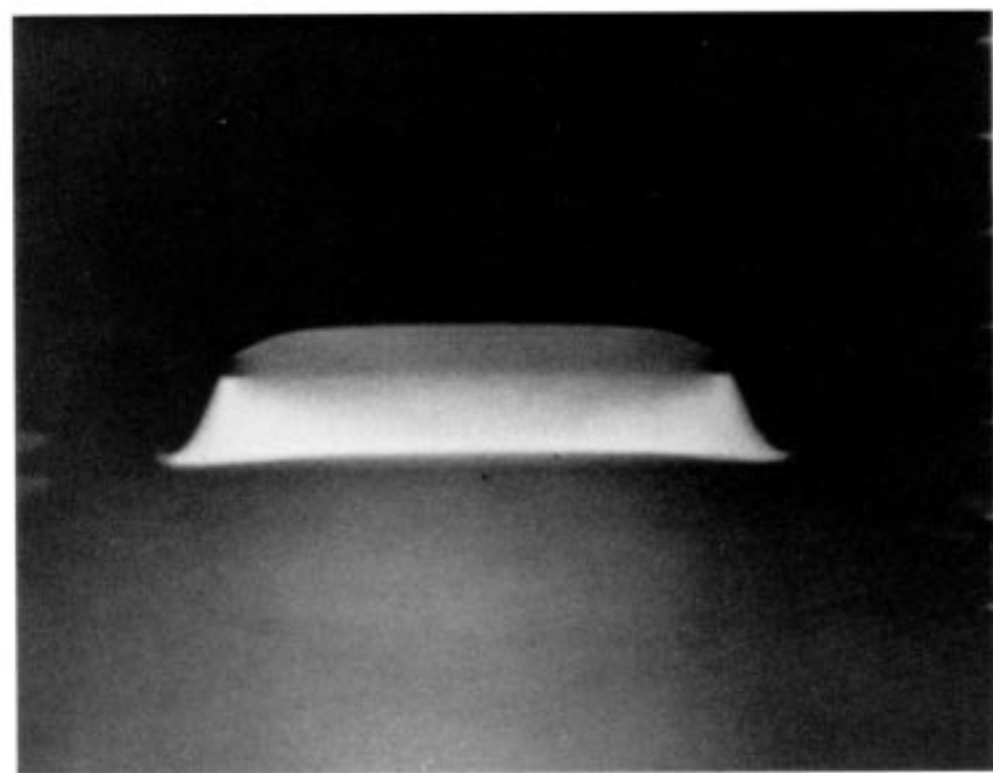
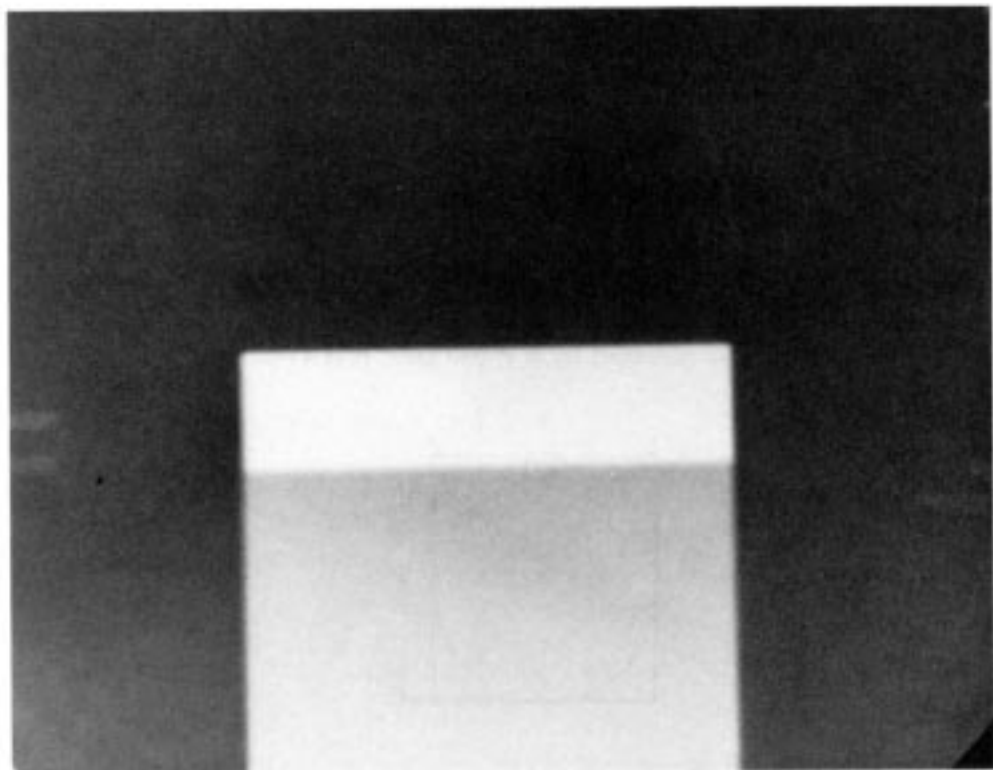
33.42 μ s

References:

Breed et al., 1967; Thurston and Mudd, 1968

Dynamic fracture of 25.0-mm-thick, t , aluminum. The plate is shocked by 101.6 mm of Composition B-3 initiated by a P-040 lens. h is 38.10 mm.





SHOT 234:

Dynamic Fracture of Aluminum

Date:

March 14, 1966

Experimenter:

Roger W. Taylor

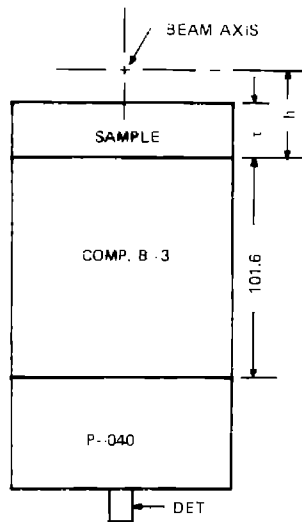
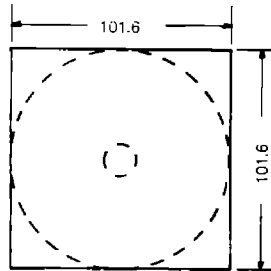
Radiographic Time:

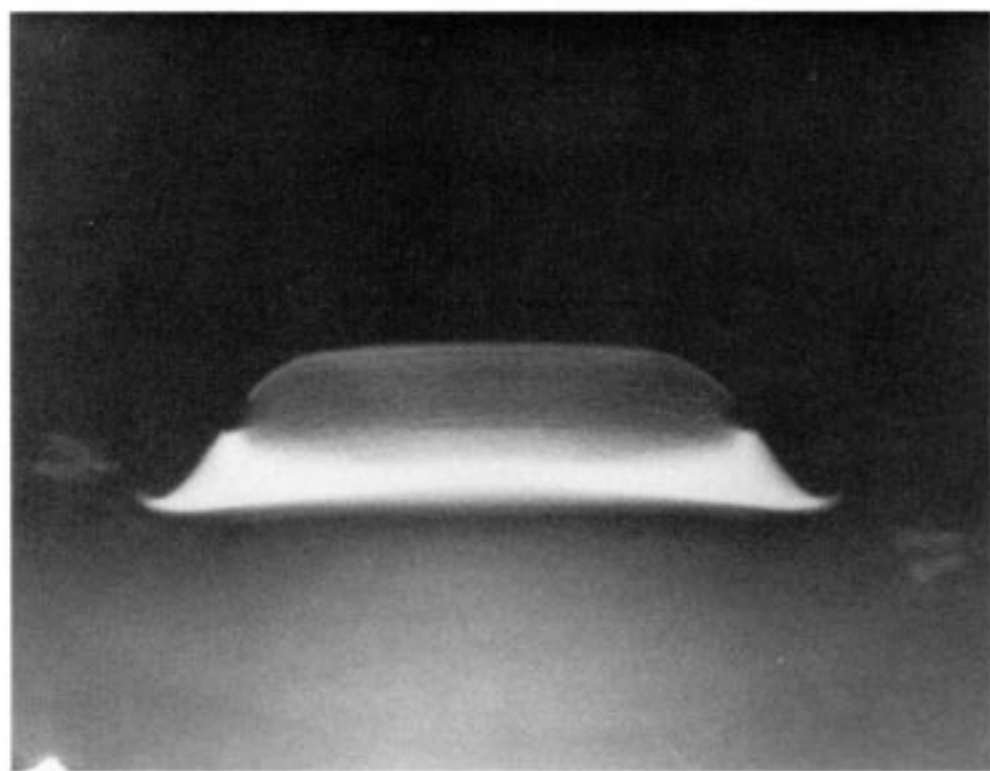
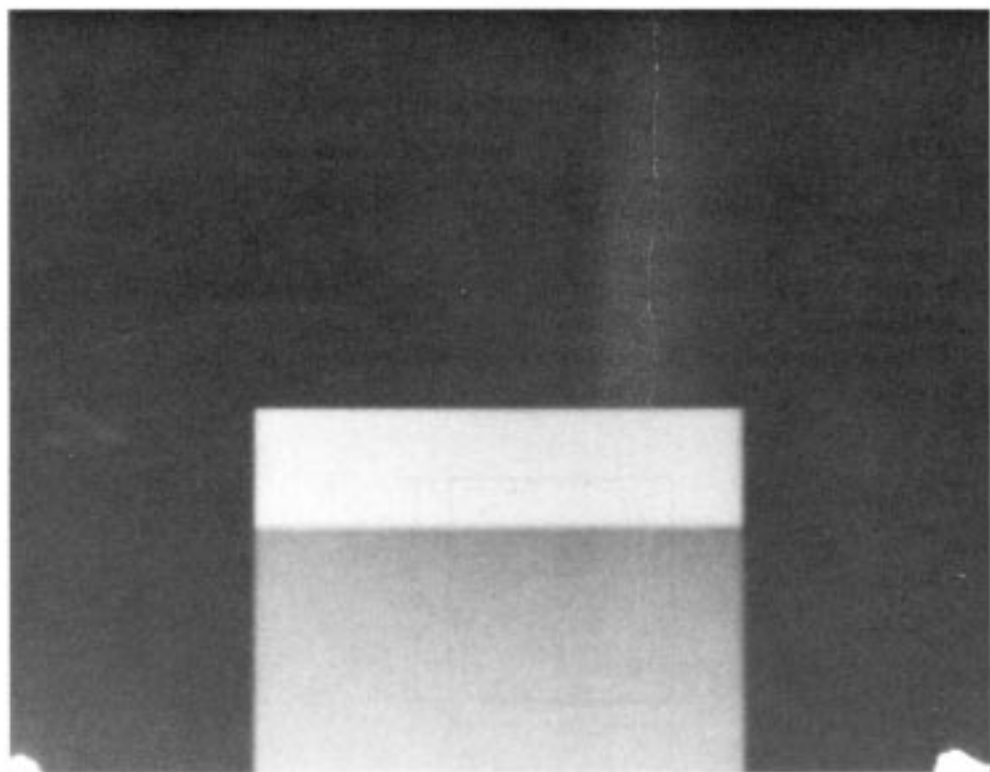
36.43 μ s

References:

Breed et al., 1967; Thurston and Mudd, 1968

Dynamic fracture of 25.0-mm-thick, t , aluminum. The plate is shocked by 101.6 mm of Composition B-3 initiated by a P-040 lens. h is 47.63 mm.





SHOT 235:

Dynamic Fracture of Aluminum

Date:

March 14, 1966

Experimenter:

Roger W. Taylor

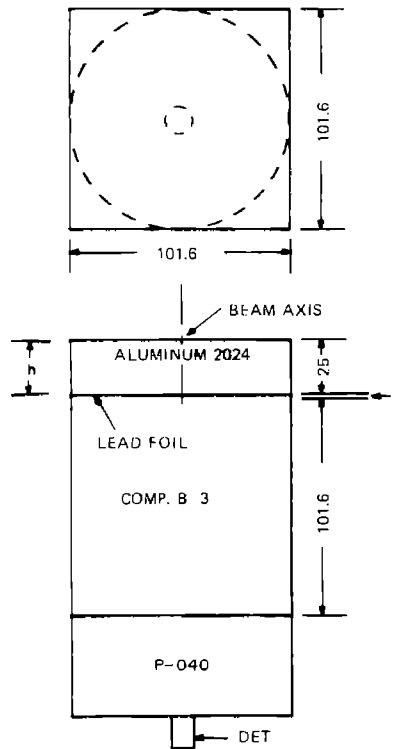
Radiographic Time:

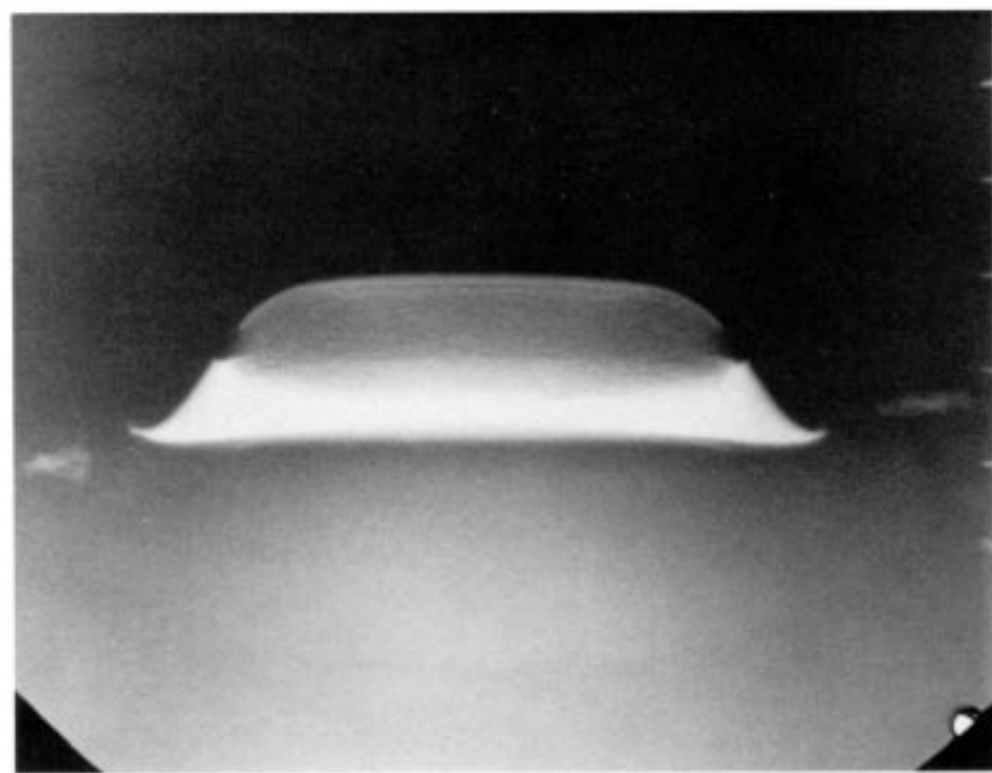
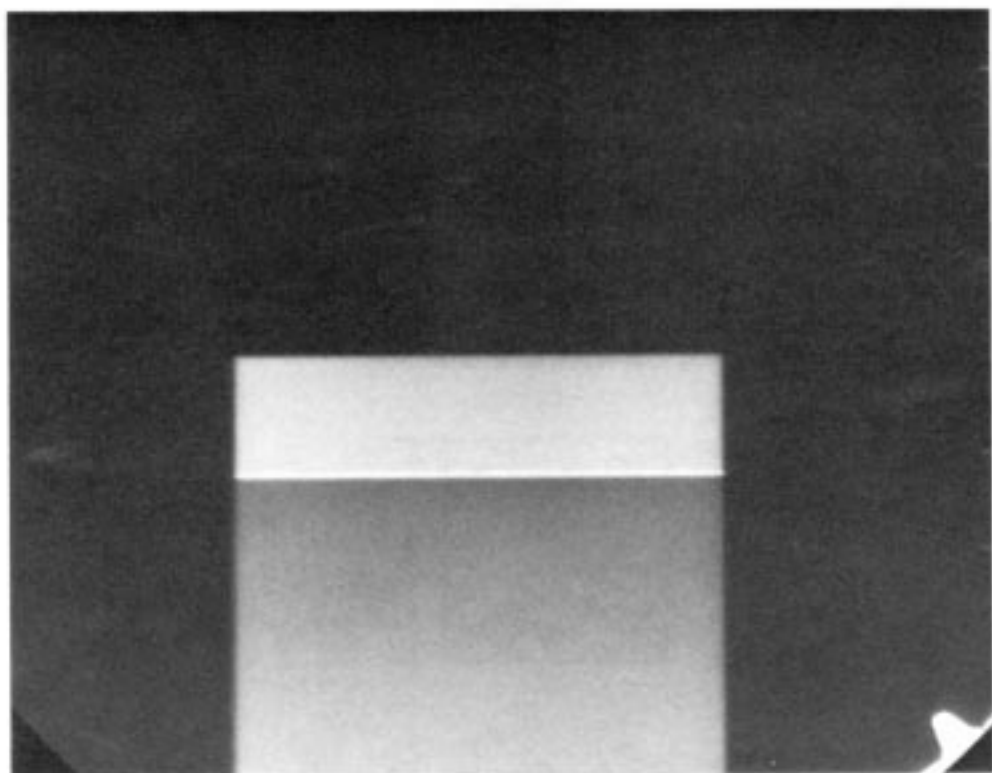
36.4 μ s

References:

Breed et al., 1967; Thurston and Mudd, 1968

Dynamic fracture of 25.0-mm-thick aluminum. The aluminum plate is shocked by 101.6 mm of Composition B-3 initiated by a P-040 lens and 0.127 mm, t , of lead. h is 47.63 mm.





SHOT 236: Dynamic Fracture of Aluminum

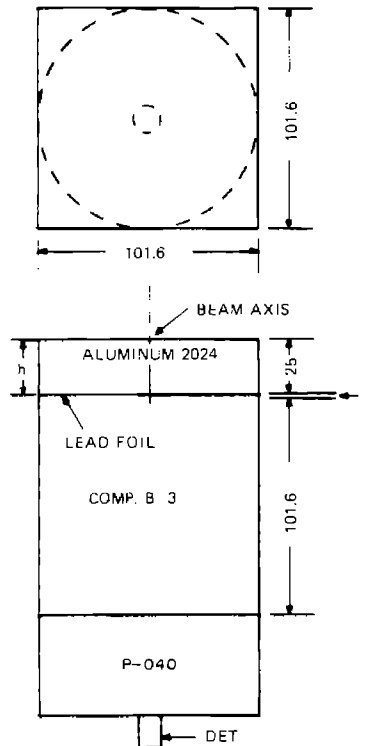
Date: March 15, 1966

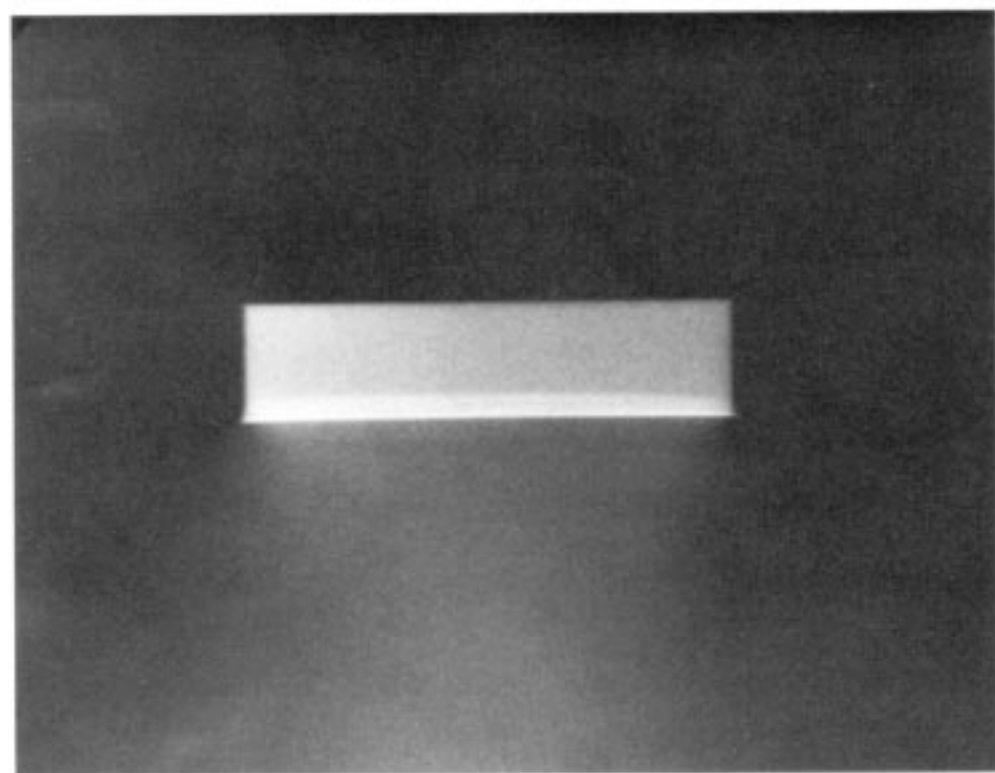
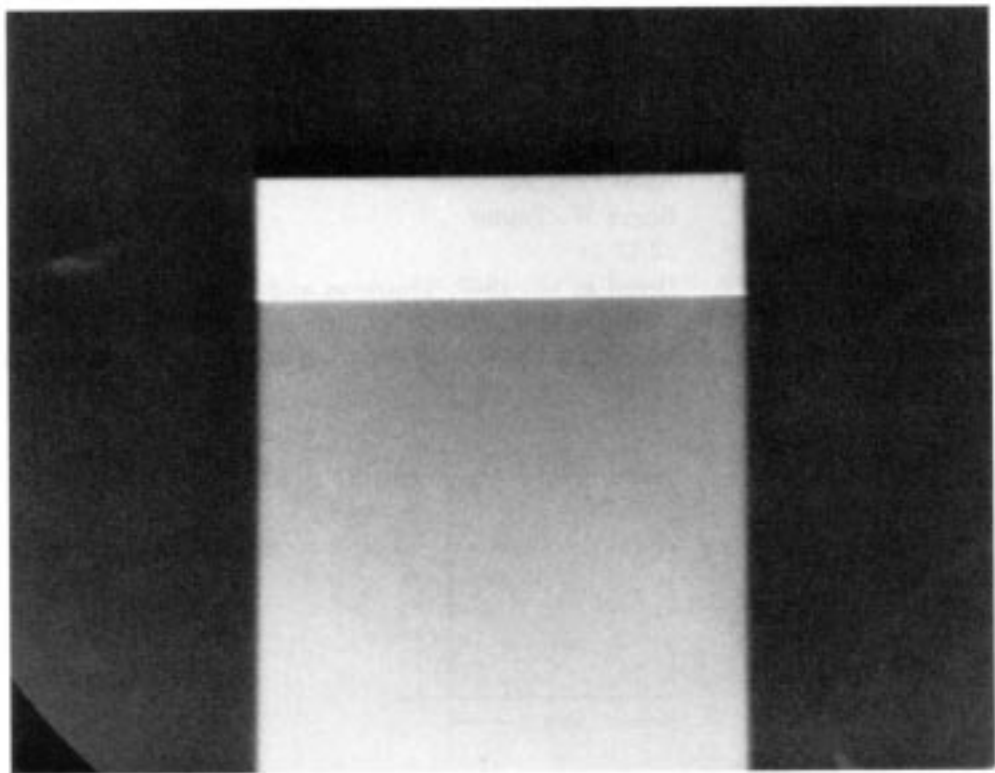
Experimenter: Roger W. Taylor

Radiographic Time: 26.93 μ s

References: Breed et al., 1967, Thurston and Mudd, 1968

The 25.0-mm-thick aluminum plate is shocked by 101.6 mm of Composition B-3 initiated by a P-040 lens and 0.127 mm, t, of lead.





SHOT 238: Dynamic Fracture of Aluminum

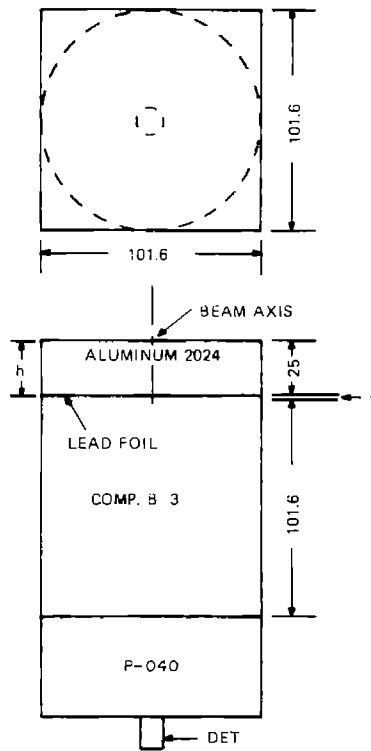
Date: April 12, 1966

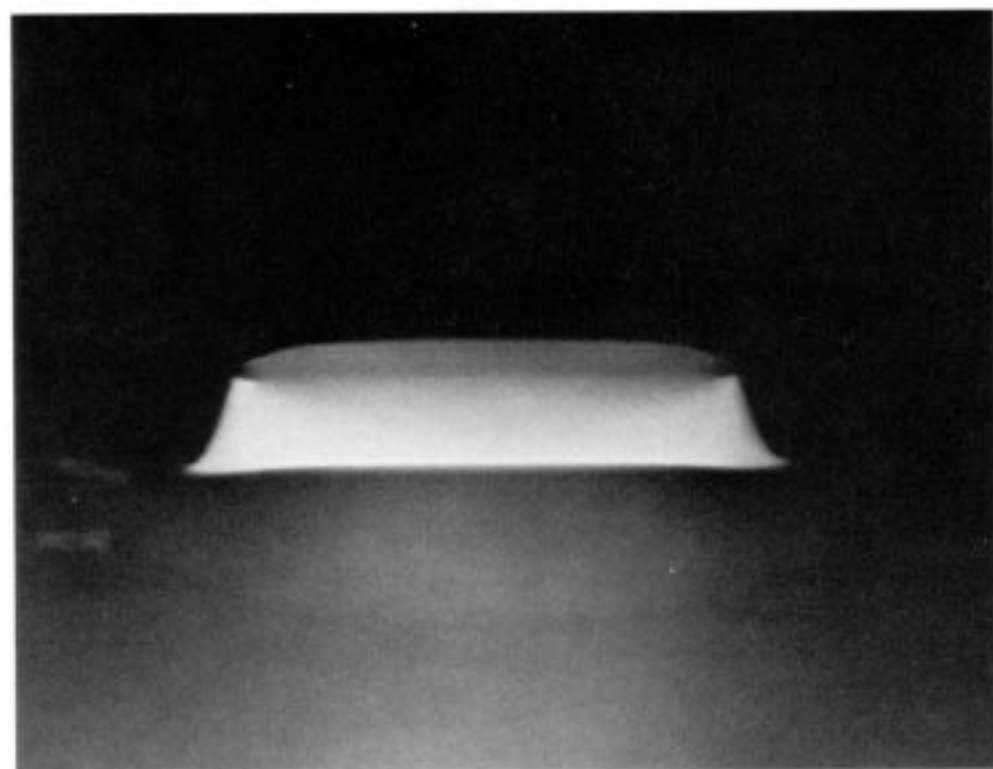
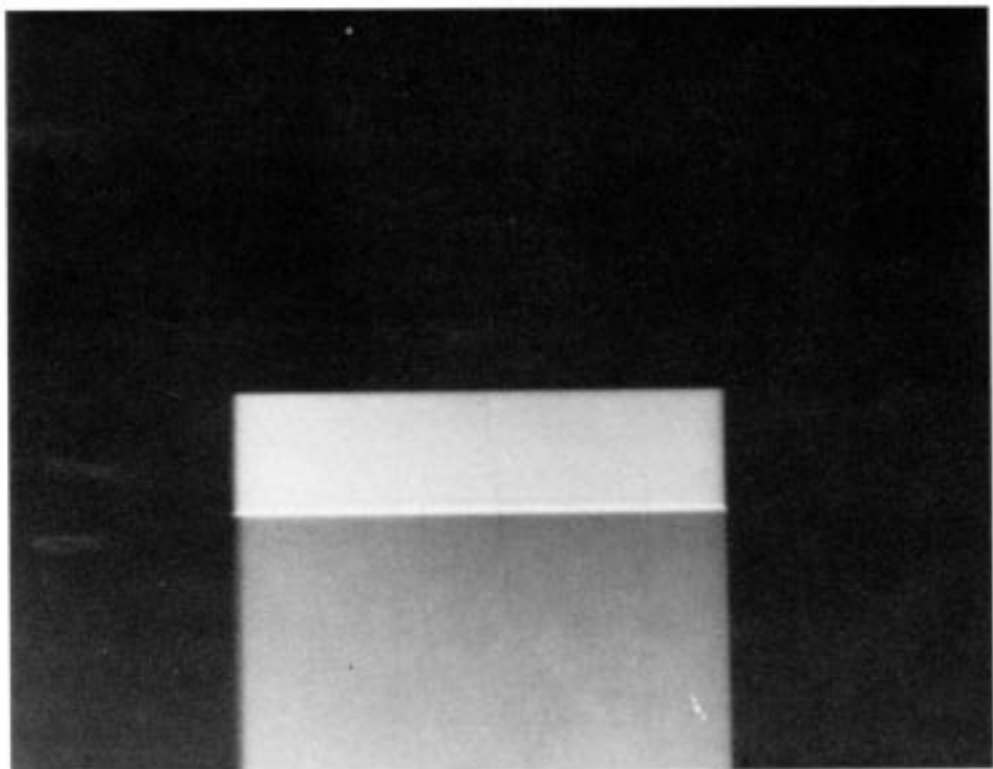
Experimenter: Roger W. Taylor

Radiographic Time: 32.43 μ s

References: Breed et al., 1967; Thurston and Mudd, 1968

Dynamic fracture of 25.0-mm-thick aluminum. The aluminum plate is shocked by 101.6 mm of Composition B-3 initiated by a P-040 lens and 0.127 mm, t , of lead. h is 34.92 mm.





SHOT 239:

Dynamic Fracture of Copper

Date:

April 18, 1966

Experimenter:

Benny Ray Breed

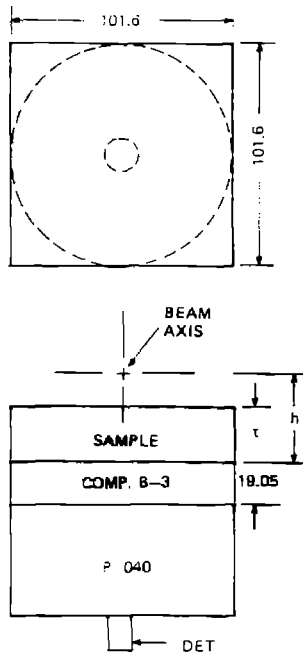
Radiographic Time:

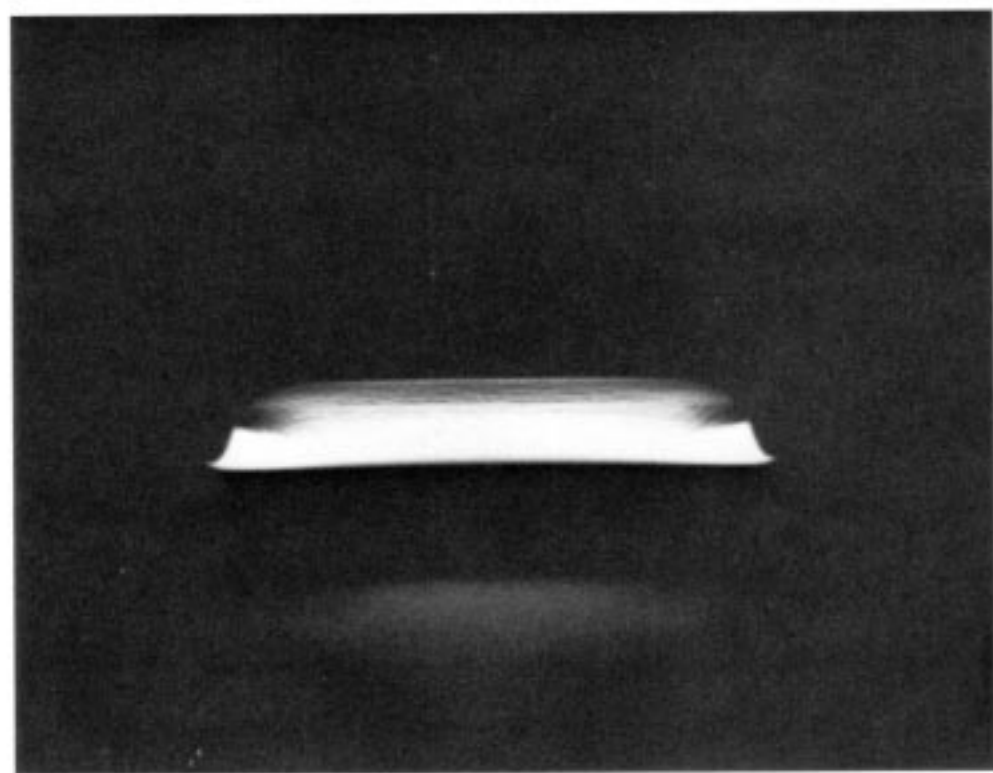
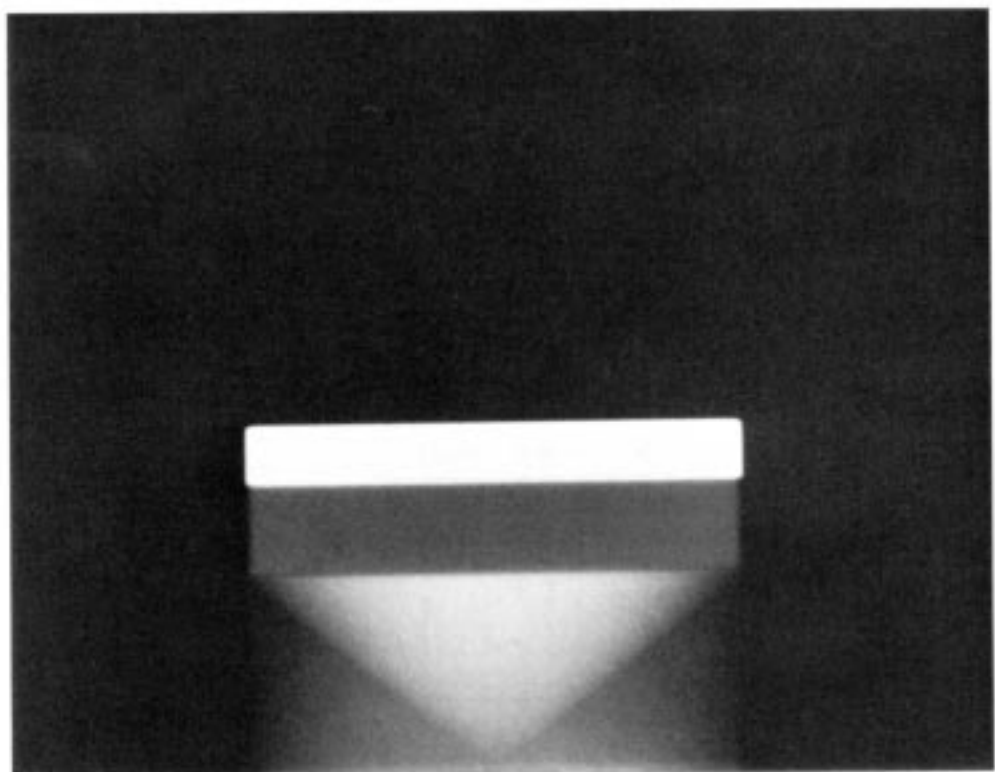
26.04 μ s

References:

Breed et al., 1967; Thurston and Mudd, 1968

Dynamic fracture of 12-mm-thick, t, copper. The plate is shocked by 19.05 mm of Composition B-3 initiated by a P-040 lens. h is 28.57 mm.





SHOT 240:

Dynamic Fracture of Copper

Date:

April 19, 1966

Experimenter:

Benny Ray Breed

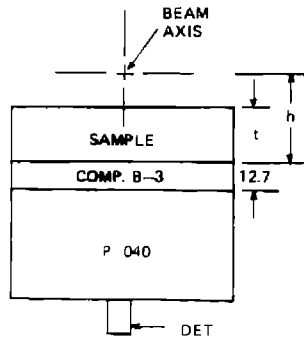
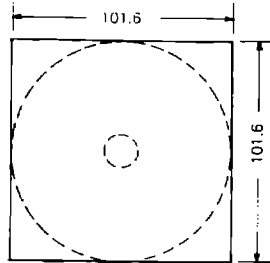
Radiographic Time:

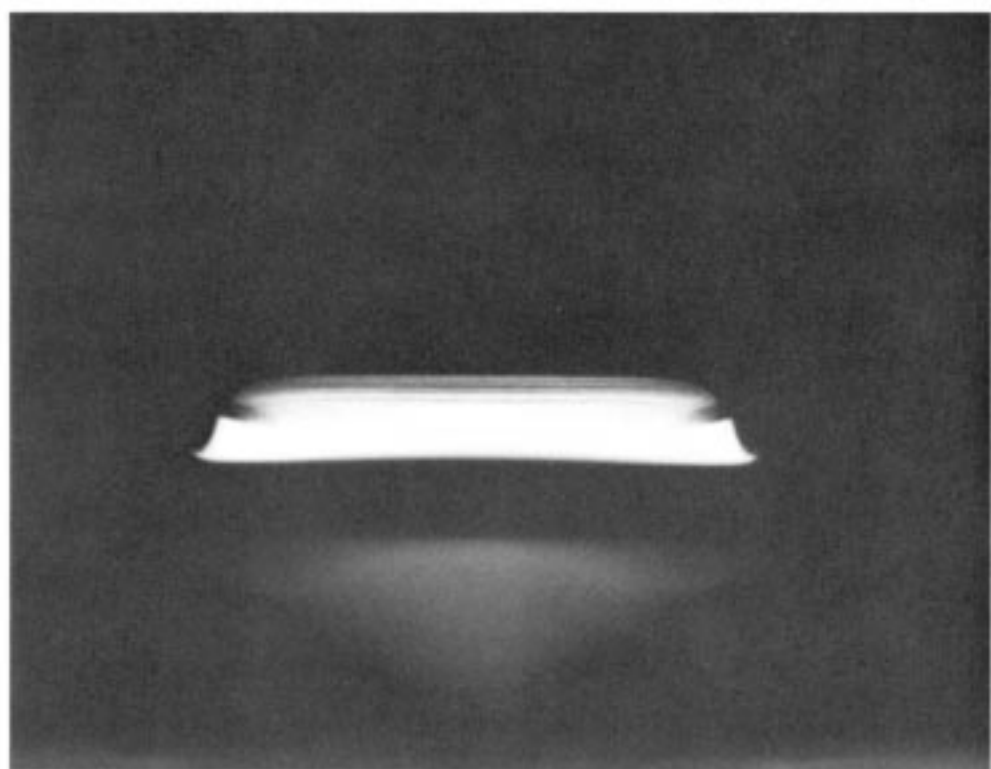
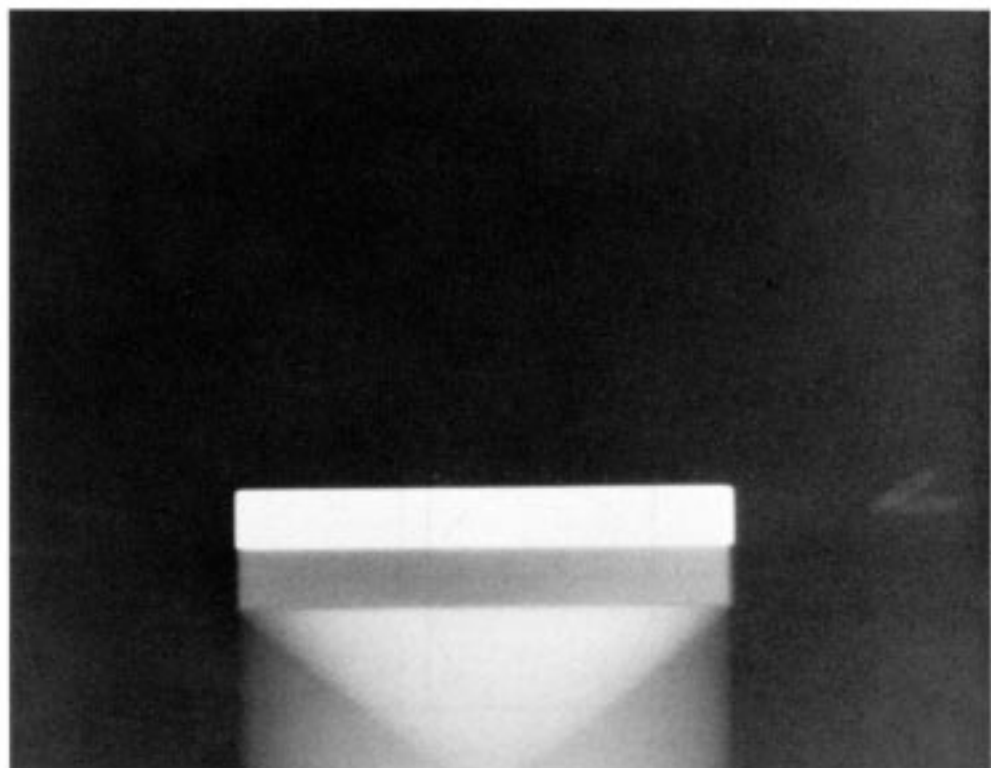
25.25 μ s

References:

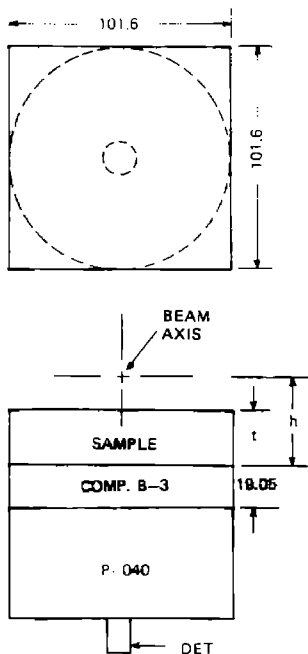
Breed et al., 1967; Thurston and Mudd, 1968

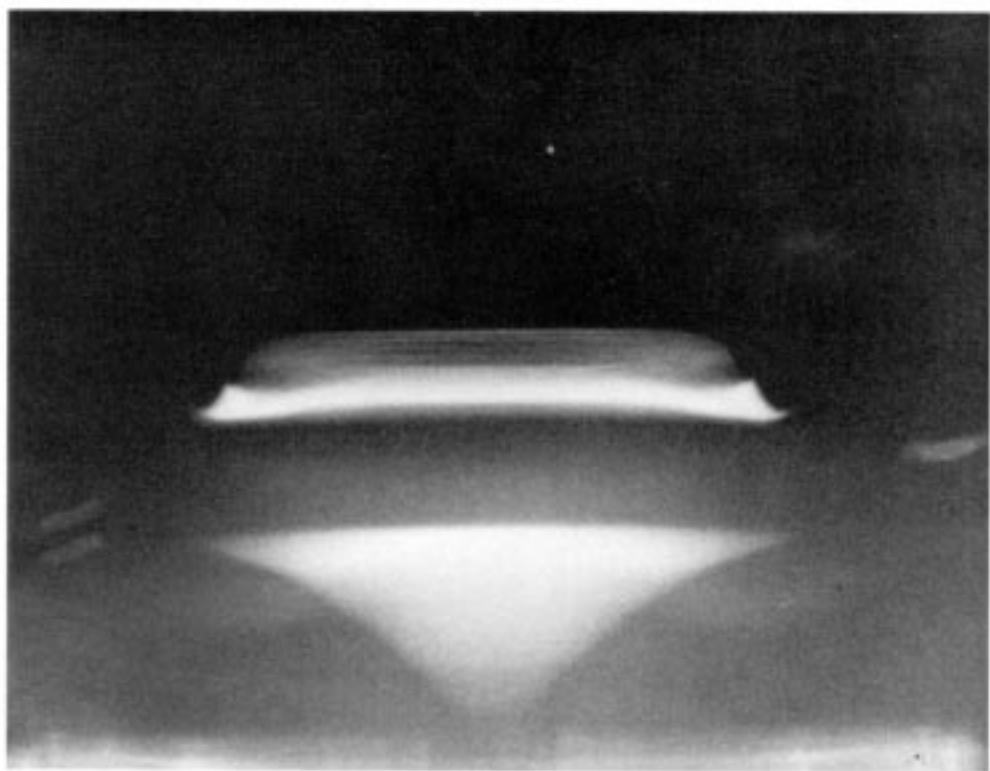
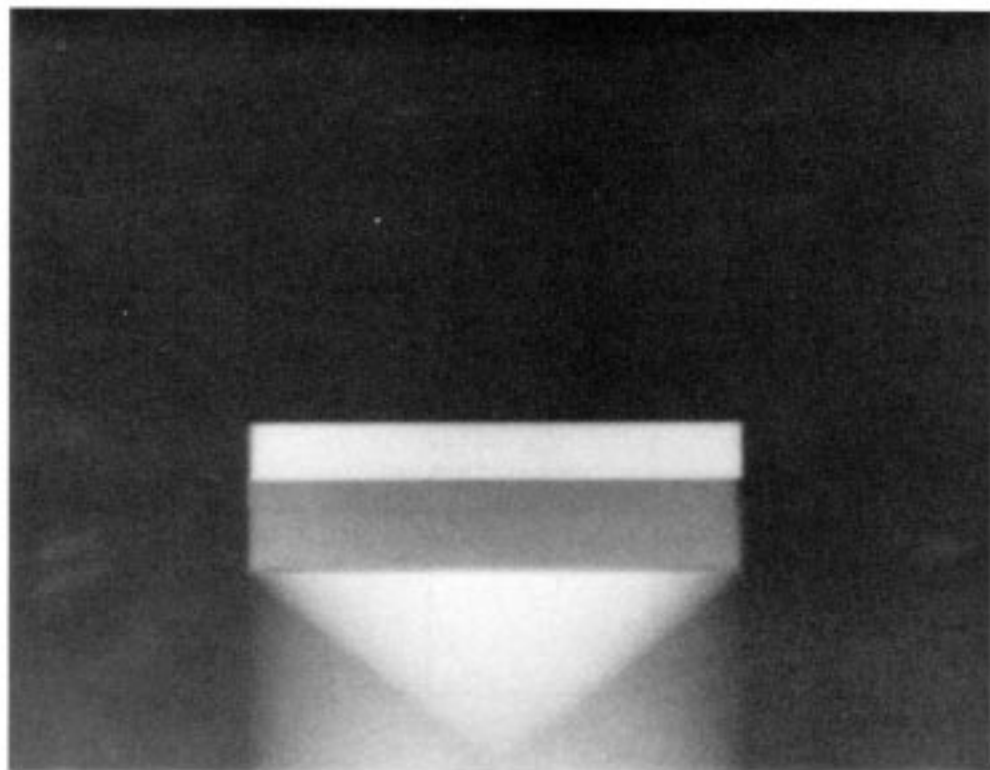
Dynamic fracture of 12.0-mm-thick, t, copper. The plate is shocked by 12.7 mm of Composition B-3 initiated by a P-040 lens. h is 28.57 mm.





SHOT 241: Dynamic Fracture of Aluminum
Date: April 5, 1966
Experimenter: Benny Ray Breed
Radiographic Time: 22.5 μ s
References: Breed et al., 1967; Thurston and Mudd, 1968
Dynamic fracture of 12.0-mm-thick, t, aluminum. The plate is shocked by 19.05 mm of Composition B-3 initiated by a P-040 lens. h is 28.57 mm.





SHOT 242:

Dynamic Fracture of Nickel

Date:

April 26, 1966

Experimenter:

Benny Ray Breed

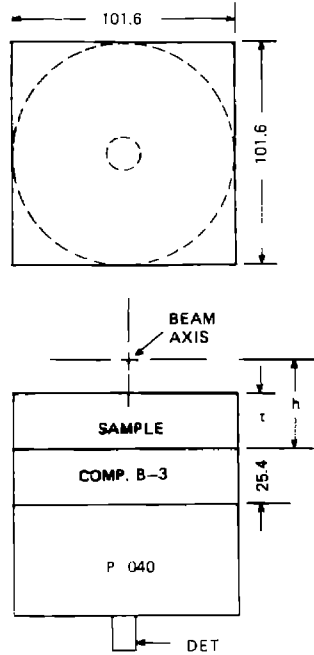
Radiographic Time:

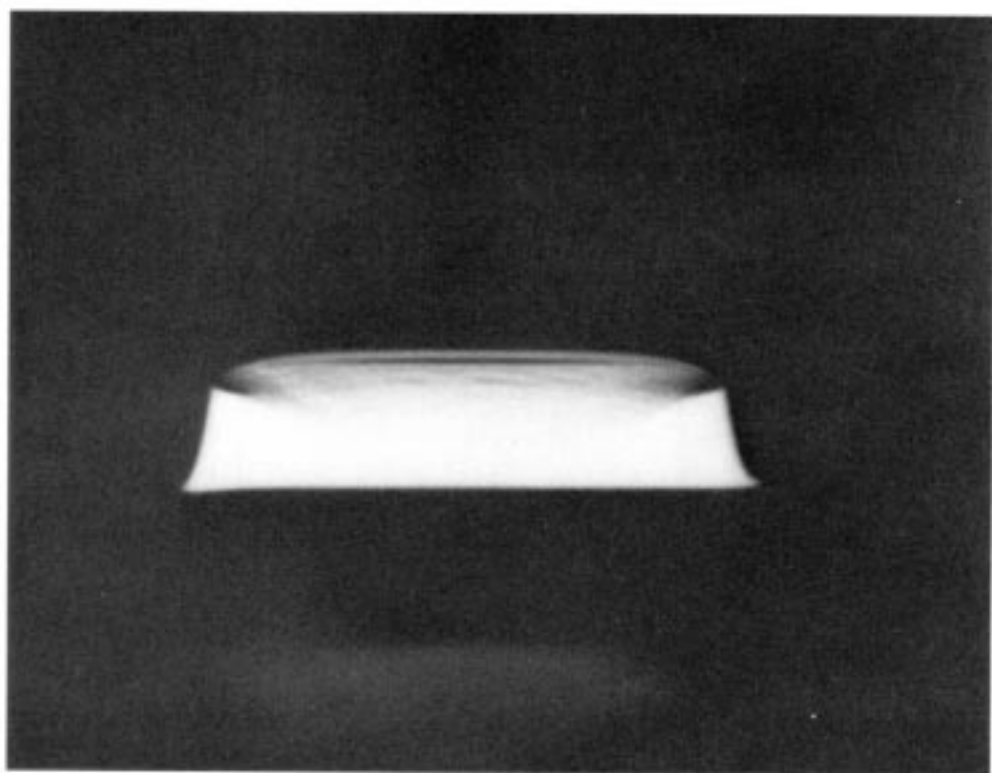
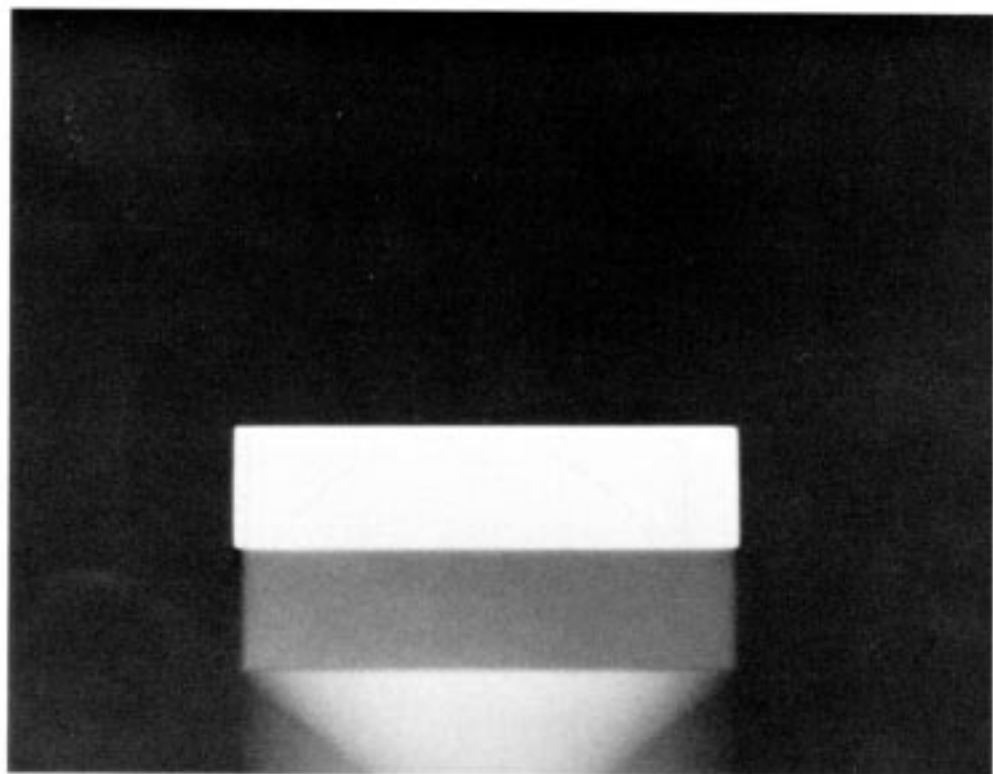
28.89 μ s

References:

Breed et al., 1967; Thurston and Mudd, 1968

Dynamic fracture of 25.0-mm-thick, *t*, nickel. The plate is shocked by 25.4 mm of Composition B-3 initiated by a P-040 lens. *h* is 41.27 mm.





SHOT 245:

Dynamic Fracture of Aluminum

Date:

February 4, 1965

Experimenter:

Douglas Venable

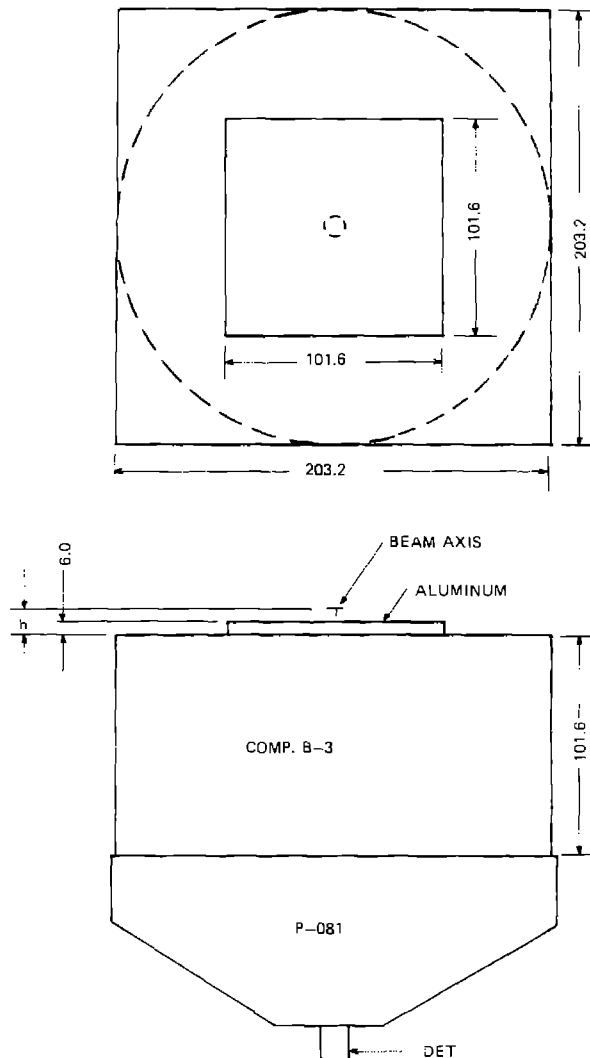
Radiographic Time:

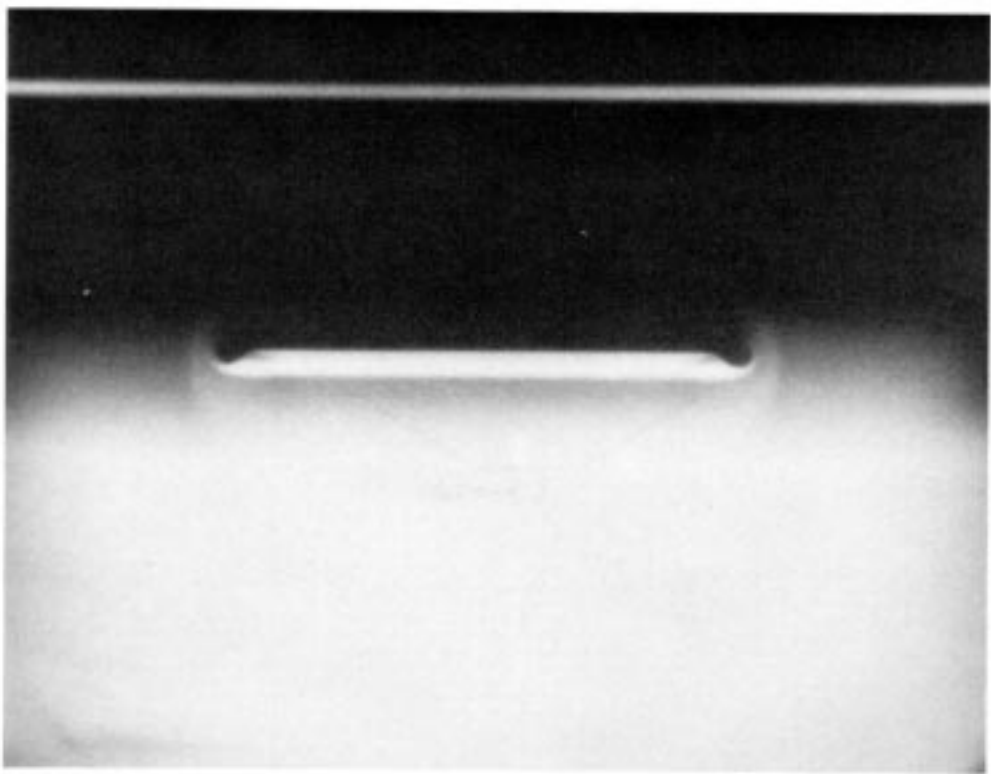
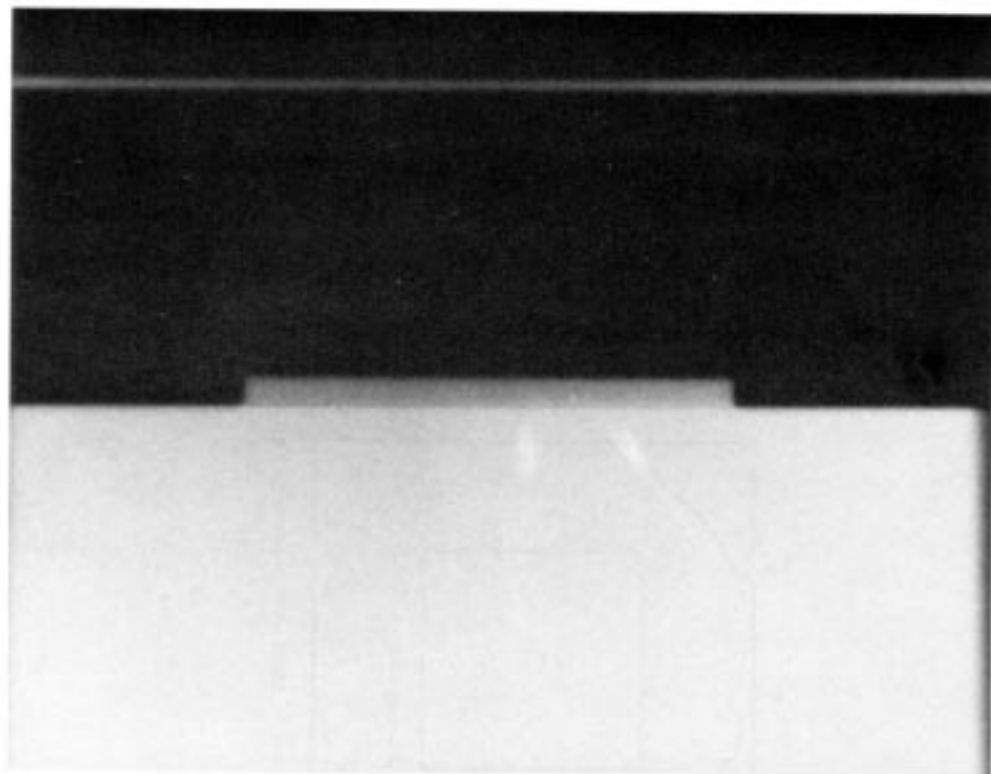
38.24 μ s

References:

Breed et al., 1967; Thurston and Mudd, 1968

Dynamic fracture of 6.0-mm-thick aluminum. The plate is shocked by 101.6 mm of Composition B-3 initiated by a P-081 lens. h is 12.7 mm.





SHOT 246:

Dynamic Fracture of Aluminum

Date:

February 9, 1965

Experimenter:

Douglas Venable

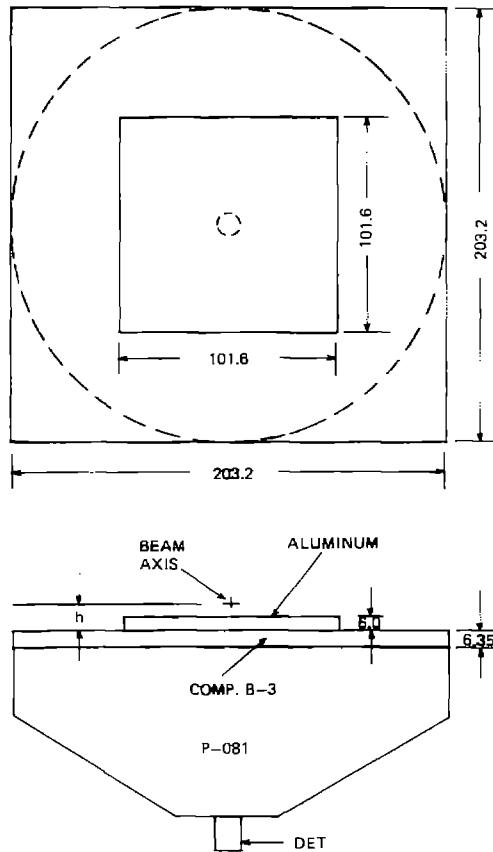
Radiographic Time:

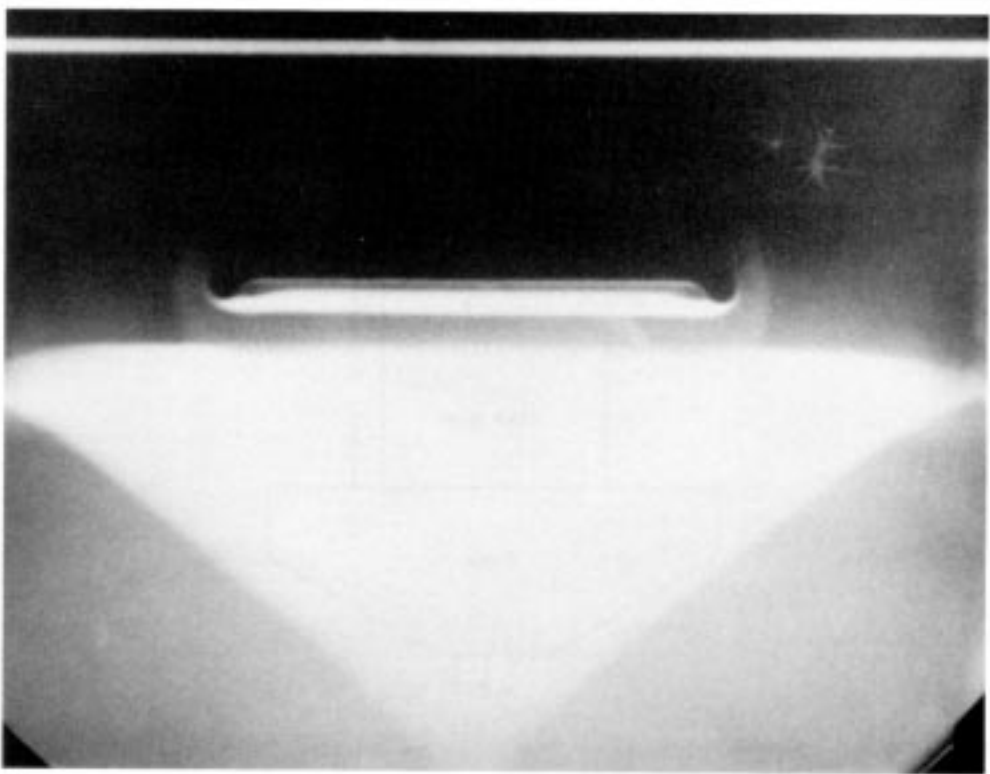
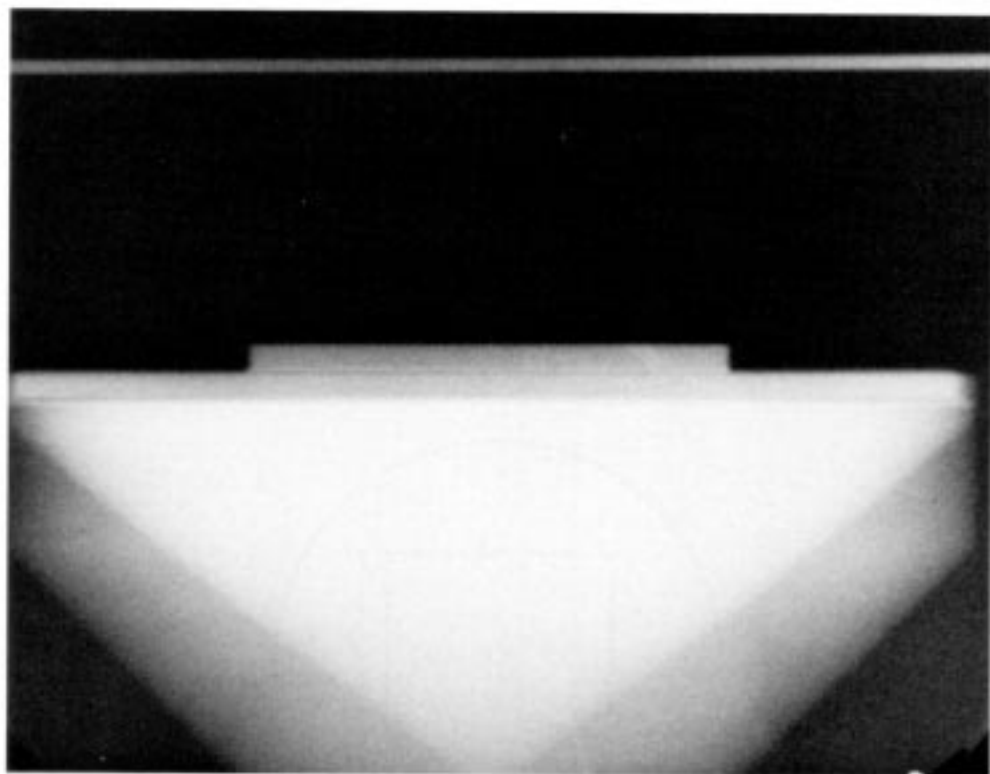
28.24 μ s

References:

Breed et al., 1967; Thurston and Mudd, 1968

Dynamic fracture of 6.0-mm-thick aluminum. The plate is shocked by 6.35 mm of Composition B-3 initiated by a P-081 lens. h is 12.7 mm.





SHOT 247:

Dynamic Fracture of Aluminum

Date:

November 3, 1965

Experimenter:

Douglas Venable

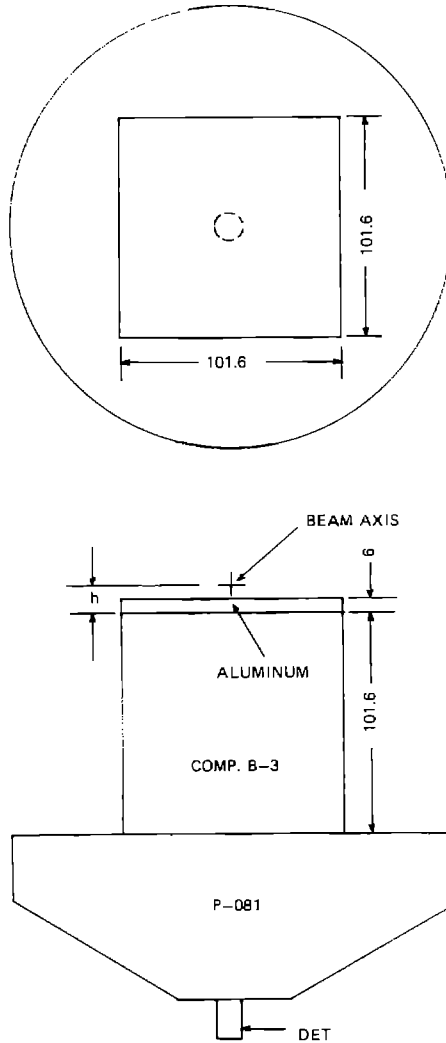
Radiographic Time:

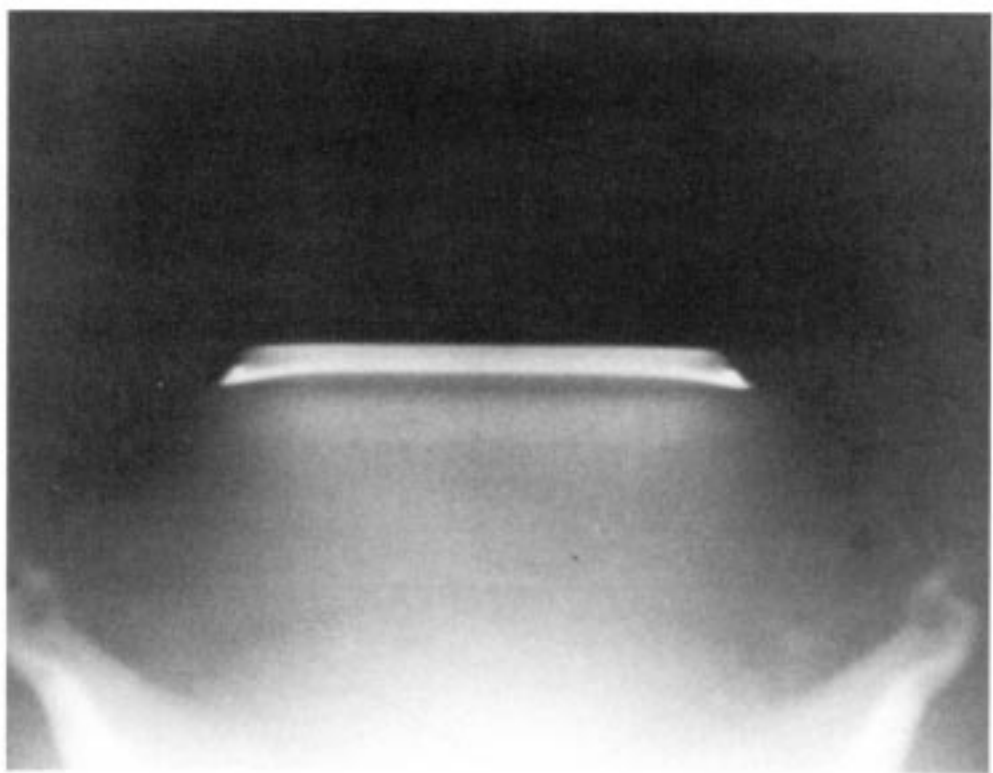
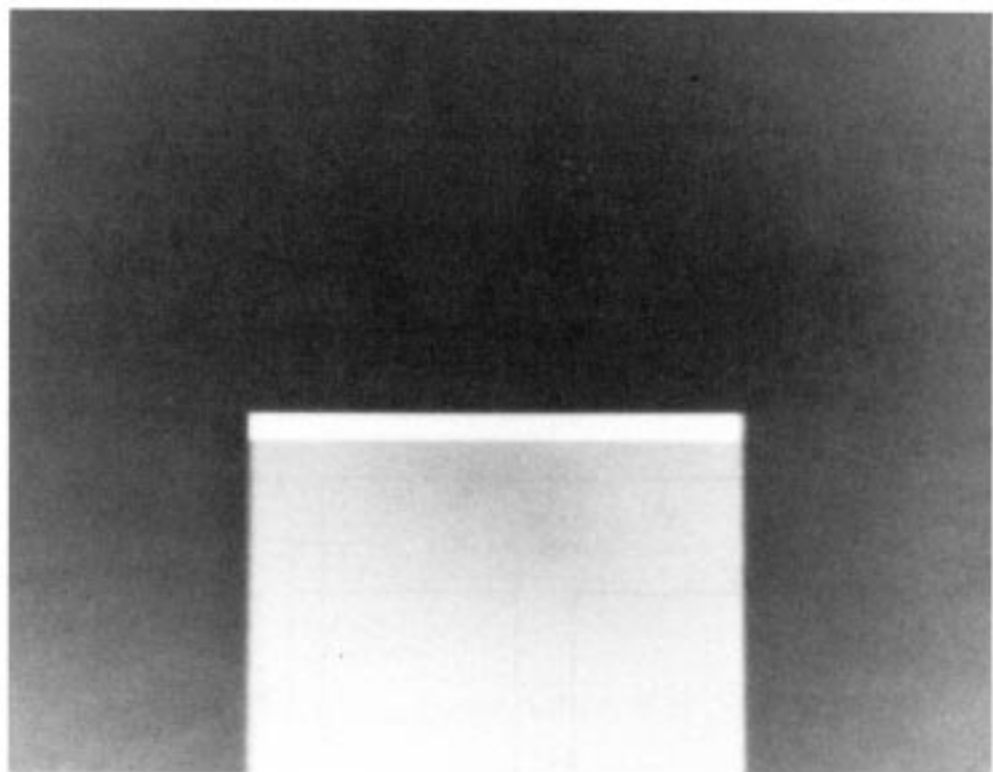
37.51 μ s

References:

Breed et al., 1967; Thurston and Mudd, 1968

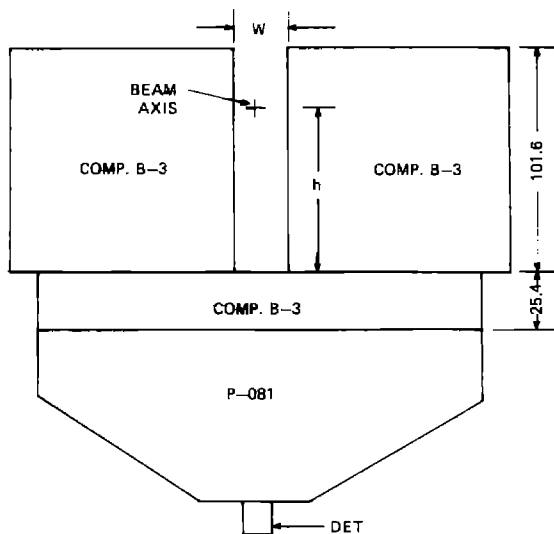
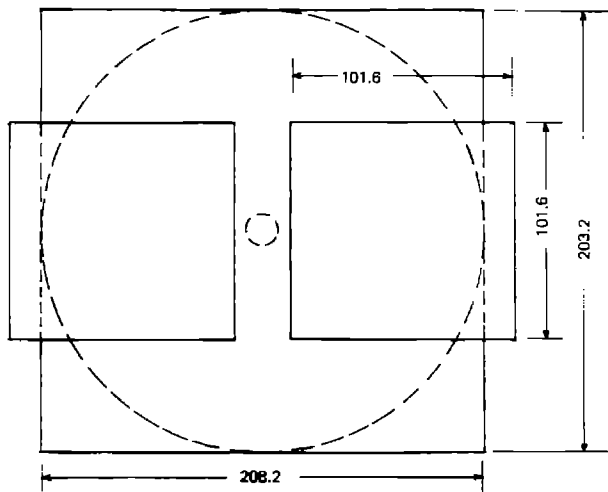
Dynamic fracture of 6.0-mm-thick aluminum. The plate is shocked by 101.6 mm of Composition B-3 initiated by a P-081 lens. h is 12.7 mm.

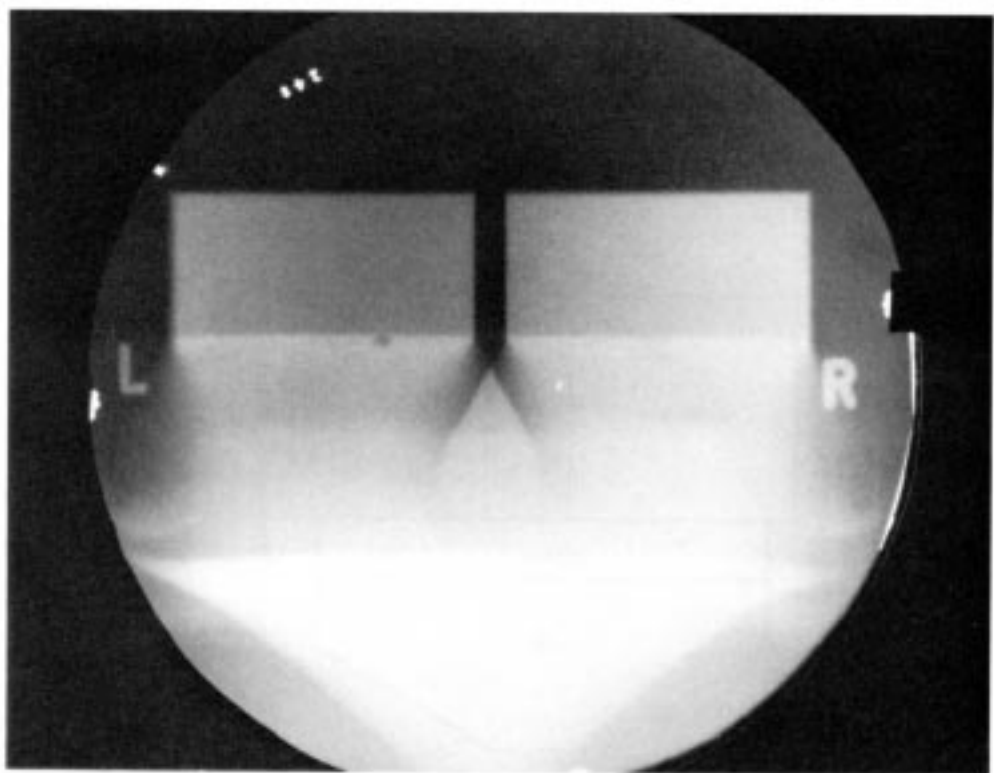
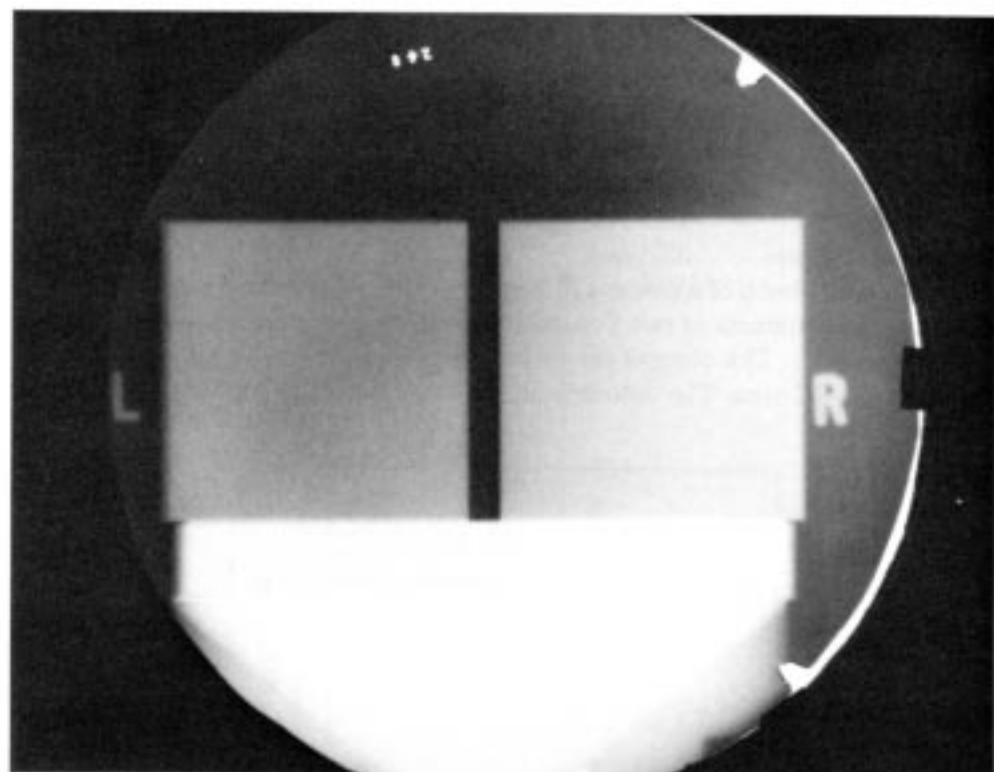




SHOT 248: Munroe Jet
Date: February 25, 1965
Experimenter: Douglas Venable
Radiographic Time: 32.37 μ s

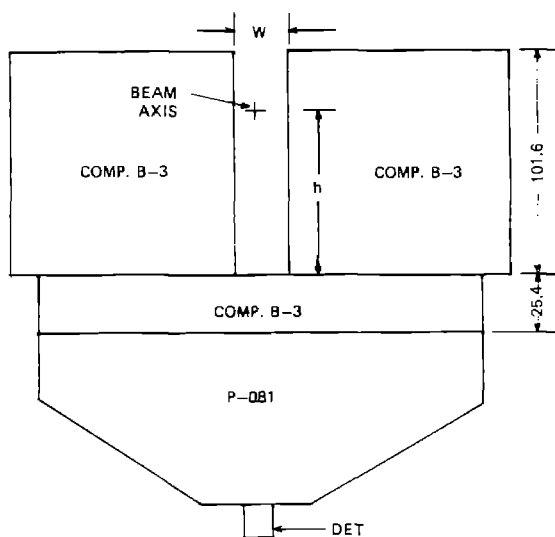
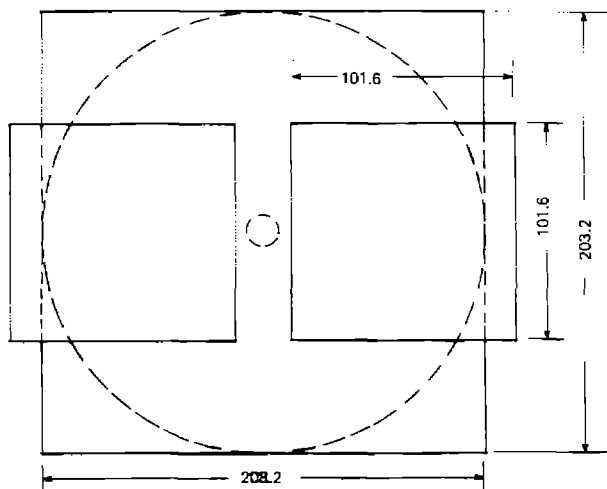
Formation and growth of a gaseous Munroe jet. This jet is formed by interaction of the detonation products of two Composition B-3 charges separated by an air gap 10.0 mm, w, wide. The charges are initiated by 25.4 mm of Composition B-3 initiated by a P-081 lens. The detonations have run along the gap for 50.8 mm. h is 50.8 mm.

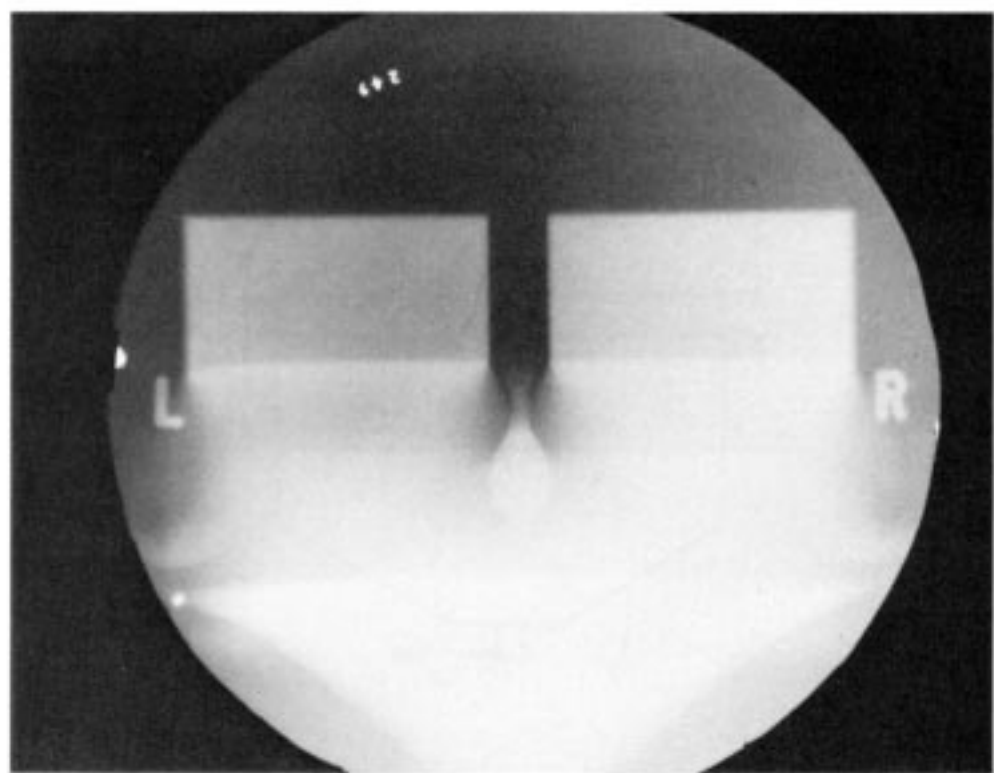
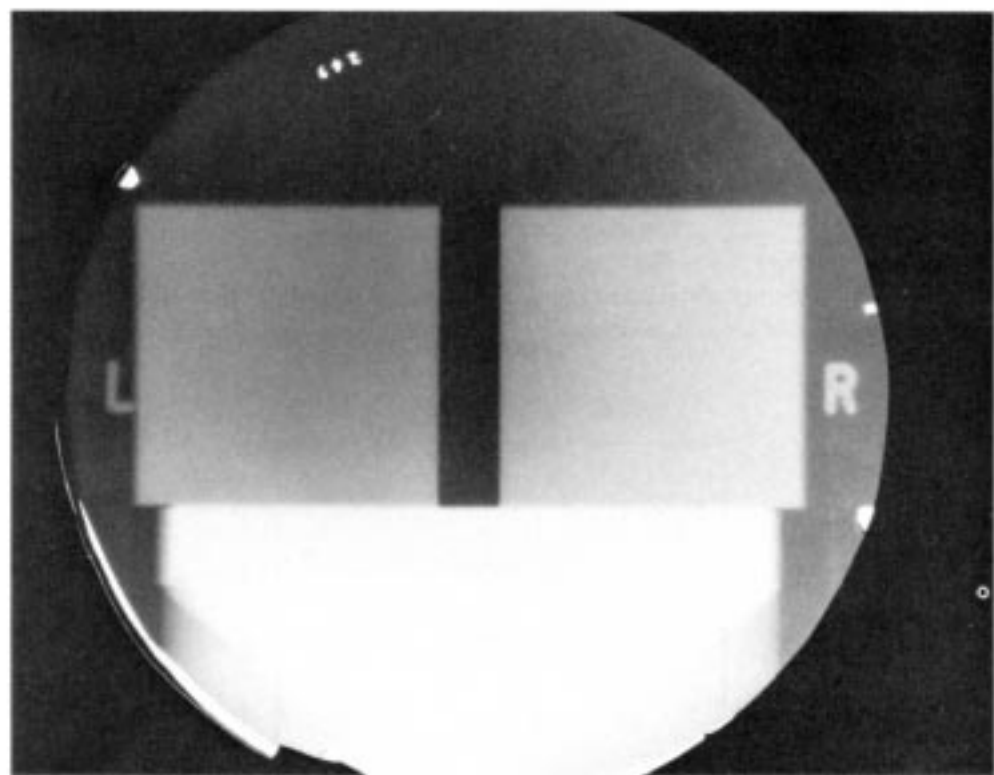




SHOT 249: **Munroe Jet**
Date: February 25, 1965
Experimenter: Douglas Venable
Radiographic Time: 32.3 μ s

Formation and growth of a gaseous Munroe jet. This jet is formed by interaction of the detonation products of two Composition B-3 charges separated by an air gap 20.0 mm, w, wide. The charges are initiated by 25.4 mm of Composition B-3 initiated by a P-081 lens. The detonations have run along the gap for 50.8 mm. h is 50.8 mm.





SHOT 250:

Plane-Wave Aluminum Gun

Date:

February 25, 1965

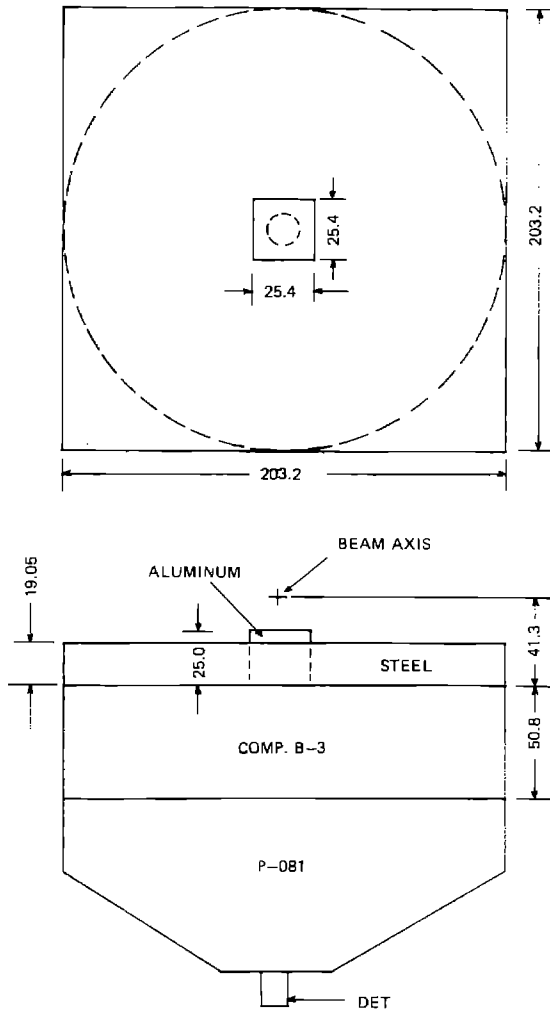
Experimenter:

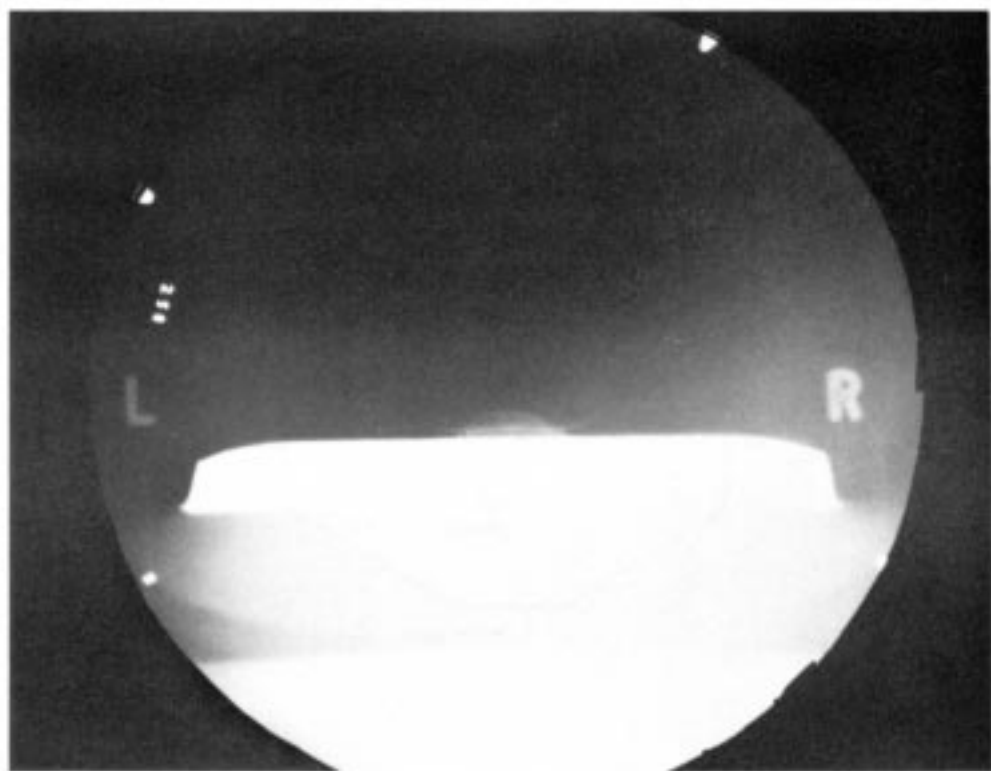
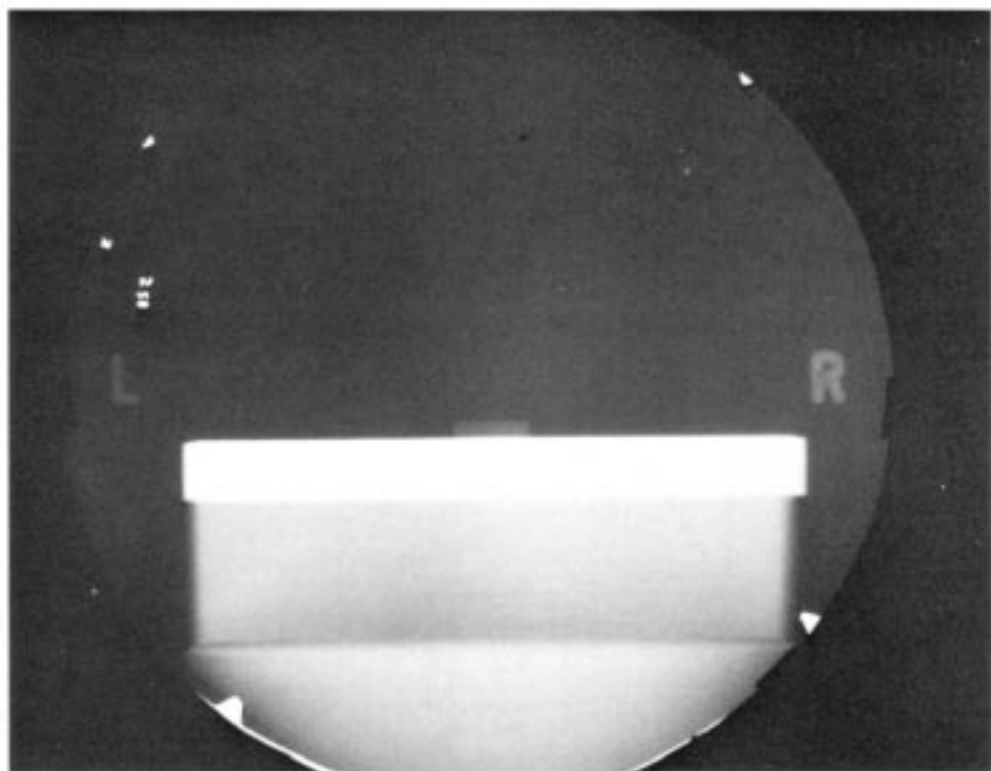
Douglas Venable

Radiographic Time:

37.13 μ s

A 25- by 25- by 25-mm aluminum cube is embedded in a 19.05-mm-thick by 203.2-mm-square block of iron. It is driven by 50.8 mm of Composition B-3 initiated by a P-081 lens.





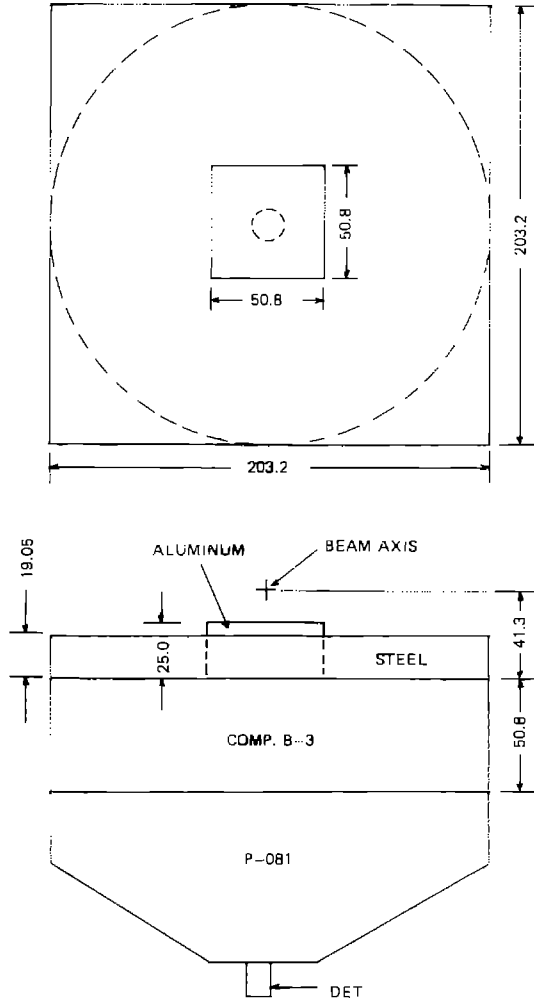
SHOT 251: Plane-Wave Aluminum Gun

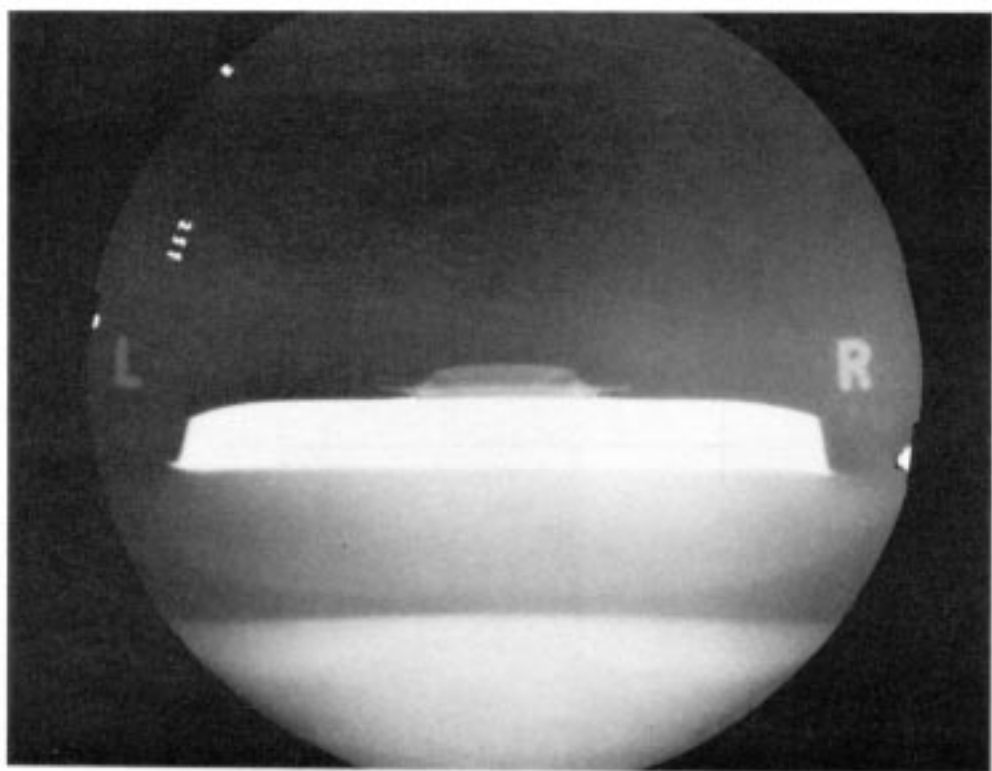
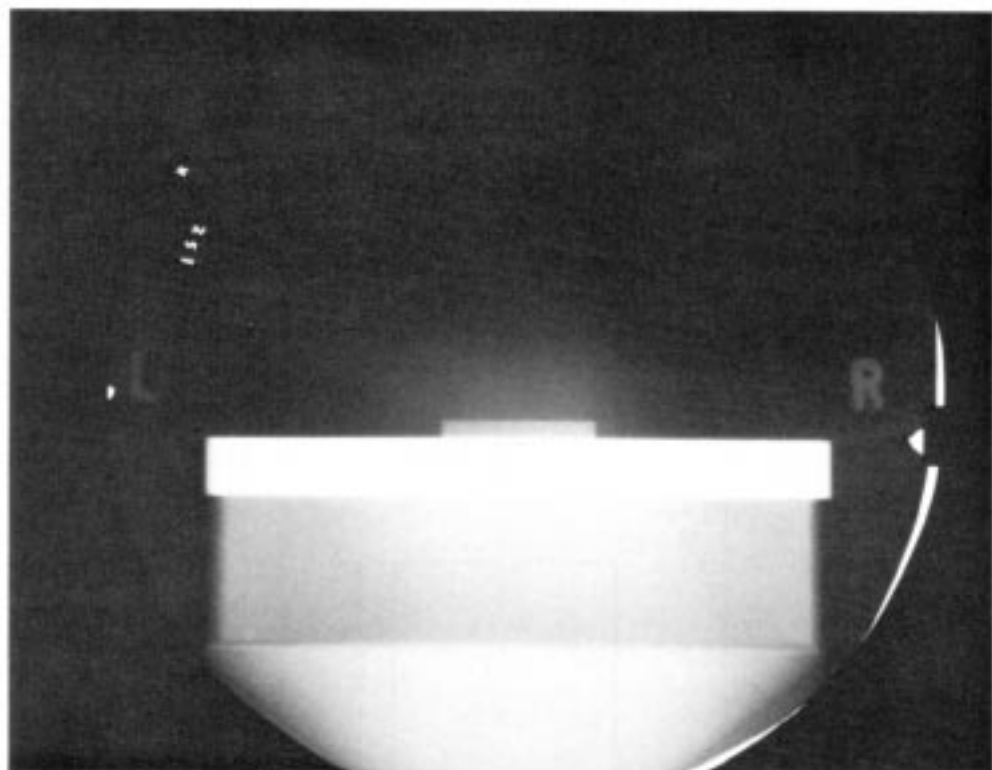
Date: February 25, 1965

Experimenter: Douglas Venable

Radiographic Time: 37.15 μ s

A 25-mm-thick by 50.0-mm-square block of aluminum is embedded in a 19.05-mm-thick by 203.2-mm-square block of iron. It is driven by 50.8-mm-thick Composition B-3 initiated by a P-081 lens.





SHOT 252:

Plane-Wave Aluminum Gun

Date:

February 25, 1965

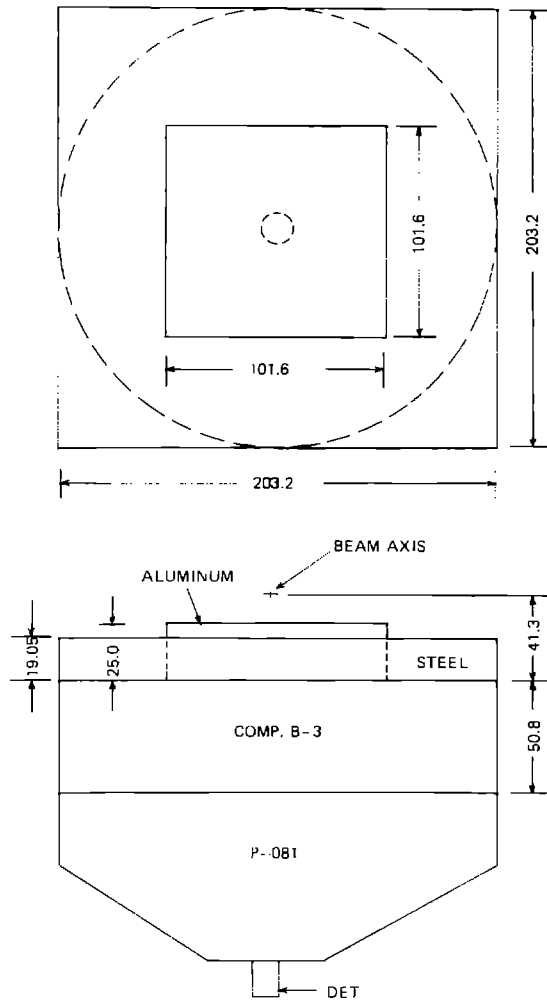
Experimenter:

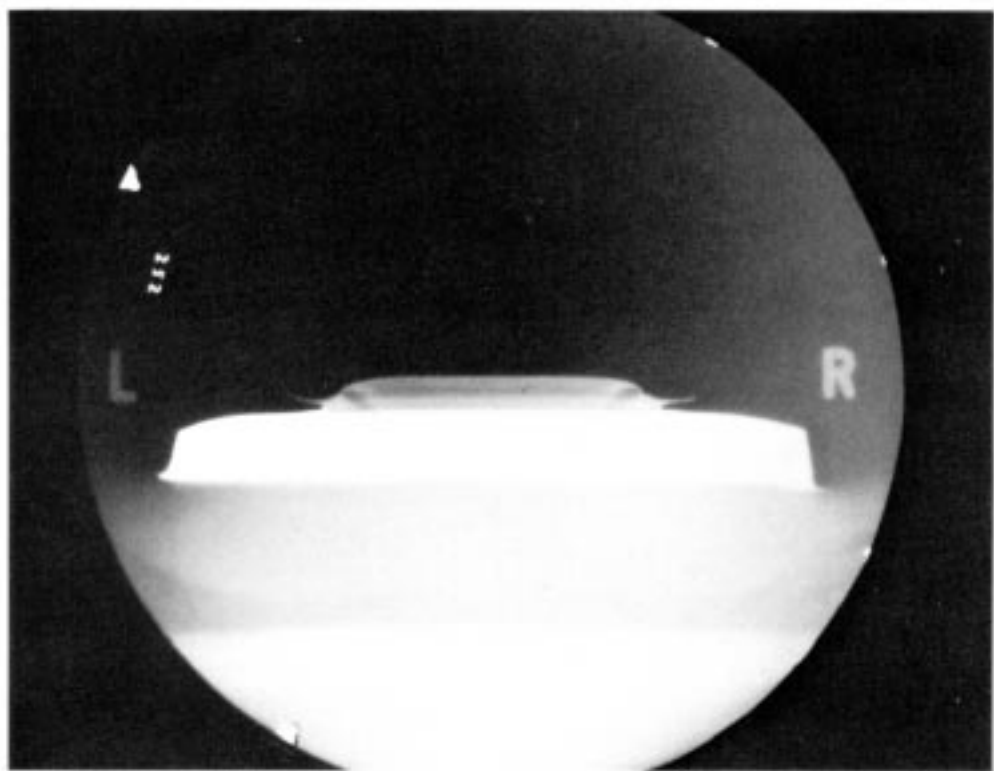
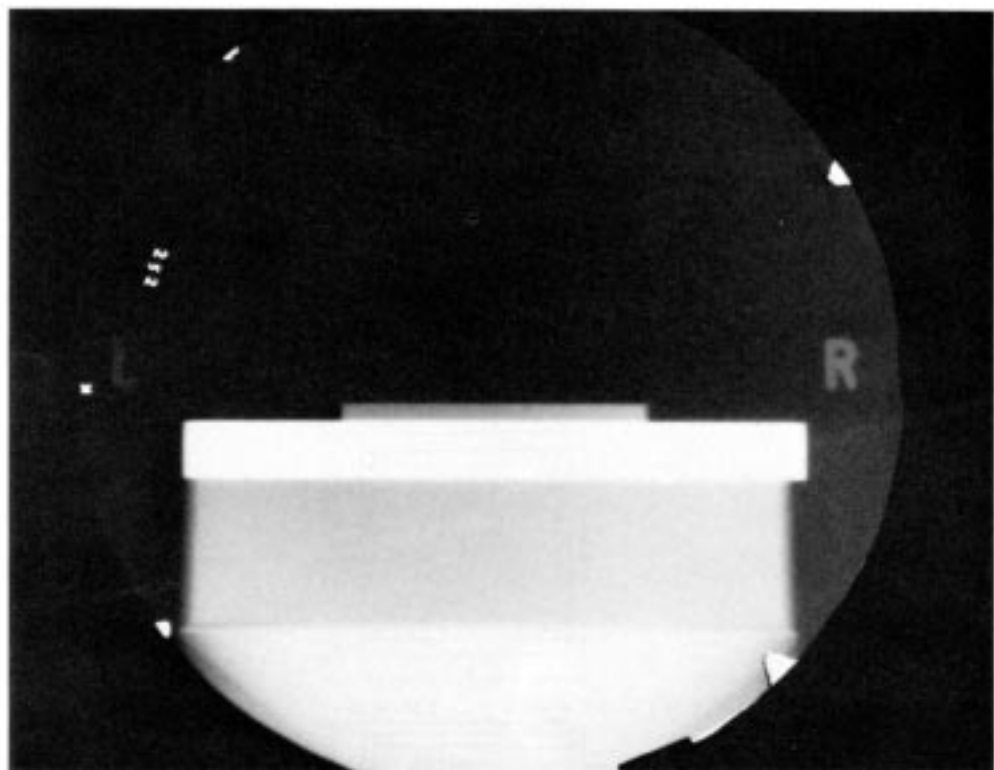
Douglas Venable

Radiographic Time:

37.13 μ s

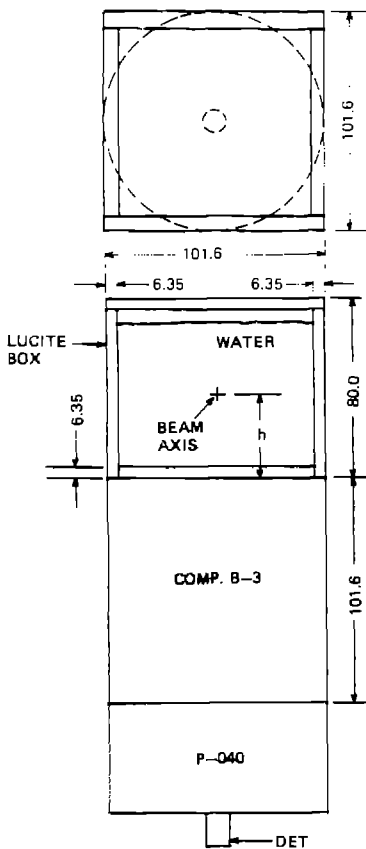
A 25-mm-thick by 101.6-mm-square block of aluminum is embedded in a 19.05-mm-thick by 203.2-mm-square block of iron. It is driven by 50.8-mm-thick Composition B-3 initiated by a P-081 lens.

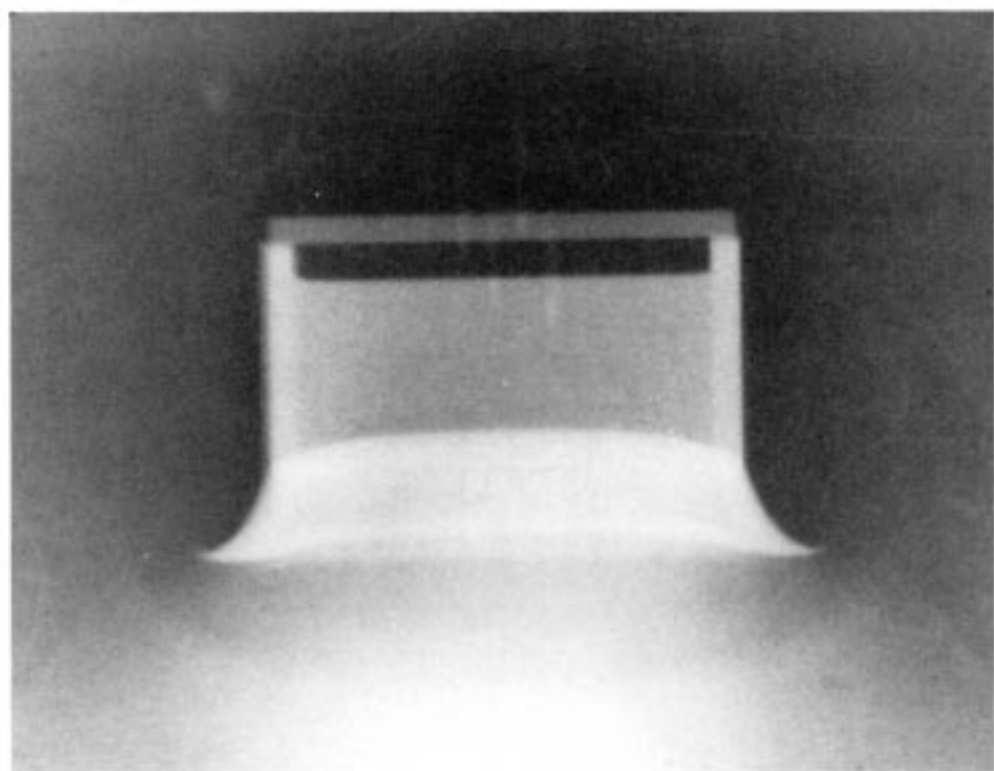
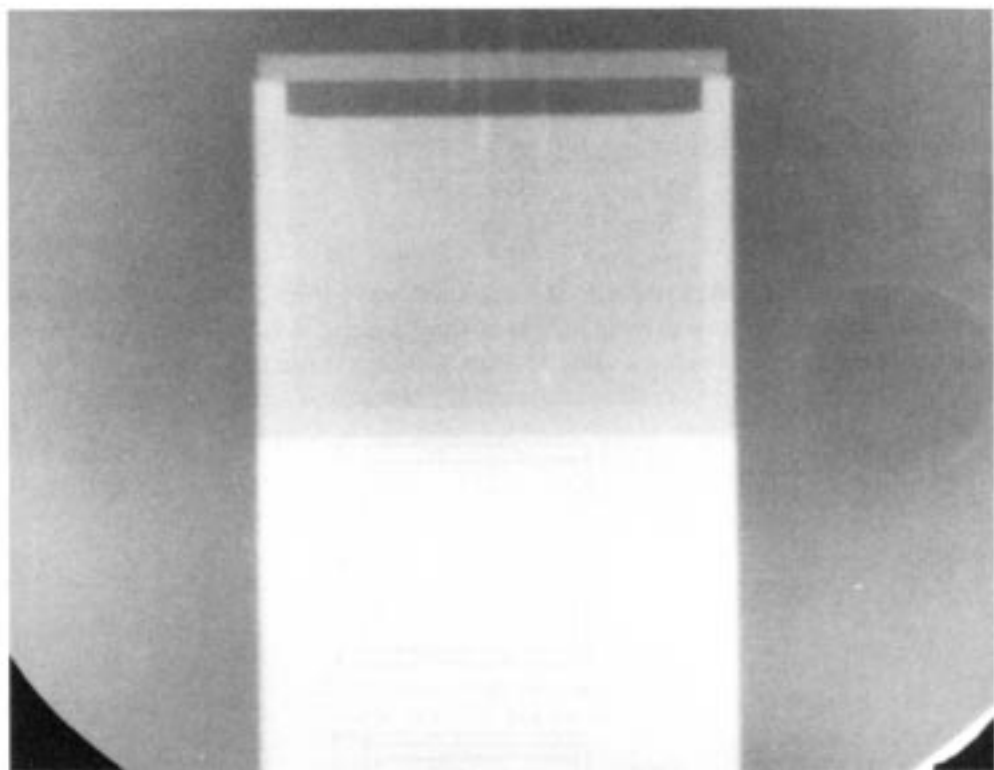




SHOT 253: **Water Shock**
Date: March 16, 1965
Experimenter: Roger W. Taylor
Radiographic Time: 32.19 μ s

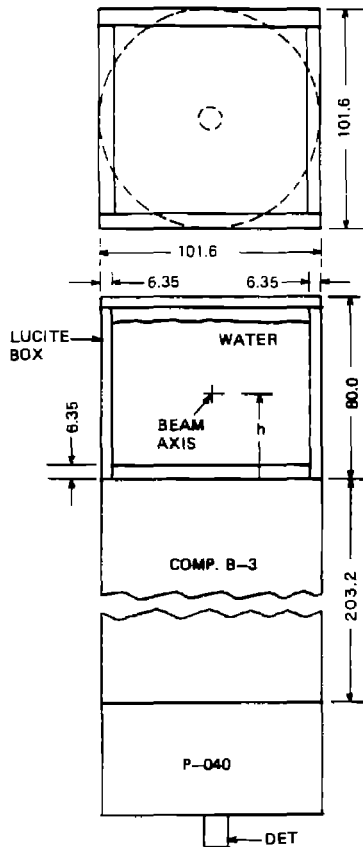
The shock wave formed in water by a detonation wave from 101.6 mm of Composition B-3 and a P-040 lens driving 6.35-mm-thick Lucite. h is 38.9 mm. Also shown are four timing pins. The shock velocity after 30.0 mm of run is 5.5 mm/ μ s.

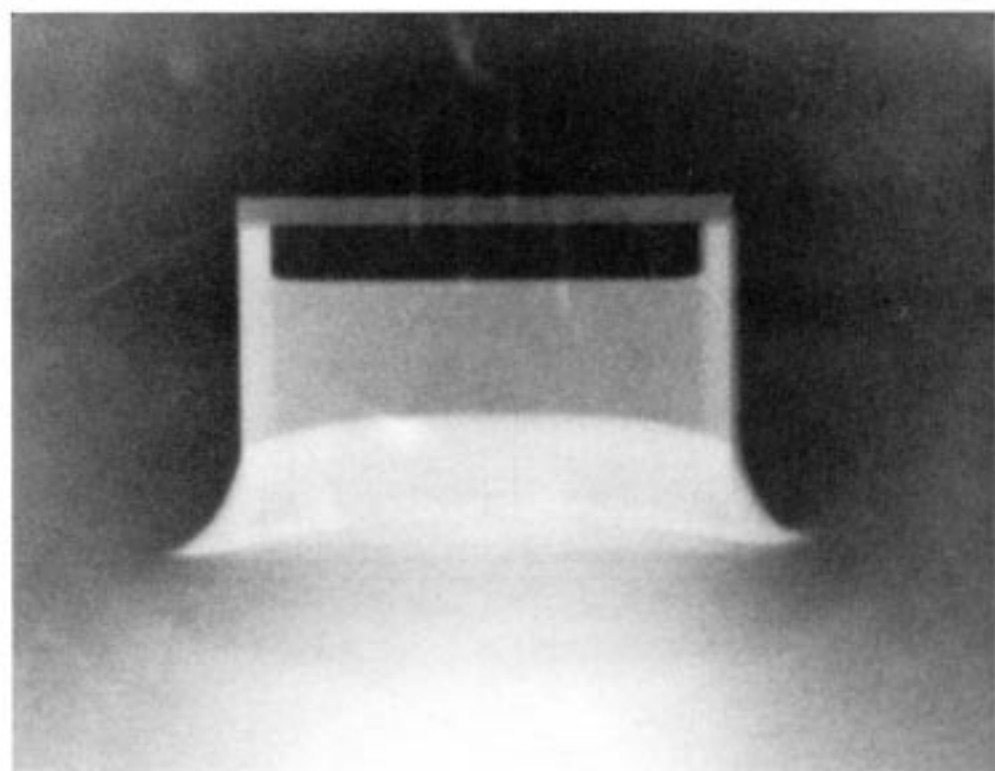
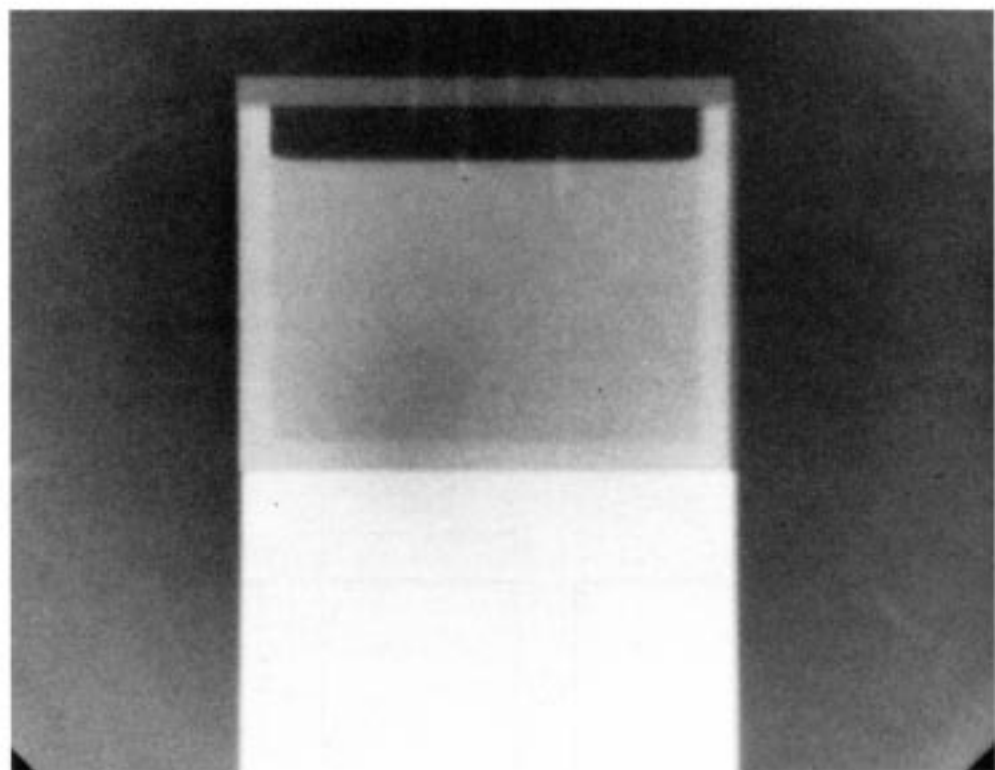




SHOT 254: **Water Shock**
Date: March 16, 1965
Experimenter: Roger W. Taylor
Radiographic Time: 44.95 μ s

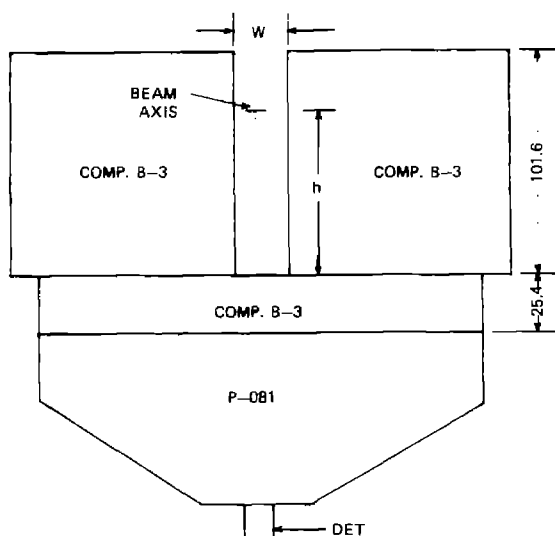
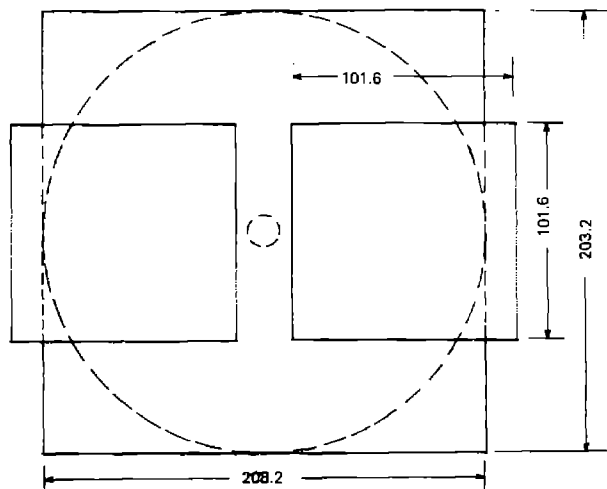
The shock wave formed in water by a detonation wave from 203.2 mm of Composition B-3 and a P-040 lens driving 6.35-mm-thick Lucite. h is 38.9 mm. Also shown are four timing pins. The shock velocity after 30.0 mm of run is 5.50 mm/ μ s.

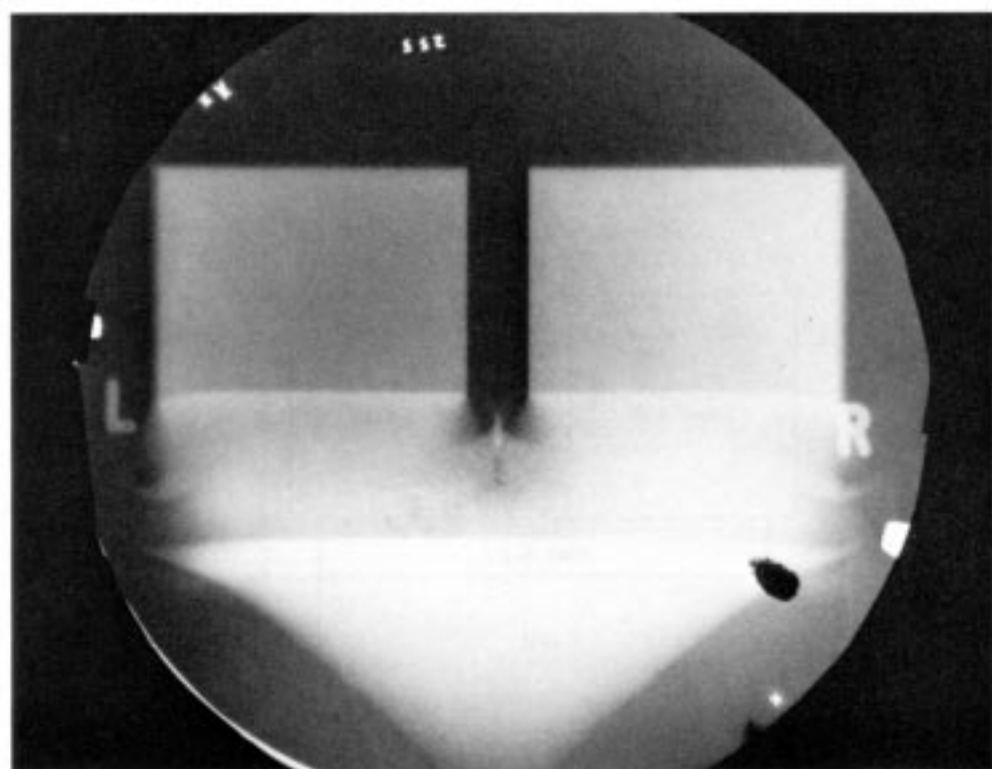
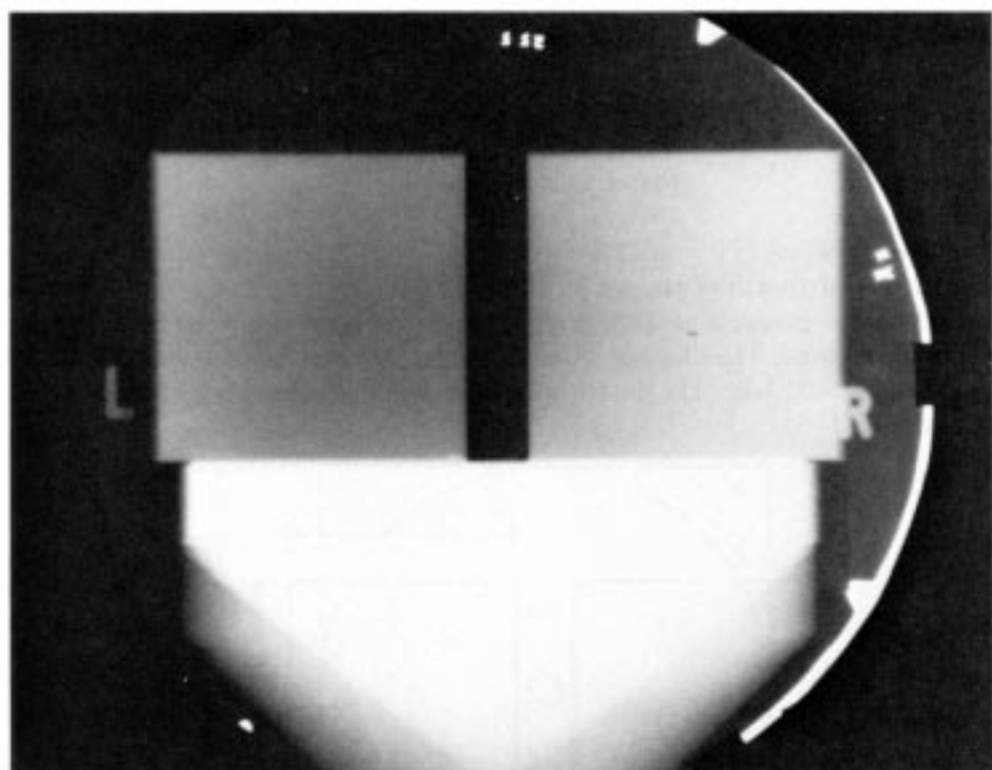




SHOT 255: **Munroe Jet**
 Date: March 2, 1965
 Experimenter: Douglas Venable
 Radiographic Time: 29.07 μ s

Formation and growth of gaseous Munroe jets. This jet is formed by interaction of the detonation products of two Composition B-3 charges separated by an air gap 20.0 mm, w, wide. The charges are initiated by 25.4 mm of Composition B-3 initiated by a P-081 lens. The detonations have run along the gap for 25.4 mm. h is 25.4 mm.





SHOT 256:**Munroe Jet**

Date:

March 2, 1965

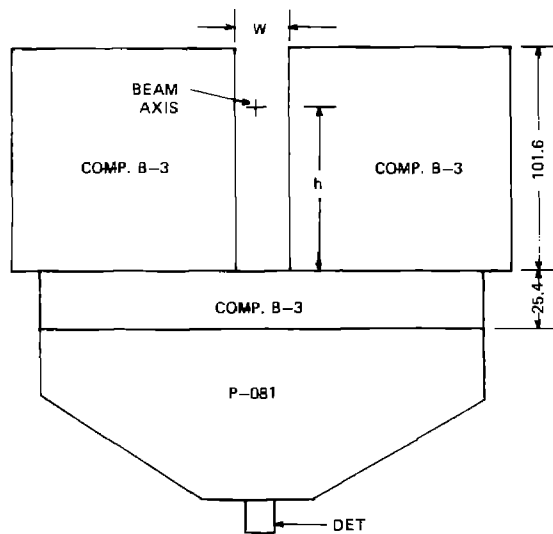
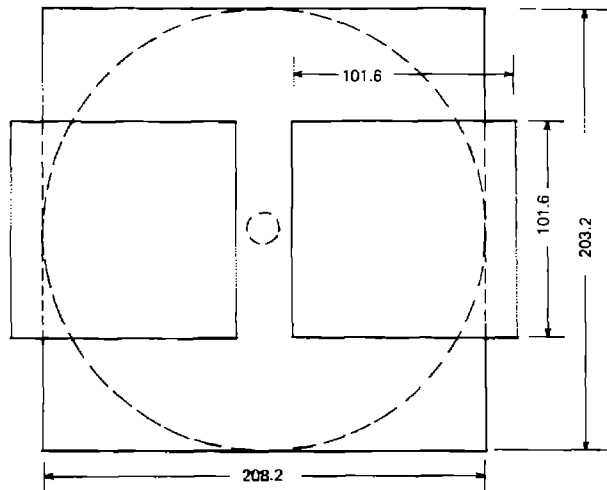
Experimenter:

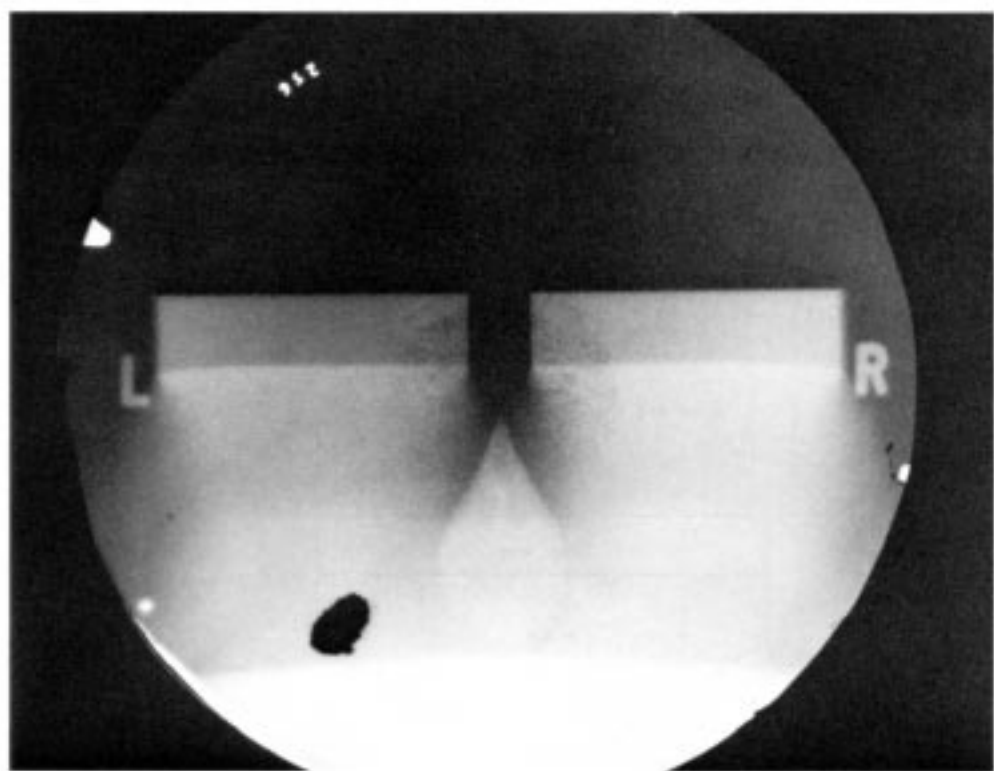
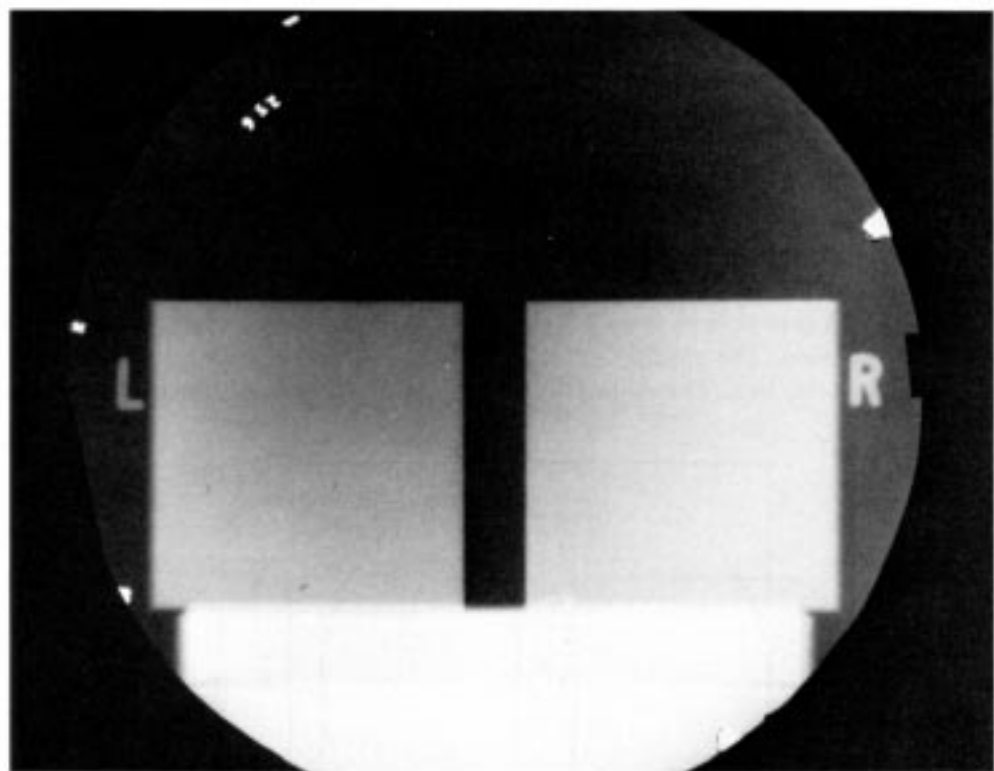
Douglas Venable

Radiographic Time:

35.45 μ s

Formation and growth of gaseous Munroe jets. This jet is formed by interaction of the detonation products of two Composition B-3 charges separated by an air gap 20.0 mm, w, wide. The charges are initiated by 25.4 mm of Composition B-3 initiated by a P-081 lens. The detonations have run along the gap for 76.2 mm. h is 76.2 mm.





SHOT 257:

Munroe Jet

Date:

March 2, 1965

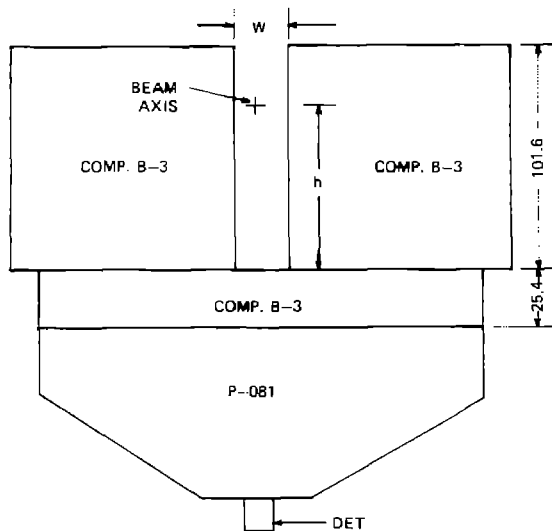
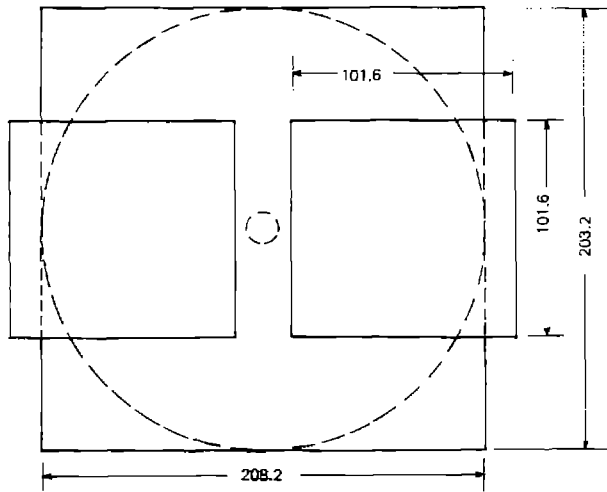
Experimenter:

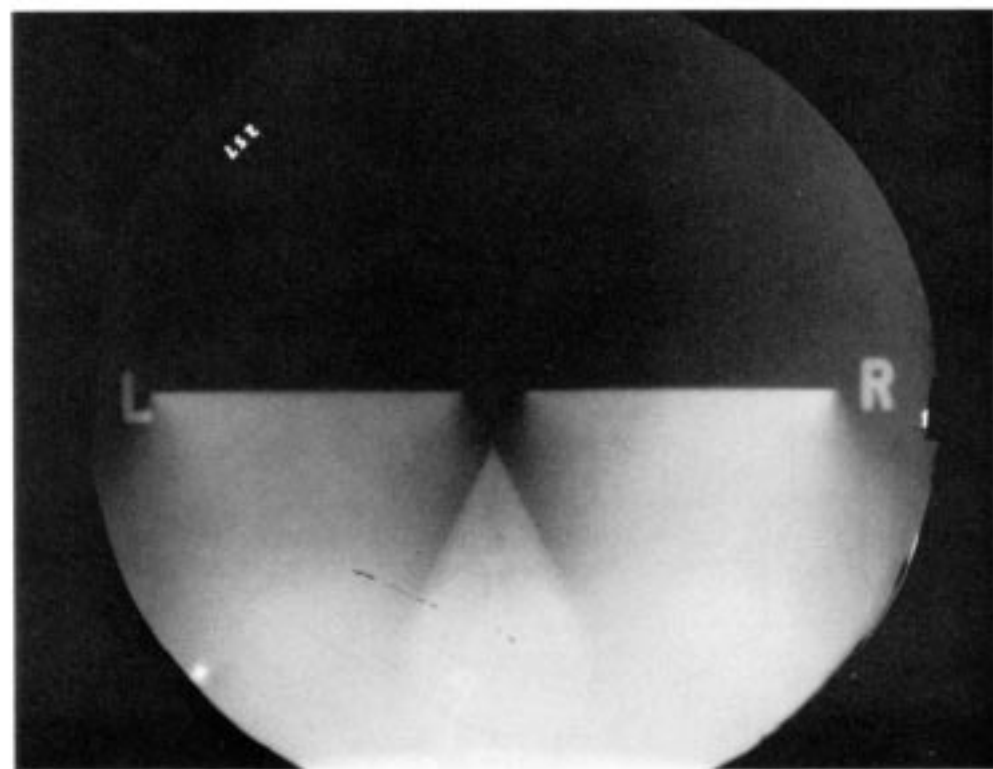
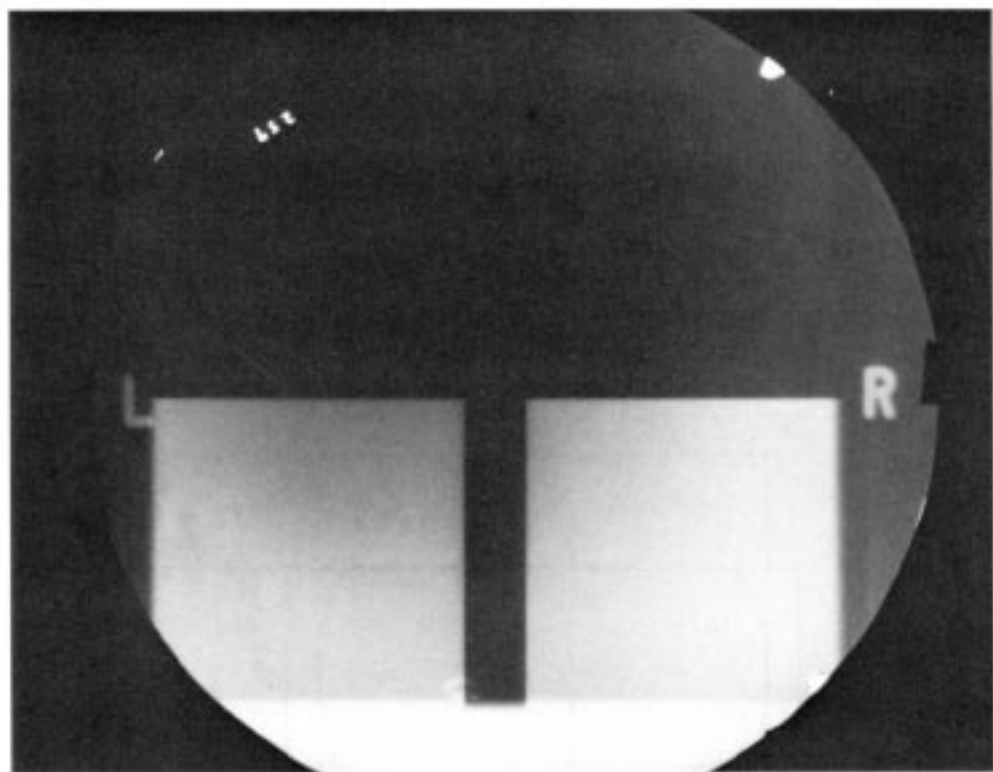
Douglas Venable

Radiographic Time:

38.65 μ s

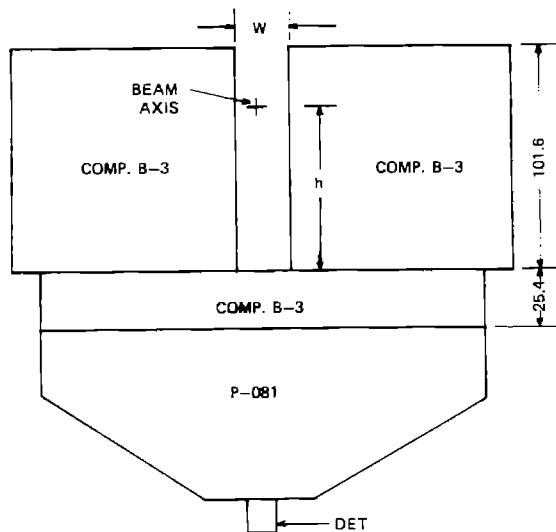
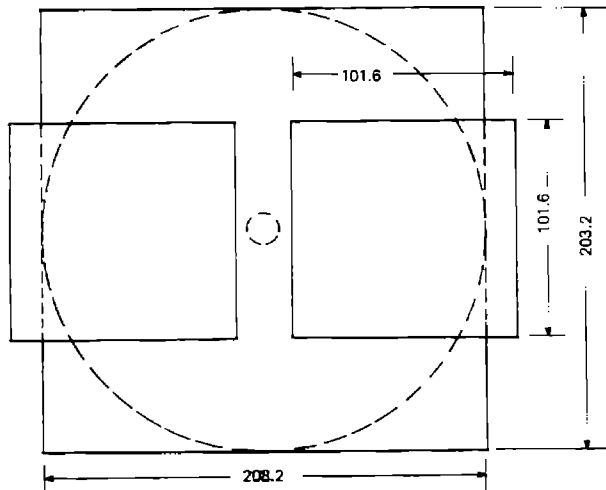
Formation and growth of gaseous Munroe jets. This jet is formed by interaction of the detonation products of two Composition B-3 charges separated by an air gap 20.0 mm, w, wide. The charges are initiated by 25.4 mm of Composition B-3 initiated by a P-081 lens. The detonations have run along the gap for 101.6 mm. h is 101.6 mm.

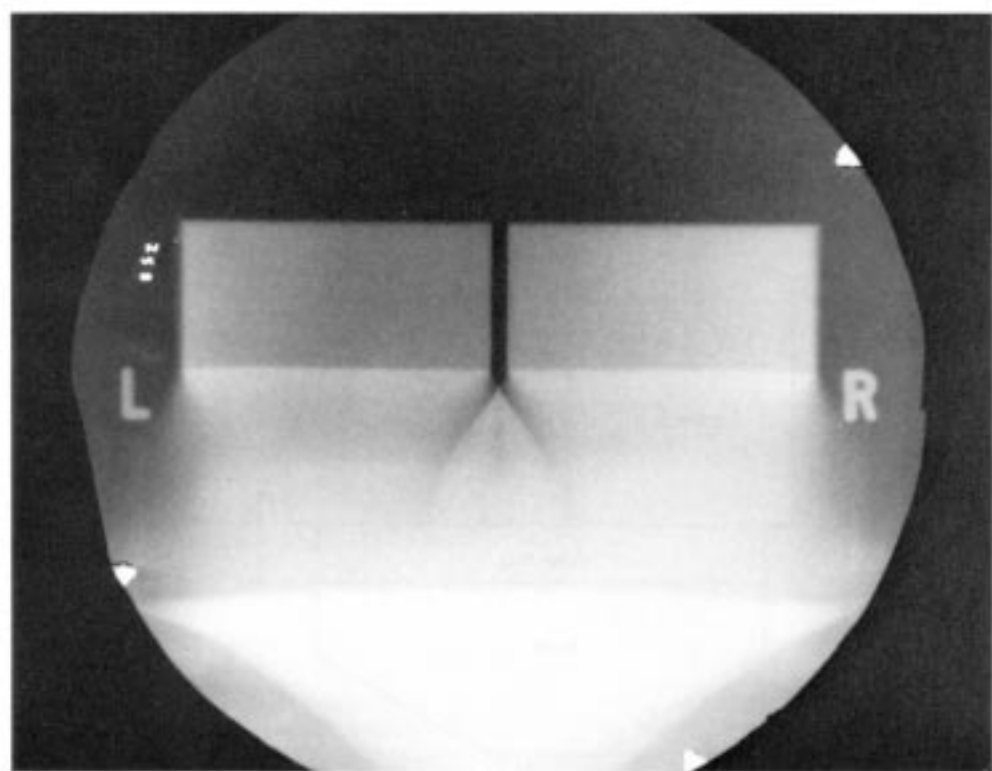
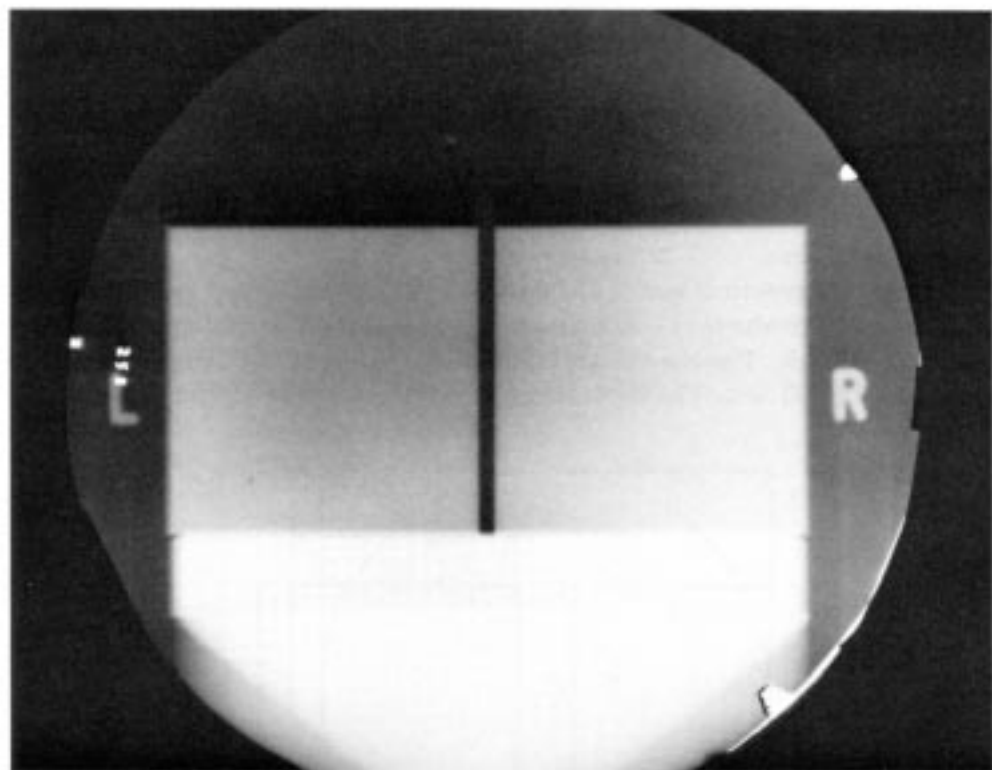




SHOT 258: **Munroe Jet**
 Date: March 4, 1965
 Experimenter: Douglas Venable
 Radiographic Time: 32.24 μ s

Formation and growth of gaseous Munroe jets. This jet is formed by interaction of the detonation products of two Composition B-3 charges separated by an air gap 5.0 mm, w, wide. The charges are initiated by 25.4 mm of Composition B-3 initiated by a P-081 lens. The detonations have run along the gap for 50.8 mm. h is 50.8 mm.





SHOT 259:

Munroe Jet

Date:

March 4, 1965

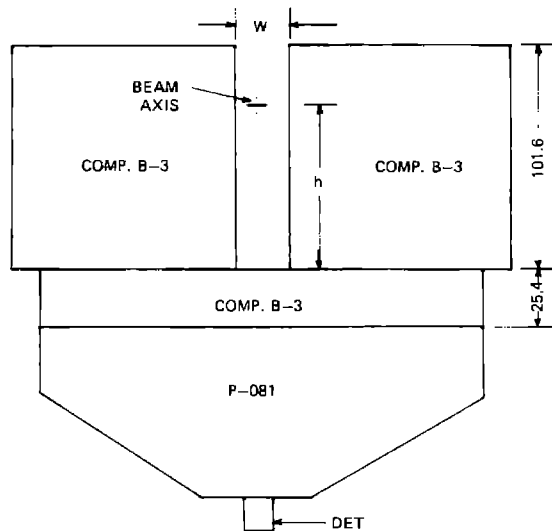
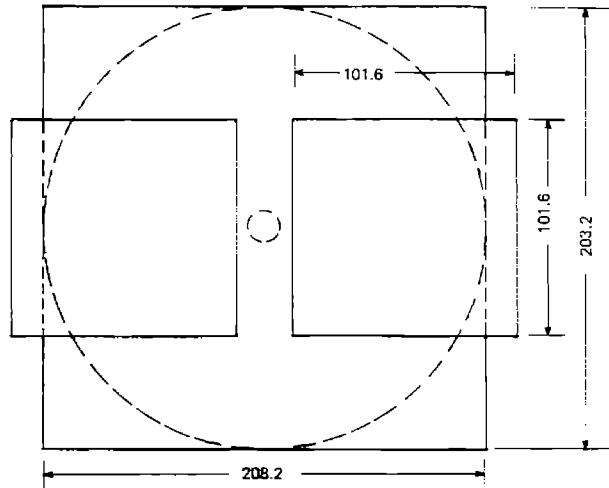
Experimenter:

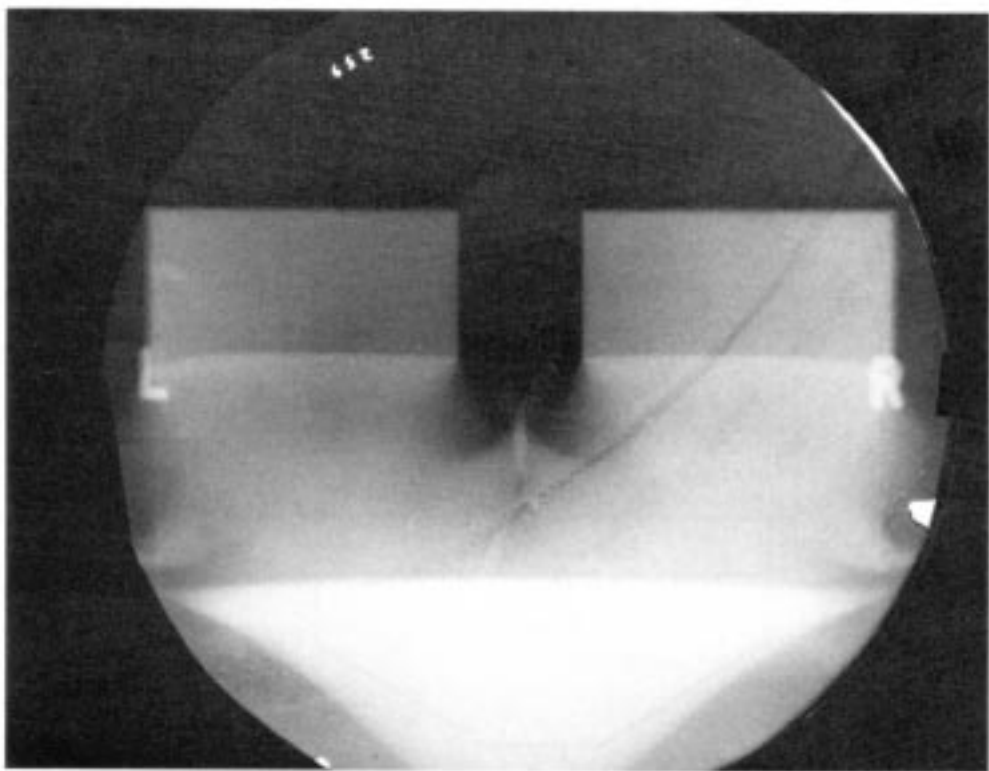
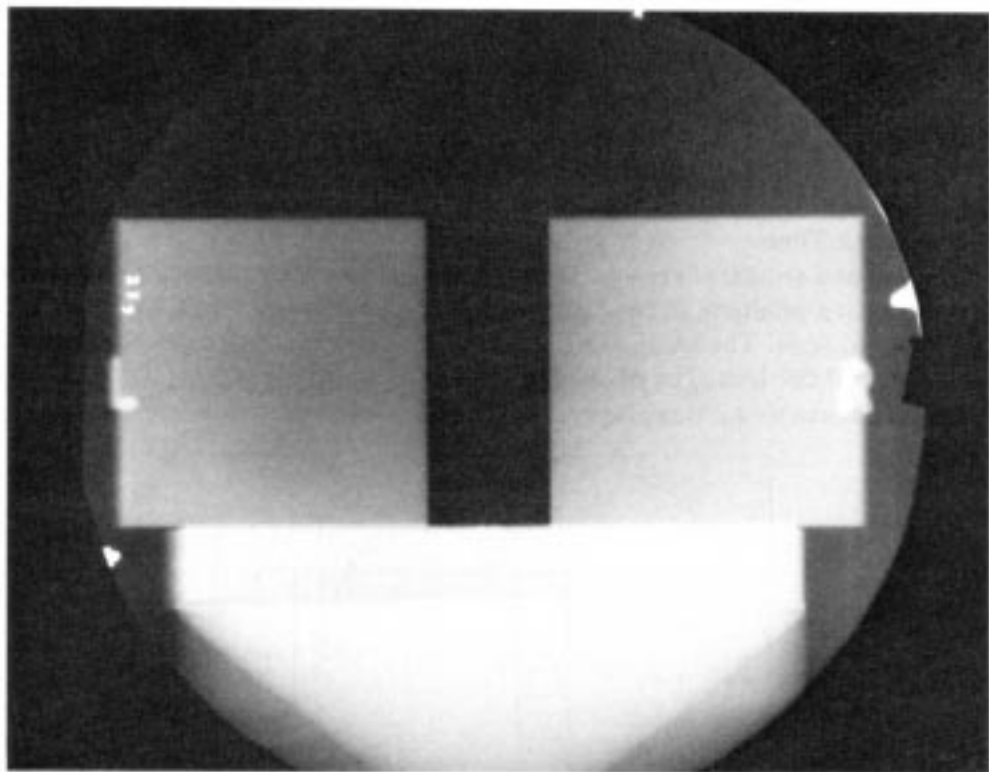
Douglas Venable

Radiographic Time:

32.24 μ s

Formation and growth of gaseous Munroe jets. This jet is formed by interaction of the detonation products of two Composition B-3 charges separated by an air gap 40.0 mm, w, wide. The charges are initiated by 25.4 mm of Composition B-3 initiated by a P-081 lens. The detonations have run along the gap for 50.8 mm. h is 50.8 mm.





SHOT 260:

Munroe Jet

Date:

March 31, 1965

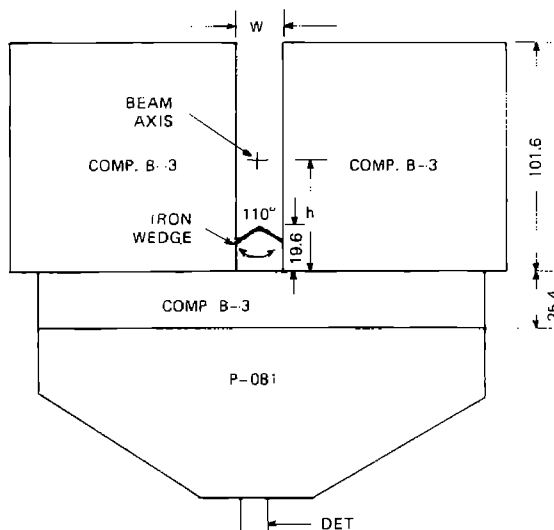
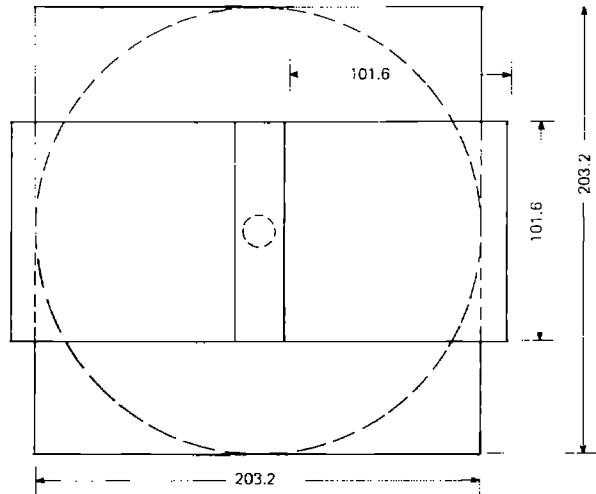
Experimenter:

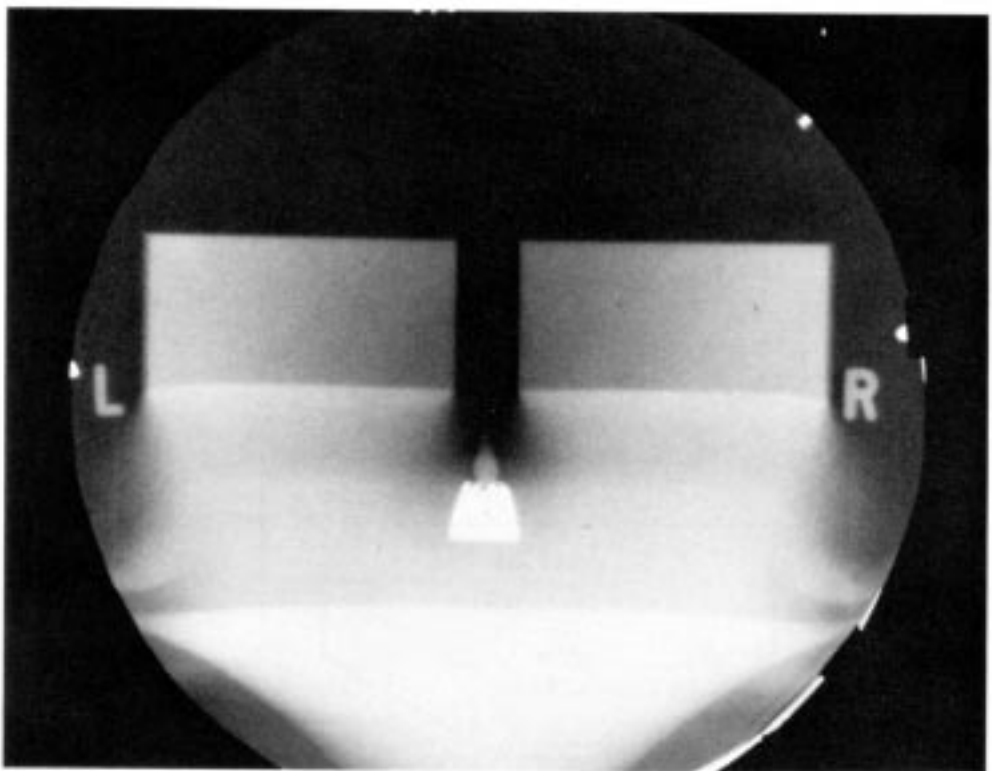
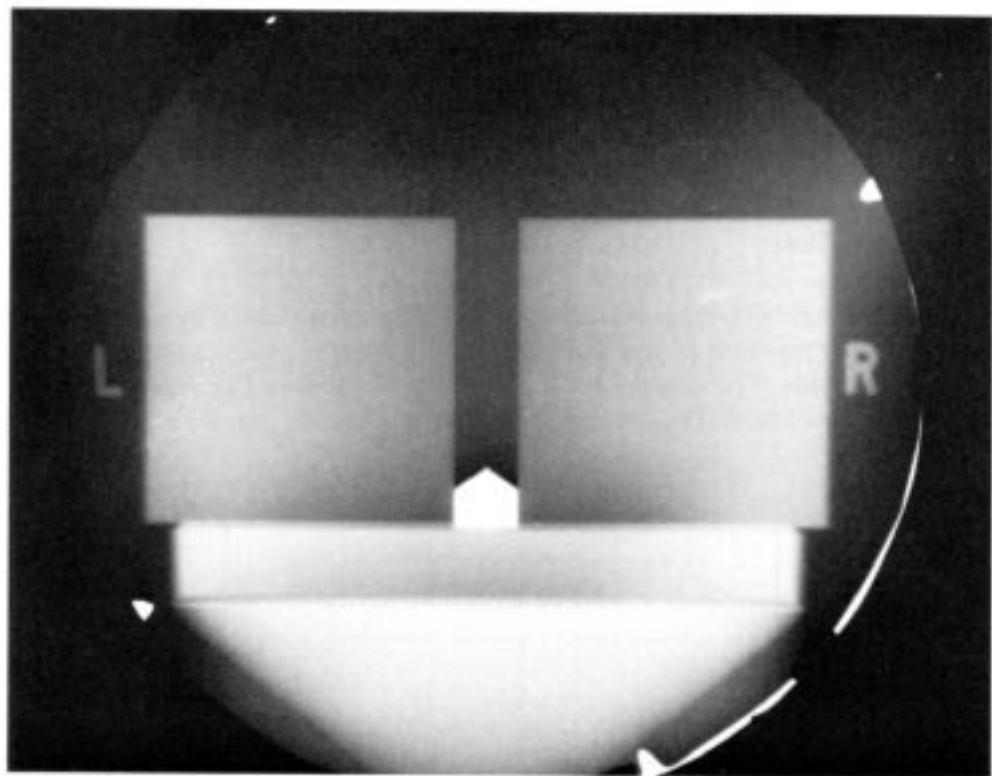
Douglas Venable

Radiographic Time:

32.36 μ s

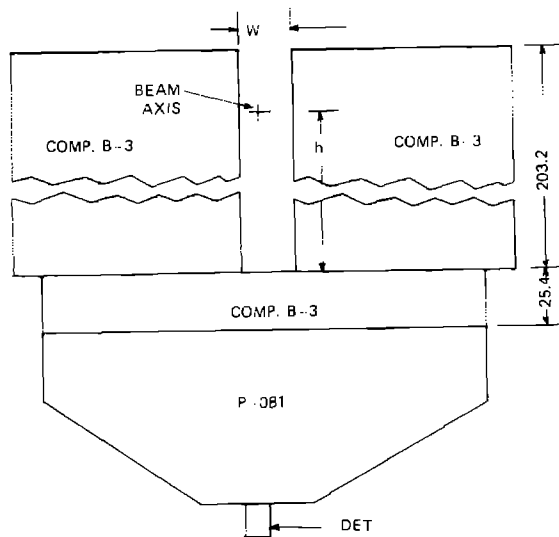
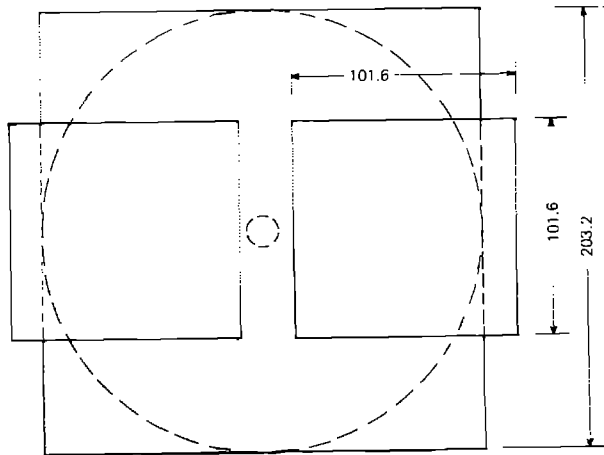
Formation and growth of gaseous Munroe jets. This jet is formed by interaction of the detonation products of two Composition B-3 charges separated by an air gap 20.0 mm, w, wide. The charges are initiated by 25.4 mm of Composition B-3 initiated by a P-081 lens. The detonations have run along the gap for 50.8 mm. h is 50.8 mm. An iron wedge was placed between the charges.

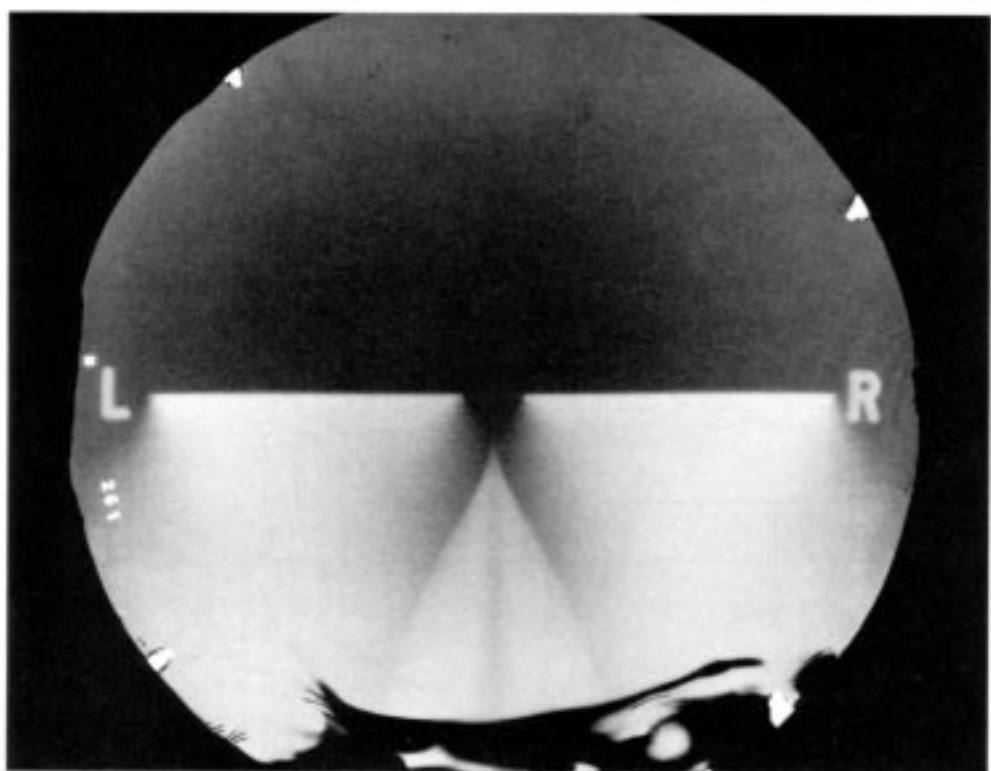
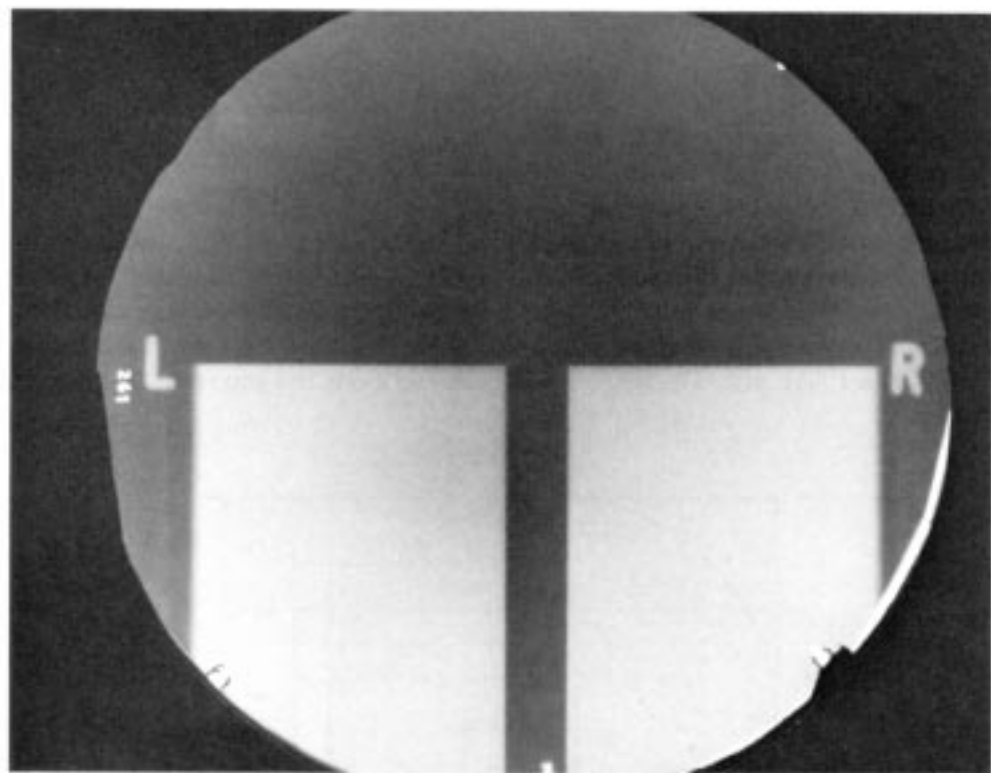




SHOT 261: **Munroe Jet**
 Date: April 7, 1965
 Experimenter: Douglas Venable
 Radiographic Time: 51.35 μ s
 Reference: Venable, 1965

Formation and growth of gaseous Munroe jets. This jet is formed by interaction of the detonation products of two Composition B-3 charges separated by an air gap 20.0 mm, w, wide. The charges are initiated by 25.4 mm of Composition B-3 initiated by a P-081 lens. The detonations have run along the gap for 203.2 mm. h is 203.2 mm.





SHOT 262:

Munroe Jet

Date:

April 15, 1965

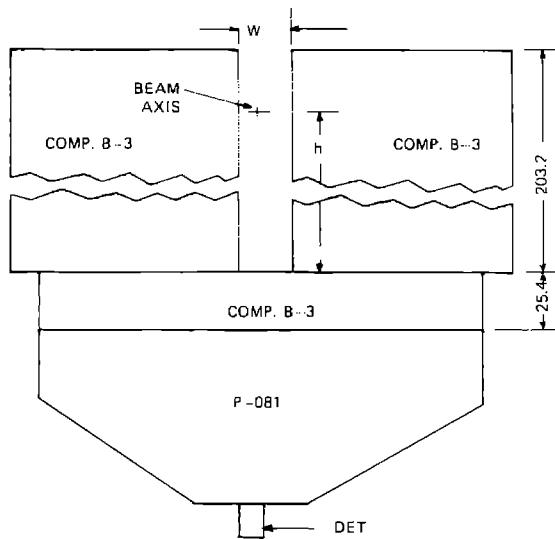
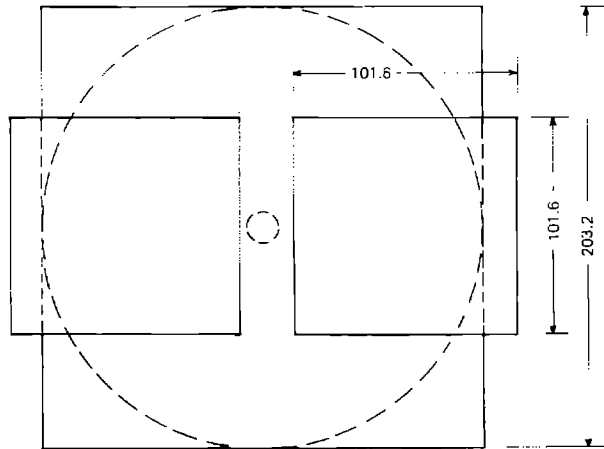
Experimenter:

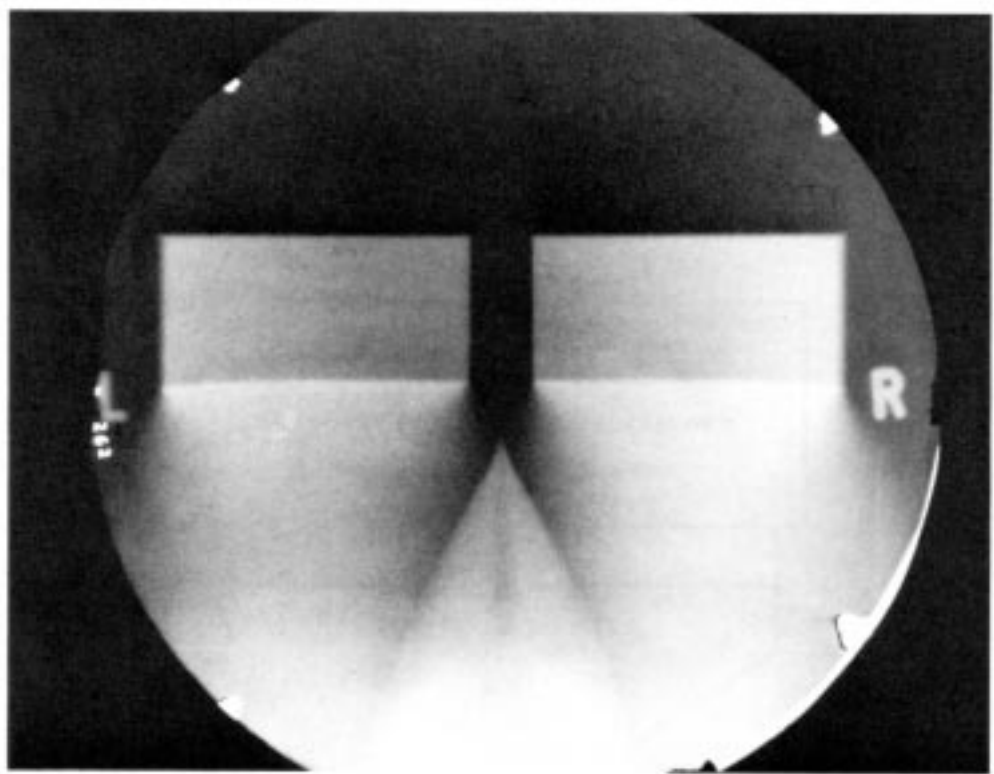
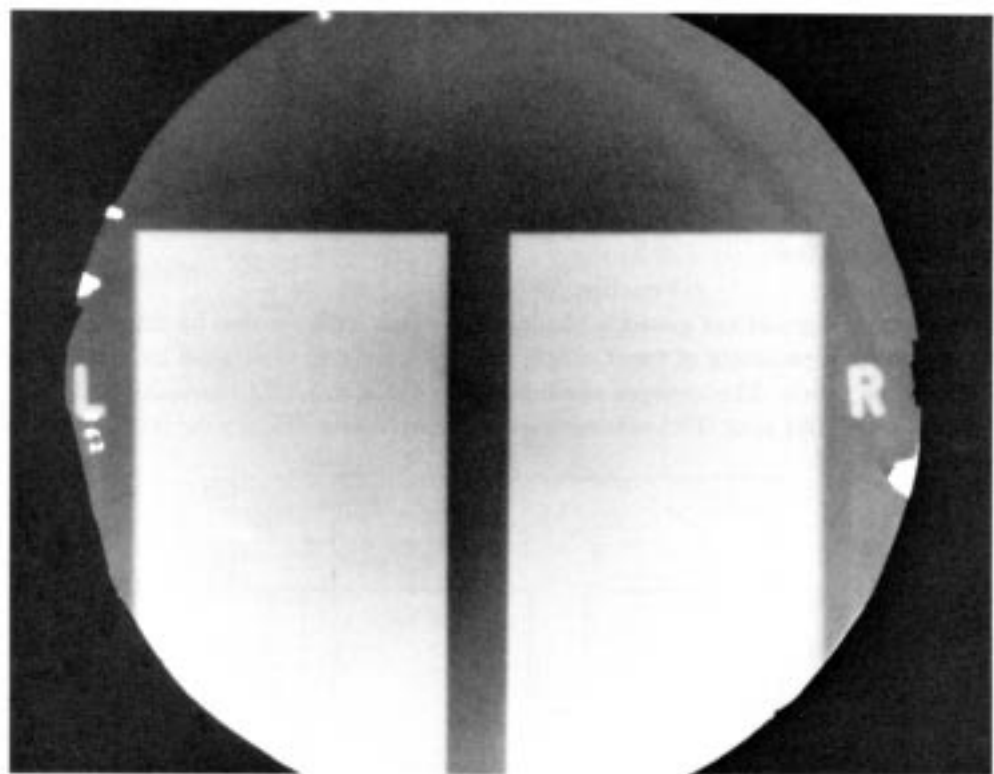
Douglas Venable

Radiographic Time:

45.1 μ s

Formation and growth of gaseous Munroe jets. This jet is formed by interaction of the detonation products of two Composition B-3 charges separated by an air gap 20.0 mm, w, wide. The charges are initiated by 25.4 mm of Composition B-3 initiated by a P-081 lens. The detonations have run along the gap for 152.4 mm. h is 152.4 mm.





SHOT 263:

Munroe Jet

Date:

April 13, 1965

Experimenter:

Douglas Venable

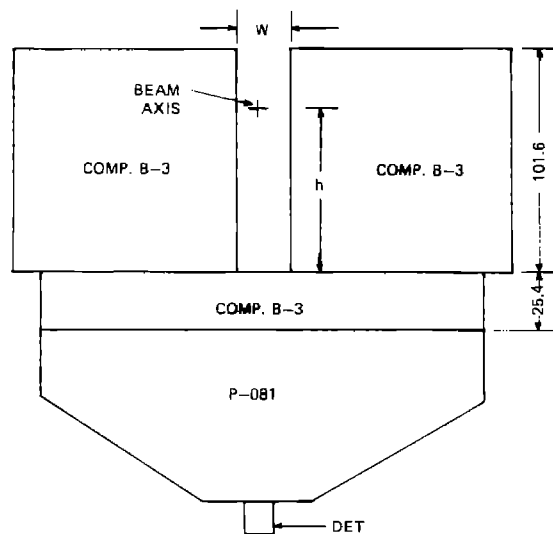
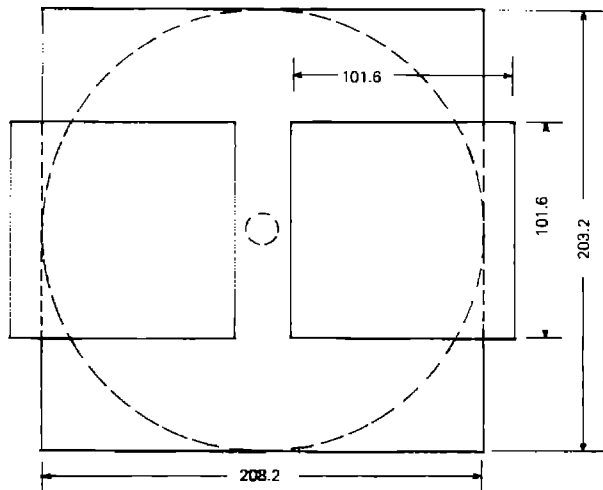
Radiographic Time:

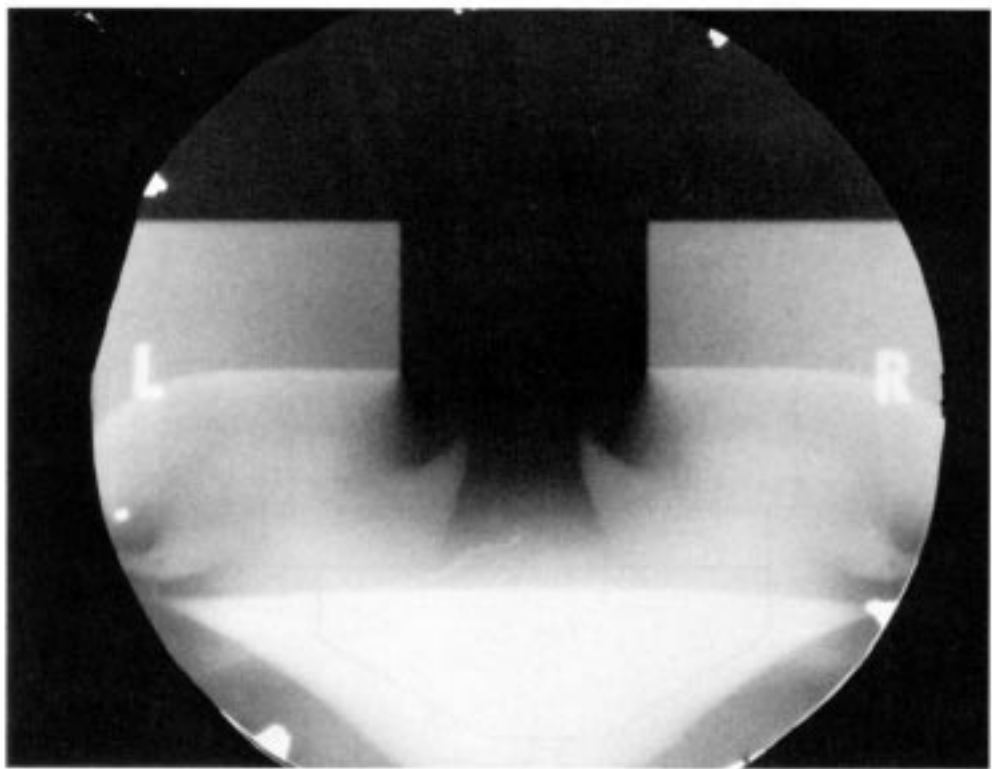
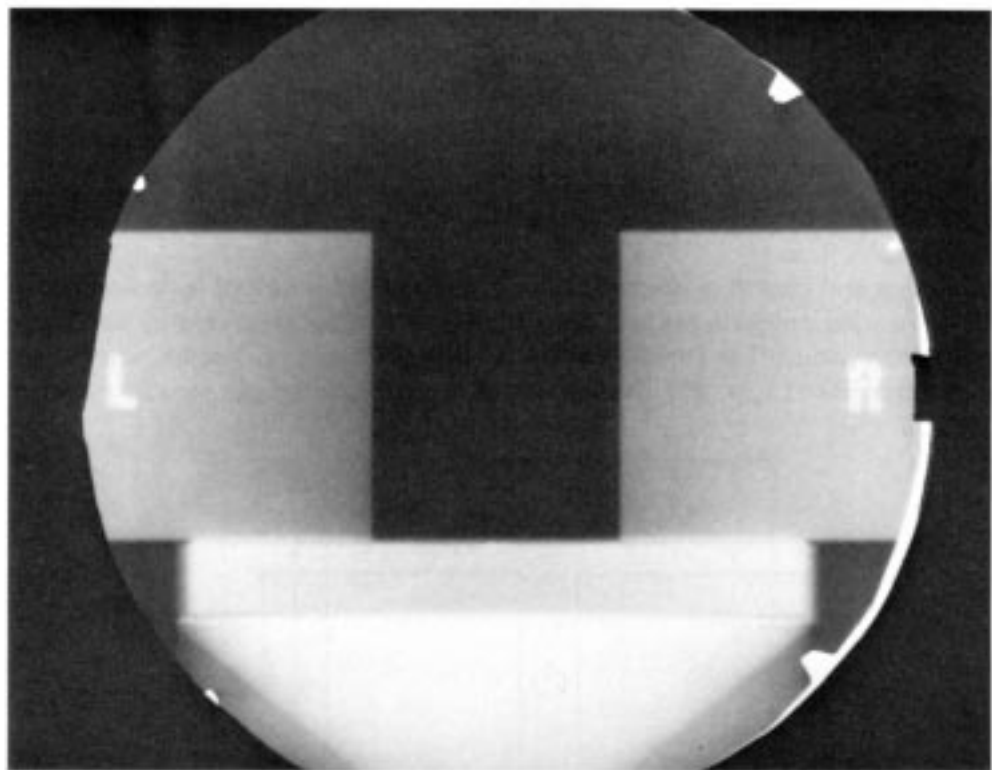
32.3 μ s

Reference:

Venable, 1965

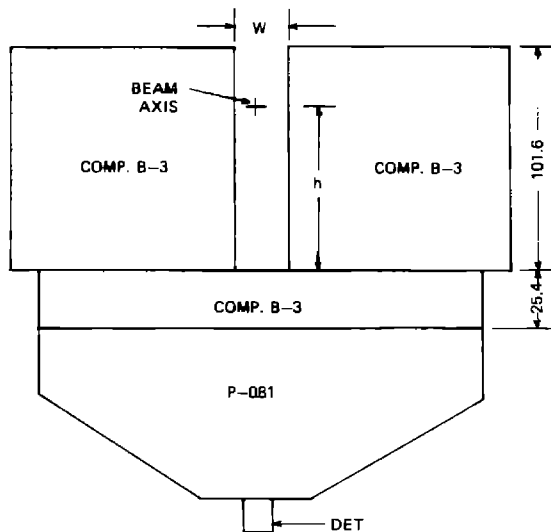
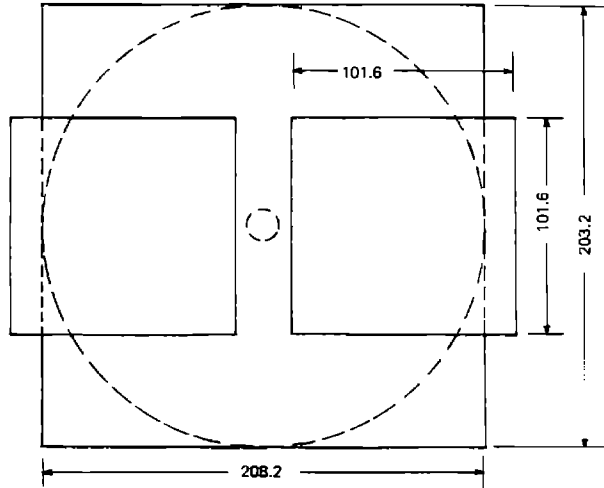
Formation and growth of gaseous Munroe jets. This jet is formed by interaction of the detonation products of two Composition B-3 charges separated by an air gap 80.0 mm, w, wide. The charges are initiated by 25.4 mm of Composition B-3 initiated by a P-081 lens. The detonations have run along the gap for 50.8 mm. h is 50.8 mm.

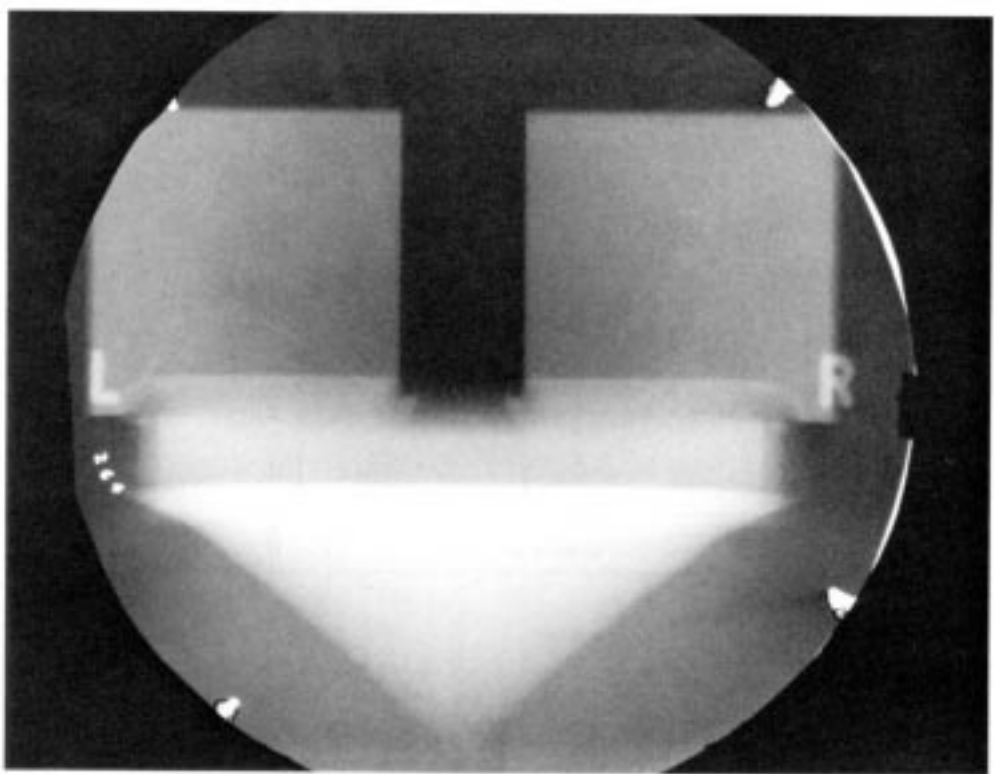
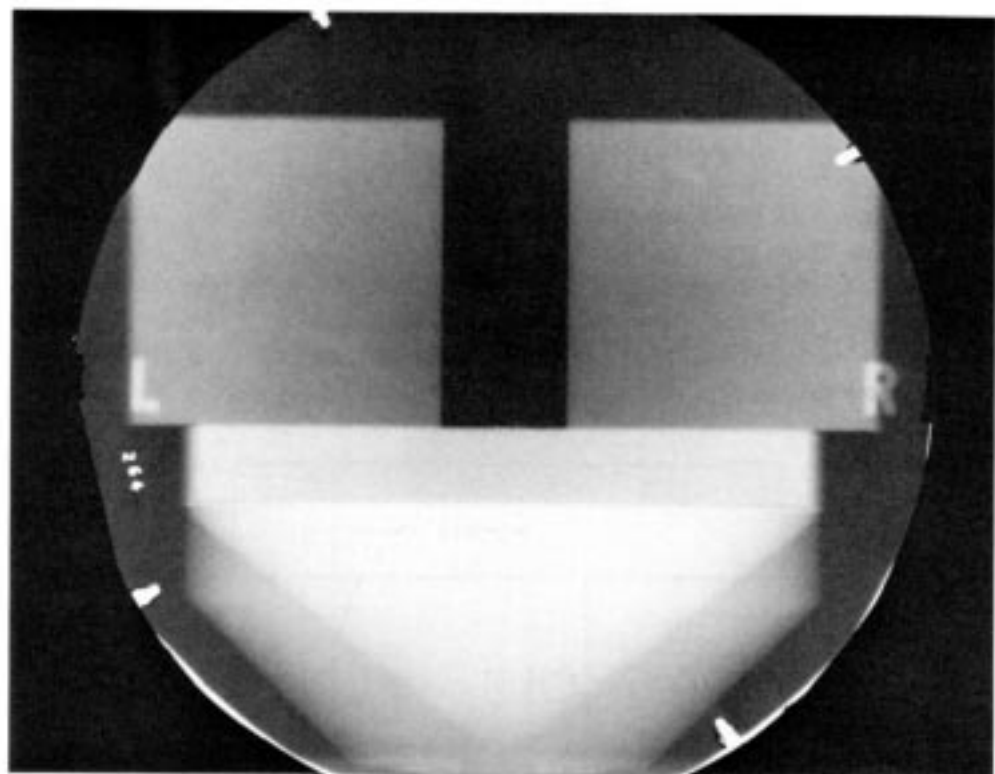




SHOT 264: **Munroe Jet**
 Date: April 13, 1965
 Experimenter: Douglas Venable
 Radiographic Time: 27.52 μ s

Formation and growth of gaseous Munroe jets. This jet is formed by interaction of the detonation products of two Composition B-3 charges separated by an air gap 40.0 mm, w, wide. The charges are initiated by 25.4 mm of Composition B-3 initiated by a P-081 lens. The detonations have run along the gap for 12.7 mm. h is 12.7 mm.





SHOT 265:

Munroe Jet

Date:

April 13, 1965

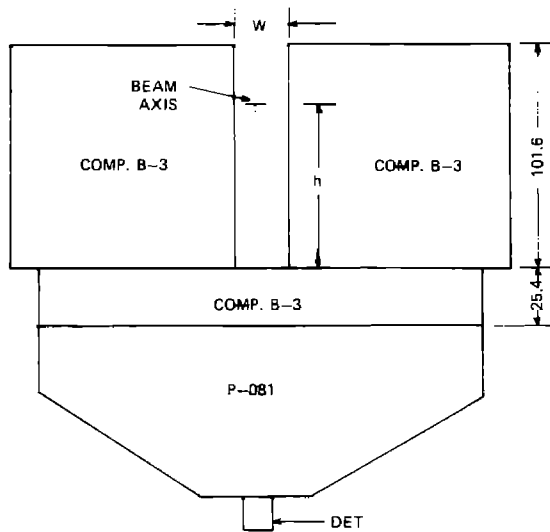
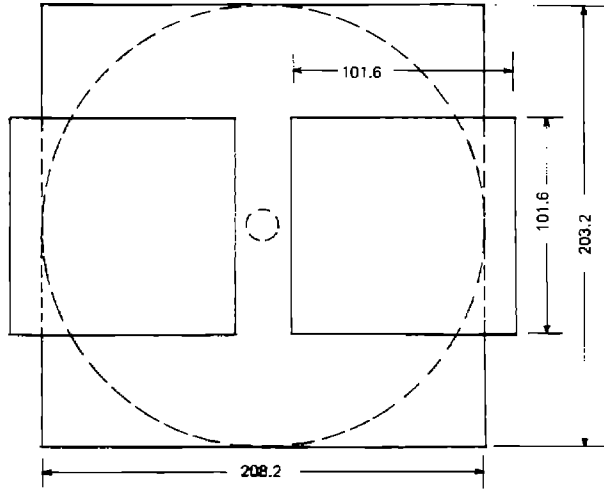
Experimenter:

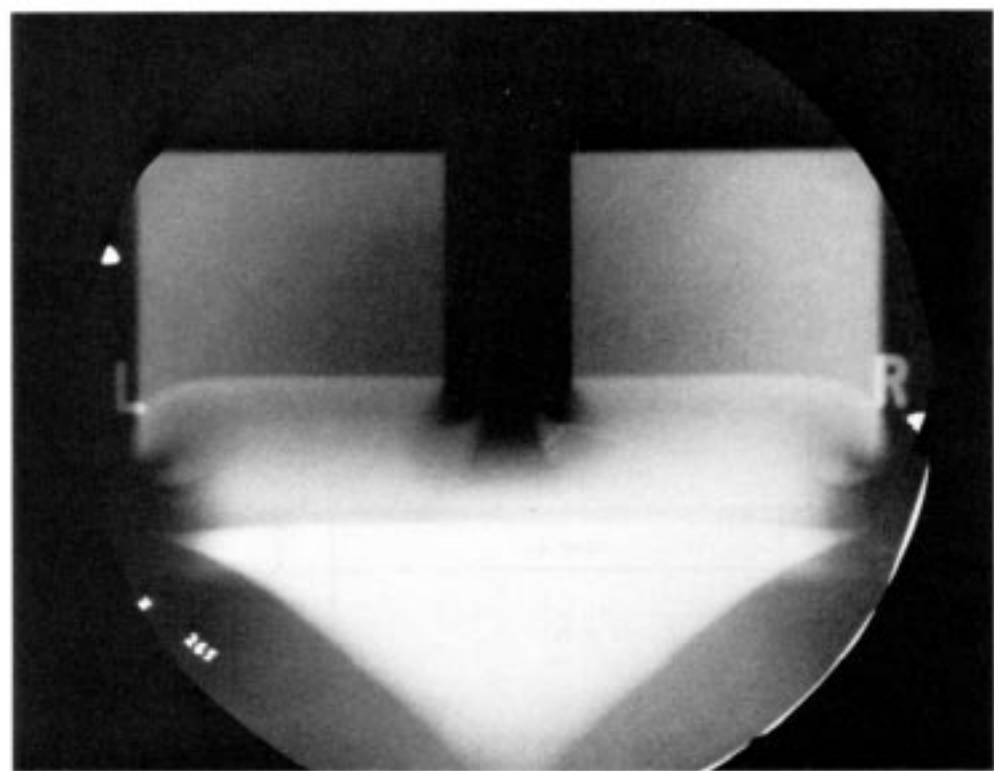
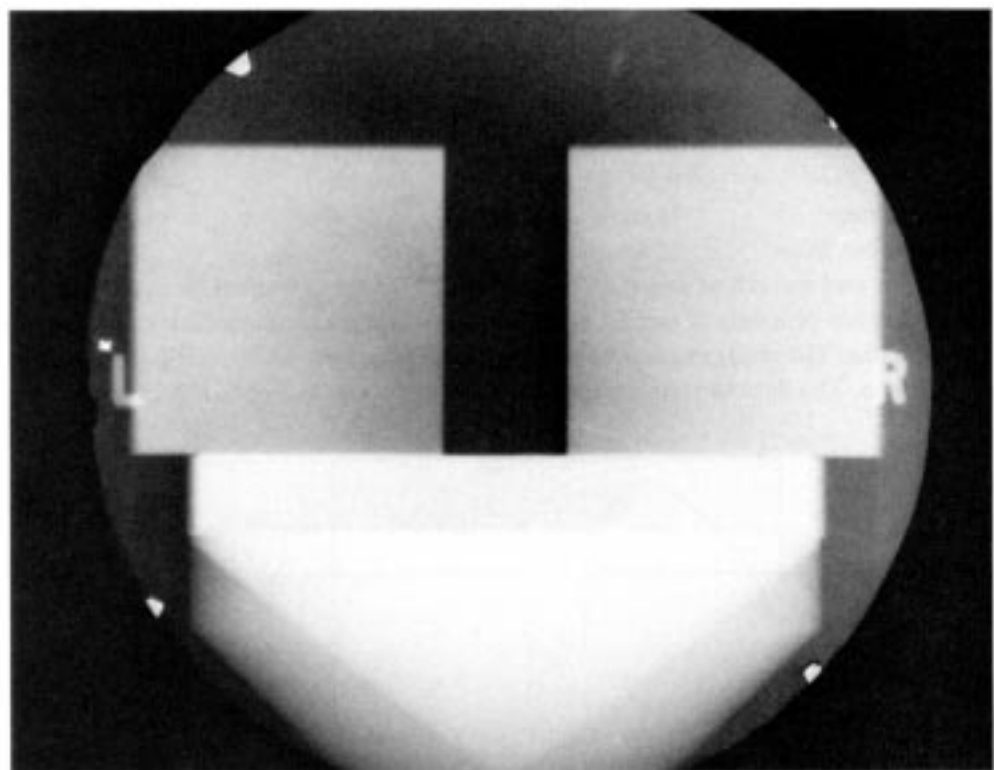
Douglas Venable

Radiographic Time:

29.15 μ s

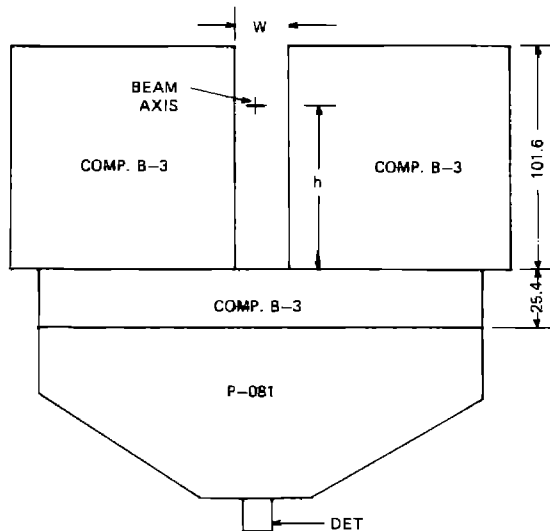
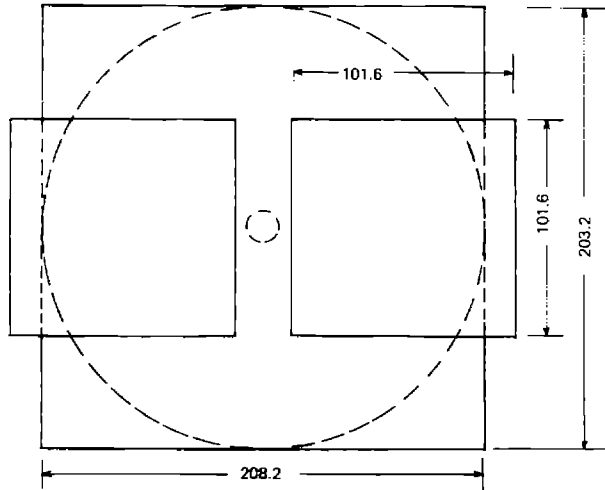
Formation and growth of gaseous Munroe jets. This jet is formed by interaction of the detonation products of two Composition B-3 charges separated by an air gap 40.0 mm, w, wide. The charges are initiated by 25.4 mm of Composition B-3 initiated by a P-081 lens. The detonations have run along the gap for 25.4 mm. h is 25.4 mm.

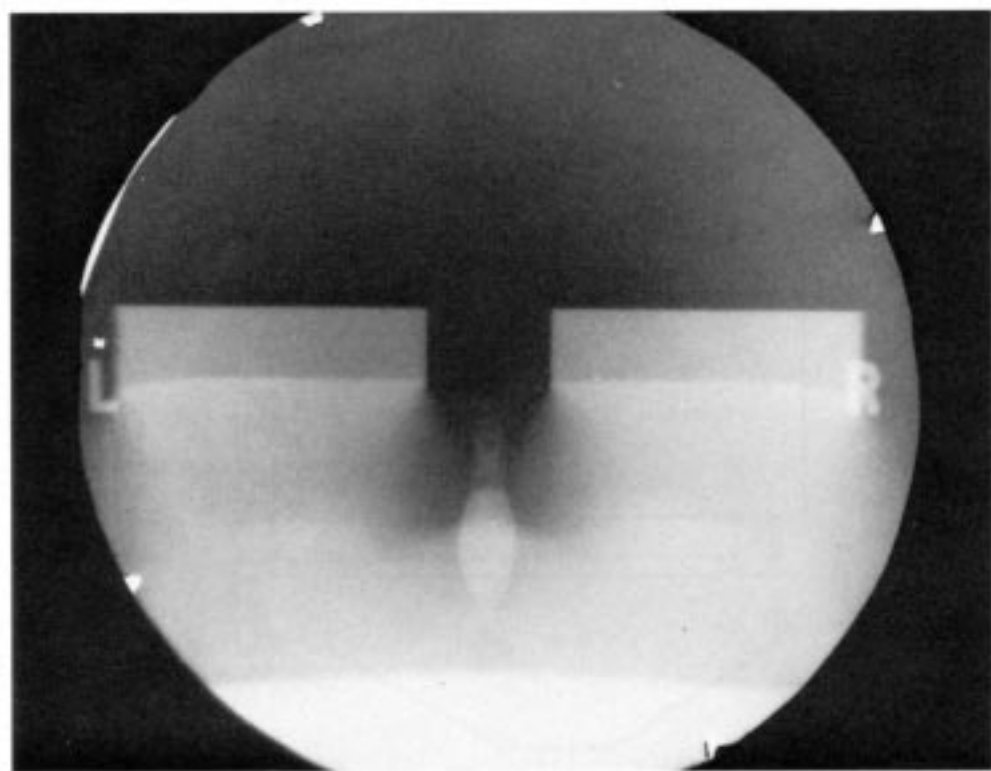
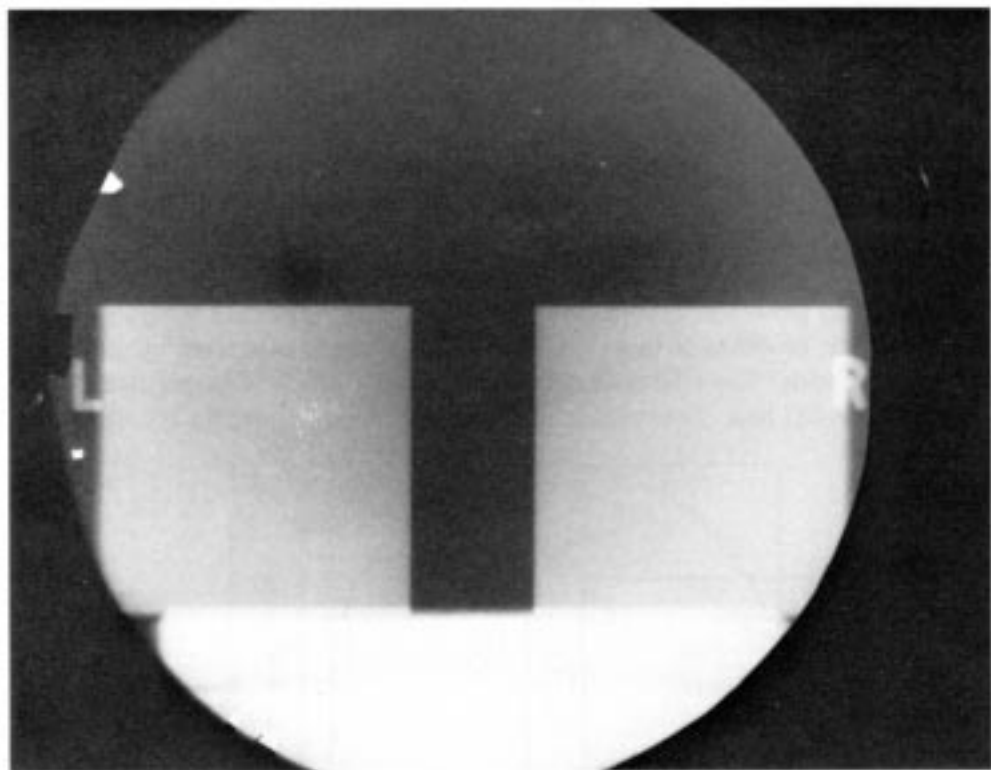




SHOT 266: **Munroe Jet**
 Date: April 20, 1965
 Experimenter: Douglas Venable
 Radiographic Time: 35.46 μ s

Formation and growth of gaseous Munroe jets. This jet is formed by interaction of the detonation products of two Composition B-3 charges separated by an air gap 40 mm, w, wide. The charges are initiated by 25.4 mm of Composition B-3 initiated by a P-081 lens. The detonations have run along the gap for 76.2 mm. h is 76.2 mm.





SHOT 267:

Munroe Jet

Date:

April 20, 1965

Experimenter:

Douglas Venable

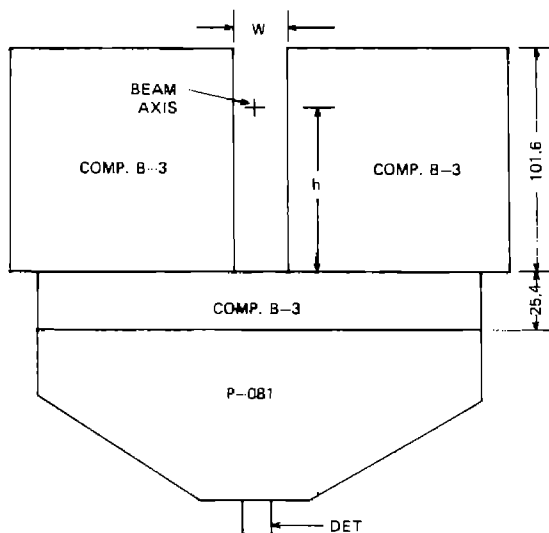
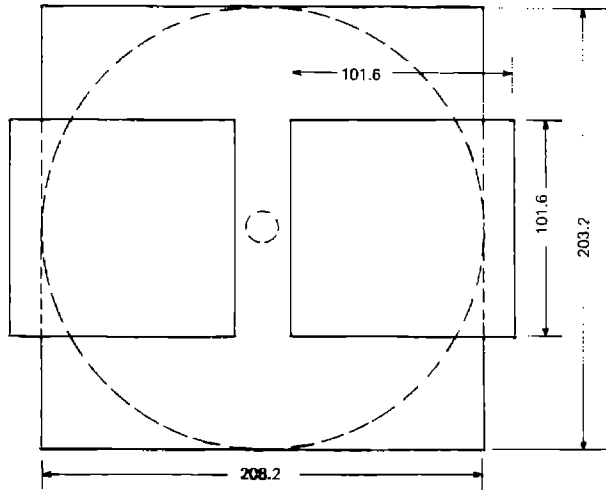
Radiographic Time:

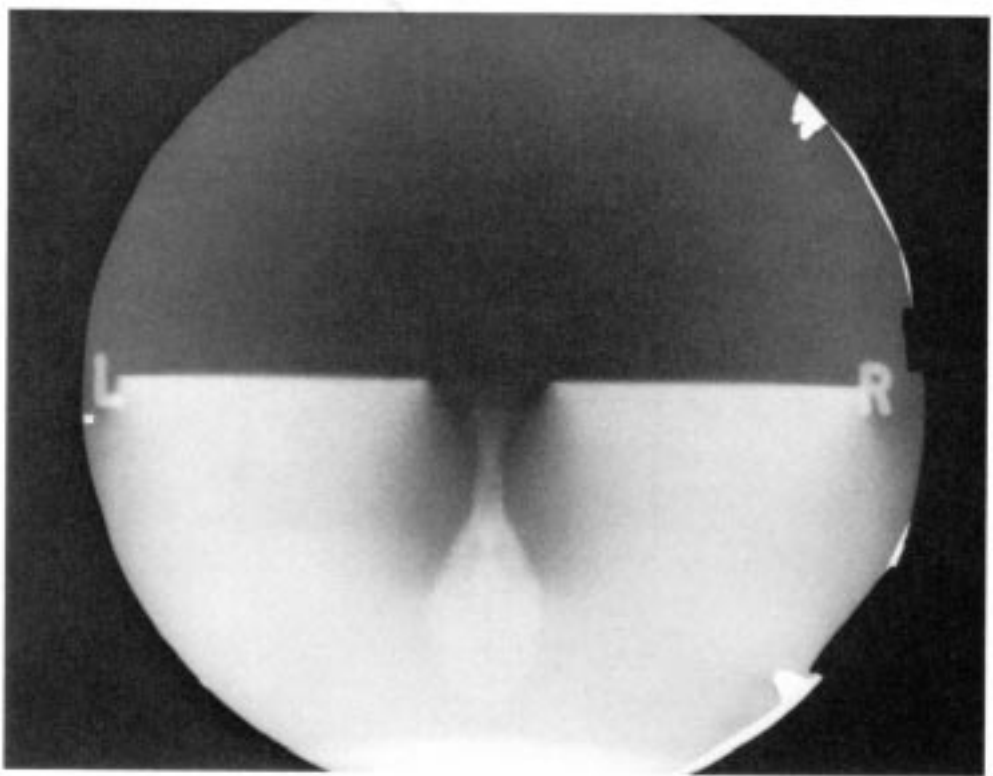
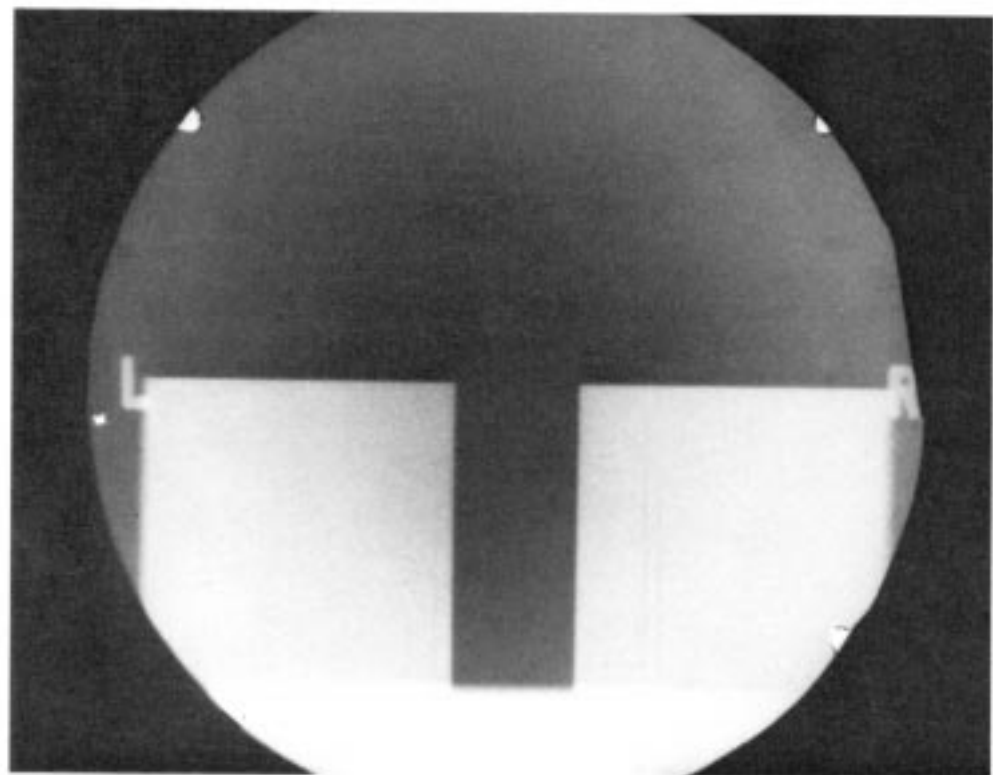
33.68 μ s

References:

Mader et al., 1967; Mader and Kershner, 1972

Formation and growth of gaseous Munroe jets. This jet is formed by interaction of the detonation products of two Composition B-3 charges separated by an air gap 40.0 mm, w, wide. The charges are initiated by 25.4 mm of Composition B-3 initiated by a P-081 lens. The detonations have run along the gap for 101.6 mm. h is 101.6 mm.





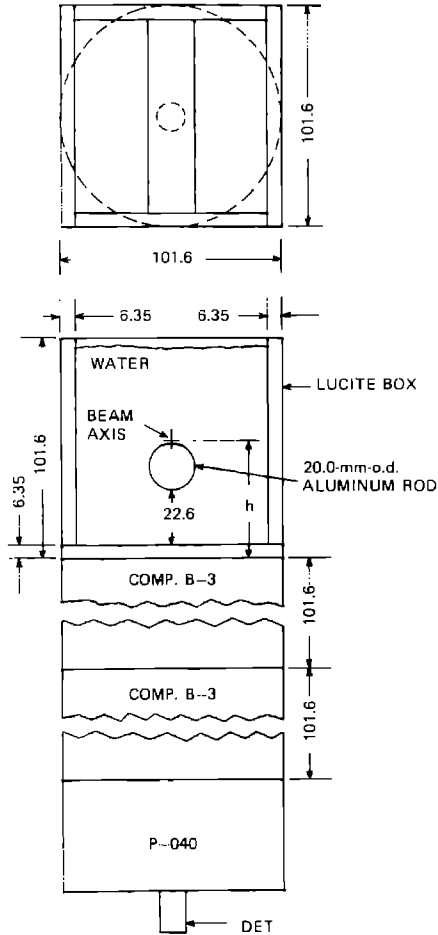
SHOT 269: Aluminum Rod in Water

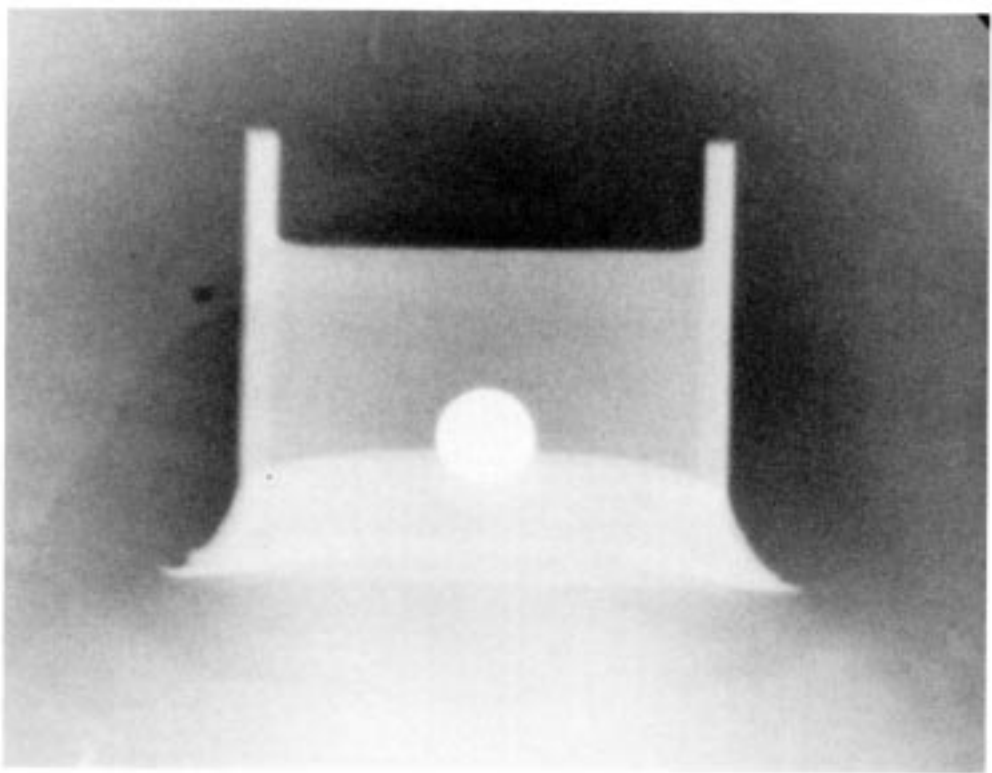
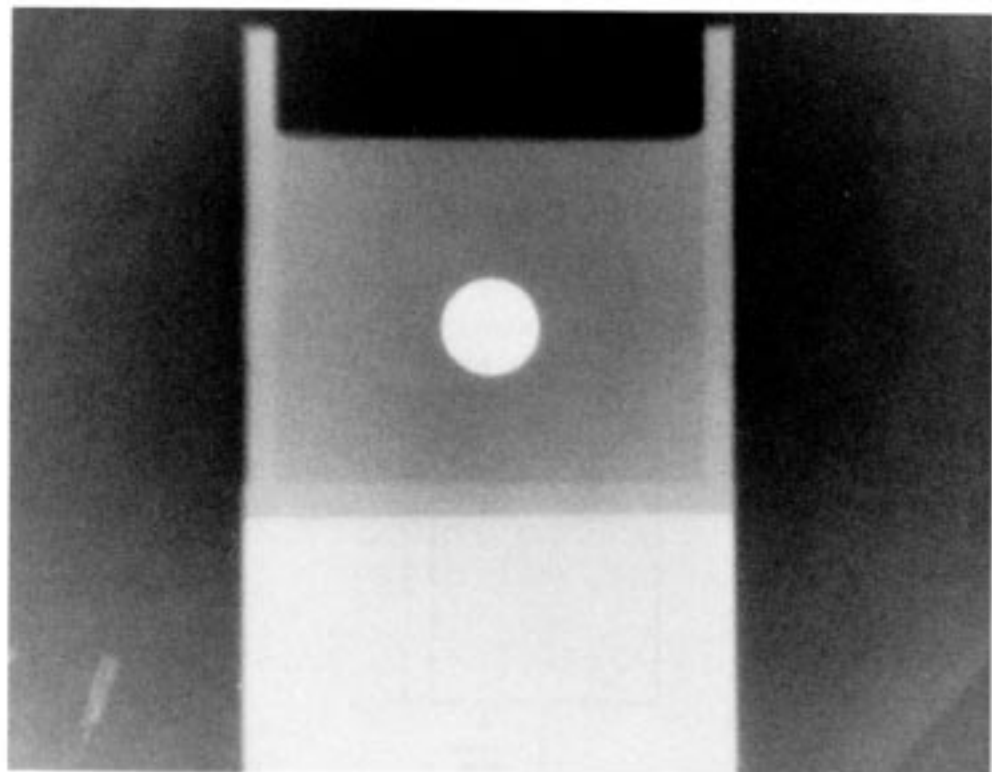
Date: March 23, 1965

Experimenter: Roger W. Taylor

Radiographic Time: 44.93 μ s

A shock wave in water interacting with a 10.0-mm-radius aluminum rod. The shock wave has traveled 4.7 μ s since the shock reached the Lucite and water interface. See Shots 189, 190, 281, and 282. h is 38.9 mm.





SHOT 270: Dynamic Fracture of Nickel

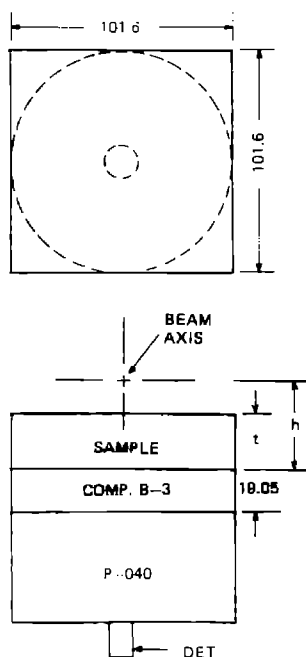
Date: May 3, 1965

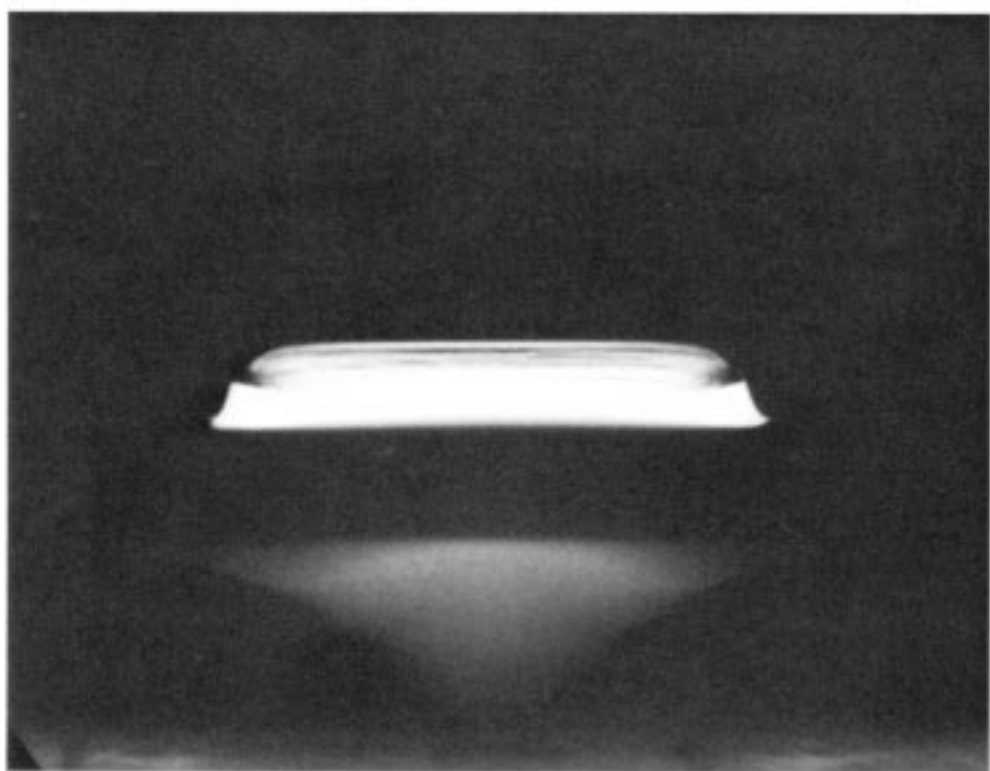
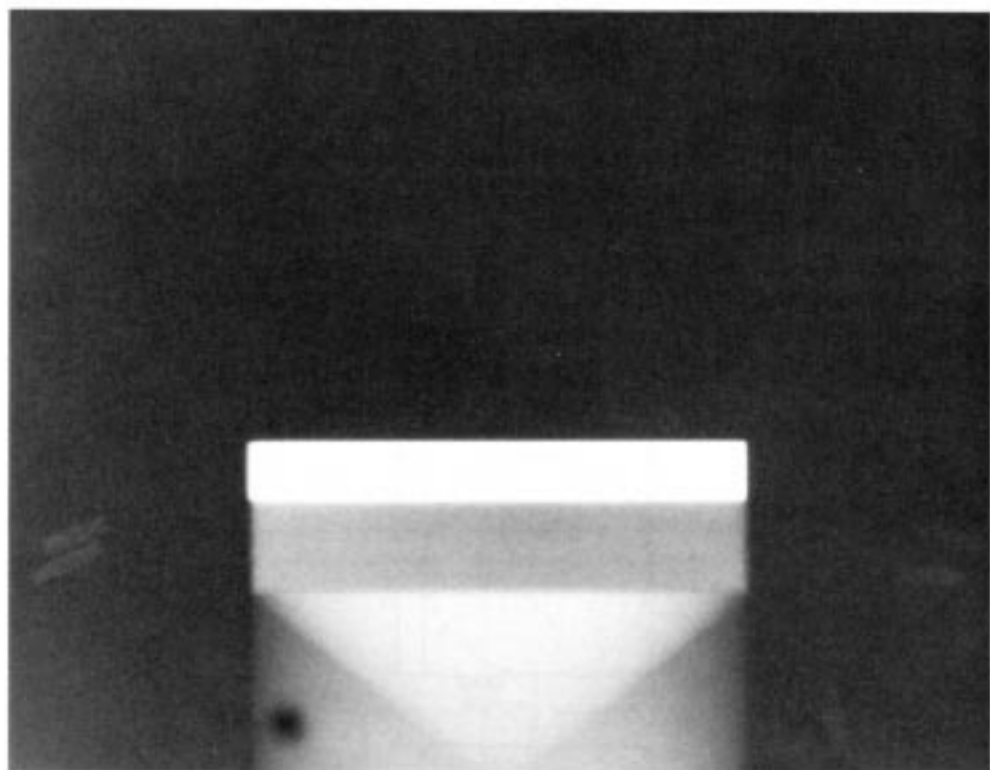
Experimenter: Benny Ray Breed

Radiographic Time: 25.91 μ s

References: Breed et al., 1967; Thurston and Mudd, 1968

Dynamic fracture of 12.0-mm-thick, t , nickel. The plate is shocked by 19.05 mm of Composition B-3 initiated by a P-040 lens. h is 28.57 mm.





SHOT 271:

Dynamic Fracture of Beryllium

Date:

April 13, 1966

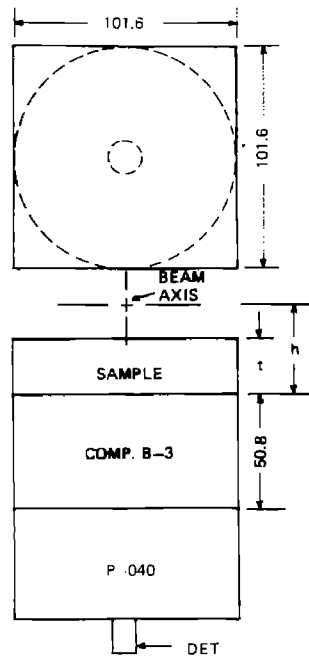
Experimenter:

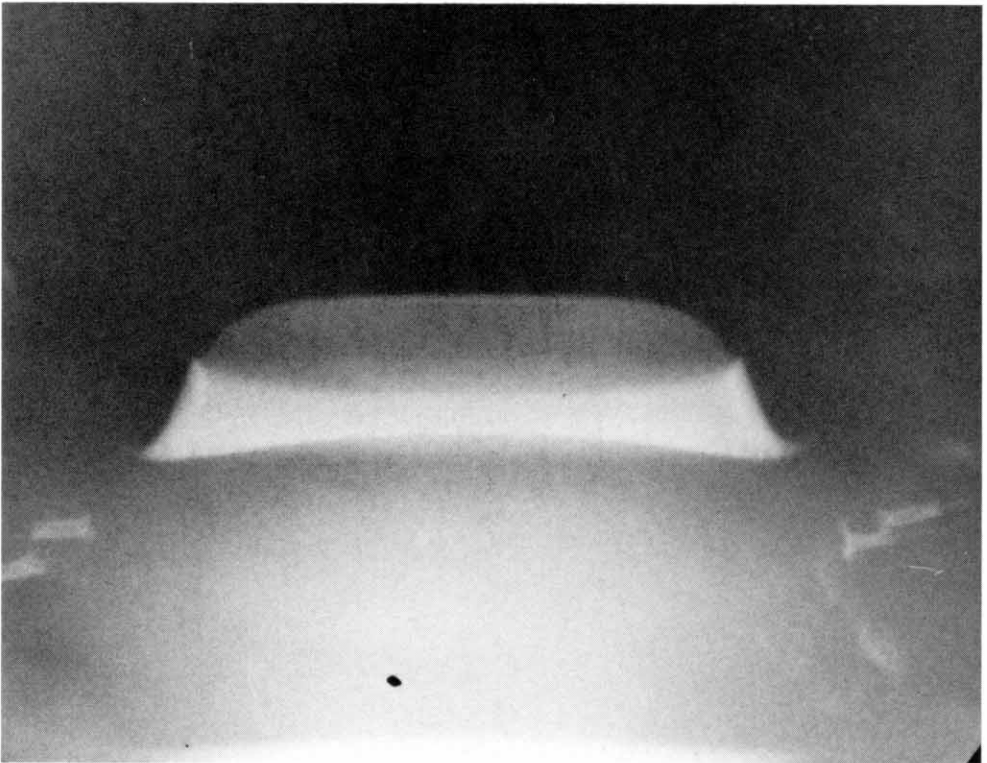
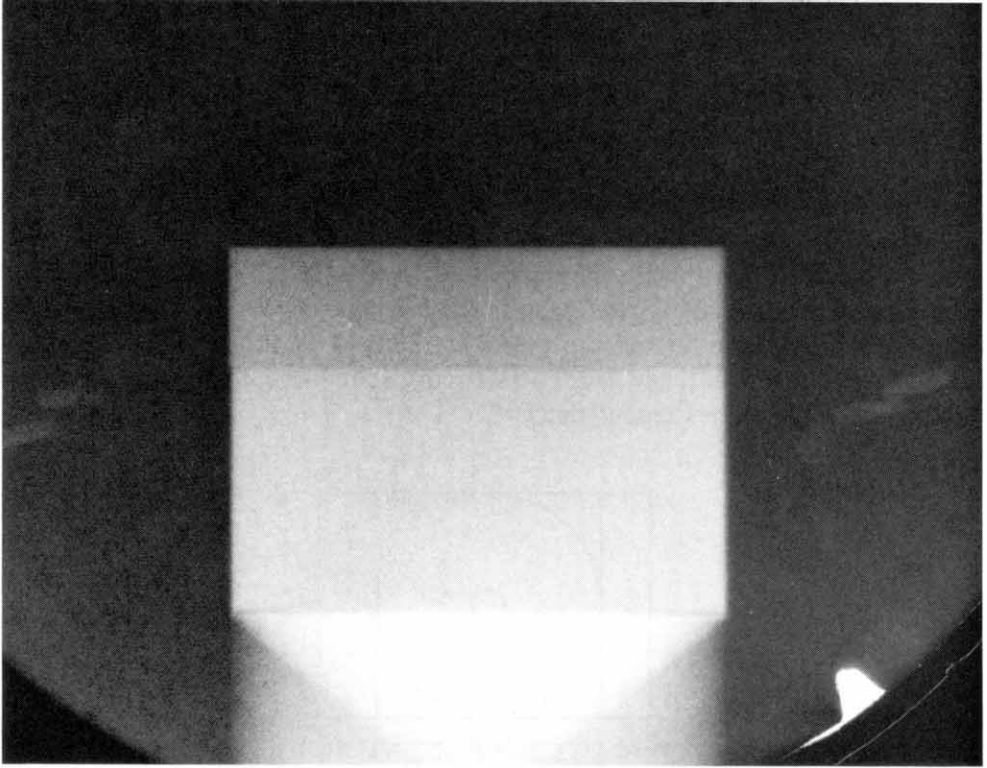
Benny Ray Breed

Radiographic Time:

28.34 μ s

Dynamic fracture of 25-mm-thick, t , beryllium. The plate is shocked by 50.8 mm of Composition B-3 initiated by a P-040 lens. h is 44.45 mm.





SHOT 272:

Composition B-3 with Embedded Tantalum Foils

Date:

April 13, 1965

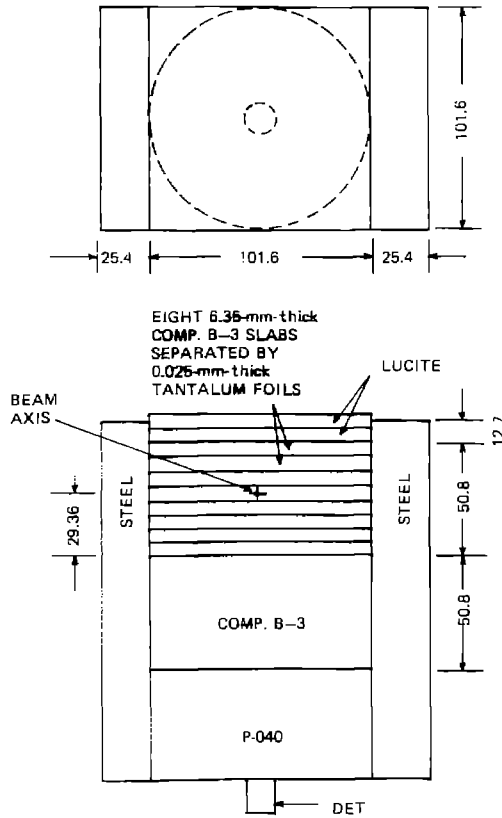
Experimenter:

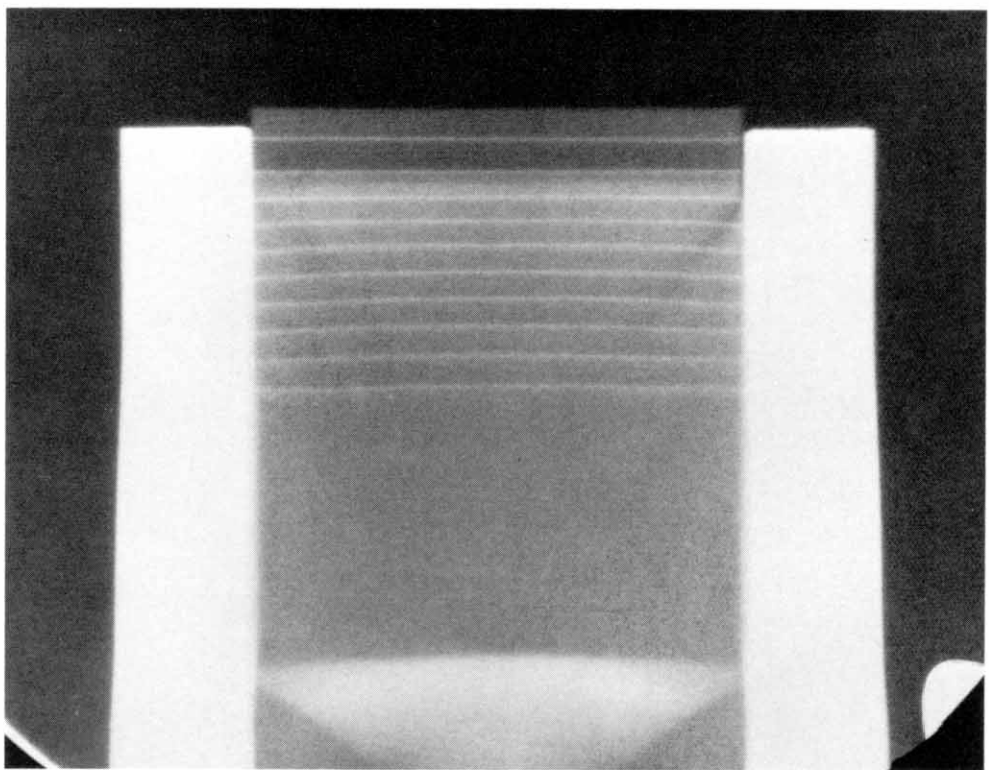
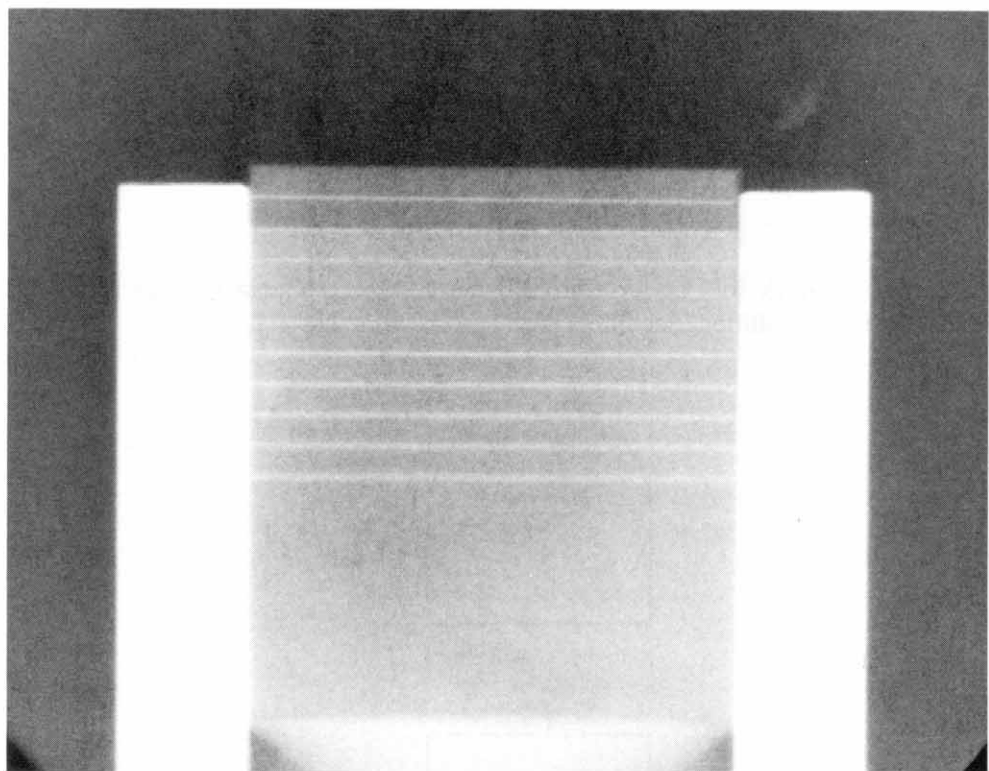
Benny Ray Breed

Radiographic Time:

26.34 μ s

Eight slabs of 6.35-mm-thick Composition B-3 separated by 0.0254-mm-thick tantalum foils were initiated perpendicular to the foils by 50.8 mm of Composition B-3 and a P-040 lens. The flow of the products confined by 25.4-mm-thick steel is shown. See Shots 220, 221, and 290. Two slabs of Lucite separated by tantalum foils were placed on top of the Composition B-3.





SHOT 273:

Colliding Composition B-3 Detonations

Date:

July 29, 1965

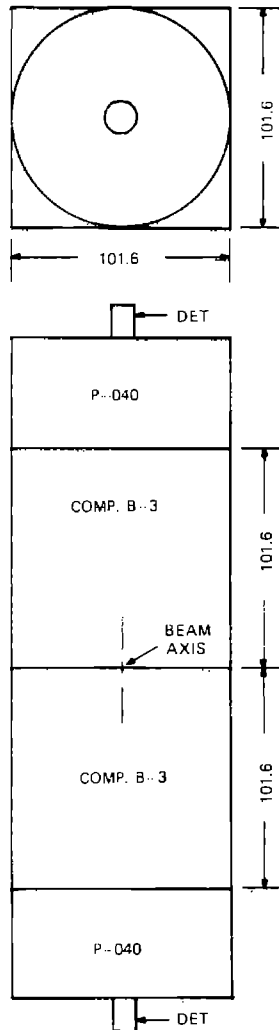
Experimenter:

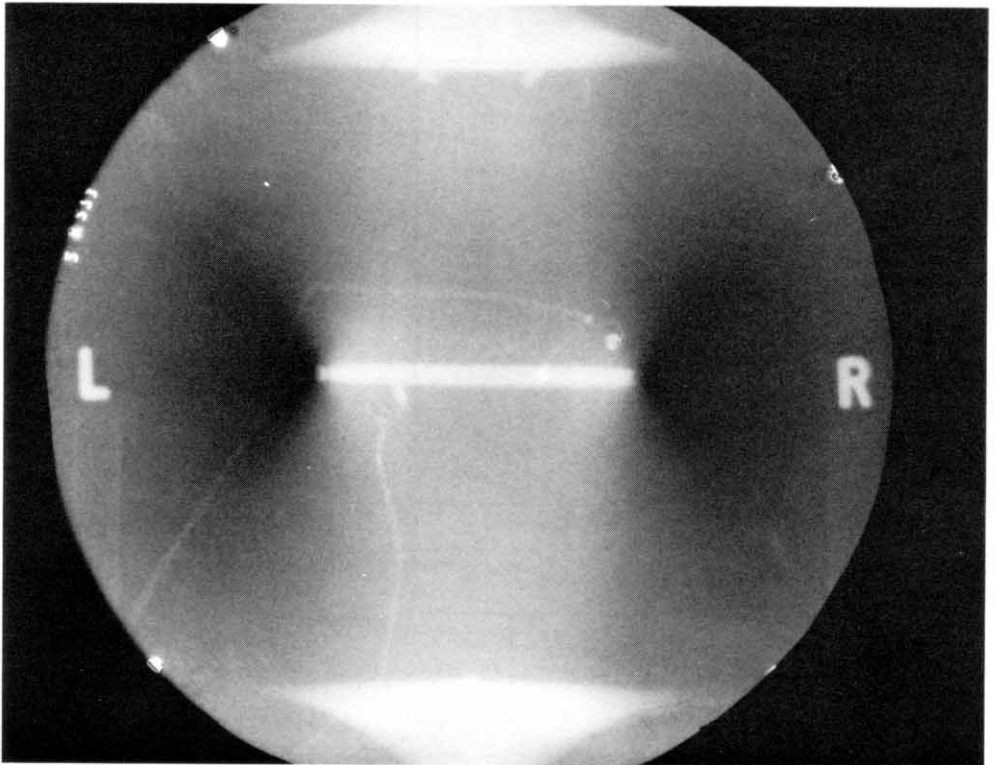
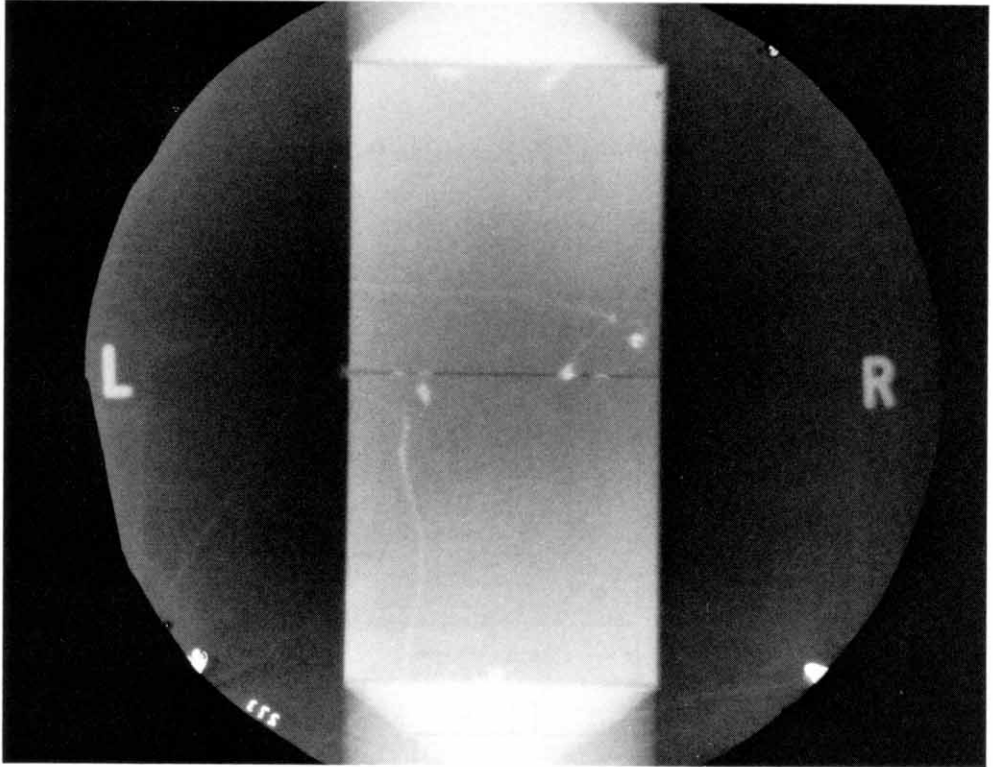
Douglas Venable

Radiographic Time:

26.97 μ s

The reflected shock in Composition B-3 detonation products 0.56 μ s after the detonation waves collided. See Shots 86, 87, 91, 92, and 274-277.





SHOT 274:

Colliding Composition B-3 Detonations

Date:

July 29, 1965

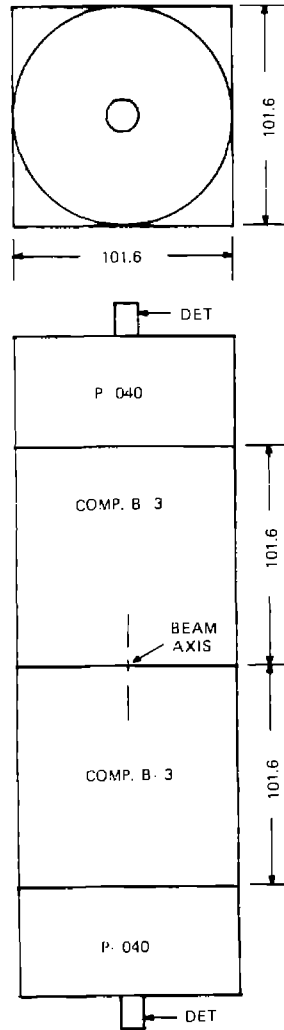
Experimenter:

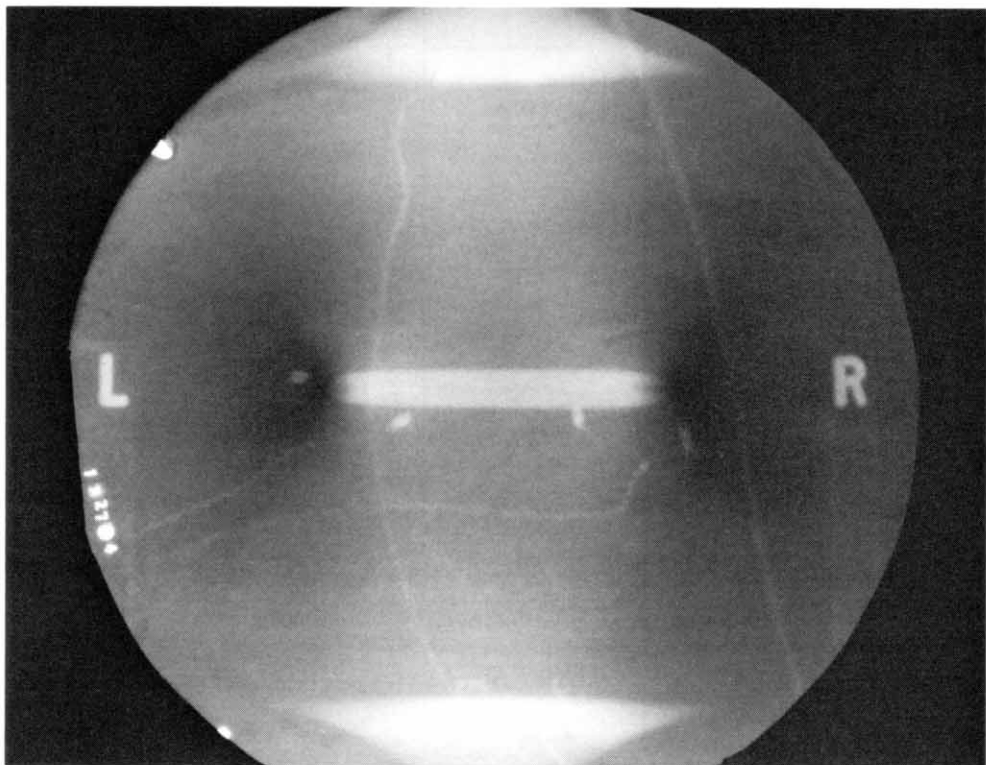
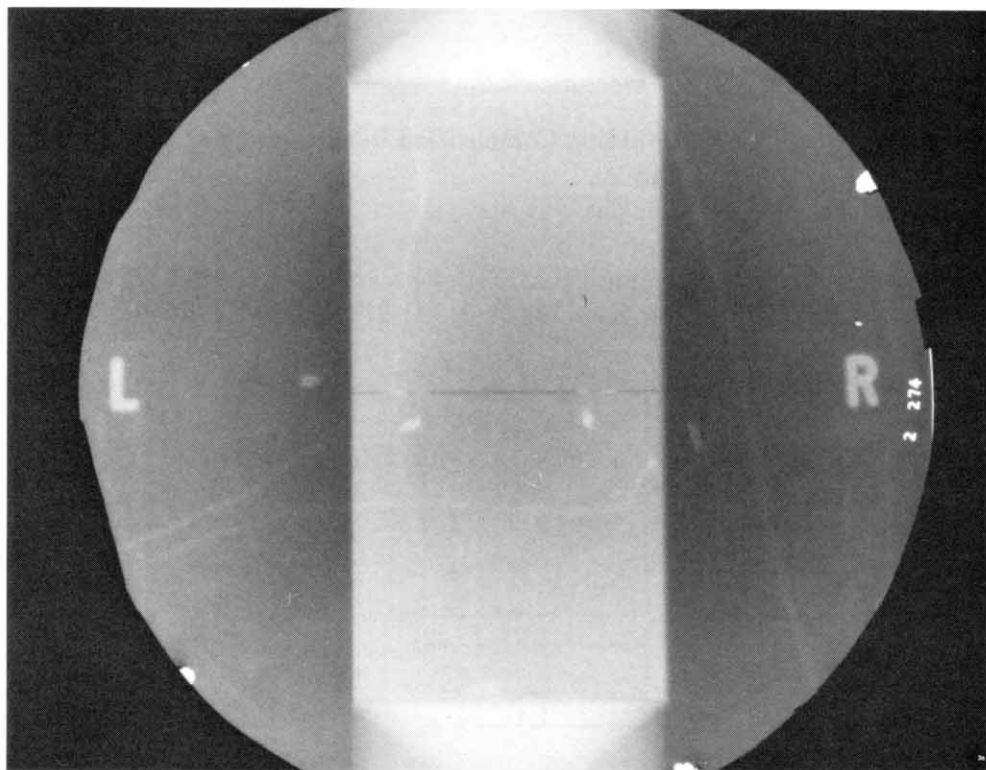
Douglas Venable

Radiographic Time:

27.42 μ s

The reflected shocks in Composition B-3 detonation products 1.02 μ s after the detonation waves collided. See Shots 86, 87, 91, 92, 273, and 275-277.





SHOT 275:

Colliding Composition B-3 Detonations

Date:

July 29, 1965

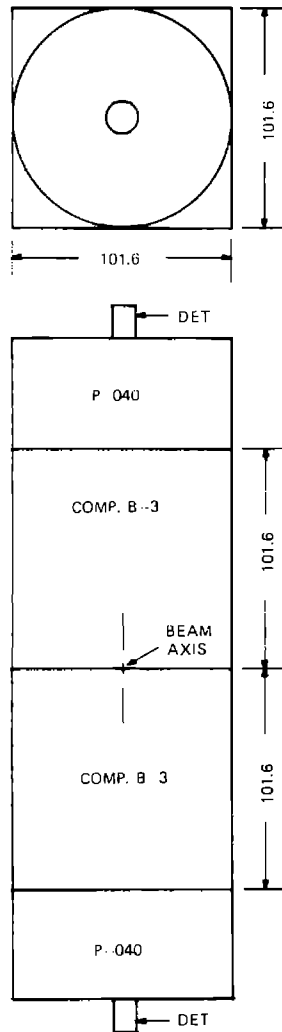
Experimenter:

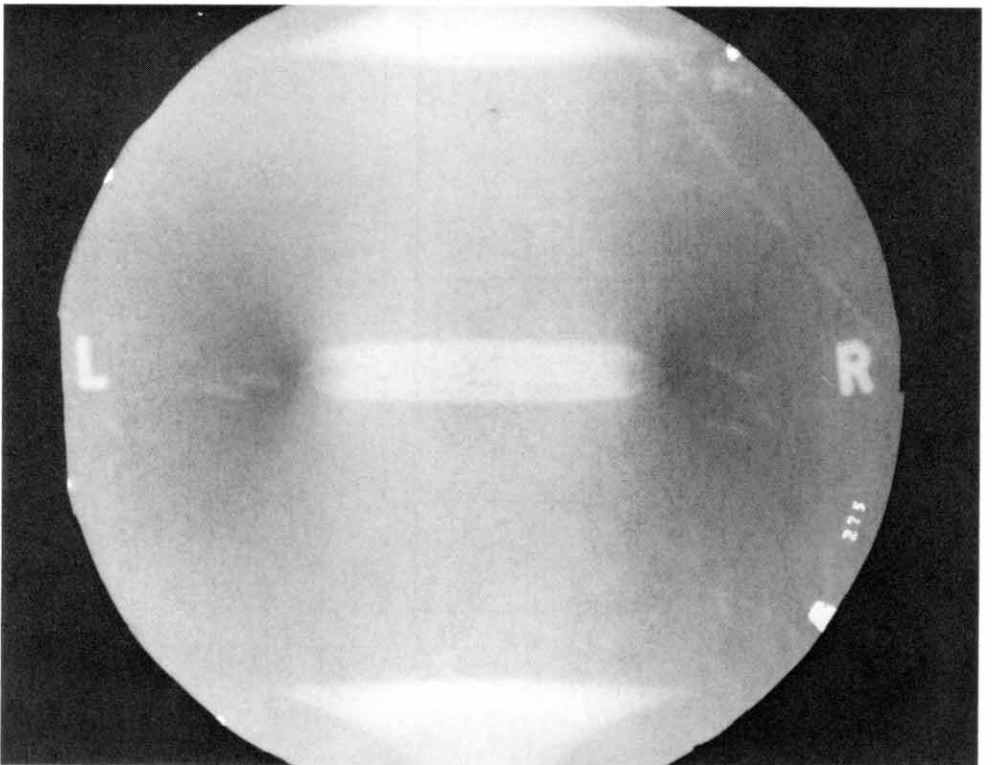
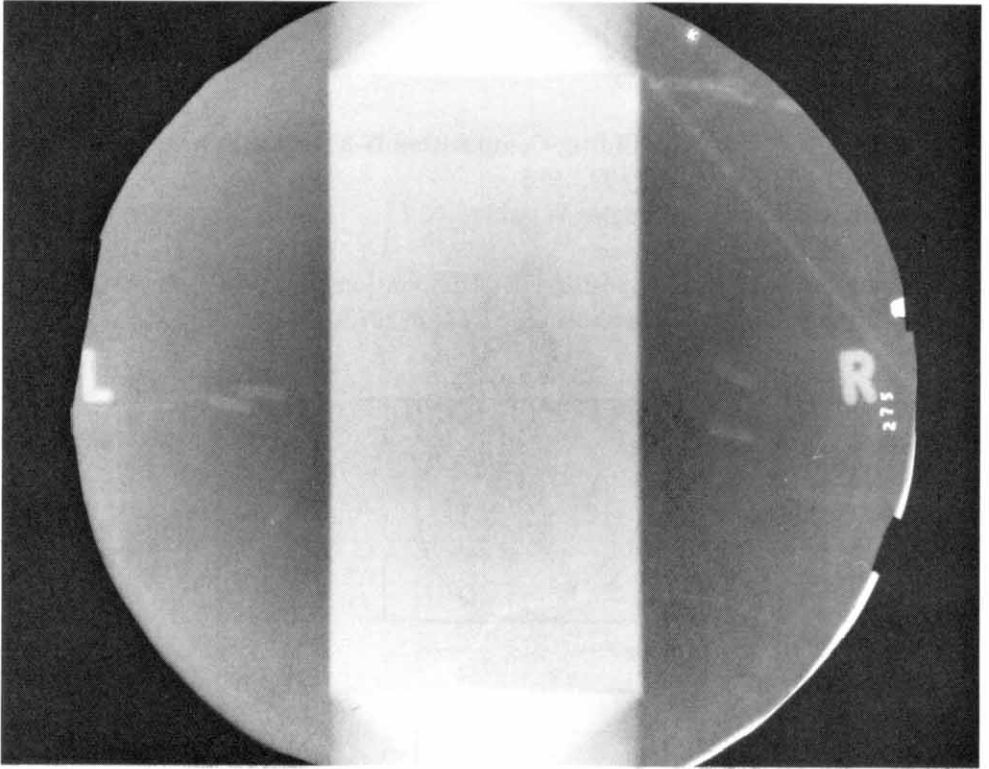
Douglas Venable

Radiographic Time:

27.94 μ s

The reflected shocks in Composition B-3 detonation products 16.3 μ s after the detonation waves collided. See Shots 86, 87, 91, 92, 273, 274, 276, and 277.





SHOT 276:

Colliding Composition B-3 Detonations

Date:

July 29, 1965

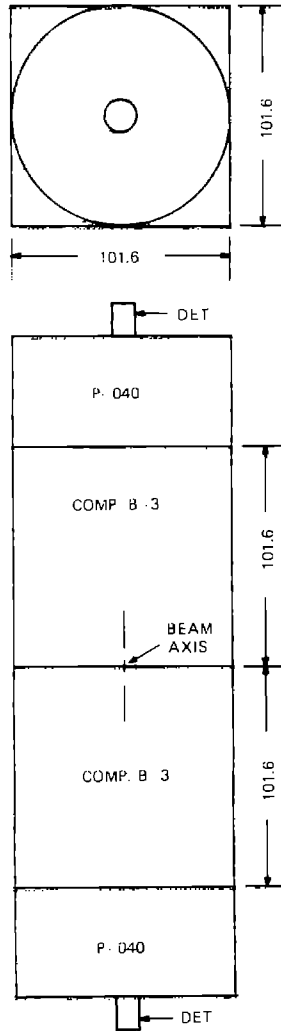
Experimenter:

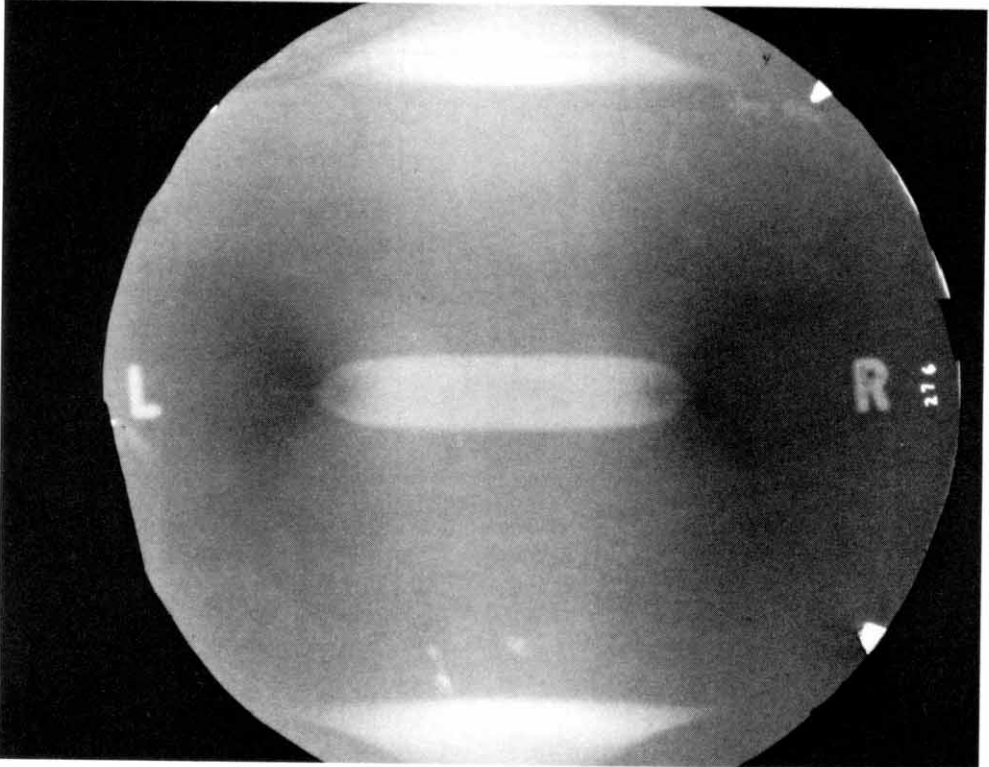
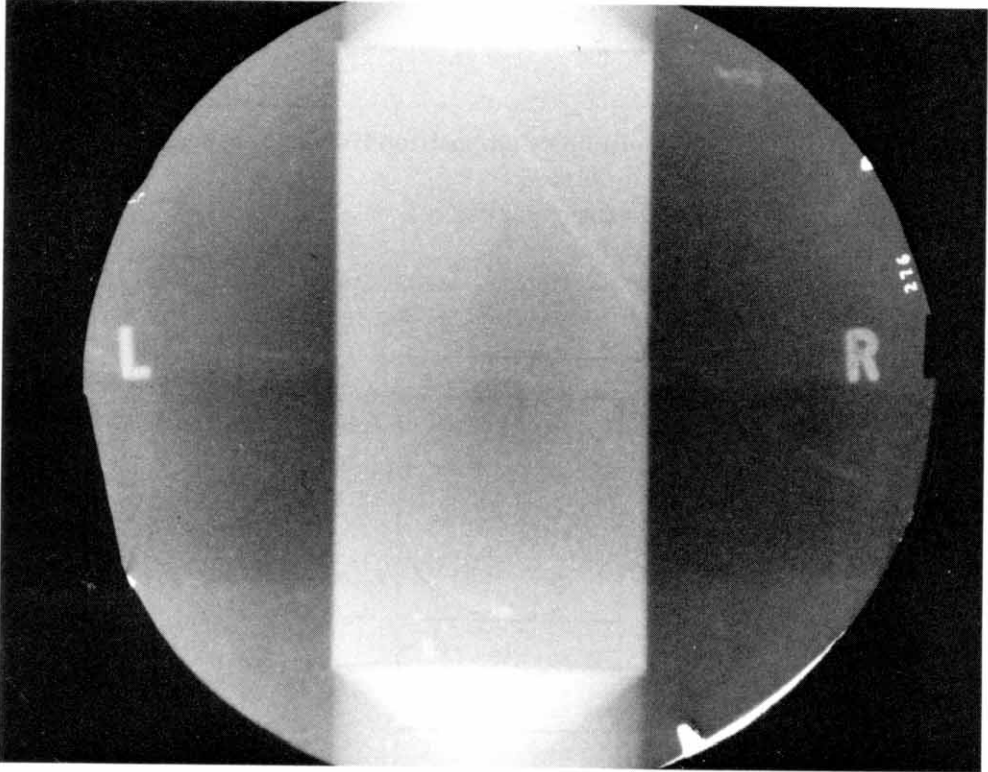
Douglas Venable

Radiographic Time:

28.4 μ s

The reflected shocks in Composition B-3 detonation products 1.96 μ s after the detonation waves collided. See Shots 86, 87, 91, 92, 273-275, and 277.





SHOT 277:

Colliding Composition B-3 Detonations

Date:

July 29, 1965

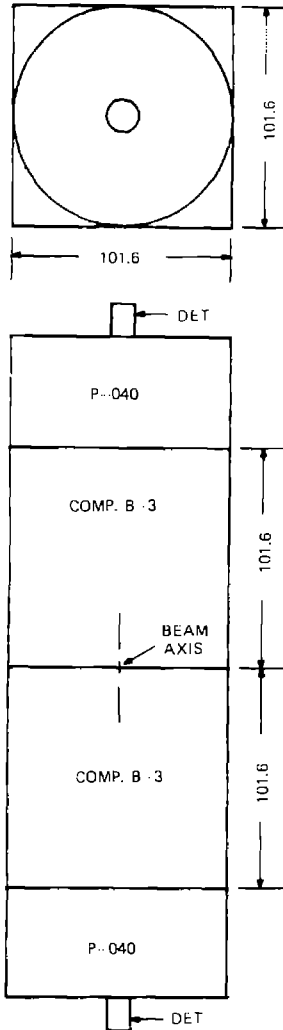
Experimenter:

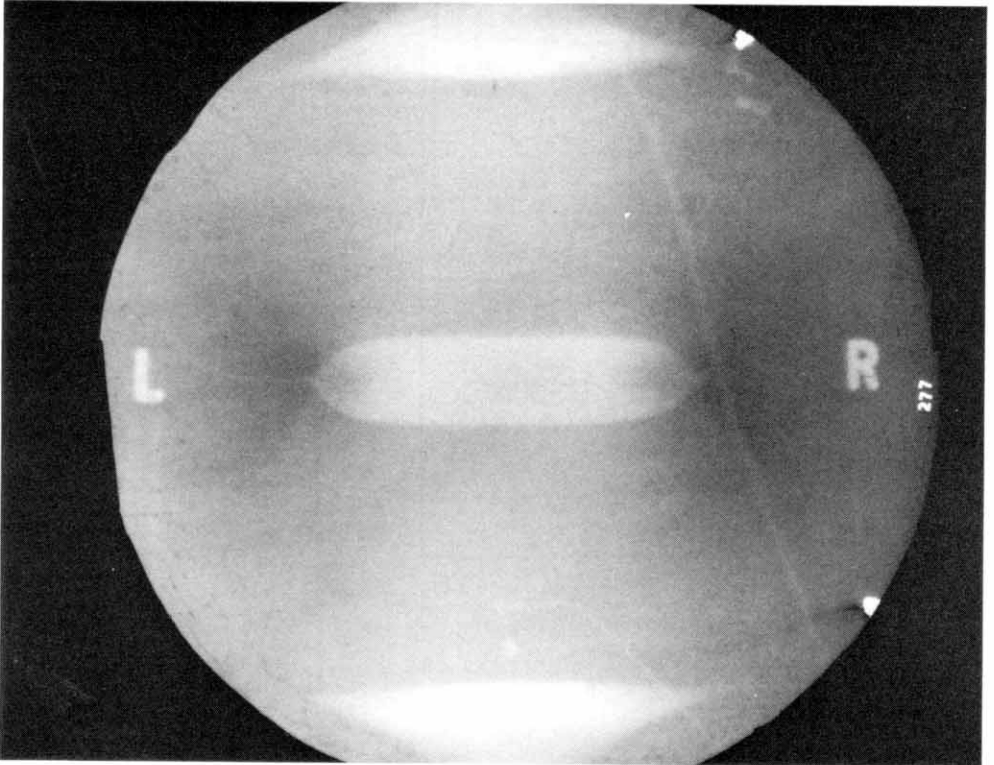
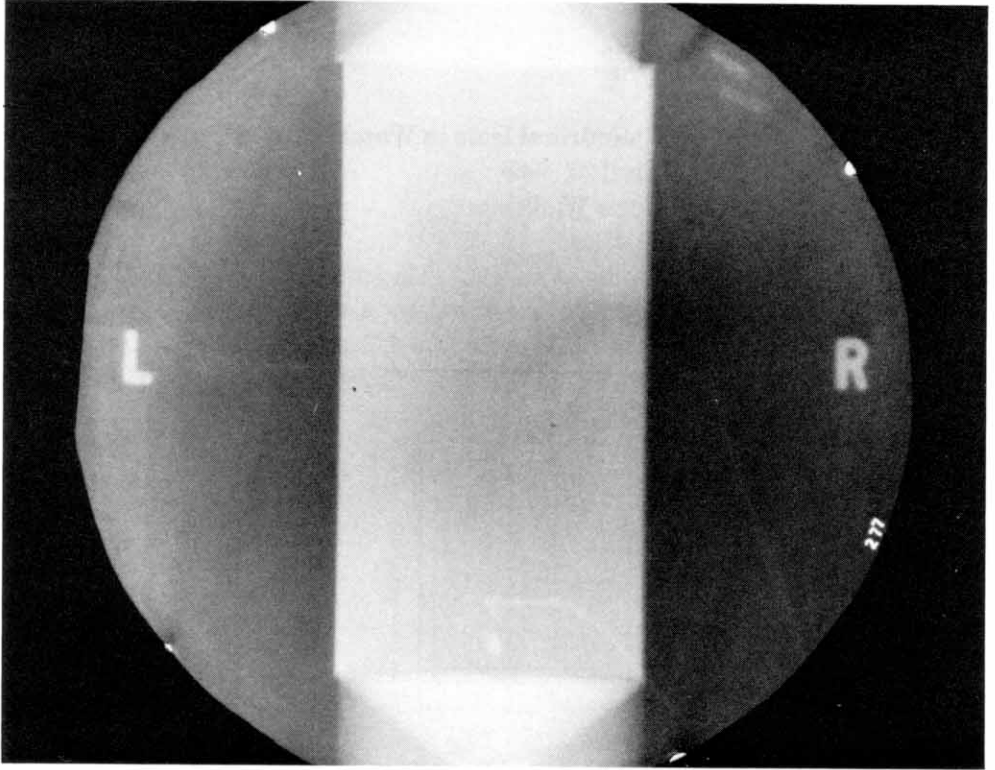
Douglas Venable

Radiographic Time:

28.91 μ s

The reflected shocks in Composition B-3 detonation products 2.48 μ s after the detonation waves collided. See Shots 86, 87, 91, 92, and 274-276.





SHOT 278:**Cylindrical Hole in Water**

Date:

April 20, 1965

Experimenter:

Roger W. Taylor

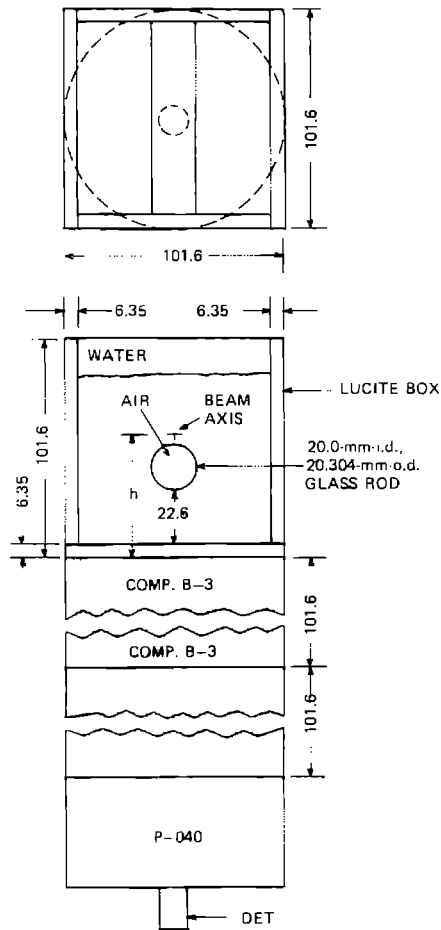
Radiographic Time:

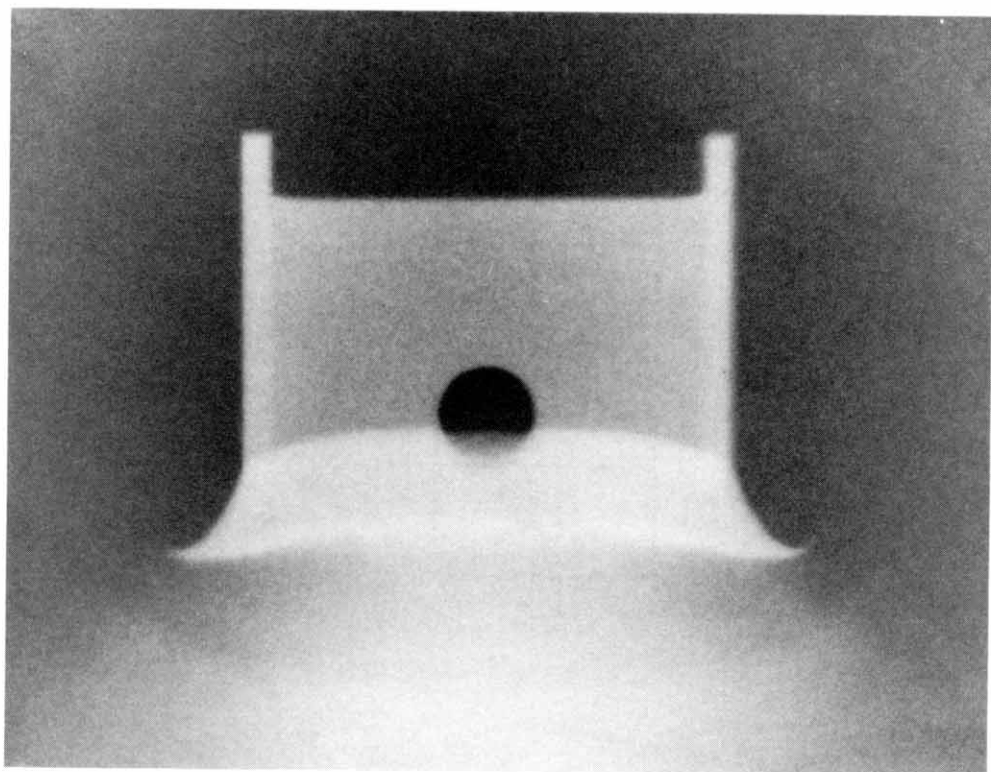
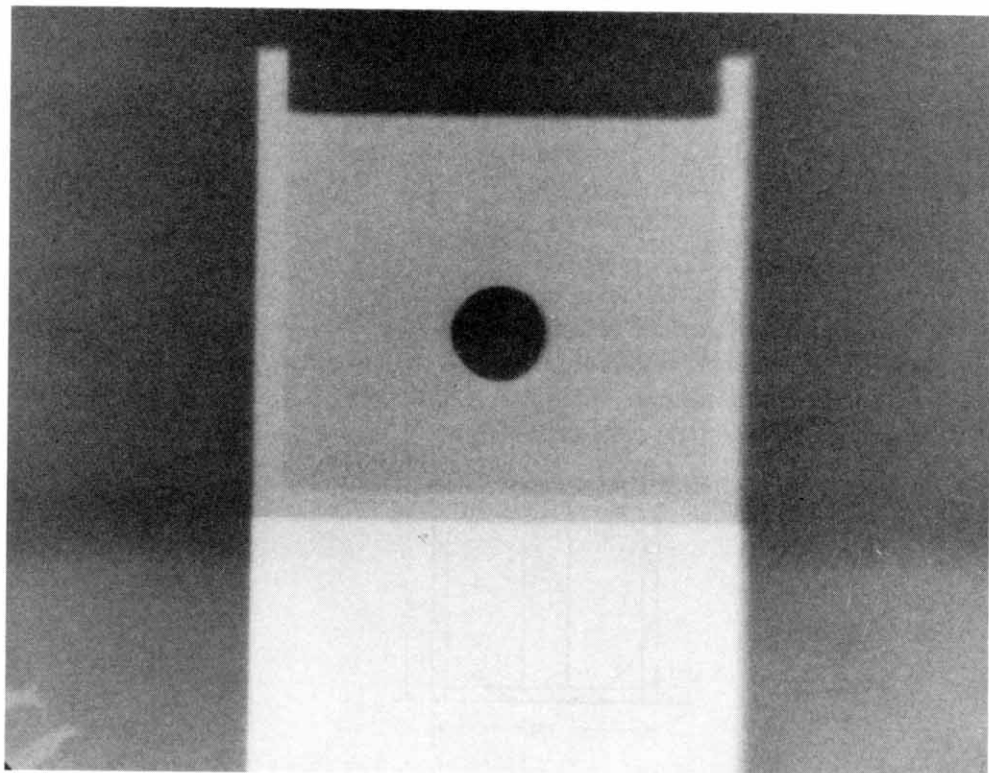
44.95 μ s

References:

Mader et al., 1967; Mader and Kershner, 1972

A 10.0-mm-radius cylindrical hole is formed by a thin-walled (0.152-mm) glass tube in water. The shock wave has traveled for 4.7 μ s since the shock reached the Lucite and water interface. See Shots 187, 188, 279-280, 300, and 318. h is 38.9 mm.





SHOT 279:

Cylindrical Hole in Water

Date:

April 20, 1965

Experimenter:

Roger W. Taylor

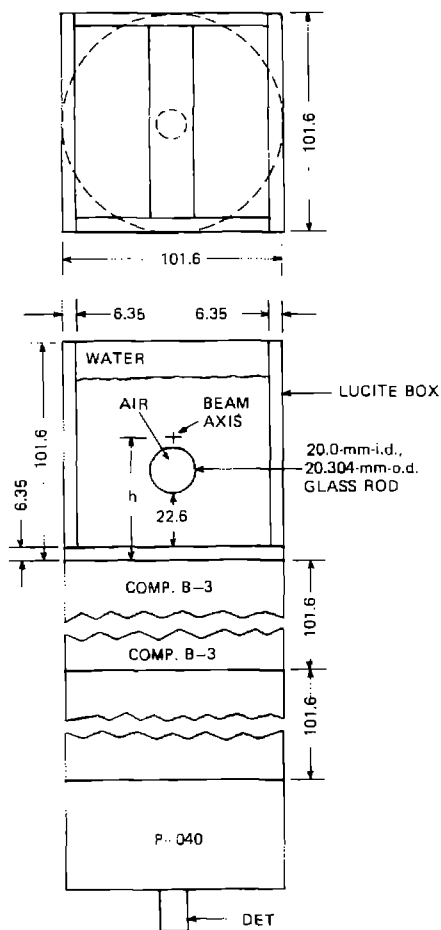
Radiographic Time:

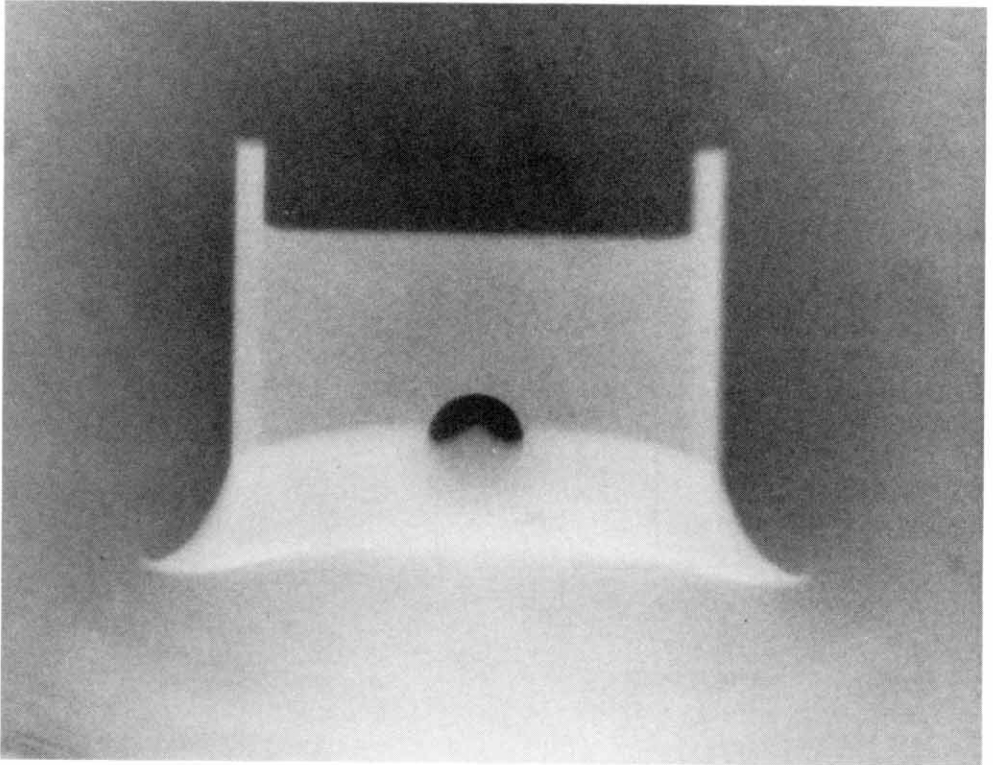
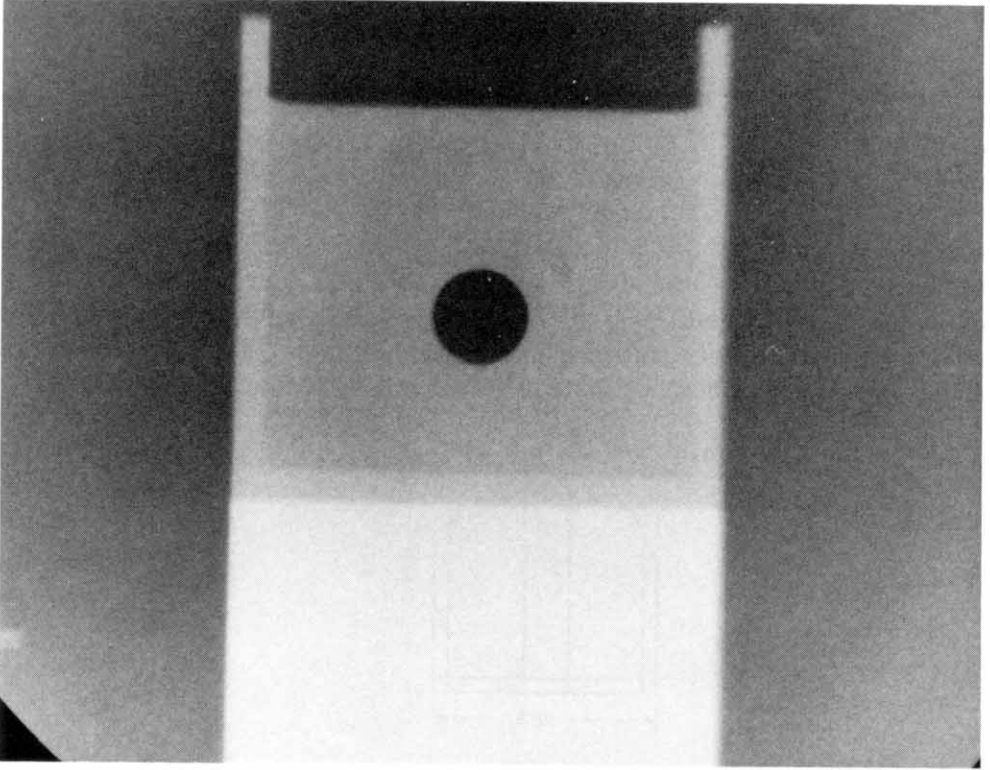
46.11 μ s

References:

Mader et al., 1967; Mader and Kershner, 1972

A 10.0-mm-radius cylindrical hole is formed by a thin-walled (0.152-mm) glass tube in water. The shock wave has traveled for 5.9 μ s since the shock reached the Lucite and water interface. See Shots 187, 188, 278, 280, 300, and 318. h is 46.0 mm.





SHOT 280: Cylindrical Hole in Water

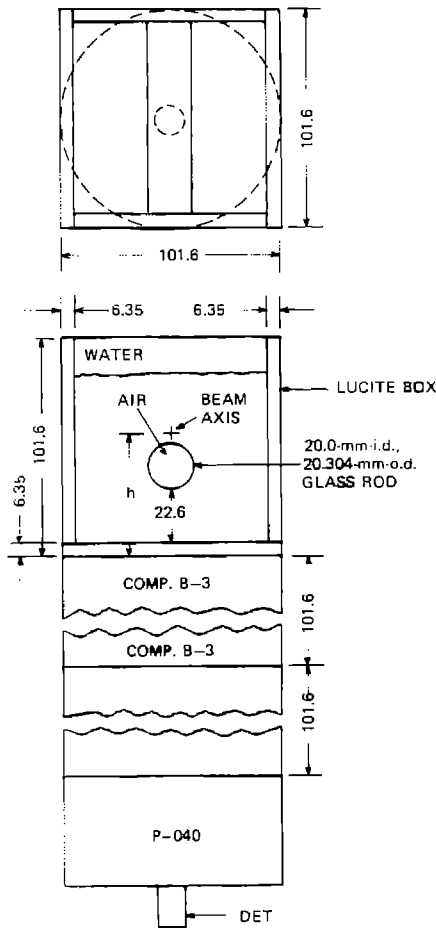
Date: April 21, 1965

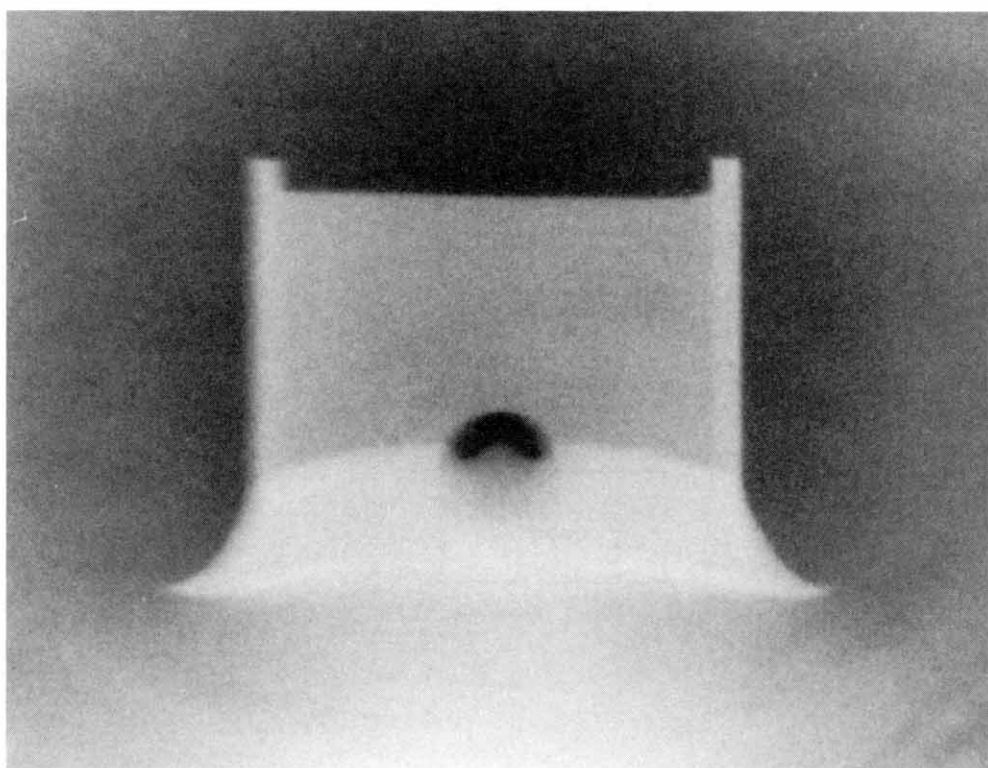
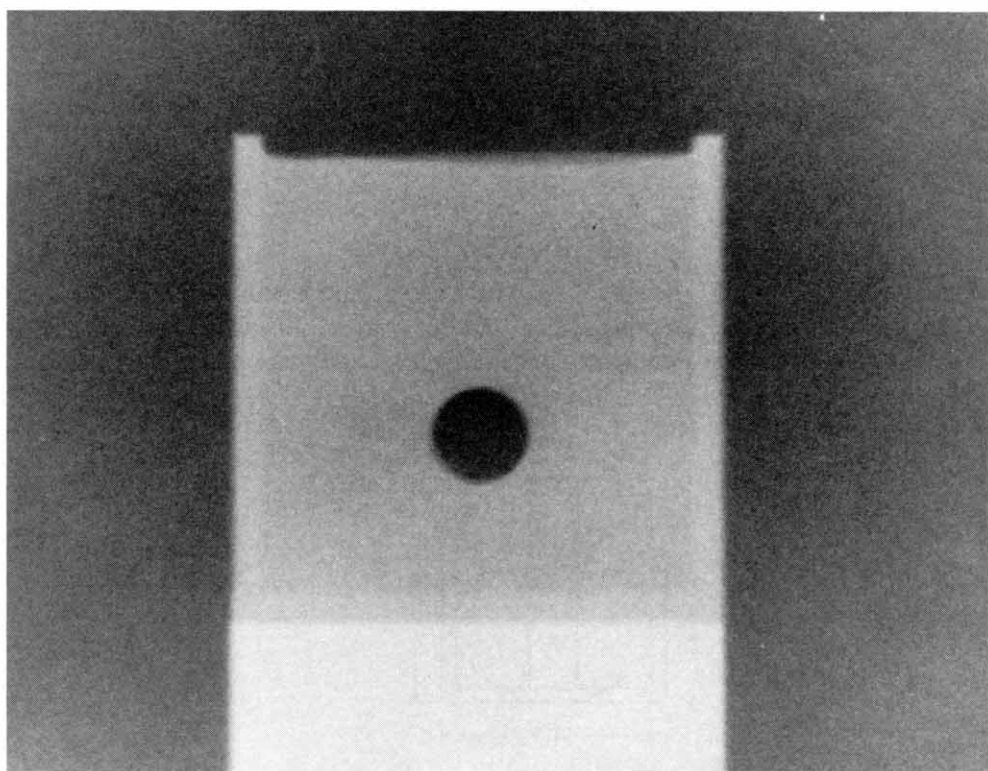
Experimenter: Roger W. Taylor

Radiographic Time: 47.3 μ s

References: Mader et al., 1967, Mader and Kershner, 1972

A 10.0-mm-radius cylindrical hole is formed by a thin-walled (0.152-mm) glass tube in water. The shock wave has traveled 7.1 μ s since the shock reached the Lucite and water interface. See Shots 187, 188, 278-279, 300, and 318. h is 54.0 mm.





SHOT 281:

Aluminum Rod in Water

Date:

April 21, 1965

Experimenter:

Roger W. Taylor

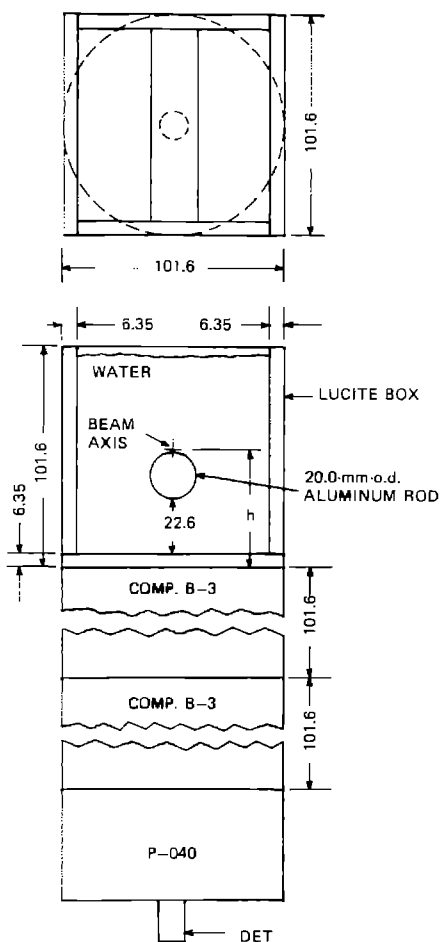
Radiographic Time:

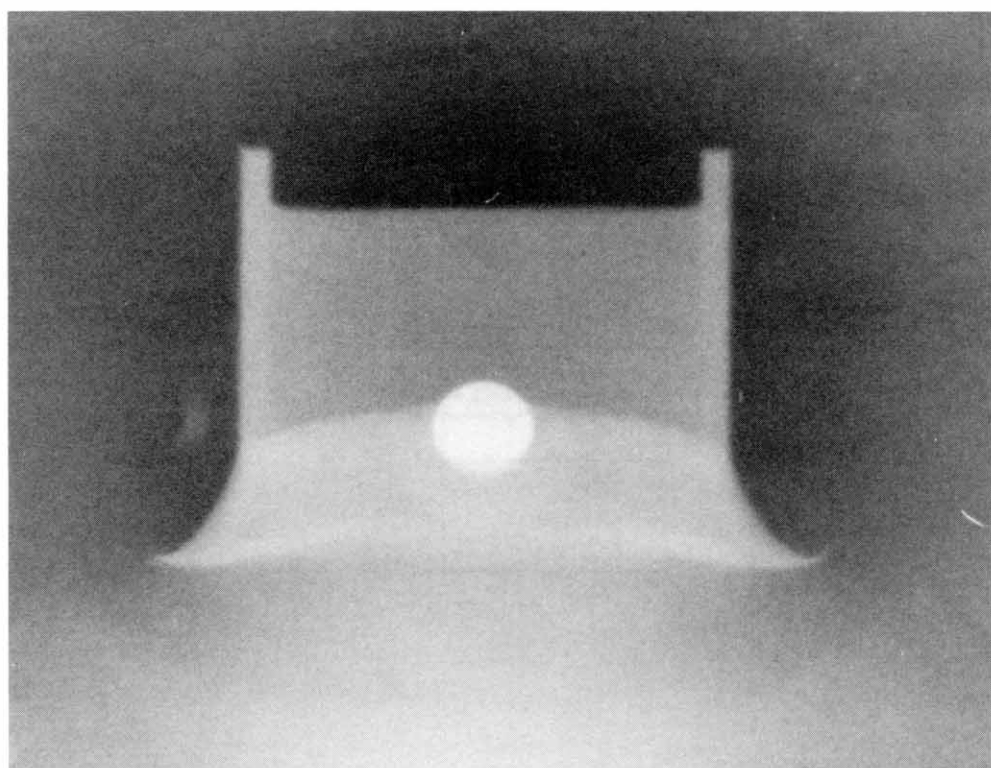
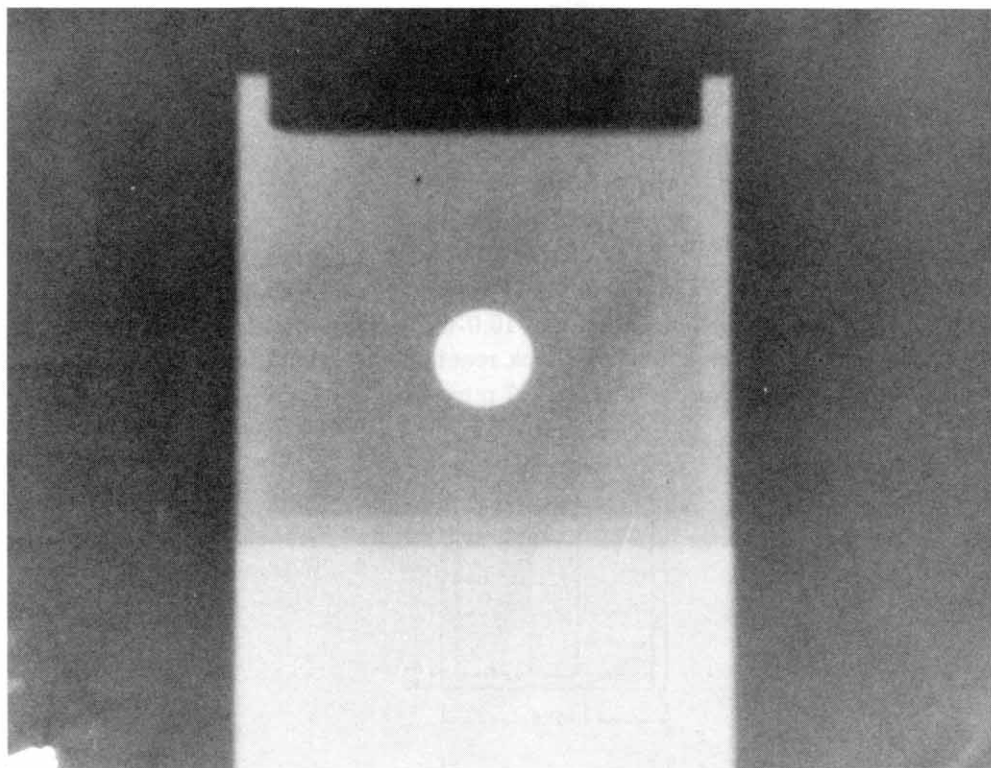
46.13 μ s

References:

Mader et al., 1967; Mader and Kershner, 1972

A shock wave in water interacting with a 10.0-mm-radius aluminum rod. The shock wave has traveled for 5.9 μ s since the shock reached the Lucite and water interface. See Shots 189, 190, 269, and 282. h is 46.0 mm.





SHOT 282:

Aluminum Rod in Water

Date:

April 21, 1965

Experimenter:

Roger W. Taylor

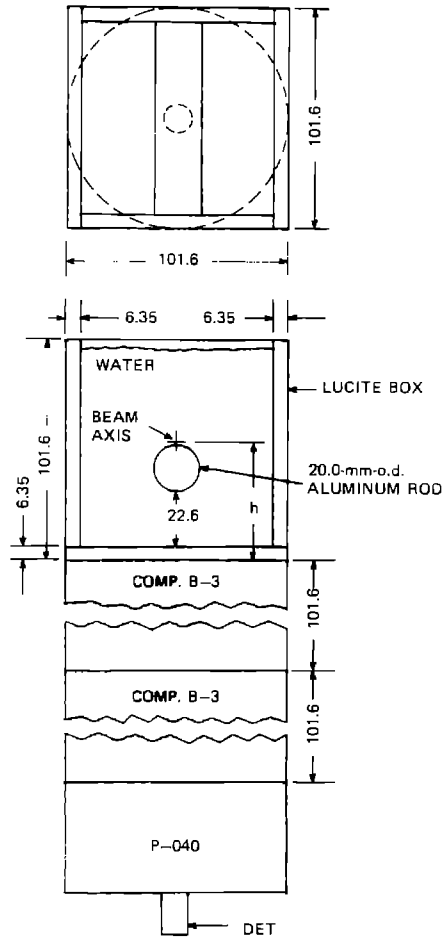
Radiographic Time:

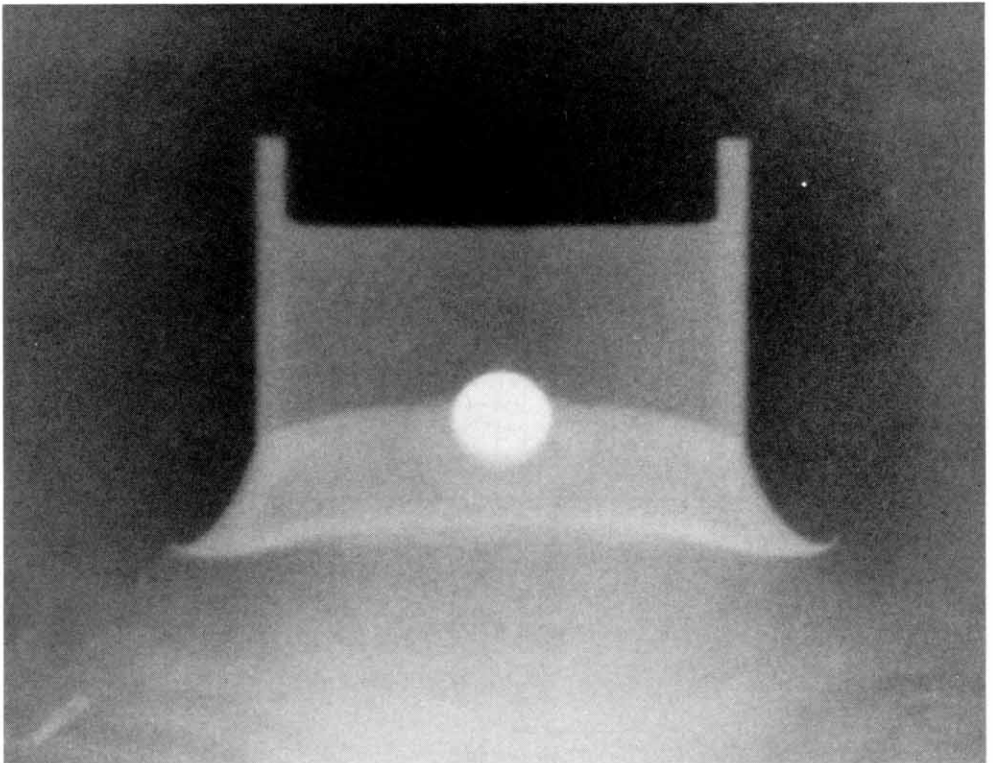
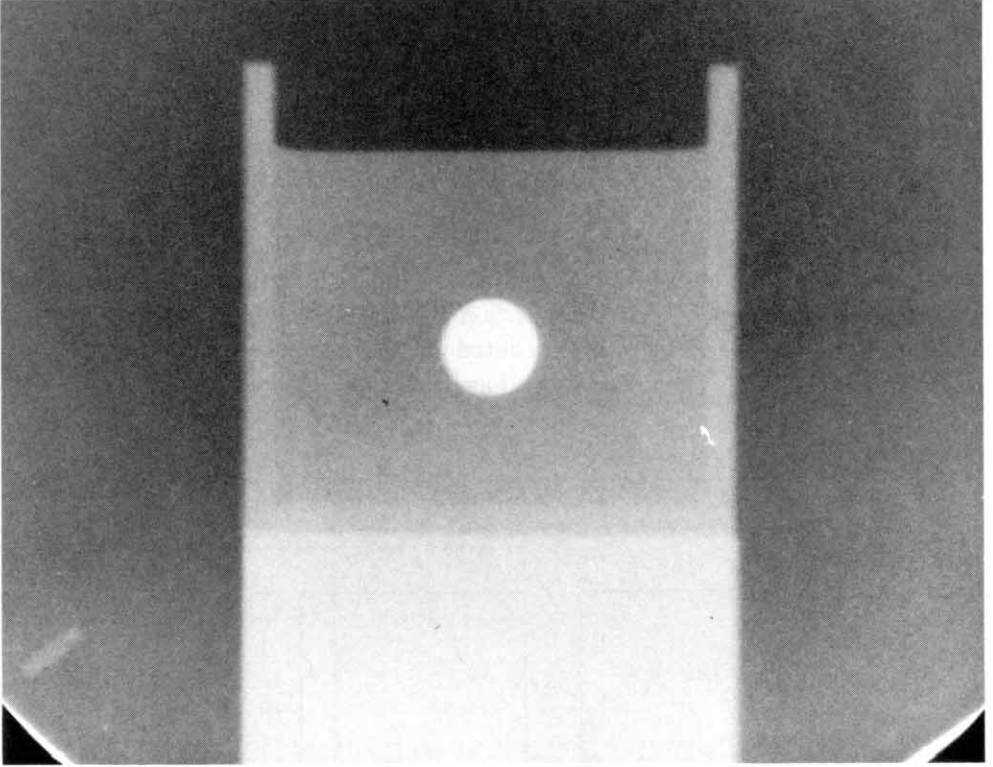
47.2 μ s

References:

Mader et al., 1969; Mader and Kershner, 1972

A shock wave in water interacting with a 10.0-mm-radius aluminum rod. The shock wave has traveled 7.0 μ s since the shock reached the Lucite and water interface. See Shots 189, 190, 269, and 281. h is 53.97 mm.





SHOT 283:

Munroe Jet

Date:

May 25, 1965

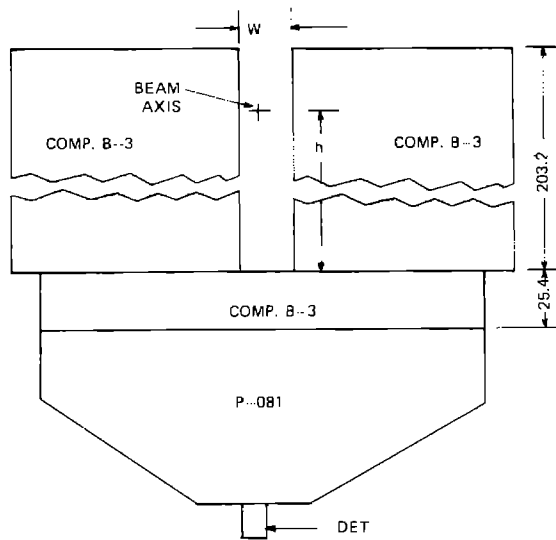
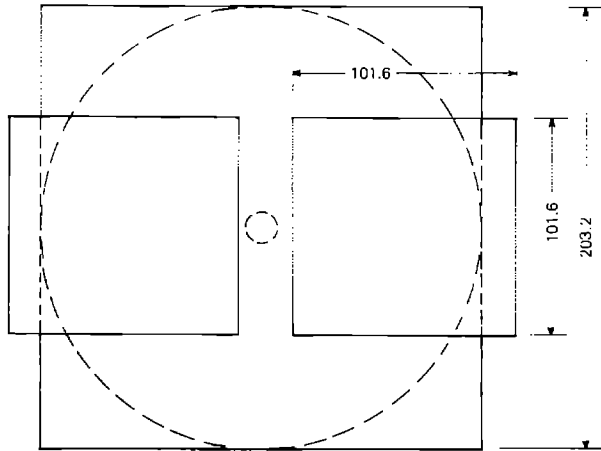
Experimenter:

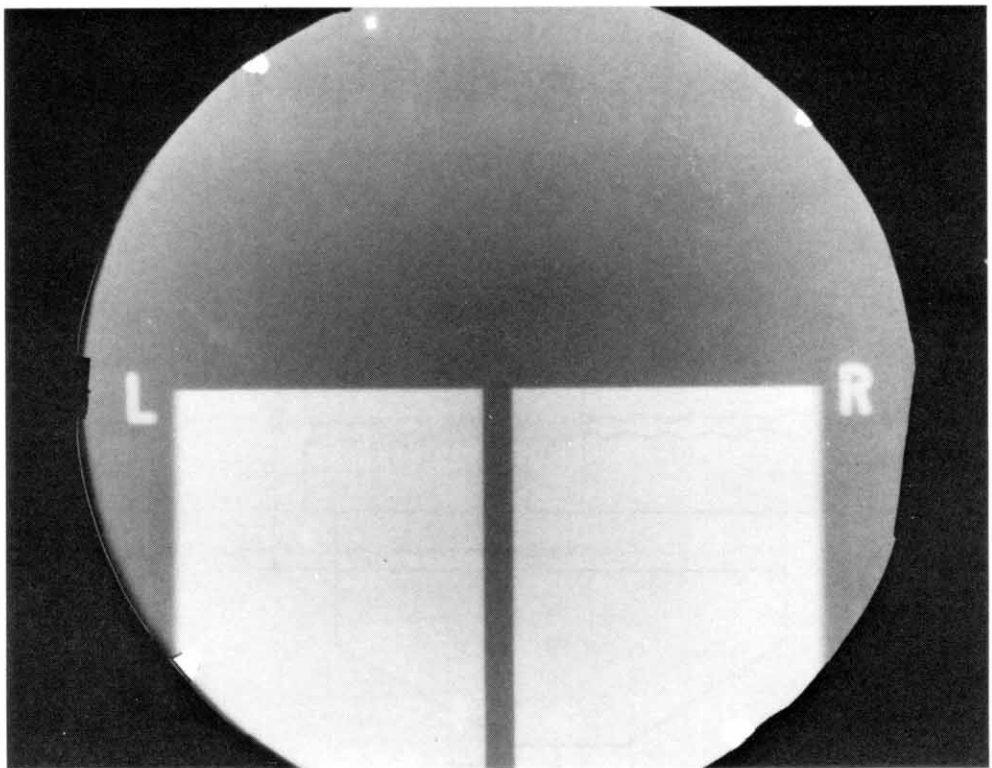
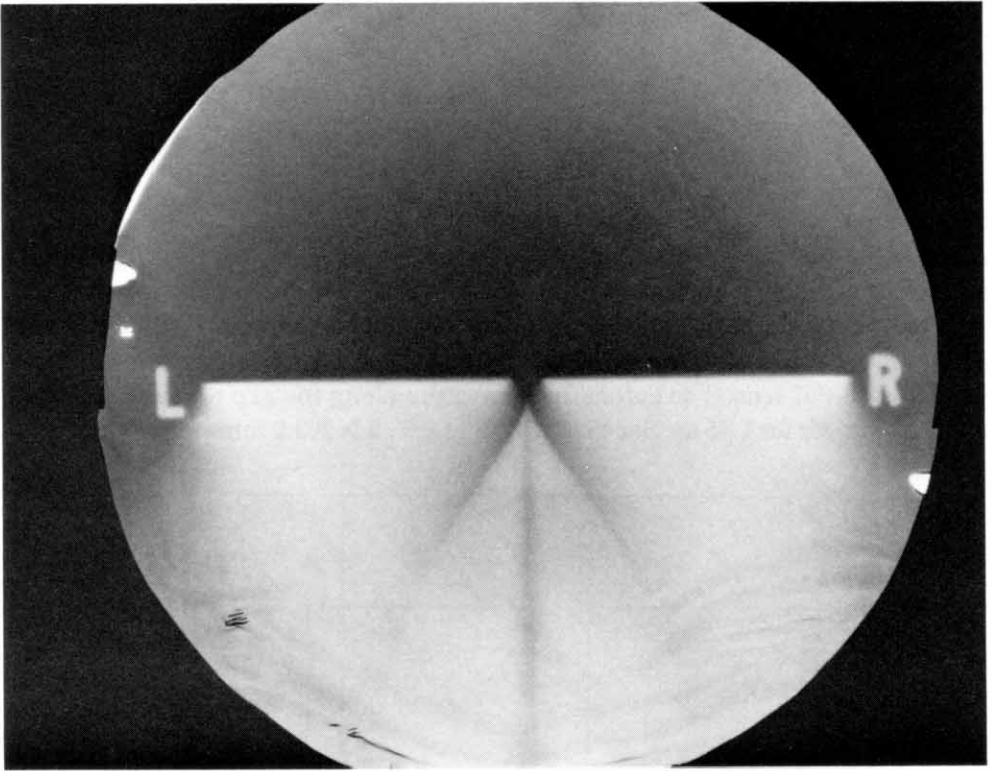
Douglas Venable

Radiographic Time:

51.47 μ s

Formation and growth of gaseous Munroe jets. This jet is formed by interaction of the detonation products of two Composition B-3 charges separated by an air gap 10.0 mm, w, wide. The charges are initiated by 25.4 mm of Composition B-3 initiated by a P-081 lens. The detonations have run along the gap for 203.2 mm. h is 203.2 mm.





SHOT 285:

Munroe Jet

Date:

May 25, 1965

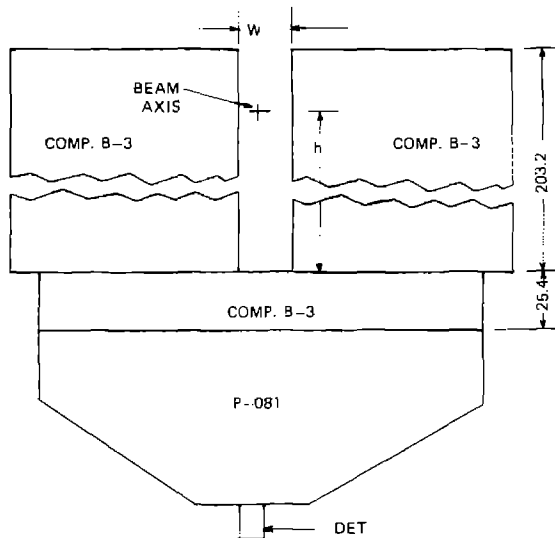
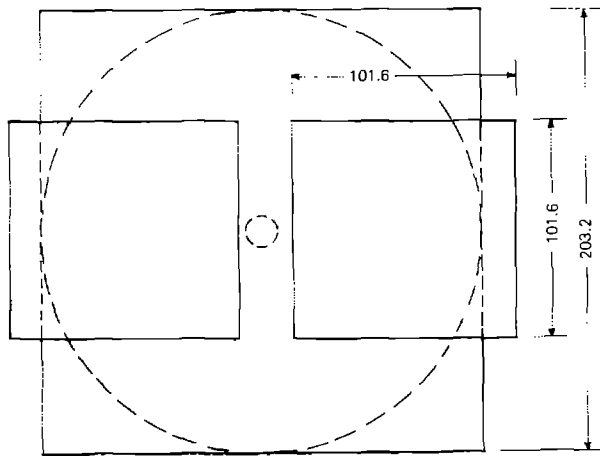
Experimenter:

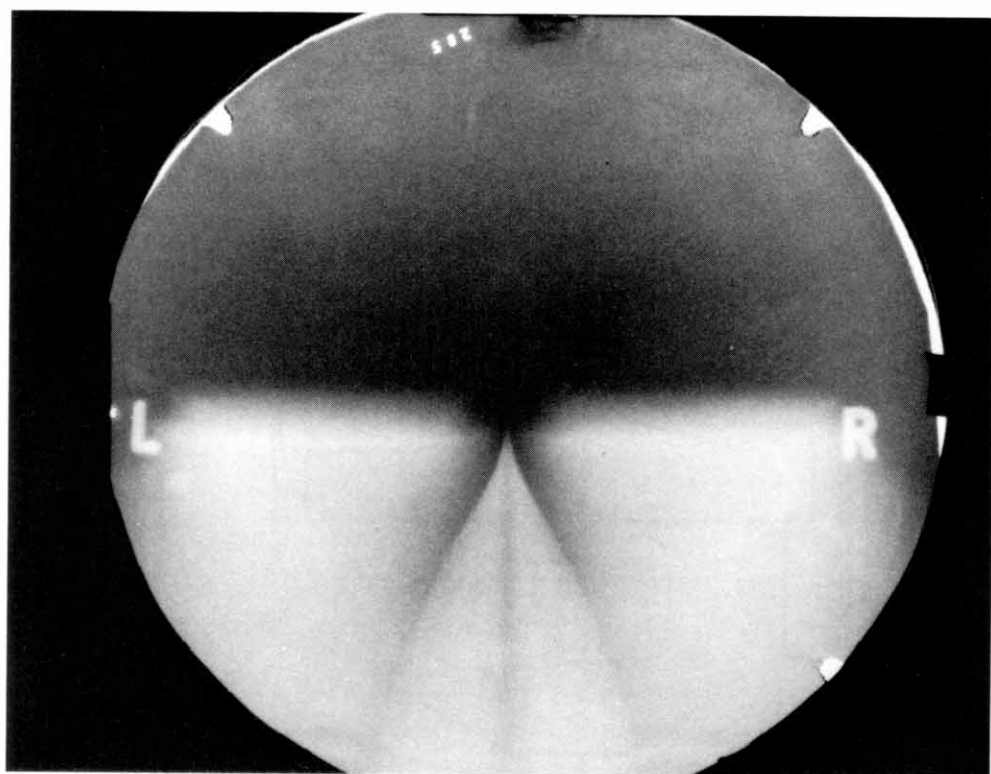
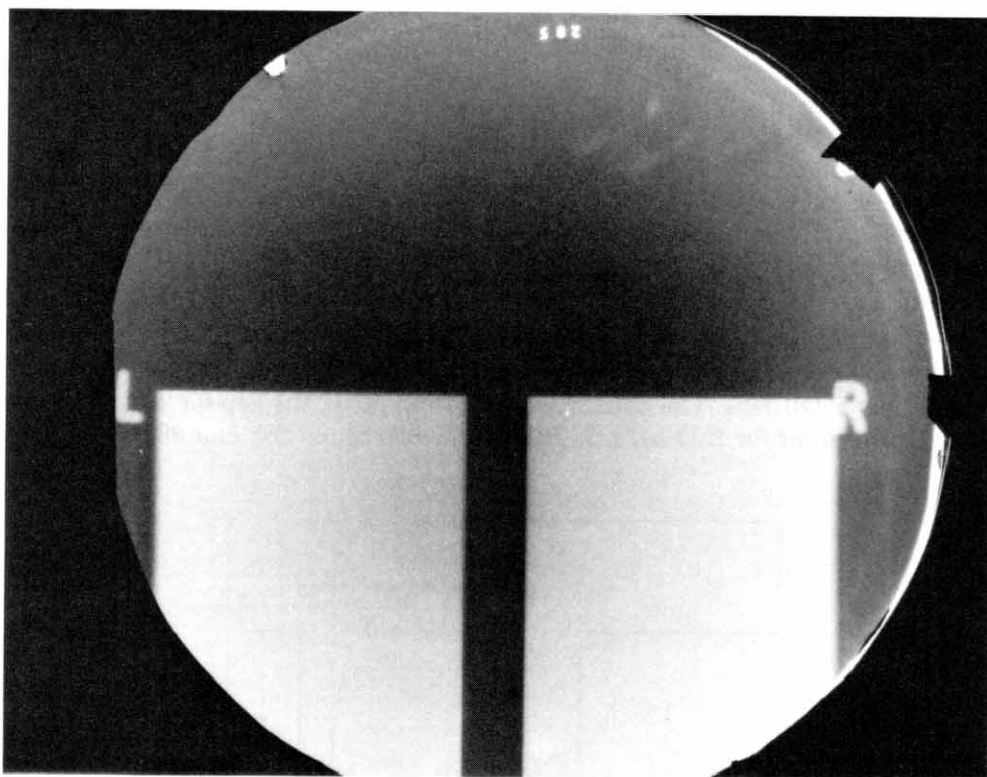
Douglas Venable

Radiographic Time:

52.92 μ s

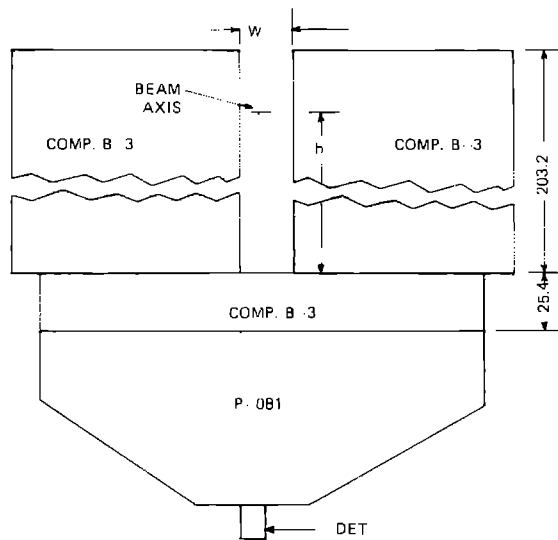
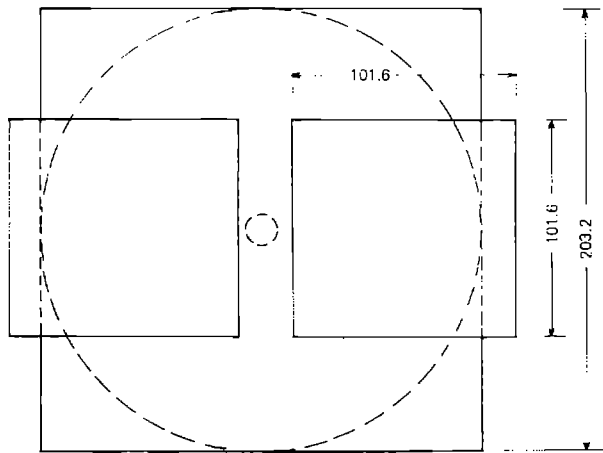
Formation and growth of gaseous Munroe jets. This jet is formed by interaction of the detonation products of two Composition B-3 charges separated by an air gap 20.0 mm, w, wide. The charges are initiated by 25.4 mm of Composition B-3 initiated by a P-081 lens. The detonations have run along the gap for 203.2 mm and expanded into air for 1.45 μ s. See Shots 286 and 287. h is 203.2 mm.

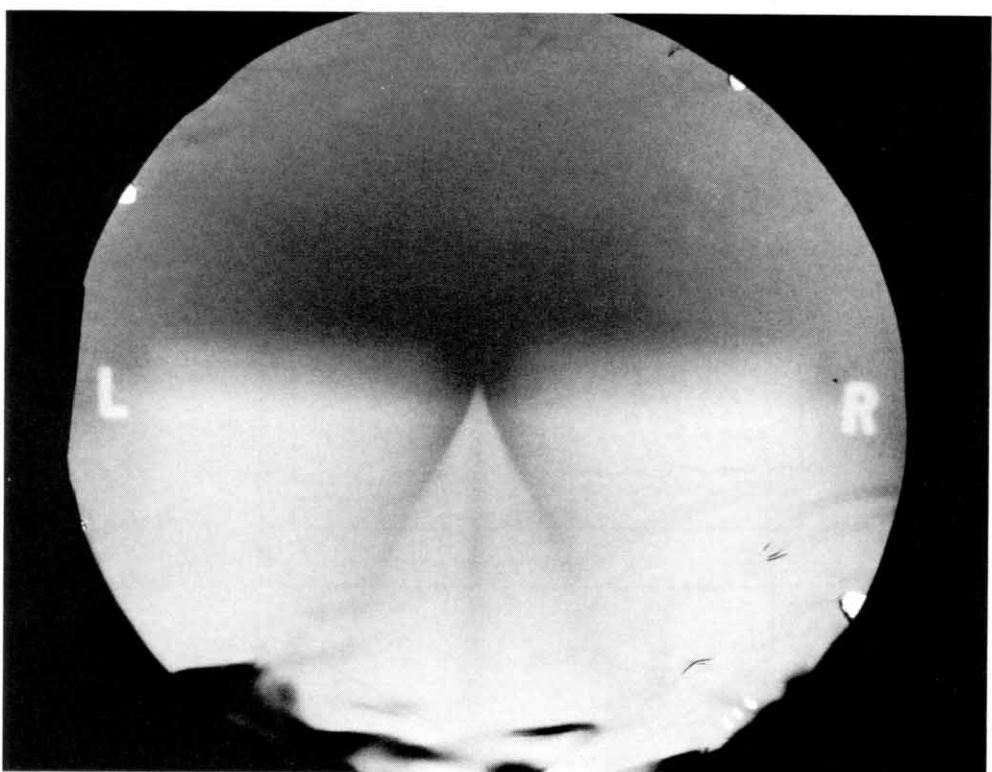
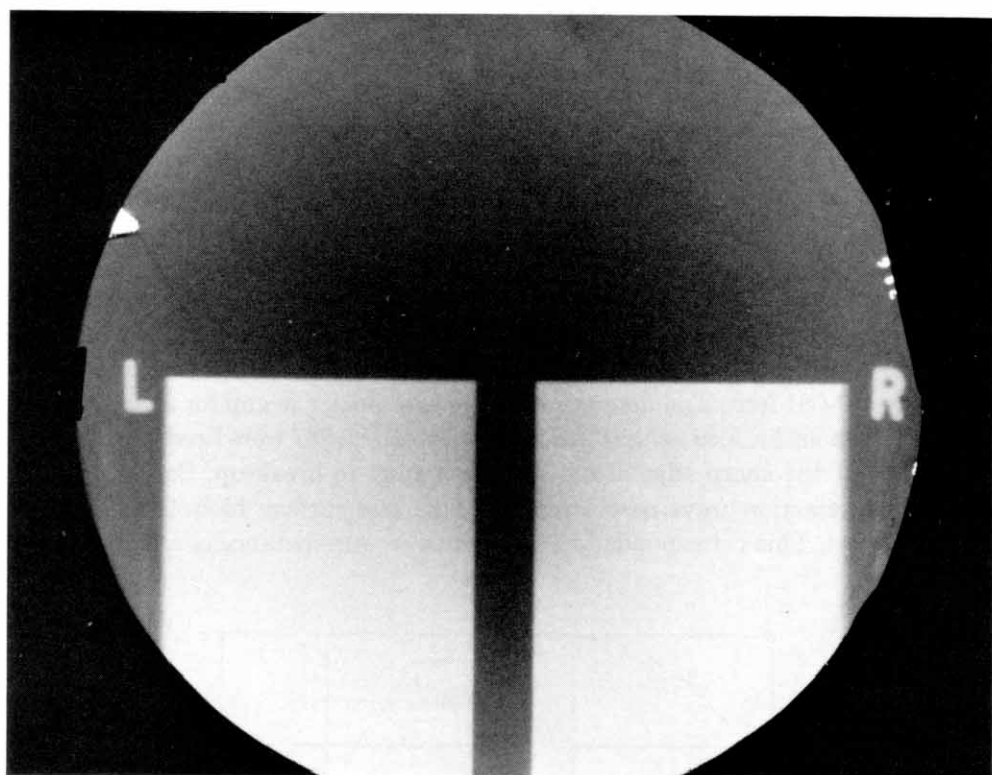




SHOT 286: **Munroe Jet**
 Date: June 15, 1965
 Experimenter: Douglas Venable
 Radiographic Time: 53.8 μ s

Formation and growth of gaseous Munroe jets. This jet is formed by interaction of the detonation products of two Composition B-3 charges separated by an air gap 20.0 mm, w, wide. The charges are initiated by 25.4 mm of Composition B-3 initiated by a P-081 lens. The detonations have run along the gap for 203.2 mm and expanded into air for 2.33 μ s. h is 203.2 mm. See Shots 285 and 287.





SHOT 287:**Munroe Jet**

Date:

June 15, 1965

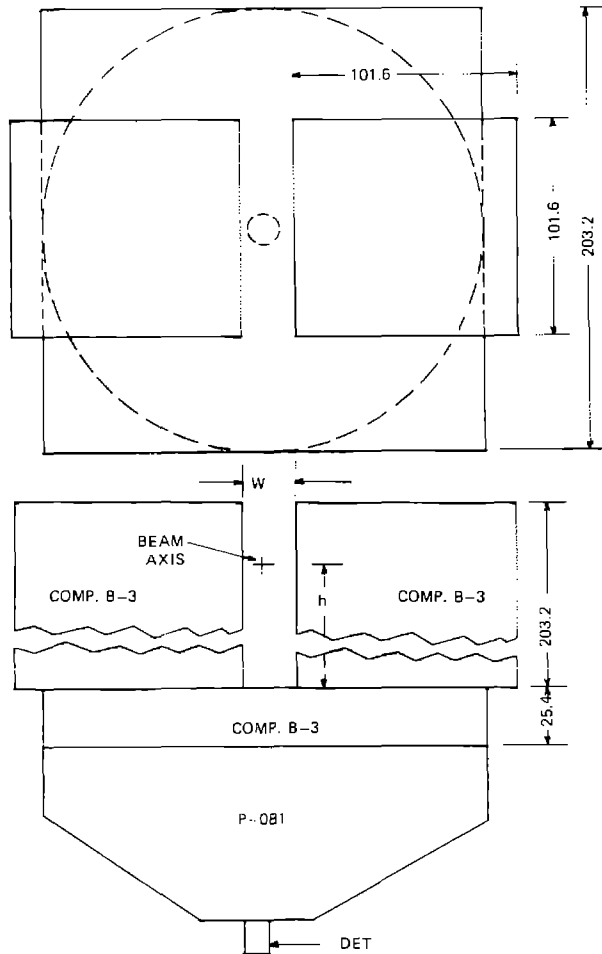
Experimenter:

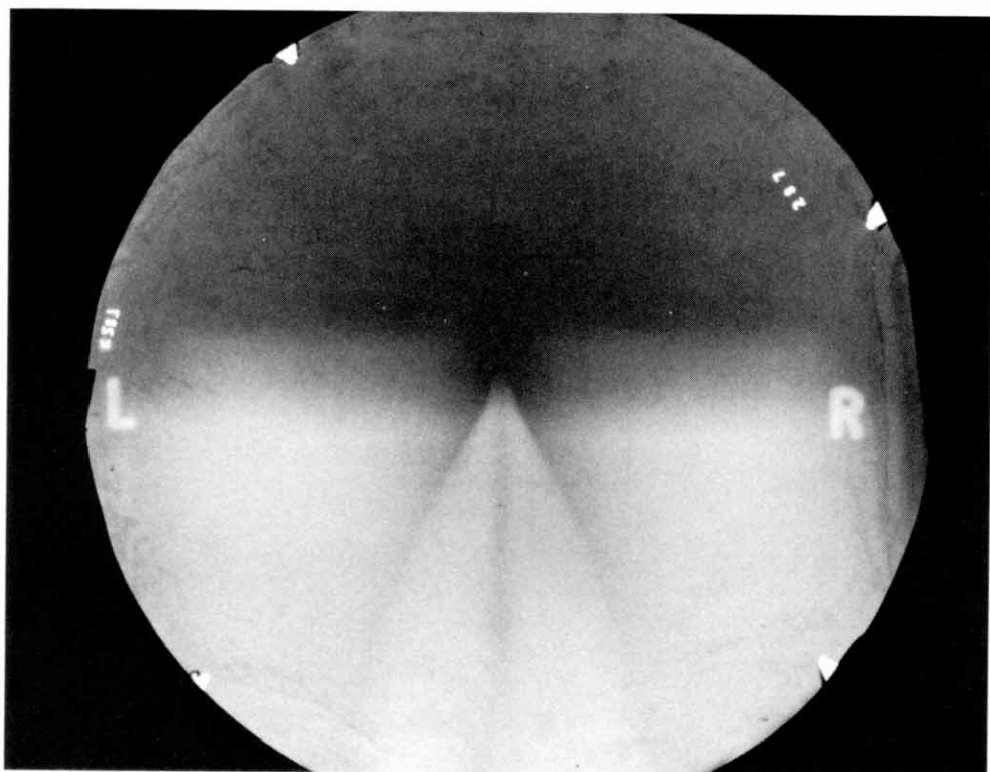
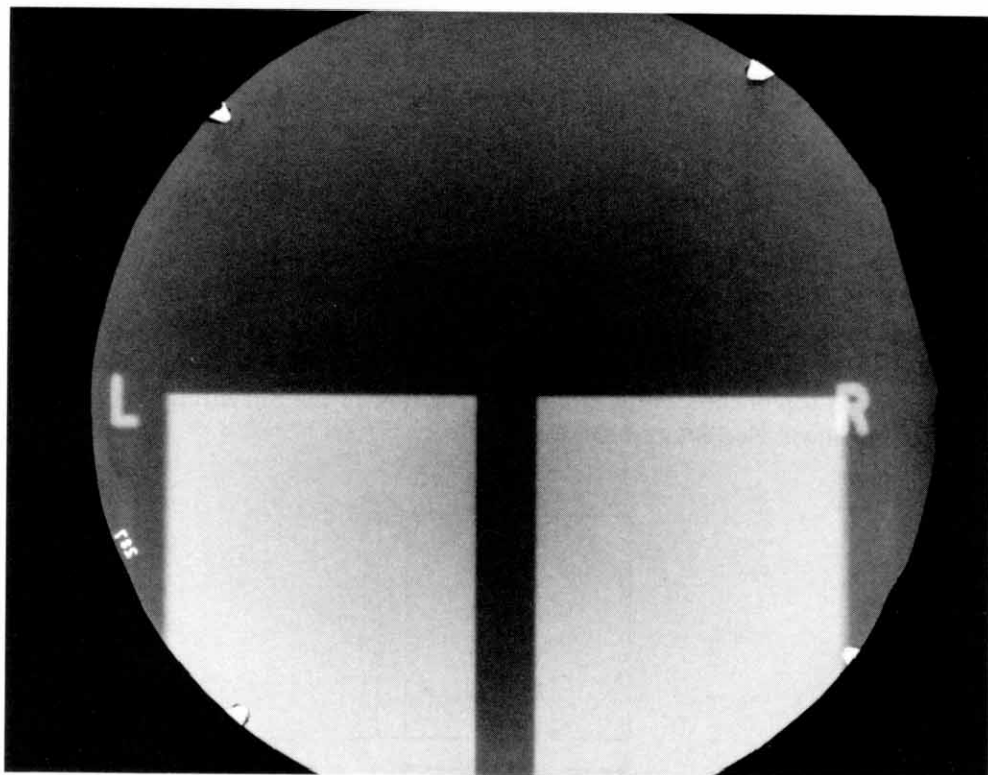
Douglas Venable

Radiographic Time:

55.06 μ s

Formation and growth of gaseous Munroe jets. This jet is formed by interaction of the detonation products of two Composition B-3 charges separated by an air gap 20.0 mm, w , wide. The charges are initiated by 25.4 mm of Composition B-3 initiated by a P-081 lens. The detonations have run along the gap for 203.2 mm and expanded into air for 3.59 μ s. h is 203.2 mm. Shots 285-287 were fired to determine at what point the sharp edge of the jet would start to break up. Breakup begins when the rarefaction wave associated with the free-surface blowoff reaches the front of the jet. This corresponds to an extended jet run distance of about one-half gap width.





SHOT 290:

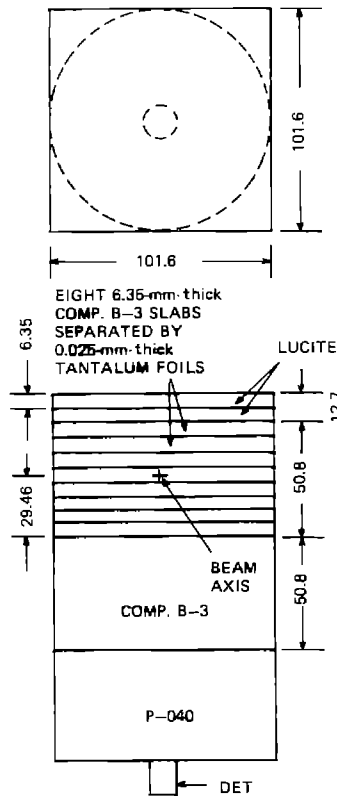
Composition B-3 with Embedded Tantalum Foils

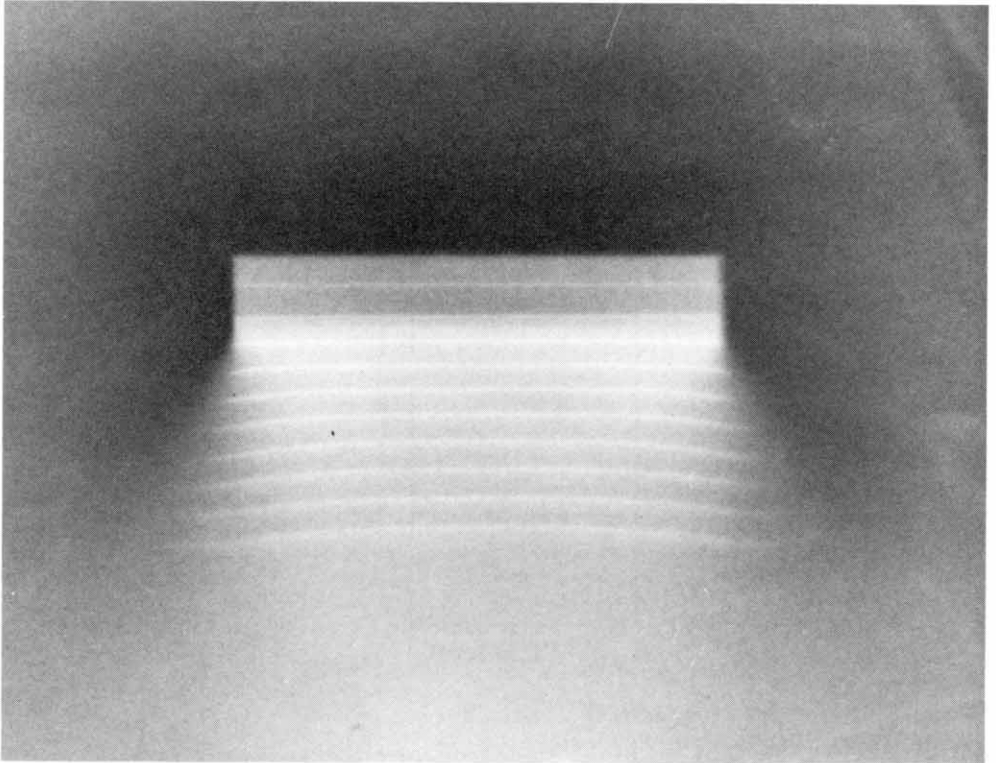
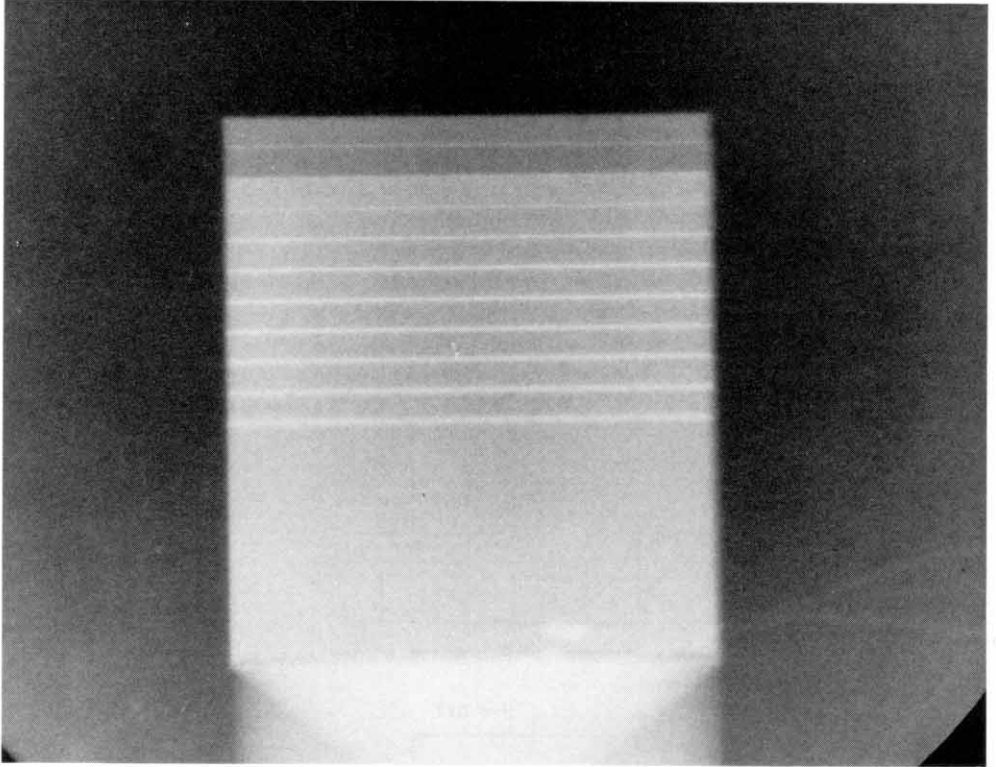
Date: August 26, 1965

Experimenter: Benny Ray Breed

Radiographic Time: 26.3 μ s

Eight slabs of 6.35-mm-thick Composition B-3 separated by 0.0254-mm-thick tantalum foils were initiated perpendicular to the foils by 50.8 mm of Composition B-3 and a P-040 lens. Two Lucite slabs separated by 0.025-mm-thick tantalum foils were placed on top of the Composition B-3. The flow of the unconfined detonation products is shown. See Shots 220 and 221.





SHOT 291:

Colliding Cyclotol Detonations

Date:

August 24, 1965

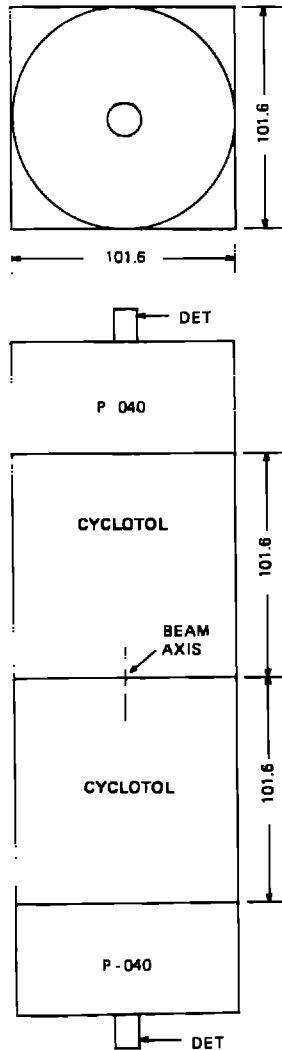
Experimenter:

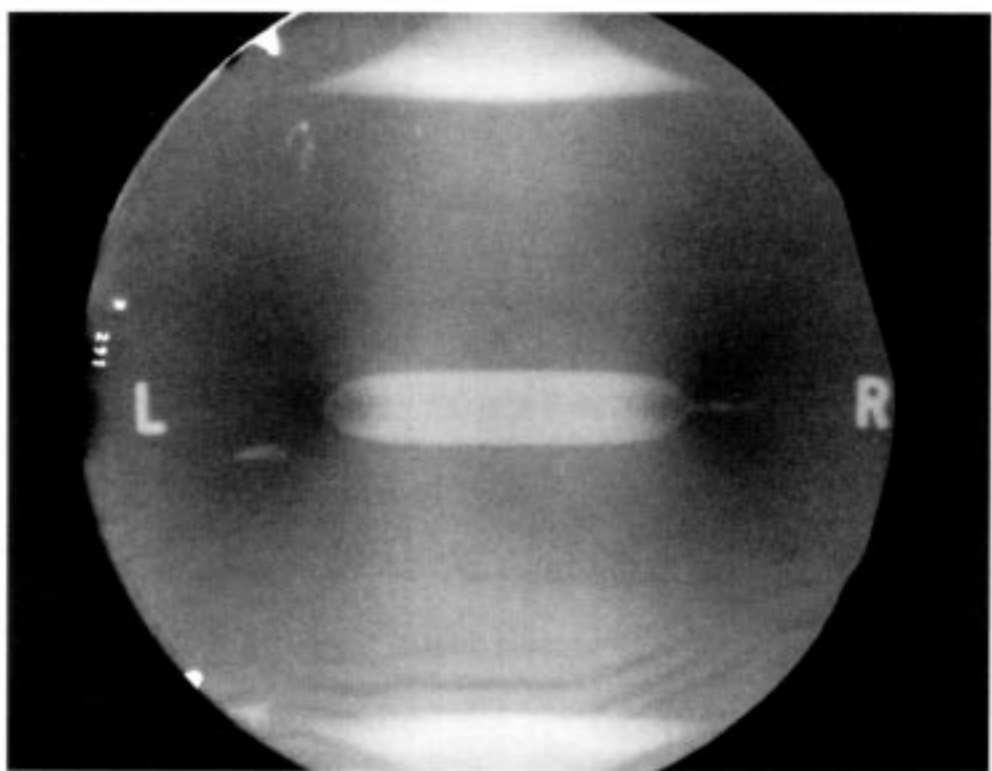
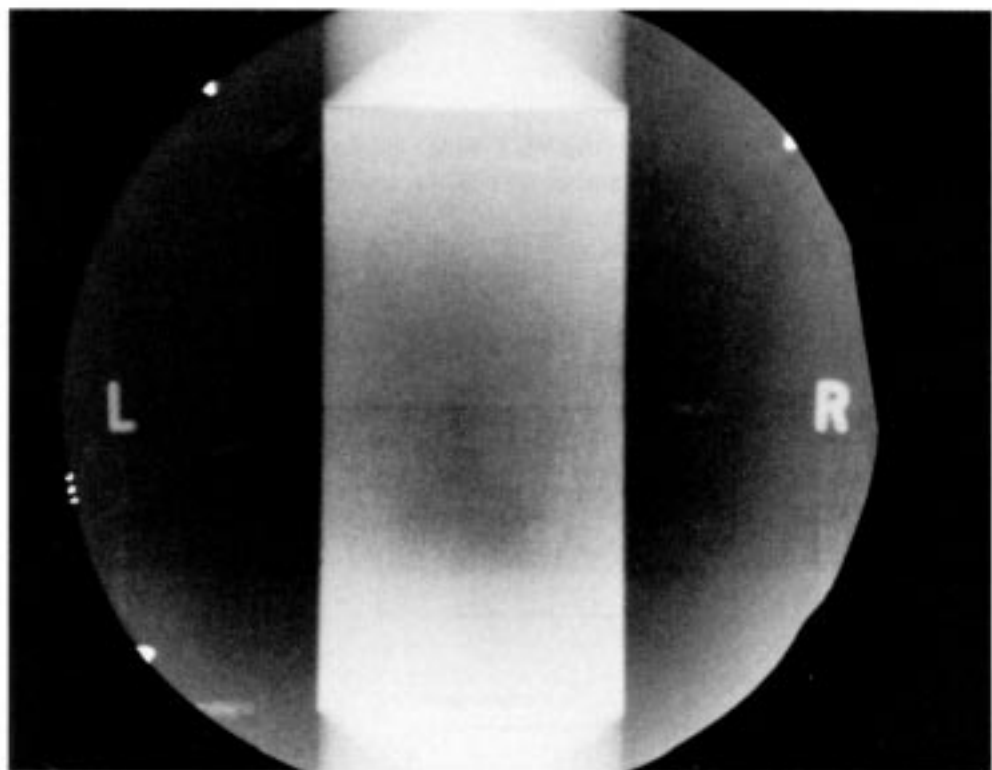
Douglas Venable

Radiographic Time:

27.79 μ s

The reflected shocks in Cyclotol detonation products 1.89 μ s after the detonation waves collided. See Shots 203-206.





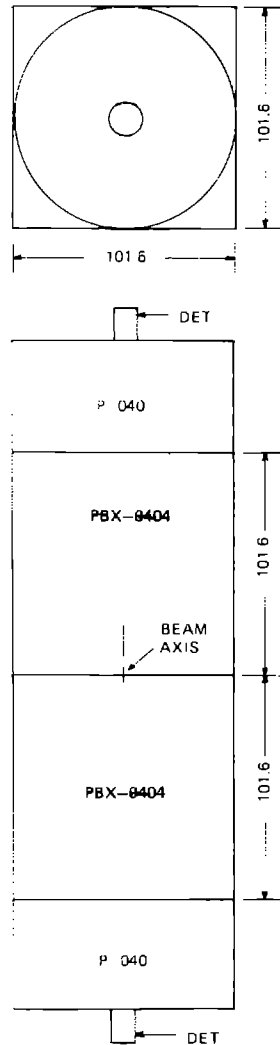
SHOT 292: Colliding PBX-9404 Detonations

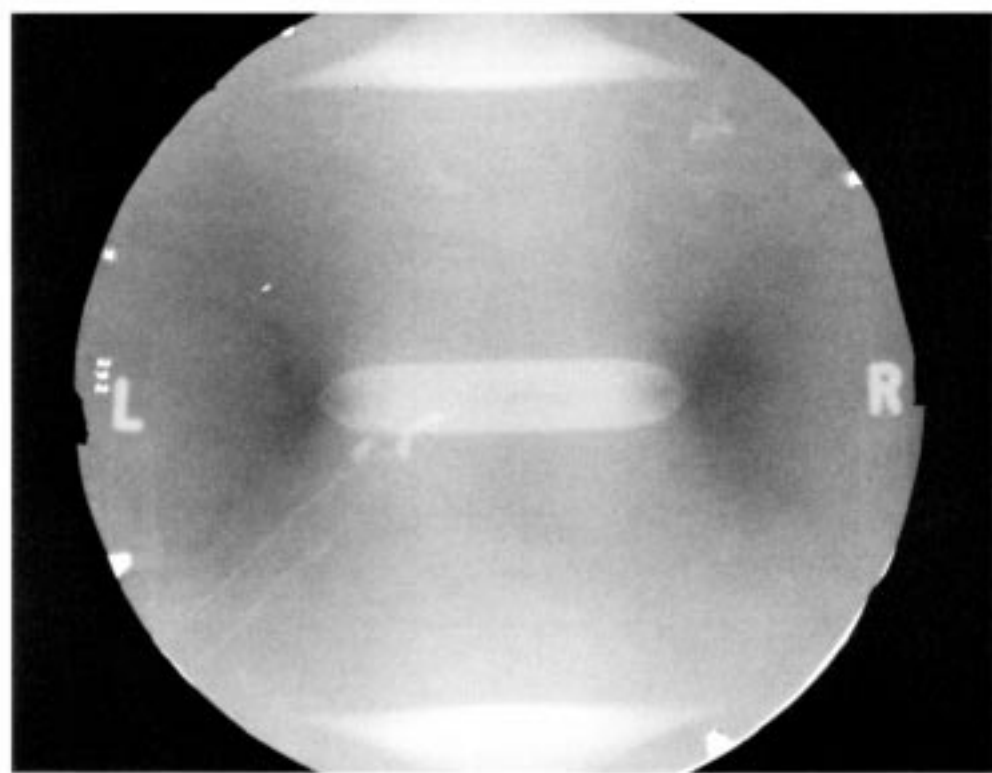
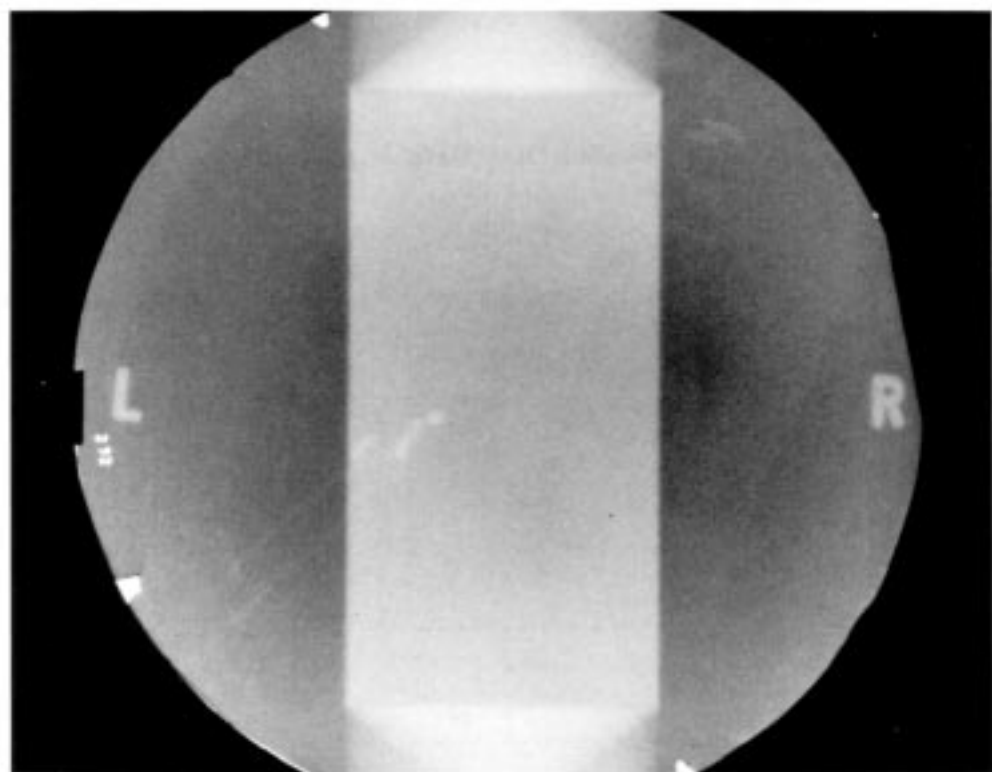
Date: September 1, 1965

Experimenter: Douglas Venable

Radiographic Time: 26.86 μ s

The reflected shocks in PBX-9404 detonation products 1.72 μ s after the detonation waves collided. See Shots 207-210.





SHOT 294:

Colliding Octol Detonations

Date:

September 14, 1965

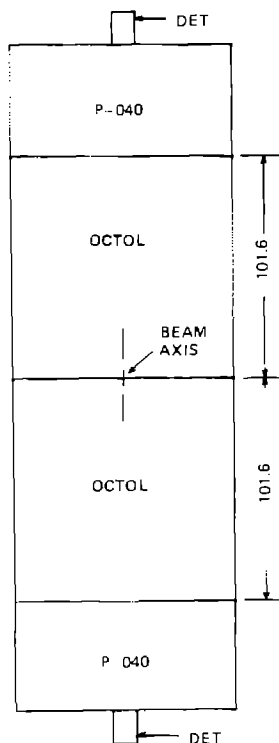
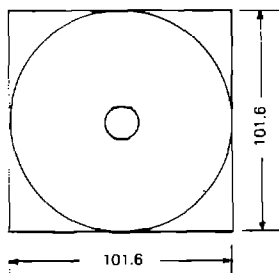
Experimenter:

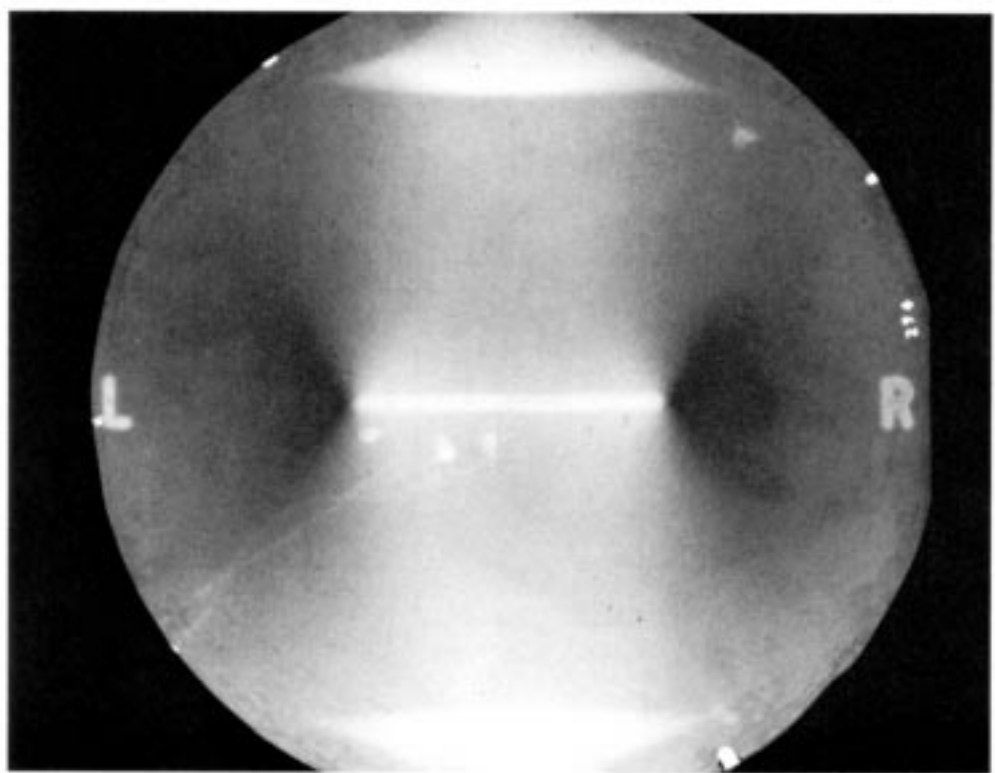
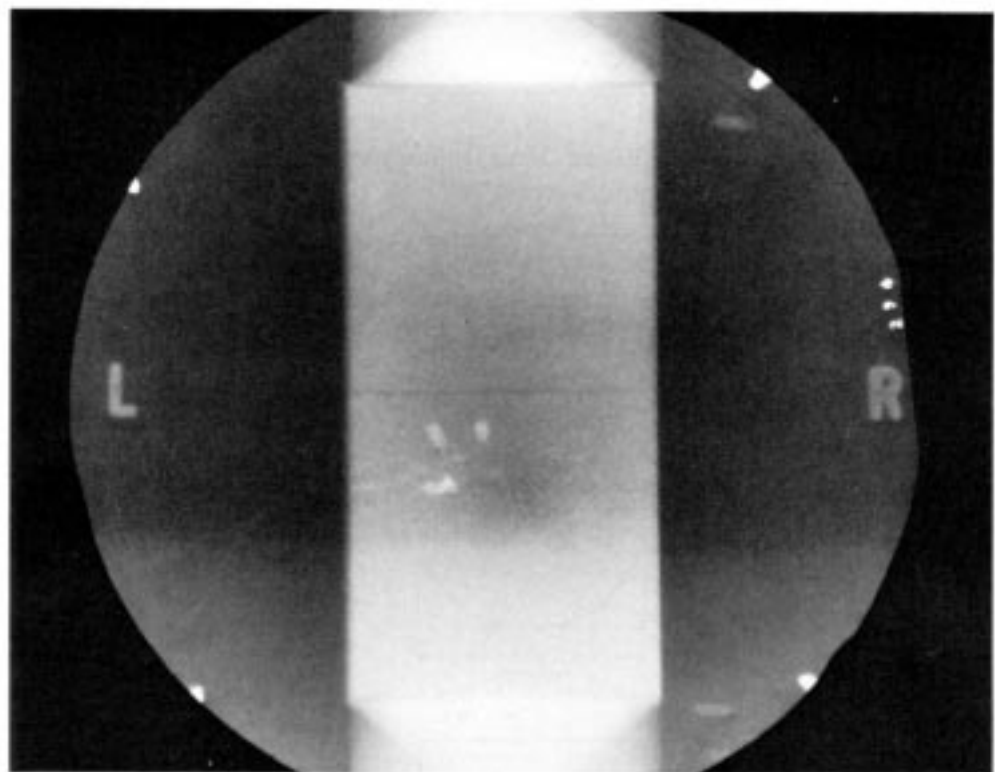
Douglas Venable

Radiographic Time:

25.86 μ s

The reflected shocks in Octol detonation products 0.34 μ s after the detonation waves collided. See Shots 295-297.





SHOT 295:

Colliding Octol Detonation Waves

Date:

September 14, 1965

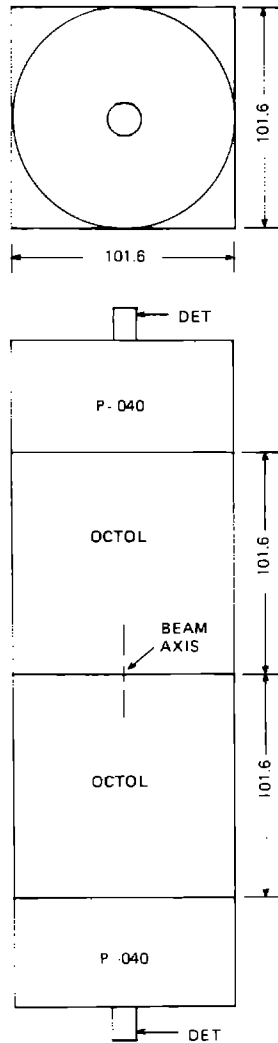
Experimenter:

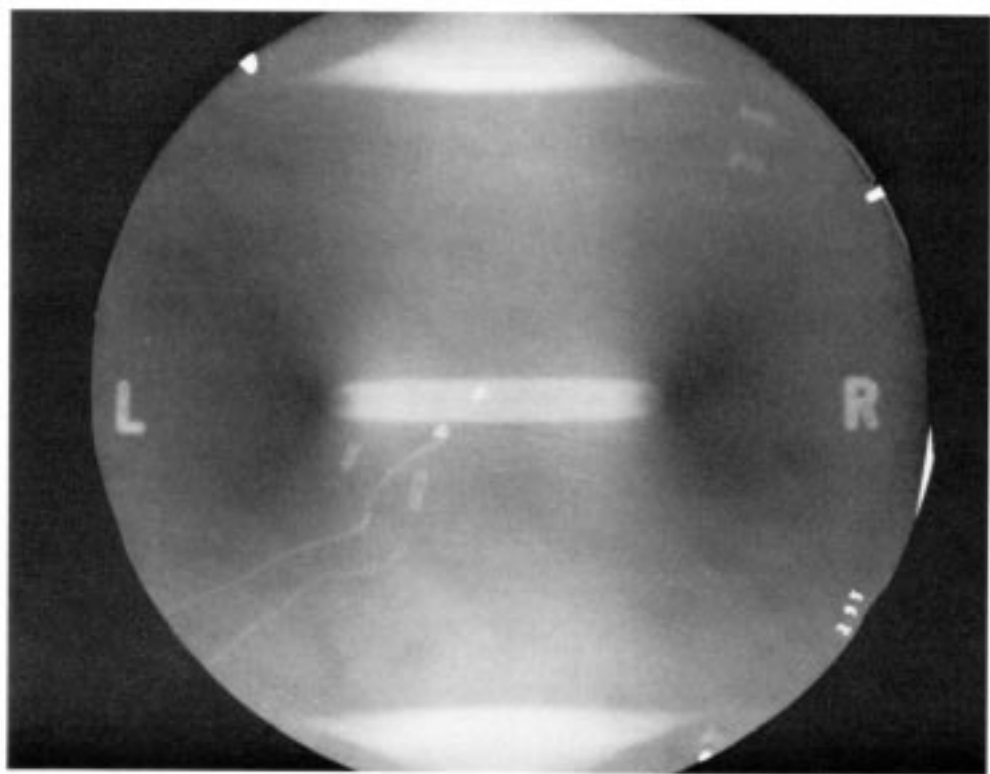
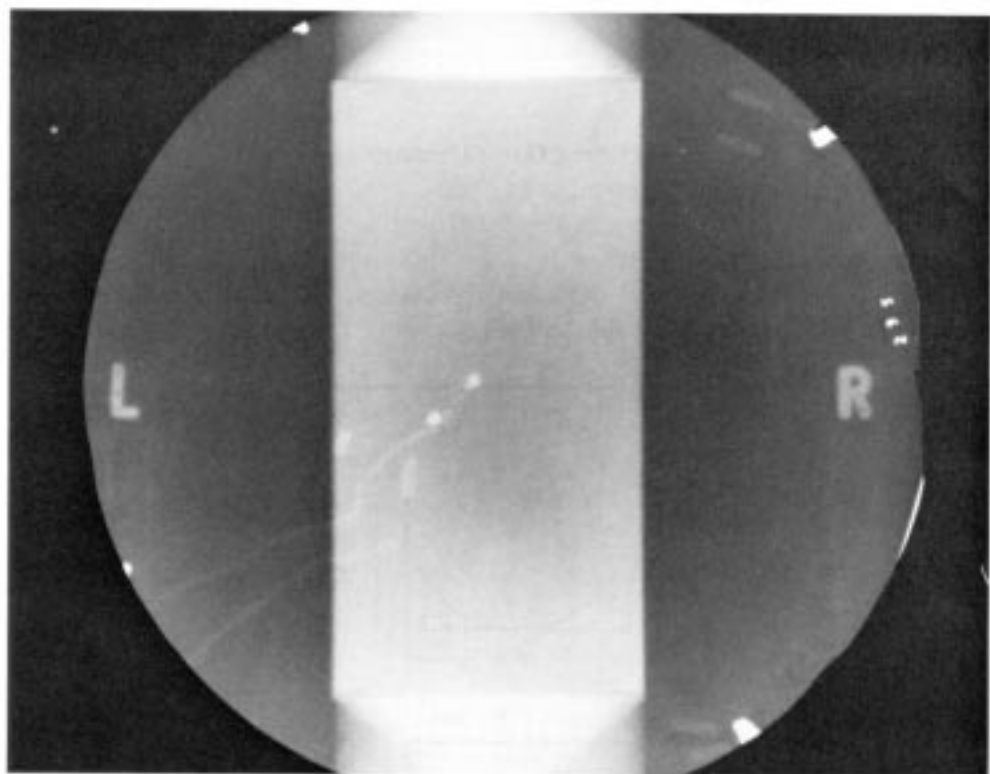
Douglas Venable

Radiographic Time:

26.51 μ s

The reflected shocks in Octol detonation products 1.03 μ s after the detonation waves collided. See Shots 294, 296, and 297.





SHOT 296:

Colliding Octol Detonation Waves

Date:

September 14, 1965

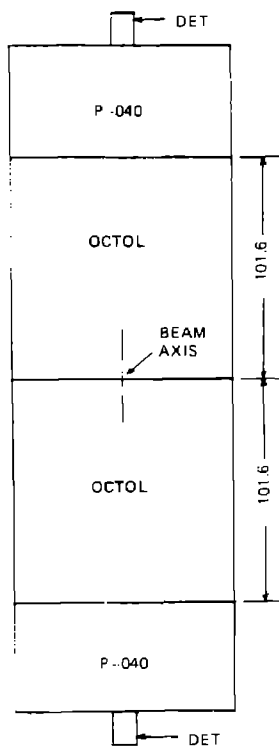
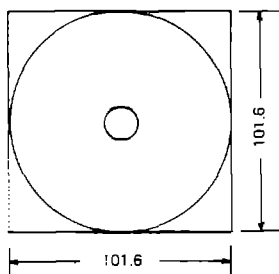
Experimenter:

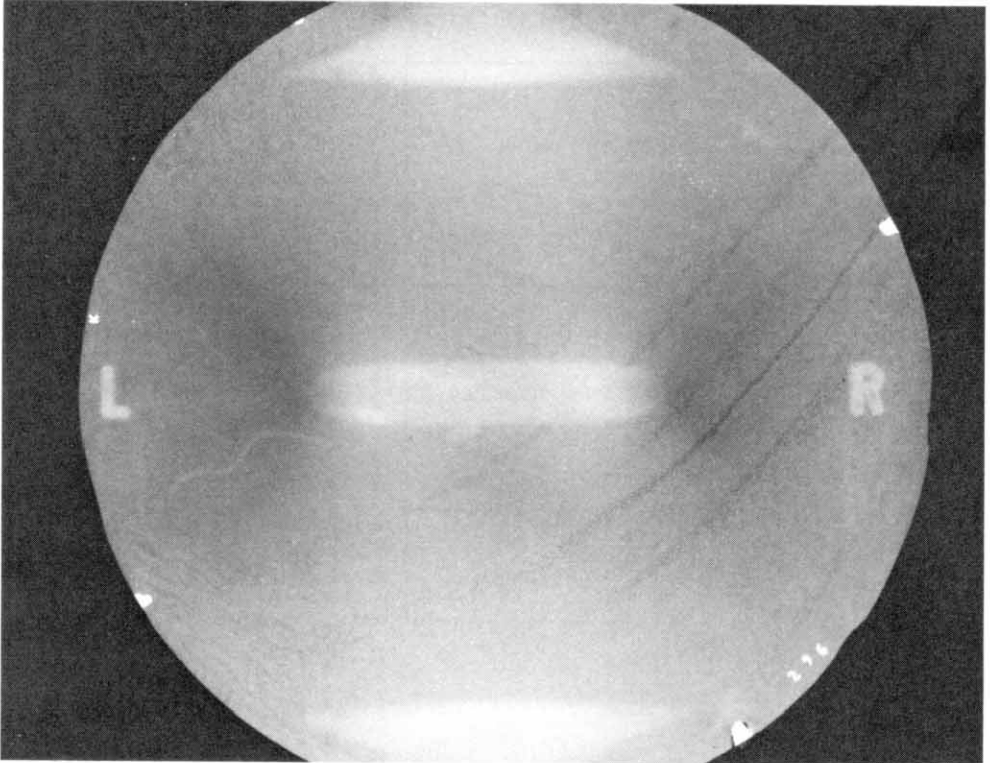
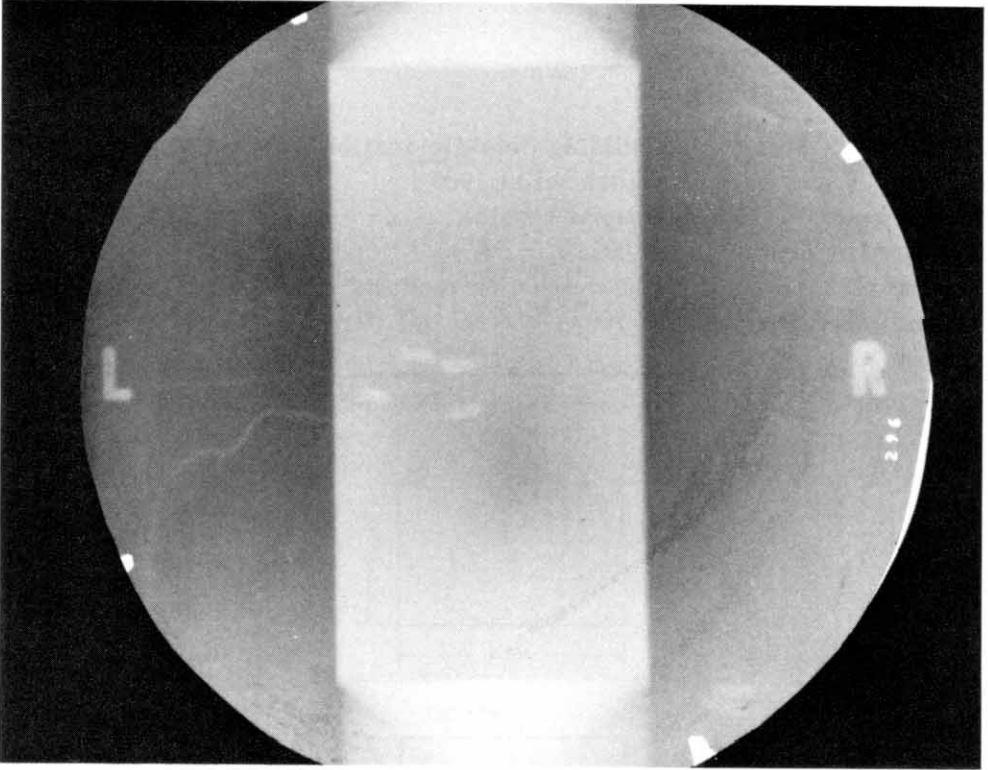
Douglas Venable

Radiographic Time:

27.02 μ s

The reflected shocks in Octol detonation products 1.55 μ s after the detonation waves collided. See Shots 294, 295, and 297.





SHOT 297:

Colliding Octol Detonation Waves

Date:

September 14, 1965

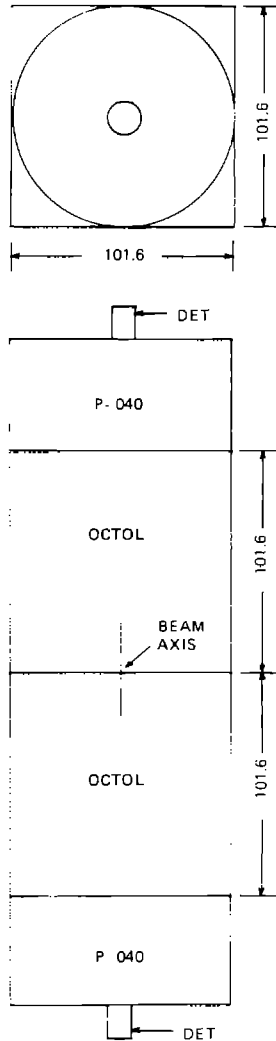
Experimenter:

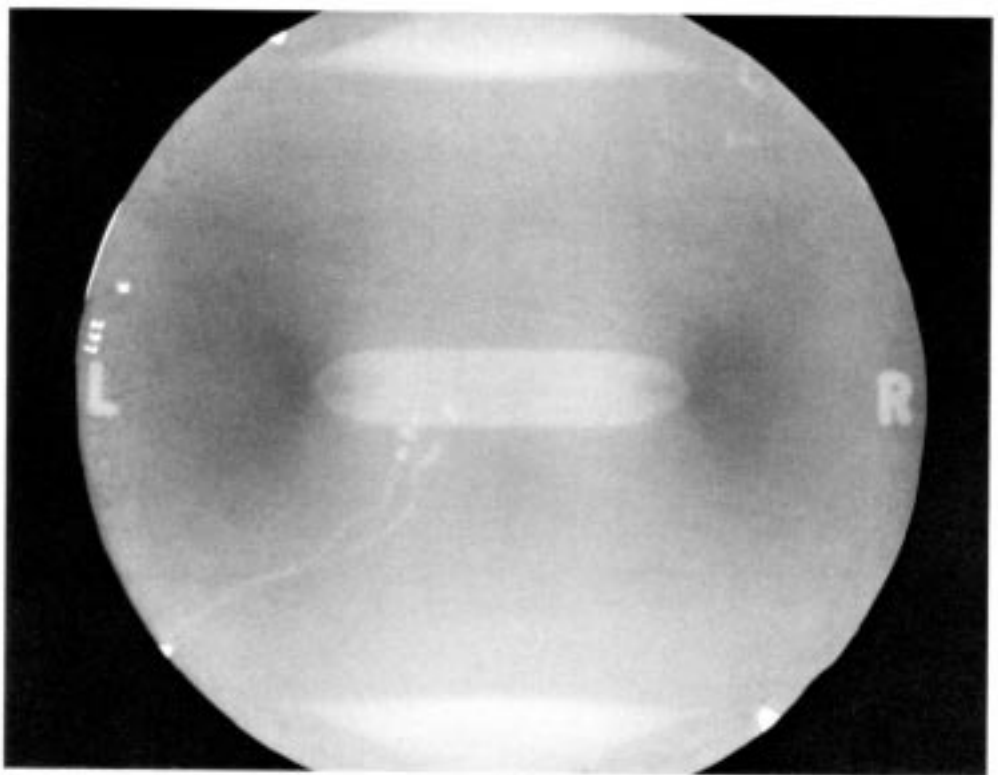
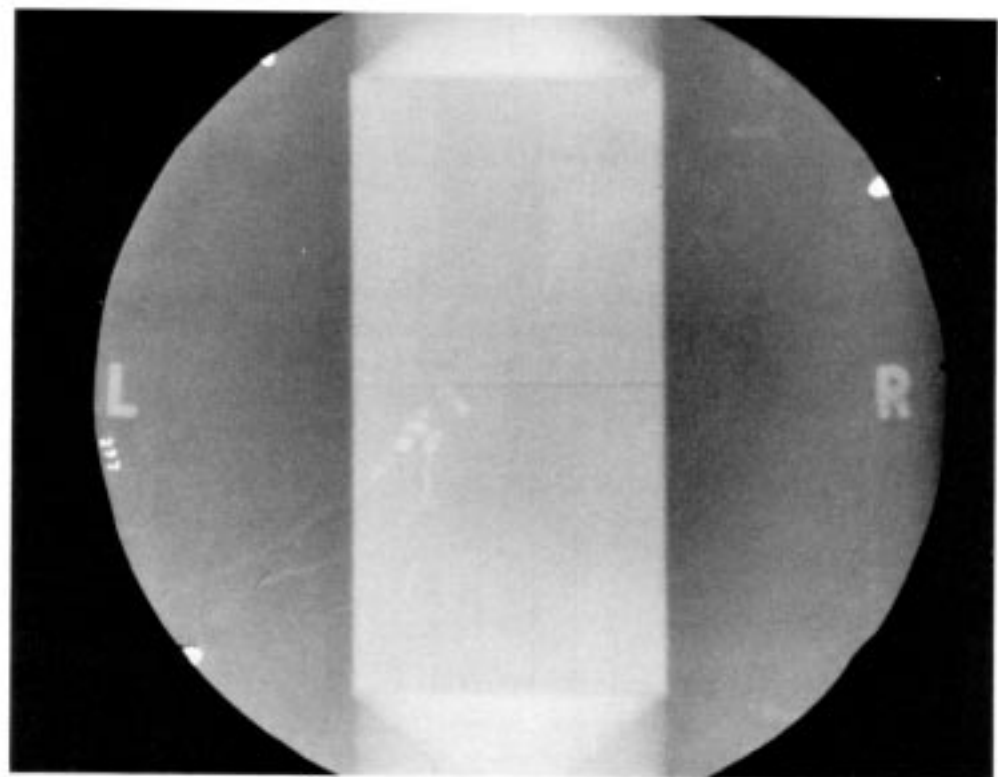
Douglas Venable

Radiographic Time:

27.49 μ s

The reflected shocks in Octol detonation products 1.98 μ s after the detonation waves collided. See Shots 294-296.





SHOT 298:

Water Jet

Date:

July 23, 1965

Experimenter:

Roger W. Taylor

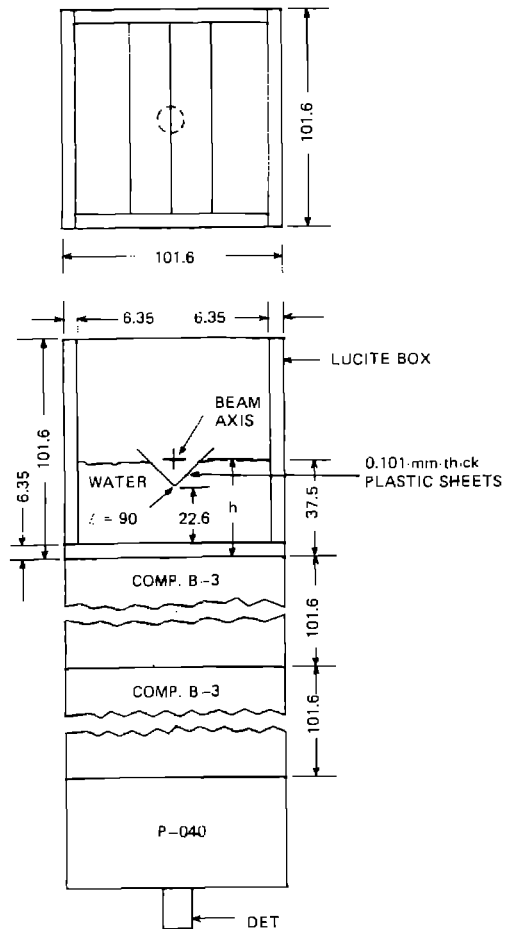
Radiographic Time:

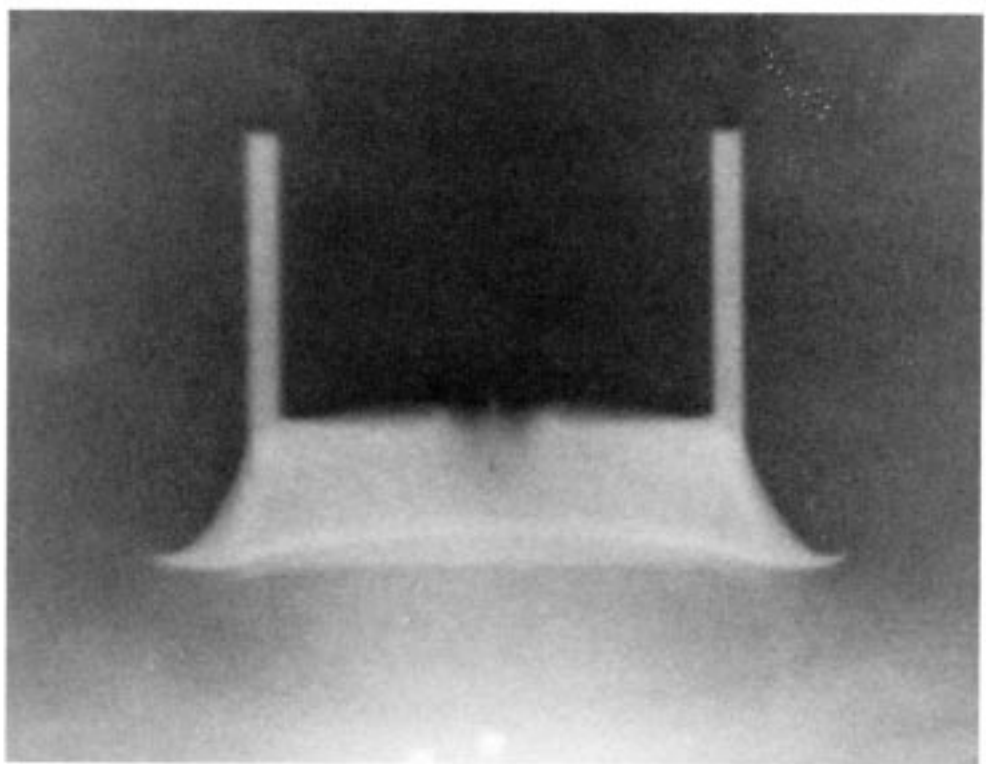
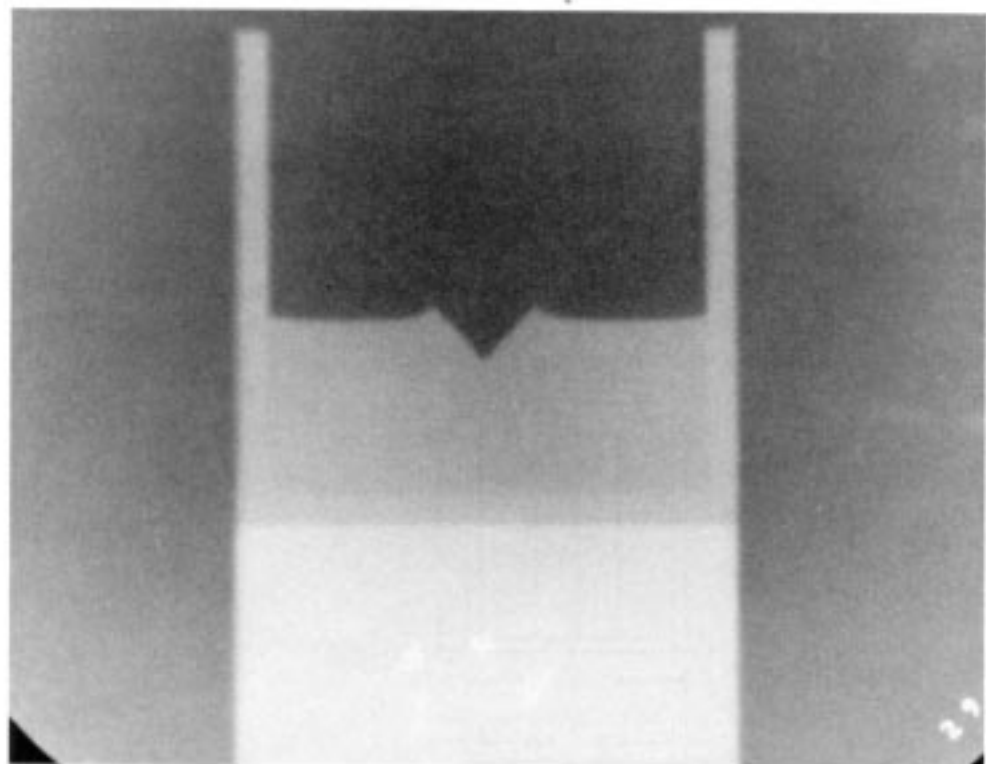
46.85 μ s

References:

Mader et al., 1967; Mader and Kershner, 1972

A shock wave in water interacts with a 9.0-mm-deep 90° groove formed by thin (0.1-mm) plastic sheets. The shock wave has traveled 6.65 μ s since the shock reached the Lucite and water interface. See Shots 192 and 299. h is 44.45 mm.





SHOT 299:

Water Jet

Date:

August 26, 1965

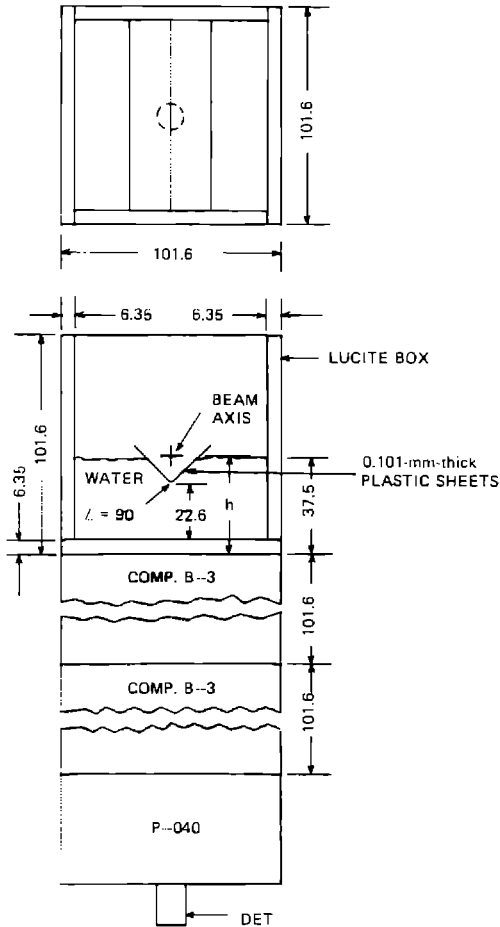
Experimenter:

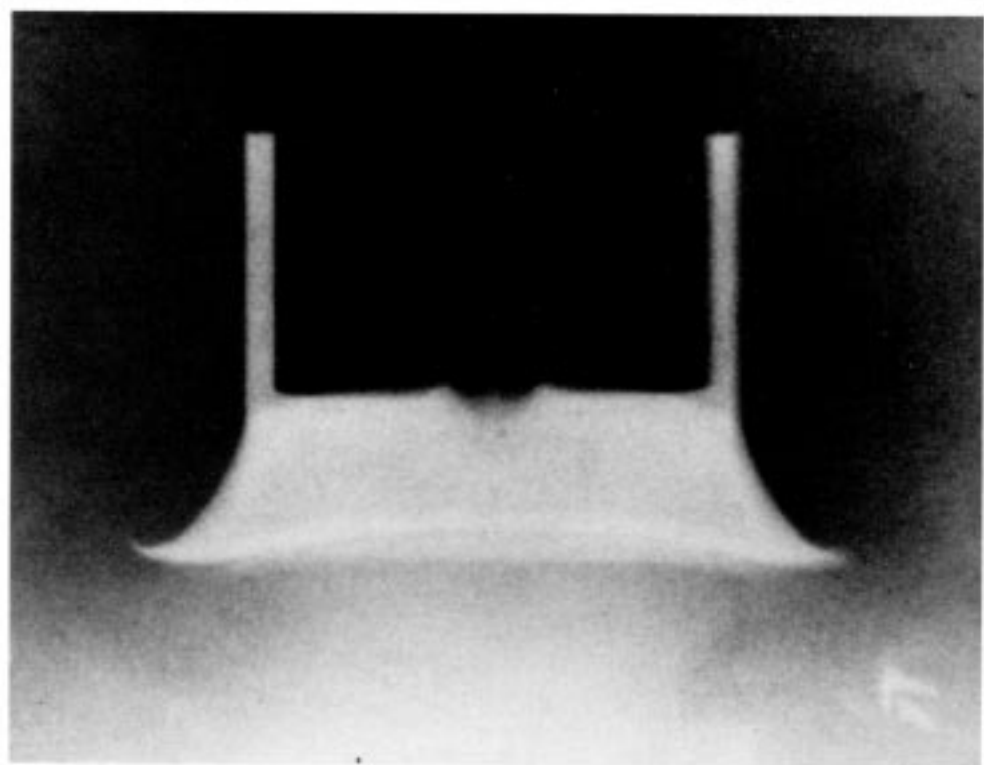
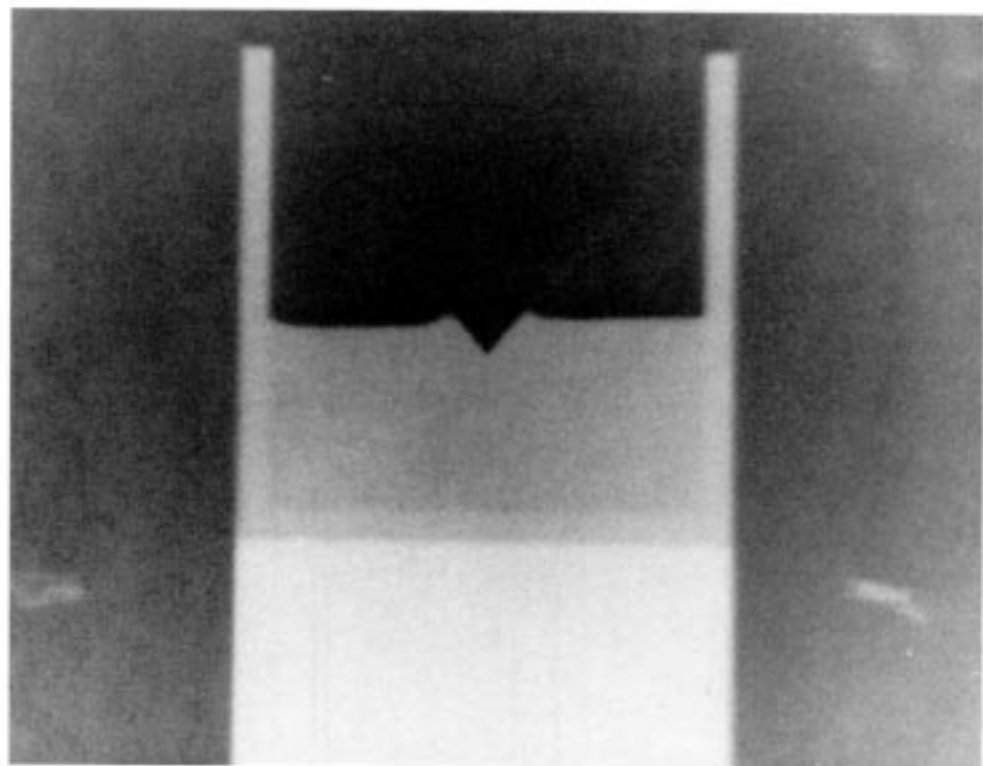
Roger W. Taylor

Radiographic Time:

47.79 μ s

A shock wave in water interacts with a 0.9-mm-deep 90° groove formed by thin (0.101-mm) plastic sheets. The shock wave has traveled 7.6 μ s since the shock reached the Lucite and water interface. See Shots 192 and 298. h is 38.1 mm.





SHOT 300: Cylindrical Hole in Water

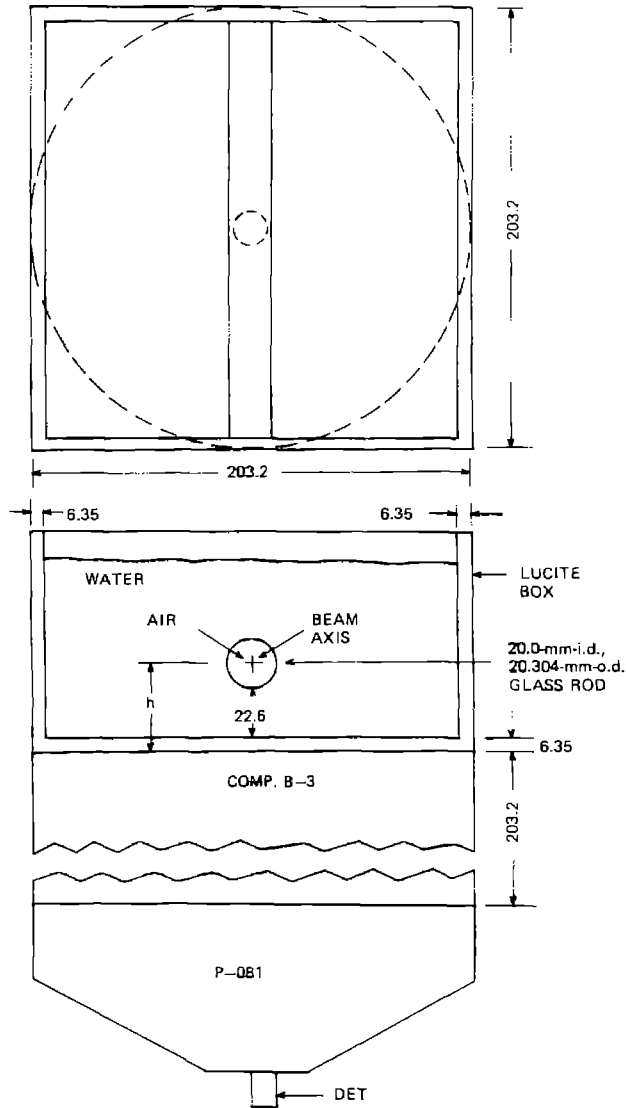
Date: July 22, 1965

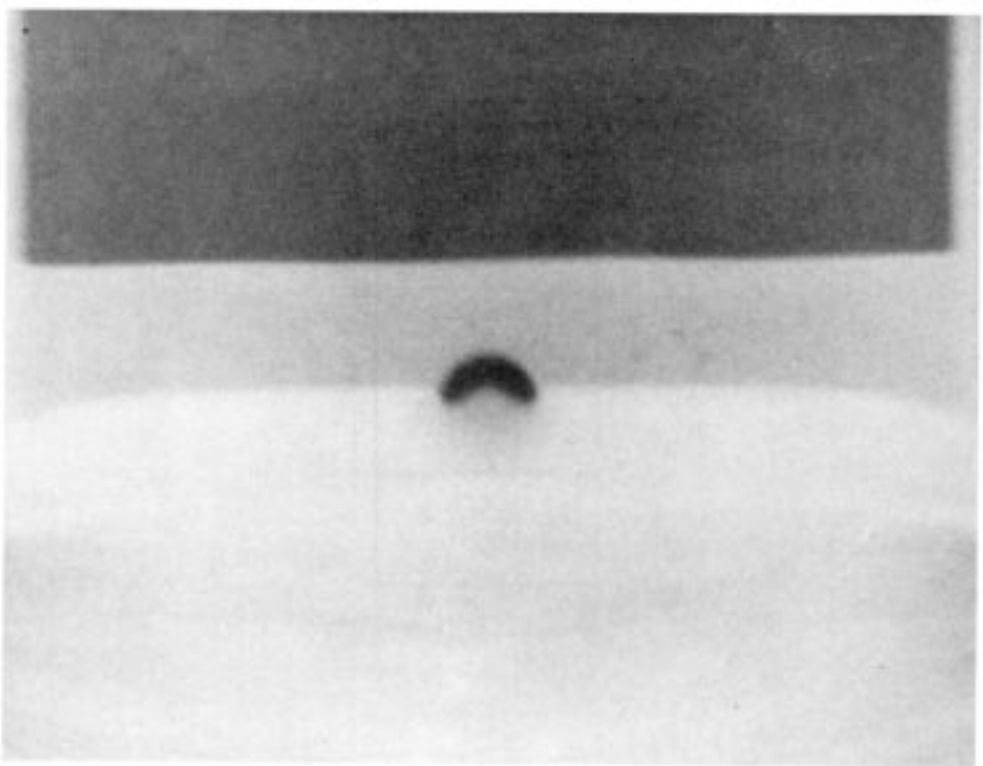
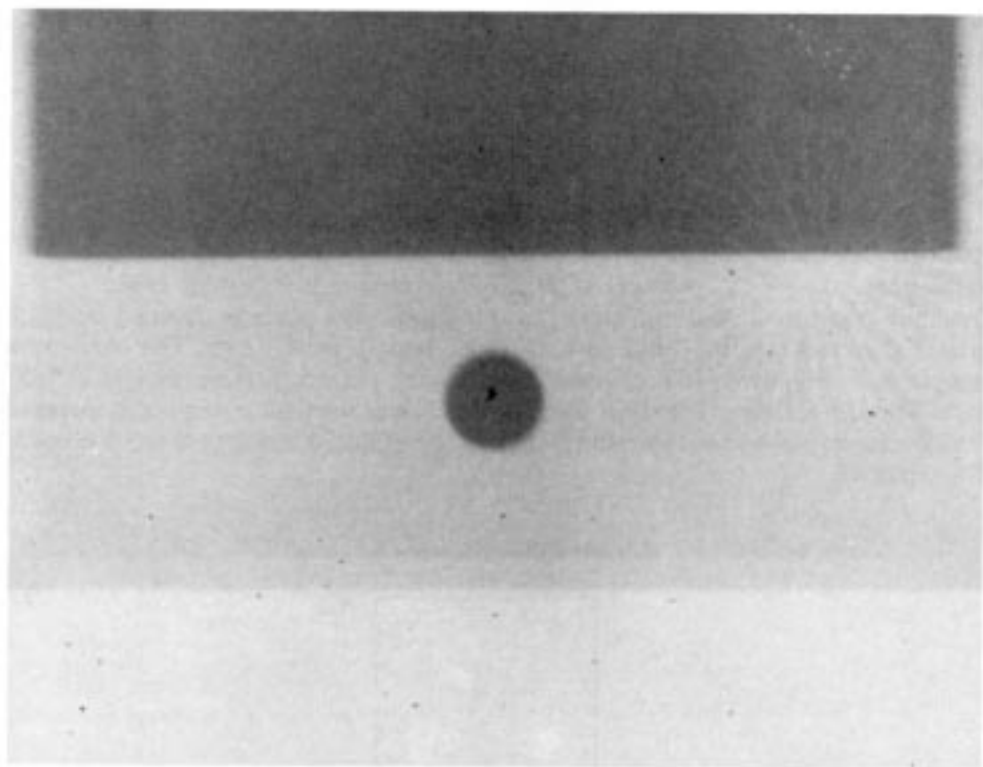
Experimenter: Roger W. Taylor

Radiographic Time: 54.78 μ s

References: Mader et al., 1967; Mader and Kershner, 1972

A 10.0-mm-radius cylindrical hole is formed by a thin-walled (0.152-mm) glass tube in water. The shock wave has traveled for 5.9 μ s since the shock reached the Lucite and water interface. This shot is similar to Shot 279 except that the water shock wave is less curved. See Shots 187, 188, 279, 280, and 318. h is 38.9 mm.





SHOT 305: Dynamic Fracture of Aluminum

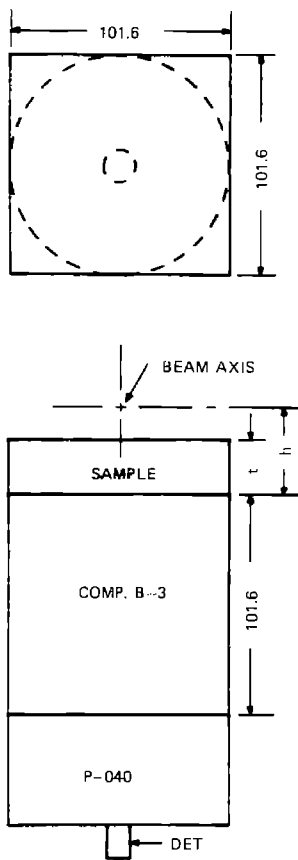
Date: November 23, 1965

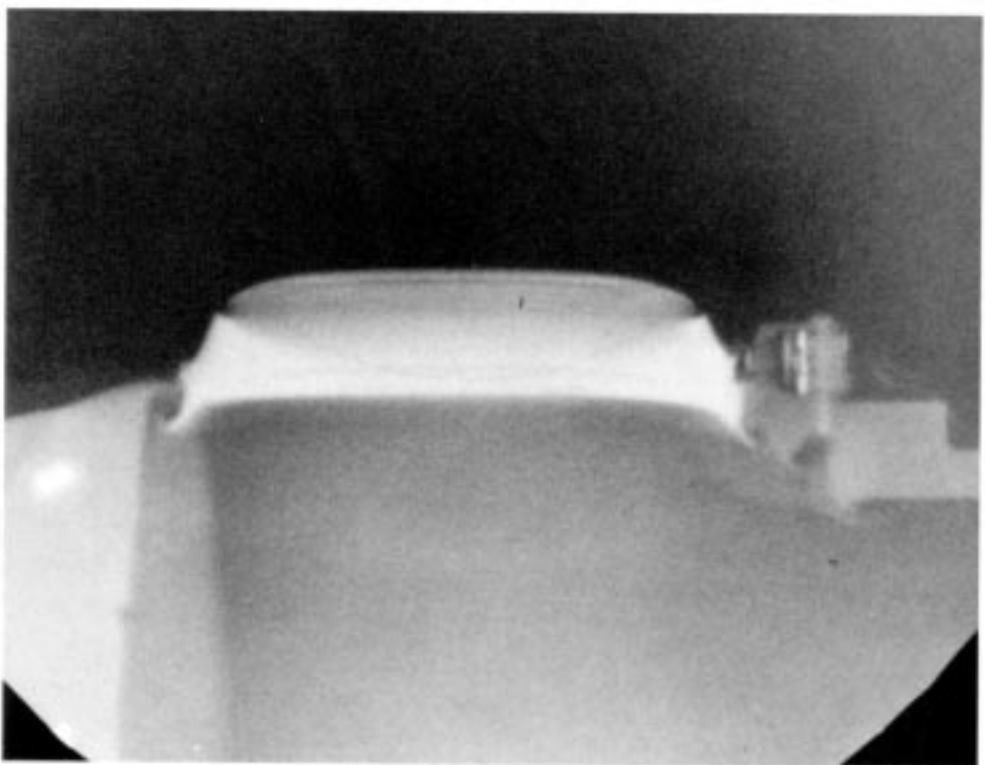
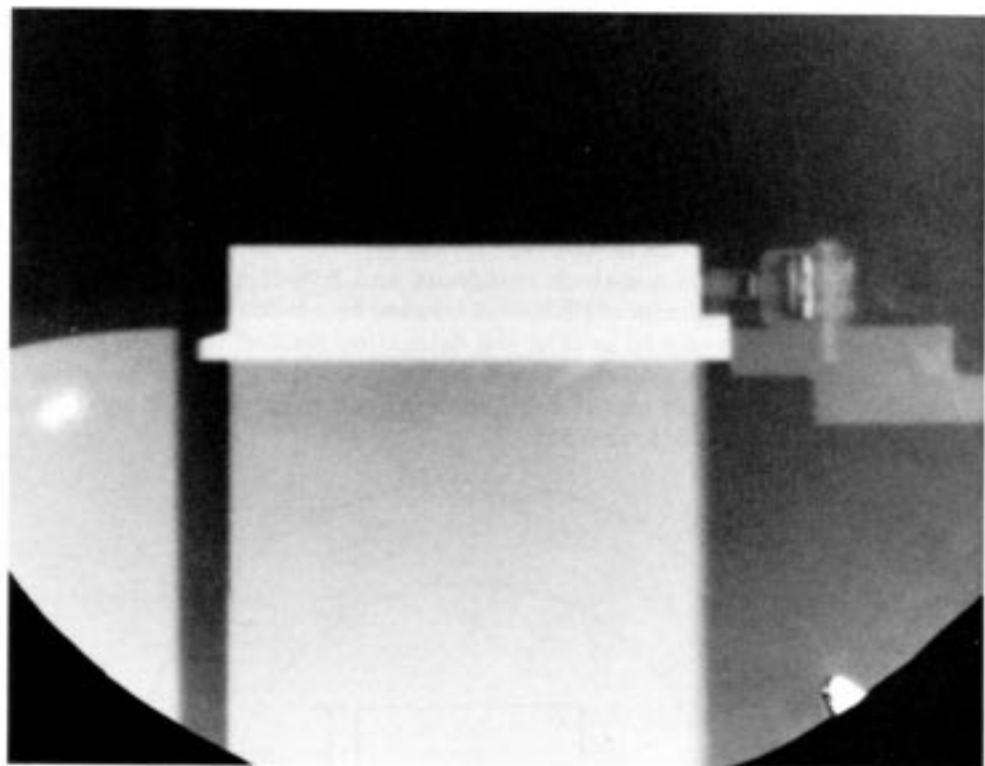
Experimenter: Benny Ray Breed

Radiographic Time: 33.38 μ s

References: Breed et al., 1967; Thurston and Mudd, 1968

Dynamic fracture of 25.0-mm-thick, t , aluminum. The plate is shocked by 101.6 mm of Composition B-3 initiated by a P-040 lens. h is 38.1 mm. The aluminum sample was cooled in liquid nitrogen before being placed on the explosive at shot time. The metal holder shown in the radiograph was part of the remotely operated device used to move the aluminum from a dewar of liquid nitrogen to the surface of the explosive.





SHOT 308:

Multiple Plate Fracture

Date:

August 30, 1965

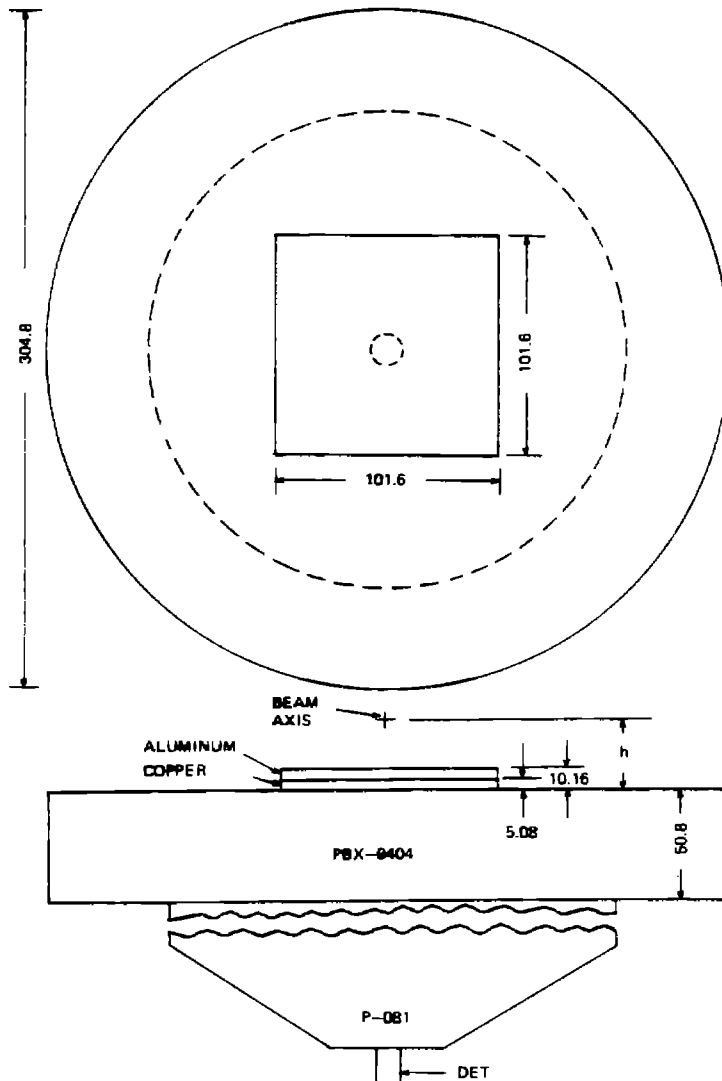
Experimenter:

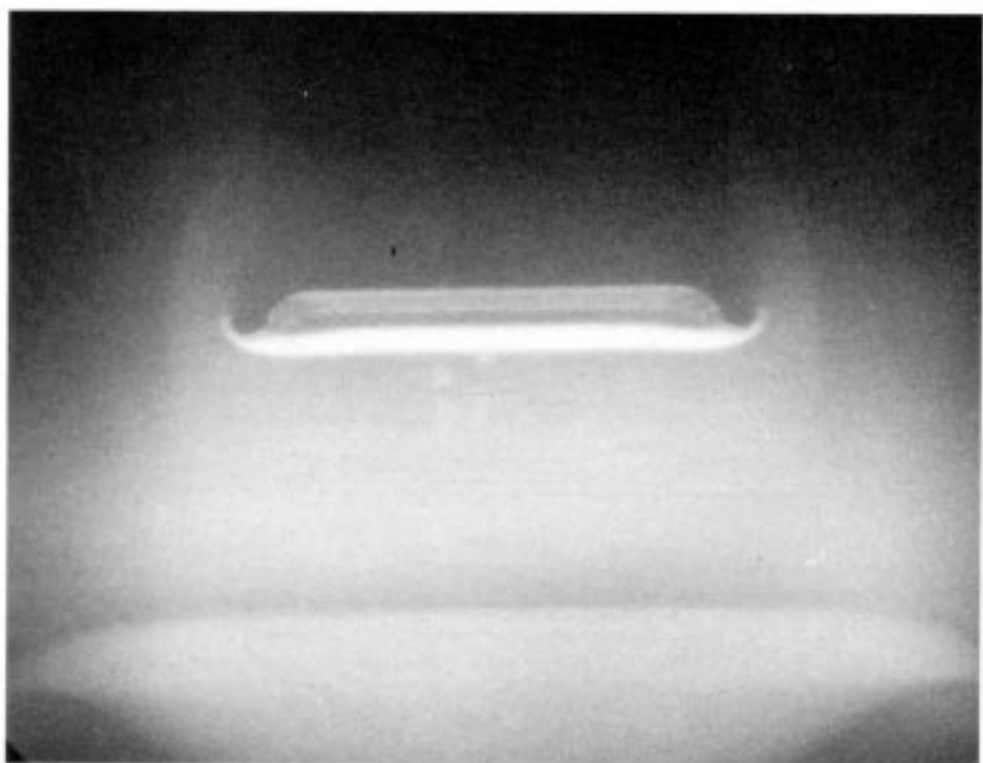
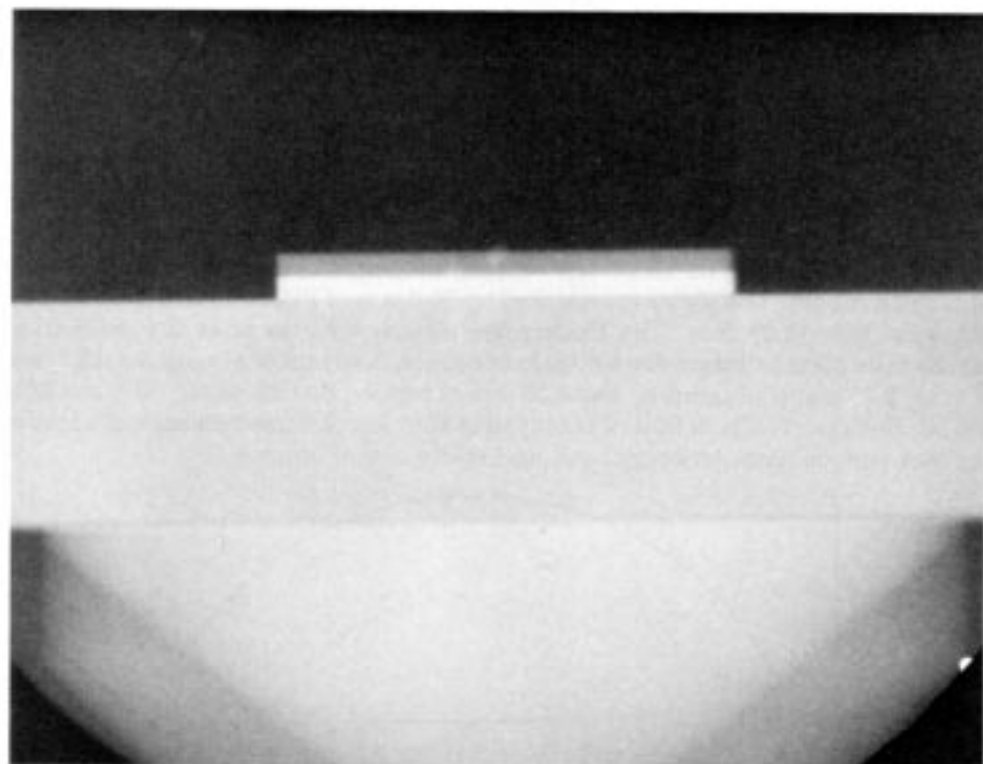
Gary W. Rodenz

Radiographic Time:

35.13 μ s

Dynamic fracture of 5.08-mm-thick aluminum and 5.08-mm-thick copper. The plates are shocked by 50.8 mm of PBX-9404 initiated by a P-081 lens. h is 17.46 mm. The thicknesses observed 6.70 μ s after the detonation reached the plate interface are 1.50 mm of aluminum, 0.75 mm of void, 1.17 mm of aluminum, 0.30 mm of void, 1.36 mm of aluminum, 3.24 mm of multiple layers and voids, and 5.92 mm of copper. See Shots 310, 311, 335, and 336.





SHOT 309:**Multiple Plate Fracture**

Date:

August 30, 1965

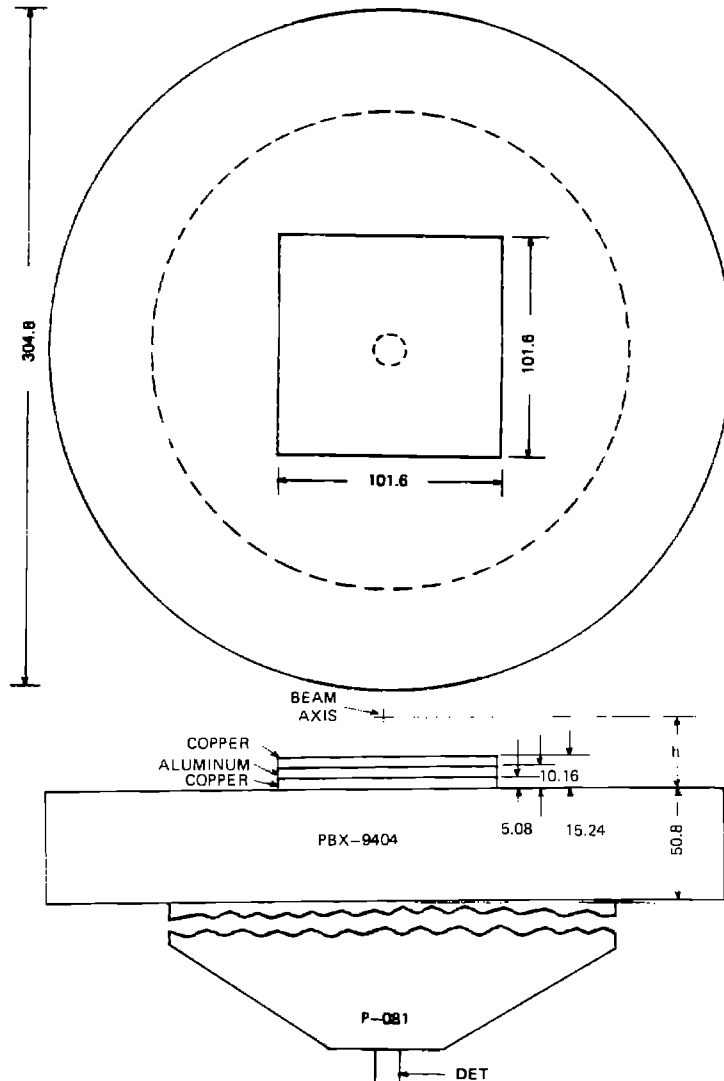
Experimenter:

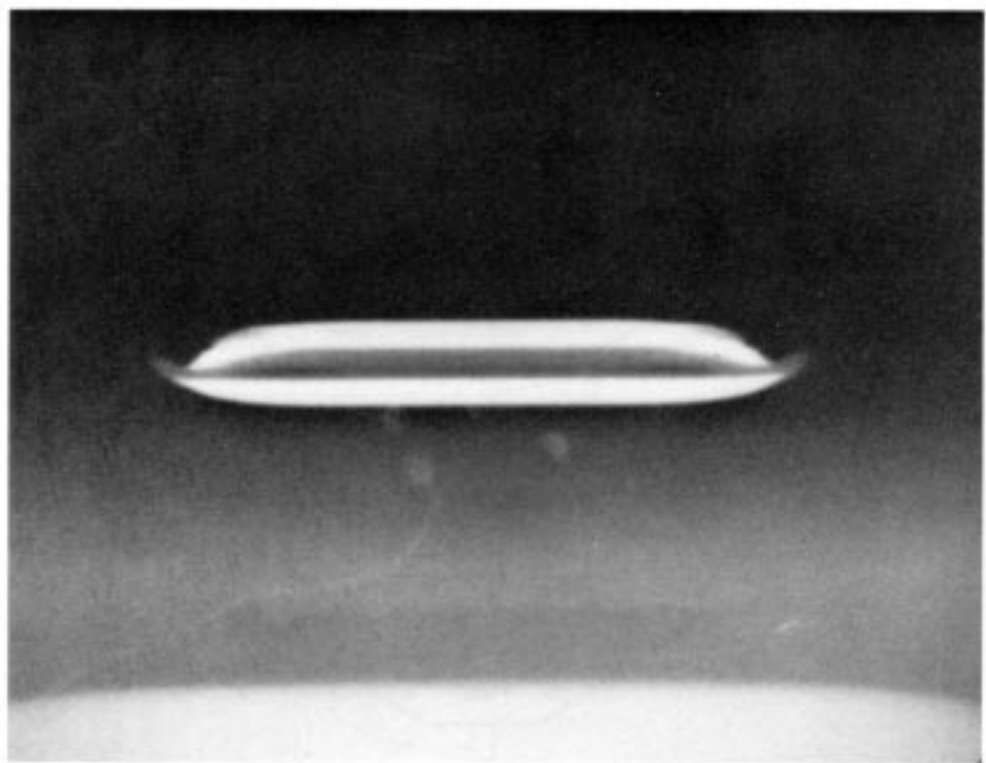
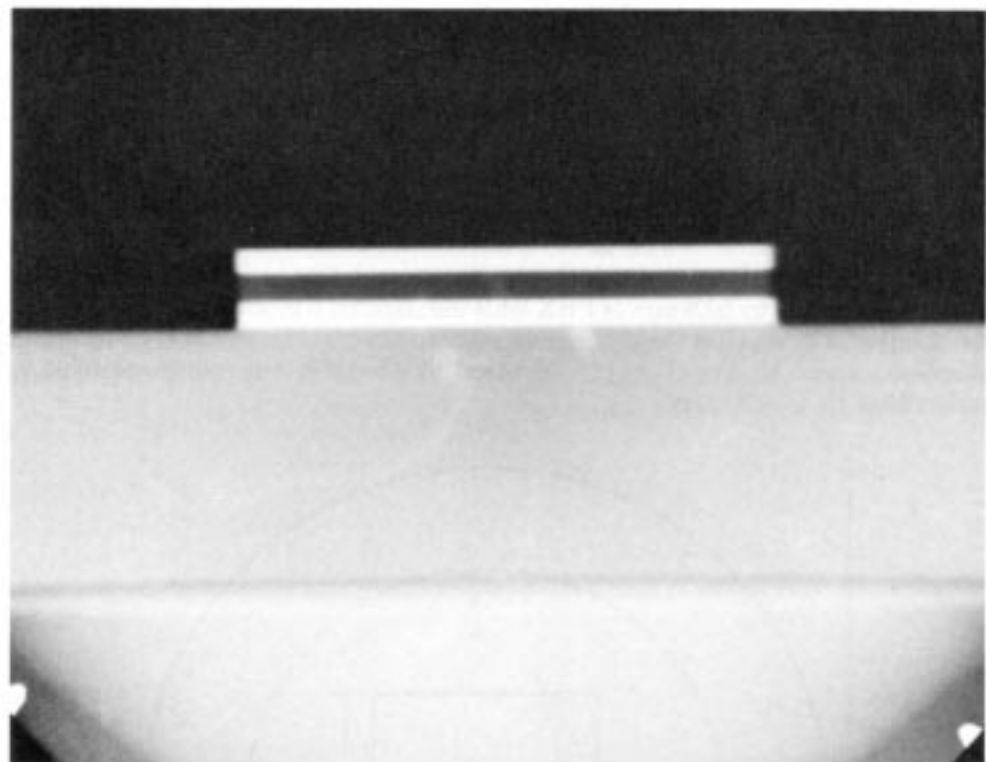
Gary W. Rodenz

Radiographic Time:

34.45 μ s

Dynamic fracture of 5.08-mm-thick copper, 5.08-mm-thick aluminum, and 5.08-mm-thick copper. The plates are shocked by 50.8 mm of PBX-9404 initiated by a P-081 lens. h is 14.29 mm. The thicknesses observed 9.0 μ s after the detonation reached the plate interface are 5.60 mm of copper, 3.20 mm of aluminum, 13.0 mm of void, 1.40 mm of aluminum, and 5.30 mm of copper. See Shots 312, 313, and 337-339. Unfortunately the details of this type of shot are obscure because the edges of the free surface plate (copper) bend and shield the aluminum.





SHOT 310:

Multiple Plate Fracture

Date:

July 6, 1965

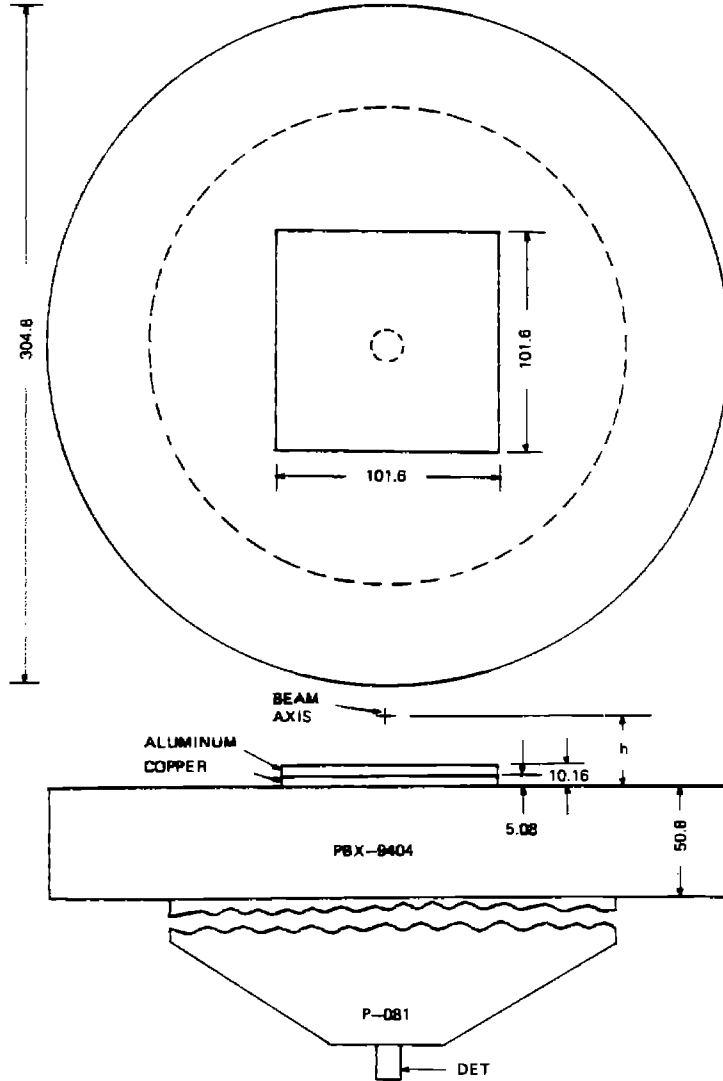
Experimenter:

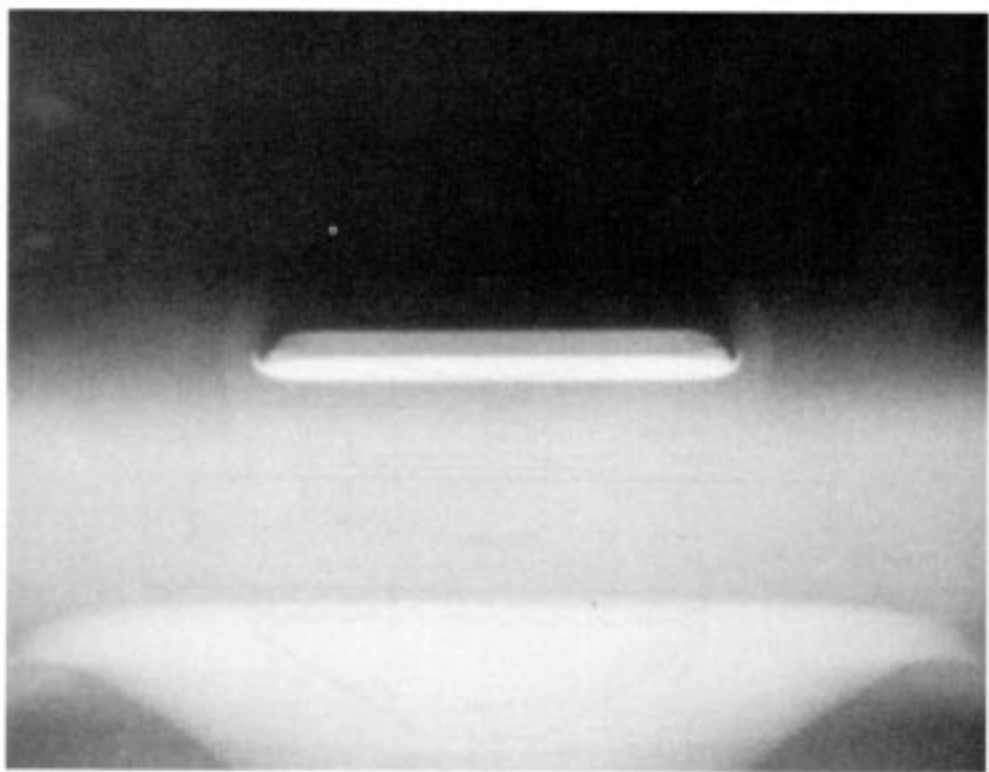
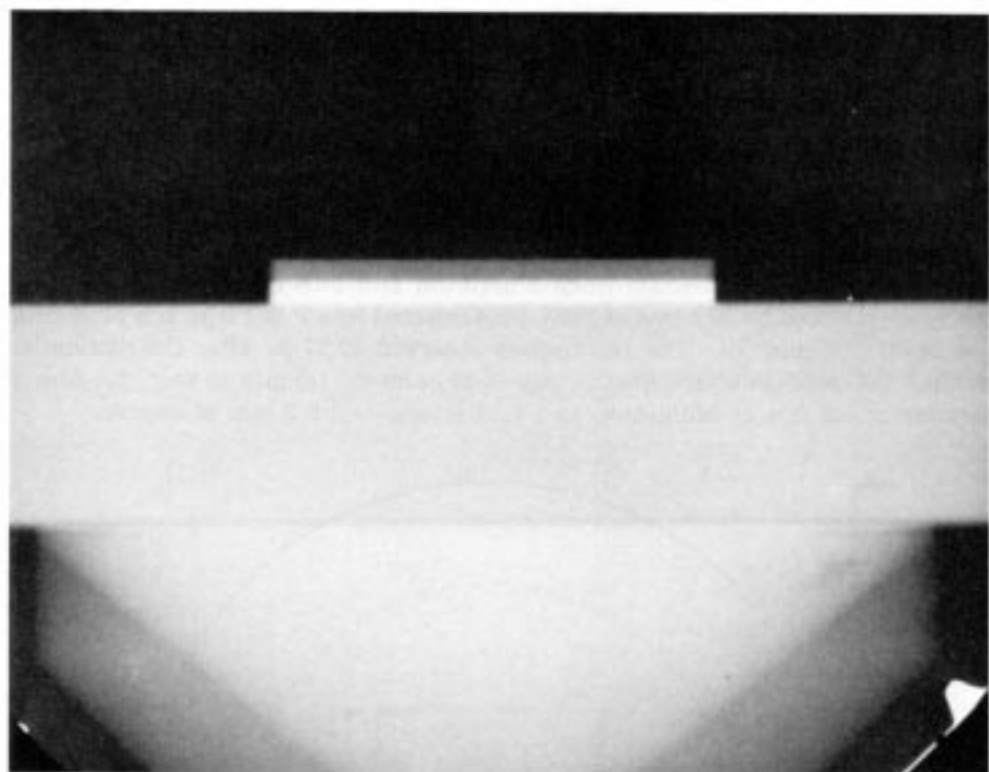
Gary W. Rodenz

Radiographic Time:

31.5 μ s

Dynamic fracture of 5.08-mm-thick aluminum and 5.08-mm-thick copper. The plates are shocked by 50.8 mm of PBX-9404 initiated by a P-081 lens. The thicknesses observed 3.24 μ s after the detonation reached the plate interface are 5.90 mm of aluminum and 5.40 mm of copper. Identical to Shot 308, but radiographed at an earlier time. h is 8.20 mm.





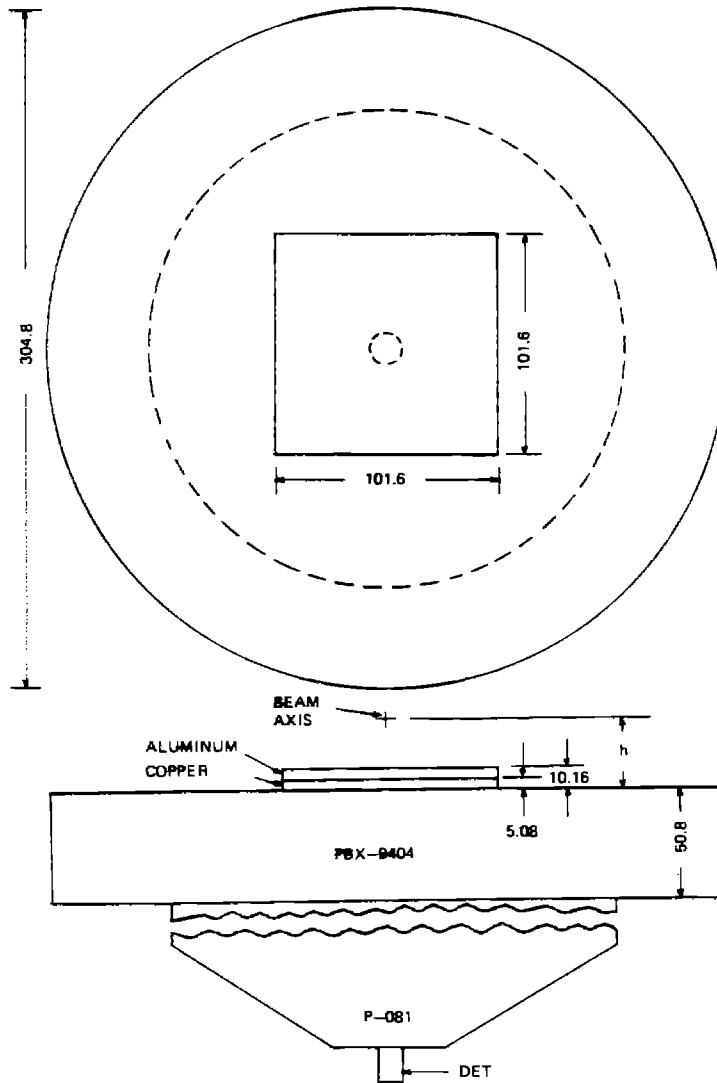
SHOT 311: Multiple Plate Fracture

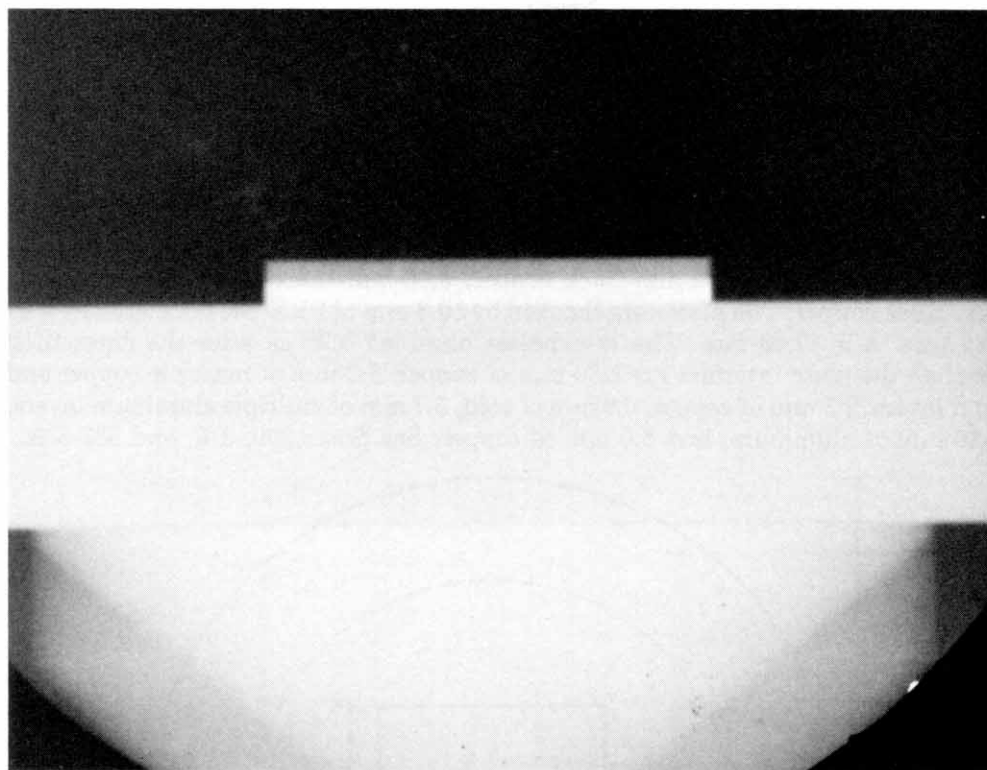
Date: July 12, 1965

Experimenter: Gary W. Rodenz

Radiographic Time: 38.46 μ s

Dynamic fracture of 5.08-mm-thick aluminum and 5.08-mm-thick copper. The plates are shocked by 50.8 mm of PBX-9404 initiated by a P-081 lens. h is 24.35 mm. See Shots 308 and 310. The thicknesses observed 10.17 μ s after the detonation reached the plate interface are 2.1 mm of aluminum, 1.0 mm of void, 1.6 mm of aluminum, 5.9 mm of aluminum and void layers, and 5.9 mm of copper.





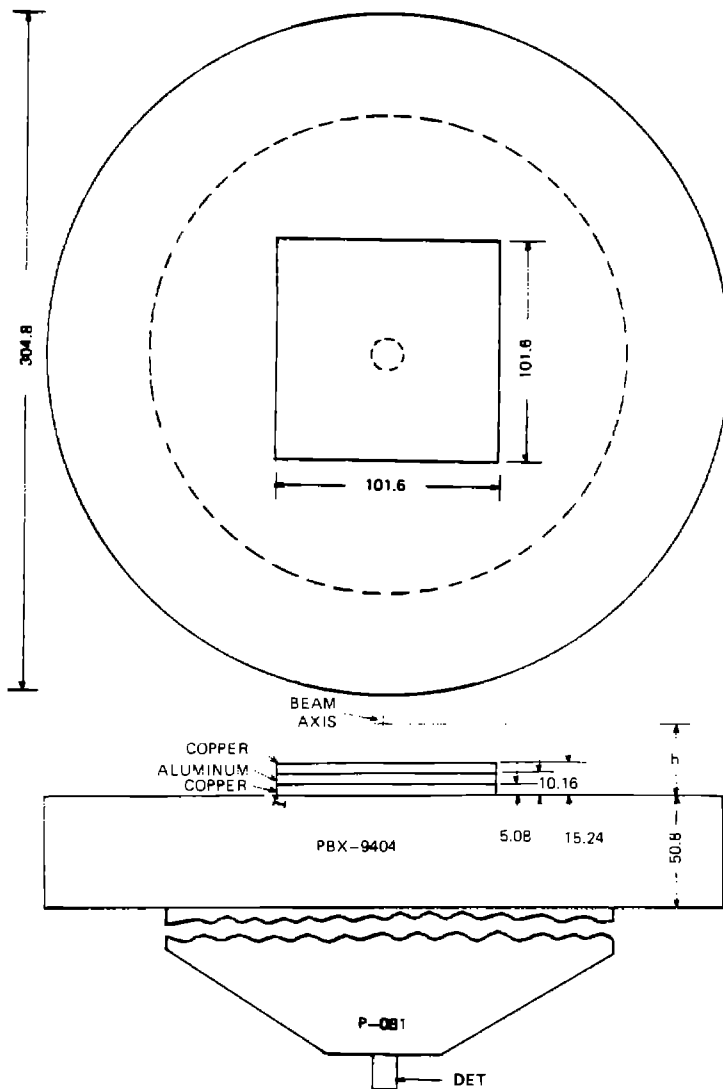
SHOT 312: Multiple Plate Fracture

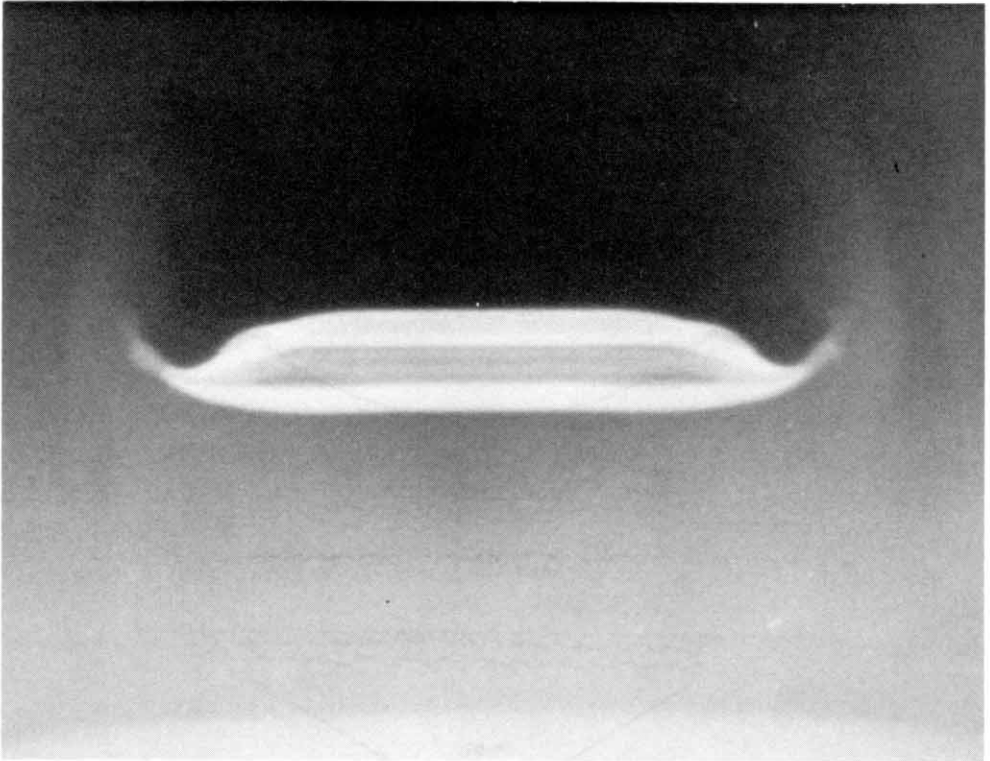
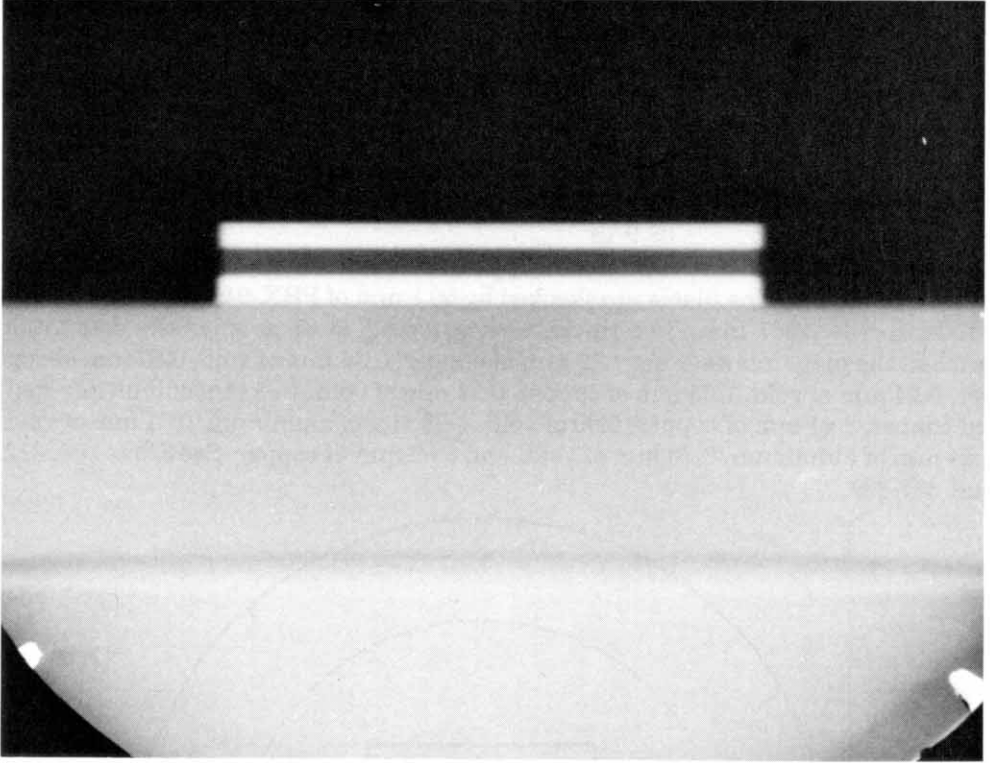
Date: September 9, 1965

Experimenter: Gary W. Rodenz

Radiographic Time: 37.49 μ s

Dynamic fracture of 5.08-mm-thick copper, 5.08-mm-thick aluminum, and 5.08-mm-thick copper. The plates are shocked by 50.8 mm of PBX-9404 initiated by a P-081 lens. h is 17.46 mm. The thicknesses observed 9.20 μ s after the detonation reached the plate interface are 1.30 mm of copper, 3.2 mm of multiple copper and void layers, 2.3 mm of copper, 0.9 mm of void, 5.7 mm of multiple aluminum layers, 1.10 mm of aluminum, and 5.0 mm of copper. See Shots 309, 313, and 337-339.





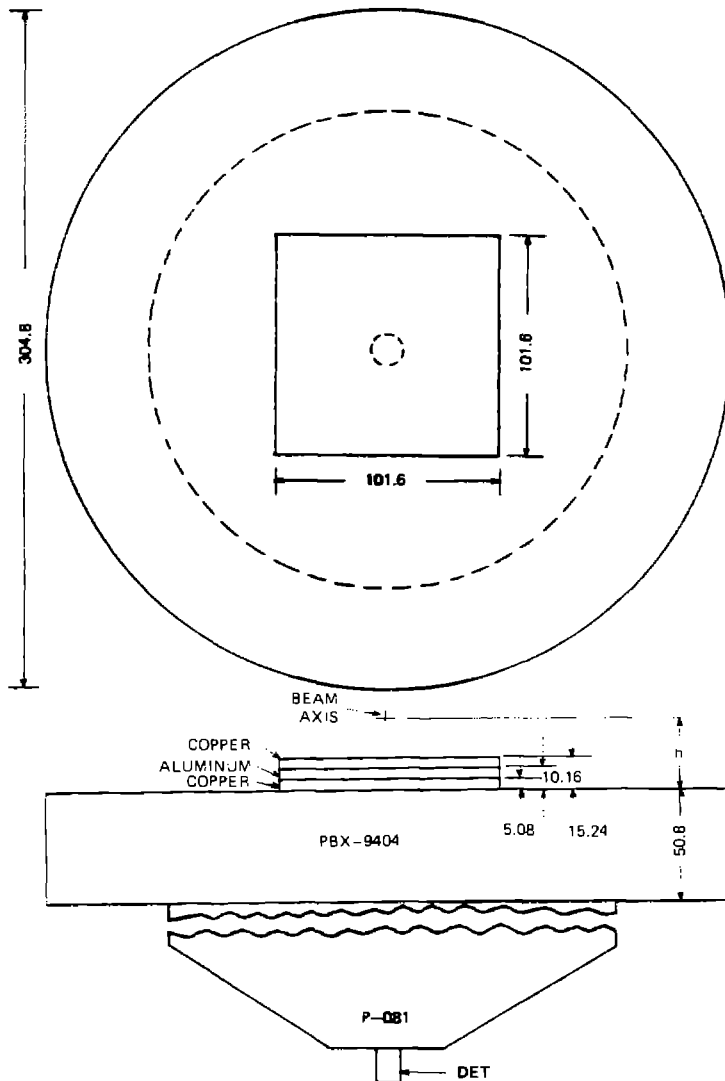
SHOT 313: Multiple Plate Fracture

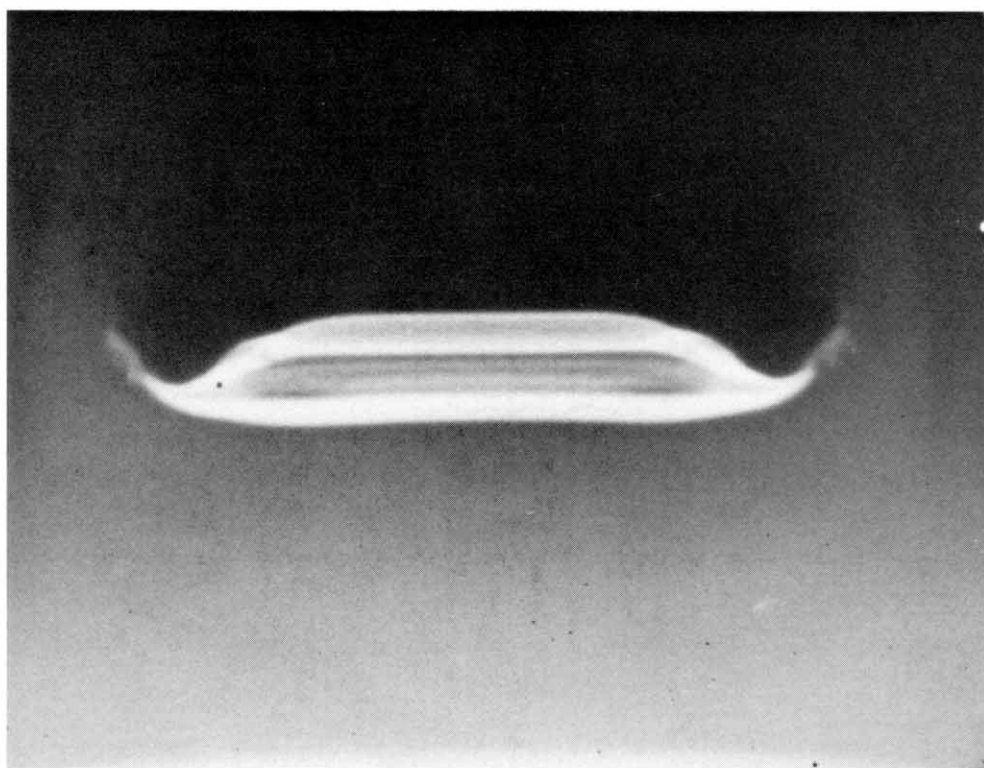
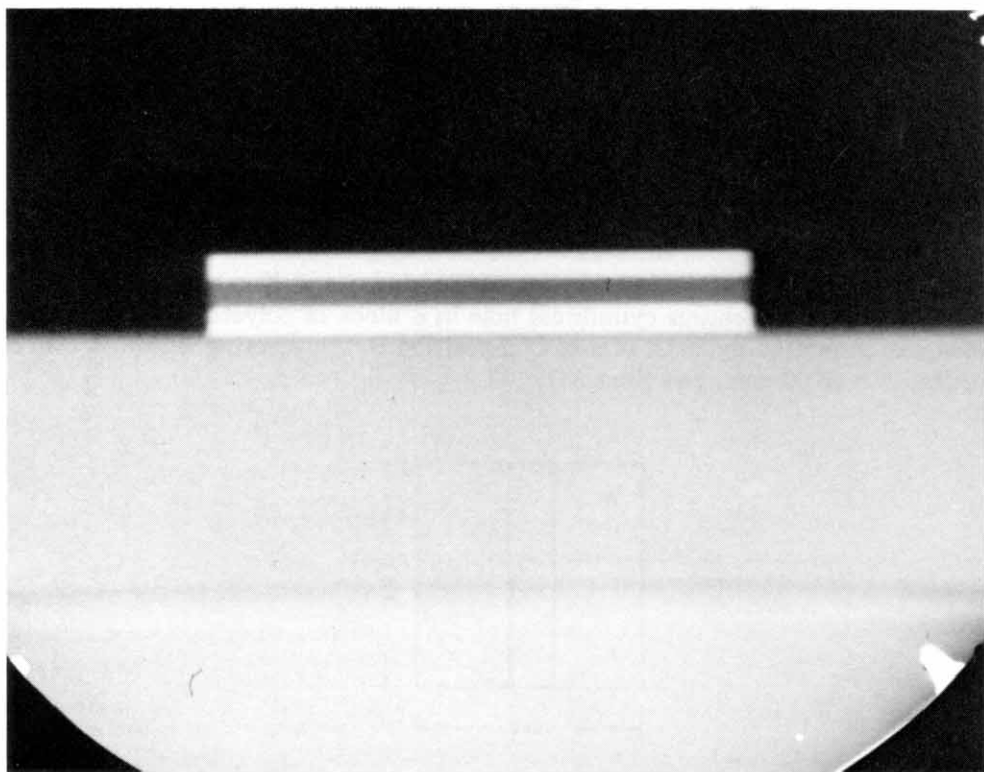
Date: September 22, 1965

Experimenter: Gary W. Rodenz

Radiographic Time: 39.9 μ s

Dynamic fracture of 5.08-mm-thick copper, 5.08-mm-thick aluminum, and 5.08-mm-thick copper. The plates are shocked by 50.8 mm of PBX-9404 initiated by a P-081 lens. h is 28.57 mm. The thicknesses observed 11.61 μ s after the detonation reached the plate interface are 1.19 mm of copper, 0.34 mm of void, 0.67 mm of copper, 0.24 mm of void, 1.05 mm of copper, 0.37 mm of void, 1.33 mm of multiple spalled copper, 2.41 mm of copper, 0.90 of void, 1.28 mm of aluminum, 0.81 mm of void, 2.84 mm of aluminum, 0.70 mm of void, and 5.57 mm of copper. See Shots 309, 312, and 337-339.





SHOT 314:

Cylindrical Hole in Polyethylene

Date:

February 23, 1966

Experimenter:

Douglas Venable

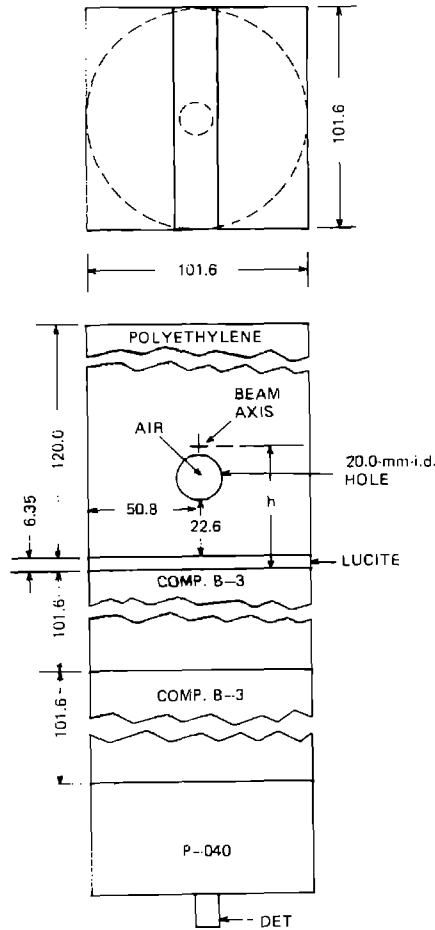
Radiographic Time:

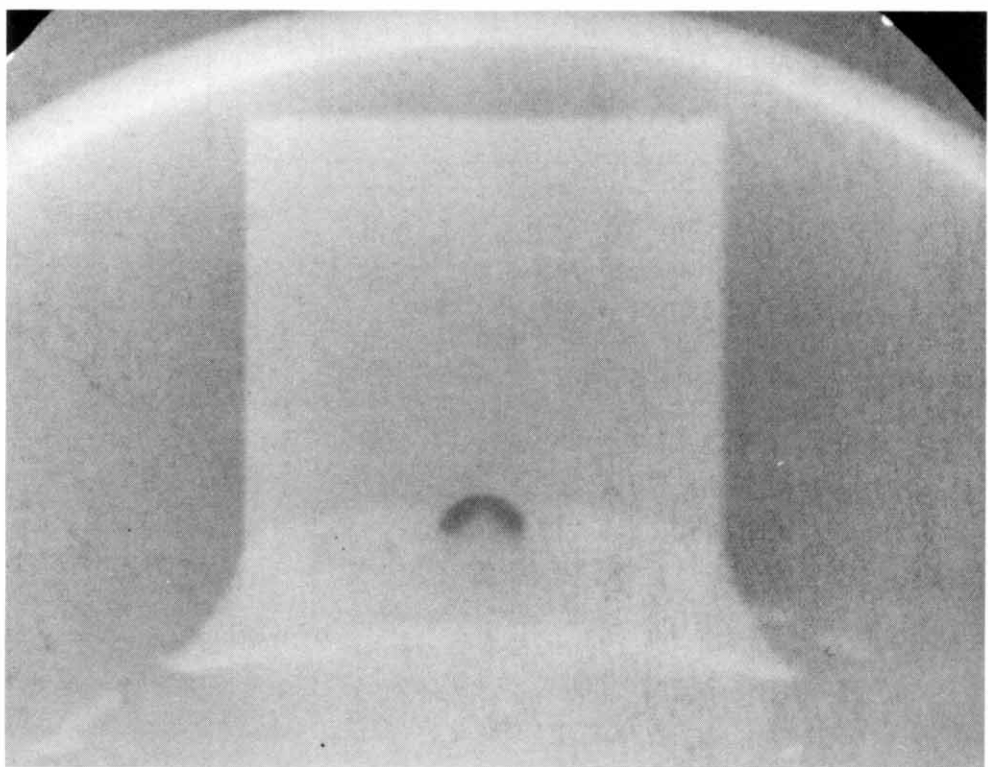
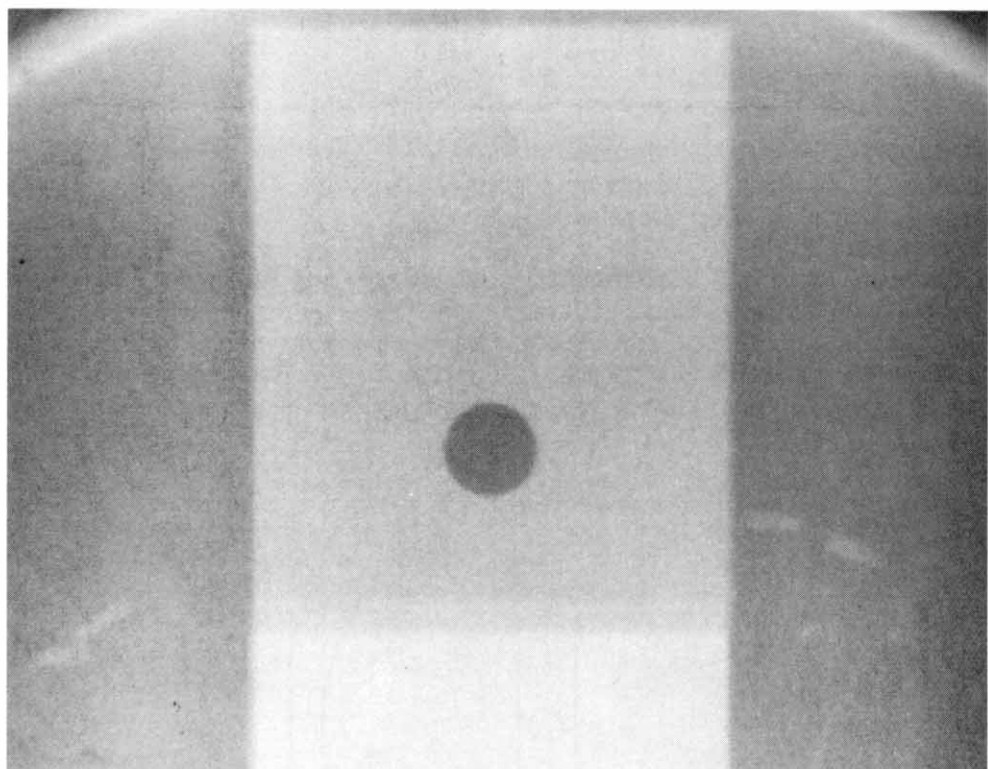
46.15 μ s

References:

Mader et al., 1967; Mader and Kershner, 1972

Study of a 10.0-mm-radius cylindrical hole in a block of polyethylene. The shock wave was generated by 203.2 mm of Composition B-3 interacting with 6.35 mm of Lucite. h is 46.03 mm. See Shot 351.





SHOT 315:

Munroe Jet

Date:

September 2, 1965

Experimenter:

Douglas Venable

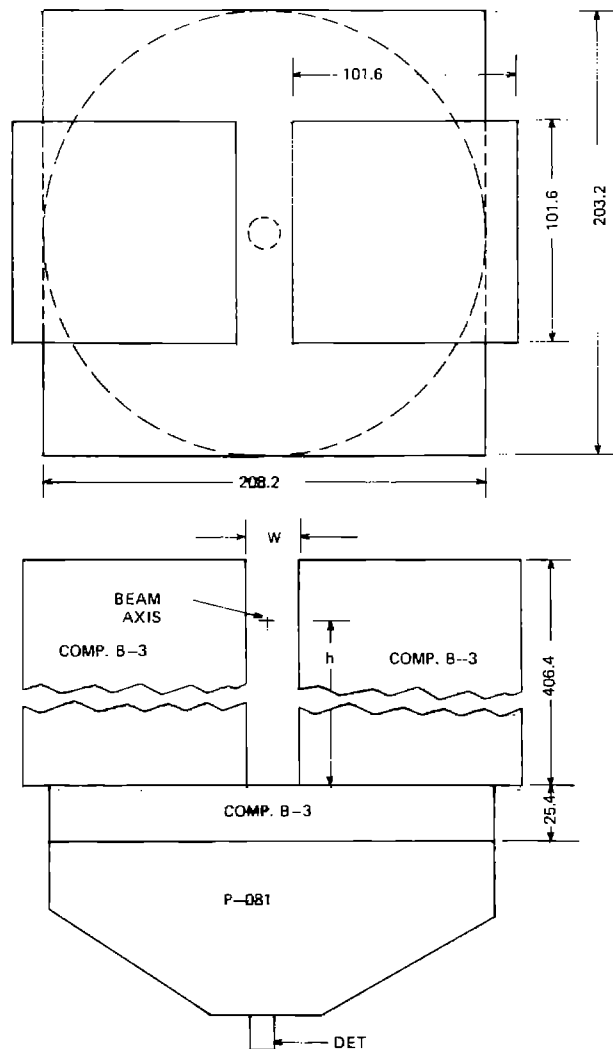
Radiographic Time:

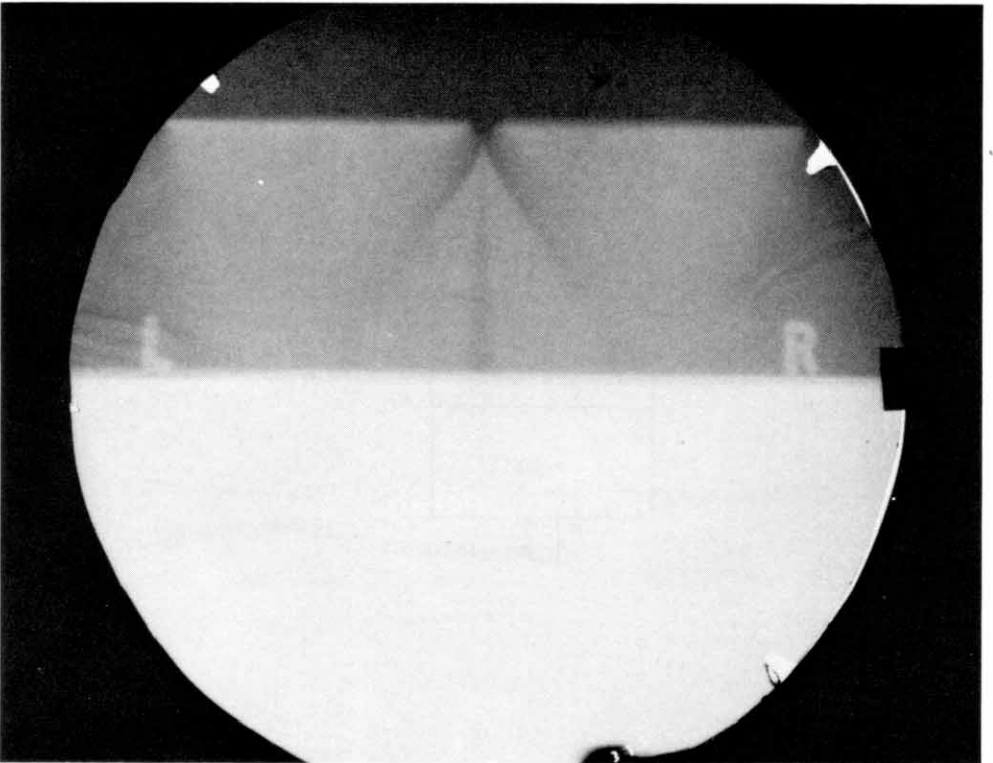
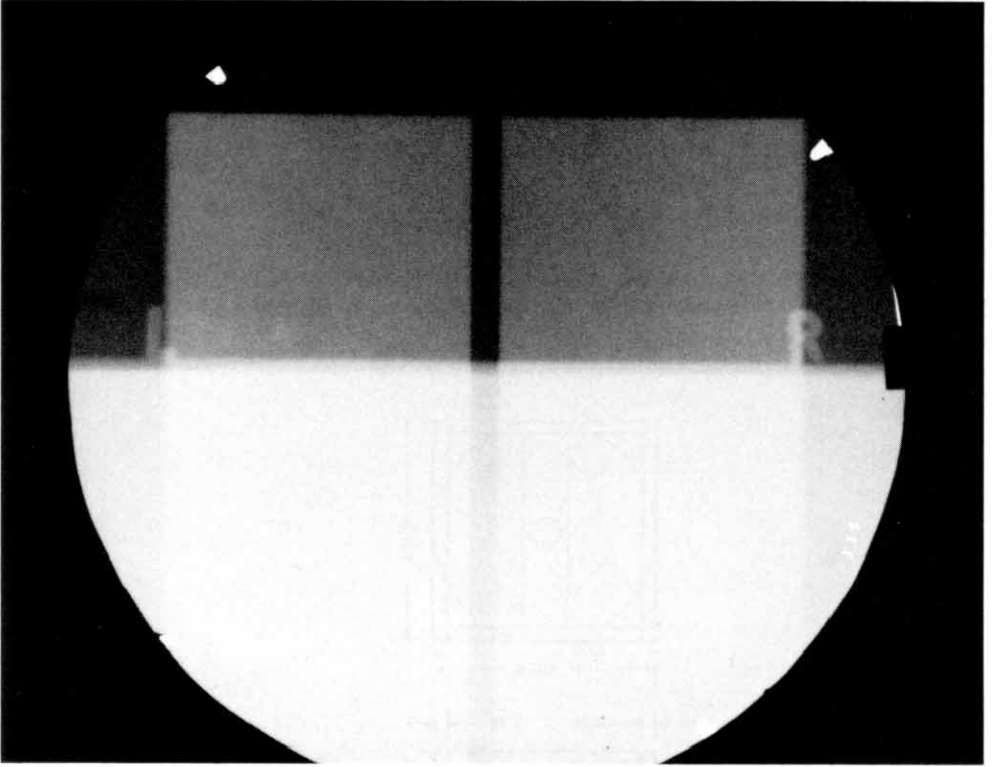
76.95 μ s

References:

Mader et al., 1967; Mader and Kershner, 1972

Formation and growth of gaseous Munroe jets. This jet is formed by interaction of the detonation products of two Composition B-3 charges separated by an air gap 10.0 mm, w, wide. The charges are initiated by 25.4 mm of Composition B-3 initiated by a P-081 lens. The detonations have run along the gap for 406.4 mm. h is 406.4.





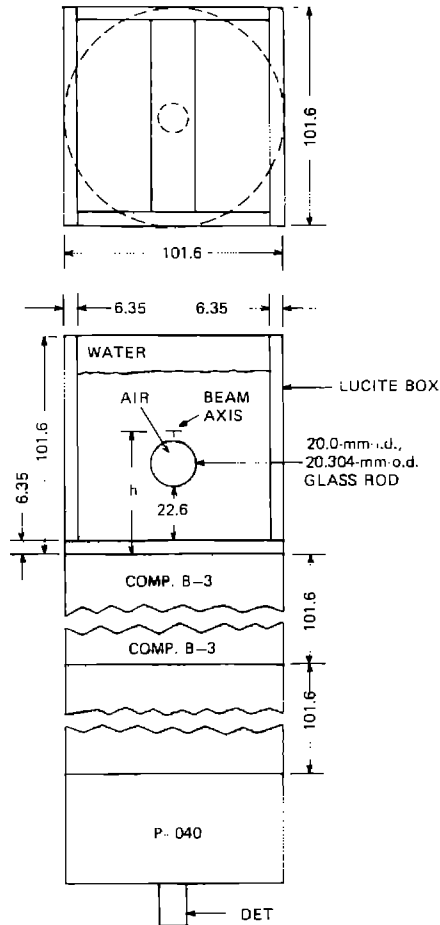
SHOT 318: Cylindrical Hole in Water

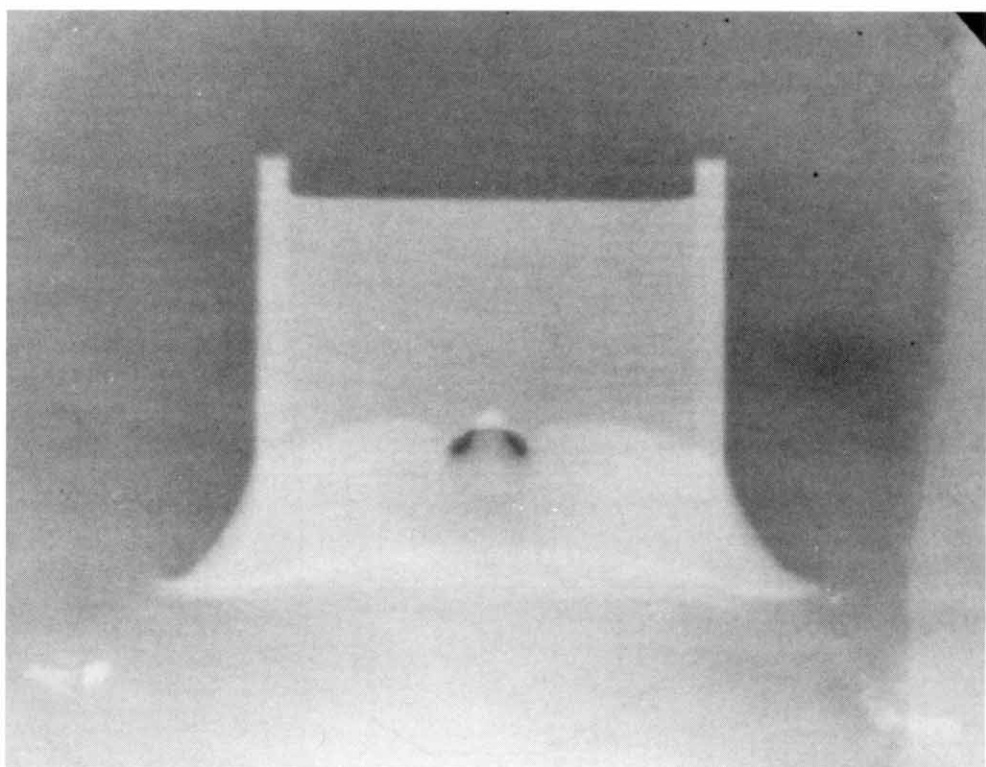
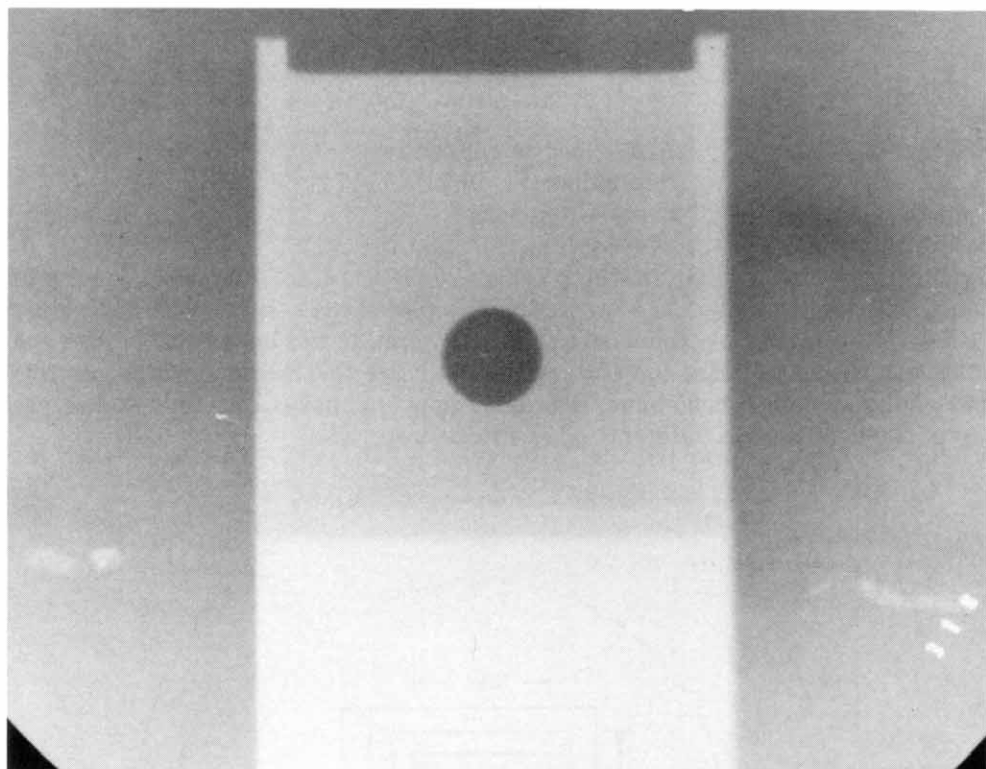
Date: September 21, 1965

Experimenter: Roger W. Taylor

Radiographic Time: 47.71 μ s

A 10.0-mm-radius cylindrical hole is formed by a thin-walled (0.152-mm) glass tube in water. The shock wave has traveled 7.5 μ s since the shock reached the Lucite and water interface. See Shots 187, 188, 278-280, and 300. h is 46.0 mm.





SHOT 319:**Multiple Plate Fracture**

Date:

September 22, 1965

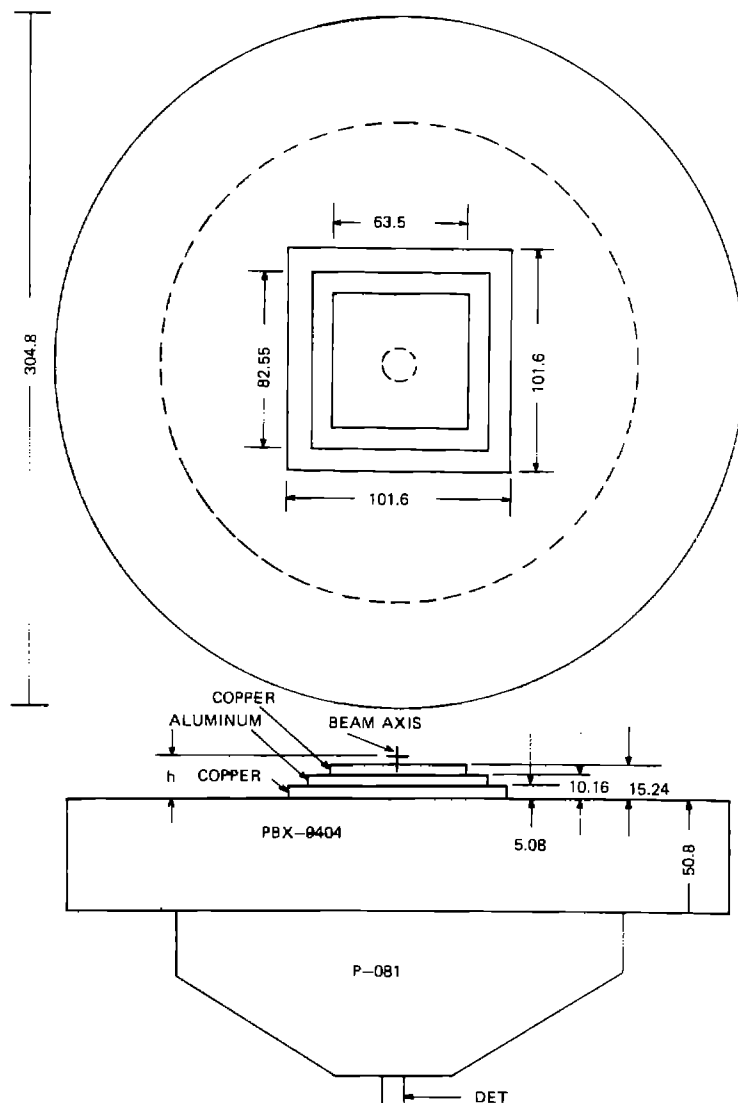
Experimenter:

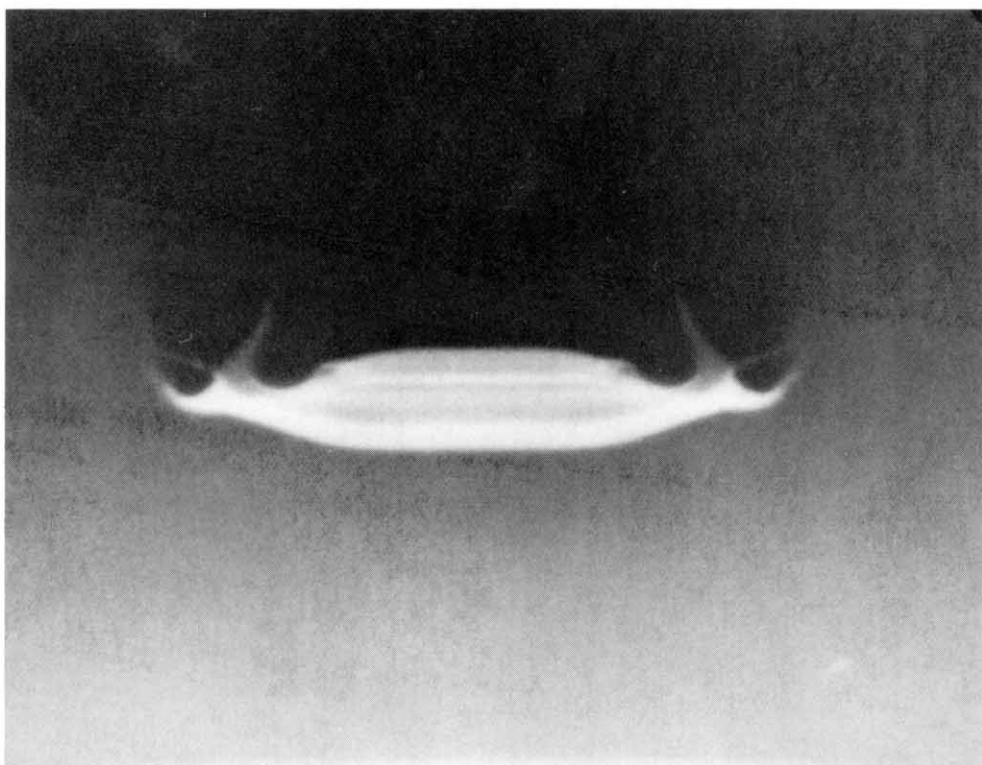
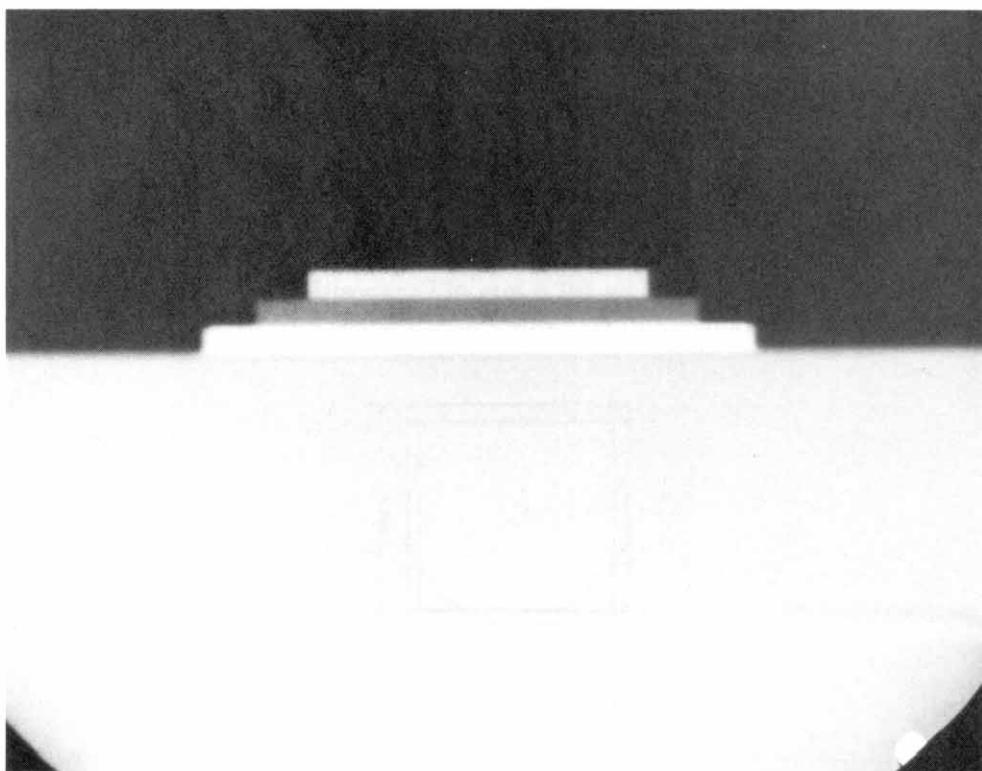
Gary W. Rodenz

Radiographic Time:

37.5 μ s

Dynamic fracture of 5.08-mm-thick copper, 5.08-mm-thick aluminum, and 5.08-mm-thick copper layered in a pyramid. The plates were shocked by 50.8 mm of PBX-9404 initiated by a P-081 lens. h is 17.46 mm. It was hoped that in this configuration the edges of the top plate would not curve and interfere with interpretation of the spalling phenomena. The technique was not successful because very complicated (although different) edge effects occurred.





SHOT 320:

Perlite Shock Velocity

Date:

September 23, 1965

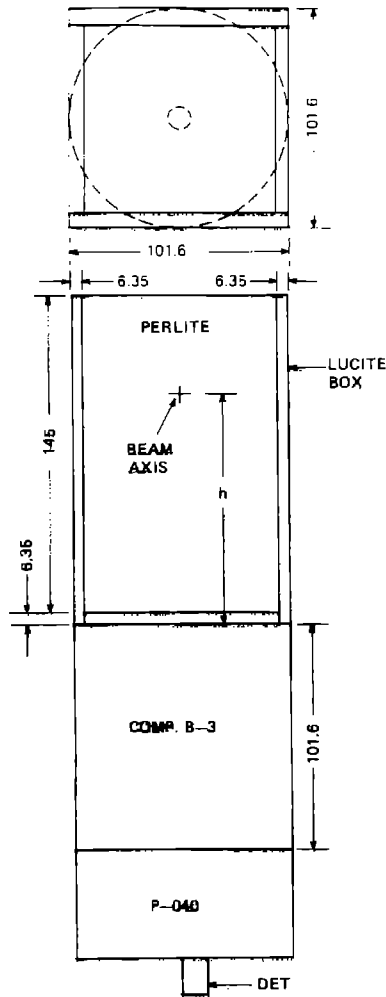
Experimenter:

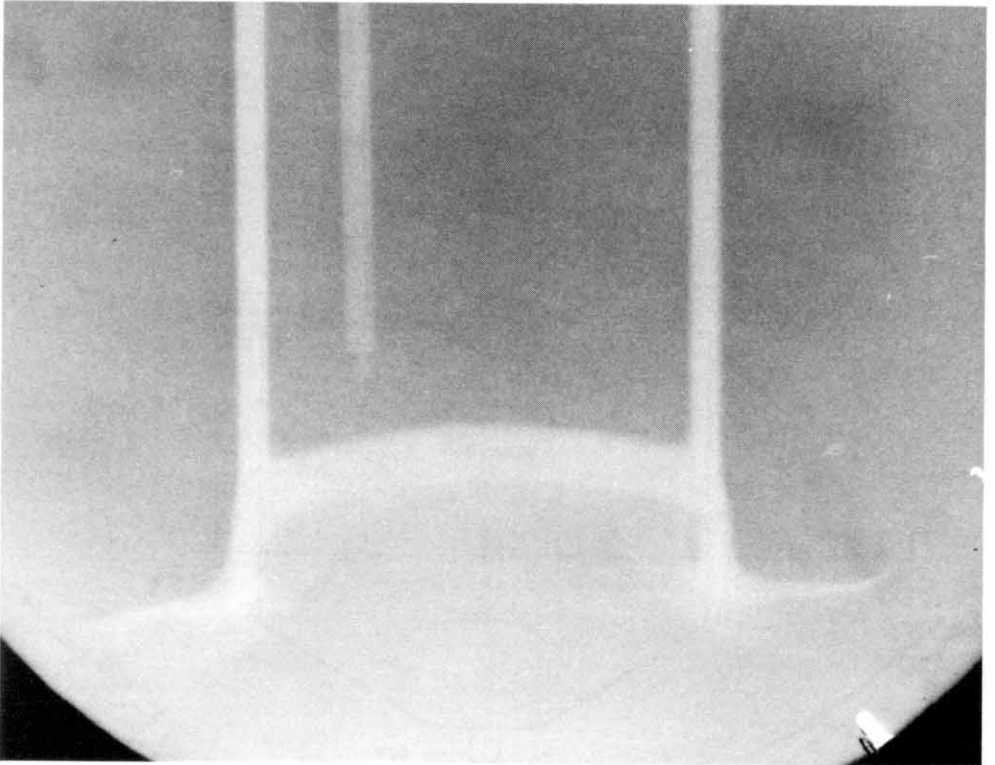
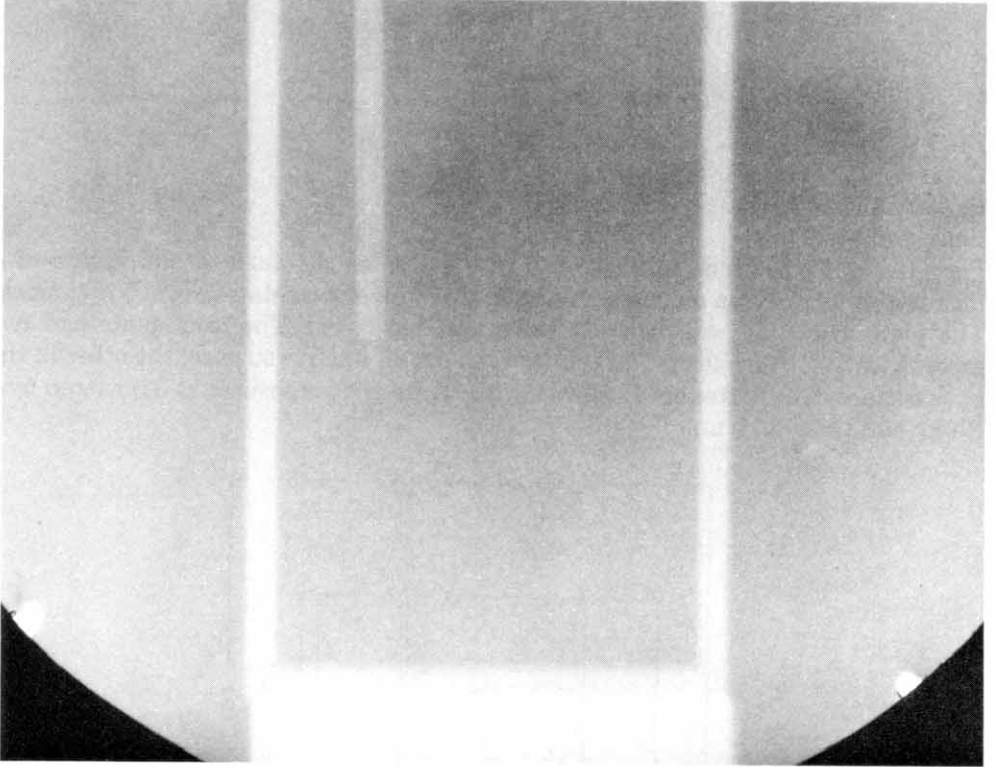
Gary W. Rodenz

Radiographic Time:

39.94 μ s

Bulk-density Perlite shocked by 101.6 mm of Composition B-3. The rod shown on the left side of the radiograph contained timing pins. h is 108 mm.





SHOT 321:

Magnesium Jets

Date:

September 1, 1965

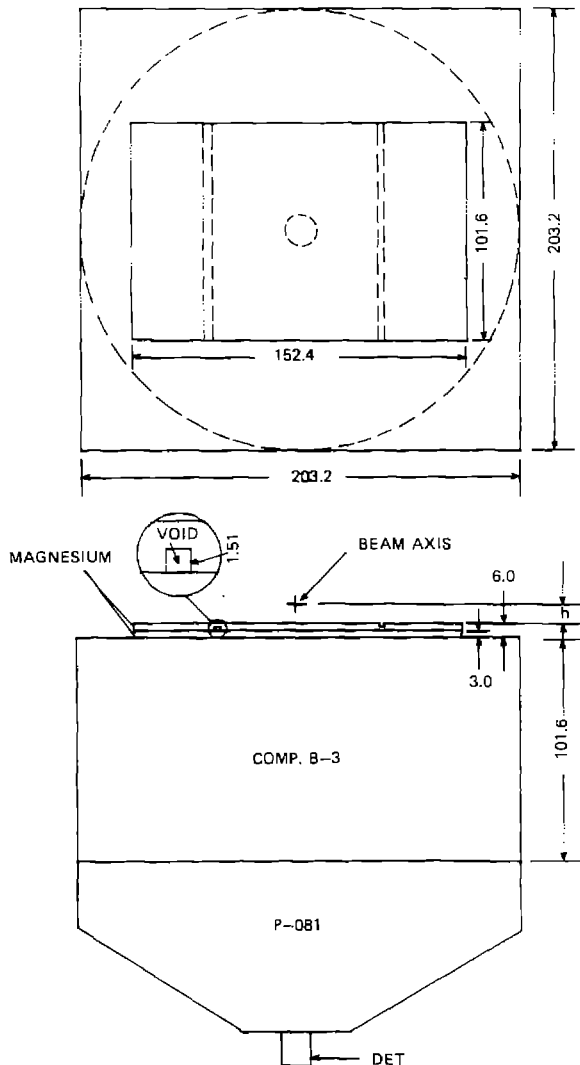
Experimenter:

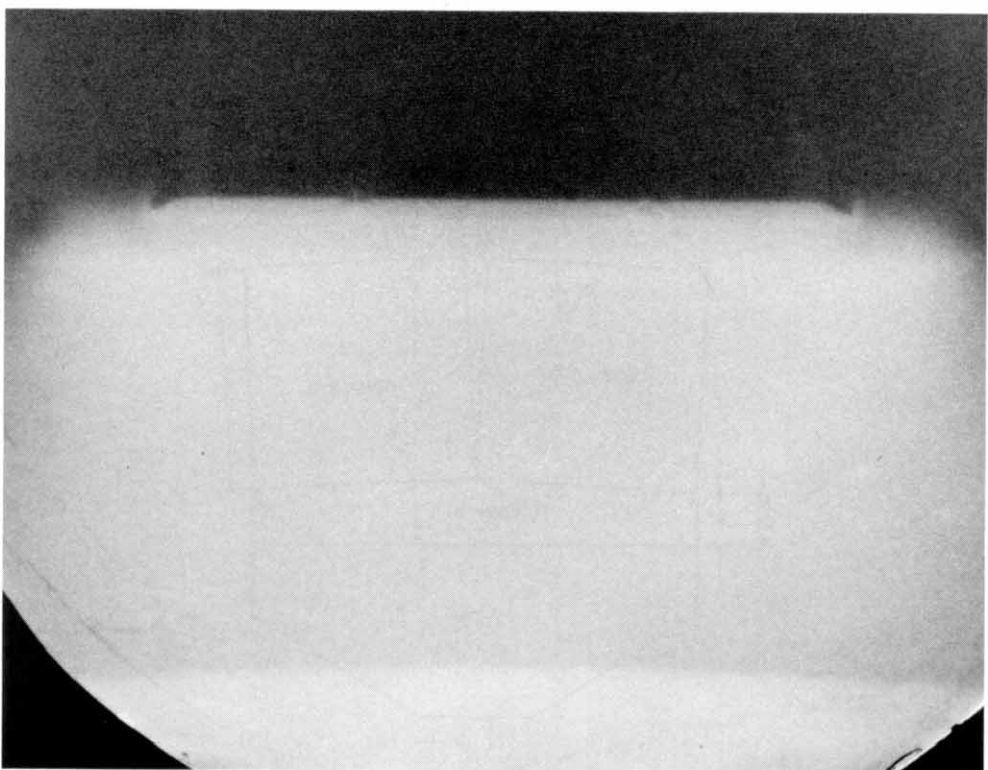
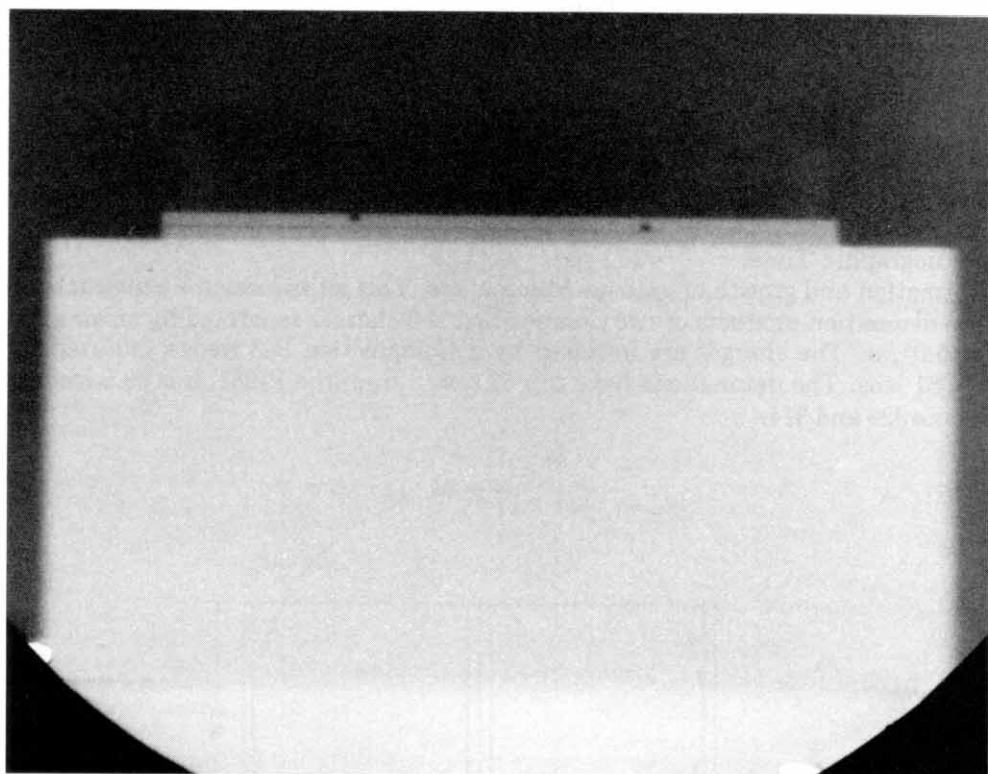
William R. Field

Radiographic Time:

36.88 μ s

Formation of jets from small rectangular holes in the surface and inside of a magnesium plate. The magnesium was in the form of two plates, each 3 mm thick. The plate in contact with the explosive was ungrooved. The front plate had two grooves, each 1.5 mm deep by 2.0 mm wide, one in the free surface, the other in the back surface. The plates are shocked by 101.6 mm of Composition B-3 initiated by a P-081 lens. h is 3.17 mm.





SHOT 322:

Diverging Munroe Jet

Date:

November 2, 1965

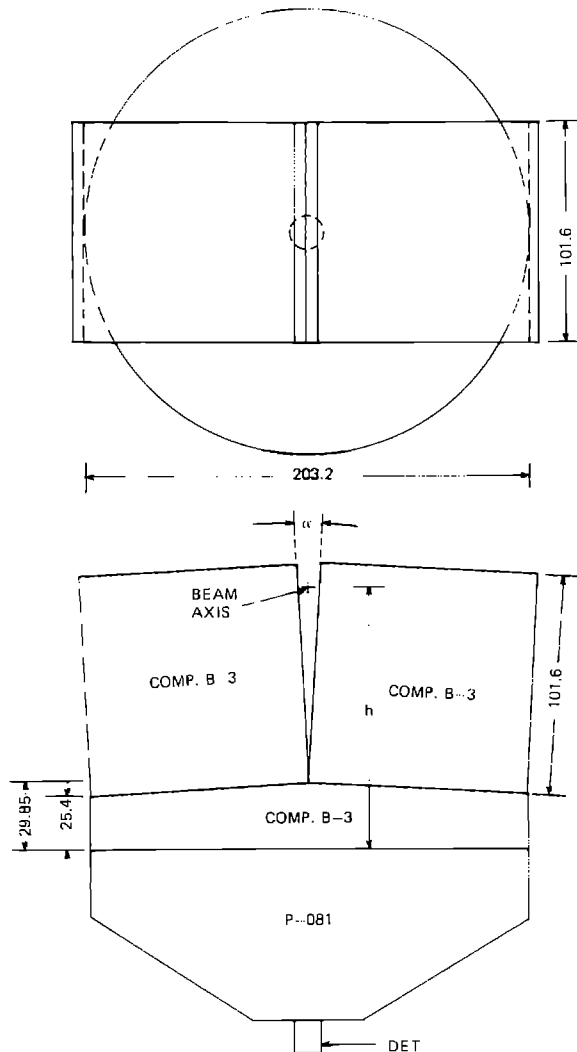
Experimenter:

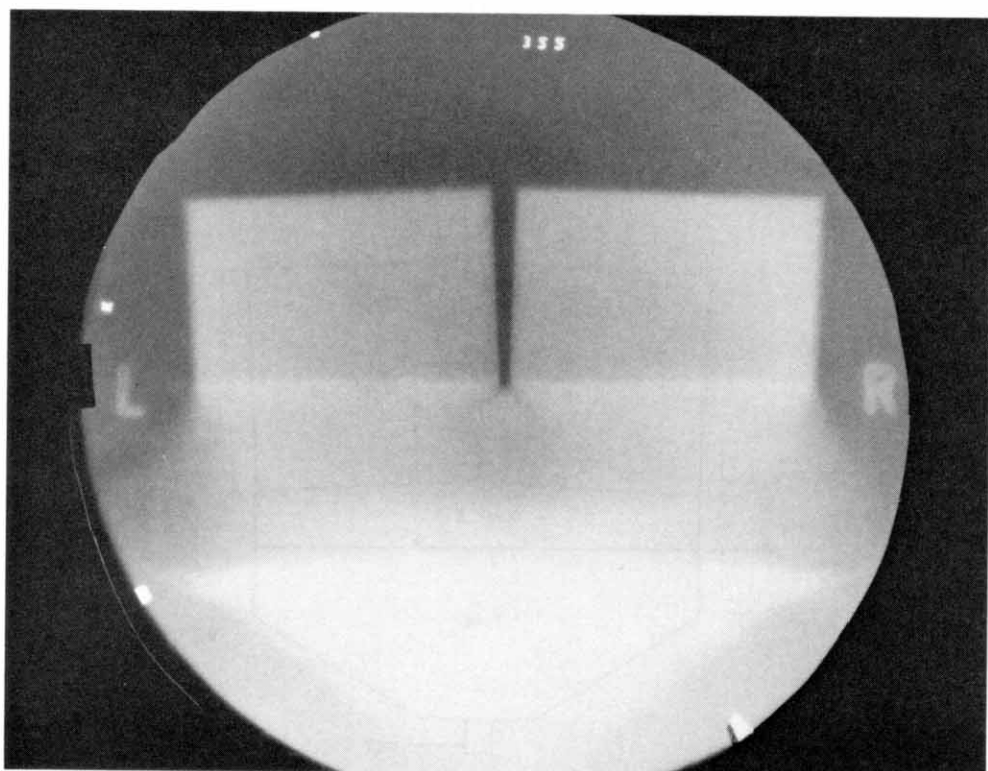
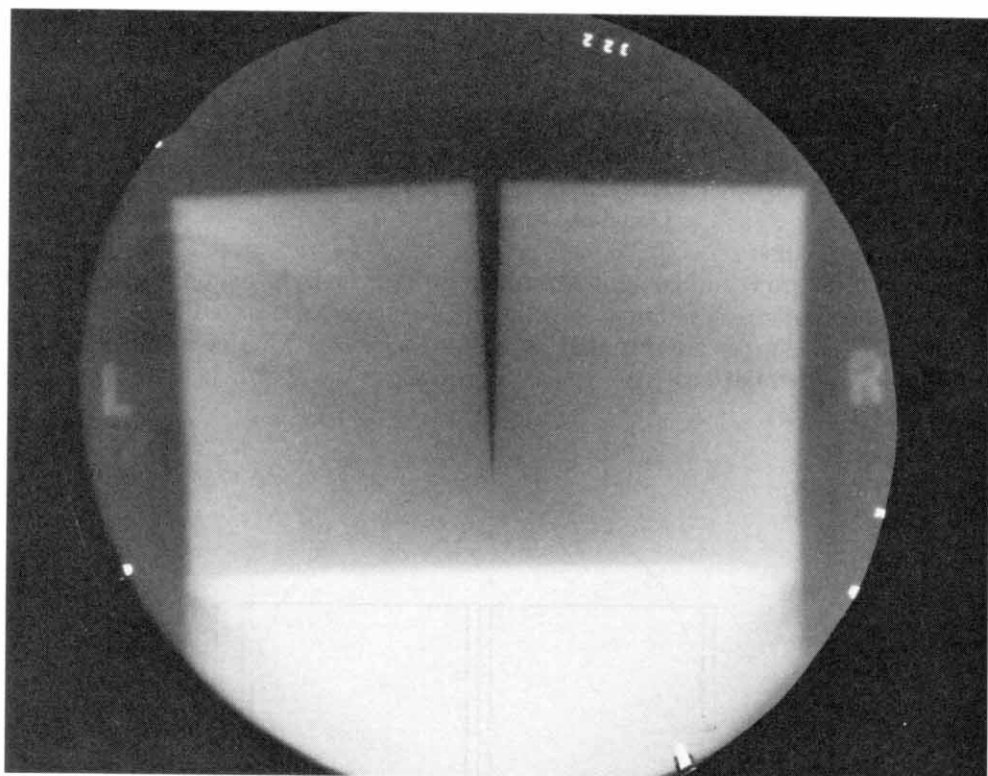
Douglas Venable

Radiographic Time:

30.71 μ s

Formation and growth of gaseous Munroe jets. This jet is formed by interaction of the detonation products of two Composition B-3 charges separated by an air groove of 5.0° , α . The charges are initiated by a Composition B-3 wedge initiated by a P-081 lens. The detonations have run 63.5 mm from the P-081. h is 63.5 mm. See Shots 323 and 324.





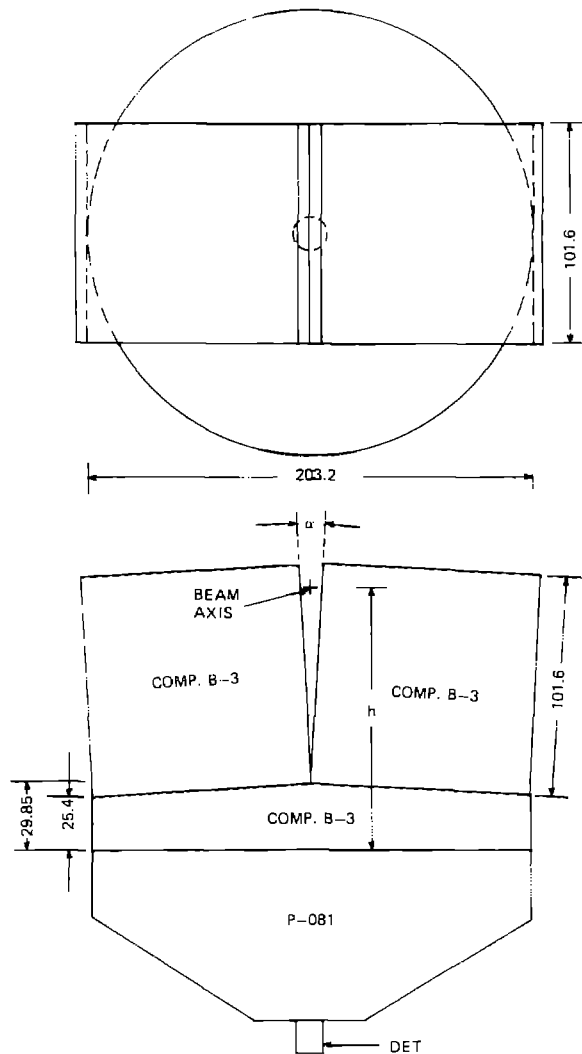
SHOT 323: Diverging Munroe Jet

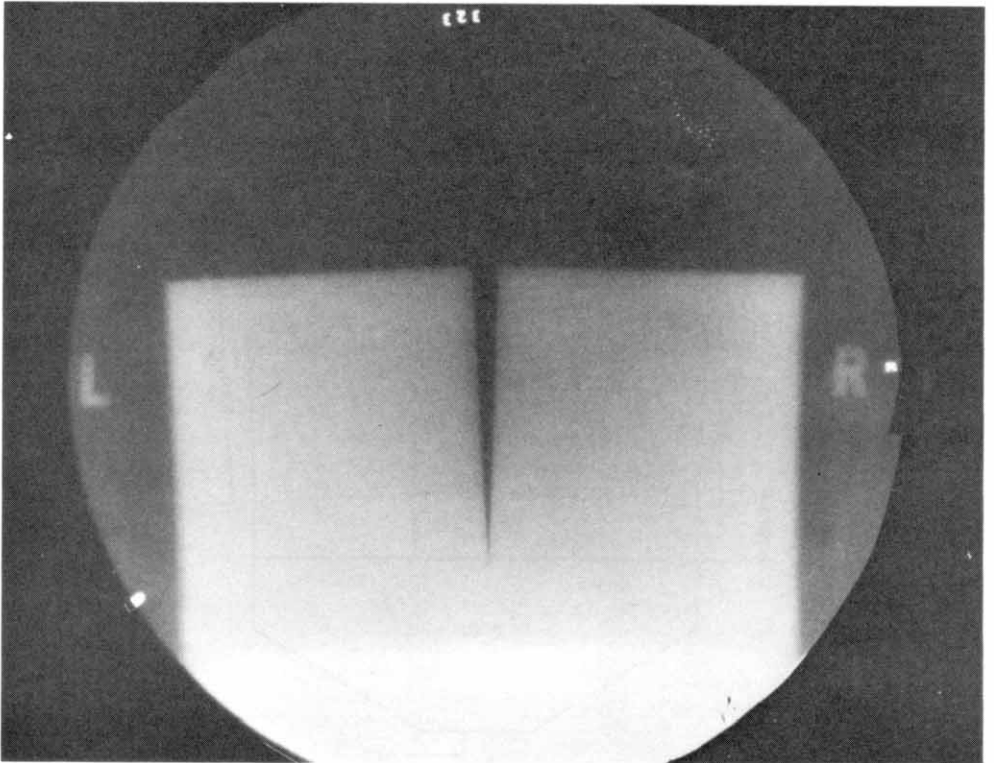
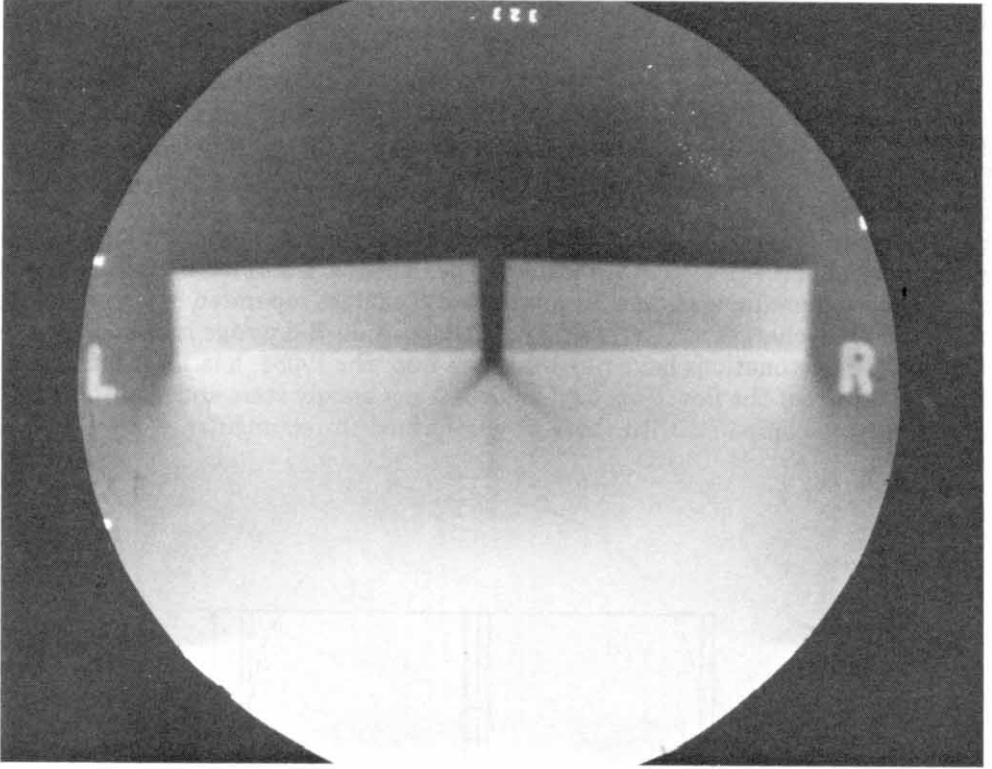
Date: November 2, 1965

Experimenter: Douglas Venable

Radiographic Time: 34.96 μ s

Formation and growth of gaseous Munroe jets. This jet is formed by interaction of the detonation products of two Composition B-3 charges separated by an air groove of 5.0° , α . The charges are initiated by a Composition B-3 wedge initiated by a P-081 lens. The detonations have run 97.6 mm from the P-081. h is 97.6 mm. See Shots 322 and 324.





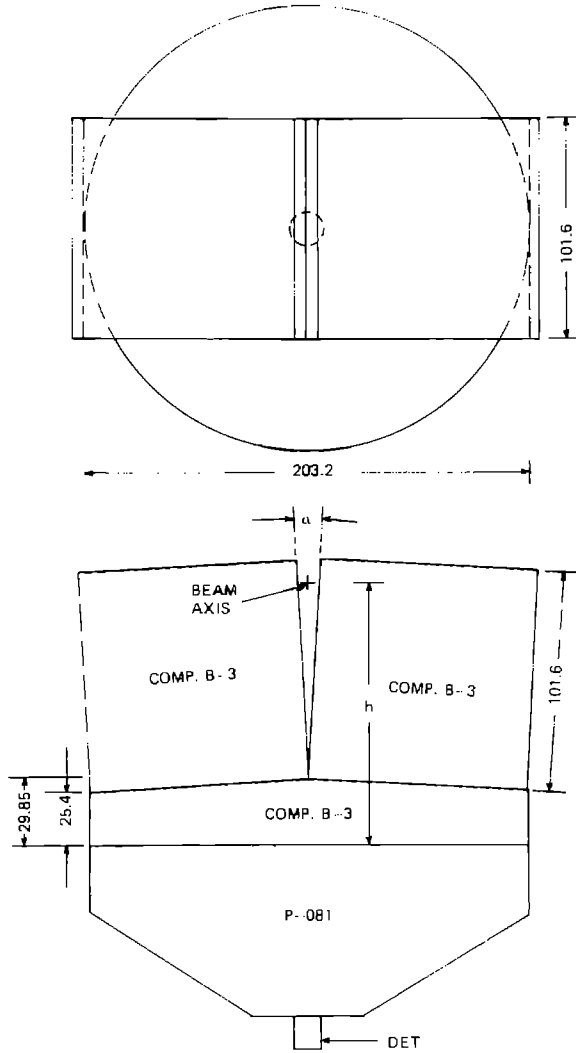
SHOT 324: Diverging Munroe Jet

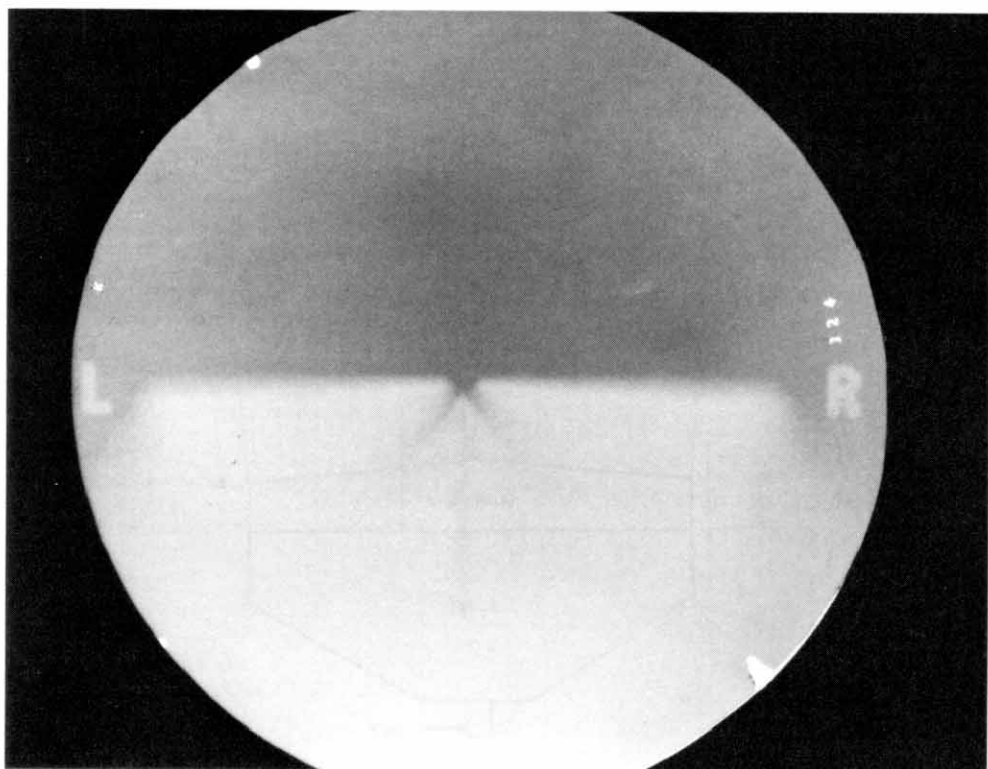
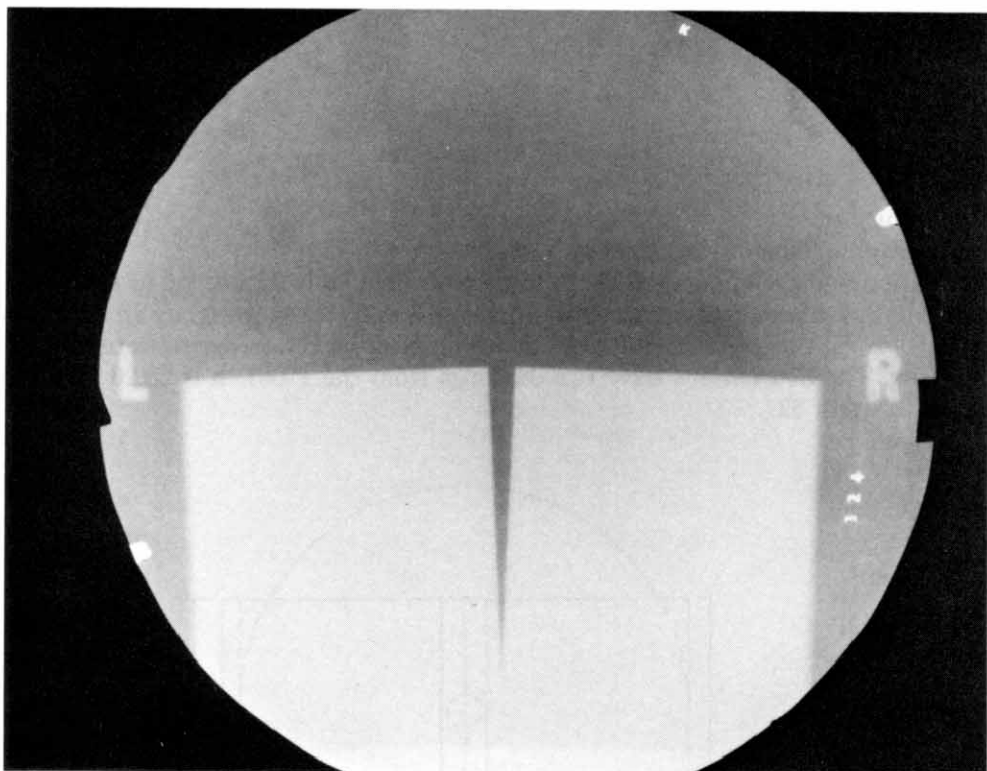
Date: September 28, 1965

Experimenter: Douglas Venable

Radiographic Time: 39.25 μ s

Formation and growth of gaseous Munroe jets. This jet is formed by interaction of the detonation products of two Composition B-3 charges separated by an air groove of 5.0° , α . The charges are initiated by a Composition B-3 wedge initiated by a P-081 lens. The detonations have run 131.7 mm from the P-081. h is 131.7 mm. Shots 322-324 show that the flow from 5.0° grooves is not steady state and that the jet tip is very diffuse compared with those of jets formed in rectangular grooves.





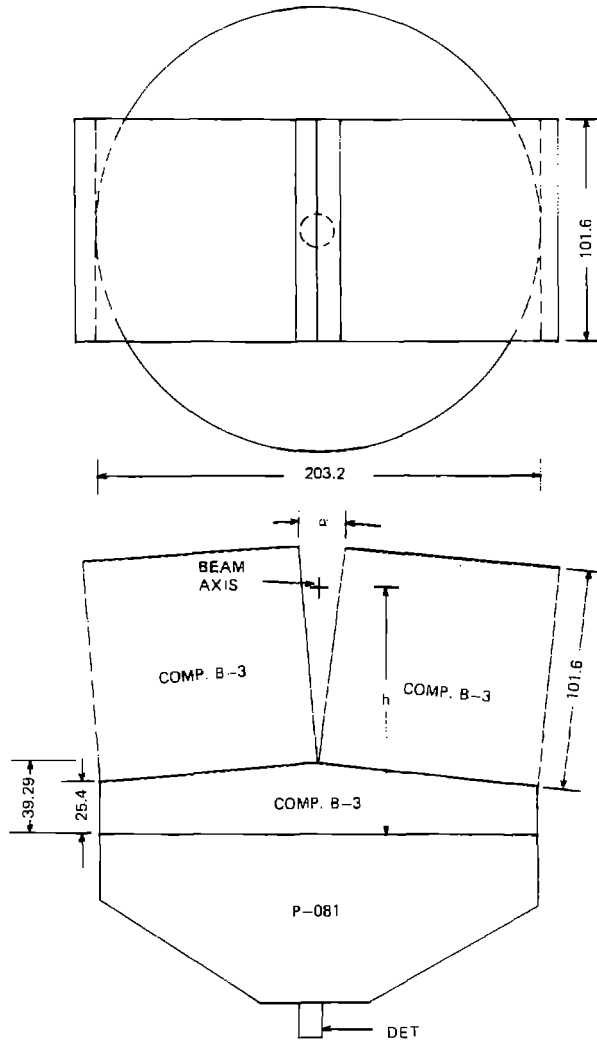
SHOT 325: Diverging Munroe Jet

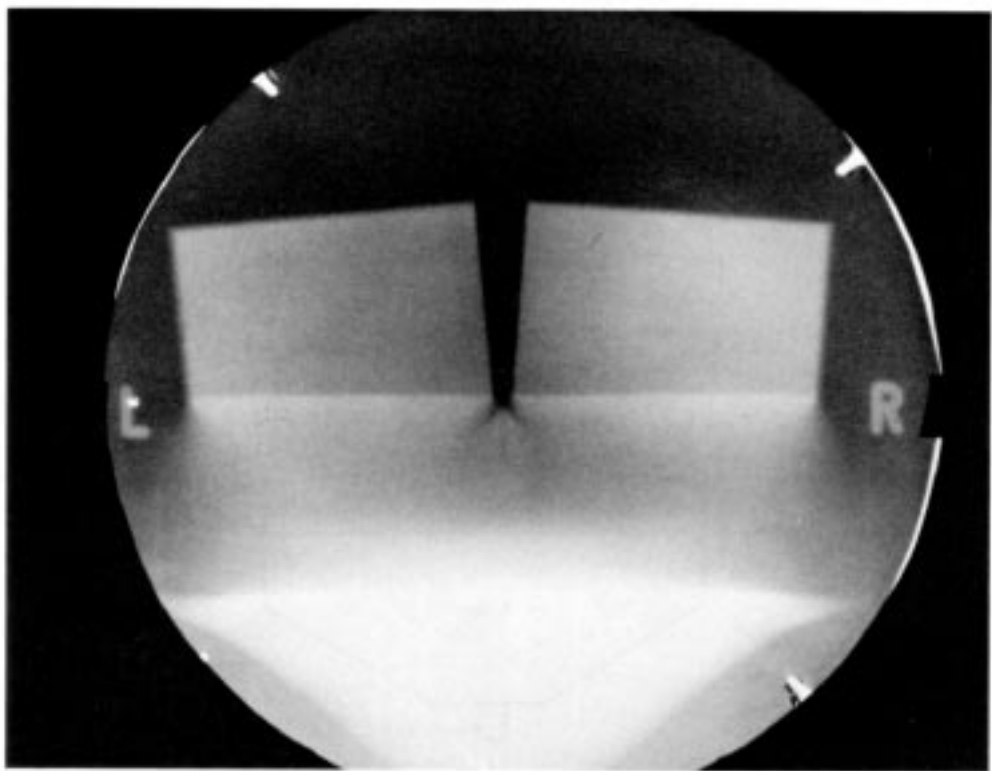
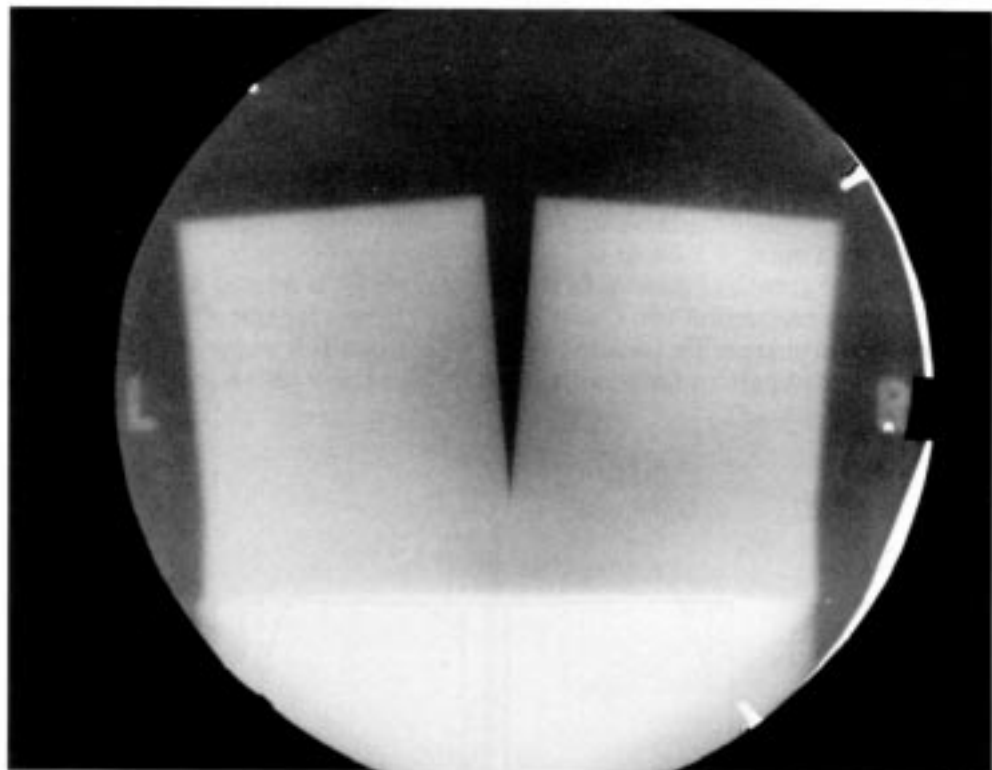
Date: October 19, 1965

Experimenter: Douglas Venable

Radiographic Time: 31.28 μ s

Formation and growth of gaseous Munroe jets. This jet is formed by interaction of the detonation products of two Composition B-3 charges separated by an air groove of 10.0° , α . The charges are initiated by a Composition B-3 wedge initiated by a P-081 lens. The detonations have run 68.0 mm from the P-081. h is 68.26 mm. See Shots 326 and 327.





SHOT 326:

Diverging Munroe Jet

Date:

October 19, 1965

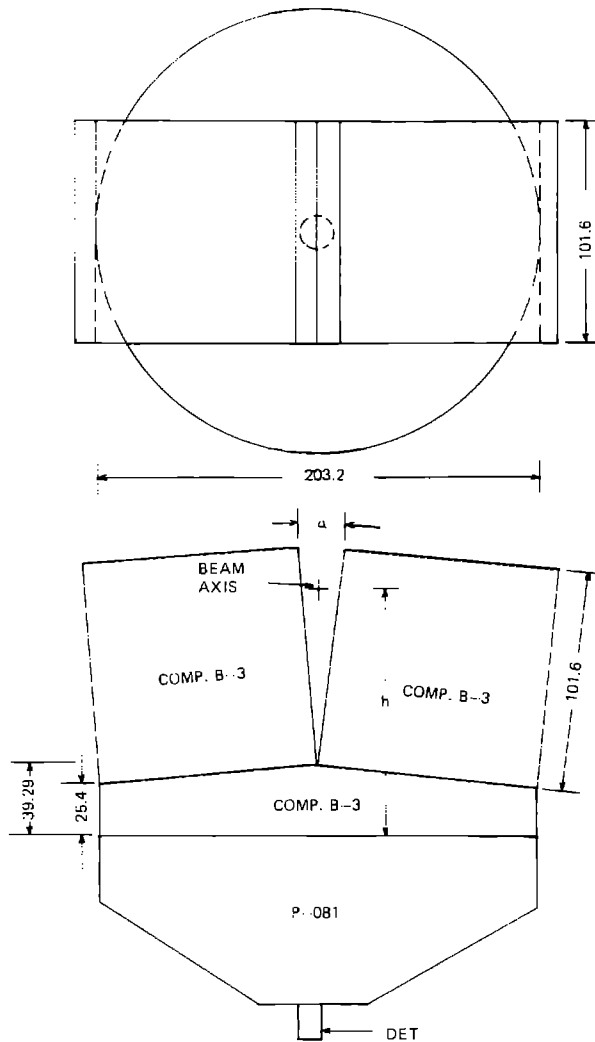
Experimenter:

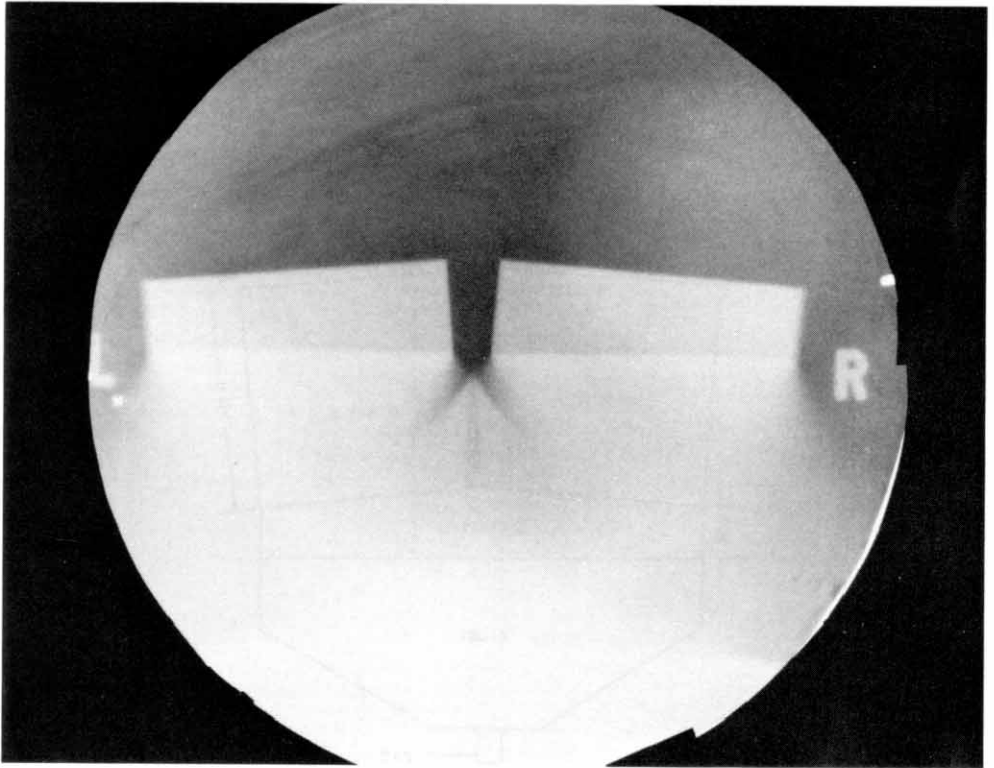
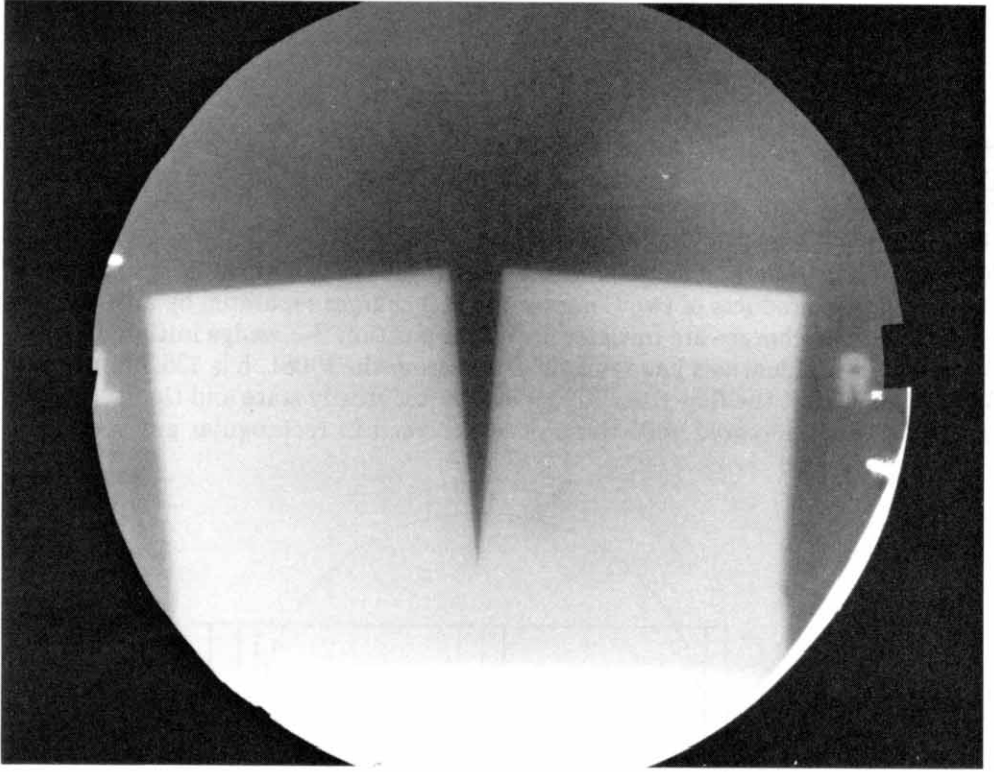
Douglas Venable

Radiographic Time:

35.49 μ s

Formation and growth of gaseous Munroe jets. This jet is formed by interaction of the detonation products of two Composition B-3 charges separated by an air groove of 10.0° , α . The charges are initiated by a Composition B-3 wedge initiated by a P-081 lens. The detonations have run 101.6 mm from the P-081. h is 101.6 mm. See Shots 325 and 327.





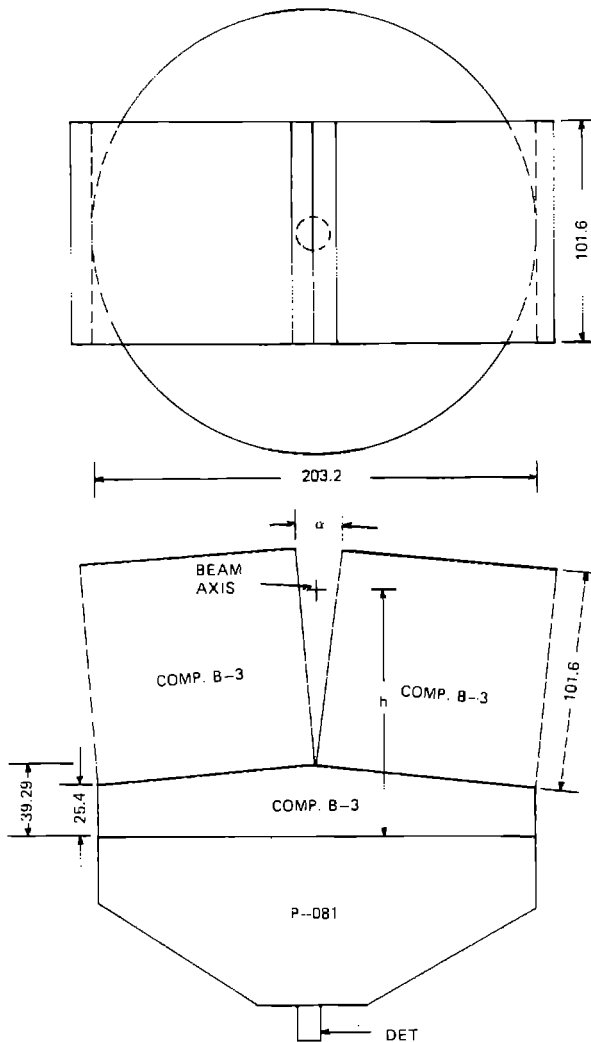
SHOT 327: Diverging Munroe Jet

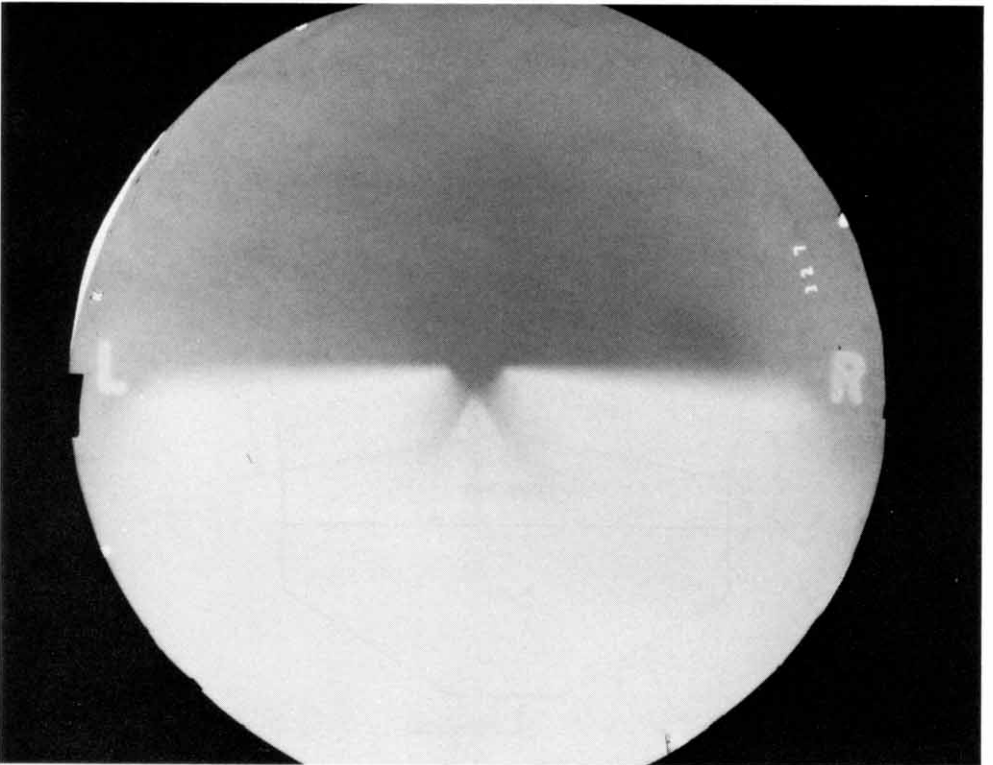
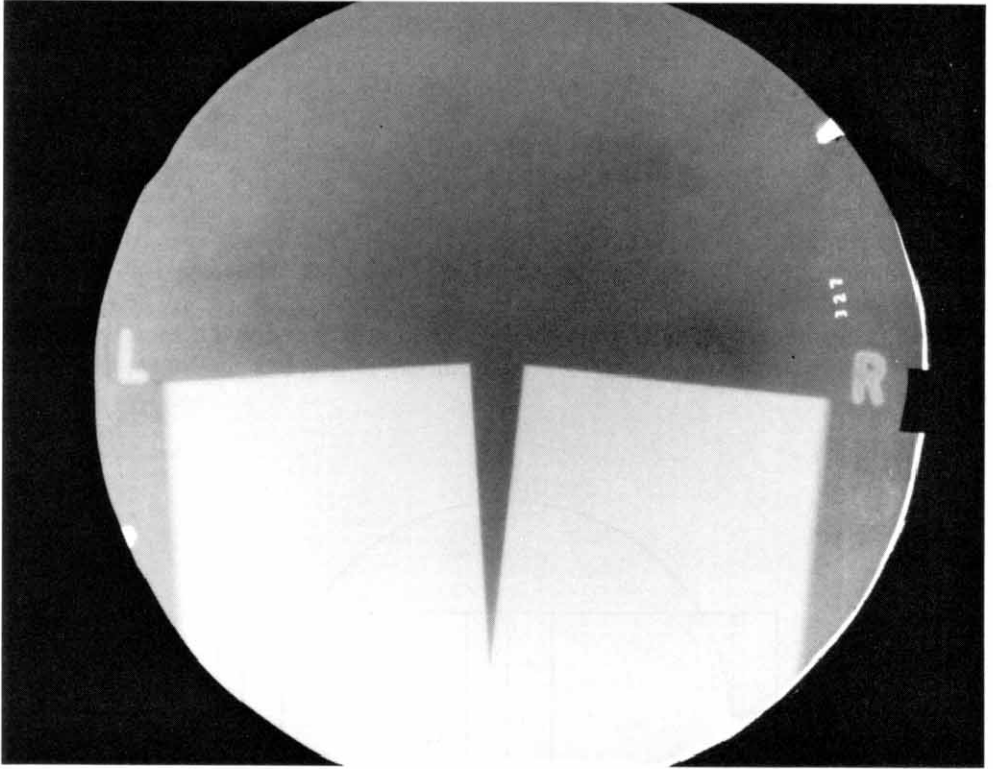
Date: September 28, 1965

Experimenter: Douglas Venable

Radiographic Time: 39.72 μ s

Formation and growth of gaseous Munroe jets. This jet is formed by interaction of the detonation products of two Composition B-3 charges separated by an air groove of 10.0° , α . The charges are initiated by a Composition B-3 wedge initiated by a P-081 lens. The detonations have run 135.0 mm from the P-081. h is 135.7 mm. Shots 325-327 show that the flow from 10° grooves is not steady state and that the jet top is very diffuse compared with those of jets formed in rectangular grooves.





SHOT 328:

Diverging Munroe Jet

Date:

October 5, 1965

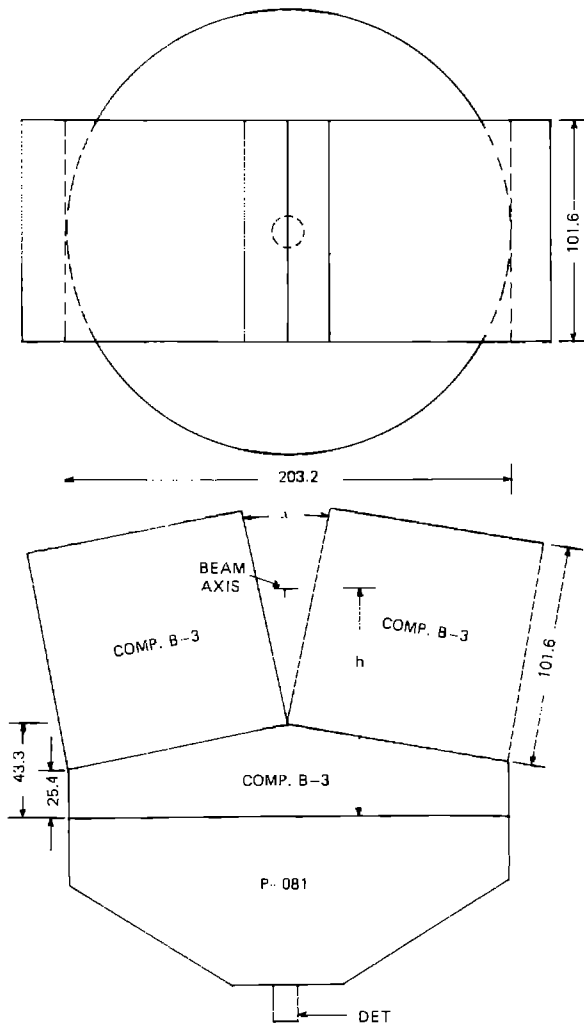
Experimenter:

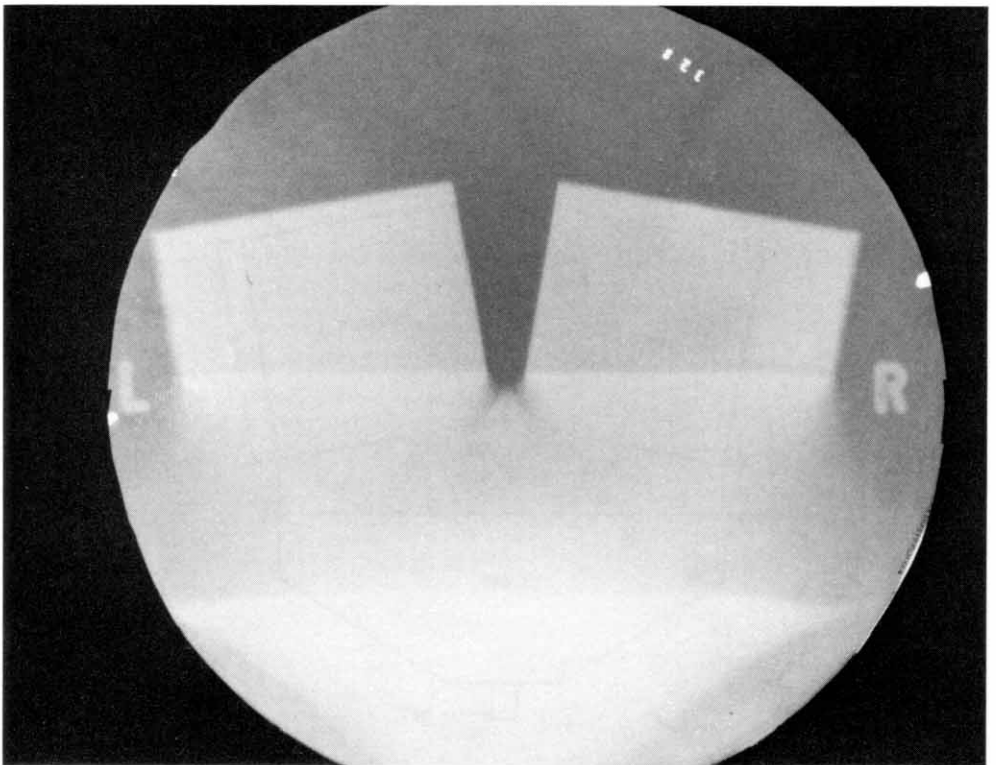
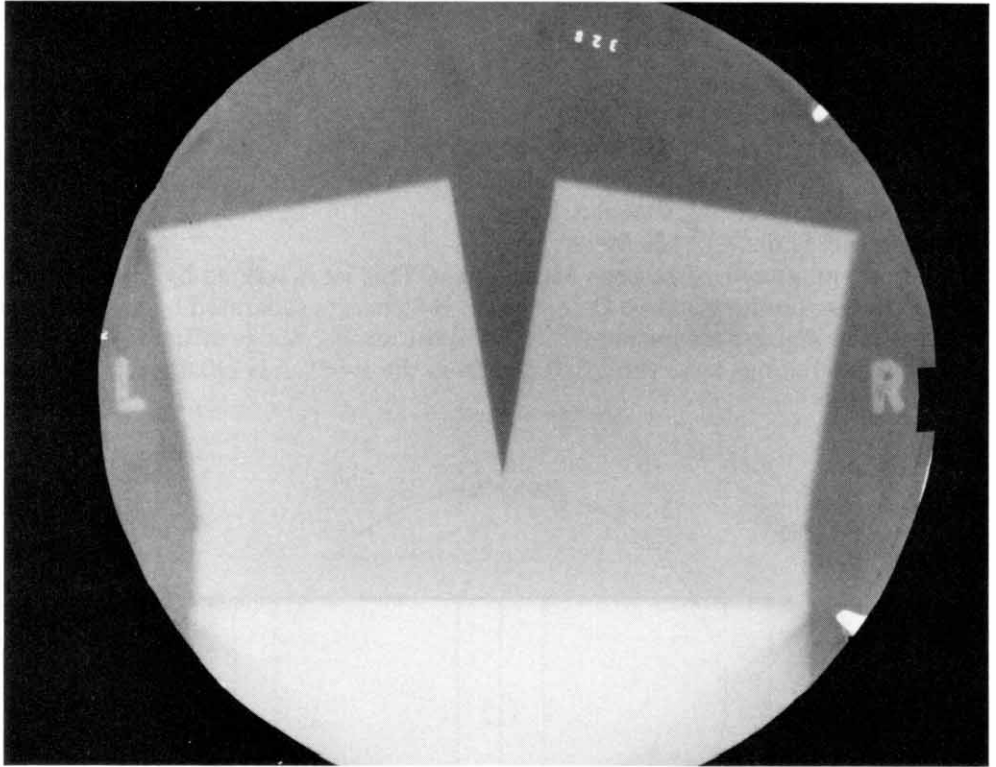
Douglas Venable

Radiographic Time:

32.4 μ s

Formation and growth of gaseous Munroe jets. This jet is formed by interaction of the detonation products of two Composition B-3 charges separated by an air groove of 20° , α . The charges are initiated by a Composition B-3 wedge initiated by a P-081 lens. The detonations have run 77.0 mm from the P-081. h is 77.0 mm. See Shots 329 and 330.





SHOT 329:

Diverging Munroe Jet

Date:

October 5, 1965

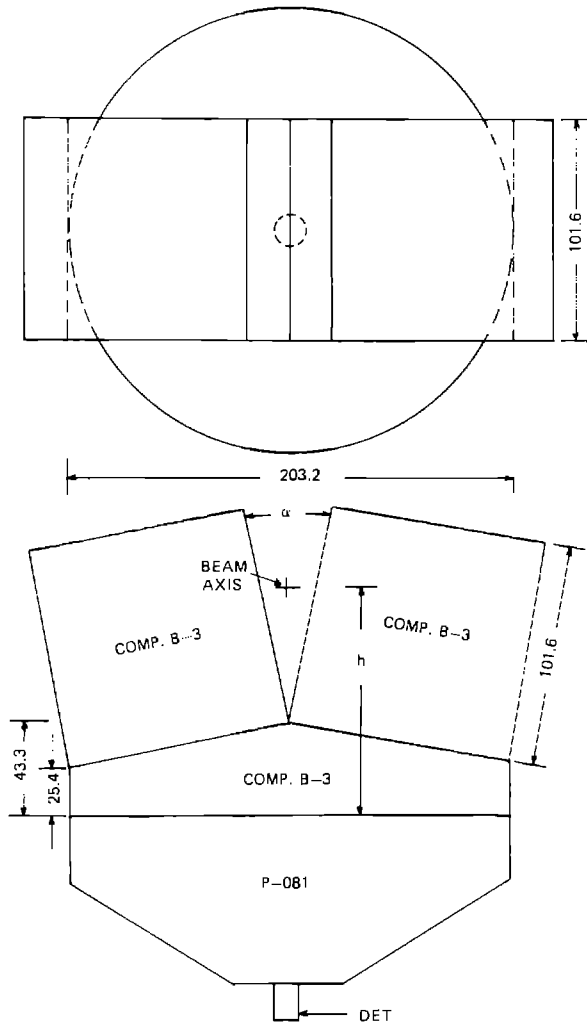
Experimenter:

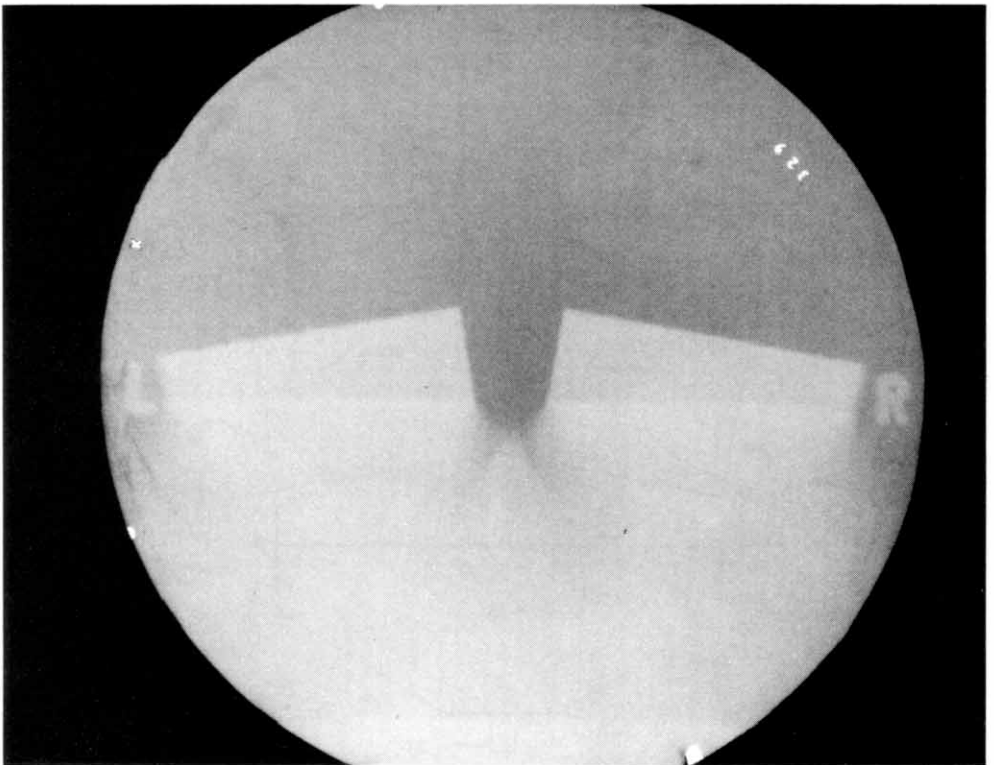
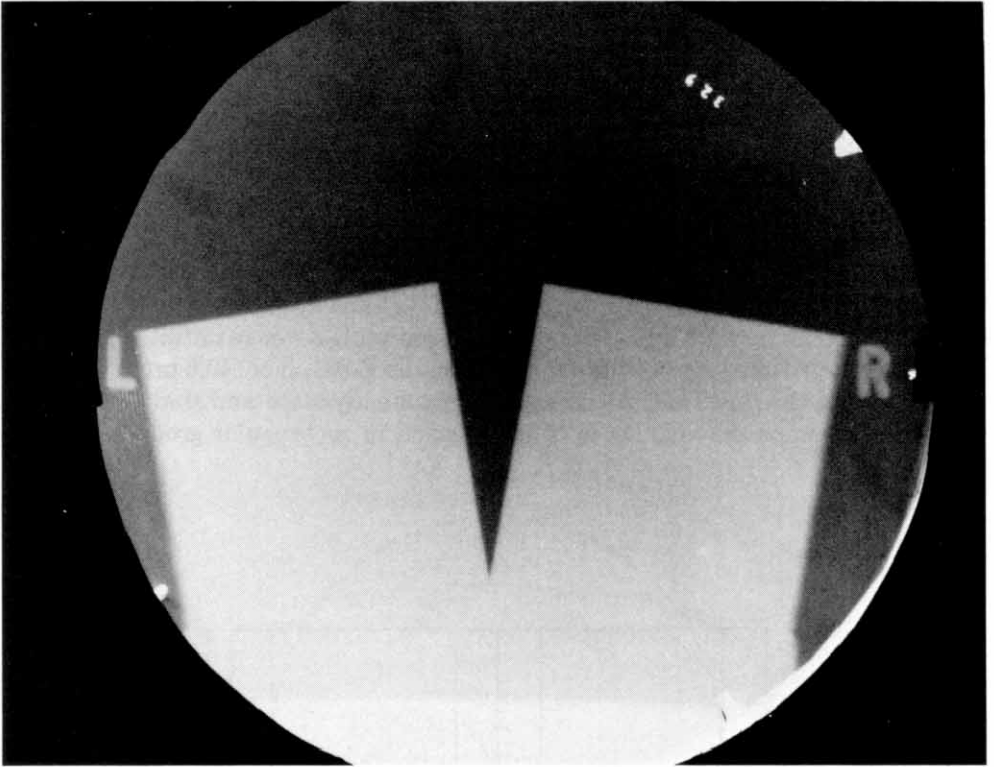
Douglas Venable

Radiographic Time:

36.54 μ s

Formation and growth of gaseous Munroe jets. This jet is formed by interaction of the detonation products of two Composition B-3 charges separated by an air groove of 20° , α . The charges are initiated by a Composition B-3 wedge initiated by a P-081 lens. The detonations have run 110.0 mm from the P-081. h is 110.3 mm. See Shots 328 and 330.





SHOT 330:**Diverging Munroe Jet**

Date:

September 28, 1965

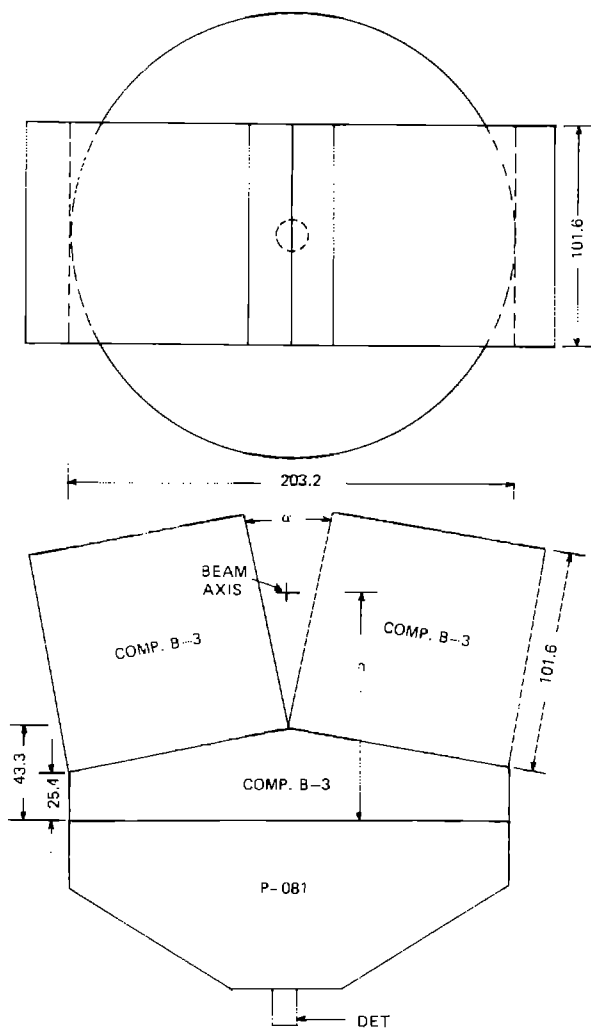
Experimenter:

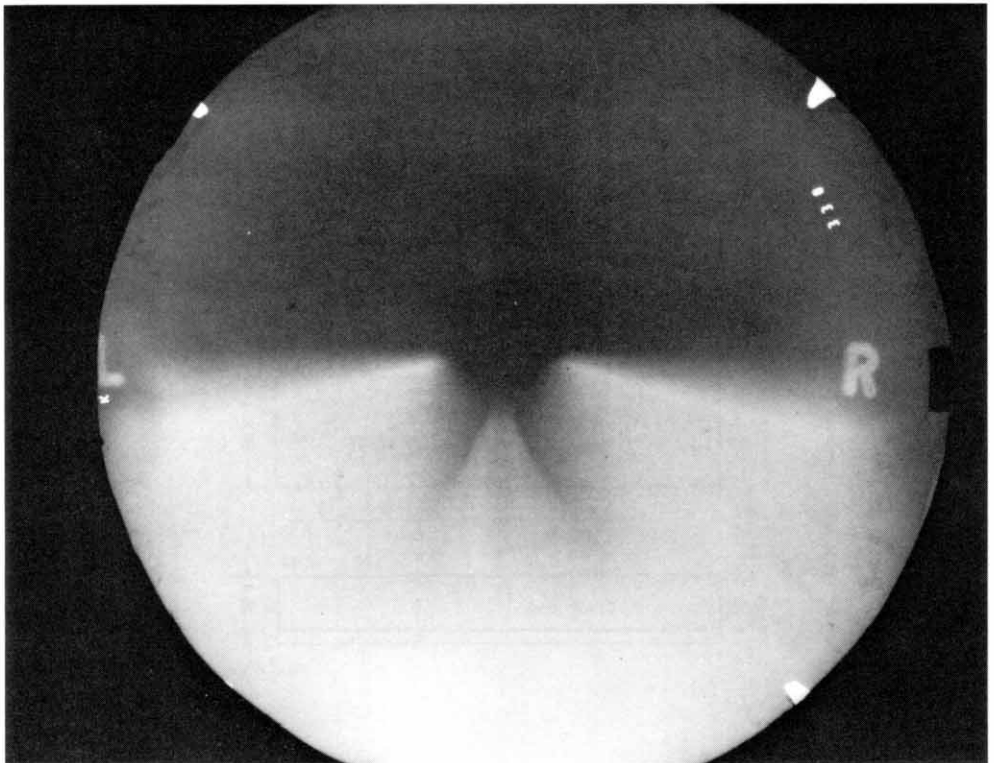
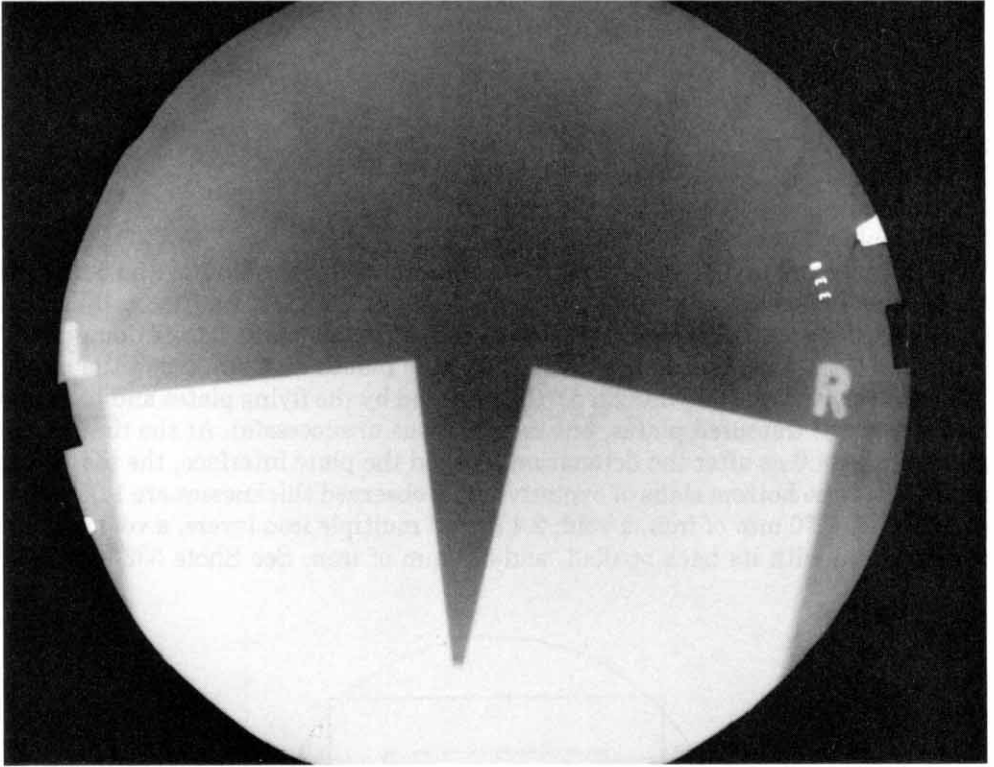
Douglas Venable

Radiographic Time:

40.77 μ s

Formation and growth of gaseous Munroe jets. This jet is formed by interaction of the detonation products of two Composition B-3 charges separated by an air groove of 20° , α . The charges are initiated by a Composition B-3 wedge initiated by a P-081 lens. The detonations have run 143.0 mm from the P-081. h is 143.6 mm. Shots 328-330 show that the flow from 20° grooves is not steady state and that the jet tip is very diffuse compared with those of jets formed in rectangular grooves.

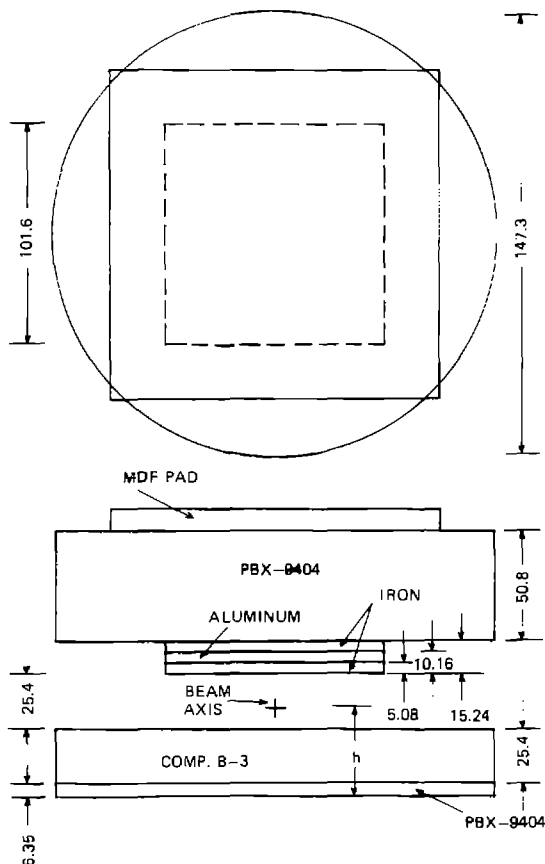


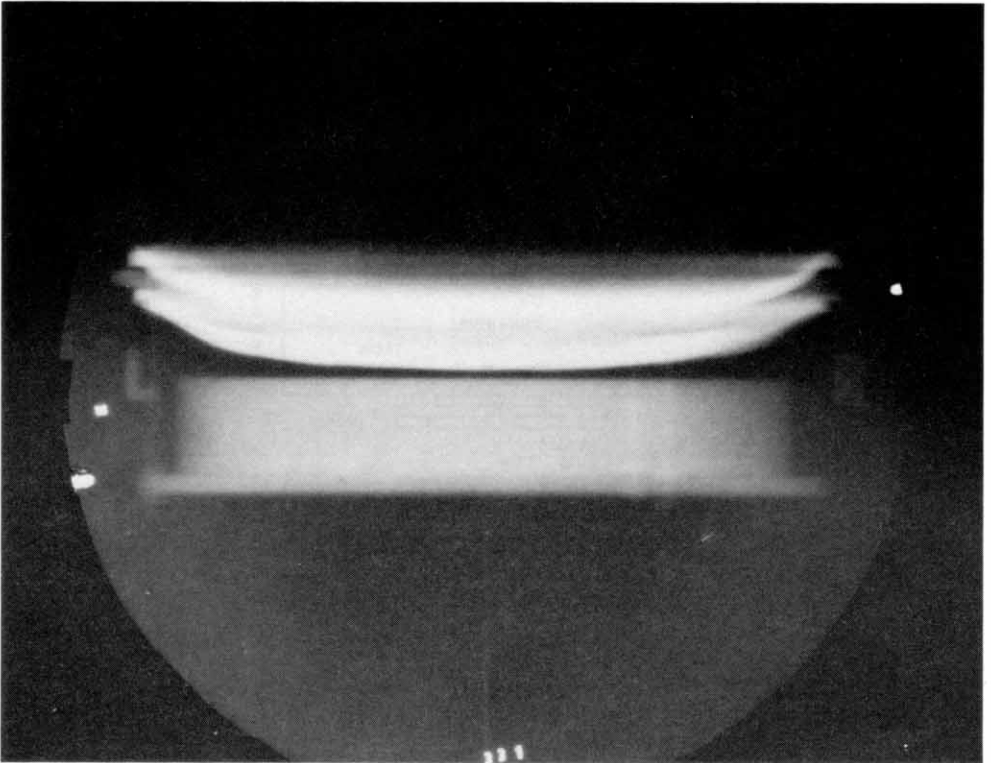
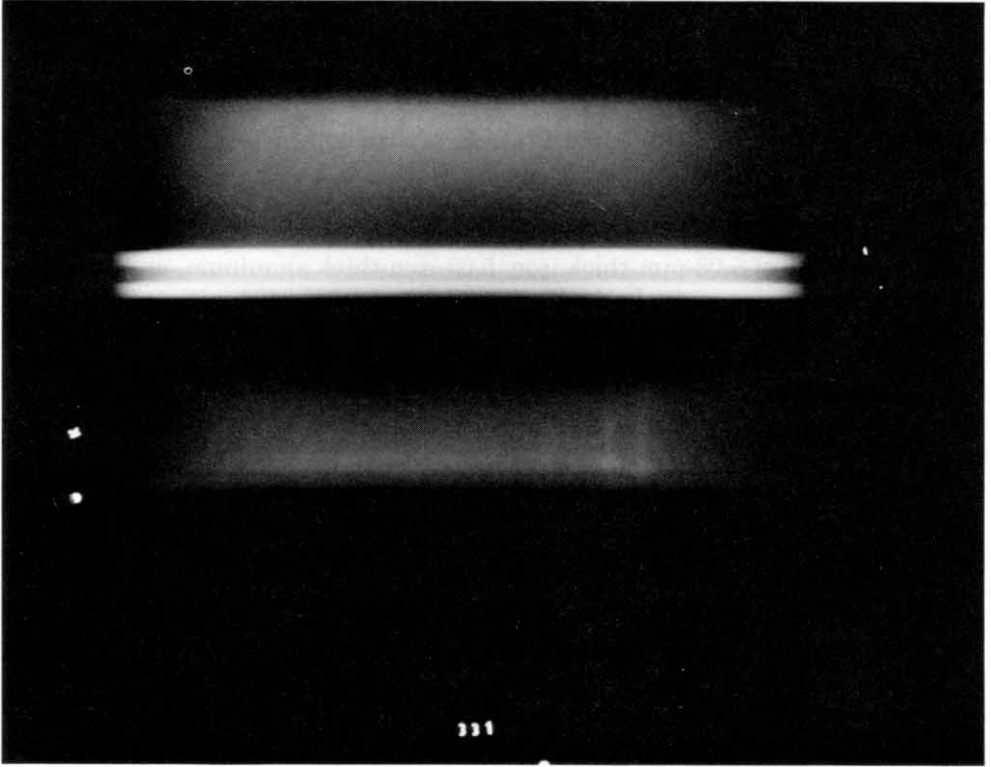


SHOT 331: Multiple Plate Fracture

Date: August 16, 1966
Experimenter: Gary W. Rodenz
Radiographic Time: 37.23 μ s

Dynamic fracture of 5.08-mm-thick iron, 5.08-mm-thick aluminum, and 5.08-mm-thick iron. The plates were shocked by 50.8 mm of PBX-9404 initiated by a mild detonating fuse (M.D.F.) pad. h is 41.93 mm. A 25.4-mm-thick slab of Composition B-3 and a 6.35-mm-thick slab of PBX-9404 were placed 25.4 mm below the plates. This explosive charge was designed to be initiated by the flying plates and to permit recovery of the fractured plates, but recovery was unsuccessful. At the time of this radiograph, 14.0 μ s after the detonation reached the plate interface, the plates had not reached the bottom slabs of explosive. The observed thicknesses are 1.50 mm of iron, a void, 1.70 mm of iron, a void, 2.4 mm of multiple iron layers, a void, 5.0 mm of aluminum with its back spalled, and 5.0 mm of iron. See Shots 332 and 333.





SHOT 332:**Multiple Plate Fracture**

Date:

August 17, 1966

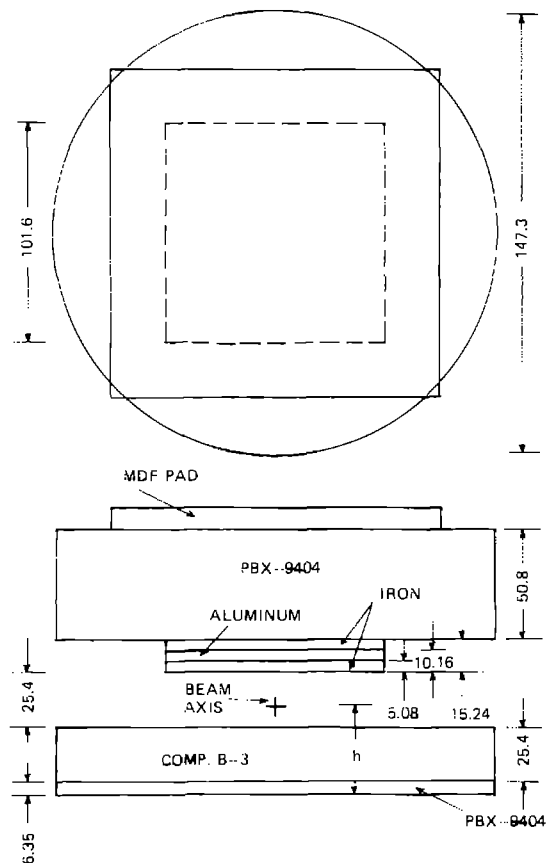
Experimenter:

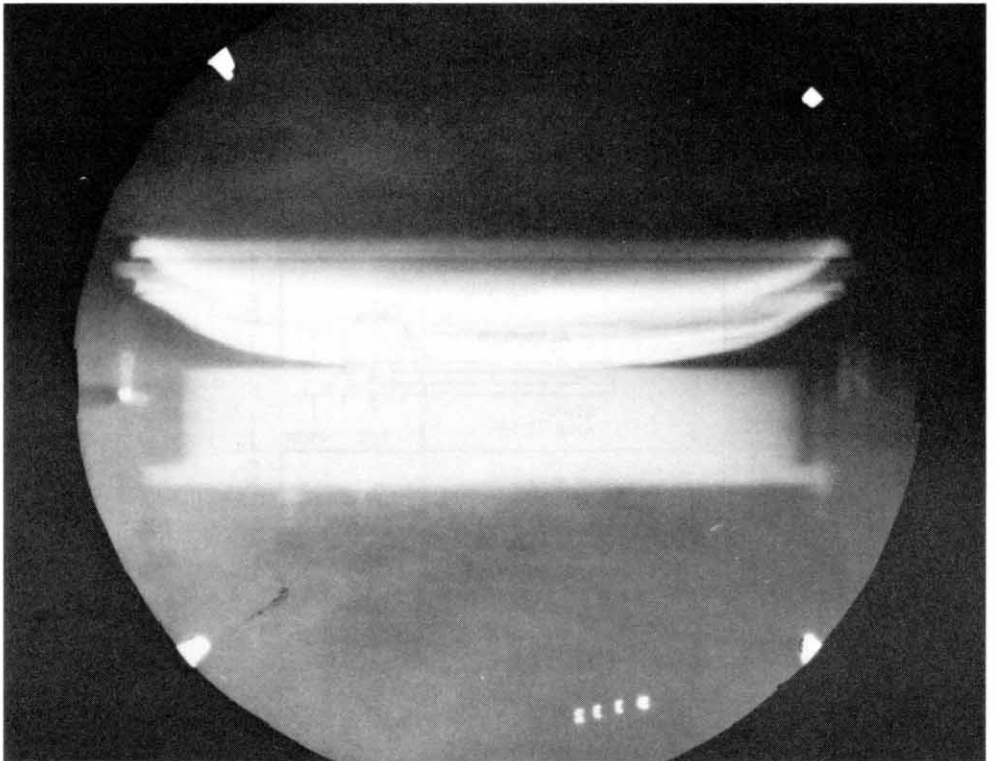
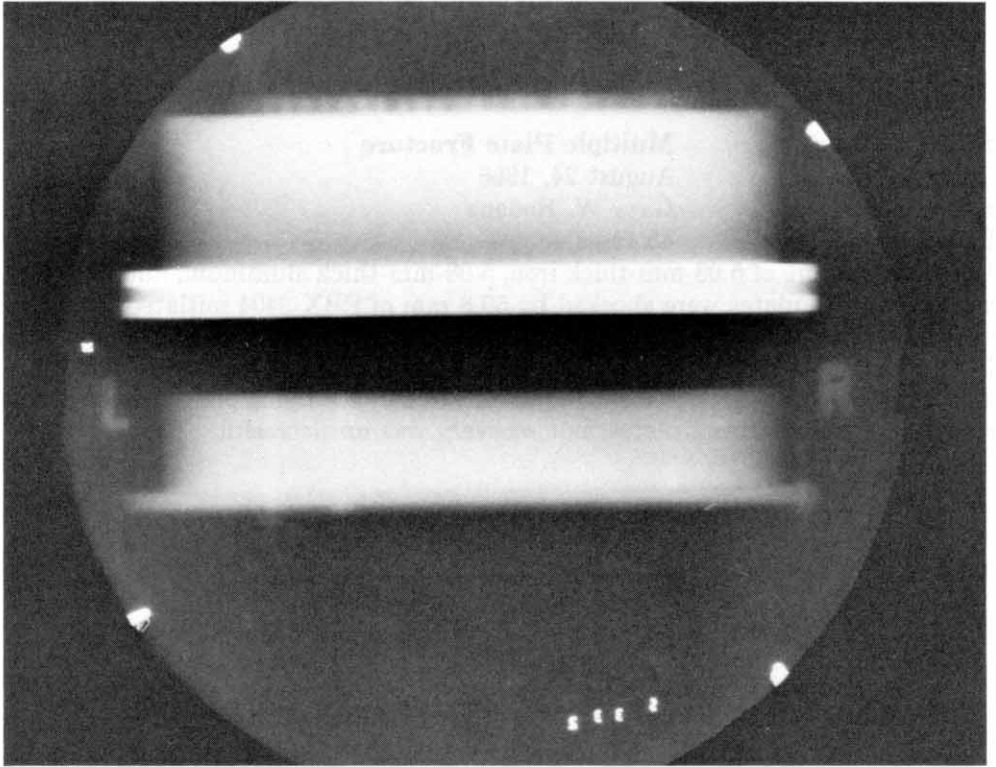
Gary W. Rodenz

Radiographic Time:

38.22 μ s

Dynamic fracture of 5.08-mm-thick iron, 5.08-mm-thick aluminum, and 5.08-mm-thick iron. The plates were shocked by 50.8 mm of PBX-9404 initiated by a mild detonating fuse (M.D.F.) pad. h is 31.75 mm. A 25.4-mm-thick slab of Composition B-3 and a 6.35-mm-thick slab of PBX-9404 were placed 25.4 mm below the plates. This explosive charge was designed to be initiated by the flying plates and to permit recovery of the fractured plates, but recovery was unsuccessful. See Shots 331 and 333.





SHOT 333:**Multiple Plate Fracture**

Date:

August 24, 1966

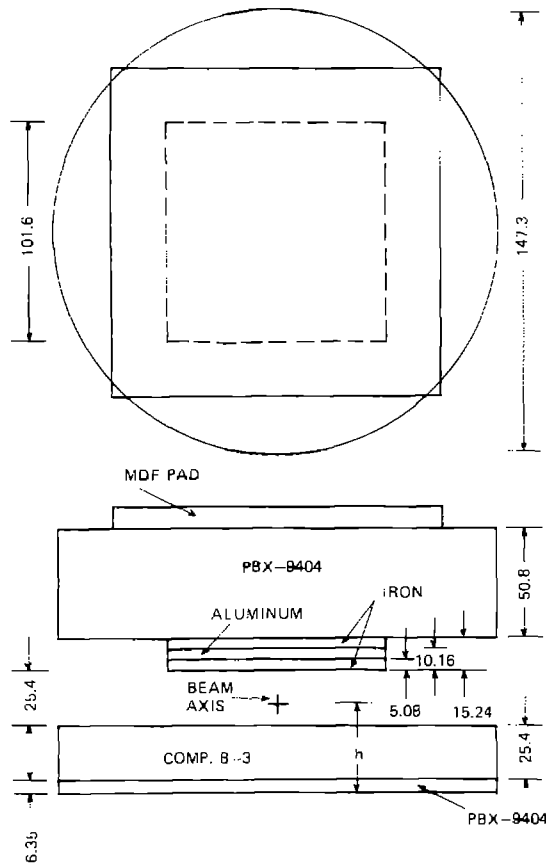
Experimenter:

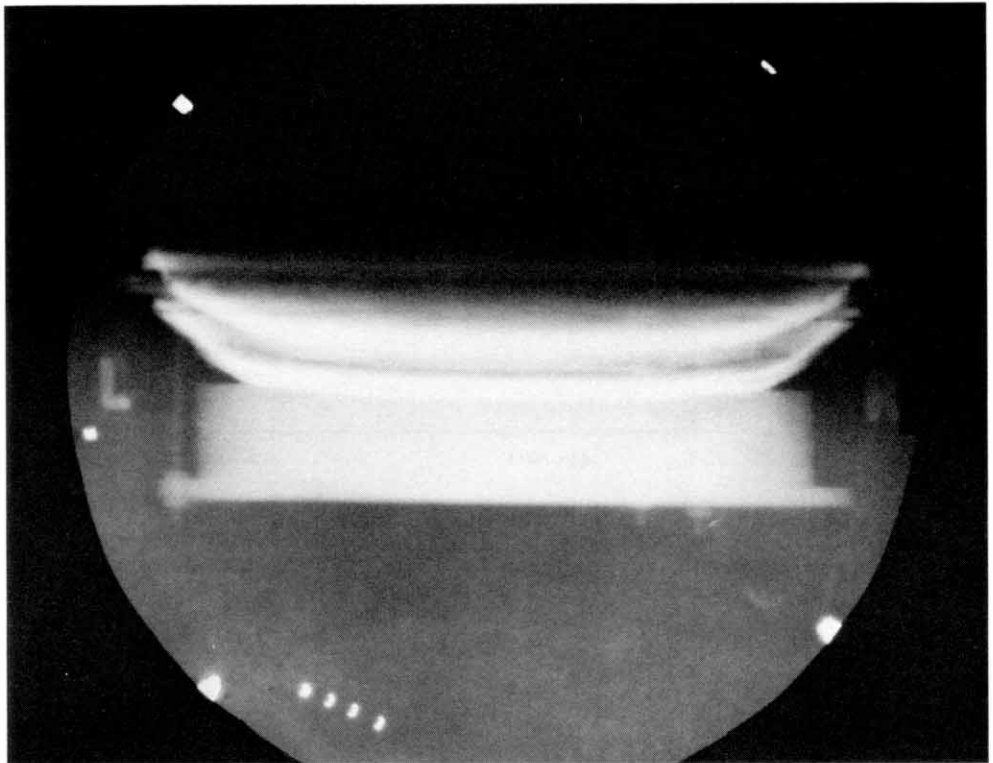
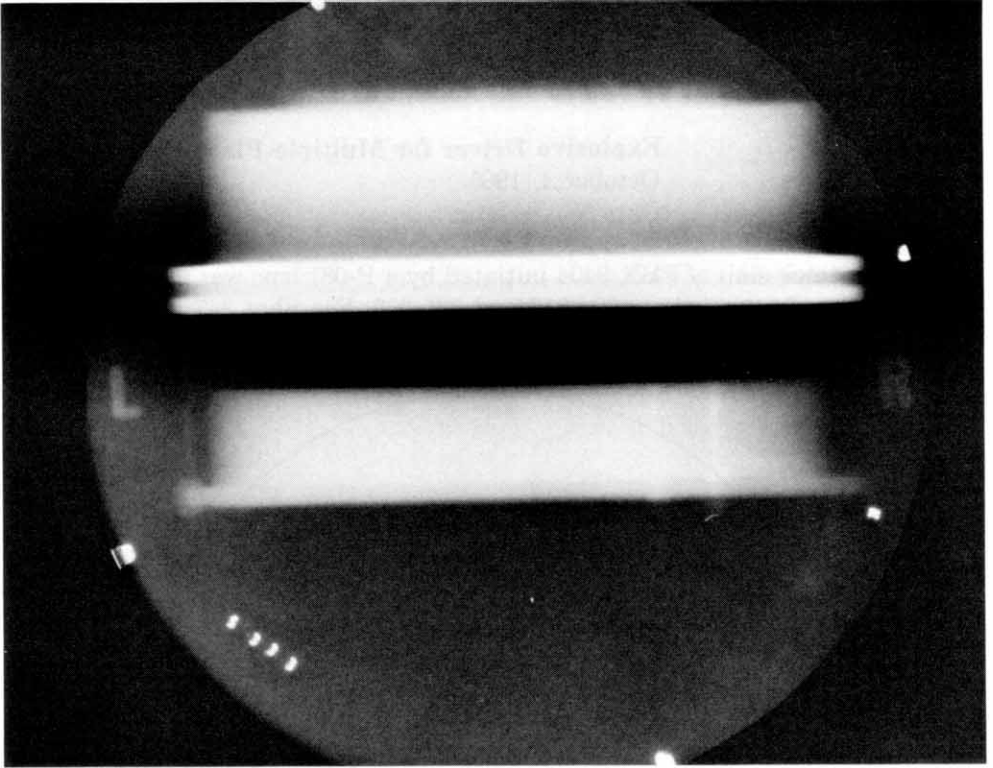
Gary W. Rodenz

Radiographic Time:

43.19 μ s

Dynamic fracture of 5.08-mm-thick iron, 5.08-mm-thick aluminum, and 5.08-mm-thick iron. The plates were shocked by 50.8 mm of PBX-9404 initiated by a mild detonation fuse (M.D.F.) pad. h is 31.75 mm. A 25.4-mm-thick slab of Composition B-3 and a 6.35-mm-thick slab of PBX-9404 were placed 25.4 mm below the plates. This explosive charge was designed to be initiated by the flying plates and to permit recovery of the fractured plates, but recovery was unsuccessful.





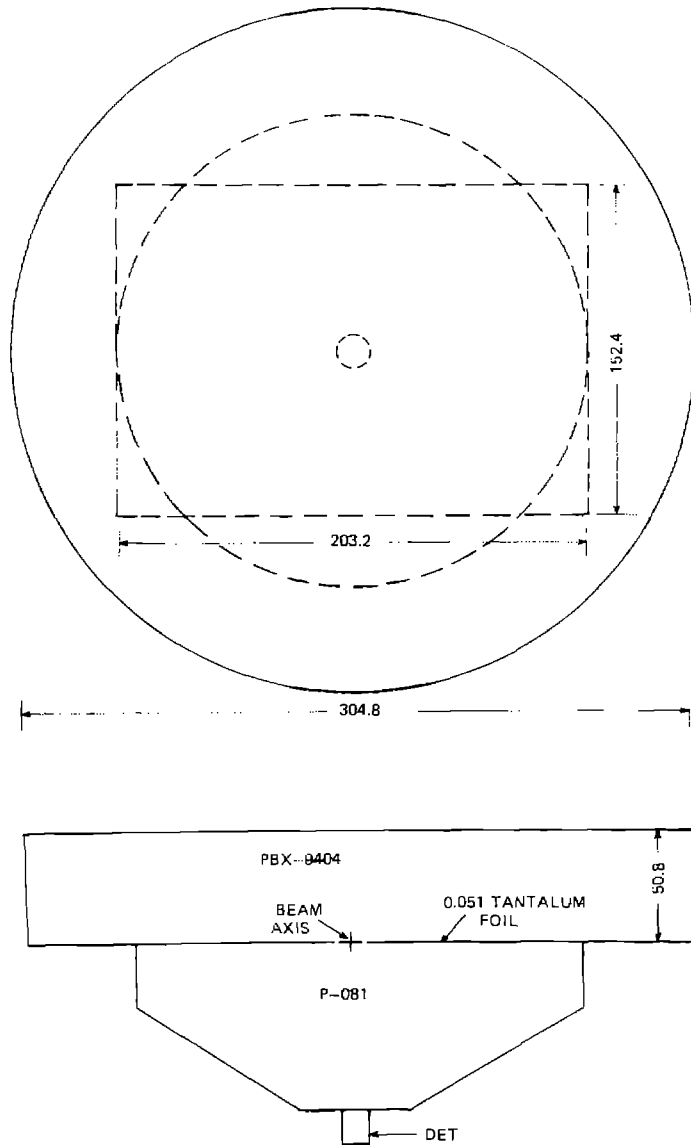
SHOT 334: Explosive Driver for Multiple Plate Fracture

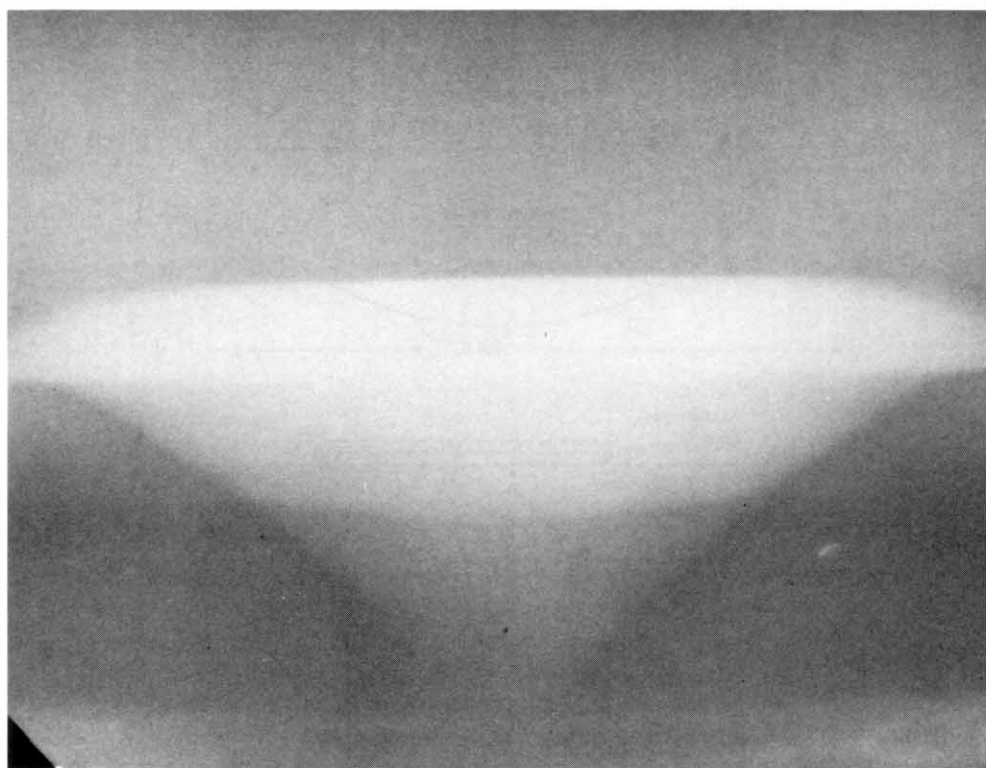
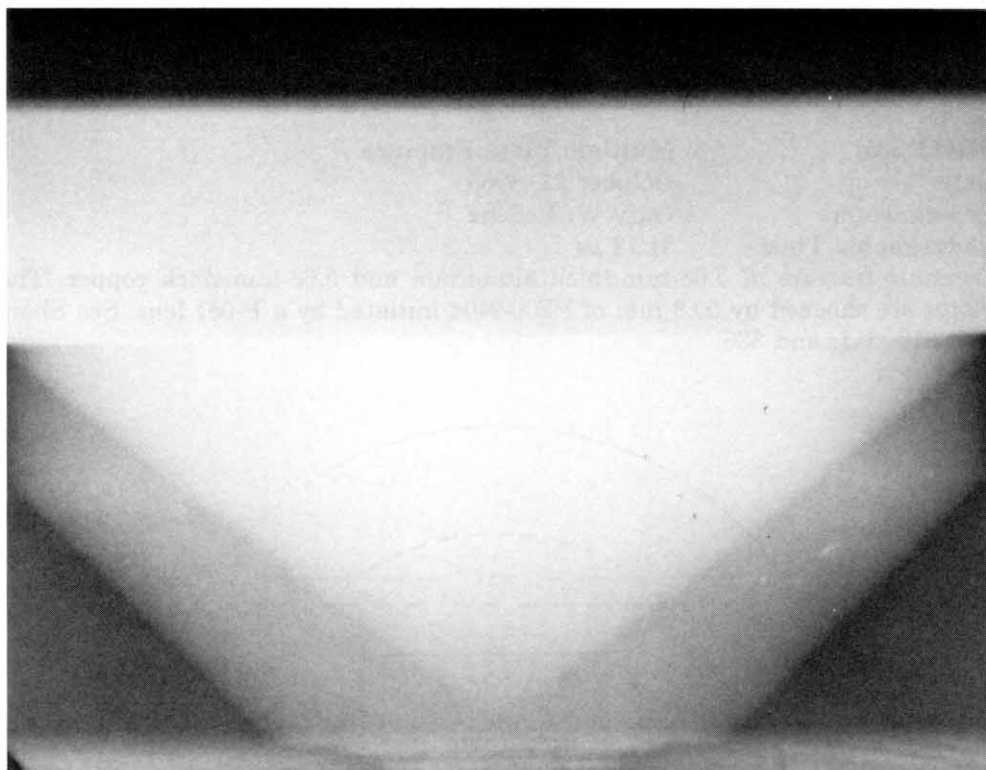
Date: October 4, 1965

Experimenter: Gary W. Rodenz

Radiographic Time: 38.48 μ s

A 50.8-mm-thick slab of PBX-9404 initiated by a P-081 lens was used to drive the multiple plate fracture shots 308-313 and 335-339. See Shot 347 also.





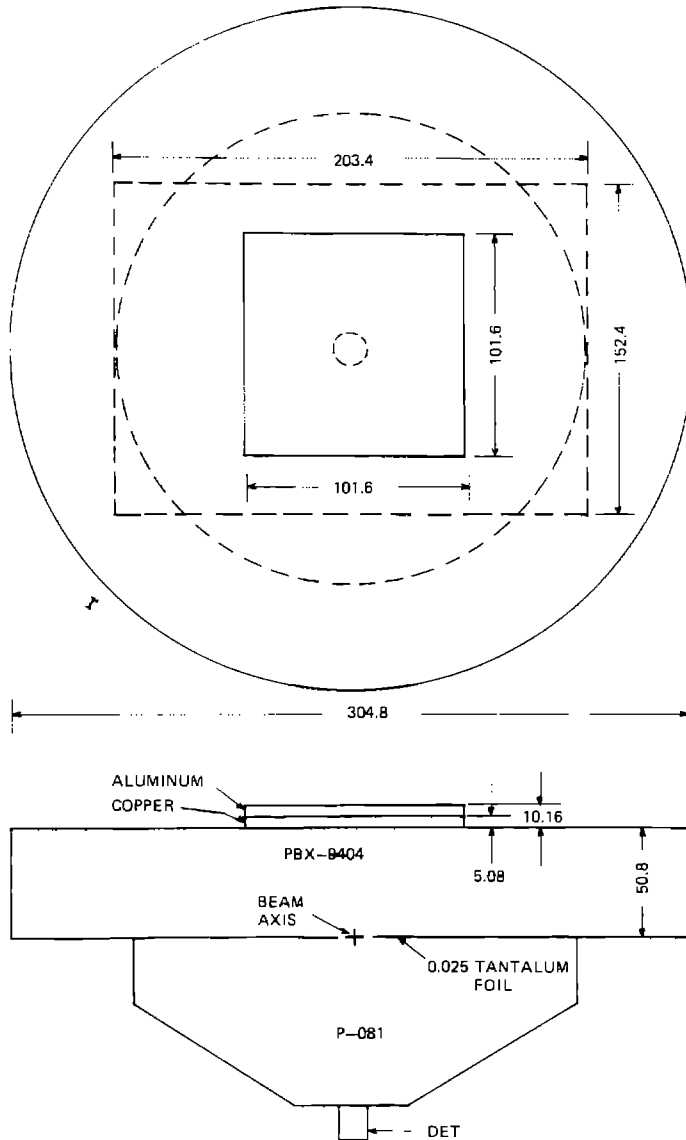
SHOT 335: Multiple Plate Fracture

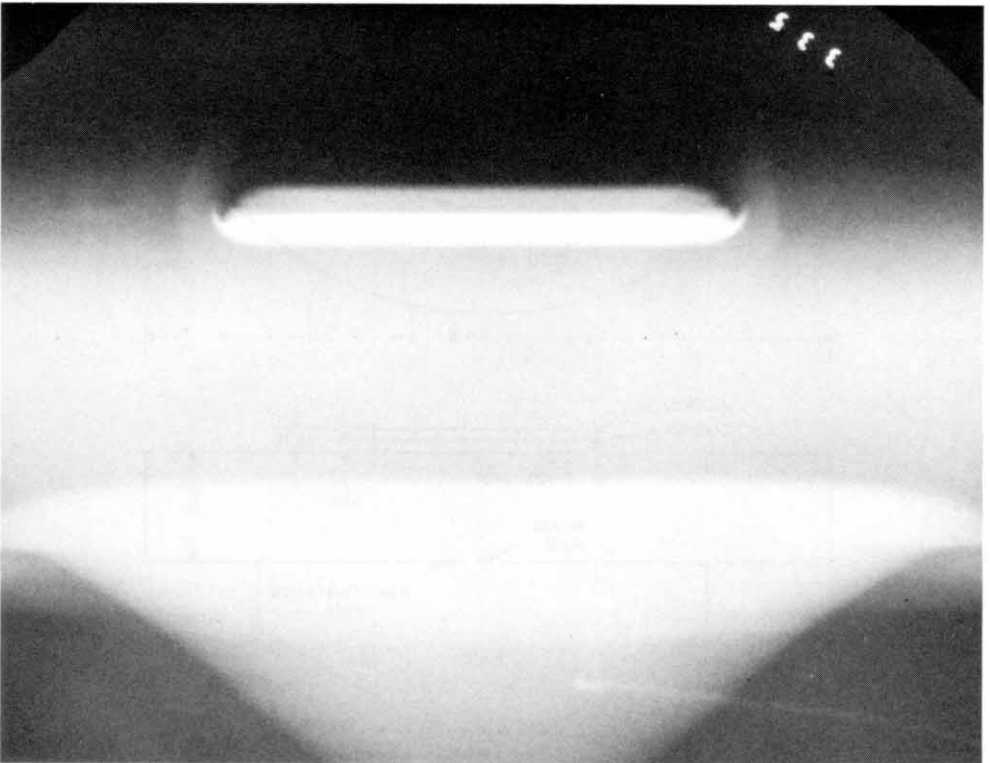
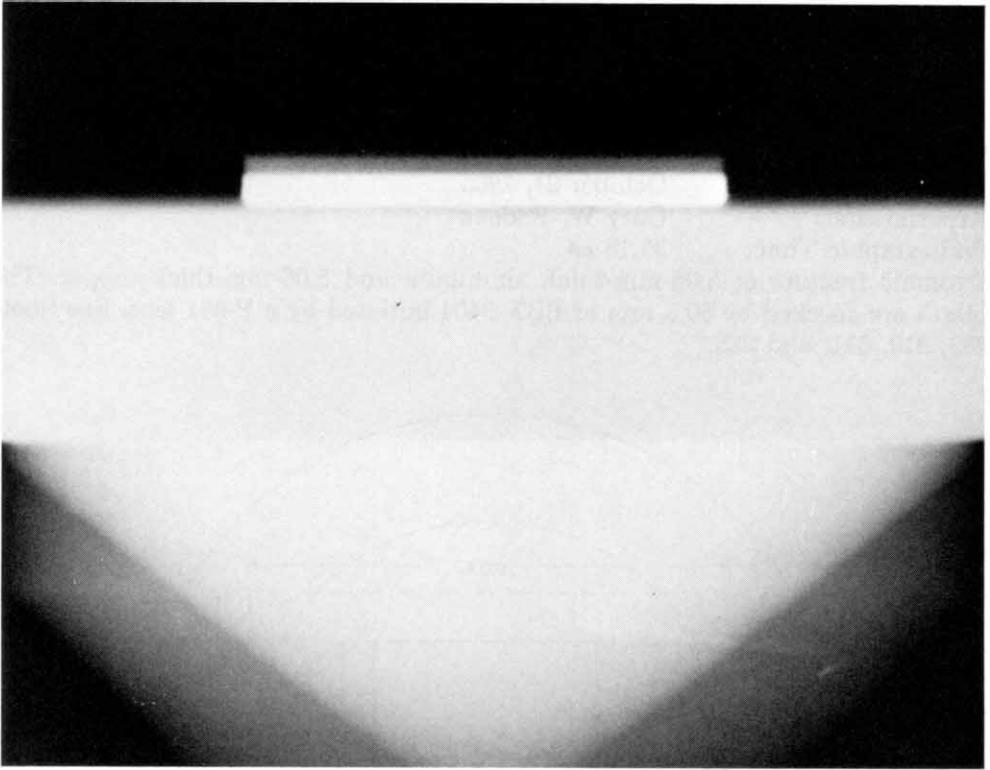
Date: October 21, 1965

Experimenter: Gary W. Rodenz

Radiographic Time: 31.72 μ s

Dynamic fracture of 5.08-mm-thick aluminum and 5.08-mm-thick copper. The plates are shocked by 50.8 mm of PBX-9404 initiated by a P-081 lens. See Shots 308, 310, 311, and 336.





SHOT 336:

Multiple Plate Fracture

Date:

October 21, 1965

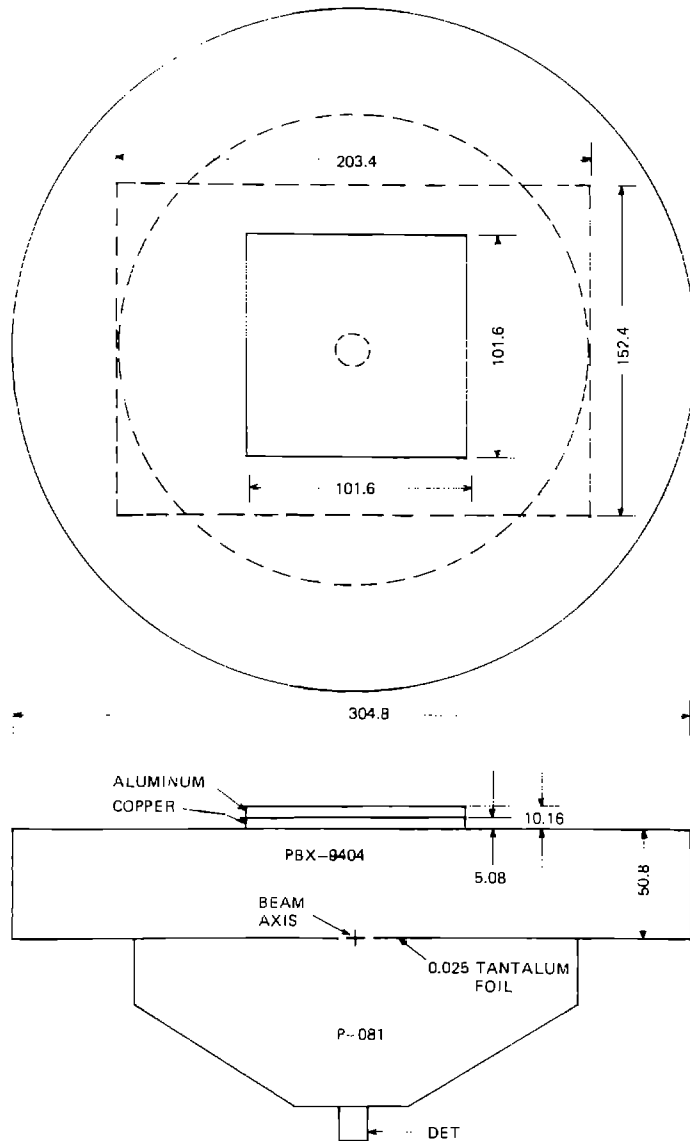
Experimenter:

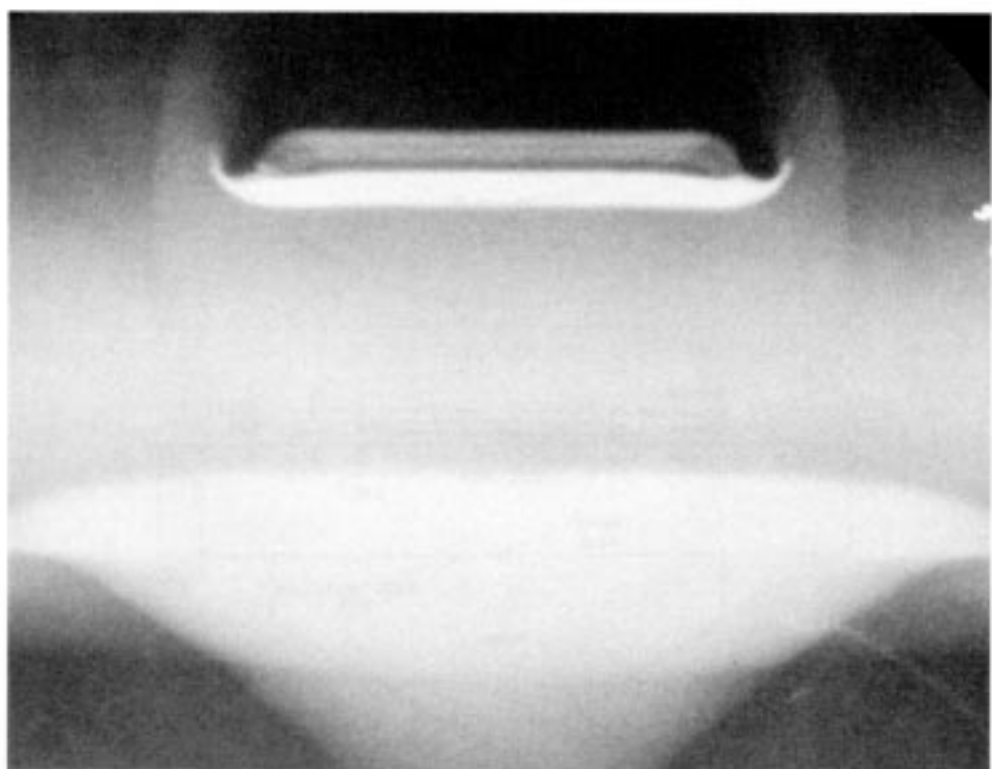
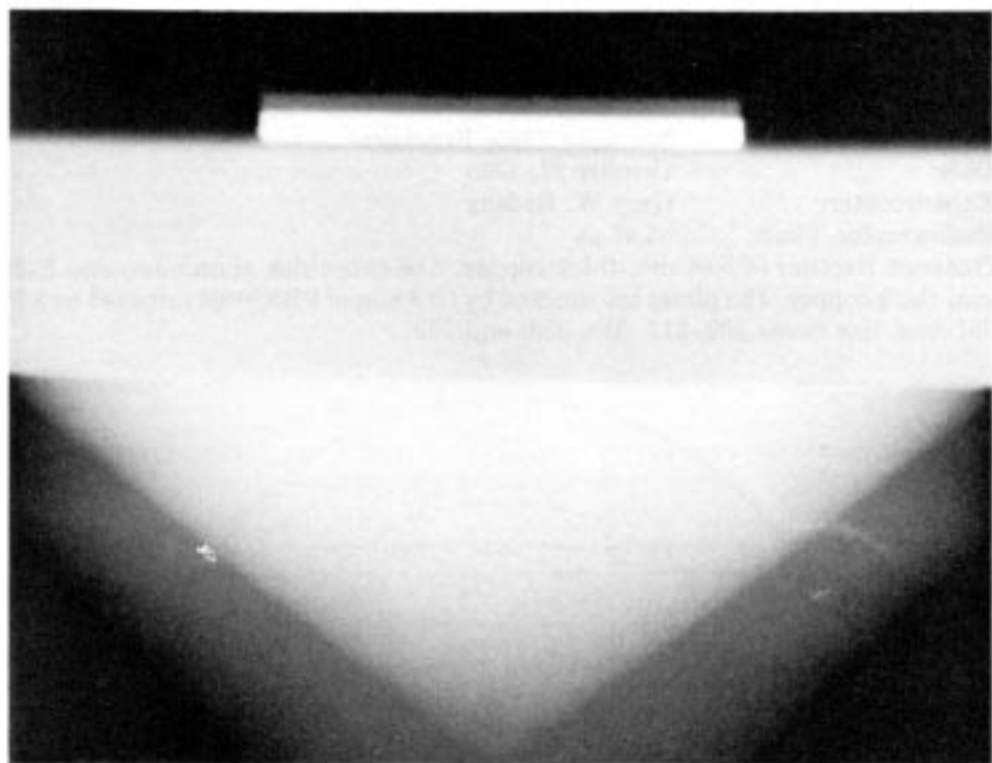
Gary W. Rodenz

Radiographic Time:

35.13 μ s

Dynamic fracture of 5.08-mm-thick aluminum and 5.08-mm-thick copper. The plates are shocked by 50.8 mm of PBX-9404 initiated by a P-081 lens. See Shots 308, 310, 311, and 335.





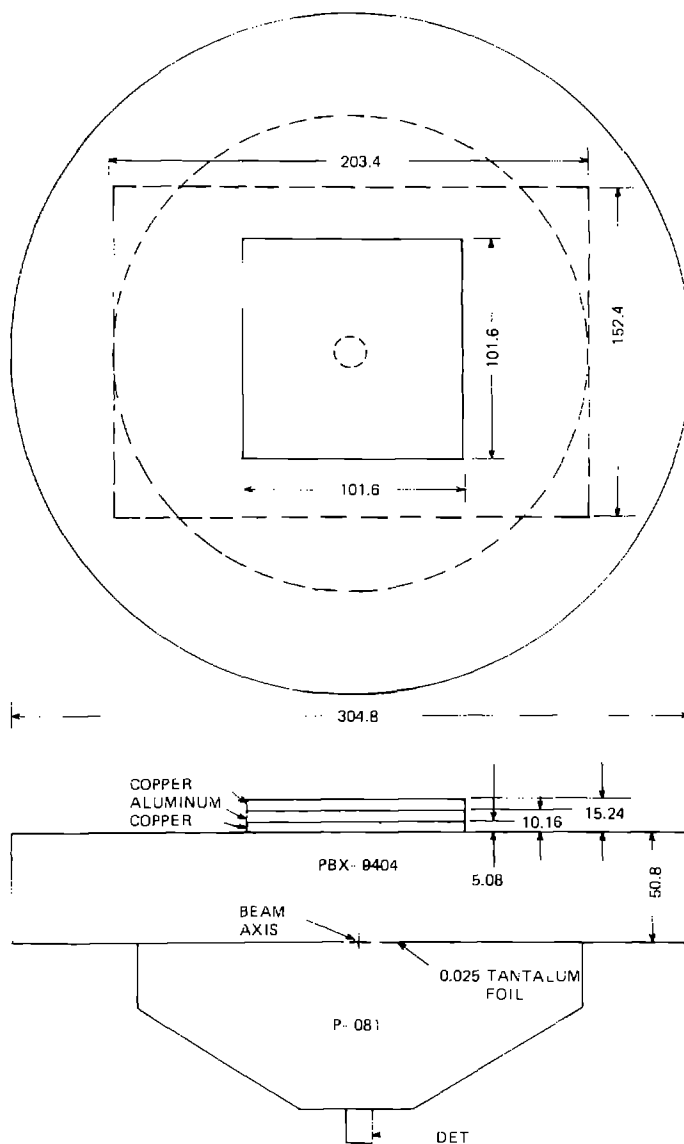
SHOT 337: Multiple Plate Fracture

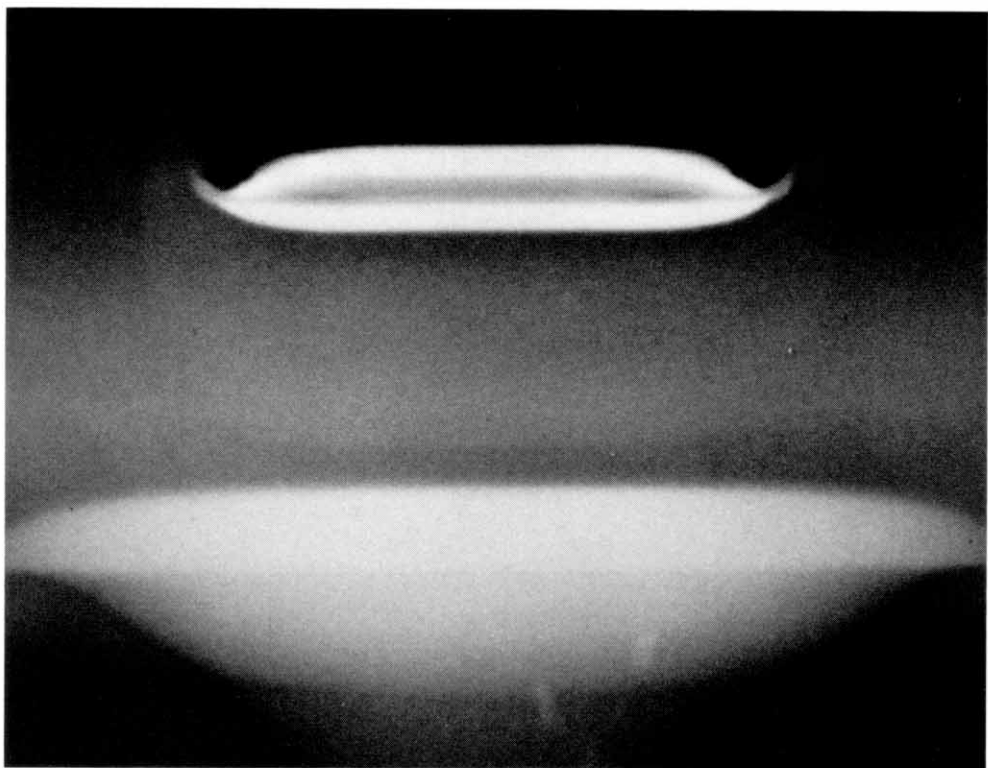
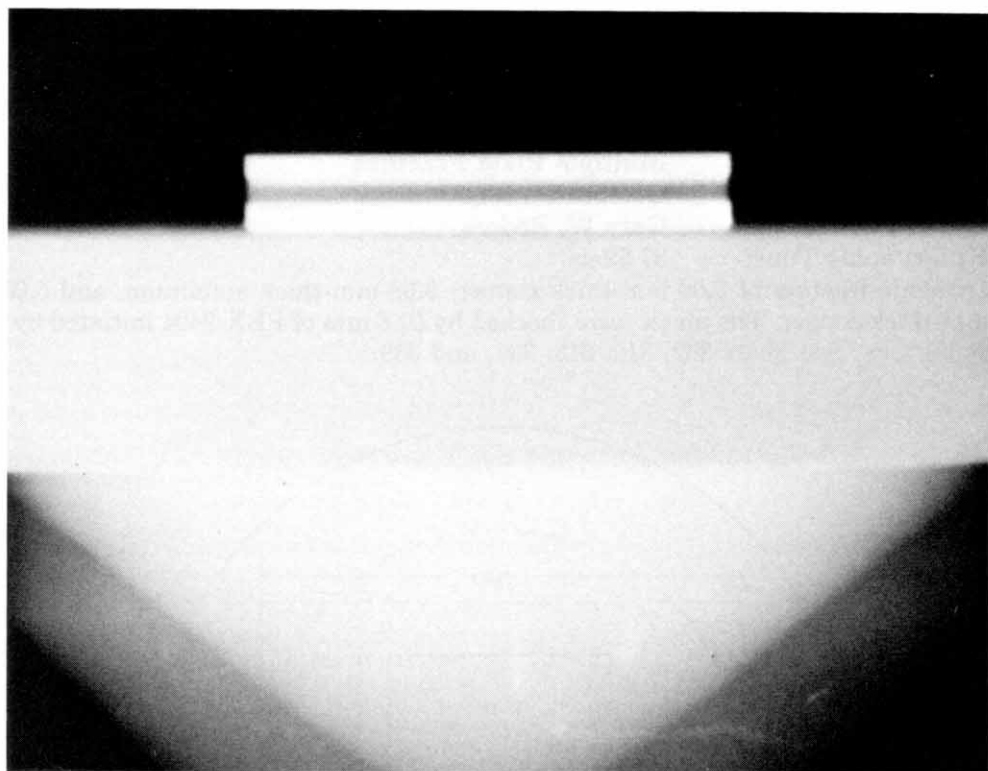
Date: October 27, 1965

Experimenter: Gary W. Rodenz

Radiographic Time: 35.47 μ s

Dynamic fracture of 5.08-mm-thick copper, 5.08-mm-thick aluminum, and 5.08-mm-thick copper. The plates are shocked by 50.8 mm of PBX-9404 initiated by a P-081 lens. See Shots 309, 312, 313, 338, and 339.





SHOT 338:

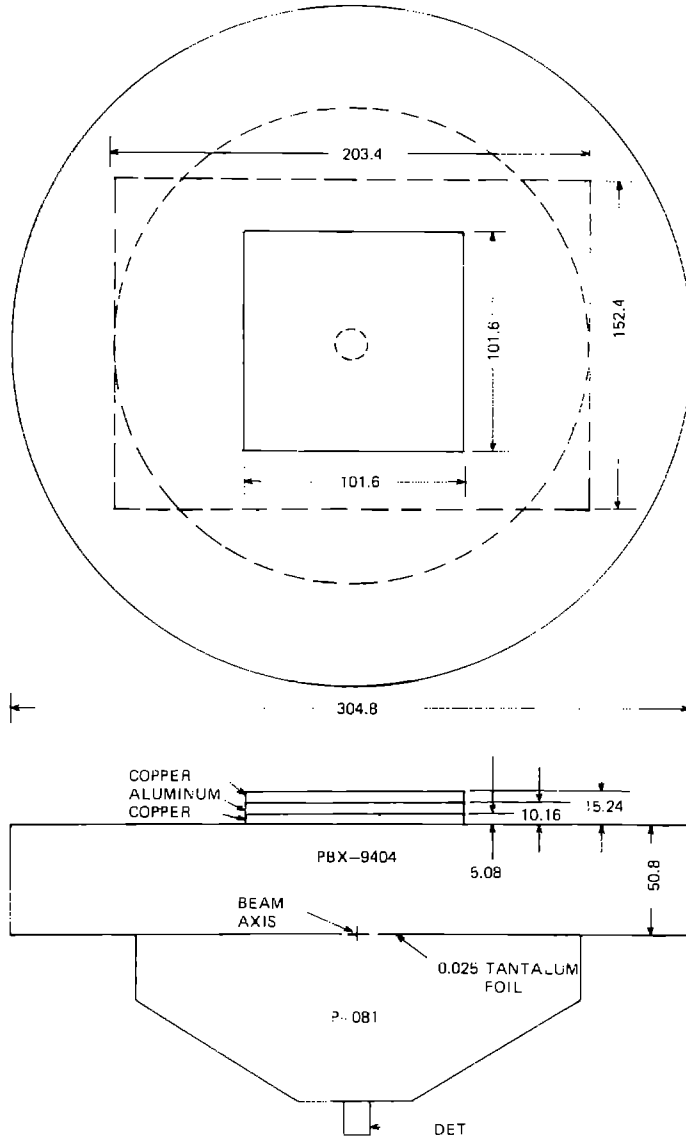
Multiple Plate Fracture

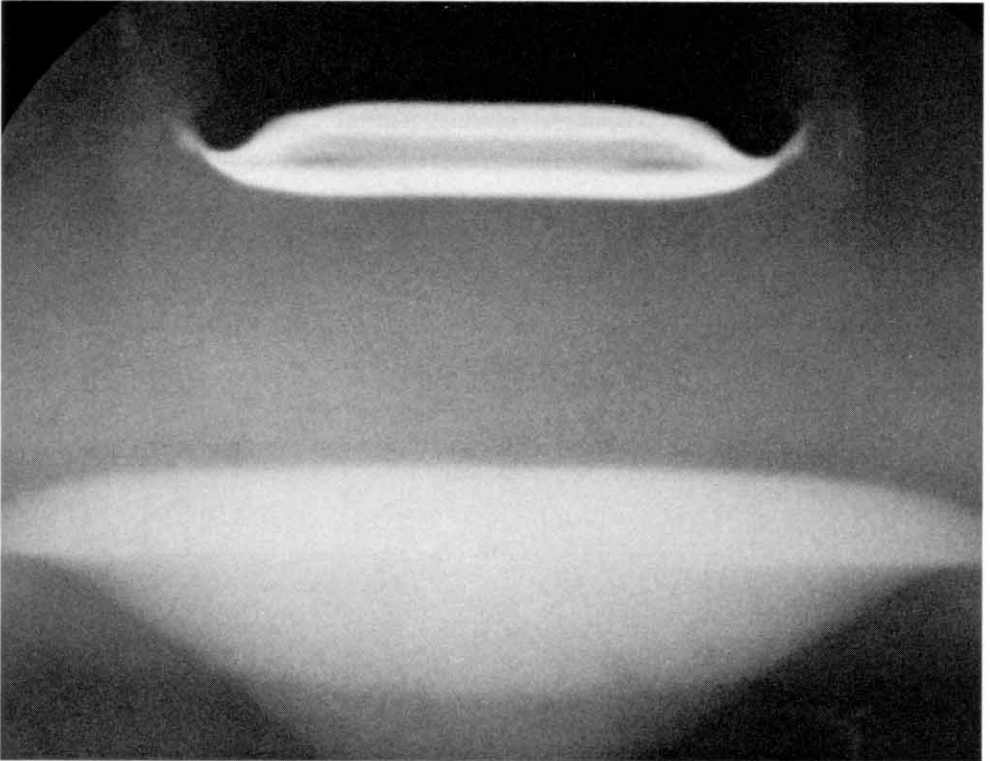
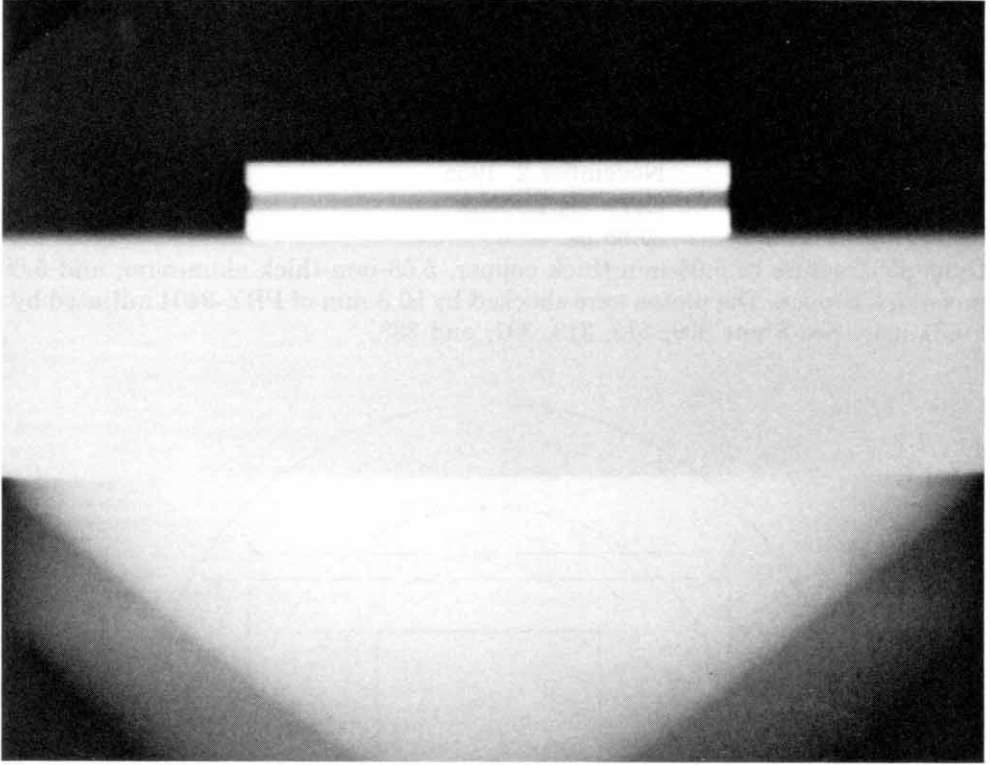
Date: October 27, 1965

Experimenter: Gary W. Rodenz

Radiographic Time: 37.52 μ s

Dynamic fracture of 5.08-mm-thick copper, 5.08-mm-thick aluminum, and 5.08-mm-thick copper. The plates were shocked by 50.8 mm of PBX-9404 initiated by a P-081 lens. See Shots 309, 312, 313, 337, and 339.





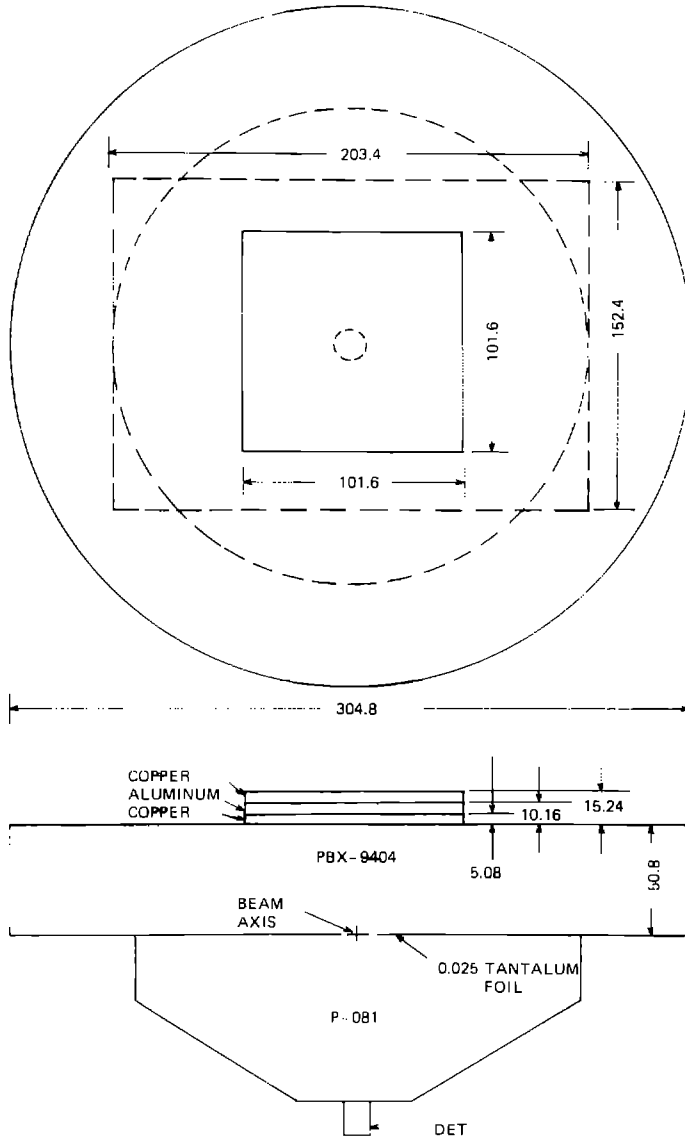
SHOT 339: Multiple Plate Fracture

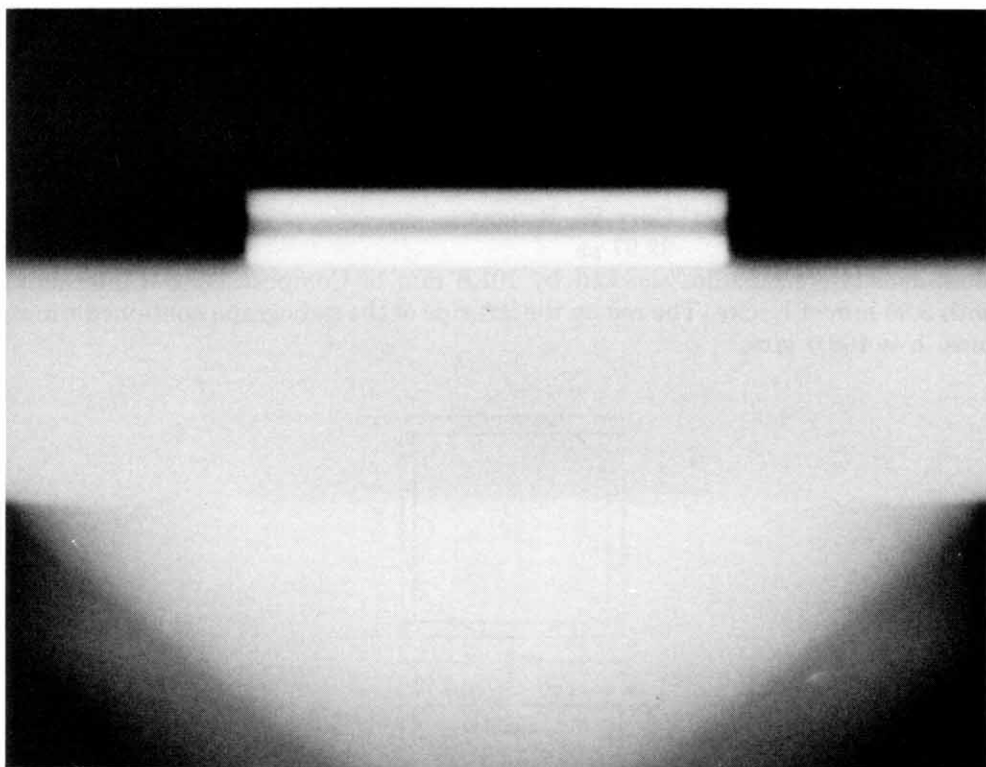
Date: November 2, 1965

Experimenter: Gary W. Rodenz

Radiographic Time: 39.88 μ s

Dynamic fracture of 5.08-mm-thick copper, 5.08-mm-thick aluminum, and 5.08-mm-thick copper. The plates were shocked by 50.8 mm of PBX-9404 initiated by a P-081 lens. See Shots 309, 312, 313, 337, and 338.





SHOT 340:

Vermiculite Shock Velocity

Date:

October 4, 1965

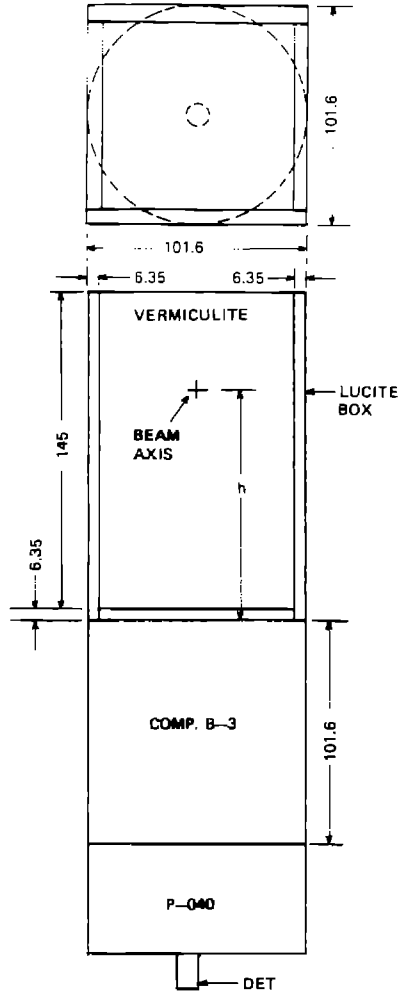
Experimenter:

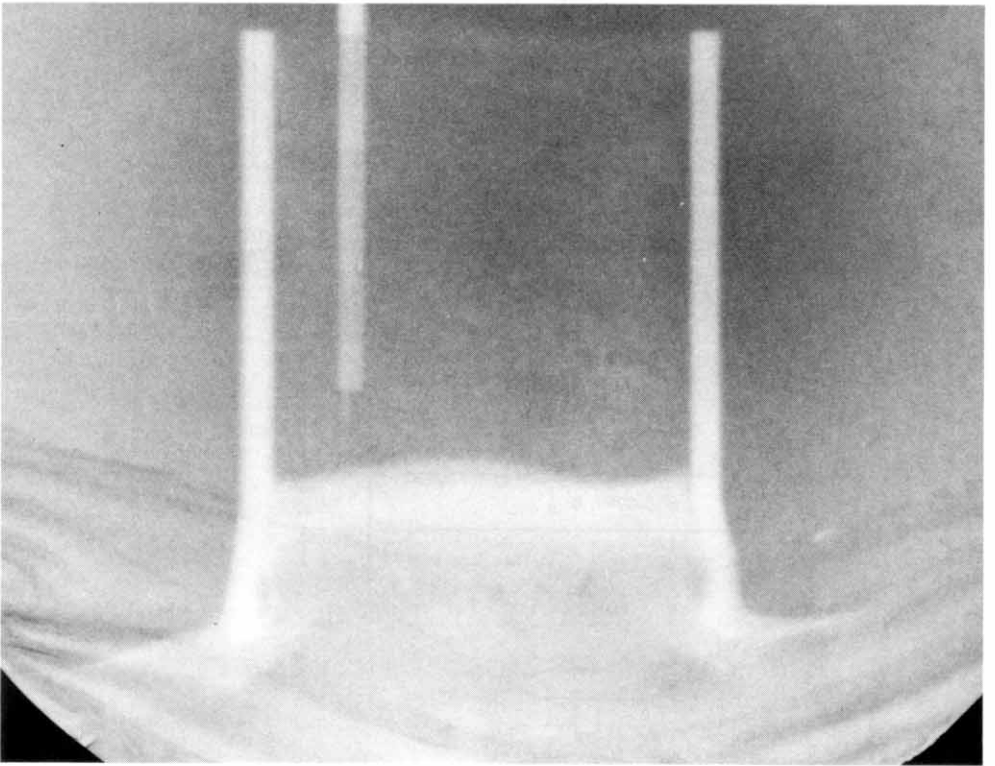
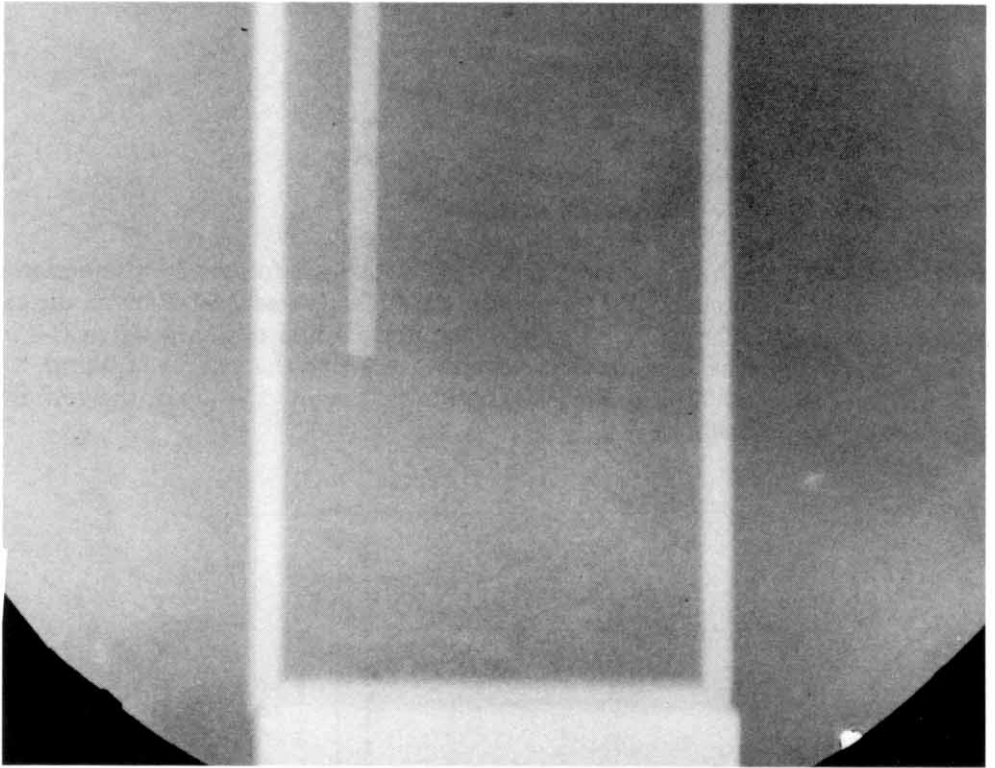
Gary W. Rodenz

Radiographic Time:

39.97 μ s

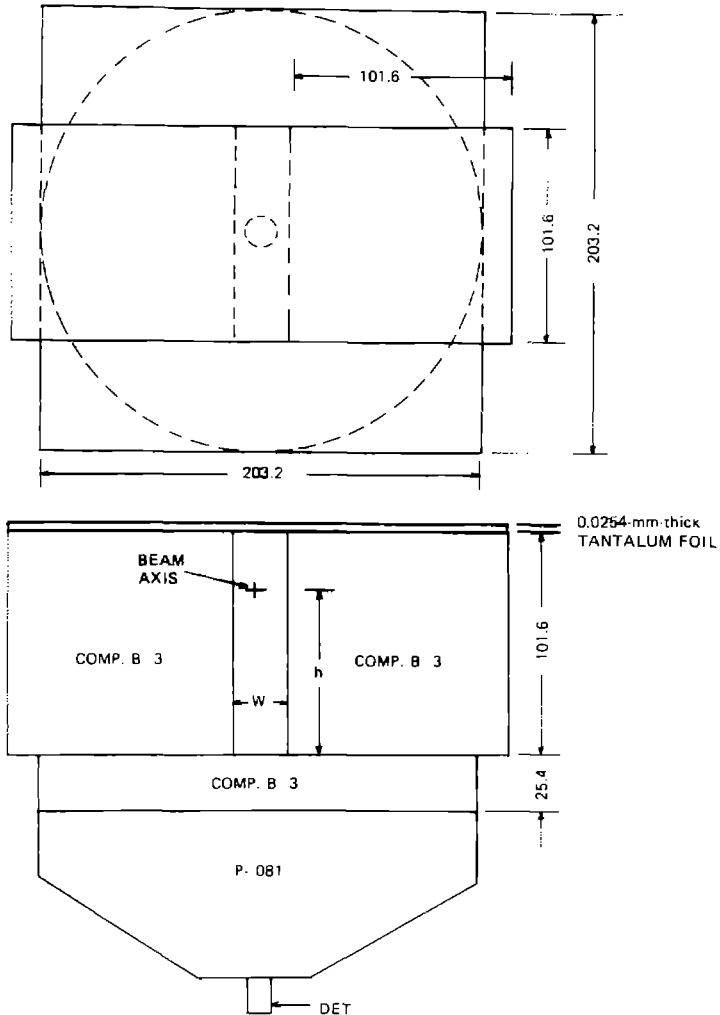
Bulk-density Vermiculite shocked by 101.6 mm of Composition B-3 interacting with 6.35 mm of Lucite. The rod on the left side of the radiograph contained timing pins. h is 108.0 mm.

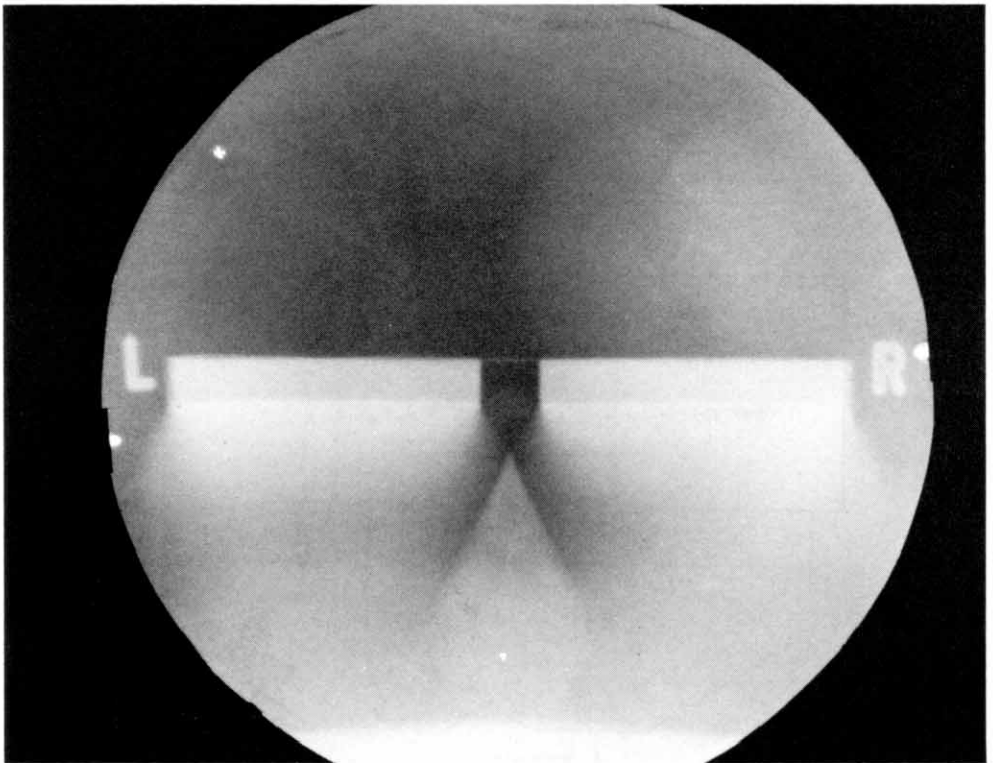
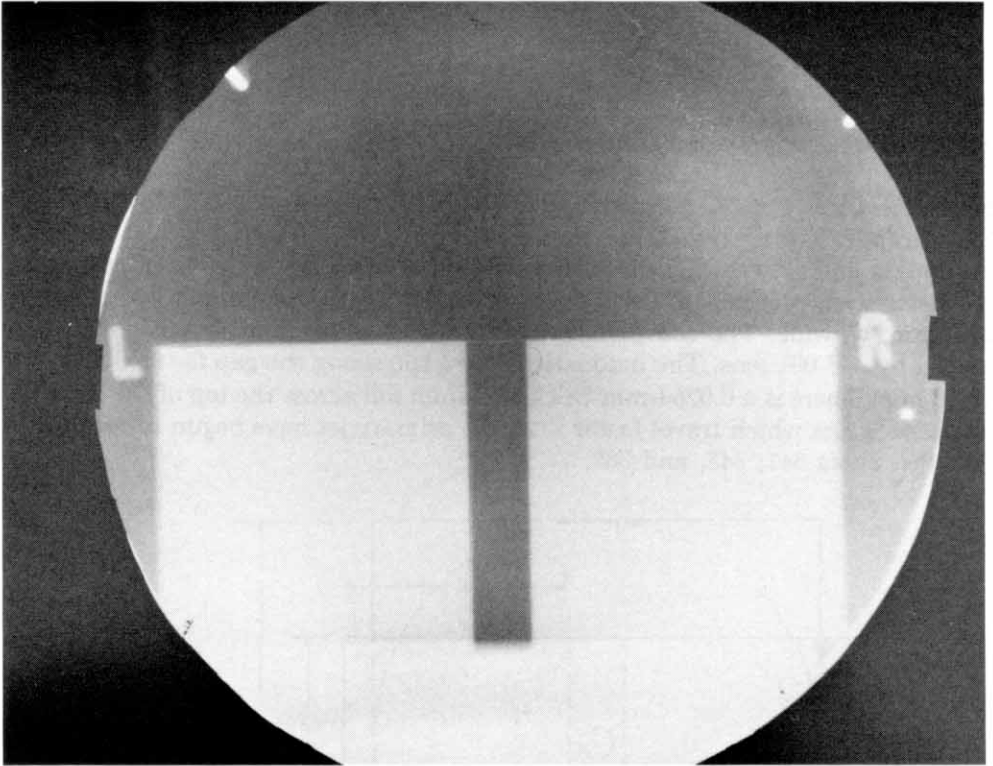




SHOT 341: **Munroe Jet**
 Date: October 19, 1965
 Experimenter: Douglas Venable
 Radiographic Time: 36.68 μ s

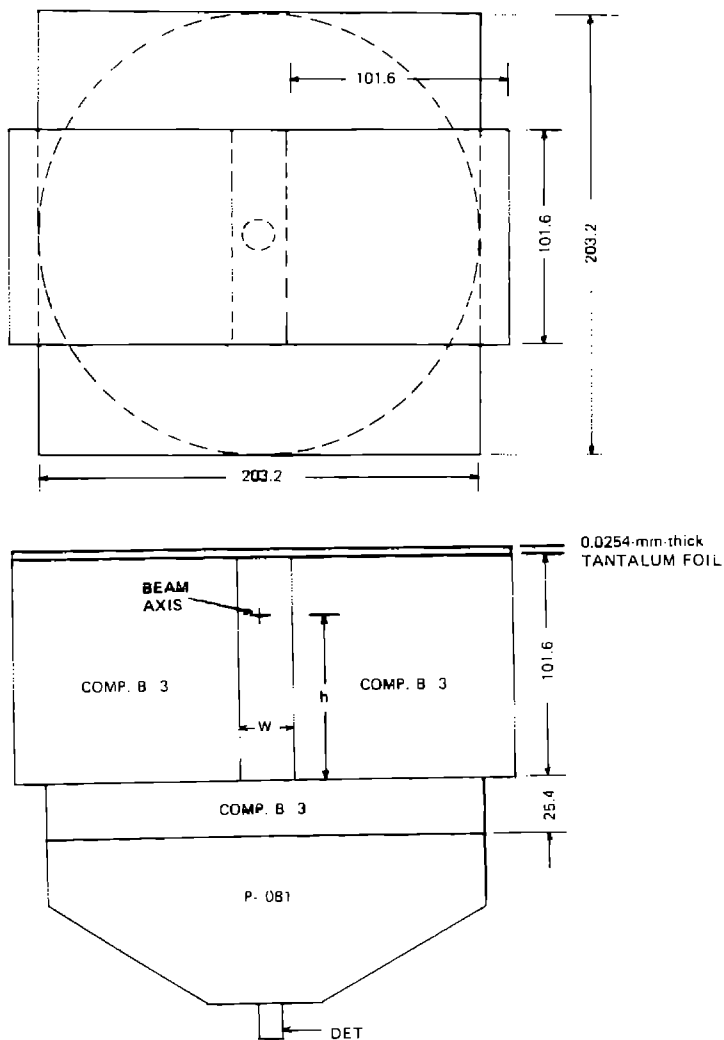
Formation and growth of gaseous Munroe jets. This jet is formed by interaction of the detonation products of two Composition B-3 charges separated by an air gap 20.0 mm, w, wide. The charges are initiated by 25.4 mm of Composition B-3 initiated by a P-081 lens. The detonations have run along the gap for 86.0 mm. h is 101.6 mm. There is 0.0254-mm-thick tantalum foil across the top of the gap. See Shots 342, 343, and 362.

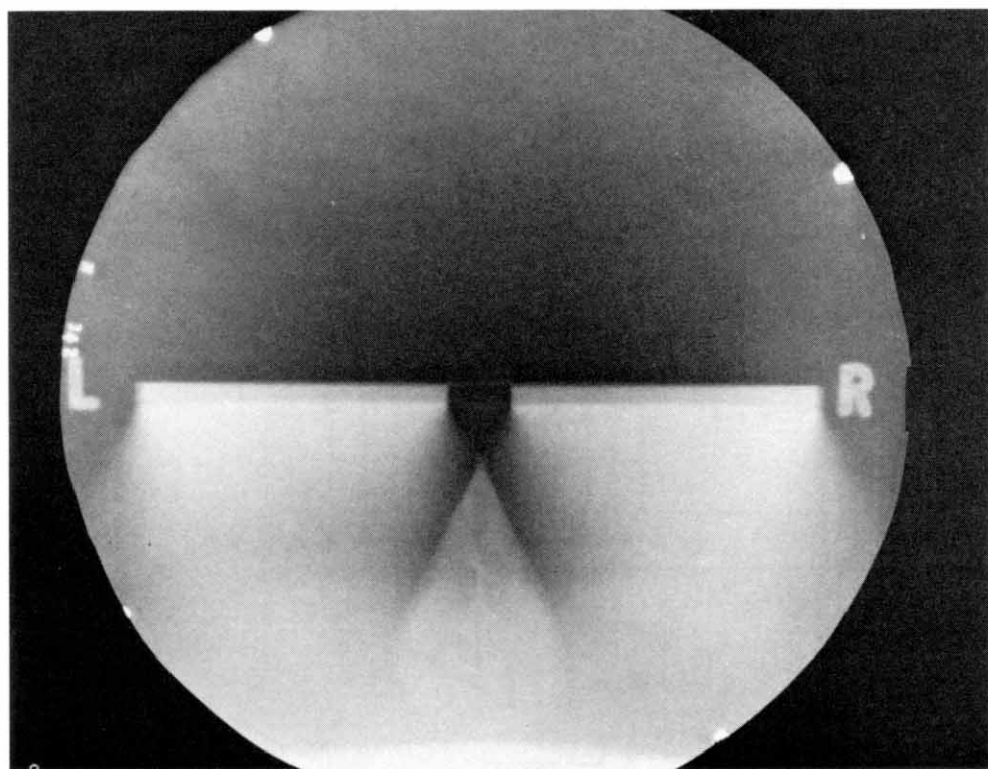
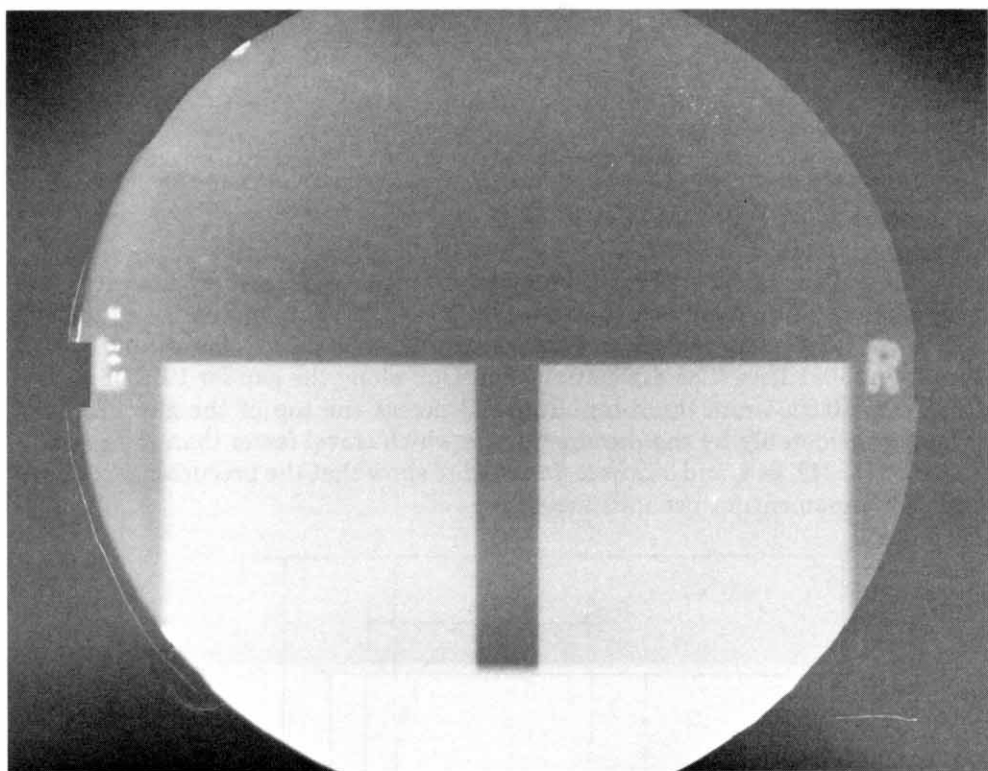




SHOT 342: Munroe Jet
 Date: October 20, 1965
 Experimenter: Douglas Venable
 Radiographic Time: 37.69 μ s

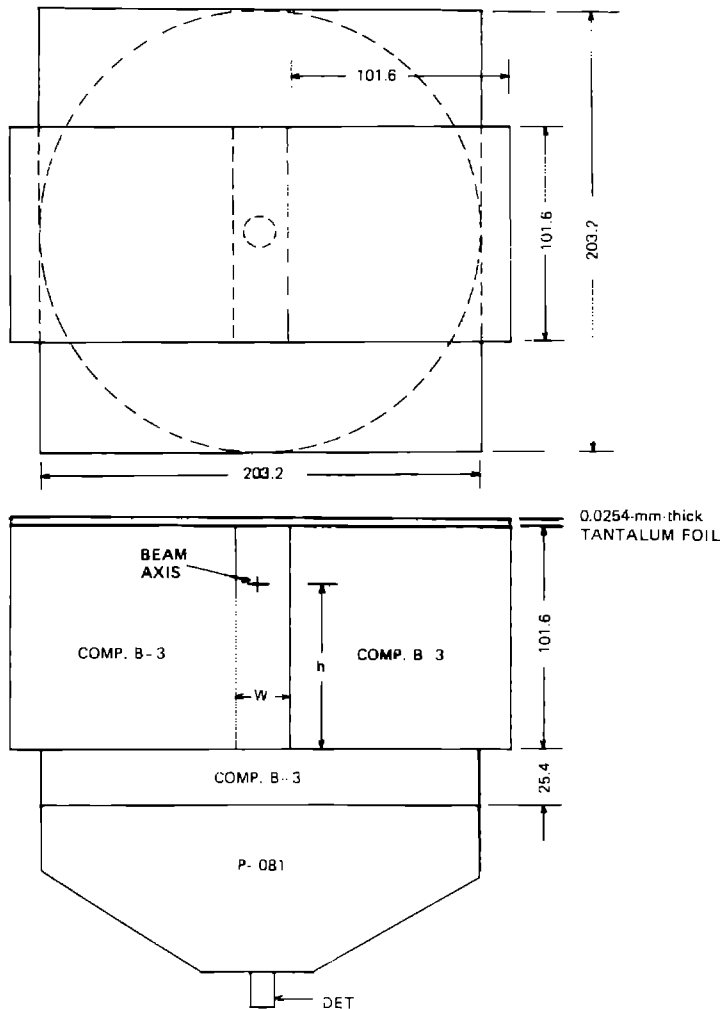
Formation and growth of gaseous Munroe jets. This jet is formed by interaction of the detonation products of two Composition B-3 charges separated by an air gap 20.0 mm, w, wide. The charges are initiated by 25.4 mm of Composition B-3 initiated by a P-081 lens. The detonations have run along the gap for 94.0 mm. h is 101.6 mm. There is a 0.0254-mm-thick tantalum foil across the top of the gap. The precursor gases which travel faster than the primary jet have begun to deform the foil. See Shots 341, 343, and 362.

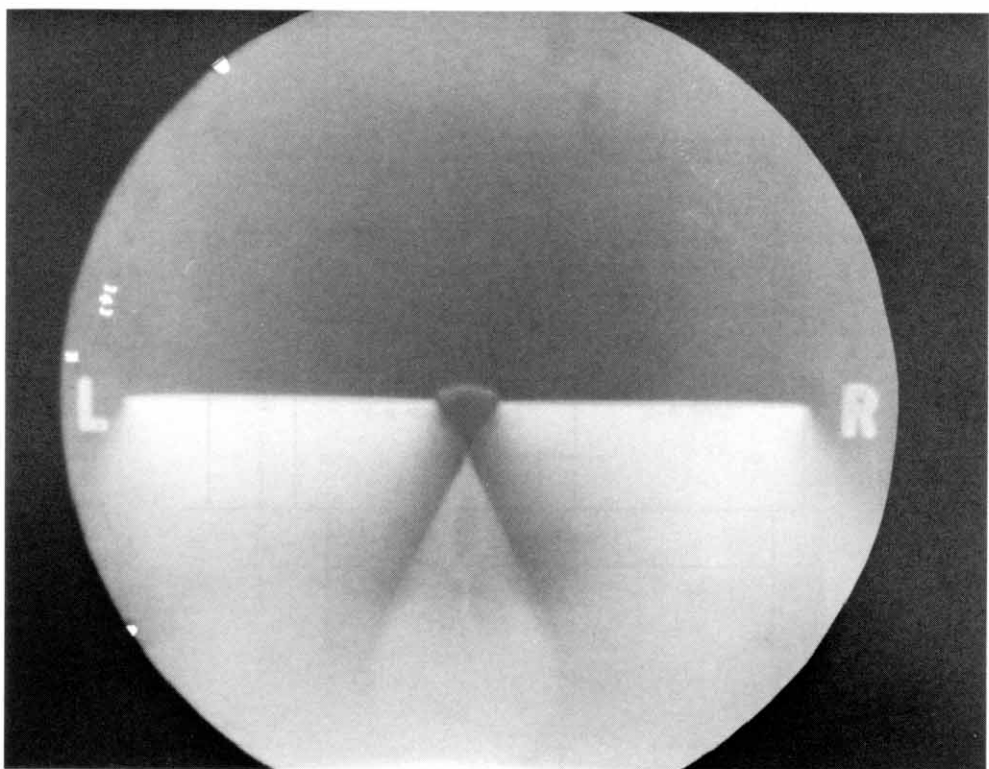
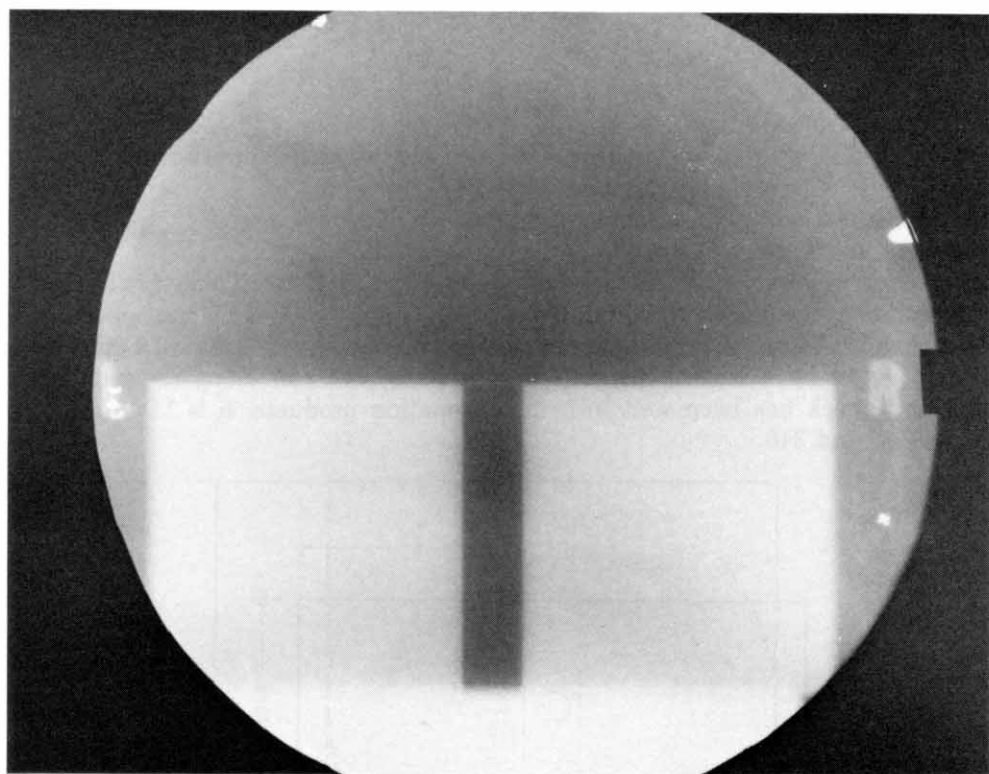




SHOT 343: **Munroe Jet**
 Date: October 26, 1965
 Experimenter: Douglas Venable
 Radiographic Time: 38.6 μ s

Formation and growth of gaseous Munroe jets. This jet is formed by interaction of the detonation products of two Composition B-3 charges separated by an air gap 20.0 mm, w, wide. The charges are initiated by 25.4 mm of Composition B-3 initiated by a P-081 lens. The detonations have run along the gap for 101.0 mm. h is 101.6 mm. A 0.0254-mm-thick tantalum foil across the top of the gap has been deformed considerably by the precursor gases which travel faster than the primary jet. Shots 341, 342, 343, and 362 were designed to show that the precursor gases have considerable momentum per unit area.





SHOT 344:

Munroe Jet Interacting with Aluminum

Date:

October 30, 1965

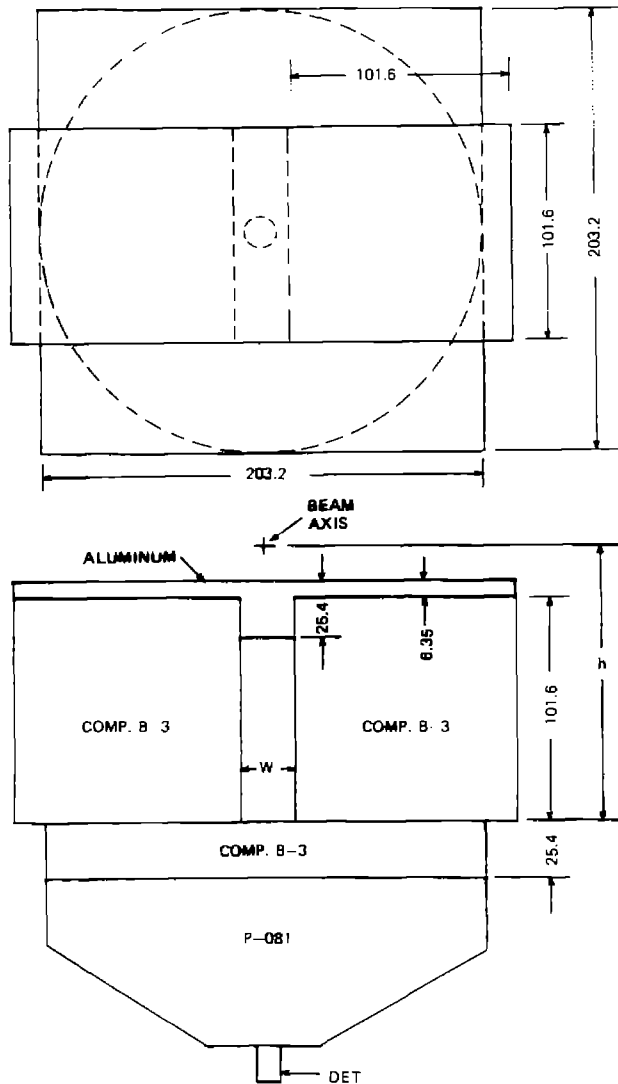
Experimenter:

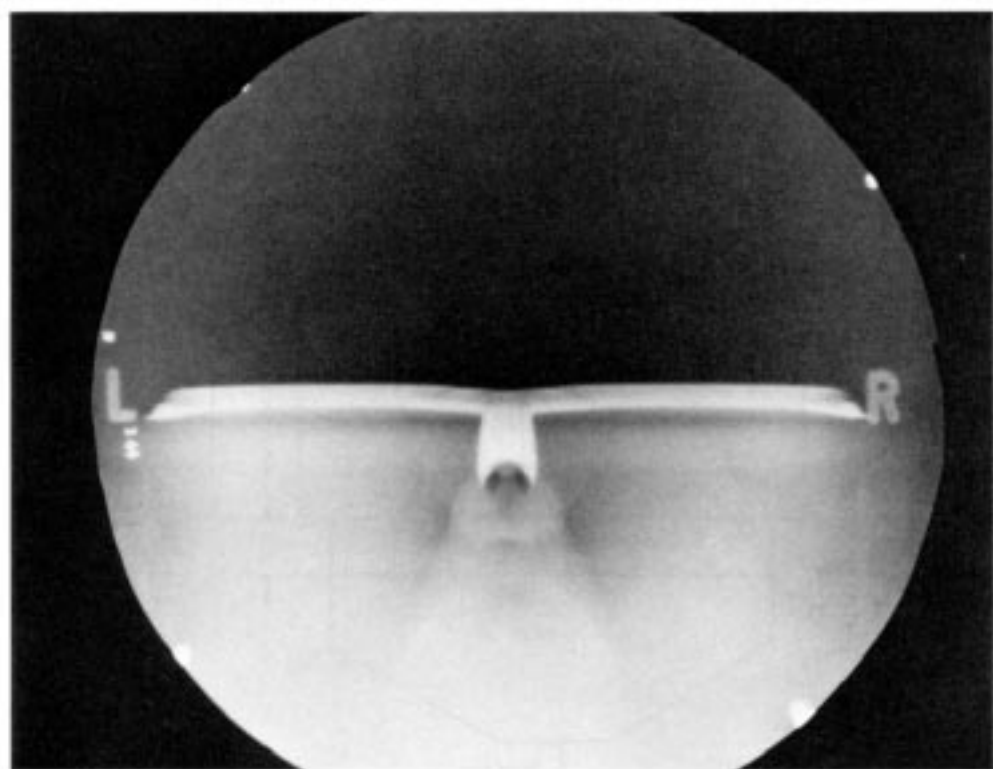
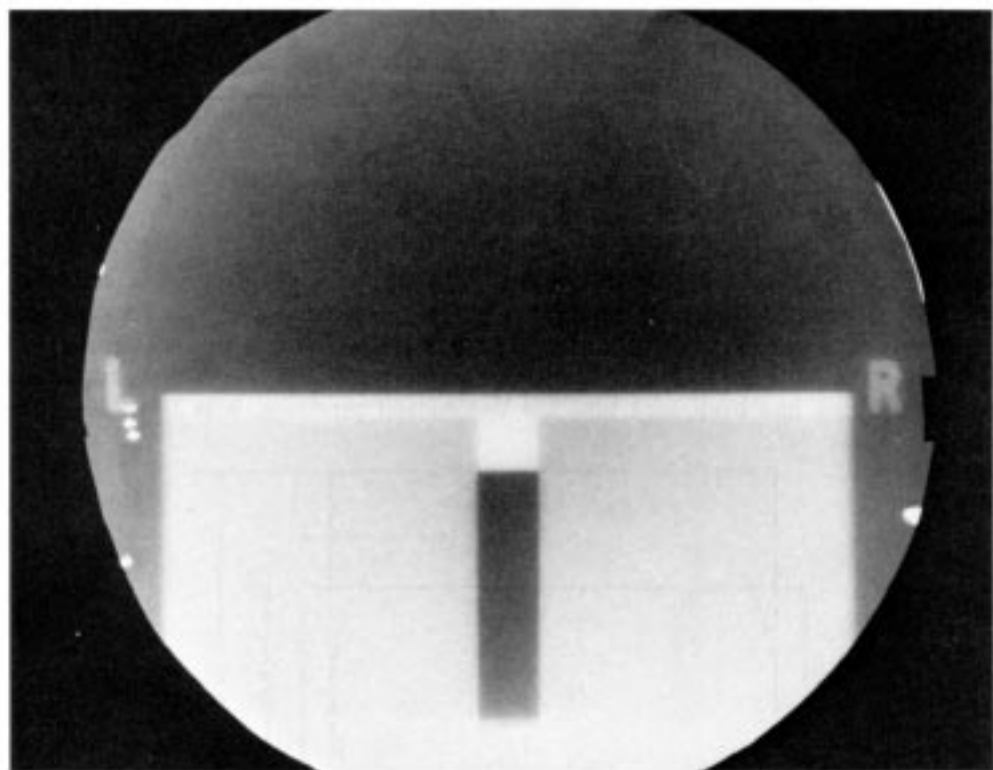
Douglas Venable

Radiographic Time:

41.65 μ s

Interaction of gaseous Munroe jets with an aluminum plate. This jet is formed by interaction of the detonation products of two Composition B-3 charges separated by an air gap 20.0 mm, w, wide. The charges are initiated by 25.4 mm of Composition B-3 initiated by a P-081 lens. The detonations have run along the gap, and a reflected shock has been sent into the detonation products. h is 114.3 mm. See Shots 345 and 346.





SHOT 345:

Munroe Jet Interacting with Aluminum

Date:

October 20, 1965

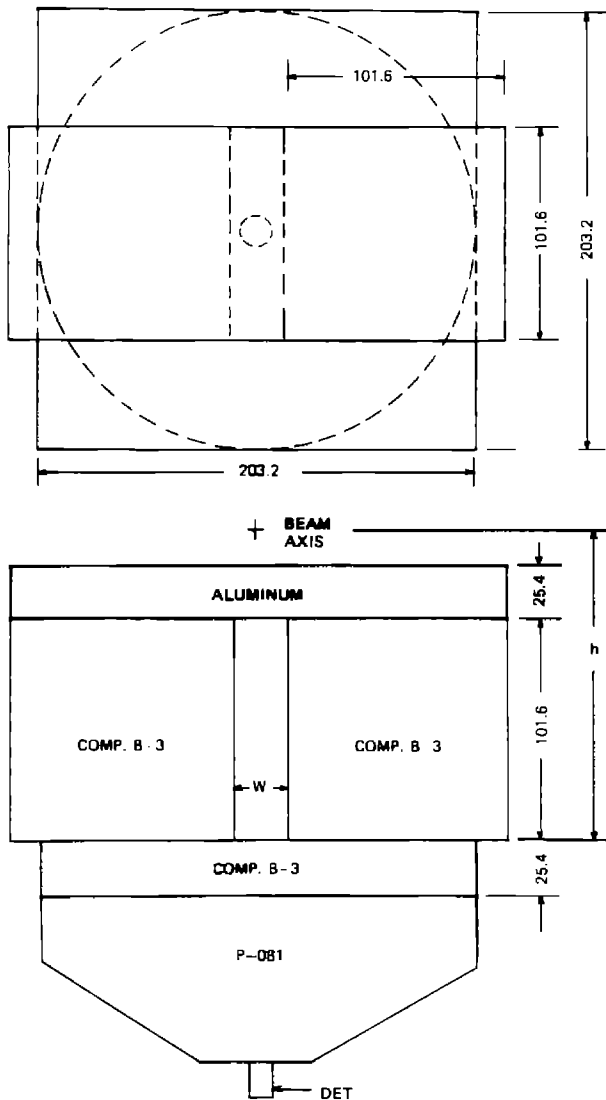
Experimenter:

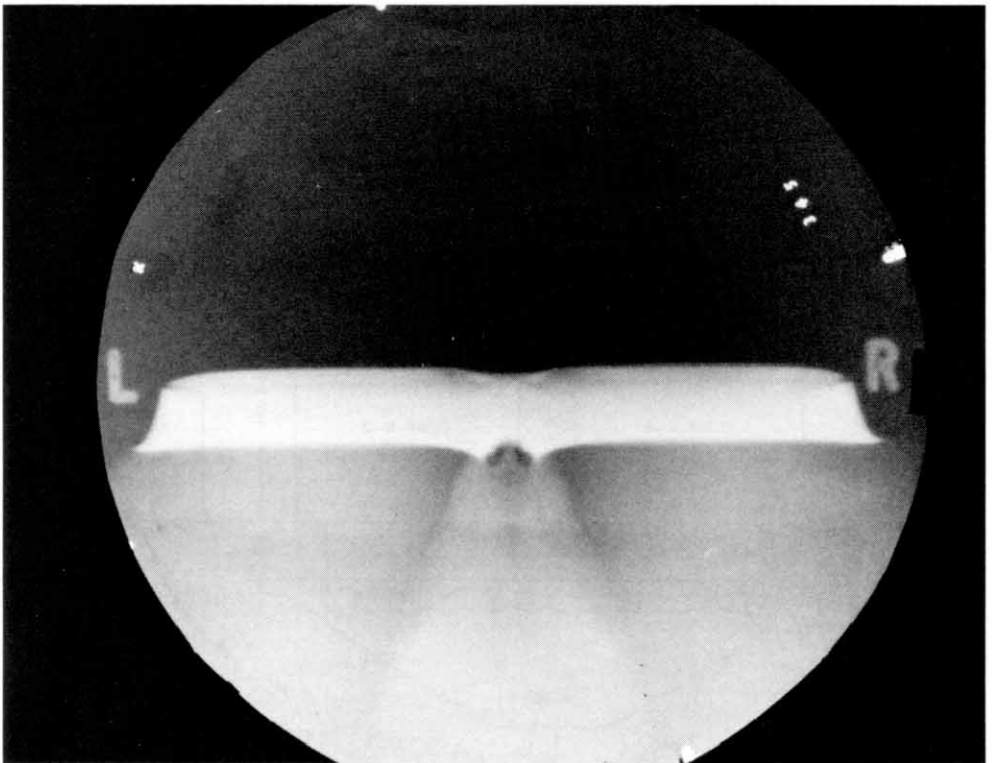
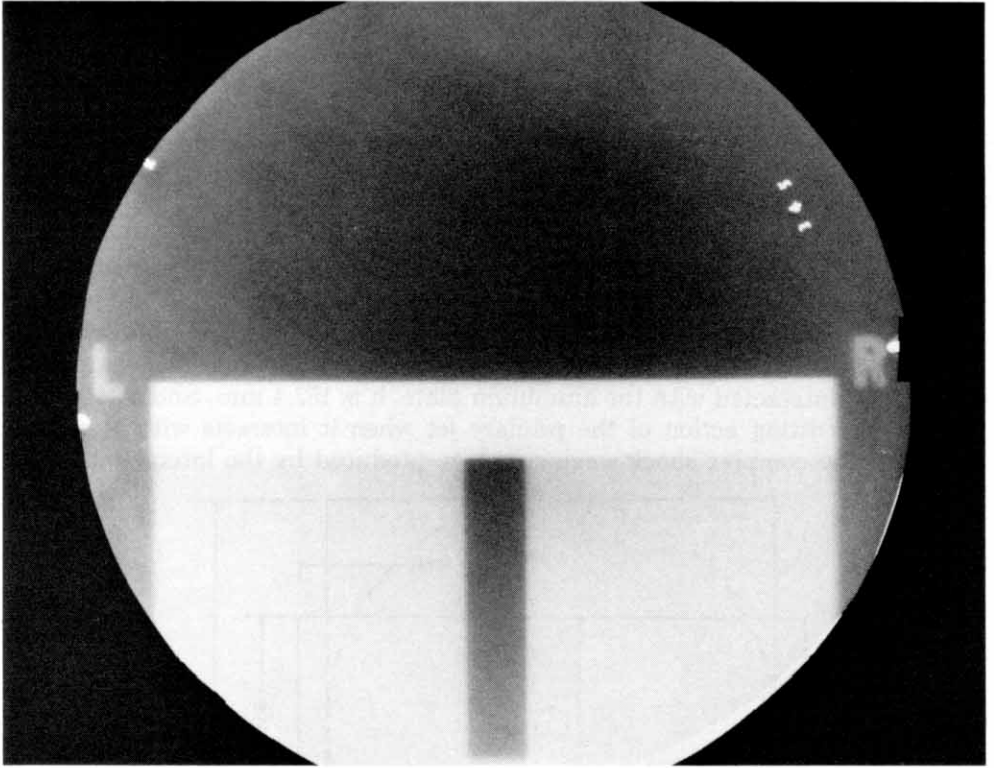
Douglas Venable

Radiographic Time:

43.97 μ s

Interaction of gaseous Munroe jets with an aluminum plate. This jet is formed by interaction of the detonation products of two Composition B-3 charges separated by an air gap 20.0 mm, w, wide. The charges are initiated by 25.4 mm of Composition B-3 initiated by a P-081 lens. The detonations have run along the gap, and a reflected shock has been sent into the detonation products. h is 133.3 mm. See Shots 343 and 346.





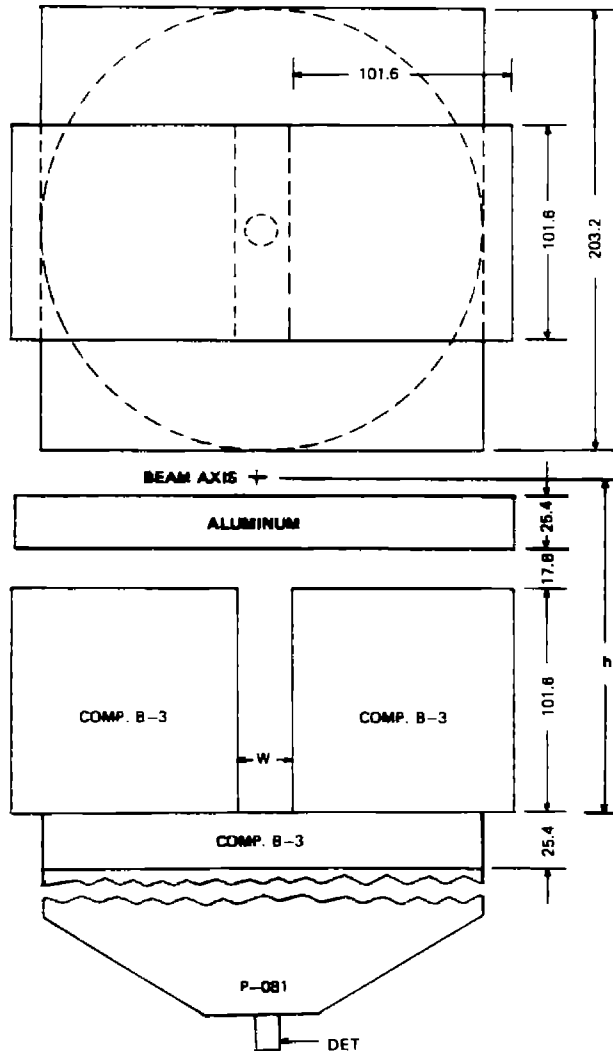
SHOT 346: Munroe Jet Interacting with Aluminum

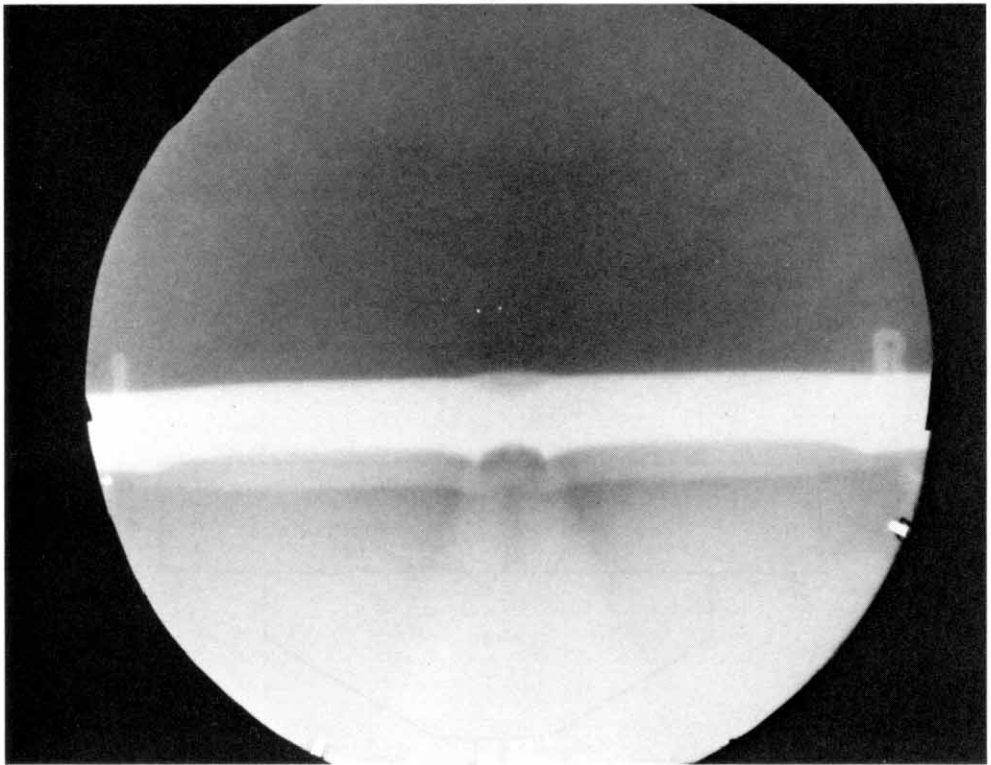
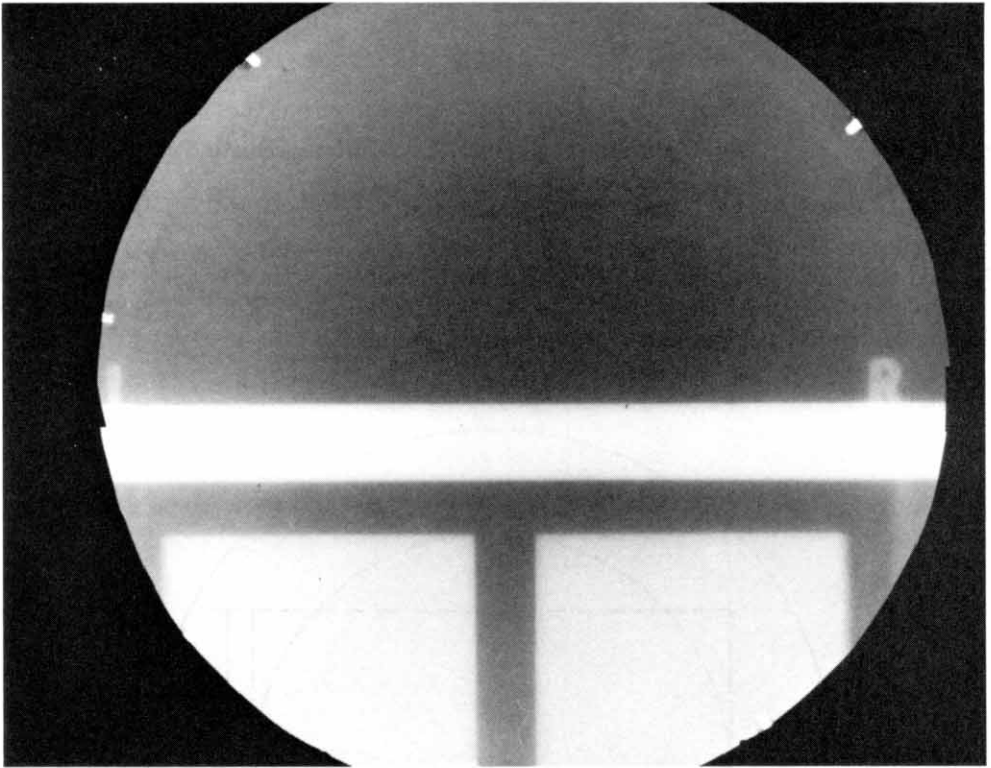
Date: October 26, 1965

Experimenter: Douglas Venable

Radiographic Time: 45.97 μ s

Interaction of gaseous Munroe jets with an aluminum plate 17.78 mm above the charges. This jet is formed by interaction of the detonation products of two Composition B-3 charges separated by an air gap 20.0 mm, w, wide. The charges are initiated by 25.4 mm of Composition B-3 initiated by a P-081 lens. The detonations and jet have interacted with the aluminum plate. h is 152.4 mm. Shots 344-346 illustrate the cutting action of the primary jet when it interacts with aluminum plates and the complex shock wave structure produced by the interaction.





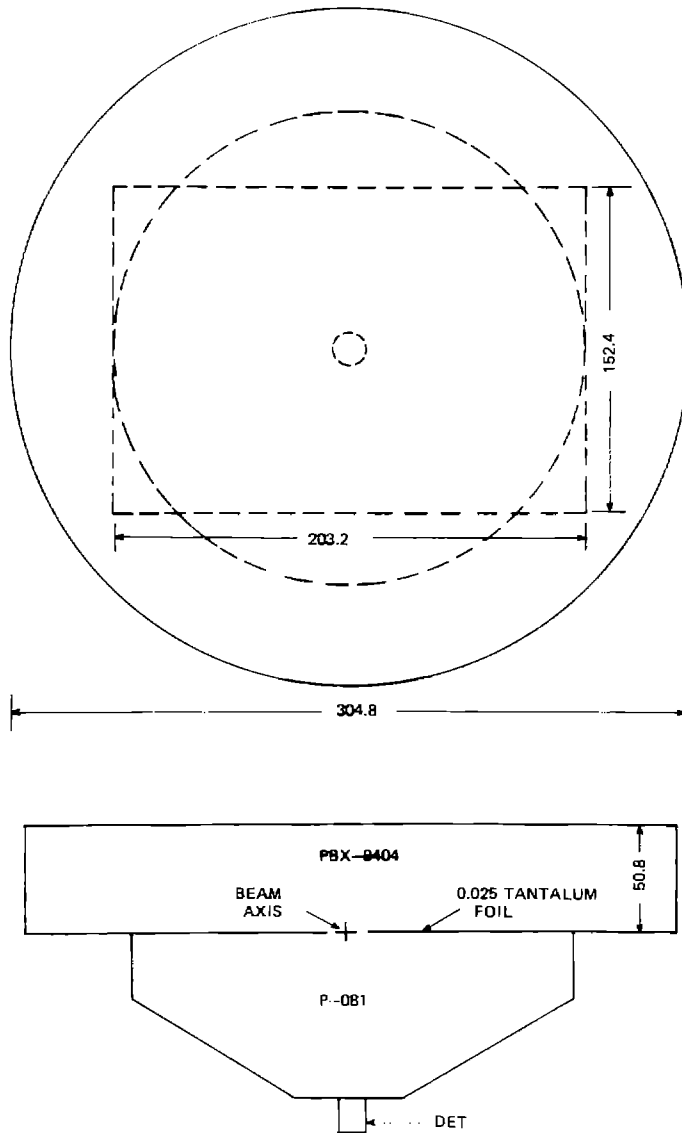
SHOT 347: Explosive Driver for Multiple Plate Fracture

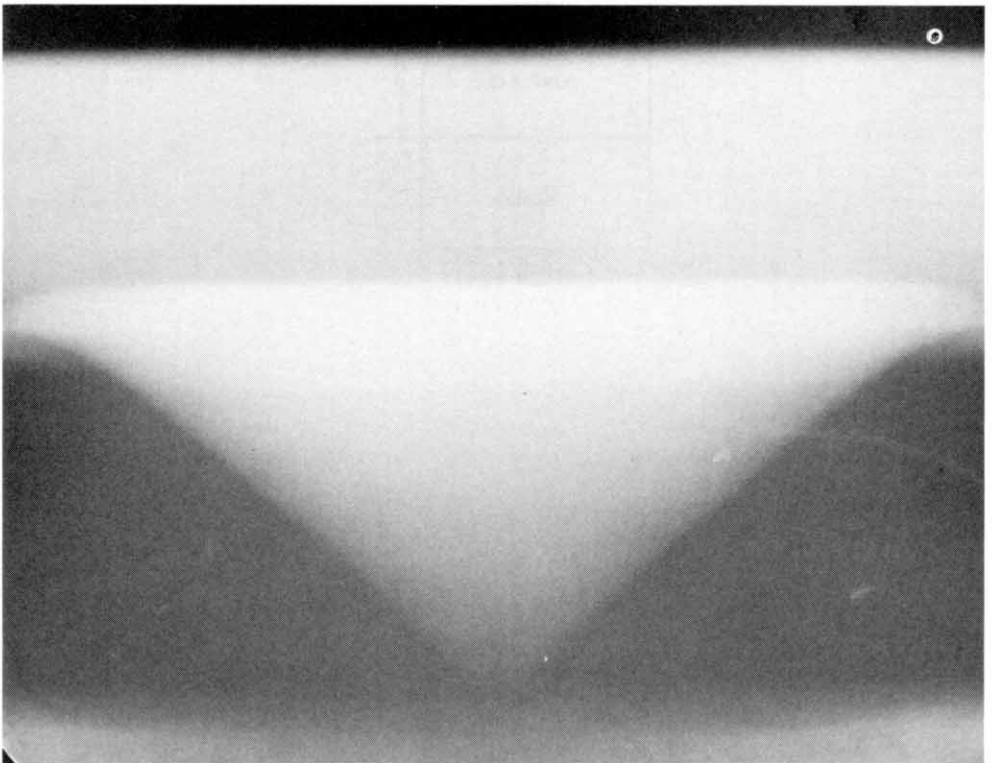
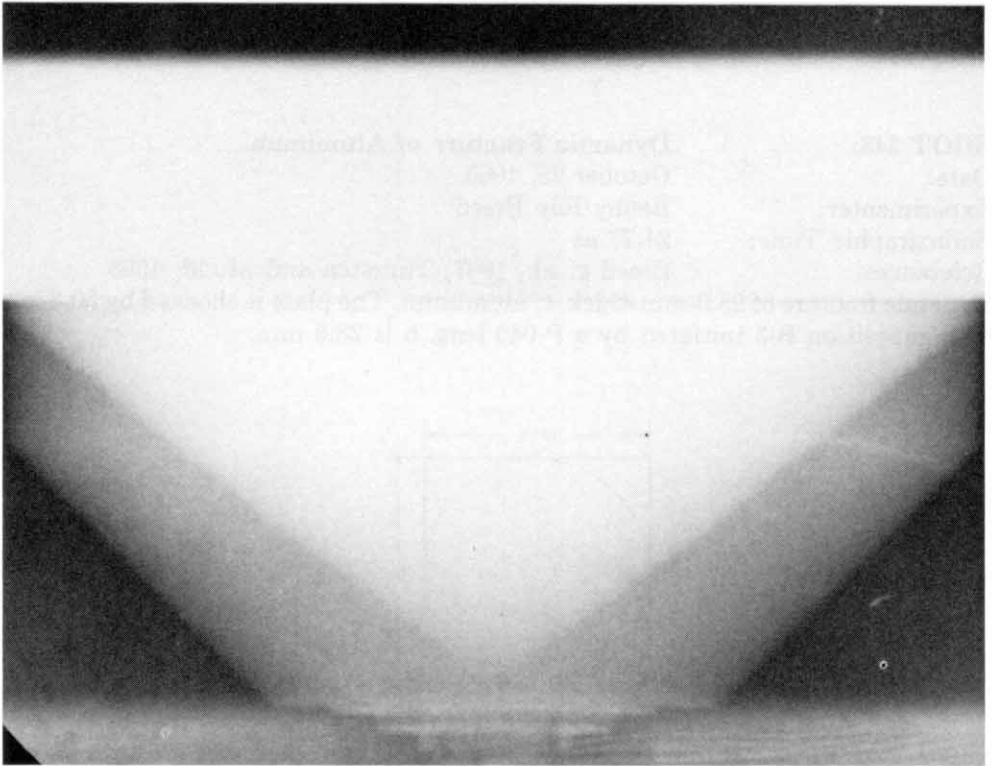
Date: October 19, 1965

Experimenter: Gary W. Rodenz

Radiographic Time: 28.53 μ s

A 50.8-mm-thick slab of PBX-9404 initiated by a P-081 lens was used to drive the multiple plate fracture shots 308-313 and 335-339. See Shot 334 for a later time. The detonation wave has reached the top surface of the PBX-9404.





SHOT 348:

Dynamic Fracture of Aluminum

Date:

October 25, 1965

Experimenter:

Benny Ray Breed

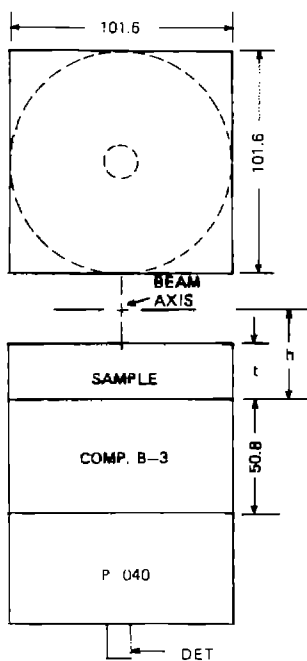
Radiographic Time:

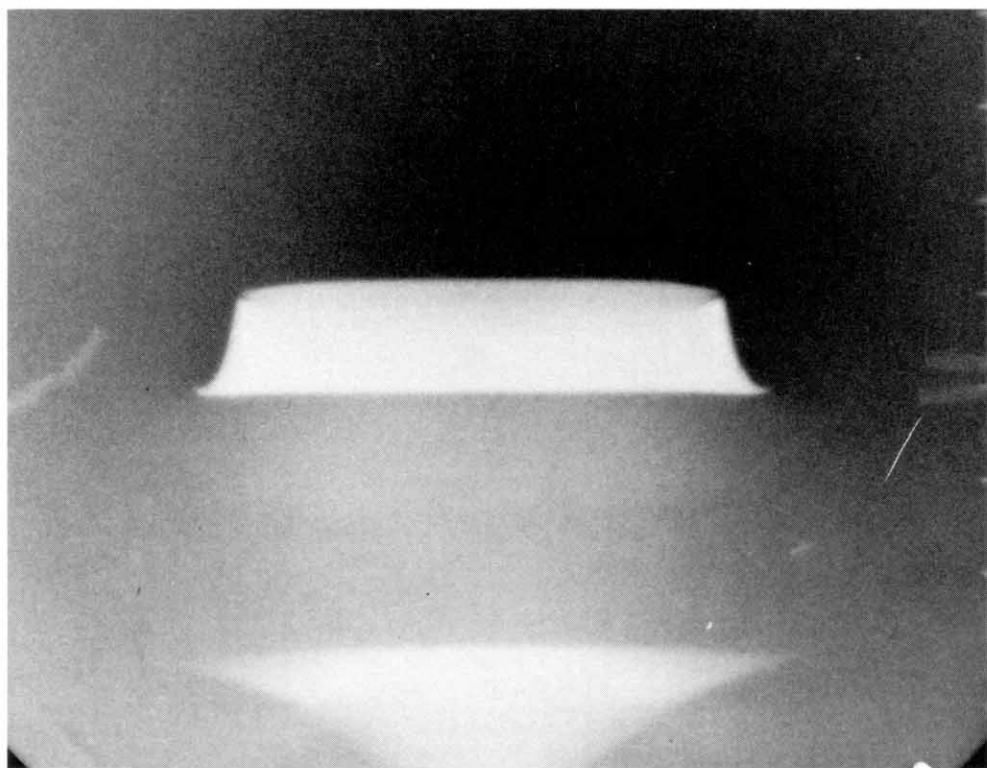
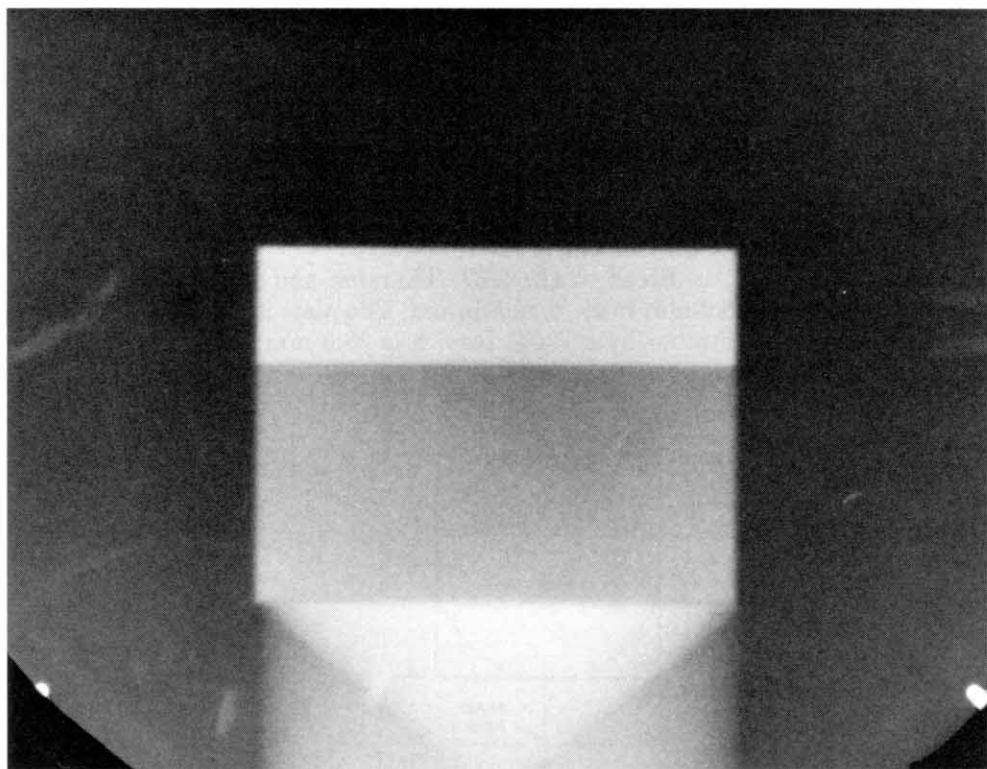
24.77 μ s

References:

Breed et al., 1967; Thurston and Mudd, 1968

Dynamic fracture of 25.0-mm-thick, t , aluminum. The plate is shocked by 50.8 mm of Composition B-3 initiated by a P-040 lens. h is 28.6 mm.





SHOT 349:

Dynamic Fracture of Aluminum

Date:

October 26, 1965

Experimenter:

Benny Ray Breed

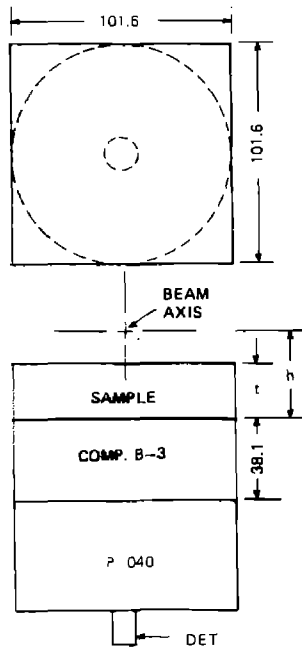
Radiographic Time:

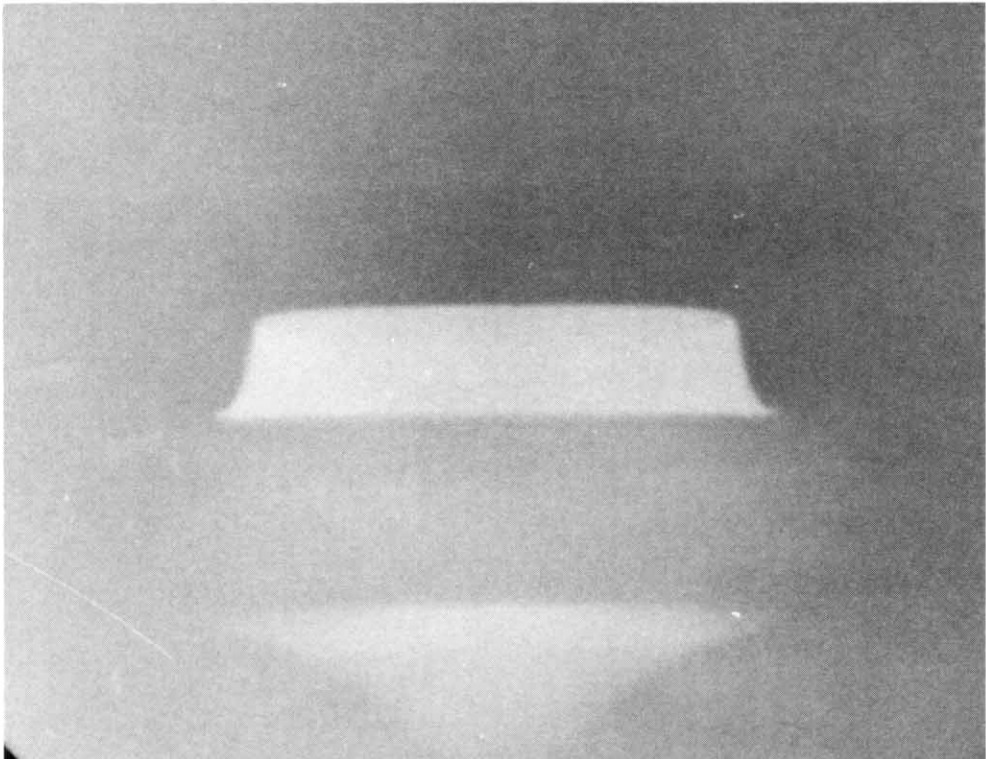
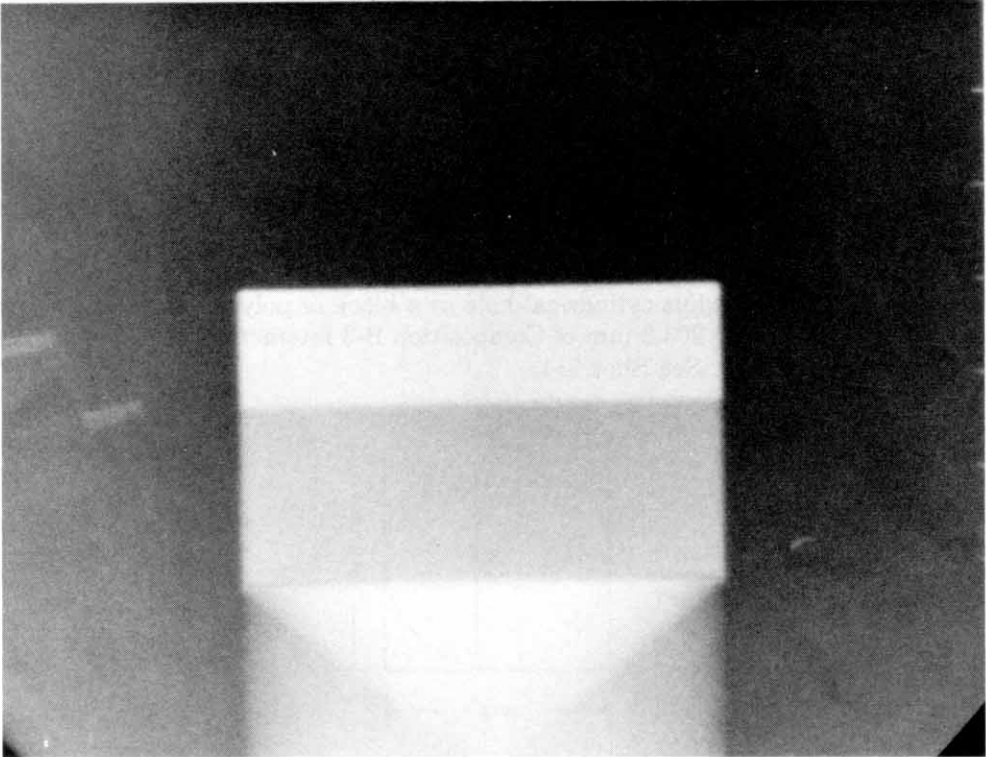
23.02 μ s

References:

Breed et al., 1967; Thurston and Mudd, 1968

Dynamic fracture of 25.0-mm thick, t , aluminum. The plate is shocked by 38.1 mm of Composition B-3 initiated by a P-040 lens. h is 28.6 mm.





SHOT 351:

Cylindrical Hole in Polyethylene

Date:

October 26, 1965

Experimenter:

Roger W. Taylor

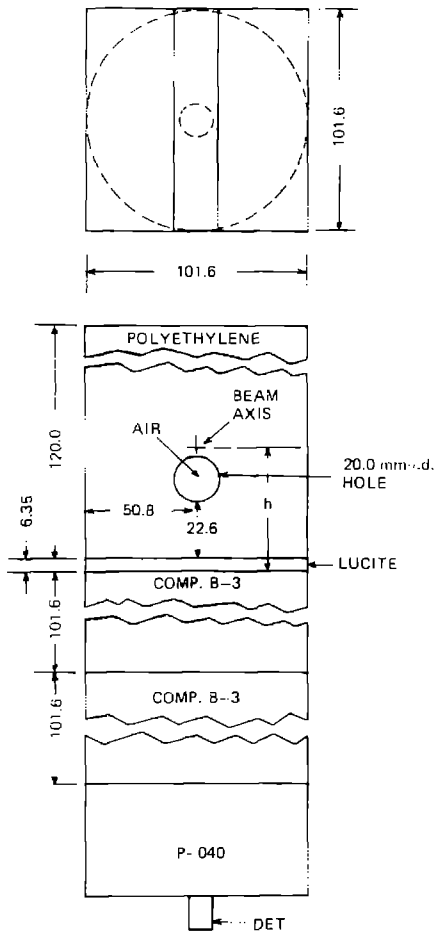
Radiographic Time:

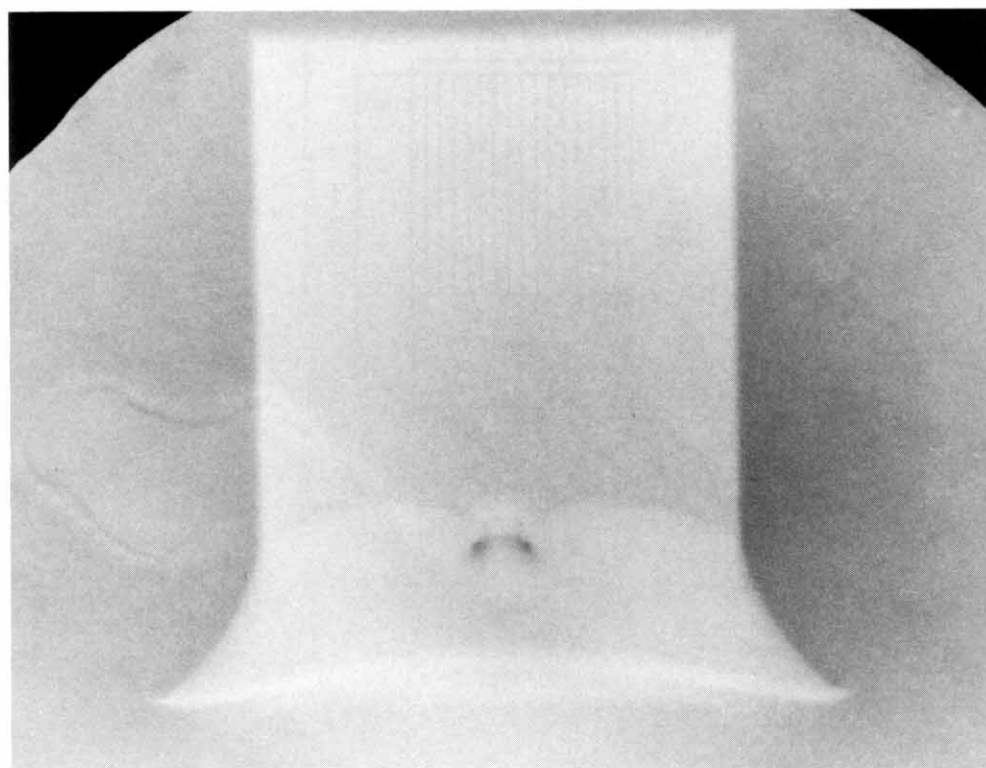
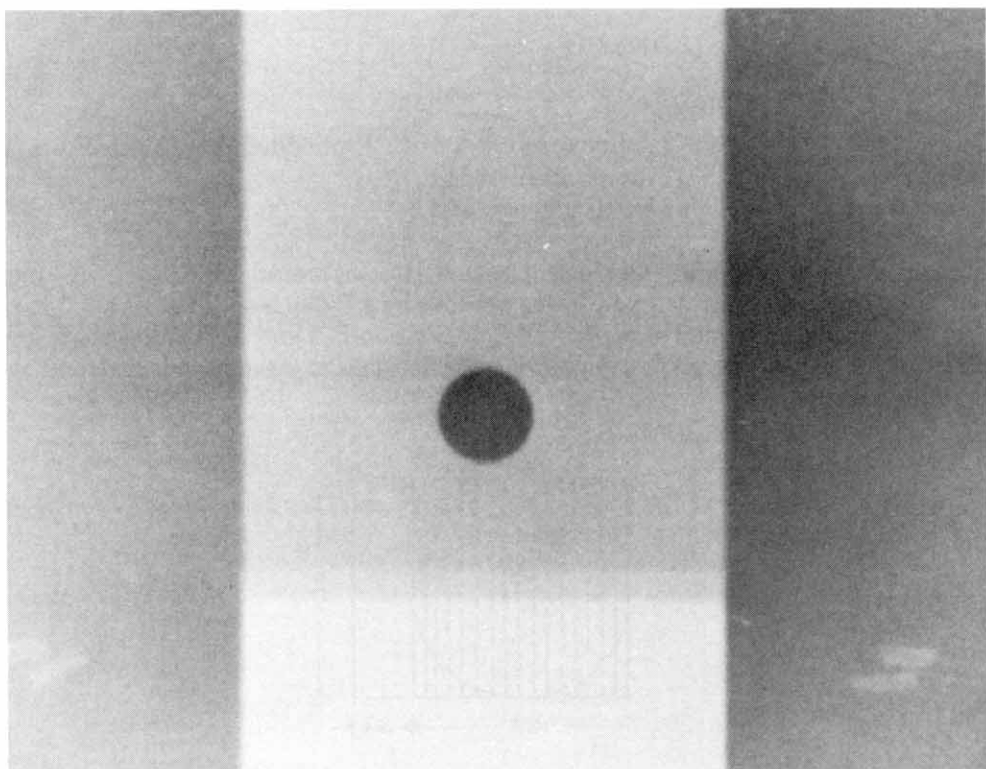
47.68 μ s

References:

Mader et al., 1967; Mader and Kershner, 1972

Study of a 10.0-mm-radius cylindrical hole in a block of polyethylene. The shock wave was generated by 203.2 mm of Composition B-3 interacting with 6.35 mm of Lucite. h is 46.03 mm. See Shot 314.





SHOT 352:

Composition B-3 with Embedded Tantalum Foils

Date:

November 8, 1965

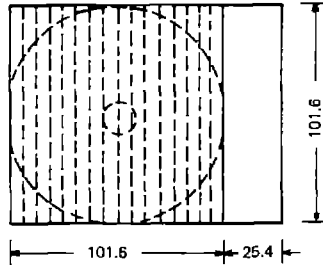
Experimenter:

Douglas Venable

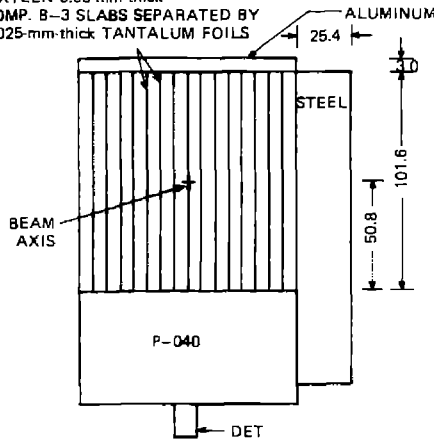
Radiographic Time:

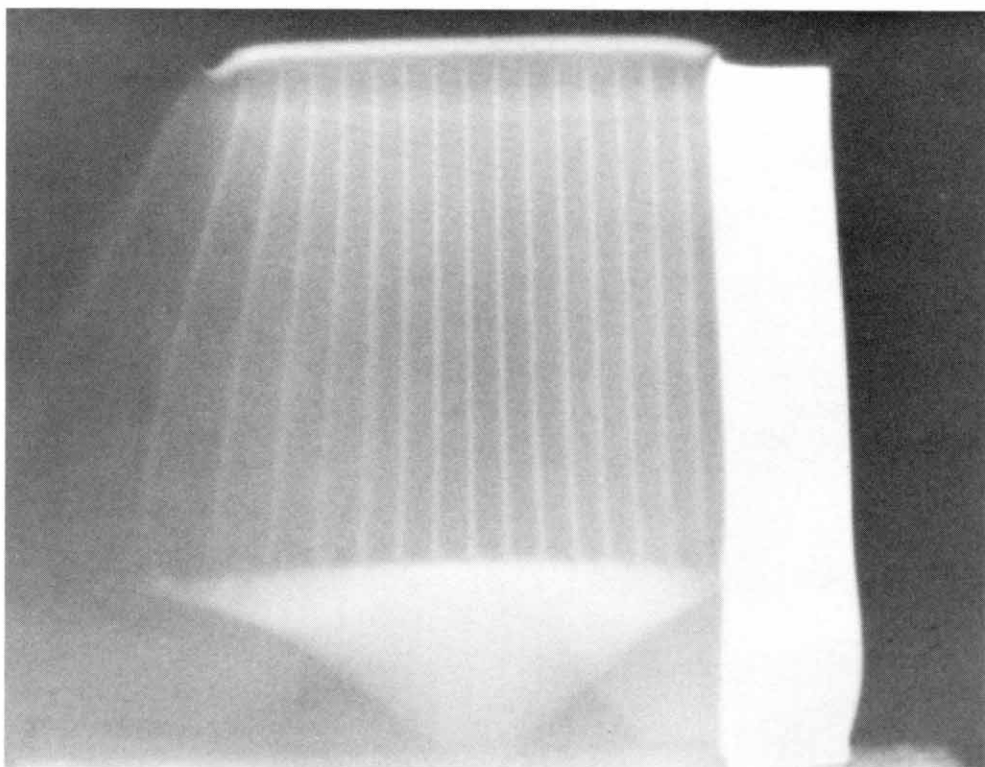
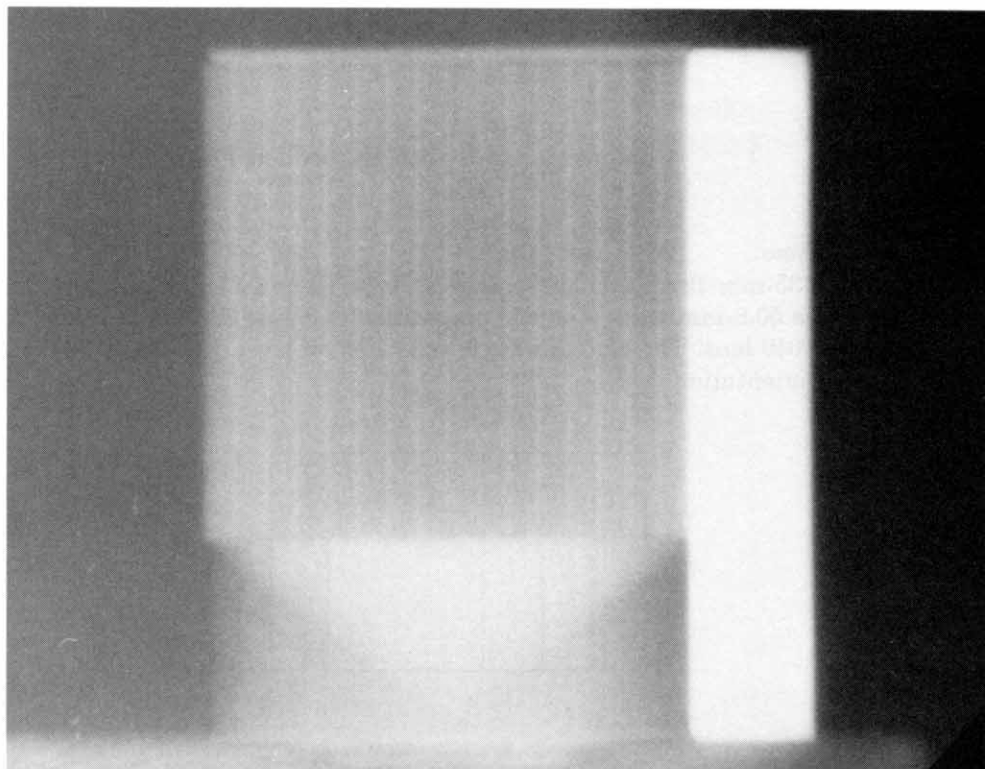
28.8 μ s

Sixteen slabs of 6.35-mm-thick Composition B-3 separated by 0.0254-mm-thick tantalum foils were initiated parallel to the foils by a P-040 lens. There is a 3.0-mm-thick aluminum plate on the top of the Composition B-3 and a 25.4-mm-thick iron plate on one side of the explosive charge. The detonation wave has reflected off the aluminum plate.



SIXTEEN 6.35-mm-thick
COMP. B-3 SLABS SEPARATED BY
0.0254-mm-thick TANTALUM FOILS





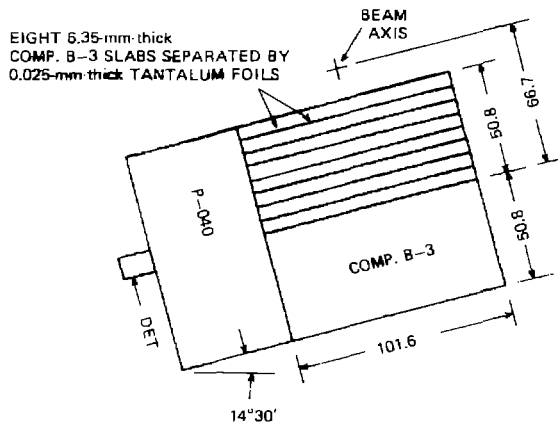
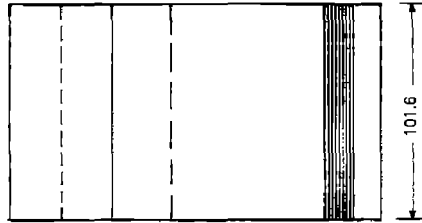
SHOT 353: Composition B-3 with Embedded Foils

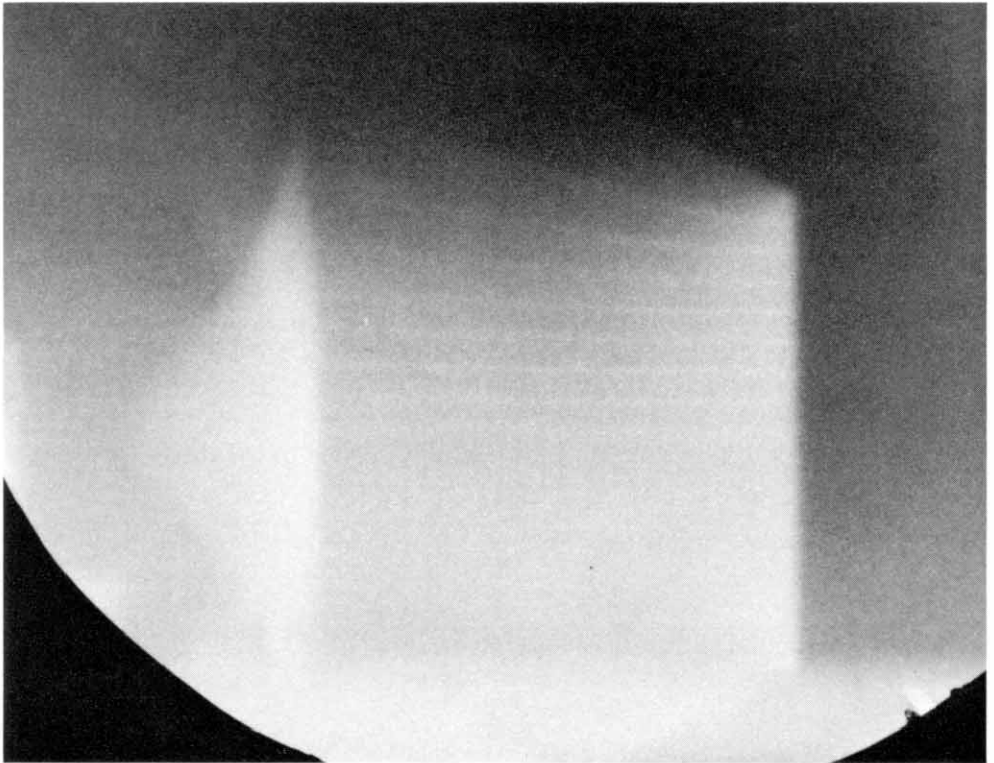
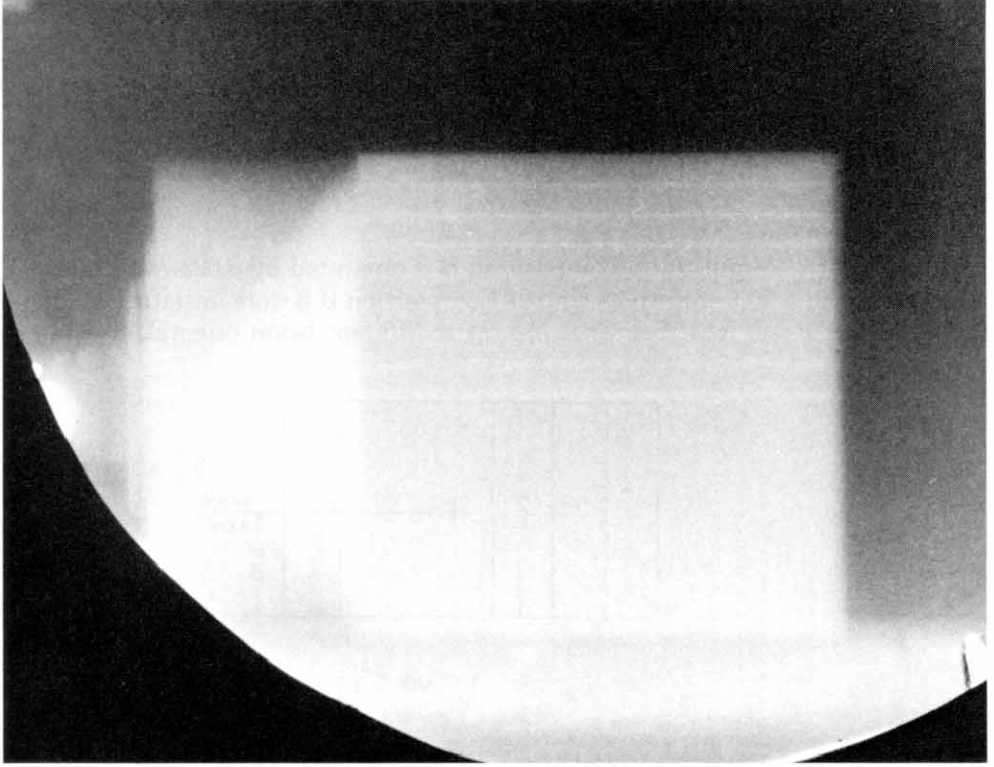
Date: November 9, 1965

Experimenter: Douglas Venable

Radiographic Time: 26.41 μ s

Eight slabs of 6.35-mm-thick Composition B-3 separated by 0.0254-mm-thick tantalum foils and a 50.8-mm-thick slab of Composition B-3 were initiated parallel to the foils by a P-040 lens. The charge was placed 14.5° off level. See Shot 354 for a different beam orientation.





SHOT 354:

Composition B-3 with Embedded Foils

Date:

November 10, 1965

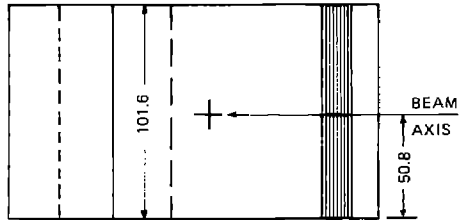
Experimenter:

Douglas Venable

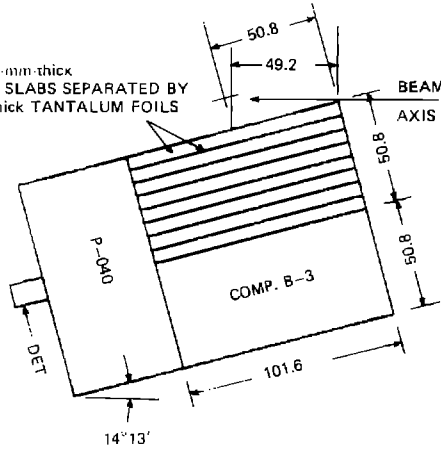
Radiographic Time:

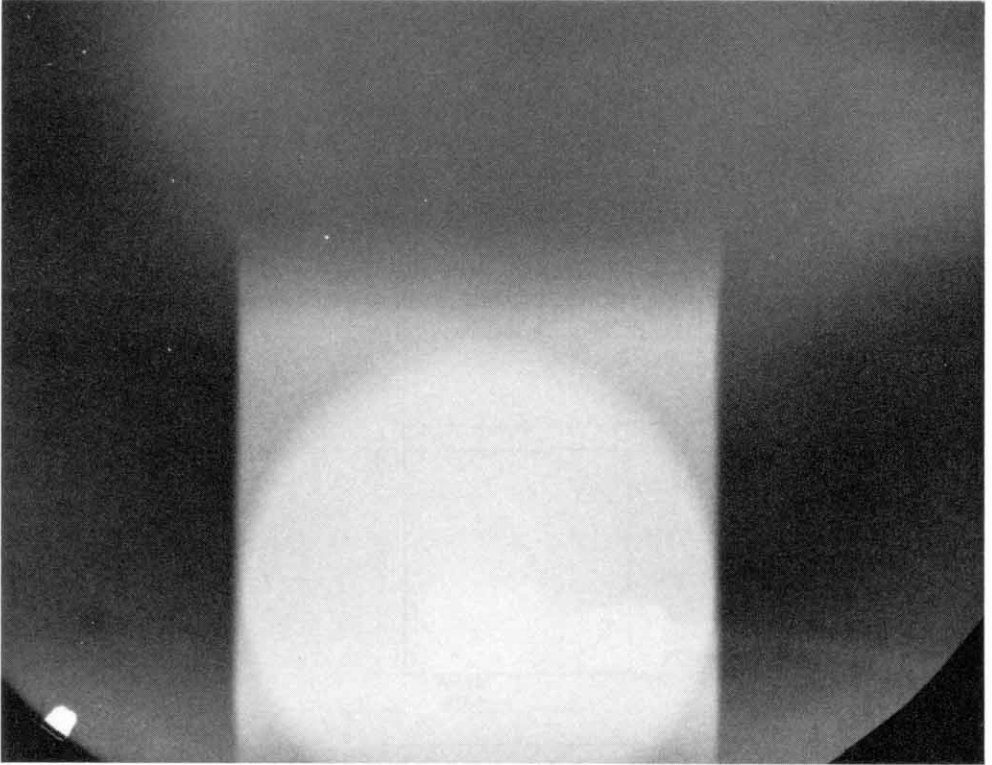
26.42 μ s

Eight slabs of 6.35-mm-thick Composition B-3 separated by 0.025-mm-thick tantalum foils and a 50.8-mm-thick slab of Composition B-3 were initiated parallel to the foils by a P-040 lens. See Shot 353 for a different beam orientation.



EIGHT 6.35-mm-thick
COMP. B-3 SLABS SEPARATED BY
0.025-mm-thick TANTALUM FOILS





SHOT 355:

Dynamic Fracture of Aluminum

Date:

November 9, 1965

Experimenter:

Benny Ray Breed

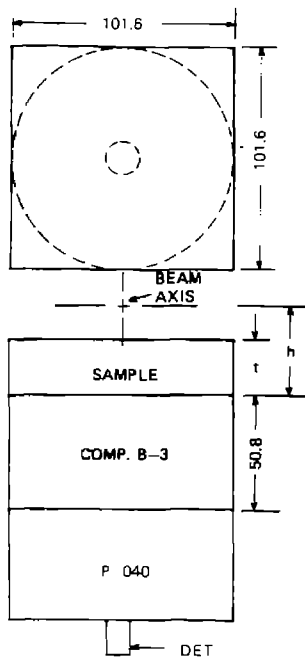
Radiographic Time:

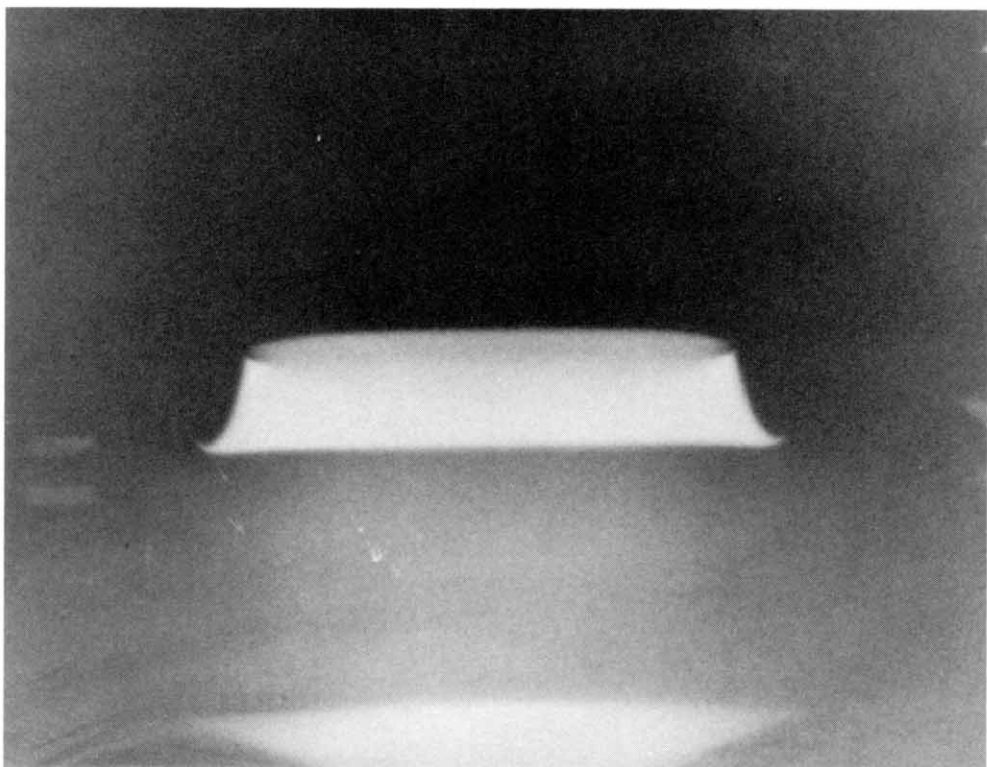
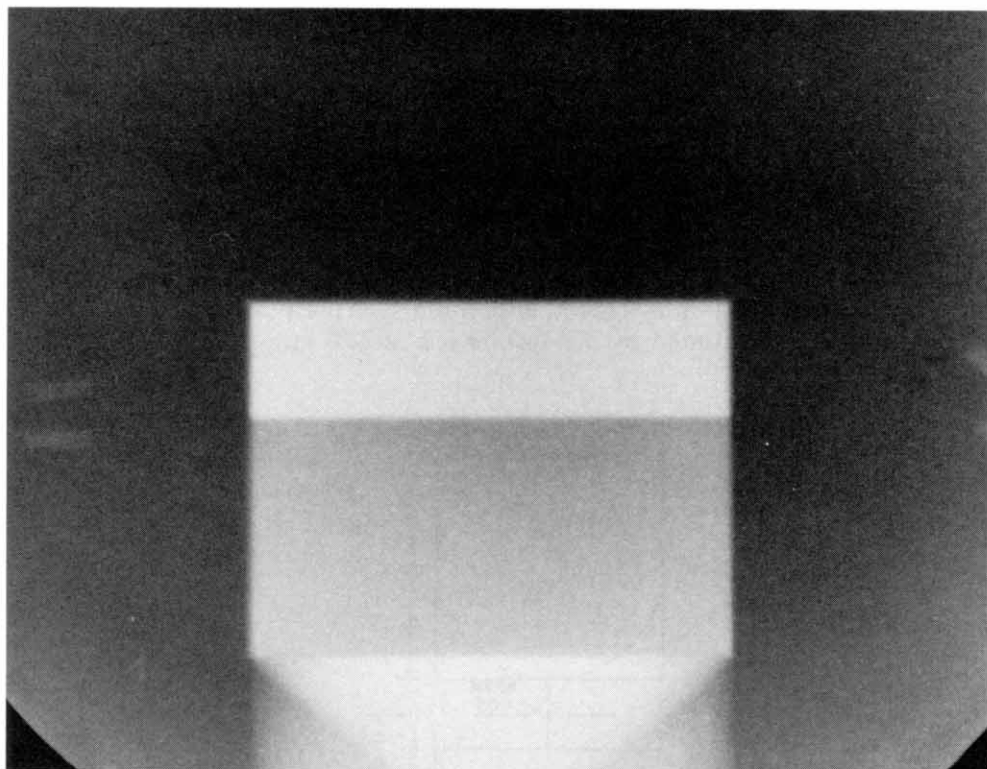
25.25 μ s

References:

Breed et al., 1967; Thurston and Mudd, 1968

Dynamic fracture of 25.0-mm-thick, t , aluminum. The plate is shocked by 50.8 mm of Composition B-3 initiated by a P-040 lens. h is 28.6 mm.





SHOT 356:

Dynamic Fracture of Aluminum

Date:

November 9, 1965

Experimenter:

Benny Ray Breed

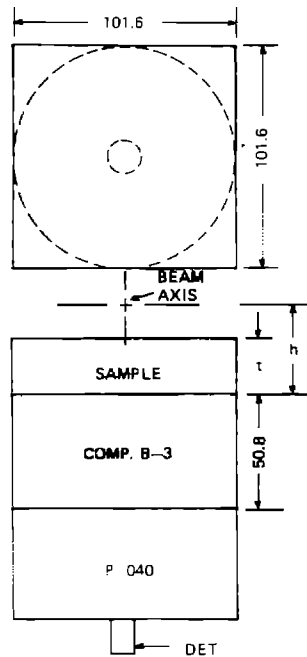
Radiographic Time:

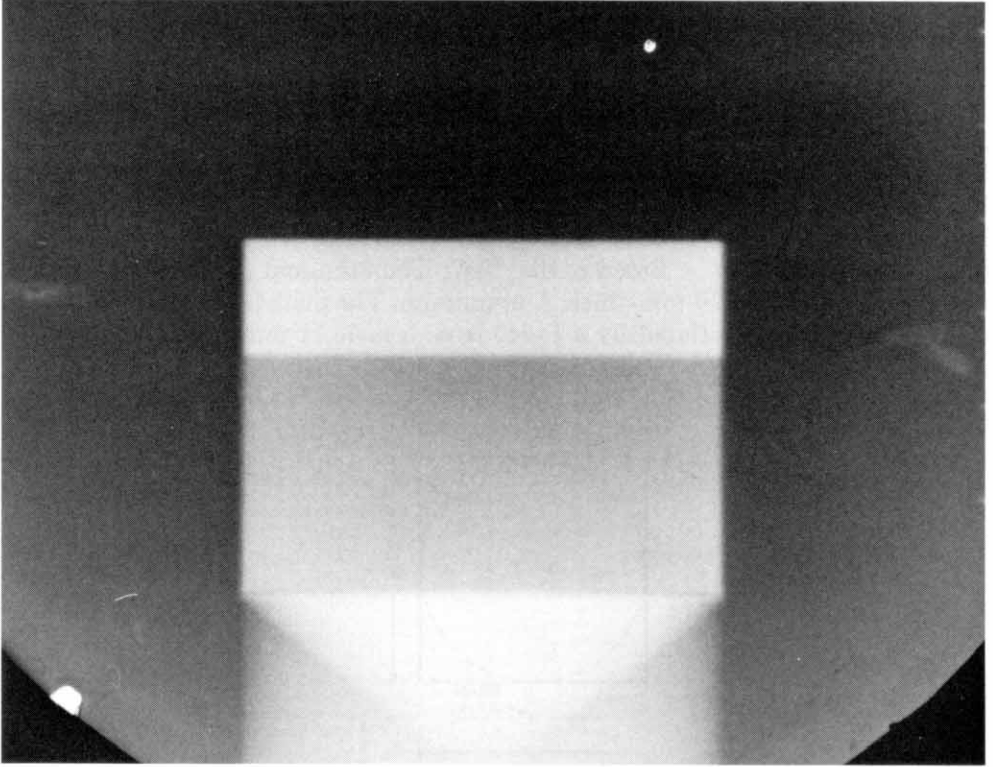
25.71 μ s

References:

Breed et al., 1967; Thurston and Mudd, 1968

Dynamic fracture of 25.0-mm-thick, t , aluminum. The plate is shocked by 50.8 mm of Composition B-3 initiated by a P-040 lens. h is 33.3 mm.





SHOT 357:

Dynamic Fracture of Aluminum

Date:

November 23, 1965

Experimenter:

Benny Ray Breed

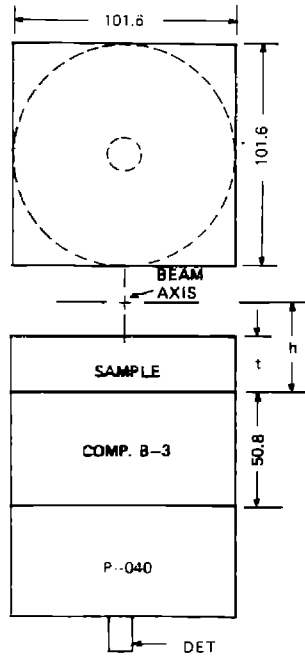
Radiographic Time:

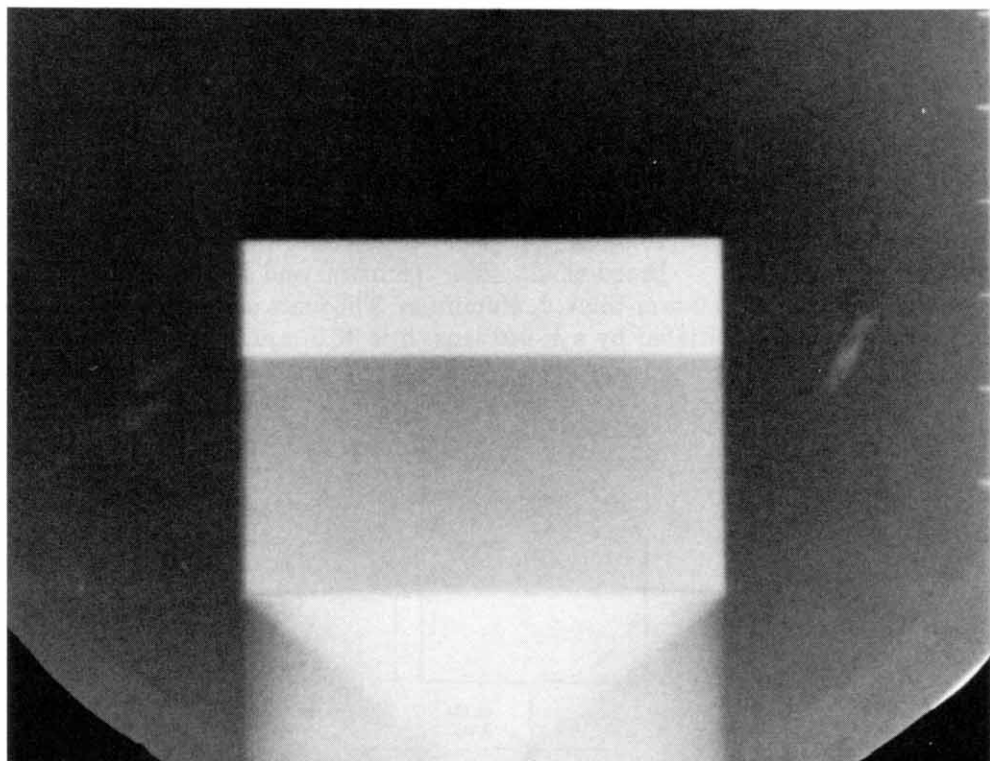
26.23 μ s

References:

Breed et al., 1967; Thurston and Mudd, 1968

Dynamic fracture of 25.0-mm-thick, t , aluminum. The plate is shocked by 50.8 mm of Composition B-3 initiated by a P-040 lens. h is 36.51 mm.





SHOT 358:

Dynamic Fracture of Aluminum

Date:

December 23, 1965

Experimenter:

Benny Ray Breed

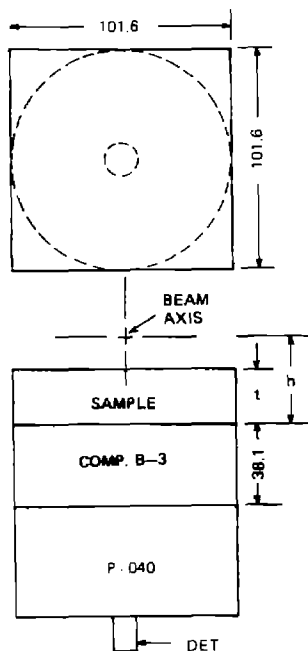
Radiographic Time:

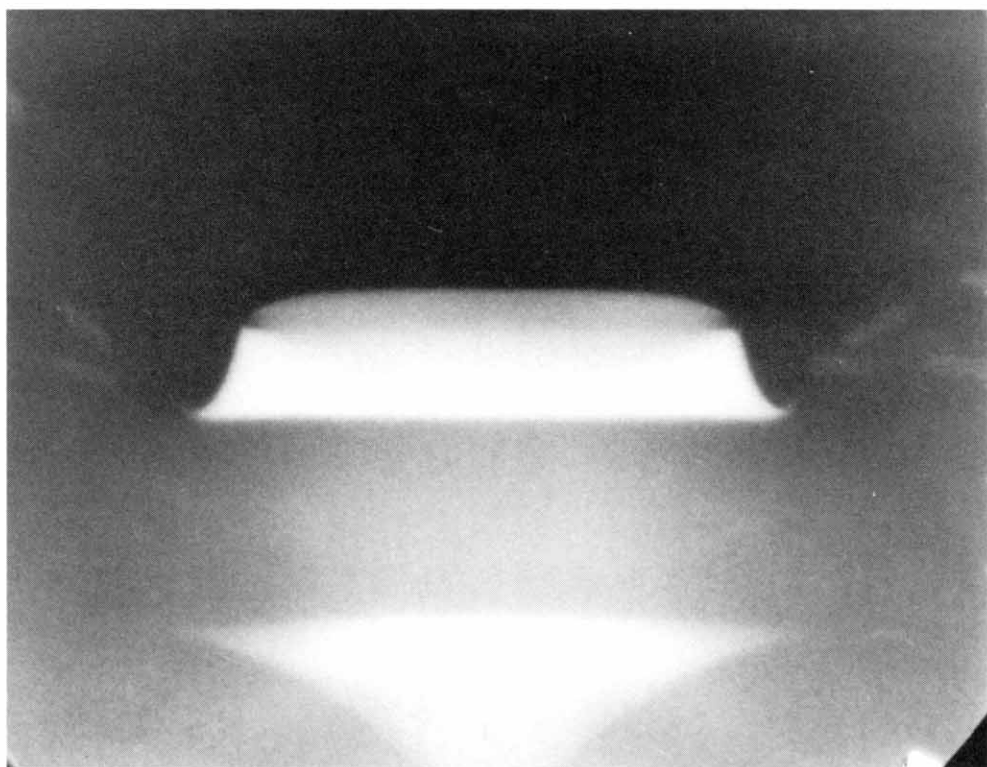
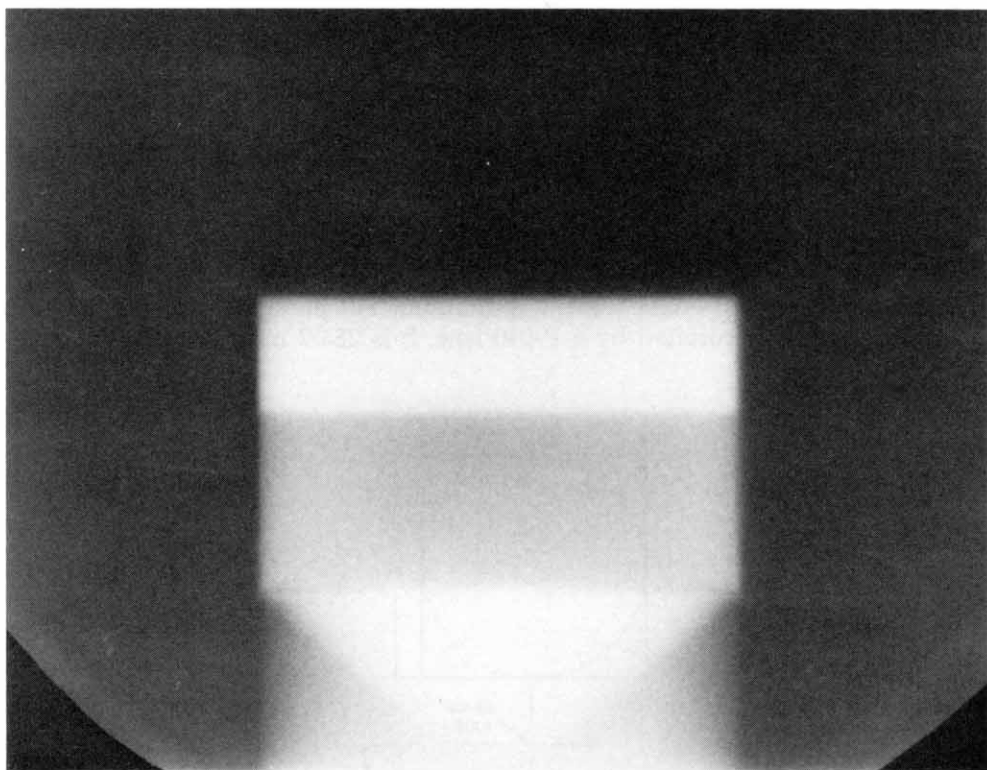
25.07 μ s

References:

Breed et al., 1967; Thurston and Mudd, 1968

Dynamic fracture of 25.0-mm-thick, t , aluminum. The plate is shocked by 38.1 mm of Composition B-3 initiated by a P-040 lens. h is 36.5 mm.





SHOT 359:

Dynamic Fracture of Aluminum

Date:

November 9, 1965

Experimenter:

Benny Ray Breed

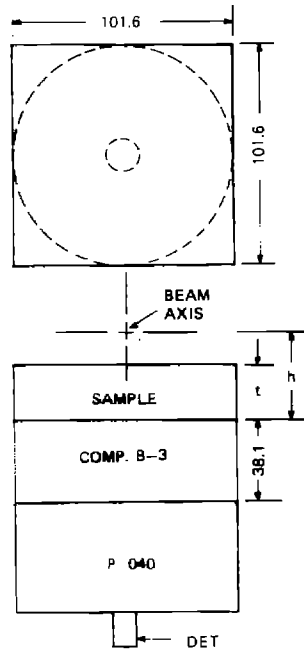
Radiographic Time:

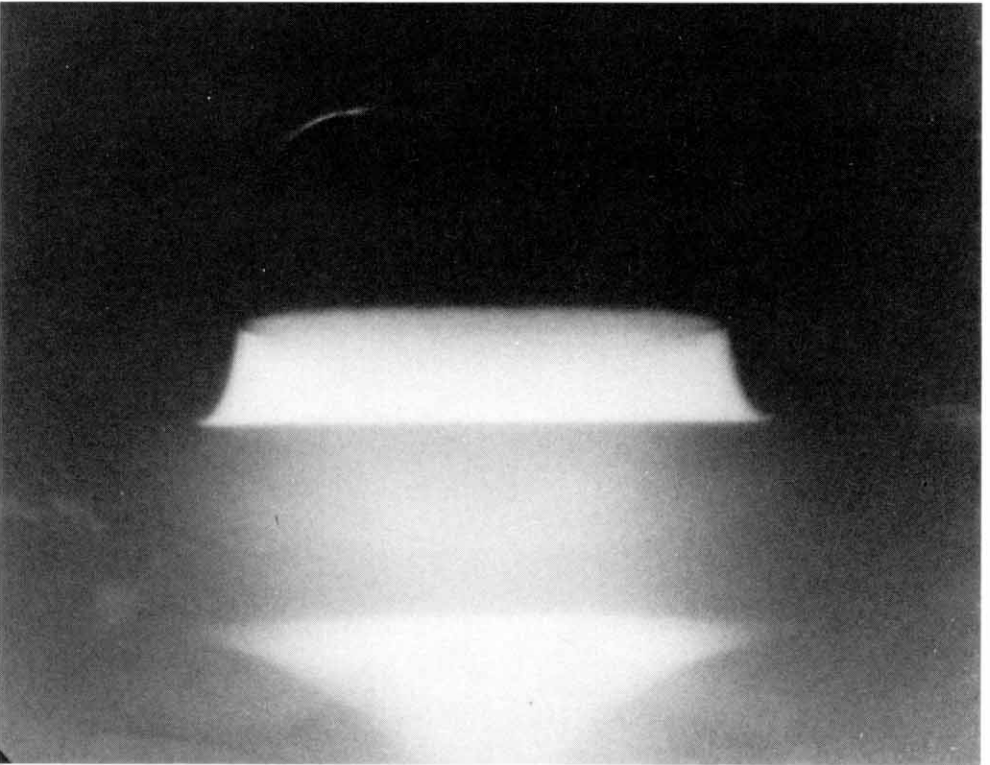
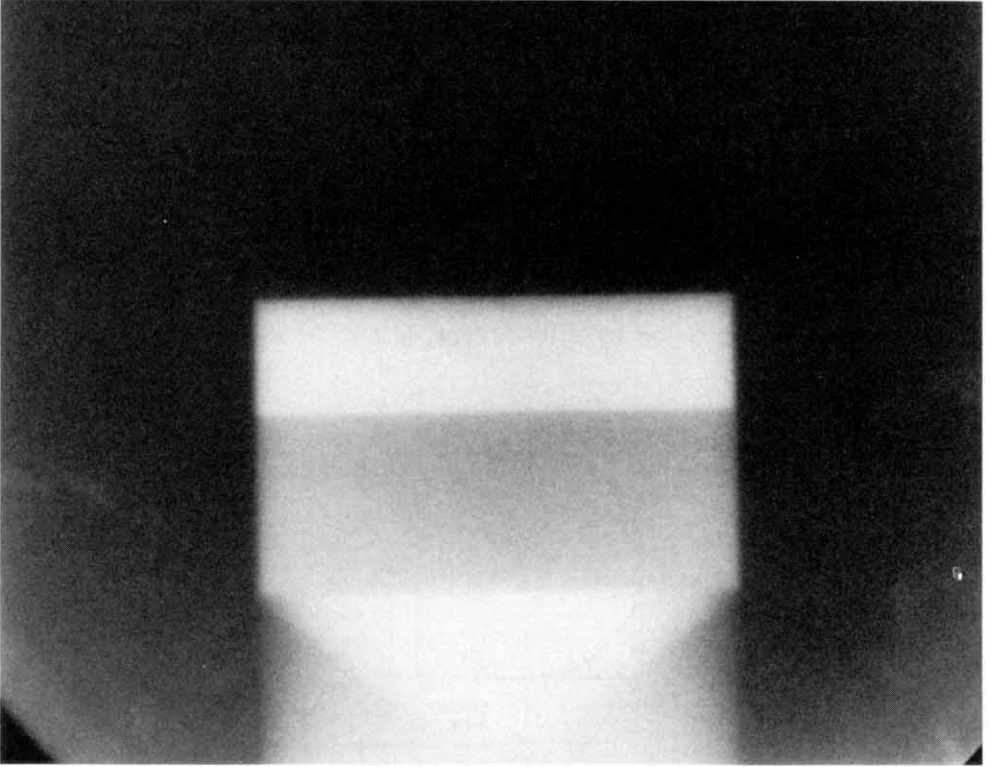
23.53 μ s

References:

Breed et al., 1967; Thurston and Mudd, 1968

Dynamic fracture of 25.0-mm-thick, t , aluminum. The plate is shocked by 38.1 mm of Composition B-3 initiated by a P-040 lens. h is 28.57 mm.





SHOT 360:

Dynamic Fracture of Aluminum

Date:

November 10, 1965

Experimenter:

Benny Ray Breed

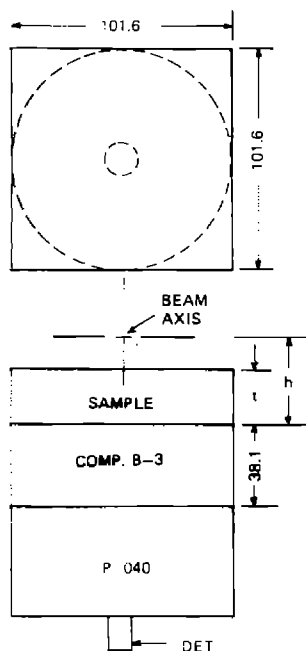
Radiographic Time:

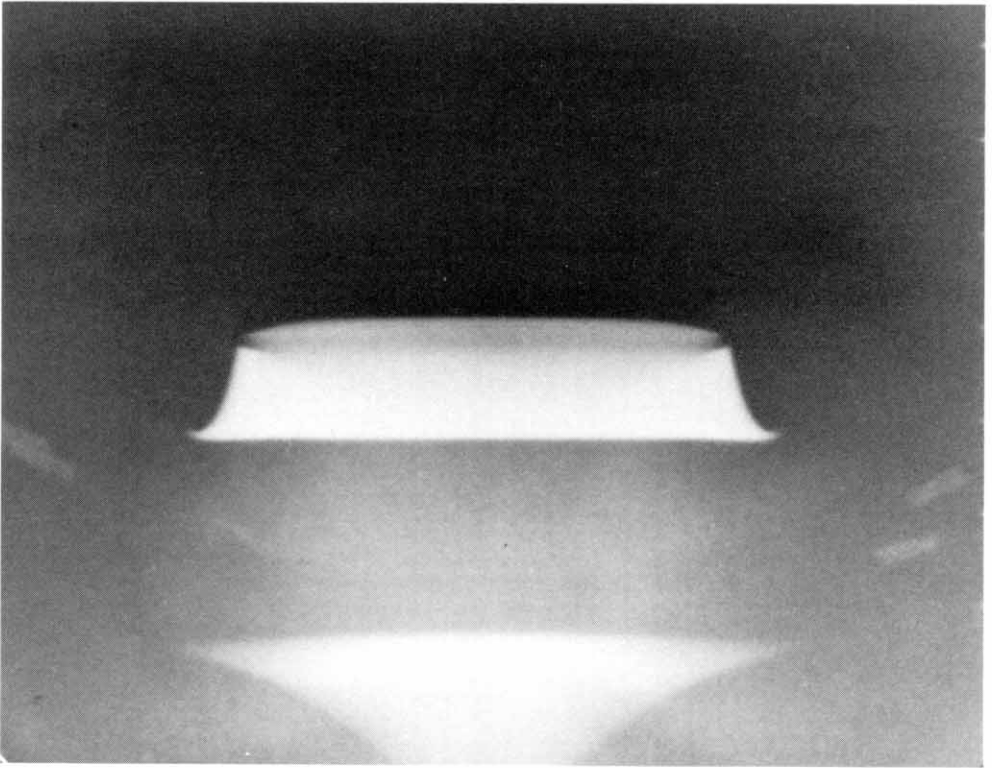
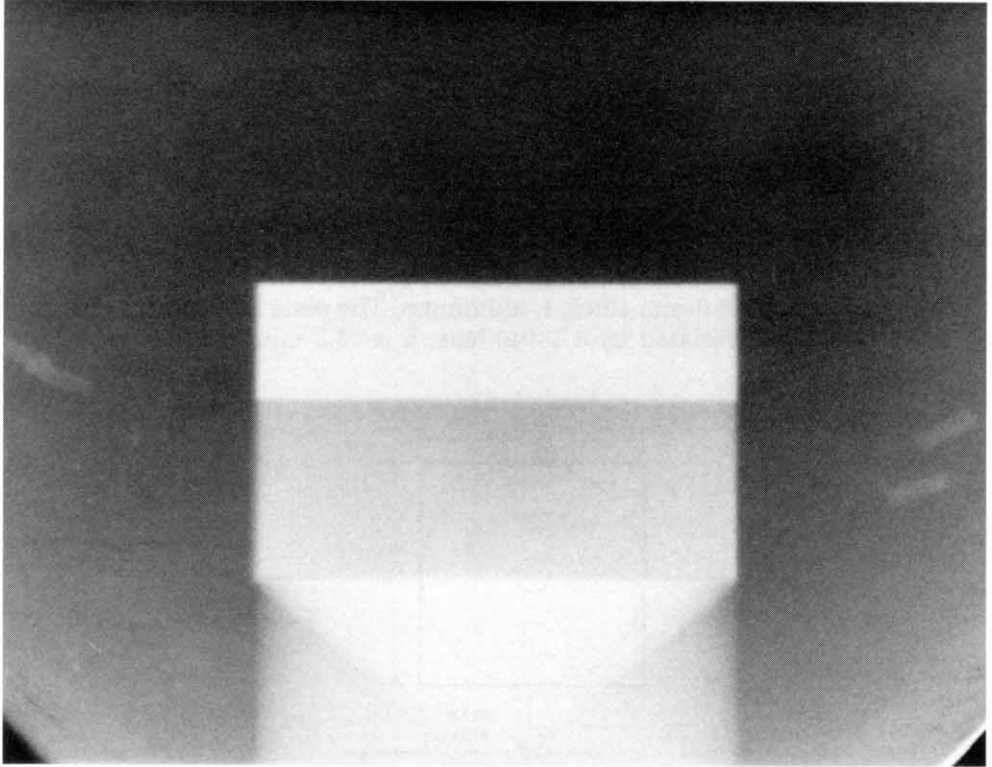
24.02 μ s

References:

Breed et al., 1967; Thurston and Mudd, 1968

Dynamic fracture of 25.0-mm-thick, t , aluminum. The plate is shocked by 38.1 mm of Composition B-3 initiated by a P-040 lens. h is 28.57 mm.





SHOT 361:

Dynamic Fracture of Aluminum

Date:

November 11, 1965

Experimenter:

Benny Ray Breed

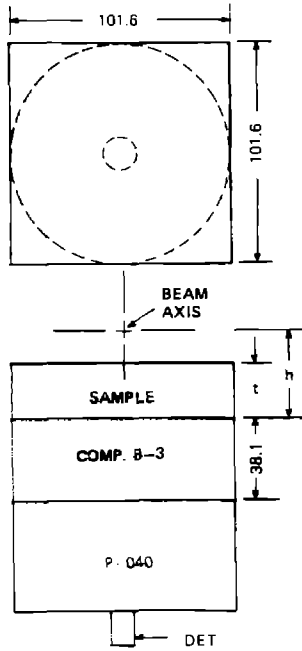
Radiographic Time:

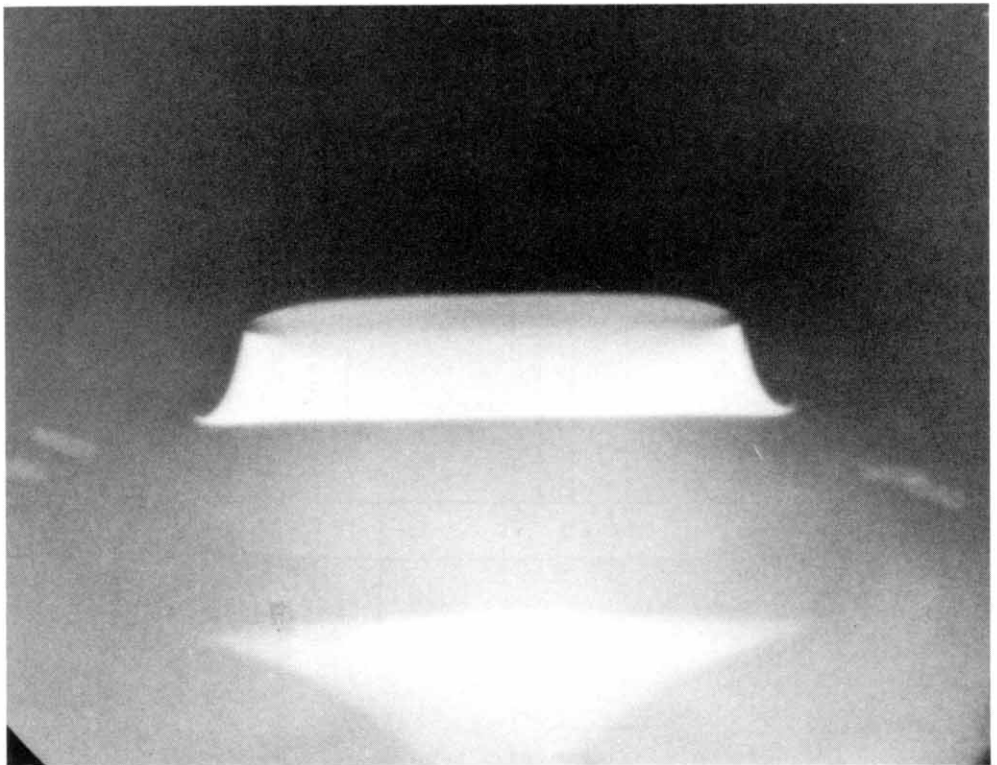
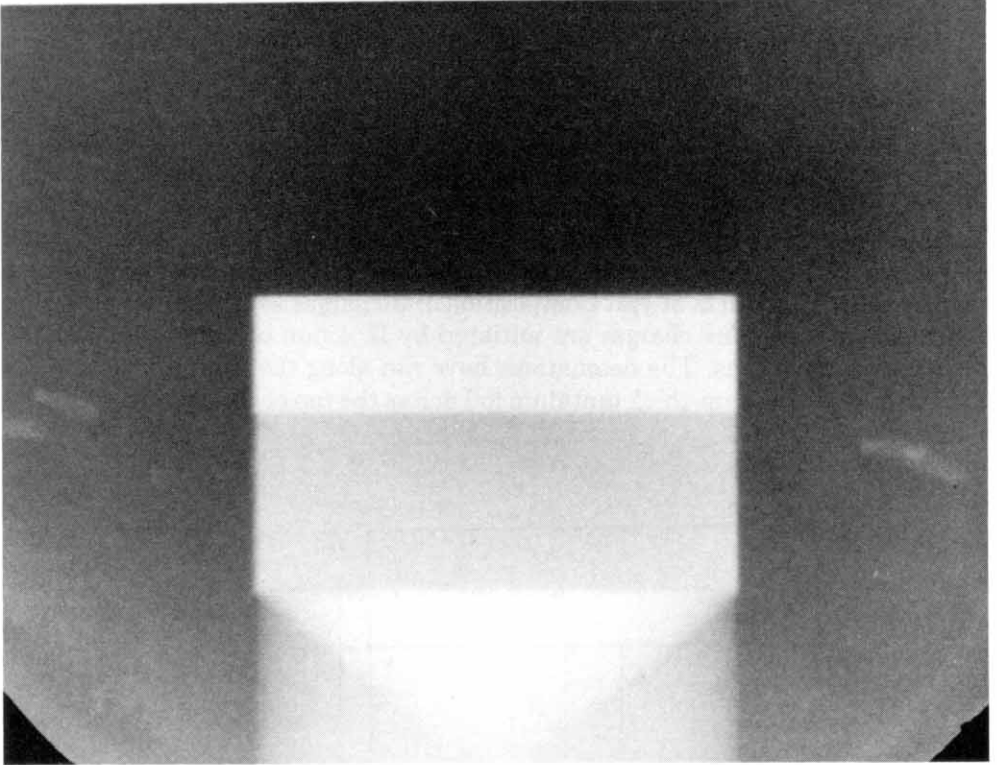
24.52 μ s

References:

Breed et al., 1967; Thurston and Mudd, 1968

Dynamic fracture of 25.0-mm-thick, t , aluminum. The plate is shocked by 38.1 mm of Composition B-3 initiated by a P-040 lens. h is 33.3 mm.





SHOT 362:

Munroe Jet

Date:

November 16, 1965

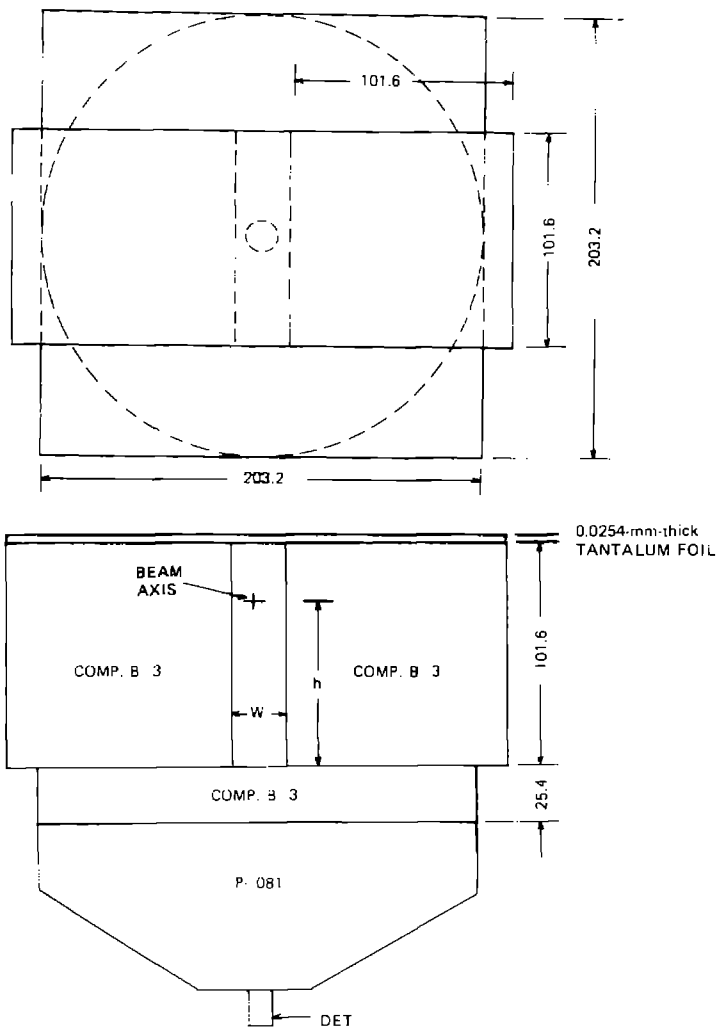
Experimenter:

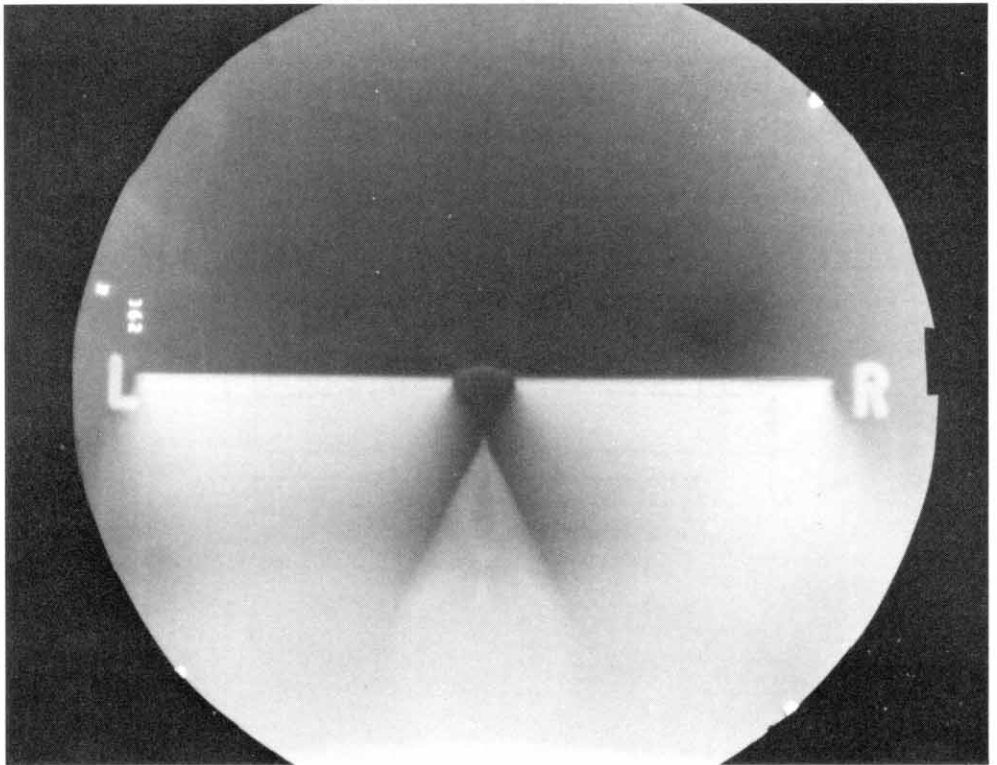
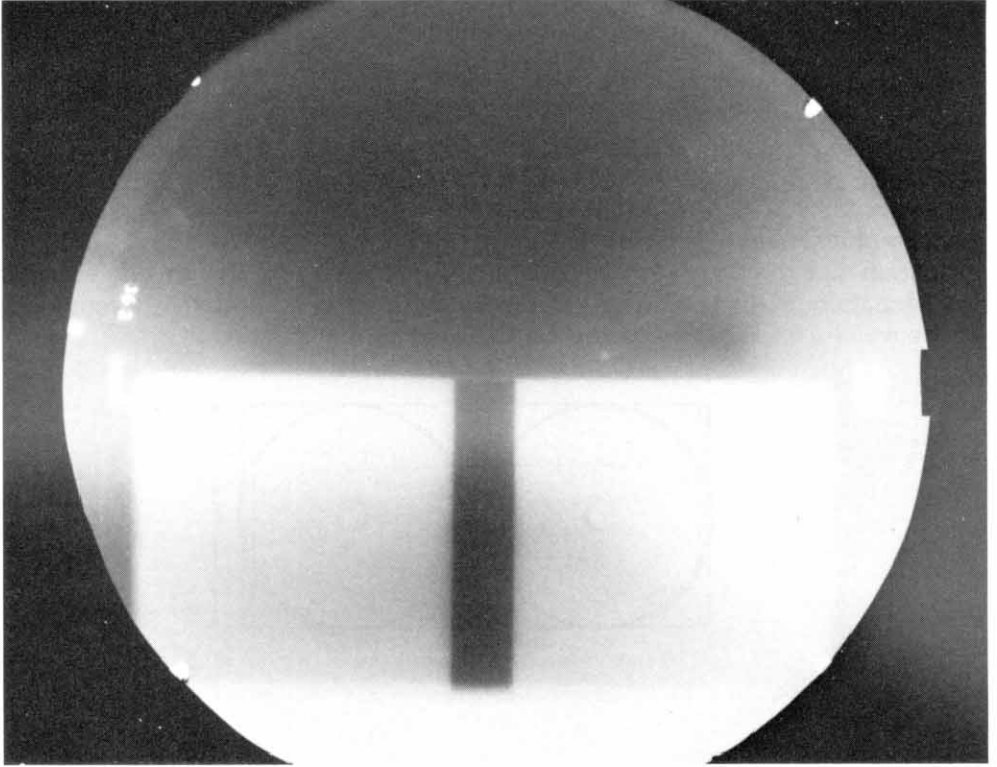
Douglas Venable

Radiographic Time:

38.18 μ s

Formation and growth of gaseous Munroe jets. This jet is formed by interaction of the detonation products of two Composition B-3 charges separated by an air gap 20.0 mm, w, wide. The charges are initiated by 25.4 mm of Composition B-3 initiated by a P-081 lens. The detonations have run along the gap for 98.0 mm. h is 101.6 mm. A 0.0254-mm-thick tantalum foil across the top of the gap is deformed by the precursor gases.





SHOT 363:

Converging Munroe Jet

Date:

November 16, 1965

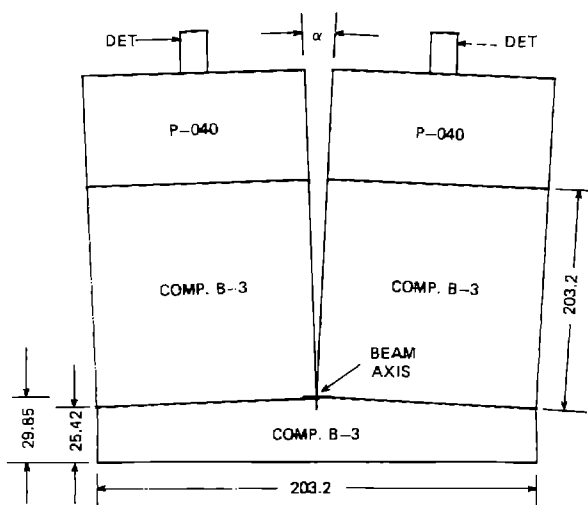
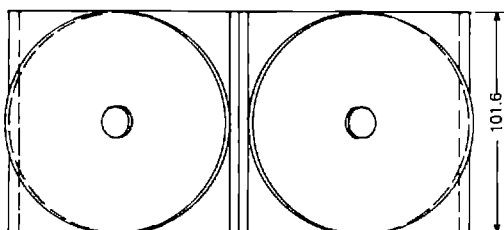
Experimenter:

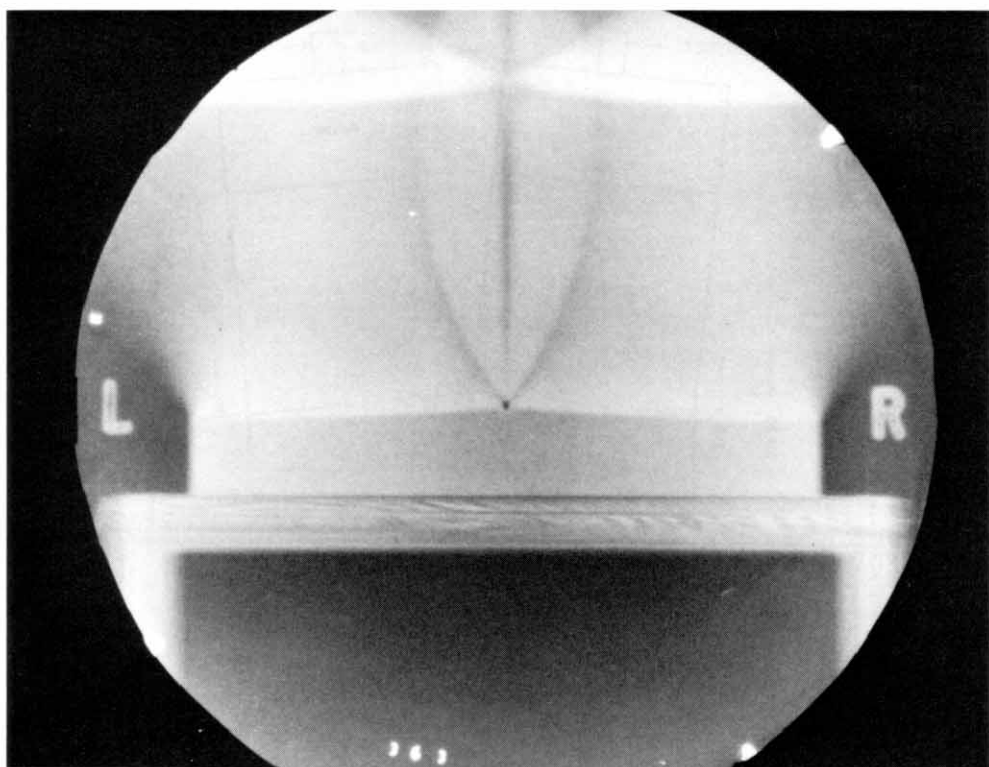
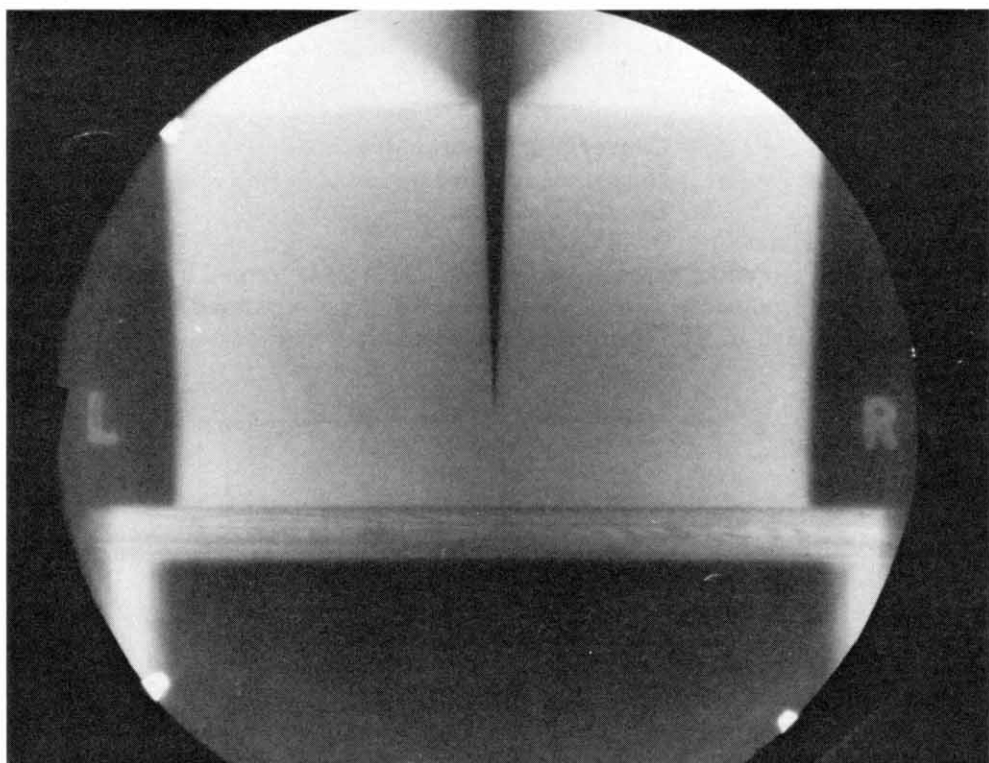
Douglas Venable

Radiographic Time:

26.41 μ s

Formation and growth of gaseous Munroe jets. This jet is formed by interaction of the detonation products of two Composition B-3 charges separated by a converging air groove of 5.0° , α . The charges are initiated by P-040 lenses.





SHOT 364:

Converging Munroe Jet

Date:

November 22, 1965

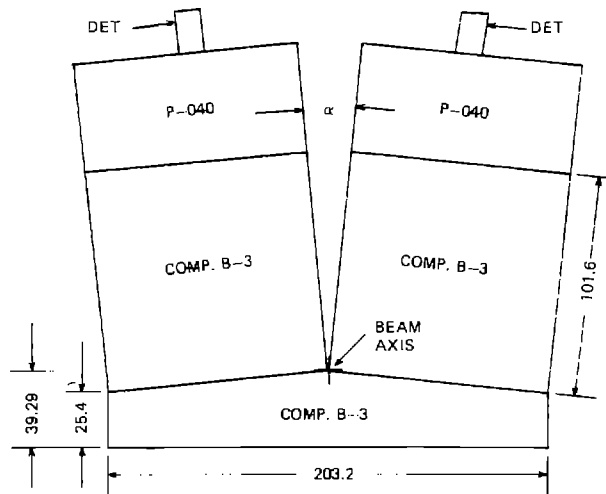
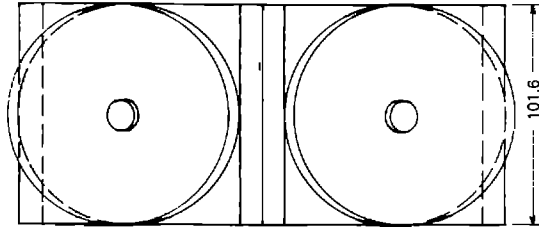
Experimenter:

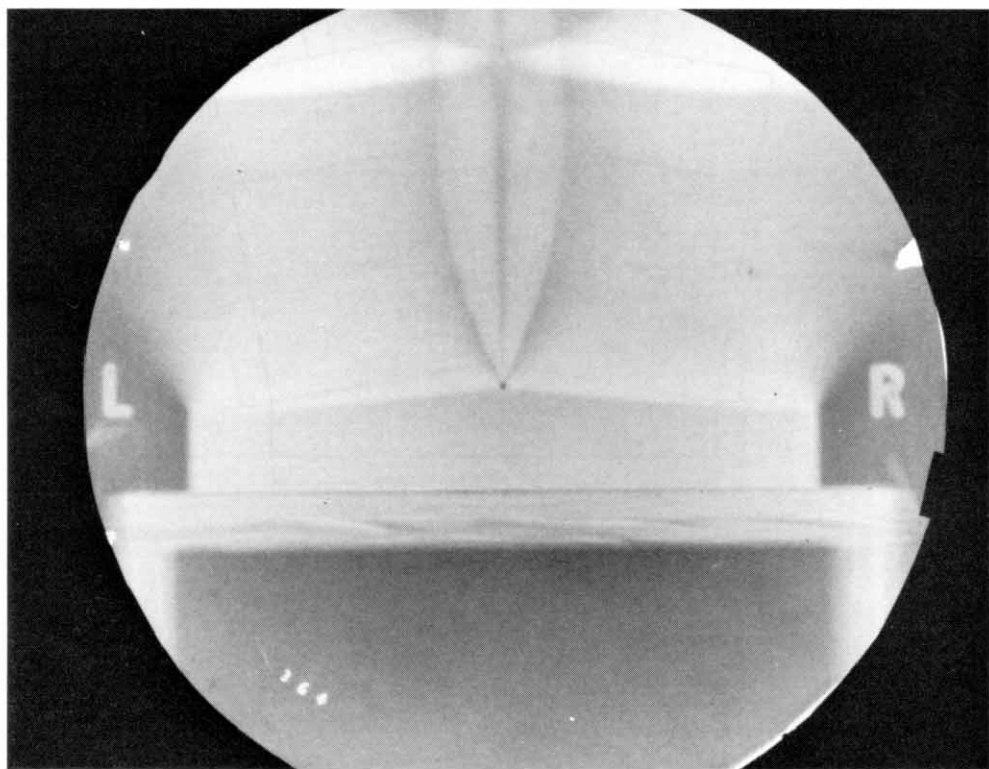
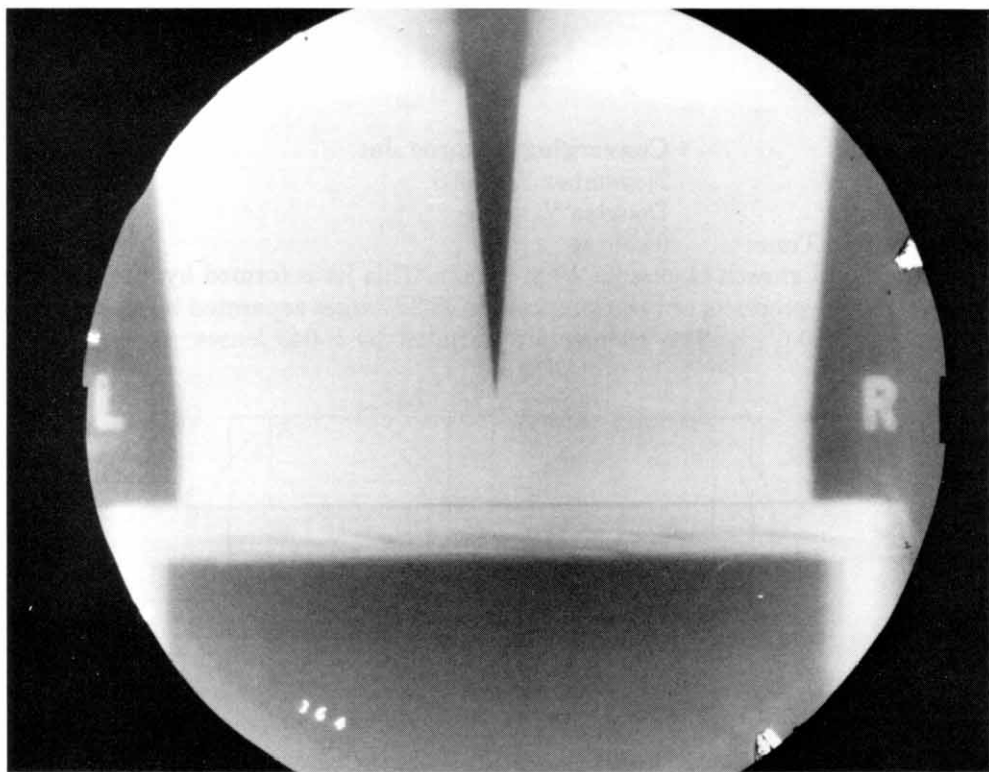
Douglas Venable

Radiographic Time:

26.43 μ s

Formation and growth of gaseous Munroe jets. This jet is formed by interaction of the detonation products of two composition B-3 charges separated by a converging air groove of 10.0° , α . The charges are initiated by P-040 lenses.





SHOT 365:

Converging Munroe Jet

Date:

November 22, 1965

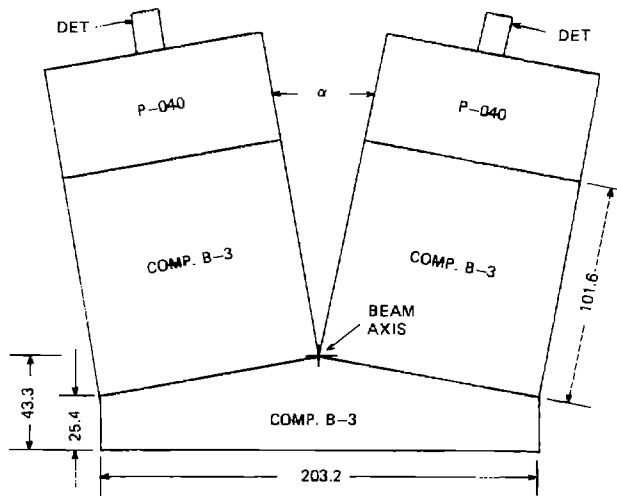
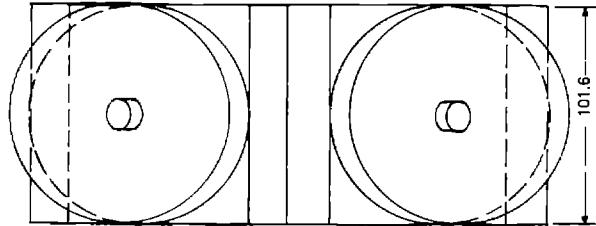
Experimenter:

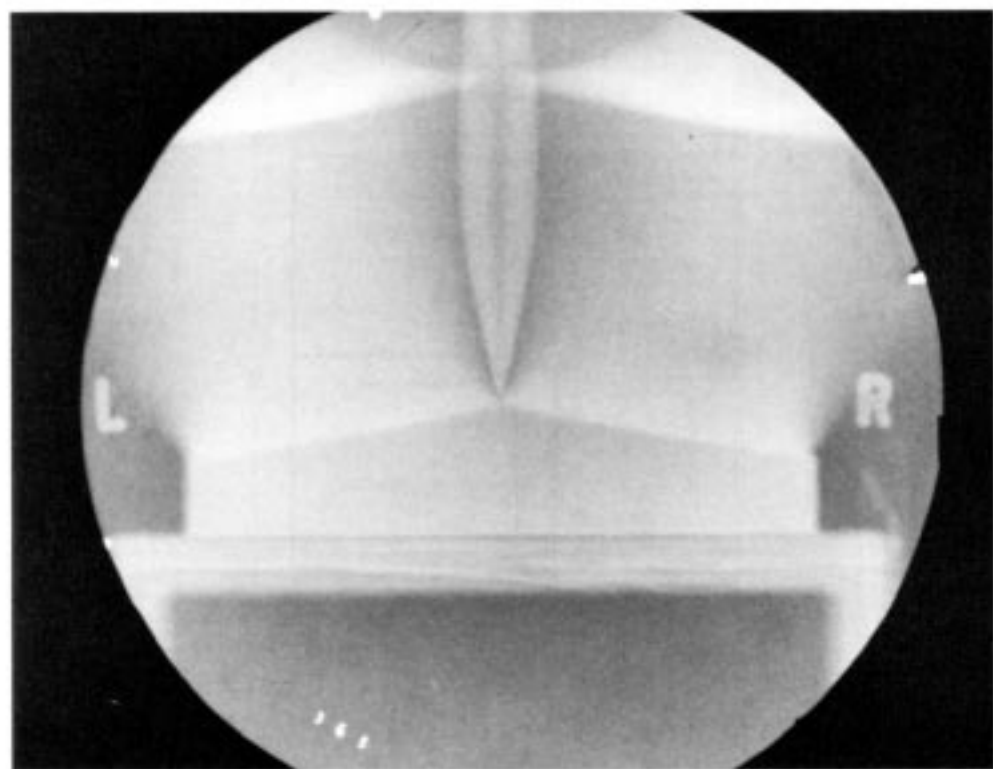
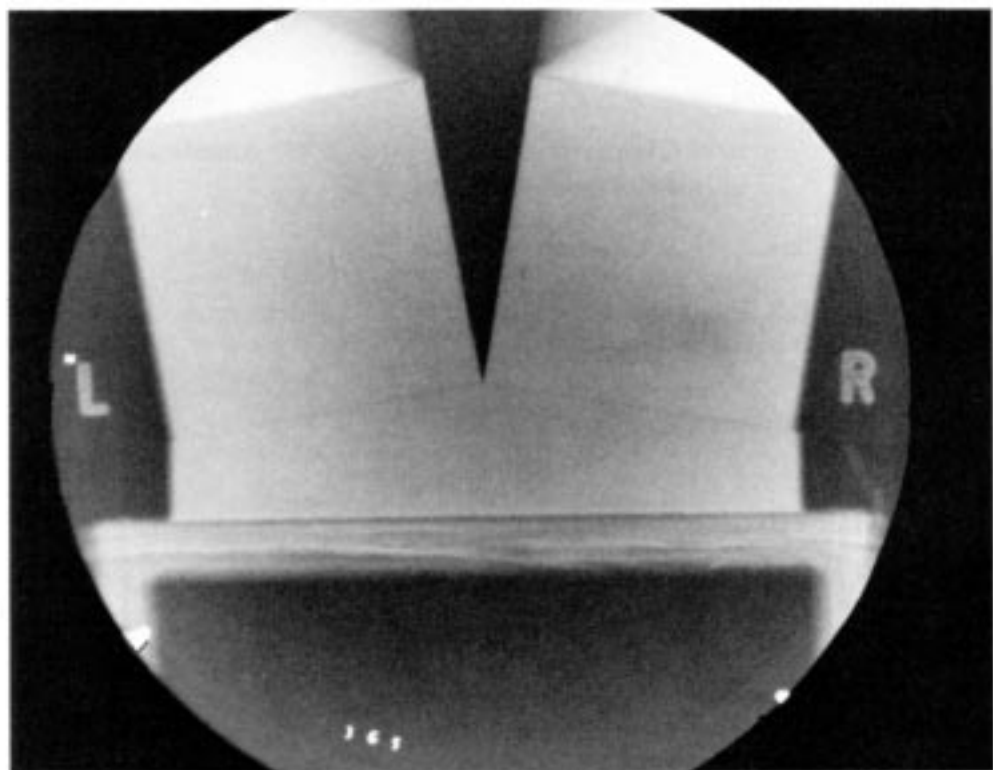
Douglas Venable

Radiographic Time:

26.39 μ s

Formation and growth of gaseous Munroe jets. This jet is formed by interaction of the detonation products of two Composition B-3 charges separated by a converging air groove of 20.0° , α . The charges are initiated by P-040 lenses.





SHOT 366:

Composition B-3 Turning a 90° Aluminum Corner

Date:

January 19, 1966

Experimenter:

Roger W. Taylor

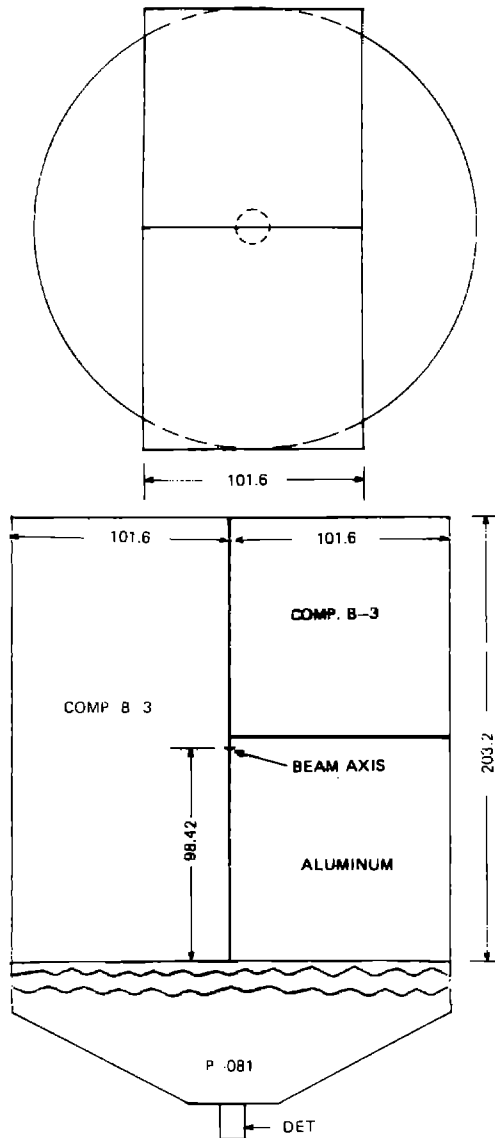
Radiographic Time:

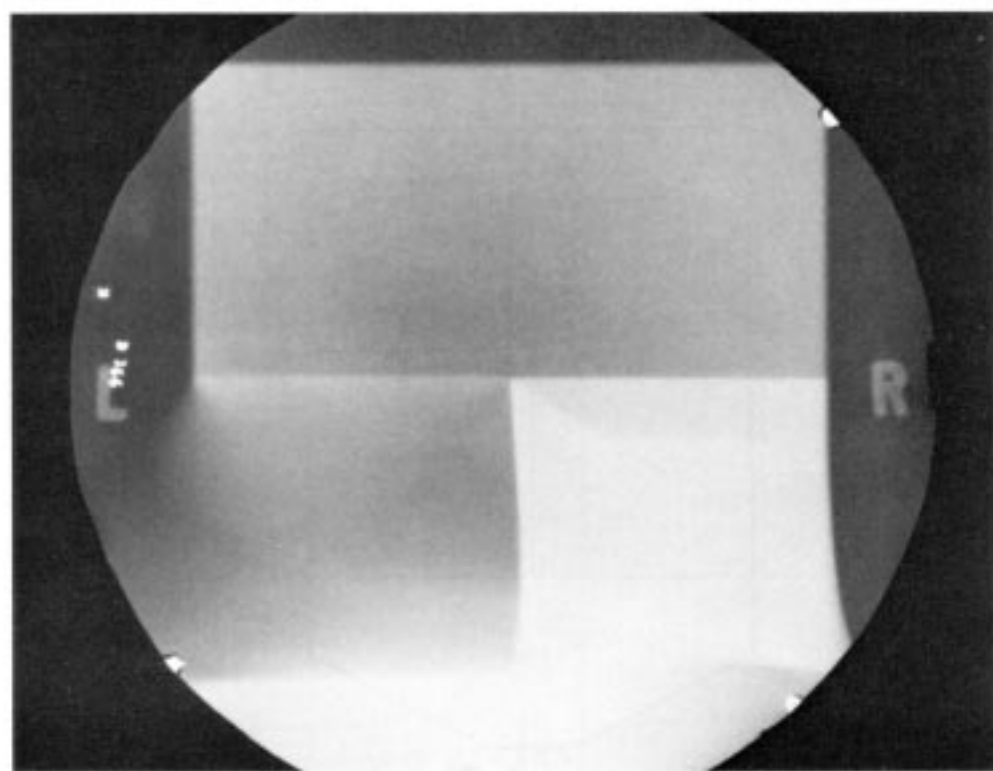
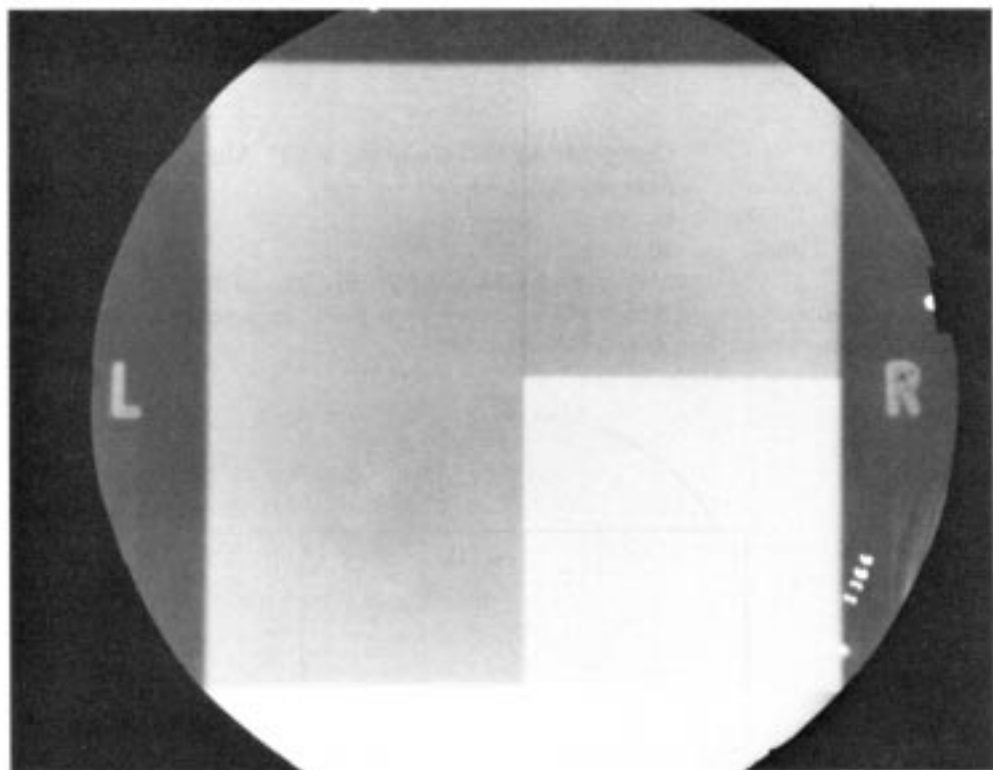
35.24 μ s

References:

Mader and Forest, 1976; Mader, 1979

A Composition B-3 detonation wave initiated by a P-081 lens turns an embedded 90° aluminum corner. The detonation wave has reached the corner. See Shots 367 and 368.





SHOT 367:

Composition B-3 Turning a 90° Aluminum Corner

Date:

January 31, 1966

Experimenter:

Roger W. Taylor

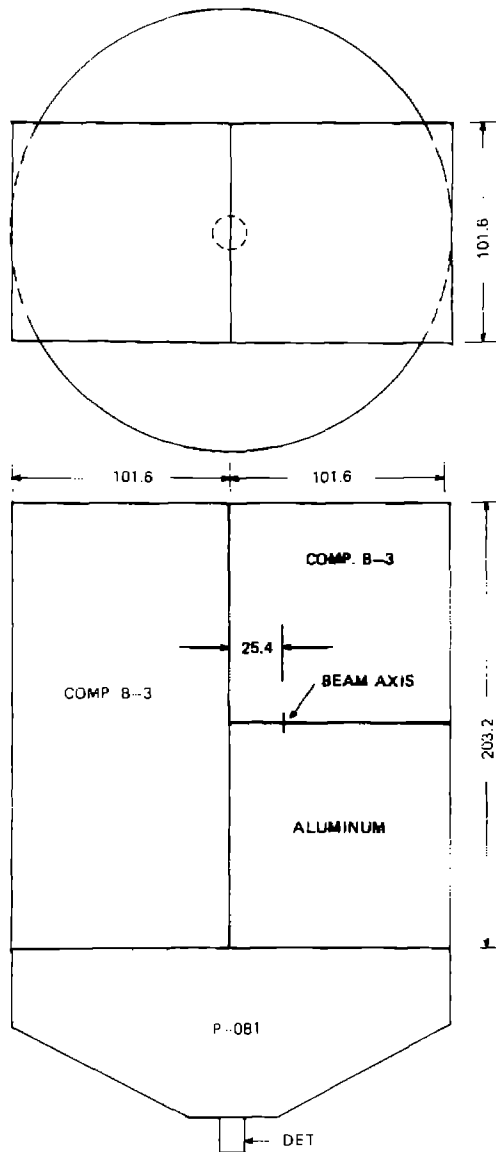
Radiographic Time:

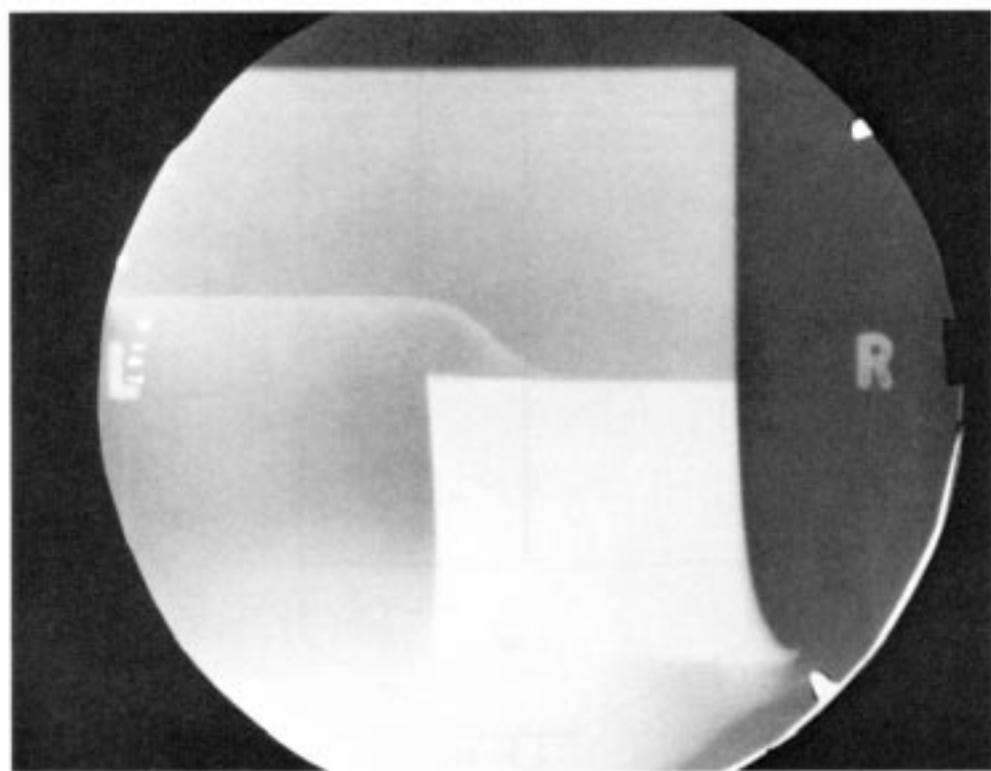
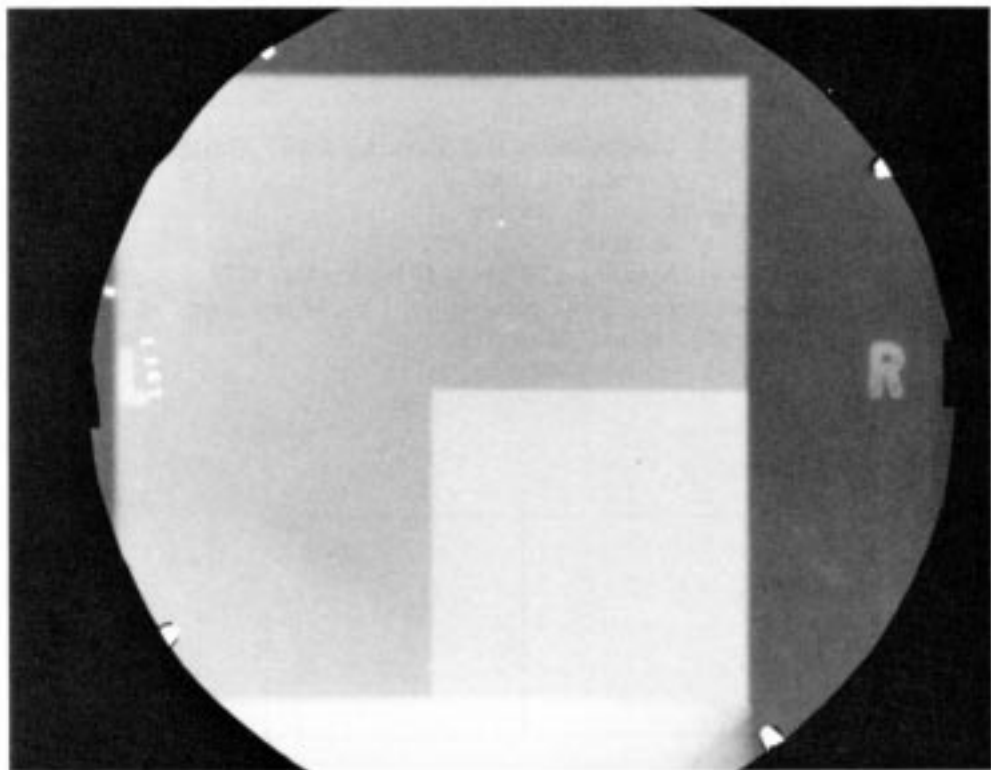
38.66 μ s

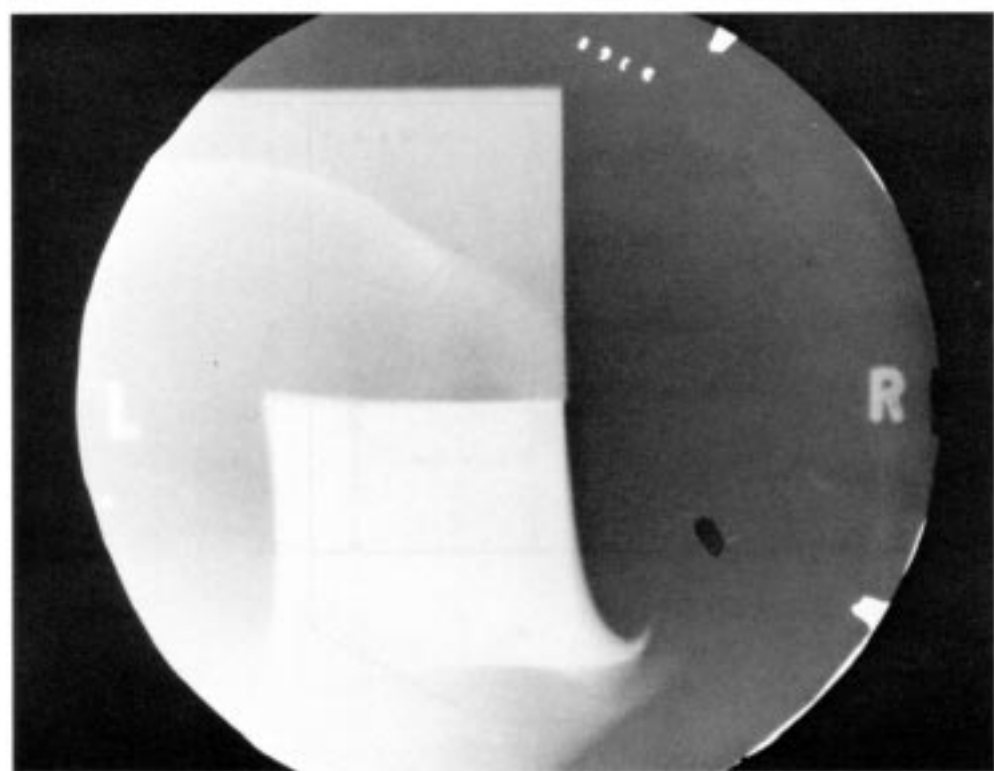
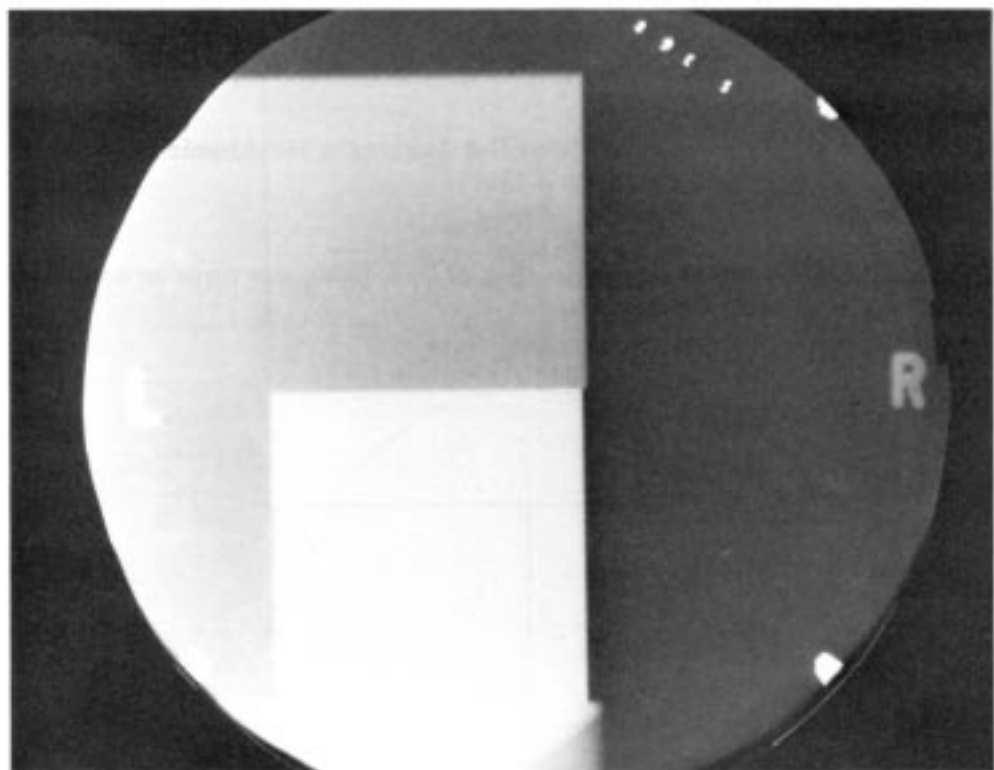
References:

Mader and Forest, 1976; Mader, 1979

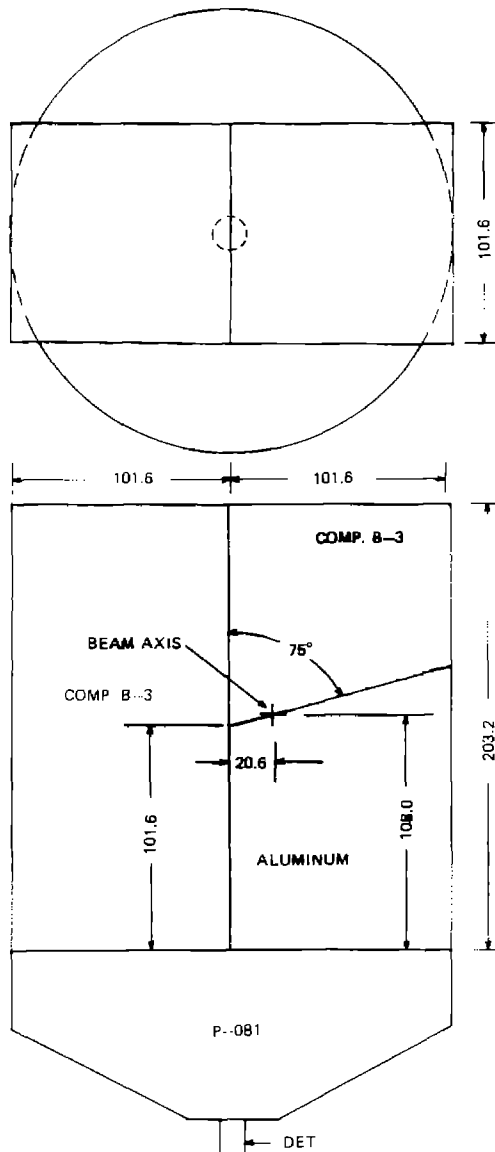
A Composition B-3 detonation wave initiated by a P-081 lens turns an embedded 90° aluminum corner. See Shots 366 and 368.

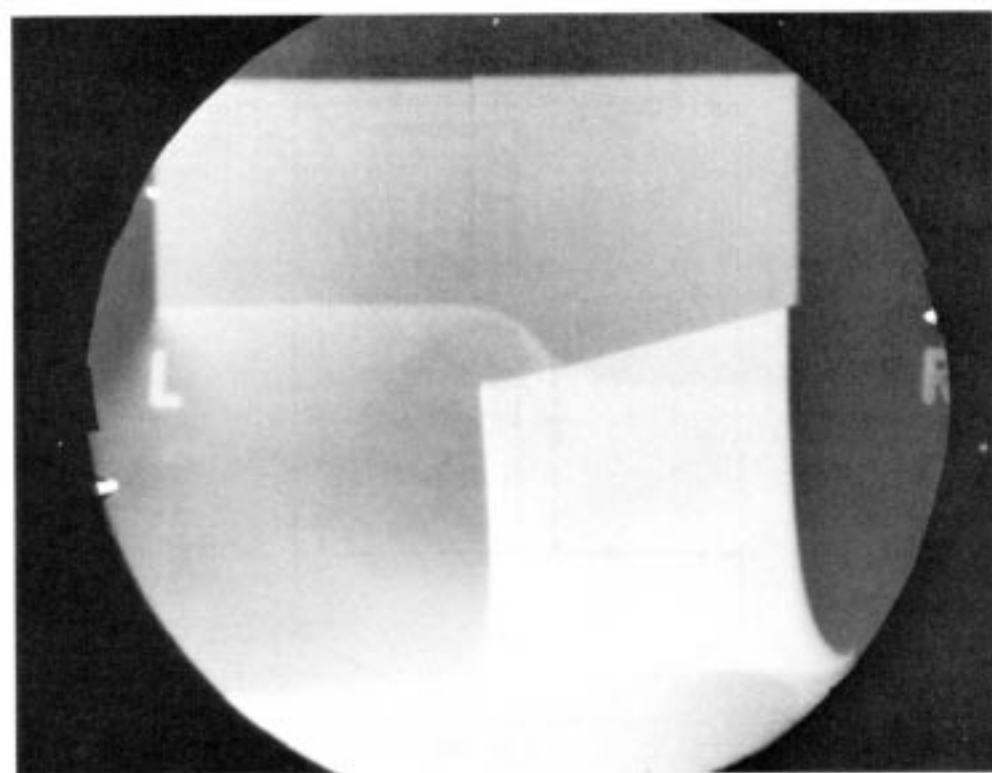
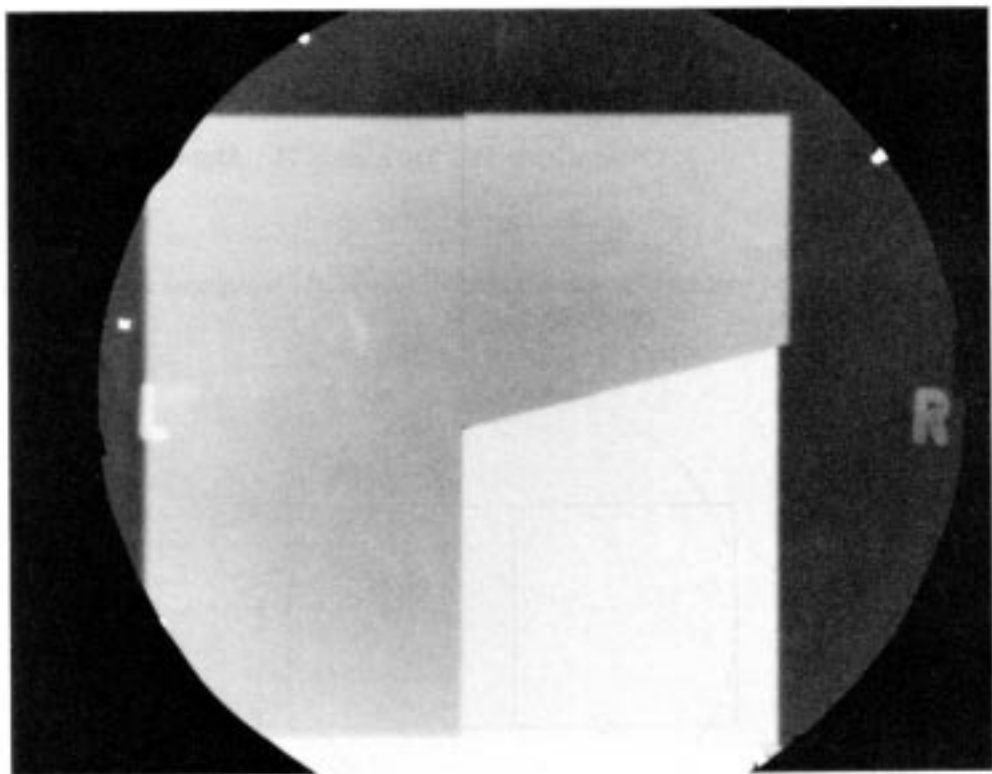


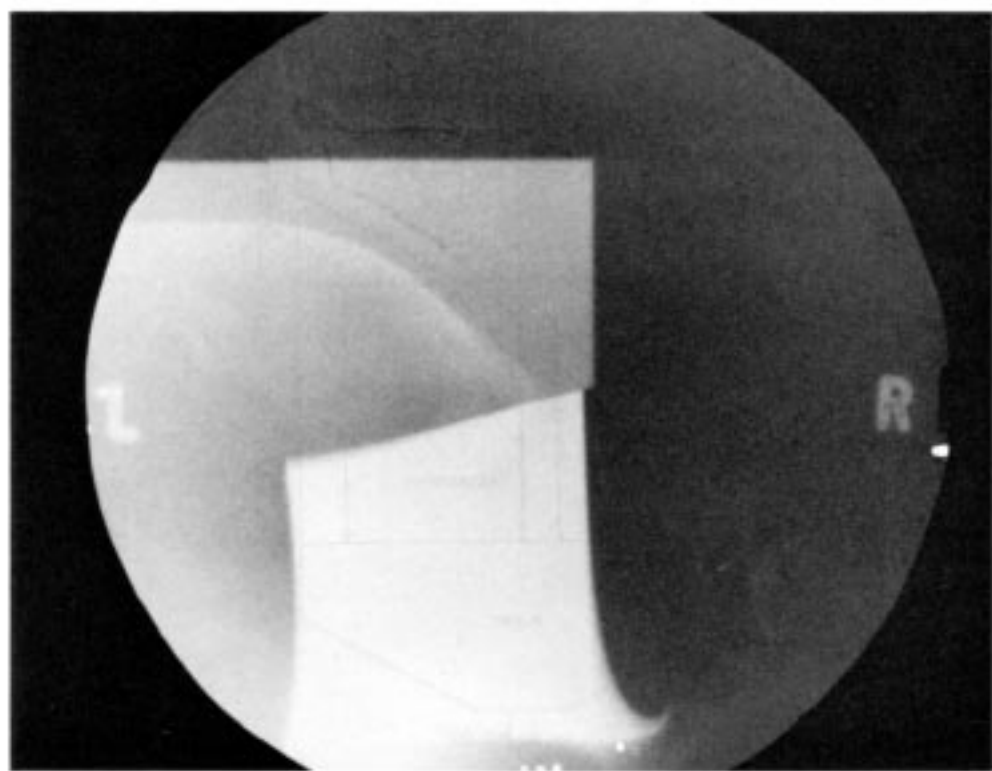
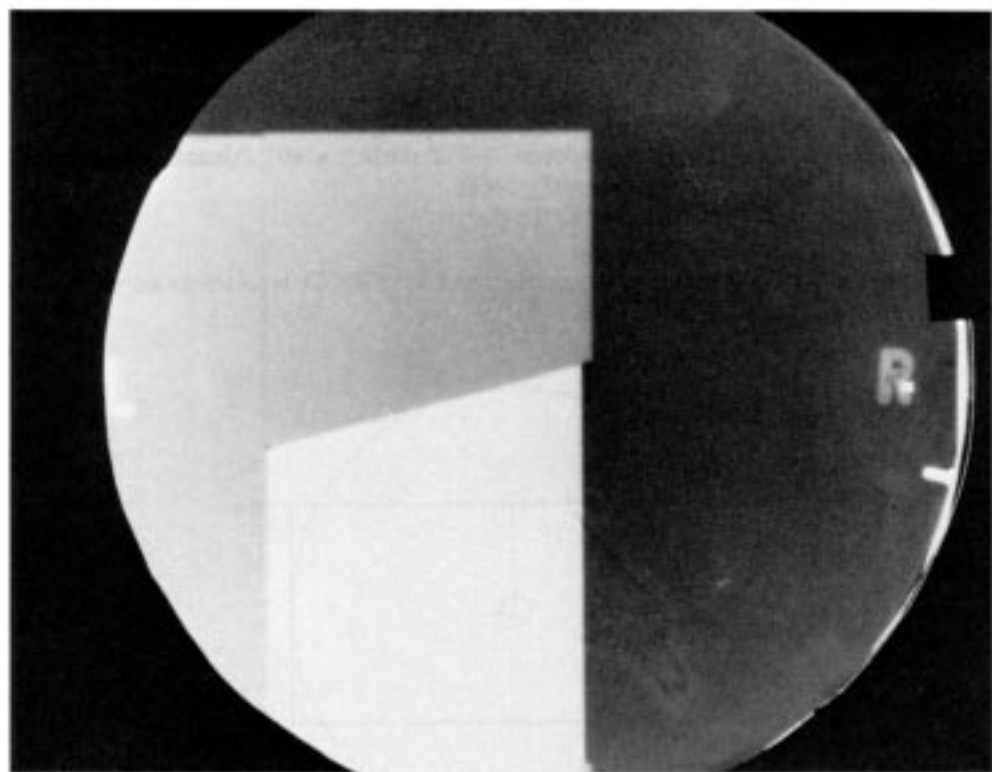




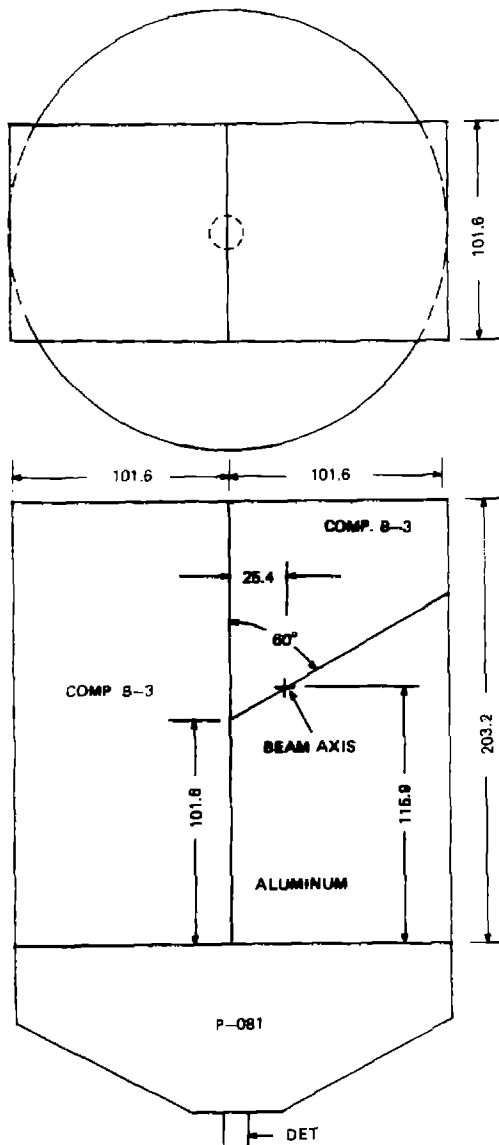
SHOT 369: **Composition B-3 Turning a 75° Aluminum Corner**
 Date: February 1, 1966
 Experimenter: Roger W. Taylor
 Radiographic Time: 38.79 μ s
 A Composition B-3 detonation wave initiated by a P-081 lens turns an embedded 75° aluminum corner. See Shot 370.

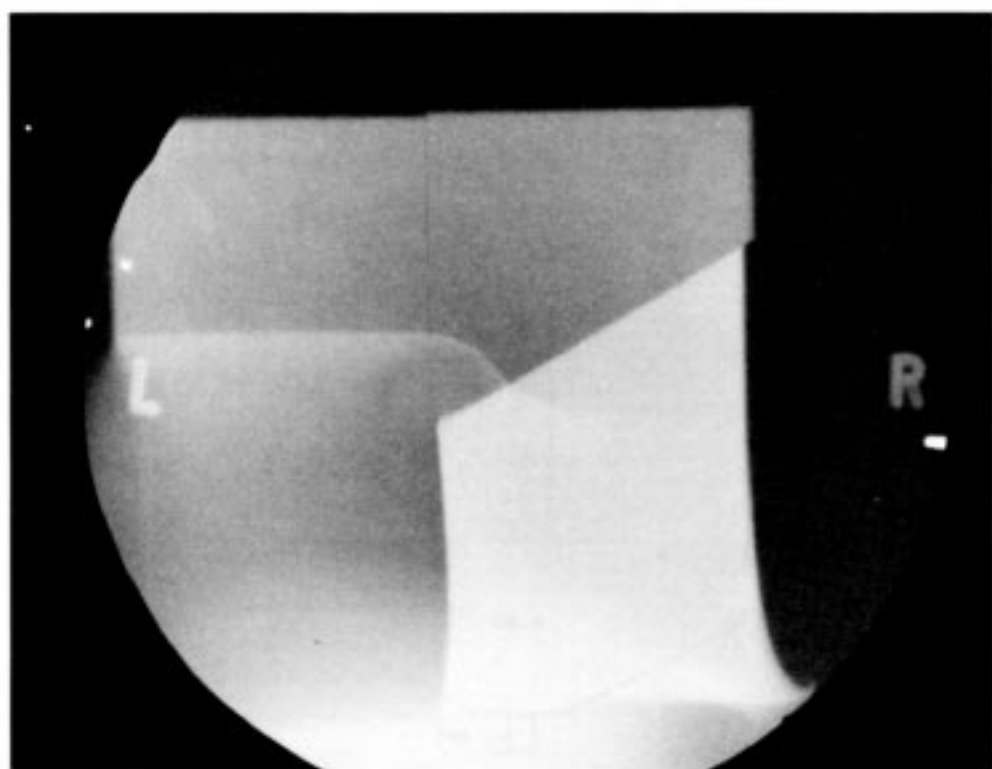
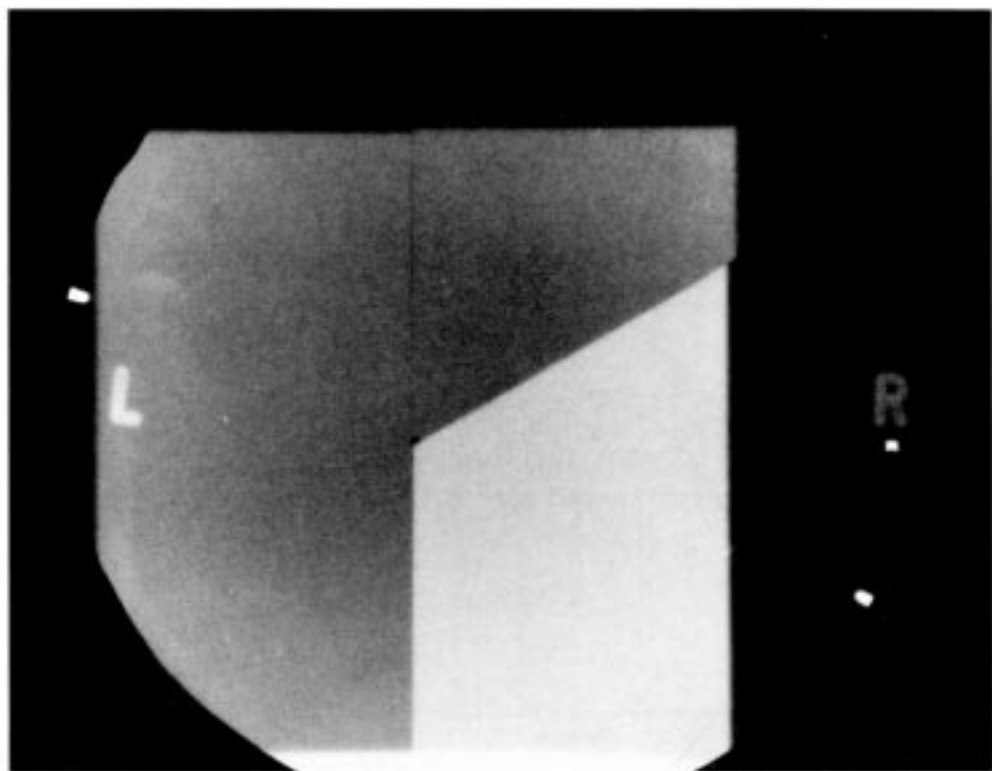






SHOT 371: **Composition B-3 Turning a 60° Aluminum Corner**
Date: **February 1, 1966**
Experimenter: **Roger W. Taylor**
Radiographic Time: **39.12 μ s**
A Composition B-3 detonation wave initiated by a P-081 lens turns an embedded 60° aluminum corner. See Shot 372.





SHOT 372:

Composition B-3 Turning a 60° Aluminum Corner

Date:

February 2, 1966

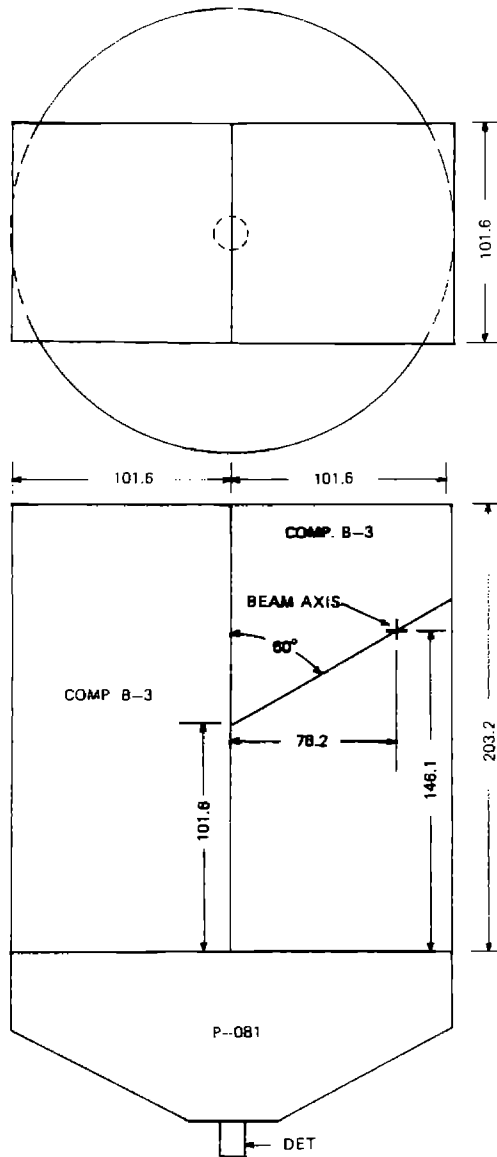
Experimenter:

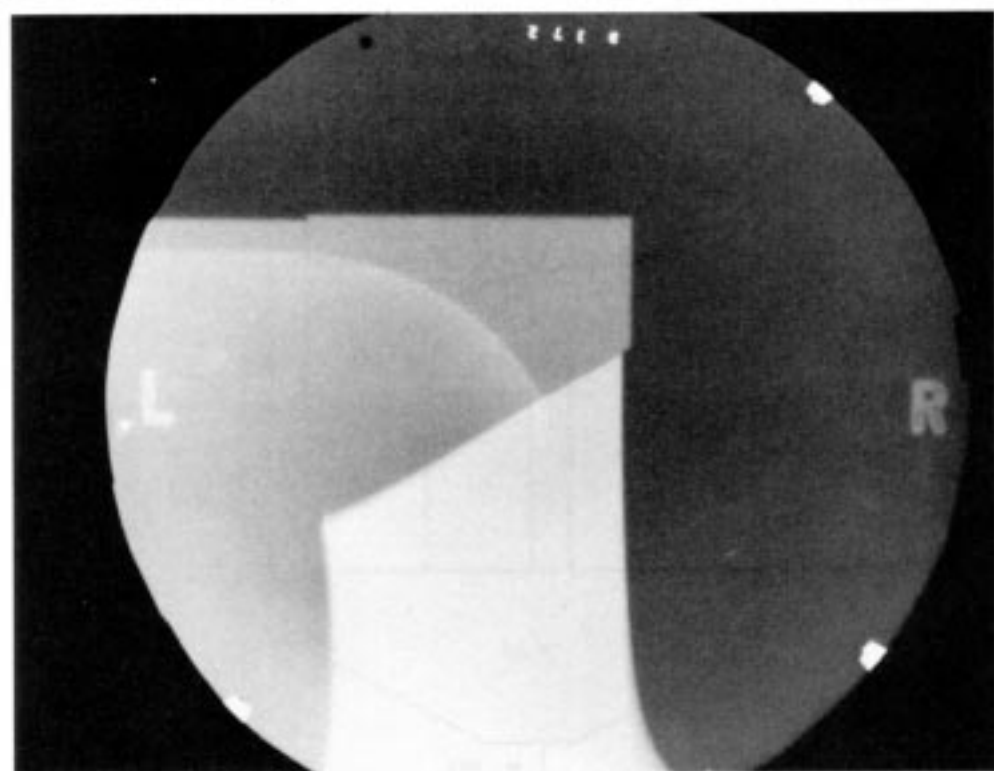
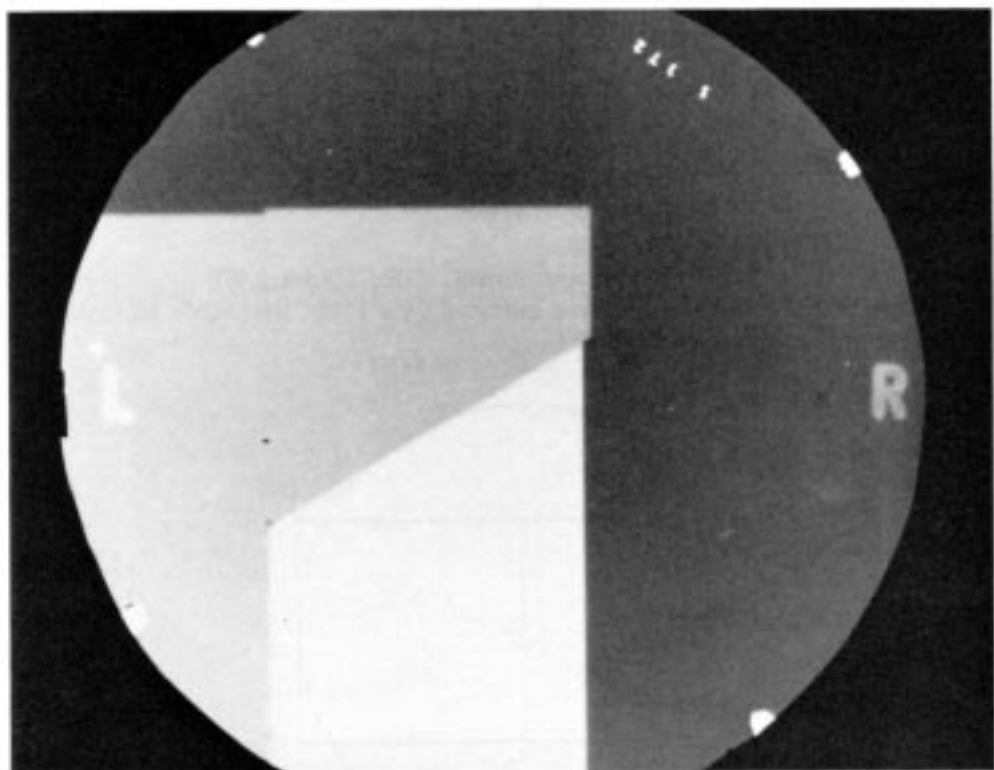
Roger W. Taylor

Radiographic Time:

46.56 μ s

A Composition B-3 detonation wave initiated by a P-081 lens turns an embedded 60° aluminum corner. See Shot 371.





SHOT 373: Composition B-3 Turning a 45° Aluminum Corner

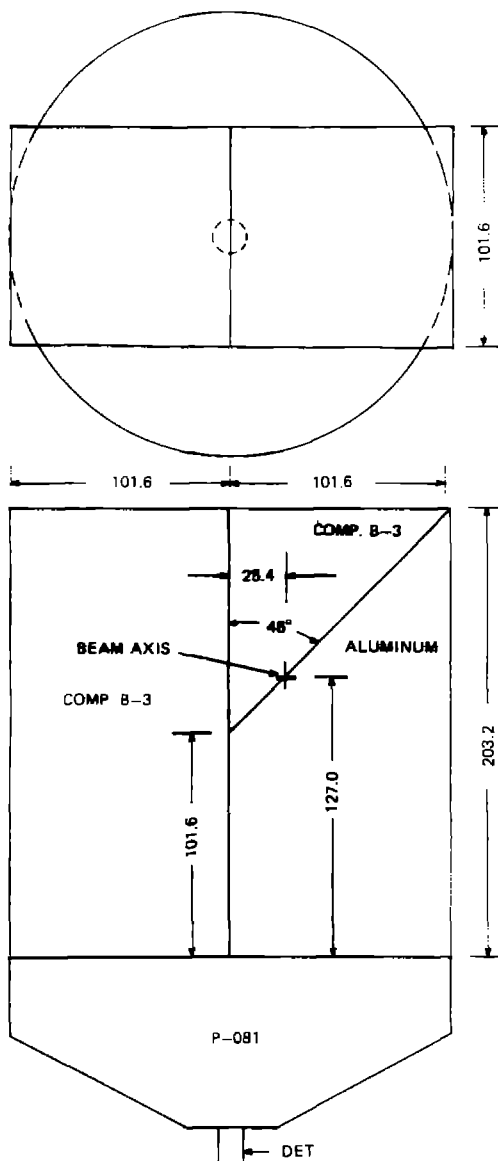
Date: February 2, 1966

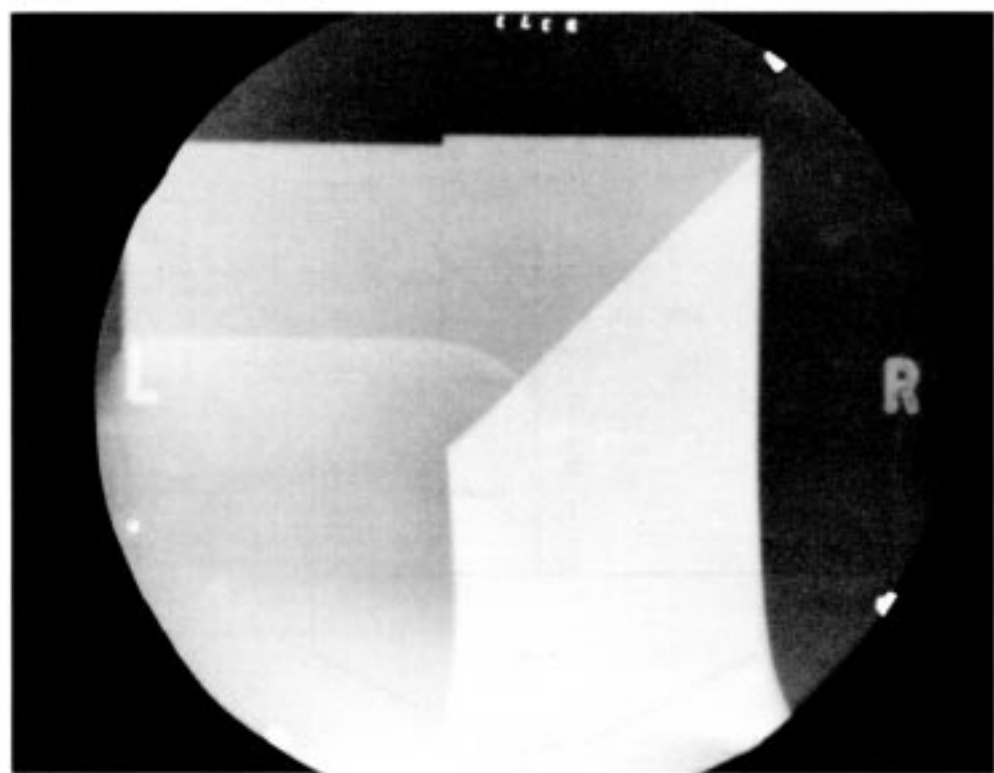
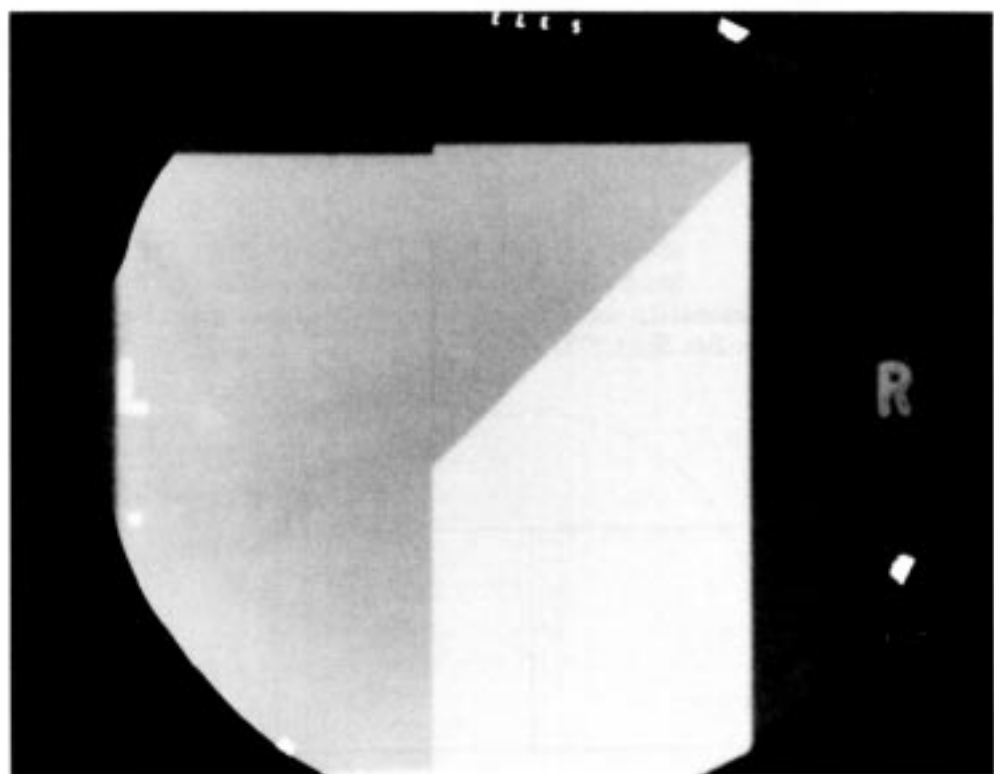
Experimenter: Roger W. Taylor

Radiographic Time: 39.98 μ s

References: Mader and Forest, 1976; Mader, 1979

A Composition B-3 detonation wave initiated by a P-081 lens turns an embedded 45° aluminum corner. See Shot 374.





SHOT 374: Composition B-3 Turning a 45° Aluminum Corner

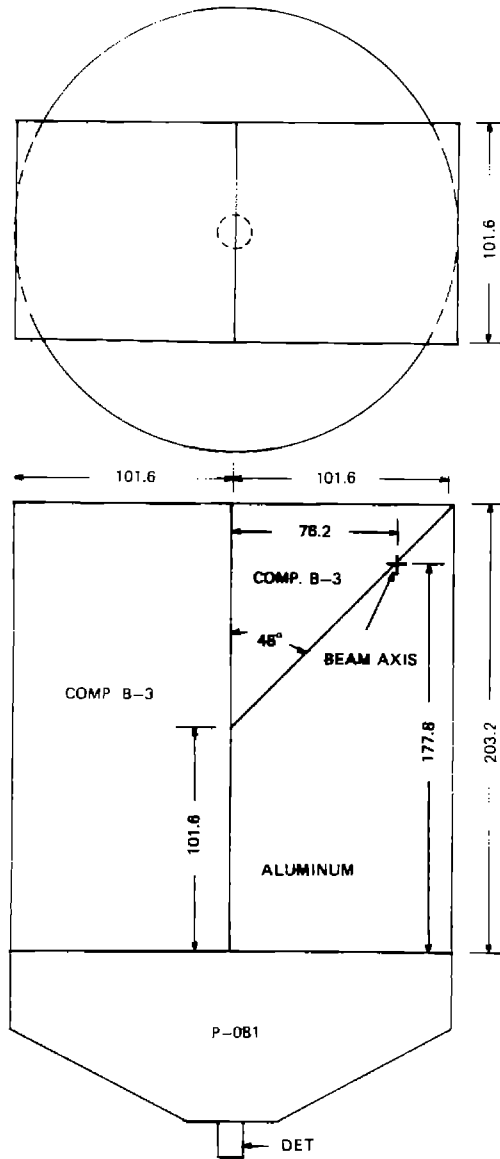
Date: February 2, 1966

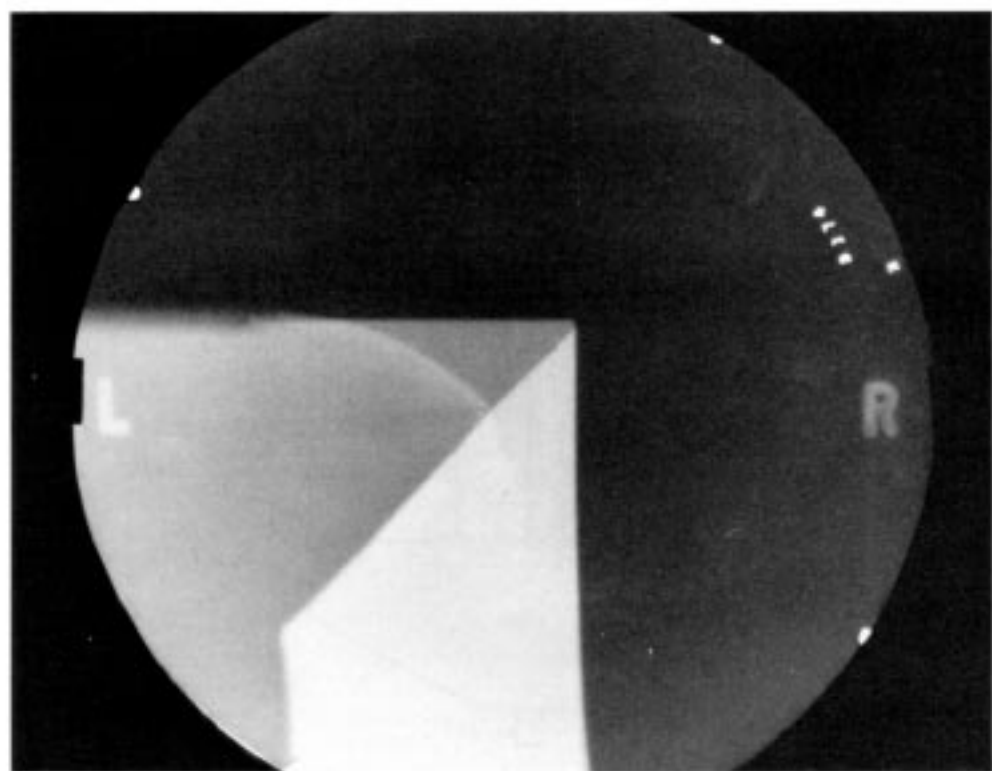
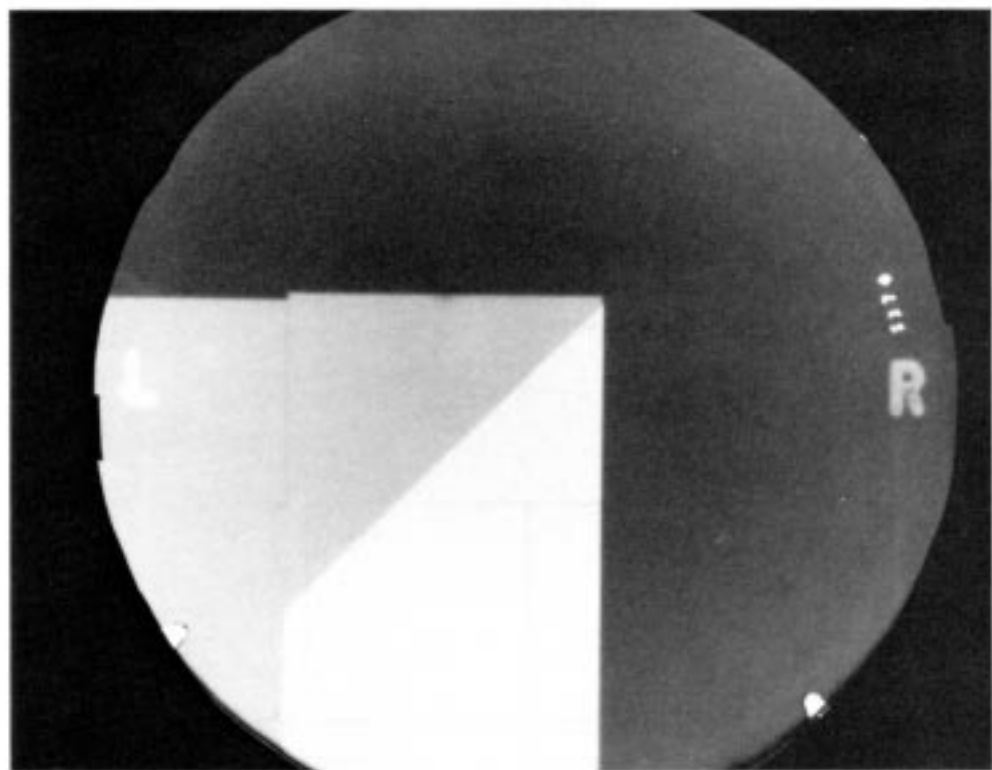
Experimenter: Roger W. Taylor

Radiographic Time: 48.94 μ s

References: Mader and Forest, 1976; Mader, 1979

A Composition B-3 detonation wave initiated by a P-081 lens turns an embedded 45° aluminum corner. See Shot 373.





SHOT 375:

Composition B-3 Turning a 30° Aluminum Corner

Date:

February 3, 1966

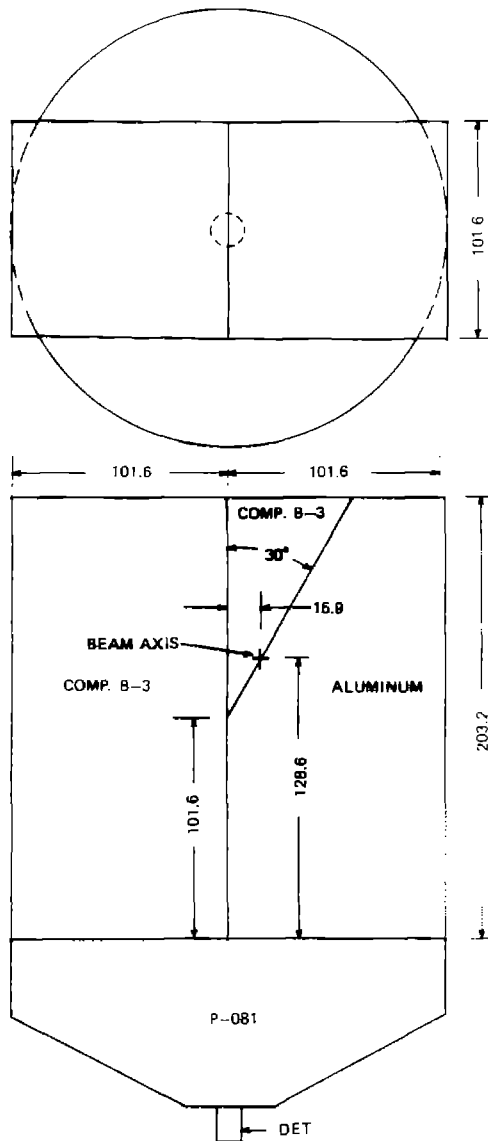
Experimenter:

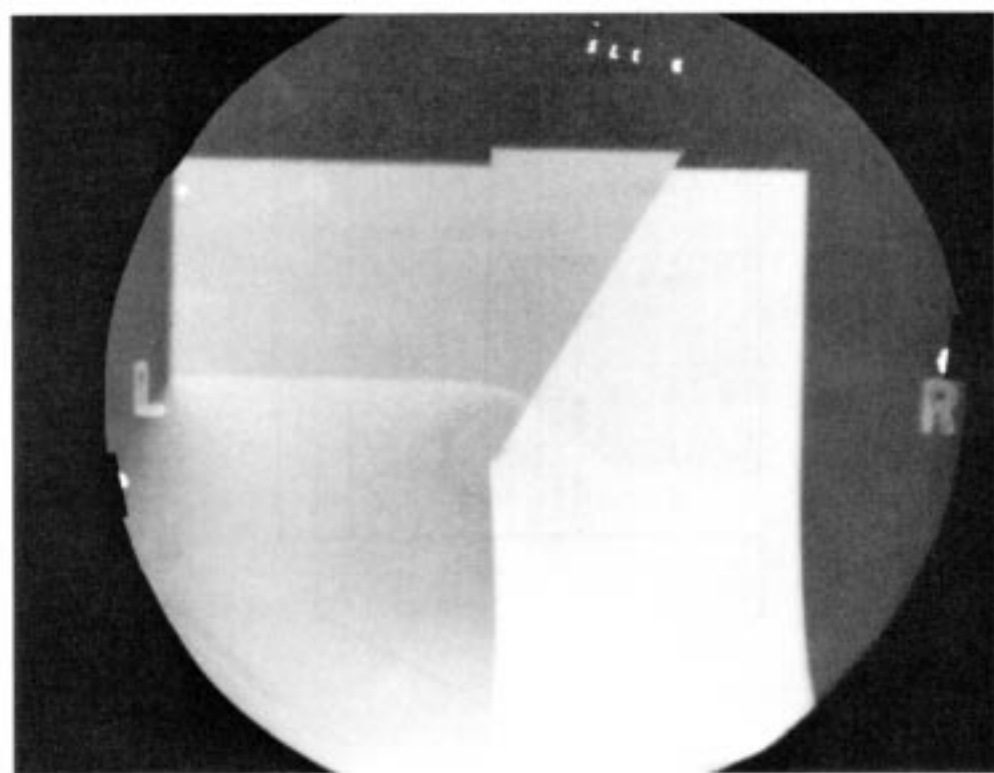
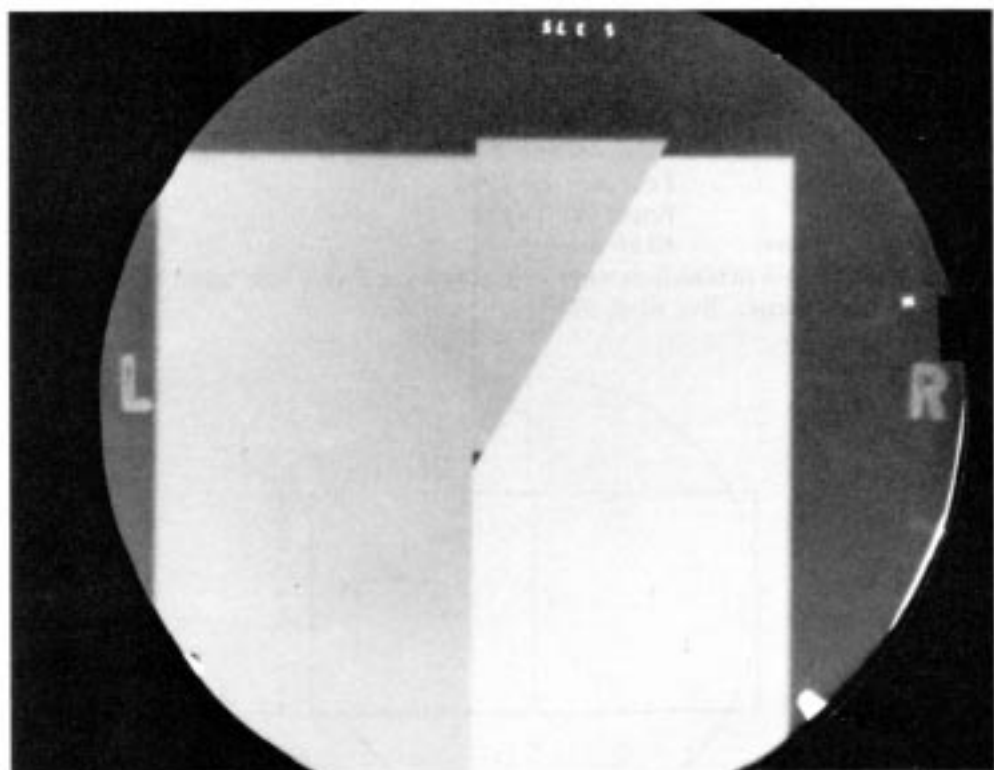
Roger W. Taylor

Radiographic Time:

39.05 μ s

A Composition B-3 detonation wave initiated by a P-081 lens turns an embedded 30° aluminum corner. See Shot 376.





SHOT 376:

Composition B-3 Turning a 30° Aluminum Corner

Date:

February 15, 1966

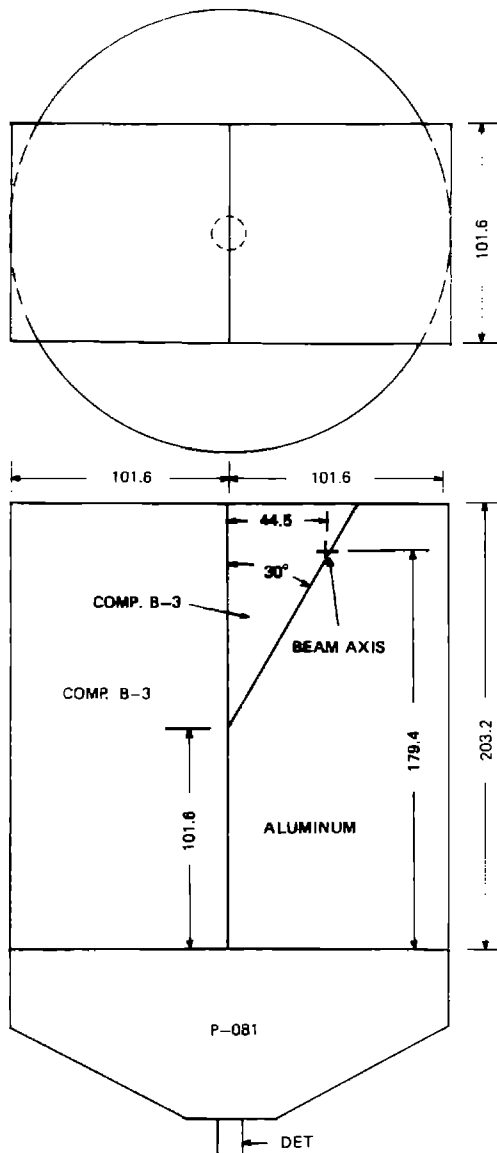
Experimenter:

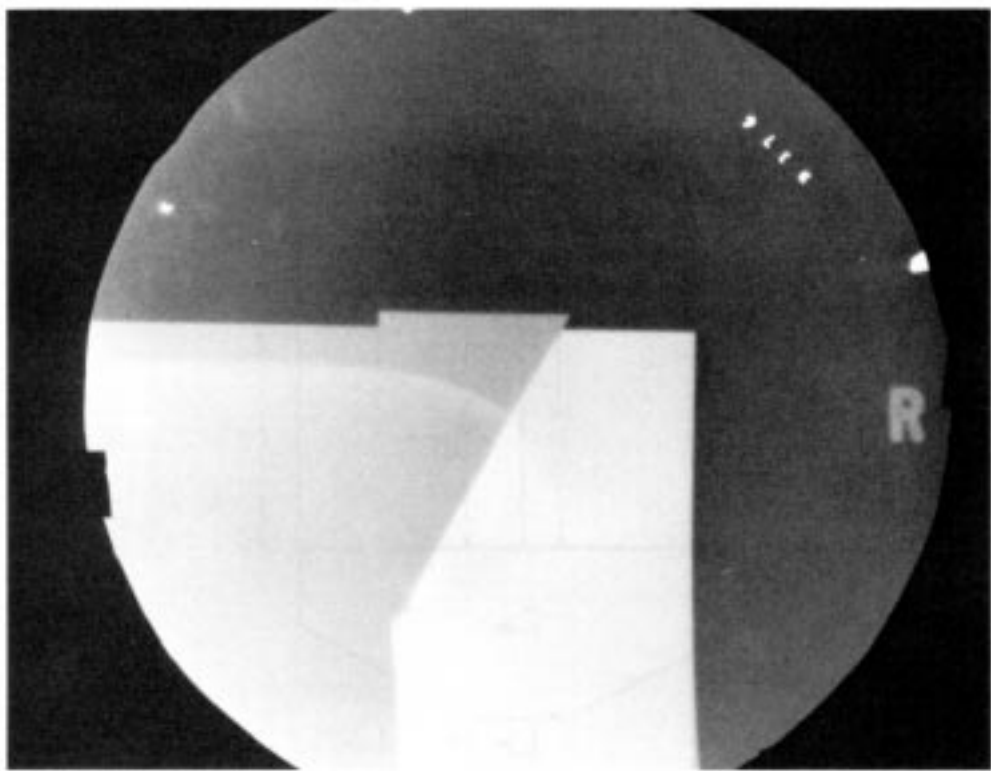
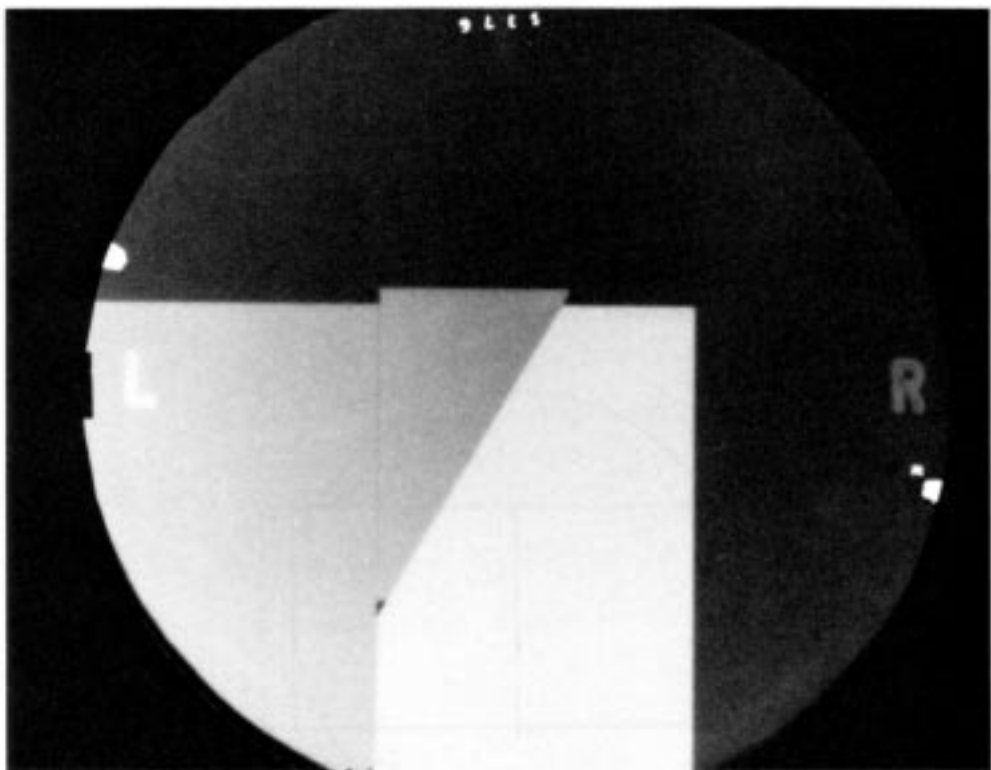
Roger W. Taylor

Radiographic Time:

46.26 μ s

A Composition B-3 detonation wave initiated by a P-081 lens turns an embedded 30° aluminum corner. See Shot 375.





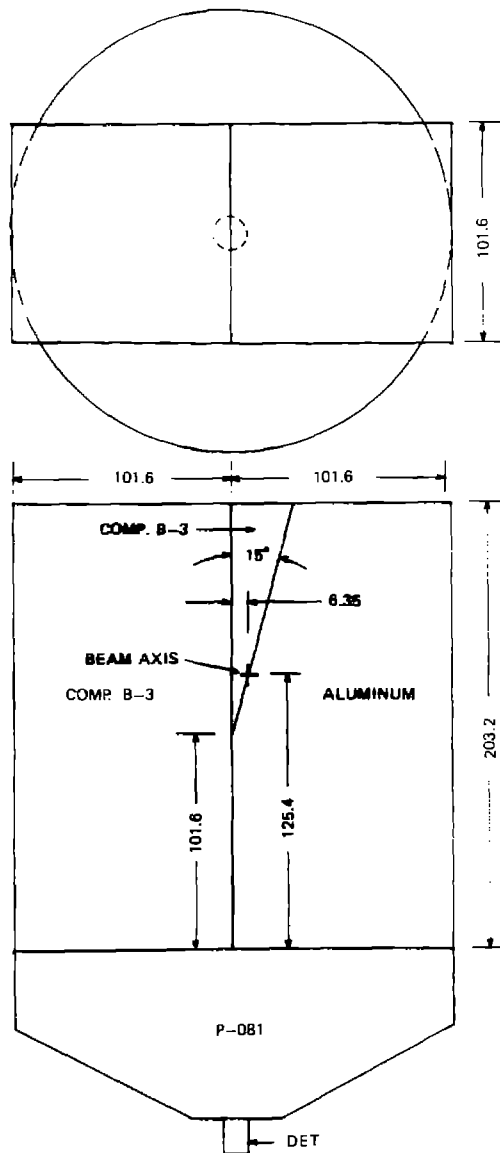
SHOT 377: Composition B-3 Turning a 15° Aluminum Corner

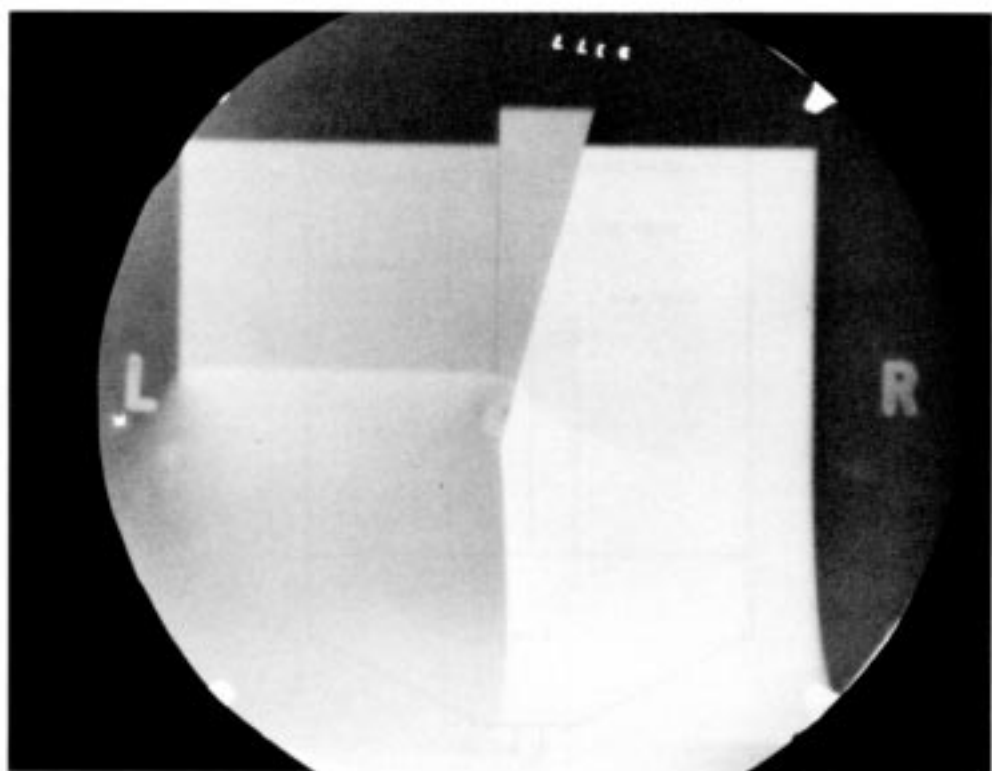
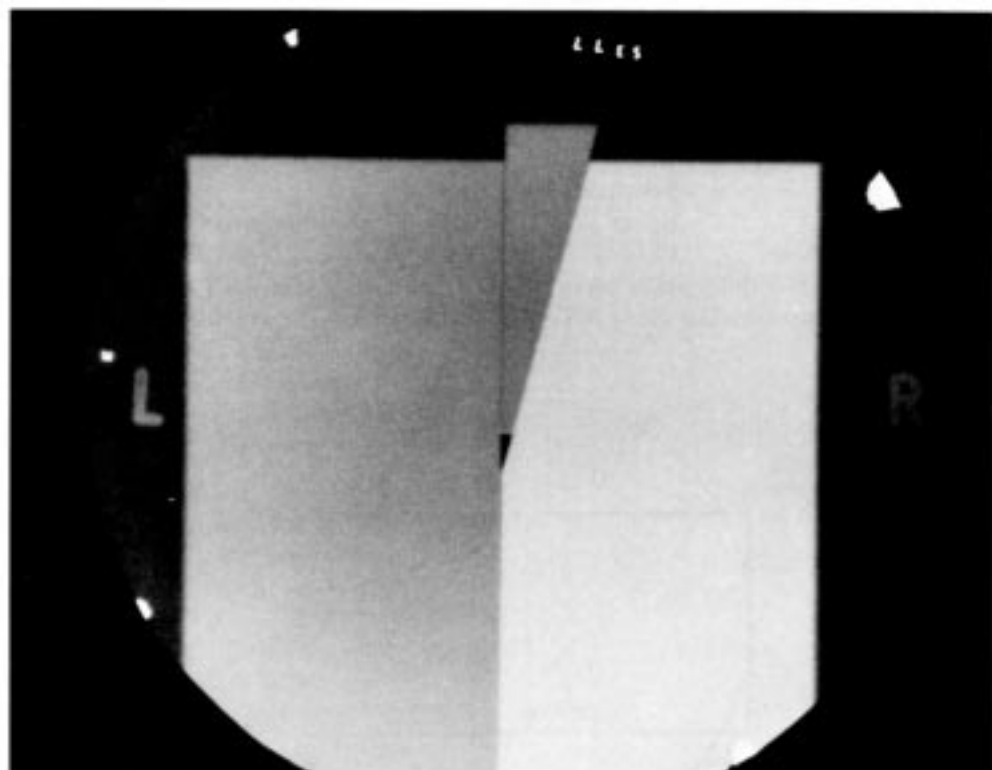
Date: February 15, 1966

Experimenter: Roger W. Taylor

Radiographic Time: 38.65 μ s

A Composition B-3 detonation wave initiated by a P-081 lens turns an embedded 15° aluminum corner. See Shot 378.





SHOT 378:

Composition B-3 Turning a 15° Aluminum Corner

Date:

February 15, 1966

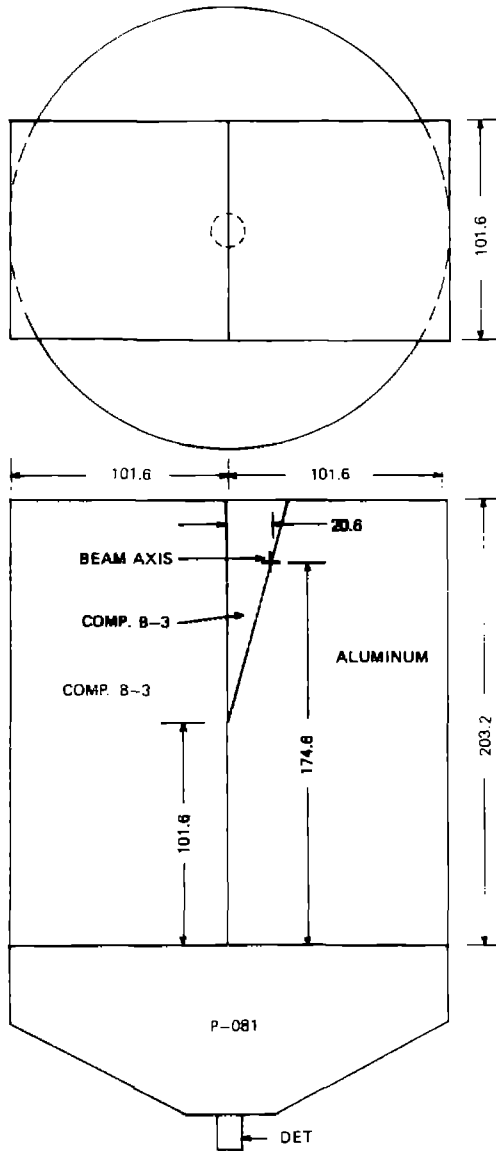
Experimenter:

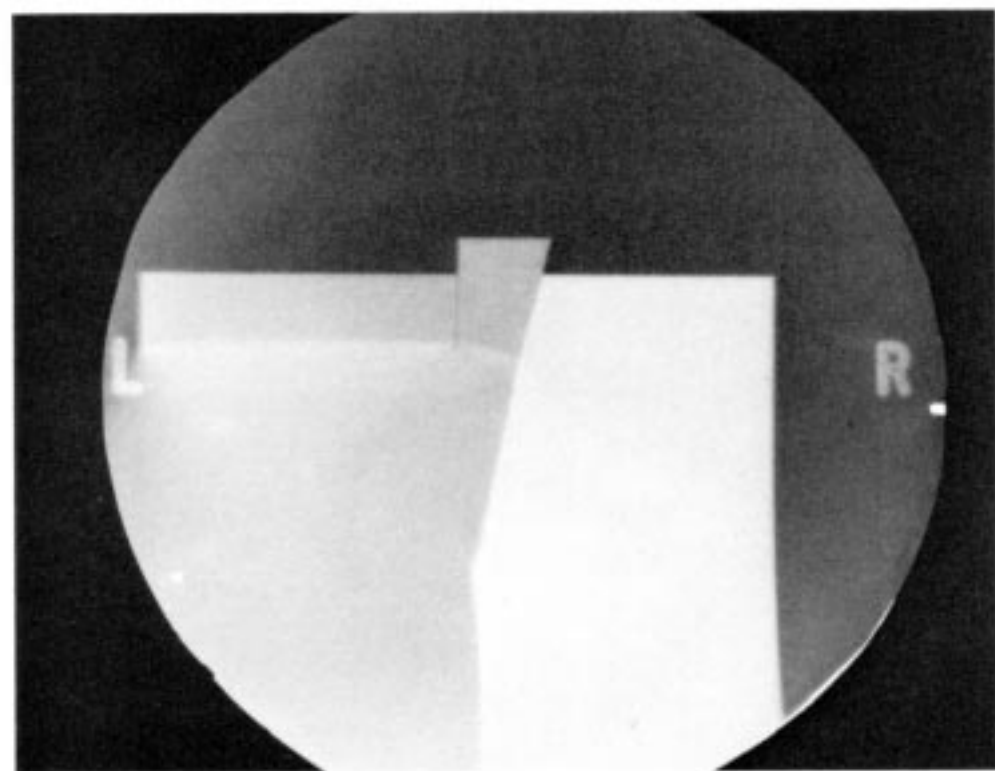
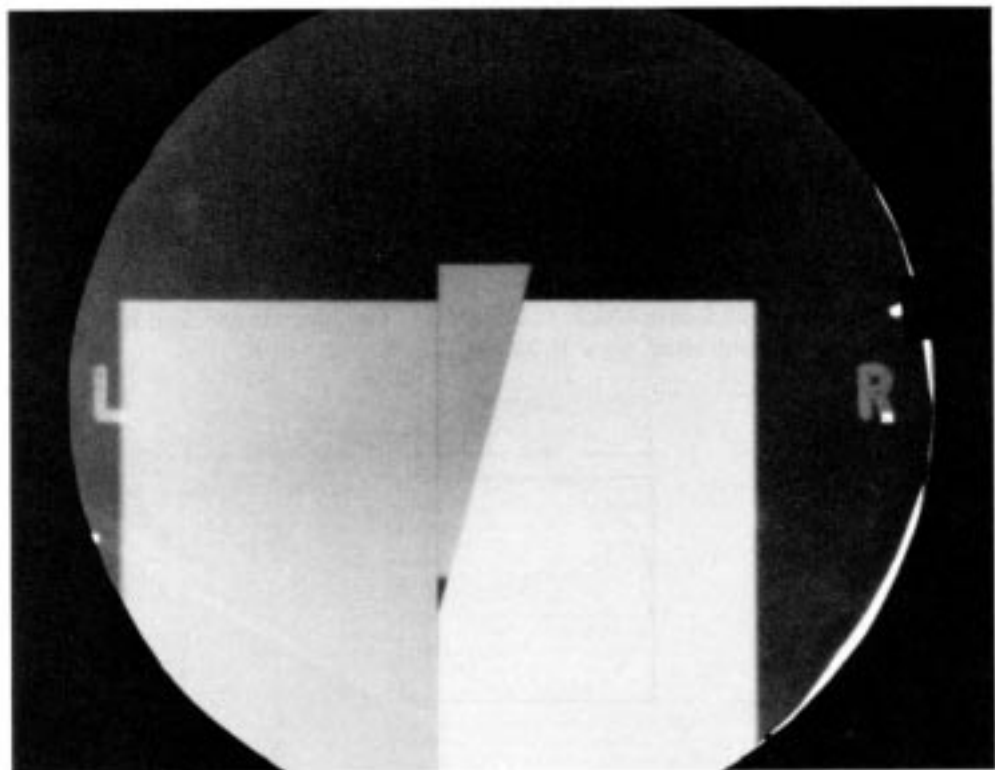
Roger W. Taylor

Radiographic Time:

45.04 μ s

A Composition B-3 detonation wave initiated by a P-081 lens turns an embedded 15° aluminum corner. See Shot 377.





SHOT 379:

Dynamic Fracture of Beryllium

Date:

November 15, 1965

Experimenter:

Benny Ray Breed

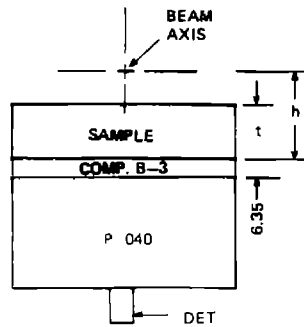
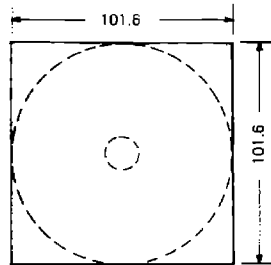
Radiographic Time:

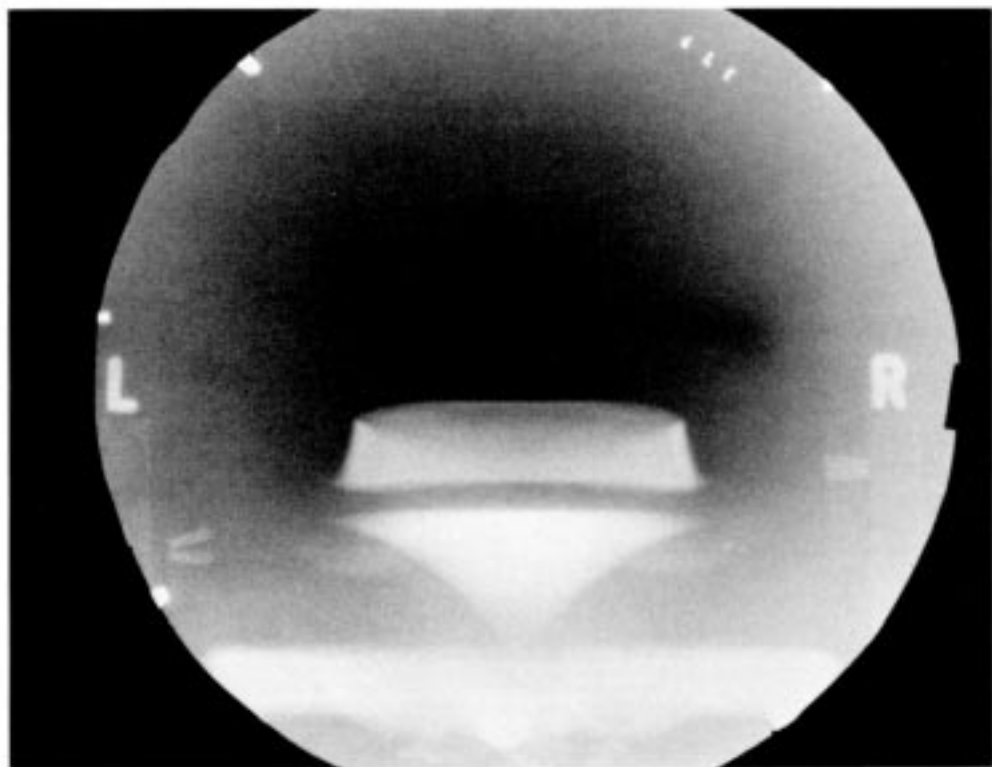
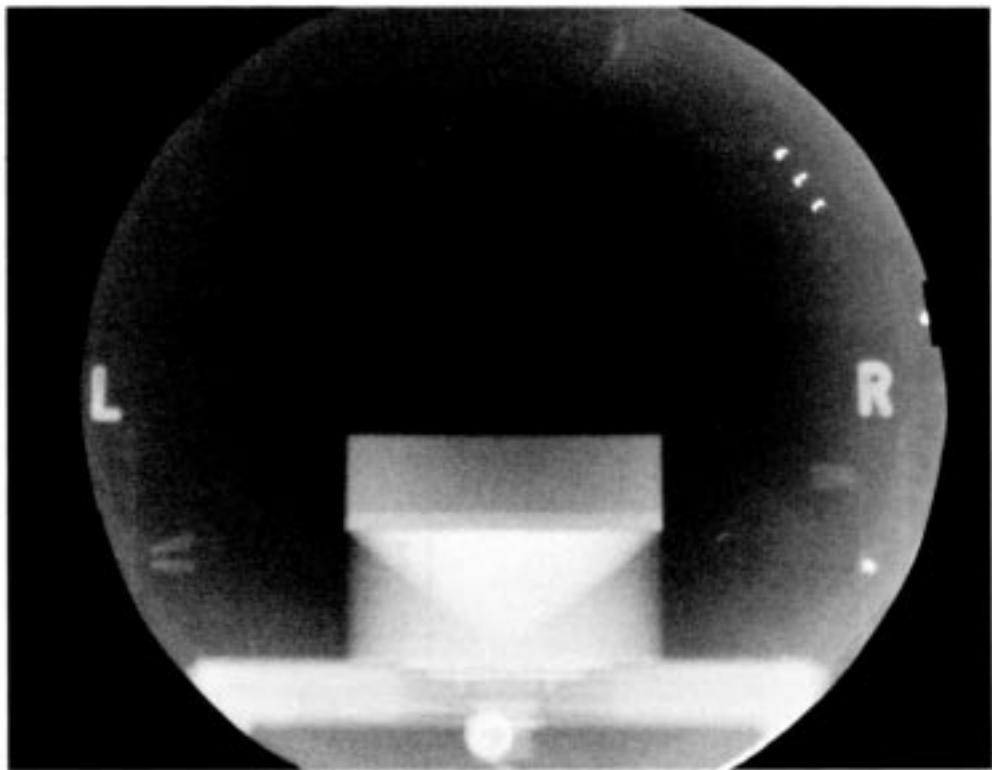
21.52 μ s

Reference:

Thurston and Mudd, 1968

Dynamic fracture of 25.0-mm-thick, t , beryllium. The plate is shocked by 6.35 mm of Composition B-3 initiated by a P-040 lens. h is 41.27 mm.





SHOT 380:

Dynamic Fracture of Beryllium

Date:

November 17, 1965

Experimenter:

Benny Ray Breed

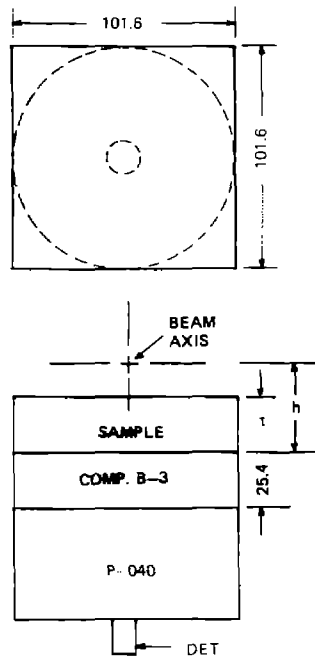
Radiographic Time:

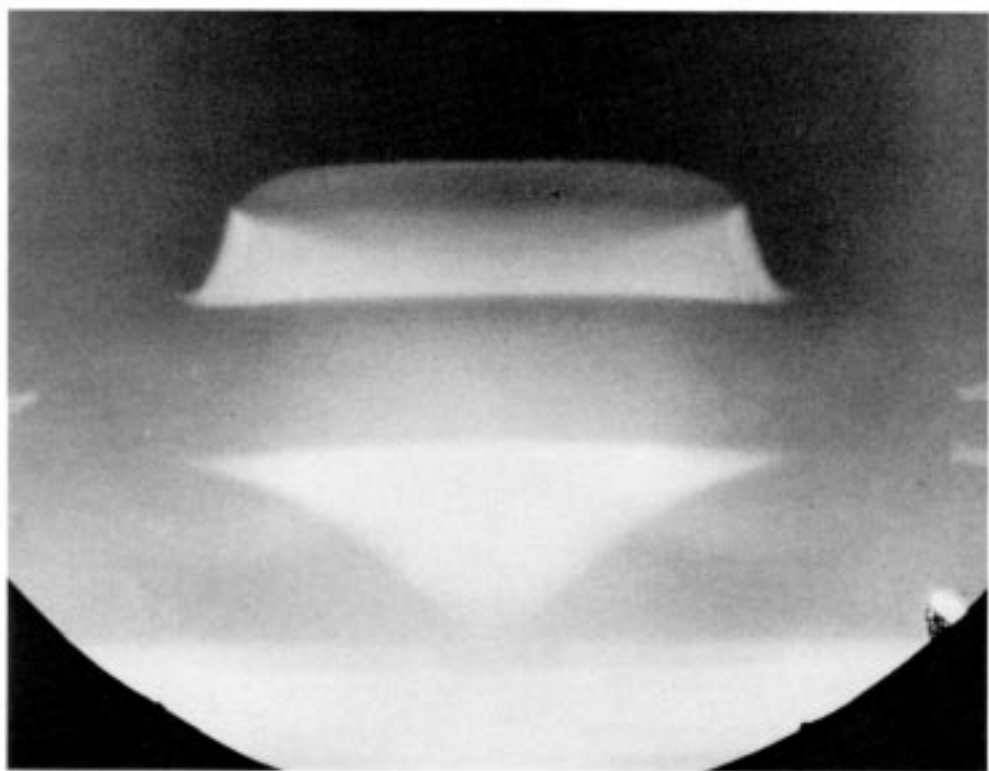
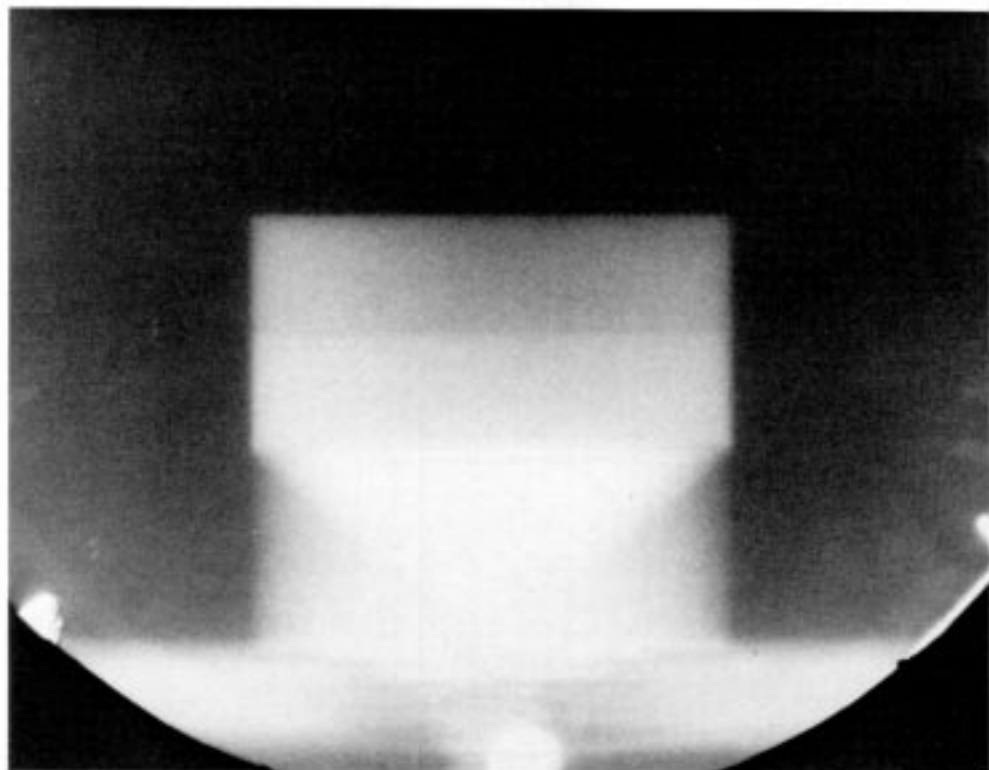
23.94 μ s

Reference:

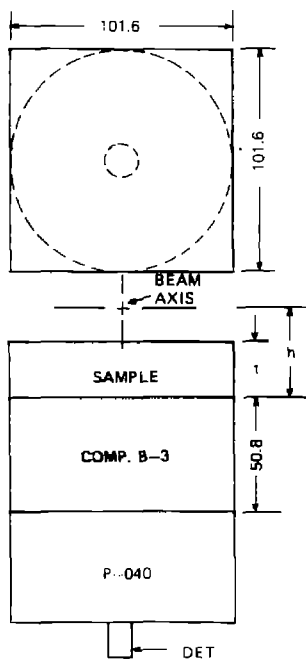
Thurston and Mudd, 1968

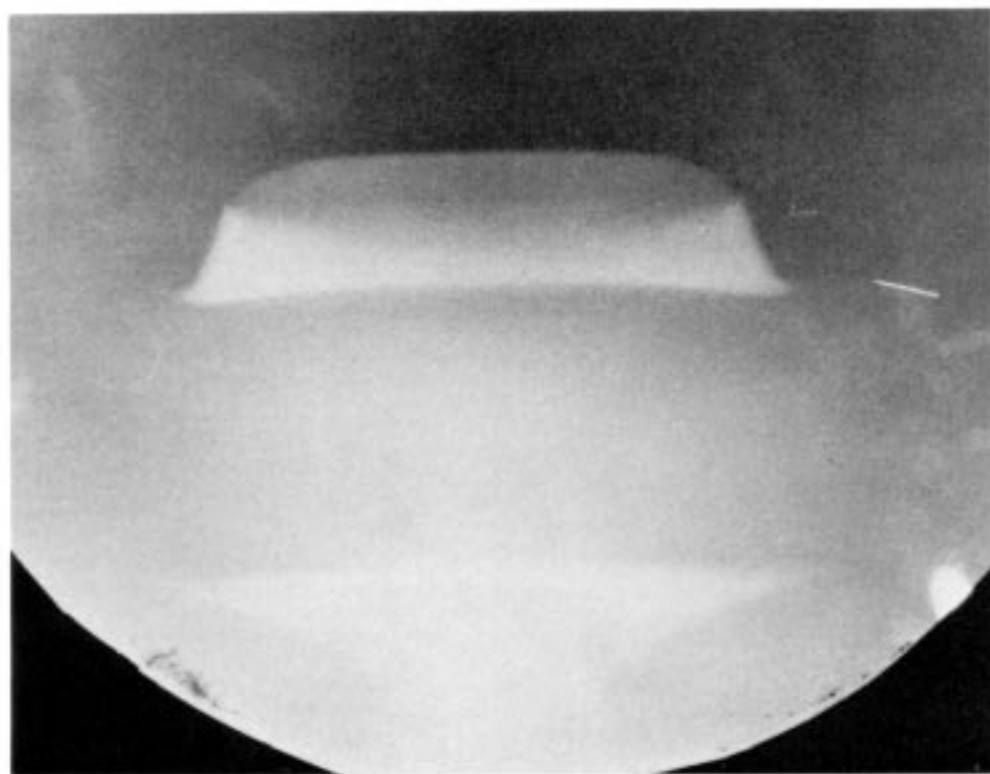
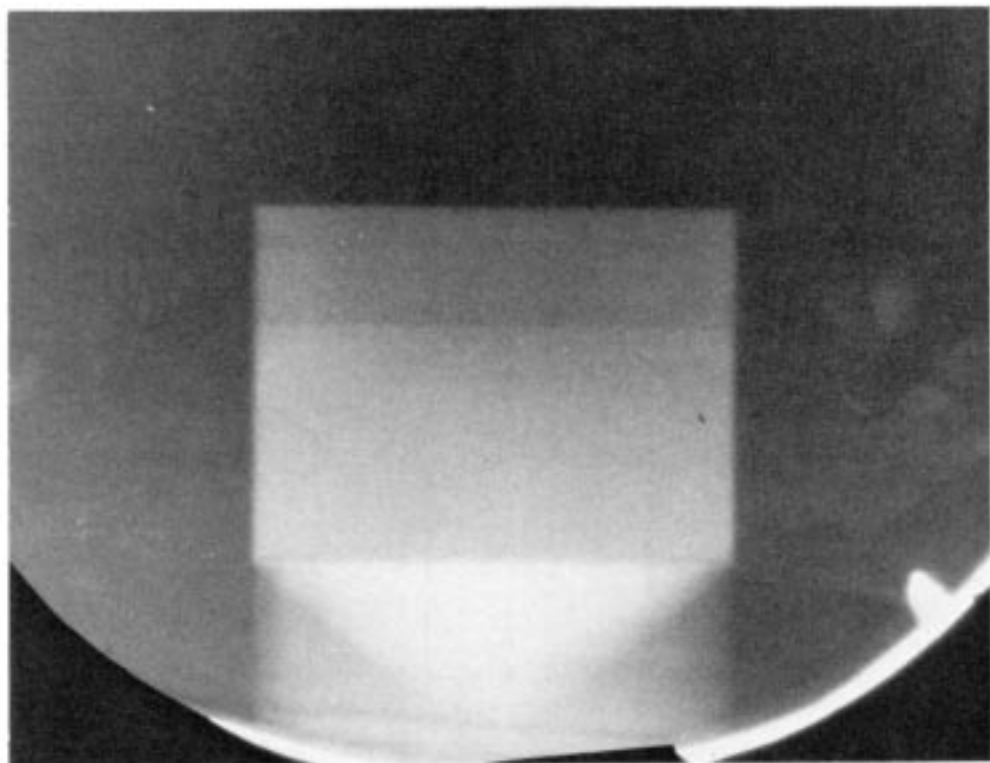
Dynamic fracture of 25.0-mm-thick, t , beryllium. The plate is shocked by 25.4 mm of Composition B-3 initiated by a P-040 lens. h is 41.27 mm.





SHOT 381: **Dynamic Fracture of Beryllium**
Date: November 18, 1965
Experimenter: Benny Ray Breed
Radiographic Time: 27.04 μ s
Reference: Thurston and Mudd, 1968
Dynamic fracture of 25.0-mm-thick, t , beryllium. The plate is shocked by 50.8 mm of Composition B-3 initiated by a P-040 lens. h is 41.27 mm.





SHOT 382:

Dynamic Fracture of Beryllium

Date:

November 24, 1965

Experimenter:

Benny Ray Breed

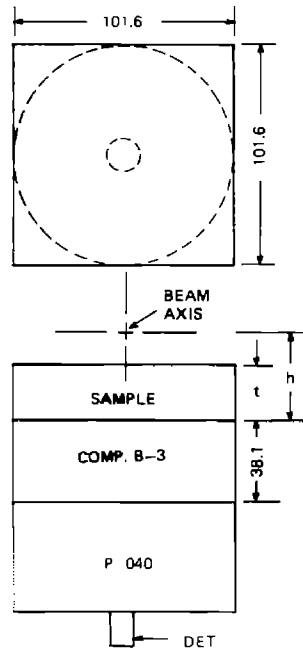
Radiographic Time:

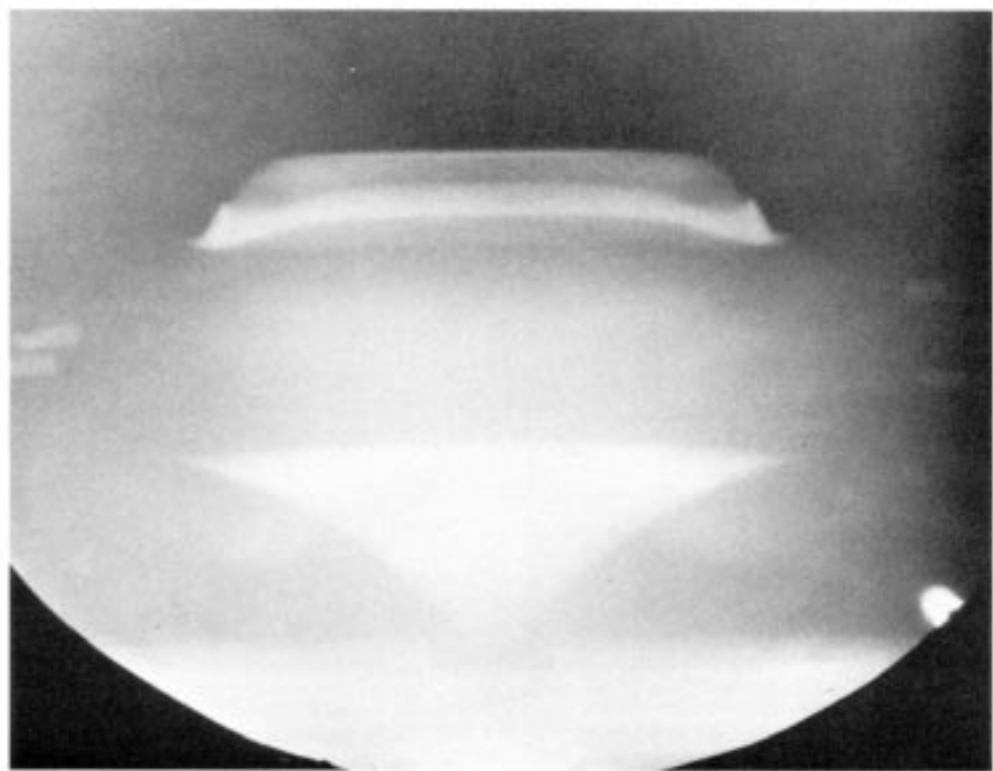
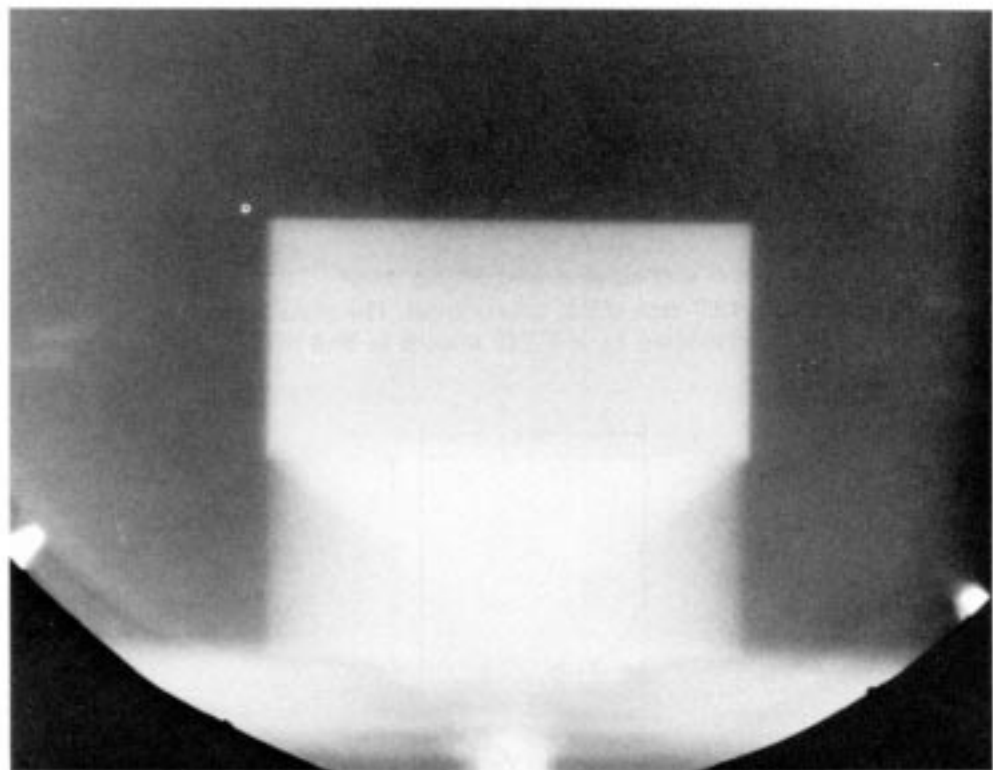
24.33 μ s

Reference:

Thurston and Mudd, 1968

Dynamic fracture of 12.0-mm-thick, t , beryllium. The plate is shocked by 38.1 mm of Composition B-3 initiated by a P-040 lens. h is 28.6 mm.





SHOT 383:

Dynamic Fracture of Beryllium

Date:

December 23, 1965

Experimenter:

Benny Ray Breed

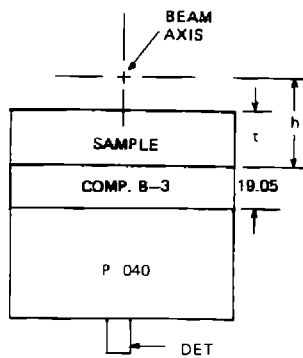
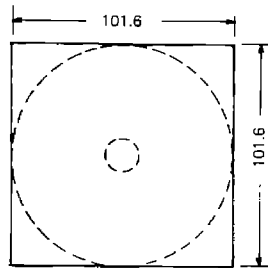
Radiographic Time:

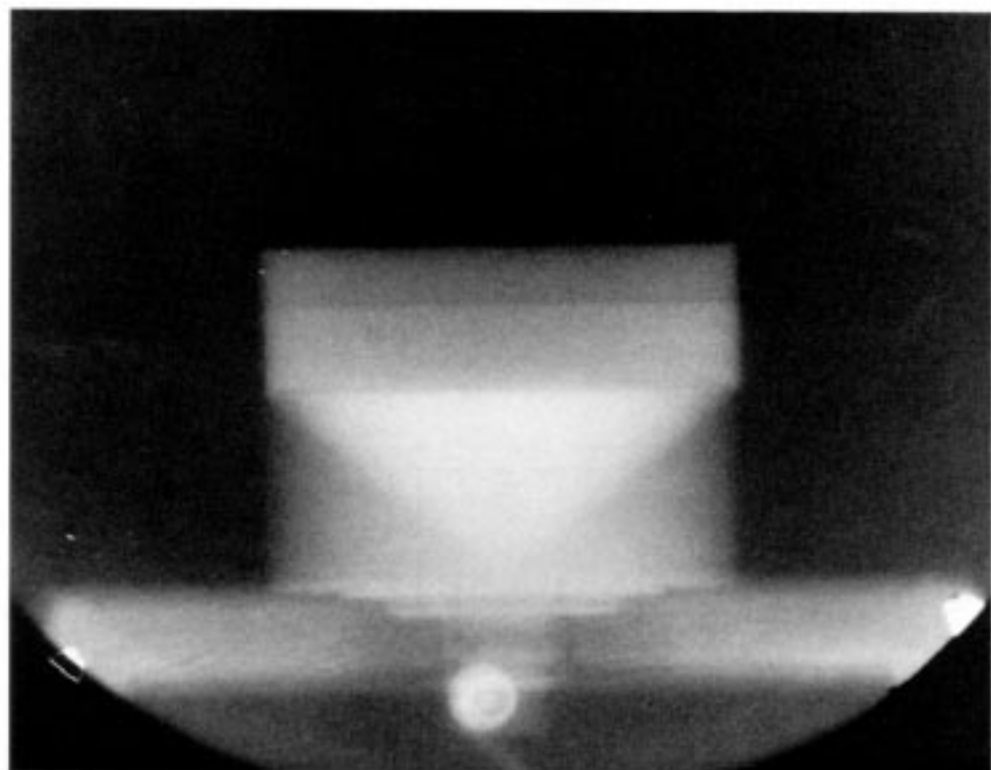
21.95 μ s

Reference:

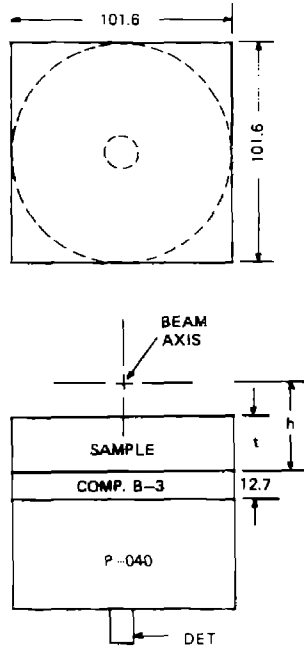
Thurston and Mudd, 1968

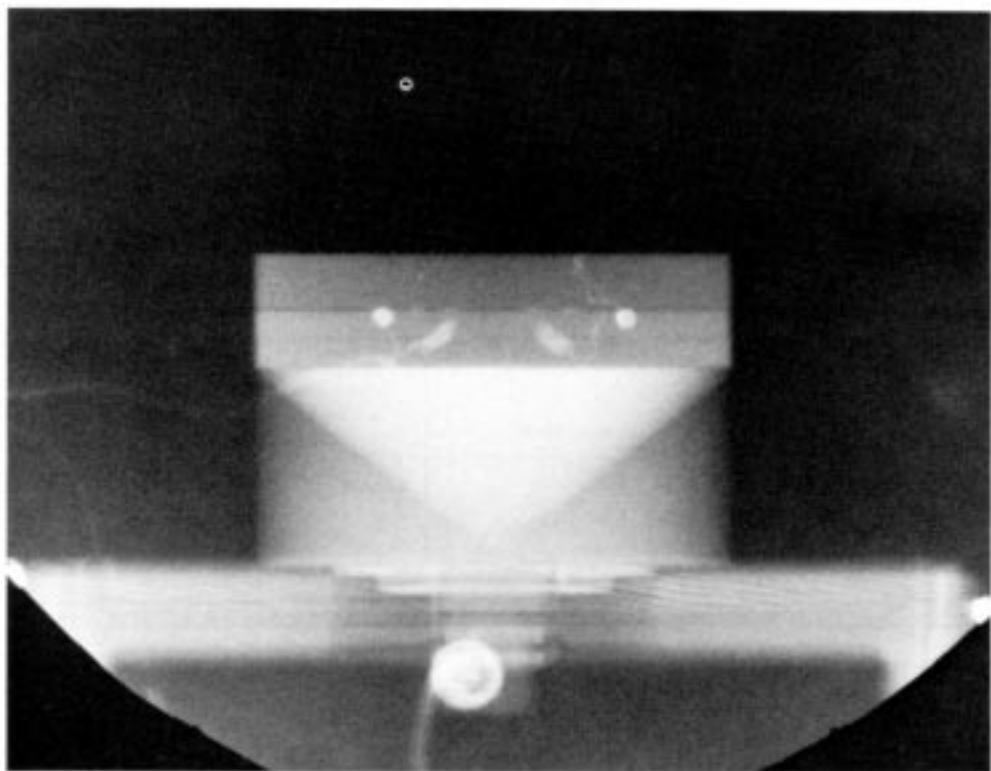
Dynamic fracture of 12.0-mm-thick, t , beryllium. The plate is shocked by 19.05 mm of Composition B-3 initiated by a P-040 lens. h is 28.6 mm.





SHOT 384: Dynamic Fracture of Beryllium
Date: February 14, 1966
Experimenter: Benny Ray Breed
Radiographic Time: 21.07 μ s
Reference: Thurston and Mudd, 1968
Dynamic fracture of 12.0-mm-thick, t, beryllium. The plate is shocked by 12.7 mm of Composition B-3 initiated by a P-040 lens. h is 28.6 mm.





SHOT 385:

Dynamic Fracture of Beryllium

Date:

February 16, 1966

Experimenter:

Benny Ray Breed

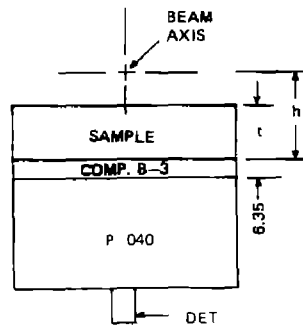
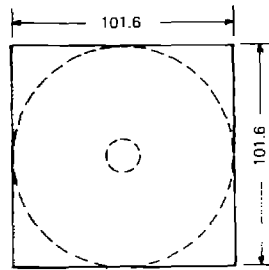
Radiographic Time:

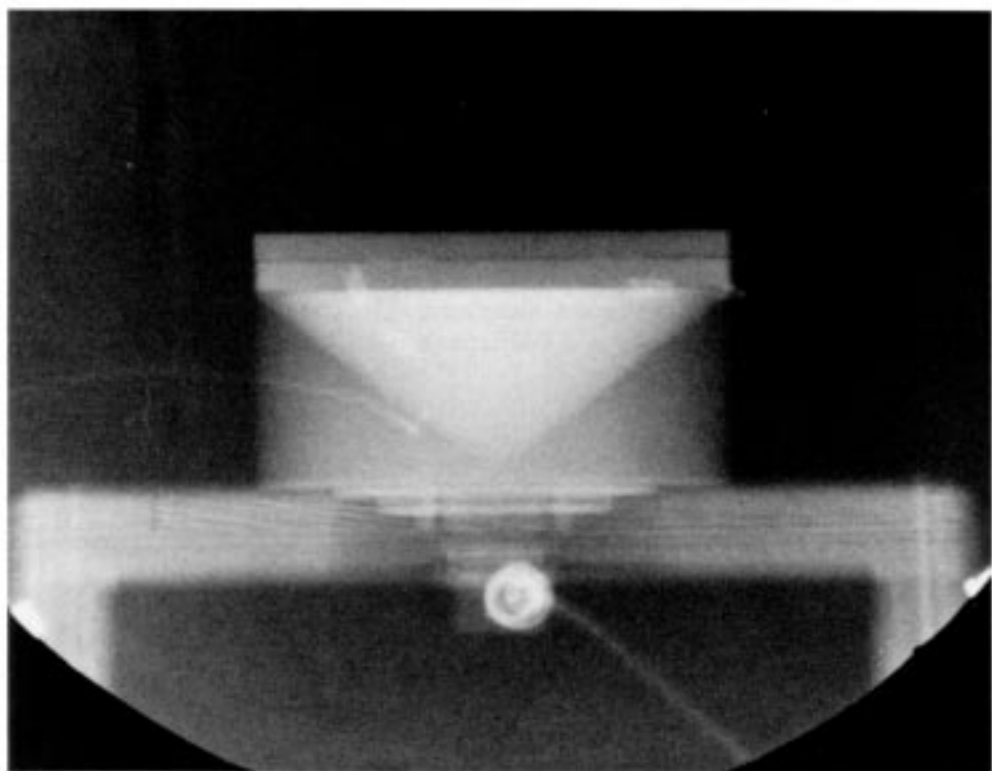
19.6 μ s

Reference:

Thurston and Mudd, 1968

Dynamic fracture of 6.0-mm-thick, t , beryllium. The plate is shocked by 6.35 mm of Composition B-3 initiated by a P-040 lens. h is 22.2 mm.





SHOT 386:

Dynamic Fracture of Aluminum

Date:

December 27, 1965

Experimenter:

Benny Ray Breed

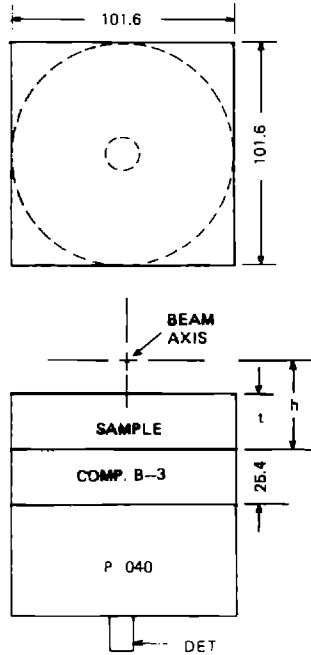
Radiographic Time:

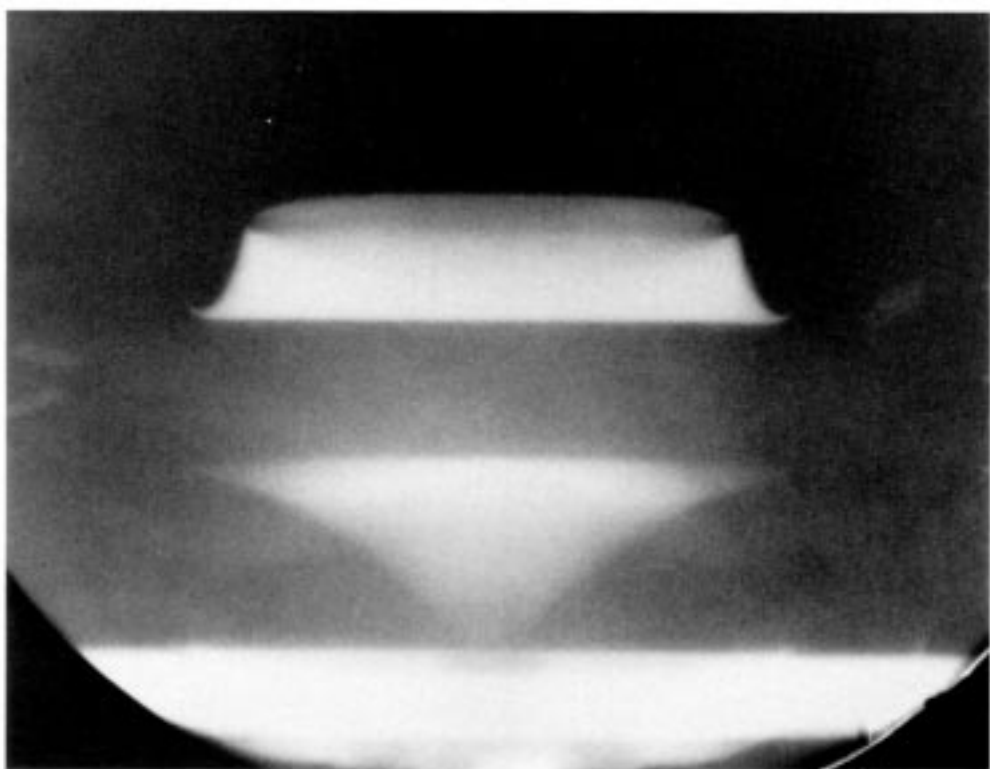
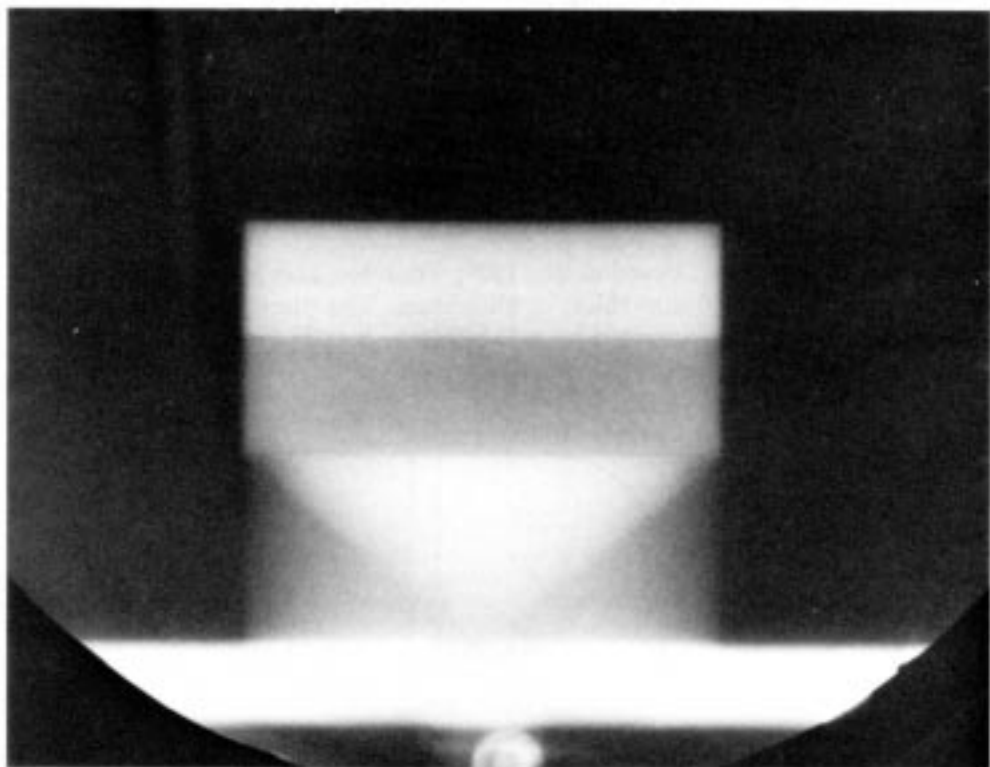
23.73 μ s

References:

Breed et al., 1967; Thurston and Mudd, 1968

Dynamic fracture of 25.0-mm-thick, t , aluminum. The plate is shocked by 25.4 mm of Composition B-3 initiated by a P-040 lens. h is 38.1 mm.





SHOT 387:

Dynamic Fracture of Aluminum

Date:

December 28, 1965

Experimenter:

Benny Ray Breed

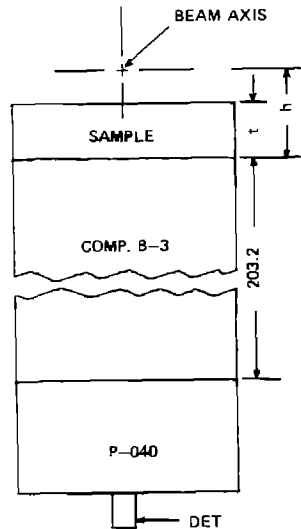
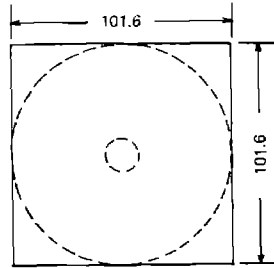
Radiographic Time:

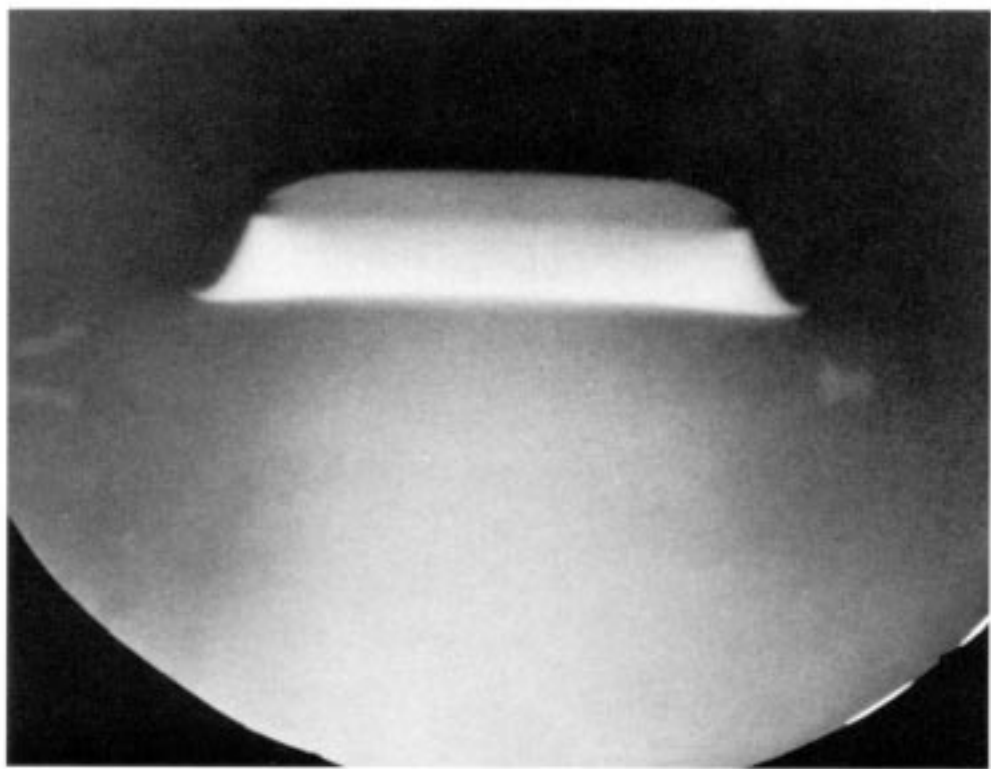
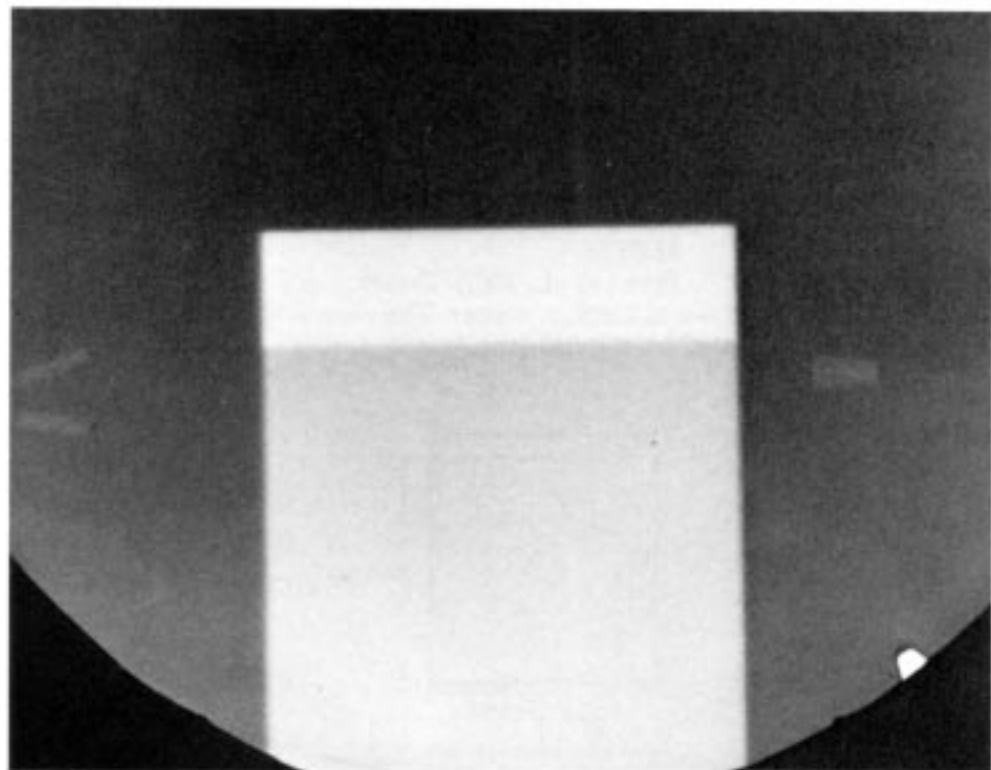
46.1 μ s

References:

Breed et al., 1967; Thurston and Mudd, 1968

Dynamic fracture of 25.0-mm-thick, t , aluminum. The plate is shocked by 203.2 mm of Composition B-3 initiated by a P-040 lens. h is 38.1 mm.





SHOT 389:

Dynamic Fracture of Copper

Date:

December 27, 1965

Experimenter:

Benny Ray Breed

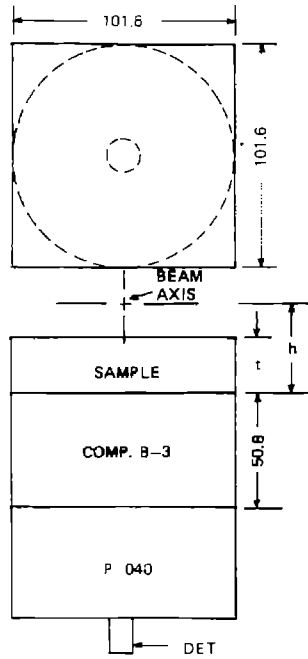
Radiographic Time:

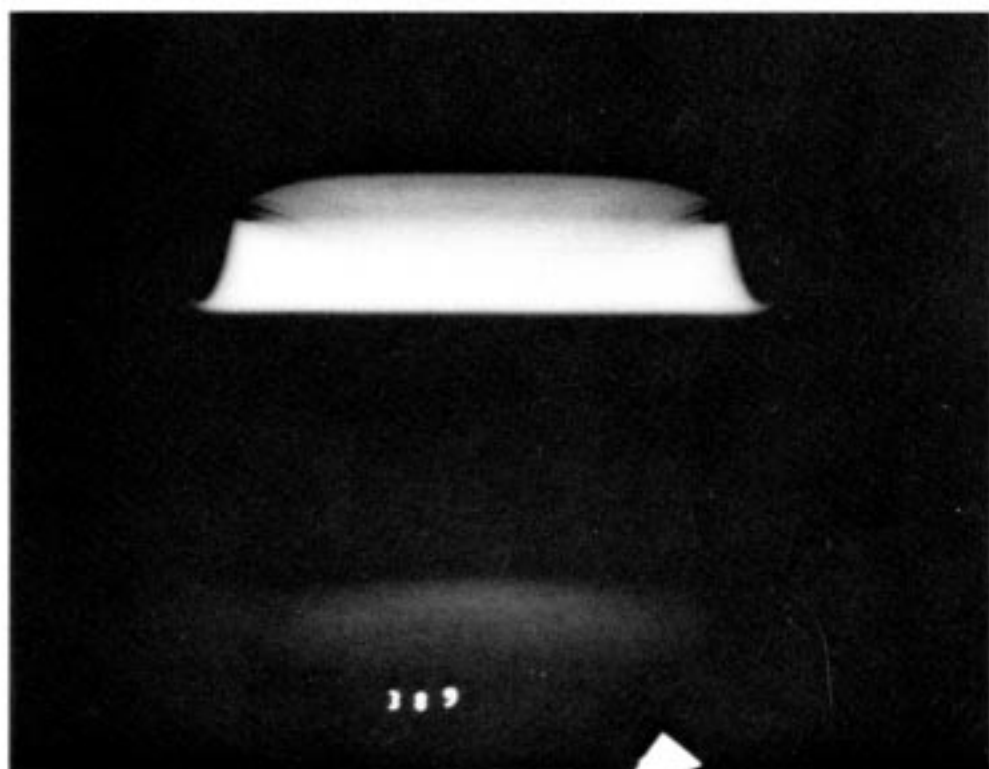
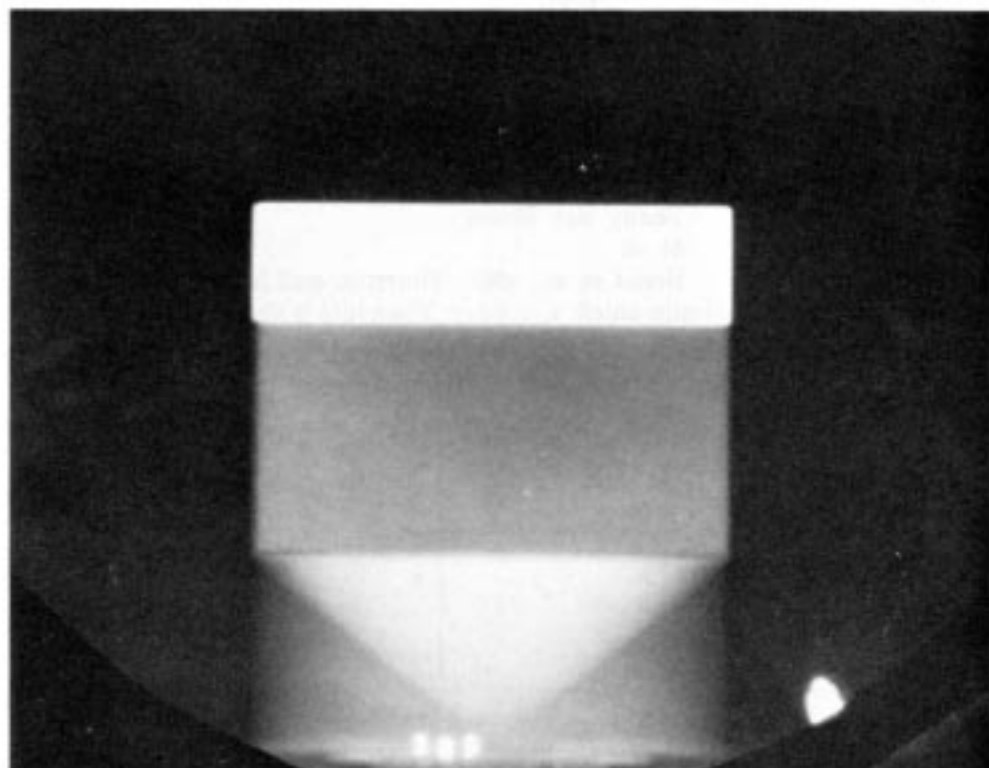
32.38 μ s

References:

Breed et al., 1967; Thurston and Mudd, 1968

Dynamic fracture of 25.0-mm-thick, t , copper. The plate is shocked by 50.8 mm of Composition B-3 initiated by a P-040 lens. h is 38.1 mm.





SHOT 390:

Dynamic Fracture of Copper

Date:

December 29, 1965

Experimenter:

Benny Ray Breed

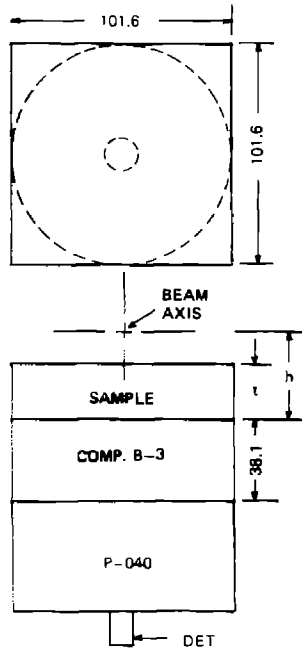
Radiographic Time:

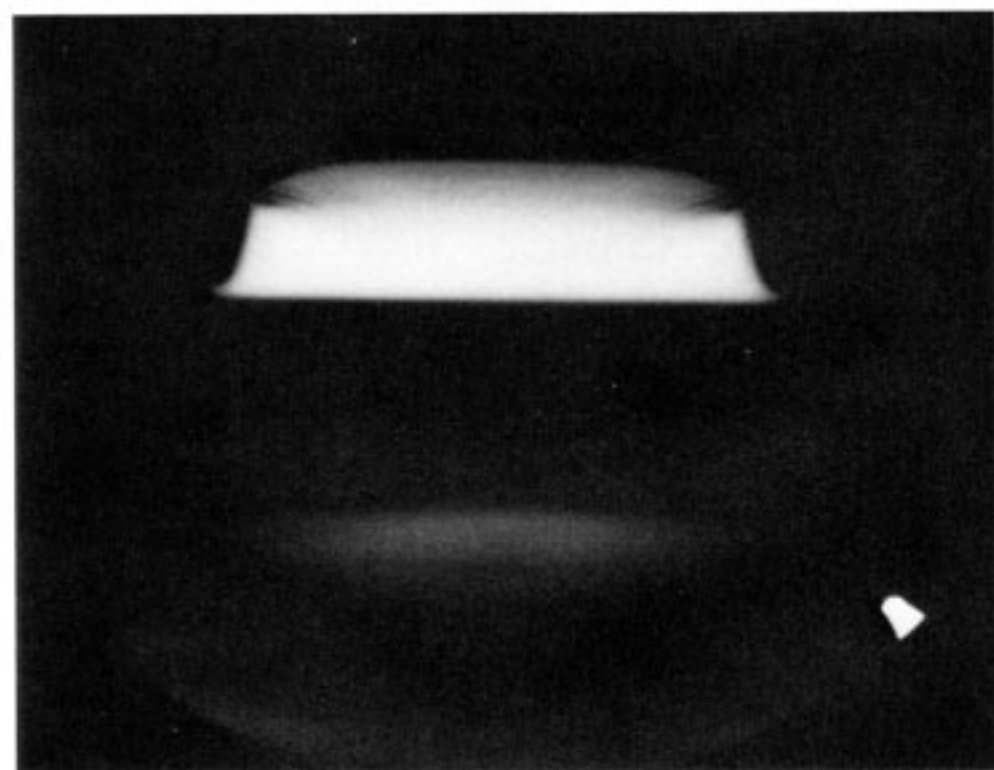
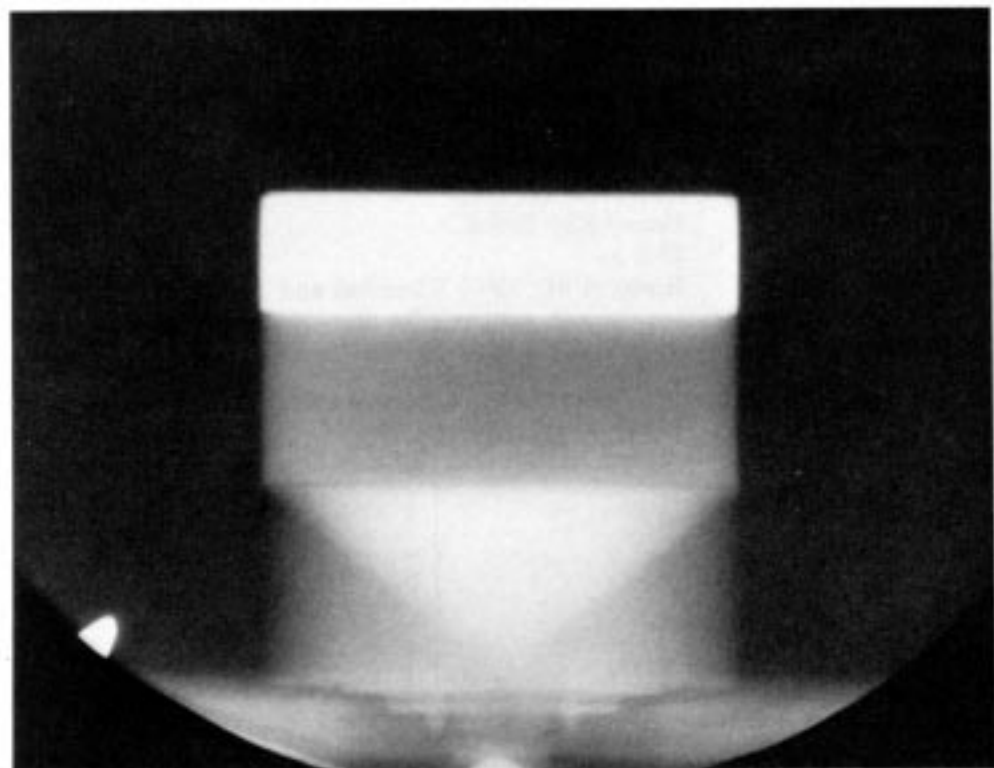
31 μ s

References:

Breed et al., 1967; Thurston and Mudd, 1968

Dynamic fracture of 25.0-mm-thick, t , copper. The plate is shocked by 38.1 mm of Composition B-3 initiated by a P-040 lens. h is 38.1 mm.





SHOT 391:

Dynamic Fracture of Copper

Date:

December 30, 1965

Experimenter:

Benny Ray Breed

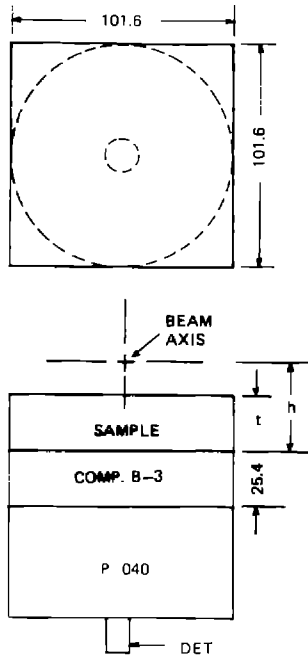
Radiographic Time:

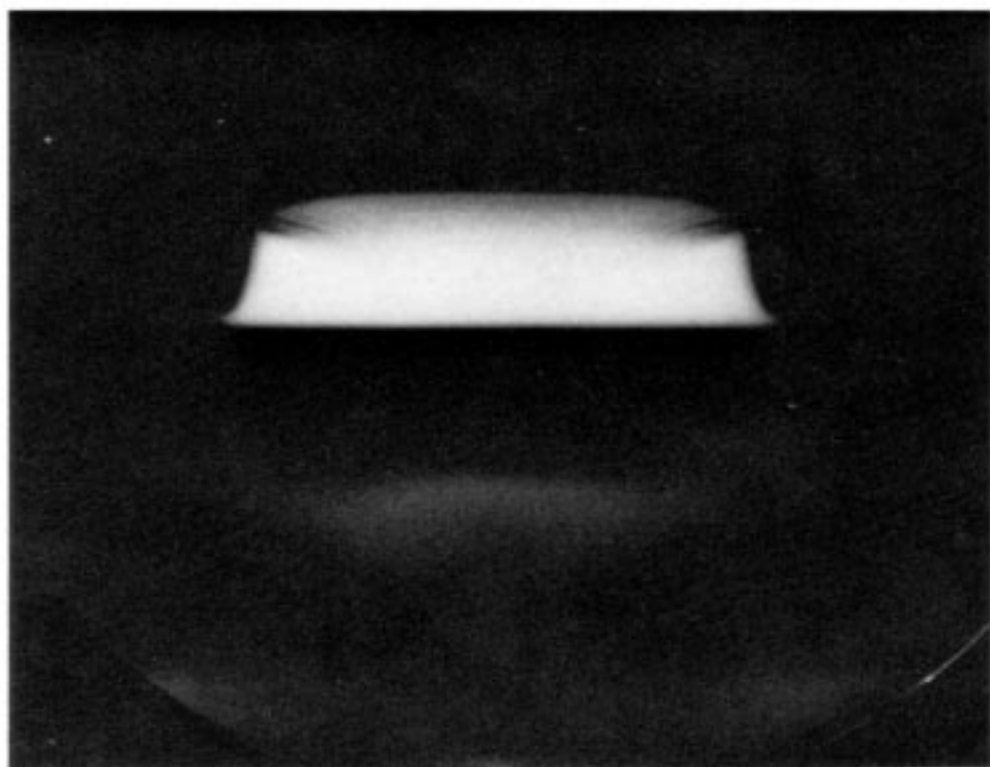
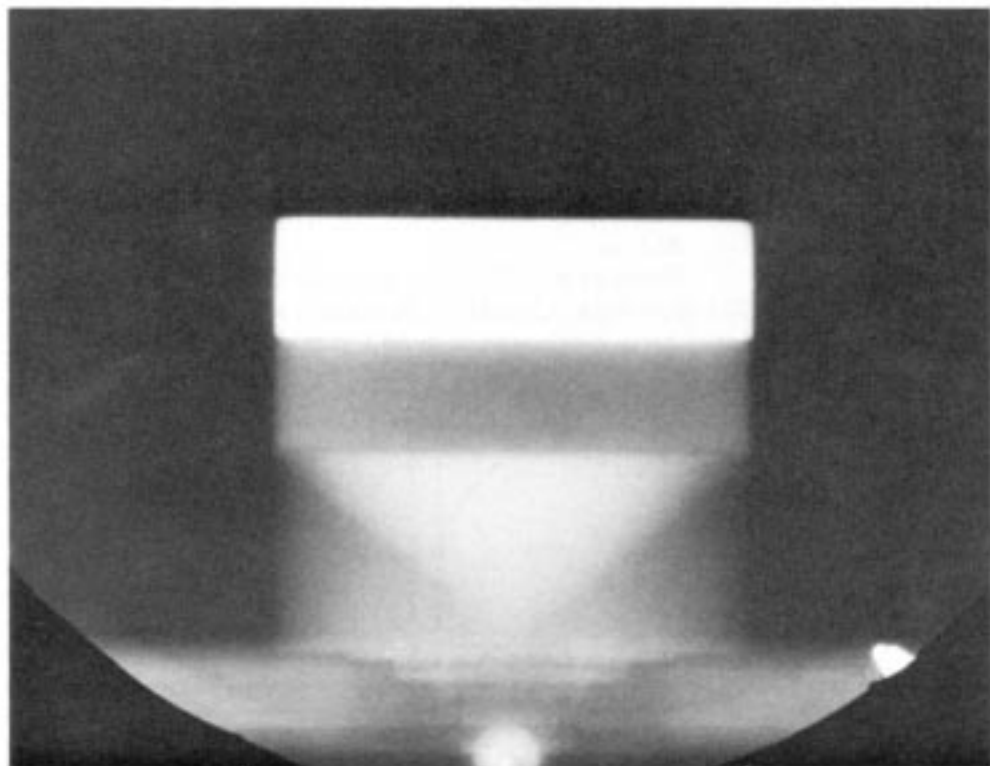
29.2 μ s

References:

Breed et al., 1967; Thurston and Mudd, 1968

Dynamic fracture of 25.0-mm-thick, t , copper. The plate is shocked by 25.4 mm of Composition B-3 initiated by a P-040 lens. h is 38.1 mm.





SHOT 392:

Dynamic Fracture of Nickel

Date:

December 22, 1965

Experimenter:

Benny Ray Breed

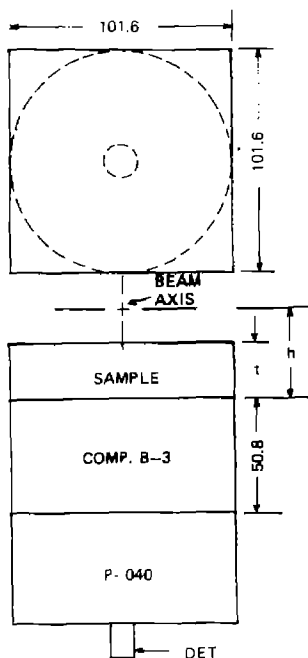
Radiographic Time:

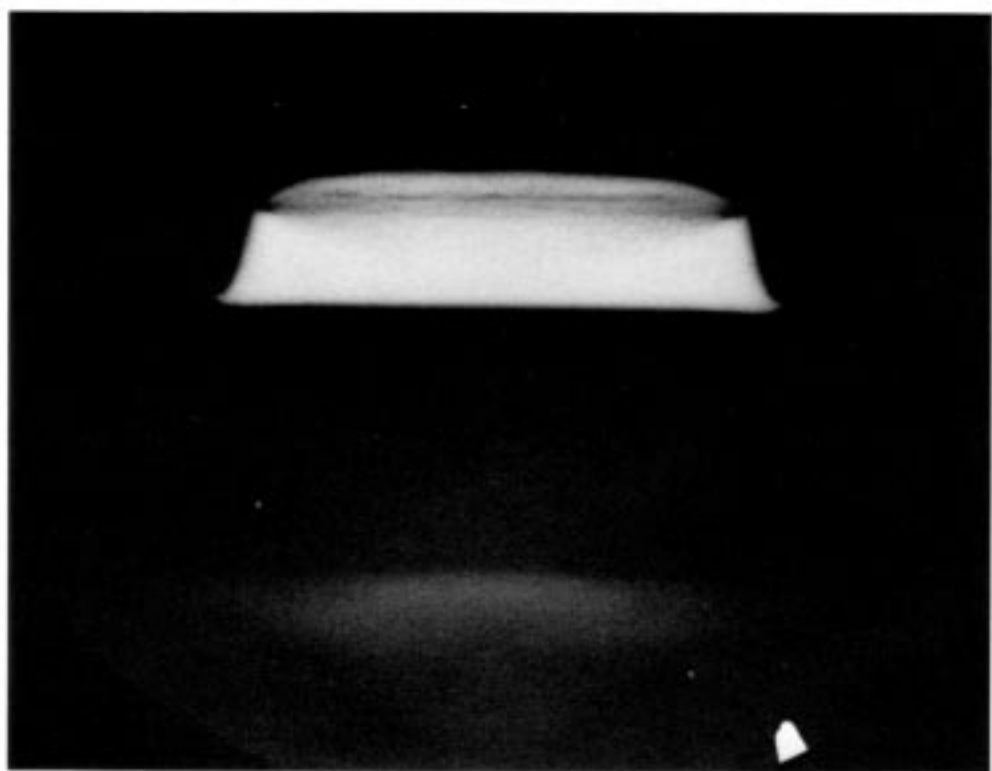
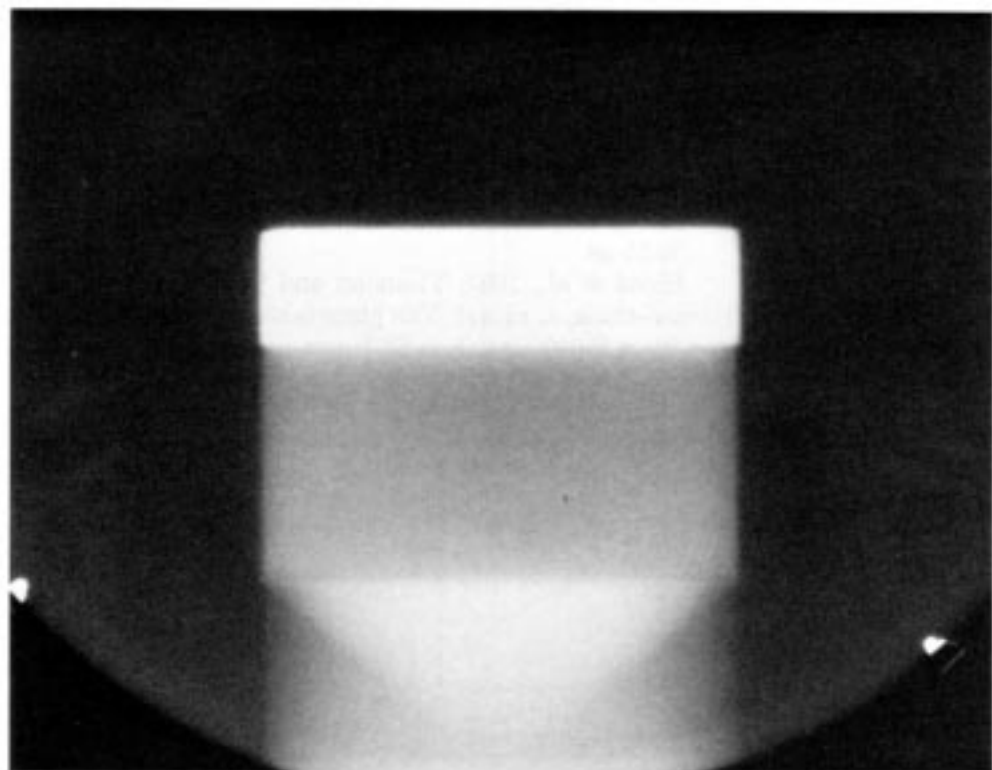
32.1 μ s

References:

Breed et al.; Thurston and Mudd, 1968

Dynamic fracture of 25.0-mm-thick, t , nickel. The plate is shocked by 50.8 mm of Composition B-3 initiated by a P-040 lens. h is 38.1 mm.





SHOT 393:

Dynamic Fracture of Nickel

Date:

January 4, 1966

Experimenter:

Benny Ray Breed

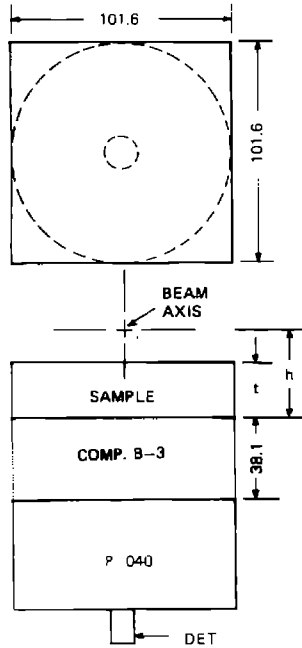
Radiographic Time:

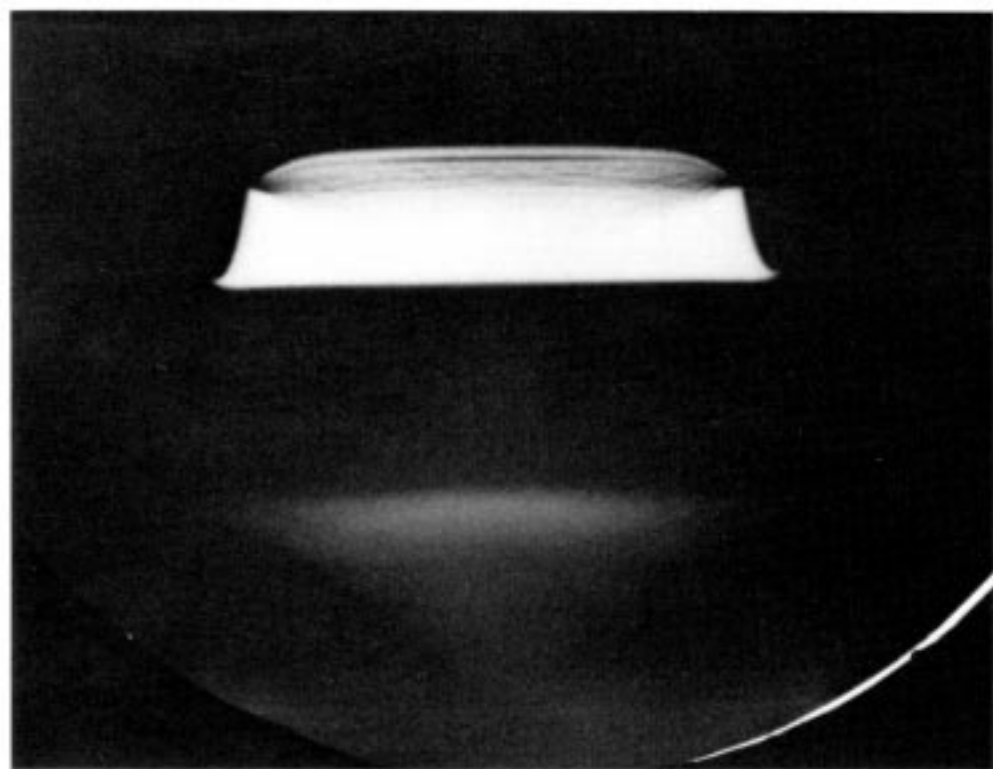
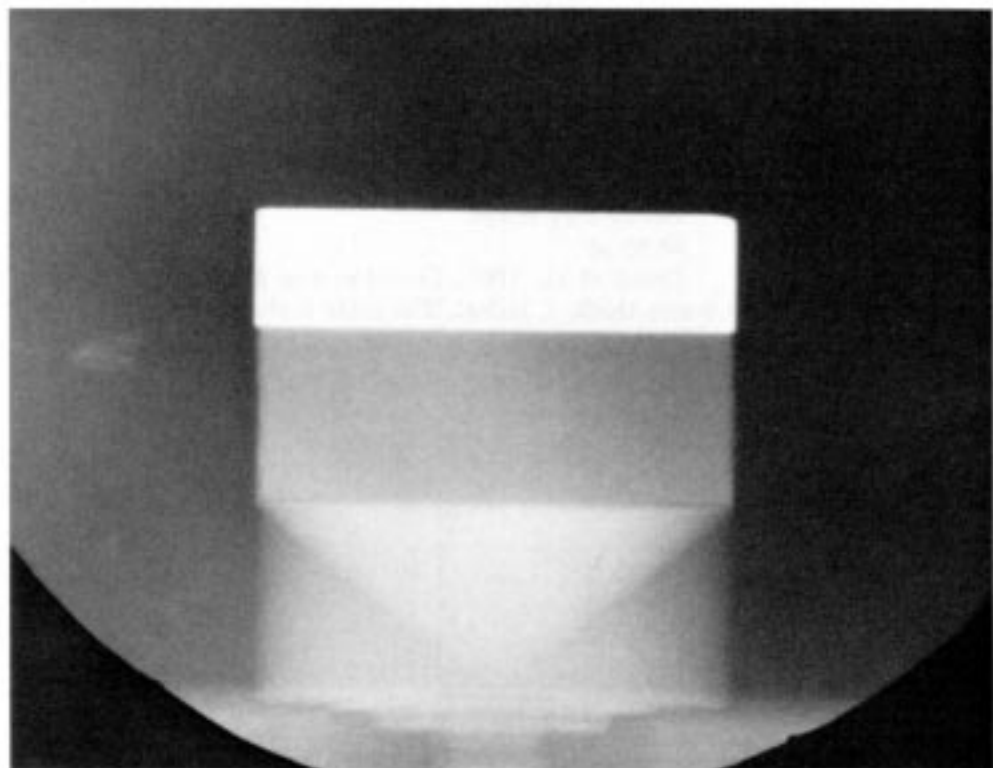
30.55 μ s

References:

Breed et al., 1967; Thurston and Mudd, 1968

Dynamic fracture of 25.0-mm-thick, t , nickel. The plate is shocked by 38.1 mm of Composition B-3 initiated by a P-040 lens. h is 38.1 mm.





SHOT 394:

Dynamic Fracture of Nickel

Date:

January 19, 1966

Experimenter:

Benny Ray Breed

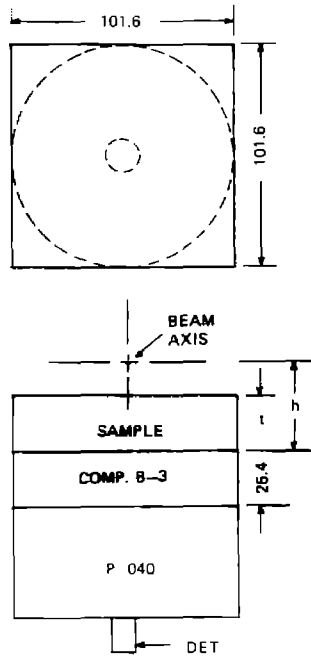
Radiographic Time:

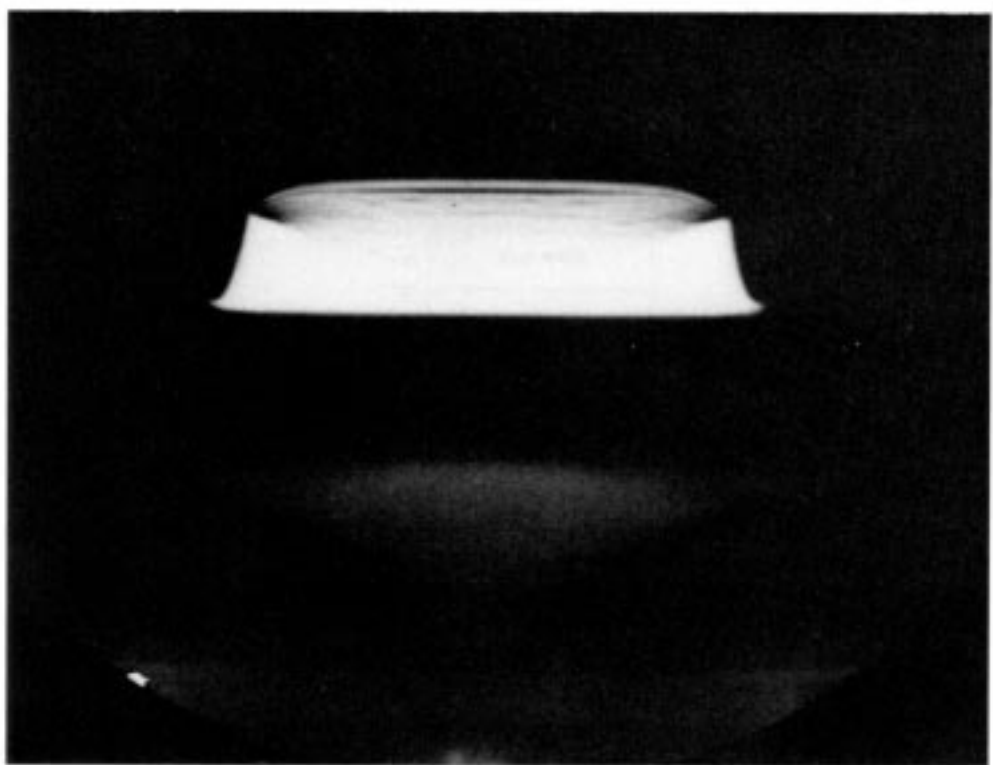
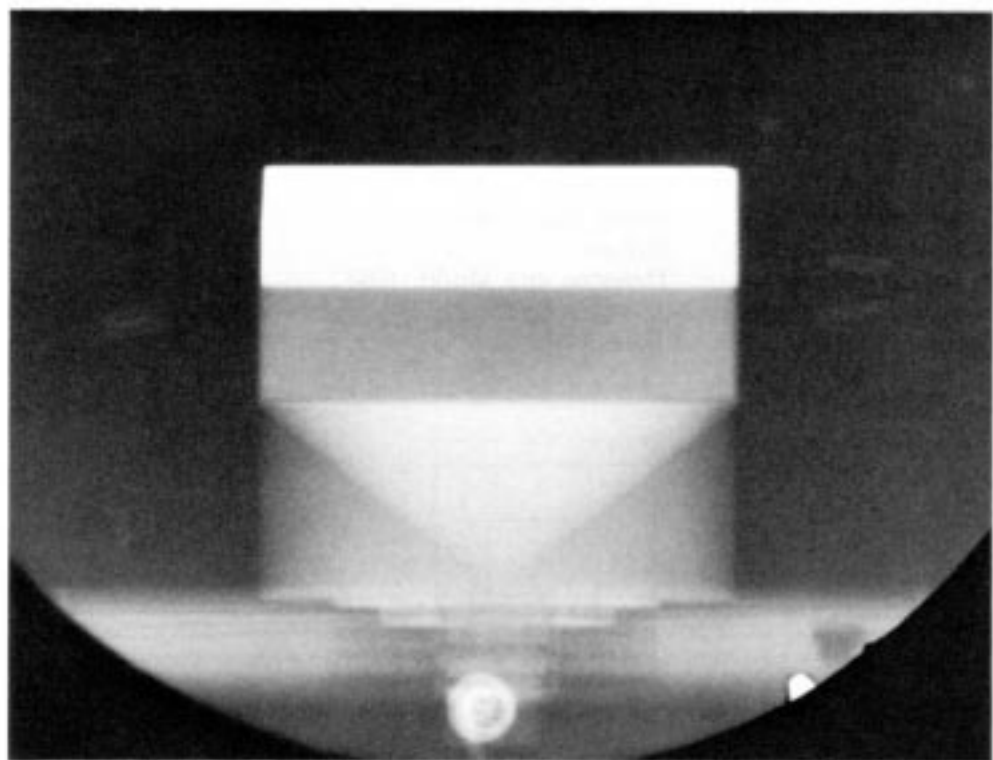
28.88 μ s

References:

Breed et al., 1967; Thurston and Mudd, 1968

Dynamic fracture of 25.0-mm-thick, t , nickel. The plate is shocked by 25.4 mm of Composition B-3 initiated by a P-040 lens. h is 38.1 mm.





SHOT 395:

Dynamic Fracture of Thorium

Date:

December 30, 1965

Experimenter:

Benny Ray Breed

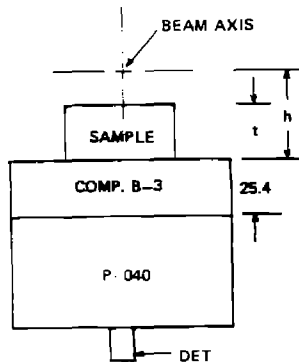
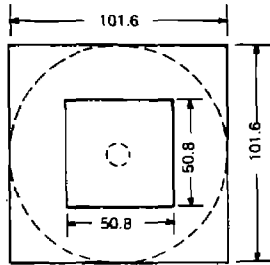
Radiographic Time:

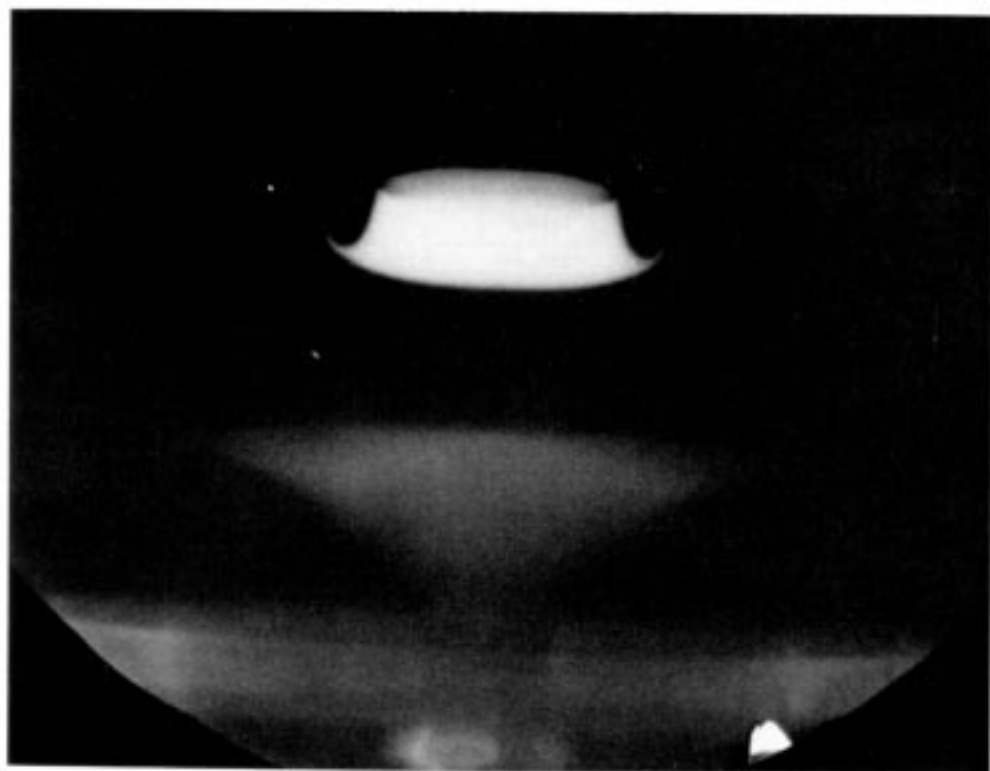
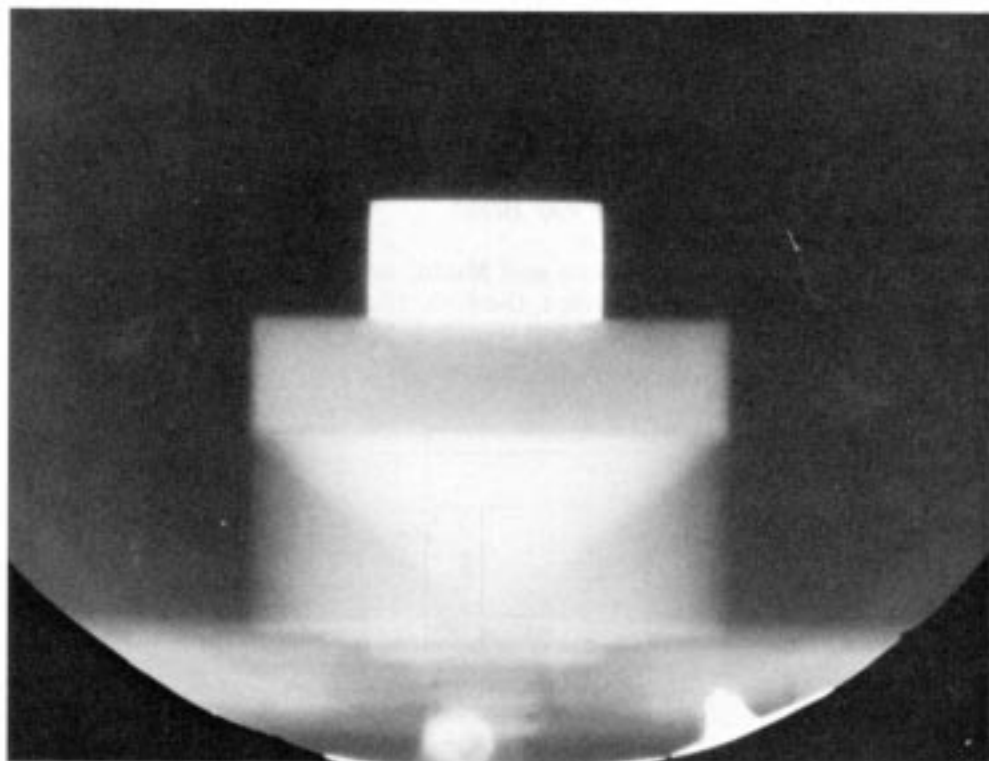
29.7 μ s

Reference:

Thurston and Mudd, 1968

Dynamic fracture of 25.0-mm-thick, t , thorium. The plate is shocked by 25.4 mm of Composition B-3 initiated by a P-040 lens. h is 38.1 mm.





SHOT 396:

Dynamic Fracture of Thorium

Date:

January 12, 1966

Experimenter:

Benny Ray Breed

Radiographic Time:

28.09 μ s

Reference:

Thurston and Mudd, 1968

Dynamic fracture of 25.0-mm-thick, t , thorium. The plate is shocked by 12.7 mm of Composition B-3 initiated by a P-040 lens. h is 38.1 mm.

